NASA Conference Publication 3270

# Third International Workshop on Squeezed States and Uncertainty Relations

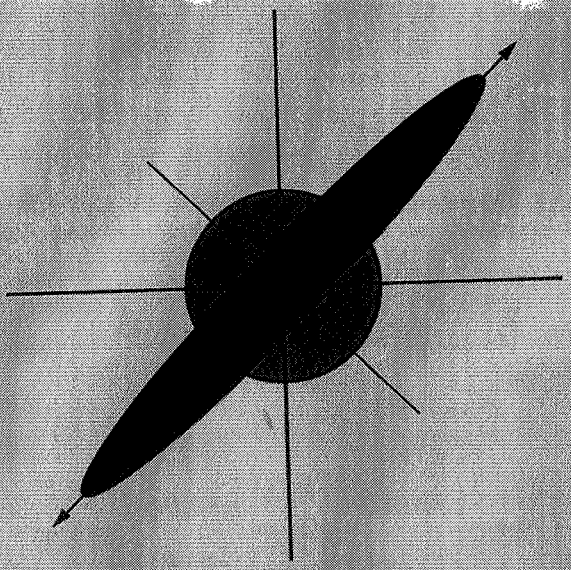

*Proceedings of a workshop held at the University of Maryland Baltimore County Baltimore, Maryland August 10 - 13, 1993*

NASA Conference Publication 3270

# Third International Workshop on Squeezed States and Uncertainty Relations

Edited by
D. Han
*Goddard Space Flight Center*
*Greenbelt, Maryland*

Y. S. Kim
*University of Maryland*
*College Park, Maryland*

N. H. Rubin
Y. Shih
*University of Maryland Baltimore County*
*Baltimore, Maryland*

W. W. Zachary
*Howard University*
*Washington, D. C.*

*Proceedings of a workshop held at the*
*University of Maryland Baltimore County*
*Baltimore, Maryland*
*August 10 - 13, 1993*


National Aeronautics and
Space Administration

**Scientific and Technical**
**Information Branch**

**1994**

Principal Organizers:

Morton H. Rubin (University of Maryland Baltimore County)
Yanhua Shih (University of Maryland Baltimore County)

Organizing Committee:

| | |
|---|---|
| C. Alley | (Univ. of Maryland, College Park) |
| V. Dodonov | (Moscow Physical Institute of Technology) |
| D. Han | (NASA Goddard Space Flight Center) |
| V. Isakov | (Lebedev Physical Institute) |
| Y. S. Kim | (Univ. of Maryland, College Park) |
| C. S. Lee | (Univ. of Maryland, College Park) |
| M .A. Man' ko | (Lebedev Physical Institute) |
| V. I. Man'ko | (Lebedev Physical Institute) |
| P. McGrath | (Laboratory for Physical Science) |
| H. S. Pilloff | (Office of Naval Research) |
| A. V. Vinogradov | (Lebedev Physical Institute) |
| W. W. Zachary | (Howard University) |

This workshop was supported by the American Physical Society, the Goddard Space Flight Center, National Aeronautics and Space Administration, The International Science Foundation, the Laboratory of Physical Sciences, the National Science Foundation, and the Office of Naval Research. Spectral Physics Corporation provided funds for refreshments.

# PREFACE

The Third International workshop on Squeezed States and Uncertainty Relations was held at the University of Maryland Baltimore County on August 10-13, 1993. This workshop was jointly organized by the University of Maryland and the Lebedev Physical Institute of the Russian Republic. These workshops were initiated by Y. S. Kim of the University of Maryland, College Park. The first of these workshops was held in 1991 at the University of Maryland, College Park and the second in Moscow in 1992.

The purpose of these workshops is to bring together an international selection of scientists to discuss the latest developments in Squeezed States in various branches of physics, and in the understanding of the foundations of quantum mechanics. At the third Workshop special attention was given to the influence that quantum optics is having on our understanding of quantum measurement theory.

The fourth meeting in this series will be held in the People's Republic of China. The principal organizer will be Q. C. Peng of the Shanxi University at Taiyun, P.R.C.

# REGISTERED PARTICIPANTS

Alley, Carroll O., Dept. of Physics, University of Maryland, College Park, MD 20742

Arnoldus, Henk, Dept. of Physics, Villanova University, Villanova, PA 19085

Artoni, Maurizo, Photonics Branch, NASA Goddard Space Flight Center, Greenbelt, MD 20771

Bandilla, Arno, Arbeitsgruppe Nichtklassische Strahlung der Humboldt Universitat, Berlin, Germany

Bly, Darren, Dept. of Physics, University of Maryland Baltimore County, Baltimore, MD 21228

Boivin, Luc, Massachusetts Institute of Technology, Room 36-497, Cambridge, MA 02139

Brandt, Howard, U.S. Army Research Laboratory, 2800 Powder Mill Road, Adelphi, MD 20783

Braunstein, Samuel, Dept. of Physics, Technion-Israel Institute of Technology, Haifa 32000, Israel

Bulatov, Alexi, Dept. of Physics, CCNY of CUNY, New York, NY 10031

Cabrera, Guillermo, Instituto de Fisica, Universidade Estadual de Campinas, Campinas, SP, Brazil, 13083-970

Cappetta, Luisa, Dept. Ing. Info. and Math. Appl., University of Salerno, Via Ponte Don Melillo, I84084 Fisciano (SA), Italy

Castaños, Octavio, Instituto de Ciencias Nucleares, UNAM, A.P. 70-543 Mexico D.F., Mexico

Ceperley, Peter, Electrical and Computer Engineering, George Mason University, Fairfax, VA 22030

Chizhov, Alexei, Laboratory of Theoretical Physics, Joint Institute for Nuclear Research, Head Post Office P.O. Box 79, Moscow 101000, Russia

D'Ariano, Giacomo, Dipartimento di Fisica "A. Volta", Universita di Pavia, Via Bassi 6, Pavia I-27100, Italy

de Muynck, Willem, Theoretical Physics, Eindhoven Institute of Technology, Eindhoven, The Netherlands

DeFacio, Brian, Department of Physics and Astronomy, University of Missouri, Columbia, MO 65211

De Martini, Francesco, Dept. of Physics, Universita di Roma, Piazza A. Moro, 2 Roma, Italy

Dowling, Jonathon, Research, Development, and Engineering Center, U.S. Army Missile Command, Redstone Arsenal, AL 35898

Enrico, Montanari, Dept. of Physics, Universita Degli Studi di Ferrara, Via Paradiso 12, Ferrara 44100, Italy

Fedele, Renato, Dept. of Physical Sciences, University of Naples, Naples I-80125, Italy

Cabrera, David Jose Fernandez, Dept. of Physics, Centro de Investigacion y Estudios, Avanzados del IPN, A.P. 14-740 07000, Mexico D.F.

Fivel, Daniel, Dept. of Physics, University of Maryland, College Park, MD 20742

Fortini, Pierluigi, Dept. of Physics, University of Ferrara, Via Paradiso 12, Ferrara 44100, Italy

Fortunato, Mauro, Dept. of Physics, University of Rome "La Sapienza", Rome 2-00185, Italy

Franson, James, Applied Physics Laboratory, Johns Hopkins University, Laurel, MD 20723

Fry, Edward, Dept. of Physics, Texas A&M University, College Station, TX 77843-4242

Gallis, Michael, Dept. of Physics, Pennsylvania State University Schuylkill, Schuylkill Haven, PA 17972

Garza, Octavio, Instituto de Ciencias Nucleares, UNAM, A.P. 70-543 Mexico D.F., Mexico

Giovannini, Massimo, Instituto Nazionale di Fisica Nucleare Torino, Italy

Greenberger, Daniel, Dept. of Physics, CCNY, New York, NY 10031

Haus, Herman, Electrical Engineering and Computer Science, Massachusetts Institute of Technology, Cambridge, MA 02139

Hegerfeldt, Gerhard, Institut für Theoretische Physik, Universität Göttingen, Germany

Hillery, Mark, Dept. of Physics and Astronomy, Hunter College of CUNY, New York, NY 10021

Horne, Michael, Dept. of Physics, Stonehill College, North Easton, MA 02357

Illuminati, Fabrizo, Dipartimento di Fisica, Universita di Salerno, Salerno, Italy

Isakov, V., Lebedev Physical Institute, Leninsky Prospect 53, Moscow 117924, Russia

Joneckis, Lance, Laboratory for Physical Sciences, University of Maryland, College Park, MD 20742

Joobeur, Adel, Electrical and Computer Engineering, University of Wisconsin, Madison, WI 53705

Jorgensen, Thomas, Chemical Physics, The Technical University of Denmark, Lyngby, Denmark

Kaertner, Franz, Research Laboratory of Electronics, Massachusetts Institute of Technology, Cambridge, MA 02139

Kakazu, Kiyotaka, Dept. of Physics, University of Maryland, College Park, MD 20742

Karassiov, V. P., Lebedev Physical Institute, Leninsky Prospect 53, Moscow 117924, Russia

Kauderer, Mark, Rome Laboratory, Griffith Air Force Base, Rome, NY 13441

Ketov, Sergei, Institute of Theoretical Physics, University of Hannover, Hannover, Germany

Kiess, Thomas, Dept. of Physics, University of Maryland, College Park, MD 20742

Kim, Abjung, Dept. of Physics, Northwestern University, Evanston, IL 60201

Kim, Chonghoon, 2145 Sheridan Road, Evanston, IL 60208-3118

Kim, Y. S., Dept. of Physics, University of Maryland, College Park, MD 20742

King, Sun-Kun, Dept. of Physics, National Tsing hua University, Hsinchu 30043, Taiwan

Klimov, Andrei, Fisico-Mathematicas, Universidad de Guadalajara, 44100 Guadalajara, Jalisco, Mexico

Klyshko, David, Dept. of Physics, Moscow State University, Moscow 119899, Russia

Kostelecky, Alan, Dept. of Physics, Indiana University, Bloomington, IN 47405

Kouznetsov, Dmitri, Centro de Instrumentos, Universidad Nacional Autonoma de Mexico, AP 70-186 Mexico DF, Mexico

Krenn, Gunther, Atominstitut der Osterreichischen Universitaten, Vienna, Austria

Kryuchkyan, G., Institute for Physical Research, Armenian Academy of Sciences, Ashtarak 2, Armenia

Kulagin, V., Steinberg Astronomical Institute, Moscow State University, Moscow 119899, Russia

Kumar, Prem, Electrical Engineering and Computer Science, Northwestern University, Evanston, IL 60208-3118

Kwiat, Paul, Dept. of Physics, University of California, Berkeley, CA 94720

Larchuk, Todd, Electrical Engineering, Columbia University, New York, NY 10027

Lee, C. T., Dept. of Physics, Alabama A&M University, Normal, AL 35762

Lee, Kang-Soo, Dept. of Physics, Sogang University, Seoul, Korea

Lerner, Peter, MS K723, Los Alamos National Laboratory, Los Alamos, NM 87545

Li, Hui, Dept. of Physics, Tsinghua University, 100084 Beijing, China

Ling, Hong Yuan, Dept. of Chemistry and Physics, Rowan College, Glassboro, NJ 08023

Lvovsky, Alexander, c/o. Dr. A. Rabinovich, 34-40 79th Street, #5, Jackson Heights, NY 11372

Man'ko, Margarita, Lebedev Physical Institute, Leninsky Prospect 53, Moscow 117924, Russia

Man'ko, Vladimir, Lebedev Physical Institute, Leninsky Prospect 53, Moscow 117924, Russia

Nancini, Stevano, Dept. of Physics, Universita di Camerino, Camerino 62032, Italy

Mandel, Leonard, Dept. of Physics and Astronomy, University of Rochester, Rochester, NY 14627

Mann, Ady, Dept. of Physics, Technion-Israel Institute of Technology, Haifa, Israel

Martens, Hans, Dept. of Physics, Eindhoven University of Technology, Eindhoven, The Netherlands

Martin, Manuel, Instituto de Fisica, Universidad Autonoma de Puebla, Puebla, Mexico

Matacz, Andrew, Dept. of Physics, University of Maryland, College Park, MD 20742

McDermott, Roger, Applied Mathematics, The Open University, Milton Keynes MK7 7BH Bucks, United Kingdom

McGrath, Paul, Laboratory for Physical Sciences, University of Maryland, College Park, MD 20742

Mertens, Christopher, Dept. of Physics, Georgia Institute of Technology, Atlanta, GA 30332-0430

Mittleman, Marvin, Dept. of Physics, The City College of New York, New York, NY 10031

Mizrahi, Solomon, Departamento de Fisica, Universidade Federal de Sao Carlos, 235 Sao Carlos, SP Brazil 13565-905

Morris, Randall, AAW System Design, Martin Marietta, Moorestown, NJ 08057

Mulhern, John, Dept. of Physics, University of New Hampshire, Durham, NH 03824

Nikonov, Dmitri, Dept. of Physics, Texas A&M University, College Station, TX 77843-4242

Orszak, Jeffrey, Dept. of Physics, University of Maryland Baltimore County, Baltimore, MD 21228-5398

Ortolan, Antonello, Laboratori Nazionali di Legnaro, Legnaro, Italy 35020

Ou, Jeffrey, Dept. of Physics, Indiana University - Purdue University at Indianapolis, Indianapolis, IN 46202

Ozawa, Masanao, Dept. of Mathematics, Nagoya University, Chikosako, Nagoya 464-01, Japan

Panunto, Michael, Dept. of Physics, University of Maryland Baltimore County, Baltimore, MD 21228-5398

Pilloff, Herschel, Office of Naval Research, 800 North Quincy Street, Arlington, VA 22217-5660

Pittman, Todd, Dept. of Physics, University of Maryland Baltimore County, Baltimore, MD 21228-5398

Popescu, Sandu, Theoretical Physics, Universite Libre de Bruxelles, Brussels, Belgium

Puri, Ravinder, Dept. of Physics and Astronomy, University of Rochester, Rochester, NY 14627

Reifler, Frank, AAW System Design, Martin Marietta, Moorestown, NY 08057

Ritus, V., Lebedev Physical Institute, Leninsky Prospect 53, Moscow 117924, Russia

Rous, Phillip, Dept. of Physics, University of Maryland Baltimore County, Baltimore, MD 21228-5398

Roger, Antoine, Genie Physique, Ecole Polytechnique, Montreal, Québec, Canada

Rubin, Morton H., Dept. of Physics, University of Maryland Baltimore County, Baltimore, MD 21228-5398

Ryff, Luiz Carlos, Instituto de Fisica, Universidade Federal do Rio de Janeiro, Rio de Janeiro, Brazil

Saleh, Bahaa, Dept. of Engineering and Computer Science, University of Wisconsin, Madison, WI 53706-1691

Sandoval, Lourdes, Instituto de Fisica, Universidad Autonoma de Puebla, Puebla, Mexico

Santos, Emilio, Fisica Moderna, Universidad de Cantabria, Santander, Spain

Schraner, Daniel, Dept. of Physics, University of Illinois, Urbana, IL 61801

Schrade, Guenter, Abteilung fur Quantenphysik, Universitat Ulm, Ulm, Germany

Scully, Marlan, Dept. of Physics, Texas A&M University, College Station, TX 77843

Sergienko, A., Dept. of Physics, University of Maryland Baltimore County, Baltimore, MD 21228-5398

Shapiro, Jeffrey, Dept. of Electrical Engineering and Computer Science, Massachusetts Institute of Technology, Cambridge, MA 02139-4307

Shepard, Scott, Dept. of Physics, Baylor University, Waco, TX 76798-7316

Shih, Yanhua, Dept. of Physics, University of Maryland Baltimore County Baltimore, MD 21228-5398

Shimony, Abner, Dept. of Physics and Philosophy, Boston University, Boston, MA 02215

Spiridonov, Vyacheslav, Centre des Recherches Mathé matique, Université de Montréal, Montréal, Québec H3C 307, Canada

Stroucken, Tineke, Dept. of Theoretical Physics, Technical University of Eindhoven, Eindhoven, The Netherlands

Sudarshan, E. C. G., Dept. of Physics, University of Texas, Austin, TX 78712

Summers, Geoffrey, Dept. of Physics, University of Maryland Baltimore County, Baltimore, MD 21228-5398

Summhammer, Johann, Atominstitut der Õ sterreichischen Universitäten, Vienna. Austria

Tanatar, Bilal, Dept. of Physics, Bilkent University, Ankara, Turkey

Tapster, Paul, Defense Research Agency, St. Andrews Road, Malvern Worcs, United Kingdom

Teich, Malvin, Dept. of Electrical Engineering, Columbia University, New York, NY 10027

Torre, Amalia, ENEA, Dip. INN, Settore Elettroottica e Laser, Frascati, Rome, Italy

Torres - Vega, Gabino, Departamento de Fisica, Centro de Investigación y de Estudios Avanzados del IPN,07000 México D.F

Tsue, Yasuhiko, Dept. of Physics, Kochi University, Kochi 780, Japan

Uffink, Jos, Dept. of History and Foundations of Mathematics and Science, University of Utrecht, The Netherlands

Vaidman, Lev, Dept. of Physics, Tel-Aviv University, Tel Aviv 69978, Israel

Vasilyev, Michael, Lebedev Physical Institute, Leninsky Prospect 53, Moscow 117924, Russia

Vitiello, Giuseppe, Dept. of Physics, University of Salerno, Salerno, Italy

Vogel, Karl, Abteilung für Quantenphysik, Universität Ulm, Ulm, Germany

Vourdas, Apostolos, Dept. of Electrical Engineering, University of Liverpool, Liverpool, United Kingdom.

Wahiddin, Mohamed, Dept. of Mathematics, University of Malaya, Kuala Lumpur, Malaysia

Wang, Lijun, Dept. of Physics, Duke University, Durham, NC 27708-0305

Wu, Ling-An, Institute of Physics, Chinese Academy of Sciences, Bejing 100080, China

Xiao, Min, Dept. of Physics, University of Arkansas, Fayetteville, AR 72701

Yeon, Kyu Hwang, Dept. of Physics, Chungbuk National University, Cheongju, Korea

Yilmaz, Huseyin, Hamamatsu Photonics, 105 Church Street, Winchester, MA 01890

Youn, Sun-Hyun, Dept. of Physics, Seoul National University, Seoul, Korea

Yu, Li-Hua, Brookhaven National Laboratory, NSLS, Upton, NY 11973

Yuen, Horace, Dept. of Electrical Engineering and Computer Science, Northwestern University, Evanston, IL 60208

Zachary, Woodford W., Computational Science and Engineering Research Center, Howard University, Washington, D.C. 20059

Zeilinger, Anton, Institute for Experimental Physics, University of Innsbruck, Innsbruck, Austria

Zhang, Yuhong, Center for Biologies and Evaluation Research, Food and Drug Administration, 8800 Rockville Pike, Bethesda, MD 20892

## TABLE OF CONTENTS

**SECTION 1 SQUEEZED STATES**

## SECTION 2 QUANTUM MEASUREMENT THEORY



## SECTION 3 AMPLIFLIER AND CAVITY ELECTRODYNAMICS

## SECTION 5 UNCERTAINTY RELATIONS



## SECTION 6 FIELD THEORY AND GENERAL INTEREST

## SECTION 8 EPR PROBLEM, BELL'S INEQUALITIES AND MULTIPHOTON INTERFEROMETRY

**BANQUET TALK**

# SECTION 1

# SQUEEZED STATES

# PROPERTIES OF TWO–MODE SQUEEZED NUMBER STATES

A. V. Chizhov and B. K. Murzakhmetov
*Bogolubov Theoretical Laboratory, Joint Institute for Nuclear Research*
*Head Post Office, P.O. Box 79, 101000 Moscow, Russian Federation*

**Abstract**

Photon statistics and phase properties of two–mode squeezed number states are studied. It is shown that photon number distribution and Pegg–Barnett phase distribution for such states have similar $(N+1)$–peak structure for nonzero value of the difference in the number of photons between modes. Exact analytical formulas for phase distributions based on different phase approaches are derived. The Pegg–Barnett phase distribution and the phase quasiprobability distribution associated with the Wigner function are close to each other, while the phase quasiprobability distribution associated with the $Q$ function carries less phase information.

## 1 Introduction

Recent developments in quantum optics have led to new proposals to generate number states of the electromagnetic field using conditioned measurements techniques [1] or the properties of atom–field interactions in microwave cavities in the micromaser [2]. The precisely defined two–mode photon number state $|N+q,N\rangle$ can be used as an input field in a squeezing device, such as a parametric amplifier. The model involves a signal and an idler modes driven by a classical pump. The Hamiltonian for the two coupled modes is taken to be [3, 4] (we set $\hbar=1$)

$$\hat{H}=\omega_a\hat{a}^\dagger\hat{a}+\omega_b\hat{b}^\dagger\hat{b}-i\{g\hat{a}\hat{b}\exp(i\omega t)-g^*\hat{b}^\dagger\hat{a}^\dagger\exp(-i\omega t)\},$$

where $\omega$ is the pump frequency and $g$ is the effective intermode coupling constant. If we consider exact resonance $\omega=\omega_a+\omega_b$ then the Hamiltonian may be transformed into the interaction picture

$$\hat{H}_I=-i\{g\hat{a}\hat{b}-g^*\hat{b}^\dagger\hat{a}^\dagger\}.$$

In this picture the time–evolution operator is

$$\exp(-i\hat{H}_I t)=\exp\{-gt\hat{a}\hat{b}+g^*t\hat{b}^\dagger\hat{a}^\dagger\},$$

and is immediately identifiable as a time–dependent two–mode squeezed operator:

$$\exp(-i\hat{H}_I t)=\hat{S}(gt).$$

with squeezing parameter $\xi=gt$. The output state at time $t$ will be the two–mode squeezed number state

$$|\xi\rangle=\exp(-\xi\hat{a}\hat{b}+\xi^*\hat{b}^\dagger\hat{a}^\dagger)|N+q,N\rangle.$$

The properties of this state are phase dependent and it should be interesting to study them.

The problem of the quantum description of the optical field phase has been the subject of considerable study for many years [5]. This is connected with the difficulty in constructing a Hermitian phase operator. Within the past few years the notion of phase variables in quantum systems has been greatly clarified. Pegg and Barnett [6]–[8] have shown how such an operator can be defined for quantized electromagnetic fields. This new formalism makes it possible to describe the quantum properties of optical phase in a direct way within quantum mechanics on the basis of the Hermitian phase operator and its eigenstates.

A quite different approach to the concepts of the phase variable has also been widely used in quantum optics [9]–[11] and which involves quantum quasiprobability distributions such as the $Q$ function and the Wigner function rather than Hermitian operators and their eigenstates. These quasiprobability distributions depend upon the complex eigenvalue $\alpha$ of the non-Hermitian annihilation operator, which can be expressed in terms of a radial variable $|\alpha|$ and a "phase" $\theta$ both of which are real. If we integrate over the radius, the resulting distributions are periodic in the phase angle and, for the most of states they satisfy all properties required by a proper phase distribution. In recent papers, the Pegg–Barnett phase distribution have been compared with those distributions obtained from the Wigner and $Q$ functions by integrating them over the radius for the multi–photon down–conversion [12], displaced number states and displaced thermal states [13], squeezed number states and squeezed thermal states [14]. In this paper we extend such comparison onto two–mode case.

The purpose of this paper is to study photon statistics and phase properties of the two–mode squeezed number states which can be considered as a natural generalization of a two–mode squeezed vacuum state.

## 2 Photon number statistics

Consider two modes of the electromagnetic field, which have annihilation operators $\hat{a}$ and $\hat{b}$. A two–mode squeezed number state (TMSNS) is defined by acting with the squeeze operator $\hat{S}(r,\varphi)$ on the two–mode number state $|N+q,N\rangle$, that is

$$|N+q,N\rangle_{(r,\varphi)} = \hat{S}(r,\varphi)|N+q,N\rangle, \quad q \geq 0, \tag{1}$$

where $q$ is the difference in the number of photons between two modes and

$$\hat{S}(r,\varphi) \equiv \exp[r(\hat{a}\hat{b}\mathrm{e}^{-2i\varphi} - \hat{b}^{\dagger}\hat{a}^{\dagger}\mathrm{e}^{2i\varphi})]. \tag{2}$$

In problems in which photons are either created in pairs or destroyed in pairs the value of $q$ remains constant. Note that in many applications where pair creation occurs starting from vacuum, the parameter $q$ will be zero. The number state decomposition of TMSNS can be written as

$$\begin{aligned} |N+q,N\rangle_{(r,\varphi)} &= \sum_n |n+q,n\rangle\langle n+q,n|N+q,N\rangle_{(r,\varphi)} = \\ &= \sum_n b_n \mathrm{e}^{i\varphi_n}|n+q,n\rangle, \end{aligned} \tag{3}$$

where

$$b_n = \frac{(\tanh r)^{N+n}}{(\cosh r)^{1+q}} (N!(N+q)!n!(n+q)!)^{1/2} \times \sum_{k=0}^{\min(n,N)} \frac{(-1)^{n-k}(\sinh r)^{-2k}}{k!(n-k)!(N-k)!(q+k)!} \tag{4}$$

and

$$\varphi_n = (n-N)\varphi \tag{5}$$

with $\varphi$ being a phase of squeezing. The above amplitude is obtained by using the factored form of the two–mode squeeze operator [15]

$$\hat{S}(r,\varphi) = (\cosh r)^{-1} \exp[-\hat{a}^\dagger \hat{b}^\dagger e^{2i\varphi} \tanh r] \times \exp[-(\hat{a}^\dagger \hat{a} + \hat{b}^\dagger \hat{b}) \ln(\cosh r)] \exp[\hat{a}\hat{b} e^{-2i\varphi} \tanh r]. \tag{6}$$

The mean number of photons in the TMSNS is

$$\langle \hat{a}^\dagger a + \hat{b}^\dagger b \rangle = (2N+q+1)\cosh 2r - 1. \tag{7}$$

The joint probability to find $n_a$ photons in mode $a$ and $n_b$ photons in mode $b$ is given by

$$P(n_a, n_b) = |\langle n_a, n_b | N+q, N \rangle_{(r,\varphi)}|^2. \tag{8}$$

Using (3) and (4), we get

$$P(n_a, n_b) = P(n+q, n)\delta_{n_a, n+q}\delta_{n_b, n}, \tag{9}$$

where

$$P(n+q, n) \equiv P_q(n) = |b_n|^2. \tag{10}$$

As we can see in Fig. 1, photon number distribution $P_q(n)$ has an oscillatory behaviour. Such a behaviour is a consequence of interference in four–dimensional phase space [16]. We would like to emphasize a presence of $(N+1)$ peaks in the photon number distribution. The similar behaviour of the photon number distribution was observed for the displaced number states [17]. It should be stressed that such a peak structure for TMSNS can be revealed only for those values of the parameter $q$ greater than a certain number. This number depends on the value of $N$ and for large $N$ we ought to choose large values for such a number. Otherwise, some adjacent peaks in the photon number distribution might overlap and thus $(N+1)$–peak structure cannot be certainly discerned.

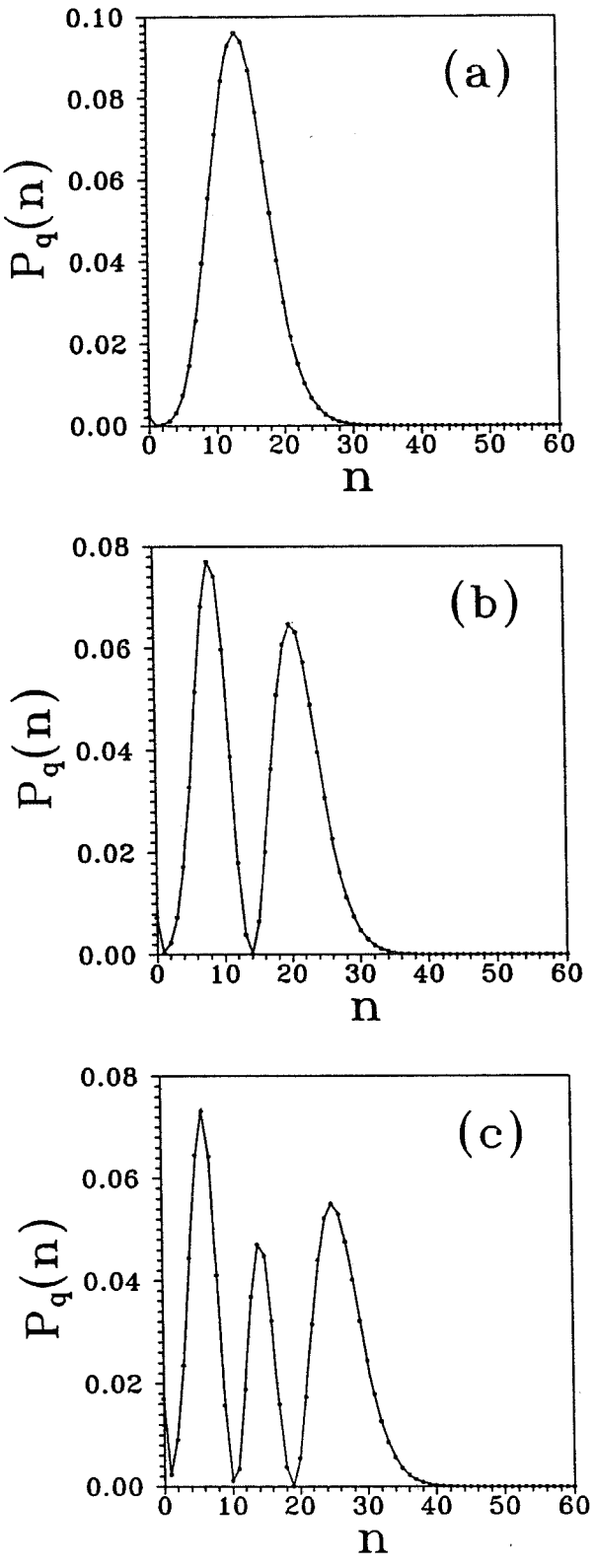


FIG. 1. Photon number distribution for the two-mode squeezed number state with $r = 0.5$, $q = 50$ and (a) $N = 0$, (b) $N = 1$, (c) $N = 2$.

# 3 Quasiprobability distributions

In this section we examine the representation of TMSNS by quasiprobability phase-space distributions. For convenience we choose the squeezing parameter to be real, $\xi = r$. The two-mode quasiprobability distributions are formed by a natural generalization of those for the single-mode fields [18]. The Glauber-Sudarshan $\mathcal{P}$ function, the Wigner function and the $Q$ function are obtained by evaluating the Fourier transforms

$$V^{(s)}(\alpha,\beta) = \frac{1}{\pi^4}\int_{-\infty}^{\infty} d^2\eta d^2\xi \exp(\alpha\eta^* - \alpha^*\eta)\exp(\beta\xi^* - \beta^*\xi)C^{(s)}(\eta,\xi), \tag{11}$$

from the characteristic functions

$$C^{(s)}(\eta,\xi) = \exp\left(\frac{s}{2}(|\eta|^2+|\xi|^2)\right)\mathrm{Tr}\left\{\hat{\rho}\exp(\eta\hat{a}^\dagger - \eta^*\hat{a})\exp(\xi\hat{b}^\dagger - \xi^*\hat{b})\right\} \tag{12}$$

where $s = 1$ if $V = \mathcal{P}$, $s = 0$ if $V = W$ and $s = -1$ if $V = Q$. We would like to notice that there no exists well-defined Glauber-Sudarshan $\mathcal{P}$ function for states under consideration owing to their nonclassical nature [18, 19].

According to ref. [20], the $Q$ function can alternatively be defined as

$$Q(\alpha,\beta) = \frac{1}{\pi^2}\langle\alpha,\beta|\hat{\rho}|\alpha,\beta\rangle. \tag{13}$$

From this definition we see that the $Q$ function is always non-negative. Using the definition of the density matrix of TMSNS

$$\hat{\rho} = \hat{S}(r)|N+q,N\rangle\langle N+q,N|\hat{S}^\dagger(r) \tag{14}$$

and the factored form of the squeeze operator (6), we obtain

$$\begin{aligned} Q(\alpha,\beta) &= \frac{|\alpha|^{2q}}{\pi^2(\cosh r)^{4N+2q+2}}\exp[-(\alpha\beta+\alpha^*\beta^*)\tanh r]\exp[-(|\alpha|^2+|\beta|^2)] \\ &\times\sum_{n=0}^{N}\sum_{k=0}^{N}\frac{(\frac{1}{2}\sinh r)^{n+k}N!(N+q)!(\alpha^*\beta^*)^{N-n}(\alpha\beta)^{N-k}}{n!k!(N-n)!(N-k)!(N+q-n)!(N+q-k)!}. \end{aligned} \tag{15}$$

As to the Wigner function, it can also be represented as [20]

$$W(\alpha,\beta) = \frac{4}{\pi^2}Tr\left\{\hat{\rho}\hat{D}_a(2\alpha)\hat{D}_b(2\beta)\exp[i\pi(\hat{a}^\dagger\hat{a}+\hat{b}^\dagger\hat{b})]\right\}, \tag{16}$$

where $D_a(\gamma)$ and $D_b(\gamma)$ are the displacement operators for modes $a$ and $b$ respectively. It is straightforward to evaluate the Wigner function using eq. (14) and the operator transformations [15]

$$\hat{S}^\dagger(r)\hat{a}\hat{S}(r) = \hat{a}\cosh r - \hat{b}^\dagger\sinh r, \tag{17}$$

$$\hat{S}^\dagger(r)\hat{b}\hat{S}(r) = \hat{b}\cosh r - \hat{a}^\dagger\sinh r, \tag{18}$$

and their Hermitian conjugates. We find a quite simple analytical form for the Wigner function

$$\begin{aligned} W(\alpha,\beta) &= \frac{4}{\pi^2}(-1)^q \exp[-2\cosh 2r(|\alpha|^2+|\beta|^2) - 2\sinh 2r(\alpha\beta+\alpha^*\beta^*)] \\ &\times L_N\left((2\sinh r|\alpha|)^2 + (2\cosh r|\beta|)^2 + 2\sinh 2r(\alpha\beta+\alpha^*\beta^*)\right) \\ &\times L_{N+q}\left((2\cosh r|\alpha|)^2 + (2\sinh r|\beta|)^2 + 2\sinh 2r(\alpha\beta+\alpha^*\beta^*)\right). \end{aligned} \tag{19}$$

where $L_n(x)$ is the Laguerre polynomial of order $n$. From eqs. (15) and (19) one can see that the $Q$ function and the Wigner function depend on the sum of the phases $\theta_a+\theta_b$ only. This fact clearly exhibits the correlated nature of the two–mode squeezed number states. In the next section we will employ the quasiprobability functions in consideration of phase properties of these states.

# 4 Phase distributions

Now we employ the two–mode Pegg–Barnett phase formalism [21], [22] to find the phase distribution function for such states. This formalism is based on the observation that the Hermitian phase operator can be defined in a finite–dimensional state space, spanned by the number states. The main idea of the Pegg–Barnett formalism is to evaluate all necessary expectation values on this finite–dimensional state space, and only after that the dimension of the space is allowed to tend to infinity. Having the number state decomposition (3) of TMSNS we can determine the continuous joint phase probability distribution for the continuous phase variables $\theta_a$ and $\theta_b$, which is given by

$$P(\theta_a,\theta_b) = \frac{1}{(2\pi)^2}\left\{1 + 2\sum_{n>k}^{\infty} b_n b_k \cos[(n-k)(\theta_a+\theta_b)]\right\}, \tag{20}$$

where $b_n$ are given by Eq. (4). The distribution (20) is normalized such that

$$\int_{-\pi}^{\pi}\int_{-\pi}^{\pi} P(\theta_a,\theta_b)d\theta_a d\theta_b = 1. \tag{21}$$

One important phase property of TMSNS is seen directly from the form of formula (20). It is clear that the joint probability distribution depends on the sum of the two phases only

$$P(\theta_a,\theta_b) = P(\theta_+ = \theta_a+\theta_b). \tag{22}$$

This means the strong correlations of the two modes. Integrating $P(\theta_a,\theta_b)$ over one of the phases gives a marginal phase distribution $P(\theta_a)$ or $P(\theta_b)$ for the phases $\theta_a$ or $\theta_b$, which are uniformly distributed

$$P(\theta_a) = \int_{-\pi}^{\pi} P(\theta_a,\theta_b)d\theta_b = \frac{1}{2\pi}. \tag{23}$$

$$P(\theta_b) = P(\theta_a) = \frac{1}{2\pi}. \tag{24}$$

Thus the phases $\theta_a$ or $\theta_b$ of the individual modes are uniformly distributed, and the only nonuniformly distributed phase quantity is the phase sum $\theta_+ = \theta_a + \theta_b$. In Fig. 2 we plot the Pegg–Barnett phase distribution for TMSNS in polar coordinates for different values of parameter $q$. For nonzero values of $q$ the phase distribution shows $(N+1)$–lobe structure, and the greater $q$ the more distinct lobes become. However, when $q = 0$ the phase distribution has only one lobe for all $N$. It is important to notice a remarkable resemblance in a behaviour of the phase distribution and the photon number distribution for TMSNS: they both display the $(N+1)$–peak structure. Another significant feature of the joint phase distribution is a property of the phase locking — the phase sum is locked to the argument of the squeezing parameter in the limit of large squeezing [21, 23].

Now consider phase quasiprobability distributions which can be obtained by integrating quasiprobability distribution functions (11) over the radial variables [9], [10]. As we have noticed above, $\mathcal{P}$ function is not well–defined function for the states under consideration and therefore it is impossible to determine corresponding phase quasiprobability distribution. As a result of integration of $Q(\alpha,\beta)$ and $W(\alpha,\beta)$ over $|\alpha|$ and $|\beta|$, we arrive to the following formula:

$$P^{(V)}(\theta_+) = \frac{1}{(2\pi)^2}\left\{1 + 2\sum_{n>k} b_n b_k \cos[(n-k)\theta_+] G^{(V)}(n,k) G^{(V)}(n+q,k+q)\right\}, \tag{25}$$

where the coefficients $G^{(V)}(n,k)$ distinguish between two distributions. and they are:

(i) for the $Q$ function

$$G^{(Q)}(n,k) = \frac{\Gamma[(n+k)/2+1]}{\sqrt{n!k!}}, \tag{26}$$

(ii) for the Wigner function

$$\begin{aligned} G^{(W)}(n,k) &= \sum_{m=0}^{\lambda} (-1)^{\lambda-m} 2^{(|n-k|+2m)/2} \\ &\times \sqrt{\binom{\lambda}{m}\binom{\nu}{\lambda-m}}\, G^{(Q)}(m,|n-k|+m), \end{aligned} \tag{27}$$

where $\lambda = \min(n,k), \nu = \max(n,k)$. All the coefficients $G^{(V)}(n,k)$ are symmetrical, $G^{(V)}(n,k) = G^{(V)}(k,n)$, and $G^{(V)}(n,n) = 1$. Note, that such expressions (20), (25) for the phase distributions are valid for all two–mode states with the number state decomposition like in (3). In Fig. 3, we show the plots of the three phase distributions in polar coordinates for TMSNS calculated according to formulas (20) and (25) with the coefficients (26) and (27) for different values of $N$ and nonzero $q$. It is seen that the Pegg–Barnett phase distribution and $P^{(W)}(\theta_+)$ are similar and have the $N+1$ lobes, while $P^{(Q)}(\theta_+)$ is much broader and has only one lobe. In the case $q = 0$ all three distributions have the same form of one lobe. So, as in the case of displaced number states [13], there is an essential difference in the phase information carried by $P^{(Q)}(\theta_+)$ and $P^{(W)}(\theta_+)$. Because of the averaging procedure with the "probabilities" $G^{(Q)}(n,k)G^{(Q)}(n+q,k+q)$

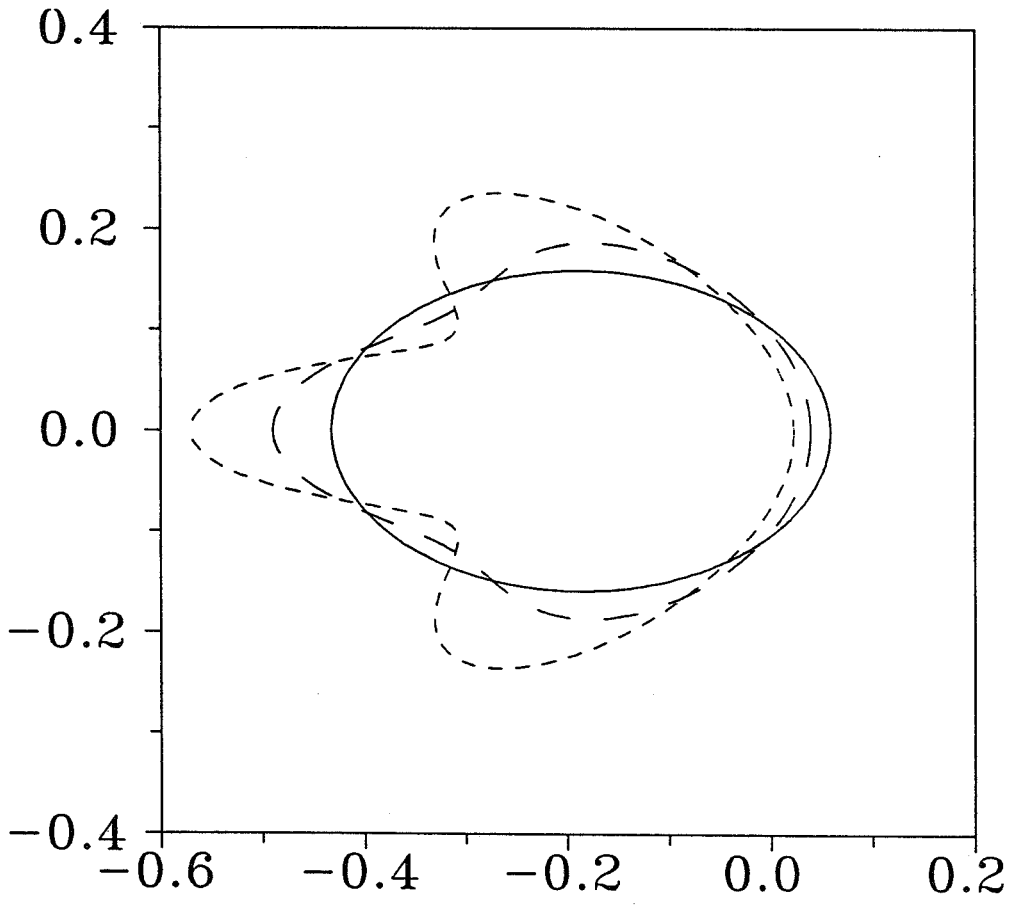


FIG. 2. Phase distribution $P^{(\mathrm{PB})}(\theta_+)$ for the two-mode squeezed number state with $r = 0.5$, $N = 2$ and $q = 0$ (solid line), $q = 3$ (long-dashed line) and $q = 6$ (short-dashed line).

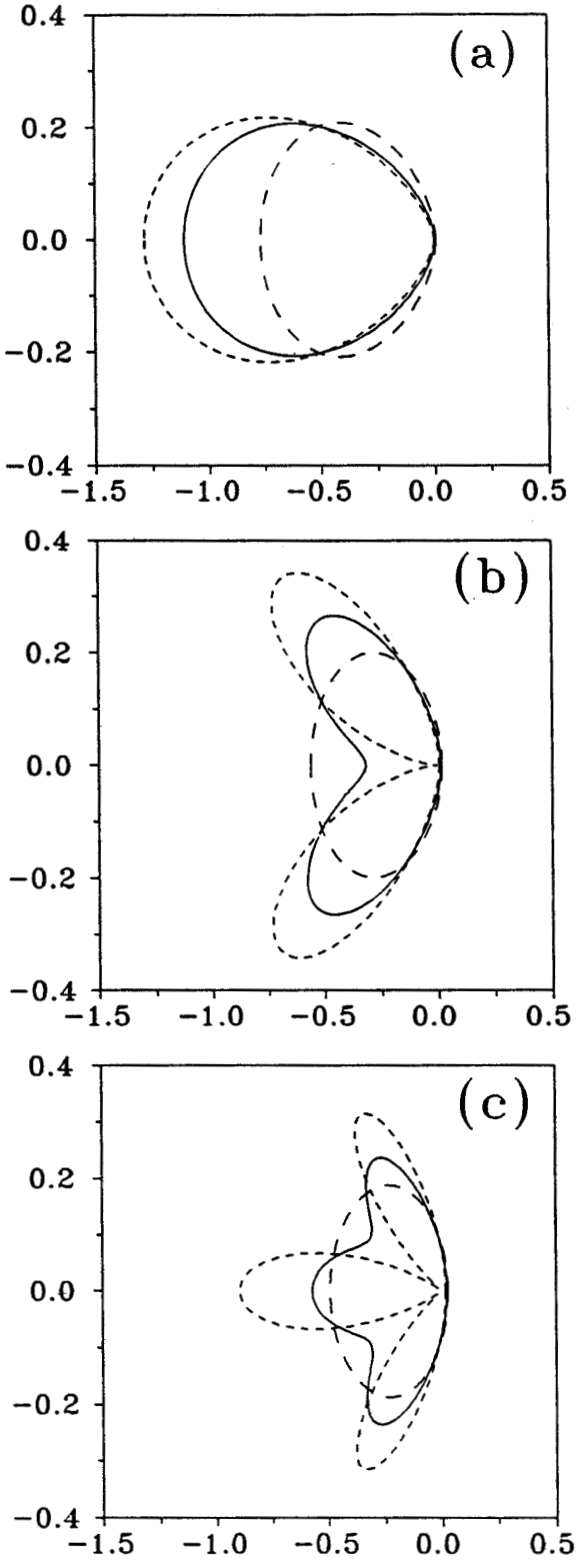


FIG. 3. Phase distribution $P^{(\mathrm{PB})}(\theta_+)$ (solid line) and phase quasiprobability distributions $P^{(W)}(\theta_+)$ (short-dashed line) and $P^{(Q)}(\theta_+)$ (long-dashed line) for the two-mode squeezed number state with $r = 0.5$, $q = 6$ and (a) $N = 0$, (b) $N = 1$, (c) $N = 2$.

some phase information is lost in $P^{(Q)}(\theta_+)$. The Pegg–Barnett phase distribution is very close to the distribution $P^{(W)}(\theta_+)$, although it is not identical to it. The phase peaks of $P^{(W)}(\theta_+)$ are slightly narrower than those of $P^{(\mathrm{PB})}(\theta_+)$. The greater the difference in number of photons $q$ the closer these two distributions. Basically they carry the same phase information. This similarity is in agreement with the area of overlap in phase space arguments, which are that the Wigner function represents quantum states in the phase space [10]. However, the Wigner function can take on negative values and the positive definiteness of $P^{(W)}(\theta_+)$ is not automatically guaranteed, while there are no such problems with the Pegg–Barnett phase distribution.

# 5 Conclusions

We have discussed photon statistics and phase properties of the two-mode squeezed number states showing that the photon number distribution and the Pegg–Barnett phase distribution for such states exhibit the similar $N+1$–peak structure for nonzero values of the difference in the number of photons $q$ between modes. We have compared the Pegg–Barnett phase distribution with the phase quasiprobability distributions $P^{(Q)}(\theta_+)$ and $P^{(W)}(\theta_+)$ obtained by integrating the $Q$ function and the Wigner function over the radial coordinates. We have shown that the Pegg–Barnett phase distribution and the distribution $P^{(W)}(\theta_+)$ carry basically the same phase information, while the distribution $P^{(Q)}(\theta_+)$ loses an essential part of the phase information.

# References


[1] C. K. Hong and L. Mandel, Phys. Rev. Lett. **56**, 58 (1986).

[2] P. Filipowicz, J. Javanainen and P. Meystre, J. Opt. Soc. Am. B **3**, 906 (1986).

[3] S. M. Barnett and P. L. Knight, J. Opt. Soc. Am. B **2**, 467 (1985).

[4] W. H. Louisell, A. Yariv and A. E. Siegman, Phys. Rev. **124**, 1646 (1961).

[5] P. Carruthers and M. M. Nieto, Rev. Mod. Phys. **40**, 411 (1968);
S. M. Barnett and D. T. Pegg, J. Phys. A **19**, 3849 (1986).

[6] D. T. Pegg and S. M. Barnett, Europhys. Lett. **6**, 483 (1988).

[7] S. M. Barnett and D. T. Pegg, J. Mod. Opt. **36**, 7 (1989).

[8] D. T. Pegg and S. M. Barnett, Phys. Rev. A **39**, 1665 (1989).

[9] S. L. Braunstein and C. M. Caves, Phys. Rev. A **42**, 4115 (1990).

[10] W. Schleich, R. J. Horowicz and S. Varro, Phys. Rev. A **40**, 7405 (1989).

[11] W. Schleich, A. Bandilla and H. Paul, Phys. Rev. A **45**, 6652 (1992).

[12] R. Tanaś and Ts. Gantsog, Phys. Rev. A **45**, 5031 (1992).

[13] R. Tanaś, B. K. Murzakhmetov, Ts. Gantsog and A. V. Chizhov, Quantum Optics **4**, 1 (1992); A. V. Chizhov, Ts. Gantsog, B. K. Murzakhmetov and R. Tanaś, J. Quant. Nonlinear Phenomena (in press).

[14] A. V. Chizhov, Ts. Gantsog and B. K. Murzakhmetov, Quantum Opt. **5**, 85 (1993).

[15] C. M. Caves and B. L. Schumaker, Phys. Rev. A **31**, 3068 (1985); B. L. Schumaker and C. M. Caves, Phys. Rev. A **31**, 3093 (1985).

[16] C. M. Caves, Chang Zhu, G. J. Milburn and W. Schleich, Phys. Rev. A **43**, 3854 (1991).

[17] F. A. M. de Oliveira, M. S. Kim, P. L. Knight and V. Bužek Phys. Rev. A **41**, 2645 (1990).

[18] S. M. Barnett and P. L. Knight, J. Mod. Opt. **34**, 841 (1987).

[19] B. R. Mollow and R. J. Glauber, Phys. Rev. **160**, 1076 (1967); **160**, 1097 (1967).

[20] K. E. Cahill and R. J. Glauber, Phys. Rev. **177**, 1857 (1969); **177**, 1883 (1969).

[21] S. M. Barnett and D. T. Pegg, Phys. Rev. A **42**, 6713 (1990).

[22] Ts. Gantsog and R. Tanaś, Opt. Commun. **82**, 145 (1991).

[23] Ts. Gantsog and R. Tanaś, Phys. Lett. A **152**, 251 (1991).

# SUPERSYMMETRY AND RADIAL SQUEEZED STATES FOR RYDBERG WAVE PACKETS

Robert Bluhm[a] and V. Alan Kostelecký[b1]

[a] *Physics Department, Colby College*
*Waterville, ME 04901, U.S.A.*

[b] *Physics Department, Indiana University*
*Bloomington, IN 47405, U.S.A.*

Atomic supersymmetry provides an analytical effective-potential model useful for describing certain aspects of Rydberg atoms. Experiments have recently demonstrated the existence of Rydberg wave packets localized in the radial coordinates with p-state angular distribution. This talk shows how atomic supersymmetry can be used to treat radial Rydberg wave packets via a particular analytical type of squeezed state, called a radial squeezed state.

## 1. Introduction

Irradiation of a Rydberg atom with a short laser pulse can produce a radially localized wave packet with a p-state angular distribution. The time evolution of such a state initially exhibits some attributes of the classical radial motion, including the Kepler period [1, 2, 3, 4]. After several radial oscillations, the packet disperses. At various later times, the quantum wave recombines into single- or multiple-component packets called revivals [5, 6, 7, 8, 9].

The localization of the initial packet suggests a theoretical description via a coherent or squeezed state [10]. However, a direct approach meets technical obstacles [11] or generates quantum packets that do not describe the characteristics of radial p-state excitations of Rydberg atoms in the absence of external fields.

This talk provides a summary of our recently developed framework for the analytical study of Rydberg wave packets [12, 13]. Our approach incorporates non-hydrogenic aspects of the packets using atomic supersymmetry [14, 15]. This provides an effective central potential along with analytical wavefunctions $R_{n^*l^*}$ and exact Rydberg eigenenergies $E_{n^*}$ for a Rydberg electron, expressed in terms of shifted quantum numbers $n^*$ and $l^*$. Recent summaries of the methods and results of atomic supersymmetry and references to the literature can be found in Ref. [16].

[1] Speaker

We use the analytical wavefunctions of atomic supersymmetry to construct a family of analytical squeezed states, called radial squeezed states, that form representations of radial Rydberg wave packets. The procedure begins by mapping the classical physics associated with the effective potential into the form of a harmonic oscillator. After the conversion to quantum physics, squeezed states can be derived for the resulting uncertainty relation. The method is based on an extension of the approach of Ref. [17] for cirular states of hydrogen. The procedure is outlined in sections 2 and 3 below. The time evolution of the resulting radial squeezed states is briefly discussed in section 4. In what follows, we use atomic units with $\hbar = e = m_e = 1$.

The reader is referred to Refs. [12, 13] for more details about the subjects presented in this talk and for more references to the background material.

## 2. Classical Physics

The classical theory corresponding to atomic supersymmetry uses a central potential that leads to the effective one-particle radial hamiltonian

$$H^* \equiv \tfrac{1}{2}p_r^2 + \frac{l^{*2}}{2r^2} - \frac{1}{r} = E^* \equiv -\frac{1}{2n^{*2}} \quad , \tag{1}$$

where $p_r = \dot{r}$ is the radial momentum. The classical continuous variable $l^*$ is a shifted value of the classical angular momentum $l$, arising from the incorporation of the effects of the central potential. At the quantum level, $l^{*2}$ becomes the quantized quantity $l^*(l^*+1)$ of atomic supersymmetry. The energy $E^*$ has for convenience been expressed in terms of a continuous classical variable $n^*$, which at the level of quantum physics converts to the quantized, shifted principal quantum number of atomic supersymmetry.

When $E^*$ is negative, the particle is bound and oscillates between outer and inner apsidal points, $r_1$ and $r_2$, say. The classical orbital period $T^*_{\rm cl}$, which is the time taken to move from $r_1$ to $r_2$ and back, is given via Eq. (1) as

$$T^*_{\rm cl} = 2\pi n^{*3} \tag{2}$$

The classical orbit can be shown from Eq. (1) to be a precessing ellipse, obeying the equation

$$\frac{1}{r} = \frac{1}{l^{*2}}\left(1 + e\cos[f(\theta - \theta_0)]\right) \tag{3}$$

Here, $e = \sqrt{1 - l^{*2}/n^{*2}}$, $\theta_0$ is a constant of the integration, and $f = l^*/l$. For the radial Rydberg wave packets we discuss below, $l^*/n^*$ is small and so the corresponding classical orbits are highly elliptical. For simplicity in what follows, we impose $f\theta_0 = \frac{\pi}{2}$.

Direct efforts to obtain coherent or squeezed states based on this model face technical obstacles. Instead, we map the theory into a harmonic-oscillator formalism. We convert to a new set of classical variables, $R$ and $P$, chosen to have sinusoidal variation with the angle $\theta$ and given by

$$R \equiv \frac{1}{r} - \frac{1}{l^{*2}} = \frac{e}{l^{*2}} \sin f\theta \quad , \qquad P \equiv -\frac{r^2}{f}\dot{R} = -\frac{el}{l^{*2}} \cos f\theta \quad . \tag{4}$$

In terms of these variables, the classical equations of motion become

$$\dot{R} = -\frac{f}{r^2}P \quad , \qquad \dot{P} = \frac{l^2 f}{r^2}R \quad . \tag{5}$$

Equation (1) then takes the form of the energy equation for a simple harmonic oscillator of frequency $l$ and energy $e^2/2f^2$:

$$\tfrac{1}{2}P^2 + \tfrac{1}{2}l^2R^2 = \frac{e^2}{2f^2} \quad . \tag{6}$$

## 3. Quantum Physics

At the quantum level, the new classical variables $R$, $P$ become quantum operators given by

$$R = \frac{1}{r} - \frac{1}{l^*(l^*+1)} \quad , \qquad P = \frac{p_r}{f} = -\frac{i}{f}(\partial_r + \frac{1}{r}) \quad , \tag{7}$$

obeying the commutation relation

$$[R, P] = -\frac{i}{f}\frac{1}{r^2} \quad . \tag{8}$$

The uncertainty product $\Delta R \Delta P$ is

$$\Delta R \Delta P \geq \frac{1}{2f}\langle\frac{1}{r^2}\rangle \quad . \tag{9}$$

At a given time, any minimum-uncertainty wavefunctions must therefore obey the equation

$$(R - \langle R\rangle)\psi = iA(P - \langle P\rangle)\psi \quad , \tag{10}$$

where the real constant $A$ is given by

$$A = \frac{2f(\Delta R)^2}{\langle\frac{1}{r^2}\rangle} = \frac{\Delta R}{\Delta P} \quad . \tag{11}$$

For convenience in what follows, we introduce the quantities

$$\alpha = \frac{f}{A} - 1 \quad , \quad \gamma_0 = \frac{f}{A}\langle\frac{1}{r}\rangle \quad , \quad \gamma_1 = -\langle p_r\rangle \quad . \tag{12}$$

In terms of these quantities, the normalized minimum-uncertainty solutions to Eq. (10) are given by

$$\psi(r) = \frac{(2\gamma_0)^{2\alpha+3}}{\Gamma(2\alpha+3)} r^{\alpha} e^{-\gamma_0 r} e^{-i\gamma_1 r} \quad . \tag{13}$$

These wavefunctions form a three-parameter family of squeezed states, called radial squeezed states. Their construction shows they are suitable candidates for radial Rydberg wave packets in any atom correctly modeled by atomic supersymmetry.

The relatively simple analytical form of the radial squeezed states permits the derivation of a number of useful results. Among these are the following expectation values:

$$\langle r\rangle = \frac{2\alpha+3}{2\gamma_0} \quad , \quad \langle p_r\rangle = -\gamma_1 \quad , \tag{14}$$

and

$$\langle H\rangle = \frac{\gamma_0^2}{2(\alpha+1)(2\alpha+1)}\left(2\gamma_0^2 l^*(l^*+1)+\alpha+1\right) - \frac{\gamma_0}{\alpha+1} + \frac{{\gamma_1}^2}{2} \quad . \tag{15}$$

Requiring finiteness of these expressions and the separate normalizability of the kinetic and potential energies of the radial squeezed states restrict the parameters to $\alpha > -\frac{1}{2}$ and $\gamma_0 > 0$.

The uncertainty relation for the usual variables $r$ and $p_r$ can be calculated for the radial squeezed states. It is

$$\Delta r \Delta p_r = \tfrac{1}{2}\sqrt{\frac{2\alpha+3}{2\alpha+1}} \quad . \tag{16}$$

As expected, this is *not* a minimum-uncertainty product. However, a relatively large value of $\alpha$ is needed to reproduce the experimental situation as the wave packet makes its first pass through the outer apsidal point, so the uncertainty product is close to $\frac{1}{2}$ at that time.

## 4. Time Evolution

The analytical nature of the radial squeezed states has made it possible for us to study their time evolution both analytically and numerically. Here, we restrict ourselves to describing briefly some results and providing a few representative figures to illustrate the key features.

Specifying a particular radial squeezed state means selecting values for the three quantities $\alpha$, $\gamma_0$, and $\gamma_1$ at some initialization time. Since the uncertainty product

$\Delta r \Delta p_r$ is expected to be minimized at the first pass through the outer turning point [1] we choose this as the initialization time and define it as $t = 0$. The three parameters $\alpha$, $\gamma_0$, and $\gamma_1$ are determined by imposing conditions on the three physical quantities $\langle p_r \rangle$, $\langle r \rangle$, and $\langle H \rangle$ at $t = 0$:

$$\langle r \rangle = r^*_{\rm out} \quad , \qquad \langle p_r \rangle = 0 \quad , \qquad \langle H \rangle = E_{\bar{n}^*} \quad . \tag{17}$$

Here, $r^*_{\rm out}$ is the outer apsidal point of the quantum orbit, and $E_{\bar{n}^*} = -1/2\bar{n}^{*2}$ is the energy expectation of the central state $\bar{n}$ excited by the short laser pulse.

In the context of radial squeezed states for atomic supersymmetry, our analysis shows that the radial squeezed state initially oscillates with the classical orbital period $T^*_{\rm cl}$ and gradually disperses. For a radial squeezed state dominated by shifted principal quantum number $\bar{n}^*$ and including a range of shifted principal quantum numbers $\delta n^*$, the packet is effectively dispersed at an interference time $t^*_{\rm int} \simeq \bar{n}^* T^*_{\rm cl}/3\delta n^*$. Much later, near the revival time $t^*_{\rm rev} \simeq \bar{n}^* T^*_{\rm cl}/3$, the radial squeezed state recombines into a packet called a full revival that is similar to the initial one and that orbits with a period $T^*_{\rm cl}$. At times $t^*_r = t^*_{\rm rev}/r$ between $t^*_{\rm int}$ and $t^*_{\rm rev}$, the radial squeezed state combines into $r$ spatially separated packets called fractional revivals, with wavefunction period $T^*_r = \frac{1}{r} T^*_{\rm cl}$.

Some of these behaviors are illustrated in Figure 1, which plots the unnormalized radial probability density $f(r) = r^2 |\psi_{\bar{n},l=1}(r)|^2$ at different times, for a hydrogenic radial squeezed state with $\bar{n}^* = \bar{n} = 85$ and $l^* = l = 1$. In this case, the initialization parameters are $\alpha \simeq 168.225$, $\gamma_0 \simeq 0.0117465$, and $\gamma_1 = 0$. This corresponds to a classical orbit of high eccentricity, $e \simeq 1$, and periodicity $T^*_{\rm cl} \simeq 93.3$ psec.

Figure 1a displays the radial squeezed state at $t = 0$. It is situated near the outer quantum apsidal point $r^*_{\rm out} \simeq 14450$ a.u. The initial uncertainty product is $\Delta r \Delta p_r \simeq 0.501$, which is close to the minimum of 0.5, as expected for a smooth packet. Initially, the packet moves towards the origin. Figure 1b shows its shape at $t = T^*_{\rm cl}/4$, while Figure 1c shows it at $t = T^*_{\rm cl}/2$. As the packet approaches the origin it spreads and develops oscillations in the radial probability distribution, thereby indicating the transition from a classical to a quantum object. The uncertainty product halfway through the first classical period is $\Delta r \Delta p_r \simeq 59.5$.

After reflection off the inner apsidal point, the packet recombines into a more classical object as it moves towards the outer apsidal point. Figures 1d and 1e show the packet at $t = 3T^*_{\rm cl}/4$ and $t = T^*_{\rm cl}$, respectively. Some decoherence is visible, but the packet is still well defined. The amount of dispersion increases with successive orbits, until a time of order $t^*_{\rm int} \simeq 4T^*_{\rm cl}$. Subsequently, the probability distribution no longer exhibits a unique and well-defined peak at any point in the orbit. For illustration, the situation at $t = 5T^*_{\rm cl}$ is displayed in Figure 1f.

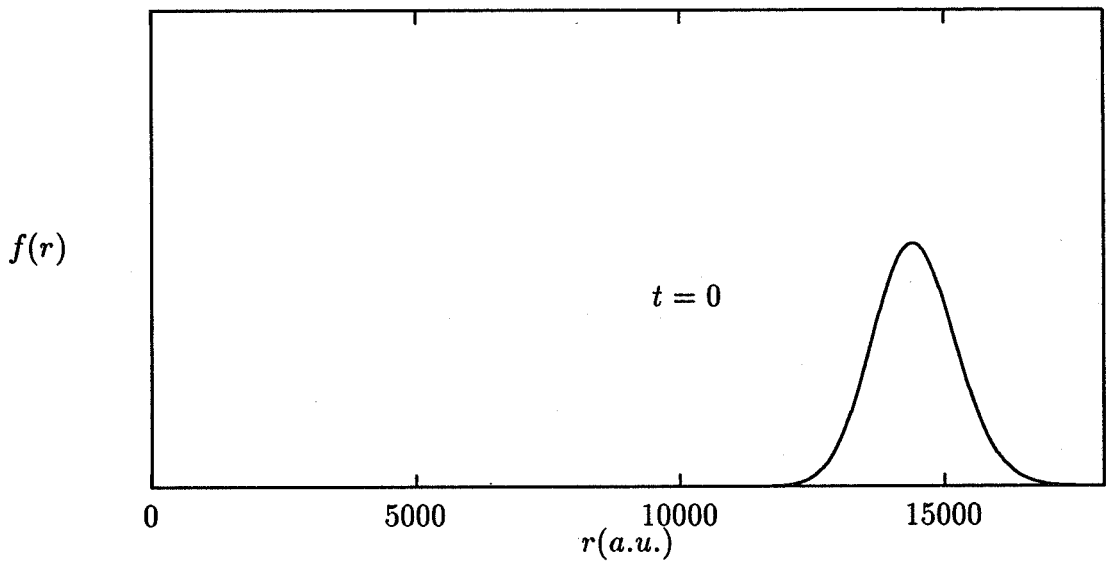


(a)

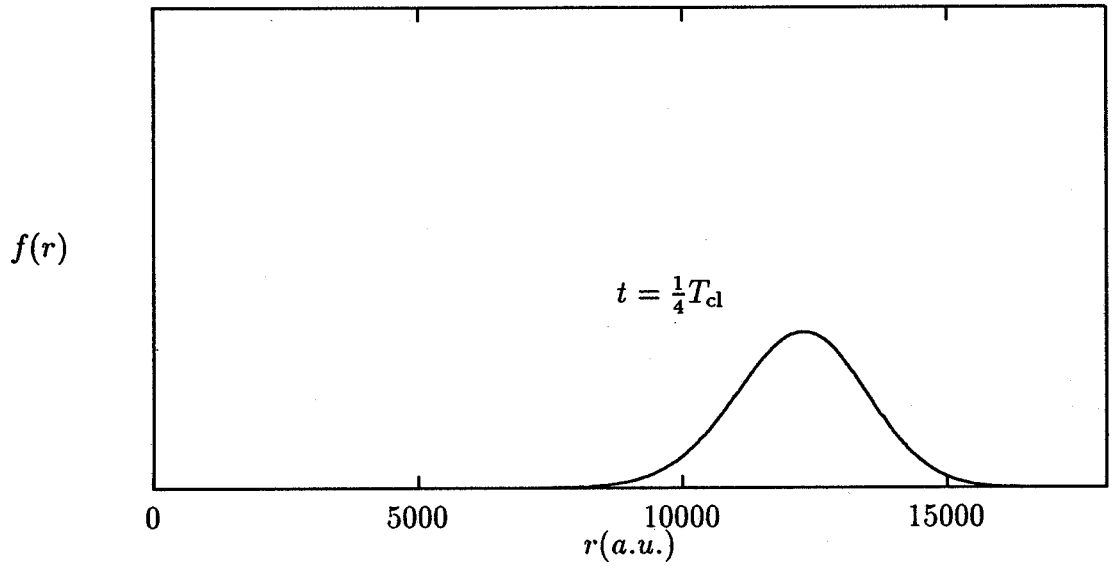


(b)

Figure 1

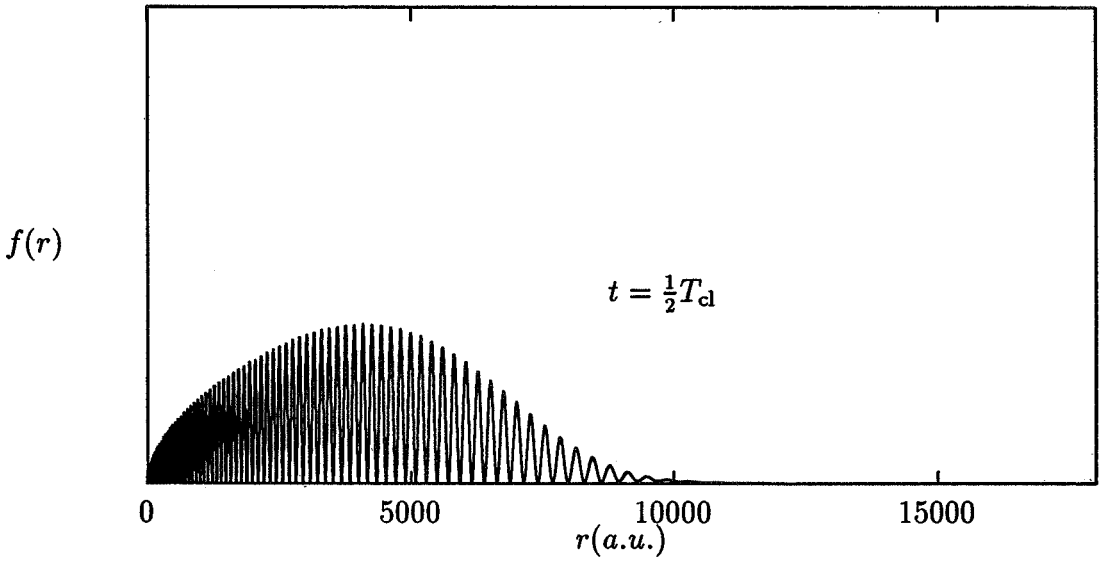
$f(r)$
$t = \frac{1}{2}T_{\rm cl}$
0
5000
10000
15000
$r(a.u.)$

(c)

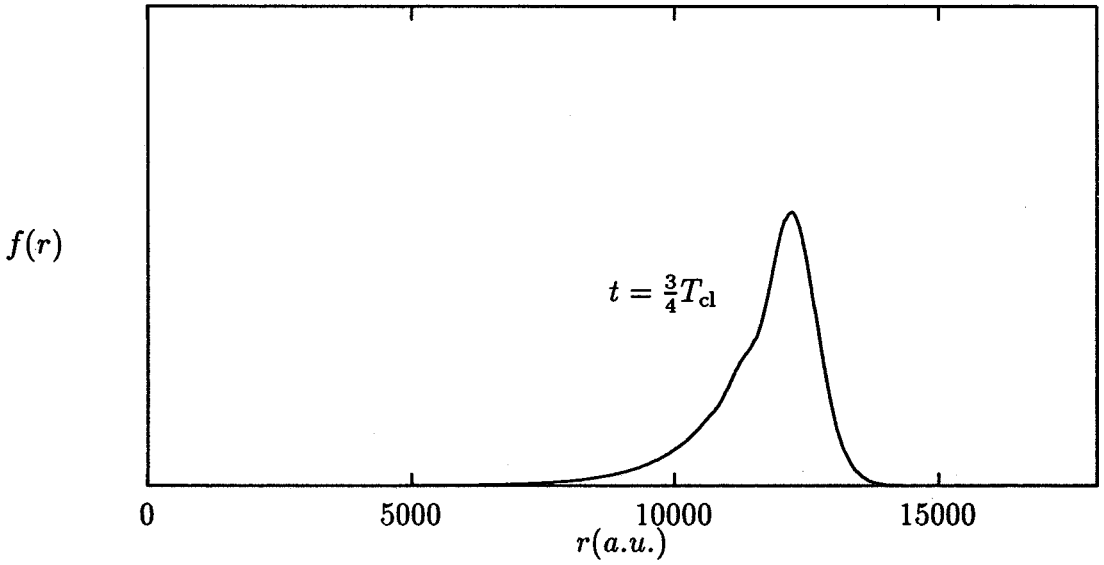
$f(r)$
$t = \frac{3}{4}T_{\rm cl}$
0
5000
10000
15000
$r(a.u.)$

(d)

Figure 1

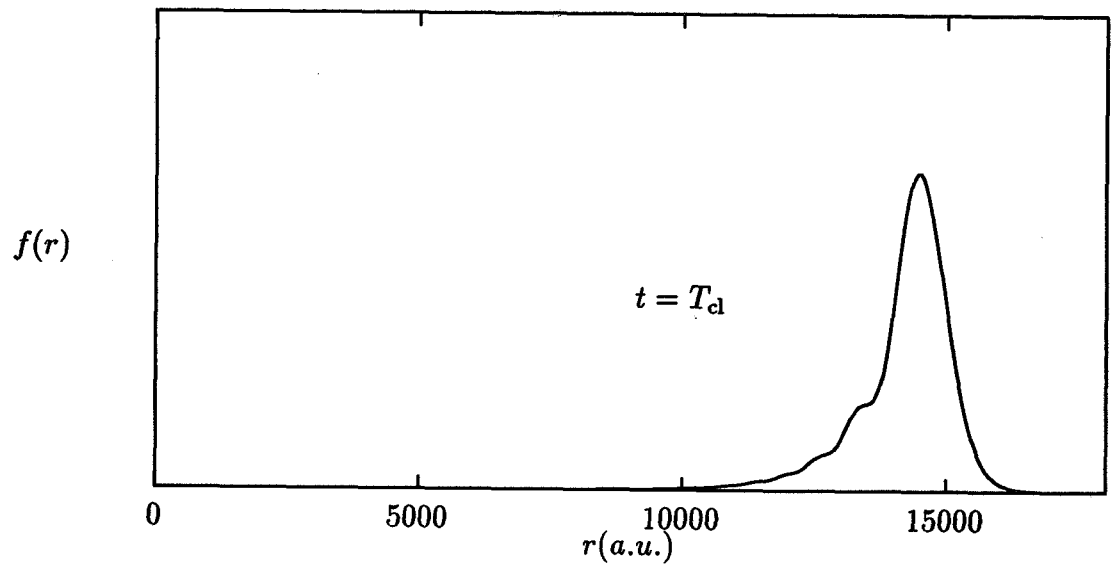


(e)

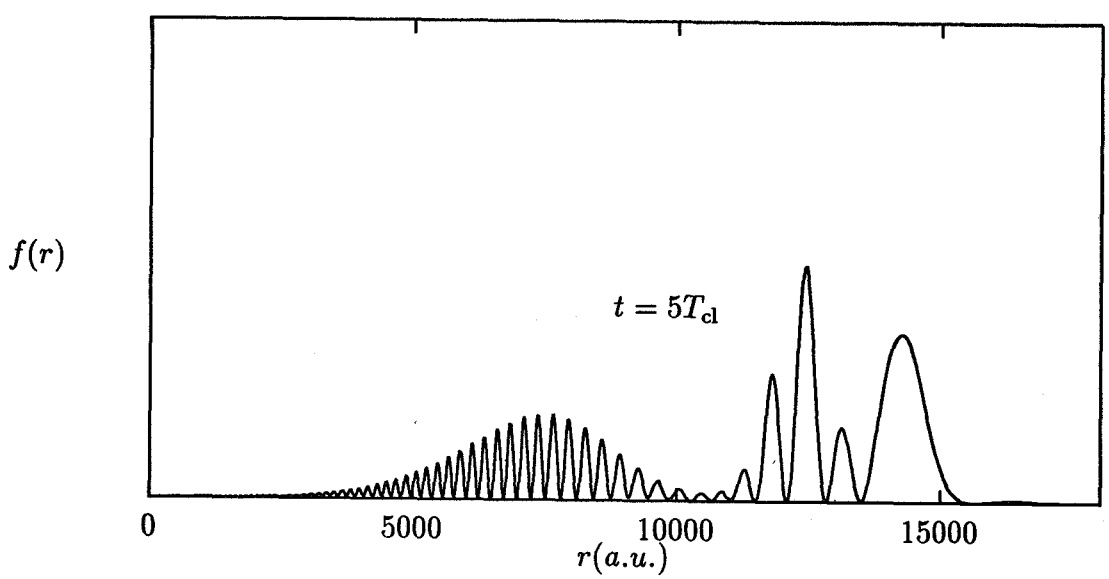


(f)

Figure 1

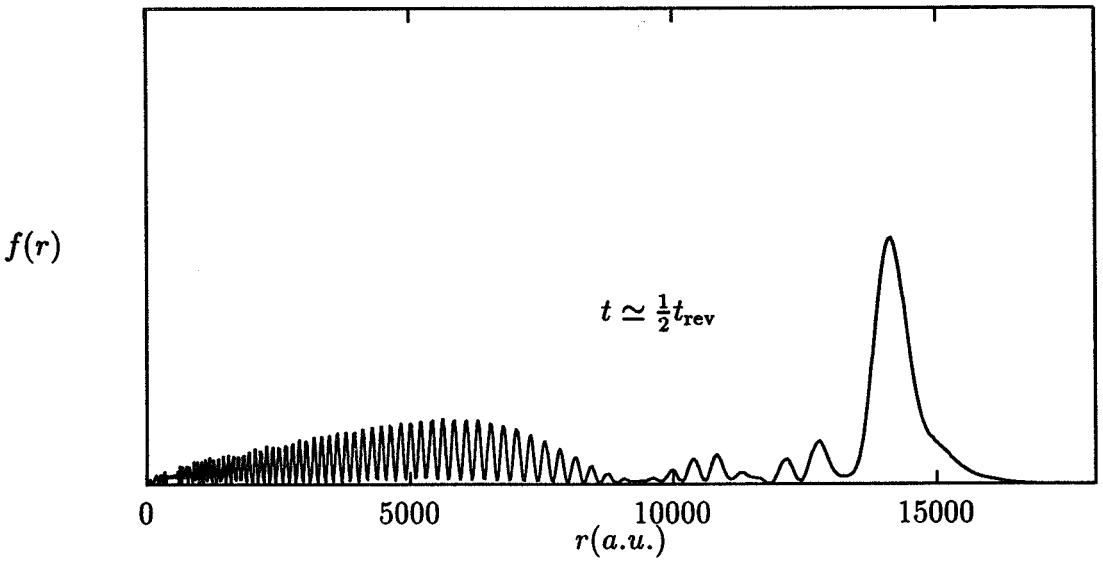
$f(r)$
$t \simeq \frac{1}{2} t_{\mathrm{rev}}$
0
5000
10000
15000
$r(a.u.)$

(g)

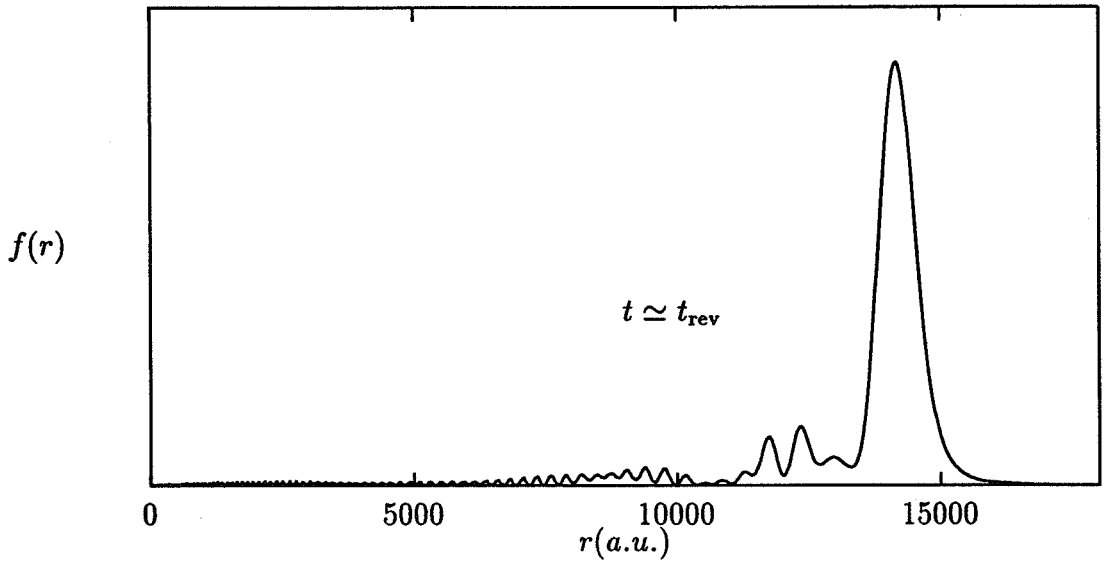
$f(r)$
$t \simeq t_{\mathrm{rev}}$
0
5000
10000
15000
$r(a.u.)$

(h)

Figure 1

At later times, fractional and full revivals appear. The fractional revival consisting of two separate peaks, which appears at $t_r^* = t_{\rm rev}^*/2 \simeq 1.3$ nsec., is shown in Figure 1g, while the full revival appearing at $t_{\rm rev}^* \simeq 2.6$ nsec. is shown in Figure 1h. These revivals exhibit all the features expected from the classical analysis, including, for example, the expected values for the wavefunction periodicity.

Along with the additional analysis contained in Refs. [12, 13], these results indicate that radial squeezed states are useful models for radial Rydberg wave packets.

## 5. References


1. J. Parker and C.R. Stroud, Phys. Rev. Lett. **56**, 716 (1986); Phys. Scr. **T12**, 70 (1986).
2. G. Alber, H. Ritsch, and P. Zoller, Phys. Rev. A **34**, 1058 (1986); G. Alber and P. Zoller, Phys. Rep. **199**, 231 (1991).
3. A. ten Wolde, L.D. Noordam, A. Lagendijk, and H.B. van Linden van den Heuvell, Phys. Rev. Lett. **61**, 2099 (1988).
4. J.A. Yeazell, M. Mallalieu, J. Parker, and C.R. Stroud, Phys. Rev. A **40**, 5040 (1989).
5. J.A. Yeazell, M. Mallalieu, and C.R. Stroud, Phys. Rev. Lett. **64**, 2007 (1990); J.A. Yeazell and C.R. Stroud, Phys. Rev. A **43**, 5153 (1991).
6. D.R. Meacher, P.E. Meyler, I.G. Hughes, and P. Ewart, J. Phys. B **24**, L63 (1991).
7. A. ten Wolde, L.D. Noordam, H.G. Muller, and H.B. van Linden van den Heuvell, in F. Ehlotzky, ed., *Fundamentals of Laser Interactions II* (Springer-Verlag, Berlin, 1989).
8. I.Sh. Averbukh and N.F. Perelman, Phys. Lett. **139A**, 449 (1989).
9. M. Nauenberg, J. Phys. B **23**, L385 (1990).
10. See, for example, J.R. Klauder and B.-S. Skagerstam, eds., *Coherent States* (World Scientific, Singapore, 1985); D. Han, Y.S. Kim, and W.W. Zachary, eds., *Squeezed States and Uncertainty Relations* (NASA, Washington, D.C., 1992).
11. E. Schrödinger, Naturwissenschaften **14**, 664 (1926).
12. R. Bluhm and V.A. Kostelecký, *Radial Squeezed States and Rydberg Wave Packets,* Phys. Rev. A, Rapid Communications, in press.
13. R. Bluhm and V.A. Kostelecký, *Atomic Supersymmetry, Rydberg Wave Packets, and Radial Squeezed States,* Indiana University preprint IUHET 256 (August 1993).

14. V. A. Kostelecký and M. M. Nieto, Phys. Rev. Lett. **53**, 2285 (1984); Phys. Rev. A **32**, 1293 (1985).

15. V. A. Kostelecký and M. M. Nieto, Phys. Rev. A **32**, 3243 (1985).

16. V.A. Kostelecký, in D. Han, Y.S. Kim, and W.W. Zachary, eds., *Proceedings of the Workshop on Harmonic Oscillators* (NASA, Washington, D.C., 1993), p. 443; *Supersymmetry, Coherent States, and Squeezed States for Rydberg Atoms,* Indiana University preprint IUHET 254 (July 1993), to appear in the Proceedings of the International Symposium on Coherent States, Oak Ridge, TN, June 1993.

17. M.M. Nieto, Phys. Rev. D **22**, 391 (1980); V.P. Gutschick and M.M. Nieto, Phys. Rev. D **22**, 403 (1980).

# EFFECT OF DISPERSION FORCES ON SQUEEZING WITH RYDBERG ATOMS

S.K. Ng
M.R. Muhamad
*Department of Physics, University of Malaya, 59100 Kuala Lumpur, Malaysia*

M.R.B. Wahiddin
*Department of Mathematics, University of Malaya, 59100 Kuala Lumpur, Malaysia*

**Abstract**

We report exact results concerning the effect of dipole-dipole interaction (dispersion forces) on dynamic and steady-state characteristics of squeezing in the emitted fluorescent field from two identical coherently driven two-level atoms. The atomic system is subjected to three different damping baths in particular the normal vacuum, a broad band thermal field and a broad band squeezed vacuum. The atomic model is the Dicke model, hence possible experiments are most likely to agree with theory when performed on systems of Rydberg atoms making microwave transitions. The presence of dipole-dipole interaction can enhance squeezing for realisable values of the various parameters involved.

## 1 Introduction

The fundamental importance of squeezed light and its interaction with matter as well as potential applications have become the focus of considerable attention in the last few years both theoretically and experimentally. Indeed, the coupling of a two-level atomic system to squeezed light for example can lead to interesting new phenomena as reported by a number of authors [1,2,3]. In this paper we consider the possibility of generating squeezing in the emitted fluorescent field from two identical coherently driven two-level atoms with dipole-dipole interaction (dispersion forces). The atomic system is subjected to three different damping baths in particular, the normal vacuum, a broad band squeezed vacuum and a broad band thermal bath. We report exact results concerning the time evolution as well as steady-state emitted field quadratures which may lead to squeezing. It is shown that squeezing may be enhanced for certain realisable values of the system parameters.

The dipole-dipole coupling is expected to play a significant role especially in the high atomic density limit [4]. It is especially important because it generally breaks the permutation symmetry of the atom-field coupling [5] which is the basic assumption of the collective spontaneous emission process (superradiant) involving $N_A$-atom system. As a consequence, the $S^2$ conservation (where $S$ is the total 'spin' of $N_A$ two-level atoms) which appear inherently in the point like Dicke model [6] is affected significantly. Since the atomic model is the coherently driven two-atom Dicke model, possible experiments are most likely to agree with theory when performed on systems of Rydberg atoms making microwave transitions – see e.g. [7] and references therein.

## 2 Description of the model

Our starting point is the master equation for the reduced atomic density operator in a frame rotating at $\omega_L$, the laser frequency – see equation (5) of ref. [8]:

$$\begin{aligned}\frac{\partial\rho}{\partial t} &= -i\Delta[S^z,\rho]+i\Omega[S^+ + S^-,\rho]-i\alpha_+[S^+S^-,\rho]\\ &+\frac{\gamma}{2}(N+1)(2S^-\rho S^+ - S^+S^-\rho-\rho S^+S^-)\\ &+\frac{\gamma N}{2}(2S^+\rho S^- - S^-S^+\rho-\rho S^-S^+)\\ &-\frac{\gamma|M|\exp(-i\Phi)}{2}(2S^+\rho S^+ - S^+S^+\rho-\rho S^+S^+)\\ &-\frac{\gamma|M|\exp(+i\Phi)}{2}(2S^-\rho S^- - S^-S^-\rho-\rho S^-S^-)\end{aligned}$$

where $S^{\pm}$, $S^z$ are the usual collective atomic operators; $2\Omega$ is the Rabi frequency characterizing the strength of the driving field, $\gamma$ is the single atom Einstein $A$ coefficient, $\alpha_+$ is the static dipole-dipole interaction potential such that

$$\alpha_+ = \Omega_{ij} = \Omega_{ji} \simeq \frac{3\gamma}{2(kr_{ij})^3}[1-3(\hat{\mu}\cdot\hat{r}_{ij})^2],$$

and $\Delta = \omega_A - \omega_L - \alpha_+$ ($\omega_A$ is the atomic transition frequency).

Note that $\Delta = -\alpha_+$ represents the on-resonant case. $N$ and $M$ are parameters of the squeezed vacuum describing squeezing with $|M|^2 = N(N+1)$ holding for minimum uncertainty squeezed state. $\Phi$ is the relative phase between the squeezed vacuum and the laser. In what follows we set $|M|^2 = N(N+1)$. Note that if $N = 0$, then the atoms are damped by the normal vacuum whilst the case $N \neq 0$, $M = 0$ corresponds to the atoms damped by a broad band thermal field such that $N \rightarrow \bar{n}$ which is the mean occupation number of the resonant field mode. The master equation is solved using the fourth order Runge-Kutta method.

## 3 Squeezing in resonance fluorescence

We now discuss the possibility of generating squeezing in the emitted fluorescent radiation field and the effect of $\alpha_+$ on it. The "in phase" and "phase quadrature" components of the emitted fluorescence field denoted by $F_x$ and $F_y$ are respectively

$$\begin{aligned}F_x &= (\Delta S^x)^2 - \frac{1}{2}|\langle S^z\rangle|\\ F_y &= (\Delta S^y)^2 - \frac{1}{2}|\langle S^z\rangle|\end{aligned}$$

with

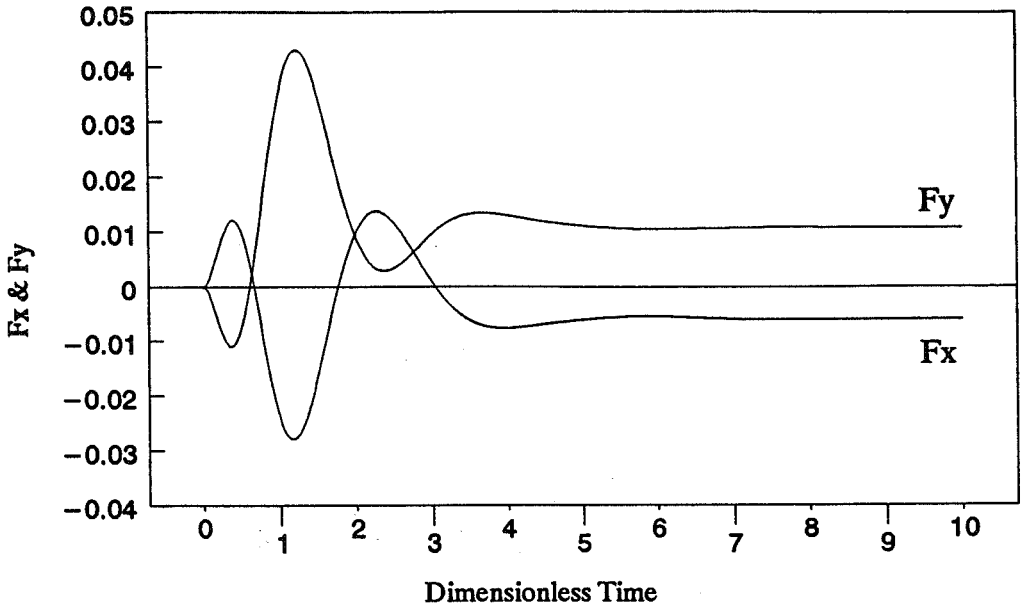


Fig.1 Fx and Fy against $\tau$ for atoms damped by a normal vacuum ; $\frac{\Omega}{\gamma}$ =0.5 , $\frac{\alpha_+}{\gamma}$ =1.0 and $\frac{\Delta}{\gamma}$ =0.0

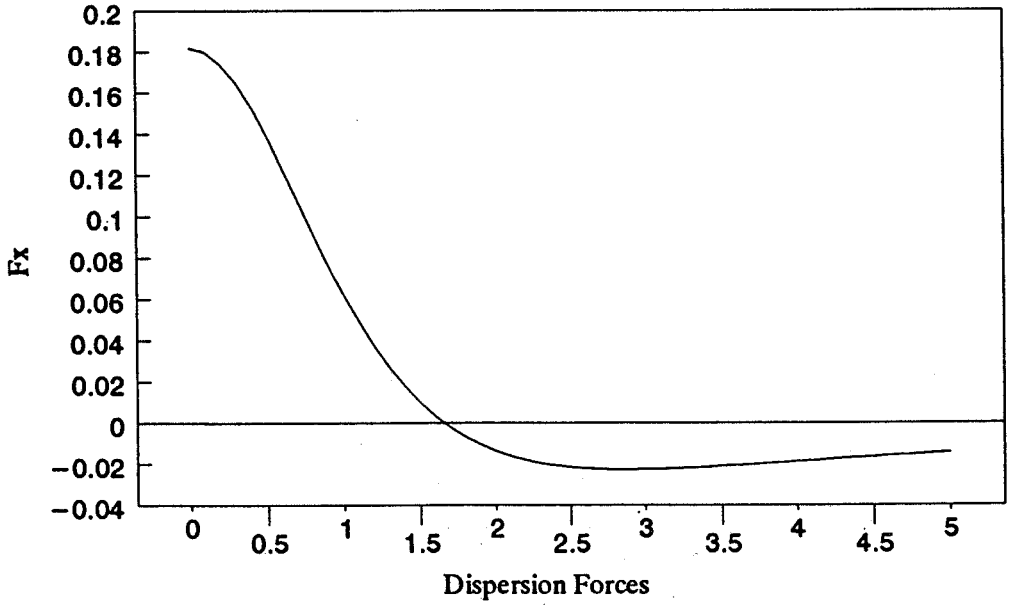


Fig.2 Steady−state Fx versus $\frac{\alpha_+}{\gamma}$ for atoms damped by a normal vacuum ; $\frac{\Omega}{\gamma}$ =0.5 and $\frac{\Delta}{\gamma}$ =− $\frac{\alpha_+}{\gamma}$

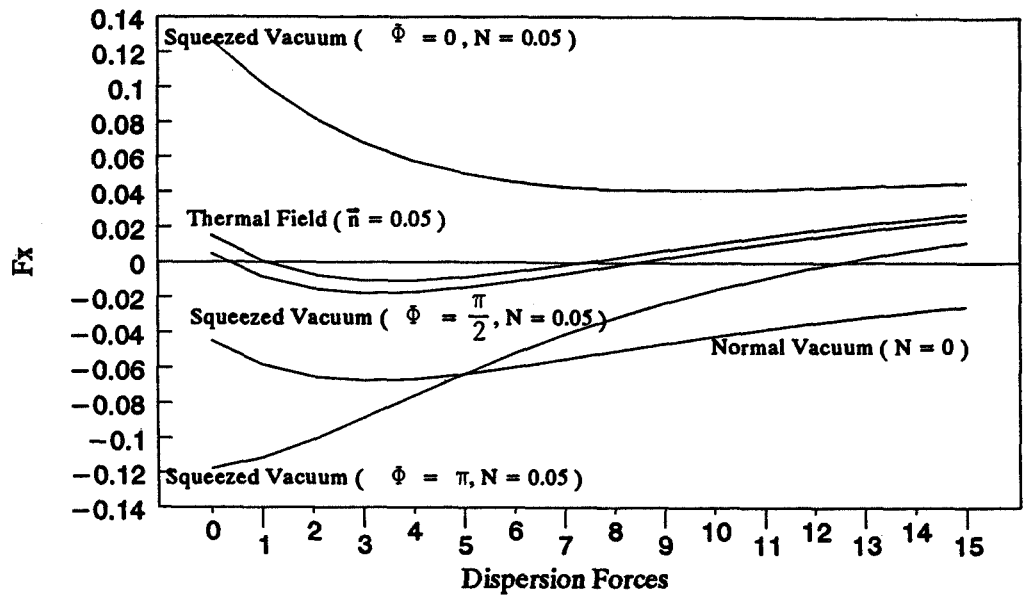


Fig.3 Steady–state Fx versus $\frac{\alpha_+}{\gamma}$ for atoms damped either by a normal vacuum, a broad band thermal field or a broad band squeezed vacuum ; $\frac{\Omega}{\gamma}$ =10 and $\frac{\Delta}{\gamma}$ =15

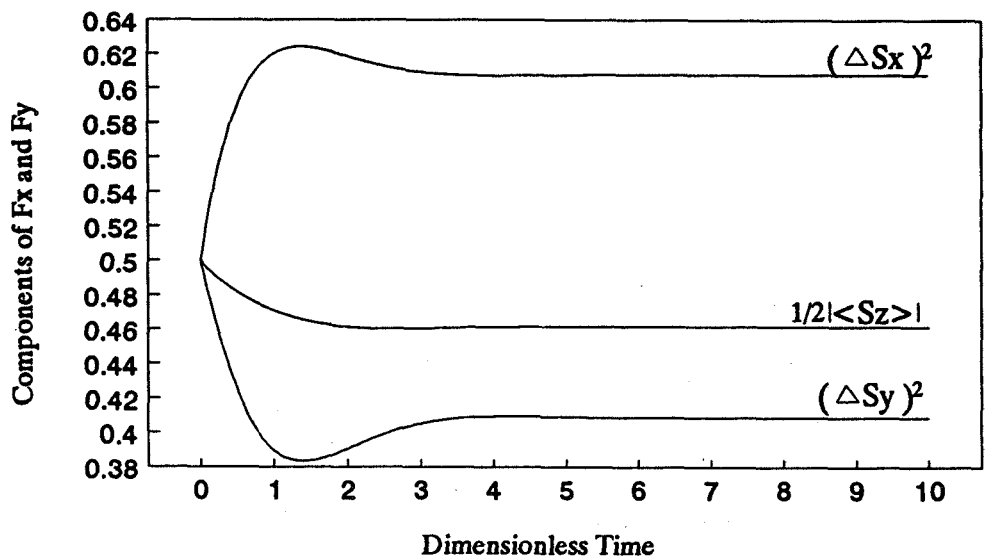


Fig.4 Components of Fx and Fy as functions of $\tau$ for atoms damped by a broad band squeezed vacuum ; $\frac{\Omega}{\gamma}$ =0.1 , $\frac{\alpha_+}{\gamma}$ =0.5 , $\frac{\Delta}{\gamma}$ =0 , N=0.05 and $\Phi$ =0

$$(\Delta S^x)^2 = \frac{1}{4}\{\langle S^+S^-\rangle + \langle S^-S^+\rangle - \langle S^+\rangle^2 - \langle S^-\rangle^2 - 2\langle S^+\rangle\langle S^-\rangle + \langle S^+S^+\rangle + \langle S^-S^-\rangle\}$$

$$(\Delta S^y)^2 = \frac{1}{4}\{\langle S^+S^-\rangle + \langle S^-S^+\rangle + \langle S^+\rangle^2 + \langle S^-\rangle^2 - 2\langle S^+\rangle\langle S^-\rangle - \langle S^+S^+\rangle - \langle S^-S^-\rangle\}$$

as there is a linear functional relation between the atomic operators and the field operators [9]. Squeezing occurs whenever $F_x$ or $F_y < 0$.

Fig. 1 shows the time evolution of $F_x$ and $F_y$ for the atomic system damped by the normal vacuum ($N = 0$) and driven by an off-resonant weak laser with weak dipole-dipole interaction: $\frac{\Omega}{\gamma} = 0.5$; $\frac{\alpha_+}{\gamma} = 1.0$. In transient, both $F_x$ and $F_y$ display squeezing but do not occur at the same time due to Heisenberg Uncertainty relation, with maximum squeezing occurring in $F_x$. In this case steady-state squeezing is only predicted in $F_x$. Increasing $\alpha_+$ further suppresses the squeezing in $F_x$ while $F_y$ is positive in the steady-state. In Fig. 2 all the parameters are the same as in Fig. 1 but now the atoms are driven by a resonant laser ($\Delta = -\alpha_+$). There the steady-state $F_x$ is plotted against $\frac{\alpha_+}{\gamma}$. Clearly, squeezing is obtained when $\frac{\alpha_+}{\gamma} > 1.7$ and the squeezing keep increasing with $\alpha_+$ and reaches its maximum value at $\frac{\alpha_+}{\gamma} \approx 2.5$. But it is reduced when $\alpha_+$ is increased further.

The effects of an off-resonant strong laser ($\frac{\Omega}{\gamma} = 10$) on steady-state squeezing in $F_x$ for the three damping baths are shown in Fig. 3. The role of the dispersion forces (dipole-dipole interaction) to produce optimum squeezing is best seen for the normal vacuum, thermal field and squeezed vacuum ($\Phi = \pi/2$, $N = 0.05$) cases. In Fig. 4 we plot the the components of $F_x$ and $F_y$ as functions of dimensionless time ($\tau = \gamma t$) for a detuned weak laser ($\frac{\Omega}{\gamma} = 0.1$, $\frac{\alpha_+}{\gamma} = 0.5$) driving the atomic system and damped by a broad band squeezed vacuum ($N = 0.05, \Phi = 0$). Here, squeezing is evident in $F_y$ in the transient as well as in the steady-state since it satisfies the squeezing condition $(\Delta S^y)^2 < \frac{1}{2}|\langle S^z\rangle|$. The steady-state squeezing achieved is estimated about 12%.

In conclusion, the dipole-dipole interaction proves to be important in the analysis of squeezing in the emitted fluorescent field from a cooperative system coherently driven and damped either by a normal vacuum, broad band thermal field or a broad band squeezed vacuum.

# 4 Acknowledgement

This research is supported by the Malaysia IRPA R&D 04-07-04-169. MRBW is grateful to University of Malaya for the support to attend the present conference.

# References

[1] C.W. Gardiner, Phys. Rev. Lett. **56**, 1917 (1986)

[2] G.M. Palma and P.L. Knight, Phys. Rev. A **39**, 1962 (1989)

[3] G.S. Agarwal and R.R. Puri, Phys. Rev. A **41**, 3782 (1990)

[4] G.S. Agarwal, L.M. Narducci and E. Apostolidis, Optics Commun. **36**, 285 (1981)

[5] B. Coffey and R. Friedberg, Phys. Rev. A **17**, 1033 (1978)

[6] R.H. Dicke, Phys. Rev. **93**, 99 (1954)

[7] G.P. Hildred, R.R. Puri, S.S. Hassan and R.K. Bullough, J. Phys. B **17**, L535 (1984)

[8] W.A.M. Othman and M.R.B. Wahiddin, J. Mod. Opt. **40**, 7 (1992)

[9] M.R.B. Wahiddin, B.M. Garraway and R.K. Bullough J. Mod. Opt. **34**, 1007 (1987)

# Higher–order squeezing of the quantum electromagnetic field and the generalized uncertainty relations in two–mode squeezed states

*Li Xizeng* *Su Baoxia*
*Department of Physics, Tianjin University, Tianjin 300072, P.R.China*

It is found that the two–mode output quantum electromagnetic field in two–mode squeezed states exhibits higher–order squeezing to all even orders. And the generalized uncertainty relations are also presented for the first time.

The concept of higher–order squeezing of the single–mode quantum electromagnetic field was first introduced and applied to several processes by Hong and Mandel in 1985[1,2]. Lately Li Xizeng and Shan Ying have calculated the higher–order squeezing in the process of degenerate four–wave mixing[3] and presented the higher–order uncertainty relations of the fields in single–mode squeezed states[4]. In this paper we generalize the above work to the higher–order squeezing in two–mode squeezed states. The generalized uncertainty relations are also presented for the first time.

## 1 Definition of higher–order squeezing in two–mode squeezed states

The definition of two–mode squeezed states was given by Caves and Schumaker[5]:

$$|\alpha_+, \alpha_-; \varsigma >= \hat{S}(\varsigma)|\alpha_+, \alpha_- > . \tag{1}$$

Where $\hat{S}(\varsigma)$ is the two–mode squeezed operator

$$\hat{S}(\varsigma) = exp[\frac{1}{2}(\varsigma^* \hat{a}_+ \hat{a}_- - \varsigma \hat{a}_+^+ \hat{a}_-^+)], \tag{2}$$

$|\alpha_+, \alpha_- >$ is the two–mode coherent state, $\hat{a}_\pm$ are two–mode annihilation operators, $\alpha_\pm$ are eigenvalues of $\hat{a}_\pm$ in $|\alpha_+, \alpha_- >$.

Define the two–mode squeezed annihilation operators by $\hat{A}_\pm$,

$$\hat{A}_\pm = \hat{S}(\varsigma)\hat{a}_\pm \hat{S}^+(\varsigma) = \mu \hat{a}_\pm + \nu \hat{a}_\mp^+. \tag{3}$$

where

$$\mu = coshr, \qquad \nu = e^{i\theta} sinhr, \tag{4}$$

$\varsigma = re^{i\theta}$ is the squeeze parameter.

Then the two−mode squeezed states are the eigenstates of $\hat{A}_{\pm}$,

$$\hat{A}_{\pm}|\alpha_+,\alpha_-;\varsigma>=\alpha_{\pm}|\alpha_+,\alpha_-;\varsigma>, \tag{5}$$

and $\alpha_{\pm}$ are the eigenvalues of $\hat{A}_{\pm}$.

The real two−mode output field $\hat{E}$ can be decomposed into two quadrature components $\hat{E}_1$ and $\hat{E}_2$, which are canonical conjugates. The output field $\hat{E}$ exhibits higher−order squeezing to any higher−order (Nth order) in $\hat{E}_1$, if there exists such a phase angle $\phi$ that the higher−order moment $<(\Delta\hat{E}_1)^N>$ in a two−mode squeezed state is smaller than its value in a completely tow−mode coherent state, viz.,

$$<(\Delta\hat{E}_1)^N>_{S.S\ \ two-mode} \ < \ <(\Delta\hat{E}_1)^N>_{C.S\ \ two-mode}.$$

This is the definition of higher−order squeezing in two−mode squeezed states.

# 2 The quadrature components of the two−mode output field $\hat{E}$

The electric field operator for the two−mode output field has the form of

$$\hat{E}(x,t)=\hat{E}^{(+)}(x,t)+\hat{E}^{(-)}(x,t). \tag{6}$$

Where

$$\hat{E}^{+}(x,t) = \sqrt{\frac{\omega_+}{2}}\hat{a}_+e^{-i\omega_+(t-x)}+\sqrt{\frac{\omega_-}{2}}\hat{a}_-e^{-i\omega_-(t-x)}, \tag{7}$$

$$\hat{E}^{-}(x,t) = \sqrt{\frac{\omega_+}{2}}\hat{a}_+^{+}e^{i\omega_+(t-x)}+\sqrt{\frac{\omega_-}{2}}\hat{a}_-^{+}e^{i\omega_-(t-x)}. \tag{8}$$

We now introduce two Hermitian quadrature components $\hat{E}_1$ and $\hat{E}_2$ of the electric field defined by

$$\hat{E}_1(x,t)=\hat{E}^{(+)}e^{i[\Omega(t-x)-\phi]}+\hat{E}^{(-)}e^{-i[\Omega(t-x)-\phi]}, \tag{9}$$

$$\hat{E}_2(x,t)=\hat{E}^{(+)}e^{i[\Omega(t-x)-(\phi+\frac{\pi}{2})]}+\hat{E}^{(-)}e^{-i[\Omega(t-x)-(\phi+\frac{\pi}{2})]}. \tag{10}$$

Then, $\hat{E}(x,t)$ can be decomposed into two quadrature components $\hat{E}_1$ and $\hat{E}_2$, which are canonical comjugates

$$\hat{E}(x,t)=\hat{E}_1 cos[\Omega(t-x)-\phi]+\hat{E}_2 sin[\Omega(t-x)-\phi], \tag{11}$$

$$[\hat{E}_1,\hat{E}_2]=2iC_0,$$

Where $\Omega$ is the carrier frequency

$$\Omega=\frac{\omega_++\omega_-}{2},$$

and $\phi$ is an arbitrary phase angle that may be chosen at will.

The units are chosen so that $\hbar = c = 1$.

Substituting Eqs.(7) and (8) into (9), we obtain

$$\hat{E}_1(x,t) = g_+\hat{a}_+ + g_-a_- + g_+^*\hat{a}_+^+ + g_-^*\hat{a}_-^+. \tag{12}$$

where

$$g_\pm = \sqrt{\frac{\omega \pm \epsilon}{2}} e^{-i[\phi \pm \epsilon(t-x)]}, \tag{13}$$

and

$$\epsilon = \omega_+ - \Omega = \Omega - \omega_- \tag{14}$$

is the modulation frequency.

From Eq.(3), we get

$$\hat{a}_\pm = \mu^* \hat{A}_\pm - \nu \hat{A}_\mp^+. \tag{15}$$

Substituting (15) to (12), we obtain $\hat{E}_1$ in terms of $\hat{A}_\pm$

$$\hat{E}_1(x,t) = (h_+\hat{A}_+ + h_-\hat{A}_-) + (h_+^* A_+^+ + h_-^*\hat{A}_-^+). \tag{16}$$

Where

$$h_\pm = g_\pm \mu^* - g_\mp^* \nu^*. \tag{17}$$

Define

$$\hat{B} = h_+\hat{A}_+ + h_-\hat{A}_-, \tag{18}$$

Then

$$\hat{E}_1 = \hat{B} + \hat{B}^+. \tag{19}$$

# 3 Higher−order noise moment $< (\Delta\hat{E}_1)^N >$ and Higher−order squeezing

By using the Campbell−Baker−Hausdorff formula, we get

$$\begin{aligned} < (\Delta\hat{E}_1)^N > \;=\; & <:: (\Delta\hat{E}_1)^N ::> + \frac{N^{(2)}}{1!}(\frac{1}{2}C_0) <:: (\Delta\hat{E}_1)^{N-2} ::> + \frac{N^{(4)}}{2!}(\frac{1}{2}C_0)^2 <:: (\Delta\hat{E}_1)^{N-4} ::> \\ & + \cdots + (N-1)!!C_0^{N/2}. \qquad \text{(N is even)} \end{aligned} \tag{20}$$

where $N^{(r)} = N(N-1)\cdots(N-r+1)$, $C_0 = \frac{1}{2i}[\hat{E}_1, \hat{E}_2] = [\hat{B}, \hat{B}^+]$, " :: " denotes normal ordering with respect to $\hat{B}$ and $\hat{B}^+$.

Now we take the two−mode squeezed states, then

$$<:: (\Delta\hat{E}_1)^N ::> = < \alpha_+, \alpha_-; \varsigma | :: (\Delta\hat{E}_1)^N :: | \alpha_+, \alpha_-; \varsigma > = \sum_{\gamma=0}^{N} \begin{bmatrix} N \\ \gamma \end{bmatrix} <:: (\Delta\hat{B}^+)^\gamma (\Delta\hat{B})^{N-\gamma} ::> = 0, \tag{21}$$

and

$$C_0 = [\hat{B}, \hat{B}^+] = |h_1|^2 + |h_2|^2 = (|g_+|^2 + |g_-|^2)(|\mu|^2 + |\nu|^2) - \Omega\sqrt{1 - \frac{\epsilon^2}{\Omega^2}}(\mu^*\nu e^{-2i\phi} + \mu\nu^* e^{2i\phi}). \quad (22)$$

From (20), (4) and (13), we get

$$< (\Delta\hat{E}_1)^N >= (N-1)!!\Omega^{N/2}[cosh(2r) - \sqrt{1 - \frac{\epsilon^2}{\Omega^2}}sinh(2r)cos(\theta - 2\phi)]^{N/2}. \quad (23)$$

If $\phi$ is chosen to satisfy $cos(\theta - 2\phi) = 1$, then Eq(23) leads to the result

$$< (\Delta\hat{E}_1)^N >= (N-1)!!\Omega^{N/2}[cosh(2r) - \sqrt{1 - \frac{\epsilon^2}{\Omega^2}}sinh(2r)]^{N/2}. \quad (24)$$

when $coshr < \frac{\Omega}{\epsilon}$, the right hand side is smaller than $(N-1)!!\Omega^{N/2}$, which is the corresponding Nth order moment for two−mode coherent states.

It follows that the two−mode output field exhibits higher−order squeezing to all even orders.

# 4 The generalized uncertainty relations

[A]. Higher−order noise moment $< (\Delta\hat{E}_2)^N >$

$\hat{E}_2$ can be regarded as a special case of $\hat{E}_1$, in which if $\phi$ is replaced by $\phi + \pi/2$, then from (23) it follows that

$$< (\Delta\hat{E}_2)^N >= (N-1)!!\Omega^{N/2}[cosh(2r) + \sqrt{1 - \frac{\epsilon^2}{\Omega^2}}sinh(2r)cos(\theta - 2\phi)]^{N/2}. \quad (25)$$

If $\phi$ is chosen to satisfy $cos(\theta - 2\phi) = 1$, then

$$< (\Delta\hat{E}_2)^N >= (N-1)!!\Omega^{N/2}[cosh(2r) + \sqrt{1 - \frac{\epsilon^2}{\Omega^2}}sinh(2r)]^{N/2}. \quad (26)$$

When $coshr < \frac{\Omega}{\epsilon}$, the right hand side is greater than $(N-1)!!\Omega^{N/2}$.

[B]. Generalized uncertainty relations

From (24) and (26), we obtain

$$< (\Delta\hat{E}_1)^N > \cdot < (\Delta\hat{E}_2)^N >= [(N-1)!!]^2\Omega^N[1 + \frac{\epsilon^2}{\Omega^2}sinh^2(2r)]^N. \quad (27)$$

Equation (27) shows that $< (\Delta\hat{E}_1)^N >$ and $< (\Delta\hat{E}_2)^N >$ in two−mode squeezed states can not be made arbitraily small simultaneously. We call Eq.(27) the generalized uncertainty relations in two−mode squeezed states, and the right hand side (constant) is dependent on $N, \epsilon, \Omega$, and r.

Since

$$1 + \frac{\epsilon^2}{\Omega^2} sinh^2(2r) > 1$$

so

$$< (\Delta\hat{E}_1)^N > \cdot < (\Delta\hat{E}_2)^N > \; > \; [(N-1)!!]^2 \Omega^N. \tag{28}$$

If $r = 0$, the two−mode squeezed states become two−mode coherent states, then

$$< (\Delta\hat{E}_1)^N >_{c,s} \cdot < (\Delta\hat{E}_2)^N >_{c,s} = [(N-1)!!]^2 \cdot \Omega^N. \tag{29}$$

This is the generalized uncertainty relations in two−mode coherent states.

If $\epsilon = 0, N = 2$, we obtain

$$< (\Delta\hat{E}_1)^2 > \cdot < (\Delta\hat{E}_2)^2 > = \Omega^2. \tag{30}$$

This is just the usual Heisenberg uncertainty relations in relevant references[1,2,4,5].

# 5 Application

As an application of the above result, we calculate the generation of higher−order squeezing by non−degenerate four−wave mixing (NDFWM). It can be shown that the field of the combined mode of the probe wave and the phase−conjugate wave exhibits higher−order squeezing to all even orders, and the generalzied uncertainty relations still hold in NDFWM process.

# 6 Acknowledgments

This research was supported by the National Natural Science Foundation of China.

# References

[1] C.K.Hong and L.Mandel, Phys. Rev. Lett. **54**, 323 (1985)

[2] C.K.Hong and L.Mandel, Phys. Rev. A**32**, 974 (1985)

[3] Li Xizeng and Shan Ying, Phys. Rev. A**40**, 7384 (1989)

[4] Li Xizeng and Shan Ying, Technical Digest of the XVI International Conference on Quantum Electronics, Tokyo, Japan (July 1988) p.180

[5] C.M.Caves and B.L.Schumaker, Phys. Rev. A**31**, 3086(1985)

# Q-DERIVATIVES, COHERENT STATES AND SQUEEZING

E.Celeghini [1], S.De Martino [2], S.De Siena [2], M.Rasetti [3] and G.Vitiello [2]

[1] *Dipartimento di Fisica - Università di Firenze and INFN–Firenze, I50125 Firenze, Italy*
[2] *Dipartimento di Fisica - Università di Salerno and INFN–Napoli, I84100 Salerno, Italy*
[3] *Dipartimento di Fisica and Unità INFM - Politecnico di Torino, I10129 Torino, Italy*

**Abstract**

We show that the $q$-deformation of the Weyl-Heisenberg ($q$-WH) algebra naturally arises in discretized systems, coherent states, squeezed states and systems with periodic potential on the lattice. We incorporate the $q$-WH algebra into the theory of (entire) analytical functions, with applications to theta and Bloch functions.

## 1 Introduction

The general properties of $q$-algebras [1] [2] have been widely studied, in particular in connection with specific physical models. In this paper we will show [3] that the $q$-deformation of the Weyl-Heisenberg ($q$-WH) algebra naturally arises in discretized quantum systems, coherent states, squeezed coherent states and systems with periodic potential on the lattice.

$q$-algebras are deformations of enveloping algebras of Lie algebras and, like the latter, they have Hopf algebras properties. The $q$-deformation of the Weyl-Heisenberg algebra ($q$-WH), as well as the WH algebra, is not even a Hopf algebra; it has only the properties of a Hopf superalgebra [4].

In our study of $q$-deformations we want to preserve the analytic structure of the corresponding Lie algebras and therefore we need to operate in a frame where analyticity is ensured: this is guaranteed by working in the Fock-Bargmann representation (FBR). In this representation it is immediate to show that finite difference operators possess the algebraic structure of $q$-WH algebra: As a result we recognize that a $q$-deformation of the algebra occurs whenever a finite length is involved in a physical system, the $q$-parameter being related with the finite spacing. The $q$-deformation is also expected in the presence of periodic conditions, since periodicity is a special form of invariance under finite difference operators.

We use the well known mapping of the $q$-algebra into the universal enveloping algebra of a corresponding Lie structure; to be specific, the mapping of finite difference operators into functions of differential operators, which can be indeed achieved only by operating on $C^\infty$ functions, namely by working in the FBR.

We would like to stress that we succeed into incorporating $q$-deformation of the WH algebra into the theory of (entire) analytical functions, with specific applications to theta functions and to Bloch functions, a result which may deserve by itself much attention.

In this paper we will use dimensionless units for all physical quantities.

## 2 Finite difference operators

The FBR operators, solution of the WH commutation relations $[a, a^\dagger] = 1, [N, a] = -a, [N, a^\dagger] = a^\dagger$ , are [5]:

$$N \rightarrow z\frac{d}{dz} \ , \qquad a^\dagger \rightarrow z \ , \qquad a \rightarrow \frac{d}{dz} \ . \tag{2.1}$$

The Hilbert space $\mathcal{F}$ is identified with the space of the entire analytical functions. Wave-functions are expressed as $\psi(z) = \sum_{n=0}^{\infty} c_n u_n(z)$, $\sum_{n=0}^{\infty} |c_n|^2 = 1$, $u_n(z) = \frac{z^n}{\sqrt{n!}}$, $(n \in Z_+)$ . The set $\{u_n(z)\}$ provides an orthonormal basis in $\mathcal{F}$. The finite difference operator $\mathcal{D}_q$

$$\mathcal{D}_q \ f(z) \ = \ \frac{f(qz) - f(z)}{(q-1)\ z} \ , \quad f \in \mathcal{F} \ , \tag{2.2}$$

with $q = e^\varsigma$, $\varsigma \in C$, may be written on $\mathcal{F}$ as $\mathcal{D}_q = ((q-1)z)^{-1}(q^{z\frac{d}{dz}} - 1)$. $\mathcal{D}_q$ is the well known [6] [7] [8] [9] $q$-derivative operator and, for $q \rightarrow 1$ (i.e. $\varsigma \rightarrow 0$), it reduces to the standard derivative. We have the algebra

$$[\mathcal{D}_q \ , \ z] \ = \ q^{z\frac{d}{dz}} \ , \quad [z\frac{d}{dz}, \ \mathcal{D}_q] \ = \ -\mathcal{D}_q \ , \quad [z\frac{d}{dz}, \ z] \ = \ z \ , \tag{2.3}$$

and observe that it is nothing but the $q$-deformation of the WH algebra. In fact, this can be seen by introducing the following operators in the space $\mathcal{F}$

$$N \rightarrow z\frac{d}{dz} \ , \quad \hat{a}_q \ \rightarrow \ z \ , \quad a_q \ \rightarrow \ \mathcal{D}_q \ , \tag{2.4}$$

where clearly $\hat{a}_q = \hat{a}_{q=1} = a^\dagger$ and $\lim_{q\rightarrow 1} a_q = a$. The quantum version of the Weyl-Heisenberg algebra is thus realized in terms of these operators $\{a_q, \hat{a}_q, N; \ q \in C\}$ with relations [1] [2]:

$$[N, a_q] = -a_q \ , \quad [N, \hat{a}_q] = \hat{a}_q \ , \quad [a_q, \hat{a}_q] \equiv a_q\hat{a}_q - \hat{a}_q a_q = q^N. \tag{2.5}$$

Equivalently, by introducing $\bar{a}_q \equiv \hat{a}_q q^{-N/2}$ , the $q$-WH algebra eq. (2.5) is rewritten in the more familiar form as $[N, a_q] = -a_q$ , $[N, \bar{a}_q] = \bar{a}_q$ , $a_q\bar{a}_q - q^{-\frac{1}{2}}\bar{a}_q a_q = q^{\frac{1}{2}N}$.

The finite difference operator algebra (2.3) in the FBR thus provides a realization of the $q$-WH algebra (2.5).

The notion of hermiticity associated with (2.5) has been studied in ref. [10] in connection with the discussion of the squeezing of the generalized coherent states $(GCS)_q$, defined in the usual Fock space $\mathcal{F}$.

We note that the commutator $[a_q, \hat{a}_q]$ acts in $\mathcal{F}$ as follows

$$[a_q, \hat{a}_q]f(z) \ = \ q^{z\frac{d}{dz}}f(z) \ = \ f(qz) \ . \tag{2.6}$$

In conclusion, the strict relation of the $q$-WH algebra with the finite difference operator $\mathcal{D}_q$ $(q \neq 1)$ suggests that whenever one deals with some lattice or discrete structure, then a deformation of the operator algebra acting on $\mathcal{F}$ should arise.

# 3 Coherent states, theta functions and squeezing

We summarize now the relation of $q$-WH algebra with the customary coherent states (CS) $|z>$ [5], with theta functions and with squeezing. Eq.(2.6) is the key relation to establish our results.

For sake of shortness we only report the relevant relations [3]:

$$< n|q^N|z > = \exp\left(-\frac{|z|^2}{2}\right) u_n(qz) \ , \tag{3.1}$$

$$< n|[a_q, \hat{a}_q]|z > = \exp\left(-(1-\bar{q})(1+q)\frac{|z|^2}{2}\right) < n|\mathcal{D}((q-1)z)|z > \ , \tag{3.2}$$

$$\exp\left((1-|q|^2)\frac{|z|^2}{2}\right)[a_q, \hat{a}_q]|z > = |qz > \ , \tag{3.3}$$

$$[a_q, \hat{a}_q]\ f(z) \ = \ \exp\left(-(1-\bar{q})(1+q)\frac{|z|^2}{2}\right)\ \mathcal{D}((1-\bar{q})\bar{z})\ f(z) \ , \tag{3.4}$$

where $\mathcal{D}(z)$ denotes the usual CS generator.

We observe that $[a_q, \hat{a}_q]$ acts as mapping operator from $|z>$ to $|qz>$ up to a phase factor. On the other hand, it acts the $z$-dilatation operator $(z \to qz)$ in the space of entire analytic functions. When $q = e^{\varsigma}$ , with $\varsigma$ pure imaginary, $\varsigma = i\theta$, then $[a_q, \hat{a}_q] : z \to e^{i\theta}z$ , generates the $U(1)$ group of phase transformations in the $z$-plane. We also observe that eqs. (3.2) and (3.3) provide a non linear realization of the quantum algebra (2.5) in terms of $a$ and $a^\dagger$. Vice-versa, the nonlinear operator $\mathcal{D}(z)$ is represented by the linear form $[a_q, \hat{a}_q]$.

In the framework of the formalism of CS on the von Neumann lattice $L$ the defining functional equation for the theta function is [5]

$$\theta_\epsilon(z+z_m) \ = \ \exp(i\pi F_\epsilon(-m))\ \exp\left(\frac{|z|^2}{2}\right)\ \exp(\bar{z}_m z)\ \theta_\epsilon(z) \ , \tag{3.5}$$

with $z_m = m_1\omega_1 + m_2\omega_2$ an arbitrary lattice vector and $F_\epsilon(m) \ = \ m_1m_2 + m_1\epsilon_1 + m_2\epsilon_2$ . A solution of (3.5) can be expressed as

$$\theta_\epsilon(z) \ = \ \sum_m e^{-i\pi F_\epsilon(m)} \exp\left(-\frac{|z_m|^2}{2}\right) \exp(-\bar{z}_m\ z) f(z) \ , \tag{3.6}$$

where $f(z)$ is an arbitrary entire function such that the series (3.6) is converging.

To establish the relation between $q$-WH algebra and theta functions, we write $q = q_m = e^{\varsigma_m}$ , with $\varsigma_m$ a vector on the lattice $L$ and, by setting $z_m = (q_m - 1)z$, we have [3]

$$\theta_\epsilon(q_m z) \ = \ [a_{q_m}, \hat{a}_{q_m}]\ \theta_\epsilon(z) \ , \tag{3.7}$$

$$[a_{q_m}, \hat{a}_{q_m}]\ \theta_\epsilon(z) \ = \ \exp(i\pi F_\epsilon(-m)) \exp\left(-(1-\bar{q}_m)(1+q_m)\frac{|z|^2}{2}\right)\theta_\epsilon(z) \ , \tag{3.8}$$

$$\theta_\epsilon(z) = \sum_m \exp(-i\pi F_\epsilon(m)) \exp\left((1-\bar{q}_m)(1+q_m)\frac{|z|^2}{2}\right)[a_{q_m}, \hat{a}_{q_m}]\ f(z) \ . \tag{3.9}$$

Eqs. (3.7-9) show that theta functions span indeed a space of representations for the $q$-algebra (2.5).

Finally, we study the relation of $q$-WH algebra with squeezing. Let $\hat{p}_z = -i\frac{d}{dz}$ and $[\hat{z}, \hat{p}_z] = i$, over a Hilbert space of states $\psi(z)$ identified with the space of entire analytic functions $\mathcal{F}$. Introduce the operators $\alpha = \frac{1}{\sqrt{2}}(\hat{z} + i\hat{p}_z)$ , $\alpha^\dagger = \frac{1}{\sqrt{2}}(\hat{z} - i\hat{p}_z)$ , $[\alpha, \alpha^\dagger] = I$. It is immediate to observe that

$$[a_q, \hat{a}_q]\ \psi(z) \ = \ \exp\Big(\varsigma z\frac{d}{dz}\Big)\ \psi(z) \ = \frac{1}{\sqrt{q}}\exp\Big(\frac{\varsigma}{2}(\alpha^2 - \alpha^{\dagger 2})\Big)\ \psi(z) \tag{3.10}$$

$$= \frac{1}{\sqrt{q}}\hat{S}(\varsigma)\psi(z) = \frac{1}{\sqrt{q}}\psi_s(z)\ ,$$

with $\hat{S}(\varsigma)$ denoting the squeezing generator [11], $\varsigma = \log q$ the squeezing parameter and $\psi_s(z)$ the squeezed state. We therefore conclude that the operator $[a_q, \hat{a}_q]$ *is* the squeezing generator for CS in the FBR, thus confirming the conjecture previously [10] formulated whereby $q$-groups are the natural candidates to study the squeezed CS.

# 4 Quantum mechanics on the lattice

Our purpose is now to show that $q$-WH algebra is underlying the physics of lattice quantum systems. Lattice Quantum Mechanics (LQM) is characterized by the E(2) commutator algebra, which in the momentum space is written as [3] [12]

$$[\hat{x}_\epsilon, \hat{p}_\epsilon] = [i\frac{d}{dk}, \epsilon^{-1}\sin(k\epsilon)] = i\cos(k\epsilon)\ ,$$

$$[\hat{x}_\epsilon, \cos(k\epsilon)] = [i\frac{d}{dk}, \cos(k\epsilon)] = -i\epsilon\sin(k\epsilon)\ . \tag{4.1}$$

$$[\hat{p}_\epsilon, \cos(k\epsilon)] = [\epsilon^{-1}\sin(k\epsilon), \cos(k\epsilon)] = 0\ .$$

where $\hat{x}_\epsilon$ and $\hat{p}_\epsilon$, denote the (one-dimensional) lattice position operator and the lattice momentum operator, respectively (extension to higher dimensions is straightforward). The corresponding uncertainty relations are

$$\Delta^2(\hat{x}_\epsilon)\Delta^2(\hat{p}_\epsilon) \geq \frac{1}{4}(\langle\cos(k\epsilon)\rangle^2)\ , \tag{4.2}$$

$$\Delta^2(\hat{x}_\epsilon)\Delta^2(\cos(k\epsilon)) \geq \frac{1}{4}(\epsilon^2\langle\sin(k\epsilon)\rangle^2)\ , \tag{4.3}$$

where $\Delta^2(\hat{A}) = \langle\hat{A}^2\rangle - \langle\hat{A}\rangle^2$ with $= \langle\hat{A}\rangle = \int dk\Psi^*(k)\hat{A}\Psi(k)$. We observe that these relations go, in the continuum limit $\epsilon \to 0$, to the usual ones. In this connection we observe that the continuum limit is, in fact, an isometric and conformal mapping of the torus on the plane.

Following the usual procedure [13], the states minimizing the uncertainties (4.2) and (4.3) are found to be, in momentum space

$$\Psi(k) = G^{-\frac{1}{2}}\ \exp\left[\bar{\gamma}\cos(\epsilon k) - i\bar{\lambda}\epsilon k\right]\ . \tag{4.4}$$

The normalization constant $G$ is given by $G = \frac{2\pi}{\epsilon} I_0(2\bar{\gamma})$ , $I_0$ denoting the modified Bessel function of the first kind of order 0. We adopted the notation: $\bar{\lambda} = \lambda\epsilon^{-1}$ , $\bar{\gamma} = \gamma\epsilon^{-2}$ , $\lambda = \langle\hat{x}_\epsilon\rangle + i\gamma\langle\hat{p}_\epsilon\rangle$ , and $\gamma$ is connected with the mean square roots of position and momentum.

In the continuum limit, i.e. for small $\epsilon$, one recovers in the space of configurations, $\tilde{\Psi}(x) = (\gamma\pi)^{-\frac{1}{4}} \exp\left\{-\left[(2\gamma)^{-1}(x - \langle\hat{x}\rangle)^2 + i\langle\hat{p}\rangle(x - \langle\hat{x}\rangle)\right]\right\}$ , which is the minimum uncertainty wave-function given by Schrödinger [14]. The $\Psi(k)$'s are the lattice coherent states.

In order to see the relation with the $q$-algebra we consider the conformal image $\tilde{\mathcal{H}}$ of the Hilbert space obtained upon introducing the variable $z = e^{i\phi}$ ($\phi = k\epsilon$ , $-\pi \leq \phi \leq \pi$), such that $-i\frac{d}{dk} = -i\epsilon\frac{d}{d\phi} = \epsilon z\frac{d}{dz}$ . The functions in $\tilde{\mathcal{H}}$ are assumed to be entire square-integrable analytic functions. We have

$$L_3 f(\phi) = -i\frac{d}{d\phi} f(\phi) = z\frac{d}{dz}\tilde{f}(z) = N\tilde{f}(z) \quad , \quad \tilde{f} \in \tilde{\mathcal{H}} \quad , \tag{4.5}$$

$$f(\phi + \epsilon) = e^{i\epsilon L_3} f(\phi) = q^N \tilde{f}(z) = \tilde{f}(qz) \quad , \tag{4.6}$$

with $q = e^{i\epsilon}$. The realization (2.4) has been adopted in the FBR, with $z$ restricted tó the unit circle. The $E(2)$ algebra (4.1) is realized by

$$[L_1, L_3]\tilde{f}(z) = -iL_2\tilde{f}(z) \, , \quad [L_2, L_3]\tilde{f}(z) = iL_1\tilde{f}(z) \, , \quad [L_1, L_2]\tilde{f}(z) = 0 \, , \tag{4.7}$$

with $\tilde{f} \in \tilde{\mathcal{H}}$, and the identifications

$$L_1 = \frac{z + \bar{z}}{2} \, , \quad L_2 = \frac{z - \bar{z}}{2i} \, , \quad L_3 = z\frac{d}{dz} \, , \quad L_+ = z \, , \quad L_- = \bar{z} \, . \tag{4.8}$$

One can see that $[a_q, \hat{a}_q]$ is nothing but the group element $e^{i\epsilon L_3}$ of $E(2)$. The algebraic structure of LQM is thus intimately related with the $q$-WH algebra, the deformation parameter $q$ being determined by the discrete lattice length $\epsilon = -i \log q$.

We finally note that $z^n = e^{in\phi}$, $n$ integer, is the eigenfunction of $L_3$ associated with the eigenvalue $n$ of the number operator in the FBR: $L_3 z^n = Nz^n = nz^n$ .

The functions $z = e^{i\phi}$ play also a rôle in the Bloch functions theory. Suppose we have a periodic potential $V(x_n) = V(x_n + \epsilon)$ on the lattice. Bloch theorem ensures the existence of solutions of the related Schrödinger equation of the form $\psi(x_n) = e^{\pm ikx_n} v_k(x_n)$, with $v_k(x_n) = v_k(x_n + \epsilon)$. $\psi(x_n)$ is the Bloch function. Let us limit ourself to consider for simplicity the plus sign in the exponentials. $\psi(x_n)$ has the property

$$\psi(x_n + \epsilon) = e^{ik\epsilon}\psi(x_n) = z\psi(x_n) \, . \tag{4.9}$$

The choice of the variable $z = e^{ik\epsilon}$ turns out to be natural in the case of periodic potentials:

$$\psi(x_n) = z^n v_k(x_n) \, , \quad \psi(x_n + \epsilon) = z^{n+1} v_k(x_n) \, . \tag{4.10}$$

Since $z^n = (z_n)^k$ and $q^N (z_n)^k = (qz_n)^k = e^{ik\epsilon(n+1)} = z^{n+1}$,

$$\psi(x_n + \epsilon) = [a_q, \hat{a}_q](z_n)^k v_k(x_n) = [a_q, \hat{a}_q]\psi(x_n) \, , \tag{4.11}$$

which shows that the Bloch functions provide indeed a representation for the $q$-WH algebra.

# References


[1] L.C Biedenharn, J. Phys. **A22**, 117 (1989).

[2] A.J. Macfarlane, J. Phys. **A22**, 4581 (1989).

[3] E.Celeghini, S.De Martino, S.De Siena, M. Rasetti, and G.Vitiello, Mod. Phys. Lett **B**, (1993), to be published; Florence University Preprint DFF188/9/93.

[4] E.Celeghini, T.D.Palev and M.Tarlini, Mod. Phys. Lett **B5**, 187 (1991).

[5] A. Perelemov, *Generalized Coherent States and Their Applications*, (Springer-Verlag, Berlin Heidelberg, 1986).

[6] L.C. Biedenharn, and M.A. Lohe , Comm. Math. Phys. **146**, 483 (1992).

[7] F.H. Jackson, Messenger Math. **38**, 57 (1909).

[8] T.H. Koornwinder, Nederl. Acad.. Wetensch. Proc. Ser. **A92**, 97 (1989).

[9] D. I. Fivel, J. Phys. **A24**, 3575 (1991).

[10] E. Celeghini, M. Rasetti, and G. Vitiello, Phys. Rev. Lett. **66**, 2056 (1991).

[11] H.P. Yuen, Phys. Rev. **A13**, 2226 (1976).

[12] F.Guerra, *Statistical Mechanics Methods in Quantum Field Theory*, Proceedings of the *International School of Mathematical Physics*, G. Gallavotti ed., Universita' di Camerino (1974).

[13] P.Carruthers, and M.N. Nieto, Rev. Mod. Phys. **40**, 411 (1968).

[14] E.Schrödinger, Naturwissenschaften **14**, 664 (1926).

# SUM-FREQUENCY GENERATION FROM PHOTON NUMBER SQUEEZED LIGHT

Ling-An Wu
*Institute of Physics, Chinese Academy of Sciences,*
*P.O.Box 603, Beijing 100080, China*

Congshi Du Meijuan Wu Shiqun Li
*Department of Modern Applied Physics, Tsinghua University,*
*Beijing 100084, China*

**Abstract**

We investigate the quantum fluctuations of the fields produced in sum-frequency (SF) generation from light initially in the photon number squeezed state. It is found that, to the fourth power term, the output SF light is sub-Poissonian whereas the quantum fluctuations of the input beams increase. Quantum anticorrelation also exists in SF generation.

## 1 Introduction

In recent years squeezed states of light have been successfully produced in several laboratories and certain applications also demonstrated.[1] In future applications it may be desirable to change the frequency of a light beam already in the squeezed state, for example by frequency doubling, parametric down conversion or four wave mixing. Three wave processes are preferable since the second order nonlinear susceptibility is much larger than the third order susceptibility. Second harmonic generation from a pump beam initially in a squeezed state has been discussed [2,3] as well as SF/DF generation and degenerate parametric down conversion of quadrature squeezed light.[3,4] In this paper we shall consider SF generation from input fields initially in the photon number squeezed or sub-Poissonian state.

## 2 Sum-frequency generation

As shown in Fig. 1 we take both input fields, of frequency $\omega_1$ and $\omega_2$, and the sum-frequency $\omega_3$ field ($\omega_3 = \omega_2 + \omega_1$) to be in a collinear geometry. The input beams are incident on a nonlinear medium such as a crystal with an effective second order nonlinear coefficient $\chi'$. The field Hamiltonian for ideal SF generation ignoring losses is

$$H = \hbar\omega_1 a_1^\dagger a_1 + \hbar\omega_2 a_2^\dagger a_2 + \hbar\omega_3 a_3^\dagger a_3 + \hbar\chi'(a_1 a_2 a_3^\dagger + \text{h.c.}) \tag{1}$$

where $a_1$, $a_2$ and $a_3$ are the annihilation operators for the two input beams and the resultant SF beam, respectively.

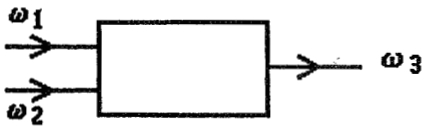


FIG. 1 Sum-frequency generation in a nonlinear crystal.

We introduce the slowly varying operators

$$c_j(t) = a_j\, e^{i\omega_j t} \tag{2}$$

where the subscript $j = 1, 2$ or 3 refers to the two input or SF waves, respectively, as throughout our paper. For propagation along the $z$-axis at a velocity $u$ in a lossless medium we make the conversion $z = ut$. Since $\omega_3 = \omega_1 + \omega_2$ and substituting $\chi = \chi'/u$ we deduce the equations of motion for the slowly varying operators from Eq. (1) to be

$$\begin{aligned} \tfrac{dc_1(z)}{dz} &= -i\chi c_2^\dagger(z)c_3(z), \\ \tfrac{dc_2(z)}{dz} &= -i\chi c_1^\dagger(z)c_3(z), \\ \tfrac{dc_3(z)}{dz} &= -i\chi c_1(z)c_2(z). \end{aligned} \tag{3}$$

In the short path approximation for $\chi z \ll 1$ we assume the solution of Eq. (3) to take the form

$$c_j(z) = c_j(0) + (\chi z)B_j + (\chi z)^2 C_j + (\chi z)^3 D_j + (\chi z)^4 E_j + \cdots \tag{4}$$

where $c_j(0)$ denotes the incident fundamental field at $t = 0$. It may be seen that $c_j(z)$ still satisfies the commutation relation

$$[c_i(z), c_j^\dagger(z)] = \delta_{ij}. \tag{5}$$

Substituting into Eq. (3) we obtain the solutions for $c_1(z)$, $c_2(z)$ and $c_3(z)$.

To discuss the photon number fluctuations of the quantized fields we consider the variance $\langle \Delta n_j^2(z) \rangle$ or the Fano factor

$$\sigma_j = \frac{\langle \Delta n_j^2(z) \rangle}{\langle n_j(z) \rangle} \tag{6}$$

where $n_j(z) = c_j^\dagger(z)c_j(z)$, and $\langle \Delta n_j^2(z) \rangle \equiv \langle n_j^2(z) \rangle - \langle n_j(z) \rangle^2$. To obtain the above expressions we need to solve for the factors $c_k^\dagger c_k$, $c_k^{\dagger 2} c_k^2$ and $c_k^{\dagger 3} c_k^3$, where $c_k = c_k(0)$ and $k = 1$ or 2, then find their expectation values. If the input fields are in a photon number squeezed state we adopt the formalism given by Kitagawa and Yamamoto[5], that is,

$$c_k = e^{i\gamma_k n_k} a_k + \xi_k, \qquad \xi_k = -i\eta_k \alpha_k e^{i\phi_k}. \tag{7}$$

Here $n_k = a_k^\dagger a_k$ is the number operator and $\gamma_k$, $\eta_k$ are constants chosen to maximise the squeezing for a given input field intensity proportional to $|\alpha_k|^2$. Using Eqs. (7) and after some tedious calculations we may obtain the expectation values $\langle c_k^\dagger c_k \rangle$ and higher terms with respect to the

eigenstates of $a_k$, noting that $c_3(0)$ is a vacuum field. The Fano factors may thus be computed numerically for explicit values of $\alpha_k$, $\gamma_k$ and $\eta_k$. It is evident that the expressions for the Fano factors of the two input beams are identical if the subscripts $k = 1$ and 2 are interchanged.

Another quantity that reflects the quantum fluctuations of the light fields is the quantum correlation between the sum of the input photon numbers, $n_1(z) + n_2(z)$, and the SF photon number $n_3(z)$. That is, if we define $\langle n(z)\rangle = \langle n_1(z) + n_2(z) + n_3(z)\rangle$, then

$$\langle \Delta n^2(z)\rangle = \langle \Delta(n_1 + n_2)^2(z)\rangle + \langle \Delta n_3^2(z)\rangle + 2[\langle (n_1 + n_2)(z) n_3(z)\rangle - \langle (n_1 + n_2)(z)\rangle\langle n_3(z)\rangle], \quad (8)$$

and we define the Fano factor for the total sum of the photon numbers as

$$\sigma(z) = \frac{\langle \Delta n^2(z)\rangle}{\langle n(z)\rangle}. \quad (9)$$

The Fano factors for different pairs of the two input beam intensities are plotted against the effective interaction length $\chi z$ in Figs. 2 to 4. It can be seen that $\sigma_3$ becomes less than 1 in all three cases, that is, the SF produced becomes sub-Poissonian. Moeover, as the interaction length increases the photon number fluctuations are reduced even further but at the expense of the input fields.

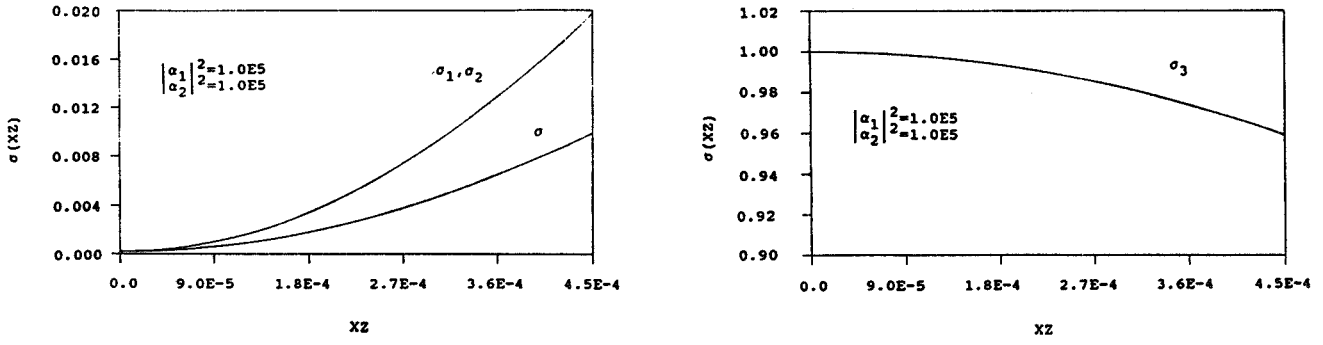


FIG. 2 Fano factors of the input and SF beams versus effective interaction length for sub-Poissonian inputs of equal intensity. Subscripts 1,2 and 3 denote the two inputs and the SF beam, respectively. $\sigma$ is the Fano factor for the total photon number of the three beams.

As shown in Fig. 2, when the two input beams are of the same intensity, that is, $|\alpha_1|^2 = |\alpha_2|^2$ and assuming that their initial statistical properties are identical, then $\sigma_1$ and $\sigma_2$ are always the same, as may be expected. However, when one frequency e.g. $\omega_2$ has a greater number of photons than the other, its Fano factor is less affected (see Fig. 3) since there is a greater number of unconverted photons left. The Fano factor $\sigma$ for the sum of all three intensities also increases with interaction length, but it is always better i.e. less than that for the individual beams. This can be understood from the correlation between the three beams, since the creation of one SF photon is always associated with the annihilation of two input photons, one from each input beam.

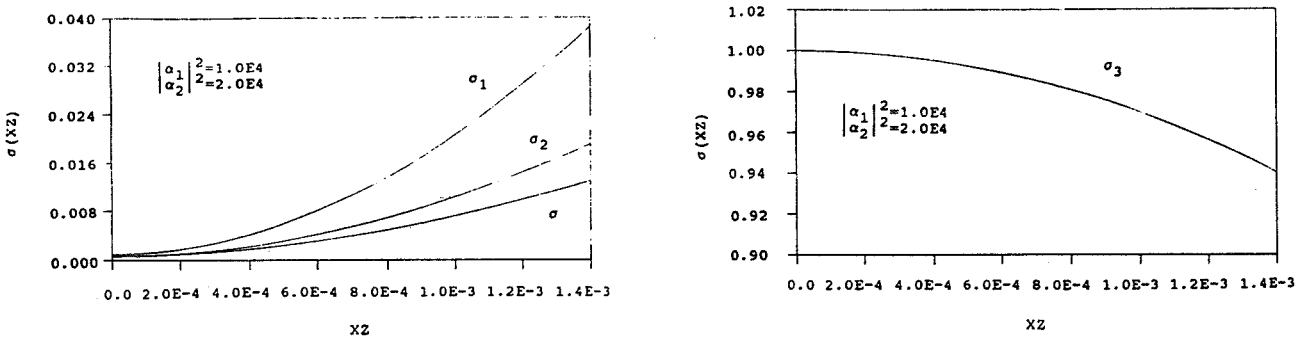


FIG. 3 Fano factors of the input and SF beams versus effective interaction length for sub-Poissonian inputs of different intensities. Subscripts 1,2 and 3 denote the two inputs and the SF beam, respectively. $\sigma$ is the Fano factor for the total photon number of the three beams.

In Fig. 4 we have taken one input beam $\omega_2$ to be sub-Poissonian whilst the other $\omega_1$ is in a coherent state, with both having the same intensity. It can be seen that the curves of $\sigma_2$ and $\sigma_3$ behave similarly to those in the previous figure, but $\sigma_1$ remains constant at 1. This implies that the coherent input beam remains coherent throughout the interaction, with only the originally squeezed beam suffering increased quantum fluctuations. The physical reason for this is yet to be fully understood.

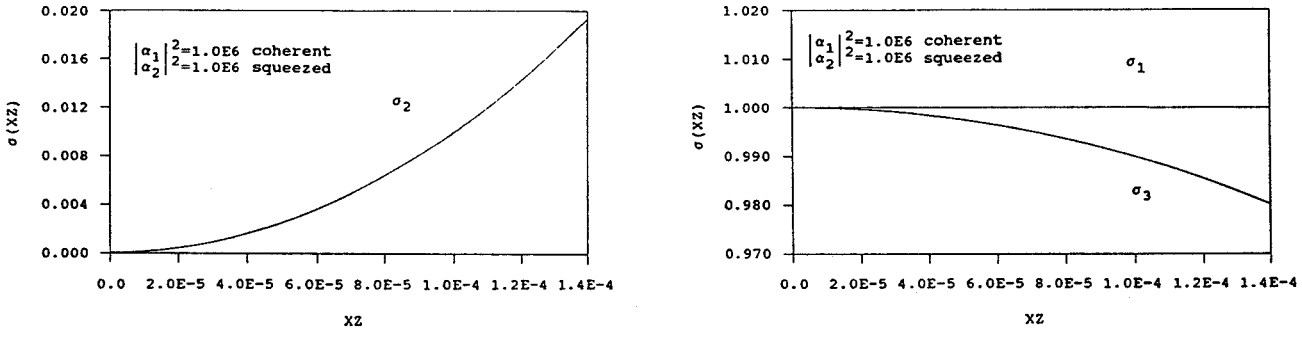


FIG. 4 Fano factors of the input and SF beams versus effective interaction length for inputs of equal intensities but different statistical nature. Subscripts 1,2 and 3 denote the two inputs and the DF beam, with $\omega_1$ in a coherent state and $\omega_2$ in a sub-Poissonian state. $\sigma$ is the Fano factor for the total photon number of the three beams.

# 3 Conclusion

We have investigated the photon number fluctuations in SF generation with sub-Poissonian light as input and small effective interaction length. We find that the generated SF beam becomes sub-Poissonian and the quantum fluctuations decrease as the effective interaction length increases, but at the expense of the two input beams which become noisier. The Fano factor of the sum of the intensities of the three beams increases also with interaction length, but it will always be less than that of the other beams. This can be understood on the grounds of the quantum correlation between the input and SF fields. When one of the input beams is coherent and the other sub-Poissonian, the coherent beam remains coherent throughout the interaction, whilst the other becomes noisier. The generated SF beam, however, still becomes sub-Poissonian.

# 4 Acknowledgments

This work was supported by the National Natural Science Foundation of China.

## References

[1] See the feature issues J. Opt. Soc. Am. B4 (10), (1987); Appl. Phys. B55 (3), (1992).

[2] A.V. Belinskii and A.S.Chirkin, Opt. Spectrosc. (USSR) 66, 695, (1989).

[3] Wu Ling-An, Zhang Weidong, Wu Meijuan and Li Shiqun, Proc. Shanghai Int. Symp. Quantum Optics, SPIE 1726, p.151 (Shanghai 1992); Wu Meijuan, Li Shiqun and Wu Ling-An, *ibid* p.92.

[4] Li Shiqun and Wu Ling-An, Chinese Phys. Lett. 8, 222, (1991).

[5] M. Kitagawa and Y. Yamamoto, Phys. Rev. A34, 3974, (1986).

# SPECTRAL, NOISE AND CORRELATION PROPERTIES OF INTENSE SQUEEZED LIGHT GENERATED BY A COUPLING IN TWO LASER FIELDS

Gagik Yu.Kryuchkyan and Karen V.Kheruntsyan

*Institute for Physical Research, National Academy of Sciences, Ashtarak-2, 378410, Republic of Armenia*

Abstract

Two schemes of four-wave mixing oscillators with nondegenerate pumps are proposed for above-threshold generation of squeezed light with nonzero mean-field amplitudes. Noise and correlation properties and optical spectra of squeezed-light beams generated in these schemes are discussed.

## 1. Introduction

The squeezed light generated to date has been in the main either squeezed vacuum or squeezed light with an extremely small mean field amplitude. Therefore there is much current interest in searching of new schemes to generate squeezed light with a large coherent component of the field.

In this report we would like to present some nonlinear optical schemes for generation of intense squeezed light with nonzero mean amplitude. This type of coherent squeezed-state light is called sometimes bright squeezed light.

One of the important schemes for the generation of squeezed light, realized experimentally, is based the process of nondegenerate four-wave mixing (FWM) in a cavity. In this process an intense pump field with frequency $\omega_0$ (for certainty) interacts via a nonlinear medium with two modes of radiated field with frequencies $\omega_1$, $\omega_2$, such that $2\omega_0 \rightarrow \omega_1 + \omega_2$.

In contrast with this standard scheme of FWM, we propose to consider the process of FWM under the pumping by two laser fields of different frequencies $\omega_1$, $\omega_2$. As a result of coupling in nonlinear

medium, a pair of photons of two pump fields $\omega_1$, $\omega_2$ transform to a pair of photons of spontaneously generated signal field with degenerate frequency $\omega_o$, such that $\omega_1+\omega_2 \rightarrow 2\omega_o$.

We study two different four-wave mixing configurations. The first of them (see Fig.1) consists of a nonlinear medium in a ring cavity, which couples two monochromatic copropagating pump beams of different colors (frequencies $\omega_1$, $\omega_2$) with an intracavity signal mode at the half-sum freguency $\omega_o=(\omega_1+\omega_2)/2$. We consider the case of spontaneous excitation of a single cavity-resonant mode. So we have dealing with a nearly collinear wave-vector matching condition $\vec{k}_1+\vec{k}_2\simeq 2\vec{k}_o$.

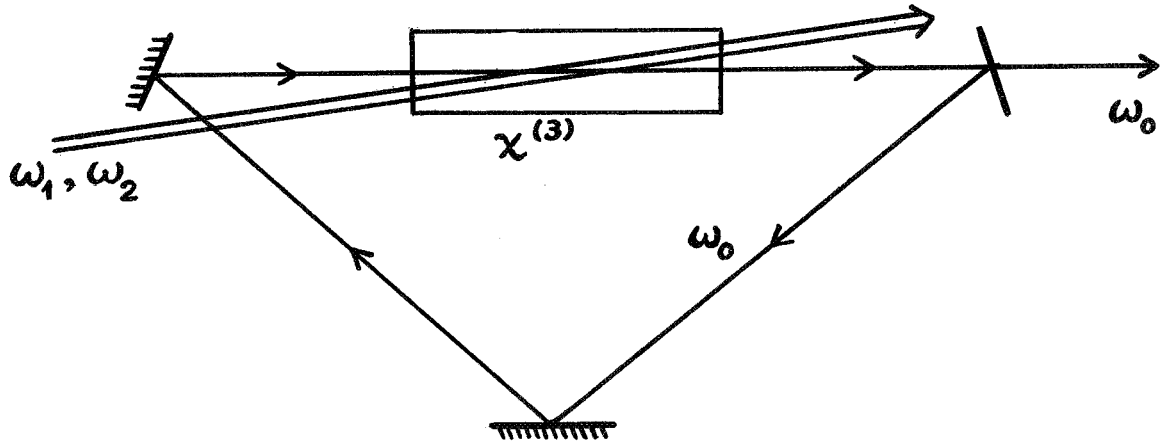


Fig.1. Scheme of the double-color-pumped FWM oscillator with a single cavity-mode excitation.

In the first part of our report (see Section 2) we shall present the results, related to the configuration of Fig.1. At the beginning of this part we would like to describe briefly some of the below-threshold results [1,2].

## 2.1. Squeezing of the central line of the resonance fluorescence in a bichromatic field in a cavity

We consider an ensemble of two-level atoms interacting in an optical cavity with a bichromatic pump field and with a cavity mode of radiation field. This pump field is treated classically and chosen

in the following form

$$E(t) = E_o \, \mathrm{Re}\left[ e^{-i(\omega_o+\delta)t-2i\phi} + e^{-i(\omega_o-\delta)t} \right] . \qquad (1)$$

It contains two components with equal amplitudes $E_o/2$, relative phase $2\phi$ and frequencies $\omega_{1,2}=\omega_o \pm \delta$, symmetrically detuned from the atomic transition frequency $\omega_o$.

We have calculated the cavity-output intensity in the process of resonance fluorescence [1]. At this we do not require the execution of any phase-matching conditions. The result for the inelastic part of the intensity is shown in Fig.2 as a function of the detuning of the cavity resonance frequency $\omega_c$ from the atomic transition frequency $\omega_o$. The curve is plotted for particular values of the pump intensity parameter $\xi=2V/\delta$ and parameters $\Gamma/\sigma$, $\delta/\gamma$ ( $V$ is the matrix element of the dipole transition, $\sigma$ is the atomic absorption coefficient, $\gamma$ is the atomic spontaneous wight, $\Gamma$ is the cavity decay rate)

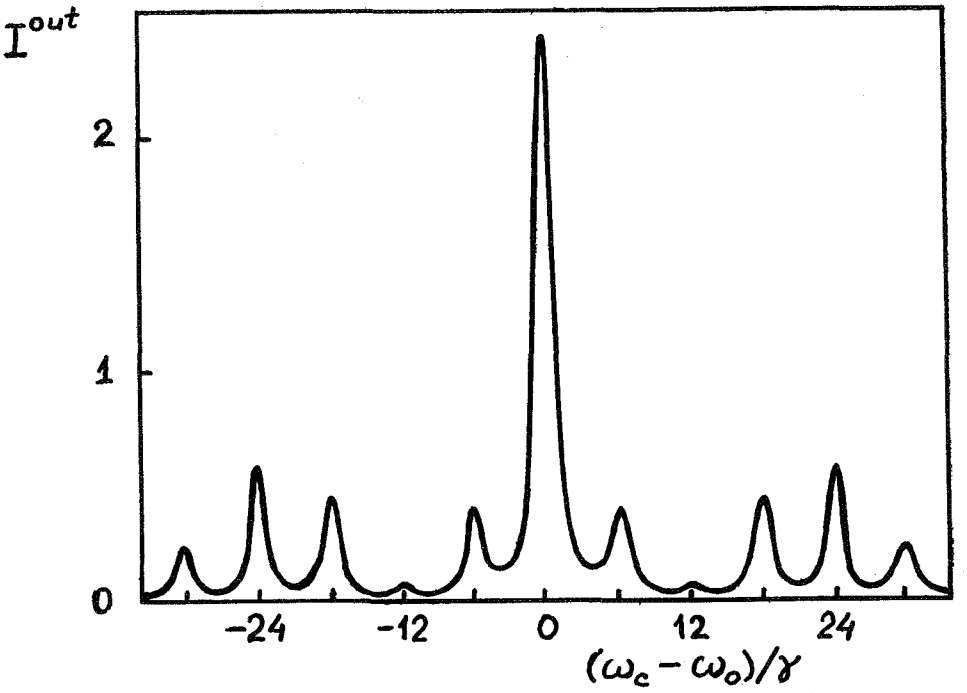


Fig.2. Cavity output intensity versus $(\omega_c-\omega_o)/\gamma$ : $\xi=5$, $\delta/\gamma=6$, $\Gamma/\sigma=0,1$.

We see that the intensity consist of a series of peaks with a constant spacing $\delta$. They are symmetrically located about a central peak, coinciding with the atomic transition frequency $\omega_o$. This intensity spectrum was experimentally studied by Y.Zhu et al. [3] for

two-level-like Ba atoms driven by two strong, equal-amplitude fields with frequency separation $2\delta$. Note that the results of our calculations are in agreement with the experimental curves.

Let us turn now to the results, related to the quantum fluctuations in the process of FWM. We consider a generation of the mode with frequency equal to the resonance fluorescence central line $\omega_o=(\omega_1+\omega_2)/2$. The calculation of the quadrature-phase fluctuations show that this $\omega_o$-mode is excited in a squeezed state. The optimal value of the squeezing spectrum $S(\omega)$ is realized at zero frequency and the maximal squeezing may reach 35%. The dependence of the quantity $S_{min}(\omega=0)$ on the pump intensity parameter $\xi=2V/\delta$ is plotted in Fig.3 [2].

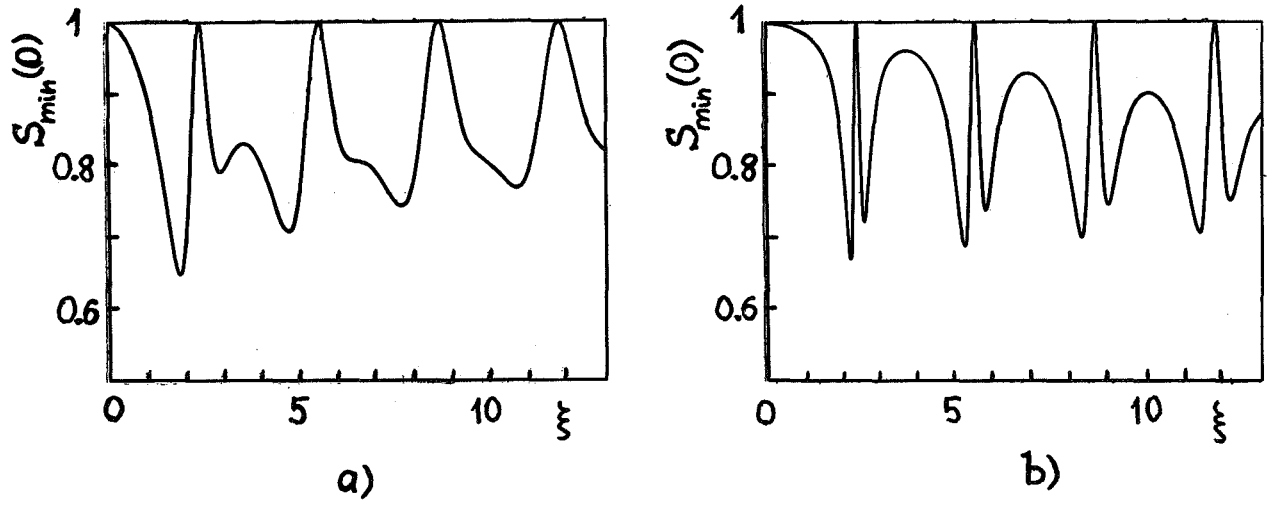


Fig.3. Peak squeezing $S_{min}(0)$ versus $\xi$ for $\Gamma/\sigma=0.1$ - (a), $\Gamma/\sigma=0.01$ - (b). The squeezing is absent for values of $\xi$, for which the probabilities of one and twin $\omega_o$-photon radiation processes cancell each other.

In order to interpret this result, note that the excitation of the $\omega_o$-mode in a cavity is caused by a nonlinear spontaneous process of two-photon radiation by an atom in a bichromatic field. In a low order of interaction it may be represented by the following graphs (see Fig.4). It is essential that there is a strong pair correlation between the photons of frequency $\omega_o$. This correlation has a super-bunching behavior and manifests itself in the reduction of quadrature fluctuations below the shot-noise level.

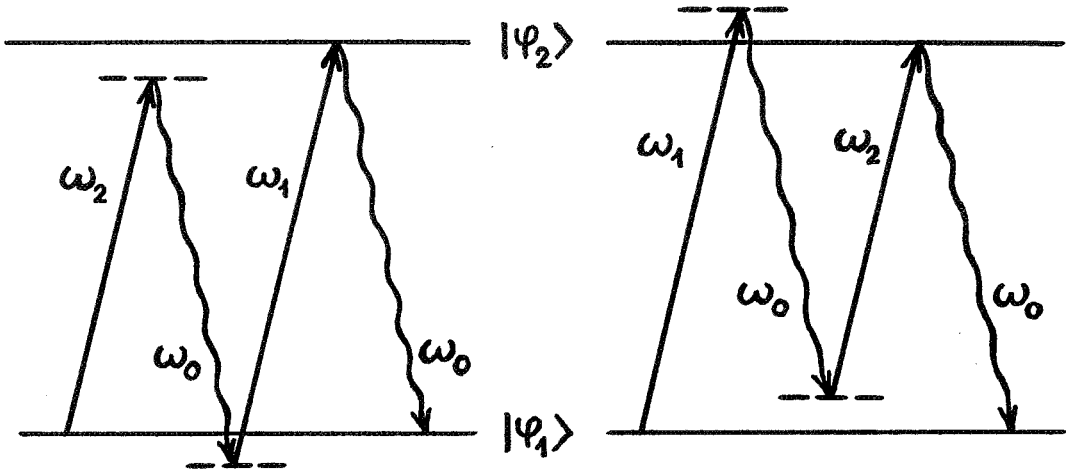


Fig.4. Illustration of the process of two-photon absorption at frequencies $\omega_{1,2}=\omega_o\pm\delta$ of the pump fields with the emission of two photons at frequenciy $\omega_o=(\omega_1+\omega_2)/2$.

## 2.2. Above threshold results in a parametric model of FWM in the presence of phase modulation

Now we consider a simple parametric model of four-wave mixing under bichromatic pumping in order to obtain the squeezing results above the generation threshold. In our analysis we include the effects of self-phase modulation and cross-phase modulation.

We describe the nonlinear medium phenomenologically by the third order susceptibility $\chi^{(3)}$. So we start from the following Hamiltonian

$$H = \hbar\omega_c a^+ a + \frac{\hbar\chi}{2} a^2 E_1^* E_2^* + a^{+2} E_1 E_2 + \frac{\hbar\chi}{4} a^{+2} a^2 +$$

$$+ \hbar\chi\left(|E_1|^2+|E_2|^2\right) a^+ a + (a^+\Gamma + a\Gamma) , \qquad (2)$$

where $a^+, a$ are creation and annihilation operators of the intracavity mode, $\omega_c$ is the cavity resonant frequency. The second term in Eq.(2) describes the four-wave interaction with coupling constant $\chi$, proportional to $\chi^{(3)}$. The third and forth term describe the self-phase modulation and cross-phase modulation. The fifth term accounts for the coupling of the cavity mode with reservoir, which will give rise to the cavity damping constant $\gamma$. The quantities $E_1$, $E_2$ are the

complex amplitudes of the pump fields at frequencies $\omega_1$, $\omega_2$. At nearly collinear phase matching condition these pump fields generate an intracavity signal mode with frequency $\omega_0=(\omega_1+\omega_2)/2$. In this configuration the pump fields travel through the medium only once. So it is possible to neglect the pump depletion and treat $E_1$, $E_2$ as a fixed constants.

With use of standard methods, we obtain the following differential equations for the stochastic amplitude of the signal mode $\omega_0$:

$$\frac{d\alpha}{dt} = -\gamma\alpha + i\left[\Delta-\chi\left(|E_1|^2+|E_2|^2\right)\right]\alpha - \frac{i\chi}{2}\alpha^+\alpha^2 - i\chi E_1E_2\alpha^+ + R_0(t), \quad (3)$$

where $\Delta=\omega_0-\omega_c$ is the cavity detuning parameter. The noise term $R_0$ has the following correlator

$$\langle R_0(t)R_0(t')\rangle = -\chi\left(E_1E_2 + \frac{1}{2}\alpha^2\right)\delta(t-t') \quad (4)$$

Note that without the phase-modulation terms equations of motion would be the same as for the degenerate parametric oscillator and degenerate four-wave mixing below threshold. The novel features and results in our system are connected with the incorporation of the self-phase modulation term. This term results in the above-threshold generation of the signal field. Let us consider the stable steady-state solution for the output intensity. It is equal to

$$I^{out} = 2\gamma\langle a^+a\rangle = 2\gamma\left[\frac{\Delta}{\gamma} - \frac{\chi}{\gamma}\left(|E_1|^2+|E_2|^2\right) + \sqrt{\left(\frac{\chi}{\gamma}\right)^2|E_1|^2|E_2|^2-1}\right]. \quad (5)$$

In Fig.5 we plot the normalized output intensity as a function of the parameter $\varepsilon^2=E^2\chi/\gamma$ for the case of equal amplitudes of the pump fields $|E_1|=|E_2|=E$.

The zero intensity solution is stable below the generation threshold at $\varepsilon^2<\varepsilon_A^2$ and well above-threshold at $\varepsilon^2>\varepsilon_B^2$, where

$$\varepsilon_A^2 = \frac{1}{3}\left[\frac{2\Delta}{\gamma} - \sqrt{\left(\frac{\Delta}{\gamma}\right)^2-3}\right], \quad \varepsilon_B^2 = \frac{1}{3}\left[\frac{2\Delta}{\gamma} + \sqrt{\left(\frac{\Delta}{\gamma}\right)^2-3}\right]. \quad (6)$$

The nonzero-intensity solution given by Eq.(5) is stable in the region $1<\varepsilon^2<\varepsilon_B^2$ and have a meaning for $\Delta$ less than $\gamma\sqrt{3}$. We see that a bistable behaviour of the output is realized in the region $1<\varepsilon^2<\varepsilon_A^2$.

Now let us turn out to the problem of squeezing. The spectrum of the output field above threshold is obtained in a standard linearized treatment of quantum fluctuations. Curves for squeezing spectra $S(\omega)$ versus $\omega/\gamma$ and the spectral value $S(\omega_{opt})$ at the points of

optimal frequency $\omega=\omega_{opt}$ versus the pump field intensity parameter $\varepsilon^2=E^2\chi/\gamma$ ($E=|E_1|=|E_2|$) are plotted in Fig.6-(a),(b).

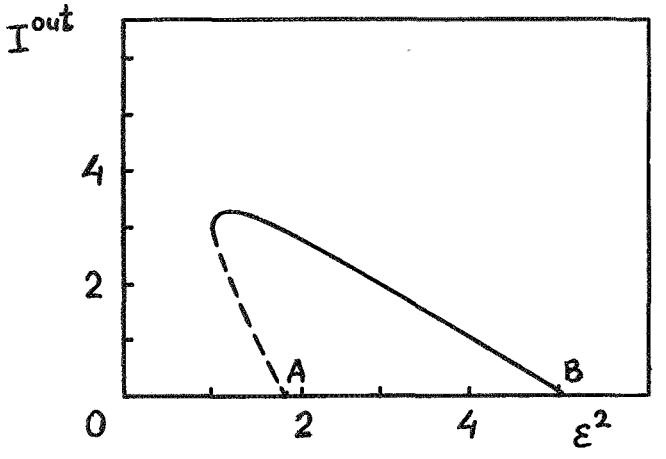


Fig.5. Output intensity of the FWM oscillator versus the intensity of the pump fields: $\Delta/\gamma=5$.

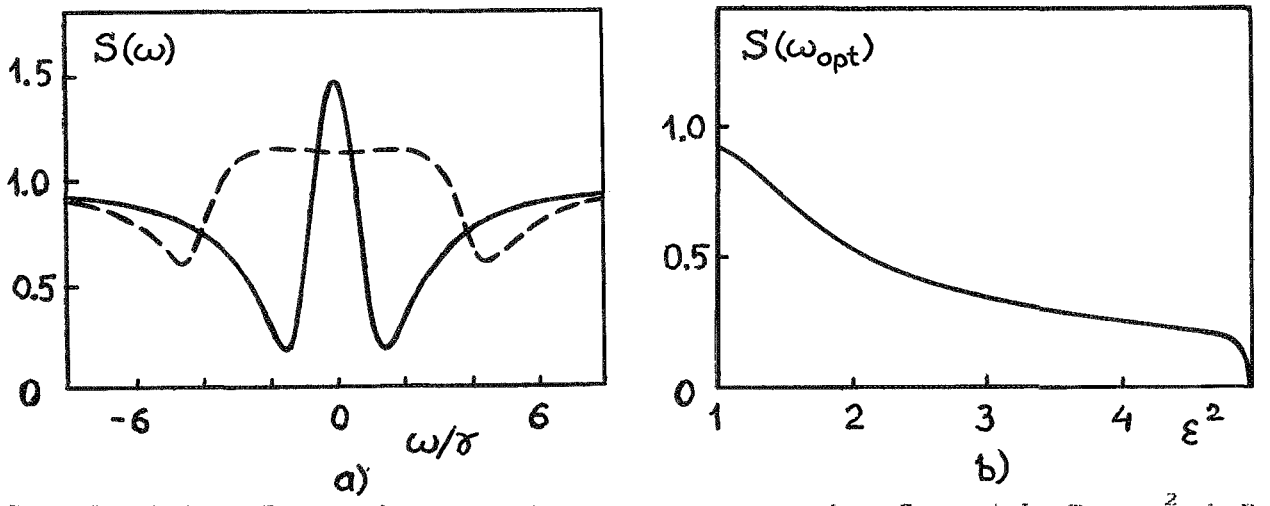


Fig.6. (a) - Squeezing spectrum versus $\omega/\gamma$ for $\Delta/\gamma=5$, $\varepsilon^2=1.8$ (dotted line) and $\varepsilon^2=4.8$ (solid line); (b) - dependence of the quantity $S(\omega_{opt})$ on $\varepsilon^2$ for $\Delta/\gamma=5$.

It should be noted that the experimental measurement of the noise on the qudrature component in a similar FWM configuration has been carried out by D.Grandclement et al [4]. They did not find the squeezed noise reduction. This is not so surprising because, as follows from our analysis, squeezing is realized for properly chosen values of parameters $\Delta/\gamma$ and $\varepsilon^2$.

## 3. Intracavity parametric FWM with nondegenerate pumps. Above-threshold results on bright squeezing of the three intracavity modes

This part of our report is devoted to the results on bright squeezing in the configuration of FWM, where the two laser driving fields propagate in the direction of the cavity axis (see Fig.7). These driving fields feed two intracavity pump modes at the frequencies $\omega_1$, $\omega_2$. The pump modes generate a signal mode at their half-sum frequency $\omega_0=(\omega_1+\omega_2)/2$ and the wave-vector matching condition are executed exactly ($\vec{k}_1+\vec{k}_2=2\vec{k}_0$). So the configuration of FWM with tree intracavity resonant modes of frequencies $\omega_1$, $\omega_2$ and $\omega_0$ is realized.

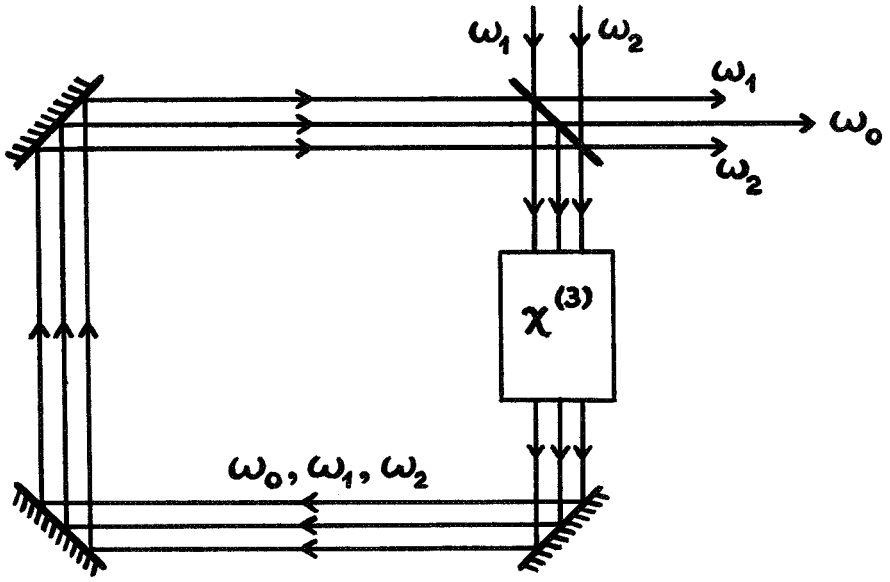


Fig.7. Scheme of the double-color-pumped FWM oscillator with three intracavity modes $\omega_1$, $\omega_2$, $\omega_0$ ($\omega_1+\omega_2=2\omega_0$).

In this configuration the effects of mutual influence of the pump and signal modes are essential. So we take into account the pump depletion. The consideration is simplified however in that we ignore the phase modulation terms.

Note that the advantages of this scheme of FWM, as compared to the standard nondegenerate FWM with a single pump mode, are caused by the following. As shown below the effect of phase diffusion is absent here. As a result, the output field for each of the three

modes have nonzero mean amplitudes with a definite phases.

Thus we start from the following Hamiltonian

$$H = \sum_{j=0}^{2} \hbar\omega_j a_j^+ a_j + i\hbar \frac{\chi}{2} \left[ a_1 a_2 a_0^{+2} - a_1^+ a_2^+ a_0^2 \right] +$$

$$+ i\hbar \sum_{k=1}^{2} \left[ E_k e^{-i\omega_k t} a_k^+ - E_k^* e^{i\omega_k t} a_k \right] + \sum_{j=0}^{2} \left[ a_j^+ \Gamma_j + a_j \Gamma_j^+ \right] \qquad (7)$$

As compared to the previous model, now we take into account the quantization of the pump modes and incorporate: (*i*) the coupling of the pump modes with two external coherent driving fields of amplitudes $E_1$, $E_2$ and (*ii*) the decay of the three cavity modes due to the coupling with reservoirs.

With use of standard methods, a Fokker-Planck equation in positive $P$-representation for the system is found, from which stochastic differential equations for the complex field amplitudes are obtained

$$\dot{\alpha}_0(t) = -\gamma_0 \alpha_0 + \chi \alpha_1 \alpha_2 \alpha_0^+ + R_0(t)$$

$$\dot{\alpha}_1(t) = -\gamma \alpha_1 - \frac{1}{2} \chi \alpha_0^2 \alpha_2^+ + E\exp(i\phi_1) + R_1(t) \qquad (8)$$

$$\dot{\alpha}_2(t) = -\gamma \alpha_2 - \frac{1}{2} \chi \alpha_0^2 \alpha_1^+ + E\exp(i\phi_2) + R_2(t)$$

Here $\gamma_0$, $\gamma \equiv \gamma_1 = \gamma_2$ are the damping constants for the modes $\omega_0$ and $\omega_1$, $\omega_2$ respectively, $E$ is the amplitude of the driving fields $E_{1,2} = E\exp(i\phi_{1,2})$, and $\phi_1$, $\phi_2$ are arbitrary phases of the driving fields. $R_j$ are Gaussian noise terms with the following nonzero correlations

$$\langle R_0(t) R_0(t') \rangle = \chi \alpha_1 \alpha_2 \delta(t-t'), \quad \langle R_1(t) R_2(t') \rangle = -\frac{\chi}{2} \alpha_0^2 \delta(t-t'). \qquad (9)$$

In order to analyze the quantum fluctuations of the modes we apply a linearized treatment of fluctuations about the stable steady-state solutions. It is worth noting that, as opposed to the standard scheme of FWM, for the present system there exist three types of stable steady-state solutions. They correspond to the three possible regimes of oscillation: one below the generation threshold $E < E_t$ and two different above-threshold regimes at $E_t < E < 2E_t$ and $E < 2E_t$. The threshold value of the amplitude $E$ is $E_t = \gamma (\gamma_0 / \chi)^{1/2}$.

The results for the cavity-output intensities $N_j^{out}$ (in photon number units per unit time) for the modes $\omega_j$ in the above-threshold regime are following. In the region $1<\varepsilon<2$ ($\varepsilon \equiv E/E_t$) we have [5,6]:

$$N_0^{out} = \frac{4\gamma\gamma_0}{\chi}(\varepsilon-1) \ , \quad N_1^{out}=N_2^{out}=\frac{2\gamma\gamma_0}{\chi}\left[1-\frac{\varepsilon}{2}\right]^2 \ ; \tag{10.a}$$

and in the region $\varepsilon>2$:

$$N_0^{out} = \frac{4\gamma\gamma_0}{\chi} \ , \quad N_1^{out}=N_2^{out}=\frac{2\gamma\gamma_0}{\chi}\left[\frac{\varepsilon^2}{2}-1\right] \tag{10.b}$$

The steady-state phases $\psi_j$ of all the three modes are defined above threshold and equal to

$$\psi_1=\phi_1 \ , \quad \psi_2=\phi_2 \ , \quad \psi_0=(\phi_1+\phi_2)/2 \tag{11}$$

So, they are determined by the phases of the driving fields $\phi_1$, $\phi_2$.

## Squeezing spectra above threshold

We calculate the quadrature fluctuation variance for all the three intracavity modes and corresponding squeezing spectra for the cavity-output fields. We would like to point out at once that an effective squeezing occurs for each of the three modes above threshold [5,6]. This is an extremely interesting feature of the double-color-pumped FWM oscillator.

The maximal squeezing is realized for the phase of the local oscillator equal to $\vartheta_j=\psi_j+\frac{\pi}{2}$ and is determined by the fluctuations of phase variables

$$S_j(\omega) = 1 + 8\gamma_j n_j \, \langle \delta\psi_j(-\omega)\delta\psi_j(\omega)\rangle \ , \tag{12}$$

where $n_j$ is the intracavity steady-state photon number of the $\omega_j$-mode.

Examples of the curves of the squeezing spectrum for the signal mode are plotted in Fig.8 for different values of parameters $\varepsilon$ and $r=\gamma_0/\gamma$.

Our analysis show that a noise reduction below the shot-noise level may reach approximately 100% in the whole above-threshold region $\varepsilon>1$ and for $r\geq 10$. The higher $\gamma_0/\gamma$ the better the squeezing. However, the intensity of this field is limited by the value $N_0=4\gamma_0\gamma/\chi$. Generation of more intense light in the squeezed state occurs at the

pump field frequencies. The corresponding output intensities grow with increase of the incident fields. However the maximal squeezing may reach approximately 50% for certain values of the ratio $\gamma_0/\gamma$.

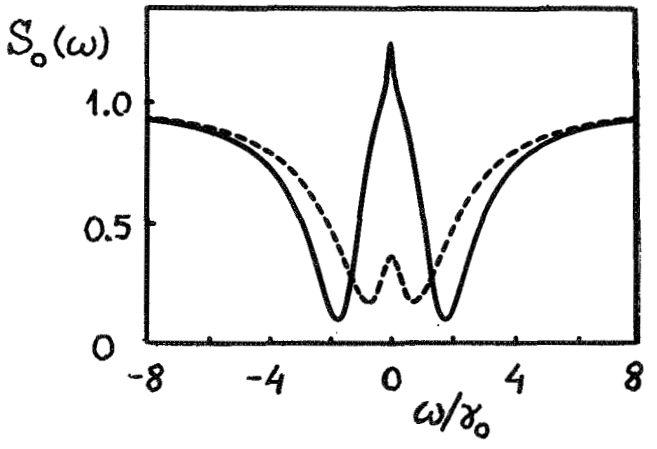


Fig.8. Squeezing spectrum $S_0(\omega)$ versus $\omega/\gamma_0$: $\varepsilon$=1.1, $r$=2 - (solid line); $\varepsilon$=4, $r$=10 - (dotted line).

We restrict ourselves by representation of the squeezing spectrum $S_{1,2}(\omega_{opt})$ at the points of minima $\omega=\omega_{opt}$. The dependence of this quantity on the parameter $r$ is plotted in Fig.9.

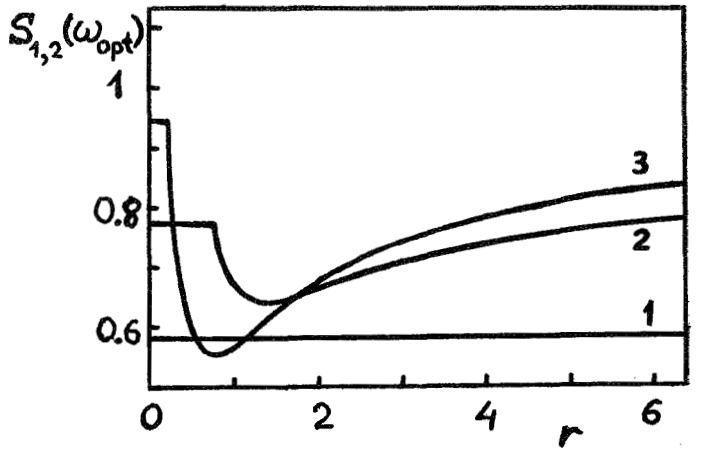


Fig.9. Dependence of the quantity $S_{1,2}(\omega_{opt})$ on $r$: (1) $\varepsilon$=2.2, (2) $\varepsilon$=2; (3) $\varepsilon$=6.

Thus we find that the double-color-pumped FWM oscillators is extremely promising for the above-threshold generation of one-mode bright squeezed light.

Sub shot-noise correlations of bright squeezed-light beams

Now we shall present the results on the sub shot-noise correlations in the above-threshold regime. We consider the correlations between both the intensities and the phases of the interacting modes.

In the well-known processes of nondegenerate FWM and parametric down-conversion, the photons of two generated modes are created in pairs and a positive correlation $\langle \delta n_1 \delta n_2 \rangle \gg 0$ between the photon number fluctuations of these modes occurs. It results in the reduction of quantum fluctuations below the shot-noise level in the intensity difference of the modes. This phenomena has been observed for the first time in intracavity nondegenerate parametric oscillator by A.Heidmann et al [7].

In our nonlinear system we have found another manifestation of such an effect. It consists of the reduction of quantum noise in the intensity sum of the pump modes [8]. The explanation of this phenomena is following. The photons of two pump modes are annihilated in pairs and the pump modes acquire correlated statistical properties, which are characteristic for two-photon absorption. As a result, the correlation between initially uncorrelated coherent pump fields becomes negative $\langle \delta n_1 \delta n_2 \rangle < 0$. And this fact results in the sub shot-noise fluctuations in the intensity sum of the cavity output beams. We shall not dwell on the particular quantitative results. Note only that the maximal noise reduction may reach approximately 100% in the limit $\varepsilon \to 2$, when the pump depletion is maximal.

A more interesting feature of our FWM configuration is connected with the correlations between the phases of the pump modes. They are studied in terms of the quadrature phase operators, as applied to the twin homodying experimental measurements.

In general the variance of the sum or difference of the quadrature component operator

$$V_{12}^{(\pm)}(\vartheta_1,\vartheta_2) = \left\langle \left[ \Delta \left[ X_1^{\vartheta_1} \pm X_1^{\vartheta_1} \right] \right]^2 \right\rangle , \quad ( X^{\vartheta} = a e^{-i\vartheta} + a^{+} e^{i\vartheta} ) \qquad (13)$$

contains the contributions from both the intensity and phase variable fluctuations of the modes.

In our system we can select properly the phases of the local os-

cillators and to get the variance as expressed in terms of the phase fluctuations only. The result can be written as follows

$$V_{12}^{(\pm)} = 2+4n\,\langle\delta(\psi_1 \pm \psi_2)^2\rangle \qquad (14)$$

Note, that such a possibility do not exist in parametric processes with phase diffusion effect. The nonclassical correlations between the phase fluctuations are manifested in the variance $V_{12}^{(\pm)}$

In our system the variance of the phase difference fluctuations is negative (in positive $P$-representation)

$$\langle\delta(\psi_1 - \psi_2)^2\rangle = -\frac{\chi}{2\gamma}\frac{\varepsilon-1}{\varepsilon}, \quad (1<\varepsilon<2) \qquad (15)$$

and so we obtain a reduction of quantum fluctuations below the shot-noise level in the difference of the quadrature phases: $V_{12}<2$.

A simple analytical result is obtained also for the measured cavity-output fields. The corresponding spectrum of the quadrature phase difference fluctuations in the region $1<\varepsilon<2$ is following

$$S_{12}^{(-)}(\omega)/S_{shot} = 1 + 4\gamma n\langle\delta\psi_1(-\omega)\delta\psi_1(\omega)\rangle + 4\gamma n\langle\delta\psi_2(-\omega)\delta\psi_2(\omega)\rangle -$$

$$- 8\gamma n\,\mathrm{Re}\langle\delta\psi_1(-\omega)\delta\psi_2(\omega)\rangle = 1 - \frac{4(\varepsilon-1)}{\varepsilon^2+(\omega/\gamma)^2} \qquad (16)$$

We see that the noise reduction up to 100% is possible in the limit $\varepsilon\to 2$ at zero frequency. In the region $\varepsilon>2$ the shape of the spectrum is complicated and the noise level is increased.

Finally we present some results concerning the optical spectra of the cavity-output squeezed light. We consider the intensity spectra of each of the three nonclassical light beams around the frequencies $\omega_j$ $(j=0,1,2)$. These spectra contain a delta-function peak corresponding to coherent part of radiation and a broadened noncoherent part. The broadened parts of spectra are caused by the quantum fluctuations of the field. In the lowest order in quantum fluctuations they contain two contributions, arising from the temporal correlations of the phase and intensity fluctuations $\langle\delta n_j(t+\tau)\delta n_j(t)\rangle$, $\langle\delta\psi_j(t+\tau)\delta\psi_j(t)\rangle$. Depending on the contribution strength, a two- or four-peaked structure of noncoherent part of spectra arise in the case of oscillating character of these correlations.

An example of four-peaked spectrum for the pump field is represented in Fig.10. Here the one pair of the peaks is caused by the

phase fluctuations and the other one - by the intensity fluctuations. The fact, that is interesting here, is the separation in frequency of these two contributions. So it seems to be possible to infer the information about the phase fluctuations from the usual optical spectrum.

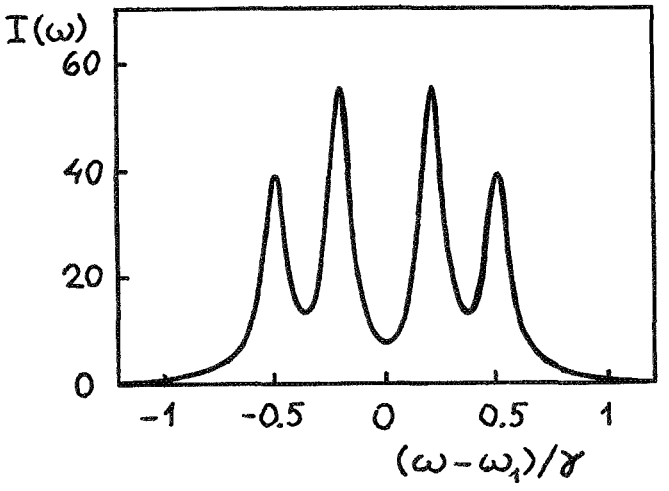


Fig.10. The noncoherent part of the intensity spectrum of the pump mode $\omega_1$: $\varepsilon$=2.2, $r$=0.05.

## REFERENCES


1. G.Yu Kryuchkyan, Quantum Optics 3, 209 (1991)
2. G.Yu Kryuchkyan and K.V.Kheruntsyan, Opt.Comm. 87, 181 (1992)
3. Y.Zhu, Q.Wu, A.Lezama, D.J.Gauthier, and T.W.Mossberg, Phys.Rev. A41, 6574 (1990)
4. D.Grandclement, M.Pinard, and G.Grynberg, IEEE J.Quant.Electron. 25, 580 (1989),
5. G.Yu Kryuchkyan and K.V.Kheruntsyan, Quantum Optics 4, 289 (1992)
6. G.Yu Kryuchkyan and K.V.Kheruntsyan, JETP 76, 9 (1993)
7. A.Heidmann, R.J.Horowics, S.Reynaud, E.Giacobino, C.Fabre, and G.Camy, Phys.Rev.Lett. 59, 2555 (1987)
8. G.Yu Kryuchkyan and K.V.Kheruntsyan, Opt.Comm. 93, 328 (1992)

# MULTIMODE SQUEEZING, BIPHOTONS AND UNCERTAINTY RELATIONS IN POLARIZATION QUANTUM OPTICS

V. P. Karassiov
*Lebedev Physical Institute,*
*Leninsky Prospect 53, Moscow 117924, Russia*

**Abstract**

The concept of squeezing and uncertainty relations are discussed for multimode quantum light with the consideration of polarization. Using the polarization gauge $SU(2)$ invariance of free electromagnetic fields, we separate the polarization and biphoton degrees of freedom from other ones, and consider uncertainty relations characterizing polarization and biphoton observables. As a consequence, we obtain a new classification of states of unpolarized (and partially polarized) light within quantum optics. We also discuss briefly some interrelations of our analysis with experiments connected with solving some fundamental problems of physics.

## 1 Introduction

Polarization properties of light were widely investigated long ago when examining some fundamental problems of quantum mechanics including "hidden" variable theories, Bell's inequalities and Einstein-Podolsky-Rosen (EPR) paradox, different topological phases etc. (see, e.g., [1-8] and references therein). Herewith, as a rule, the polarization structure of light has been described in terms of the field correlation functions, associated Stokes parameters and the Poincare sphere which are well adapted to classical optics experiments [7,9] but are not quite adequate to specific quantum ones (photon counting)[3]. Such a description also ignores a polarization $SU(2)$ symmetry[10-12] of light fields though it has been widely used implicitly - through the Stokes parameters $s_{\hat{a}}$ which determine, in particular, the polarization degre $degP = [s_1^2 + s_2^2 + s_3^2]^{1/2}/s_0$ of monochromatic plane wave light beams[1,3,9,13].

But recently a new formalism[10-12] was proposed for a description of polarization structure of multimode quantum light fields using the polarization $SU(2)$ symmetry and a related concept of the $P$-quasispin which generalizes the Stokes vector notion at the quantum level and is closely related to the Stokes operators defined in [13]. This approach enabled us to gain a new insight into the polarization structure of light and quantum mechanisms of its depolarization[12,13].

At the same time, so-called squeezed states of light are intensively examined now within quantum optics (see, e.g.,[10,14-17] and references therein) since these states have attractive properties of the "noise reduction" in measurements of some quantum mechanical observables. However, we note that squeezed states have been studied sufficiently well only for the single-mode fields[15,14] whereas for multimode fields it is not the case since even the definition of the concept of multimode squeezing is not unique that is due to a lot of the choices of measurable quantities[16,17].

The aim of this report is to give an analysis of the concept of squeezing of the multimode light related to polarization degrees of freedom by using the above mentioned formalism of $P$-quasispin. Specifically, we will show that there exist new quantum states of light beams exhibiting , in a sense, an absolute squeezing in polarization degrees of freedom. Such states are generated by specific unpolarized biphoton clusters and have all characteristics of usual unpolarized light, but unlike the latter, new quantum states of unpolarized light are "polarizationally noiseless" [10-12,18]. Besides we discuss briefly some generalizations and applications of new non-classical states of light to setting up new optical experiments related to some fundamental problems of physics.

# 2 Polarization $P$-quasispin of electromagnetic fields and unpolarized biphotons

In quantum optics the free transverse electromagnetic(em) field with "m" spatiotemporal modes is described by the vector potential[1,3,12,13]

$$\vec{A}(\vec{r},t) = \vec{A}^{(-)}(\vec{r},t) + \vec{A}^{(+)}(\vec{r},t) = c\sum_{j=1}^{m}(\frac{2\pi\hbar}{\omega_j V})^{1/2}\{\vec{A}^{(-)}(j)\exp[i(\vec{k}_j\vec{r}-\omega_j t)] + h.c.\},$$

$$\vec{A}^{(-)}(j) = \sum_{\alpha=+,-,3}\vec{e}_\alpha(j)a_\alpha^+(j), \vec{A}^{(+)} = (\vec{A}^{(-)})^+ \tag{2.1}$$

where $a_\alpha(j)/a_\alpha^+(j)$ are destruction/creation operators for $j$-th spatiotemporal and $\alpha$-th polarization modes of the field, $\vec{e}_\alpha(j)$ are the polarization unit vectors adapted to the helicity basis, $\vec{e}_3(j) = \vec{k}_j/\omega_j$, $V$ is a quantization volume, etc. With the help of Eq. (2.1) one determines correlation tensors[3]

$$G^{(s,p)}_{i_1\ldots i_s;j_1\ldots j_p}(\{\vec{r}_a,t_a\};\{\vec{r}'_b,t'_b\}) = Tr[\rho E^{(-)}_{i_1}(\vec{r}_1,t_1)\ldots E^{(-)}_{i_s}(\vec{r}_s,t_s)E^{(+)}_{j_1}(\vec{r}'_1,t'_1)\ldots E^{(+)}_{j_p}(\vec{r}'_p,t'_p)],$$

$$\vec{E}^{(\pm)} = c^{-1}\partial\vec{A}^{(\pm)}/\partial t \tag{2.2}$$

which correspond to different physical quantities, measurable in optical experiments, and are expressed in terms of quantum expectations of ordered polynomials in operators $a_\alpha(j)$ and $a_\alpha^+(j)$[6]. We note that quantum expectations of any physical quantities are calculated by averaging on the space $L_{phys} = L_F(m)$ spanned by basis vectors

$$|\{n_i^\sigma\}> = N(\{n_i^\sigma\})\ \prod_{i=1}^{m}\ \prod_{\sigma=-,+}\ [n_i^\sigma!]^{-1/2}\ \ (a_\sigma^+(i))^{n_i^\sigma}\ \ |0> \tag{2.3}$$

which are generated by the creation operators $a_\alpha^+(i)$ of photons with transverse ($\alpha = +,-$) polarizations (helicities) only (that corresponds to a standard form of the gauge condition for transverse radiation fields in quantum electrodynamics[12,13]).

The most important of such measurable quantities is the field Hamiltonian

$$H_f = \sum_{i=1}^{m}\omega_i\sum_{\alpha=+,-,3}a_\alpha^+(i)a_\alpha(i) \tag{2.4}$$

which determines the time-evolution of other field observables[3]. But in polarization quantum optics there are specific observables which characterize proper polarization properties of light beams and correspond to to the group $U(2)$ of a specific polarization gauge invariance of the Hamiltonian (2.4)[10-12]. This continious polarization group $U(2)$ is closely related to discrete symmetries of em fields(mirror reflection $\hat{\sigma} : a^{\dagger}_{\pm}(j) \to a^{\dagger}_{\mp}(\hat{j}), \vec{k}_{\hat{j}} = -\vec{k}_j$ and the spatial inversion $\hat{P}$) since all these (chiral) symmetries act in a natural manner on a 2-dimensional "polarization spinor" $\{\vec{e}_{\alpha}(i), \alpha = \pm\}$ spaces[11,13].

The generators of the polarization group $U(2)$ are of the form

$$P_0 = \frac{1}{2}\sum_{i=1}^{m}[a^{\dagger}_{+}(i)a_{+}(i) - a^{\dagger}_{-}(i)a_{-}(i)] = \sum_i P_0(i),$$

$$P_{\pm} = \sum_{i=1}^{m} a^{\dagger}_{\pm}((i)a_{\pm}(i) = \sum_i P_{\pm}(i), \quad N = \sum_{i=1}^{m}\sum_{\alpha=+,-} a^{\dagger}_{\alpha}(i)a_{\alpha}(i) = \sum_i N(i) \tag{2.5}$$

where $N$ is the total photon number operator and operators $P_{\alpha}$ are generators of the $SU(2)$ subgroup defining the polarization ($P$) (quasi)spin [10-12]. The operators $P_{\beta}$ and $N$ satisfy commutation relations

$$[N, P_{\alpha}] = 0, \quad [P_0, P_{\pm}] = \pm P_{\pm}, \quad [P_+, P_-] = 2P_0 \tag{2.6}$$

and in the case $m = 1$ coincide up to the factor $1/2$ with Stokes operators $\Sigma_{\alpha} : \Sigma_1 = 2P_2, \Sigma_2 = -2P_0, \Sigma_3 = -2P_1$ [13]. As is clear from Eqs (2.5) the total $P$-quasispin of the em field is obtained by adding of the appropriate quasispin quantities for single spatiotemporal modes. However, from the experimental viewpoint the total $P$-quasispin of the em field enable us to examine new interesting physical phenomena connected with correlations of different modes, in particular, with so-called "entangled states" which are widely discussed in multiparticle interferometry [2,5,19].

Note that the operators $P_{\alpha}$ do not commute with components $S_{\alpha}$ of the gauge non-invariant (and hence locally non-observable) ordinary spin $\vec{S} = (S_1, S_2, S_3)$ of the em field wich define the field transformations with respect to the $SO(3) \subset SL(2C)$ group of rotations in the usual 3-dimensional space and are expressed in terms of the $\vec{A}(\vec{r}, t)$ Fourier components $A^{(\pm)}_a(j)$ as follows [13,12]

$$S_a = -i\sum_j\sum_{b,c}\epsilon_{abc}A^{(-)}_b(j)A^{(+)}_c(j) \tag{2.7}$$

where $\epsilon_{abc}$ is the fully antisymmetric tensor ( $\epsilon_{123} = 1$). Specifically, from Eqs.(2.1),(2.7) one easily finds relations specifying "rotation" properties of different physical operators[12]. For example, in the case of plane wave beams, when in (2.1) $e_{3a}(j) = \delta_{3a}, a = 1, 2, 3, e_{\pm 3}(j) = 0$ ($e_{\alpha a}(i)$ is the projection (directing cosine) of $\vec{e}_{\alpha}(i)$ on the "$a$"-th axis of a fixed spatial frame of reference with the axe $O\vec{X}_3$ being parallel to all $\vec{k}_j$) and $S_3 = 2P_0$, one finds a relation

$$exp(i\phi S_3)P_{\alpha}exp(-i\phi S_3) = exp(i2\alpha\phi)P_{\alpha}, \alpha = 0, \pm, \tag{2.8}$$

defining transformations of $P$-spin components under rotations around the light beam axis.

From Eqs (2.5), (2.7) it follows that the $P$-quasispin formalism has evident advantages in comparison with the ordinary spin for describing properly polarization properties of light since its components have a clear physical meaning and are measurable in quantum optics polarization experiments related to counting photons with definite polarizations[12]. In particular, the total

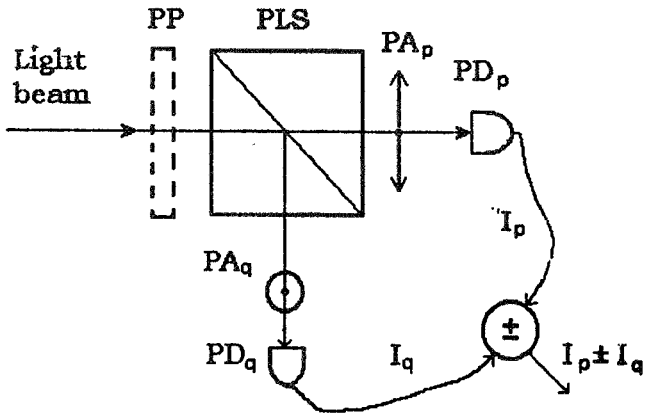


Figure 1: Scheme of the measurement of $P$-quasispin components

helicity $2P_0$ of the field is the difference $(N_+ - N_-)$ of the right- and left- handed photon numbers and Hermitian operators $2P_1 = (P_+ + P_-)$ and $2P_2 = i(P_+ - P_-)$ determine (cf.[9,6]) differences of photon numbers for two pairs of orthogonal linear polarizations which are connected with the helicity basis by the linear transformations[12]

$$a) \quad a_1^+(j) = \frac{1}{\sqrt{2}}\{a_-^+(j) - a_+^+(j)\}, \quad a_2^+(j) = \frac{i}{\sqrt{2}}\{a_+^+(j) + a_-^+(j)\} \tag{2.9a}$$

$$b) \quad \hat{a}_1^+(j) = \frac{1}{\sqrt{2}}\{a_1^+(j) + a_2^+(j)\}, \quad \hat{a}_2^+(j) = \frac{1}{\sqrt{2}}\{-a_1^+(j) + a_2^+(j)\} \tag{2.9b}$$

implemented, for example, with the help of phase plates and polarization rotators [9,6,7]. (From the formal viewpoint components $P_1$ and $P_2$ correspond to the choice of different subgroups $SO(2) \subset SU(2)$ unlike the helicity subgroup $U(1)$ for $P_0$. Moreover, basis wave functions with linear polarization defined by Eqs (2.9) are eigenstates of operators describing the abovementioned discrete symmetries $\hat{\sigma}, \hat{P}$ of light fields.)

A typical principal scheme[18] of the measurement of components $P_\alpha$ of $P$-quasispin is presented on Fig. 1, where we use the following notations: $PP$ denotes phase plates, $PLS$ stands for polarization light beam splitters, $PA_a$ and $PD_a$ are, respectively, polarization analyzers and photodetectors for polarization modes "$a$". We note that this scheme can be realized in both single-mode ($m = 1$) and multimode ($m > 1$) regimes. However, as it will be seen later, the use of multimode regimes enables us to reveal new interesting physical phenomena, in particular, an absolutely unpolarized quantum light[10-12].

Since in the case of the monochromatic plane waves quantum expectations $< P_\alpha >$ are proportional to the Stokes parameters $s_\alpha =< \Sigma_\alpha >, \alpha = 1,2,3; s_0 =< N >$ [13], then in general cases one can consider that quantities $< P_\alpha >, < N >$ determine the polarization degree $degP$ of light beams with arbitrary wave fronts and frequencies by the relation

$$degP = 2[\sum_{\alpha=0,1,2} (< P_\alpha >)^2]^{1/2} / < N > \tag{2.10}$$

generalizing the appropriate definition for one-mode light beams[3]. At the same time the quantum averages $< |P^2| >= \bar{P}(\bar{P}+1)$ of the $SU(2)_{pol}$ Casimir operator $P^2 = (1/2)(P_+P_- + P_-P_+) + P_0^2$

are connected by the relation

$$< |P^2| >= \bar{P}(\bar{P}+1) = \sum_{\alpha=0,1,2} [\sigma_\alpha + (< |P_\alpha| >)^2] \tag{2.11}$$

with the variances $\sigma_\alpha =< |P_\alpha^2| > -(< |P_\alpha| >)^2$ determining "polarization noises" [3,12,18] and different uncertainty measures for operators $P_\alpha$(cf. [20-22]).

Therefore, one may use $P$-spin ($P_\alpha$) as an adequate tool for studying proper polarization properties of quantum light fields in parallel to the usual apparatus of the correlation functions and Stokes vector $\vec{s} = (s_1/s_0, s_2/s_0, s_3/s_0)$ running on the Poincare sphere[3]. But unlike the latter, the use of the $P$-spin formalism allows us to gain a more deep insight into the inner nature of the polarization struture of light beams with arbitrary wave fronts.

Indeed,as it was shown in [10-12], one can decompose the Fock space $L_F(m)$ spanned by the vectors (2.3) into the direct sum

$$L_F(m) = \sum_{P,\pi} L(P\pi) \tag{2.12}$$

of infinite-dimensional subspaces $L(P\pi)$ which are specified by eigenvalues $P, \pi$ of the $P$-spin and $P_0$ respectively and spanned by basis vectors $|P\pi; n, \lambda >$ of the form

$$|P\pi; n, \lambda >= \sum C(\{\alpha_i, \beta_{ij}, \gamma_{ij}\}) \prod_i (a_\pm^+(i))^{\alpha_i} \prod_{i \le j} (Y_{ij}^+)^{\beta_{ij}} (X_{ij}^+)^{\gamma_{ij}} |0 > \tag{2.13}$$

where $\sum \alpha_i = 2|\pi|, \sum \beta_{ij} = (P - |\pi|), \sum \gamma_{ij} = n/2 - P$. For example, in the cases $m = 1$ and $m = 2$ we have the following expressions[23]

$$a)|P\pi >= [(P-\pi)!(P+\pi)!]^{-1/2} (a_+^+(1))^{|\pi|+\pi} (a_-^+(1))^{|\pi|-\pi} (Y_{11}^+)^{P-|\pi|} |0 >, \tag{2.14a}$$

$$b)|P\pi = \pm P; n, t >= [(n+1)!(n-2P)!(P-t)!(P+t)!/(2P+1)!]^{-1/2}$$
$$(a_\pm^+(1))^{P+t} (a_\pm^+(2))^{P-t} (X_{12}^+)^{n/2-P} |0 >, 2t = n(1) - n(2) \tag{2.14b}$$

for some of such vectors. In general, the coefficients $C(...)$ in (2.13) are determined from the defining equations

$$P^2 |P\pi; n, \lambda >= P(P+1)|P\pi; n, \lambda >; \quad P_0 |P\pi; n, \lambda >= \pi |P\pi; n, \lambda >,$$
$$N \mid P\pi; n, \lambda >= n \mid P\pi; n, \lambda > \tag{2.15}$$

and some equations for fixing an extra (vector) label $\lambda$ (see [12,11] and references therein). Operators

$$Y_{ij}^+ = \frac{1}{2}(a_+^+(i)a_-^+(j) + a_-^+(i)a_+^+(j)), X_{ij}^+ = a_+^+(i)a_-^+(j) - a_-^+(i)a_+^+(j) \tag{2.16}$$

in (2.13), (2.14) are the solutions of the operator equations

$$[P_0, Y_{ij}^+] = 0; \quad [P_\alpha, X_{ij}^+] = 0, \quad \alpha = 0, +, - \tag{2.17}$$

and may be interpreted as creation operators of $P_0$-scalar and $P$-scalar biphoton kinematic clusters, respectively.

From Eqs(2.16), (2.17) one easily obtains that $< P_\alpha >= 0, \alpha = 0,1,2$, in states generated by actions on the vacuum vectors $|0>$ of operators $(X_{ij}^+)^a(Y_{ij}^+)^b$ only ( and spanned by vectors (2.13) with $\pi = 0$); these states are examples of entangled states of multiparticle interferometry[5,19]. In general, the states (2.13) describe light beams representing a mixture of both usual (uncoupled) photons $a_\alpha^+(j)$ and unpolarized $P$- and $P_0$-scalar biphoton clusters $X_{ij}^+, Y_{ij}^+$ [10-12]. As it follows from (2.13), the total number operators $N_{ph}, N_X, N_Y$, respectively, of uncoupled photons and $X$-and $Y$-type biphotons are given as follows,

$$N_{ph} = 2|P_0| = 2\sqrt{(P_0)^2}, N_X = N/2 - P, N_Y = P - |P_0|, P = -1/2 + \sqrt{1/4 + P^2} \qquad (2.18)$$

We, however, note that biphotons $Y_{ij}^+$ exist for any number "m" of spatiotemporalal modes whereas $X_{ij}^+ \neq 0$ only for "$m$" $\geq 2$. We also emphasize that in contrast to the usual photon operators $a_\alpha^+(j), a_\alpha(j)$ the operators $X_{ij} = (X_{ij}^+)^+, X_{ij}^+, Y_{ij} = (Y_{ij}^+)^+, Y_{ij}^+$ satisfy not the canonical commutation relations but trilinear commutation relations for quanta of generalized parastatistical fields (these operators, however, can be transformed in some "particle-like" quanta ones)[11].

Further, the decomposition (2.12) is invariant with respect to the Lie algebra $so^*(2m)$ generated by biphoton operators $X_{ij}, X_{ij}^+$ and commuting with the polarization invariance algebra $su(2) = Span\{P_\alpha\}$[12,11]. Therefore, states $|\psi >$ belonging to a subspace $L(P\pi)$ with given $P, \pi$ at initial time will be in it for the time evolution governed by the interaction Hamiltonians $H_{int} = H_i'(\{X_{ij}, X_{ij}^+\})$ what is similar to the situation in the theories with spontaneosly broken symmetry; examples of such Hamiltonians are given by those of some parametric processes [10-12]. Extending the algerbra $so^*(2m)$ by adding operators $Y_{ij}, Y_{ij}^+$ we get the algebra $u(m,m)$ commuting with the polariztion subalgebra $u(1) = Span\{P_0\} \subset su(2)$ and associated with interaction Hamiltonians $H_{int} = H_{int}''(\{Y_{ij}, Y_{ij}^+; X_{ij}, X_{ij}^+\})$ (describing, for example, light propagation in Kerr media) which keep invariant for time evolution subspaces $L'(\pi) = \sum_{P \geq ||\pi|} L(P\pi)$ (with fixed $\pi$)[12]. If we restict ourselves by biphoton operators $Y_{ij}, Y_{ij}^+$ only we obtain the subalgebra $sp(2m, R) \subset u(m,m)$. So, algebras $so^*(2m), sp(2m, R)$ and $u(m,m)$ describe specific $P$-and $P_0$-scalar degrees of freedom of light fields which are complementary, in a sense, to polarization ones.

# 3 Squeezing in polarization quantum optics. A new classification of unpolarized light

The decomposition (2.12) implies a new classification of the polarization states of quantum light fields from the physical viewpoint [11,12]. This classification is closely related to a specific sort of squeezing of multimode light beams with consideration of polarization.

In fact, a definition of squeezing in quantum mechanics is based on an analysis of different uncertainty relations for expectations $< |(A_i)^s| >$ of a set $\{A_i, i = 1, ..., r > 1\}$ of non-commuting Hermitian operators $A_i$ representing some quantum observables[1,14-17,20-25]. These relations are connected with specific measures of admissible quantum fluctuations ("noises") for *joint measurements of all observables* $A_i$ in a state $|>$ which characterize differences betveen quantum observables and their classical analogs($< |A_i| >$) and are displayed with the help of different quasiprobability functions[3,14,25] and generalized coherent states[3,10,20-22]. Specifically, the most widespread uncertainty relation (of the Heisenberg type) has the form[1,14,20-22]

$$\Delta A_i \Delta A_j \geq 1/2| < |[A_i, A_j]| > | \qquad (3.1)$$

where $(\Delta A)^2 \equiv \sigma_A =< |(A)^2| > -(< |A| >)^2$ is a standard quadratic measure (variance) of a deviation of the quantum quantity $A$ from its classical analog. Then the problem of squeezing consists in finding quantum states minimizing both the product $\Delta A_i \Delta A_j$ of two "individual" uncertainty measures (the condition of a *joint* quasiclassical behaviour of $A_i$ and $A_j$) and one (say, $\Delta A_i$) of them (the condition of properly squeezing).

If the right side of inequality (3.1) is a $c$-number this problem is easily solved and leads to a definition of the usual concept of squeezing related to generalized coherent states of the group $SU(1,1)$[14-17]. For example, it is the case for single-mode em field when we use as observables $A_i$ two quadrature components $A_1 \equiv X_1 = (a^+_\alpha(j) + a_\alpha(j))/\sqrt{2}, A_2 \equiv X_2 = i(a^+_\alpha(j) - a_\alpha(j))/\sqrt{2}(\alpha, j$ are fixed) [14,15]. However, for multimode em fields the situation becomes more complicated since in this case we have a more vast set of observables which obey non-trivial commutation relations[10,16,17]. Therefore, there are many possibilities of definition of squeezing related to a choice (from physical considerations) of some subsets of observables (and adequate joint uncertainty meausures for them) for which a solution of this problem is comparatively simple. As we established above, in polarization quantum optics it is natural to take as such subsets components $P_\alpha$ of the $P$-quasispin obeying the commutation relations (2.6) of the $su(2)$ algebra as well as subsets of unpolarized biphoton operators (2.16) of $X$- and $Y$- types (related to the "biphoton algebras" $so^*(2m), sp(2m, R)$ and $u(m, m)$). That enables us to define a specific polarization squeezing which is closely related to a new physical phenomenon of biphoton unpolarized light(UL)[12].

Since operators $P_\alpha$ are similar to angular momentum operators $J_\alpha, \alpha = 1, 2, 3$ obeying the $su(2)$ commutation relations, one can apply analysis[20,21,24] of uncertainty relations and an appropriate concept of squeezing for operators$J_\alpha$ to analysis of those for operators $P_\alpha, \alpha = 1, 2, 3(P_3 = P_0)$. As is known[20-22], the Heisenberg uncertainty relations (3.1) for $A_i = J_i (i = 1, 2, 3)$ are minimized on the $SU(2)$ generalized coherent states[20] $|\zeta; \pm j >= exp(\zeta J_+ - \zeta^* J_-)|j; \pm j >, \zeta = -\frac{\theta}{2} exp(-i\phi)$ where $|j; \pm j >$ is the highest (or lowest) vector of the $SU(2)$ irreducible representation $D^j$. The states $|\zeta; \pm j >$ are maximally close to classical ones[20] and minimize a $SU(2)$-invariant (cf. (2.11)) "radial" uncertainty meausure $\sum_i \sigma_{J_i}$ ($\sum_i \sigma_{J_i} = min = j$ on the states $|\zeta; \pm j >$) which is an adequate characteristic of quasiclassical behaviour of a whole set $\{J_i\}$[20,21]. Besides, these states are used for a definition of polarization analogs $Q(\theta, \phi; \rho)_{\pm P} = | < \zeta; \pm P|\rho|\zeta; \pm P > |^2 (\rho$ is a density matrix of a light beam) [23] of $Q$-functions of quasiprobability[3,14] which are well adapted for displaying squeezing properties of oscillator systems. Evidently, for physical systems with a fixed value of $j$ (e.g., for usual spin systems) we obtain an "absolute" squeezing for $\{J_i\}$, characterized by relations

$$\sum_i \sigma_{J_i} = 0, \Delta J_i = 0 =< |J_i| > \forall i, \qquad (3.2a)$$

only for the unique vector $|\zeta; 0 >= |0; 0 >$. But for em fields the situation is quite different because of the decomposition (2.12) for $L_F(m)$.

Specifically, as is seen from Eqs (2.13), (2.17), the states $| > \in L(00) = Span\{|00; n, \lambda >\}$ satisfy Eqs (3.2a) and provide an "absolute" minimum of both the aforementioned "radial" uncertainty measure $\sum_i \sigma_{P_i}$ as well as uncertainty relations of the (3.1) type for operators $P_i$; besides these states form the infinite-dimensional space on which three non-commuting operators $P_\alpha$ behave themselves as $c$-numbers exhibiting an "absolute squeezing" and totally *classical* behaviour in polarization degrees of freedom (that it is of interest for designing different experiments related to the EPR-paradox and "hidden variable" theories[1,2,5,11]). We note that in $L_F(m)$ there exists

another class of quantum states displaying a similar (though more weak, than (3.2a)) property of polarization squeezing. Namely, for states $|>\in L'(\pi=0)$ we find from (2.12)-(2.14)

$$\Delta P_0 = 0 =< |P_i| >, \sum_i \sigma_{P_i} = \bar{P}(\bar{P}+1) \neq 0 \tag{3.2b}$$

As it follows from Eqs (3.2), states $|P0;...>\in L(P0) \subset L'(\pi=0)$ and $|00;...>\in L(00)$ possess the characteristic property ($< |P_\alpha| >= 0$) of UL (cf.[3,9]). Besides, the calculations [11] showed that $< |S_\alpha| >= 0$ for all $\alpha$ and correlation tensors $G_{ij}^{(1,1)}(\vec{r},\vec{t};\vec{r},\vec{t})$ have for these states a form corresponding to UL beams with, in general, arbitrary wave fronts. But unlike classical (chaotic) UL, for the states $|00;...>$ and $|P0;...>$ we have additional characteristics of light depolarization which follow from Eqs (2.12)-(2.14), (2.17) and are expressed in terms of higher moments for $P_\alpha$:

$$< |(P_0)^s| >= 0 \forall s = 1,2,...,| >\in L'(\pi=0);$$

$$< |(P_\alpha)^s| >= 0 \forall \alpha = 0,+,-, s = 1,2,...,| >\in L(00) \tag{3.3}$$

showing the absence of appropriate polarization "noises" ($< |(P_\alpha)^s| > -(< |(P_\alpha)| >)^s_{cr}$, $\alpha = 0,1,2$ for $| >\in L(00)$ and $\alpha = 0$ for $| >\in L'(\pi=0)$) of any order measured by appropriate noises of difference photocurrents in schemes of Fig. 1; herewith, as it follows from Eq. (2.8), for axial (plane wave) light beams results of measurements do not depend on rotations of analyzers around beam axis.

So, for states $| >\in L(00)$ all proper polarization properties are identical with those for vacuum state $|0>$, but unlike the latter the light intensity $< |H_f| >$ in these states(with the Hamiltonian $H_f$ from Eq. (2.3)) is not equal to zero. Consequently, they may be recognized as states describing absolutely unpolarized light while the states $| >\in L'(0)$ have a hidden polarization structure revealed in measurements of linear polarization noises. Therefore, states $|\phi>\in L'(0)$ generated by biphotons $Y_{ij}^+, X_{ij}^+$ and $|\psi>\in L(00) \subset L'(0)$ generated only by biphotons $X_{ij}^+$ describe new types of UL due to strong quantum phase correlations rather than random mixing light beams as it is the case for the classical UL [3,9]. Examples of such states are yielded by generalized coherent states of the above biphoton algebras (and appropriate groups) related with interaction Hamiltonians $H_{int} = H_{int}^1 + H_{int}^2$ where $H_{int}^1 = \sum_{i<j}(g_{ij}X_{ij} + g_{ij}^* X_{ij}^+)$, $H_{int}^2 = \sum_{i,j}(f_{ij}Y_{ij} + f_{ij}^* Y_{ij}^+)$ describing some specific parametric processes[11]. In particular, generalized coherent states of the $SO^*(2m)$ group orbit type

$$|\{\gamma_{ij}\}>_P = S_X(\{\gamma_{ij}\})|0> = \exp[\sum(\gamma_{ij}X_{ij} - \gamma_{ij}^* X_{ij}^+)]|0> \tag{3.4}$$

discussed together with some related models in [10-11] are generated by $H_{int}^1$ whereas $H_{int}^2$ produces generalized coherent states of the group $Sp(2m,R) \subset U(m,m)$

$$|\{\beta_{ij}\}>_{P_0} = S_Y(\{\beta_{ij}\})|0> = \exp[\sum(\beta_{ij}Y_{ij}^+ - \beta_{ij}^* Y_{ij})]|0> \tag{3.5}$$

coinciding in the case $m=1$ with two-mode squeezed states introduced in [15] and related to the $SU(1,1)$ group [11,12]. In general cases states (3.4), (3.5) display some properties of specific multimode squeezing associated with biphoton algebras $so^*(2m), sp(2m,R), u(m,m)$ (cf.[10-12,16]). Therfore, operators $S_X, S_Y$ can be called as biphoton squeezing operators. Without dwelling here

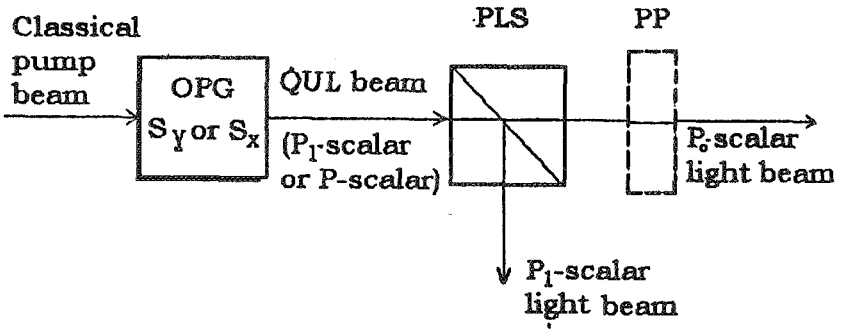


Figure 2: Scheme of production of biphoton unpolarized light

on analysis of all their properties we note that operators $S_X$ commute with the "proper" polarization squeezing operators $S_P(\zeta) = exp(\zeta P_+ - \zeta^* P_-)$ while it is not the case for the operators $S_Y$.

Physical realizations of such states, connected with actions of $P_0$- and $P$-scalar biphoton squeezed operators $S_Y(\{\beta_{ij}\})$ and $S_X(\{\gamma_{ij}\})$ on the vacuum vectors $|0>$, are represented schematically on Fig. 2 where $POG$ stands for parametric oscillator generators corresponding to the operators $S_Y, S_X$ and other notations are the same as on Fig 1. We note that, in practice, it is easier to realize such schemes corresponding to Eq. (3.5) rather than Eq. (3.4) because the latter require parametric oscillator crystals with highly anisotropic properties. Therefore, for production of $P$-scalar light it is preferable to combine more simple schemes of production of $P_0$-scalar light together with some interferometric schemes[5,18,19].

Thus, our analysis displays inner mechanisms of the light depolarization at the quantum level by contrast to the generally accepted viewpoint [9] that randomization is the only way of obtaining UL. Besides, the $P$-spin formalism yields (see (2.17) and (2.18)) some new natural measurable quantitative characteristics of light depolarization, namely, degrees $dep_P = (1 - 2\bar{P}/\bar{N})$ and $dep_{P_0} = (1 - |2\bar{\pi}|/\bar{N})$ of the content of $P$-scalar and of $P_0$-scalar biphotons where $\bar{P}, \bar{\pi} = \bar{P}_0, \bar{N}$ denote expectation values of appropriate operators; herewith $\bar{P} = -1/2 + [1/4 + < |P^2| >]^{1/2}$ is determined from Eqs (2.10), (2.11) as a function of $degP$, $\bar{N}$ and variances $\sigma_\alpha$. Evidently, $dep_{P_0}$ is connected with thewell-known degree of circular polarization $| < N_+ > - < N_- > |/ < N >$ whereas $dep_P$ provides a new quantitative characteristic of polarization structure of light related to measurements of polarization noises.

We also note that analysis above can be extended by considering modifications of the decomposition (2.12) where any other Hermitian operator $P_{\vec{n}} = S_P(\zeta(\vec{n}))P_0(S_P(\zeta(\vec{n})))^+$ is diagonalized instead of $P_0$ ($S_P(\zeta(\vec{n})) = exp(\zeta(\vec{n})P_+ - \zeta^*(\vec{n})P_-)$, $\zeta(\vec{n}) = -\frac{\theta}{2}exp(-i\phi)$ and vector $\vec{n} = (\sin\theta\cos\phi, \sin\theta\sin\phi, \cos\theta)$ corresponds to a position of the Stokes vector $\vec{s}$ on the Poincare sphere). Specifically, one can diagonalize Hermitian operators $P_\alpha, \alpha = 1, 2$ corresponding to a linear polarization basis of light beams[12]. Such extensions lead to new states of quantum UL generated by $P_{\vec{n}}$(e.g., $P_1$- or $P_2$) - scalar biphotons $Y^+_{ij}(\vec{n}) = (S_P(\zeta(\vec{n})))^+ Y^+_{ij} S_P(\zeta(\vec{n}))$ of the (2.16) type and having characteristics similar to those described by Eqs (3.2)-(3.3) but with some peculiarities concerning their "rotation" properties determined by Eqs (2.8); for example, the condition $\Delta P_{1(2)} = 0$ is valid only for quite definite angle positions of polarization analyzers. We also note that usual multimode Glauber coherent states $|\{\alpha^+_i, \alpha^-_j\}> = \prod_i exp(\alpha^+_i a^+_+(i) + \alpha^-_i a^+_-(i) - \alpha^{+*}_i a_+(i) - \alpha^{-*}_i a_-(i))|0>, \alpha^\pm_i \neq 0$, which are in general cases states

of partially polarized light, contain ( for special values of parameters $\alpha_i^{\pm}$) a subclass of states corresponding to UL. In particular, all such states display properties($< |P_\alpha| >= 0, \sigma_{P_\alpha} \neq 0 \forall \alpha$) of usual UL, when the condition $|\alpha_i^+| = |\alpha_i^-|$ is fulfilled[8,18].

All this leads to a new classification of states of UL within quantum optics which can be represented by a chain of embedded subsets

$$UL^0 \supset UL^c \supset UL^{bp} \supset UL^{P_0} \supset UL^P \tag{3.6}$$

with the following typical density matrices for each subset:

$$a) UL^0 \rightarrow \rho_{th}, \tag{3.7a}$$

$$b) UL^c \rightarrow \rho_c = |\{\alpha_\pm\} >< \{\alpha_\pm\}|, |\alpha_+| = |\alpha_-|, \tag{3.7b}$$

$$c) UL^{bp} \rightarrow \rho_{bp} = |\lambda >< \lambda|, |\lambda >= exp(\lambda P_+ - \lambda P_-)| >, | >\in L'(\pi = 0), \tag{3.7c}$$

$$d) UL^{P_0} \rightarrow \rho_{P_0} = | >< |, | >= S_Y(\{\beta_{ij}\})|0 >\in L'(\pi = 0), \tag{3.7d}$$

$$e) UL^P \rightarrow \rho_P = | >< |, | >= S_X(\{\gamma_{ij}\})|0 >\in L(00) \tag{3.7e}$$

where $\rho_{th}$ is a density matrix for the thermal radiation[3], $\rho_c$ describes coherent UL whereas $\rho_{bp}, \rho_{P_0}, \rho_P$ correspond to different kinds of biphoton UL[12]. We note that all these classes of UL are distinguished by values of $dep_P = (1 - 2\bar{P}/\bar{N})$ and $dep_{P_0} = (1 - |2\bar{\pi}|/\bar{N})$.

# 4 Generalizations and conclusion

Thus, in the previous sections we have shown that in the Fock space $L_F(m)$ of multimode light with consideration of polarization one can pick out with the help of Eq. (2.12) subspaces ($L(P = 0\pi = 0), L'(\pi = 0)$ and someones related to them) of quantum states describing different new types of UL light and, simultaneously, manifesting specific forms of squeezing in polarization optics. All other subspaces $L(P\pi), L'(\pi), \pi > 0$, in the decomposition (2.12) describe, generally speaking, states of partially depolarized quantum light (see [10,11] where we also examined various types of polarization generalized coherent states of light).

However, in real physical experimental situations states of light beams do not belong to a single subspace $L(P\pi)$ but are superpositions of states from different subspaces $L(P\pi)$. Therefore, it is of interest to study polarization squeezing properties (with using measurement devices of schemes on Fig. 1) of partially polarized light beams obtained by actions of the biphoton squeezing operators $S_Y, S_X$ together with the "proper" polarization squeezing operators $S_P(\zeta)$ on states $|in >_{phys}$ of some physical input light beams

$$|PPSL >_{X/Y} = S_P(\zeta)(S_X(\{\gamma_{ij}\})/S_Y(\{\beta_{ij}\}))|in >_{phys} \tag{4.1}$$

that is presented schematically on Fig 3. As a result we can obtain new (non-classical) sets of states of partially polarized light which can be called as partially polarized squeezed light(PPSL). Specifically, taking as $|in >_{phys}$ usual multimode Glauber coherent states $|\{\alpha_i^+, \alpha_j^-\} >, \alpha_i^{\pm} \neq 0$, we get in such a manner states of PPSL which contain (at the condition $|\alpha_i^+| = |\alpha_i^-|$) a subclass of states corresponding to $UL^c$ in the classification above. In general, transmitting different input

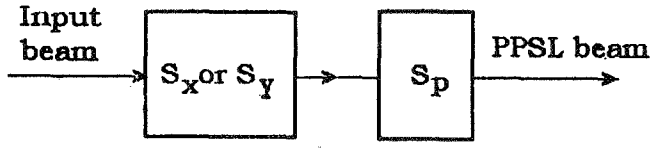


Figure 3: Scheme of production of partially polarized squeezed light

beams through physical devices corresponding to different combination of the above squeezing operators in (4.1), one can obtain new classes of partially polarized light distinguished by values of $dep_P = (1 - 2\bar{P}/\bar{N})$ and $dep_{P_0} = (1 - |2\bar{\pi}|/\bar{N})$ by analogy with UL.

In conclusion we emphasize that the above results give a more deep insight into polarization structure of light beams enabling to determine new nonusual states in quantum optics. In a sense, the results of section 2,3 and those of papers [10-12] yield all necessary prerequisites for developing a quantum description of unpolarized light waves whose existence has not yet an adequate solution within the classical optics[26]. All this opens some possibilities in setting new optical experiments related, in particular, to "hidden" variables, "entangled states" and EPR paradox [1,2,5,6,19], polarization chaos, spontaneous symmetry breaking and bistability [8,11,12], "optical atoms" and reduction of quantum noises [4,6,11,12,19] etc. From other lines of possible applications of the results above we point out precise measurements in spectroscopy of anisotropic media[18] and studies of interaction of light in different new polarization states with optically active biological macromolecules (using the interrelations between the above chiral symmetries $su(2), \hat{\sigma}, \hat{P}$ of em fields and chiral properties of such molecules)[27].

# 5 Acknowledgements

The author thanks V.P. Bykov and A.V. Masalov for stimulating discussions and M.H. Rubin and Y. Shih for interest in the work. A partial financial support of the American Physical Society is acknowledged. The gratitude is also expressed to the staff of Facultad de Ciencias Fisico-Matematicas de Universidad de Guadalajara, where the final version of the paper was prepared, for hospitality.

# References

[1] D. Bohm, *Quantum theory*, (Prentice-Hall, N.Y., 1951)

[2] J.F. Clauser and A. Shimony, Rep.Progr.Phys. **41**, 1881 (1978)

[3] J. Perina, *Coherence of light*, (Van Nostrand, London, 1972); *Quantum statistics of linear and nonlinear optical phenomena*, (D. Reidel, Dordrecht, 1984)

[4] S. Frieberg, C.K. Hong and L. Mandel, Phys. Rev. Lett., **54**, 2011 (1985); A. Heidmann, R.J. Horowicz, S.Reynaud, E. Giacobino, C. Fabre and C. Camy, Phys. Rev. Lett.,**59**, 2555 (1987)

[5] Y.H. Shih and C.O. Alley, Phys. Rev. Lett., **61**, 2921 (1988)

[6] D.N. Klyshko, Phys.Lett.**A163**, 349 (1992)

[7] R. Bhandari and J. Samuel, Phys. Rev. Lett., **60**, 1211 (1988); T.F. Jordan, Phys. Rev., **A38** 1590 (1988)

[8] H.-H. Ritze and A. Bandilla, Phys.Lett., **A78**, 447 (1980)

[9] A. Gerrard and J.M. Burch, *Introduction to matrix methods in optics*, (Wiley, London, 1975)

[10] V.P.Karassiov and V.I Puzyrevsky, J. Sov. Laser Research **10**, 229 (1989); Trudy FIAN (Proc. P.N. Lebedev Phys. Inst.), **211**, 161 (1991)

[11] V.P. Karassiov, J. Sov. Laser Research, **12**, 147 (1991); ibidem, 431 (1991)

[12] V.P. Karassiov, J. Phys., **A26**, 00 (1993); Preprint FIAN N 63,(Moscow, 1992)

[13] J.M. Jauch and F. Rohrlich, *Theory of photons and electrons*, (Addison-Wesley, London, 1959)

[14] D. Stoler, Phys. Rev., **D4**,1925 (1971); H.P. Yuen, Phys. Rev., **A13**, 2226 (1976)

[15] R. Loudon and P.L. Knight, J. Mod. Opt., **34**, 709 (1987)

[16] X. Ma and W. Rhodes, Phys. Rev., **A41**, 4625 (1990)

[17] C.K. Hong and L. Mandel, Phys. Rev., **A32**, 974 (1985)

[18] V.P. Karassiov and A.V. Masalov, Optika and Spectr., **74**, N 4 (1993)[Russian]

[19] D. Greenberger, M. Horne and A. Zeilinger, Phys. Today,**46**, N8, Pt.1, 22 (1993)

[20] A.M. Perelomov, *Generalized coherent states and their applications*,(Nauka, Moscow, 1987)

[21] R. Delbourgo, J. Phys.,**A10**, 1837 (1977)

[22] V.V. Dodonov and V.I. Man'ko, Trudy FIAN, **183**, 5 (1987)

[23] V.P. Karassiov, Bull. Lebedev Phys. Inst., N 5/6, 00 (1993)

[24] C. Aragone, E. Chalbaud and S. Salamo, J. Math Phys., **17**, 1963 (1976)

[25] G.S. Agarwal, D. Home and W. Schleich, Phys. Lett., **A 170**, 359 (1992)

[26] H. Hepp and H. Jensen, Sitzber. Heidelberg. Acad. Wiss., Mat.-Naturw. Kl.,**4**, 89 (1971)

[27] S.F. Mason, *Molecular optical activity and the chiral discrimination*, (University Press, Cambridge, 1982)

# A NEW APPROACH TO THE PHOTON LOCALIZATION PROBLEM

D. Han
*National Aeronautics and Space Administration, Goddard Space Flight Center, Code 902.3, Greenbelt, Maryland 20771*

Y. S. Kim
*Department of Physics, University of Maryland, College Park, Maryland 20742*

Marilyn E. Noz
*Department of Radiology, New York University, New York, New York 10016*

**Abstract**

Since wavelets form a representation of the Poincaré group, it is possible to construct a localized superposition of light waves with different frequencies in a Lorentz-covariant manner. This localized wavelet satisfies a Lorentz-invariant uncertainty relation, and also the Lorentz–invariant Parseval's relation. A quantitative analysis is given for the difference between photons and localized waves. It is then shown that this localized entity corresponds to a relativistic photon with a sharply defined momentum in the non–localization limit. Waves are not particles. It is confirmed that the wave–particle duality is subject to the uncertainty principle.

## 1 Introduction

We propose a quantitative approach to the photon localization problem. Photons are relativistic particles requiring a covariant theoretical description. Classical optics based on the conventional Fourier superposition is not covariant under Lorentz transformations [1]. On the other hand, wavelets can be regarded as representations of the Lorentz group [2, 3, 4]. In Ref. [1], we discussed the difference between waves and wavelets without mentioning the word "wavelet." We have seen there that the lack of covariance of light waves is due to the lack of Lorentz invariance of the integral measure. We concluded there that an extra multiplicative factor is needed to make the Fourier optics covariant. We would like to point out that this procedure corresponds to the wavelet formalism of wave optics.

In spite of the covariance of wavelets, photons are not wavelets. Instead, we shall make a quantitative analysis of the difference between these two clearly defined physical concepts. The advantage of this quantitative approach is that we can see how close they are to each other. In this way, we can assert that photons are waves with a proper qualification.

Another convenient feature of the localized wavelet representation is that it is possible to introduce an cut–off procedure in a covariant manner, so as to preserve the information given in

the distribution. By introducing the concept and word "window" [5, 6, 7, 8], it is possible to define the region in which the frequency distribution is non–zero. We can then compare the "windowed" wavelet to the photon operators in quantum field theory to pinpoint the difference between the photons and wavelets.

## 2 Localized Light Wavelets

For light waves, we start with the usual expression

$$F(z,t) = \frac{1}{\sqrt{2\pi}} \int g(k) e^{i(kz-\omega t)} dk \; . \tag{1}$$

Unlike the case of the Schrödinger wave, $\omega$ is equal to $k$, and there is no spread of wave packet. The velocity of propagation is always that of light. We might therefore be led to think that the problem for light waves is simpler than that for nonrelativistic Schrödinger waves. This is not the case. In Ref.[1], we have considered the following questions.

(1). We would like to have a wave function for light waves. However, it is not clear which component of the Maxwell wave should be identified with the quantal wave whose absolute square gives a probability distribution. Should this be the electric or magnetic field, or should it be the four–potential?

(2). The expression given in Eq.(1) is valid in a given Lorentz frame. What form does this equation take for an observer in a different frame?

(3). Even if we are able to construct localized light waves, does this solve the photon localization problem?

(4). The photon has spin 1 either parallel or antiparallel to its momentum. The photon also has gauge degrees of freedom. How are these related to the above-mentioned problems?

Even though light waves do not satisfy the Schrödinger equation, the very concept of the superposition principle was derived from the behavior of light waves. Furthermore, it was reconfirmed recently that light waves satisfy the superposition principle [9]. It is not difficult to carry out a spectral analysis on Eq.(1) and give a probability interpretation. The question then is whether this probability interpretation is covariant. We addressed this question in Ref. [1]. We concluded in effect that the localized light wave is covariant if we use the wavelet form. We regret however that we were not aware of the word "wavelet" at that time. In this section, we shall translate what we did in Ref. [1] into the language of wavelets.

The expression given in Eq.(1) is not covariant if $g(k)$ is a scalar function, because the measure $dk$ is not invariant. If $g(k)$ is not a scalar function, what is its transformation property? We shall approach this problem using the light-cone coordinate system. We define the light-cone variables as

$$s = (z+t)/2, \qquad u = (z-t) \; . \tag{2}$$

The Fourier-conjugate momentum variables are

$$k_s = (k-\omega) \; , \qquad k_u = (k+\omega)/2 \; . \tag{3}$$

If we boost the light wave (or move against the wave with velocity parameter $\beta$), the new coordinate variables become

$$s' = \alpha_+ s \; , \quad u' = \alpha_- u \; , \quad k'_s = \alpha_- k_s \quad k'_u = \alpha_+ k_u \; , \tag{4}$$

where

$$\alpha_{\pm} = [(1 \pm \beta)/(1 \mp \beta)]^{1/2} \ . \tag{5}$$

If we construct a phase space consisting of $s$ and $k_s$ or $u$ and $k_u$, the effect of the Lorentz boost will simply be the elongation and contraction of the coordinate axes. If the coordinate $s$ is elongated by $\alpha_+$, then $k_s$ is contracted by $\alpha_-$ with $\alpha_+\alpha_- = 1$.

In the case of light waves, $k_s$ vanishes, and $k_u$ becomes $k$ or $\omega$. In terms of the light-cone variables, the expression of Eq.(1) becomes

$$F(u) = \left(\frac{1}{2\pi}\right)^{1/2} \int g(k) e^{iku} dk \ . \tag{6}$$

We are interested in a unitary transformation of the above expression into another Lorentz frame. In order that the norm

$$\int |g(k)|^2 dk \tag{7}$$

be Lorentz-invariant, $F(u)$ and $g(k)$ should be transformed like

$$F(u) \rightarrow \sqrt{\alpha_+} F(\alpha_+ u) \ , \qquad g(k) \rightarrow \sqrt{\alpha_-} g(\alpha_- k) \ . \tag{8}$$

Then Parseval's relation:

$$\int |F(u)|^2 du = \int |g(k)|^2 dk \tag{9}$$

will remain Lorentz-invariant.

It is not difficult to understand why $u$ in Eq.(2) and $k = k_u$ in Eq.(3) are multiplied by $\alpha_+$ and $\alpha_-$ respectively. However, we still have to give a physical reason for the existence of the multipliers $(\alpha_{\pm})^{1/2}$ in front of $F(u)$ and $g(k)$. In Ref. [10], Kim and Wigner pointed out that the multipliers in Eq.(8) come from the requirement that the Wigner phase–space distribution function be covariant under Lorentz transformations [11, 7].

Let us illustrate this point using a Gaussian form. We can consider the g(k) function of the form

$$g(k) = \left(\frac{1}{\pi b}\right)^{1/4} \exp\left\{-(k-p)^2/2b\right\} \ , \tag{10}$$

which leads to the $F(u)$ of the form

$$F(u) = \left(\frac{b}{\pi}\right)^{1/4} \exp\left(bu^2/2\right) \exp\left(ipu\right) \ , \tag{11}$$

where $b$ is a constant and specifies the width of the distribution, and $p$ is the average momentum:

$$p = \frac{\int k|g(k)|^2 dk}{\int |g(k)|^2 dk} \ . \tag{12}$$

Under the Lorentz boost according to Eq.(8), $g(k)$ becomes

$$\left(\frac{1}{\pi b}\right)^{1/4} \sqrt{\alpha_-} \exp\left\{-\alpha_-(k - \alpha_+ p)^2/2b\right\} \ . \tag{13}$$

Thus, according to the transformation law given in Eq.(8), the transformed F(u) becomes

$$F(u) = \left(\frac{b}{\pi}\right)^{1/4} \sqrt{\alpha_+} \exp\left(b(\alpha_+ u)^2/2\right) \exp\left(i(\alpha_+ p)u\right) . \tag{14}$$

We note here that the average momentum $p$ is now increased to $\alpha_+ p$. The average momentum therefore is a covariant quantity, and $\alpha_-$ can therefore be written as

$$\alpha_- = \sigma/p , \tag{15}$$

where $\sigma$ is the average momentum in the Lorentz frame in which $\alpha_\pm = 1$, and $\beta = 0$.

As a consequence, in order to maintain the covariance, we can replace $F(u)$ and $g(k)$ by $F'(u)$ and $g'(k)$ respectively, where

$$F'(u) = \sqrt{\frac{p}{\sigma}} F(u) , \qquad g'(k) = \sqrt{\frac{\sigma}{p}} g(k) . \tag{16}$$

These functions will satisfy Parseval's equation:

$$\int |F'(u)|^2 du = \int |g'(k)|^2 dk \tag{17}$$

in every Lorentz frame without the burden of carrying the multipliers $\sqrt{\alpha_+}$ and $\sqrt{\alpha_-}$. We can simplify the above cumbersome procedure by introducing the form

$$G(u) = \frac{1}{\sqrt{2\pi p}} \int g(k) e^{iku} dk . \tag{18}$$

where the procedure for the Lorentz boost is to replace $p$ by $\alpha_+ p$, and $k$ in $g(k)$ by $\alpha_- k$. This is precisely the wavelet form for the localized light wave, and this definition is consistent with the form given in earlier papers on wavelets [2, 3].

# 3 Windows

There are in physics many distributions, and we have a tendency to choose "smooth" or analytic functions to describe them. These functional forms usually extend from minus infinity to plus infinity. However, the distribution function of physical interest is usually concentrated within a finite interval. On the other hand, it is not uncommon in physics that mathematical difficulties in theory come from the region in which the distribution function is almost zero and is physically insignificant. Thus, we are tempted to ignore contributions from outside of the specified region. This is called the "cut–off" procedure.

One of the difficulties of this procedure is that a good cut-off approximation in one Lorentz frame may not remain good in different frames. The translational symmetry of wavelets allows us to define the cut-off procedure which will remain valid in all Lorentz frames.

We can allow the function to be nonzero within the interval

$$a \leq x \leq a + w , \tag{19}$$

while demanding that the function vanish everywhere else. The parameter w determines the size of the window. The window can be translated or expanded/contracted according to the operation of the affine group [8]. Indeed, it is possible to define the window in such a way that the boundary condition be covariant, and the information contained in the window be preserved [8].

# 4 Photon Localization Problem

The wavelet formalism allows the description of a localized wave function for light waves in a Lorentz covariant manner with Lorentz-invariant normalization. We shall now examine how close the wavelet can be to photons. First of all, it should be noted that there are no physical laws which dictate the functional form for $a(k)$ or $g(k)$. This depends on initial conditions. If we choose an analytic function, this is purely for mathematical convenience. If we choose functions which vanish near $k = 0$ and $k$ greater than a certain value, this also satisfies our criterion for mathematical convenience. Indeed, the concept of window plays a decisive role in this form of localization.

In quantum electrodynamics, we start with the form

$$A(z,t) = \int \frac{1}{\sqrt{2\pi\omega}} a(k) e^{i(kz-\omega t)} dk \, . \tag{20}$$

This is a covariant expression in the sense that the norm

$$\int \frac{|a(k)|^2}{2\pi\omega} dk \tag{21}$$

is invariant under Lorentz transformations, because the integral measure $(1/\omega)dk$ is Lorentz-invariant.

We are quite familiar with the expression of Eq.(1) for wave optics, and with that of Eq.(20) for quantum electrodynamics. The wavelet form of Eq.(18) satisfies the same superposition principle as Eq.(1), and has the same covariance property as Eq.(20). It is quite similar to both Eq.(1) and Eq.(20), but they are not the same. The difference between $F(u)$ of Eq.(1) and the wavelet $G(u)$ is insignificant. Other than the factor $\sqrt{\sigma}$ where $\sigma$ has the dimension of the energy, the wavelet $G(u)$ has the same property as $F(u)$ in every Lorentz frame [1]. However, the difference between $G(u)$ and $A(u)$ is still significant.

It is possible to give a particle interpretation to Eq.(20) after second quantization. However, $A(z,t)$ cannot be used for the localization of photons. On the other hand, it is possible to give a localized probability interpretation to $F(z,t)$ of Eq.(1), while it does not accept the particle interpretation of quantum field theory.

$A(u)$ of Eq.(20) and $G(u)$ of Eq.(18) are numerically equal if

$$a(k) = \sqrt{\frac{k}{p}} g(k) \, , \tag{22}$$

where the window is defined over a finite interval of $k$ which does not include the point $k = 0$. It is thus possible to jump from the wavelet $G(u)$ to the photon field $A(u)$ using the above equation.

However, the above equality does not say that $a(k)$ is equal to $g(k)$. The photon intensity distribution is not directly translated into the photon–number distribution. This is the quantitative difference between wavelets and photons.

Of course, this difference becomes insignificant when the window becomes narrow. The narrower window in $k$ means a wider distribution of the wave in the $u$ coordinate system. We conclude therefore that photons become waves in non–localization limit. Particles are not waves. The wave–particle duality is subject to the uncertainty principle. The relation given in Eq.(22), together with the appropriate window, is a statement of this uncertainty relation.

## Acknowledgments

We would like to thank B. DeFacio and G. Hegerfeldt for very helpful comments and criticisms. We thank also G. Kaiser for sending us reprints of his articles.

## References

[1] D. Han, Y. S. Kim, and M. E. Noz, Phys. Rev. A **35**, 1682 (1987).

[2] E. W. Aslaksen and J. R. Klauder, J. Math. Phys. **9**, 206 (1968) and **10**, 2267 (1969).

[3] I. Daubechies, *Ten Lectures on Wavelets* (Society for Industrial and Applied Mathematics, Philadelphia, PA, 1992).

[4] G. Kaiser, Phys. Lett. A **168**, 28 (1992).

[5] G. Kaiser, in *Wavelets and Applications* (Toulouse, 1994), Proceedings (1992), and the references contained in this paper.

[6] H. H. Szu and H. J. Caulfield, Optical Engineering **31**, 1823 (1992).

[7] For the phase–space picture of wavlets, see B. DeFacio, C. R. Thompson, and G. V. Welland, in *Digital Image Synthesis and Inverse Optics*, Proc. of SPIE – The International Society for Optical Engineerg (Society of Photo–Optical Instrumentation Engineers, Bellingham, WA 1992). See also B. DeFacio, in *Workshop on Squeezed States and Uncertainty Relations*, Proceedings, D. Han, Y. S. Kim, and W. W. Zachary, eds. (NASA Conference Publications No. 3135, 1992).

[8] D. Han, Y. S. Kim, and M. E. Noz, in *Second International Workshop on Squeezed States and Uncertainty Relations*, edited by D. Han, Y. S. Kim, V. I. Man'ko (NASA Conference Publications No. 3219, 1993).

[9] A. Aspect, P. Grangier, and G. Roger, J. Optics (Paris) **20**, 119 (1989).

[10] Y. S. Kim and E. P. Wigner, Phys. Rev. A **36**, 1293 (1987).

[11] Y. S. Kim and M. E. Noz, *Phase Space Picture of Quantum Mechanics* (World Scientific, Singapore, 1991).

N95-13906

# PRODUCTION OF SQUEEZED STATES FOR MACROSCOPIC MECHANICAL OSCILLATOR

V.V. Kulagin
*Sternberg Astronomical Institute, Moscow State University,*
*Universitetsky prospect 13, 119899, Moscow, Russia.*

**Abstract**

**The possibility of squeezed states generation for macroscopic mechanical oscillator is discussed. It is shown that one can obtain mechanical oscillator in squeezed state via coupling it to electromagnetic oscillator (Fabry-Perot resonator) and pumping this Fabry-Perot resonator with a field in squeezed state. The degradation of squeezing due to mechanical and optical losses is also analysed.**

Realization of quantum states such as squeezed, amplitude squeezed and others in real physical systems is of great importance for confirmation of predictions of quantum mechanics and its future development. There are a lot of papers concerning generation of squeezed states of electromagnetic fields [1, 2, 3]. However realization of such states in other systems, for example, mechanical is also of great importance. This problem arises in different high precision measurements, especially in gravitational wave experiment [4].

Let's consider a system of two coupled oscillators [5, 6]: electromagnetic (represented by Fabry-Perot resonator with a laser pump beam amplitude $E_L$ and frequency $\omega_p$ near one of the resonant frequencies of resonator $\omega_0$) and mechanical (represented by a moving mirror of Fabry-Perot resonator connected to a spring). Pump beam enters the resonator through fixed mirror with reflectance approaching 1 (this assumption is not critical for results and used only for simplicity, we also suppose that $\mid t_f \mid \to 0$ but $E_L \cdot \mid t_f \mid$=const., where $t_f$ is amplitude transmittance coefficient of fixed mirror). Usually one treats such a system in Hamiltonian formalism framework [7] when equations of motion are conservative and the system is in free evolution. However in our case it is more convenient to use Langevin approach with evolution of the system under the action of input fields: $E_L$ (classical laser field) and $E_{ba}$ (quantum field from field controller - device allowing to generate electromagnetic field in appropriate state). In our analysis $E_{ba}$ is squeezed noise with two point of squeezing and it enters the resonator through moving mirror with nonzero amplitude transmittance coefficient $t_m$. Then linearised equations of motion for such system have the following form:

$$\begin{aligned} \ddot{\hat{x}} + \omega_\mu^2 \hat{x} &= -2\gamma \cdot [\hat{E}_1 \sin(\Delta t + \phi) + \hat{E}_2 \cos(\Delta t + \phi)] \\ \dot{\hat{E}}_1 + \delta_e \hat{E}_1 + 2\beta \hat{x} \cos(\Delta t + \phi) &= 2\delta_e \hat{E}_{b1} \\ \dot{\hat{E}}_2 + \delta_e \hat{E}_2 - 2\beta \hat{x} \sin(\Delta t + \phi) &= 2\delta_e \hat{E}_{b2} \end{aligned} \qquad (1)$$

where the following parameters are introduced

$$\beta = \frac{\omega_0 E_0}{2l} \qquad \gamma = \frac{S E_0}{4\pi m t_m^2} \qquad \Delta = \omega_p - \omega_0 \qquad (2)$$

$E_0$ and $\phi$ are the amplitude and the phase of the field inside optical resonator due to the action of "laser force" $E_L$ with mirrors fixed, $S$ is the beam cross section, $l$ is the length of optical resonator, $\delta_e$ is optical damping of resonator due to the leakage of inside field through moving mirror (with reflectivity less than 1), $m$ and $\omega_\mu$ are mass and frequency of mechanical oscillator and $\hat{x}$ is its coordinate operator. For simplicity we assume that one can omit the damping of mechanical system. We also assume that the fields could be represented in terms of their quadrature component operators with usual commutation relations [8, 9]:

$$\begin{aligned} \hat{E}_{ba} &= \hat{E}_{b1}\cos\omega_0 t + \hat{E}_{b2}\sin\omega_0 t \\ \hat{E}_{out} &= \hat{E}_1\cos\omega_0 t + \hat{E}_2\sin\omega_0 t \end{aligned} \tag{3}$$

Index "ba" fits a field entered the system from field controller and index "out" means that the field outputs from Fabry-Perot resonator through moving mirror.

Introducing quadrature components for mechanical oscillator through equation

$$\hat{x} = \hat{x}_c\cos(\Delta t + \phi) + \hat{x}_s\sin(\Delta t + \phi) \tag{4}$$

(frequency $\Delta \approx \omega_\mu$ is not exactly equal to the frequency $\omega_\mu$ of single mechanical oscillator and matches the presence of coupling between two oscillators) one can easily obtain the following equations of motion (we suppose that the system is in steady state therefore $d\hat{x}_{c,s}/dt = 0$)

$$\begin{aligned} &(\hat{x}_c\cos(\Delta t + \phi) + \hat{x}_s\sin(\Delta t + \phi))(\omega_\mu^2 - \Delta^2) = -2\gamma\cdot[\hat{E}_1\sin(\Delta t + \phi) + \hat{E}_2\cos(\Delta t + \phi)] \\ \dot{\hat{E}}_1 + \delta_e\hat{E}_1 &= 2\delta_e\hat{E}_{b1} - \beta\cdot[\hat{x}_c + \hat{x}_c\cos(2\Delta t + 2\phi) + \hat{x}_s\sin(2\Delta t + 2\phi)] \\ \dot{\hat{E}}_2 + \delta_e\hat{E}_2 &= 2\delta_e\hat{E}_{b2} + \beta\cdot[\hat{x}_s - \hat{x}_s\cos(2\Delta t + 2\phi) + \hat{x}_c\sin(2\Delta t + 2\phi)] \end{aligned} \tag{5}$$

It is obvious from (5) that fluctuations of $\hat{x}_c$ and $\hat{x}_s$ depend on fluctuations of controller field quadrature components only near frequencies $\omega \approx 0$ and $\omega \approx 2 \mid \Delta \mid$ that means that controller field must consist of two modes with different frequencies $\omega_0$ and $\omega_0 + 2\Delta$. Then one can introduce the following form for $\hat{E}_{ba}$:

$$\hat{E}_{ba} = \hat{E}_c\cos\omega_0 t + \hat{E}_s\sin\omega_0 t + \hat{E}_{2c}\cos((\omega_0 + 2\Delta)t + \chi) + \hat{E}_{2s}\sin((\omega_0 + 2\Delta)t + \chi) \tag{6}$$

where $\hat{E}_c$, $\hat{E}_s$, $\hat{E}_{2c}$, $\hat{E}_{2s}$ are quadrature component operators of two modes in narrow non overlapping bandwidths ($\delta\omega \ll \mid \Delta \mid$) near left and right sidebands which are detuned from the pump frequency $\omega_p$ by $\Delta$ : $\omega_0 = \omega_p - \Delta$ and $\omega_0 + 2\Delta = \omega_p + \Delta$. Then introducing the coefficients

$$A = \omega_\mu^2 - \Delta^2 - \frac{4\beta\gamma\Delta}{\delta_e^2 + 4\Delta^2} \qquad B = \frac{8\beta\gamma\Delta^2}{\delta_e(\delta_e^2 + 4\Delta^2)} \tag{7}$$

one could obtain the following system of equations

$$\begin{aligned} A\hat{x}_c + B\hat{x}_s &= -4\gamma\hat{E}_s - 4\gamma\delta_e(\delta_e^2 + 4\Delta^2)^{-1/2}[\hat{E}_{2c}\cos(\chi - \zeta - 2\phi) + \hat{E}_{2s}\sin(\chi - \zeta - 2\phi)] \\ A\hat{x}_s - B\hat{x}_c &= -4\gamma\hat{E}_c + 4\gamma\delta_e(\delta_e^2 + 4\Delta^2)^{-1/2}[\hat{E}_{2c}\sin(\chi - \zeta - 2\phi) - \hat{E}_{2s}\cos(\chi - \zeta - 2\phi)] \end{aligned} \tag{8}$$

where phase $\zeta = \arctan(2\Delta/\delta_e)$ represents the delay of the pump field inside the cavity with respect to the laser field.

Let's assume that controller field $E_{bc}$ is in squeezed state with $< \hat{E}_{bc} >= 0$ and dispersions of quadrature components [8, 9]

$$< \Delta\hat{E}_s^2 >= N_0/g_0 \qquad < \Delta\hat{E}_c^2 >= N_0 g_0 \tag{9}$$

where $g_0 > 1$ is the squeezing coefficient of back action field for mode with frequency $\omega_0$, $N_0$ is vacuum level of dispersion and we use the fact that $2 \mid \Delta \mid \approx 2\omega_\mu \ll \omega_0$. The same expressions are valid for $\hat{E}_{2s}, \hat{E}_{2c}$ with obvious substitution $g_0 \to g_2$ and correlations between $\hat{E}_s, \hat{E}_c$ and $\hat{E}_{2s}, \hat{E}_{2c}$ are zero. Factors $g_0$ and $g_2$ depends on the structure of back action field controller.

The mechanical oscillator would be in squeezed state only if the following special conditions are valid. The first condition concerns the detuning $\Delta$ of the system: it must satisfy the equation

$$A = 0 \qquad \omega_\mu^2 - \Delta^2 - \frac{4\gamma\beta\Delta}{\delta_e^2 + 4\Delta^2} = 0 \tag{10}$$

In this case contribution of "noisy component" $\hat{E}_c$ to $\hat{x}_s$ vanishes. For the contribution of another "noisy component" $\hat{E}_{2c}$ would be also unimportant one must choose the phase $\phi$ according to the following equation:

$$\chi - \zeta - 2\phi = k\pi/2 \qquad k = 0, \pm 1, \pm 2 \ldots \tag{11}$$

that means that special phase correspondence must take place. In physical language this means that one must compensate the delay of electromagnetic field inside Fabry-Perot resonator with regard to the pump field. This can be done by appropriate phase correspondence between the pump beam and the field $E_{bc}$ from the squeezed state controller. Then the system equations of motion occur ($k = 1$)

$$\begin{aligned} B\hat{x}_s &= -4\gamma\hat{E}_s - 4\gamma\delta_e(\delta_e^2 + 4\Delta^2)^{-1/2}\hat{E}_{2s} \\ B\hat{x}_c &= 4\gamma\hat{E}_c - 4\gamma\delta_e(\delta_e^2 + 4\Delta^2)^{-1/2}\hat{E}_{2c} \end{aligned} \tag{12}$$

Therefore we obtain special quantum nondemolition coupling between optical and mechanical oscillator: one quadrature component of mechanical oscillator couples only with one quadrature component of optical field (on frequencies $\omega_0$ and $\omega_0 + 2\Delta$) and the larger the squeezing of the field of two electromagnetic modes (with frequency $\omega_0$ and $\omega_0 + 2\Delta$) the greater the squeeze factor of mechanical oscillator. It is worth mentioning that the squeezing $g_2$ of the mode with frequency $\omega_0 + 2\Delta$ could be smaller than the squeezing $g_0$ of the mode with frequency $\omega_0$ of electromagnetic field provided $\delta_e < \Delta$ (because of the filtration of fluctuations by narrow bandwidth optical resonator) otherwise the squeezing of two modes must be equal.

Let's discuss the time of operating regime achievement and the influence of mechanical $\delta_\mu$ and optical coherent (due to difraction and mirror absorbtion) $\delta_c$ losses. In practice optical damping $\delta_e$ due transmittance through moving mirror is much greater than mechanical damping $\delta_\mu$. Then the field inside resonator becomes squeezed through time $\delta_e^{-1}$. After that through time $(2\beta\gamma/\omega_\mu)^{-1/2}$ (that is inverse value of coupling constant) the state of mechanical oscillator becomes also squeezed and the initial state is forgotten. It is obvious that mechanical losses must not be very large: $\delta_\mu < (2\beta\gamma/\omega_\mu)^{1/2}/g$ ($g$ - required squeezing factor for mechanical oscillator) otherwise the rate of coherent pumping through losses would be larger than the rate of squeezing through action of controller field. Similarly $\delta_c$ must be smaller than $\delta_e/\max(g_0, g_2)$.

In conclusion let's discuss the structure of back action field controller. In accordance with the ideas of papers [10, 11, 12] it must contain two circulators for uncoupling the fields $E_{out}$ and $E_{ba}$, the load (absorber black body with zero temperature) and two squeezers with pump frequencies $2\omega_0$ and $2(\omega_0+2\Delta)$ (for example, degenerate parametric amplifiers or four wave mixers). Then the field $E_{out}$ comes through moving resonator mirror and two circulators to the load and dissipates in it. Zero fluctuations of the load enters through first circulator the squeezer with pump frequency $2\omega_0$, then gets through second circulator to the squeezer with pump frequency $2(\omega_0 + 2\Delta)$ and then enters the system through moving mirror.

# References


[1] D. F. Walls, Nature (L), **306**, 141 (1983).

[2] B. Yurke, Phys. Rev. A, **32**, 300 (1985).

[3] H. A. Haus, Y. Yamamoto, Phys. Rev. A, **34**, 270 (1986).

[4] C. M. Caves, K. S. Thorne, R. W. P. Drever, V. D. Sandberg, M. Zimmermann, Rev. Mod. Phys., **52**, 341 (1980).

[5] V. V. Kulagin, V. N. Rudenko, Nuovo Cimento C, **10**, 601 (1987).

[6] V. V. Kulagin, V. N. Rudenko, Sov. Phys. JETP, **67**, 677 (1988).

[7] G. J. Milburn, A. S. Lane, D. F. Walls, Phys. Rev. A, **27**, 2804 (1983).

[8] C. M. Caves, Phys. Rev. D, **26**, 1817 (1982).

[9] C. M. Caves, B. L. Schumaker, Phys. Rev. A, **31**, 3008 (1985).

[10] B. Yurke, J. Opt. Soc. Am. B, **2**, 732 (1985).

[11] B. Yurke, J. Denker, J. Physica B, **108**, 1359 (1981).

[12] B. Yurke, L. R. Corruccini, Phys. Rev. A, **30**, 895 (1984).

# SQUEEZING IN A 2-D GENERALIZED OSCILLATOR

Octavio Castaños and Ramón López-Peña
*Instituto de Ciencias Nucleares, UNAM*
*Circuito Exterior, C.U., Apdo. Postal 70-543*
*04510 México, D. F., México*

Vladimir I. Man'ko
*Physical Institute of the Russian Republic*
*Leninsky Prospect 53. Moscow, Russia*

**Abstract**

A two-dimensional generalized oscillator with time-dependent parameters is considered to study the two-mode squeezing phenomena. Specific choices of the parameters are used to determine the dispersion matrix and analytic expressions, in terms of standard hermite polynomials, of the wavefunctions and photon distributions.

## 1 Introduction

In the middle of the sixties and beginning of the seventies a set of quantum states of the electromagnetic field were observed which have less uncertainty in one quadrature than a coherent state [1-3]. These one-mode squeezed states have generated big expectations in optical communication systems [4]. In some quantized fields, the interaction hamiltonians occur only between pairs of modes and then to understand the main features of the system, one restricts to study one and two normal modes . In the last decade two-mode squeezing phenomena have attracted attention to study properties of noise and correlations [5-8]. Recently the accidental degeneracy of a two-dimensional (2-D) harmonic oscillator with frequency $\omega_0$ plus an interaction proportional to the z-th projection of the angular momentum was studied [9]. This system was called the generalized 2-D harmonic oscillator because presents a bigger accidental degeneracy depending on the strength $\lambda$ of the angular momentum interaction. This model was generalized [10] to include time-dependent parameters, $m = m_0 f(t)$ and $\lambda = \omega_0 \lambda_0(t)$. If we take $f(0) = \lambda_0(0) = 1$; the hamiltonian, for $t = 0$, represents a charged particle moving in a constant magnetic field .

The aim of this work is to study two-mode squeezing phenomena with this model because it demonstrates the change of dispersions due to variation of the mass and coupling constant during the evolution. In the framework of quantum optics the hamiltonian is built by: the operator $(1/f + f)\vec{a}^\dagger \cdot \vec{a}$, that causes a time-dependent exchange of kinetic and potential energies within each mode; the interaction $1/2(1/f - f)(\vec{a}^\dagger \cdot \vec{a}^\dagger + \vec{a} \cdot \vec{a})$, which describes a degenerate two-photon interaction; and the potential $i\lambda_0(t)(a_2^\dagger a_1 - a_1^\dagger a_2)$, that is a mode mixing operator.

The solution of the corresponding time dependent Schroedinger equation is obtained through the theory of integrals of motion [11]. By means of Noether's theorem, using a special variation

[10], we construct the linear time dependent integrals of the motion. The resulting quantum invariants are given in terms of the positions and momenta operators [10,11] by

$$\vec{P}(t) = \lambda_1 \vec{p} + \lambda_2 \vec{q}, \quad \vec{Q}(t) = \lambda_3 \vec{p} + \lambda_4 \vec{q}, \tag{1}$$

with the initial conditions $\vec{P}(0) = \vec{p}$ and $\vec{Q}(0) = \vec{q}$, so that the $2 \times 2$ matrices previously introduced satisfy $\lambda_1(0) = \lambda_4(0) = I_2$ and $\lambda_3(0) = \lambda_2(0) = 0$. The operators $\vec{A}(t) = 1/\sqrt{2}\,[\vec{Q}(t)/l + il/\hbar \vec{P}(t)]$ and its hermitean conjugate, can be constructed with the matrices

$$\lambda_p = \frac{1}{l}\lambda_3 + \frac{il}{\hbar}\lambda_1, \quad \lambda_q = \frac{1}{l}\lambda_4 + \frac{il}{\hbar}\lambda_2\,, \tag{2}$$

with $l = \sqrt{\frac{\hbar}{m_0\omega_0}}$ defining the oscillator length. These integrals of motion also are given in terms of the creation and annihilation photon operators

$$\vec{A}(t) = M_1 \vec{a} + M_2 \vec{a}^\dagger, \quad \vec{A}^\dagger(t) = \quad M_3 \vec{a} + M_4 \vec{a}^\dagger\,. \tag{3}$$

With the initial conditions $\vec{A}(0) = \vec{a}$ and $\vec{A}^\dagger(0) = \vec{a}^\dagger$, the matrices defined in (3) comply with $M_1(0) = M_4(0) = I_2$ and $M_3(0) = M_2(0) = 0$. The $\lambda_k$'s, $M_k$'s, $\lambda_p$ and $\lambda_q$ are entries of symplectic matrices in four dimensions because the invariants (1) and (3) satisfy the commutation relations of Heisenberg-Weyl algebras.

In the present work, we study the behavior of the model for $\lambda_0(t)$ an arbitrary function of time and considering two kinds of varying masses, *i.e.*, two choices for the function $f(t)$, namely:

$$f(t) = \exp(\gamma t) \;\; ; \tag{4}$$

$$f(t) = \begin{cases} 1 & , \;\; t \leq 0 \\ \cosh^2 \Omega_0 t & , \;\; 0 \leq t \leq T \\ \{\Omega_0(t-T)\sinh\Omega_0 T + \cosh\Omega_0 T\}^2 & , \;\; T \leq t \end{cases} . \tag{5}$$

For these two cases the $\lambda_k$ matrices take the general form

$$\lambda_k = \mu_k\, \mathbf{R} = \mu_k \begin{pmatrix} \cos\theta & \sin\theta \\ -\sin\theta & \cos\theta \end{pmatrix}; \;\; k = 1,\, 2,\, 3,\, 4; \tag{6}$$

where the definition $\theta = \int_0^t \omega_0 \lambda_0(\tau) d\tau$ was used. The analytic expressions for the $\mu_k$'s functions are given in Ref. [10]. In the next sections we determine the coherent and Fock-like states, the photon distributions and the dispersion matrices in terms of these $\mu_k$'s.

# 2 Squeezed Coherent and Fock States

The coherent-like states are obtained by solving the differential equation $\vec{A}(t)\Phi_0(\vec{q},t) = 0$ with $\vec{A}(t)$ given in Eq. (3). This solution yields the vacuum state of the physical system, and its phase is chosen to guarantee that satisfies the time dependent Schroedinger equation. The expression for the ground state wavefunction is

$$\Phi_0(\vec{q},t) = \frac{1}{\sqrt{2\pi\hbar^2\mu_p}} \exp\left\{-\frac{i}{2\hbar}\frac{\mu_q}{\mu_p}\vec{q}\cdot\vec{q}\right\} \;. \tag{7}$$

To get the last expression the relation (2) was used and the functions $\mu_p = \frac{1}{\sqrt{2}}\left(\frac{il}{\hbar}\mu_1 + \frac{1}{l}\mu_3\right)$ and $\mu_q = \frac{1}{\sqrt{2}}\left(\frac{il}{\hbar}\mu_2 + \frac{1}{l}\mu_4\right)$ were defined. To obtain the general expression for the eigenstates in the coordinate representation one needs to apply the unitary operator $\hat{D}(\alpha) = \exp\{\vec{\alpha}\cdot\vec{A}^{\dagger} - \vec{\alpha}^{*}\cdot\vec{A}\}$, which an invariant, to the vacuum wavefunction (7), *i.e.*,

$$\Phi_{\alpha}(\vec{q},t) = \exp\left\{-\frac{|\alpha|^2}{2} + \frac{1}{2}\frac{\mu_p^*}{\mu_p}\vec{\alpha}\cdot\vec{\alpha} + \frac{i}{\hbar\mu_p}\vec{q}\,\tilde{\mathbf{R}}\vec{\alpha}\right\}\Phi_0(\vec{q},t) \quad . \tag{8}$$

These are expressed in terms of multi-dimensional Hermite polynomials [12] through the relation

$$\exp\left(-\frac{1}{2}u\,\vec{\alpha}^{*}\cdot\vec{\alpha}^{*} + v\,\vec{\alpha}^{*}\,\tilde{\mathbf{R}}\,\vec{\gamma}\right) = \sum_{n_1,n_2=0}^{\infty}\frac{\alpha_1^{*n_1}}{n_1!}\frac{\alpha^{*n_2}}{n_2!}\mathbf{H}_{n_1,n_2}^{\{u\mathbf{I_2}\}}\left(\frac{v}{u}\tilde{\mathbf{R}}\vec{\gamma}\right) \quad . \tag{9}$$

Substituting the last expression into (8) and using the form of the coherent-like states in the Fock-like representation, we get the Fock-like eigenstates in the coordinate representation:

$$\langle\vec{q}|n_1n_2\rangle = \Phi_0(\vec{q},t)\;\mathbf{H}_{n_1,n_2}^{\left\{-\frac{\mu_p^*}{\mu_p}\mathbf{I_2}\right\}}\left(-\frac{i}{\hbar\mu_p^*}\mathbf{R}\vec{q}\right) . \tag{10}$$

These multi-dimensional Hermite polynomials are rewritten as a product of two standard one-dimensional Hermite polynomials [12] as follows:

$$\begin{aligned}\mathbf{H}_{n_1,n_2}^{\left\{\frac{\mu_p^*}{\mu_p}\mathbf{I_2}\right\}}\left(-\frac{i}{\hbar\mu_p^*}\mathbf{R}\vec{q}\right) &= \left(-\frac{\mu_p^*}{2\mu_p}\right)^{(n_1+n_2)/2} H_{n_1}\left(\frac{1}{\sqrt{2}\hbar|\mu_p|}[\cos\theta\;q_1 + \sin\theta\;q_2]\right)\\ &\quad\times H_{n_2}\left(\frac{1}{\sqrt{2}\hbar|\mu_p|}[-\sin\theta\;q_1 + \cos\theta\;q_2]\right) ,\end{aligned} \tag{11}$$

where we use the explicit expression of matrix $\mathbf{R}$. These Fock (10) and coherent (8) -like states represent squeezed and correlated eigenstates of the system as it will be shown further.

# 3 Propagator

The propagator in the coherent state representation is given by the matrix elements of the evolution operator $U(t)$, which will be obtained by means of the theory of time dependent integrals of motion [11]. If $\vec{I}(t)$ is an integral of motion then satisfies $\vec{I}(t)\hat{U}(t) = \hat{U}(t)\vec{I}(0)$. Taking its matrix elements with respect to the coherent states, we get a linear system of differential equations, which can be solved. Thus the propagator takes the form

$$G(\vec{\alpha}^{*},\vec{\gamma},t) = \frac{\exp\left(-|\vec{\alpha}|^2/2 - |\vec{\gamma}|^2/2\right)}{\sqrt{detM_1}}\exp\left(-\frac{1}{2}\vec{\alpha}^{*}M_1^{-1}M_2\vec{\alpha}^{*} + \vec{\alpha}^{*}M_1^{-1}\vec{\gamma} + \frac{1}{2}\vec{\gamma}M_3M_1^{-1}\vec{\gamma}\right) \quad . \tag{12}$$

For the cases (4) and (5), the following relations are satisfied

$$\sqrt{detM_1} = \frac{1}{\sqrt{2}}\left(l\mu_q - \frac{i\hbar}{l}\mu_p\right) \equiv g_1, \quad M_1^{-1}M_2 = \frac{1}{\sqrt{2}g_1}\left(l\mu_q + \frac{i\hbar}{l}\mu_p\right)\mathbf{I_2} \equiv g_2\mathbf{I_2} \quad , \tag{13}$$

$$M_1^{-1} = \frac{1}{g_1}\tilde{\mathbf{R}}\ , \quad M_3 M_1^{-1} = \frac{1}{\sqrt{2}g_1}\Big(l\mu_q^* + \frac{i\hbar}{l}\mu_p^*\Big) I_2 \equiv g_4 \mathbf{I_2}\ . \tag{14}$$

Substituting these relations into the Eq.(12) we get the propagator, which through Eq. (9) can be expressed in terms of multi-dimensional Hermite polynomials. If we compare with the power series expansion of the propagator we get the probability amplitude for having $n_1$ and $n_2$ photons in the coherent-like state $|\vec{\gamma}, t\rangle$, *i.e.*,

$$\langle n_1 n_2|\vec{\gamma}, t\rangle = \frac{1}{g_1\sqrt{n_1! N_2!}} \exp\Big(-\frac{|\vec{\gamma}|^2}{2} + \frac{1}{2}g_4\vec{\gamma}\cdot\vec{\gamma}\Big)\mathbf{H}_{n_1,n_2}^{\{g_2\mathbf{I_2}\}}\Big(\frac{1}{g_1 g_2}\tilde{\mathbf{R}}\vec{\gamma}\Big)\ . \tag{15}$$

By means of the Eq.(12) this amplitude can be rewritten in terms of standard Hermite polynomials [12]. The squared absolute value of this amplitude yields the photon distribution function of the system, $W_{n_1 n_2}(\vec{\gamma}, t) = |\langle n_1 n_2|\vec{\gamma}, t\rangle|^2$. This will let us calculate, at least formally, the mean, $\langle N_k\rangle$, and the mean squared fluctuation of the number of photons, $(\Delta N_k)^2$, in direction $k$, which are present in the coherent state $|\vec{\gamma}, t\rangle$. The expectation values of $N_k$ and $N_k^2$ are evaluated directly using the expressions of the creation and annihilation photon operators in terms of the integrals of the motion (3), and the commutation properties for these invariants. For the vacuum state one has

$$\langle N_k\rangle = \frac{1}{4}\Big\{(\mu_1 - \mu_4)^2 + \Big(m_0\omega_0\mu_3 + \frac{1}{m_0\omega_0}\mu_2\Big)^2\Big\}, \tag{16}$$

$$\begin{aligned}\langle N_k^2\rangle \ = \ & \frac{1}{8}\Big\{(\mu_1 - \mu_4)^2 + (m_0\omega_0\mu_3 + \frac{1}{m_0\omega_0}\mu_2)^2\Big\} \\ & \Big\{(\mu_1 + \mu_4)^2 + (m_0\omega_0\mu_3 - \frac{1}{m_0\omega_0}\mu_2)^2\Big\} + \frac{1}{16}\Big\{(\mu_1 - \frac{1}{m_0\omega_0}\mu_2)^2\Big\}^2 .\end{aligned} \tag{17}$$

With these expressions, we evaluate the ratio of the mean squared fluctuation $(\Delta N_k)^2$ and the mean number of photons $\langle N_k\rangle$, which determines the nature of the distribution function of the system:

$$\frac{(\Delta N_k)^2}{\langle N_k\rangle} = \frac{1}{2}\Big\{(\mu_1 + \mu_4)^2 + \Big(m_0\omega_0\mu_3 - \frac{1}{m_0\omega_0}\mu_2\Big)^2\Big\} \tag{18}$$

For the cases (4) and (5) the ratio is greater than one when $t > 0$, which implies that we have a super-Poissonian photon distribution function. For $t = 0$, there is a discontinuity in the ratio, which is obtained by comparing the following limiting procedures: making $t \to 0$ and then $\vec{\alpha} \to 0$, and conversely.

# 4 Dispersion Matrices

The dispersion matrix can be written in terms of $2 \times 2$ matrices characterizing the dispersions in the positions and momenta operators and the correlation between them. Besides for the cases under study, due to (6), they take the form

$$\sigma_{pp}^2(t) = \frac{1}{2}\hbar m_0\omega_0\Big(\frac{1}{(m_0\omega_0)^2}\mu_2^2 + \mu_4^2\Big)\ \mathbf{I_2}\ , \tag{19}$$

$$\sigma^2_{qp}(t) = -\frac{\hbar}{2}\Big(\frac{1}{m_0\omega_0}\mu_1\mu_2 + m_0\omega_0\mu_3\mu_4\Big)\,\mathbf{I_2}\ , \tag{20}$$

$$\sigma^2_{qq}(t) = \frac{1}{2}\frac{\hbar}{m_0\omega_0}(\mu_1^2 + (m_0\omega_0)^2\mu_3^2)\,\mathbf{I_2}\ . \tag{21}$$

The corresponding correlation matrices for the creation and annihilation operators are obtained immediately from the last expressions; they are given by

$$\sigma^2_{aa} = \frac{1}{4}\Big\{\mu_1^2 - \mu_4^2 + (m_0\omega_0)^2\mu_3^2 - \frac{\mu_2^2}{(m_0\omega_0)^2} - 2i\Big(\frac{1}{m_0\omega_0}\mu_1\mu_2 + m_0\omega_0\mu_3\mu_4\Big)\Big\}\ , \tag{22}$$

$$\sigma^2_{a^\dagger a} = \frac{1}{4}\Big(\mu_1^2 + \mu_4^2 + (m_0\omega_0)^2\mu_3^2 + \frac{\mu_2^2}{(m_0\omega_0)^2}\frac{m_0\omega_0}{\hbar}\Big), \tag{23}$$

$$\sigma^2_{a^\dagger a^\dagger} = \frac{1}{4}\Big\{\mu_1^2 - \mu_4^2 + (m_0\omega_0)^2\mu_3^2 - \frac{\mu_2^2}{(m_0\omega_0)^2} + 2i\Big(\frac{1}{m_0\omega_0}\mu_1\mu_2 + m_0\omega_0\mu_3\mu_4\Big)\Big\}\ . \tag{24}$$

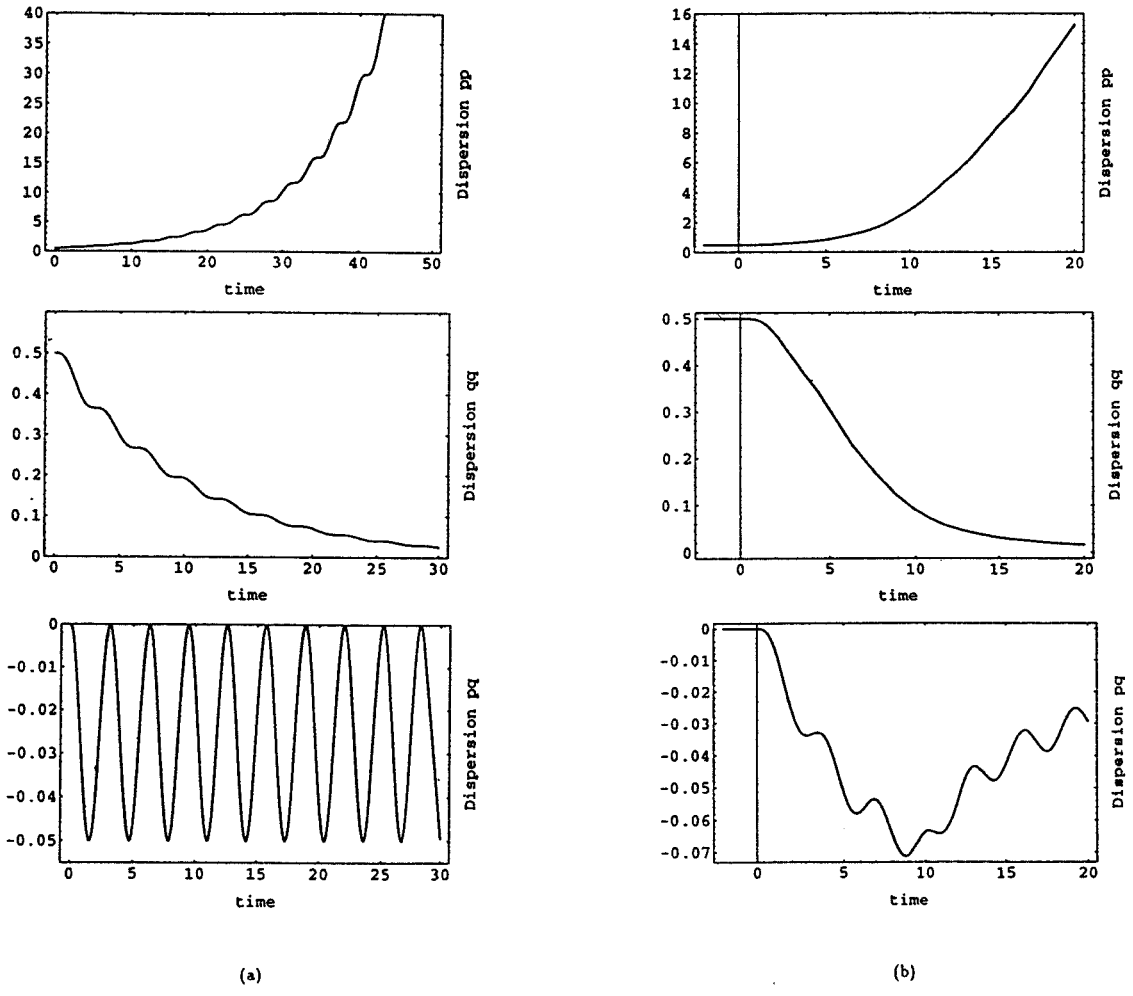


Fig. 1. Dispersion and correlation matrices behavior in positions and momenta space for the studied cases in this paper: (a) corresponds to Eq.(4), and (b), to Eq.(5).

The behavior of the dispersion matrices is illustrated in Fig. 1. For the case (4), we choose the parameters $\gamma = 0.1$ and $m_0 = \omega_0 = 1$. It is seen that there is squeezing for the coordinates and stretching for the momenta. Also one notes that $\sigma_{pq}$ is a negative function and therefore there are one-mode correlations between the coordinates and the momenta. If we reverse the sign of $\gamma$, the roles between the dispersion for coordinates and momenta are interchanged, and $\sigma_{pq}$ becomes positive. In the case (5), we use the parameters $\Omega_0 = 0.15$, $T = 10$, and $m_0 = \omega_0 = 1$. In spite of the mass is different that in the previous example, the general trends are similar. For example, the $\sigma_{pp}$ is an increasing function of time starting from its minimum value at $t \leq 0$, and there is squeezing for the $\sigma_{qq}$. The main difference appears in the correlation $\sigma_{pq}$: in this case, it can be positive for large times, while in the previous one is negative or zero for any time.

# 5 Acknowledgments

Work supported in part by projects UNAM-DGAPA IN-103091 and CONACYT 1570-E9208.

# References

[1] D. R. Robinson, *Commun. Math. Phys.* **1**, 159 (1965).

[2] D. Stoler, *Phys. Rev. D* **4**, 1925 (1971).

[3] E. Y. C. Lu, *Lett. Nuovo Cimento* **2**, 1458 (1971); **4**, 585 (1972).

[4] H. P. Yuen and J. H. Shapiro, *IEEE Trans. Inform. Theory IT* **24**, 657 (1978); **26**, 78 (1980).

[5] C. M. Caves and B. L. Schumaker, *Phys. Rev. A* **31**, 3068 (1985); B. L. Schumaker and C. M. Caves. *Phys. Rev. A* **31**, 3093 (1985).

[6] B. Yurke, S. L. McCall and J. R. Klauder. *Phys.Rev. A* **33**, 4033 (1986).

[7] Y. S. Kim and V. I. Man'ko, *Phys. Lett. A* **157** (1991), 226.

[8] R. Glauber, in *Proc. of Quantum Optics Conference*, Hyderabad, January 5-10, 1991, Eds. G. S. Agarwal and R. Ingua, Plenum Presss, 1993.

[9] O. Castaños and R. López-Peña, *J. Phys. A: Math. Gen.* **25**, 6685 (1992).

[10] O. Castaños, R. López-Peña, and V. I. Man'ko: *Noether's Theorem and Time-Dependent Quantum Invariants.* Submitted for publication.

[11] V. V. Dodonov and V. I. Man'ko, in: Proc. P. N. Lebedev Physical Institute, Vol. 183. *Invariants and evolution of non-stationary quantum systems*, Ed. M. A. Markov (Nova Science, Commack, N. Y., 1987).

[12] V. V. Dodonov, V. I. Man'ko, and V. V. Semjonov, *Nuovo Cimento B* **83**, 145 (1984).

# SIMULTANEOUS TWO COMPONENT SQUEEZING IN GENERALIZED q–COHERENT STATES

Roger J. McDermott and Allan I.Solomon
*Faculty of Mathematics, Open University*
*Walton Hall, Milton Keynes, MK7 6AA, U.K.*

**Abstract**

Using a generalization of the q-commutation relations, we develop a formalism in which it is possible to define generalized q-bosonic operators. This formalism includes both types of the usual q-deformed bosons as special cases. The coherent states of these operators show interesting and novel noise reduction properties including simultaneous squeezing in both field components, unlike the conventional case in which squeezing is permitted in only one component. This also contrasts with the usual quantum group deformation which also only permits one component squeezing.

## 1 Deformed Commutation Relations

Consider the single particle deformed commutation relation [1]

$$aa^\dagger - f(N)a^\dagger a = 1 \tag{1}$$

where $a^\dagger$ and $a$ are generalized creation and annihilation operators, $N$ is the number operator such that $N|n\rangle = n|n\rangle$, $f$ is a real function, and the vacuum $|0\rangle$ is defined by $a|0\rangle = 0$. We define a normalized one-particle state by $a^\dagger|0\rangle = |1\rangle$. This formalism incorporates the deformation schemes previously encountered in the literature as special cases.

**Examples:**

1. $f(N) = 1$.
   This is the usual commutation relation of the Heisenberg–Weyl algebra and describes ordinary quantum mechanical bosonic systems such as the the harmonic oscillator.

2. $f(N) = q$.
   The so–called q–oscillator, first suggested by Arik and Coon [2]. It has since been studied in detail by several authors e.g. Jannussis et al [3], Kuryshkin [4], Kulish and Damaskinsky [5].

3. $f(N) = \frac{q^{N+2}+1}{q(q^N+1)}$.
   This gives a deformed commutation relation equivalent to that of the q–boson first discovered by Macfarlane [6] and Biedenharn in connection with the representation theory of quantum groups.

4. This form of deformed commutation relation can also be related to the extensive work of Bonatsos, Daskaloyannis and others,[7] and refs. therein, on the generalized oscillator formalism as well as the recent work of Jannussis [8].

Building up normalized eigenstates of the number operator $N$ by repeated application of the generalized creation operators in (1), we obtain

$$|n\rangle = \frac{(a^\dagger)^n}{([n]!)^{\frac{1}{2}}}|0\rangle. \tag{2}$$

where the function $[n]$ is defined recursively by

$$[n+1] = 1 + f(n)[n] \tag{3}$$

with initial condition $[0] = 0$.

Explicitly, we see

$$\begin{aligned} [n] &= 1 + f(n-1) + f(n-1)f(n-2) + f(n-1)f(n-2)f(n-3) \\ &\quad + \cdots + f(n-1)f(n-2)\cdots f(2)f(1) \end{aligned} \tag{4}$$

$$= \sum_{k=0}^{n-1} \frac{f(n-1)!}{f(k)!}. \tag{5}$$

The functions $[n]$ can be thought of as generalizations of the basic numbers of q-analysis [9]. They obey a highly non–linear arithmetic but for appropriate choice of the function $f$, they tend in some limit to the ordinary integers.

# 2 Coherent States

Conventional coherent states of the oscillator obeying the undeformed commutation relation ($f(N) = 1$) may be defined by

$$a|\lambda\rangle = \lambda|\lambda\rangle \tag{6}$$

or equivalently

$$|\lambda\rangle = \frac{1}{\exp(|\lambda|^2)} \exp(\lambda a^\dagger)|0\rangle \tag{7}$$

where the exponentional function, by definition, has the property

$$\frac{d}{dx}\exp(\lambda x) = \lambda \exp(\lambda x) \tag{8}$$

These definitions of coherent states have been used to generalize the concept to the cases where the commutation relations have been deformed.

Given the q–commutation relation $aa^\dagger - q\,a^\dagger a = 1$, we may define coherent states $|\lambda\rangle$ by

$$a|\lambda\rangle = \lambda|\lambda\rangle \tag{9}$$

To achieve the alternative definition given by (7), it is necessary to introduce a q–derivative operator [9], ${}_qD_x$ such that

$${}_qD_x E_q(\lambda x) = \lambda E_q(\lambda x) \tag{10}$$

where $E_q(x)$ is the Jackson q–exponential. When this is done, we see that

$$|\lambda\rangle = \frac{1}{E_q(|\lambda|^2)} E_q(\lambda a^\dagger)|0\rangle \tag{11}$$

The same procedure can also be used to define q–coherent states for the Macfarlane–Biedenharn oscillator (although in this case the generalization of the exponential function is different from that of Jackson).

For $[n]$ (defined by (5)), an analytic function of the variable $n$, it is possible to extend the above analysis to the case of bosonic creation and annihilation operators obeying the general commutation relations (1).

We define an operator $D_x$ such that

$$D_x = \frac{1}{x}\left[x\frac{d}{dx}\right]. \tag{12}$$

This acts as a generalized differential operator
e.g.

$$D_x\, x^n = [n]x^{n-1}. \tag{13}$$

The eigenfunctions of $D_x$ given by

$$E(x) = \sum_{n=0}^{\infty} \frac{x^n}{[n]!}. \tag{14}$$

are well–defined provided the function $f$ satisfies the appropriate convergence criteria. If $f(n) \geq 1$ as $n \to \infty$ then $E(x)$ converges for all real values of $x$. If $f(n) < 1$ as $n \to \infty$ then convergence is ensured for a certain range of $x$ dependent on the precise nature of the function $f$.

Since $a\,E(\lambda a^\dagger)|0\rangle = \lambda E(\lambda a^\dagger)|0\rangle$, we can use $E(x)$ to define analogues of coherent states as normalized eigenstates of the generalized annihilation operator.

$$|\lambda\rangle = \{E(|\lambda|^2)\}^{-\frac{1}{2}} E(\lambda a^\dagger)|0\rangle \tag{15}$$

# 3 Noise Reduction Properties

We consider conventional (undeformed) bosons.

The electromagnetic field components $x$ and $p$ are given by

$$x = \frac{1}{\sqrt{2}}(a + a^\dagger) \quad \text{and} \quad p = \frac{1}{i\sqrt{2}}(a - a^\dagger). \tag{16}$$

As usual, we define the variances $(\Delta x)$ and $(\Delta p)$ by

$$(\Delta x)^2 = \langle x^2 \rangle - \langle x \rangle^2 \quad \text{and} \quad (\Delta p)^2 = \langle p^2 \rangle - \langle p \rangle^2. \tag{17}$$

In the vacuum state

$$(\Delta x)_0 = \frac{1}{\sqrt{2}} \quad \text{and} \quad (\Delta p)_0 = \frac{1}{\sqrt{2}}. \tag{18}$$

and so

$$(\Delta x)_0 (\Delta p)_0 = \frac{1}{2}. \tag{19}$$

The commutation relation for $a$ and $a^\dagger$ leads to the following uncertainty principle

$$(\Delta x)(\Delta p) \geq \frac{1}{2} |\langle [x, p] \rangle| = \frac{1}{2}. \tag{20}$$

Thus the vacuum state attains the lower bound for the uncertainty, as do the coherent states.

While it impossible to lower the product $(\Delta x)(\Delta p)$ below the vacuum uncertainty value, it is nevertheless possible to define *squeezed* states [11] for which (at most) one quadrature lies below it's vacuum value, i.e.

$$(\Delta x) < (\Delta x)_0 = \frac{1}{\sqrt{2}} \quad \text{or} \quad (\Delta p) < (\Delta p)_0 = \frac{1}{\sqrt{2}} \tag{21}$$

If we now consider the generalized bosonic operators given by (1), using the same definitions for the the field quadratures, $x$ and $p$, as in (16) we find that, just as in the conventional case, the vacuum uncertainty product $(\Delta x)_0 (\Delta p)_0 = \frac{1}{2}$ is a lower bound for all *number* states.

*However, unlike the conventional case, it is not a global lower bound.*

Consider the quadrature values in eigenstates of the generalized annihilation operator.

Then

$$\langle x \rangle_\lambda = \langle \lambda | \frac{1}{\sqrt{2}} (a^\dagger + a) | \lambda \rangle = \frac{1}{\sqrt{2}} (\lambda + \bar{\lambda}) \tag{22}$$

and

$$\langle x^2 \rangle_\lambda = \langle \lambda | \frac{1}{2} ((a^\dagger)^2 + a^2 + a^\dagger a + a a^\dagger) | \lambda \rangle \tag{23}$$

$$= \frac{1}{2} \{ (\bar{\lambda} + \lambda)^2 + 1 - \varepsilon_{f,\lambda} |\lambda|^2 \} \tag{24}$$

where

$$\varepsilon_{f,\lambda} = 1 - \langle f(N+1) \rangle_\lambda \tag{25}$$

If we choose $0 < f(n) < 1$, then it can be shown that $\varepsilon_{f,\lambda}|\lambda|^2 \in (0,1)$ for $\lambda$ within the radius of convergence of the generalized exponential.

Hence

$$(\Delta x)^2_\lambda = \frac{1}{2}\{1 - \varepsilon_{f,\lambda}|\lambda|^2\} \tag{26}$$

Evaluating the variance for the other component, we find that $(\Delta p)^2_\lambda = (\Delta x)^2_\lambda$ so

$$(\Delta x)_\lambda(\Delta p)_\lambda = \frac{1}{2}\{1 - \varepsilon_{f,\lambda}|\lambda|^2\} < \frac{1}{2} \tag{27}$$

However, it can also be shown that

$$\frac{1}{2}\{1 - \varepsilon_{f,\lambda}|\lambda|^2\} = \frac{1}{2}|\langle[x,p]\rangle_\lambda| \tag{28}$$

so

$$(\Delta x)_\lambda(\Delta p)_\lambda = \frac{1}{2}|\langle[x,p]\rangle_\lambda| \tag{29}$$

Thus we see that these generalized q–coherent states satisfy a restricted form of the Minimum Uncertainty Property (M.U.P.) of the conventional coherent states. Additionally we see that there is a general noise reduction in both quadratures compared to their vacuum value. In conventional coherent states there is no noise reduction relative to the vacuum value. In conventional squeezed states, there is noise reduction in only one component.

# 4 Special Cases

We can apply the preceding analysis to the q-deformed bosons recently studied in connection with quantum groups (e.g. [5]).

**a). 'Physics' q–bosons**

First consider the q-bosons described by Macfarlane and Biedenharn [6].
These use the definition of the generalised number, $[n]$, recently discussed in the Physics literature and so will be termed '*physics*' q–bosons. They are characterised by the deformed commutation relation

$$aa^\dagger - q\,a^\dagger a = q^{-N}. \tag{30}$$

This can be rewritten [1] as

$$aa^\dagger - f(N)\,a^\dagger a = 1 \tag{31}$$

where $f(N) = \frac{q^{N+2}+1}{q(q^N+1)}$
In this case, for normalizable eigenstates, the function $\varepsilon_{f,\lambda}$ is negative and so noise reduction does not take place. This is in agreement with the findings of Katriel and Solomon [12].

**b). 'Maths' q–bosons**

We now consider the q-boson described by Arik and Coon [2]. This uses the generalized number function found in classical q–analysis and will therefore be termed a '*maths*' q–boson. It is characterised by the deformed commutation relation

$$aa^\dagger - q\,a^\dagger a = 1 \tag{32}$$

For $q \in (0,1)$, the Jackson q-exponential $E_q(|\lambda|^2)$ converges, provided $\varepsilon_q|\lambda|^2 = (1-q)|\lambda|^2 < 1$. Given this condition on $\lambda$, we have normalizable q-analogue coherent states satisfying (6) in which

$$(\Delta x)^2_\lambda = (\Delta p)^2_\lambda = (\Delta x)_\lambda(\Delta p)_\lambda = \frac{1}{2}\{1 - \varepsilon_q|\lambda|^2\} < \frac{1}{2} \tag{33}$$

Hence, for this type of q–boson, we do obtain noise reduction in both quadratures with respect to the vacuum value.

# 5 Acknowledgements

One of us (R.J.M.) would like to thank the organizers of the workshop for their generous financial assistance.

# References

[1] A.I. Solomon and J.L. Birman *Symmetries in Science VII* ed. B. Gruber, (Plenum Press, N.Y., 1993).

[2] M. Arik and D.D. Coon *J. Math. Phys.* **17** 524 (1976).

[3] A. Jannussis, L.C. Papaloucas and P.D. Siafarikas *Had. J.* **3** 1622 (1980)

[4] V.V. Kuryshkin *Ann. Fond. L. de Broglie* **5** 111 (1980).

[5] P.P. Kulish and E.V. Damaskinsky *J. Phys. A.* **23** 415 (1990).

[6] A.J. Macfarlane *J. Phys. A.* **22** 4581 (1989).
L.C. Biedenharn *J. Phys. A.* **22** L873 (1989).

[7] C. Daskaloyannis *J. Phys. A.* **25** 2261 (1992).
D. Bonatsos and C. Daskaloyannis *J. Phys. A.* **26** 1589 (1993).

[8] A. Jannussis *J. Phys. A.* **26** L233 (1993)

[9] F.H. Jackson *Mess. Math.* **38** 62 (1909).
H. Exton *q-Hypergeometric Functions and Applications*, (Ellis Horwood, Chichester, 1983)

[10] R.J. Glauber *Phys. Rev.* **131** 27 66 (1963).

[11] H.P. Yuen *Phys. Rev. A.* **13** 2226 (1976).

[12] J. Katriel and A.I. Solomon *J. Phys. A.* **24** 2093 (1991).

# PHOTON STATISTICS OF A TWO-MODE SQUEEZED VACUUM

G. Schrade, V. M. Akulin [1], W. P. Schleich [2]
*Abt. für Quantenphysik, Universität Ulm*
*D-89069 Ulm, Germany*

V. I. Man'ko [3]
*Dipartimento di Scienze Fisiche*
*Universita di Napoli Federico II*
*80125 Napoli, Italy*

**Abstract**

We investigate the general case of the photon distribution of a two-mode squeezed vacuum and show that the distribution of photons among the two modes depends on four parameters: two squeezing parameters, the relative phase between the two oscillators and their spatial orientation. The distribution of the total number of photons depends only on the two squeezing parameters. We derive analytical expressions and present pictures for both distributions.

## 1 Introduction

Squeezing the quantum fluctuations of the radiation field has been demonstrated experimentally using various optical systems [1]. Most of them rely on two-mode squeezing [2, 3, 4]. Therefore the properties of a two-mode squeezed state have been studied extensively [5, 6]. However it appears, that the photon statistics of such a state has not been investigated in all details. Only some particular cases have been considered (see for example Refs. [7] and [8]). In the present paper we therefore extend these considerations to an arbitrary two-mode squeezed vacuum and address the following questions: (i) What is the most general case of the squeezed vacuum of a two-mode oscillator, and how many independent parameters are needed to describe this state? (ii) What is the photon statistics in this state? This is of interest in the context of the degenerate parametric amplifier [9] since the mathematical structure of the two-mode distribution function coincides with the transition probability function of a two-dimensional parametric oscillator [10].

[1] also Moscow Institute of Physics and Technology Dolgoprudny, Moscow, Russia
[2] also Max-Planck-Institut für Quantenoptik, D-85748 Garching, Germany
[3] permanent address: Lebedev Institute of the Academy of Sciences, Moscow, Russia

## 2 general case of the squeezed vacuum of a two-mode oscillator

We start our considerations with the question (i). The linear canonical transformation

$$(a^\dagger, a; b^\dagger, b) \longrightarrow (A^\dagger, A; B^\dagger, B) \tag{1}$$

of the creation operators $a^\dagger$, $b^\dagger$ and the annihilation operators $a$, $b$ to their new counterparts $A^\dagger$, $B^\dagger$ and $A$, $B$ corresponding to the two modes suggests a set of 10 parameters. Indeed, the generic transformation (1) of the four-dimensional vector $(a^\dagger, a, b^\dagger, b)$ into $(A^\dagger, A, B^\dagger, B)$ via a $4 \times 4$ matrix brings in 16 complex values, that is 32 parameters. Since $a$ and $a^\dagger$, $b$ and $b^\dagger$ ,$A$ and $A^\dagger$, $B$ and $B^\dagger$ are hermitian conjugate of each other, only half of these parameters are independent. Therefore the number of parameters reduces to 16. The condition to preserve the commutation relation $[A, B] = 0$, $[A, B^\dagger] = 0$, $[A, A^\dagger] = 1$, and $[B, B^\dagger] = 1$ provides additional constraints. Since the commutator of an operator with its hermitian conjugate is always real, the last two conditions provide only two constraints, whereas the first two conditions must hold for the real and the imaginary part separately. This decreases the number of parameters by six leaving us indeed with 10 parameters.

This finding is in accordance with the results of group theory. Reference [11] shows, that the group of rotations and squeezing of the four-dimensional phase space, that preserves the phase space volume of the two degrees of freedom, consists of 10 generators. Hence there are 10 parameters determining the elements of the real symplectic group Sp(4,R).

But what is the physical meaning of these parameters? They are associated with rotation and squeezing transformation of phase space of two oscillators. Generic rotations of four-dimensional phase space are described by 6 parameters but the symplectic rotations in four-dimensional space, that is the transformation preserving the commutation relations, are described by 4 parameters. They can be represented as a sequence of four rotations. The first rotation given by the transformation $e^{i\hat{M}\phi_1}$, where $\hat{M} = i(a^\dagger b - b^\dagger a)$ is the angular momentum operator, corresponds to the rotation in the coordinate space by the angle $\phi_1$. The second and the third rotations are given by the operator $e^{i\psi a^\dagger a}$ and $e^{i\chi b^\dagger b}$, and correspond to rotations by the angles $\psi$ and $\chi$ in the respective phase-spaces of the two oscillators. The last rotation again can be taken in the form $e^{i\hat{M}\phi_2}$. Thus the angles $\phi_1$, $\phi_2$, $\psi$ and $\chi$ are chosen to be the parameters of the symplectic rotation. The general symplectic transformation also includes squeezing. We can represent the generic real symplectic transformation (1) as consisting of three consecutive transformations: symplectic rotation (4 parameters), followed by independent squeezing of the two modes given by the squeezing operators

$$\hat{S}_1 = e^{r_1(a^2 - a^{\dagger 2})/2}, \qquad \hat{S}_2 = e^{r_2(b^2 - b^{\dagger 2})/2}, \tag{2}$$

(2 squeezing parameters $r_1$ and $r_2$) and followed by another real symplectic rotation (4 parameters more). But how many of these parameters govern the two-dimensional squeezed vacuum state? The first four parametric rotation acting on the completely symmetric vacuum state leaves this state unchanged. Hence 2 squeezing parameters and 4 parameters associated with the second rotations define the two-dimensional squeezed vacuum state. In addition we can include an overall quantum phase factor $e^{i\rho}$ of this state. An explicit calculation of the general case of a two-mode squeezed vacuum wave function is given in Ref. [12].

# 3 Photon statistics for the total number of photons

We now address the question: how many of these parameters govern the photon statistics of such a two-dimensional squeezed vacuum state? In particular, how many of them determine the probability of (i) counting a total number $n$ of photons in the two modes, and (ii) counting the number $n_1$ and $n_2$ of photons in the individual modes?

In this section we consider the case of (i) and ask for the total number $n$ of photons in both modes, which corresponds to the surface of a four-dimensional sphere, $\frac{1}{2}(p_1^2 + x_1^2 + p_2^2 + x_2^2) = n$, centered at the origin of the four-dimensional phase space. The rotation of the phase space does not alter this sphere and hence only two squeezing parameters are essential. The probability of counting the total number $n$ of photons for the case of two independently squeezed oscillators reads

$$W_n(s_1, s_2) = \sum_{n_1=0}^{n} W_{n_1}(s_1) W_{n-n_1}(s_2), \tag{3}$$

where $W_{n_j}(s_j)$ is the one-dimensional photon statistics [13]

$$W_{n_j}(s_j) = \begin{cases} 0 & \text{for } n_j \text{ odd} \\ \sqrt{1-s_j}\, s_j^{n_j/2} 2^{-n_j} \binom{n_j}{n_j/2} & \text{for } n_j \text{ even} \end{cases} \tag{4}$$

of the squeezed vacuum wave function

$$\Psi_{sq}(x_j) = \frac{e^{r_j/2}}{\pi^{1/4}} \exp(-\frac{1}{2} e^{2r_j} x_j^2) \tag{5}$$

where

$$s_j = \tanh^2(r_j). \tag{6}$$

Equation (4) reduces Eq. (3) to

$$W_n(s_1, s_2) = \begin{cases} W_{2k}(s_1, s_2) = \mathcal{N} 4^{-k} \sum_{n_1=0}^{k} s_1^{n_1} s_2^{k-n_1} \binom{2n_1}{n_1} \binom{2(k-n_1)}{k-n_1} \\ W_{2k+1}(s_1, s_2) = 0 \end{cases} \tag{7}$$

where the normalization factor $\mathcal{N}$ reads

$$\mathcal{N} = \sqrt{1-s_1}\sqrt{1-s_2}. \tag{8}$$

The odd terms of $W_n$ vanish because of Eq. (4) . The sum in Eq. (7) has been calculated in [12] and the probability of counting $n = 2k$ photons then reads

$$W_{2k}(s_1, s_2) = \mathcal{N} s_2^k \, {}_2F_1(-k, 1/2, 1; 1 - s_1/s_2) \tag{9}$$

where ${}_2F_1$ describes the hypergeometric function. For the special case of identical squeezing in the two modes, that is, $s_1 = s_2 = s$, Eq. (9) yields

$$W_{2k}(s) = \mathcal{N} s^k. \tag{10}$$

In Fig. 1 we show the photon statistics (9) for various magnitudes of the squeezing parameters $s_1$ and $s_2$. The solid and dashed curves correspond to weak and strong symmetric squeezing ($s_1 = s_2$), respectively. In accordance with Eq. (10) the photon distribution then displays an exponential dependence. Stronger squeezing results in a higher amount of quanta involved. The dotted curve shows the photon statistic for an asymmetric squeezing.

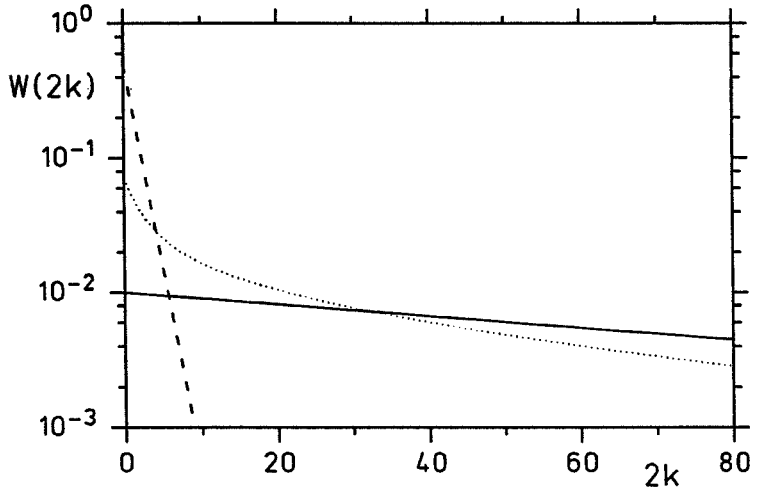


Fig. 1. Probability of counting $n = 2k$ photons in a two-mode squeezed vacuum as given by Eq. (9). For symmetric squeezing (dashed line for $s_1 = s_2 = 0.5$ and solid line for $s_1 = s_2 = 0.99$) the curve is a straight line and hence exponential whereas for asymmetric squeezing (dotted line for $s_1 = 0.5$ and $s_2 = 0.99$ ) the photon statistics is non-exponential. Here we have not specified the distribution of the $n = 2k$ photons among the two modes. Note that $W_{n=2k+1} = 0$ which we have omitted for simplicity.

# 4 Photon statistics in the individual modes

We now turn to the second case and calculate the photon statistics $W(n_1, n_2) = |< n_1, n_2|\Psi_{sq}>|^2$ in the individual modes. For this purpose we start from the generic expression of a squeezed vacuum state $|\Psi_{sq}>$, which we produce in the following way:

$$\begin{aligned}\Psi_{sq}(x_1, x_2) &= e^{i\rho}\, e^{-i\phi\hat{M}}\, \hat{\Gamma}(\gamma)\, \hat{S}_1(r_1)\, \hat{S}_2(r_2)\, \Psi_{0,0}(x_1, x_2) \\ &= \sqrt{\frac{2}{\pi}}\, (A_1 B_1 - C_1^2)^{1/4}\, e^{-Ax_1^2 - Bx_2^2 + 2Cx_1x_2 + i\rho} \end{aligned} \tag{11}$$

with the vacuum wave function of the two-dimensional oscillator $\Psi_{0,0}(x_1, x_2) = \Psi_0(x_1)\, \Psi_0(x_2)$, the angular momentum operator $\hat{M} = i\,(a^\dagger b - b^\dagger a)$ and the operator $\hat{\Gamma}(\gamma) = \exp(i\gamma(b^\dagger b - a^\dagger a))$ which describes a mutual phase shift $2\gamma$ between the oscillators. The wave function of a two-dimensional squeezed vacuum state is a Gaussian described by the three complex numbers $A$, $B$, and $C$, which are functions of the four real parameters $r_1$, $r_2$, $\phi$, and $\gamma$. Their explicit dependence is given in [12]. One also finds there the generic two-mode squeezed vacuum wave function depending on two more parameters that do not affect the photon distribution.

We contract Eq. (11) with the probability amplitude of the photon energy states $\psi_{n_1}(x_1)$ and $\psi_{n_2}(x_2)$ and arrive after calculating the resulting double integral [12] at

$$
\begin{aligned}
W(n_1,n_2) \;=\; & \frac{8\,\exp(-|\ln(n_1!/n_2!)|)}{|(2A+1)(2B+1)-4C^2|}\,(A_1B_1-C_1^2)^{1/2}\;\times \\
& \times\left|\frac{4AB+2A-2B-1-4C^2}{4AB-2A+2B-1-4C^2}\right|^{(n_1-n_2)/2}\;\times \\
& \times\left|\frac{4AB-2A-2B+1-4C^2}{4AB+2A+2B+1-4C^2}\right|^{(n_1+n_2)/2}\;\times \\
& \times\left|P^{|n_1-n_2|/2}_{|n_1+n_2|/2}\left(\frac{-4C}{\sqrt{4AB+2A+2B+1-4C^2}\sqrt{4C^2-4AB+2A+2B-1}}\right)\right|^2 .
\end{aligned}
\tag{12}
$$

Here $P_l^k$ denotes the associated Legendre Polynomial. As in Eq. (7) the total number of photons $n = n_1+n_2$ must be an even number hence $n_1$ and $n_2$ are either both even or both odd. Otherwise the photon distribution function vanishes.

In Fig. 2 we display the probability to find $n_1$ photons in mode 1 and $n_2$ photons in mode 2. This is the generic case of the photon distribution of a two-mode squeezed vacuum. It depends on four parameters: two squeezing parameters, the orientation of the distribution function with respect to our laboratory system, and the correlation between the two modes. Beside the even-odd oscillations the maxima lie on curves which are symmetric with respect to the main diagonal $n_1 = n_2$. This behavior is similar to the distribution function of a displaced two-mode squeezed state discussed in Ref. [7, 8].

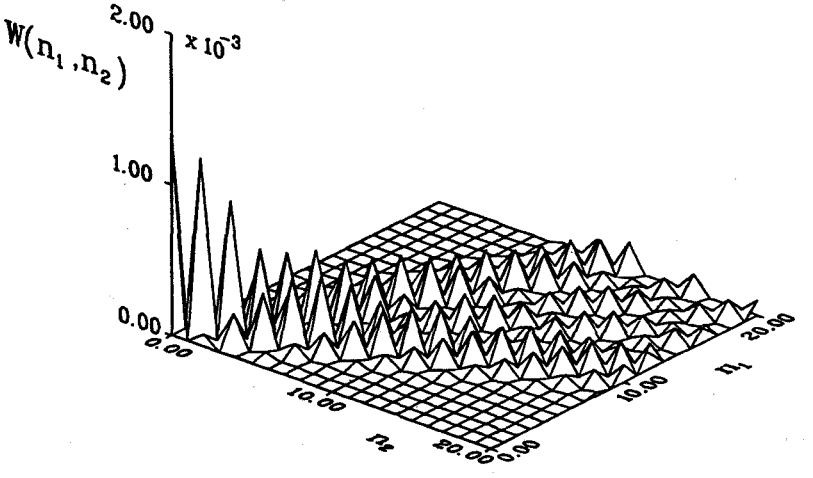


Fig. 2. Probability of counting $n_1$ and $n_2$ photons in the two-mode squeezed vacuum calculated via Eq. (12). We have chosen $r_1 = 3$, $r_2 = 5$, $\phi = \frac{\pi}{5}$, and $\gamma = \frac{2\pi}{9}$. The wavy structure of this distribution is confined to an angle in the photon number plane.

# 5 Conclusion

We conclude by summarizing our main results. The wave function of the two-mode squeezed vacuum depends on 6 parameters (besides the phase factor). However only 4 of them, – the squeezing parameters $r_1$ and $r_2$ of the two modes, the phase difference $\gamma$ between the two oscillators, and the rotation of the reference system by the angle $\phi$ – manifest themselves in the generic case in the distribution of the photons among the two modes. This distribution function can be expressed explicitly in terms of Legendre polynomials. Only two parameters $r_1$ and $r_2$ govern the distribution of the total number of photons, which we express explicitly in terms of a hypergeometric function. In conclusion we want to make the remark that similar consideration for $N$-mode squeezed vacuum state shows that the photon distribution $W(n_1, n_2, ..., n_N)$ depends on $N^2$ parameters.

# 6 Acknowledgments

One of the authors (V.I.M.) thanks the University of Ulm and in particular the Hans-Kupczyk Foundation for the support which made this research possible.

# References

[1] For a review on squeezed states see, for example, special issues on squeezed states in J. Opt. Soc. Am. B **4**, No. 10 (1987); and Appl. Phys. B **55**, No. 3 (1992).

[2] C. M. Caves and B.L. Schumaker, Phys. Rev. A **31**, 3068 (1985).

[3] S. M. Barnett and P. L. Knight, J. Opt. Soc. Am. B **2**, 467 (1985).

[4] B. Yurke, S. McCall, and J. R. Klauder, Phys. Rev. A **33**, 4033 (1986).

[5] B. L. Schumaker, Phys. Rep. **135**, 317 (1986).

[6] A. K. Ekert and P. L. Knight, Am. J. Phys. **57**, 692 (1989).

[7] C. M. Caves, C. Zhu, G. J. Milburn, and W. Schleich, Phys. Rev. A **43**, 3854 (1991).

[8] M. Artoni, U. P. Ortiz, and J.L. Birman, Phys. Rev. A **43**, 3954 (1991).

[9] For the photon statistics of a parametric oscillator see for example R. Vyas and S. Singh, Phys. Rev. A **40**, 5147 (1989); and Opt. Lett. **14**, No. 20, 1110 (1989);

[10] I. A. Malkin, V.I. Man'ko, and D. A. Trifonov, J. Math. Phys. **14**, 576 (1973); V. V. Dodonov and V. I. Man'ko in *Invariants and the evolution of nonstationary quantum systems*, ed. by M. A. Markov, (Nova Science Publ., New York, 1989).

[11] G. J. Milburn, J. Phys. A **17**, 737 (1984).

[12] G. Schrade, V. M. Akulin, V. I. Man'ko, and W. P. Schleich, Phys. Rev. A **48**, 2398 (1993).

[13] W. Schleich and J. A. Wheeler, Nature **326**, 574 (1987).

# SECTION 2

# QUANTUM MEASUREMENT THEORY

# ON THE THEORY OF QUANTUM MEASUREMENT

Hermann A. Haus
Franz X. Kärtner
*Department of Electrical Engineering and Computer Science*
*Research Laboratory of Electronics*
*Massachusetts Institute of Technology*
*Cambridge, MA 02139*

**Abstract**

Many so called paradoxes of quantum mechanics are clarified when the measurement equipment is treated as a quantized system. Every measurement involves nonlinear processes. Selfconsistent formulations of nonlinear quantum optics are relatively simple. Hence optical measurements, such as the quantum nondemolition (QND) measurement of photon number, are particularly well suited for such a treatment. It shows that the so called "collapse of the wave function" is not needed for the interpretation of the measurement process. Coherence of the density matrix of the signal is progressively reduced with increasing accuracy of the photon number determination. If the QND measurement is incorporated into the double slit experiment, the contrast ratio of the fringes is found to decrease with increasing information on the photon number in one of the two paths.

## 1 Introduction

The Theory of Quantum Measurement has a long and venerable history. Many of the original discussions of the founders of quantum mechanics are contained in the reprint volume of Wheeler and Zurek[1]. Yet, inspite of its long history, the issues raised in these well known discussions have not been fully settled.

In this paper we attempt to make a modest contribution to this weighty problem. In doing so we are guided by a quote of Niels Bohr which reads: "... one sometimes speaks of "disturbance of phenomena by observation" or "creation of physical attributes to atomic objects by measurement." Such phrases, however, are apt to cause confusion, since words like phenomena and observation, just as attributes and measurements, are here used in a way incompatible with common language and practical definition. On the lines of objective description, [I advocate using] the word *phenomenon* to refer only to observations obtained under circumstances whose description includes an account of the whole experimental arrangement. In such terminology, the observational problem in quantum physics is deprived of any special intricacy and we are, moreover, directly reminded that every atomic phenomenon is closed in the sense that its observation is based on registrations obtained by means of suitable amplification devices with irreversible functioning such as, for example, permanent marks on a photographic plate, caused by the penetration of

electrons into the emulsion" [Ref. 1, p. 3]. We have underlined the words that we consider particularly worthy of note. Bohr requires a description of the whole experimental arrangement. Further, if one is to state the outcome of the experiment in classical language, large amplification is required.

At the risk of making statements that may be considered even more controversial by the adherents of the Einsteinian school, we should like to strengthen Bohr's quote by saying: "*Physical reality* cannot be formulated until the measurement equipment used to determine the observables is specified and treated as a quantum system. The *large gain* of the measurement equipment provides the classical interface at the *output* of the measurement apparatus."

Much of the controversy involving quantum measurements is the consequence of the fact that it is very difficult to describe well the measuring equipment, according to our interpretation, to describe it quantum mechanically.

In quantum optics we have made great progress in describing optical components quantum mechanically. The theory has been well tested experimentally. The squeezing by a parametric amplifier is well understood theoretically and amply confirmed experimentally[2-6]. Less extensively explored, yet also tested, is the self-phase modulation and squeezing in optical fibers via the optical Kerr effect[7-9]. Hence it appears natural to use the well tested quantum description of optical devices to construct a measurement apparatus and test some of the predictions of quantum mechanics using such a measurement apparatus. This is the main objective of this paper. We start by describing a Quantum Nondemolition Measurement of the photon number of a signal via a nonlinear Mach-Zehnder interferometer. We follow the development of the composite wave function of the signal and measurement apparatus to the output. We shall see that the photon number in the signal can be determined with a negligible probability of error if the gain of the measurement apparatus is large enough. Further, when this is the case, the density matrix of the signal, obtained by tracing over the (Hilbert) coordinates of the measurement equipment, is diagonalized. Finally, since the probability of error of measuring a particular photon number approaches zero, each measurement, and not the whole ensemble, can be interpreted as yielding an interpretable result. This corresponds to the von Neumann projection operator interpretation. However, when the gain is not very large, the signal density matrix does not decohere, it is not diagonalized. This is consistent with Bohr's dictum that we can put the measurement results into classical language only if the gain of the measurement equipment is very large.

When no measurement is performed, and the signal and "measurement" beams are passed on into a second nonlinear Mach-Zehnder interferometer with a Kerr coefficient of opposite sign, the entire action of the first interferometer can be undone; the wave functions emerge disentangled! This confirms the reversibility of quantum mechanics.

We conclude with the double slit experiment. We put a nonlinear Mach-Zehnder measurement apparatus in each of the two light beams. As the accuracy of the photon number determination is systematically increased, the contrast of the interference fringes decreases accordingly.

## 2 The Quantum Nondemolition Measurement

Figure 1 shows a nonlinear Mach-Zehnder interferometer. The signal beam $\hat{a}_s^{in}$ at one frequency and the probe beam $\hat{b}^{in}$ at another frequency enter a Kerr medium through a dichroic mirror. At the end of the Kerr medium they are again separated by another dichroic mirror. A portion of the probe beam has been passed on directly for interference. Classically, the Kerr medium produces a phase shift on the probe beam that can be measured giving an indication of the intensity of the signal beam. Quantum mechanically, the process is described by the Hamiltonian of the Kerr medium[10]

$$\hat{H} = \hbar\kappa\hat{a}_s^\dagger\hat{a}_s\hat{b}^\dagger\hat{b} \tag{1}$$

where $\kappa$ is a factor proportional to the Kerr coefficient; $\hat{a}_s$ is the annihilation operator of the signal photons, $\hat{b}$ that of the probe photons. They obey the usual commutation relations:

$$[\hat{a}_s, \hat{a}_s^\dagger] = 1 \tag{2}$$

$$[\hat{b}, \hat{b}^\dagger] = 1 \tag{3}$$

It should be noted that the Hamiltonian (1) does not account for a self-phase shift. This has been left out for convenience. A medium resonant at the sum frequency of signal and probe would be described by such a simplified Hamiltonian.

The two portions of the probe beam are combined by a beam splitter with the Hamiltonian:

$$\hat{H} = \hbar M[\hat{b}^\dagger\hat{c} + \hat{c}^\dagger\hat{b}] \tag{4}$$

As usual, one may consider the wave packets to evolve in time as they propagate along the system. If the beam splitter is 50/50, the parameter $M$ must be chosen

$$\frac{M\ell}{v_g} = \frac{\pi}{4} \tag{5}$$

where $\ell$ is the length of the medium and $v_g$ is the group velocity, $\ell/v_g$ is the travel time.

From the known Hamiltonian one may determine the evolution of the wave function $|\psi\rangle_s|\beta\rangle|0\rangle$ of the three input ports. They are products at the input, and become entangled at the output. We denote the output annihilation operators by $\hat{f}$ and $\hat{g}$. The balanced photodetector measures the expectation values of the difference current operator $\hat{I} = \hat{f}^\dagger\hat{f} - \hat{g}^\dagger\hat{g}$ and its moments[11].

$$\langle\hat{I}\rangle = |\beta|^2\sin(\kappa\hat{a}_s^\dagger\hat{a}) \simeq \kappa|\beta|^2\hat{a}_s^\dagger\hat{a}_s \tag{6}$$

The expectation value traced over the Hilbert space of the probe yields the sine of the signal photon operator. If the sine function can be expanded to first order, it becomes the photon operator. The mean square fluctuations follow from the second moment and are[11]

$$\langle|\Delta\hat{I}|^2\rangle = |\beta|^2 \tag{7}$$

if the signal is in a photon number state. This is shot noise since $|\beta|^2$ is the photon number in the probe beam.

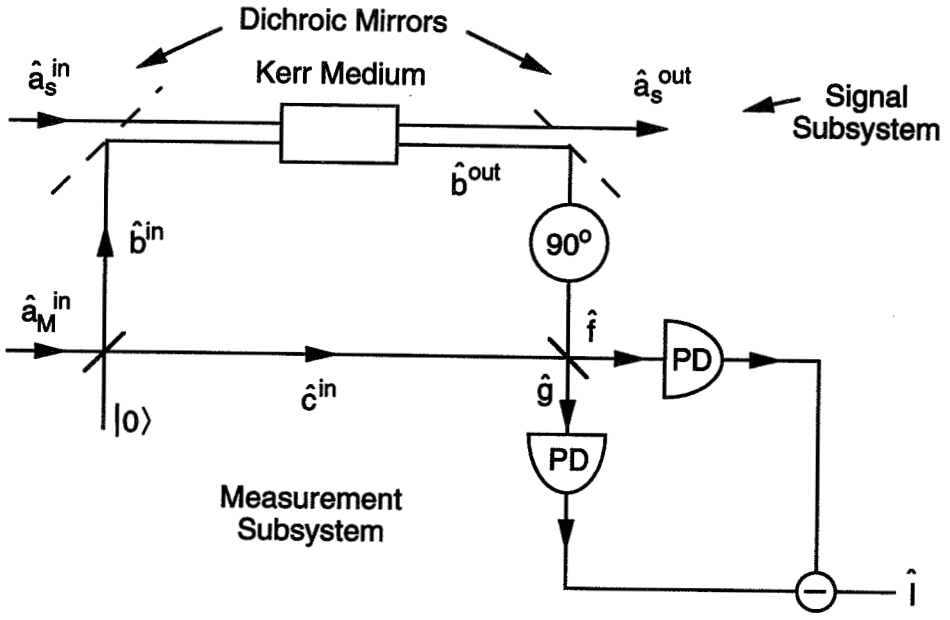


FIG. 1. Schematic of nonlinear Mach-Zehnder interferometer and balanced detector.

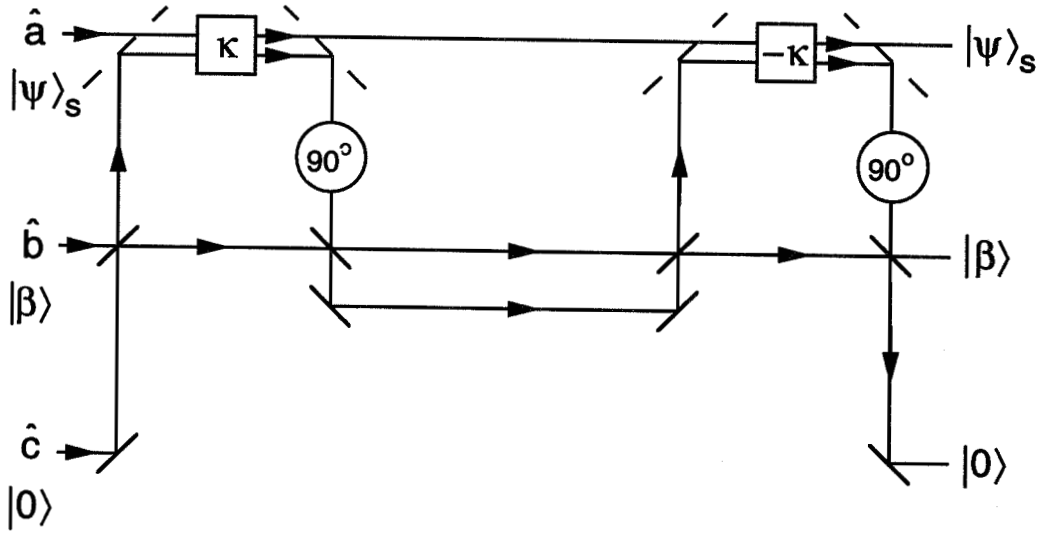


FIG. 2. Two nonlinear Mach-Zehnder interferometers with media of equal and opposite Kerr coefficients.

The probability of error follows from the mean square fluctuations (7) that approach gaussians in the large photon number limit[11]:

$$P_{\text{error}} \simeq 2\sqrt{\frac{2}{n}}\frac{1}{|\kappa\beta|}e^{-|\kappa\beta|^2/8} \tag{8}$$

If $|\kappa\beta|^2 \gg 1$, the probability of error can be made arbitrarily small. The physical meaning of this quantitity can be fathomed as follows. $\kappa|\beta|^2$ is the phase shift due to the probe photons, $\kappa$ itself is the phase shift due to one photon. The geometric mean of these two products has to be made very large. If we used fiber interferometers, these operating parameters are not easily achieved. Here, however, we are not concerned with the practical realization of the measurement apparatus, but only with the theoretical conclusions that can be drawn from it. In particular, we find that the probability of error can be made arbitrarily small, for $|\kappa\beta| = 10$, it is $10^{-6}$. This means that each measurement has vanishing error probability. Hence one may interpret every measurement, and not only the ensemble, as yielding a definite result. This is analogous to the von Neumann projection postulate which interprets a measurement as projecting the state into an eigenstate. Pursuing this interpretation further, we can say that a measurement with the Mach-Zehnder interferometer at large gain projects the signal into a photon state.

# 3 The Density Matrix

The trace of the density matrix over the measurement system part at the output of the signal-measurement system of Fig. 1 can be evaluated for a signal wave function[11]:

$$|\psi\rangle_s = \sum_n c_n|n\rangle \tag{9}$$

It is

$$\begin{aligned}\langle\rho_s\rangle &= \sum_{n=0}^{\infty} e^{-\frac{|\beta|^2}{2}}\frac{|\beta/\sqrt{2}|^{2n}}{n!}e^{i\kappa n\hat{a}^\dagger\hat{a}}|\psi\rangle_s^{\text{in}}\,{}_s^{\text{in}}\langle\psi|e^{-i\kappa n\hat{a}^\dagger\hat{a}} \\ &\simeq \sum_{m,\ell=0}^{\infty}\hat{c}_m^* c_\ell|m\rangle\langle\ell|\underbrace{e^{-\frac{|\kappa\beta|^2}{8}(m-\ell)}}_{\text{error probability}}e^{i\frac{|\beta|^2}{2}\kappa(m-\ell)}\end{aligned} \tag{10}$$

In the limit of large gain, the density matrix traced over the measurement equipment becomes diagonal at the same rate as the probability of error approaches zero (note the exponential factor!). Hence, again, we see that the signal acquires a classical (decohered) appearance when the gain of the measurement system ($|\kappa\beta|$) is made very large.

# 4 Reversibility

If one does not perform a measurement on the probe beam, but reintroduces it in the second Mach-Zehnder as shown in Fig. 2, which has a Kerr coefficient of opposite sign, one can disentangle entirely the wave functions. This shows, of course, the reversibility of quantum

mechanics if no measurement intervenes in the process. Of course, no measurement could have been undertaken, because the probe beam was completely recycled. This brings us back to the act of measurement. A measurement is an irreversible process that prevents recycling. Indeed, in the present example the probe beam is passed into a balanced detector in which it is absorbed. Only then can one apply the homodyne photon detection formula to evaluate the current operator statistics.

# 5 Tracing, Decoherence and the Act of Measurement

The density matrix of the signal system becomes diagonal in the signal Hilbert space when traced over the probe space. Tracing is a mathematical operation which, according to the postulates of quantum mechanics, evaluates expectation values. In the context of the derivation of the signal density matrix, the reduced density matrix can be interpreted as a "Gedankenexperiment" on the density matrix of the signal after passage through the Mach-Zehnder. Accompanied by the statement that the signal and probe systems would never be combined again, the entanglement that in fact exists between the two systems could never be reversed. In this sense, the reversibility of quantum mechanics is broken. In an actual measurement, of course, the apparatus works on the probe subspace, causes partial or total decoherence in that space, and leads "de facto" to an irreversible action.

# 6 Two Slit Experiment

Finally, let us look at the "two-slit" interference experiment of Fig. 3. The two slits are here replaced by the two arms of an interferometer. A phase shifter in one of the arms changes the phase of the superimposed beams. If the two beams were perfectly coherent, the intensity at the detector would have to show perfect extinction. However, we mount two QND apparati in each of the arms to ascertain the number of photons passing through them individually. The gain of the apparati can be adjusted, thus changing the accuracy of the measurement of the photon number passing through each arm. One can then compute the expectation value of the contrast and finds it to be[11] (see Fig. 4)

$$\langle \hat{I} \rangle = e^{-|\kappa\beta|^2/4} \cos\theta \tag{11}$$

Thus, a similar exponential factor as the one that appears in the error probability determines the extinction of the contrast. The factor is squared, because two measurements are being performed. Here again we find that the transition between the behavior of the photon as a wave and that of a particle is a continuous one. The accuracy of the determination of the photon number determines how much the photon behaves as a particle.

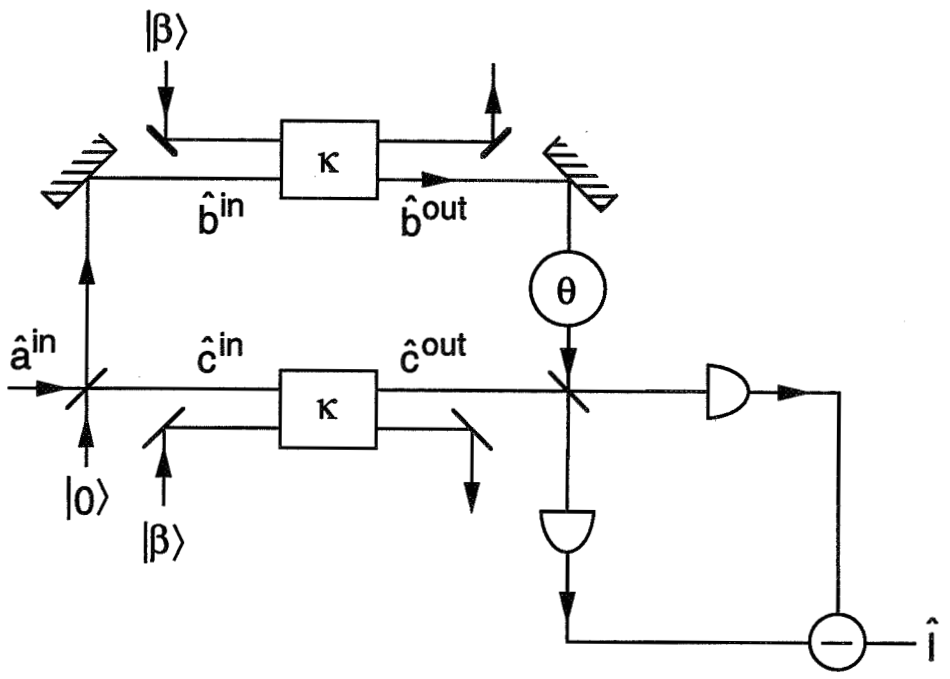


FIG. 3. An interferometer representing two-slit interference and attached QND measurement apparati.

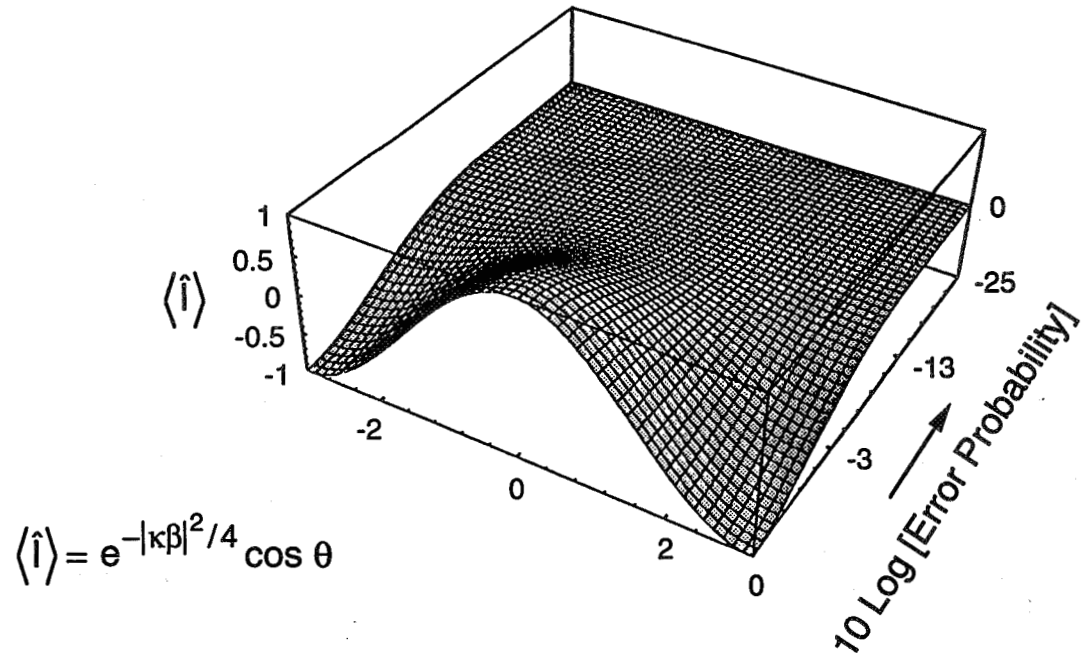


FIG. 4. Expectation value of detector current versus phase and error probability of photon number determination.

# 7 Conclusion

We started with the postulate that a proper formulation of a quantum measurement has to quantize the measuring apparatus as well. The quantum formalisms developed for optical components enable one to do a full quantum analysis of an optical measurement apparatus. The measurement apparatus of photon number with infinite gain yields results that can be described in classical language: photons behave as particles (since we chose a particle measurement apparatus). When the gain is not infinite, the behavior is more duplicitous, it is not what one would call the behavior of a classical particle. This confirms Bohr's statement that it is necessary to have large gain to obtain measurement results that can be put into classical language. We also found that a measurement with infinite gain is equivalent to a projection operation on the signal.

If no measurement is undertaken, the entanglement of the signal and probe states can be fully undone by an inverse apparatus.

Finally, the "double-slit" experiment can also be described in terms of partial knowledge of the photon number in each of the paths. If the knowledge is only partial, there can still be interference of the two beams.

# 8 Acknowledgments

This work was supported by the Office of Naval Research, Grant N00014-92-J-1302.

# 9 References

[1] *Quantum Theory and Measurement*, J. A. Wheeler and W. H. Zurek, Eds., Princeton University, Princton, NJ, 1983.

[2] R. E. Slusher, L. W. Hollberg, B. Yurke, J. C. Mertz, and J. F. Valley, Phys. Rev. Lett. **55**, 2409 (1985).

[3] L. W. Wu, H. J. Kimble, J. L. Hall, and H. Wu, Phys. Rev. Lett. **57**, 2520 (1986).

[4] M. G. Raizen, L. A. Orozco, M. Xiao, T. L. Boyd, and H. J. Kimble, Phys. Rev. Lett. **59**, 2520 (1987).

[5] M. W. Maeda, P. Kumar, and J. H. Shapiro, Opt. Lett. **12**, 161 (1987); J. Opt. Soc. Am. B **4**, 1501 (1987).

[6] B. Yurke, P. Grangier, R. E. Slusher, and M. J. Potasek, Phys. Rev. A **35**, 3586 (1987).

[7] R. M. Shelby, M. D. Levenson, S. H. Perlmutter, R. G. DeVoe, and D. F. Walls, Phys. Rev. Lett. **57**, 691 (1986).

[8] M. Shirasaki and H. A. Haus, J. Opt. Soc. Am. B **7**, 30 (1990).

[9] K. Bergman and H. A. Haus, Opt. Lett. **16**, 663 (1991).

[10] N. Imoto, H. A. Hans, and Y. Yamamoto, Phys. Rev. A **32**, 2287 (1985).

[11] F. X. Kärtner and H. A. Haus, Phys. Rev. A **47**, 4585 (1993).

# UNCERTAINTY RELATIONS AS HILBERT SPACE GEOMETRY

Samuel L. Braunstein
*Department of Physics, Technion—Israel Institute of Technology,*
*32 000 Haifa, Israel*

**Abstract**

Precision measurements involve the accurate determination of parameters through repeated measurements of identically prepared experimental setups. For many parameters there is a "natural" choice for the quantum observable which is expected to give optimal information; and from this observable one can construct an Heisenberg uncertainty principle (HUP) bound on the precision attainable for the parameter. However, the classical statistics of multiple sampling directly gives

us tools to construct bounds for the precision available for the parameters of interest (even when no obvious natural quantum observable exists, such as for phase, or time); it is found that these direct bounds are more restrictive than those of the HUP. The implication is that the natural quantum observables typically do not encode the optimal information (even for observables such as position, and momentum); we show how this can be understood simply in terms of the Hilbert space geometry.

Another striking feature of these bounds to parameter uncertainty is that for a large enough number of repetitions of the measurements *all* $V$ quantum states are "minimum uncertainty" states — not just Gaussian wave-packets. Thus, these bounds tell us what precision is achievable as well as merely what is allowed.

## 1 Introduction

I want to start by pointing out that the very term "precision measurement" implicitly refers to an idealization of our use of quantum theory. It assumes that there are some c-number parameters (ordinary commuting numbers instead of operators) "out there" in the laboratory which have no, or at least negligible, quantum uncertainty for their values. For instance, in the case of the precision interferometric measurement of some path difference it is thus assumed that the end-mirror masses are so heavy that the initial uncertainty in their location and the quantum "diffusion" of their position throughout the entire measurement procedure are negligible. In this talk I will discuss the fundamental limits quantum theory places on our ability to determine c-number parameters through measurement. We might, for instance, be interested in the precision determination of fundamental constants such as the gravitational coupling $G$, the speed of light $c$, etc., or of laboratory parameters such as a time difference $T$, some path difference $D$, a phase difference $\Phi$, etc. These latter parameters are just settings on some machine in our laboratory.

The type of machine we envision is one which has an inexhaustible supply of raw material which it uses to make a "train" of identical quantum states. These states will have encoded in them in some way the value of the parameter we seek. Thus, if our machine has some setting

which controls the value of a parameter $X$, then it will generate an inexhaustible supply of states $|\psi_X\rangle$; alternatively, if the setting is $X'$ then it will generate a supply of new states $|\psi_{X'}\rangle$. Our job is to use some observable $\hat{\xi}$ to determine the parameter's value.

Let us consider a simple example where our machine sets some "location" parameter $X$ which determines the location of the center of the peak of the wavefunctions generated:

$$\psi_X(x_i) = \frac{1}{(2\pi\sigma^2)^{1/4}} \exp\left[\frac{-(x_i - X)^2}{4\sigma^2}\right],$$

where $i$ is a sequential label for replicas of our state generated by the laboratory machine at some fixed setting $X$. Because we are seeking the "location" of the state we might expect that the natural observable of position $\hat{\xi} = \hat{x}$ is optimal, so this is the observable we shall use. In seeking fundamental limits to measurement in quantum theory it is worth seeing what the Heisenberg uncertainty principle (HUP) says. For a single measurement we would simply take the value of position measured and use that as our estimate of the location parameter $X$ of our state. In this way, the uncertainty for the parameter $X$ would just be the uncertainty in our observable for this state, so

$$\Delta X = \Delta x \geq \frac{\hbar}{2\Delta p},$$

by the HUP, for a single measurement. Alternatively, for $N$ measurements (each on a new replica of our state) we might take the average location we observe $\hat{x} = (\hat{x}_1 + \cdots + \hat{x}_N)/N$ as an estimate for our parameter, which is an operator with conjugate momentum $\hat{p} = \hat{p}_1 + \cdots + \hat{p}_N$ so the $N$-shot HUP will read

$$\Delta X = \Delta x \geq \frac{1}{\sqrt{N}} \frac{\hbar}{2\Delta p_1},$$

in terms of the uncertainty $\Delta p_1$ for a single state. This result shows a simple $1/\sqrt{N}$ improvement over the single-measurement HUP.

To summarize, we have learned that precision measurements deal with the language of c-number parameters — this being an idealization. We have learned that we must make some choice of observable to determine our parameter of interest, and where it exists we might choose the natural observable. Finally, we saw that the process of extraction of an estimate for our parameter from observation requires some form of data analysis — even if it be only the completely transparent procedure of using the value observed.

# 2 Bounds to data analysis

The previous section considered a crude multiple measurement uncertainty principle. It is surprising that much more powerful versions may be obtained from well known classical bounds to the efficiency of performing data analysis. The simplest of such bounds is called the Cramér-Rao lower bound [1], which we shall derive here. (Helstrom [2] was the first to place this bound in quantum language and recognize its significance; in this paper we broaden our physical understanding of this bound.)

Consider an arbitrary kind of data analysis based upon the $N$ observations $x_1, \ldots, x_N$ which yields an estimate $X_{\text{est}}$ for the parameter $X$ via a function

$$X_{\text{est}} = X_{\text{est}}(x_1, \ldots, x_N)$$

which is independent of the value of the parameter sought, and for which each of the observations $x_i$ is "drawn" independently from the probability distribution

$$p(x|X) = |\psi_X(x)|^2 \, .$$

To ensure that this data analysis has some connection with our parameter we impose the condition that on average it yields the correct value for $X$, i.e.,

$$X = \int X_{\rm est}(x_1, \ldots, x_N)\, p(x_1|X) \ldots p(x_N|X)\, dx_1 \ldots dx_N \, .$$

By taking the derivative of this with respect to $X$ we obtain

$$1 = \int \Delta X_{\rm est} \sum_{i=1}^{N} \left( \frac{\partial}{\partial X} \ln p(x_i|X) \right) p(x_1|X) \ldots p(x_N|X)\, dx_1 \ldots dx_N \, ,$$

where $\Delta X_{\rm est} \equiv X_{\rm est} - X$. Then applying the Schwartz inequality yields the Cramér-Rao bound

$$\Delta X_{\rm est} \geq \frac{1}{\sqrt{NF}} \, ,$$

with $F$ the Fisher information given by

$$F \equiv \int \left( \frac{\partial}{\partial X} p(x|X) \right)^2 p(x|X)\, dx \, .$$

Before we look at the consequences for this theorem from classical data analysis, we shall state one more theorem which applies to the specific kind of data analysis called maximum likelihood (ML) analysis. Fisher's theorem [3] states that as $N \to \infty$ ML analysis is asymptotically efficient (since it asymptotes towards the Cramér-Rao bound), i.e.,

$$\Delta X_{\rm est} \longrightarrow \frac{1}{\sqrt{NF}} \, ;$$

thus, at least one method of data analysis may reach the classical bound when a large enough sample of data is used. What is not given by this theorem is just how large a data sample is required to achieves this.

The simplest implication of the Cramér-Rao bound for a quantum system involves measurements of multiple copies of the pure state

$$\psi_X(x) = \psi(x - X) = r(x - X) \exp[i\phi(x - X)/\hbar] \, ,$$

where $X$ is a so-called translation parameter. The result may be directly obtained from the uncertainty in the momentum for this state

$$(\Delta p)^2 = \frac{\hbar^2}{4} F + (\Delta \phi')^2 \, , \tag{1}$$

yielding from the Cramér-Rao bound

$$\Delta X_{\rm est} \geq \frac{\hbar}{2\sqrt{N}\sqrt{(\Delta p)^2 - (\Delta\phi')^2}} \geq \frac{\hbar}{2\sqrt{N}\Delta p} .$$

This result is rather startling, since it shows that the classical bound is *always* more restrictive than the quantum bound; even for $N = 1$ when we would expect to have no qualms about the usual HUP. Further, it directly yields a parameter uncertainty principle for an arbitrary kind of data analysis, and hence is more general than the $N$-shot HUP we discussed in the previous section. To see why the classical bound can be more restrictive than the HUP we turn now to the metric on Hilbert space.

# 3 Quantum and classical metrics

Consider two ensembles $|\psi_X\rangle$ and $|\psi_{X'}\rangle$ which differ only in their values of the parameter $X$. For pure states there is a natural metric, measuring the distance in Hilbert space between a pair of states; since pure states are just rays of unit length, any suitable function of the angle between these rays will determine a Hilbert space metric. In particular, we shall choose the Study-Fubini metric [4]

$$d\left(|\psi_X\rangle, |\psi_{X'}\rangle\right) = 1 - |\langle\psi_X|\psi_{X'}\rangle|^2 \ ;$$

as the states overlap more they become less distinguishable which is reflected in a decrease in the metric.

For the observable $\hat{\xi}$ the two ensembles we are studying can be completely characterized by the probability distributions $p(\xi|X)$ and $p(\xi|X')$ ($p$ and $p'$ respectively). We can thus construct a classical metric to behave like the quantum one with respect to the distinguishability of states. Classical distinguishability, however, is limited by the Cramér-Rao bound, so if the nearby ensembles differ in

the parameter $X$ by $\delta X$ then they are permitted to be distinguishable so long as $NF(p)\,(\delta X)^2 \geq 1$. This gives a natural classical metric for nearby ensembles as

$$d(p, p') = \frac{1}{4}F(p)\,(\delta X)^2 + \cdots ,$$

where the scale factor is chosen for convenience. This result is equivalent to the metric introduced by Wootters [5] to lowest order.

To compare these two metrics, classical and quantum, we shall write the states in a descrete basis (labeled by $j$)

$$\begin{aligned} \psi_X\rangle &= \sum j\sqrt{pj}e^{i\varphi j}Ij\rangle \\ I\psi_{X'}\rangle &= \sum j\sqrt{pj + \delta pj}e^{i(\varphi j + \delta\varphi j)}|j\rangle . \end{aligned}$$

Then to second order we may calculate the quantum metric to be

$$\begin{aligned} d\left(I\psi_X\rangle, |\psi_{X'}\rangle\right) &= (\delta X)^2\left[\frac{1}{4}\sum jpj\left(\frac{\partial}{\partial X}\ln pj\right)^2 + \sum jpj\left(\frac{\partial\varphi j}{\partial X}\right)^2 - \left(\sum jpj\frac{\partial\varphi j}{\partial X}\right)^2\right] + \cdots \\ &= (\delta X)^2\frac{(\Delta p_X)^2}{\hbar^2} + \cdots \end{aligned}$$

where $\hat{p}_X$ is the "momentum" operator generating infinitesimal translations in the parameter $X$. The first term in square brackets is just the classical metric. The second and third terms correspond to the dispersion in the rate of change of the wavefunction's phase; this is similar to Eq. (1), and reduces to it exactly when $X$ is a translation parameter.

This relationship shows that classical distances between nearby ensembles are shorter than the corresponding quantum distances. Because the ensembles are harder to distinguish classically, the Cramér-Rao bound is more restrictive than the HUP. The classical distances are shorter than the quantum ones. We might ask whether the greater distances inherent in the quantum metric are accessible at all for the purposes of precision determination of parameters? We shall see that the answer is typically yes.

# 4 Seeing a quantum distance

The quantum metric

$$d\left(|\psi\rangle, |\psi'\rangle\right) = d(p, p') + (\Delta\varphi')^2(\delta X)^2 \,,$$

exceeds the classical one only by the variance of the rate of change of the phase of the wavefunction. Thus, by a suitable choice of basis the phase can be made trivial so that the classical part of the metric makes up the entire contribution. This may seem a little strange since we typically will start with what we thought was the "natural" observable for a particular parameter. Yet since in general the phase will give some non-zero contribution this argument tells us that natural observables are rarely optimal.

We can see this surprising effect quite simply for a squeezed state. For the purposes of this example we will scale the units of position and momentum so that the ordinary HUP reads $\Delta x \Delta p \geq 1$. Suppose we wish to find the location parameter $X$ for the squeezed state

$$|\psi_X\rangle = \hat{D}(X)\hat{R}(\theta)\hat{S}(r)|0\rangle \,.$$

On a phase-space diagram this corresponds to the squeezed vacuum (squeezed by $e^{-r}$ in along the $x$-axis) rotated counter-clockwise by $\theta$ radians, and then displaced along the positive $x$-axis by the distance $X$. The natural observable for the position of the state would be $\hat{\xi} = \hat{x}$. So our mean signal would be

$$\mathcal{S} \equiv \langle \hat{x} \rangle = X \,,$$

i.e., a measurement of $\hat{x}$ directly yields an estimate for the parameter $X$. Further, the uncertainty (or "noise") in this value after a single measurement will be

$$\mathcal{N} \equiv \Delta x = \sqrt{e^{2r}\sin^2\theta + e^{-2r}\cos^2\theta} \,,$$

which includes the reduced noise from the squeezed quadrature, plus an admixture (for $\theta \neq 0$) from the amplified quadrature.

By contrast, suppose we use the observable $\hat{\xi} \equiv \hat{x}' = \hat{R}(\theta)\hat{x}\hat{R}^\dagger(\theta)$. The new signal will be on average

$$\mathcal{S}' \equiv \langle \hat{x}' \rangle = X\cos\theta \,,$$

which is reduced by a trigonometric factor, and the uncertainty in this value after a single measurement will be simply

$$\mathcal{N}' \equiv \Delta x' = e^{-r} .$$

A comparison shows that the signal-to-noise ratio has been improved by using a non-natural observable with

$$\frac{\mathcal{S}'}{\mathcal{N}'} > \frac{\mathcal{S}}{\mathcal{N}} ,$$

for $e^{2r}\sin(2\theta) > 1$ (an improvement for all $\theta \neq 0$ is possible using a more complicated rotation angle for the new observable).

In general then, so long as we can choose a basis where the phases are trivial we can "see" the full quantum distance for the new observable. In this ideal observable we will have a bound of

$$\Delta X_{\text{est, opt}} \geq \frac{\hbar}{2\sqrt{N}\Delta p_X} ,$$

which if $X$ is a translation parameter will be just our original $N$- shot HUP. Now, however, Fisher's theorem tell's us that this lower bound can always be achieved so long as we take a large enough sample size (i.e., $N \rightarrow \infty$) and that we use the maximum likelihood method for our data analysis. This means that for the proper choice of observable (typically not the natural one) *all* $V$ quantum states are minimum uncertainty states! This removal of so-called natural observables from their central place in quantum theory has practical implications for the precision measurement of time, phase, etc., where natural observables for these measurements are somewhat problematic.

# 5 Conclusion

Precision measurements naturally assume a language involving the existence of c-number parameters. The bounds to classical data analysis form a natural extension of the Heisenberg uncertainty principle from operator dispersions to parameter uncertainties; and generalize it to allow arbitrary data analysis on the results of multiple measurements of identically prepared systems. In general, it is found that the "natural" observables do not yield maximal information about the parameters sought; however, with a suitable observable and using maximum likelihood data analysis all quantum states (not just gaussian wavepackets) are minimum uncertainty states for a large enough number of measurements.

# References


[1] H. Cramér, *Mathematical Methods of Statistics* (Princeton Univ. Press, Princeton, NJ,1946) pp. 500-504.

[2] C. W. Helstrom, *Quantum Detection and Estimation Theory* (Academic, New York,1976).

[3] R. A. Fisher, Proc. Camb. Soc. **22**, 700 (1925) .

[4] J. Samuel and R. Bhandari, Phys. Rev. Lett. **60**, 2339 (1988).

[5] W. K. Wootters, Phys. Rev. D **23**, 357 (1981).

N95-13912

# TIME-DEPENDENT DISTINGUISHABILTY: CHOOSING TO BE A WAVE OR A PARTICLE

T.P. Grayson, X.Y. Zou, D. Branning, J.R. Torgerson and L. Mandel
*Department of Physics and Astronomy, University of Rochester, Rochester, NY 14627*

**Abstract**

Interference experiments with connected parametric down-converters have demonstrated that the possibility, in principle, of identifying the photon path through the interferometer is sufficient to wipe out all interference, irrespective of whether the identification is actually made. The distinguishability of the photon path can be controlled by a time-dependent shutter, which leaves the choice whether the photon behaves as a wave or as a particle in the experimenter's hands. By contrast, in some more recent experiments involving the addition of a low-Q cavity, each idler photon makes the choice whether the associated signal photon behaves like a wave and exhibits interference, or like a particle.

# 1 Introduction

In this paper we briefly review some recent interference experiments in which several non-classical and non-local effects show up. The basis for all the experiments is the process in non-linear optics known as parametric down-conversion that generates pairs of signal and idler photons simultaneously in an entangled quantum state [1, 2]. The experiments outlined below all make use of two down-converters, and the prototype of the arrangement is illustrated in Fig.1 [3, 4].

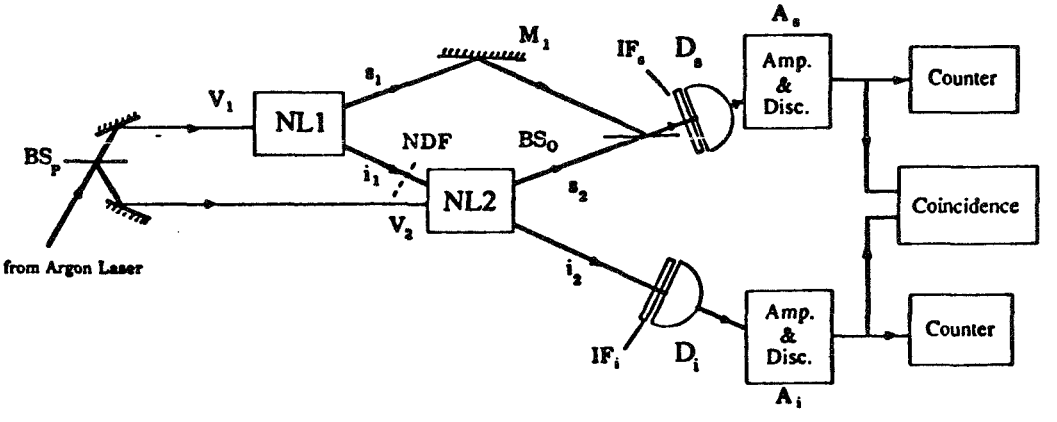


Fig. 1. Outline of the experimental set-up underlying all the experiments [Reproduced from Zou et al (1991)].

Here $NL1$ and $NL2$ are two similar crystals with a $\chi^{(2)}$ non-linear susceptibility functioning as down-converters. Both crystals are optically pumped by mutually coherent light beams of

amplitudes $V_1$, $V_2$ derived from the same laser beam. As a result down-conversion can occur at $NL1$ with the emission of a signal $s_1$ and an idler $i_1$ photon simultaneously, or down-conversion can occur at $NL2$ with the emission of a pair of $s_2$, $i_2$ photons. The crystals are so oriented that $i_1$ passses through $NL2$ and then is colinear with $i_2$. At the same time the $s_1$ and $s_2$ beams are brought together at the output beam splitter $BS_o$ where they are mixed, and the mixed signal beams fall on signal detector $D_s$. We are interested to know whether $s_1$ and $s_2$ exhibit mutual coherence and interfere. If they do, then the photon counting rate of $D_s$ will oscillate as $BS_o$ is slowly translated in a direction perpendicular to its face.

The results of the experiment are illustrated in Fig 2. [3]. It appear that $s_1$ and $s_2$ do indeed

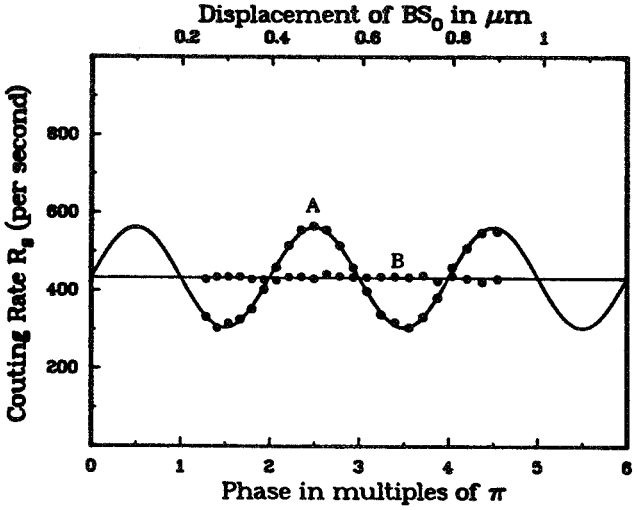


Fig. 2. Experimental Results of the Interference Experiment [Reproduced from Zou et al (1991)].

interfere (curve A ) when $i_1$ and $i_2$ are aligned, but that all interference disappears when $i_1$ is blocked by a beam stop (curve B). The average rate of photon emission is, however, the same in both cases. If we argue that $i_1$ induces coherence between $s_1$ and $s_2$ in some sense, then this induced coherence is unusual because it is not accompanied by any induced emission. If, instead of blocking $i_1$, we insert a filter $NDF$ in the path of $i_1$, as shown in fig 1, then the resulting interference pattern of $s_1$, $s_2$ is found to have a visibility proportional to the absolute transmissivity $\mathcal{T}$ of the filter. It can be shown that under somewhat idealized conditions, and with equal signal $s_1$ and $s_2$ intensities, the degree of coherence $|\gamma_{s_1 s_2}|$ between $s_1$ and $s_2$ or the visibility is given by [4]

$$|\gamma_{s_1 s_2}| = |\gamma_{DC}(\tau_0 + \tau_2 - \tau_1)||\mathcal{T}|, \tag{1}$$

where $\gamma_{DC}$ is the normalized second order auto-correlation function of the down-converted field. $\tau_0$, $\tau_2$, $\tau_1$ are propagation times from $NL1$ to $NL2$, from $NL2$ to $D_s$, and from $NL1$ to $D_s$, respectively and $\tau_0 + \tau_2 - \tau_1 = 0$ when the interferometer is balanced, in which case $\gamma_{DC}(0) = 1$. It is possible to understand the absence of mutual coherence between $s_1$ and $s_2$ when $i_1$ is blocked in terms of the potential distinguishability of the photon sources. With the help of an auxiliary measurement with detector $D_i$ shown in Fig. 1, that does not disturb the interference between $s_1$ and $s_2$, one can determine the source of the detected signal photon [3].

## 2 Effect of a Differential Time Delay

As is well known, the insertion of a differential time delay $\mathcal{T}_D$ in one interferometer arm generally lowers the visibility, and if $\mathcal{T}_D$ exceeds the coherence time $T_c$ of the light the visibility drops close to zero. But according to Eq. (1), the effect of incrementing $\tau_2$ by $\tau_D$ should be exactly the same as the effect of leaving $\tau_2$ unchanged and incrementing $\tau_0$ instead, even though $\tau_0$ relates to the $i_1$ path which is not really part of the interferometer. The reason is the quantum entanglement of signal and idler photons, which makes the effect of a delay on the signal virtually indistinguishable from the effect of the same delay on the idler. As the experimental results shown in Fig. 3 indicate, the observed visibility falls with increasing $\tau_D$ in accordance with Eq. (1), although it is the idler 1 which is being delayed [5].

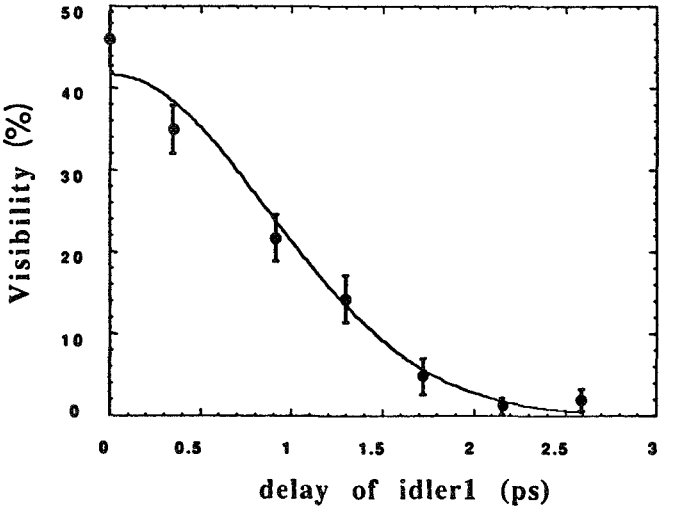


Fig. 3. Experiment Results showing the effect of a time delay imposed on the $i_1$ idler photons [Reproduced from Zou et al (1993)].

## 3 Effect of a Time-Dependent Filter

So far we have dealt only with steady state situations. An interesting variant of the foregoing arises if the filter of transmissivity $\mathcal{T}(t)$ shown in Fig. 1 is allowed to vary in time. Indeed we may think of the filter as a time-dependent shutter that opens and closes at certain times. We now ask how the transmissivity affects the visibility of the interference contributed by a signal photon which is detected by $D_s$ at time $t$.

This problem has recently been examined theoretically [6]. With the help of a spectral analysis of the fields and the filter response function it was shown that the visibility of a signal photon detected by $D_s$ at time $t$ is completely determined by the filter transmissivity $\mathcal{T}$ at the earlier time $t - \tau_2 - \tau_0''$. Here $\tau_0''$ is the propagation time of photons from the filter to $NL2$. The time $t - \tau_2 - \tau_0''$ is therefore the time at which a photon from $NL1$ on the way to $NL2$ and then on to $D_s$ would have passed the filter. Of course there is no such photon. But the time $t - \tau_2 - \tau_0''$ is the time when $i_1$ would pass the filter if the photons originate in $NL1$. Provided the filter is then open ($\mathcal{T} = 1$) this photon is indistinguishable from an $i_2$ photon from $NL2$. It does not matter at all what the transmissivity is at any other time.

# 4 Effect of a Resonant Cavity around the Idler Beams

Consider the experimental arrangement shown in Fig. 4 [7]. Here a beam splitter $BS_i$ has been inserted in the $i_1$ beam between $NL1$ and $NL2$, and light reflected from $BS_i$ is detected by an additional detector $D_i$ such that the propagation time from $NL1$ to $D_i$ is also $\tau_1$. It follows that an $s_1, i_1$ photon pair emitted by $NL1$, of which the $i_1$ photon is reflected by $BS_i$ and passed to $D_i$, will result in coincident detections by both $D_s$ and $D_i$. Needless to say, these photons do not contribute to the signal interference because their source is known. Mirrors $M3$, $M4$ are introduced so as to form an optical cavity resonant with the idlers. An $i_1$ photon which is transmitted through $BS_i$ may then propagate to $M4$, where it may be reflected and again pass through $BS_i$ ; it may then be reflected from $M3$ and return to $BS_i$, where it is reflected and passed to $D_i$. Similarly, an $i_2$ photon emitted from $NL2$ may traverse the cavity and end up being reflected by $BS_i$ and detected by $D_i$. Needless to say, an $i_1$ or $i_2$ photon which has made one or more trips around the cavity in this way will be detected by $D_i$ later that the conjugate signal photon is detected by $D_s$. Moreover, if the interferometer is balanced, the time delay between detections by $D_i$ and $D_s$ will be the same whether the photons originate in $NL1$ or $NL2$. As a result the sources of these photons are indistinguishable and interference is to be expected, whereas the sources are distinguishable for coincident signal-idler detections.

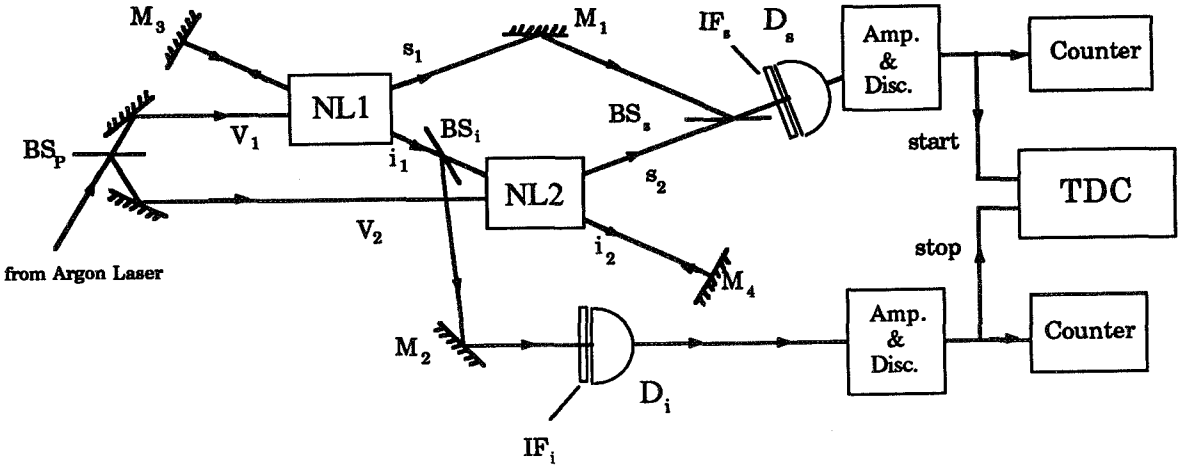


Fig. 4. Outline of the experiment with a resonant idler cavity [Reproduced from Grayson et al (1993)].

In order to measure the delay time intervals $\tau_D$ between $D_s$ and $D_i$ detections the photoelectric pulses from $D_s$ and $D_i$ are passed to the 'start' and the 'stop' inputs of a time-to-digital converter ($TDC$) that measures and digitizes the intervals and accumulates the data in channels determined by $\tau_D$. The number of events accumulated in delay channel $\tau_D$ is then a measure of how many photon pairs have a time separation $\tau_D$. In addition by varying the optical path difference through displacement of $BS_o$ we can extract the visibility of the interference pattern formed by the two signal beams.

The results of the experiment together with theoretically expected values are shown in Fig. 5. [7]. Fig. 5a gives the accumulation of photon pairs as a function of the delay $\tau_D$. The peak centered at $\tau_D = 0$ corresponds to idler $i_1$ photons that emerge from the optical cavity without

making any round trip. The observed visibility is shown in Fig. 5b. Those photons that emerge without extra delay are counted but exhibit no interference, because they originate in NL1. Those photons that emerge after one cavity roundtrip behave like waves and interfere with about 50% visibility.

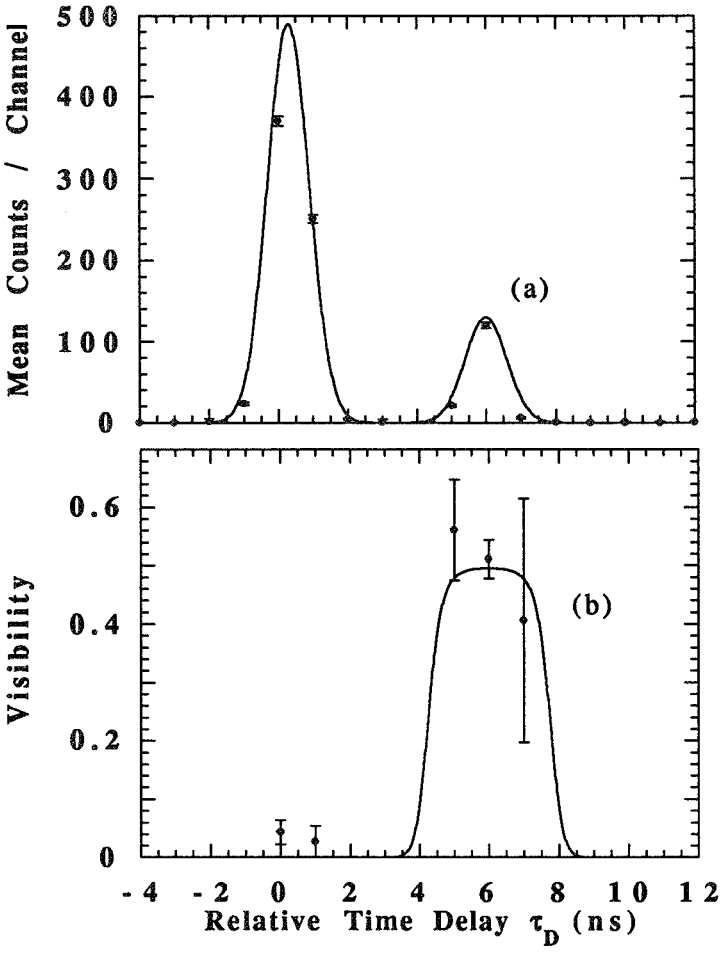


Fig. 5. Experimental results showing how the photon pair rate and the visibility vary with the delay $\tau_D$. The cavity round trip time is 6 nsec. [Reproduced from Grayson et al (1993)]

Because the idlers are registered by the $TDC$ after the signal photons, the experiment has some of the character of a delayed choice experiment. But the 'choice' is here made not by the experimenter but by the idler photons. Those idlers that are reflected by $BS_i$ at the first encounter cause the conjugate signal photons to behave like particles; those idlers that make one round trip before emerging from the cavity cause the conjugate signal photons to behave like waves and to interfere. We note that both aspects of nature are here exhibited by different photons in the same apparatus.

# 5 Acknowledgments

This research was supported by the National Science Foundation and by the U.S. Office of Naval Research.

# References

[1] D.N. Klyshdo, Zh. Eksp. Teor. Fiz. **55**,1006 (1968) [Sov. Phys. JETP **28**, 522 (1969)].

[2] D.C. Burnham and D.L. Weinberg, Phys. Rev. Lett. **25**, 84 (1970).

[3] X.Y. Zou, L.J. Wang and L. Mandel, Phys. Rev. Lett. **67**, 318 (1991).

[4] L.J. Wang, X.Y. Zou and L. Mandel, Phys. Rev. A **44**, 4614 (1991).

[5] X.Y. Zou, T.P. Grayson, G.A. Barbosa and L. Mandel, Phys. Rev A **47**, 2293 (1993).

[6] L.J. Wang, X.Y. Zou and L. Mandel, J. Opt. Soc. Am B **9**, 605 (1992).

[7] T.P. Grayson, X.Y. Zou, D. Branning, J.R. Torgerson and L. Mandel, to be published (1993).

N95-13913

# HOMODYNING AND HETERODYNING THE QUANTUM PHASE

G. M. D'Ariano, C. Macchiavello and M. G. A. Paris
Dipartimento di Fisica 'Alessandro Volta'
Via Bassi 6, I-27100 Pavia, Italy

ABSTRACT: The double-homodyne and the heterodyne detection schemes for phase shifts between two synchronous modes of the electromagnetic field are analyzed in the framework of quantum estimation theory. The probability operator-valued measures (POM's) of the detectors are evaluated and compared with the ideal one in the limit of strong local reference oscillator. The present operational approach leads to a reasonable definition of phase measurement, whose sensitivity is actually related to the output r.m.s. noise of the photodetector. We emphasize that the simple-homodyne scheme does not correspond to a proper phase-shift measurements as it is just a zero-point detector. The sensitivity of all detection schemes are optimized at fixed energy with respect to the input state of radiation. It is shown that the optimal sensitivity can be actually achieved using suited squeezed states.

## 1 Introduction

Weak forces on macroscopic bodies in interferometric arrangements or, more generally, minute variations of environmental parameters in optical fibers are detected through the induced changes in the optical paths of the light beams. The detection of the induced phase-shift represents one of the most sensitive measurement on radiation in order to monitor such small perturbations. The back-action effect on the measured parameter due to the radiation pressure imposes limitations on the radiation intensity, and improvements of the sensitivity can only be achieved by suited preparation of the input quantum state.
In this paper a narrowband analysis of some relevant phase detection schemes is presented (a multimode wideband analysis can be found in [1]). Classically a phase-shift measurement in an interference experiment can be directly related to the polar angle between two quadratures of one field-mode, which in turn are given by two output photocurrents. Quantum mechanically the quadratures of the field are noncommuting observables and their relative polar angle cannot be interpreted as a selfadjoint operator, as in the early Dirac's heuristic approach [2]. The oscillator phase is not an observable in usual sense, and the problem of identifying its quantum dynamical counterpart has provoked many discussions in the literature (see, for example, [3, 4, 5] and references therein). Among the numerous attempts the limiting procedure of Pegg and Barnett [3] has become the most popular technique, because it allows the evaluation of expected values with very simple and reliable rules. However, despite its simplicity and effectiveness as a mathematical tool, this approach has no obvious physical interpretation, and leaves most of the conceptual problems on phase detection still open. The actual problem of a phase measurement description does not concerns with a definition of a selfadjoint operator, but with an operative recipe to evaluate the phase statistics in a real measurement, starting from the knowledge of the density matrix of the input radiation. On these lines the most appropriate approach to the phase detection of the field is the quantum estimation theory of [4]. Even though it easy to show that this method is equivalent in the end to the Pegg and Barnett procedure (see [8] for more details), nevertheless it provides a physically meaningful scheme for the phase measurement where all conceptual problems disappear. Despite it has long been recognised as the most natural framework for analyzing any kind of quantum detection, the quantum estimation theory has not

gained the necessary popularity yet, perhaps due to the fact that its main ingredient—the probability operator measure (POM)—is generally a nonorthogonal spectral decomposition, and thus appears to be in conflict with the conventional dictum of quantum mechanics that only "observables "—i.e. orthogonal POM's—can be measured. This point has been well clarified in some papers (see for example [8]), where it is shown that nonorthogonal POM's correspond to actual observables on a larger Hilbert space which includes also modes pertaining the measuring apparatus (all together referred to as "probe"). It is clear that this assertion provides the proper quantum setting for the operational point of view of [11], where the dependence of the measured operator on the detection scheme just corresponds to the involvement of the probe variables in the measuring process, involvement which becomes unavoidable when the phase of the field is detected.

Any quantum measurement needs a classical final stage and for measurement on radiation this is essentially a photodetection. Moreover a proper measurement of the quantum phase has to be related to the detection of a quantity which itself is a phase, i.e. is defined on the unit circle. In this sense we distinguish between two main different classes: the genuine phase detection schemes and the measurements of a single phase-dependent observable. In the former class, the phase-shift of the field is related to the polar angle between two measured photocurrents which, in turn, correspond to a couple of two conjugated quadratures of the field. Such scheme is the only viable one for phase detection, and corresponds equivalently to either heterodyning or double-homodyning the field. This also clarifies the subtle nature of the phase itself which, despite being a single real parameter, nonetheless requires a joint measures of two conjugated operators. In contrast, in the second class of measurements, only a single observable is detected—typically, when homodyning a single-quadrature of the field. Here we want emphasize that a single-quadrature measurement cannot be used to infer the value of the phase, because the knowledge of a quadrature would require an additional measurement on the field—essentially its intensity—which unavoidably would destroy the information on phase. Thus, the single-homodyning scheme can be used only as a zero-phase monitoring technique, which, however, is the essential of a typical interferometric measurement. In order to stress the operational nature of POM approach here we also present, as an example, a numerical simulation of a real experiment, reproducing the classical output photocurrents due to a particular quantum state, and then evaluating the phase statistics as the polar angle distribution.

After selecting a measurement procedure—either ideal or feasible—the statistics of the detected phase can be further improved at fixed total energy by looking for optimal states of the field. We show that the r.m.s. phase sensitivity versus the average photon number $\bar{n}$ is bounded by the ideal limit $\Delta\phi \sim \bar{n}^{-1}$, whereas for the feasible schemes the bound is $\Delta\phi \sim \bar{n}^{-2/3}$, in between the shot noise level $\Delta\phi \sim \bar{n}^{-1/2}$ and the ideal bound. The latter can actually be achieved by single-homodyning suitable squeezed states, but only in the neighborhood of a fixed zero-phase working point. The requirement of detecting the whole phase probability distribution makes the proper phase measurement less sensitive than in the case of a zero-point detection and the state achieving the two bounds are dramatically different: they are weakly squeezed (about 2% of squeezing photons) for the double-quadrature measurement, whereas they become strongly squeezed (50%) for one-quadrature detection.

Sect.2 is devoted to the theory of phase measurements, with a detailed analysis of the various schemes. Subsect. 2.1 is a brief review of the quantum estimation approach. Subsect. 2.2 presents some remarks and criticisms about the different definitions of sensitivity. Detection of the phase through simultaneous measurement of two quadratures of the field are discussed in Subsects. 2.3 and 2.4, which are dedicated to double-homodyne and heterodyne detection (it is shown that the two schemes are fully equivalent). Subsect. 2.5 examines the measurement of the quantum sine and cosine of the phase, with a comparison between the present quantum estimation approach and earlier treatments [7].In Subsect. 2.6 we analyze the homodyne detection scheme. In Sect.3 the optimal states of the field are given, which maximize sensitivity for all the schemes of Sect.2, also indicating how to actually achieve such states.

## 2 Quantum measurement of the phase

At presently it is fairly universally accepted that the quantum description of a phase measurement on a single mode of the e. m. field cannot be approached by means of the usual concept of observable. As a matter of fact, even though selfadjoint operators can be defined on the Fock space, none of them can appropriately describe the actual statistics of phase measurements. The quantum estimation theory of Helstrom [4] provides the most general—nonetheless operational—framework to analyze any kind of measurement in the quantum context, and, in particular, the detection of a phase differences between synchronous oscillators. The main ingredient of such theory is represented by the mathematical concept of probability-operator-valued measure (POM) on the Hilbert space $\mathcal{H}_S$ of the system, which extends the conventional description by selfadjoint operators. Using a notation which is familiar to physicists—even though not strictly legitimate from the mathematical point of view [8]— given a set of (generally complex) parameters $\mathbf{z}$ to be measured, a POM $d\hat{\lambda}(\mathbf{z})$ is a self-adjoint measure with the following properties

$$d\hat{\lambda}(\mathbf{z}) \geq 0\,, \qquad \int_Z d\hat{\lambda}(\mathbf{z}) = \hat{1}\,, \tag{2.1}$$

where $Z$ denotes the space of the parameters $\mathbf{z}$. Eqs.(2.1) assure that using a POM one has an operational recipe which univocally relates the density-matrix state $\hat{\rho}$ of the system to a probability distributions of the parameters $\mathbf{z}$ corresponding to a particular experimental setup. In formulas one has

$$dP(\mathbf{z}) = \mathrm{tr}\{\hat{\rho} d\hat{\lambda}(\mathbf{z})\}\,. \tag{2.2}$$

Also a set of selfadjoint operators $\hat{\Lambda}$ can be defined

$$\hat{\Lambda} = \int_Z \mathbf{z} d\hat{\lambda}(\mathbf{z})\,, \tag{2.3}$$

and, more generally, operator functions $\widehat{f(\Lambda)}$ as

$$\widehat{f(\Lambda)} = \int_Z f(\mathbf{z}) d\hat{\lambda}(\mathbf{z})\,. \tag{2.4}$$

When the POM $d\hat{\lambda}(\mathbf{z}) = |\mathbf{z}\rangle\langle\mathbf{z}|d\mathbf{z}$ is given in terms of orthogonal $|\mathbf{z}\rangle$'s, then it corresponds to the customary measure of the commuting observables $\hat{\Lambda}$, whose corresponding selfadjoint operators obey the function calculus

$$\widehat{f(\Lambda)} = f(\hat{\Lambda})\,. \tag{2.5}$$

On the contrary, the relation (2.5) no longer holds true for a generic nonorthogonal POM. As a consequence, the selfadjoint operators $\hat{\Lambda}$ only provide the expected values of the parameters $\mathbf{z}$, whereas the higher moments of the probability distributions differ from the corresponding moments of the operators $\hat{\Lambda}$ themselves, and can be evaluated only through Eq.(2.2). One should notice that, despite the POM's generally describe measurements that do not correspond to observables in the usual sense, nonetheless there is no conflict with the basic assertion of quantum mechanics that only observables can be measured. In fact, the Naimark theorem assures that every POM can be obtained as a partial trace of a customary projection-valued measure on a larger Hilbert space [8] which itself represents the original system interacting with an appropriate measuring apparatus. Upon denoting by $|\psi(\mathbf{z})\rangle \in \mathcal{H}_S \otimes \mathcal{H}_P$ a complete orthonormal set of eigenvectors of commuting selfadjoint operators acting on the enlarged space—including also the apparatus (*probe*) space $\mathcal{H}_P$—the probability distribution

$$dP(\mathbf{z}) = \mathrm{tr}\,(\hat{\rho}_S \otimes \hat{\rho}_P |\psi(\mathbf{z})\rangle\langle\psi(\mathbf{z})|) = \mathrm{tr}_S\,[\hat{\rho}_S \mathrm{tr}_P\,(\hat{\rho}_P |\psi(\mathbf{z})\rangle\langle\psi(\mathbf{z})|)]\,, \tag{2.6}$$

corresponds to the POM on the Hilbert space $\mathcal{H}_S$ of the system only

$$d\hat{\lambda}(\mathbf{z}) = \mathrm{tr}_P\left(\hat{\rho}_P|\psi(\mathbf{z})\rangle\langle\psi(\mathbf{z})|\right) \equiv \langle\psi(\mathbf{z})|\hat{\rho}_P|\psi(\mathbf{z})\rangle\,. \tag{2.7}$$

Notice that the above extensions of the system Hilbert space—hence, physically, the experimental realization of the POM—is not necessarily unique.
In Subsect. 2.1 we review the quantum estimation theory of the phase which leads to the optimal POM representing the most accurate measurement. This, however, is only an ideal limit as no viable schemes implementing such POM has been envisaged yet. Therefore, in Subsects.2.3 and 2.4 experimentally achievable detection schemes which correspond to a sub-optimal POM (double-homodyne and heterodyne) are analyzed in detail, whereas in Subsect.2.6 the customary homodyne detection is considered. The latter exits from the present quantum estimation approach, however it is in order, due to the relevance of this scheme in any interferometric setup.

### 2.1 Canonical Measurement

The quantum estimation theory analyzes the possible strategies for estimating a parameter on the basis of an error-cost-function: the optimum POM is the one which minimizes the total average cost. For a maximum-likelihood criterion, the optimum POM for the phase is

$$d\hat{\mu}(\phi) = \frac{d\phi}{2\pi}|e^{i\phi}\rangle\langle e^{i\phi}|\,, \tag{2.8}$$

$|e^{i\phi}\rangle$ being the Susskind-Glogower phase states [7]

$$|e^{i\phi}\rangle = \sum_{n=0}^{\infty} e^{in\phi}\,|n\rangle\,. \tag{2.9}$$

It is worth noticing that in the present case the maximum likelihood criterion is equivalent to the Gaussian-cost-function one for the bounded case ($\sin^2$-cost)[4]. Such generality of the optimal POM $d\hat{\mu}(\phi)$ justifies the term *Canonical Measurement* here adopted for this POM approach. Also notice that the Pegg and Barnett [3] approach is totally equivalent to the present one as regards evaluations of statistics. However, there is no physical interpretation for the mathematical tricks on which their method relies. Some examples of commuting pairs of self-adjoint operators achieving the optimum POM (2.8) on a system-probe Hilbert space have been proposed in [9] and in [5]: however, no viable method for experimentally implementing a corresponding setup has been devised yet, and hence the POM (2.8) only represents an ideal limit.
Corresponding to the optimal POM (2.8) one defines the selfadjoint phase operator

$$\widehat{\phi} = \int_{-\pi}^{\pi} \phi\; d\hat{\mu}(\phi) = -i\sum_{n\neq m}(-)^{n-m}\frac{1}{n-m}\,|n\rangle\langle m| \tag{2.10}$$

and the squared operator

$$\widehat{\phi^2} = \int_{-\pi}^{\pi} \phi^2 d\hat{\mu}(\phi) = \frac{\pi^2}{3} + 2\sum_{n\neq m}(-)^{n-m}\frac{1}{(n-m)^2}\,|n\rangle\langle m|\,. \tag{2.11}$$

Notice that, as announced,

$$\widehat{\phi^2} \neq \widehat{\phi}^2\,, \tag{2.12}$$

and more generally $\widehat{f(\phi)} \neq f(\hat{\phi})$. Such fail of the operator function calculus also holds true for the selfadjoint operators defined through the experimentally feasible non-optimal POM's. The fact that there is no orthogonal optimum POM for the phase, physically corresponds to the impossibility of defining the measurement of the phase independently on the apparatus. This assertion clarifies and formalizes the operational nature of the phase detection which has been pointed out by Mandel et al.in [11].

## 2.2 Phase Sensitivity

Usually the sensitivity of a measurement of a parameter say $x \in \mathbf{R}$ is assumed equivalent to the r.m.s. of the experimental probability distribution $dP(x)$, namely

$$\overline{\Delta x^2} = \int_{\mathbf{R}} dP(x) x^2 - \left( \int_{\mathbf{R}} dP(x) x \right)^2 . \tag{2.13}$$

On the other hand, the phase variable $\phi$ is defined in the bounded domain $[-\pi, \pi)$ with $2\pi$-periodicity: this peculiar property of the phase has lead many authors to the conclusion that the r.m.s. of the phase is not the appropriate quantity to be considered as an evaluation of the phase sensitivity, claiming that it is not invariant under phase variable translation $\phi \longrightarrow \phi + \chi$. Thus, different definitions for the sensitivity have been adopted, which would be equivalent for an unbounded Gaussian-distributed variable. Here, after critical reviewing such quantities, we show that an operational definition of a phase measurement procedure leads unequivocally to adopt the r.m.s. itself as the correct sensitivity parameter.

*a. Phase dispersion* $D$[12, 13].
Dispersion $D$ is defined as follows

$$D \equiv (1 - \langle \cos\phi \rangle^2 - \langle \sin\phi \rangle^2)^{\frac{1}{2}} = 1 - \left| \sum_{n=0}^{\infty} c_{n+1}^* c_n \right|^2 , \tag{2.14}$$

where $c_n$ are the coefficient of the number representation of the state and the sine and cosine operators are defined according to Eq.(2.4) as follows

$$\widehat{\cos\phi} = \int_{-\pi}^{\pi} \cos\phi \, d\hat{\mu}(\phi) , \tag{2.15}$$

$$\widehat{\sin\phi} = \int_{-\pi}^{\pi} \sin\phi \, d\hat{\mu}(\phi) , \tag{2.16}$$

and coincide with the sine and cosine operators of Susskind and Glogower [7]. The definition (2.14) follows from elementary error-propagation calculus, the phase $\phi$ being regarded as a function of the two "independent variables" $\sin\phi$ and $\cos\phi$ as follows

$$\phi = -i \ln(\cos\phi + i \sin\phi) . \tag{2.17}$$

In Eq.(2.17) the correct logarithm branch is selected in order to obtain the desired domain for $\phi$. A part the minor point that Eq.(2.14) would lead to dispersion $D = 1$ for constant distributions—instead of $\overline{\Delta\phi^2} = \pi^2/3$—the main criticism is that $\sin\phi$ and $\cos\phi$ cannot be considered as independent variables, because they correspond to a noncommuting pair of operators which are jointly measured when detecting $\phi$.

*b. Reciprocal peak likelihood* $\delta\phi$[5].
The peak likelihood $P(\phi|\phi)$ is the maximum height of the probability distribution. Its inverse, namely

$$\delta\phi = \frac{1}{p(\phi|\phi)} = 2\pi \left( \sum_{n=0}^{\infty} |c_n| \right)^{-2} , \tag{2.18}$$

has been introduced in [5] as a measure of the width of the distribution, coherently with the maximum-likelihood strategy used in the quantum estimation theory. Here, the following criticisms are in order: i) $\delta\phi$ is a *local* criterion, namely it checks only one point of the distribution, whereas there is no control on the global behaviour as, for example, on the eventual occurrence of high tails. The most degenerate situation occurs when the tails are so high that the distribution itself converges to the $P(\phi) = 1/2\pi$ apart from

one point with infinite probability density and zero integral [14], thus leading to vanishing $\delta\phi$ instead of $\delta\phi = \pi^2/3$; ii) the coherence of this sensitivity definition with the maximum-likelihood strategy [5] cannot be considered as a valid argument, in view of the aforementioned equivalence between the likelihood strategy and the (quasi)-Gaussian one; iii) recent numerical results [6] have shown that the simulated sensitivity does actually not correspond to $\delta\phi$.

*c. POM r.m.s.* $\langle\widehat{\Delta\phi^2}\rangle$

Given a physical apparatus (or an ideal detector) one has a corresponding POM and, in turn, a probability distribution $dP(\phi)$ according to Eq.(2.2). Such probability has a r.m.s. error (2.13) given by

$$\langle\widehat{\Delta\phi^2}\rangle = \langle\widehat{\phi^2}\rangle - \langle\widehat{\phi}\rangle^2 \,. \tag{2.19}$$

Here $\langle\ldots\rangle$ denotes the ensemble quantum average on the system space $\mathcal{H}_S$, and the operators $\widehat{\phi}$ and $\widehat{\phi^2}$ depend on the considered POM (for the optimum POM they are given in Eqs.(2.10,2.11)). Notice that there is no ambiguity in choosing between the two operators $\widehat{\phi^2} \neq \widehat{\phi}^2$, because Eq.(2.19) directly follows from the probability (2.2). For a random-phase state—namely a constant probability distribution—one correctly has $\langle\widehat{\Delta\phi^2}\rangle = \pi^2/3$.

As regards the problem of invariance under phase shifts, here we stress that this actually is not a problem. In fact, the only concern is the correspondence between experimental and theoretical quantities, and the circular topology of the phase arises at both experimental and theoretical levels in the same way. Whatever procedure is considered for measuring the phase, the information on it has always to be inferred from a joint sine-cosine measurement, and hence the experimental equipment itself has to be tuned on a selected $2\pi$-window. Once the domain is fixed, the experimental noise is, by definition, the r.m.s. noise on such domain. Therefore, different choices of the $2\pi$-window actually lead to different experimented amounts of noise, and also theoretically the r.m.s. noise has to be evaluated on the chosen domain (hereafter we will always use the $[-\pi, \pi)$ window).

### 2.3 Double-homodyne Detection

The double-balanced-homodyne [11] (DBH) detection provides a way for simultaneously measuring a couple of field-quadratures for one mode of e. m. field. The schematic diagram of the experimental set-up is reported in Fig. 1. There are four 50-50 beam splitters and four identical photocounters, and a $\pi/2$ phase shifter is inserted in one arm. The mode supporting the phase is $a$, whereas a stable reference for the phase is provided by a local oscillator (LO) which is synchronous with $a$ and is prepared in a highly excited coherent state $|z\rangle$.

The DBH scheme can also perform a phase measurement, however with a probability distribution which does not correspond to the ideal case due to unavoidable addition of "instrumental" noise. The DBH phase distribution is obtained through the following procedure. Each experimental event consists of a simultaneous detection of the two difference photocurrents $\hat{I}_1 = \hat{n}_6 - \hat{n}_5$ and $\hat{I}_2 = \hat{n}_4 - \hat{n}_3$ which "trace" two field-quadratures. Each event thus corresponds to a point plotted in the complex plane of the field amplitude. The phase relative to the event is nothing but the polar angle of the point itself. An experimental histogram of the phase distributions is thus obtained upon dividing the plane into small ("infinitesimal") angular bins of equal width $\delta\phi$, from $-\pi$ to $\pi$, then counting the number of points which fall into each bin. In formulas, one has the statistical frequency $P_n$ for the $n$-th bin $\theta_n \equiv [-\pi + n\delta\phi, -\pi + (n+1)\delta\phi)$

$$P_n = \frac{1}{N}\{\#\text{ of events with } I_1 = \rho\cos\phi\,, I_2 = \rho\sin\phi\,, \phi \in \theta_n\}\,, \tag{2.20}$$

where $\rho = \sqrt{I_1^2 + I_2^2}$ and $N$ is the total number of experimental points.

In Fig. 2, as an example, a computer simulation of the above experimental procedure is illustrated for a squeezed state with equal number $\langle n\rangle = 10$ of signal and squeezing photons. The experimental histogram

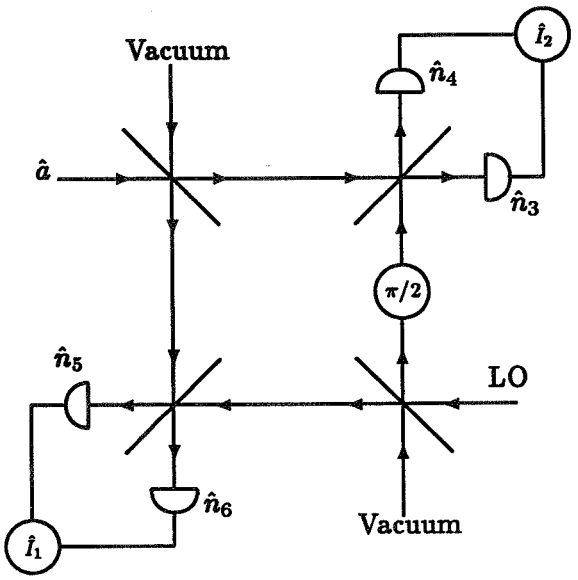


Figure 1: Outline of scheme of a double-homodyne detectors

($10^4$ events) is compared with the theoretical results from the POM for the DBH detection. This can be obtained as follows. The difference photocurrents $\hat{I}_1$ and $\hat{I}_2$ are commuting operators with factorized probability $P(I_1, I_2) = P(I_1)P(I_2)$. Introducing the *reduced current* $\hat{\mathcal{I}} = \hat{I}/|z|$ for each homodyne detector, one has the probability distribution in terms of the Fourier-transform of the generating function for the moments $\langle e^{i\lambda\hat{\mathcal{I}}} \rangle$

$$P(\mathcal{I}) = \int_{-\pi|z|}^{\pi|z|} \frac{d\lambda}{2\pi} \ \mathrm{tr}\{\hat{\rho} e^{i\lambda(\hat{\mathcal{I}}-\mathcal{I})}\}. \tag{2.21}$$

The phase distribution is the marginal probability integrated over the modulus $\rho$

$$P(\phi) = \int_0^\infty \rho d\rho \ P_1(\rho\cos\phi) P_2(\rho\sin\phi) \ . \tag{2.22}$$

Using Eq.(2.21) one has

$$P(\phi) = \int_0^\infty \rho d\rho \int_{-\pi|z|}^{\pi|z|} \frac{d\mu}{2\pi} \int_{-\pi|z|}^{\pi|z|} \frac{d\nu}{2\pi} \ \mathrm{tr}\{\hat{\rho}_S \otimes \hat{\rho}_P \ e^{i\mu(\hat{\mathcal{I}}_1 - \rho\cos\phi) + i\nu(\hat{\mathcal{I}}_2 - \rho\sin\phi)}\} \tag{2.23}$$

$\hat{\rho}_S$ being the density matrix of the mode $a$ (the system) and

$$\hat{\rho}_P = |0\rangle\langle 0| \otimes |0\rangle\langle 0| \otimes |z\rangle\langle z| \tag{2.24}$$

the density matrix of the probe. From Eqs.(2.6,2.7) one can see that the "experimental" POM is obtained upon tracing over the probe Hilbert space $\mathcal{H}_P$, thus obtaining the operator which acts solely on the system space $\mathcal{H}_S$

$$d\hat{\mu}_D(\phi) = d\phi \int_0^\infty \rho d\rho \int_{-\pi|z|}^{\pi|z|} \frac{d\mu}{2\pi} \int_{-\pi|z|}^{\pi|z|} \frac{d\nu}{2\pi} \ \mathrm{tr}_P\{\hat{1}_S \otimes \hat{\rho}_P \ e^{i\mu(\hat{\mathcal{I}}_1 - \rho\cos\phi) + i\nu(\hat{\mathcal{I}}_2 - \rho\sin\phi)}\}. \tag{2.25}$$

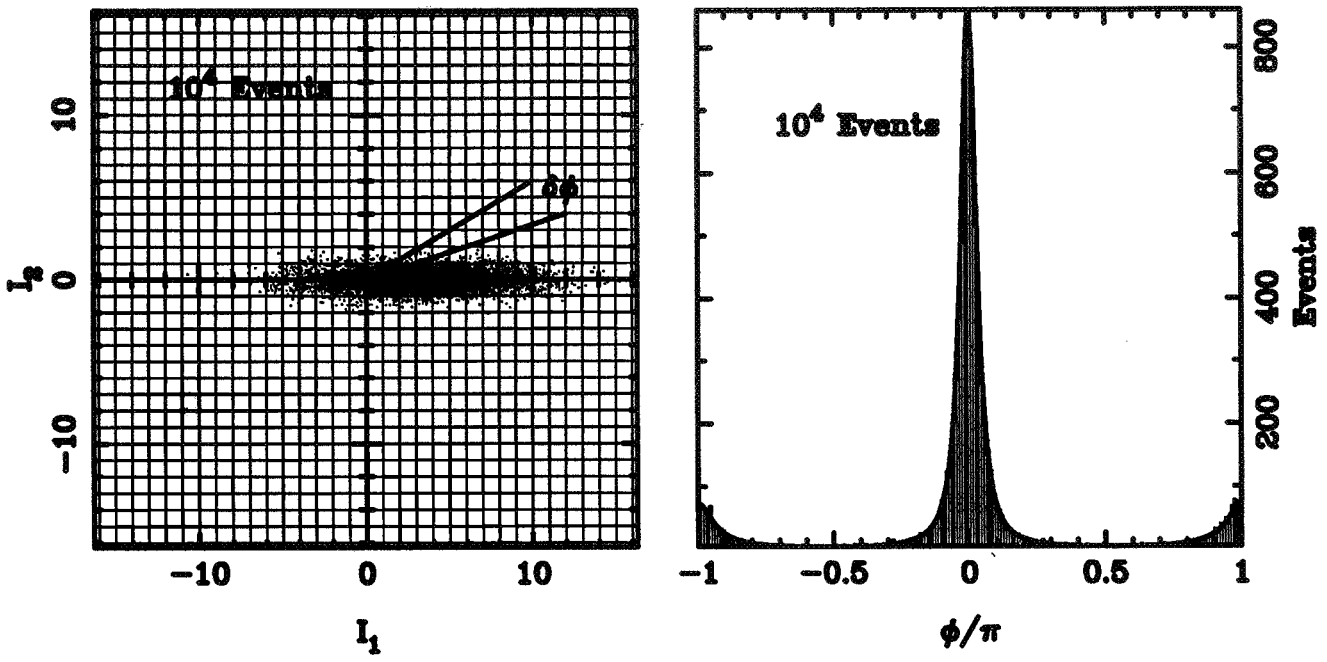


Figure 2: Computer simulation of the DBH experimental procedure for a squeezed state with equal number $\langle n \rangle = 10$ of signal and squeezing photons. The experimental histogram ($10^4$ events) is compared with the theoretical results from the POM in Eq.(2.26)

Using the coherent state resolution of the identity, the following closed formula is obtained (the detailed derivation is reported in the appendix)

$$d\hat{\mu}_D(\phi) = \frac{d\phi}{2\pi} \sum_{n \neq m} e^{i(n-m)\phi} \frac{\Gamma(\frac{n+m}{2}+1)}{\sqrt{n!m!}} |n\rangle\langle m| \,, \tag{2.26}$$

where $\Gamma(x)$ is the Eulero's gamma function.
The POM in Eq.(2.26) for the DBH detector corresponds to an *effective* measured phase operator which is given by

$$\hat{\phi}_D = \int \phi \, d\hat{\mu}_D(\phi) = -i \sum_{n \neq m} (-)^{n-m} \frac{1}{n-m} \frac{\Gamma(\frac{n+m}{2}+1)}{\sqrt{n!m!}} |n\rangle\langle m| \,, \tag{2.27}$$

and the squared one

$$\widehat{\phi_D^2} = \int \phi^2 \, d\hat{\mu}_D(\phi) = \frac{\pi^2}{3} + 2 \sum_{n \neq m} (-)^{n-m} \frac{1}{(n-m)^2} \frac{\Gamma(\frac{n+m}{2}+1)}{\sqrt{n!m!}} |n\rangle\langle m| \,, \tag{2.28}$$

needed for evaluation of the instrumental sensitivity $\langle \widehat{\Delta\phi_D^2} \rangle$. For any state of the mode $a$ one can simply verify that

$$\langle \widehat{\Delta\phi_D^2} \rangle \geq \langle \widehat{\Delta\phi^2} \rangle \,, \tag{2.29}$$

namely the DBH scheme adds extrinsic instrumental noise, as it does not implement the optimal canonical measurement of the phase. However, we stress again that the DBH detection is the best available method for detecting the phase. In Fig.3 a comparison between the canonical (ideal) and DBH (feasible) phase probability distributions is given for the same state of the computer simulation in Fig.2, showing that the former is sharper and higher than the latter.

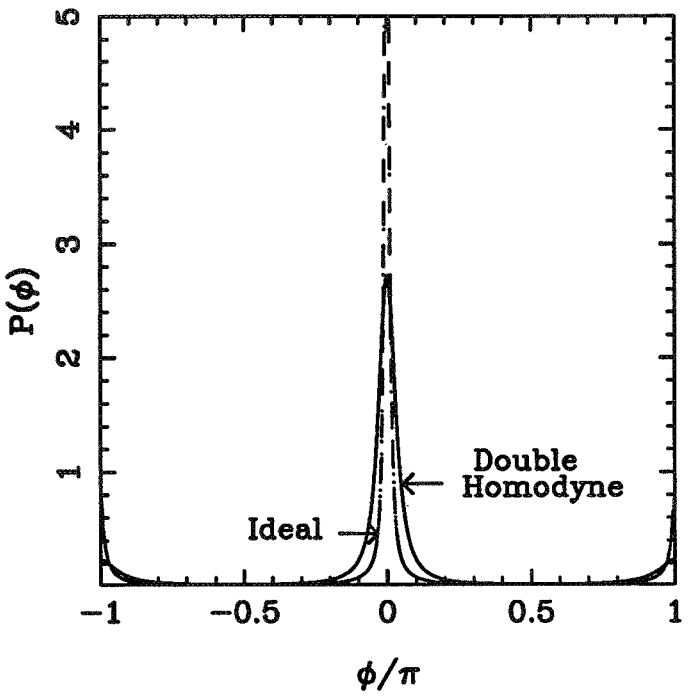


**Figure 3:** Comparison between the ideal and double-homodyne phase probability distributions for the same squeezed state of Fig.2

### 2.4 Heterodyne Detection

The first proposed method to perform simultaneous measurements of two field-quadratures was the heterodyne detection. Here we synthetically analyze this scheme, only in order to make a connection with the double-homodyne detector and show that that the two apparatus are completely equivalent from the point of view of the measured physical quantities. The input field $E_{IN}$ impinges into a beam splitter and has nonzero photon number only at the frequency $\omega_0 + \omega_{IF}$. The local oscillator works at the different frequency $\omega_0$, and the output the photocurrent $\hat{I}_{OUT}$ is measured at the *intermediate frequency* $\omega_{IF}$. The measured photocurrent is given by

$$\hat{I}_{OUT}(t) = \hat{E}^-_{OUT}(t)\hat{E}^+_{OUT}(t)\,, \tag{2.30}$$

where $E^{\pm}$ denote the usual positive and negative frequency components of the field. The component at frequency $\omega_{IF}$ is given by

$$\begin{aligned} \hat{I}_{OUT}(\omega_{IF}) &= \int dt\, \hat{I}_{OUT}(t) e^{i\omega_{IF}t} \\ &= \int d\omega \hat{E}^-_{OUT}(\omega + \omega_{IF})\hat{E}^+_{OUT}(\omega)\,. \end{aligned} \tag{2.31}$$

For a nearly transparent beam splitter, and in the limit of strong LO in the coherent state $|z\rangle$ one can define the reduced complex current $\hat{\mathcal{Y}}$

$$\hat{\mathcal{Y}} = \lim_{\substack{\eta \to 1, |z| \to \infty \\ \gamma = \text{cost.}}} \gamma^{-1} \hat{I}_{OUT}(\omega_{IF})\,, \tag{2.32}$$

where $\gamma = |z|\sqrt{\eta(1-\eta)}$. In this limit the expression of $\hat{\mathcal{Y}}$ is given by

$$\hat{\mathcal{Y}} = |z|^{-1}(a_s^\dagger b_l + a_i b_l^\dagger) + \text{ vanishing terms}\,, \tag{2.33}$$

where the subscript $s$, $l$ and $i$ refer to the signal, LO and image component of the field respectively, $a$ are signal modes, $b$ the LO modes, and the vanishing terms denote operators which do not give contributions in the strong LO limit. In the double-homodyne in the same limit the role of the complex current (2.33) is played by

$$\hat{\mathcal{I}} = \hat{\mathcal{I}}_1 + i\hat{\mathcal{I}}_2 = |z|^{-1}\left(a_2 a_1^\dagger + b_0 a_2^\dagger\right)\,, \tag{2.34}$$

where subscript 1 refers to the input signal and subscript 2 to the local oscillator, whereas $b_0$ is the vacuum mode at the unused port of the beam splitter which contains the input signal. The fully equivalence between heterodyne and double-homodyne is apparent when comparing Eq.(2.33) and Eq.(2.34). As in the double-homodyne case, now the real and imaginary parts of the current trace the two conjugated quadratures $a_{s\phi}$ and $a_{s\phi+\pi/2}$ of the signal mode. In [16] the POM of the heterodyne detector has been derived in a different context, leading to the same result obtained for the double-homodyne in Subsect.2.3. We notice that the actual sources of extrinsic added noise are the vacuum modes $a_i$ for the heterodyne detector and $b_0$ for the double-homodyne: the other vacuum modes are totally irrelevant in the limit of strong LO.

### 2.5 Measurement of the phase quadratures

The POM approach naturally leads to well defined operator functions of the phase which obey the trigonometric calculus at the operator level, and, hence, also at the level of expectation values. In particular, the sine and cosine operators are defined as in (2.16). Such definitions coincide, in the case of optimum POM, with the sine and cosine operators $\hat{s}$ and $\hat{c}$ introduced by Susskind and Glogower [7]

$$\hat{s} = \frac{1}{2i}(\hat{e}^- - \hat{e}^+)\,, \qquad \hat{c} = \frac{1}{2}(\hat{e}^- + \hat{e}^+)\,, \tag{2.35}$$

where $\hat{e}_\pm$ denote the raising and lowering operators $\hat{e}_+|n\rangle = |n+1\rangle$, $\hat{e}_- \equiv (\hat{e}_+)^\dagger$. Notice, however, that this equivalence between operators fails for higher powers, namely

$$\hat{c}^n \neq \widehat{\cos^n}\phi\,, \qquad \hat{s}^n \neq \widehat{\sin^n}\phi\,, \qquad \text{for } n > 1 \tag{2.36}$$

Here some remarks are in order, regarding relevant differences between a conventional measurement of a single phase-quadrature—say the cosine $\hat{c}$—and a joint measurement of both sine-cosine quadratures which have been analyzed in previous Subsections. A single phase-quadrature measurement leads to violation of the trigonometric calculus for expectation values. In fact, for a general density matrix state $\hat{\rho}$ one has that

$$\mathrm{Tr}[\hat{\rho}(\hat{c}^2 + \hat{s}^2)] = 1 - \frac{1}{2}\langle 0|\hat{\rho}|0\rangle\,, \tag{2.37}$$

whereas for a joint measurement one obtains

$$\mathrm{Tr}[\hat{\rho}(\widehat{\sin^2}\phi + \widehat{\cos^2}\phi)] = 1\,. \tag{2.38}$$

We stress again that, however, the linear operators coincide in the two cases, and thus one gets the same average values. However, the probability distribution of the outcomes from single phase-quadrature measurement exhibits unphysical features for nonclassical states, whereas the probability distribution from the joint measurement does not. In the single-quadrature measurement one has

$$P(c) = \mathrm{tr}\{\hat{\rho}|c\rangle\langle c|\}\,, \tag{2.39}$$

where the eigenstates of $\hat{c}$ are given by [7, 15]

$$|c\rangle = \sqrt{\frac{2}{\pi}}(1-c^2)^{-1/4}\sum_{n=0}^{\infty}\sin[(n+1)\arccos c]|n\rangle \tag{2.40}$$

On the other hand, the Radon-Nikodym derivative of the joint measurement POM's leads to

$$P(c) = \mathrm{Tr}\left[\hat{\rho}\frac{d\hat{\mu}(\phi)}{d\phi}\frac{d\phi}{dc}\right] = \frac{1}{\pi}(1-c^2)^{-\frac{1}{2}}\sum_{n,m}\langle m|\hat{\rho}|n\rangle\exp\left[i(n-m)\arccos c\right]\,, \tag{2.41}$$

for the optimum POM case, whereas for double-homodyning one obtains

$$P(c) = \mathrm{Tr}\left[\hat{\rho}\frac{d\hat{\mu}_D(\phi)}{d\phi}\frac{d\phi}{dc}\right] = \frac{1}{\pi}(1-c^2)^{-\frac{1}{2}}\sum_{n,m}\langle m|\hat{\rho}|n\rangle\frac{\Gamma(\frac{m+n}{2}+1)}{\sqrt{n!m!}}\exp\left[i(n-m)\arccos c\right]\,. \tag{2.42}$$

The differences between the single-quadrature and double-quadrature probabilities become striking for isotropic states, as, for example, the vacuum or a general number state. In this case the above distribution should be compared with the Radon-Nikodym derivative of the constant distribution

$$P(c) = \frac{1}{\pi}\frac{1}{\sqrt{1-c^2}}\,, \tag{2.43}$$

which is a concave function and has poles at the $c = \pm 1$ stationary points of the cosine. The probabilities (2.41) and (2.42) coincide with (2.43) for number states, whereas the probability (2.39) has the opposite curvature for the vacuum state, and oscillates fastly around the function (2.43) for nonvacuum number states. These undesired physical features disappear for highly excited coherent states, where, however, the main quantum features are lost.

### 2.6 Homodyne Detection

This Subsection is devoted to the customary homodyne detector, which, despite it exits from the present phase estimation treatment, however it is the most relevant device in any interferometric setup. Actually, the homodyne detector belongs to the class of the *zero-point* measurement schemes, and thus *is not a measurement of phase.* The balanced homodyne scheme measures one quadrature of a field mode, which in turn is related to its phase difference with respect to the synchronous LO. Generally one is interested in the measure of the phase shift $\chi$ of the signal state

$$|\psi\rangle_\chi = \exp(-i\chi\hat{n})|\psi\rangle_0\,, \tag{2.44}$$

where, without loss of generality, the input state is assumed of the form

$$|\psi\rangle_0 = \sum_{n=0}^{\infty}c_n|n\rangle\,,\quad c_n \geq 0\,. \tag{2.45}$$

The expectation value of the quadrature is given by

$$\langle\hat{a}_\phi\rangle_\chi = \sum_{n=0}^{\infty}\sqrt{n+1}c_nc_{n+1}\cos(\phi-\chi) = \langle\hat{a}_0\rangle_0\cos(\phi-\chi)\,. \tag{2.46}$$

The quadrature $\hat{a}_\phi$ is proportional to the cosine of the phase with a proportionality "constant " $\langle\hat{a}_0\rangle_0$ which can be evaluated from the knowledge of the fixed input state. Notice that, however, when the present scheme is regarded as a measure of the phase of the state $|\psi\rangle_\chi$ itself the state-depending "constant

" is unknown, and it cannot be preventively measured without destroying the information on phase. In this case the only point which does not need any knowledge of the "constant" is the $\phi - \chi = \pi/2$ point, namely just the maximum-derivative zero-current working point. Thus, it is not possible to detect a arbitrary phase difference, the sensitivity depending on the particular input signal, whereas a suitable feedback mechanism is needed to follow the working point. A convenient description of the homodyne detector in view of the above considerations is given in [17], where the zero-point (zero-field) probability distribution is revisited as a sort of a phase probability distribution.
The phase sensitivity of the homodyne detector can be straightforwardly obtained from error propagation calculus using the relation

$$\delta\phi = \sqrt{\langle \Delta \hat{a}_\phi^2 \rangle} \left| \frac{\delta \langle \hat{a}_\phi \rangle}{\delta \phi} \right|^{-1} , \tag{2.47}$$

which is customary in the literature on interferometry. One can see that the $\phi - \chi = \pi/2$ working point minimizes sensitivity.

## 3 Optimal states for phase measurements

The design a phase measurement needs optimization of both the detection scheme and of the quantum state which carries the phase information. The former is the main task of quantum estimation theory, which leads to an ideal scheme to be compared with the feasible ones. The latter, which is the main concern of this Section, depends on the detection scheme itself, and should account for the actual physical constraints, mainly the total power impinged into the state. Therefore, the problem is that of optimizing the r.m.s sensitivity $\Delta\phi \stackrel{\text{def}}{=} \sqrt{\langle \widehat{\Delta\phi^2} \rangle}$ for fixed average photon number, and depending on the particular detection scheme.
In the following we consider, without loss of generality, a zero average phase state, with real coefficients on the number basis, namely

$$|\psi\rangle = \sum_{n=0}^{\infty} c_n \, |n\rangle \quad c_n \in \mathbf{R}. \tag{3.1}$$

The state optimization problem is to minimize a quantity of the form

$$\langle \widehat{\Delta\phi^2} \rangle = \frac{\pi^2}{3} + 2 \sum_{n \neq m} A_{n,m} \, c_n c_m \, , \tag{3.2}$$

with the constraints

$$\sum_{n=0}^{\infty} c_n^2 = 1 \, , \qquad \sum_{n=0}^{\infty} n \, c_n^2 \equiv \langle n \rangle = \bar{n} \, . \tag{3.3}$$

The (real symmetric) matrix $\mathbf{A} = \{A_{n,m}\}$ depends on the detection scheme. In particular, for $n \neq m$ one has ($A_{n,n} = 0$)

$$A_{n,m} = \frac{(-)^{n-m}}{(n-m)^2} \, , \qquad \text{(canonical)} \tag{3.4}$$

$$A_{n,m} = \frac{(-)^{n-m}}{(n-m)^2} \, \frac{\Gamma(\frac{n+m}{2} + 1)}{\sqrt{n!m!}} \qquad \text{(DBH)} \, . \tag{3.5}$$

The method of Lagrange multipliers reduces the problem to that of minimizing the following expression

$$F(\{c_n\}; \lambda, \beta | \bar{n}) = \frac{\pi^2}{3} + 2 \sum_{n \neq m} A_{n,m} \, c_n c_m + \lambda \left( \sum_{n=0}^{\infty} c_n^2 - 1 \right) + \beta \left( \sum_{n=0}^{\infty} n c_n^2 - \bar{n} \right) \tag{3.6}$$

with respect to $\{c_n\}$, $\lambda$ and $\beta$ being the Lagrange multipliers. The variational problem (3.6) is that of a quadratic symmetric form and is equivalent to the eigenvalue problem

$$(\mathbf{M}(\beta) + \lambda \mathbf{I}) \cdot \mathbf{c} = 0 \qquad \mathbf{c} \stackrel{def}{=} (c_0, c_1, ...) \,, \tag{3.7}$$

for symmetric matrix $\mathbf{M} = \{M_{nm}\}$ given by

$$M_{n,m} = A_{nm} + \delta_{nm}\beta n \,. \tag{3.8}$$

Eq.(3.7) for the matrix (3.8) can be numerically solved upon suitable truncation of the Hilbert space $\mathcal{H}_s$. The absolute minimum corresponds to eigenvalue $\lambda = \pi^2/3$, and $\bar{n} \in [0, \dim\mathcal{H}_s/2]$ turns out to be a decreasing function of the running parameter $\beta \in [0, 1]$. Notice that one should consider only average values $\bar{n} \ll \dim\mathcal{H}_s/2$, such that the number distribution has vanishing tail at $n = \dim\mathcal{H}_s$, in order to avoid undesired numerical boundary effects.

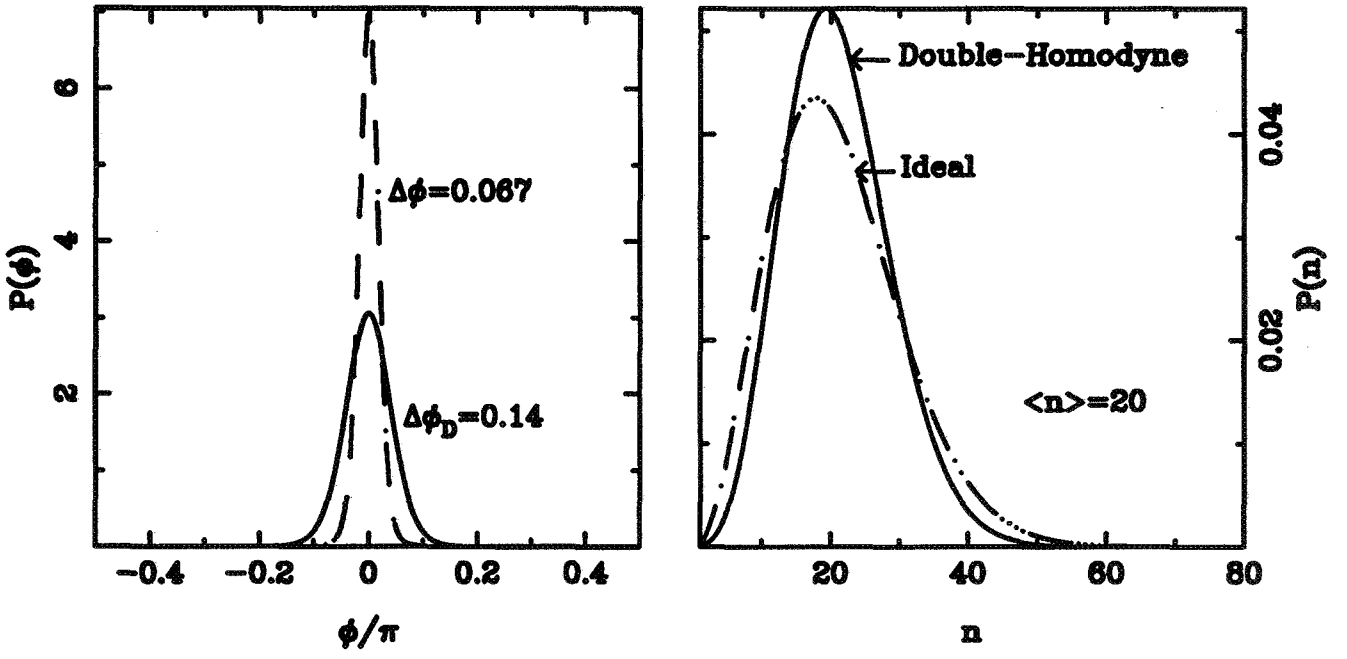


Figure 4: Phase and number probability distributions of an optimal states of $\bar{n} = 20$ for both ideal and DBH detection

### 3.1 Canonical Measurement

For ideal measurement of the phase, the best phase states obtained through the above optimization procedure, lead to the simple power-law

$$\Delta\phi \sim \frac{1.36 \pm 0.01}{\bar{n}^{1.00 \pm 0.01}} \,, \tag{3.9}$$

in agreement with results of [18]. The proportionality constant actually increases very slowly as a function of $\bar{n}$, and one has a variation of few percent for two decades of $\Delta\phi$. Eq.(3.9) can be compared with the result of [18], and with the theoretical bound $\Delta\phi \sim 1/(e\bar{n})$ [19] obtained by means of information-theory arguments. One should notice that essentially the same result can be obtained for large $\bar{n}$ ($\bar{n} > 10$) using

squeezed states where the squeezing photon number is optimized as a function of the average total number. It turns out that the optimal states have only $\sim 3.7\%$ of squeezing photons (see Fig. 5). This result is quite different from the customary 50% optimal squeezing number (which also holds true for the homodyne sensitivity of the Mack-Zehnder interferometer [20]).

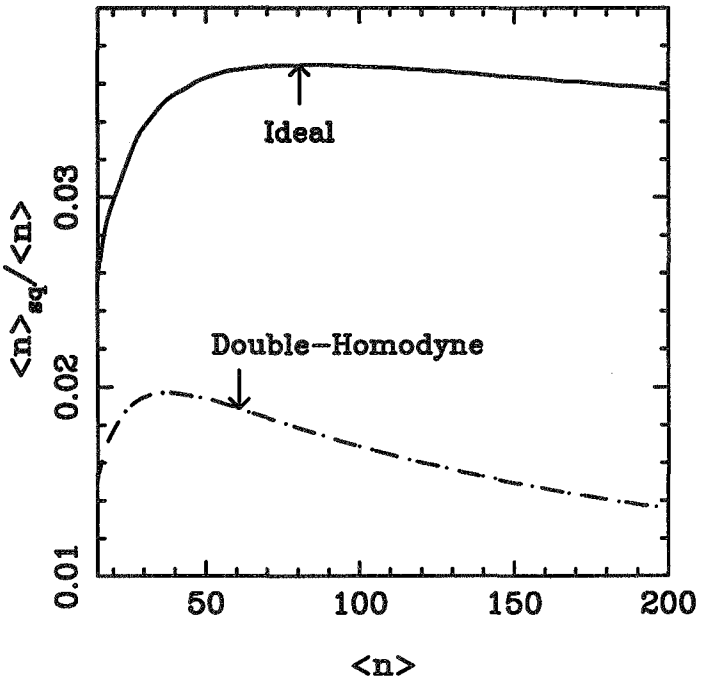


Figure 5: Optimal squeezing photon number as a function of the average total number for both ideal and DBH detection.

### 3.2 Double-homodyne

As expected, an actual measurement of the phase does not achieve the ideal sensitivity (3.9). In the case of double-homodyne (or equivalently heterodyne) phase detection, the resulting power-law is

$$\Delta\phi_D = \frac{(1.00 \pm 0.01)}{\bar{n}^{0.65\pm0.01}}\,, \tag{3.10}$$

which is obtained by numerically solving Eq.(3.7) for matrix M given in Eqs.(3.8) and (3.5). In Fig. 4 the optimized states for both canonical and DBH detection are compared for an equal fixed average photon number $\bar{n} = 20$. One can see that the number and phase probability distributions are qualitatively similar, however the DBH optimum states are slightly sharper in the number distribution and larger in the phase one. Also the best DBH states are essentially indistinguishable from squeezed states which are optimized in the squeezing photon number as a function of the average total number (see Fig. 5). In this case, only less than $\sim 2\%$ of squeezing photons turns out to be optimal.

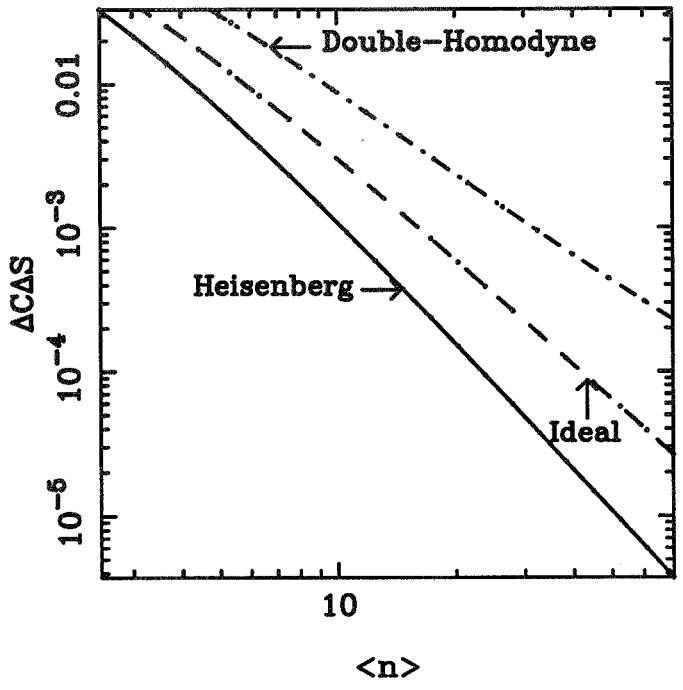


Figure 6: Uncertainty product versus the average photon number for optimal states.

### 3.3 Heisenberg Uncertainty Product for phase quadrature

The customary Heisenberg uncertainty relation

$$\Delta A \Delta B \geq \frac{1}{2} |\mathrm{Tr}\left\{\hat{\rho}[\hat{A}, \hat{B}]\right\}| \tag{3.11}$$

refers to the situation in which the quantum system is prepared in a state with fixed uncertainty say $\Delta A$ and the other observable $\hat{B}$ is measured. For the case of a joint $\hat{A}$-$\hat{B}$ measurement, however, a generalized uncertainty relation hold, where the 1/2 factor on the right side of Eq.(3.11) is dropped, corresponding to an added noise of 3 dB [21]. For the phase-quadratures one has the commutation relation

$$[\hat{c}, \hat{s}] = -\frac{i}{2} |0\rangle\langle 0| , \tag{3.12}$$

corresponding to the joint-measurement uncertainty relation

$$\Delta c \Delta s \geq \frac{1}{2} |\langle \psi | 0 \rangle|^2 . \tag{3.13}$$

In Eqs.(3.11) and (3.13) the uncertainties are defined in the usual way, namely $\Delta O^2 = \langle \hat{O}^2 \rangle - \langle \hat{O} \rangle^2$. On the other hand, in the POM approach the correct uncertainty (namely the measured quantity) is defined as $\Delta O^2 = \langle \widehat{O^2} \rangle - \langle \hat{O} \rangle^2$, where $\widehat{O^2} \neq \hat{O}^2$ is defined as in Eq.(2.4). In general, by means of Schwartz inequality, one obtains

$$\langle \widehat{O^2} \rangle - \langle \hat{O} \rangle^2 \geq \langle \hat{O}^2 \rangle - \langle \hat{O} \rangle^2 . \tag{3.14}$$

| | Ideal detection | Double-homodyne | Homodyne | Ideal Sine detection |
|---|---|---|---|---|
| | $\Delta\phi$ (Eqs.(2.10,2.11)) | $\Delta\phi_D$(Eqs.(2.27,2.28)) | $\Delta\phi$ (Eq.(2.47)) | $\Delta\phi$ (Eq.(2.47)) |
| Coherent States | $\frac{1}{2}\bar{n}^{-\frac{1}{2}}$ | $\frac{1}{\sqrt{2}}\bar{n}^{-\frac{1}{2}}$ | $\frac{1}{2}\bar{n}^{-\frac{1}{2}}$ | $\frac{1}{2}\bar{n}^{-\frac{1}{2}}$ |
| Phase-Coherent States (see [5]) | $(\ln 4)^{\frac{1}{2}}\bar{n}^{-\frac{1}{2}}$ | $(\frac{1}{2}\ln\bar{n})^{\frac{1}{2}}\bar{n}^{-\frac{1}{2}}$ | $(\frac{\ln\bar{n}}{4\pi})^{\frac{1}{2}}\bar{n}^{-1}$ | $\frac{1}{2}\bar{n}^{-\frac{1}{2}}$ |
| Optimised Squeezed States | $(1.36\pm 0.01)\bar{n}^{-1.00\pm.01}$ $\bar{n}_{sq}/\bar{n}\sim 4\%$ | $(1.00\pm 0.01)\bar{n}^{-0.65\pm.01}$ $\bar{n}_{sq}/\bar{n}\sim 2\%$ | $\frac{1}{2}\bar{n}^{-1}$ $\bar{n}_{sq}/\bar{n}=50\%$ | $(1.36\pm 0.01)\bar{n}^{-1.00\pm.01}$ $\bar{n}_{sq}/\bar{n}\sim 5\%$ |

Table 1: Asymptotic sensitivities versus the average photon number (results from numerical calculations are given with error estimation)

Therefore, one should not expect that the optimum states for phase detection achieve the minimum uncertainty product (3.13), even though phase detection corresponds to a joint sine-cosine measurement. In Fig. 6, the minimum uncertainty product in Eq.(3.13) is compared with the actual uncertainty product of the optimal states for canonical measurement. One can see that the minimum uncertainties are never achieved, despite canonical detection is ideal. In the same figure the uncertainty product of the optimal states for DBH detection is also reported for comparison, showing additional noise due to nonideal measurement.

### 3.4 Homodyne detection

For homodyne detection the well known sensitivity $\Delta\phi = \frac{1}{2}\bar{n}^{-1}$ is achieved only near the zero-current working point. As a consequence, it happens that it is better than the sensitivity achieved by the true phase measurement, either in the double-homodyne or the ideal case itself. This is due to the fact that the measurement of the field-quadrature near the zero-current working point partially underestimates the tails of the phase distribution at $\phi = \pm\pi$. The latter are enhanced by large squeezing, and thus one also finds that the optimal number of squeezing photons is only a few percent of $\bar{n}$ for the true phase measurements, whereas it is 50% for single homodyning. It is interesting to notice that the measurement of a single phase-quadrature, say $\sin\phi$, also exhibits a small optimal squeezing fraction ($\sim 5\%$), as, in some sense, it is more faithful observable than the field quadrature. In Table1 the above results are reported along with the phase sensitivity for other quantum state and different detection schemes in the limit of large average photon numbers $\bar{n}$.

## 4 Conclusion

We have analyzed ideal and actual detection schemes for the quantum phase. We have also considered the homodyne detectors as it can be used as zero-phase measurement apparatus. The working conditions for a phase detectors have been discussed showing that in an actual measurement the phase shift corresponds to the polar angle between two real output photocurrents. We have analyzed in detail the double-homodyne scheme of [11], giving the POM of the apparatus. The equivalence of this schemes with heterodyne one in detecting the phase it has also been shown.
A critical revision of various adopted definitions of sensitivity has been reported, we have concluded that the usual r.m.s. noise is the right quantity to be considered.

The sensitivity of all the detection schemes has been optimized at fixed energy with respect to input quantum states of radiation. We have shown that the sensitivity versus the average photon number $\bar{n}$ is bounded by the ideal limit $\Delta\phi \sim \bar{n}^{-1}$, whereas for double-homodyne detection the bound is $\Delta\phi_D \sim \bar{n}^{-2/3}$, in between the shot noise level $\Delta\phi \sim \bar{n}^{-1/2}$ and the ideal bound. The optimal states achieving the best sensitivity for fixed energy have been numerically obtained, and we have shown that they are very close to coherent states weakly squeezed either for ideal detection or for double-homodyne. This result, which is in contrast with the 50% of optimal squeezing photons for single-homodyning, is due to the sensitivity of the double-homodyne detection to the whole phase distribution including tails, which are enhanced by increasing squeezing.

## Appendix: Evaluation of Double-Homodyne POM

The phase distribution is the marginal probability integrated over the modulus $\rho$ , namely

$$P(\phi) = \int_0^\infty \rho d\rho \, P_1(\rho\cos\phi) P_2(\rho\sin\phi) \, . \tag{A.1}$$

Using Eq. (2.21) one has

$$P(\phi) = \int_0^\infty \rho d\rho \int_{-\pi|z|}^{\pi|z|} \frac{d\mu}{2\pi} \int_{-\pi|z|}^{\pi|z|} \frac{d\nu}{2\pi} \, \mathrm{tr}\{\hat{\rho}_P \otimes \hat{\rho}_S \, e^{i\mu(\hat{I}_1 - \rho\cos\phi) + i\nu(\hat{I}_2 - \rho\sin\phi)}\} \, , \tag{A.2}$$

$\hat{\rho}_S$ being the density matrix of the mode $a$ (the system) and

$$\hat{\rho}_P = |0\rangle\langle 0| \otimes |0\rangle\langle 0| \otimes |z\rangle\langle z| \tag{A.3}$$

the density matrix of the probe. From Eqs. (2.6) and (2.7) one can see that the POM is obtained upon tracing over the probe Hilbert space $\mathcal{H}_P$, thus obtaining the operator which acts on the system space $\mathcal{H}_S$ only

$$d\hat{\mu}_D(\phi) = d\phi \int_0^\infty \rho d\rho \int_{-\pi|z|}^{\pi|z|} \frac{d\mu}{2\pi} \int_{-\pi|z|}^{\pi|z|} \frac{d\nu}{2\pi} \, \mathrm{tr}_P\{\hat{\rho}_P \otimes \hat{1}_S \, e^{i\mu(\hat{I}_1 - \rho\cos\phi) + i\nu(\hat{I}_2 - \rho\sin\phi)}\}, \tag{A.4}$$

Using the coherent state resolution of identity one has

$$d\hat{\mu}_D(\phi) = d\phi \int_0^\infty \rho d\rho \int_{-\pi|z|}^{\pi|z|} \frac{d\mu}{2\pi} \int_{-\pi|z|}^{\pi|z|} \frac{d\nu}{2\pi} \int_{\mathbf{C}} \frac{d^2u}{\pi} \int_{\mathbf{C}} \frac{d^2w}{\pi} e^{-i\rho(\mu\cos\phi + \nu\sin\phi)} |u\rangle R \langle w| \, , \tag{A.5}$$

where $R$ is the matrix element

$$R = \langle u, z, 0, 0 | \hat{U}^\dagger e^{i(\mu\hat{I}_1 + \nu\hat{I}_2)} \hat{U} | 0, 0, z, w \rangle \, . \tag{A.6}$$

In Eq. (A.6) $\hat{U}$ denotes the unitary evolution operator of the detector, which acts on the state (A.6) as follows

$$\hat{U}|0, 0, z, w\rangle = |\frac{1}{2}(z + w), \frac{1}{2}(z - w), \frac{1}{2}(iz + w), \frac{1}{2}(iz - w)\rangle \, . \tag{A.7}$$

The explicit expression of the matrix element $R$ is given by

$$\begin{aligned} \ln R \;=\; & -|z|^2 - \frac{1}{2}|u|^2 - \frac{1}{2}|w|^2 + \frac{1}{2}|z|^2 \left(\cos\frac{\mu}{|z|} + \cos\frac{\nu}{|z|}\right) + \frac{1}{2} z\bar{u} \left(i\sin\frac{\mu}{|z|} + i\sin\frac{\nu}{|z|}\right) \\ + \; & \frac{1}{2} w\bar{z} \left(i\sin\frac{\mu}{|z|} - i\sin\frac{\nu}{|z|}\right) + \frac{1}{2} w\bar{u} \left(\cos\frac{\mu}{|z|} + \cos\frac{\nu}{|z|}\right) \, . \end{aligned} \tag{A.8}$$

Taking the strong LO limit $|z| \to \infty$ and introducing the complex variable $\alpha = \frac{1}{2}(\nu + i\mu)e^{i\arg(z)}$ one gets

$$R = \exp\left[-\frac{1}{2}|u|^2 - \frac{1}{2}|w|^2 - |\alpha|^2 + \alpha\bar{u} - w\bar{\alpha} + w\bar{u}\right] = \sum_{p=0}^{\infty}\frac{1}{p!}\langle u|\hat{a}^\dagger|\alpha\rangle\langle -\alpha|\hat{a}|w\rangle\,. \tag{A.9}$$

Substituting Eq.(A.9) into Eq.(A.5) leads to

$$\begin{aligned} d\hat{\mu}_D(\phi) &= d\phi\int_0^\infty \rho d\rho \int_{-\infty}^{\infty}\frac{d\mu}{2\pi}\int_{-\infty}^{\infty}\frac{d\nu}{2\pi}e^{-i\rho(\mu\cos\phi+\nu\sin\phi)}\sum_{p=0}^{\infty}\frac{1}{p!}\int_{\mathbf{C}}\frac{d^2u}{\pi}\,|u\rangle\langle u|\hat{a}^{p\dagger}|\alpha\rangle\langle -\alpha|\hat{a}^p\int_{\mathbf{C}}\frac{d^2w}{\pi}|w\rangle\langle w| \\ &= d\phi\sum_{p=0}^{\infty}\frac{1}{p!}\frac{1}{2\pi}\hat{a}^{p\dagger}\left[2\int_0^\infty\rho d\rho\int_{\mathbf{C}}\frac{d^2\alpha}{\pi}\exp(\rho\hat{a}e^{i\phi})|\alpha\rangle\langle\alpha|e^{i\pi\hat{n}}\exp(\rho\hat{a}^\dagger e^{-i\phi})\right]\hat{a}^p\,. \end{aligned} \tag{A.10}$$

Using the coherent resolution of the identity and integrating over $\rho$ one obtains

$$d\hat{\mu}_D(\phi) = \frac{d\phi}{2\pi}\sum_{p=0}^{\infty}\frac{1}{p!}\sum_{m,n=0}^{\infty}(-i)^{n-m}e^{i(n-m)\phi}\frac{\Gamma(\frac{n+m}{2}+1)}{n!m!}\hat{a}^{p\dagger}e^{i\frac{\pi}{2}\hat{n}}\hat{a}^{m\dagger}\hat{a}^n e^{i\frac{\pi}{2}\hat{n}}\hat{a}^p\,, \tag{A.11}$$

where $\Gamma(x)$ is Eulero's Gamma function. The normal ordered representation of the vacuum state

$$\lim_{\varepsilon\to 1}\sum_{p=0}^{\infty}\frac{(-\varepsilon)^p}{p!}\hat{a}^{p\dagger}\hat{a}^p = |0\rangle\langle 0|\,, \tag{A.12}$$

leads to

$$d\hat{\mu}_D(\phi) = \frac{d\phi}{2\pi}\sum_{m,n=0}^{\infty}(-i)^{n-m}e^{i(n-m)\phi}\frac{\Gamma(\frac{n+m}{2}+1)}{n!m!}\,e^{i\frac{\pi}{2}\hat{n}}\,\hat{a}^{m\dagger}|0\rangle\langle 0|\hat{a}^n\,e^{i\frac{\pi}{2}\hat{n}}\,. \tag{A.13}$$

From Eq.(A.13) one obtains the POM of the detector in form of a double series

$$d\hat{\mu}_D(\phi) = \frac{d\phi}{2\pi}\sum_{n,m}e^{i(n-m)\phi}\frac{\Gamma(\frac{n+m}{2}+1)}{\sqrt{n!m!}}\,|n\rangle\langle m|\,. \tag{A.14}$$

Alternatively, using the $\Gamma$-function integral representation one can write

$$d\hat{\mu}_D(\phi) = \frac{d\phi}{\pi}\int_0^\infty\rho d\rho\,e^{-\rho^2}e^{\rho e^{i\phi}a^\dagger}|0\rangle\langle 0|e^{\rho e^{-i\phi}a} = \frac{d\phi}{\pi}\int_0^\infty\rho d\rho\,|\rho e^{i\phi}\rangle\langle\rho e^{i\phi}|\,. \tag{A.15}$$

## References


[1] G. M. D'Ariano, and M. G. A. Paris, submitted to *Phys. Rev.* A

[2] P. A. M. Dirac. Proc. R. Soc. London A 114 243 (1927)

[3] D. T. Pegg, S. M. Barnett *Phys. Rev.* **A39**, 1665 (1989)

[4] C. W. Helstrom *Quantum Detection and Estimation Theory* (Academic Press, New York, 1976)

[5] J. H. Shapiro, S. R. Shepard *Phys. Rev.* **A43**, 3795 (1991), J. H. Shapiro, S. R. Shepard, N. C. Wong *Phys. Rev. Lett.* **62**, 2377 (1991), J. H. Shapiro in *The Workshop on Squeezed States and Uncertainty Relations* ed. by D.Han et al. (NASA Conf. Public. 3135, Washington DC, 1992), p.107

[6] A. S. Lane, S. Braunstein, C. M. Caves *Phys. Rev.* **A47**, 1667 (1993)

[7] L. Susskind and J. Glogower, *Physics* **1** (1964) 49.

[8] M. Ozawa, 'Operator algebras and nonstandard analysis' in *Current Topics in Operator Algebras* ed. by H. Araki et. al., World Scientific, (Singapore 1991) p.52

[9] M. Ban *J. Opt. Soc. Am.* **B9**, 1189 (1992)

[10] H. P. Yuen *Phys. Lett.* **91A**, 101 (1982)

[11] J. W. Noh, A. Fougeres, L. Mandel *Phys. Rev. Lett.* **67**, 1426 (1991); *Phys. Rev.***A45**, 424 (1992); *Phys. Rev.***A46**, 2840 (1992)

[12] Z. Hradil *Quantum Opt.* **4**, 93 (1992)

[13] A. Bandilla, H. Paul, H. H. Ritze *Quantum Opt.* **3**, 267 (1991)

[14] Z. Hradil, J. H. Shapiro *Quantum Opt.* **4**, 31 (1992)

[15] P. Carruthers, M. M. Nieto *Rev. Mod. Phys.* **40**, 411 (1968)

[16] M. J. W Hall, I. G. Fuss *Quantum Opt.* **3**, 147 (1991)

[17] W. Vogel, W. Schleich *Phys. Rev.* **A44**, 7642 (1991)

[18] G. S. Summy, D. T. Pegg, *Opt. Commun.***77**,75 (1990)

[19] H. P. Yuen, in *The Workshop on Squeezed States and Uncertainty Relations* ed. by D.Han et al. (NASA Conf. Public. 3135, Washington DC, 1992), p.13

[20] R. S. Bondurant and J. H. Shapiro, Phys. Rev. **A30** 2548 (1984)

[21] E. Arthurs, M. S. Goodman *Phys. Rev. Lett.* **60**, 2447 (1988)

# Joint and Angle-covariant Spin Measurements with a Quadrupole Magnetic Field

Hans Martens and Willem M. de Muynck
*Theoretical Physics Group, Department of Physics, Eindhoven University of Technology, PO Box 513, 5600 MB Eindhoven, The Netherlands.*

**Abstract**

We study a Stern-Gerlach type setup, with a quadrupole magnetic field, for neutral particles of arbitrary spin. The Hamiltonian is of a form proposed for joint measurements of incompatible observables. The measurement results are discussed, showing the limitation of such Hamiltonians. Some remarks are made on the relevance of covariance as a criterion for measurement schemes.

## 1 Introduction

The canonical form for the Hamiltonian of a measurement interaction is (operators are careted)

$$\hat{H}_I = \kappa \hat{a}'_p \hat{A}_o \,, \tag{1}$$

where the subscripts $o$ and $p$ denote object and pointer, respectively. The operator $\hat{A}_o$ is measured, whereas $\hat{a}'_p$ is conjugate to the read-out observable $\hat{a}_p$. One of the simplest measurement arrangements, often used as an example [1, 2, 3], is the Stern-Gerlach, where an inhomogeneous magnetic field effects an interaction amounting to [2, 4]

$$\hat{H}_I = -\kappa \hat{x} \hat{\sigma}_x \,, \tag{2}$$

Here the coupling constant $\kappa$ is proportional to the strength of the inhomogeneity. The spin degrees of freedom represent the object, and the spatial degrees of freedom are the "measuring device". Thus we measure the spin in the $x$-direction, by reading out the $x$-momentum component. If we assume both $\hat{p}_x$ and $\hat{\sigma}_x$ to be conserved in the absence of interactions, the Hamiltionian (2) causes in the Heisenberg picture ($\hbar = 1$)

$$\hat{p}_x(t) = \hat{p}_x(0) + \kappa \hat{\sigma}_x t \,. \tag{3}$$

Thus, as soon as $t$ is larger than the $\hat{p}_x$-width, the spatial part is separated into $s$ packets, according to $\hat{\sigma}_x$ eigenvalue. Conversely, a read-out of $\hat{p}_x$ means an accurate measurement of $\hat{\sigma}_x$.

In order to be able to measure two incompatible observables jointly, Arthurs & Kelly [5] extended the basic scheme (1) to

$$\hat{H}_I = \kappa_A \hat{a}'_p \hat{A}_o + \kappa_B \hat{b}'_p \hat{B}_o \,. \tag{4}$$

In this interaction Hamiltonian, $\hat{a}'_p$ and $\hat{b}'_p$ are two compatible pointer system operators, with read-outs $\hat{a}_p$ and $\hat{b}_p$, respectively. The operators $\hat{A}_o$ and $\hat{B}_o$, not necessarily compatible, are to be measured. Arthurs & Kelly applied (4) to joint position-momentum measurements. They found that the probabilities of finding a result $(a, b)$ are given by

$$\text{prob}(a,b) = \frac{1}{\pi} Tr\big(\hat{\rho}_o |\alpha\rangle\langle\alpha|\big) \ , \ \alpha = a + ib \ , \tag{5}$$

where $|\alpha\rangle$ is a coherent or squeezed state, depending on the interaction balance $\kappa_A/\kappa_B$. Therefore the $a$ marginal is related to the $x$ probability distribution by a convolution

$$\text{prob}(a) = \int_{-\infty}^{\infty} f(a-x)\ \langle x|\hat{\rho}_o|x\rangle\ \mathrm{d}x \tag{6}$$

with a Gaussian $f$, and analogously for $b$ and $p$. This relation, providing the basis for the interpretation of $b$ in terms of $x$, we have termed "non-ideality" elsewhere [6]. Sets of operators such as $\frac{1}{\pi}|\alpha\rangle\langle\alpha|$, which generate probability distributions but are not orthogonal, are called positive operator-valued measures (POVMs) [7].

If we combine (4) with (2), we get a Hamiltonian like

$$\hat{H}_I = -\kappa_x \hat{x}\hat{\sigma}_x + \kappa_y \hat{y}\hat{\sigma}_y \ . \tag{7}$$

Such a Hamiltonian may be realized using a quadrupole magnetic field, which around the origin in the $x, y$-plane satisfies

$$\vec{A} \propto (0, 0, xy) \Rightarrow \vec{B} \propto (x, -y, 0) \ . \tag{8}$$

In the present paper we will investigate the properties of a measurement scheme based on the quadrupole Stern-Gerlach (7), where $\kappa = \kappa_x = \kappa_y$. Neutral particles of arbitrary spin $s$ will be used. We shall focus especially on its relation to (6) and (5).

# 2 General description

If we consider the quadrupole Hamiltonian (7), we see that its rotational symmetry immediately implies that $\hat{\tilde{J}}_z = \hat{L}_z - \hat{\sigma}_z$ is conserved. It is therefore profitable to change into a polar momentum representation $(p, \varphi)$. Denote the eigenvalues of $\hat{\sigma}_z$ by $m_z$. Now we can eliminate $\varphi$ by writing the $m_z$ component of the state $|\Psi\rangle$ as

$$\langle m_z, p, \varphi|\Psi\rangle = \exp[i(m_{\tilde{j}} + m_z)\varphi]\ \phi_{m_z}(p) \ . \tag{9}$$

The Hamiltonian, seen as an operator on the $(2s+1)$-dimensional spin Hilbert space, then becomes

$$\hat{H} = p^2 - i\frac{\partial}{\partial p}\hat{\sigma}_x - \hat{\sigma}_y \frac{m_{\tilde{j}} + \hat{\sigma}_z}{p} \ . \tag{10}$$

We have taken $\kappa = 2m = 1$, without loss of generality [8]. Note that $\hat{\sigma}_y\hat{\sigma}_z$ is not Hermitian, but then neither is $i\frac{\partial}{\partial p}$; the overall expression (10) is Hermitian.

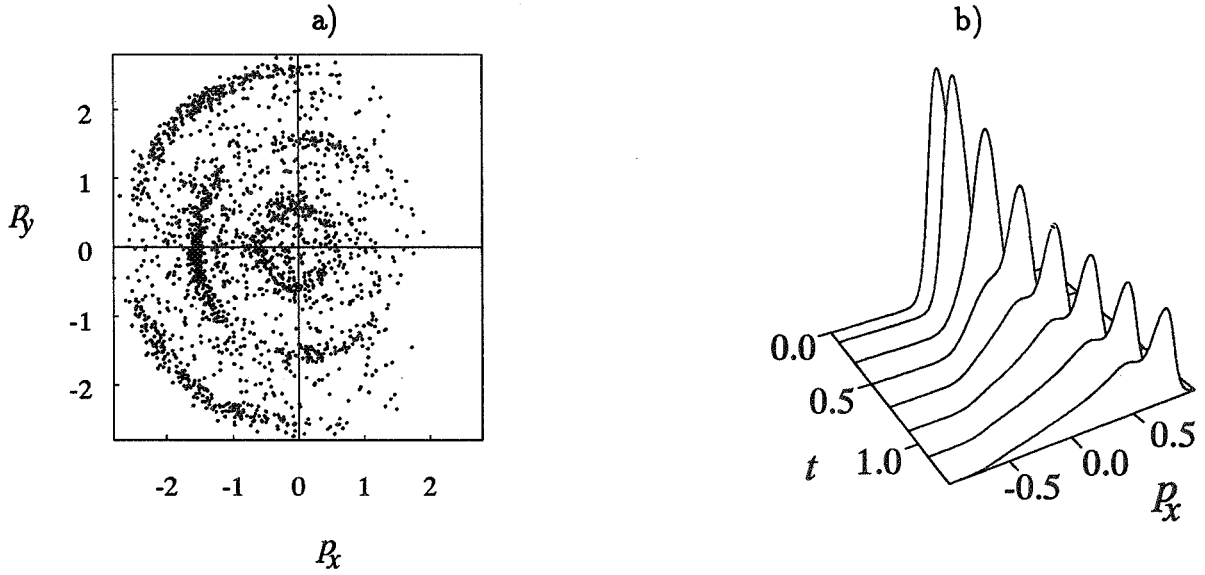


FIG. 1. Two views on the measurement results. (The Gaussian spatial part initially had variance $\Delta p^2 = 0.01$ and $L_z = 0$.)

a. Typical output distribution. The density of markers indicates the momentum probability density at $t = 1$. The input state was a $s = \frac{5}{2}$ state, with $m_x = -\frac{3}{2}$.

b. Matrix element $\langle \frac{1}{2}|\hat{M}(p_x)|\frac{1}{2}\rangle$ for $s = \frac{1}{2}$ as a function of time. The quality of the measurement can be characterized by the integral of the matrix element over $p_x > 0$. Note that this value does not approach 1.

We integrated eq. (10) numerically. In view of the fact that the process is intended as a spin measurement, we took the initial state to be a product of spatial and spin parts (denoted by subscripts $r$ and $\sigma$ when necessary),

$$|\Psi\rangle = |\phi\rangle_r \otimes |\varsigma\rangle_\sigma \,. \tag{11}$$

The spatial part $|\phi\rangle_r$ was taken to be a axially symmetric Gaussian. The final state then turned out to be structured into a number of expanding rings, one for each $|m|$; only $m = 0$ (for integral spin particles) leads to a hump remaining around the origin. Fig. 1.a is a typical example, where $s = \frac{5}{2}$, and we have 3 rings. In the figure the spin part was initially directed in the $x$-direction, with $m_x = -\frac{3}{2}$, and thus we see that the distribution is peaked in the left part of the middle ring. More generally, states with spin initially directed in the $xy$-plane lead to correspondingly oriented distributions; only spins initially in the $z$-direction evolve into complete ring distributions. In the rings the spins are directed roughly outward, with appropriate magnitude.

The scheme is meant to be seen as a spin measurement. Accordingly, we trace out the spatial variables and generate the outcome probabilities from the spin density operator $\hat{\rho}_\sigma$ by means of a POVM $\hat{M}(p,\varphi)$ on spin Hilbert space,

$$\begin{aligned} \mathrm{prob}_{\hat{\rho}_\sigma}(p,\varphi) &= Tr[\hat{\rho}_\sigma\, \hat{M}(p,\varphi)] \,; \\ \hat{M}(p,\varphi) &= {}_r\langle\phi|\, \hat{U}^\dagger(t)\Big(|p,\varphi\rangle_r\langle p,\varphi| \otimes \hat{1}_\sigma\Big)\hat{U}(t)\, |\phi\rangle_r \,;\; \hat{U}(t) = \exp(-i\hat{H}t) \,. \end{aligned} \tag{12}$$

In the next two sections we will discuss some properties of the POVM $\hat{M}(p,\varphi)$.

# 3 Marginals

The output variables of the measurement are $(p_x, p_y)$. Naively, one would suspect on the basis of (3) and (7) that a read-out of $\hat{p}_x$ can be seen as a measurement of $\hat{\sigma}_x$. Accordingly, we are interested in the $p_x$ marginal of $\hat{M}$,

$$\hat{M}(p_x) = \int_{-\infty}^{\infty} \hat{M}(p_x, p_y)\, \mathrm{d}p_y \ . \tag{13}$$

Consider first the $s = \frac{1}{2}$ case. Here the spin operators anti-commute. Thus the interaction Hamiltonian (7) satisfies

$$\hat{S}\hat{H}_I\hat{S}^\dagger = \hat{H}_I \ ; \ \hat{S} = \hat{I}_y \otimes (2\hat{\sigma}_x) \ . \tag{14}$$

Hence, if the initial spatial state is $\hat{I}_y$-symmetric, the $p_x$ marginal of the final $(p_x, p_y)$ distribution must depend only on $\hat{\sigma}_x$. Accordingly we may write (13) as

$$\hat{M}(p_x) = \sum_{m=+\frac{1}{2},-\frac{1}{2}} f_m(p_x)\hat{E}_m(0) \ , \tag{15}$$

where the $f_m$ are positive functions and $\hat{E}_m(0)$ denote the projectors onto the $\hat{\sigma}_x$ eigenstates. Thus we get an analog of the convolution (6), reproducing the basic result (3) with additional noise terms that do not depend on the spin degrees of freedom [4]. As is easily verified, an analogous relation holds between $\hat{p}_y$ and $\hat{\sigma}_y$. In fig. 1.b we plotted the probability that a particle with $m_x = +\frac{1}{2}$ will give the measurement result $p_x$. We see that the noise terms assure that the measurement quality is limited, in contrast to (3). This is necessary on account of the uncertainty principle [9, 10], as we are jointly measuring the two incompatible observables $\hat{\sigma}_x$ and $\hat{\sigma}_y$.

Nevertheless, (15) means that an unambiguous relation between the $\hat{p}_x$ and $\hat{\sigma}_x$ distributions exists. It allows for the $m_x$ estimation from $p_x$ that we aimed at [11], albeit an imperfect one. In the spin-$\frac{1}{2}$ case, the spin observables are Fourier-pairs [12] and therefore close analogs of the position-momentum pair studied by Arthurs & Kelly [5]. Accordingly, the above conclusion matches theirs.

We might think that for $s > \frac{1}{2}$ this result may be generalized. In fig. 2.a the diagonal elements of the POVM (13) in $\hat{\sigma}_x$ representation are plotted vs. $p_x$. We see that indeed the various $m_x$ values are roughly correlated to different $p_x$ regions, as expected. Thus, it appears that from $p_x$ an estimate of $m_x$ can be made, just as for $s = \frac{1}{2}$. But there is a catch: neglecting the $p^2$-term (strong or impulsive interaction approximation), it follows after some calculation that

$$\begin{aligned} \hat{p}_x(t) = \hat{p}_x(0) \ &+ \ \hat{\sigma}_x(0)[t\cos^2\theta + \frac{\sin rt}{r}\sin^2\theta] \\ &+ \ \hat{\sigma}_y(0)\frac{1}{2}[\frac{\sin rt}{r} - t]\sin 2\theta + \hat{\sigma}_z(0)\frac{\cos rt - 1}{r}\sin\theta \ ; \end{aligned} \tag{16}$$

where we used the polar position representation $(x, y) = (r\cos\theta, r\sin\theta)$. Clearly $\hat{p}_x$ contains extra spin terms that do not commute with $\hat{\sigma}_x$. Indeed the non-diagonal elements of $\hat{M}(p_x)$ are not zero, as is evidenced by fig. 2.b. Consider again (16). The desired effect, $t\hat{\sigma}_x$, is contained in the second term , whereas the last two terms are the problematic ones. As the rings expand more and more, the $\frac{1}{r}$ terms will decay roughly as $1/t^2$. Still, even as $t \to \infty$, a significant term containing $\hat{\sigma}_y$ remains: $\hat{M}$ and $\hat{\sigma}_x$ are incompatible.

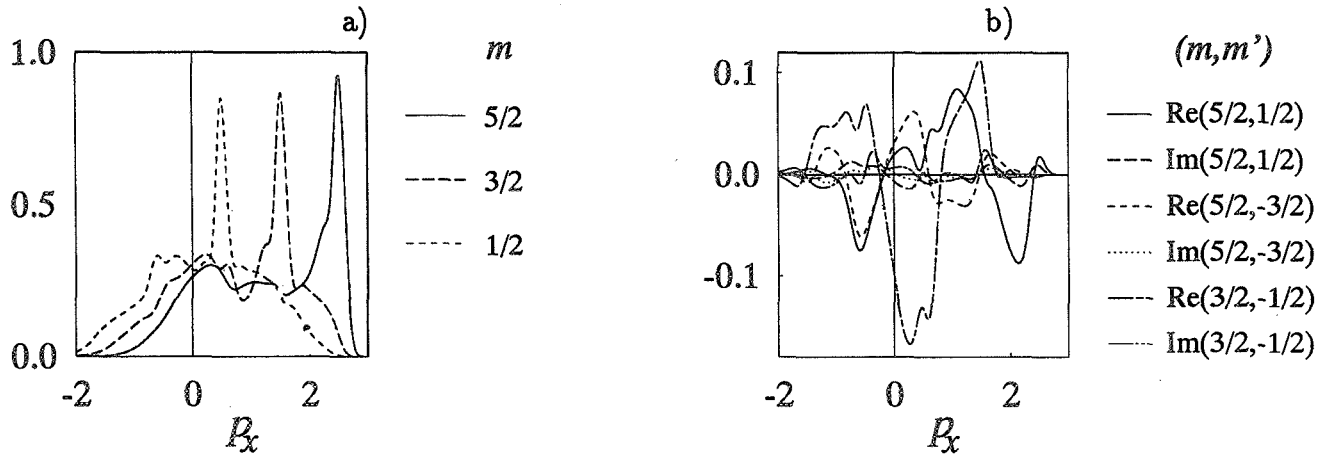


FIG. 2. The POVM $\hat{M}(p_x)$ in $\hat{\sigma}_x$ representation. (Data as in fig. 1.)
a. Diagonal matrix elements $\langle m|\hat{M}(p_x)|m\rangle = \langle -m|\hat{M}(-p_x)|-m\rangle$.
b. Independent non-zero non-diagonal matrix elements $\langle m|\hat{M}(-p_x)|m'\rangle$.

But all the problematic terms in (16) are seen to contain a factor $\sin 2\theta$ or $\sin\theta$. Denote reflection in the $xz$-plane by $\hat{I}_y$. The sine terms in $\langle\hat{p}_x\rangle$ vanish if we choose the spatial part of the initial state $\hat{I}_y$-symmetric, like we do in our calculations. But if we consider $\langle\hat{p}_x^2\rangle$, terms with factors like $\hat{\sigma}_y^2\sin^2 2\theta$ emerge. Such terms do not vanish, so that higher moments do not commute with $\hat{\sigma}_x$. Only if $s=\frac{1}{2}$, we have $\hat{\sigma}_y^2 \propto \hat{1}$ so that $\langle\hat{p}_x^2\rangle$ commutes with $\hat{\sigma}_x$ after all, in accordance with our earlier result (15).

But in what sense can we consider this scheme to be a measurement of $\hat{\sigma}_x$ if $s>\frac{1}{2}$? Clearly no analog of (15) holds; only the expectation value $\langle\hat{p}_x\rangle$ is free of incompatible spin terms, so that we can use the measurement only to estimate the $\hat{\sigma}_x$ expectation value. Higher moments, or even $m_x$ probabilities, cannot be established. Thus it is a $\hat{\sigma}_x$ measurement only in the weak sense of expectation value estimation [11].

## 4 Covariance

The measurement is therefore not generally a useful joint measurement. But it may have another use. Remember, the Hamiltonian (7) is rotationally symmetric. If we now consider the outcomes in polar coordinates, it is easily derived that the POVM $\hat{M}(p,\varphi)$ is angle covariant:

$$\hat{M}(p,\varphi+\Delta\varphi) = \hat{R}(\Delta\varphi)\hat{M}(p,\varphi)\hat{R}^\dagger(\Delta\varphi)\ ;\ \hat{R}(\Delta\varphi) = \exp(i\Delta\varphi\hat{\sigma}_z)\ . \tag{17}$$

Covariance is a criterion that is often used to characterize classes of measurements e.g. time or photon phase measurements. Here we therefore speculate that $\hat{M}(p,\varphi)$ realizes some kind of spin-angle measurement. Define the projector onto the eigenstate of the operator $\cos\theta\hat{\sigma}_x+\sin\theta\hat{\sigma}_y$ with eigenvalue $m$ as $\hat{E}_m(\theta)$. Then we choose as spin-angle observable [13]

$$\sum_m c_m\int_{-\pi}^{\pi}\hat{E}_m(\theta)\ \mathrm{d}\theta = \hat{1}\ , \tag{18}$$

where the summation runs over all relevant $|m|$ values, and $c_m = \frac{1}{2\pi}$ for $m = 0$ and $\frac{1}{\pi}$ otherwise. Accordingly, $c_m \hat{E}_m(\theta)$ defines a POVM that may be seen as a "spin-angle" observable [7]. We can now attempt to link (18) to (17). As in the previous section, this is possible for $s = \frac{1}{2}$. There a convolution-type relation between the realized angle measurement and the ideal (18) holds [4]. But, as in the previous section, this cannot be generalized to higher spins: $\hat{M}$ and 18 are incompatible, although the incompatibility is generally smaller than that of fig. 2.b. Thus, although the POVM is angle-covariant, it is not clear in what sense the "angle of spin" is measured, if at all. Analogously we may therefore conclude that photon-phase covariance and time covariance must also give many POVMs without unambiguous interpretation. Like spin-angle covariance, they are weak criterions.

# 5 Acknowledgments

This work was sponsored by the Foundation for Philosophical Research (SWON), which is financially supported by the Netherlands Organization for Scientific Research (NWO).

# References

[1] R. Feynman, R. Leighton & M. Sands, *The Feynman Lectures on Physics*, vol. 3 (Addison-Wesley, Reading, Mass., 1965).

[2] G. Ludwig, *Einführung in die Grundlagen der Theoretischen Physik*, vol. 3 (Vieweg, Braunschweig, 1976).

[3] M. Scully, B.-G. Englert & J. Schwinger, *Phys. Rev. A* **40**, 1775 (1989); R. Levine & R. Tucci, *Found. Phys.* **19**, 175 (1990).

[4] H. Martens & W. de Muynck, *J. Phys. A* **26**, 2001 (1993).

[5] E. Arthurs & J. Kelly, *Bell Syst. Techn. J.* **44**, 725 (1965).

[6] H. Martens & W. de Muynck, *Found. Phys.* **20**, 255 (1991).

[7] C.W. Helstrom, *Quantum Detection and Estimation Theory*, (Academic, NY, 1976).

[8] A suitable choice of time and position scales removes the factors in front of $\frac{\partial}{\partial t}$, $\frac{\partial}{\partial p}$ and $p$.

[9] H. Martens & W. de Muynck, *Found. Phys.* **20**, 355 (1991).

[10] P. Busch, *Phys. Rev. D* **33**, 2253 (1986).

[11] H. Martens & W. de Muynck, *Phys. Lett. A* **157**, 441 (1991).

[12] J. Schwinger, *Proc. Nat. Acad. Sc.* **46**, 570 (1960).

[13] The Fourier transform of $\hat{\sigma}_z$ is another candidate, but it fares even worse than (18) for the present (low) spin values: the incompatibility with $\hat{M}$ is much larger.

# TWO NEW KINDS OF UNCERTAINTY RELATIONS

Jos Uffink
*Department of History and Foundations of Mathematics and Science*
*University of Utrecht, P.O. Box 80.000, 3508 TA Utrecht, the Netherlands*

**Abstract**

We review a statistical-geometrical and a generalized entropic approach to the uncertainty principle. Both approaches provide a strengthening and generalization of the standard Heisenberg uncertainty relations, but in different directions.

## 1 Introduction

The purpose of this note is to introduce two approaches to the uncertainty principle which have been developed recently, a statistical-geometrical approach and a generalized entropic approach. But before we go into this, let us consider why one would need a new approach at all. In other words, what is unsatisfactory with the traditional approach to the uncertainty principle? In the standard textbook approach the uncertainty principle for position and momentum is expressed by the inequality

$$\forall \psi : \quad \Delta_\psi P \Delta_\psi Q \geq \frac{\hbar}{2} \tag{1}$$

or more generally:

$$\forall \psi : \quad (\Delta_\psi A)^2 (\Delta_\psi B)^2 \geq \frac{1}{4} \left( |\langle [A,B]_- \rangle_\psi|^2 + \langle [A - \langle A \rangle_\psi, B - \langle B \rangle_\psi]_+ \rangle^2 \right) \tag{2}$$

for arbitrary observables $A$ and $B$. Here, $\Delta_\psi A$ etc. is defined as:

$$(\Delta_\psi A)^2 = \langle (A - \langle A \rangle_\psi)^2 \rangle_\psi \tag{3}$$

There are three problems. First, uncertainty relations as (1) or (2) presuppose that all observables for which one wants to write down an uncertainty relation can be represented as self-adjoint (or at least normal [1]) operators. Unfortunately this is not always the case. Notorious examples are time and energy, and phase and photon number. Further, in relativistic quantum theory, even the status of the position observable becomes dubious. There is no self-adjoint position (vector) operator for photons [2].

Secondly, note that the right-hand side of (2) still depends on $\psi$. It may become zero, even if $A$ and $B$ do not commute. In fact, this always happens in an eigenstate of $A$ or $B$. Then, taken as a general statement about $\Delta_\psi A \Delta_\psi B$, the inequality only says that this product is greater than zero for some states and equal to zero for others. That, however, is true also in classical physics. To read off more from (2), one needs to know the state. But then, when $\psi$ is given, one can also calculate $\Delta_\psi A$ and $\Delta_\psi B$ directly, without using the inequality at all.

Even in the case where the right-hand side is always strictly greater than zero, as in relation (1), there are further problems, due to the properties of the standard deviations. In the definition (3) of the standard deviation, the probability density is integrated with a quadratic weight factor that puts most emphasis on the tails of the distribution. As a result, the standard deviation can become very high, even if 99% or more of the probability distribution is concentrated in a very small interval, and the remainder is located in long tails, as e.g. in a Breit-Wigner lineshape. Thus a large standard deviation does not necessarily prevent a probability distribution from being very sharply concentrated, and a bound on the product of standard deviations by itself does not prevent both observables from being as precisely determined as we please. In the next sections we ask whether there are more stringent inequalities that improve on the above aspects.

## 2 Statistical-geometrical approach

It is usual to assume in quantum theory that the state of the system is given. But in this section we consider an inverse problem. Suppose we don't know the state of the system. Our problem is to make a statistical inference about this state from given measurement results.

For definiteness, let us assume that some partial information about the state is given: it belongs to a given set of (pure) states labeled by an index parameter $\theta$. To be more specific, it is asumed that these states are generated by some unitary group:

$$|\psi_\theta\rangle = e^{i\theta A/\hbar}|\psi\rangle \tag{4}$$

where $A$ is a self-adjoint operator. We can think of this set of states as describing a curve in state space. The problem of statistical inference is now equivalent to that of estimating the value of $\theta$.

It is clear that a detailed discussion of this estimation problem should involve the kind of measurements performed, the results obtained, and criteria distinguishing 'good' from 'bad' estimates. However, even without going into details of statistical theory [3, 4], it can be made plausible that a fundamental bound for the estimation accuracy is obtained by considering the overlap $|\langle\psi_\theta|\psi_{\theta+\delta\theta}\rangle|$. If this overlap is high the states resemble each other much and a typical measurement result which would be probable or improbable in one state would likewise be probable or improbable in the other. Then one cannot expect to discriminate the states by any measurement procedure. It is only when the overlap begins to fall off that there are observables whose probability distributions for the states $\psi_\theta$ and $\psi_{\theta+\delta\theta}$ differ enough to allow for accurate discrimination.

This suggests the following definition. Choose some fixed value $\beta < 1$ and define the estimation inaccuracy $\delta_\psi\theta$ as the smallest value of $\delta\theta$ for which

$$|\langle\psi_\theta|\psi_{\theta+\delta\theta}\rangle| = \beta$$

Due to the particular choice (4), this overlap does not depend on the value of $\theta$. One can then show: [5, 6, 7, 8]

$$\forall\psi: \quad \delta_\psi\theta\Delta_\psi A \geq 2\hbar \arccos\beta \tag{5}$$

This then represents a useful uncertainty relation. It says that an unlimited increase in the estimation accuracy of $\theta$ is only possible at the expense of an increased spread in $A$.

Several remarks are called for. First, these relations are applicable to any one-parameter unitary group. Obvious examples are the translations in time, represented by the evolution operators

$U(t) = \exp(-itH/\hbar)$ or the translations in space, $\exp(ixP/\hbar)$, where $P$ is the momentum operator; or we can consider an angle of rotation and angular momentum, or phaseshifts and photon number. In short, we find statistical uncertainty relations of the type (5) in every case where $A$ is the generator of a unitary group and $\theta$ the group parameter. This approach is in fact ideally suited for a relativistical treatment of quantum theory in which one starts from the construction of unitary groups from the symmetries of the system.

Secondly, relation (5) is asymmetrical; $\delta_\psi\theta$ is an inaccuracy of estimation of a parameter (i.e. a *c-number*). $\Delta_\psi A$ on the other hand is the r.m.s. spread of a quantum mechanical *observable* (self-adjoint operator). Since one does not need a pair of operators to obtain relation (5) there are no problems when such a pair does not exist.

However if one does exist, e.g. in the case of non-relativistic position and momentum, it is possible to take advantage of that fact. Then there is a second, independent, uncertainty relation for the spread in position and the estimation accuracy of the parameter in the group of kicks $\{U(p) = \exp(-ipQ/\hbar)\}$, i.e. shifts in momentum. This restores symmetry between position and momentum. More importantly, we note that the position operator mimicks the parameter $x$ of the translation group in the sense that

$$\langle\psi_x|Q|\psi_x\rangle = x \tag{6}$$

(assuming $\langle\psi|Q|\psi|\rangle = 0$) i.e. the position operator acts as an unbiassed estimator of the location parameter. From this it follows: [9]

$$|\langle\psi_\theta|\psi_{\theta+\delta\theta}\rangle|^2 \leq \left(1 + (\frac{\delta\theta}{2\Delta_\psi Q})^2\right)^{-1}$$

combined with (5), where $A$ is interpreted as momentum, this result implies the standard uncertainty relation (1). In fact, as a bonus, we obtain (1) not only for the position operator proper, but for any other operator acting as unbiassed estimator of $x$ as well.

There is only one problem of those mentioned in the previous section that is not solved by the relations (5): they still rely on one standard deviation, and thus become useless for states in which this diverges. To fix this problem, the standard deviation can be replaced by an interquantile range, i.e. the smallest size $W_\psi(A)$ of an interval $W$ on which a fraction $\alpha < 1$ of the total probability distribution for $A$ is concentrated: $\int_W |\langle\psi|a\rangle|^2 da = \alpha$. A variation of the proof of (5) gives [6, 8]

$$\delta_\psi\theta W_\psi(A) \geq \hbar \arccos\frac{1+\beta-\alpha}{\alpha} \quad \text{if } \beta \geq 2\alpha - 1 \tag{7}$$

Finally we note that this concept of estimation inaccuracy fits into a general geometrical approach to statistical inference on the basis of the Fisher information metric [4]. Let it suffice here to note that this metric equips Hilbert space with a statistical distance between states which equals

$$d(\psi, \psi') = \arccos|\langle\psi|\psi'\rangle|$$

and that the geometrical background of (5) is the simple fact that the distance between $\psi_\theta$ and $\psi_{\theta'}$ (i.e. the right hand side of (5)) is less than the length of the curve (4) connecting these points. This also point the way to how the relations are to be generalized in cases where the curve is not generated by a unitary group.

# 3 Generalized entropic approach

For a discrete probability distribution $p = (p_1, \ldots p_n)$, with $p_i \geq 0$, $\sum_i p_i = 1$, the Shannon entropy

$$H(p) := -\sum_i p_i \log p_i \tag{8}$$

represents, roughly speaking, a measure of whether the distribution is 'spread out' or 'peaked'. If $A$ and $B$ are quantum observables for which an uncertainty principle holds, it is natural to ask for a lower bound of the sum of the Shannon entropies for the probabilities $|\langle\psi|a_i\rangle|^2$ and $\langle\psi|b_j\rangle|^2$ [10, 11]. Here we assume a discrete spectrum and $|a_i\rangle$ and $|b_j\rangle$ denote the eigenstates of $A$ and $B$. It turns out that

$$H(\psi, A) + H(\psi, B) := H(|\langle\psi|a_i\rangle|^2) + H(|\langle\psi|b_j\rangle|^2) \geq -2\log \sup_{ij} |\langle a_i|b_j\rangle| \tag{9}$$

This entropic uncertainty relation limits the concentration of both probability distributions by a bound which is independent of $\psi$.

There is a class of expressions that share many properties with the Shannon entropy, and also represent useful measures of 'peakedness' or concentration:

$$M_r(p) = (\sum_i p_i^{1+r})^{1/r} \tag{10}$$

Their properties have been studied extensively by Hardy, Littlewood and Pólya and by Renyi [12]. ( $-\log M_r$ is known as Renyi entropy.) Special cases are:

$$M_\infty(p) = \sup_i p_i \quad , \quad M_0(p) = e^{-H(p)} \quad , \quad M_{-1}(p) = (\#\{i \,:\, p_i > 0\})^{-1} \tag{11}$$

Where # counts the number of elements in a set. The generalized entropic uncertainty relation then reads: [11, 13]

$$M_r(|\langle\psi|a_i\rangle|^2) M_s(|\langle\psi|b_j\rangle|^2) \leq \sup_{ij} |\langle a_i|b_j\rangle|^2 \quad \text{for } r = -s/(2s+1) \;\; r, s \geq -1/2 \tag{12}$$

which contains the relations (9) as the special case with $r = s = 0$.

Remarks: The above inequalities apply to any pair of discrete observables and yield a non-trivial bound iff these observables do not share an eigenstate. (A condition which is slightly stronger than mere non-commutativity.) In the case of a two-dimensional Hilbert space, the most restrictive bounds are obtained by the choice $r = -1/2, s = \infty$ or v.v.

Secondly, in the proof of (12) it is not necessary to assume that observables are represented by self-adjoint operators. It is sufficient to demand the existence of the sets of "eigenstates" $\{|a_i\rangle\}$ and $\{|b_j\rangle\}$, possibly non-orthogonal, such that

$$\sum_i |a_i\rangle\langle a_i| = I\!I, \quad \sum_i |b_i\rangle\langle b_i| = I\!I \tag{13}$$

Thus, the approach of this section is also applicable if one accepts unitary operators [14] or even more generally, positive-operator-valued measures (POVM's) [15] as *bona fide* representations of observables. As an example, we mention a phase observable below.

In the case of continuous observables, it appears necessary to replace (8) and (10) by a relative notion of entropy:

$$M_r(p|\mu) := \left(\int (\frac{\partial p}{\partial \mu})^{1+r} d\mu\right)^{1/r} \quad , \quad H(p|\mu) = -\log M_0(p|\mu) = -\int \frac{\partial p}{\partial \mu} \log \frac{\partial p}{\partial \mu}\, d\mu \qquad (14)$$

where $\partial p/\partial \mu$ is the Radon-Nikodym derivative of a probability measure $p$ with respect to a 'background measure' $\mu$. These expressions reflect whether the probability distribution $p$ is concentrated in comparison with $\mu$. In the discrete case, the absolute entropies are recovered by choosing $\mu$ to be the counting measure $\#$. In the case of continuous observables it is natural to take for $\mu$ the Lebesgue measure, and $\partial p/\partial \mu$ becomes an ordinary probability density.

For continuous nondegenerate operators $A$ and $B$ a theorem of Haussdorf and Young analogous to (12) leads to [17, 13]

$$M_r(\psi, A|\mu) M_s(\langle \psi, Q, |\mu) := \left(\int |\langle \psi|a\rangle|^{2(1+r)} da\right)^{1/r} \left(\int |\langle \psi|b\rangle|^{2(1+s)} db\right)^{1/s} \leq \sup |\langle a|b\rangle|^2$$

(Still assuming $r = -s/(2s+1)$.) For position and momentum a slightly stronger inequality $M_r(\psi, P|\mu) M_s(\psi, Q|\mu) \geq 2(1+r)(1+2r)^{-(1+2r)/(2r)} (2\pi\hbar)^{-1}$ is obtained by a theorem of Beckner. These inequalities are all sharp for Gaussian 'minimum uncertainty' states and strictly imply the standard uncertainty relations (1).

Let $N$ be the photon number operator of a single electromagnetic field mode, with eigenstates $|n\rangle$ and $\sum |n\rangle\langle n| = I\!I$. A description of a phase observable by means of a POVM $\Phi$ was constructed by Lévy-Leblond and by Susskind and Glogower [14, 16] from the non-orthogonal improper "eigenstates"

$$|\phi\rangle = (2\pi\hbar)^{-1/2} \sum_n e^{i\phi n} |n\rangle$$

This yield a resolution of identity $\int_0^{2\pi} d\phi |\phi\rangle\langle\phi| = I\!I$ in analogy with (13). Here one finds an analogous uncertainty relation

$$M_r(\psi, \Phi) M_s(\psi, N) \leq \frac{1}{2\pi\hbar} \qquad (15)$$

where

$$M_r(\psi, \Phi) = \left(\int |\langle \psi|\phi\rangle|^{2(1+r)}\, d\phi\right)^{1/r} \quad , \quad M_s(\psi, N) = \left(\sum_{n=0}^{\infty} |\langle \psi|n\rangle|^{2(1+s)}\right)^{1/s}$$

Let us finally compare the two different approaches. Both improve on the standard approach in the sense that they yield bounds which are state independent and strictly imply $\Delta_\psi P \Delta_\psi Q \geq \hbar/2$. The statistical/geometrical approach is restricted to conjugate pairs of quantities: time/energy, location/momentum, angle/angular momentum etc. All such pairs are treated, on the same footing, as consisting of a parameter and an observable. It is essential that the observable is represented as a self-adjoint operator because of its role in (4). The approach is relativistically invariant. The entropic approach, on the other hand, is applicable to pairs of arbitrary observables, not necessarily conjugate pairs or even self-adjoint operators. It is sufficient that they do not share eigenstates. However, these uncertainty relations do not seem to have a relativistic generalization. Also, the last problem mentioned in the introduction is not completely overcome in this approach. IN the example of the Breit-Wigner distribution one still has the result $M_r(p|\mu) = 0$ for $r \leq 0$ and the inequality is not very restrictive.

# References


[1] M. Bersohn, Am. J. Phys. **34**, 62 (1966).

[2] A.S. Wightman, Rev. Mod. Phys. **34**, 845 (1962); K. Kraus, in *Uncertainty Principle and Foundations of Quantum Mechanics*, W.C. Price and S.S. Chissick (eds), (Wiley, London, 1977).

[3] A. Bhattacharyya, Bull. Calcutta Math. Soc. **35**, 99 (1943); C.R. Rao, Bull. Calcutta Math. Soc. **37**, (1945).

[4] W.K. Wootters, Phys. Rev. D **23**, 357 (1981). J. Hilgevoord and J. Uffink, Found. Phys. **21**, 323 (1991).

[5] L. Mandelstam and I. Tamm, J. Phys. (USSR) **9**, 249 (1945); G.N. Fleming, Nuovo Cimento A **16**, 263 (1973); K. Bhattacharyya, J. Phys. A **16**, 2993 (1983).

[6] J. Uffink and J. Hilgevoord, Found. Phys. **15**, 925 (1985); J. Hilgevoord and J. Uffink in *Microphysical Reality and Quantum Formalism*, A. van der Merwe et al. (eds) (Kluwer, Dordrecht, 1988) and in *Sixty-two years of Uncertainty*, A. Miller (ed), (Plenum, N.Y., 1990).

[7] J. Anandan and Y. Aharonov, Phys. Rev. Lett. **65**, 1697 (1991); L. Vaidman, Am. J. Phys. **60**, 182 (1992); A. Uhlmann, Phys. Lett. A **161**, 329 (1992).

[8] J. Uffink, Am. J. Phys. (to appear).

[9] J-M. Lévy-Leblond, *Phys. Lett. A* **111**, 353 (1985).

[10] D. Deutsch, *Phys. Rev. Lett.* **50**, 631 (1983); I.Białynicki-Birula, in*Quantum Probability and Applications II*, L. Accardi and W. von Waldenfels (eds.), (Springer, Berlin, 1984); K. Kraus, *Phys. Rev. D* **35**, 3070 (1987).

[11] H. Maassen and J. Uffink, *Phys. Rev. Lett.* **60** 1103 (1988).

[12] G.H. Hardy, J.E. Littlewood and G. Pólya, *Inequalities*, (Cambridge U.P., Cambridge, 1934); A.Renyi, *Wahrscheinlichkeitsrechnung*, (Deutscher Verlag der Wissenschaften, 1962).

[13] J. Uffink, *Measures of Uncertainty and the Uncertainty Principle*, Ph. D. thesis, University of Utrecht (1990).

[14] J-M. Lévy-Leblond, Ann. Phys. **101**, 319 (1976).

[15] E.B. Davies, *Quantum Theory of open Systems* (Academic Press, London, 1976); A.S. Holevo *Probabilistic and Statistical Aspects of Quantum Theory* (North-Holland, Amsterdam, 1982).

[16] L. Susskind and J. Glogower, Physics **1**, 49 (1964).

[17] I.I. Hirschman, Am. J. Math. **79**, 152 (1957); I. Białynicki-Birula and J. Micielski, Comm. Math. Phys. **44**, 129 (1975); W. Beckner, Ann. Math. **102**, 159 (1975).

# MEASUREMENT OF VERY SMALL PHASE FLUCTUATIONS BY MEANS OF THE OPERATIONAL APPROACH

A. Bandilla
AG "Nichtklassische Strahlung" der MPG, Humboldt–Univeristät Berlin,
Rudower Chaussee 5, O-1199 Berlin, Germany

Recently Noh, Fougères and Mandel (NFM) [1] have improved the operational approach to the quantum phase problem substantially and measured the phase dispersion of coherent light down to very small mean photon numbers of the order of $10^{-2}$. This has prompted many other investigations and clarified some important questions in relation to what is actually measured. Although their treatment is rather general, we confine ourselves here to the case of a strong local oscillator (LO) and reproduce their measurement scheme in Fig. 1. Surprisingly enough, this simultaneous measurement of the sine and the cosine of the phase difference is completely equivalent to an old proposal to measure the phase after strong linear amplification [2] realized experimentally by the Welling group [3]. The reason for this rests on the fact, that in both cases the results are determined by the $Q$ function of the signal. This was shown for amplification in [4] and for the measurement after beam splitting by Lai and Haus [5] and also in [6, 7, 8]. The measured phase dispersion is given by

$$\begin{aligned}(\delta\varphi)^2 &= 1 - \left|\ll e^{i\varphi} \gg\right|^2 . \\ &= 1 - \left|\sum_{n=0}^{\infty} c_n c_{n+1}^* b_n^1\right|^2 ,\end{aligned} \tag{1}$$

where the double brackets mean a classical average over the radius integrated $Q$ function of the signal and the $b_n^1$ are defined by

$$b_n^1 = \frac{\Gamma(n+1/2+1)}{\sqrt{n!(n+1)!}} . \tag{2}$$

These coefficients are all smaller than one and broaden therefore the phase distribution of the pure state $|\psi>$

$$|\psi>=\sum_{n=0}^{\infty} c_n |n> . \tag{3}$$

In showing that the $b_n^1$ result from the calculation of the dispersion with the help of the NFM operators we found the expansion [8]

$$b_n^1 = 1 - \frac{1}{8(n+1)} + \frac{1}{128(n+1)^2} + \frac{5}{8\cdot 128(n+1)^3} - + \cdots , \tag{4}$$

that evidently proves the above mentioned property $b_n^1 < 1$ and $\lim_{n\to\infty} b_n^1 = 1$. This expansion converges excellently and is very useful because eq. (1) reduces to the Pegg–Barnett (PB) dispersion [9] by putting all $b_n^1$ equal to one, the zeroth approximation of eq. (4).

Now, very small phase fluctuations suppose great photon number fluctuations and the last can change the interference signal. Of such kind is the situation for states near to the so–called phase optimized states (POS) [10,11] which are characterized by the relation [11]

$$(\delta\varphi)^2_{\mathrm{PB}} = \frac{1\cdot 89}{(N+1)^2}, \qquad N \gg 1 , \tag{5}$$

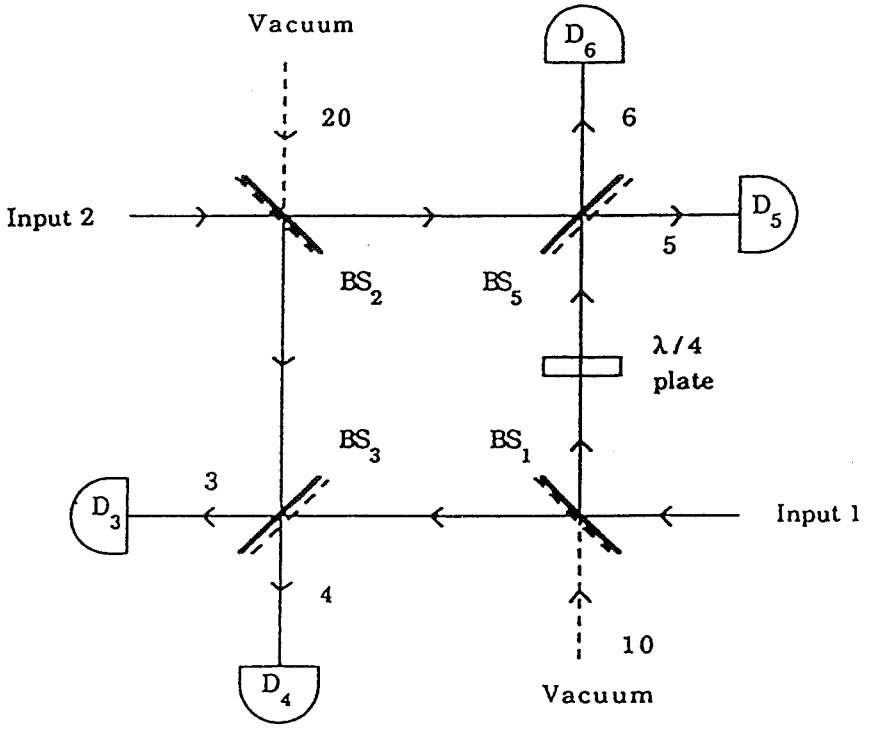


**Fig. 1** *Outline of the experimental scheme used by Noh, Fougères and Mandel where the sine and the cosine of the phase difference are measured simultaneously. $BS_i$ are identical 50/50 beam splitters and $D_j$ are photodetectors. Input 2 is the local oscillator.*

where $N$ is the mean photon number. Note that coherent states lead to

$$(\delta\varphi)^2_{\mathrm{PB}} = \frac{1}{4N}, \quad N \gg 1\,. \tag{6}$$

For clarity the subscripts PB indicate that eqs. (5) and (6) are Pegg–Barnett dispersions i. e., they are calculated by replacing the classical average in eq. (1) by the quantum ensemble average $< e^{i\hat{\varphi}} >$ with the Hermitian phase operator $\hat{\varphi}$ [9].

The question is now how to determine such small dispersions from measurements in the operational approach, i. e., by measuring via the radius integrated $Q$ function (eqs. (1), (2) and (4)). The answer is that with the help of the expansion (4), some limitations and an additional measurement of the photon distribution in the scheme of Fig. 1 it is possible to infer the PB dispersion of states with a $(\delta\varphi)^2$ comparable to the value of eq. (5). Note that the measurement of eq. (1) alone cannot give adequate information about phase dispersions near to POS. This is illustrated in Fig. 2 for two-photon coherent states (TCS) that can be optimized to come close to POS for certain degrees of squeezing $s$ at a fixed mean photon number $N$ [12].

The following investigations are rather analogous to calculations made by Ritze [13] in his different proposal to measure extremely small phase fluctuations. First, one has to find a suitable reference phase in order to make the $c_n$ in eq. (1) real. This corresponds to $< \sin\hat{\varphi} >= 0$, where we suppress the phase of the $LO$. Second, only such input fields can be admitted that allow a truncation of the expansion (4):

$$\ll \cos\varphi \gg_Q = \sum_{n=0}^{\infty} c_n c_{n+1} - \frac{1}{8}\sum_{n=0}^{\infty}\frac{c_n c_{n+1}}{n+1} + \frac{1}{128}\sum_{n=0}^{\infty}\frac{c_n c_{n+1}}{(n+1)^2}\,. \tag{7}$$

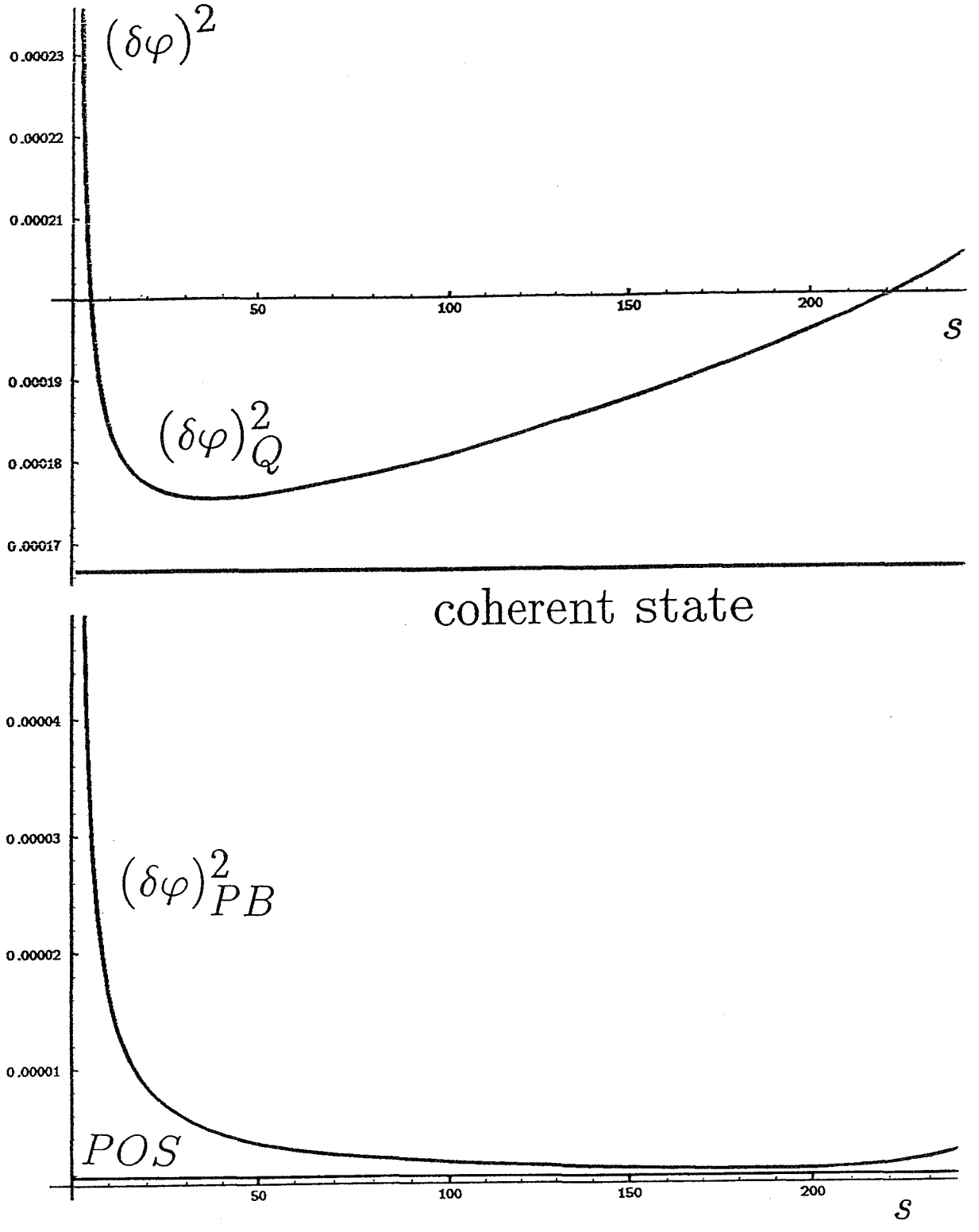


**Fig. 2** *Phase dispersions for TCS at a mean photon number of* $N = 1500$ *and increasing squeezing parameter* $s$. *Note that* $s = 1$ *describes coherent light. The Q function based dispersion* $(\delta\varphi)^2_Q$ *starts at* $1/2N$, *comes close to the coherent state value* $1/4N$ *and increases again. The Pegg–Barnett dispersion* $(\delta\varphi)^2_{PB}$ *begins at* $1/4N$ *for* $s = 1$, *decreases sharply and reaches its minimum near to the POS level at strongly different* $s$ *values than* $(\delta\varphi)^2_Q$.



C-3.

Third, we assume a smooth $c_n$ distribution and approximate the $c_{n+1}$ by

$$c_{n+1} = c_n + c_n' , \tag{8}$$

where $c_n'$ denotes the derivative of $c_n$ with respect to $n$. With eq. (8) we can determine the second sum in eq. (7):

$$\begin{aligned} \sum_{n=0}^{\infty} \frac{c_n c_{n+1}}{n+1} &\cong \sum_{n=0}^{\infty} \frac{c_n^2}{n+1} + \frac{1}{2}\int_0^{\infty} \frac{d(c_n^2)}{n+1} \\ &= \left\langle \frac{1}{\hat{n}+1} \right\rangle - \frac{1}{2}c_0^2 + \frac{1}{2}\int_0^{\infty} \frac{c_n^2}{(n+1)^2} dn , \end{aligned} \tag{9}$$

where $\hat{n}$ is the photon number operator and $< \ldots >$ the normal quantum average. Due to the Schwarz inequality we find in addition [14,2]

$$\left( \sum_{n=0}^{\infty} c_n c_{n+1} \right)^2 \leq \sum_{n=0}^{\infty} c_n^2 \sum_{n=0}^{\infty} c_{n+1}^2 \tag{10}$$

and therefore $(\delta\varphi)^2_{PB} \geq c_0^2$. It turns out that POS fulfil $(\delta\varphi)^2_{PB} \gg c_0^2$ and our truncation assumption requires the same. Therefore $c_0^2$ can be neglected in eq. (9) and we obtain eventually

$$\ll \cos\varphi \gg_Q = \ll \cos\varphi \gg_{PB} - \frac{1}{8}\left\langle \frac{1}{\hat{n}+1} \right\rangle - \frac{7}{128}\left\langle \frac{1}{(\hat{n}+1)^2} \right\rangle . \tag{11}$$

It is evident that for the determination of the averages over the number operator expressions on the right–hand side of eq. (11) we need the knowledge of the photon number distribution. This is not surprising because very small phase fluctuations require enhanced photon number fluctuations that affect the interference signal. During the measurement of such phase dispersions we must consequently also monitor the photon number fluctuations.

The situation changes remarkably, if we omit the first beam splitter in Fig. 1 and put the signal into each channel as illustrated in Fig. 3. This makes sense if we confine ourselves to two– photon coherent states (TCS) because than the radius integrated Wigner function is measured as was shown for coherent states by Freyberger and Schleich [6] and generalized to TCS by Leonhardt and Paul [15]. The measured dispersion is now

$$(\delta\varphi)^2_W = 1 - \left| \sum_{n=0}^{\infty} c_n c_{n+1}^* A_n^1 \right|^2 , \tag{12}$$

where the subscript $W$ points to the Wigner function and the $A_n^1$ can be expanded into the series

$$A_n^1 = 1 + \frac{(-1)^n}{4(n+1)} + \frac{1}{32(n+1)^2} - \frac{(-1)^n \cdot 5}{128(n+1)^3} - + \cdots . \tag{13}$$

Eq. (13) shows clearly the oscillations about one what amounts to the fact that eqs. (12) and (6) give exactly corresponding results in this order $(1/N)$. However, for TCS's near to POS (eq. (5)), as introduced in [12], the next order, $1/N^2$, is dominating. Here, the term $1/32(n+1)^2$ of the $A_n^1$ plays an important role. The result is that the measured dispersion $(\delta\varphi)^2_W$ can be smaller than the corresponding PB result. Thus the measurement following the scheme of Fig. 3 yields for coherent states with $N \gg 1$ the Pegg–Barnett result while second–order effects can change the measured dispersion for optimized TCS drastically for moderate $N(\cong 50)$. For very large $N$ $(\delta\varphi)^2_{PB}$ and $(\delta\varphi)^2_W$ coincide for TCS [16].

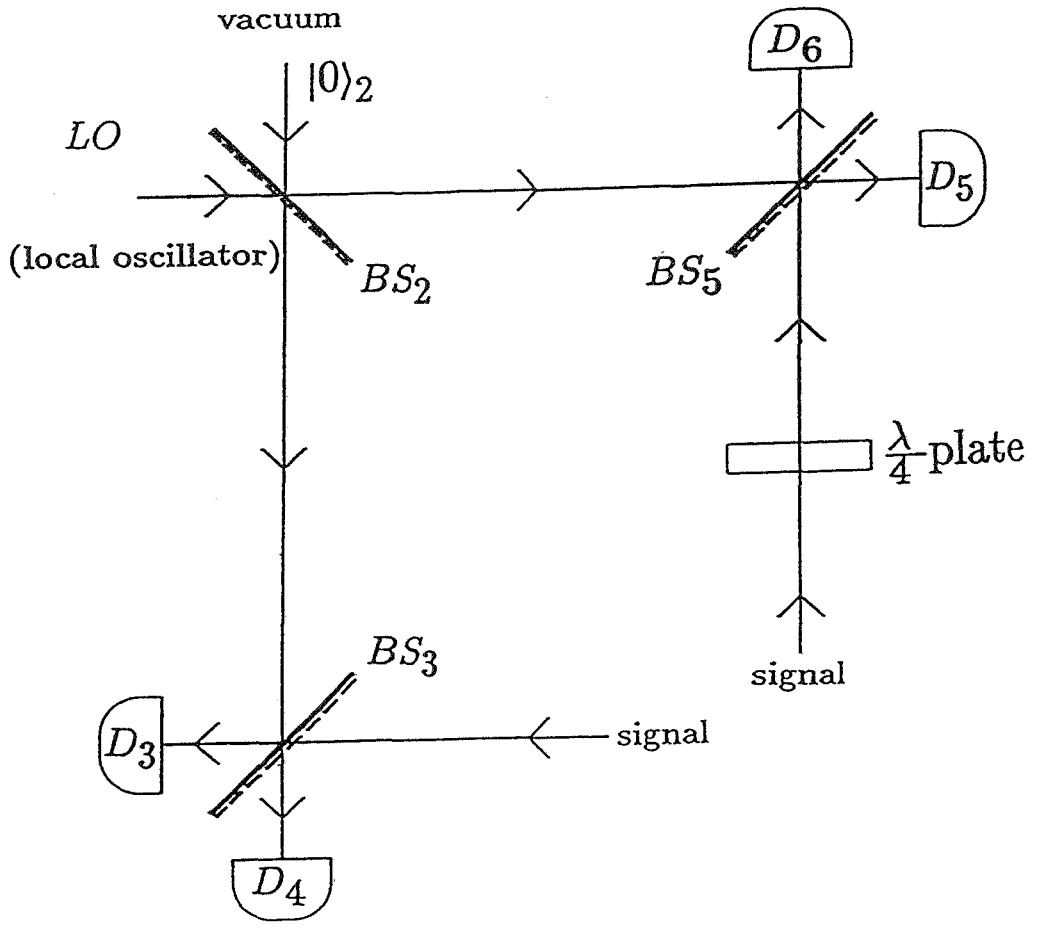


**Fig. 3** *Modified homodyne detection scheme with two input ports where two identically prepared signals are incident. The $\lambda/4$–plate makes, as in Fig. 1, a $\pi/2$ phase shift in order to measure simultaneously the sine and the cosine of the phase difference. The signal is here not contaminated by the vacuum from the unused port. Thus, there is no physical reason for any broadening as in Fig. 1.*


[1] J. W. Noh, A. Fougères and L. Mandel, Phys. Rev. Lett. **67**, 1426 (1991); Phys. Rev. A **45**, 424 (1992) and Phys. Rev. A **46**, 2840 (1992).

[2] A. Bandilla and H. Paul, Ann. Physik **23**, 323 (1969)

[3] H. Gerhardt, H. Welling and D. Frölich, Appl. Phys. **2**, 91 (1973) and H. Gerhardt, U. Büchler and G. Litfin, Phys. Lett. **49 A**, 199 (1974)

[4] W. Schleich, A. Bandilla and H. Paul, Phys. Rev. A **45**, 6652

[5] Y. Lai and H. A. Haus, Quantum Opt. **1**, 99 (1989)

[6] M. Freyberger and W. Schleich, Phys. Rev. A**47**, R 30 (1993)

[7] U. Leonhardt and H. Paul, to be published in Phys. Rev. A, 1992

[8] A. Bandilla, to be published in the Special Issue of Physica Scripta, 1993

[9] D. T. Pegg and S. M. Barnett, Europhys. Lett. **6**, 483 (1988) and S. M. Barnett and D. T. Pegg, J. mod. Opt. **36**, 7 (1989)

[10] G. S. Summy and D. T. Pegg, Opt. Commun. **77**, 75 (1990)

[11] A. Bandilla, H. Paul and H.–H. Ritze, Quantum Opt. **3**, 267 (1991)

[12] A. Bandilla, Opt. Commun. **94**, 273 (1992)

[13] H.–H. Ritze, Opt. Commun. **92**, 127 (1992)

[14] H. Paul, W. Brunner u. G. Richter, Ann. Physik **12**, 325 (1963)

[15] U. Leonhardt and H. Paul, to be published in Phys. Rev. Lett., 1993

[16] A. Bandilla a. H.-H. Ritze, submitted for publication

# THE QUANTUM MEASUREMENT OF TIME

**Scott R. Shepard**
*Department of Physics,*
*Baylor University, Waco, Texas 76798-7316*

**Abstract**

Traditionally, in non-relativistic Quantum Mechanics, time is considered to be a *parameter*, rather than an *observable* quantity like space. In relativistic Quantum Field Theory, space and time are treated equally by reducing space to also be a parameter. Herein, after a brief review of other measurements, we describe a third possibility, which is to treat time as a directly observable quantity.

## 1 The Measurements of Space and Momentum

Here we postulate the existence of position eigenstates, such that their corresponding eigenkets (defined by $\hat{x}|x\rangle = x|x\rangle$, where $\hat{x}$ is the position operator) resolve the identity operator

$$\hat{I}_x = \int_{-\infty}^{+\infty} dx |x\rangle\langle x| \tag{1}$$

for the Hilbert space that they span, $\mathcal{H}_x \leftrightarrow \{|x\rangle : x \subset [-\infty,+\infty]\}$. Thus, any state $|\psi\rangle \in \mathcal{H}_x$ can be expressed as a weighted sum of position eigenstates:

$$|\psi\rangle = \int_{-\infty}^{+\infty} dx |x\rangle\, \psi(x) \tag{2}$$

where $\psi(x) \equiv \langle x|\psi\rangle$ is Schrodinger's time independent wavefunction, the magnitude-square of which gives the probability of obtaining the value $x$ in what we call the *measurement of* $\hat{x}$.

An infinitesimal translation in physical space, denoted by $\hat{T}(\delta x)$, is defined by its mapping of the position eigenstates:

$$\hat{T}(\delta x)|x\rangle = |x+\delta x\rangle, \tag{3}$$

and linear canonical momentum, denoted as $\hat{p}$, is defined to be the generator of these translations:

$$\lim_{\delta x \to 0} \hat{T}(\delta x) = \hat{I}_x - i\hat{p}\delta x/\hbar. \tag{4}$$

It is important to note that in writing equation (3) we are assuming that space is unbounded, i.e. $x \subset [-\infty,+\infty]$. From equations (3) and (4) we can easily prove [1] that there is a Fourier transform relation between $\psi(x)$ and $\varphi(p) \equiv \langle p|\psi\rangle$, where $\hat{p}|p\rangle = p|p\rangle$. Rayleigh's theorem [2] then guarantees that $|\varphi(p)|^2$ is a normalizable distribution and

hence (since it must also be positive semi-definite) it corresponds to a probability distribution function (pdf) that describes the "measurement of $\hat{p}$." This can also be seen by virtue of the fact that a normalized $|\varphi(p)|^2$ implies that the momentum eigenkets must also resolve the identity operator:

$$\int_{-\infty}^{+\infty} dp|p\rangle\langle p| = \hat{I}_x. \tag{5}$$

In the case of the measurements of space and momentum our descriptions are complete in the sense that both operators are Hermitian thereby ensuring that each has an orthogonal set of eigenkets so that the corresponding wavefunctions can collapse.

## 2 "Time-like" Measurements

Time evolution, by an infinitesimal amount, $\delta t$, denoted as $\hat{U}(\delta t)$, is defined by

$$\hat{U}(\delta t)|\psi,t\rangle = |\psi,t+\delta t\rangle, \tag{6}$$

where $|\psi,t\rangle$ is the ket $|\psi\rangle$ when the time *parameter* takes on the value *t*. This is very different than the interpretation of equation (3), i.e. we are NOT postulating that $|\psi,t\rangle$ is an eigenket of a time operator. Thus, Schrodinger's time-dependent wavefunction, $\psi(x,t) \equiv \langle x|\psi,t\rangle$, still describes the measurement of **space** (not time) as is clear from the fact that it is still the completeness of the position eigenkets that allows us to interpret $|\psi(x,t)|^2$ as a pdf **for** $x$ so that at each instant in time we have

$$\int_{-\infty}^{+\infty} dx\,|\psi(x,t)|^2 = 1. \tag{7}$$

We can obtain "time-like" information by performing this measurement of space (on identically prepared systems) at different values of the time parameter, but we are only *inferring* time information from the spatial measurement.

Similarly, we can perform measurements of other quantities, such as a spin component (e.g. $\hat{S}_z$) at different times, but here again we would be inferring rather than directly measuring the temporal information. For example, consider a particle of spin *s*. We have an identity operator

$$\hat{I}_s = \sum_{m=-s}^{s} |m\rangle\langle m| \tag{8}$$

for the spin part of our state space, $\mathcal{H}_s \leftrightarrow \{|m\rangle : m = -s,-s+1,\ldots,s-1,s\}$, where $\hat{S}_z|m\rangle = m\hbar|m\rangle$. Thus the measurement of $\hat{S}_z$ (performed at time *t*) is still described by a

probability mass function for $m$, so that for every instant in time we have $\sum_{m=-s}^{s} P_t(m) = 1$, where $P_t(m) \equiv |\langle m|\psi,t\rangle|^2$.

## 3 The Direct Measurement of Time

We can parallel the discussion of the spatial measurement given in section 1 under the substitutions of $t$ for $x$, the Hamiltonian $\hat{H}$ for $\hat{p}$, and $\hat{U}(\delta t)$ for $\hat{T}(\delta x)$, thereby obtaining a *temporal wavefunction* [3], $\psi(t)$, that is complementary to the energy representation: $\psi(t) \overset{\mathcal{F}}{\Leftrightarrow} \psi(E)$, i.e.

$$\psi(t) = \int_0^\infty dE\ \psi(E)\, e^{-iEt/\hbar} \tag{9}$$

where $\psi(E) \equiv \langle E|\psi\rangle$ and $\hat{H}|E\rangle = E|E\rangle$. As it stands however, this rather obvious approach does not give a complete description of the measurement of time [4] due to the existence of a lower bound on the energy eigenspectra (i.e. a "ground state").

For the sake of definiteness, consider a single harmonic oscillator of ("rigged") Hilbert space $\mathcal{H}_1 \leftrightarrow \{|n_1\rangle : n_1 = 0,1,2,...\infty\}$, where $\hat{n}_1|n_1\rangle = n_1|n_1\rangle$, $\hat{H}_1 = \hbar\omega\left(\hat{n}_1 + \frac{1}{2}\hat{I}_1\right)$, and $\hat{I}_1 = \sum_{n_1=0}^{\infty} |n_1\rangle\langle n_1|$. The temporal wavefunction in this case is

$$\psi(t) = e^{-i\phi/2} \sum_{n_1=0}^{\infty} \psi_{n_1}\, e^{-in_1\phi} \;=\; e^{-i\phi/2}\, \psi(\phi), \tag{10}$$

where $\phi \equiv \omega t$, $\psi_{n_1} \equiv \langle n_1|\psi\rangle$, and the gauge-induced topological phase, $e^{-i\phi/2}$, is not observable without performing interference with another system since $|\psi(t)|^2 = |\psi(\phi)|^2$. Clearly the lower bound on photon number $(n_1 \geq 0)$ prevents $\psi(t)$ (or $\psi(\phi)$) from collapsing to a delta-function. This implies that the underlying phase kets $\{|\phi\rangle\}$ are not orthogonal, $\langle\phi_1|\phi_2\rangle \neq \delta(\phi_1 - \phi_2)$ (where $\psi(\phi) = \langle\phi|\psi\rangle$) and yet

$$\int_{-\pi}^{\pi} \frac{d\phi}{2\pi} |\phi\rangle\langle\phi| = \sum_{n_1=0}^{\infty} |n_1\rangle\langle n_1| = \hat{I}_1 \tag{11}$$

so that $\frac{1}{2\pi}|\psi(\phi)|^2$ is a perfectly valid pdf (as can also be seen from Parseval's theorem [2]). This pdf must somehow correspond to a realizable quantum measurement (as can also be seen from the formalism of *probability operator measures* or POMs [5]) and yet our description of the measurement is "incomplete" in the sense that we do not have wavefunction collapse (the $\{|\phi\rangle\}$ is not an orthogonal set) and likewise, the non-Hermitian operator associated with this measurement does not commute with its adjoint.

## 4 The Complete Description of The Direct Measurement of Time

In order to get a complete description of the direct measurement of time we *must* deal with a Hilbert space that is larger than $\mathcal{H}_1$. For example, we can use the product space for *two* oscillators, $\mathcal{H}_{1\otimes 2} \equiv \mathcal{H}_1 \otimes \mathcal{H}_2$. If we are willing to restrict our states to a subset of $\mathcal{H}_{1\otimes 2}$ where each value of the energy difference ($m \equiv n_1 - n_2$) occurs with a *unique* value of the energy sum ($j \equiv n_1 + n_2$) then there are an infinite number of Hermitian time operators since there is an infinite number of such subsets (one such example, where we restrict to $\mathcal{H}' \subset \{\mathcal{H}_{1\otimes 2} : n_1 n_2 = 0\}$, is discussed in [6], [7], and [8]). If we do **not** wish to restrict our states, then there are two physically reasonable alternatives. We perform a *relative time measurement* that treats the different $j$ states as either: (1) distinguishable; or (2) indistinguishable. These two procedures *also* correspond to performing: (1) a "marginal measurement" in which we average over all values of absolute time; and (2) a "conditional measurement" in which we determine the relative time distribution at an instant in absolute time, as we now demonstrate.

Complementarity suggests that for an arbitrary two-mode excitation, with number representation $\psi_{n_1,n_2} \equiv {}_1\langle n_1|\,{}_2\langle n_2\|\,\psi\rangle_{1\otimes 2}$, we take a two-dimensional Fourier transform

$$\Psi(\phi_1,\phi_2) \equiv {}_1\langle\phi_1|\,{}_2\langle\phi_2\|\,\psi\rangle_{1\otimes 2} = \sum_{n_1=0}^{\infty}\sum_{n_2=0}^{\infty} \psi_{n_1,n_2}\, e^{-in_1\phi_1}\, e^{-in_2\phi_2}. \tag{12}$$

Rewriting this in terms of $\phi_\Sigma \equiv (\phi_1+\phi_2)/2$ and $\phi_\Delta \equiv (\phi_1-\phi_2)/2$, we have

$$\psi(\phi_\Delta,\phi_\Sigma) \equiv \langle\phi_\Delta,\phi_\Sigma\|\,\psi\rangle_{1\otimes 2} = \sum_{j=0}^{\infty}\sum_{m=-j}^{+j} \psi_{j,m}\, e^{-im\phi_\Delta}\, e^{-ij\phi_\Sigma} \tag{13}$$

where

$$|\phi_\Delta,\phi_\Sigma\rangle \equiv \sum_{j=0}^{\infty}\sum_{m=-j}^{+j} |j,m\rangle\, e^{im\phi_\Delta}\, e^{ij\phi_\Sigma} \quad \text{and} \quad |j,m\rangle \equiv |n_1\rangle_1|n_2\rangle_2\Big|_{j=n_1+n_2,\, m=n_1-n_2}. \tag{14}$$

We see that the $\phi_\Sigma$ part of $\psi(\phi_\Delta,\phi_\Sigma)$ cannot collapse due to the boundedness of its complement, the energy sum ($j \geq 0$).

We can eliminate $\phi_\Sigma$ to obtain a complete description of the measurement of $\phi_\Delta$ on $\mathcal{H}_{1\otimes 2}$ by applying an "absolute time average" to $|\phi_\Delta,\phi_\Sigma\rangle\langle\phi_\Delta,\phi_\Sigma|$ resulting in

$$\begin{aligned}(2\pi)d\hat{\Pi}_1(\phi_\Delta) \equiv \int_{-\pi}^{+\pi} \frac{d\phi_\Sigma}{2\pi} |\phi_\Delta,\phi_\Sigma\rangle\langle\phi_\Delta,\phi_\Sigma| = \\ \sum_{j=0}^{\infty}\left[\left(\sum_{m=-j}^{+j} |j,m\rangle e^{im\phi_\Delta}\right)\left(\sum_{m'=-j}^{+j} \langle j,m'|e^{-im'\phi_\Delta}\right)\right].\end{aligned} \tag{15}$$

Note that since both of the inner sums use the same value of $j$, interference among the different $j$ states is excluded and we have (for pure states) the pdf

$$P_1(\phi_\Delta) = Tr\left(\hat{\rho}\, d\hat{\Pi}_1(\phi_\Delta)\right) = \frac{1}{2\pi}\sum_{j=0}^{\infty}\left|\psi^{(j)}(\phi_\Delta)\right|^2 \tag{16}$$

where: $Tr()$ denotes trace; $\hat{\rho}$ is the density matrix; and

$$\psi^{(j)}(\phi_\Delta) \equiv \sum_{m=-j}^{+j} \psi_{j,m}\, e^{-im\phi_\Delta} \quad . \tag{17}$$

This procedure treats the $j$ states as distinguishable (**adding** the non-interfering **probabilities** that each contributes to the measurement of $\phi_\Delta$).

We can also eliminate $\phi_\Sigma$ by conditioning $|\phi_\Delta, \phi_\Sigma\rangle\langle\phi_\Delta, \phi_\Sigma|$ to $\phi_\Sigma = 0$ resulting in

$$\begin{aligned}(2\pi)\, d\hat{\Pi}_2(\phi_\Delta) &\equiv \frac{1}{P(\phi_\Sigma = 0)}|\phi_\Delta, \phi_\Sigma = 0\rangle\langle\phi_\Delta, \phi_\Sigma = 0| \quad = \\ &\frac{1}{P(\phi_\Sigma = 0)}\left(\sum_{j=0}^{\infty}\sum_{m=-j}^{+j}|j,m\rangle e^{im\phi_\Delta}\right)\left(\sum_{j'=0}^{\infty}\sum_{m'=-j'}^{+j'}\langle j',m'|e^{-im'\phi_\Delta}\right)\end{aligned} \tag{18}$$

where the renormalization constant is

$$P(\phi_\Sigma = 0) = \sum_{m=-\infty}^{\infty}\left\{\left|\left(\sum_{j=0}^{\infty}\psi_{j,m}\right)\right|^2\right\} \quad . \tag{19}$$

Herein we are taking a "snapshot" in absolute time so that the inner sums use different values of $j$ thereby permitting interference among the different $j$ states so that (for pure states) we have the pdf

$$P_2(\phi_\Delta) = Tr\left(\hat{\rho}\, d\hat{\Pi}_2(\phi_\Delta)\right) = \frac{1}{2\pi\, P(\phi_\Sigma = 0)}\left|\sum_{j=0}^{\infty}\psi^{(j)}(\phi_\Delta)\right|^2 . \tag{20}$$

This measurement treats the $j$ states as indistinguishable (**adding** the interfering **amplitudes** that each contributes).

## 5 Discussion

It may be of interest to note that in the "marginal measurement" defined by equation (15) (which reduces to equation (16) for pure states) we are **directly** measuring the relative phase angle between our two "clock arms." Thus, two uniformly (randomly) distributed clocks result in a uniform (random) distribution in $\phi_\Delta$. This is different than what one would obtain from the *marginal pdf* calculated from the joint distribution of our two clock arms. Rather than directly measuring a phase difference, the marginal pdf

would describe the procedure of *first* measuring $\phi_1$ and $\phi_2$, and *then* subtracting the results of these two measurements (resulting in a non-uniform distribution for the case of two random clocks, due to the mod $2\pi$ range of $\phi_1$ and $\phi_2$).

It may also be of interest to note that physical intuition regarding the connection between the issue of *distinguishability* and "absolute time average" versus "snapshot" can be reinforced by contrasting electromagnetic field moments with the angular measurement (which is equivalent to the measurement of $\phi_\Delta$ when the two oscillators are the right and left circularly polarized modes of an electromagnetic wave [3]). Furthermore, in the case of the "snapshot" (equations (18) and (19)) we determine the angular distribution of the field vectors (and their quantum fluctuations) at a point in absolute time, whereas the "absolute time average" (equations (15) and (16)) traces out the quantum version of the polarization ellipse.

## 6 References


[1] J. J. Sakurai, *Modern Quantum Mechanics* (Benjamin/Cummings, Menlo Park, CA, 1985).

[2] A. B. Carlson, *Communication Systems* (McGraw-Hill, New York, NY, 1975).

[3] S. R. Shepard, Workshop on Harmonic Oscillators (NASA CP-3197, Washington, D. C. 1992).

[4] Actually, the measurement of space suffers the same limitation since any experiment must be performed in a room of finite extent. The mathematical procedures and physical interpretations presented herein are therefore applicable to $x$ as well as $t$.

[5] C. W. Helstrom, *Quantum Detection and Estimation Theory* (Academic Press, New York, NY, 1976).

[6] S. R. Shepard, Ph.D. Thesis Proposal (Massachusetts Institute of Technology, Cambridge, MA, 1990).

[7] J. H. Shapiro, S. R. Shepard, and N. C. Wong, *Coherence and Quantum Optics VI*, L. Mandel, E. Wolf, and J. H. Eberly, eds. (Plenum, New York, NY, 1990).

[8] S. R. Shepard, Workshop on Squeezed States and Uncertainty Relations (NASA CP-3135, Washington, D. C., 1991).

N95-13918

# MANIPULATION OF QUANTUM EVOLUTION

David J. Fernández C.
*Departamento de Física, CINVESTAV*
*A.P. 14-740, 07000 México D.F., MEXICO*

Bogdan Mielnik
*Institute of Theoretical Physics, Warsaw University*
*Warszawa, ul. Hoża 69, POLAND*
*and*
*Departamento de Física, CINVESTAV*
*A.P. 14-740, 07000 México D.F., MEXICO*

**Abstract**

The free evolution of a non–relativistic charged particle is manipulated using time–dependent magnetic fields. It is shown that the application of a programmed sequence of magnetic pulses can invert the free evolution process, forcing an arbitrary wave packet to "go back in time" to recover its past shape. The possibility of more general operations upon the Schrödinger wave packet is discussed.

## 1 Introduction

We expect that in a near future the problem of particle trapping will be replaced by a wider manipulation problem concerning the purposeful operations on quantum states. This involves the inverse evolution problem: given a unitary operator acting in the Hilbert space of states of a quantum system, one asks if there exists a realistic (possibly time–dependent) Hamiltonian inducing this operator as a result of a dynamical evolution process. The importance of the subject: the unitary operations which can be dynamically induced, can also be used to control the wave–like behaviour of quantum objects, e.g. during the preparation of a measurement. The so defined subject was put forward by Lamb [1] and it has been subsequently developed by his followers (Lubkin [2], Mielnik [3, 4], Royer [5], Brown [6], Fernández [7], and other authors.) A key to the manipulation of a quantum state lies in the possibility of trapping the particle in a circular dynamical process called an *evolution loop* [4] (EL). In an EL the evolution operator $U(t)$ becomes the identity for a finite time interval. The subsequent perturbation of the EL can induce arbitrary unitary operations on the wave packet as the result of the cummulative process involving the small precessions of the distorted loop [3].

The unitary transformations that will be discussed in this paper are:

$$\begin{cases} \text{evolution loop} & U(\tau) = \mathbf{1},\ \tau > 0, \\ \text{rigid displacement of the wave packet} & U(\tau) = e^{i\mathbf{a}\cdot\mathbf{p}/\hbar}, \\ \text{the quantum time machine} & U(\tau) = e^{-iT'\mathbf{p}^2/2m\hbar},\ -\infty < T' < \infty. \end{cases}$$

## 2 The evolution loops

Consider a non–relativistic spinless particle of charge $e$ evolving under the action of a homogeneous time–dependent magnetic field $\mathbf{B}(t)$. The Hamiltonian of the system can be expressed as:

$$H(t) = \frac{1}{2m}\left(\mathbf{p} + \frac{e}{2c}\mathbf{r}\times\mathbf{B}(t)\right)^2 = \frac{1}{2m}\left[\mathbf{p}^2 + \left(\frac{e\mathbf{B}(t)}{2c}\right)^2 \mathbf{r}_\perp^2\right] - \frac{e\mathbf{B}(t)\cdot\mathbf{L}}{2mc}, \tag{1}$$

where $\mathbf{L}$ is the angular momentum operator and $\mathbf{r}_\perp = \mathbf{r} - \left(\mathbf{r}\cdot\frac{\mathbf{B}(t)}{|\mathbf{B}(t)|}\right)\frac{\mathbf{B}(t)}{|\mathbf{B}(t)|}$ is the part of $\mathbf{r}$ orthogonal to $\mathbf{B}(t)$. Here, $\mathbf{B}(t)$ will be taken as the sequence of identically shaped orthogonal pulses in the three directions $x_1$, $x_2$, $x_3$ defined by the right–handed orthonormal set of basis vectors $\{\mathbf{e_1}, \mathbf{e_2}, \mathbf{e_3}\}$:

$$\mathbf{B}(t) = \begin{cases} B(t)\mathbf{e_1} & \text{for } t\in[0,T), \\ B(t-T)\mathbf{e_2} & \text{for } t\in[T,2T), \\ B(t-2T)\mathbf{e_3} & \text{for } t\in[2T,3T), \end{cases} \tag{2}$$

with $B(t) = B\beta(t/T)$, $\int_0^1 \beta(t')dt' = 0$. The generic evolution can be determined through the operator $U(3T,0) = U(3T,2T)U(2T,T)U(T,0)$. In dimenssionless units ($t' = t/T$, $\tilde{\mathbf{q}} = \sqrt{m/\hbar T}\,\mathbf{q}$, $\tilde{\mathbf{p}} = \sqrt{T/m\hbar}\,\mathbf{p}$) it takes the form:

$$\begin{aligned} U(t'=3,0) &= W_1W_2W_3, \\ W_1 &= \Omega(\tilde{x}_1,\tilde{p}_1)^2\exp(-i\tilde{p}_1^2/2), \\ W_2 &= \Omega(\tilde{x}_2,\tilde{p}_2)\exp(-i\tilde{p}_2^2/2)\Omega(\tilde{x}_2,\tilde{p}_2), \\ W_3 &= \exp(-i\tilde{p}_3^2/2)\Omega(\tilde{x}_3,\tilde{p}_3)^2. \end{aligned} \tag{3}$$

Above, $\Omega(q,p) = \mathcal{T}\left\{\exp\left(-i\int_0^1 \tilde{H}(t')dt'\right)\right\}$ is the evolution operator induced by the one–dimensional harmonic oscillator of variable frequency $\alpha(t') = \left(\frac{eBT}{2mc}\right)\beta(t') = \alpha\beta(t')$ and Hamiltonian $\tilde{H}(t') = p^2/2 + \alpha(t')^2q^2/2$, $q$ and $p$ are two canonically conjugated operators such that $[q,p] = i$ and $\mathcal{T}$ is the time ordering operator.

Now, because $W_i$ depends on Hamiltonians which are quadratic in the canonical variables $(\tilde{x}_i,\tilde{p}_i)$ but it doesn't involve $(\tilde{x}_j,\tilde{p}_j)$ $j\neq i$, it is possible to represent it by a $2\times 2$ matrix $w_i$ (the "Heisenberg picture"):

$$W_i^\dagger \begin{bmatrix}\tilde{x}_i \\ \tilde{p}_i\end{bmatrix} W_i = w_i \begin{bmatrix}\tilde{x}_i \\ \tilde{p}_i\end{bmatrix}, \tag{4}$$

where $i = 1,2,3$. The kind of dynamical process (3) depends on the algebraic type of the matrices $w_i$, and due to the form of the operators $W_i$ it is determined just by one c–number invariant called *the discriminant*:

$$\Delta(\alpha\beta) = Tr(w_1) = Tr(w_2) = Tr(w_3). \tag{5}$$

Whenever this invariant accepts one of the distinguished values:

$$\Delta(\alpha\beta) = 2\cos\frac{2\pi l}{n}, \quad l,n = \pm1,\pm2,\cdots, \tag{6}$$

the matrices $w_i$ fulfill the algebraic identity $w_i^n = 1$ [4] $\Rightarrow$ $W_i^n = \mathbf{1}$. Hence:

$$U(t' = 3n, 0) = U(3, 0)^n = \mathbf{1}. \tag{7}$$

It can be shown [8] that for any piece–wise continuous bounded real function $\beta(t')$, $0 \leq t' \leq N$ with $N$ finite, there exist pulse amplitudes $\alpha$ for which the discriminant $\Delta(\alpha\beta)$ accepts any of the special values (6). Whenever this happens, the $n$ repetitions of our magnetic pulse pattern (2) generate the evolution loops in the space of states $L^2(\mathbf{R}^3)$ at the loop period $\tau = 3nT$.

As an illustration we restrict the discussion to the case of rectangular pulses:

$$\beta(t') = \theta(1/2 - t')\theta(t') - \theta(t' - 1/2)\theta(1 - t'), \tag{8}$$

where $\theta(x)$ is the step function. In this case, the discriminant $\Delta(\alpha\beta)$ can be analytically determined taking the form $\Delta(\alpha\beta) = 2\cos 2\alpha - \alpha \sin 2\alpha$. The simplest EL is achieved making $n = 4$, $l = 1$ in (6); the solution for $\alpha$ becomes:

$$\alpha = 0.632295 \cdots. \tag{9}$$

The loop period is $\tau = 12T$, and the orders of magnitude of the field strenght and $T$ must satisfy the relation $B = 2\alpha mc/eT$ with the value of $\alpha$ in (9).

# 3 Rigid displacement of the wave packet

The evolution loops provide a convenient method to generate arbitrary unitary transformations of quantum states. Suppose, e.g., we want to produce a rigid displacement of the wave packet. To this end, we take the loop induced by the rectangular pulses (8) with the $\alpha$–value (9) as the unperturbed system. The loop is then perturbed by a homogeneous time–dependent external force $\mathbf{F}(t) = e\mathbf{E}(t)$. The total Hamiltonian becomes $H(t) = H_0(t) - e\mathbf{r} \cdot \mathbf{E}(t)$, where $H_0(t)$ is the loop part and $-e\mathbf{r} \cdot \mathbf{E}(t)$ is the perturbation. The evolution operator within one loop period $\tau = 12T$ can be evaluated in the interaction picture. Hence:

$$U(\tau) = \exp\left(\frac{i}{\hbar}\int_0^\tau \mathbf{F}(t) \cdot \mathbf{r}_0(t)dt\right) = \exp\left[\frac{i}{\hbar}(\mathbf{a} \cdot \mathbf{p} + \mathbf{b} \cdot \mathbf{r})\right], \tag{10}$$

where $\mathbf{r}_0(t)$ is the triplet of canonical operators $x_1(t)$, $x_2(t)$, $x_3(t)$ in the Heisenberg frame of $H_0(t)$. By taking $\mathbf{F}(t) = \mathbf{F} \sin 2\pi t/\tau$ it is possible to obtain explicitly $\mathbf{a}$ and $\mathbf{b}$ in (10) [8]. With the aim of produce the pure rigid displacement, with $\mathbf{b} = 0$, we selected $\mathbf{F}(t)$ as a sequence of pulses of rectangular force. It was found that a single pulse of rectangular force $\mathbf{F} = e\mathbf{E}$ in the $x_1$–direction acting within the interval $[9T, 10T]$ displaces the packet *against* the applied force by $a_x = -1.658693FT^2/m$ (the *boomerang effect*). Other possibilities are discussed elsewhere [8].

# 4 The quantum time machine

As the next example we shall discuss the *quantum time machine*. In this scheme, the acceleration, slowing or inversion of the free evolution of the charged particle is possible. Once again, the

technology is based on a sequence of pulses of homogeneous magnetic field of the form:

$$\mathbf{B}(t) = \begin{cases} B(t)\mathbf{e}_1 & \text{for } t \in [0, 2T), \\ B(t-2T)\mathbf{e}_2 & \text{for } t \in [2T, 4T), \\ B(t-4T)\mathbf{e}_3 & \text{for } t \in [4T, 6T), \quad \int_0^{2T} B(t)dt = 0, \end{cases} \tag{11}$$

with $B(t)$ given by:

$$B(t) = \begin{cases} B_1 & \text{for } t \in [0, t_1), \qquad (0 < t_1 < T) \\ B_2 & \text{for } t \in [t_1, T), \\ -B_2 & \text{for } t \in [T, T+t_2), \ (t_2 = T - t_1), \\ -B_1 & \text{for } t \in [T+t_2, 2T). \end{cases} \tag{12}$$

The key evolution operator $U(\tau = 6T, 0)$ in dimensionless coordinates and time $t' = t/T$ takes a similar form as in (3):

$$U(6,0) = \Omega^2 G \otimes \Omega G \Omega \otimes G\Omega^2, \tag{13}$$

where $\Omega = \Omega(2)$ and $G = G(2)$ describe the evolution of the oscillator of variable frequency and the free evolution in $[0,2]$ respectively. All the calculations are made in the matrix representation, working with the angular parameters $\gamma_1 = \alpha_1 t_1'$ and $\gamma_2 = \alpha_2 t_2'$, where $\alpha_1 = eB_1T/2mc$, $\alpha_2 = eB_2T/2mc$, $t_1' = t_1/T$, $t_2' = t_2/T$. It turns out that when the amplitudes and times of the pulses of magnetic field satisfy the relations [8]:

$$\begin{aligned} \alpha_1 &= \frac{\gamma_1 \tan\gamma_1 - \gamma_2 \tan\gamma_2}{\tan\gamma_1}, \\ \alpha_2 &= \frac{\gamma_1 \tan\gamma_1 - \gamma_2 \tan\gamma_2}{-\tan\gamma_2}, \\ t_1' &= \frac{\gamma_1 \tan\gamma_1}{\gamma_1 \tan\gamma_1 - \gamma_2 \tan\gamma_2}, \\ t_2' &= \frac{-\gamma_2 \tan\gamma_2}{\gamma_1 \tan\gamma_1 - \gamma_2 \tan\gamma_2}, \end{aligned} \tag{14}$$

the free evolution operator is produced at the end time of the sequence (11):

$$U(\tau) = \exp\left(-\frac{i}{\hbar}\frac{p^2}{2m}T'\right) = \exp\left(-\frac{i}{\hbar}\frac{p^2}{2m}\tau\chi\right), \tag{15}$$

where the "effective" time $T' = \tau\chi = 6T\chi$ depends on the *distorsion coefficient*:

$$\chi = \frac{1}{3} + \frac{2}{3}\cos^2\gamma_2 \frac{\tan^2\gamma_1 - \tan^2\gamma_2}{\gamma_1\tan\gamma_1 - \gamma_2\tan\gamma_2}. \tag{16}$$

As from definition $t_1'$ and $t_2'$ must be positive, then $\gamma_1$ and $\gamma_2$ must lie in intervals of different parity, i.e. $n\pi < \gamma_1 < (n+1/2)\pi$ and $(m-1/2)\pi < \gamma_2 < m\pi$, $m, n \in \mathbf{Z}^+$ or vice versa. The distorsion coefficient $\chi$ as function of $\gamma_1$ and $\gamma_2$ is plotted in the Fig.1. As can be seen, one can generate three different situations:

$$\begin{cases} \chi > 1 & \text{free evolution acceleration} \\ 0 < \chi \leq 1 & \text{free evolution slowing} \\ \chi \leq 0 & \text{free evolution regression} \end{cases}$$

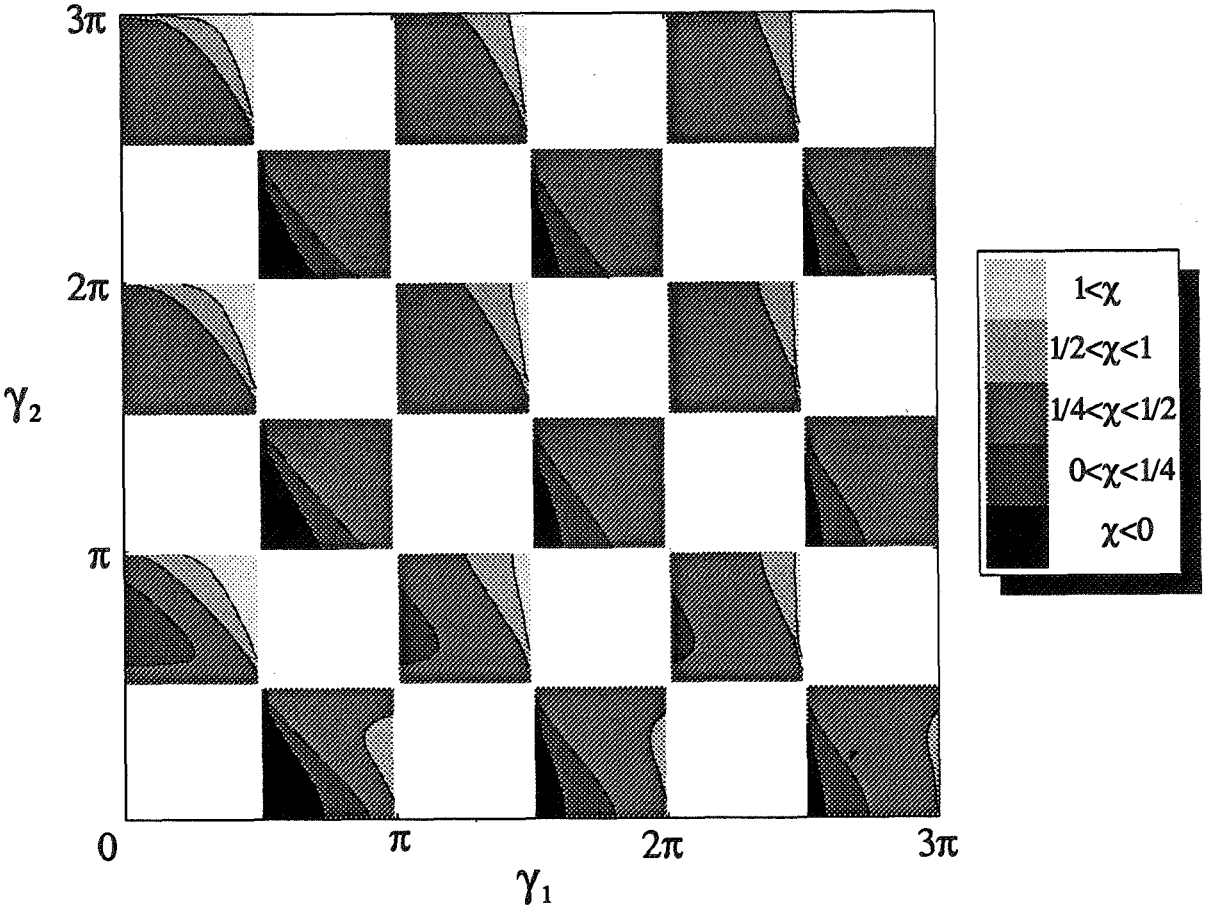


FIG. 1. The "chessboard of distorted time" for the free evolution of a charged particle manipulated by the magnetic field (11–12). The level curves for the distorsion coefficient $\chi$ are ploted as functions of the angles $\gamma_1$ and $\gamma_2$ and mark the zones for which at $\tau = 6T$ we obtain the acceleration ($\chi > 1$), slowing ($0 < \chi \leq 1$) or regression ($\chi \leq 0$) of the free evolution.

As a final remark we would like to point out that this kind of manipulations is not restricted to rectangular pulses of magnetic field. The same possibilities can be found if smooth fields are used, although we won't have analytic expressions for the discriminant anymore.

# Acknowledgments

The authors acknowledge to CONACYT, México for financial support.

# References


[1] W.E. Lamb Jr., Phys. Today **22**(4), 23 (1969).

[2] E. Lubkin, J. Math. Phys. **15**, 663 (1974); *ibid* **15**, 673 (1974).

[3] B. Mielnik, Rep. Math. Phys. **12**, 331 (1977).

[4] B. Mielnik, J. Math. Phys. **27**, 2290 (1986).

[5] A. Royer, Phys. Rev. A **36**, 2460 (1987).

[6] L.S. Brown, Phys. Rev. A **36**, 2463 (1987).

[7] D.J. Fernández C., Nuovo Cim. **107B**, 885 (1992).

[8] D.J. Fernández C. and B. Mielnik, *Controling Quantum Motion*, (preprint CINVESTAV, 1993).

# SECTION 3

# AMPLIFIER AND CAVITY ELECTRODYNAMICS

# QUANTUM STATE ENGINEERING

K. Vogel, V. M. Akulin[1], and W. P. Schleich[2]
*Abteilung für Quantenphysik, Universität Ulm*
*Albert-Einstein-Allee 11, D-89069 Ulm, Germany*

**Abstract**

We show how to create an arbitrary field state in a cavity by sending appropriately prepared two–level atoms through the cavity and subsequently detecting them in their ground state.

## 1 Introduction

Two typical questions in quantum mechanics are (i) how does a given initial quantum state evolve in time? (ii) what are the properties of a given quantum state? Usually, the question of how to prepare these states is not answered. One notable exception is the operational approach by W. E. Lamb [1]. He prepares an arbitrary quantum state of a particle by "catching" it in an appropriate potential constructed out of the corresponding wave function. In quantum optics, however, quantum states of the radiation field are of central interest. Here this scheme does not work, since there is only a limited variety of Hamiltonians describing the interaction between matter and the radiation field. During the last few years, the preparation of nonclassical states of the radiation field has attracted a lot of interest. However, the investigations were limited to certain classes of quantum states. In particular, the generation of squeezed states [2], number states[3, 4] and Schrödinger cat states [4, 5] was discussed.

So far two approaches have been used: (i) Find an appropriate Hamiltonian which transforms via unitary time evolution a given (simple) initial state to the desired final state. (ii) Make a measurement on one of two entangled quantum systems and obtain the state of the other system by the corresponding state reduction. Although in principle we can always construct the necessary Hamiltonians and entanglements, the variety of states which we can obtain in this way is limited since the Hamiltonians and entanglements based on physical interactions are limited by nature. Nevertheless, we give a recipe how to construct an *arbitrary* quantum state of the radiation field starting from the vacuum state by repeatedly using a simple Hamiltonian and subsequent state reduction [6].

## 2 The Ingredients for Quantum State Engineering

The ingredients for our method of creating an arbitrary quantum state are two–level atoms and a cavity for the electromagnetic field. The atoms interact with a resonant mode of the cavity via

[1] also Moscow Institute of Physics and Technology, Dolgoprudny, Moscow, Russia.
[2] also Max-Planck-Institut für Quantenoptik, D-85748 Garching, Germany.

the Jaynes-Cummings Hamiltonian. We start with a cavity field which is initially in the vacuum state and consecutively inject atoms in such a way that there is at most one atom in the cavity at a time. Before an atom enters the cavity we prepare it in a specific superposition of the excited state $|a\rangle$ and the ground state $|b\rangle$. This superposition has to be chosen appropriately [7] in order to drive the state of the cavity field towards the desired state. A measurement of the internal state of each atom after it has passed through the cavity leaves the quantum field in a pure state.

Let us consider one step of this process, that is, the interaction of the $k$-th atom with the cavity field. Before we inject the $k$-th atom the cavity field is in a state

$$|\varphi^{(k-1)}\rangle = \sum_n \varphi_n^{(k-1)} |n\rangle \,. \tag{1}$$

The $k$-th atom enters the cavity in the superposition state $|a\rangle + i\varepsilon_k|b\rangle$ controlled by the complex number $\varepsilon_k$ [8]. During its flight through the cavity the atom interacts with the cavity field according to the Jaynes–Cummings Hamiltonian. After it has left the cavity, the state of the combined atom-field system reads

$$\begin{aligned} |\Phi^{(k)}\rangle \;=\; & \sum_n \varphi_n^{(k-1)} \left[ C_n^{(k)} |n,a\rangle - i S_n^{(k)} |n+1,b\rangle \right. \\ & \left. + i\varepsilon_k C_{n-1}^{(k)} |n,b\rangle + \varepsilon_k S_{n-1}^{(k)} |n-1,a\rangle \right] . \end{aligned} \tag{2}$$

Here $C_n^{(k)} = \cos(g\tau_k\sqrt{n+1})$ and $S_n^{(k)} = \sin(g\tau_k\sqrt{n+1})$, where $\tau_k$ is the interaction time of the $k$-th atom with the field and $g$ is the atom-field coupling constant.

Obviously the state (2) is an entangled state. In order to obtain a pure field state we make a measurement on the $k$-th atom and detect it either in the excited state or in the ground state. If we detect the atom in the excited state our method cannot create the desired field state. We therefore have to go back to the vacuum state and start the procedure again. However, if we find the $k$-th atom in the ground state we continue the process. In this case the new field state [8] reads

$$|\varphi^{(k)}\rangle = \sum_n \varphi_n^{(k)} |n\rangle \,. \tag{3}$$

The coefficients for the new state, $\varphi_n^{(k)}$, and the coefficients for the old state, $\varphi_n^{(k-1)}$, are related via the recurrence relation

$$\varphi_n^{(k)} = S_{n-1}^{(k)} \varphi_{n-1}^{(k-1)} - \varepsilon_k C_{n-1}^{(k)} \varphi_n^{(k-1)} \tag{4}$$

which follows from Eq. (2).

# 3 The Art of Quantum State Engineering

Each atom which has passed through the cavity and has been detected in the ground state increases the number of Fock states building up the cavity field state by one. Therefore, after $N$ atoms have passed through the cavity, the field state which initially was the vacuum state $|\varphi^{(0)}\rangle$, is a superposition of the $N+1$ number states $|0\rangle, |1\rangle, \ldots, |N\rangle$. But how do we get a desired combination

$$|\psi_d\rangle = \sum_{n=0}^{N} d_n |n\rangle \;\; ? \tag{5}$$

The key idea of our method is to find a combination

$$|\varphi^{(N-1)}\rangle = \sum_{n=0}^{N-1} \varphi_n^{(N-1)} |n\rangle \tag{6}$$

of $N$ number states $|0\rangle$, $|1\rangle$, ..., $|N\rangle$ which yields the field state $|\psi_d\rangle$ after the $N$-th atom prepared in an appropriate internal state $|a\rangle + i\varepsilon_N|b\rangle$ has passed through the cavity and has been detected in the ground state. From Eq. (4) we find for the $N+1$ unknowns, that is, the $N$ coefficients $\varphi_n^{(N-1)}$ and the parameter $\varepsilon_N$, the following set of $N+1$ equations:

$$\begin{aligned} d_N &= S_{N-1}^{(N)} \varphi_{N-1}^{(N-1)} \\ &\vdots \quad\quad \vdots \\ d_n &= S_{n-1}^{(N)} \varphi_{n-1}^{(N-1)} - \varepsilon_N C_{n-1}^{(N)} \varphi_n^{(N-1)} \\ &\vdots \quad\quad \vdots \\ d_0 &= -\varepsilon_N \varphi_0^{(N-1)} . \end{aligned} \tag{7}$$

We express the unknown values $\varphi_n^{(N-1)}$ in terms of the known values $d_n$, starting with the first equation of the set (7), and obtain

$$\varphi_n^{(N-1)} = \sum_{\nu=1}^{N-n} \left[ \prod_{\mu=n}^{n+\nu-2} \frac{C_\mu^{(N)}}{S_\mu^{(N)}} \right] \frac{d_{n+\nu}}{S_{n+\nu-1}^{(N)}} \varepsilon_N^{\nu-1} . \tag{8}$$

In addition we have to satisfy the last equation of the set (7). We therefore substitute the coefficients $\varphi_0^{(N-1)}$ into the last equation of the set (7) and obtain

$$d_0 + \sum_{\nu=1}^{N} \left[ \prod_{\mu=0}^{\nu-2} \frac{C_\mu^{(N)}}{S_\mu^{(N)}} \right] \frac{d_\nu}{S_{\nu-1}^{(N)}} \varepsilon_N^\nu = 0 \tag{9}$$

as the characteristic equation for $\varepsilon_N$.

We solve the characteristic equation numerically and choose one value $\varepsilon_N$ from the $N$ roots of Eq. (9). Equation (8) immediately gives us the corresponding coefficients $\varphi_n^{(N-1)}$ of the state $|\varphi^{(N-1)}\rangle$. We take $|\varphi^{(N-1)}\rangle$ as a new desired state which we have to obtain by sending $N-1$ atoms through the cavity. For the state $|\varphi^{(N-1)}\rangle$ we do the same calculations as for the state $|\psi_d\rangle$ and obtain the parameter $\varepsilon_{N-1}$ and state $|\varphi^{(N-2)}\rangle$ with $N-1$ coefficients $\varphi_n^{(N-2)}$. We repeat the calculations until we end up with the vacuum state. A string of complex numbers $\varepsilon_1$, $\varepsilon_2$, ..., $\varepsilon_N$ defines the internal states of a sequence of $N$ atoms we have to inject into the cavity in order to obtain the desired state $|\psi_d\rangle$ from the vacuum state.

We illustrate this method by creating a superposition of the number states $|2\rangle$ and $|7\rangle$,

$$|\psi_d\rangle = \frac{1}{\sqrt{2}}\big(|2\rangle + |7\rangle\big) . \tag{10}$$

In Table I we give the values $\varepsilon_1$, $\varepsilon_2$, ..., $\varepsilon_7$ calculated for identical interaction parameters $g\tau_k = \pi/5$. In order to give an impression about the individual steps of the evolution of the field state from the

TABLE I. Internal state $|a\rangle + i|\varepsilon_k|\, e^{i\beta_k}|b\rangle$ of the $k$-th atom needed to obtain the state $\big(|2\rangle + |7\rangle\big)/\sqrt{2}$, Eq. (10), for a fixed interaction parameter $g\tau = \pi/5$. The right column gives the probability $P_b^{(k)}$, Eq. (14), to find the $k$-th atom in state $|b\rangle$ after its interaction with the cavity field provided all earlier atoms have been detected in the state $|b\rangle$. In this case the probability $\mathcal{P}_7$, Eq. (16), to find all atoms in the ground state is $\mathcal{P}_7 = P_b^{(1)} \cdot P_b^{(2)} \cdots P_b^{(7)} = 0.00801$.

| $k$ | $\lvert\varepsilon_k\rvert$ | $\beta_k/\pi$ | $P_b^{(k)}$ |
|---|---|---|---|
| 1 | 0.6066 | 0.2105 | 0.5215 |
| 2 | 0.7482 | 0.9820 | 0.4284 |
| 3 | 0.9320 | -0.5961 | 0.4379 |
| 4 | 1.2036 | -0.1964 | 0.5546 |
| 5 | 1.6243 | 0.6000 | 0.4294 |
| 6 | 0.0000 | 0.0000 | 0.4590 |
| 7 | 0.0000 | 0.0000 | 0.7495 |

vacuum state to the desired state, Eq. (10), we plot in Figure 1 the $Q$-function for the field state $|\varphi^{(k)}\rangle$ after the $k$-th atom has passed through the cavity and has been detected in the ground state.

# 4 Probabilities

But what is the probability to create the state, that is, what is the probability $\mathcal{P}_N$ to find all atoms in the ground state after they have passed through the cavity? So far we have used unnormalized states for the atoms and the field because it was convenient for calculating $\varepsilon_k$ and $\varphi_n^{(k)}$. However, when we need probabilities we have to use normalized field states

$$|\psi^{(k)}\rangle = \sum_{n=0}^{k} \psi_n^{(k)} |n\rangle \tag{11}$$

and atomic field states $\left(|a\rangle + i\varepsilon_k|b\rangle\right)/\sqrt{1+|\varepsilon_k|^2}$.

For the coefficients $\psi_n^{(k)}$ we obtain equations similar to Eqs. (7) which read

$$\begin{aligned}
\psi_k^{(k)} &= \mathcal{N}_k\, S_{k-1}^{(k)}\, \psi_{k-1}^{(k-1)} \\
&\vdots \qquad\quad \vdots \\
\psi_n^{(k)} &= \mathcal{N}_k \left[ S_{n-1}^{(k)}\, \psi_{n-1}^{(k-1)} - \varepsilon_k\, C_{n-1}^{(k)}\, \psi_n^{(k-1)} \right] \\
&\vdots \qquad\quad \vdots \\
\psi_0^{(k)} &= -\mathcal{N}_k\, \varepsilon_k\, \psi_0^{(k-1)} \,.
\end{aligned} \tag{12}$$

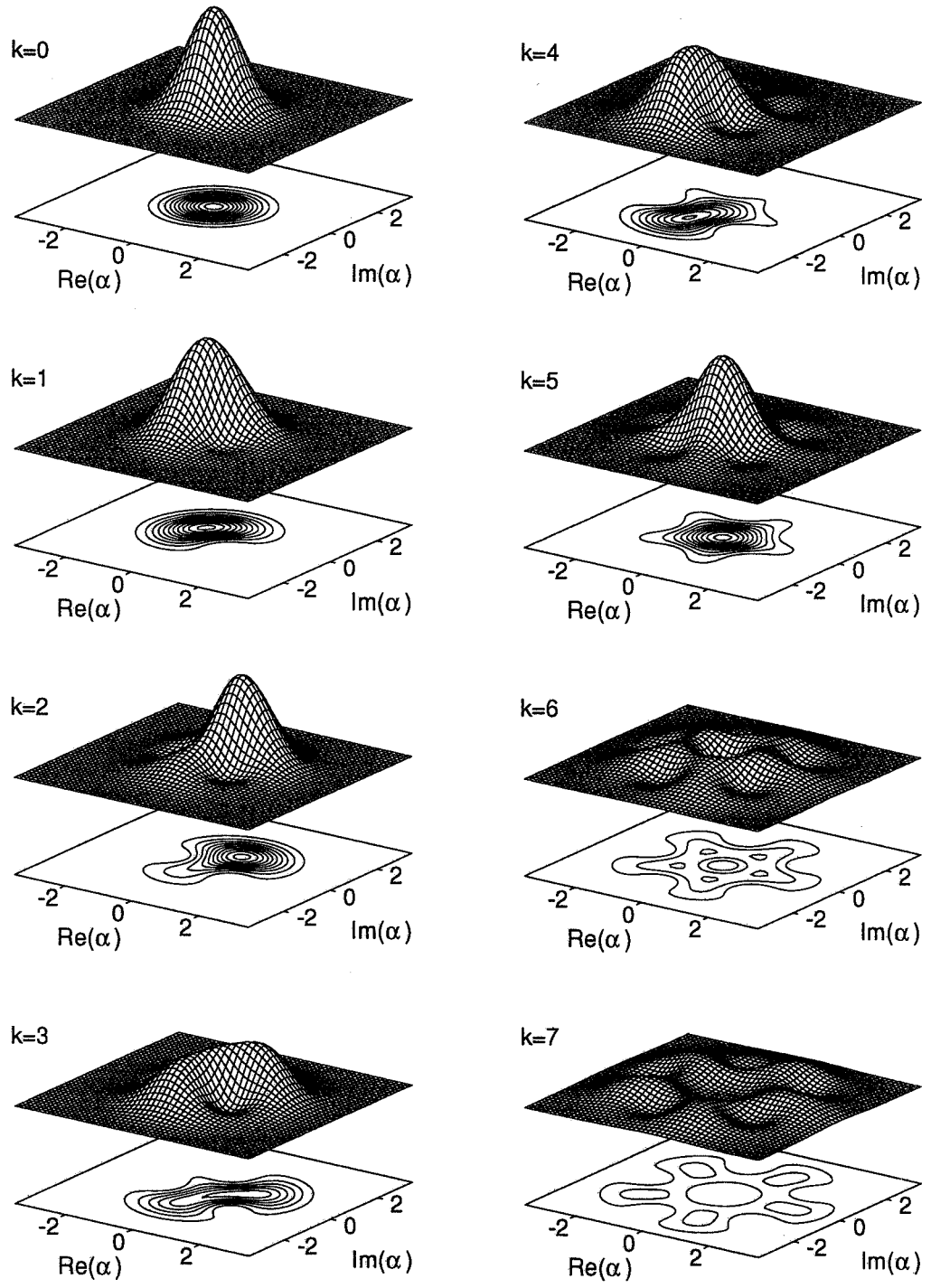


FIG. 1. $Q$-function $Q(\alpha) = |\langle\alpha|\varphi^{(k)}\rangle|^2/\pi$ for the field state $|\varphi^{(k)}\rangle$ after the $k$-th atom has interacted with the field and has been detected in the ground state. The parameters for the internal states of the incoming atoms are given in Table I.

Here the normalization constant

$$\mathcal{N}_k = \frac{1}{\sqrt{P_b^{(k)}\,(1+|\varepsilon_k|^2)}} \tag{13}$$

consists of two parts: The factor $1/\sqrt{1+|\varepsilon_k|^2}$ which takes into account the normalization of the internal state of the $k$-th atom, and the factor $1/\sqrt{P_b^{(k)}}$ which is due to the normalization of the field state after the state reduction. Here

$$P_b^{(k)} = \frac{\sum_{n=0}^{k} \left| S_{n-1}^{(k)}\,\psi_{n-1}^{(k-1)} - \varepsilon_k\, C_{n-1}^{(k)}\,\psi_n^{(k-1)} \right|^2}{1+|\varepsilon_k|^2} \tag{14}$$

is the probability to find the $k$-th atom in the ground state. From the first equation of (12) follows

$$\psi_N^{(N)} = \prod_{k=1}^{N} \left( \mathcal{N}_k S_{k-1}^{(k)} \right) \psi_0^{(0)} . \tag{15}$$

Since we start from the vacuum state we have $\psi_0^{(0)} = 1$. Moreover, we note that for a normalized desired state we have $\psi_n^{(N)} = d_n$. We substitute $\mathcal{N}_k$ from Eq. (13) into Eq.(15) and obtain for the probability $\mathcal{P}_N$ to find all $N$ atoms in the ground state

$$\mathcal{P}_N = \prod_{k=1}^{N} P_b^{(k)} = \frac{1}{|d_N|^2} \prod_{k=1}^{N} \left[ \frac{(S_{k-1}^{(k)})^2}{1+|\varepsilon_k|^2} \right] . \tag{16}$$

The probability $\mathcal{P}_N$ depends on the choice of roots of the characteristic equation, Eq. (9), and the interaction times $\tau_k$. Can we use these "degrees of freedom" to optimize the probability $\mathcal{P}_N$? To get an idea of the possibilities of this optimization let us consider the simplest case of identical interaction times $\tau_k = \tau$ for the example of a superposition of the number states $|2\rangle$ and $|7\rangle$, Eq. (10). The dependence of the probability $\mathcal{P}_7$ on the interaction parameter $g\tau$ is shown in Figure 2. For this curve we have chosen for each atom the $\varepsilon_k$ with the smallest absolute value. We note that $\mathcal{P}_7$ increases for increasing interaction parameter $g\tau$ and reaches its maximum $\mathcal{P}_7 \approx 0.00944$ at $g\tau \approx 0.2219\pi$ and then decreases. Moreover, trapping states, that is, interaction parameters $g\tau$ with $\sin(g\tau\sqrt{n}) = 0$ $(n = 1, 2, \ldots, 7)$, manifest themselves in vanishing probabilities $\mathcal{P}_7$ as apparent from Eq. (16). As a general rule the maximum value for the probability occurs for interaction parameters smaller than those corresponding to trapping states.

In the next step of the optimization we allow each atom to have its individual interaction time $\tau_k$ with the cavity field. In Table II we have chosen $\tau_k$ such that the probability $\mathcal{P}_7$ to find all seven atoms in the ground state has a maximum. Using this strategy we increase $\mathcal{P}_7$ up to the value $\mathcal{P}_7 \approx 0.02630$.

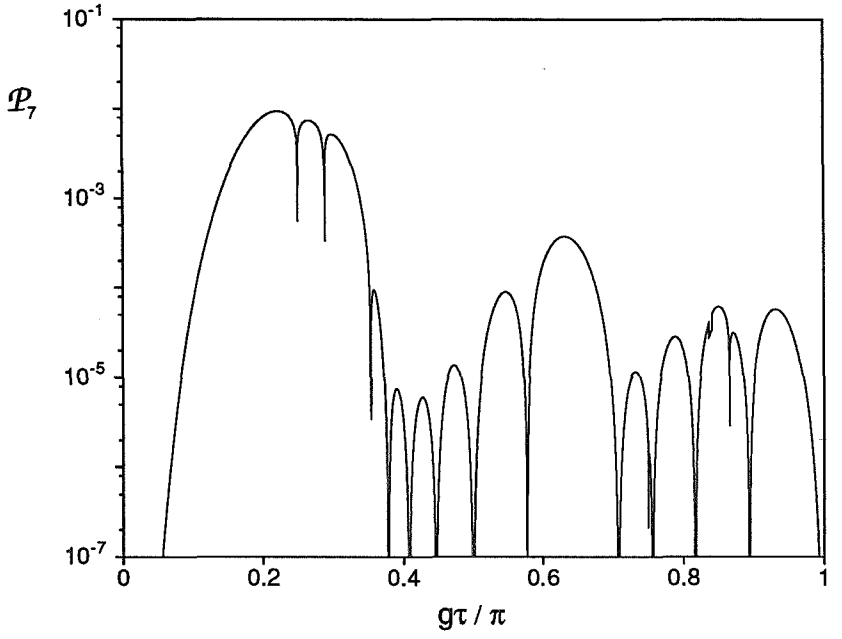


FIG. 2. Probability $\mathcal{P}_7$ to find all seven atoms in the ground state as a function of the interaction parameter $g\tau$ for the superposition state, Eq. (10). Here we have chosen $\varepsilon_k$ with the smallest absolute value. Note the occurrence of trapping states where, according to Eq. (16), the probability $\mathcal{P}_7$ vanishes.

TABLE II. Internal state $|a\rangle + i|\varepsilon_k|\, e^{i\beta_k}|b\rangle$ of the $k$-th atom needed to obtain the state $\big(|2\rangle + |7\rangle\big)/\sqrt{2}$, Eq. (10). Here we have optimized the interaction parameters $g\tau_k$ as to maximize the probability $\mathcal{P}_7$, Eq. (16), to find all atoms in the ground state. The right column gives the probability $P_b^{(k)}$, Eq. (14), to find the $k$-th atom in state $|b\rangle$ after its interaction with the cavity field provided all earlier atoms have been detected in the state $|b\rangle$. In this case we have $\mathcal{P}_7 = 0.02630$.

| $k$ | $\lvert\varepsilon_k\rvert$ | $\beta_k/\pi$ | $g\tau_k/\pi$ | $P_b^{(k)}$ |
|---|---|---|---|---|
| 1 | 0.7157 | -0.5870 | 0.5000 | 1.0000 |
| 2 | 1.0031 | -0.2310 | 0.3078 | 0.8041 |
| 3 | 1.1683 | -0.9769 | 0.2479 | 0.5559 |
| 4 | 1.1891 | 0.1949 | 0.2043 | 0.3311 |
| 5 | 1.2350 | 0.6000 | 0.1808 | 0.3527 |
| 6 | 0.0000 | 0.0000 | 0.2566 | 0.6297 |
| 7 | 0.0000 | 0.0000 | 0.2301 | 0.8000 |

# 5 Conclusion

In conclusion we emphasize that we can construct *any* superposition of the first $N+1$ number states from the vacuum state by injecting $N$ appropriately prepared atoms into a cavity and detecting all of them in the ground state after they have interacted with the field. Furthermore, we note that the Jaynes-Cummings Hamiltonian is not crucial for this method. Similar interactions between field and atom can also be used provided that they allow for energy exchange between field and atoms.

# 6 Acknowledgments

One of us (K. V.) wants to thank the Deutsche Forschungsgemeinschaft for travelling support. The work of W. P. S. was partially supported by QED Associates.

# References

[1] W. E. Lamb, Physics Today **22** (4), 23 (1969).

[2] For a review on squeezed states, see the special issues J. Mod. Opt. **34**, (1987), J. Opt. Soc. Amer. B **4** (10) (1987), and Appl. Phys. B **55** (3) (1992).

[3] J. Krause, M. O. Scully, and H. Walther, Phys. Rev. A **36**, 4547 (1987); J. Krause, M. O. Scully, T. Walther, and H. Walther, Phys. Rev. A **39**, 1915 (1989); P. Meystre, Opt. Letters **12**, 669 (1987); P. Meystre, in: *Squeezed and Nonclassical Light*, edited by P. Tombesi and E. R. Pike (Plenum, New York, 1988); H. Paul, J. Mod. Opt. **38**, 515 (1989); M. Brune, S. Haroche, V. Lefevre, J. M. Raimond, and N. Zagury, Phys. Rev. Lett. **65**, 976 (1990); M. J. Holland, D. F. Walls, and P. Zoller, Phys. Rev. Lett. **67**, 1716 (1991).

[4] P. Meystre, in: *Progress in Optics XXX*, 261 (North–Holland, Amsterdam, 1992).

[5] M. Brune, S. Haroche, J. M. Raimond, L. Davidovich, and N. Zagury, Phys. Rev. A **45**, 5193 (1992); P. Meystre, J. J. Slosser, and M. Wilkens, Opt. Commun. **79**, 300 (1990).

[6] These results have been published in: K. Vogel, V. M. Akulin, and W. P. Schleich, Phys. Rev. Lett. **71**, 1816 (1993); another method to create an arbitrary quantum state in a cavity uses the adiabatic passage of atoms to transfer the coherence between atomic Zeeman sublevels to the cavity field, see: A. S. Parkins, P. Marte, P. Zoller, and H. J. Kimble, Phys. Rev. Lett. **71**, 3095 (1993).

[7] We can obtain any superposition of the excited state $|a\rangle$ and the ground state $|b\rangle$ from the state $|a\rangle$ or $|b\rangle$ by applying an appropriate classical field.

[8] In order to keep the mathematics simple we use here unnormalized atomic states and field states.

N95-13920

# SQUEEZED LIGHT FROM MULTI-LEVEL CLOSED-CYCLING ATOMIC SYSTEMS

Min Xiao
*Department of Physics, University of Arkansas*
*Fayetteville, Arkansas 72701*

Yi-fu Zhu
*Schlumberger-Doll Research*
*Ridgefield, CT 06877*

**Abstract**

Amplitude squeezing is calculated for multi-level closed-cycling atomic systems. These systems can lase without atomic population inversion in any atomic bases. Maximum squeezing is obtained for the parameters in the region of lasing without inversion. A practical four-level system and an ideal three-level system are presented. The latter system is analysed in some detail and the mechanism of generating amplitude squeezing is discussed.

# 1 INTRODUCTION

Generation of squeezed states of light has attracted lots of attention in the past decade due to the posssible applications in various fields of physics. Squeezed light was generated in several different systems (atomic multi-wave mixing, degenerate parametric oscillator, optical fibers, optical diodes, second harmonic generation, and et al) and in several different forms (c.w. and pulsed) in laboratories around the world.[1] Although, this kind of quantum state is generated routinely in the laboratories, to make a compact, efficient, reliable, and cw squeezed coherent light source is still a challenge. Diode laser is a very good device to generate amplitude squeezed light with high efficiency[2], but the wavelength selection is very limited for applications in atomic spectroscopy.

Another area of recent interest in physics is to achieve lasing without atomic population inversion in multi-level atomic systems.[3-7] The possible applications of these new lasers include reaching new wavelengths and getting "quiter" laser output intensity. Several theoretical works were published in studying quantum statistical properties of $\Lambda$-type three-level atomic system and multi-level Raman systems.[8-11] In this paper, we discuss quantum statistical properties of multi-level closed-cycling atomic systems, which exhibits lasing without atomic population inversion.

We have studied two particular atomic systems. The first one is a practical four-level closed-cycling atomic system.[11] A brief discussion of the steady-state behaviors and linearized fluctuations in this system are given. Conditions achieving good squeezing are described.

To understand the mechanism of generating squeezing in this relatively complicated system, we constructed a simple, idealized three-level model which eliminates the intermediate level |4> and neglects decay from the upper lasing level |2> to the ground state |1>. After adiabatic elimination of extra atomic variables (under condition $\gamma_{32} >> \kappa$, with $\kappa$ as cavity decay rate), we obtain a set of equations which are similar to an effective two-level atomic system. Then steady-state correlation functions of the amplitude fluctuations are calculated, analytically, to find best conditions for maximum squeezing. Some interesting effects are discussed and compared to the results of previous four-level model

# 2 Four-Level Cycling System

Our model consists of an essemble of N closed four-level atoms confined in a single-mode cavity with photon loss rate $2\kappa$. The transition $|1> \leftrightarrow |3>$ of frequency $\omega_{31}$ is driven by a laser of frequency $\omega_1$ with Raby frequency $2\Omega$. $2\gamma_{ij}$ (i, j=1–4) are the spontaneous decay rates from state |i> to state |j>. Using standard procedure, a set of stochastic differential equations are derived. The steady state behaviour and conditions to achieve lasing without inversion were discussed in our earlier publication.[11] When $\gamma_{21}/\gamma_{34}<1$, lasing will start from population inversion. As the laser intensity building up, the population of the upper lasing level |2> will be depleted and the lasing will be sustained by the coherence induced between levels |2> and |3>. This transition from lasing with inversion to lasing without inversion in the same system is an interesting phenomena to study. At the opposite limit, i.e. $\gamma_{21}/\gamma_{34}>1$, the laser will always operate with no population inversion.

We calculated, numerically, the amplitude fluctuations of the system by linearization around steady-state solutions and found that large degree of squeezing (about 80%) at the laser output can be obtained with relative low pumping power and very small decay rate from the upper lasing state |2> to the lower lasing state |1>.

# 3 Three-Level Idealized Cycling System

Due to the complication in the four-level system, numerical calculation has to be used in calculating the laser intensity fluctuations. In order to understand the mechanism and the limiting conditions for achieving optimal squeezing, we simplify the four-level model to be an ideal three-level closed-cycling system.

Since we are only interested in the optimal conditions for generating squeezing, the decay from upper lasing level |2> to the lower lasing level |1> is neglected. To simplify our calculation, we also eliminate the intermediate state |4> and neglect decay from level |3> to level |1>. Since the effective coupling between the atomic transition and the intracavity field is $\sqrt{N}$g instead of g, we can increase the coupling by putting large number of atoms in the cavity mode, which is usually true for a laser system. This will justify the approximation of neglecting decay rates but of keeping finite dipole coupling between level |3> and level |1> and between level |2> and level |1>. Careful choice of the atomic element as the gain medium can also help to satisfy this approximation. The decay rate $\gamma$ from level |3> to level |2> is the only one to keep.

Using the same standard procedure, we derive a set of stochastic differential equations for this system from Hamiltonian, as following:

$$\begin{aligned}
\dot{J}_{12} &= i\Omega J_{23}^{\dagger} + i\alpha g(J_{22} - J_{11}) + \Gamma_3(t), \\
\dot{J}_{12}^{\dagger} &= -i\Omega J_{23} - i\alpha^{\dagger} g(J_{22} - J_{11}) + \Gamma_{10}(t), \\
\dot{J}_{13} &= -\gamma J_{13} + i\Omega(J_{33} - J_{11}) + i\alpha g J_{23} + \Gamma_4(t), \\
\dot{J}_{13}^{\dagger} &= -\gamma J_{13}^{\dagger} - i\Omega(J_{33} - J_{11}) - i\alpha^{\dagger} g J_{23}^{\dagger} + \Gamma_9(t), \\
\dot{J}_{23} &= -\gamma J_{23} + i\Omega J_{12}^{\dagger} + i\alpha^{\dagger} g J_{13} + \Gamma_5(t), \\
\dot{J}_{23}^{\dagger} &= -\gamma J_{23}^{\dagger} - i\Omega J_{12} - i\alpha g J_{13}^{\dagger} + \Gamma_8(t), \\
\dot{J}_{22} &= 2\gamma J_{33} - i\alpha g J_{12}^{\dagger} + i\alpha^{\dagger} g J_{12} + \Gamma_6(t), \\
\dot{J}_{33} &= -2\gamma J_{33} + i\Omega J_{13} - i\Omega J_{13}^{\dagger} + \Gamma_7(t), \\
\dot{\alpha} &= -\kappa\alpha - igJ_{12} + \Gamma_1(t), \\
\dot{\alpha}^{\dagger} &= -\kappa\alpha^{\dagger} + igJ_{12}^{\dagger} + \Gamma_2(t),
\end{aligned} \tag{1}$$

where $< \Gamma_i(t)\Gamma_j(t') > \equiv D_{ij}\delta(t-t')$ describing the correlation of the fluctuations. There are 36 nonzero $D_{ij}$ terms for this particular system. To save space, these nonzero diffusion terms are not given explicitly here. For a closed system, we have condition

$$J_{11} + J_{22} + J_{33} = N. \tag{2}$$

These ten differential equations are still too complicated to calculate correlations for the fluctuations analytically. However, in good cavity limit, i.e. $\gamma >> \kappa$ (which is a good approximation in a realistic laser system), some of the atomic variables ($J_{13}$, $J_{13}^{\dagger}$, $J_{23}$, $J_{23}^{\dagger}$, $J_{22}$, and $J_{33}$) can be adiabatically eliiminated from equation (1). We can do it by letting time derivatives over these atomic variables go to zero, because they decay much faster to their steady-state values comparing to $J_{12}$, $J_{12}^{\dagger}$, and the field variables. We can then solve $J_{13}$, $J_{13}^{\dagger}$, $J_{23}$, $J_{23}^{\dagger}$, $J_{22}$, and $J_{33}$ together with their corresponding fluctuation terms from equation (1) and substitute them into equations for $J_{12}$, $J_{12}^{\dagger}$, $\alpha$, and $\alpha^{\dagger}$. After some algebra, we arrive at

$$\begin{aligned}
\frac{\partial J_{12}}{\partial \tau} &= ixN - \left[\frac{Y(X+2)}{2(X+1)} + \frac{X(X+1)}{Y}\right] J_{12} + x^2 \left[\frac{Y}{2(X+1)} + \frac{X+1}{Y}\right] J_{12}^{\dagger} \\
&\quad + \Gamma_{12}(t), \\
\frac{\partial J_{12}^{\dagger}}{\partial \tau} &= -ix^{\dagger}N + x^{*2}\left[\frac{Y}{2(X+1)} + \frac{X+1}{Y}\right] J_{12} - \left[\frac{Y(X+2)}{2(X+1)} + \frac{X(X+1)}{Y}\right] J_{12}^{\dagger} \\
&\quad + \Gamma_{12}^{\dagger}(t), \\
\frac{\partial x}{\partial \tau} &= -i\frac{1}{n_0} J_{12} - \kappa x,
\end{aligned} \tag{3}$$

$$\frac{\partial x^\dagger}{\partial \tau} = i\frac{1}{n_0}J_{12}^\dagger - \kappa x^\dagger.$$

Where the new normalized variables and parameters are defined as

$$X = x^* x \equiv \frac{\alpha^\dagger \alpha}{n_0}, \quad Y \equiv \left(\frac{\Omega}{\gamma}\right)^2, \quad \tau \equiv \gamma t,$$

$$n_0 \equiv \frac{\gamma^2}{g^2}, \quad k \equiv \frac{\kappa}{\gamma}. \tag{4}$$

The new fluctuation terms are still quite complicated.

The steady-state equation can be easily solved to give

$$X_o = \frac{1}{2}\left[-1 + \sqrt{2YG + 1 - 2Y^2}\right], \tag{5}$$

where G≡$Ng^2/\kappa\gamma$ is the normalized coupling strength between the field and atoms. In this calculation, we have assumed the resonance condition between the cavity mode and the transition frequency from level |2> to level |1>. The normalized steady-state population distributions are

$$\frac{J_{11}}{N} = \frac{1}{2} - \frac{Y}{2G},$$

$$\frac{J_{22}}{N} = \frac{1}{2} + \frac{Y}{2G} - \frac{1}{2G}\left(-1 + \sqrt{2YG + 1 - 2Y^2}\right), \tag{6}$$

$$\frac{J_{33}}{N} = \frac{1}{2G}\left(-1 + \sqrt{2YG + 1 - 2Y^2}\right).$$

To calculate correlation fuctions of the fluctuations, we need to linearize equation (3) around their steady-state solutions. From the numerical calculation of the four-level system and the steady-state solutions of this system, we can determine the area in the parameter space where best squeezing occurs. For $X_0$>>1, and small, but finite, Y, equations in (3) can be linearized to give

$$\frac{d}{d\tau}\begin{pmatrix} \delta x \\ \delta x^\dagger \\ \delta J_{12} \\ \delta J_{12}^\dagger \end{pmatrix} = -\begin{pmatrix} k & 0 & i\frac{1}{n_o} & 0 \\ 0 & k & 0 & -i\frac{1}{n_o} \\ -iA & iB & C & -C \\ -iB & iA & -C & C \end{pmatrix}\begin{pmatrix} \delta x \\ \delta x^\dagger \\ \delta J_{12} \\ \delta J_{12}^\dagger \end{pmatrix}$$

$$+\begin{pmatrix} 0 & 0 & 0 & 0 \\ 0 & 0 & 0 & 0 \\ 0 & 0 & D & -D \\ 0 & 0 & -D & D \end{pmatrix}^{\frac{1}{2}}\begin{pmatrix} \xi_1(\tau) \\ \xi_2(\tau) \\ \xi_3(\tau) \\ \xi_4(\tau) \end{pmatrix}, \tag{7}$$

where

$$A \equiv kn_o(G - \frac{5X_o^2}{Y} - \frac{Y}{2}),$$

$$B \equiv kn_o(\frac{3X_o^2}{Y} - \frac{Y}{2}),$$
$$C \equiv \frac{X_o^2}{Y} + \frac{Y}{2}, \tag{8}$$
$$D \equiv kn_o(-20\frac{X_o^2}{Y} + 16X_o^2 - X_oY - Y^2 + \frac{4X_o^4}{Y^2}).$$

The intracavity correlation functions and, therefore the amplitude squeezing is easily calculated by standard method. The intracavity squeezing is given by

$$S_+ = 2n_o(< \delta x \delta x^\dagger > + < \delta x \delta x >)$$
$$\approx \frac{-20\frac{X_o^3}{Y} + 16X_o^2 - X_oY - Y^2 + \frac{4X_o^4}{Y^2}}{(\frac{X_o^2}{Y} + \frac{Y}{2})(G - \frac{10X_o^2}{Y} - Y)}. \tag{9}$$

The steady-state intensity $X_o$ is related to the pumping intensity Y and coupling strength G through the steady-state equation (5).

It is easy to show that $S_+$ is limited to the minimum value of -0.5, which corresponding to a 50% squeezing inside cavity. The output spectrum of squeezing has also been calculated numerically. The maximum squeezing is also limited to a 50% level at around carrier frequency.

# 4 Discussion

We have calculated two atomic models for generating squeezed states of light and conditions for lasing without inversion. The four-level system can start to lase with or without population inversion depending on the relative decay rates. Far above threshold the lasing is only sustained by the coherence induced between level |3> and level |2>. For the three level ideal model, the laser will always operate without the population inversion.

The four-level system can generate 80% squeezing at the output for relatively low pumping power. As for the simplified and idealized three-level cycling system, even without decay from the upper lasing state to the lower lasing state, the maximum output squeezing and the total intracavity squeezing are both limited to the 50% level. we realize that 50% squeezing comes from the suppression of spontaneous emission of the upper lasing level. The extra 30% squeezing is due to the pumping regulation through the incoherent decay processes between level |3> & level |4> and between level |4> & level |2>. So, the extra level |4> actually enhances the available squeezing for the laser output.

**References**

[1] See, e.g., the feature issue on Squeezed States of the Electromagnetic Field, J. Opt. Soc. Am. B4, 1450-1741, (1987); and Quantum Fluctuations in Optical Systems, Progress in Optics, XXX, 1-85 (1992).

[2] Y. Yamamoto, S. Machida, and Y. Itaya, Phys. Rev. Lett. 58, 1000 (1987).

[3] S.E. Harris, Phys. Rev. Lett. 62, 1033 (1989); A. Imanoglu, Phys. Rev. A40, 4135 (1989).

[4] M.O. Scully, S.Y. Zhu, and A. Gavrielides, Phys. Rev. Lett. 62, 2813 (1989); E.F. Fill, M.O. Scully, and S.Y. Zhu, Opt. Commun. 77, 36 (1990).

[5] A. Nottelmann, C. Peters, and W. Lange, Phys. Rev. Lett. 70, 1783 (1993).

[6] E.S. Fry, el al, Phys. Rev. Lett. 70, 3235 (1993).

[7] W.E. van der Veer, el al, Phys.Rev.Lett.70,3243 (1993).

[8] G.S. Agarwal, Phys. Rev. Lett. 67, 980 (1991).

[9] K.M. Gheri and D.F. Walls, Phys. Rev. Lett. 68, 3428 (1992); Phys. Rev. A45, 6675 (1992).

[10] H. Ritsch, M.A.M. Marte, and P. Zoller, Europhys. Lett. 19, 7 (1992); H. Ritsch, M.A. Marte, Phys. Rev. A47, 2354 (1993).

[11] Yifu Zhu and Min Xiao, Phys. Rev. A48, 3895 (1993).

# A METHOD OF MEASURING THE AMPLITUDE-MODULATED VACUUM FIELD NEAR A CONDUCTING MIRROR

Sun-Hyun Youn, Jai-Hyung Lee, Joon-Sung Chang
*Department of Physics*
*Seoul National University, Seoul 151-742, Korea*

**Abstract**

Electromagnetic fields of the vacuum mode near a conducting mirror are modified with respect to those in free space, with their amplitudes having a sinusoidal spatial dependence from the mirror. Therefore if we combine this spatially amplitude-modulated vacuum field mode and intense corehent light with a beam splitter, we may detect this fluctuation of the vacuum mode in a homodyne detection scheme. It will give new method to produce squeezed states of light with a single mirror placed close to an unused port of a beam splitter. We show that the amplitude fluctuation of the combined light can be reduced by a factor of 2 below that of the coherent light. We also discuss the limitations due to the finite line width of the laser and the effective absorption length of the photodiodes.

## 1 Squeezed light generation with a conducting mirror

The characteristics of vacuum fluctuations in a confined space have been studied in several cases, for example near an infinite plane conducting mirror [1], between two parallel mirrors and in a spherical cavity [3]. Here we consider a tangential vacuum-field mode with its wave vector k normal to the conducting surface ( z-direction) [2], and we choose the polarization and the propagation of the electric field along the x and z-axis, respectively. Then the electric field operator for the vacuum field entering the beam splitter (see Fig. 1) becomes

$$\hat{E}_s = \sum_k \sqrt{\frac{\hbar\omega_k}{\varepsilon_o V}} \sin(kz)(\hat{a}_k e^{-i\omega_k t} - a_k^\dagger e^{i\omega_k t})\vec{x}, \tag{1}$$

where $\omega_k$ is the frequency for the mode $k(\omega_k = ck)$, $\hbar$ and $\varepsilon_o$ have the usual meanings, and $V$ is the normalization volume [1]. Note that the sinusoidal spatial-dependence $\sin(kz)$ for the field amplitude comes from the boundary condition that the tangential components of the electric field modes on the conducting surface should vanish.

We now consider a homodyne detection scheme to measure the quantum mechanical noise of the signal (i.e. amplitude-modulated vacuum field ) as shown in Fig. 1. Let us assume, for simplicity, that the electric field for the local oscillator has a single mode(we will consider the multimode effects in the next section). Then the local oscillator field can be written as

$$\hat{E}_l = \hat{E}_{cl} + \hat{E}_q \tag{2}$$

with

$$\hat{E}_{cl} = i\sqrt{\frac{\hbar\omega}{2\varepsilon_o V}}(\alpha\, e^{-i(\omega t-k_o z)} - \alpha^*\, e^{i(\omega t-k_o z)})\,\vec{x}, \tag{3}$$

$$\hat{E}_q = i\sum_k \sqrt{\frac{\hbar\omega_k}{2\varepsilon_o V}}(\hat{b}_k\, e^{-i(\omega_k t-kz)} - \hat{b}_k^\dagger\, e^{-i(\omega_k t-kz)})\,\vec{x}, \tag{4}$$

where $\omega$ is the laser frequency ( $\omega = ck_o$). Here we have decomposed the coherent light $\hat{E}_l$ into $\hat{E}_{cl}$ and $\hat{E}_q$ [4]. $\hat{E}_{cl}$ is the classical analogy of the coherent light which has a definite amplitude and phase, whereas $\hat{E}_q$ is the quantum fluctuation in the electric field of the coherent light which is simply equivalent to the vacuum fluctuation.

Considering the vacuum mode relation in the Fig. 2, we can get the electric field in fluctuating vacuum modes at the detector 1

$$\begin{aligned}\hat{E}^{(+)}_{vac,1} &= \sum_k i\sqrt{\frac{\hbar\omega_k}{4\varepsilon_o V}}\,\{\sqrt{T}\hat{b}_k^\dagger e^{i(\omega_k t-kZ_1)} + \hat{a}^\dagger_{1,k}e^{i(\omega_k t+kz_1)} \\ &- R\hat{a}^\dagger_{1,k}e^{i(\omega_k t-kz_1)} - \sqrt{RT}\hat{a}^\dagger_{2,k}e^{i(\omega_k t-kz_1)}\},\end{aligned} \tag{5}$$

where $z_1(Z_1)$ represents the length for the beam path between the single mirror (laser) and the detector 1. We have separated the electric field into positive- $\hat{E}^{(+)}$ ($\sim e^{i\omega t}$) and a negative-frequency components $\hat{E}^{(-)}$ ($\sim e^{-i\omega t}$), and note the propagation-direction of traveling wave. We also add the factor $\frac{1}{\sqrt{2}}$ for the normalization of the vacuum fluctuation.

Using photodetection theory [5], we obtain the photocurrent $\hat{I}$ as

$$\hat{I} = \int_{-\infty}^{t} dt' h(t-t')\hat{E}^{(+)}(z,t')\,\hat{E}^{(-)}(z,t'), \tag{6}$$

where $h(t-t')$ is the photodetector response function [6]. Assuming instantaneous response of the detector, we can approximate $h(t-t')$ as $h\delta(t-t')$. Then the photocurrent induced on the detector 1 is

$$\hat{I}_1(z,t) = h\{\sqrt{T}\hat{E}^{(+)}_{cl}(Z_1,t) + \hat{E}^{(+)}_{vac,1}\} \times \{\sqrt{T}\hat{E}^{(-)}_{cl}(Z_1,t) + \hat{E}^{(-)}_{vac,1}\}. \tag{7}$$

Since the expectation value of $\alpha^*\alpha$ is much greater than that of $\hat{a}^\dagger\hat{a}$ and $\hat{b}^\dagger\hat{b}$, we keep only the terms which contain $\alpha$ or $\alpha^*$. If the reflectivity ($R$) of the beam splitter approaches to 1, the Eq. (5) surely represents the positive frequency part of the Eq. (1). In that case, $\hat{a}_1$ and $\hat{a}_2$ are totally decoupled and we can find the standing vacuum mode in the port 1.

Using the condition in Eq. (5), $\hat{I}_1$ is obtained as

$$\begin{aligned}\hat{I}^o_1(z_1,Z_1) = \frac{|\,\alpha\,|}{\sqrt{2}}\{&\sqrt{T}e^{i\phi}(T + e^{-ik_o(Z_1+z_1)} - Re^{-ik_o(Z_1-z_1)})\hat{a}_1 - T\sqrt{R}e^{i\phi}(1 + e^{-ik_o(Z_1-z_1)})\hat{a}_2 \\ &+\sqrt{T}e^{-i\phi}(T + e^{ik_o(Z_1+z_1)} - Re^{ik_o(Z_1-z_1)})\hat{a}_1^\dagger - T\sqrt{R}e^{-i\phi}(1 + e^{ik_o(Z_1-z_1)})\hat{a}_2^\dagger\},\end{aligned} \tag{8}$$

where $\hat{I}^o_1$ is the time-averaged photocurrent which is normalized with respect to $h$, and we have replaced $\alpha$ with $|\,\alpha\,|\,e^{i\phi}$. Note that in Eq. (8) we have included only one vacuum field mode

identical to the laser light with its wavevector $k$ and frequency $\omega = ck_o$ since only that mode survives as a result of the time average effect on the detector. We have neglected the $\alpha^*\alpha$ term in $\hat{I}_1^o$ , since it does not include any fluctuation and corresponds to a constant dc current which can be filtered out by ac coupling. And the average values of $\hat{I}_1^o$ are expected to be zero, since the operators $\hat{a}_1$ and $\hat{a}_2$ both represent the fluctuating vacuum field modes.

The sum and difference of these photocurrents $I_1^o, I_2^o$ are obtained from the Eq. (8). It becomes

$$\begin{aligned}
\hat{I}_1^o \pm \hat{I}_2^o &= \frac{|\alpha|}{\sqrt{2}}[\sqrt{T}e^{i\phi}\{T + e^{-ik_o(Z_1+z_1)} - Re^{-ik_o(Z_1-z_1)} \pm R \pm Re^{-ik_o(Z_2-z_2)}\}\hat{a}_1 \\
&+ \sqrt{T}e^{-i\phi}\{T + e^{ik_o(Z_1+z_1)} - Re^{ik_o(Z_1-z_1)} \pm R \pm Re^{ik_o(Z_2-z_2)}\}\hat{a}_1^\dagger \\
&- \sqrt{R}e^{i\phi}\{T + Te^{-ik_o(Z_1-z_1)} \pm R \pm e^{-ik_o(Z_2+z_2)} \mp Te^{-ik_o(Z_2-z_2)}\}\hat{a}_2 \\
&- \sqrt{R}e^{-i\phi}\{T + Te^{ik_o(Z_1-z_1)} \pm R \pm e^{ik_o(Z_2+z_2)} \mp Te^{ik_o(Z_2-z_2)}\}\hat{a}_2^\dagger]. \qquad (9)
\end{aligned}$$

We now evaluate the square of each quantity to find its fluctuations. Squaring the Eq. (8), we gather the terms $(\hat{a}_i\hat{a}_i^\dagger)$ which contains the nonzero vacuum expectation value. Then the results become

$$[I_1^o(z_1, Z_1)]^2 = \frac{T\,|\,\alpha\,|^2}{2}\{T^2 + 2T\cos[k_o(Z_1 + z_1)] + 1 + R^2 - 2R\cos(2k_o z_1) + 2RT\}, \qquad (10)$$

and the modulation effect due to the $\cos(Z_i + z_i)$ term will vanish , since the origins of the $Z_1$ and $Z_2$ are not an absolute one for the traveling local oscillator mode. However, the origin of the $z_1$ and $z_2$ is absolutely fixed to the mirror position so we will keep only this modulation effect due to $\cos(2z_{1,2})$ term. Together with the relation $R + T = 1$, Eq. (10) finally become

$$\overline{I_1^2(z_1)} = T\,|\,\alpha\,|^2\,\{1 - R\cos(2k_o z_1)\}, \qquad (11)$$

These results , Eq. (11), clearly show that the intensity fluctuations measured at each photodetector exhibit a sinusoidal spatial dependence. The photocurrent fluctuations for each detector comes partly from the vacuum field in the local oscillator itself, and partly from the vacuum field modified by the perfect mirror. Note that the sinusoidal modulation in Eq. (11), which is responsible for amplitude squeezing, is totally due to the vacuum field mode that has the same frequency as the laser oscillator but is altered by the perfect mirror.

For the balanced homodyne detection, assuming $T = R = 1/2$ , the resulting quantum fluctuation of the *modulated* light may fall below that of the coherent state i.e. become squeezed as shown in Fig. 2. The fluctuation of the coherent state without the perfect mirror can be calculated by replacing $\cos(k_o z_{1,2})$ by its average value zero so that Eq. (11) simply becomes a constant value $\frac{|\alpha|^2}{2}$ as the result of the usual beam splitter . On the other hand, if we consider the situation such that the distance $z_i (i = 1, 2)$ between the perfect mirror and each detector is well resolved and satisfies $k_o z_i = n\pi$($n$: positive integer), then Eq. (11) reduces to $\frac{|\alpha|^2}{4}$. In other words, the measured quantum fluctuations may fall below that of the coherent vacuum state by as much as 50%. This squeezing limit comes from the intrinsic fluctuations of the coherent state of the laser itself, which is combined with the modified vacuum field with its amplitude suppressed at the detector position such that $k_o z_i = n\pi (i = 1, 2)$.

The quantum fluctuations of the square of the sum and difference of the photocurrents $I_1^o$ and $I_2^o$ are similarly obtained from Eq. (9). Squaring this Eq. (9) and keeping the non vanishing terms, we can obtain

$$\begin{aligned} &< (I_1^o \pm I_2^o)^2 > \equiv \overline{(I_1 \pm I_2)^2} \\ &= \frac{T \mid \alpha \mid^2}{2}[T^2 \pm 2TR + 3R^2 + 1 - 2R\cos(2k_o z_1) \pm 2R\cos(2k_o z_1) \mp 2R^2] \\ &+ \frac{R \mid \alpha \mid^2}{2}[R^2 \pm 2TR + 3T^2 + 1 - 2T\cos(2k_o z_2) \pm 2T\cos(2k_o z_2) \mp 2T^2], \end{aligned} \tag{12}$$

where we have used the relation $Z_1 - z_1 = Z_2 - z_2$. Using the relation $T + R = 1$ , we simplify this equation (12) like this,

$$\overline{(I_1 \pm I_2)^2} = \mid \alpha \mid^2 [1 - (1 \mp 1)TR\{\cos(2k_o z_1) + cos(2k_o z_2)\}]. \tag{13}$$

We find that fluctuations of the sum of $I_1^o$ and $I_2^o$ in Eq. (13) is not dependent on $z_1, z_2$, since this fluctuation has come from the local oscillator. On the other hand, as in the case of $\overline{I_1^2}$ and $\overline{I_2^2}$, the fluctuation of $\overline{(I_1 - I_2)^2}$ which comes from the modulated vacuum field contains the important spatial modulation with a period of $\pi/k_o$. The spatially-averaged fluctuation of $\overline{(I_1 - I_2)^2}$ is $\mid \alpha \mid^2$, which is just the quantum fluctuation of the free-space vacuum field without the mirror. However, the fluctuation of the difference at the detector position such that $k_o z_i = n\pi (i = 1, 2)$ becomes zero. The resulting fluctuations of $\overline{(I_1 - I_2)^2}$ in Eq. (13) are also plotted in Fig. 2. In this Fig. 2, we have replaced the $\cos(k_o z_2)$ with zero, which represents the average value, and have plotted $\overline{(I_1 - I_2)^2}$ as a function of $z_1$.

# 2 Practical limits: finite linewidth and absorption length

So far, we have considered a monochromatic coherent light for the local oscillator. The laser light, however, always has a finite linewidth, so that the modulation depth in Eqs.(11) and (13) may be decreased as the linewidth increases. In this section, we will consider the practical limits to squeezing due to the finite active layer depth of the photodetector as well as the finite laser linewidth.

The effects of the line broadening can be calculated from the Gaussian probability density function [7]

$$P(k) = \frac{1}{(\sqrt{\pi}\Delta k)} e^{[-(k-k_o)^2/\Delta k^2]}. \tag{14}$$

Another practical limit comes from the finite thickness of effective absorption-layer of the photodetectors. The period of the spatial modulation of the quantum fluctuations is of the order of the optical wavelength, whereas the effective depth of the detectors is typically much larger than the wavelength. The probability that a photon is converted into an electron-hole pair at a distance $\xi$ from the surface of the detector's active region can be written as [8]

$$P_D(\xi) = \kappa e^{-\kappa\xi}, \tag{15}$$

where $\kappa$ the absorption coefficient of the detector material.

We can evaluate the expectation values of the fluctuations in Eqs. (11) and (13), with respect to this probability function and obtain

$$\overline{I_1^2} = T \mid \alpha \mid^2 [1 - Re^{-z_1^2 \Delta k^2} \times \frac{\kappa\{\cos(2k_o z_1 + \phi_o) - e^{-\kappa D}\cos[2k_o(z_1 + D) + \phi_o]\}}{\sqrt{4k_o^2 + \kappa^2}}] \quad (16)$$

and

$$\overline{(I_1 - I_2)^2} = \mid \alpha \mid^2 (1 - 2TR \times [ \frac{\kappa e^{-z_1^2 \Delta k^2}\{cos(2k_o z_1 + \phi_o) - e^{-\kappa D}\cos[2k_o(z_1 + D) + \phi_o]\}}{\sqrt{4k_o^2 + \kappa^2}} + \frac{\kappa e^{-z_2^2 \Delta k^2}\{cos(2k_o z_2 + \phi_o) - e^{-\kappa D}\cos[2k_o(z_2 + D) + \phi_o]\}}{\sqrt{4k_o^2 + \kappa^2}}]). \quad (17)$$

where $\phi_o = \arctan(\frac{2k_o}{\kappa})$ and $D$ is the thickness of the depletion layer of the photo detector. Note that we also have used the fact that the variation of $e^{-(Z+\xi)^2 \cdot \Delta k^2}$ in the region [0,D] is so small that we can extract this term as a constant out of the integrand in the above equations.

We can easily see from Eqs. (16) and (17) that all the modulation terms which have $z_1, z_2$ dependence are reduced by a scale factor $e^{-z_i^2 \Delta k^2}\kappa/\sqrt{4k_o^2 + \kappa_2}$. In Figure 3, we plot the fluctuations of $\overline{I_1^2}$ and $\overline{(I_1 - I_2)^2}$ in Eqs.(16) and (17) with respect to the absorption coefficient $\kappa$ and $\Delta z_1$. To observe deep modulations more than anything else, we need a large absorption coefficient $\kappa$ for the detector. For an $Ar^+$ laser light ($\lambda = 514.5nm$ or $k_o = 122\,122cm^{-1}$ ), the absorption coefficients of the Si and Ge are about $10^4 cm^{-1}$ and $4 \times 10^5 cm^{-1}$, respectively. The scale factors are thus 0.04 and 0.85 for Si and Ge detectors. Therefore it would be possible to observe the squeezing effects with a Ge type detector. However, it might be hard to measure a modulation of the quantum fluctuations for the $Ar^+$ ion laser with a silicon detector . If we make a very thin depletion layer for the silicon detector in order not to wash out the spatial modulation, the quantum efficiency $\eta$ will decrease, which implies the fact that all the photons are not converted into electron-hole pairs. Some extra noise will then add up with a relative amplitude $(1 - \eta)$, and this extra noise will also degrade the modulation of the quantum fluctuations.

The linewidth of a single-mode frequency-stabilized $Ar^+$ laser is better than 1 MHz , which is equivalent $\Delta k = 0.0002cm^{-1}$. The scale factor for this linewidth $e^{-\Delta k^2 z^2}$ is 0.9996 for $z \approx 100cm$. Therefore the practical limit to the modulation or squeezing effects is mainly due to the characteristics of the photodetectors in use.

# 3 Conclusion

We have proposed the possibility to produce squeezed state of light simply with a single conducting mirror without elaborate experimentation to produce squeezed vacuum. The electromagnetic field modes near a perfect mirror are modified with respect to those in free space due to the cavity QED effects: the modes of the vacuum fluctuations have sinusoidal spatial dependence from the

mirror. These modified vacuum-field modes, when combined with a coherent light, may produce spatially modulated squeezing effects for the coherent light, which can be measured in a balanced homodyne detection scheme. If we divide a coherent local oscillator with a 50:50 beam splitter and combine with the modulated vacuum field, we estimate that the quantum fluctuations of the combined light are reduced by as much as 50% below the intrinsic fluctuations of the coherent light at distances $z = n\lambda$ (n : positive integer) between the photodetectors and the perfect mirror. Moreover, at those position, we reduced the fluctuation of the difference of two beams which are come from the unused beam splitter. In other words, we can obtain the highly sub-Poissonian fluctuation of the difference which may come from the totally correlated beams such as photon twins generated by the parametric amplification [9].

The finite laser linewidth degrades the spatial modulation by a factor $e^{-z_2\Delta k^2}$, but this factor can be neglected if we use a narrow linewidth laser. Decreasing the distance between the perfect mirror and the detector will also help. The imperfect reflectivity of the mirror may slightly decrease the modulation of the vacuum field. But, since the reflectivity of a metal-coated mirror at the optical frequency is about 97% , this also gives negligible effects. The most important practical limit comes from the characteristics of the photodetector. We need a detector whose quantum efficiency is close to unity and whose absorption coefficient is large enough that the depth of the effective absorption region is smaller than the wavelength (e.g., Ge type photo detector). Including all these limits we have calculated the quantum fluctuation of the light intensity in the last section and shown in Fig. 3. The results indicate that we may increase the ratio of the average intensity to the intensity fluctuation using this homodyne detector with a good conducting mirror.

# References


[1] D. Meschede, W. Jhe and E.A. Hinds, Phys. Rev. A. **41**,1587 (1990)

[2] We consider only the tangential components with the wave vector $\vec{k}$ normal to the mirror, which can couple with the local oscillator at the detector in our experimental configuration of Fig. 1.

[3] W. Jhe, D. Meschede, and E.A. Hinds, to be published.

[4] B. Yurke,*Squeezed Light* , (AT&T Bell Laboratories Murray Hill, New jersey,1989)

[5] P.D. Drummond, Phys. Rev. A **35**, 4253 (1987)

[6] B. Yurke, Phys. Rev. A **32**, 311 (1985)

[7] A.E. Siegman, *Laser* (Oxford University Press, Oxford, 1986)

[8] S.M. Sze , *Semiconductor Devices Physics and Technology* (AT&T Bell Laboratories Murray Hill, New Jersey,1985)

[9] A. Heidmann, R.J. Horowicz, S. Reynaud, E. Giacobino, C. Fabre and G. Camy, Phys. Rev. A **31**, 2049 (1987)

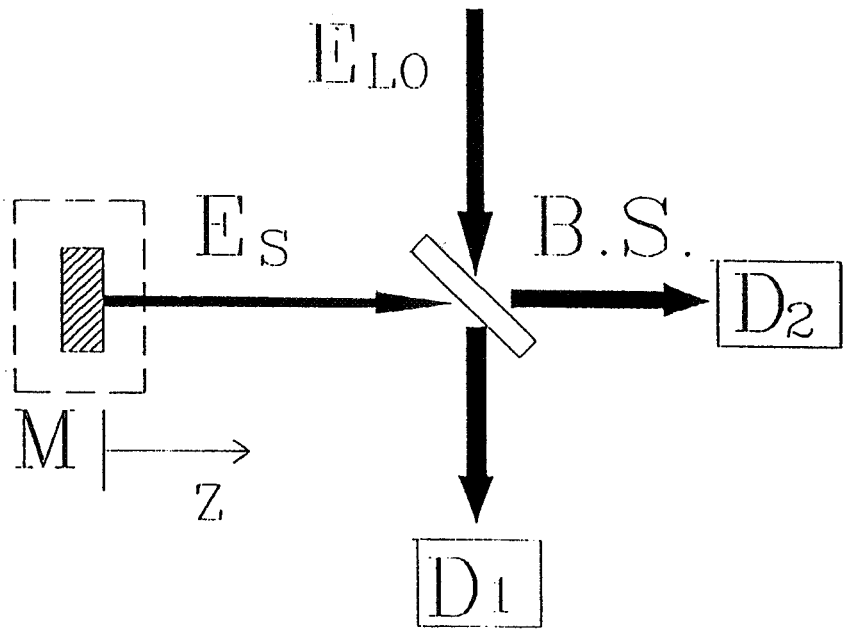


Fig. 1 Homodyne detector. $D_1, D_2$ : photo detector, B.S. : beam splitter. $E_s$ and $E_L$ represent the signal and local oscillator, respectively.

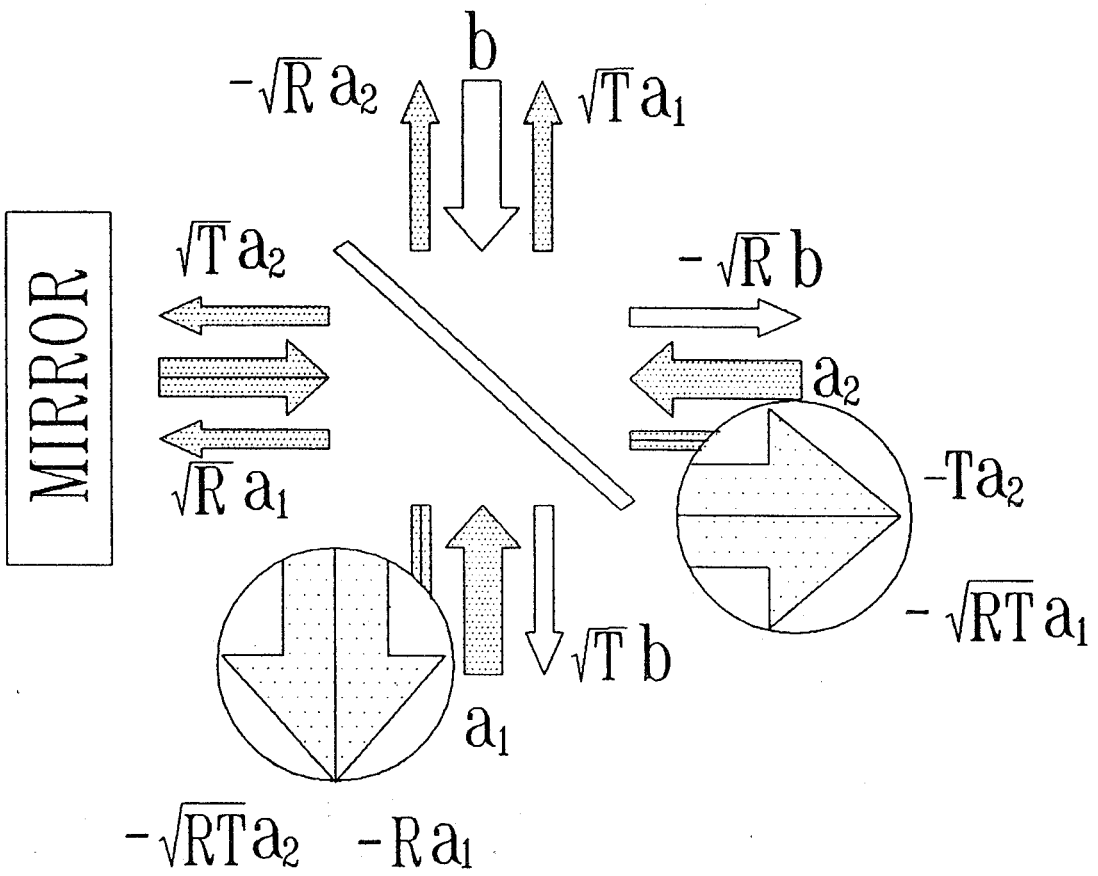


Fig. 2 The vacuum mode relations in the beam splitter with a conducting mirror.

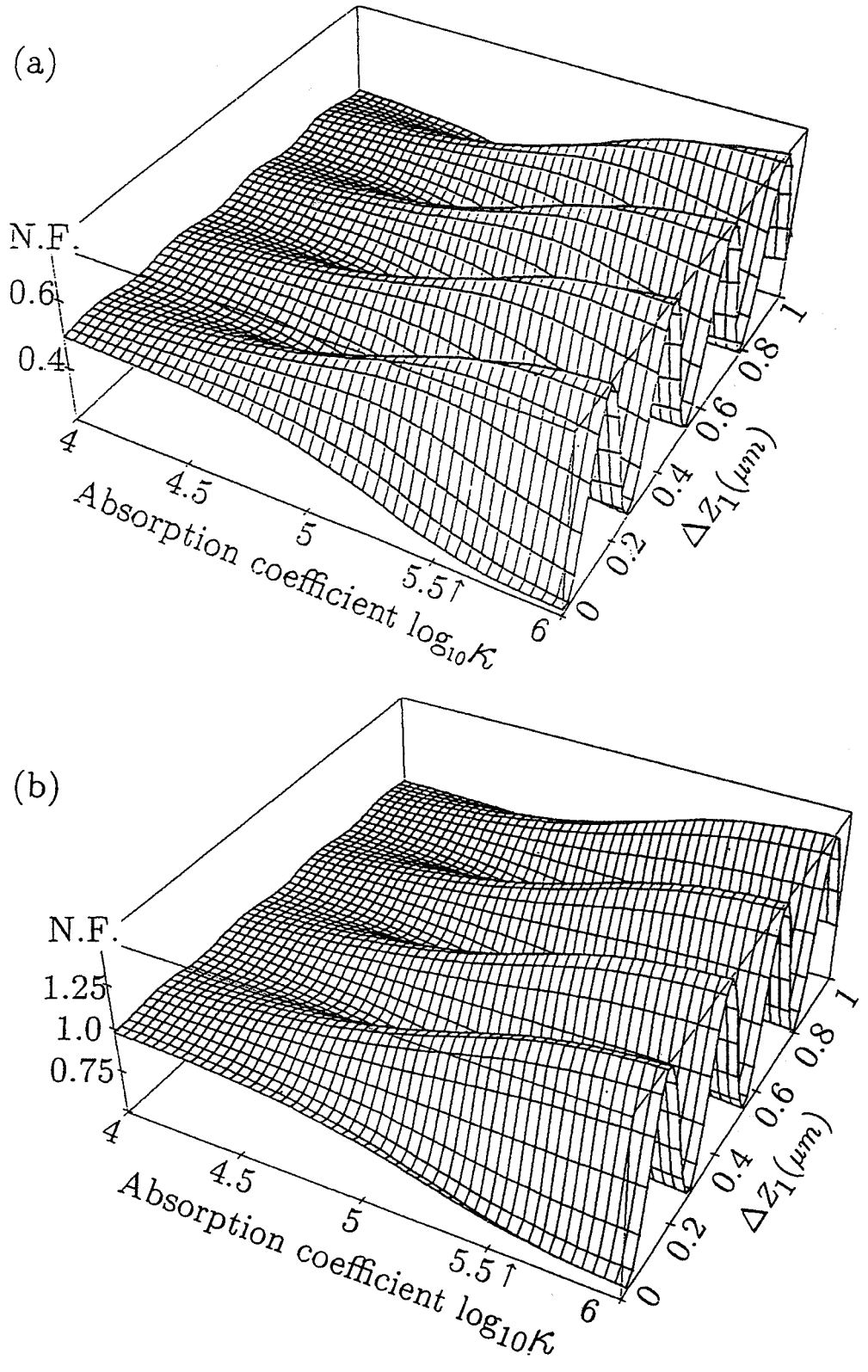


Fig. 3 The amplitude fluctuation of (a)$\overline{I_1^2}$ and (b) $\overline{(I_1 - I_2)^2}$, ,normalized to $\mid \alpha \mid^2$, as a function of $\log \kappa$ ( $\kappa$ : absorption coefficient in units of $cm^{-1}$ and $\Delta z_1$ is displacemen.) Note that the intrinsic quantum fluctuation without the mirror correspond to 0.5 in (a) and 1.0 in (b) on the vertical axis. The arrow indicates for the Ge detector which has $\kappa = 4 \times 10^5 cm^{-1}$ (N.F. : Normalized Fluctuation )

# HOW TO CHARACTERIZE THE NONLINEAR AMPLIFIER?

Dmitri Kouznetsov Kallistratova
*Centro de Instrumentos, UNAM, Ap. 70-186 Cd. Universitaria 04510 DF, Mexico*
*and Lebedev Physical Institute, Leninsky 54, 117924 Moscow*

Carlos Flores Cotera
*Centro de Instrumentos, UNAM, Ap. 70-186 Cd. Universitaria 04510 DF, Mexico*

**Abstract**

The conception of the amplification of the coherent field is formulated. The definition of the coefficient of the amplification as the relation between the mean value of the field at the output to the value at the input and the definition of the noise as the difference between the number of photons in the output mode and square of the modulus of the mean value of the output amplitude are considered. On the simple example it is shown that by these definitions the noise of the nonlinear amplifier may be less than the noise of the ideal linear amplifier of the same amplification coefficient. Proposals to search the other definition of basic parameters of the monlinear amplifiers are discussed. This definition should enable us to formulate the universal fundamental lower limit of the noise which should be valid as for linear quantum amplifiers as for nonlinear ones.

## 1 Introduction

In the development of the modern communication systems the tendencies to reduce the energy of the signal and to increase their frequency take place. The question about the minimal energy of the signal which can carry the information without the significant bit error rate is important. If the amplitude coding, the phase of the field carries no information, and there is no fundamental limit on the noise of amplifiers: in principle it is possible to count the number $n$ of photons and to construct the state of $G^2 n$ photons, where $G^2$ is the intensity amplification coefficient. The uncertainty of the number of photons at the output in the ideal case should be exactly $G^2$ times greatly than at the input. But the face of the field sometimes is important. For example, if the 3-dimensional picture should be transferred, the "exact" amplification of number of photons in each mode causes the complete loss of the phase information, and the output picture is plane. So, the question of the phase properties of quantum states and their amplification is very important. For the case of the linear amplification the inicially coherent state the minimal fundamental noise is determined [1] by the amplification coefficient:

$$N_{min} = GG^* - 1, \tag{1}$$

where $N$ is the intensity of the output noise

$$N = < a^+ a >_{out} - < a^+ >_{out} < a >_{out}, \tag{2}$$

while $G$ is the amplification coefficient:

$$G = < a >_{out} / < a >_{in} . \tag{3}$$

Here subscripts "in" and "out" denote the initial state (before the amplification) and the output state (after the amplification). We assume that these states are related by the unitary transformation

$$| >_{out} = U| >_{in}; U^+U = 1. \tag{4}$$

In the simplest case of the single-mode linear amplifier the transformation of the field operator is linear:

$$U^+aU = Ga + F, \tag{5}$$

where $G$ is a c-number amplification coefficient and $F$ is an operator which transforms the state of the amplifier only and does not touch the mode of the field. So, all commutators and correlators of all degrees of $F$ and $F^+$ with all degrees of $a$ and $a^+$ are zero.

The aim of this work is to apply the definitions (1-4) to the example of the nonlinear amplifier. (For the nonlinear amplifier the relation (5) is not valid). Here we don't interested by the squeezing properties discussed in [4],[1], the fundamental limit of the noise is the problem which should be investigated.

# 2 The parametric amplification the saturation

Consider the model example of the quantum amplifier with small nonlinearity. The parametric amplifier with the saturation of the pump may be considered as the nonlinear amplifier. In the two-mode approximation the Hamiltonian can be written in the form

$$H =: i(a^+b^+ - ab)(1 - \epsilon b^+b) :, \tag{6}$$

where $a$ is the operator of the mode of the field, $b$ is the operator of the idler mode, and the symbol :...: denotes the normal ordering. All correlators and all commutators of all degrees of $a, a^+$ with all degrees of $b, b^+$ are zero because the amplifier knows nothing about the phase of the field which should be amplified. The c-number parameter $\epsilon$ describes the depletion of the classical pump. In the ordered form the hamiltonian (6) can be rewritten as

$$H = i(a^+b^+ - ab - \epsilon a^+b^{+2}b + \epsilon ab^+b^2). \tag{7}$$

In the following consideration the parameter $\epsilon$ is assumed to be small. Consider the transformation of the field defined by the operator

$$U = exp(-iHt), \tag{8}$$

where $t$ is the c-number parameter. It may be considered as dimensionless time of the interaction. The Heisenberg equations have the form

$$da\ dt = b^+ - \epsilon b^{+2}b, \tag{9}$$

$$db\ dt = a^+ - \epsilon(2a^+b^+b - ab^2). \tag{10}$$

Consider the perturbation theory by the parameter $\epsilon$. Let

$$a(t) = a_0(t) - \epsilon a_1(t) + O(\epsilon^2). \tag{11}$$

In the 0-th order of the perturbation theory the introduction of (11) into (9),(10) gives:

$$a_0(t) = a(0)cosh(t) + b(0)^+ sinh(t), \tag{12}$$

$$b_0(t) = b(0)cosh(t) + a(0)^+ sinh(t); \tag{13}$$

Use notations $a = a(0)$, $b = b(0)$ , $s = sinh(t)$, $c = cosh(t)$; for the first order:

$$a_1(t) = b^{+2}b(s^3/3 + s) + (2b^+ba + a^+b^{+2})(c^3 - 1)/3$$

$$+ (a^2b + 2b^+a^+a + 2b^+)s^3/3 + (a^+a^2 + 2a)(c^3/3 - c + 2/3). \tag{14}$$

Let the input we have the coherent state with amplitude $\alpha$; the mean value of the number of photons $x = \alpha\alpha^*$ . The calculation of the amplification coefficient (3) and of the mean value of photons at the output gives:

$$G = c - \epsilon(2 + x)(c^3/3 - c + 2/3) + O(\epsilon^2), \tag{15}$$

$$< a^+a >_{out} = c^2x + s^2 - 2\epsilon(x(2 + x)c(c^3/3 - c + 2/3) + 2(x + 1)s^4/3) + O(\epsilon^2). \tag{16}$$

By the formula (1) the output noise of the amplifier is

$$N = s^2 - 4\epsilon(1 + x)s^4/3 + O(\epsilon^2), \tag{17}$$

while the noise of the ideal linear amplifier with same amplification coefficient $G$ by formula (15) is

$$N_{lin} = G^2 - 1 = c^2 - 1 - \epsilon 2c(2 + x)(c^3/3 - c + 2/3) + O(\epsilon^2). \tag{18}$$

The difference of two last formulas gives

$$N - N_{lin} = -1.5\epsilon(c - 1)^2(2 + (c^2 + 2c + 2)x) + O(\epsilon^2). \tag{19}$$

This difference is negative at positive $\epsilon$ and all values of $x$. It proves that the noise of the nonlinear amplifier may be less than the noise of the ideal linear one with the same amplification coefficient.

# 3 Discussion

The example of the "better than linear" quantum amplifier is constructed in the previous section. During the discussion at the Workshop it was suggested to consider another example of the nonlinear amplifier - the system of identical resonant 2-level atoms interacting with the single mode of the boson field. This system has the "exact" solution [3] and the dependence of the noise intensity on the amplification coefficient and the input intensity may be presented also in the extremely nonlinear case. It indicates the same possibility to realize the "better than linear" amplifier. Infortunately, the consideration is not yet finished at the time of the deadline of the submission.

The paper on the noise properties of the "Tavis-Cummings amplifier" [3] should be published elsewhere. Formulas of the previous section based on the simplest generalization of definition of the amplification coefficient and the noise intensity to the case of the nonlinear amplifier. Formula (19) shows that in the sense of these definitions the nonlinear amplifier may be better then the ideal linear one. Either the real system with "better then linear" information capabilities can be constructed or the another, more appropriate definition of the amplification coefficient and (or) the noise of the nonlinear amplifier should be investigated. One of the alternative possibilities was suggested at the Workshop - to define the amplification coefficient by

$$G(\alpha\alpha^*) = d < a >_{out} / d\alpha \tag{20}$$

instead of formula (3). It is under investigation now. The possibility of the other definition of the noise (instead of (2)) may be considered too. Of course, no "better then linear" amplifier should break information limits of quantum states ground in [4]. So it is important to work out appropriate parameters to characterize the nonlinear quantum amplifier of general kind.

# Asknowledgments

We are grateful to Roberto Ortega, Javier Mondragon, Marvin Mittelman, Alexei Bulatov and other participants of the Workshop for the discussions. This work is partially supported by the Comitet Nacional de Ciencia y Technologia, Mexico.

# References

[1] C. Caves, Phys. Rev. D **26**, 1817 (1982).

[2] H. Haus, G. Mullen, Phys. Rev. **128**, 2407 (1962).

[3] M. Tavis, F. W. Cummings, Phys. Rev. **170**, 379 (1968).

[4] Y. Yamamoto, H. Haus, Rev. of Modern Physics, **58**, 1001 (1986).

N95-13923

# PHASE PROPERTIES OF MULTICOMPONENT SUPERPOSITION STATES IN VARIOUS AMPLIFIERS

K.S.Lee and M.S.Kim
*Department of Physics, Sogang University, CPO BOX 1142, Seoul, 121-742, Korea*

**Abstract**

There have been theoretical studies for generation of optical coherent superposition states. Once the superposition state is generated it is natural to ask if it is possible to amplify it without losing the nonclassical properties of the field state. We consider amplification of the superposition state in various amplifiers such as a sub-Poissonian amplifier, a phase-sensitive amplifier and a classical amplifier. We show the evolution of phase probability distribution functions in the amplifier.

# 1 INTRODUCTION

The superposition principle lies at the heart of quantum mechanics according to Dirac [1]. In this paper we consider the amplification of optical superposition states. As a result of interaction of a single mode coherent state with a nonlinear Kerr medium, the coherent state input becomes a generalized coherent state [2 - 3]. The dynamics of a single mode field propagating in the Kerr medium is governed by the effective Hamiltonian [2] $\hat{H} = \omega\hat{n} + \lambda\hat{n}^2$, where $\lambda$ is the non-linear factor and $\hat{n}$ is the photon number operator. Under the influence of the nonlinear interaction the initial coherent state $|\alpha\rangle$ of the amplitude $\alpha$ evolves at time $t$ into the state

$$|\Psi(t)\rangle = \exp\left(-\frac{|\alpha|^2}{2}\right)\sum_{k=0}^{\infty}\frac{\alpha^k e^{-i\Phi_k}}{\sqrt{k!}}|k\rangle, \quad \Phi_k = \lambda t k^2, \tag{1}$$

where $|k\rangle$ is a Fock state. At the interaction time $t = \pi/N\lambda$, we can rewrite Eqn(1) as a form

$$|\Psi\rangle = \frac{1}{\sqrt{N}}\sum_{n=1}^{N} e^{i\zeta_n}|-\alpha e^{2in\pi/N}\rangle, \tag{2}$$

which is a superposition of N coherent component states located on a circle with the centre at the origin of phase space. If we decompose the state (2) into the Fock basis and compare it with Eqn(1) we obtain an equation for the arguments, $\zeta_n$, of the coefficients of coherent components for an arbitrary value of $N$. For example when $N = 4$ we have

$$|\Psi\rangle = \frac{1}{2}\left(e^{-i\pi/4}|\alpha\rangle - e^{-i\pi/4}|-\alpha\rangle + |i\alpha\rangle + |-i\alpha\rangle\right), \tag{3}$$

which we call the Yurke-Stoler state throughout the paper.

Such superpositions of multicomponent coherent states may be generated not only in the amplitude dispersive medium but also in the micromaser type experiment. Recently Garraway et al. have proposed a method to prepare quantum superposition of multicomponent states [4, 5]

for the eventual goal of preparation of a Fock state. A stream of three-level atoms are injected into a high-Q micromaser cavity. It is assumed that there is just one atom at a time in the cavity and the initial coherent cavity field is tuned to the two-photon resonance with the atomic transition. A superposition state of two coherent component states is generated by a conditional measurement of the atomic excitation after an interaction time that determines the relative phase of the component states. By a sequence of the conditional measurements the superposition of multicomponent coherent states may be generated. As a special case, the initial interaction time is chosen to create a superposition state of two component states separated in phase space by $\pi$ and the interaction times are reduced by one half after each interaction. The second conditional measurement creates a superposition of four component states

$$|\Psi\rangle = \frac{1}{\sqrt{\aleph}}\left[e^{i\frac{9}{4}\pi}|\alpha e^{i\frac{3}{4}\pi}\rangle + e^{-i\frac{9}{4}\pi}|\alpha e^{-i\frac{3}{4}\pi}\rangle + e^{i\frac{3}{4}\pi}|\alpha e^{i\frac{1}{4}\pi}\rangle + e^{-i\frac{3}{4}\pi}|\alpha e^{-i\frac{1}{4}\pi}\rangle\right], \tag{4}$$

where $\aleph$ is a normalization constant. Eventually, the Nth measurement creates the superposition of $2^N$ components separated by $2\pi/2^N$ in phase space. We call the state (4) as the Garraway state.

# 2 PHASE PROBABILITY DISTRIBUTION FUNCTION

There are quasiprobability distributions according to ordering of system operators. One is the Glauber P representation which is quasi probability distribution function for the normal ordering of the system operators and another is the $Q$ function $Q(re^{i\theta})$ for antinormal ordering of system operators [6]. The Wigner function $W(re^{i\theta})$for the symmetrical ordering can be negative. Since the P function cannot be defined in the nonclassical regime, the P function is not dealt with in this paper.

We can study the phase probability of the system with help of the quasiprobabilities. We derive two phase probability distributions from the $Q$ and Wigner quasiprobability distributions [7]:

$$P^{(W)}(\theta) = \int_0^\infty rW(re^{i\theta})dr \tag{5a}$$

$$P^{(Q)}(\theta) = \int_0^\infty rQ(re^{i\theta})dr \tag{5b}$$

Buzek et al. [7] compare these two probability distributions with phase probability defined by Pegg and Barnett [8]. As for the Wigner function, the Wigner phase probability distribution can have negative values, which indicate nonclassical nature of the system. For the quantum superposition state, the quantum interference between component states are best illustrated by the Wigner phase distribution as it can become negative for the quantum interference of component states. As shown in Fig.1a the quantum interference for the Yurke-Stoler state is reflected by the negative values of the Wigner phase probability function. However the Wigner function for the Garraway state is always positive as in Fig.1b. We can therefore conclude that the quantum interference is not necessarily represented by negative values in the Wigner phase distribution. The $Q$ phase distribution function is always positive differently from the Wigner phase distribution function as shown in Fig.1.

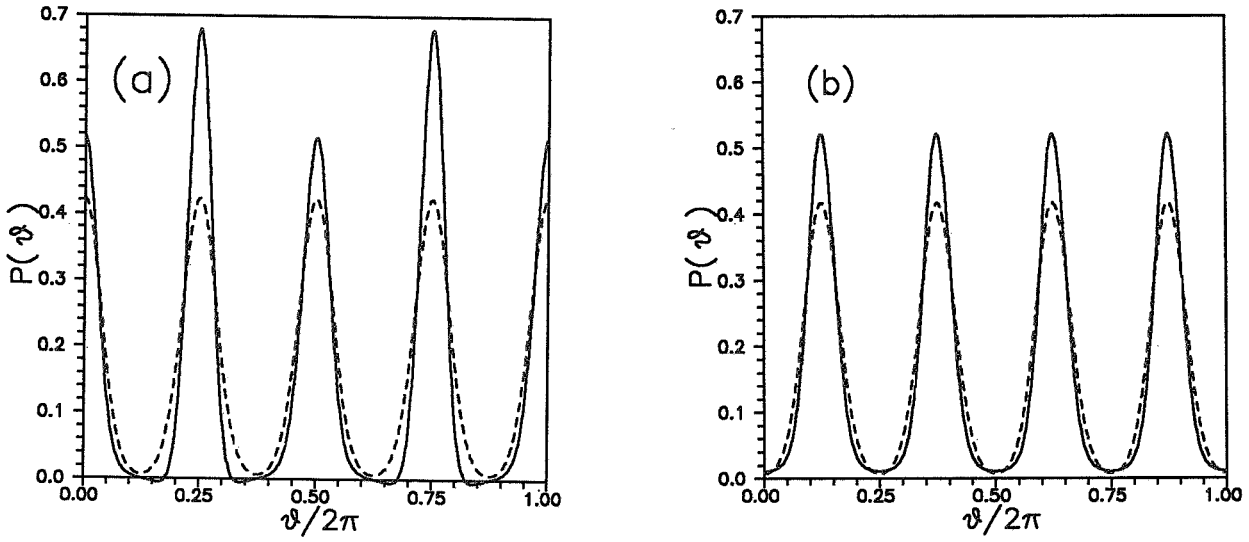


Fig.1. Wigner and $Q$ phase distribution of the Yurke-Stoler (a) and Garraway (b) state. Solid line shows the Wigner phase distribution and dashed line shows the $Q$ phase distribution. ($\alpha = 3$)

# 3 AMPLIFIED SUPERPOSITION STATES

The simplest way to amplify the state of the single-mode field is to displace it by the displacement operator $\hat{D}(\sigma)$ [6]. This operator shifts a field state by a given amplitude in phase space. The displacement of a field state can be implemented by driving the field by a classical current. The displaced superposition state is expressed by

$$|\Psi\rangle = \hat{D}(\sigma)|\psi_0\rangle, \quad \hat{D} = \exp\left(\sigma\hat{a}^\dagger - \sigma^*\hat{a}\right), \tag{6}$$

where $|\psi_0\rangle$ is the initial superposition state. From definitions of the quasiprobability distributions it follows that their shapes are invariant with respect to the action of the displacement operator. The only difference consists in the shift of the Wigner function of the state in phase space along the action of the displacement operator. One of consequences of this invariance is that the displacement of the state does not change the quadrature-squeezing properties associated with the original state. As the whole picture is displaced along one direction in phase space the phase distribution will be differed by the action of displacement as shown in Fig.2. The Wigner phase distribution becomes to have negative values by displacement.

Recently the correlated (phase-sensitive) amplifier has been realized experimentally [9]. In this section we study the evolution of the phase probability distribution of the superposition states amplified by the phase-sensitive amplifier. The dynamics of the field mode coupled to the phase-sensitive amplifier is in the Born and Markov approximation governed by the Fokker-Planck equation for the $Q$ function, which in the interaction picture can be written as [10]

$$\frac{\partial Q(\alpha,t)}{\partial t} = \gamma\left[N_0\frac{\partial^2}{\partial\alpha^*\partial\alpha} - \frac{1}{2}\left(\frac{\partial}{\partial\alpha^*}\alpha^* + \frac{\partial}{\partial\alpha}\alpha\right) + \frac{M_0^*}{2}\frac{\partial^2}{\partial\alpha^2} + \frac{M_0}{2}\frac{\partial^2}{\partial\alpha^{*2}}\right]Q(\alpha,t), \tag{7}$$

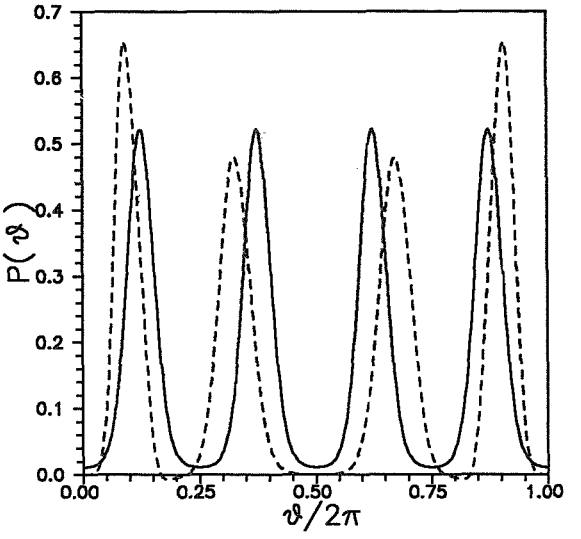


Fig.2. Wigner phase distribution for the displaced Garraway superposition state. Solid line is for the initial state and dashed line is for the displaced state ($\sigma = 1, \alpha = 3$).

where $\gamma$ is proportional to the coupling between the field mode and the environment, and $N_0$ and $M_0$ are the parameters determined by nature of the amplifier. If the phase-sensitive parameter $M_0$ is equal to zero then the Fokker-Planck equation (8) reduces into the equation describing the phase-insensitive amplification of the single mode field. The gain $G$ of the amplifier is defined as $G = \exp(\gamma t)$.

Fig.3 clearly shows that the choice of the $M$ value determines into which quadrature noise should be added. When $M$ is positive the phase information at $\vartheta = 0$ and $\pi$ is kept while the phase information at $\vartheta = \pi/2$ and $3\pi/2$ is lost very rapidly. However, when $M$ is negative the information at $\vartheta = \pi/2, 3\pi/2$ is kept at the expense of the rapid loss of the information at the other quadrature.

We consider a stream of atoms injected into a micromaser cavity with an infinite Q. We assume that there is just one atom at a time in the cavity and the atom makes the two-photon transition of frequency $\omega_0$ between the nondegenerate ground and excited states via a single intermediate level. The cavity is assumed to be tuned to the two-photon resonance with the excited and ground levels and the intermediate level is so detuned not to be excited, so that one photon transitions can be neglected which means that the transition between the ground and excited levels can be considered as a two-photon process.

Let us assume that the field mode is initially prepared in a pure state

$$|\Psi(0)\rangle = \sum_{k=0}^{\infty} C_0(k)|k\rangle. \tag{8}$$

and the atom is prepared in the excited state. During the time evolution the atom and the field become strongly entangled [4]. Nevertheless, at some particular moments they become dynamically disentangled and are again in their pure states. One of those moments is identical to the revival

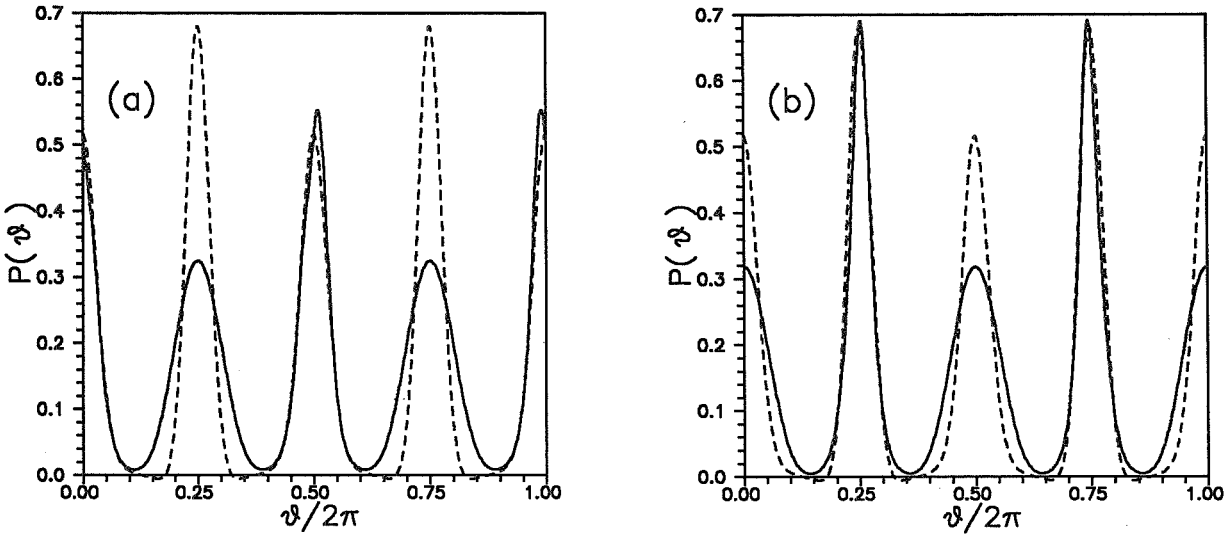


Fig.3. Wigner phase distribution for the Yurke-Stoler state in the phase sensitive amplifier characterized by $N_0 = 3, M_0 = \sqrt{12}$ (a) and by $N_0 = 3, M_0 = -\sqrt{12}$ (b). Dashed line is for the initial state and solid line is for the state at $G = 1.22$ ($\alpha = 3$)

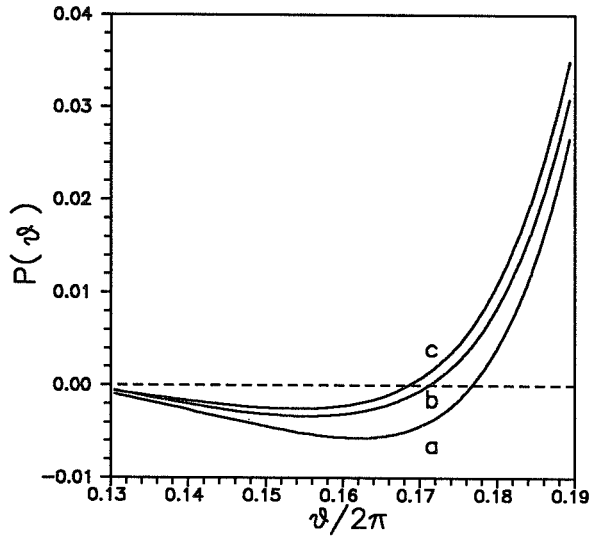


Fig.4. Part of the Wigner phase distribution of the Yurke-Stoler state in the sub-Poissonian amplifier. Line a is for the initial state, line b is for the state with two extra photons and line c is for the state with four extra photons. ($\alpha = 3$)

time $t_R$ (see ref.[4] for details) when the atom is (approximately) in its ground state and the field can be described by the state vector

$$|\Psi(1)\rangle = \sum_{k=0}^{\infty} C_0(k)|k+2\rangle. \tag{9}$$

At this moment exactly two photons are transferred from the atom to the field, so the mean photon number of the field is $\bar{n}(1) = \bar{n}(0) + 2$, where $\bar{n}(i)$ is the mean photon number of the cavity field after $i$ atoms pass the cavity. Analogously, after a sequence of $M$ atoms each of which interacts for time $t_R$ with the cavity field, the state vector of the field can be written as:

$$|\Psi(M)\rangle = \sum_{k=0}^{\infty} C_0(k)|k+2M\rangle. \tag{10}$$

We call the process during which the exact number of photons are transferred to the field as the sub-Poissonian (amplitude-squeezed) amplification.

In Fig.4 we can see that the Wigner phase distribution function is smoothened by the amplification. This means that the phase uncertainty is enlarged as the number uncertainty (so that the energy uncertainty) is reduced by the sub-Poissonian amplification.

This paper was supported by NON DIRECTED RESEARCH FUND, Korea Research Foundation, 1993.

# References

[1] P.A.M. Dirac, *Principles of Quantum Mechanics, 4th Ed.*, (Oxford University Press, London, 1954).

[2] B. Yurke and D. Stoler, Phys. Rev. Lett., **57**, 13(1986).

[3] Ts. Gansog and R. Tanas, Phys. Rev. **A 44**, 2086(1991).

[4] K.S. Lee, M.S. Kim, S.-D. Lee and V. Buzek, J. Korean Phys. Soc., **26**, 197(1993); K.S. Lee, M.S. Kim and V. Buzek, submitted to J.Opt.Soc.Am.

[5] B.M. Garraway, B. Sherman, H. Moya-Cessa, P.L. Knight and G. Kurizki, submitted to Phys.Rev.A.

[6] R.J. Glauber, Phys.Rev., **131**, 2766(1963).

[7] V. Buzek, Ts. Gantsog, M.S. Kim, submitted to Phys.Scrip.

[8] D. T. Pegg and S. M. Barnett, Europhys.Lett. **6**, 483 (1988)

[9] A.Y. Ou, S.F. Pereira and H.J. Kimble, Phys.Rev.Lett. **70** 3239 (1993).

[10] M. S. Kim, K. S. Lee and V. Buzek, Phys. Rev. **A 47**, 4302(1993).

N95- 13924

# SUB-POISSONIAN LIGHT AND PHOTOCURRENT SHOT-NOISE SUPPRESSION IN CLOSED OPTO-ELECTRONIC LOOP

A.V.Masalov, A.A.Putilin, M.V.Vasilyev
*Lebedev Physical Institute, Leninsky pr.53, 117924 Moscow, Russia*

**Abstract**

We examine experimentally photocurrent noise reduction in the opto-electronic closed loop. Photocurrent noise density 12.5 dB below the shot-noise level was observed. So large suppression was not reached in previous experiments [1, 2, 3, 4] and can not be explained in terms of an ordinary sub-Poissonian light in the loop. We propose the concept of anticorrelation state for the description of light in the loop.

We study closed opto-electronic loop consisting of light source (single-mode, single-frequency argon laser with 1W output power at the wavelength 514 nm), electro-optical modulator with half-wavelength voltage 170V, *p-i-n* photodiode having quantum efficiency 0.68 and electronic feedback circuit including two amplifiers with total 62-63 dB amplification in the 1-100MHz frequency range and noise temperature less than 300K (Fig.1). The modulator operates in the regime of the amplitude modulation, where feedback strength $A$ is proportional to the light power and can be easily changed. The feedback strength has been controlled by the value of average photocurrent: $A/\langle i\rangle$ = 0.6-0.7 mA.

Experimental noise spectra of the feedback photodiode current (Fig.2) are in a good agreement with formula

$$\frac{\langle \delta i^2 \rangle}{\langle \delta i^2_{SNL} \rangle} = \frac{1}{|1 + Ae^{2\pi j f \tau}|^2} , \qquad (1)$$

where $\langle \delta i^2_{SNL} \rangle$ is the standard shot-noise level, $\tau$ is loop round-trip time. Eliminating the noise amplification areas by a narrow-bandpass filter we have obtained the photocurrent noise reduction up to 12.5 dB (=factor 17.8), i.e. 94.4% of standard shot noise has been suppressed (Fig.3). This noise reduction is beyond the limit imposed by non-unity quantum efficiency of the feedback photodiode: $\langle \delta i^2 \rangle / \langle \delta i^2_{SNL} \rangle$ should be larger than $1 - \eta$. Photocurrent noise reduction does not depend on the quantum efficiency of the feedback photodiode and can be made arbitrary large (Fig.4). Our data can not be explained in terms of an ordinary sub-Poissonian light in the loop and require an introduction of the new concept of light.

The light beam extracted from the loop exhibits a noise above the standard quantum limit (Fig.5). This noise is shown in Fig.6 versus the feedback strength for two values of the feedback photodiode quantum efficiency. The data are in a good agreement with the theory [5], shown by solid line.

To describe the state of light in the loop we offer the concept of anticorrelation state: the temporal variations of average light intensity produced by electrically driven modulator are anti-correlated to its quantum fluctuations. Due to this anticorrelation the total fluctuations of in-loop

light intensity can be suppressed:

$$\frac{\langle \delta I^2 \rangle}{\langle \delta I^2_{SQL} \rangle} = \frac{1 + |A|^2 \frac{(1-\eta)}{\eta}}{|1+A|^2}, \tag{2}$$

where $\langle \delta I^2_{SQL} \rangle$ is the standard quantum level. In addition the part of the intensity modulation component is *a posteriori* anticorrelated to photocurrent fluctuations arising in the diode due to non-unity quantum efficiency. Thus the photocurrent noise is suppressed, and this suppression is more effective than in the light because the closed opto-electronic loop is a device stabilizing the fluctuations of the current at the modulator. The light here serves only as a feedback signal carrier.

When a beam splitter is inserted into the loop to extract the light, the intensity modulation component contains a term anticorrelated to the quantum fluctuations brought by the beam splitter. However in the extracted beam the corresponding quantum fluctuations are correlated rather than anticorrelated to this modulation term. Therefore extracted beam noise is always super-Poissonian:

$$\frac{\langle \delta I'^2 \rangle}{\langle \delta I'^2_{SQL} \rangle} = 1 + \frac{A}{1+A} \frac{1-T}{T\eta} \tag{3}$$

The principal difference between the anticorrelation light and ordinary sub-Poissonian light is seen from the following example: the ordinary sub-Poissonian light decreases its sub-Poissonian quality when passes through a beam splitter; the anticorrelation light with sub-Poissonian noise passes through a beam splitter and improves its sub-Poissonian factor while the reflected beam gains super-Poissonian statistics. In principle, this paradoxical situation may be observed by QND measurements.

# References


[1] S.Mashida, Y.Yamamoto. Optics Commun. 57, 290 (1986).

[2] Y.Yamamoto, N.Imoto, S.Mashida. Phys. Rev. A 33, 3243 (1986).

[3] P.R.Tapster, J.G.Rarity, J.S.Satchell. Phys. Rev. A 37, 2963 (1988).

[4] Ya.A.Fofanov. Kvantovaya Elektronika (Russian) 16, 2593 (1989).

[5] J.H.Shapiro, G.Saplakoglu, S.-T.Ho, P.Kumar, B.E.A.Saleh, M.C.Teich. JOSA B 4, 1604 (1987).

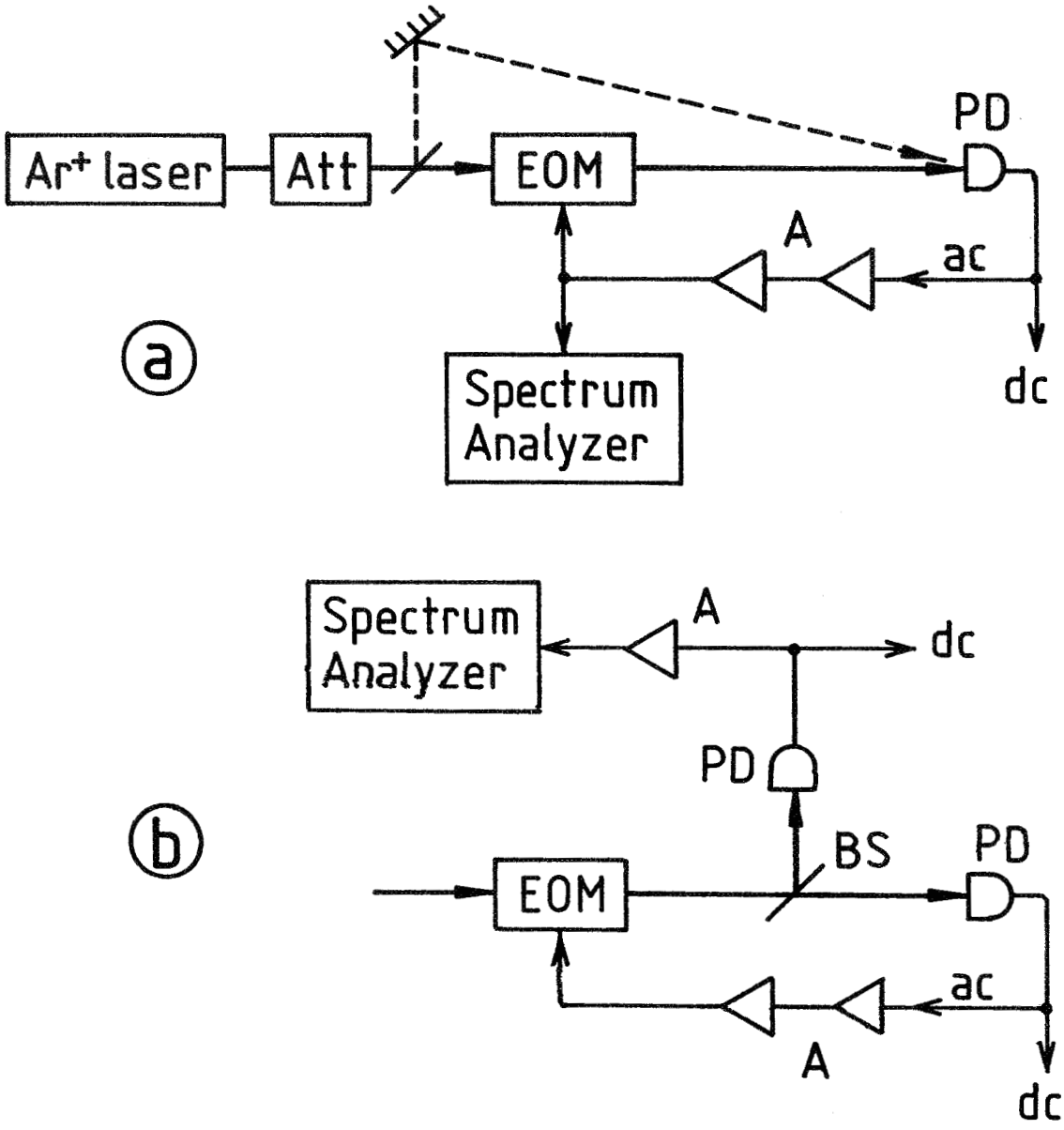


Fig. 1. Experimental setup: *a* - measurements of photocurrent noise in the closed opto-electronic loop, *b* - the same for the beam extracted from the loop. *PD* - photodiodes, *EOM* - electro-optical modulator, *BS* - beam splitter, *A* - amplifiers, *Att* attenuator.

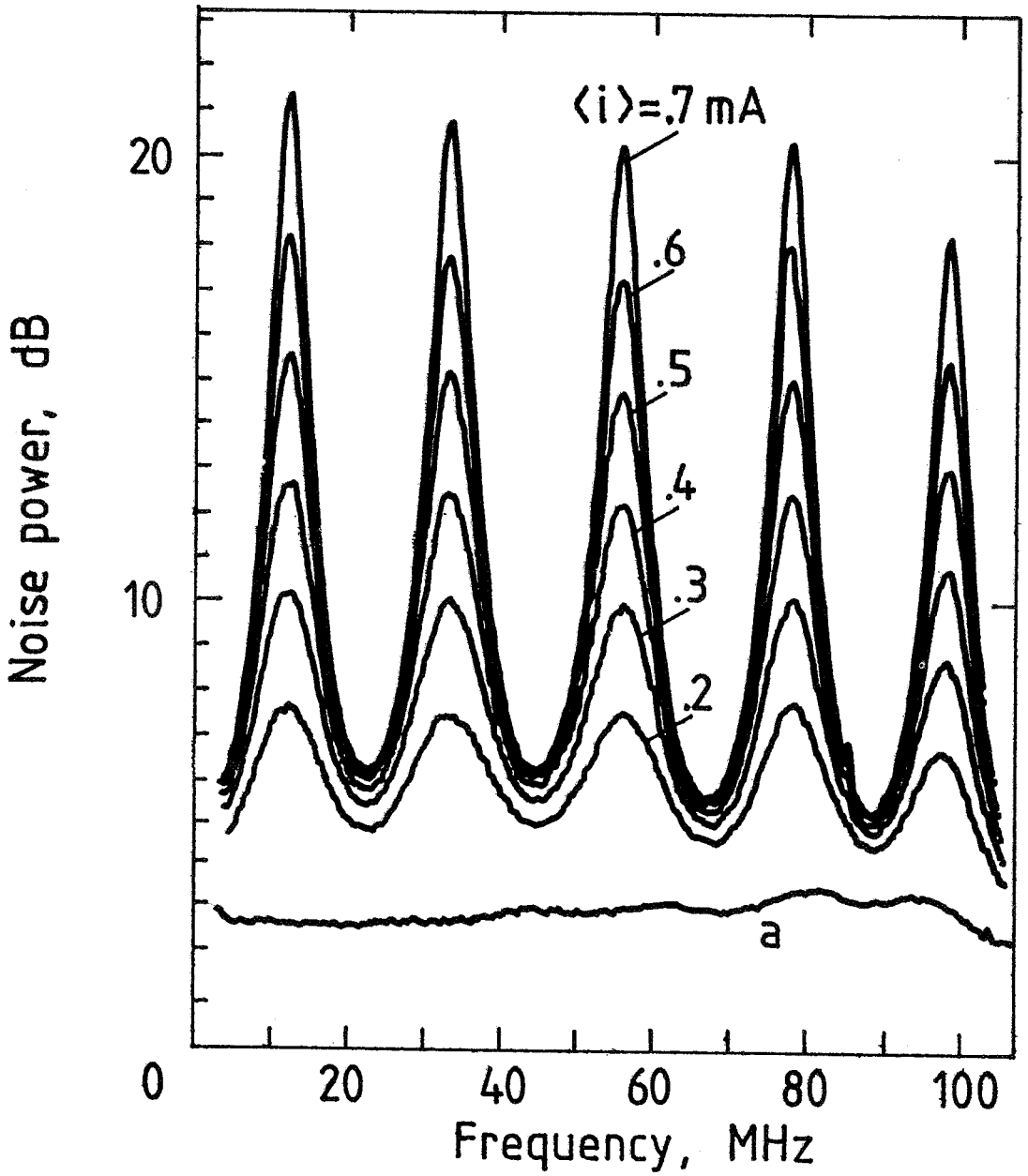


Fig. 2. Noise spectra of the feedback photodiode current at different values of the feedback strength; $a$ - amplifier noise, loop round-trip time $\tau = 47ns$.

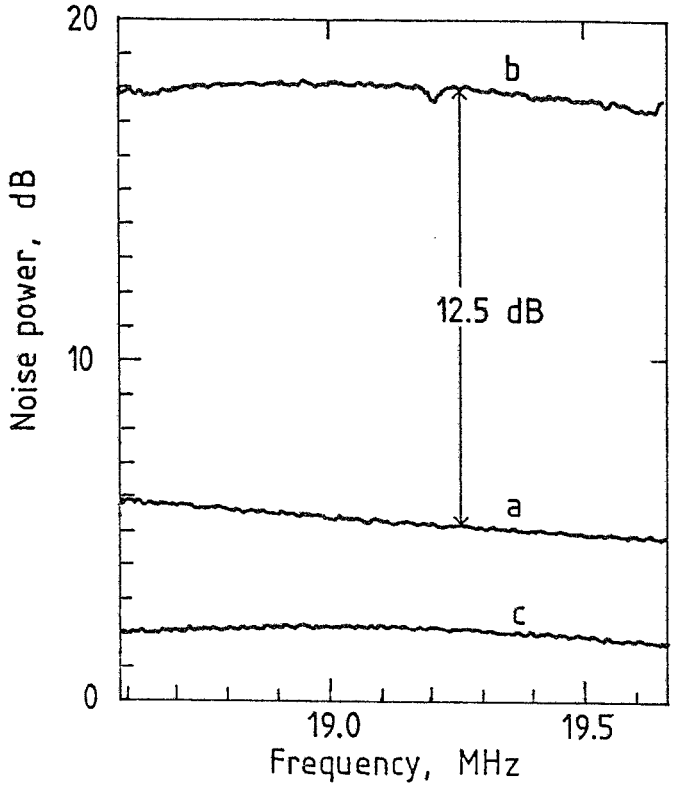


Fig. 3. *a* - photocurrent noise spectral density in the loop with a narrow-band filter in the feedback circuit, *b* - standard shot-noise level, *c* - amplifier noise.

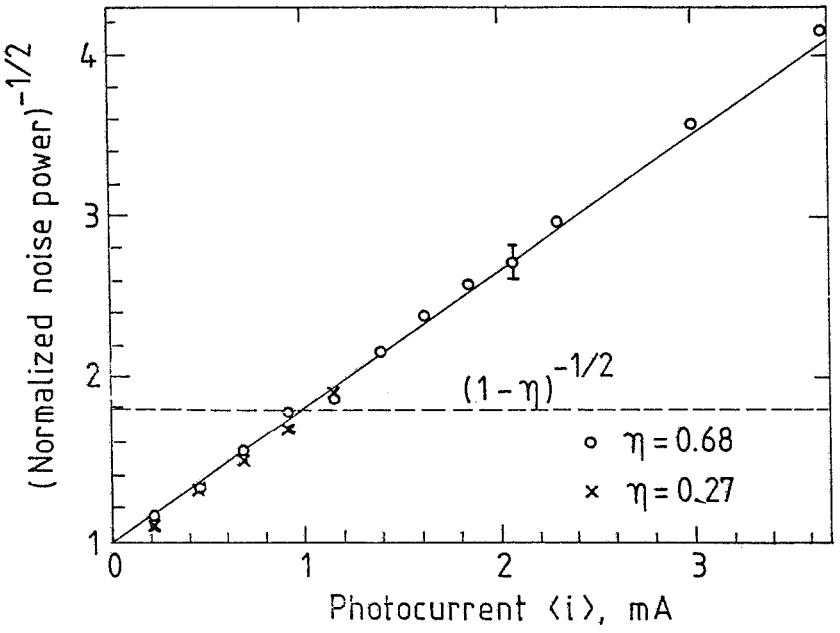


Fig. 4. Shot-noise suppression factor at the frequency 19.2 MHz versus feedback strength in the units of average photocurrent. Dashed line is the limit due to the quantum efficiency of the feedback photodiode $\eta = 0.68$.

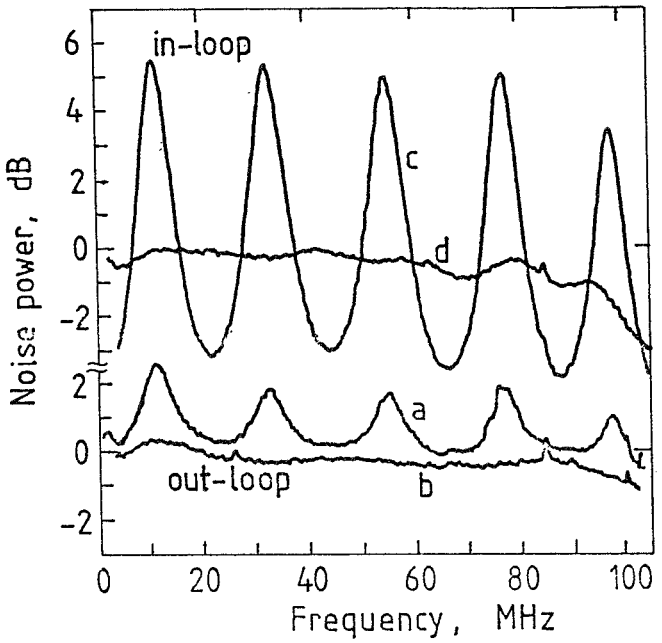


Fig. 5. Photocurrent noise spectrum for the photodiode in the extracted beam ($a$) and the relevant standard shot-noise level ($b$); $c$ and $d$ are those for feedback photodiode.

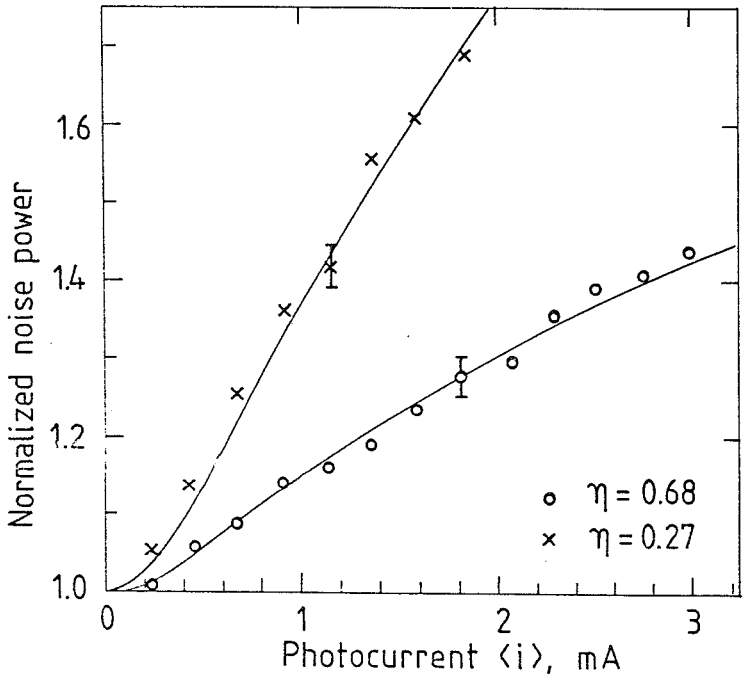


Fig. 6. Noise spectral density of the extracted beam photocurrent, normalized to the standard shot-noise level, versus the feedback strength (in the units of the average feedback photocurrent).

N95- 13925

# MODES IN LIGHT WAVE PROPAGATING IN SEMICONDUCTOR LASER

M. A. Man'ko
*Lebedev Physics Institute, Leninsky pr.,53, Moscow,117333 Russia*

**Abstract**

The study of semiconductor laser based on an analogy of the Schrödinger equation and an equation describing light wave propagation in nonhomogeneous medium is developed.The active region of semiconductor laser is considered as optical waveguide confining the electromagnetic field in the cross-section $(x, y)$ and allowing waveguide propagation along the laser resonator $(z)$.The mode structure is investigated taking into account the transversal and what is the important part of the suggested consideration longitudinal nonhomogeneity of the optical waveguide.It is shown that the Gaussian modes in this case correspond to spatial squeezing and correlation.Spatially squeezed two-mode structure of nonhomogeneous optical waveguide is given explicitly.Distribution of light among the laser discrete modes is presented.Properties of the spatially squeezed two-mode field are described. The analog of Franck-Condon principle for finding the maxima of the distribution function and the analog of Ramsauer effect for control of spatial distribution of laser emission are discussed.

## 1 Introduction

The aim of the talk is to study the possible modes of the electromagnetic field propagating in a semiconductor laser taking into account nonhomogeneous longitudinal structure of the medium in the optical waveguide of the laser.The Gaussian modes in such structures may demonstrate a squeezing phenomenon in the electromagnetic field distribution in transversal cross-section of the semiconductor laser.We will consider the light propagation along the active layer of the semiconductor laser understanding that the refractive index of the media of this layer has such dependence on the transversal coordinates $x$ and $y$ that provides the waveguiding conditions confining the electromagnetic field in the transversal section of the laser waveguide.We also assume that the value of the longitudinal coordinate $z$ which varies along the laser resonator axis influences the refractive index.Our goal is to show that the refractive index dependence on the longitudinal coordinate z produces the change of the widths of the Gaussian electromagnetic field beam that may influence the far field distribution.The equation for propagating field of the fixed frequency $\omega$ in paraxial approximation is derived from the Helmholz equation

$$\Delta\psi + k^2(x, y, z)\psi = 0 \tag{1}$$

for which the structure of the field looks as the amplitude $A$ which has slow dependence on the longitudinal coordinate $z$ and the fast oscillating exponential.Due to this the equation for the

amplitude $A(x,y,z)$ is reduced to the Schrödinger-like equation (Fock-Leontovich approximation [1],or parabolic approximation)

$$i\frac{\partial A}{\partial z} = -\frac{1}{2}(\frac{\partial^2}{\partial x^2} + \frac{\partial^2}{\partial y^2})A + k^2(x,y,z)A \tag{2}$$

in which formally the coordinate $z$ plays the role of time and the refractive index plays the role of the potential energy.If there is no dependence of refrective index on the coordinate $z$ the equation (2) is equivalent to the Schrödinger equation for the stationary states which in case of waveguide describe the possible modes of electromagnetic field propagating along the laser resonator. If the z-dependence of refractive index takes place the structure of the modes changes essentially.For optical fibers this phenomenon has been discussed,for example,in [2]. Our aim is to consider this phenomenon for the semiconductor laser waveguide since the physical picture of the light propagation in semiconductor laser has its own specifics and applications.

# 2 Spatial Squeezing of Semiconductor Laser Beam

As a model we will suppose that the refractive index has parabolic profile in transversal coordinates with $z$-dependences of the formal "frequency"-coefficients in parabolic terms $\omega_x^2(z)x^2/2$ and $\omega_y^2(z)y^2/2$.We will apply the result known in the theory of nonstationary quantum oscillator to the case of optical waveguide of semiconductor laser with the parabolic refractive index of the active layer.It was shown [3] that the width of the Gaussian packet describing at the initial moment the ground state of quantum oscillator due to the time dependence of the frequency has the following value at $t$-moment

$$(\Delta x)^2 = \frac{|e|^2}{2}(\frac{\hbar}{m\omega}), \tag{3}$$

where the function $e$ satisfies the equation

$$\ddot{e} + \omega^2 e = 0, \tag{4}$$

$$e(0) = 1, \tag{5}$$

$$\dot{e}(0) = i\omega(0). \tag{6}$$

Dots mean time-derivatives.We can use the complete analogy of our equation for the light propagation with Schrödinger equation for the nonstationary oscillator.Due to this analogy the following conclusion may be made for the influence of $z$-dependence of the refractive index on the behaviour of the fundamental mode.Its width in transversal coordinate $x$ has the form

$$(\Delta x)^2 = |e_x|^2(\Delta x_0)^2 \tag{7}$$

and in transversal coordinate $y$ it has the form

$$(\Delta y)^2 = |e_y|^2(\Delta y_0)^2, \tag{8}$$

where the functions $e_x(z)$ and $e_y(z)$ satisfy the equations

$$e_x''(z) + \omega_x^2(z)e_x(z) = 0, \tag{9}$$

$$e_y''(z) + \omega_y^2(z)e_y(z) = 0 \tag{10}$$

and the initial conditions

$$e_x(0) = 1, \qquad e_x'(0) = i\omega_x(0), \tag{11}$$

$$e_y(0) = 1, \qquad e_y'(0) = i\omega_y(0), \tag{12}$$

where $z = 0$ is the coordinate of the left mirror of the laser resonator. The formulae (7) and (8) are given in dimensionless variables. It is known that the functions $e_x$ and $e_y$ may become less than 1 for appropriate $z$-dependence.In our case it means that for appropriate refractive index we may obtain squeezing of the light spot on the right mirror of laser resonator in comparison with the width of the field distribution on the left mirror in both transversal directions.Opposite phenomenon also may be present.It means that changing somehow the media properties along the resonator axis we could form the far field distribution.In particular there may exist spatial squeezing in the light beam propagating in semiconductor laser.

# 3 Spatially Squeezed Two-Mode Structure in the Optical Waveguide of Semiconductor Laser

We have discussed above the spatial squeezing for Gaussian modes,because the squeezing for modes which differ from fundamental one are described by the same formulae (7) and (8).Now we will consider the spatial squeezing in discrete modes of semiconductor laser using the same analogy with time-dependent oscillator.In generic case these discrete modes $\psi_{nm}$ are described by Hermite polynomials of two variables.In our case it may be shown that the widths of light spots on the right mirror of the laser resonator may be given by formulae

$$(\Delta x)^2 = (\Delta x_0)^2(2n+1)|e_x|^2, \qquad n = 0, 1, 2, ... \tag{13}$$

and

$$(\Delta y)^2 = (\Delta y_0)^2(2m+1)|e_y|^2, \qquad m = 0, 1, 2, ... \tag{14}$$

We see that the width in both direction may be essentially reduced by choosing an appropriate $z$-dependence of refractive index.This spatial squeezing may be achieved both for Gaussian modes and discrete modes simultaneously.The appropriate $z$-dependence of the refractive index corresponds to such behaviour of the function $e_x$ and $e_y$ for which their moduli become much less than 1 on the right mirror.In these cases we have the spectral squeezing of the light patterns related to the discrete mode structure of the semiconductor laser beam.

# 4 Analogs of Franck-Condon Principle and Ramsauer Effect for Semiconductor Laser Nonhomogeneous along the Optical Axis

Since we have established that for the field in the semiconductor laser the formal role of potential in Schrödinger equation is played by the dielectric constant,while the role of time is played by the coordinate along the cavity axis [4], [5],[6] we have a complete analogy of the character of a

stepwise change in the properties of the active region along the laser optical axis to the character of change in vibrational motion of nuclei after the electron transition in a polyatomic molecule.In order to use this analogy,we will exploit existing results in quantum mechanics to explain the various operating conditions of a laser emphasizing that the role of the field is played by the wave function $\Psi$.In quantum mechanics, bound states exist when the probability density $|\Psi|^2$ diminishes exponentially away from the potential energy minimum.For a semiconductor laser,these bound states with quantum energy levels correspond to mode solutions of the wave equation.Hence,any conclusion regarding the transitions between energy levels due to changes in a potential over time may be reformulated analogously for the case of light redistribution among the modes when two (or more) different parts of the active region are joined corresponding to inhomogeneity of the dielectric constant along the cavity axis.A continuous junction (slow change of refractive index along the cavity) is possible together with stepwise junction (a step in refractive index profile in the vicinity of the junction).In quantum mechanics of nonstationary potential the Schrödinger equation is solved in some cases for varying potential,but such cases are few and they include a specific dependence of the potential on the coordinates(see [7]). For time irregular changes in potential,in quantum mechanics the behavior of a system for the case of polyatomic molecules is predicted by the Franck-Condon principle for potentials arbitrary depending on the coordinates.Hence,this formulation of the analog of the Franck-Condon principle for semiconductor laser operation is of interest, since the qualitative predictions obtained on the basis of this principle are independent of models describing the dielectric constant of the laser active region [8].

For taking into account the nonhomogeneities of heterojunction laser along the resonator we proposed in [4], [5] the model in which the active region was considered as a set of several optical waveguides with different refractive indices connected to each other in such a way that the coupling between the separate sections of the active region was achieved with the help of mode coupling coefficients $C_{nm}$.Let us consider the laser consisting of two end-joined active regions (each one homogeneous along the optical axis).So,we consider in fact two connected lasers each having their own refractive index described by their own "potential curve". Each of these connected lasers is described by its own "potential well" with the "energy levels" corresponding to the descrete laser modes. If both potential wells are plotted in the same figure the analog of the Franck-Condon principle can predict which mode in the second laser (the second part of the laser) will be excited with the maximal probability,when the field energy was contained in a given mode of the first laser (the first part of the laser).This analog of the Franck-Condon principle produces a qualitative prediction for finding the maximum of the square of the modulus of the mode coupling coefficient of two lasers (two parts of the laser)

$$C_{nm} = \int Y_n^*(y) Y_m(y) dy, \tag{15}$$

i.e.,an analog of the Franck-Condon factor

$$W_{nm} = |C_{nm}|^2 \tag{16}$$

for diatomic molecules (the overlap integral of the vibration wave functions before and after the electron transition).This factor describes the portion of energy contained in $n$-mode of the second laser (the second part of the laser) if all energy of the first laser (the first part of the laser) was

concentrated in its $m$- mode.Let us note that this rule is valid in a semiconductor laser when the imaginary part of the dielectric constant of its optical waveguide does not significantly change the spectrum of mode "levels" (in language of quantum mechanics,the imaginary part of the complex potential does not change the energy level spectrum, but rather is responsible only for broadening of the levels and their lifetime; however, the widths of the levels are small compared to the distance between levels).

Another analogy that would allow using results from quantum mechanics in the physics of nonhomogeneous semiconductor lasers is the analog of the Ramsauer effect [9].Let us discuss the practical important case when distribution of dielectric constant in one transverse direction (along the $x$-axis) has the step-like form (in the case of heterojunction laser,the distribution of $\epsilon(x)$ in the direction of current flow is determined by the difference between the refractive indices of the active region and the wide-band layers of the heterostructure) and in the other direction (along the $y$-axis) it is approximated by parabola (symmetric waveguide). The dielectric constant in the resonator is described by the formula:

$$\epsilon(y,z) = \epsilon_0 + a(z)y^2, \tag{17}$$

and the equation for electromagnetic field in the laser formally coincides with the Schrödinger equation for the harmonic oscillator with variable frequency.The analog of the Franck-Condon factor (15),(16) for our model of longitudinal nonhomogeneous laser consisting of two homogeneous parts may be presented in the form,calculated in [7]:

$$W_{nm} = \frac{n!}{m!}\sqrt{1-R}|P^{(m-n)/2}_{(m+n)/2}(\sqrt{1-R})|^2, \qquad m > n, \tag{18}$$

where $P^l_k(x)$ are the Legendre polynomials,and the parameter $R$ can be interpreted formally as the reflection coefficient from a potential whose form is determined by the time dependence of the oscillator frequency.In our case the role of time dependent frequency is formally played by the longitudinal dependence $a(z)$ in formula (17).It is possible to find such dependence of the "potential" $a(z)$ to satisfy the conditions for which the equality $R = 0$ takes place (analogue of the Ramsauer effect in quantum mechanics) and $W_{nm} = \delta_{nm}$ (there is no redistribution of the energy of the electromagnetic field over the modes).In this case the structure of nonhomogeneity of such longitudinal nonhomogeneous laser is such that there is "transparency" in the point of connection of two lasers (two parts of the laser).With a specific dependence of $\epsilon(y,z)$ at the connection between two part of the laser one can regulate the transparency of the connection.It is possible to use this effect for control of the output characteristics of the semiconductor laser.In the presence of dielectric insert in such a laser one can control the output characteristics of the laser by varying the characteristics of the dielectric insert [10].

The formula (18) may be considered as the mode distribution function of the laser light energy in the second laser (the second part of the laser) between its modes with index $m$, $(m = 0, 1, 2, ...)$ if the light in the first laser (the first part of the laser) is exactly in the mode state labeled by the index $n$.Such distribution function emerges if the connection of two lasers is described by the change of the discussed above "frequency" related to $z$-dependence of the refractive index along the laser optical waveguide. More general mode distribution function may be expressed in terms

of Hermite polinomials of two variables in complete analogy with the parametric oscillator theory given in [11],[12].

## Acknowledgments

The author would like to acknowledge the University of Maryland at Baltimore County for kind hospitality and the American Physical Society for travel support.

## References

[1] A. M. Leontovich and V. A. Fock, JETP **16**, 557 (1946).

[2] V. I. Man'ko, *Lie Methods in Optics*, Lectures Notes in Physics, **250**,p.193,eds.J.S.Mondragon and K.-B. Wolf, (Springer Verlag,1986).

[3] V. V. Dodonov and V. I. Man'ko, *Invariants and Evolution of Nonstationary Quantum Systems*, Proceedings of Lebedev Physics Institute,**183**,ed. M. A. Markov, (Nova Science Publishers, Commack, N.Y.,1989).

[4] M. A. Man'ko and G. T. Mikaelyan, Sov. J. Quantum Electron., **16**, 985 (1986).

[5] M. A. Man'ko and G. T. Mikaelyan, *Nonlinear Optics of Semiconductor Lasers*, Proceedings of Lebedev Physics Institute, **166**,p.126,ed. N. G. Basov,(Nova Science Publishers,Commack,N.Y., 1987).

[6] M. A. Man'ko, *ECOOSA-90 Quantum Optics*, p.247, ed. M. Bertolotti, (IOP Publishers Ltd., 1991).

[7] I. A. Malkin and V. I. Man'ko, *Dynamical Symmetries and Coherent States of Quantum Systems* (Nauka, Moscow, 1979, in Russian).

[8] M. A. Man'ko and G. T. Mikaelyan, Sov. J. Quantum Electron., **16**, 201, (1986).

[9] M. A. Man'ko,*Group Theoretical Methods in Fundamental and Applied Physics*, p.247, U.H.Kopvillem, ed. (Nauka ,Moscow,1988, in Russian).

[10] M. A. Man'ko, Soviet Physics–Lebedev Physics Institute Reports, **N12**, p.38, (Allerton Press,N.Y.,1985).

[11] V. V. Dodonov, V. I. Man'ko, and V. V. Semjonov, Nuovo Cimento, **B83**, 145 (1984).

[12] V. V. Dodonov, O. V. Man'ko, and V. I. Man'ko, Phys. Rev.A (1993 submitted).

# SECTION 4

# DISTRIBUTIONS IN PHASE SPACE

# SQUEEZING GENERATED BY A NONLINEAR MASTER EQUATION AND BY AMPLIFYING-DISSIPATIVE HAMILTONIANS

V.V. Dodonov
*Moscow Institute of Physics and Technology*
*16, Gagarin street, 140160 Zhukovskiy, Moscow region, Russia*

M.A. Marchiolli, S.S. Mizrahi and M.H.Y. Moussa
*Departamento de Física, Universidade Federal de São Carlos*
*Via Washington Luiz km 235, 13565-905, São Paulo, SP, Brasil*

**Abstract**

In the first part of this contribution we show that the master equation derived from the generalized version of the nonlinear Doebner-Goldin equation leads to the squeezing of one of the quadratures. In the second part we consider two familiar Hamiltonians, the Bateman – Caldirola – Kanai and the optical parametric oscillator; going back to their classical Lagrangian form we introduce a stochastic force and a dissipative factor. From this new Lagrangian we obtain a modified Hamiltonian that treats adequately the simultaneous amplification and dissipation phenomena, presenting squeezing, too.

## 1 The nonlinear master equation

Our search for a new class of equations was inspired by the model proposed recently by Doebner and Goldin [1]. They looked for the most general Schrödinger equation compatible with the Fokker-Planck equation for the probability density $\rho(\mathbf{x},t) = \mid \psi(\mathbf{x},t) \mid^2$,

$$\rho_t \; + \; \nabla \cdot \mathbf{j} \; = \; D \, \nabla^2 \rho \tag{1}$$

(where $D$ is a constant positive diffusion coefficient), and derived the nonlinear equation

$$\begin{aligned} i\hbar \partial\psi(\mathbf{x},t)/\partial t \; &= \; [-(\hbar^2/2m)\nabla^2 + V(\mathbf{x})]\psi(\mathbf{x},t) \\ &+ \; i\hbar D \left[ \frac{\nabla^2 \; + \; \mid \nabla\psi(\mathbf{x},t) \mid^2}{\mid \psi(\mathbf{x},t) \mid^2} \right] \psi(\mathbf{x},t) \qquad , \end{aligned} \tag{2}$$

for a particle with mass $m$ moving in a scalar potential $V(\mathbf{x})$. The advantage of eq. (2), comparatively to other ones [2], is its group theoretical origin, the nonlinear term was not simply added to the usual Schrödinger equation *ad hoc*, but its structure was derived from the analysis of representations of the $Diff(\mathbf{R}^3)$ group, proposed as a "universal quantum kinematical group" [1]. The only drawback of eq. (2) is its limited range of applicability, since it can be used only in

the coordinate representation. It is desirable to have a more general equation valid in arbitrary representations. To obtain such a generalization (heuristically), first, we remove the Cartesian coordinates dependence, introducing an arbitrary set of states $\mid z\rangle$, which form a complete system with respect to some measure $d\mu(z)$, i.e.,

$$\int \mid z\rangle\langle z \mid d\mu(z) = \hat{1}. \tag{3}$$

Secondly, we replace the two $\nabla$ - operators in the additional term of eq. (2) by two *arbitrary* (linear) operators $\hat{A}$ and $\hat{B}$. By this way we arrive at the equation, whose nonlinear part, in general, is neither Hermitian, nor anti-Hermitian,

$$i\hbar\frac{\partial}{\partial t}\langle z \mid \psi\rangle = \langle z \mid \hat{H} \mid \psi\rangle + i\hbar D\left[\langle z \mid \psi\rangle\frac{\langle\psi \mid \hat{B} \mid z\rangle\langle z \mid \hat{A} \mid \psi\rangle}{\langle\psi \mid z\rangle\langle z \mid \psi\rangle} - \langle z \mid \hat{B}\hat{A} \mid \psi\rangle\right]. \tag{4}$$

Multiplying both sides of this equation by $\langle\psi \mid z\rangle$ and integrating over $d\mu(z)$ with account of (3), one can check that the normalization of the wave function is preserved in time since

$$\int\langle\psi \mid z\rangle\langle z \mid \Omega\{\psi\}\rangle\, d\mu(z) = 0, \tag{5}$$

where $\langle z \mid \Omega\{\psi\}\rangle$ is the non-Hamiltonian term in the right-hand side of eq. (4). Evidently, the new equation satisfies the homogeneity condition. Moreover, the "separability property" also holds: the wave function of noninteracting particles is factorized for all times, if it was factorized at the initial moment. Nonetheless, the form (4) is not the most general, in [3] we showed that the more general form for $\Omega\{\psi\}$ is

$$\Omega\{\mid\psi\rangle\} = i\hbar D\left[\frac{\langle\psi \mid \hat{B} \mid z\rangle\langle z \mid \hat{A} \mid \psi\rangle}{\langle\psi \mid z\rangle\langle z \mid \psi\rangle} - r\frac{\langle\psi \mid \hat{B}\hat{A} \mid z\rangle}{\langle\psi \mid z\rangle} - \lambda\hat{B}\hat{A} \mid \psi\rangle\right], \tag{6}$$

where $\lambda$ and $r$ may be arbitrary complex numbers satisfying the restriction $\lambda + r = 1$. In papers [4, 5] we investigated eq. (4) with $\hat{B} = \hat{A}^+$, $\hat{A}$, $\hat{B}$ being lowering and rising operators for the two-level system and for the harmonic oscillator. It was demonstrated that this equation, written in the discrete energy (Fock) basis $\mid n\rangle$, describes the relaxation to "pseudothermal" stationary states, possessing the Planck distribution for the populations of energy levels, but nonzero off-diagonal elements of the density matrix. This is not surprising, since eq. (4) relates to *pure quantum states*. However, it is more natural to describe relaxation processes in terms of *density matrices*, in order to investigate the evolution of *mixed quantum states*. Therefore, our next goal is to obtain *nonlinear master equations* originating from eq. (6) and its special cases.

Starting from equation (6) and considering the evolution of the pure state density matrix $\langle z \mid \rho_\psi \mid z'\rangle = \langle z \mid \psi\rangle\langle\psi \mid z'\rangle$ governed by this equation and replacing $\mid\psi\rangle\langle\psi \mid$ by $\hat{\rho}$ we obtain

$$\begin{aligned}\frac{\partial}{\partial t}\langle z \mid \hat{\rho} \mid z'\rangle &= D\Big\{\frac{\langle z \mid \hat{A}\,\hat{\rho}\,\hat{B} \mid z\rangle}{\langle z \mid \hat{\rho} \mid z\rangle} + \frac{\langle z' \mid \hat{B}^+\,\hat{\rho}\,\hat{A}^+ \mid z'\rangle}{\langle z' \mid \hat{\rho} \mid z'\rangle} \\ &- r\frac{\langle z' \mid \hat{\rho}\,\hat{B}\,\hat{A} \mid z\rangle}{\langle z' \mid \hat{\rho} \mid z\rangle} - r^*\frac{\langle z' \mid \hat{A}^+\,\hat{B}^+\,\hat{\rho} \mid z\rangle}{\langle z' \mid \hat{\rho} \mid z\rangle}\Big\}\langle z \mid \hat{\rho} \mid z'\rangle \\ &- D\lambda\langle z \mid \hat{B}\,\hat{A}\,\hat{\rho} \mid z'\rangle - D\lambda^*\langle z \mid \hat{\rho}\,\hat{A}^+\,\hat{B}^+ \mid z'\rangle - \frac{i}{\hbar}\langle z \mid \left[\hat{H}\,,\,\hat{\rho}\right] \mid z'\rangle,\end{aligned} \tag{7}$$

which preserves the trace, normalization and hermiticity for an arbitrary initial density matrix.

## 2 Application: The harmonic oscillator in the coordinate representation

This section is devoted to investigating a special case of the general equation derived in Sect. 1. We shall limit ourselves to one dimension, identifying the ket-vector $\mid z\rangle \equiv \mid x\rangle$ and apply the new equation to the harmonic oscillator Hamiltonian

$$\hat{H} = -\frac{\hbar^2}{2m}\frac{\partial^2}{\partial x^2} + \frac{m}{2}\omega^2 x^2 - fx \quad , \tag{8}$$

we choose operators $\hat{A}$ and $\hat{B}$ as $\hat{A} = \hat{B}^+ = \frac{\partial}{\partial x} + sx$, where $s, D, r, \lambda$, are assumed to be real constants. Now, designating the elements of the density matrix in the coordinate representation as $\rho(x,y) = \rho^*(y,x)$ and introducing the notation

$$\begin{aligned} \mathcal{H}\{\rho\} &= -\frac{i}{\hbar}\langle x \mid \left[\hat{H}, \hat{\rho}\right] \mid y\rangle \\ &= \frac{i\hbar}{2m}(\rho_{xx}(x,y) - \rho_{yy}(x,y)) - \frac{i}{\hbar}(V(x) - V(y)) \quad , \end{aligned} \tag{9}$$

$$\rho_x \equiv \frac{\partial \rho}{\partial x}\,,\ \rho_y \equiv \frac{\partial \rho}{\partial y}\,,\ \rho_{xx} \equiv \frac{\partial^2 \rho}{\partial x^2}, \ldots \tag{10}$$

we can write eq. (7) as

$$\begin{aligned} \frac{\partial \rho(x,y)}{\partial t} &= \mathcal{H}\{\rho\} + D\Big\{\frac{\rho_{xy}(x,x) + sx\,[\rho_x(x,x) + \rho_y(x,x)]}{\rho(x,x)} \\ &+ \frac{\rho_{xy}(y,y) + sy\,[\rho_x(y,y) + \rho_y(y,y)]}{\rho(y,y)} + 2s \\ &+ r\,\frac{\rho^*_{xx}(x,y) + \rho^*_{yy}(x,y)}{\rho^*(x,y)}\Big\}\rho(x,y) + \lambda D\,[\rho_{xx}(x,y) + \rho_{yy}(x,y)]\,. \end{aligned} \tag{11}$$

All derivatives in this equation must be calculated for the *independent* variables $x$ and $y$, and only after that one should consider $x = y$ in the functions $\rho_x, \rho_y$, and $\rho_{xy}$.

For the probability density $P(x) \equiv \rho(x,x)$ eq. (11) results in the following Fokker-Planck equation

$$\frac{\partial P}{\partial t} + \frac{\partial J}{\partial x} = D\left\{\frac{\partial^2 P}{\partial x^2} + 2s\,\frac{\partial}{\partial x}(xP)\right\} \quad , \tag{12}$$

where $J(x) = -\frac{i\hbar}{2m}[\,\rho_x(x,x) - \rho_y(x,x)\,]$ is the current density, $2sDx$ is the drift velocity, and $D$ is the diffusion coefficient. Eq. (12) clearly shows that the total probability is conserved in time. Eq. (11) admits a special class of solutions in the form of Gaussian exponentials,

$$\rho(x,y) = \exp\left[-\frac{1}{2}ax^2 + cxy - \frac{1}{2}a^*y^2 + bx + b^*y + \Phi\right] \quad , \tag{13}$$

with $c$ and $\Phi$ being real functions of time, while $a$ and $b$ may be, in general, complex. Putting expression (13) into eq. (11) we get the equations for the coefficients $a(t)$ and $c(t)$, which do not

contain neither the force $f(t)$, nor the function $b(t)$. Therefore, let us assume, for simplicity, that $f = b = 0$. Then, instead of eq. (11) we have the following set of ordinary differential equations for the *real* functions $\alpha = \mathrm{Re}a$, $\beta = \mathrm{Im}a$, $c$, and $\Phi$,

$$\dot{\alpha} = 2\frac{\hbar}{m}\alpha\beta + 4D\left\{\alpha c - c^2 - \alpha^2 + s(\alpha - c)\right\} \quad , \tag{14}$$

$$\dot{\beta} = \frac{m}{\hbar}\omega^2 + \frac{\hbar}{m}(c^2 - \alpha^2 + \beta^2) + 4\xi D\alpha\beta \quad , \tag{15}$$

$$\dot{c} = 2\frac{\hbar}{m}\beta c - 4D\alpha c \quad , \tag{16}$$

$$\dot{\Phi} = \frac{\hbar}{m}\beta + 2D(c - \alpha + s) \quad . \tag{17}$$

Here the parameter $\xi = r - \lambda$ is introduced .

The trace of the Gaussian density matrix equals

$$Tr\hat{\rho} = \left[\frac{\pi}{\alpha - c}\right]^{1/2} e^{\Phi} \quad , \tag{18}$$

consequently, the condition of its conservation is the equation

$$\dot{\Phi} - \frac{1}{2}\frac{\dot{\alpha} - \dot{c}}{\alpha - c} = 0 \quad , \tag{19}$$

and it is easy to check that this equation is fulfilled. The difficulty of treating the equations for the coefficients $\alpha, \beta, c$ is connected with their nonlinearity even in the absence of nonlinear terms in the master equations (i.e., when $D = 0$). It is well known, however, that in the latter case the equations of motion for *average values* and the *second order moments* are *linear* for any quantum system with quadratic Hamiltonian. Therefore we replace the equations for coefficients $\alpha, \beta, c$, by the equivalent equations for the variances

$$\sigma_{xx} = \langle\hat{x}^2\rangle - \langle\hat{x}\rangle^2 \, , \; \sigma_{pp} = \langle\hat{p}^2\rangle - \langle\hat{p}\rangle^2 \, , \; \sigma_{xp} = \frac{1}{2}\langle\hat{x}\hat{p} + \hat{p}\hat{x}\rangle - \langle\hat{x}\rangle\langle\hat{p}\rangle \, , \tag{20}$$

these quantities are related to the coefficients of the Gaussian density matrix (13) by

$$\sigma_{xx} = \frac{1}{2(\alpha - c)} \quad , \tag{21}$$

$$\sigma_{xp} = -\hbar\beta\sigma_{xx} = -\frac{\hbar\beta}{2(\alpha - c)} \quad , \tag{22}$$

$$\sigma_{pp} = \frac{\hbar^2}{2}(\alpha + c) + \frac{\sigma_{xp}^2}{\sigma_{xx}} = \frac{\hbar^2}{2}\frac{\alpha^2 + \beta^2 - c^2}{\alpha - c} \quad . \tag{23}$$

Another quantity characterizing the quantum state is

$$\Delta = \frac{4}{\hbar^2}\left(\sigma_{xx}\sigma_{pp} - \sigma_{xp}^2\right) = \frac{\alpha + c}{\alpha - c} \quad . \tag{24}$$

Its importance is explained by two factors. First, any quantum state must satisfy the *generalized Robertson – Schrödinger uncertainty relation* [6] $\Delta \geq 1$. Second, any positively definite density operator must satisfy the inequality

$$\frac{Tr(\hat{\rho}^2)}{[Tr(\hat{\rho})]^2} \leq 1 \quad , \tag{25}$$

but for any Gaussian state [7]

$$\frac{Tr(\hat{\rho}^2)}{[Tr(\hat{\rho})]^2} = \Delta^{-1/2} \quad . \tag{26}$$

Consequently, the parameter $\Delta$ characterizes the "degree of coherence" of the Gaussian state: $\Delta = 1$ for pure states, and $\Delta > 1$ for mixed states.

The relations inverse to eqs. (21) – (23) read

$$\alpha = \frac{1+\Delta}{4\sigma_{xx}} \, , \; c = \frac{\Delta - 1}{4\sigma_{xx}} \, , \; \beta = -\frac{\sigma_{xp}}{\hbar\sigma_{xx}} \quad , \tag{27}$$

so one can check that eqs. (14) – (16) result in the following equations for the variances,

$$\dot{\sigma}_{xx} = \frac{2}{m}\sigma_{xp} - 4Ds\,\sigma_{xx} + 2D \quad , \tag{28}$$

$$\dot{\sigma}_{xp} = \frac{1}{m}\sigma_{pp} - \omega^2 m\,\sigma_{xx} - 4Ds\,\sigma_{xp} + D\frac{\sigma_{xp}}{\sigma_{xx}}\left[2 + \xi(1+\Delta)\right] , \tag{29}$$

$$\dot{\sigma}_{pp} = -2\omega^2 m\,\sigma_{xp} + \frac{Ds}{\sigma_{xx}}\left(\hbar^2 - 4\sigma_{xp}^2\right) + \frac{2D}{\sigma_{xx}^2}\left\{\sigma_{xp}^2\left[1 + \xi(1+\Delta)\right] - \frac{\hbar^2}{8}\left[1 + \Delta^2\right]\right\} . \tag{30}$$

As a consequence, the equation for the parameter $\Delta$ is

$$\dot{\Delta} = -D(\Delta - 1)\left[4s + \frac{\Delta - 1}{\sigma_{xx}}\right] \quad . \tag{31}$$

We perceive that $\Delta$ is conserved in time if $D = 0$. Alternatively, if $D \neq 0$, then $\Delta$ tends to the unit value at $t \to \infty$, provided both coefficients, $D$ and $s$, are positive. This means that any initial state exhibits the relaxation to a *pure state*!

The advantage of the equations for the variances is clear: The nonlinear terms are multiplied by the diffusion coefficients, which are small in all reasonable situations. Therefore we may use the solutions corresponding to $D = 0$ as the zero approximation, and develop some perturbative scheme.

If $D = 0$, getting rid of $\sigma_{xp}$ and $\sigma_{pp}$, one arrives at a single third-order equation for the coordinate variance,

$$\frac{d^3\sigma_{xx}}{dt^3} + 4\omega^2\frac{d\sigma_{xx}}{dt} = 0 \quad , \tag{32}$$

whose solution reads

$$\sigma_{xx}(t) = A + B\,e^{2i\omega t} + B^*\,e^{-2i\omega t} \quad , \tag{33}$$

where $A$ and $B$ are constant coefficient. It is natural to suppose that for $D \to 0$ the evolution of $\sigma_{xx}$ is given by the same expression, but with the *slowly varying in time* coefficients:

$$\sigma_{xx}(t) = A(t) + B_+(t) \quad , \tag{34}$$

where

$$B_\pm(t) = B(t)\, e^{2i\omega t} \pm B^*(t)\, e^{-2i\omega t} \quad . \tag{35}$$

Now inserting (33) into eq. (28) and neglecting terms of the order of $O(D^2)$ (guessing that the $n$-th derivatives of $A(t)$ and $B(t)$ are proportional to $D^n$), we can express the covariance $\sigma_{xp}$ as follows,

$$\sigma_{xp} = i\omega\, m\, B_- + \frac{m}{2}\left(\dot{A} + \dot{B} e^{2i\omega t} + \dot{B}^*\, e^{-2i\omega t}\right) + 2mDs\,(A + B_+) - mD\,, \tag{36}$$

and with the same accuracy we find the momentum variance for eq. (30):

$$\begin{aligned} \sigma_{pp} &= (\omega m)^2 (A - B_+) + 8i\omega m^2 DsB_- + 2i\omega m^2 \left(\dot{B}\, e^{2i\omega t} - \dot{B}^*\, e^{-2i\omega t}\right) \\ &- \frac{i\omega m^2 D B_-}{A + B_+}\left[2 + \xi(1+\Delta)\right] \quad . \end{aligned} \tag{37}$$

Since in this expression the function $\Delta$ is multiplied by the small parameter $D$, we must calculate it in the zeroth approximation. Thus we get

$$\Delta = \left(\frac{2\omega m}{\hbar}\right)^2 \left(A^2 - 4\,|\,B\,|^2\right) \equiv R^2 \quad , \tag{38}$$

being both, $R$ and $\Delta$, slowly varying functions of time.

Now, we make the crucial step first proposed in [8, 9]: we put the expression for $\sigma_{pp}$ in terms of $A$ and $B$ into eq. (30) and average both sides with respect to the fast oscillations of frequency $\omega$ . Then we arrive at the equation, which contains functions $A$ and $R$ only

$$\begin{aligned} \dot{A} &= 2\Gamma\omega\left\{\left[-4\sigma_0 s + \left(\xi - \frac{1}{2}\right) R + \frac{1+\xi}{R} - \frac{1}{2R^3}\right] A \right. \\ &\left. + \left(1 + R^2\right)\left(\frac{2\sigma_0 s}{R} - \xi\right)\sigma_0\right\} \quad , \end{aligned} \tag{39}$$

and where $\sigma_0 = \hbar/(2\omega m)$ is the coordinate variance in the oscillator ground state, while $\Gamma = mD/\hbar$ is the dimensionless diffusion coefficient.

Now, averaging eq. (31) we arrive at a *closed* equation for $R(t)$,

$$\dot{R} = -\Gamma\omega\left(R - \frac{1}{R}\right)\left(4\sigma_0\, s + R - \frac{1}{R}\right) \quad . \tag{40}$$

Consequently, eq. (39) actually is the *first order linear nonuniform equation* with respect to function $A(t)$, which can be easily solved provided the solution to eq. (40) is known.

Thus, averaging the equations for the variances over the fast oscillations leads to the effective linearization of the equations governing the evolution of the coefficients of the Gaussian density matrix. To get the equation for $B(t)$, one should first multiply both sides of the equation for $\dot{\sigma}_{pp}$,

by $\exp(-2i\omega t)$, and then average over the fast oscillations. We confine ourselves, however, to the evolution of functions $\Delta(t)$ and $A(t)$ (the absolute value of $B(t)$ can be extracted from eq. (38)). It is worth to mention that $A(t)$ is nothing but the energy of quantum fluctuations (up to the constant factor and small corrections of the order of $O(D)$):

$$\delta E(t) = \frac{\omega^2 m}{2}\sigma_{xx} + \frac{1}{2m}\sigma_{pp} = \omega^2 m A(t) . \tag{41}$$

Now if we consider a pure state, $R = 1$, then the solution for eq. (39) is

$$A(t) = \sigma_0 + [A(0) - \sigma_0]\exp[-4\Gamma\omega(2\sigma_0 s - \xi)t] \quad . \tag{42}$$

We see that the energy of fluctuations can increase or decrease, depending on the sign of the term in the exponential:

1)If $2\sigma_0 s - \xi > 0$, we verify that $A(\infty) = \sigma_0$ , $\delta E(\infty) = \hbar\omega/2$ and $B(\infty) = 0$, therefore asymptoticaly $\sigma_{xx}$ and $\sigma_{pp}$ do not oscillate.

2)If $2\sigma_0 s - \xi < 0$ and since reasonably $\Gamma\omega \ll 1$, $A(t)$ becomes a slowly increasing function with time (the same for $\delta E(t)$). From eq. (38), asymtoticaly we have $A(t) \simeq 2B(t) \gg \sigma_0^2$. If $B(t)$ is real at $t = 0$ then it is real for any $t > 0$, so from eqs. (34) and (35) $\sigma_{xx}(t) = A(t) + 2B(t)\cos(2\omega t)$ or $A(t) - 2B(t) \leq \sigma_{xx} \leq A(t) + 2B(t)$. But from eq. (38) $A(t) - 2B(t) = \sigma_0^2/(A(t) + 2B(t)) \sim \sigma_0^2/(2A(t))$. Therefore asymtoticaly $\sigma_{xx}$ oscillates between two values,

$$\frac{\sigma_0^2}{2A(t)} \leq \sigma_{xx} \leq 2A(t) \quad , \tag{43}$$

thence, as time goes on the solution of the nonlinear Schrödinger equation becomes highly squeezed. Note that a similar behavior of the variances (i.e., an exponential increase of the squeezing coefficient) is observed in the case of the usual Schrödinger equation for the parametrically excited oscillator, when its frequency changes in time [7]. However, in the present case all the coefficients in the generalized Schrödinger equation with the functional (6) (or its master equation counterpart eq.(7)) do not depend on time, and the increase of fluctuations is caused by the nonlinear terms.

# 3 Amplifying – Dissipative Hamiltonians

Here we shall consider the theory developed many years ago by P. Havas [10], which is quite suited to construct Hamiltonians that take into account dissipation and apply it to two examples, confining ourselves to the one-dimensional case.

## 3.1 The Bateman-Caldirola-Kanai (BCK) Hamiltonian

The harmonic oscilator with an exponential time-dependent mass $m(t) = m_0\exp(\zeta t)$, is known as the BCK Hamiltonian [11] and we shall introduce the phenomenon of friction in it. According to [10] when friction is present the Lagrangian that describes the motion, ( that reproduces the classical equation of motion) is

$$L(q,\dot{q};t) = \left(\frac{1}{2}m(t)\,\dot{q}^2 - V(q;t) + qF(t)\right)\exp[\gamma(t)] \quad . \tag{44}$$

Here $V(q;t) = \frac{1}{2}m(t)\omega_0^2\, q^2$ and $F(t)$ is a time-dependent external force. The exponential factor introduces the friction effects (also external) on the system and for the specific Lagrangian one has

$$\gamma(t) = \frac{\gamma_0}{\zeta}(1 - \exp(-\zeta t)) \quad , \tag{45}$$

as $\lim_{t\to\infty}\gamma(t) = \gamma_0/\zeta$ and $\lim_{\zeta\to 0}\gamma(t) = \gamma_0 t$, so, recovering previous results [12]. We shall consider $F(t)$ as being a stochastic force whose mean in an *ensemble* is null, $\langle F(t)\rangle = 0$, and that its correlation is *Markovian*, $\langle F(t)F(t')\rangle = 2d\delta(t-t')$.

According to the quantization procedure of [12] one obtains the system Hamiltonian

$$\hat{H}(\hat{P},\hat{Q};t) = \frac{\hat{P}^2}{2m_0}\exp(-\zeta t) + \frac{1}{2}m_0\omega_0^2\hat{Q}^2\exp(\zeta t) + \frac{\gamma_0}{4}\{\hat{Q},\hat{P}\}\exp(-\zeta t) + \hat{Q}F(t)\exp(\gamma(t)/2) \tag{46}$$

where $\hat{P},\hat{Q}$ are canonicaly conjugated operators, $[\hat{Q},\hat{P}] = i\hbar$. The physical position and momentum operators are related to those through

$$\hat{q}_{phys} = \hat{Q}\exp(-\gamma(t)/2) \quad , \quad \hat{p}_{phys} = \hat{P}\exp(-\gamma(t)/2) \tag{47}$$

In order to obtain the equations of motion for the operators $\hat{P}$ and $\hat{Q}$ in the Heisenberg picture we first do an unitary transformation in Schrödinger equation with operator $\mathbf{S}(\zeta t/2) = \exp(-\frac{\zeta t}{4}\{\hat{Q},\hat{P}\})$, which leads to the new Hamiltonian

$$\begin{aligned}\hat{K}(\hat{\pi},\hat{x};t) &= \frac{\hat{\pi}^2}{2m_0} + \frac{1}{2}\,m_0\omega_0^2\hat{x}^2 + \frac{1}{4}\,(\gamma_0\exp(-\zeta t) + \zeta)\{\hat{x},\hat{\pi}\} \\ &+ \hat{x}F(t)\exp\left[\frac{1}{2}(\gamma(t) - \zeta t)\right]\end{aligned} \tag{48}$$

with

$$\begin{aligned}\hat{q}_{phys} &= \hat{x}\exp\left[-\frac{1}{2}(\gamma(t)+\zeta t)\right] \\ \hat{p}_{phys} &= \hat{\pi}\exp\left[-\frac{1}{2}(\gamma(t)-\zeta t)\right] \quad .\end{aligned} \tag{49}$$

The equations of motion for $\hat{x}(t)$ and $\hat{\pi}(t)$ are solved assuming $\hat{x}_H = u(t)\hat{x}_0 + v(t)\hat{\pi}_0 + w(t)$, leading to the set of linear differential equations

$$\frac{d^2u}{dt^2} - \left[\Omega_0^2 + \frac{\gamma_0^2}{4}\exp(-2\zeta t)\right]u = 0 \tag{50}$$

$$\frac{d^2v}{dt^2} - \left[\Omega_0^2 + \frac{\gamma_0^2}{4}\exp(-2\zeta t)\right]v = 0 \tag{51}$$

$$\frac{d^2w}{dt^2} - \left[\Omega_0^2 + \frac{\gamma_0^2}{4}\exp(-2\zeta t)\right]w = -\frac{F(t)}{m_0}\exp\left[\frac{1}{2}(\gamma(t) - \zeta t)\right] \tag{52}$$

where $\Omega_0^2 = \frac{\zeta^2}{4} - \omega_0^2$ and with the following initial conditions

$$u(0) = 1 \quad \text{and} \quad \dot{u}(0) = \frac{1}{2}(\gamma_0 + \zeta) \tag{53}$$

$$v(0) = 0 \quad \text{and} \quad \dot{v}(0) = \frac{1}{m_0} \tag{54}$$

$$w(0) = \dot{w}(0) = 0 \quad . \tag{55}$$

The exact solutions of the above differential equations are :

$$
\begin{aligned}
u(t) &= \left[\left(\nu - \frac{\gamma_0}{2\zeta} - \frac{1}{2}\right)\mathbf{K}_\nu\left(\frac{\gamma_0}{2\zeta}\right) + \frac{\gamma_0}{2\zeta}\mathbf{K}_{\nu-1}\left(\frac{\gamma_0}{2\zeta}\right)\right]\mathbf{I}_\nu\left(\frac{\gamma_0}{2\zeta}\exp(-\zeta t)\right) \\
&- \left[\left(\nu - \frac{\gamma_0}{2\zeta} - \frac{1}{2}\right)\mathbf{I}_\nu\left(\frac{\gamma_0}{2\zeta}\right) - \frac{\gamma_0}{2\zeta}\mathbf{I}_{\nu-1}\left(\frac{\gamma_0}{2\zeta}\right)\right]\mathbf{K}_\nu\left(\frac{\gamma_0}{2\zeta}\exp(-\zeta t)\right) \qquad (56) \\
v(t) &= \frac{1}{m_0\zeta}\left[\mathbf{I}_\nu\left(\frac{\gamma_0}{2\zeta}\right)\mathbf{K}_\nu\left(\frac{\gamma_0}{2\zeta}\exp(-\zeta t)\right) - \mathbf{K}_\nu\left(\frac{\gamma_0}{2\zeta}\right)\mathbf{I}_\nu\left(\frac{\gamma_0}{2\zeta}\exp(-\zeta t)\right)\right] \qquad (57) \\
w(t) &= \frac{1}{m_0\zeta}\int_0^t \exp\left\{\frac{1}{2}\left[\gamma(t_1) - \zeta t_1\right]\right\}\left[\mathbf{I}_\nu\left(\frac{\gamma_0}{2\zeta}\exp(-\zeta t)\right)\mathbf{K}_\nu\left(\frac{\gamma_0}{2\zeta}\exp(-\zeta t_1)\right)\right. \\
&- \left.\mathbf{K}_\nu\left(\frac{\gamma_0}{2\zeta}\exp(-\zeta t)\right)\mathbf{I}_\nu\left(\frac{\gamma_0}{2\zeta}\exp(-\zeta t_1)\right)\right] F(t_1)\,dt_1 \quad , \qquad (58)
\end{aligned}
$$

where $\mathbf{I}_\nu(.)$ and $\mathbf{K}_\nu(.)$ are the modified Bessel functions of the first and third kind, respectively [13]. The parameter $\nu$ is

$$
\nu = \begin{cases} \frac{\Omega_0}{\zeta} & \text{if } \frac{\zeta}{2} > \omega_0 \\ 0 & \text{if } \frac{\zeta}{2} = \omega_0 \\ i\frac{\Omega_0}{\zeta} & \text{if } \frac{\zeta}{2} < \omega_0 \end{cases} \quad . \qquad (59)
$$

Similarly the momentum operator in the Heisenberg picture is $\hat{\pi}_H(t) = \mu(t)\hat{x}_0 + \beta(t)\hat{\pi}_0 + \xi(t)$, where

$$
\begin{aligned}
\mu(t) &= m_0\left[\dot{u}(t) - \frac{1}{2}\left[\gamma_0\exp(-\zeta t) + \zeta\right]u(t)\right] \\
\beta(t) &= m_0\left[\dot{v}(t) - \frac{1}{2}\left[\gamma_0\exp(-\zeta t) + \zeta\right]v(t)\right] \\
\xi(t) &= m_0\left[\dot{w}(t) - \frac{1}{2}\left[\gamma_0\exp(-\zeta t) + \zeta\right]w(t)\right] \quad . \qquad (60)
\end{aligned}
$$

Considering that the energy increasing prevails over energy dissipation, $\gamma_0/\zeta \ll 1$, one has the approximative solutions,

$$
\begin{aligned}
\hat{x}_H(t) &= \left(\cosh(\Omega_0 t) + \frac{\gamma_0 + \zeta}{2\Omega_0}\sinh(\Omega_0 t)\right)\hat{x}_0 + \left(\frac{1}{m_0\Omega_0}\sinh(\Omega_0 t)\right)\hat{\pi}_0 \\
&- \frac{1}{m_0\Omega_0}\exp\left(\frac{\gamma(t)}{2}\right)\int_0^t \exp\left(\frac{-\zeta t_1}{2}\right)\sinh[\Omega_0(t-t_1)]\,F(t_1)\,dt_1 \qquad (61) \\
\hat{\pi}_H(t) &= \left[-\frac{m_0\omega_0^2}{\Omega_0}\sinh(\Omega_0 t) + \frac{m_0\gamma_0}{2}\left(\cosh(\Omega_0 t) - \frac{\zeta}{2\Omega_0}\sinh(\Omega_0 t)\right)\right]\hat{x}_0 \\
&+ \left(\cosh(\Omega_0 t) - \frac{\zeta}{2\Omega_0}\sinh(\Omega_0 t)\right)\hat{\pi}_0 \\
&+ \exp\left(\frac{\gamma(t)}{2}\right)\int_0^t \exp\left(\frac{-\zeta t_1}{2}\right)\left[\frac{\zeta}{2\Omega_0}\sinh[\Omega_0(t-t_1)] - \cosh[\Omega_0(t-t_1)]\right]F(t_1)dt_1 \qquad (62)
\end{aligned}
$$

and the variances for $\hat{q}_{phys}$ and $\hat{p}_{phys}$ become

$$\lim_{t\to\infty}\langle\Delta\hat{X}^2_{1,H}\rangle \sim \frac{\zeta}{16\Omega_0}\exp[-(\zeta-2\Omega_0)t]\left\{\frac{\gamma_0}{\zeta}\left(\frac{\zeta}{2\Omega_0}-1\right)\coth\left(\frac{\hbar\omega_0}{2k_BT}\right)+\exp\left(-\frac{\gamma_0}{\zeta}\right)\left(\frac{\zeta}{2\Omega_0}+1\right)\left(1+\frac{\gamma_0}{\zeta}\right)\right\}\to 0\left(\frac{\zeta}{2\Omega_0}>1\right) \tag{63}$$

$$\lim_{t\to\infty}\langle\Delta\hat{X}^2_{2,H}\rangle \sim \frac{\zeta}{16\Omega_0}\exp[(\zeta+2\Omega_0)t]\left\{\frac{\gamma_0}{\zeta}\left(\frac{\zeta}{2\Omega_0}+1\right)\coth\left(\frac{\hbar\omega_0}{2k_BT}\right)+\exp\left(-\frac{\gamma_0}{\zeta}\right)\left(\frac{\zeta}{2\Omega_0}-1\right)\left(1+\frac{\gamma_0}{\zeta}\right)\right\}\to\infty\left(\frac{\zeta}{2\Omega_0}>1\right) \quad , \tag{64}$$

verifying squeezing even in occurence of a weak dissipation.

## 3.2 The optical parametric oscillator (OPO)

Using the same method we can treat the OPO introducing in the Hamiltonian the dissipation of the cavity, hence,

$$H(A^+,\,A,\,t) := f_1(t)A^+A + \left\{f_2(t)(A^+)^2 + f_3(t)A^+ + h.c.\right\} \tag{65}$$

where the mathematical operators $A^+$ and $A$ are related to the physical creation and destruction operators by $a = A\exp(-\lambda t/2)$ and $a^+ = A^+\exp(-\lambda t/2)$. Moreover, $f_1(t) = \omega_0$ is the mode frequency in the cavity, $f_2 = \kappa\exp(-2i\omega t) + i\lambda/4$, where $\kappa$ and $\omega$ are, respectively, the intensity and the frequency of the pumping field, while $\lambda$ is the damping constant of the cavity. $f_3(t) = F(t)\,e^{\lambda t}/(2\omega_0)^{1/2}$. The force $F(t)$ is assumed to be a *Markovian* stochastic force: $< F(t) >= 0$, $< F(t)F^*(t') >=< F(t)^*F(t') >= 2d\delta(t-t')$ and $< F(t)F(t') >= 0$, and the parameter $d$ is related to the temperature of the cavity,

$$d = \frac{\lambda\omega_0}{2}\coth\left(\frac{\omega_0}{2k_BT}\right) \quad . \tag{66}$$

Considering the pumping at resonance, $\omega_0 = \omega$, and for $\kappa\lambda/\omega_0 \ll 1$, the solution of Heisenberg equations for operator $A_H(t)$ is

$$A_H(t) = u(t)A(t) + v(t)A^+(t) + w(t) \tag{67}$$

where

$$u(t) = e^{-\imath\omega_0 t}\cosh(2\kappa t) + \left[e^{-\imath\omega_0 t}\left(\sinh^2\gamma\,\cosh(2\kappa t) - \imath\,\sinh\gamma\cosh\gamma\sinh(2\kappa t)\right) - c.c.\right] \tag{68}$$

$$v(t) = \imath\,\sinh(2\kappa t)\left(\cosh^2\gamma\,e^{-\imath\omega_0 t} - \sinh^2\gamma\,e^{\imath\omega_0 t}\right) - \imath\,\sinh(2\gamma)\sinh(2\kappa t)\cos(2\omega_0 t) \tag{69}$$

$$w(t) = -\cosh(\gamma-2\kappa t)\left[\int_0^t f_3(t')\exp[-\imath\omega_0(t-t')]\,dt' - c.c.\right] \tag{70}$$

and $\tanh(2\gamma) = \lambda/(2\omega_0)$.

With the above solution we present the asymptotic ($t \to \infty$) mean values of several quantities, after taking the average over the high frequency oscillations of the field ($\omega_0$) and considering $4\kappa/\lambda < 1$:

1)Energy,

$$\lim_{t\to\infty} \langle \hat{E} \rangle = \omega_0 e^{-\lambda t} \langle A_H^+ A_H \rangle_{\omega_0} \sim \frac{d}{\lambda} \frac{1}{1-(4\kappa/\lambda)^2} \tag{71}$$

2)Variances of the two quadratures,

$$\lim_{t\to\infty} \langle \Delta \hat{X}_{1,2} \rangle_t \sim \frac{d}{2\lambda\omega_0} \frac{1}{1-(4\kappa/\lambda)^2} \tag{72}$$

Although the asymptotic values of the variances of the quadratures are both above the value 1/2, at initial times squeeze is seen in the fast oscillations (before averaging over the mode frequency). In eqs. (71) and (72) one verifies the effects of the dissipation-amplification process through the quantity $4\kappa/\lambda$:

i) If $4\kappa/\lambda \ll 1$ (very weak pumping compared with the cavity dissipation), the thermalization, represented by the parameter $d$, dominates in the physiçal expressions at equilibrium.

ii) On the other side, when $4\kappa/\lambda$ is close to 1 (strong pumping) the factor $(1-(4\kappa/\lambda)^2)^{-1}$ dominates the strenghts of the asymptotic values, increasing dramatically the energy and fluctuations, as is expected to occur at resonance.

# 4 Summary

We have presented two different formulations of quantum dynamical equations that show squeezing in the variances of the conjugate canonical operators. In the first one we considered a generalization of the Doebner-Goldin nonlinear extension of the Schrödinger equation and we verified that although the parameters that enter the nonlinear part of the equation are constant in time, squeezing occurs, essentially due to the nonlinearity. Moreover, the master equation shows the surprising feature that any initial mixed state relax to a pure state!

In the other approach we introduced the dissipation phenomenon into the Hamiltonian formalism by starting with a conveniently defined Lagrangian, as proposed by P. Havas [10]. We considered two familiar time-dependent Hamiltonians, the BCK and the OPO. The BCK Hamiltonian has a time-dependent mass and it displays amplification of energy and squeezing of variance of momentum or of position, although uncertainty is preserved. The dissipation was introduced and the effects are seen in eqs. (63)–(64).

The second Hamiltonian is the OPO, describing a single mode in an electromagnetic cavity with pumping at resonance. Dissipation is introduced to take into account the loss in the cavity walls. As an expressive result we verify that the asymtotic physical expressions depend, essentially, on the factor $4\kappa/\lambda$, $\kappa$ representing the pumping and $\lambda$, the dissipation.

# 5 Acknowledgments

V.V.D. and M.A.M. are grateful to the Fundação de Amparo à Pesquisa do Estado de São Paulo (FAPESP) for full financial support to elaborate the present work, and S.S.M. acknowledge travel

financial support. S.S.M. also acknowledge partial financial support from the Conselho Nacional de Desenvolvimento Científico e Tecnológico (CNPq), Brasil.

# References

[1] H.-D. Doebner and G.A. Goldin, Phys. Lett. A**162**, 397 (1992); G.A. Goldin, Int. J. Mod. Phys. B**6**, 1905 (1992).

[2] M.D. Kostin, J. Chem. Phys. **57**, 3589 (1973); J. Stat. Phys. **12**, 145 (1975)
R.W. Hasse, J. Math. Phys. **16**, 2005 (1975)
N. Gisin, J. Phys. A**14**, 2259 (1981); Found. Phys. **13**, 643 (1983)
D. Schuch, K.-M. Chung, H. Hartmann, J. Math. Phys. **24**, 1652 (1983)
G. Crespo, D. Otero, A. Plastino and A.N. Proto, Phys. Rev. A**39**, 2133 (1989)
I. Bialynicki-Birula and J. Mycielski, Ann. Phys. **100**, 62 (1976).

[3] V.V. Dodonov and S.S. Mizrahi, *Uniform nonlinear evolution equations for pure and mixed quantum states*, preprint UFSCar.

[4] V.V. Dodonov and S.S. Mizrahi, *A new class of nonlinear generalisations of the Schroedinger equation* to appear in J. Phys. A.

[5] V.V. Dodonov and S.S. Mizrahi, *Pseudothermal relaxation of quantum systems induced by a new nonlinear Schroedinger equation* preprint UFSCar.

[6] H.P. Robertson, Phys. Rev. **35**, 667 (1930)
E. Schrödinger, Sitzungsber. Preuss. Akad. Wiss, Phys. Math. **24**, 296 (1930).

[7] V.V. Dodonov and V.I. Man'ko, *Invariants and the evolution of nonstationary quantum systems*, (Proc. Lebedev Phys. Inst., vol. **183**, Nova Science, Commack, 1989).

[8] V.V. Dodonov, Comm. Theor. Phys. (Allahabad, India) **2**, 61 (1993).

[9] V.V. Dodonov and S.S. Mizrahi, *Doebner-Goldin nonlinear model of quantum mechanics for a damped harmonic oscillator in a magnetic field* to appear in Phys. Lett. A.

[10] P. Havas, Nuovo Cimento Suppl. **5**, 363 (1957).

[11] H. Bateman, Phys. Rev. **38**, 815 (1931)
P. Caldirola, Nuovo Cimento **18**, 393 (1941)
E. Kanai, Prog. Theor. Phys. **3**, 440 (1948).

[12] J.R. Brinati and S.S. Mizrahi, J. Math. Phys. **21**, 2154 (1980).

[13] N.N. Lebedev, *Special Function and their Applications*, (Dover Publ. Inc., New York, 1972).

# PHASE–SPACE ANALYSIS OF CHARGED AND OPTICAL BEAM TRANSPORT: WIGNER ROTATION ANGLE

G. Dattoli and A. Torre
*ENEA, Dip. INN., Settore Elettroottica e Laser,*
*CRE Frascati, C.P. 65 - 00044 Frascati, Rome, Italy*

**Abstract**

The possibility of using the phase space formalism to establish a correspondence between the dynamical behaviour of squeezed states and optical or charged beams, propagating through linear systems, has received a great deal of attention during the last years. In this connection, it has been indicated how optical experiments may be conceived to measure the Wigner rotation angle. In this paper we address the topic within the context of the paraxial propagation of optical or charged beams and suggest a possible experiment for measuring the Wigner angle using an electron beam passing through quadrupoles and drift sections. The analogous optical system is also discussed.

## 1 Introduction

Lorentz group is the basic language of special relativity [1]. It has been recognized as a powerful tool in many other fields of modern physics as well. Many dynamical symmetry groups, underlying specific branches of physics, as quantum optics, classical and quantum mechanics, Hamiltonian optics, are locally isomorphic to the group $SO(2,1)$ of Lorentz transformations in two–space and one–time dimensions.

Actually, the $(3+1)$–dimensional Lorentz group $SO(3,1)$ is the full space–time symmetry group. However, we seldom discuss Lorentz transformations in the three–dimensional coordinate system, since computing for instance velocity additions and successive Lorentz boosts is quite complicated, $4 \times 4$ matrices being involved. Restricting thereby the problem from $SO(3,1)$ to $SO(2,1)$ may simplify significantly calculations.

Furthermore $SO(2,1)$ has both a physical and mathematical interest. It is indeed the little group, which leaves a space–like four–momentum invariant. Accordingly, studying $SO(2,1)$ amounts to studying free particles travelling faster than light (the so–called tachyons), which are intrinsically interesting from a theoretical point of view.

Above all, the group $SO(2,1)$ gave rise to a great amount of interest, since, as already remarked, it is locally isomorphic to other groups, as $Sp(2)$, $SU(1,1)$, $SL(2,C)$, and has therefore a very rich mathematical and physical content. The isomorphism with the above quoted groups offers many advantages from both analytical and theoretical point of view. In fact, it allows further simplification in the calculations involving Lorentz transformations, the groups $Sp(2)$, $SU(1,1)$, $SL(2,C)$ consisting of $2 \times 2$ matrices. In particular, the algebraic analogy with the symplectic

group $Sp(2)$ offers a further advantage, as $Sp(2)$ consists of real matrices. Hence, it is possible to visualize Lorentz transformations in terms of transformations in a two–dimensional geometry, making a correspondence between Lorentz transformations in real space and linear canonical transformations in phase–space or, equivalently, between volume–preserving transformations and area–preserving transformations.

In addition, as firstly recognized by Han, Kim and Noz [2], the quoted isomorphism allows to conceive a kind of analog computer for testing the Lorentz group properties. In particular, as is well known, instead of rotations, pure Lorentz transformations do not form a subgroup. As a consequence, the product of two boosts along different directions is not a boost but a boost preceded or followed by a rotation. The angle of rotation is known as the Wigner angle and provides the kinematic basis for Thomas precession in atomic physics [1, 2].

Many suggestions have indeed proposed in order to perform optical experiments to observe the optical analog of the Wigner angle [3, 4].

In this connection, the paper is devoted at suggesting a possible experiment for measuring the Wigner angle within the context of electron beam transport [5]. The paraxial propagation of a charged particle along a magnetic channel is indeed governed by the symplectic symmetry. It can be therefore conceived an experiment involving electron beams for measuring the Wigner angle. The formal analogy between the propagation of charged beams and that of light beams through optical systems in the Gaussian approximation suggests to discuss the topic in full generality. However, the specific language used through the paper is that usually adopted in accelerator physics, whilst the symbology is just that of ray–optics.

The paper is organized as follows. Sec. 2 is devoted to a preliminary analysis of the problem, in order to introduce the formalism relevant to symplectic symmetry. In Sec. 3 the analogy between linear canonical transformations and optical systems is developed, thus leading to a specific design of the experiment for measuring the Wigner angle within the electron–beam optics, as illustrated in Sec. 4. Concluding remarks are given in Sec. 5.

## 2 $SO(2,1)$ and $Sp(2)$

As remarked in ref. [6], the *symplectic group*, originally introduced by Weyl in 1938, plays a central role in many branches of physics, as a consequence of that symplectic transformations preserve the skew symmetric products, which frequently appear in physics. In particular, symplectic geometry is the mathematical theory underlying Hamiltonian mechanics. It emerges especially in phase–space picture. The phase–space of a mechanical system is indeed recognized as a symplectic manifold and the time evolution of a conservative dynamical system is a one–parameter family of symplectic diffeomorphisms, or, linear canonical transformations.

Phase space formalism is becoming the unifying language for both classical and quantum mechanics.It is basic to the Hamiltonian formulation of classical mechanics. Within this context, indeed, the evolution of a dynamical system is described by a number $n$ of independent coordinate variables and on the same number of canonically conjugate momenta. The cartesian space of these $2n$ coordinates is just the *phase–space*.

Correspondingly, phase space picture of quantum mechanics is becoming increasingly popular. Although, the concept of phase–space is not compatible with quantum mechanics, $\hat{q}$ and $\hat{p}$ being noncommuting operators, the Wigner phase–space representation allows to overcome this prob-

lem, since in this representation both the coordinate and momentum variables are $c$–numbers. Accordingly, it is possible to perform phase–space canonical transformations as in the case of classical mechanics, which correspond to unitary transformations in the Schrödinger picture of quantum mechanics.

Phase space concept appears therefore as the unifying context, where classical as well as quantum mechanics can be naturally framed, thus suggesting the possibility to transfer concepts and methods from quantum to classical mechanics and viceversa.

Furthermore, as discussed in ref. [2], phase–space picture provides the natural language for quantum optics as well, offering a geometrical view to coherent and squeezed states as circles and ellipses respectively. In this respect, taking advantages from the symmetry of the relevant Wigner phase space distribution function it is possible to calculate expectation values and transition probabilities for the above quoted states [2].

In the present paper, we are interested in the paraxial propagation of optical or charged–particle beams through *optical* systems [7, 8]. We are thereby led to consider the harmonic oscillator–type Hamiltonian

$$H = \frac{1}{2}\{p^2 + k(s)q^2\} \ , \tag{1}$$

with $q$ and $p$ being canonically conjugate variables. As noticed, the Hamiltonian (1) models the paraxial propagation of electron beams as well as light beams through optical systems. The $p^2$–term describes the free propagation for both electron beams and light rays, the variable $p$ being understood as the particle–momentum and the ray reduced slope, respectively. On the other hand, the $q^2$–term accounts for the propagation through optical systems as quadrupoles or lens–like medium, the corresponding *strength* being measured by the coefficient $k(s)$. The coordinate $s$ is measured along the symmetry axis of the system, also assumed as the direction of the beam propagation.

The basic tools of classical mechanics are the Poisson brackets and the canonical transformations. The latter can be derived from the former.

The properties of Poisson brackets, indeed, as the antisymmetry, the derivation property and the Jacobi's identity, assure that Poisson brackets make any commutative ring of functions defined on a domain $X \subset R^{2n}$ into a Lie algebra. It is thereby possible to associate with any Hamiltonian $H$ the operator $\hat{\xi}_H \equiv \{H, \ldots\}$, which for the one–degree of freedom writes as

$$\hat{\xi}_H = \frac{\partial H}{\partial q}\frac{\partial}{\partial p} - \frac{\partial H}{\partial p}\frac{\partial}{\partial q} \ . \tag{2}$$

Accordingly, the dynamics ruled by (1) is naturally framed within the group structure generated by the operators associated with the quadratic polynomials:

$$\begin{aligned} &\frac{1}{2}p^2 \rightarrow -p\frac{\partial}{\partial q} \ , \\ &\frac{1}{2}q^2 \rightarrow q\frac{\partial}{\partial p} \ , \\ &pq \rightarrow p\frac{\partial}{\partial q} - q\frac{\partial}{pq} \ . \end{aligned} \tag{3}$$

Embedding the above operators into the following

$$\begin{aligned} \hat{K}_1 &= \frac{1}{2}\left(q\frac{\partial}{\partial p} - p\frac{\partial}{\partial q}\right) , \\ \hat{K}_2 &= \frac{1}{2}\left(q\frac{\partial}{\partial p} + p\frac{\partial}{\partial q}\right) , \\ \hat{K}_3 &= \frac{1}{2}\left(p\frac{\partial}{\partial p} - q\frac{\partial}{\partial q}\right) , \end{aligned} \tag{4}$$

it is easy to recognize the symplectic structure of the corresponding group, as displayed by the commutation relations obeyed by the above introduced operators:

$$[\hat{K}_1, \hat{K}_2] = \hat{K}_3 , \quad [\hat{K}_1, \hat{K}_3] = -\hat{K}_2 , \quad [\hat{K}_2, \hat{K}_3] = -\hat{K}_1 . \tag{5}$$

As elements of $Sp(2)$, the operators $\hat{K}_1$, $\hat{K}_2$, $\hat{K}_3$ are amenable of the matrix representation

$$K_1 = \frac{1}{2}\begin{pmatrix} 0 & 1 \\ -1 & 0 \end{pmatrix} , \quad K_2 = \frac{1}{2}\begin{pmatrix} 0 & 1 \\ 1 & 0 \end{pmatrix} , \quad K_3 = \frac{1}{2}\begin{pmatrix} 1 & 0 \\ 0 & -1 \end{pmatrix} . \tag{6}$$

Finally, let us say that the operators (4) are the generators of the canonical transformations in phase–space, which will be analysed with some details in the next section, within the context of the specific problem of charged beam motion in magnetic fields.

# 3 Linear canonical transformations and optical systems

Before analysing the specific role of the operators $\hat{K}_i$, $i = 1, 2, 3$ and discussing the optical analogs of the associated canonical transformations, let us make some preliminary considerations in order to visualize the phase–space canonical transformations within the specific context of electron–beam transport physics.

As is well known, an invariant quadratic form

$$\mathcal{I} = \underline{x}^T \underline{\underline{T}}(s) \underline{x} \tag{7}$$

can be associated to any dynamics described by quadratic Hamiltonians in canonical coordinates and momenta. In passing, it is worth stressing that within a quantum context the quadratic form $\mathcal{I}$ is reported as the Ermakov–Lewis invariant [9], the vector $\underline{x}$ containing obviously the position and momentum operators, whilst in classical mechanics it is known as the Courant–Snyder invariant [10], firstly introduced in the analysis of electron beam motion through magnetic channels. In the above expression, the two component vector $\underline{x} \equiv \begin{pmatrix} q \\ p \end{pmatrix}$ is acted by the real $2 \times 2$ matrix $\underline{\underline{T}}$, which furthermore is required to be symmetric and unimodular: $\det \underline{\underline{T}} = 1$. Just to share the language of accelerator physics, we refer to $\underline{\underline{T}}$ as the *Twiss* matrix[1] and write it in the form

$$\underline{\underline{T}} = \begin{pmatrix} \gamma & \alpha \\ \alpha & \beta \end{pmatrix} . \tag{8}$$

[1]The quadratic form (7) can also be regarded as the transcription in phase space of the quantum invariant, the vector $\underline{x}$ being formed by the expectation values of the position and momentum operators and the matrix $\underline{\underline{T}}$ being linked to the *quantum covariance* matrix.

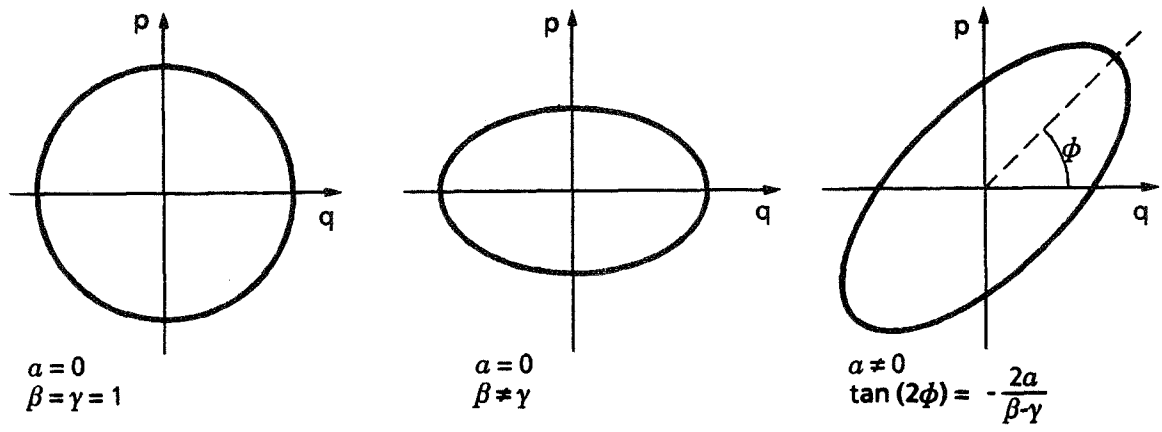


Figure 1: Phase–space ellipses for different values of the Twiss parameters $\alpha, \beta, \gamma$.

The entries $\alpha, \beta, \gamma$ usually named as *Twiss* parameters, play an important role in designing transport channels.

The quadratic form (7) can be depicted in the phase space as an ellipse, whose size and orientation are determined by the Twiss coefficients. The area of the ellipse, which is just the value of the invariant $\mathcal{I}$, is usually denoted in accelerator physics as $\mathcal{I} = \pi\varepsilon$, $\varepsilon$ being referred to as the *beam emittance*. It plays a crucial role in characterizing the quality and the dynamics of the $e$–beam. In a single particle analysis, $\alpha, \beta$ and $\gamma$ define the particle trajectory, as in an ensemble analysis they define the second order momentum of the phase space distribution function, thus providing information on its extent and maximum localization. Explicitly,

$$\begin{aligned} \varepsilon\gamma &= \sigma_{pp}^2 \equiv \langle p^2 \rangle - \langle p \rangle^2 \,, \\ \varepsilon\beta &= \sigma_{qq}^2 \equiv \langle q^2 \rangle - \langle q \rangle^2 \,, \\ \varepsilon\alpha &= -\sigma_{qp}^2 \equiv -(\langle qp \rangle - \langle q \rangle \langle p \rangle) \,, \end{aligned} \tag{9}$$

the averages being understood on the distribution function. Accordingly, the emittance can be given the further meaning:

$$\varepsilon^2 = \sigma_{qq}^2 \sigma_{pp}^2 - \sigma_{qp}^2 \,. \tag{10}$$

According to the above considerations,the dynamics of charged beams passing through transport channels naturally leads to a visualization of the problem in terms of circles and ellipses in the phase–space, which on the other hand have been recognized as useful pictures for the coherent and squeezed states of quantum optics as well (Fig. 1).

Acting on the vector $\underline{x}$ amounts to acting on the phase–space ellipse and correspondingly on the Twiss parameters. To be more precise, let us say that a linear canonical transformation $U$, represented by the matrix $\underline{\underline{U}} = \begin{pmatrix} A & B \\ C & D \end{pmatrix}$, change the Twiss parameters as [8]

$$\begin{pmatrix} \alpha' \\ \beta' \\ \gamma' \end{pmatrix} = \begin{pmatrix} AD + BC & -AC & -BD \\ -2AB & A^2 & B^2 \\ -2DC & C^2 & D^2 \end{pmatrix} \begin{pmatrix} \alpha \\ \beta \\ \gamma \end{pmatrix} \,. \tag{11}$$

After these introductory remarks, let us consider the specific effect of the transformations generated by the operators $\hat{K}_i$, $i = 1, 2, 3$ and recognize the corresponding *optical* systems.

Using the matrix representation (6), we immediately get

$$e^{\eta \hat{K}_3} \equiv S(\eta, 0) = \begin{pmatrix} e^{\eta/2} & 0 \\ 0 & e^{-\eta/2} \end{pmatrix} \,, \tag{12}$$

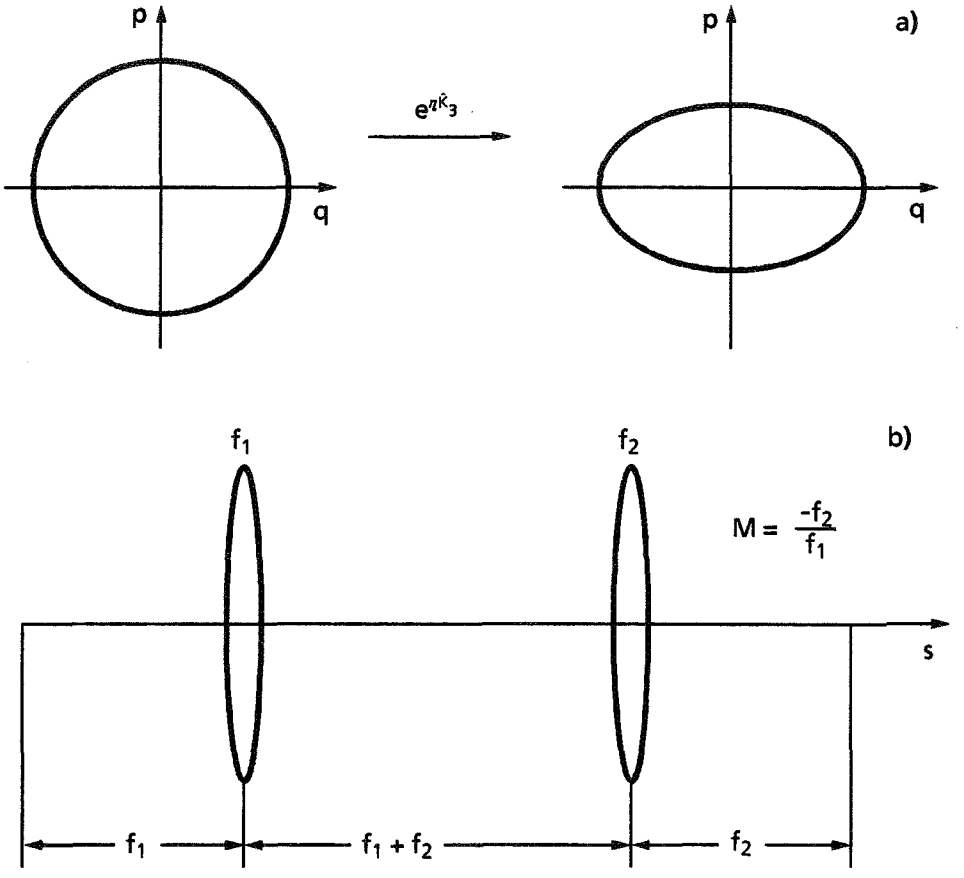


Figure 2: Phase–space canonical transformation (a) and optical system (b) corresponding to the operator $e^{\eta \hat{K}_3}$.

which represents an elongation in the $q$–direction and correspondingly a stretching in the $p$–direction, turning for instance a circle into an ellipse, as sketched in Fig. 2a.

It is needless to say that the transformation (12) preserves phase–space area, as a consequence of that $Sp(2)$ matrices leave invariant the cross products, naturally associated with areas.

In the optics of electron or light beams the transformation described by $S(\eta, 0)$ is realized by means of telescopic systems, consisting of two thin lenses appropriately combined, according to the scheme shown in Fig. 2b. In this regard, let us recall that the symbology for optics of electron beams and light beams is the same. Hence, thin lenses in ray optics correspond to quadrupoles in electron–beam optics.

The parameter $M$, which is just equal to minus the ratio of the foci of the two lenses, is reported in optics as the *magnification* of the system. It produces indeed an *image magnification* and a *ray–angle demagnification.*

As to the operator $\hat{K}_1$, it is easy to obtain the associated transformation as

$$e^{-\phi \hat{K}_1} \equiv R(\phi) = \begin{pmatrix} \cos \phi/2 & -\sin \phi/2 \\ \sin \phi/2 & \cos \phi/2 \end{pmatrix} , \tag{13}$$

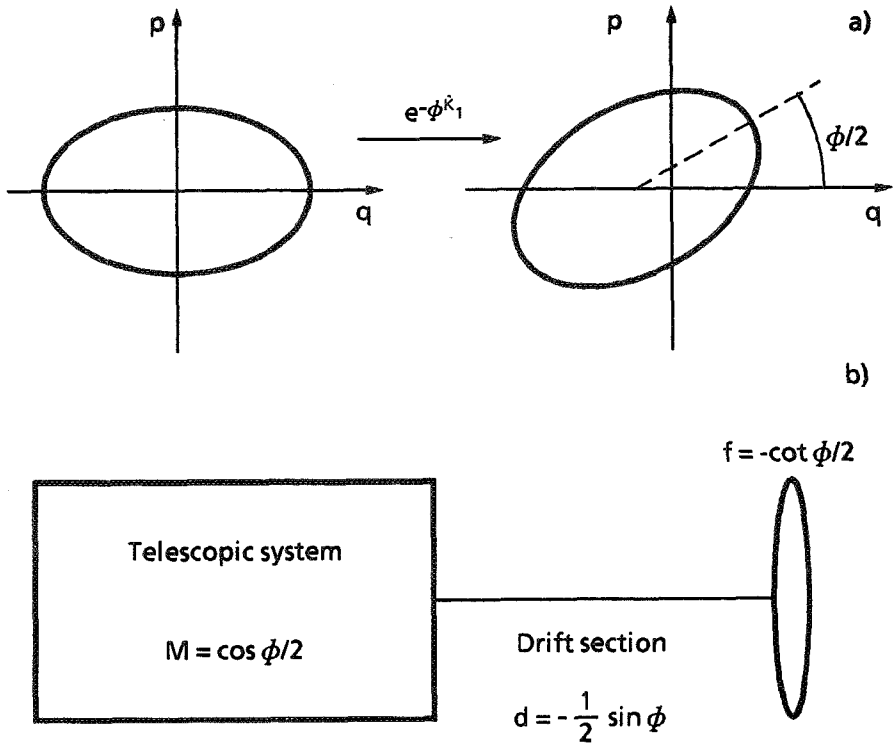


**Figure 3: Phase–space canonical transformation (a) and optical system (b) corresponding to the operator $e^{-\phi \hat{K}_1}$.**

immediately recognized to describe the rotation around the origin in the phase space by the angle $\phi/2$, as further confirmed by the transformation law (11) for the Twiss parameters according to which the associated ellipse rotates in the counterclockwise direction by $\phi/2$.

Since any group elements can be appropriately factorized, the canonical transformation corresponding to the matrix $R(\phi)$ can be realized by means of an appropriate sequence of the basic optical elements, that is thin lenses, drift sections and telescopic systems, which however are just a combination of the first two.

Accordingly, the optical system corresponding to a rotation in phase–space can be realized by means of the following sequence (Fig. 3):

1. telescopic system with magnification $M = \cos \phi/2$
2. drift section of length $d = -\frac{1}{2} \sin \phi$
3. thin lens of focus $f = -\cot \phi/2$

In this connection, it is worth stressing that the above scheme is only one of the possible ones, which can be obtained changing the ordering in the operator factorization, thus allowing to satisfy specific requests on the parameters of the optical components.

Finally, the operator $e^{\eta \hat{K}_2}$, which can be represented by the matrix:

$$e^{\eta \hat{K}_2} \equiv S(\eta, 90°) = \begin{pmatrix} \cosh \eta/2 & \sinh \eta/2 \\ \sinh \eta/2 & \cosh \eta/2 \end{pmatrix} , \tag{14}$$

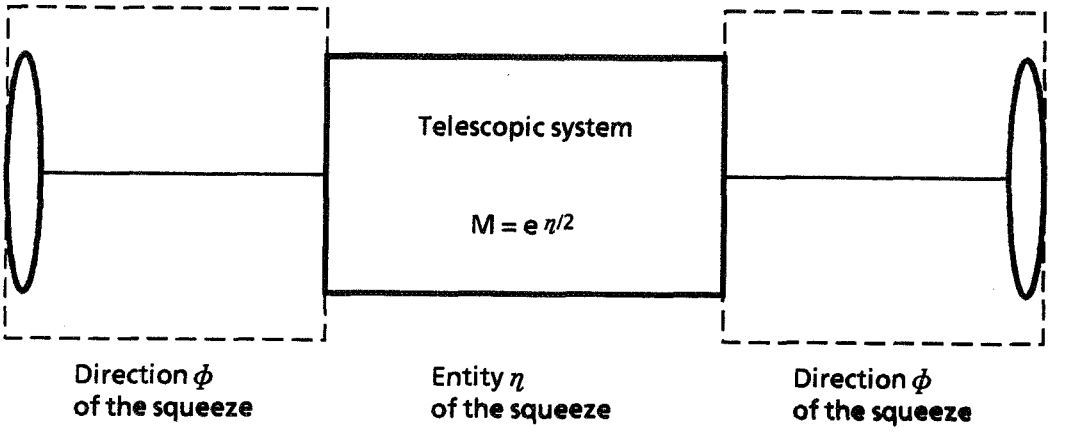


Figure 4: Optical analog of the squeeze $S(\eta, \phi)$.

is easily identified according to the transformation law (11) as producing a squeeze in the direction making an angle of 45° with the $q$–axis.

The optical analog can be realized for instance by the same sequence as before, the relevant parameters being now $M = \cosh \eta/2$, $d = \sinh \eta/2$, $f = \tanh^{-1} \eta/2$.

Finally, let us discuss the squeeze $S(\eta, \phi)$ in the direction making an angle $\phi/2$ with respect to the $q$–axis. Since it can be obtained combining rotations and squeeze along the $q$–axis, as formally expressed by the composition

$$S(\eta, \phi) = R(\phi) S(\eta, 0) R(-\phi) \ , \tag{15}$$

it is easy to get the well known matrix representation [2]

$$S(\eta, \phi) = \begin{pmatrix} \cosh \eta/2 + \cos \phi \sinh \eta/2 & \sin \phi \sinh \eta/2 \\ \sin \phi \sinh \eta/2 & \cosh \eta/2 - \cos \phi \sinh \eta/2 \end{pmatrix} . \tag{16}$$

According to the above discussion, a possible optical configuration can be realized by a telescopic system, preceded and followed by the same sequence of thin lens–drift section, symmetrically disposed. It is worth stressing that the magnification of the telescopic system is determined by the entity $\eta$ of the squeeze as the parameters of the optical system drift section–thin lens are determined by the squeeze direction $\phi$ (Fig. 4). The quantities $\eta, \phi$ are usually combined into the squeeze parameter $\zeta \equiv \eta e^{i\phi}$, so that $\eta$ and $\phi$ can be regarded as the modulus and the phase of the squeeze parameter $\zeta$.

In conclusion, we have stated a correspondence between the linear canonical transformations in phase–space, as squeezes and rotations, and *optical systems*, which can be conceptually conceived as realizing such transformations, acting effectively on electron or light beams.

# 4 Electron–beam transport channels and Wigner angle

The correspondence between linear canonical transformations and Lorentz transformations has been already recognized [2]. Boosts correspond indeed to squeezes in phase–space and rotations in real space to rotations in phase–space and rotations in real space to rotations in phase–space. Similarly, as the product of two boosts along different directions is not a boost, but a boost preceded or followed by a rotation, so the product of two squeeze along different directions does not result into a single squeeze, but into a squeeze and a rotation. It can be verified that

$$S(\lambda,\phi)S(\eta,0) = S(\xi,\theta)R(\omega)\ . \tag{17}$$

The parameters $\xi,\theta$, specifying the entity and the direction of the resulting squeeze, and the angle $\omega$, referred to as the Wigner angle, are determined by $\lambda,\phi,\eta$ according to the well–known formulae:

$$\begin{aligned}
\cosh\xi &= \cosh\eta\cosh\lambda + \cos\phi\sinh\lambda\sinh\eta\ , \\
\tan\theta &= \frac{\sin\phi[\sinh\lambda + \cos\phi\tanh\eta(\cosh\lambda-1)]}{\cos\phi\sinh\lambda + \tanh\eta[1+\cos^2\phi(\cosh\lambda-1)]}\ , \\
\tan\frac{\omega}{2} &= \frac{\sin\theta\sinh\frac{\eta}{2}\sinh\frac{\lambda}{2}}{\cosh\frac{\lambda}{2}\cosh\frac{\eta}{2} + \cos\phi\sinh\frac{\lambda}{2}\sinh\frac{\eta}{2}}\ .
\end{aligned} \tag{18}$$

Within the context of the optical analogy, developed in the previous section, the above relations can be recast in terms of the parameters of the optical systems corresponding to $S(\lambda,\phi)$ and $S(\eta,0)$, according to

$$\begin{aligned}
\cosh\xi &= \frac{1}{4M_\eta^2M_\lambda^2}\left\{(M_\eta^4+1)(M_\lambda^4+1) + \left(1-\frac{2d}{f}\right)(M_\eta^4-1)(M_\lambda^4-1)\right\}\ , \\
\tan 2\theta &= 2d\frac{(M_\lambda^4-1)(M_\eta^4+1) - \left(1-\frac{2d}{f}\right)(M_\eta^4-1)(M_\lambda^2-1)^2}{(M_\lambda^4-1)(M_\eta^4+1)\left(1-\frac{2d}{f}\right) + (M_\eta^4-1)\left[2M_\lambda^2 + \left(1-\frac{2d}{f}\right)(M_\lambda^2-1)^2\right]}\ , \\
\tan\frac{\omega}{2} &= 2d\frac{(M_\eta^2-1)(M_\lambda^2-1)}{(M_\eta^2+1)(M_\lambda^2+1) + \left(1-\frac{2d}{f}\right)(M_\eta^2-1)(M_\lambda^2-1)}\ ,
\end{aligned} \tag{19}$$

where $M_\eta$ specifies the magnification of the optical system $S(\eta,0)$, whilst $M_\lambda, d$ and $f$ denote the parameters of the system $S(\lambda,\phi)$ according to the scheme of Fig. 4.

Accordingly, one can design an appropriate sequence of quadrupoles and drift sections to perform the transformation represented by the product of three squeeze:

$$S(-\xi,\theta)S(\lambda,\phi)S(\eta,0)\ , \tag{20}$$

with $\xi,\theta$ given according to (19).

As stated in (17), such a transformation does not leave unchanged the Twiss parameters of the beam, which indeed change as in a rotation of the angle $\omega/2$. Explicitly,

$$\begin{aligned}
\alpha_2 &= \alpha_1 - \frac{1}{2}(\beta_1-\gamma_1)\sin\omega\ , \\
\beta_2 &= \alpha_1\sin\omega + \beta_1\cos^2\frac{\omega}{2} + \gamma_1\sin^2\frac{\omega}{2}\ , \\
\gamma_2 &= -\alpha_1\sin\omega + \beta_1\sin^2\frac{\omega}{2} + \gamma_1\cos^2\frac{\omega}{2}\ .
\end{aligned} \tag{21}$$

It is evident that if $\alpha_1 = 0$ and $\gamma_1 = \beta_1 = 1$, that is depicted in phase–space by a circle of unitary radius, the rotation does not have any effect, since $\alpha_2 = 0$ and $\gamma_2 = \beta_2 = 1$ as well. As a consequence, a beam having different variance in the $q$ and $p$ directions should be used; in other words, sharing the language of quantum optics, a *squeezed* beam should be used to produce a rotation of the beam ellipse.

In that case, indeed, the initial ellipse will rotate in the phase–space just by the angle $\omega/2$. Measuring then the Twiss parameters of the electron beam before and after being acted by the optical system, performing the transformation (20), it is possible to infer the Wigner angle, $\omega$, for which the following link with the Twiss parameters can be deduced:

$$\tan\omega = 2\frac{\alpha_2(\beta_1 - \gamma_1) - \alpha_1(\beta_2 - \gamma_2)}{(\beta_2 - \gamma_2)(\beta_1 - \gamma_1) + 2\alpha_1\alpha_2} \,. \tag{22}$$

# 5 Concluding remarks

The consideration developed in the previous sections are basically grounded on the algebraic analogy between the $SO(2,1)$ Lorentz group and the symplectic group $Sp(2)$, which is basic to the Hamiltonian dynamics. Exploiting this analogy, it is possible to conceive and design an optical system for electron beams, which allows to get a measure of the Wigner angle by detecting the variations occurred in the electron–beam Twiss parameters as a result of the motion through the magnetic channel. In this connection, the two–slits method [11] may offer an appropriate tool to visualize the rotation of the beam ellipse and thus to measure the Wigner angle. However, the measure is strongly limited by space–charge effects and transverse coupling, induced by sextupolar contributions to the quadrupole magnetic field.

The discussion has been put forward in full generality comprehending also light beams, whose paraxial propagation through optical systems is governed by the symplectic symmetry as well. An experiment using light beams can be conceptually conceived, but its realization is rather difficult, since the measure of the corresponding Twiss parameters, which in the specifically optical context, can be understood as linked to the beam spot–size and divergence, is limited by diffraction effects.

In conclusion, let us stress the relevance of the above results, according to which an analog computer for the Lorentz group can be recognized within the purely classical context of electron beam transport or optical ray propagation.

# References


[1] Y.S. Kim and M.E. Noz, *Theory and Applications of the Poincarè Group*, (Reidel, Dordrecht, 1986); F.R. Halpern, *Special Relativity and Quantum Mechanics*, (Prentice–Hall, Inc., Englewood Cliffs, N.J., 1968).

[2] D. Han, Y.S. Kim and M.E. Noz, *Phys. Rev.* **A37**, 807 (1988); D. Han, Y.S. Kim and M.E. Noz, *Phys. Rev.* **A40**, 902 (1989); D. Han, Y.S. Kim and M.E. Noz, *Phys. Rev.* **A41**, 6233 (1990); Y.S. Kim and M.E. Noz, *Phase Space Picture of Quantum Mechanics*, (World Publ., Co., Singapore 1991).

[3] D. Han, E.E. Hardekopf and Y.S. Kim, *Phys. Rev.* **A39**, 1269 (1989).

[4] P.K. Aravind, *Phys. Rev.* **A42**, 4077 (1990).

[5] F. Ciocci, G. Dattoli, C. Mari and A. Torre, *Phys. Rev.* **A46**, 5149 (1992).

[6] Y.S. Kim and M.E. Noz, *Am. J. Phys.* **51**, 368 (1983).

[7] V. Guillemin and S. Sternberg, *Symplectic Techniques in Physics* (Cambridge University Press, Cambridge, 1984).

[8] G. Dattoli and A. Torre, "A general view to Lie Algebraic Methods in Applied Mathematics, Optics and Transport Systems for Charged Beam Accelerators", in *Dynamical Symmetries and Chaotic Behaviour in Physical Systems* (World Publ. Co., Singapore, 1991).

[9] H.R. Lewis Jr., *Phys. Rev. Lett.* **18**, 510 (1967); H.R. Lewis Jr., *J. Math. Phys.* **9**, 1976 (1968); H.R. Lewis Jr. and W.B. Reisenfeld, *J. Math. Phys.* **10**, 1458 (1969).

[10] E.D. Courant and H.S. Snyder, *Ann. Phys.* **3**, 1 (1958).

[11] F. Bordoni, T. Letardi and M. Placidi, *Nucl. Instr. and Meth.* **65**, 72 (1968).

# PHASE SPACE FLOW OF PARTICLES IN SQUEEZED STATES

Peter H. Ceperley
*Physics Department*
*George Mason University, Fairfax, VA 22030*

**Abstract**

**The manipulation of noise and uncertainty in squeezed states is governed by the wave nature of the quantum mechanical particles in these states. This paper uses a deterministic model of quantum mechanics in which *real* guiding waves control the flow of localized particles. This model will be used to examine the phase space flow of particles in typical squeezed states.**

## 1 Introduction

The study of squeezed states and uncertainties is exciting. It is exciting because of its potential applications to low-noise instrumentation and communication. It is exciting because it represents a new frontier of physics, giving us new understanding of quantum mechanics. However I hear again and again that the end of many new experiments is to verify quantum mechanics. Should it really be so exciting to re-verify quantum mechanics for the ten thousandth and first time if we are so sure that the present ideas of quantum mechanics are indeed correct. Or perhaps we are still haunted by the ghosts of de Broglie and Einstein and their insistence that quantum mechanics be deterministically based. The non-verbalized and forbidden question seems to be "Is it possible to construct a localizable, deterministic model that is consistent with the observations that quantum mechanics explains so well?" And in spite of the repeated claims by physicists that they are ardent non-determinists, their pursuits seems to be strongly focused at finding a weakness in quantum mechanics or at least some inkling of a microscopic, deterministic world that has been previously hidden to physics. Certainly modern quantum optics experiments have this potential.

It is not that there is anything incorrect with quantum mechanics. It is just that it is a statistical theory and there are many situations and many applications in which it would be very useful to have a deterministic, single particle theory also. At any rate, it would seem that this workshop would be incomplete without at least one person reiterating the challenge of de Broglie and Einstein. In this vein, I will present one possible deterministic model for quantum mechanics, and then go on to relate this model to squeezed states and uncertainties. Phase diagrams will be included.

## 2 The Model

To begin with, this model assumes that particles have real, and localizable, continuous, existence. This is consistent with the feelings of many, if not most, physicists. However, the model also

assumes, contrary to popular belief, that the waves of quantum mechanics are also *real.* After a century of discussing wave-like phenomena, perhaps the physics community might allow the possible existence of some *real* waves. I assume that a source that emits particles, also emits waves in rough proportion to the wave intensity, and anything that absorbs particles also absorbs the waves in proportion. The model also assumes that the waves entrap the ensemble (or phase space of) emitted particles and force them to flow along with the wave energy, such that a setup that splits the waves will also split the particles in rough (or statistical) proportion to the split of wave energy, thereby insuring that the particle density stays proportional to $\psi^2$. In a sense, the particles are nearly massless specks, carried at will by the flow of waves. All large-scale dynamics are controlled by the waves. What is there left for the particles to do? Without them, the wave fields would pass through each other. The particles represent small local, non-linear mixing sites that allow wave fields to interact with each other for the processes of scattering, transitions, absorption, emission, and detection. Thus in this model[1] propagation is determined by the waves while interactions are determined by the particles. This model is similar to models by de Broglie[2], Bohm[3], Einstein[4], and others, although it is generally more specific and physical than the previous models.

What about a wave equation? I find the easiest wave equation to work with is the Klein-Gordon Equation:

$$-\hbar^2 \frac{\partial^2 \psi}{\partial t^2} = -\hbar^2 c^2 \nabla^2 \psi + m^2 c^4 \psi \tag{1}$$

which can be changed into a plasma equation:

$$\nabla^2 \psi - \frac{1}{c^2} \frac{\partial^2 \psi}{\partial t^2} - \frac{\omega_o^2}{c^2} \psi = 0 \tag{2}$$

with the substitution of:

$$m = \frac{\hbar \omega_o}{c^2} \tag{3}$$

An interpretation of this is: for each species of particle, such as electrons, space supports an associative guiding wave governed by (2) with the 'plasma' frequency given by (3). There need not be any real plasma, only a space resonance at this frequency which may be fundamentally linked to the existence of the particles themselves. Furthermore, I am not hypothesizing agreement of two independent, physical quantities in (3), the mass and the plasma frequency. In quantum mechanics there is no physical, classical mass and the mass is used only as a number in various equations. In this model also there is no physical mass associated with the classical mass numbers, but instead the physics is tied up in the 'plasma frequencies'.

One can hypothesize an interaction potential between the waves and particles, and generate the phase space orbits shown in Fig. 1. In order that the orbits stay bound to the waves, even as the waves spread out and decline in amplitude, it is necessary to assume that the microscopic mass of the particles be in proportion to the waves. This can be rationalized[1] as a mass due to the energy content of a local resonance centered about the particle. Fig. 1a shows phase space orbits for particles trapped in a standing wave field. Fig. 1b shows similar orbits for traveling waves hitting a finite height barrier. Evanescent waves partially penetrate the barrier, causing some particle orbits to be carried into the barrier, while a fraction of these waves and particles tunnel completely through the barrier.

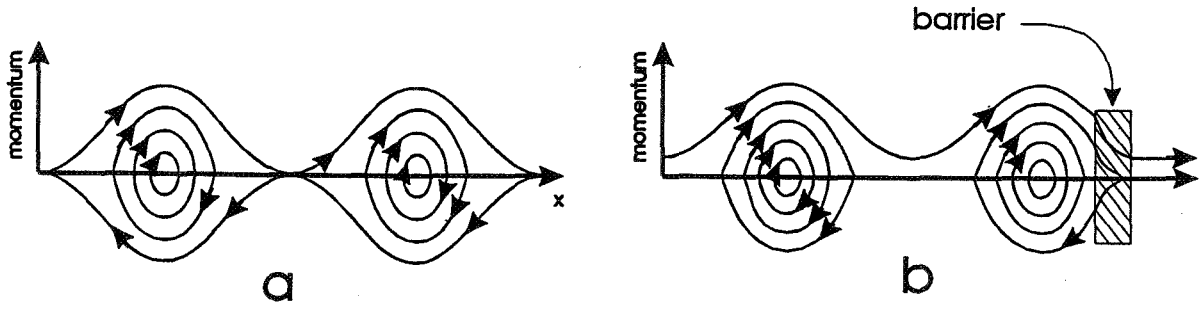


FIG. 1. Phase space orbits for particles captured in a) standing wave fields, and b) a tunneling situation. On the vertical axis is plotted the microscopic momentum of the particles which is very different from the macroscopic, observable momentum.

Just to mention a few more details of this model from Ref.1: mixing equations show that during interactions, frequency sums and vectorial wave number sums are conserved and form the basis for macroscopic energy and momentum conservation. Microscopic energy and momentum, are not so useful since the waves and the associated microscopic energy tend to spread out while propagating. The spread out remnant wave energy creates the vacuum fields, as well as being redeposited around particles, i.e. in populated states.

# 3 Uncertainties

The Heisenberg uncertainty principle states that;

$$\Delta x \, \Delta p \geq \hbar \, . \tag{4}$$

However, since in this model, waves control particle motion, in order to localize a particle or group of particles, we need to first localize the entrapping *wave*. The correct uncertainty relation for localizing waves is given by:

$$\Delta x \, \Delta k \geq 2\pi \, , \tag{5}$$

where $\delta k$ is the spread in wave number. Just as quantum mechanics operationally does, this model replaces macroscopic momentum with wave number. Similarly, the related uncertainty:

$$\Delta t \, \Delta E \geq \hbar \, , \tag{6}$$

can be visualized as in Fig. 2, where a traveling wave pulse is entrapping particle orbits to itself. Suppose there is a detector at some point to the right that the pulse will impinge on and that we are discussing the $\delta t$ in the time spread of the detected particles. In order to narrow the time spread of particles, we must narrow the time duration the *wave* pulse will be at the detector and this requires use of the relationship:

$$\Delta t \, \Delta \omega \geq 2\pi \, . \tag{7}$$

This is again like conventional quantum mechanics (at least operationally): in this case replacing energy with a frequency. So we see that the Heisenberg uncertainty relations fall out very naturally from this model.

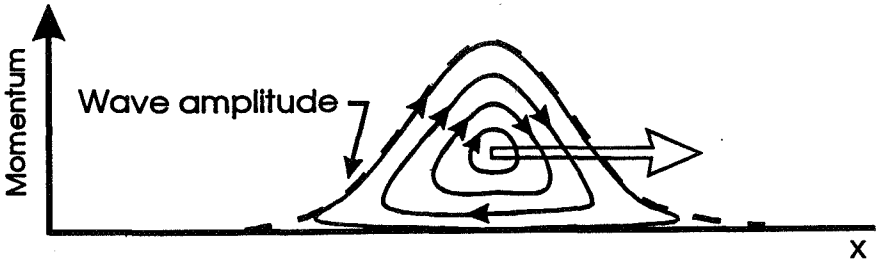


FIG. 2. Sketch of phase space of particles trapped in a traveling wave pulse.

# 4 Squeezed States: Amplitude and Phase

One of the most common squeezing operations involves reducing the amplitude fluctuations in a beam of particles. Fig. 3 shows a hypothetical micro-phase space of a beam. Here we assume a perfectly level traveling wave field (of completely well defined amplitude and phase) and illustrate the statistical distribution of particles that might be filling this wave field. The particles are randomly placed with respect to position and microscopic phase, and move horizontally to the right (on unplotted) orbits on the plot. The irregular line plots the fluctuating density of these particles as a function of position, which 'squeezing' is often called on to smooth out. If we selectively amplify or attenuate certain parts of the beam to level the density of particles, two undesirable things will also occur. First, we will not (in most cases we cannot) also homogenize the beam in the microscopic momentum coordinate. This will adversely effect certain other measurements, such as phase as we shall shortly see. Secondly, any attenuation or amplification process that changes particle density necessarily also attenuates or amplifies the associated wave. If the wave started out perfect, it will be degraded by this process.

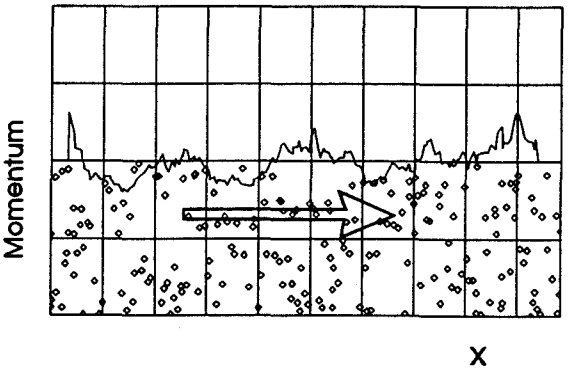


FIG. 3. Hypothetical micro-phase space of a beam of particle entrapped by a uniform traveling wave field.

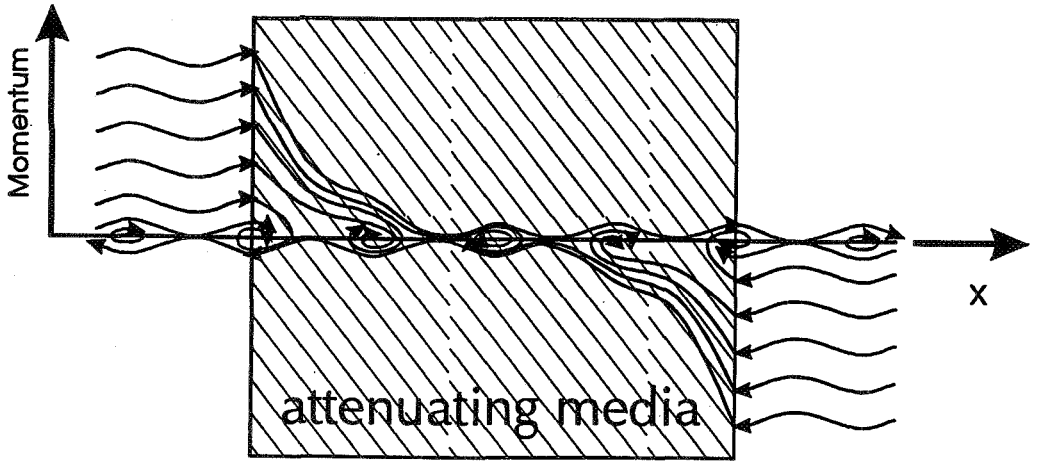


FIG. 4. Elemental phase detector showing mapping of various regions of phase space of the incoming beams into different parts of the interference pattern.

Figure 4 shows an elemental or simplistic phase detector. It involves injecting two signals into opposite ends of an attenuating medium and looking for spacial interference in the middle. A moving detector would be used to map out the particle density as a function of position to determine the relative phase of the two beams. Changing the relative phase of the two signals will move the interference maxima. This scheme was chosen because, unlike most other schemes, all particle paths are along a single line, i.e. in one dimension. This frees the other dimension for plotting microscopic momentum and greatly simplifies our phase space plotting. The interesting feature of the plot is that the phase space orbits map different microscopic momentum regions of the incoming signals into different interference maxima. In the figure here, only the uppermost momentum particles make it into the central, most useful maximum. This illustrates that inhomogeneities in the particle density in the momentum direction will adversely effect the interference pattern and thus the phase. Irregularities in the waves themselves will also have a similar adverse effect.

# 5 Postscript: Modern Non-local Experiments

Dr. Shimony raised the question about recent non-locality experiments being in conflict with the model presented here. My answer was that the experiments I had examined carefully[5] are in fact not inconsistent with this model. I wish to expand on that here. For example, the Franson experiment can be explained deterministically[6][7]. Even with delayed choice experiments where beams are changed after they become separated from each other, a change in the beam will affect both the particles in that beam and the waves around the particles. Since the waves determine the dynamics, it is not surprising that we get wave-like behavior in going through subsequent filters, beam splitters, and polarizers.

Surprisingly, the hardest experiments to reconcile with this model are photon cancellation experiments[8]. However even for this there is a possible classical explanation [5]: the IF filters,

which most quantum optics experiments use, are resonators and as such selectively accept and reject photons. The math of the time correlation of this classical acceptance and rejection process has an uncanny resemblance to the math of entangled states. In a nutshell, when a Mach-Zehnder interferometer is balanced so as to prevent coincident detection through its outputs, the wave fields (of this model, as well as those of normal quantum mechanics) are phased so as to load up only one IF filter at a time, thereby preventing the passage photons through the IF filters of both detectors simultaneously. The conclusion is that these experiments are not conclusive proof of non-locality, particularly if one has a local model, such as the one presented here, where the particles are entrapped by and guided by waves.

These effects of IF filters also should be considered with reference to the Franson and the delayed choice type experiments discussed above to give mathematically correct agreement between this model and experiments. We shall all look forward to the day when the quantum optics experiments are done with no IF filters after the down conversion process. Also, detection of practically all photons entering the experimental apparatus is essential if one wishes to analyze the system one-dimensionally (with branches). This requires large (no lost beam due to collimation or finite detectors, etc), high-efficiency detectors with large angular acceptance. Like good accountants, we need to see where everything is going.

# References


[1] P. H. Ceperley, Annales de la Foundation Louis de Broglie **18**, 197 (1993).

[2] Louis de Broglie, *Non-Linear Wave Mechanics, A Causal Interpretation*, (Elsevier Publishing Co., Amsterdam, 1960).

[3] D. Bohm, Phys. Rev. **85** 166 (1952).

[4] Einstein, Podolsky, and Rosen, Phys. Rev. **47**, 777 (1933).

[5] P. H. Ceperley, Bull. Am. Phys. Soc., **38** No. 2, 1004 (1993).

[6] J. D. Franson, "Quantum Phase Uncertainties and the Classical Limit", Third International Workshop on Squeezed States and Uncertainity Relations, 1993.

[7] P. G. Kwiat, W. A. Vareka, C. K. Hong, H. Nathel, and R. Y. Chiao, Phys. Rev. A **41**, 2910 (1990).

[8] C. K. Hong, Z. Y. Ou, and L. Mandel, Phys. Rev. Lett. **59**, 2044 (1987).

# MULTIVARIABLE HERMITE POLYNOMIALS AND PHASE–SPACE DYNAMICS

G. Dattoli, A. Torre
*ENEA, Dip. INN., Settore Elettroottica e Laser,*
*CRE Frascati, C.P. 65 - 00044 Frascati, Rome, Italy*

S. Lorenzutta, G. Maino
*ENEA, INN.SVIL Divisione Calcolo, Bologna, Italy*

C. Chiccoli
*INFN, Sezione di Bologna and CNAF, Bologna, Italy*

**Abstract**

The phase–space approach to classical and quantum systems demands for advanced analytical tools. Such an approach characterizes the evolution of a physical system through a set of variables, reducing to the canonically conjugate variables in the classical limit. It often happens that phase–space distributions can be written in terms of quadratic forms involving the above quoted variables. A significant analytical tool to treat these problems may come from the generalized many–variables Hermite polynomials, defined on quadratic forms in $\mathcal{R}^n$. They form an orthonormal system in many dimensions and seem the natural tool to treat the harmonic oscillator dynamics in phase–space. In this contribution we discuss the properties of these polynomials and present some applications to physical problems.

# 1 Introduction

Classical special functions play a central role in both pure and applied mathematics. Usually conceived for the solution of very specific problems, they gave rise to a far–reaching theory, being part of, and frequently motivation for, important general theories.

The trigonometric functions, for instance, originally introduced to deal with specific problems of astronomy and navigation, are the basis for the theory of Fourier series and Fourier integral, which have applications to many parts of physics.

Similarly, Bessel functions firstly appeared in mathematical physics in the 1738 Bernoulli's memoir, containing enunciations of theorems on the oscillations of heavy chains. Then, they reappeared in mechanical problems as the vibration of a stretched membrane or the symmetrical and unsymmetrical propagation of heat in solid cylinders and spheres, as well as in astronomical problems, related for instance to the elliptic motion of a planet about the sun. Presently, Bessel functions have a very wide field of applications, from abstract number theory and theoretical astronomy to concrete problems of physics and engineering [1].

Correspondingly, classical orthogonal polynomials (Jacobi, Legendre, Hermite), also introduced in connection with astronomical problems, are now of great importance in mathematical physics, approximation theory as well as in the theory of mechanical quadrature. In addition, they find significant applications in quantum mechanics on the determination of discrete energy spectra and the corresponding wave functions in fundamental problems [2]. Orthogonal polynomials are indeed essential tool to deal with the problems of the harmonic oscillator and the motion of particles in a central field. Furthermore, the classical orthogonal polynomials of a discrete variable are of interest in the theory of difference methods [2].

Theory of classical special functions is rather well settled [3]. Recursion relations, addition theorems, integral representations, generating functions, asymptotic formulae, differential equations are collected in an organic body, which is however continuously refined and enriched by new investigations and new theoretical approaches [4].

Let us recall for instance the method illustrated in ref. [1], which suggests a generalization of the Rodriguez formula for the classical orthogonal polynomials, thus allowing to obtain explicit integral representations of all the special functions and to derive their basic properties. Similarly, the possibility of framing special functions within the context of group theory [4, 5] revealed a powerful tool permitting derivation of new results and a rational classification of old results, as well as suggesting to introduce new classes of functions, related to the recently discovered algebraic systems, such as the supergroups and the quantum groups [6].

Furthermore, we note the description of orthogonal polynomials by their recursion relations, which once regarded as eigenvalue equations allow to look at orthogonal polynomials from the viewpoint of scattering theory [4, 7].

Recently, interest in special functions has greatly increased in connection with the possibility of *generalizing* the well known functions of mathematical physics to more than one variable and/or more than one index. In this regard, the generalization amounts to introducing functions with properties analogous to those of the one–variable counterpart. Generating functions are usually the key–note for many–variable generalizations of special functions.

The multivariable Bessel functions, for instance, originally introduced by Appell [8] in connection with the problem of the elliptic motion of planets [9], have revealed a wealth of possible applications to physical and/or purely mathematical problems, as the scattering of laser radiation by free or weakly bounded electrons, the emission of e.m. radiation by relativistic electrons passing through magnetic undulators [10] as well as problems related to the queuing theory [11]. Also, they proved their relevance in multiphoton emission and absorption processes by quantum systems, which are of interest for the investigation of squeezed states, the relevant Hamiltonian operator containing indeed powers of the annihilation and creation operators [12].

Correspondingly, the multivariable generalization of orthogonal polynomials has attracted a great amount of interest. In particular, as to the Hermite polynomials, let us recall that in ref. [13] a procedure has been developed, which generalizing that proposed by Gould and Hopper [14] allows to define multivariable generalized Hermite polynomials, providing a complete orthonormal set in $\mathcal{L}_2(R^n)$ space of square sommable functions with $n$ variables.

The present paper concerns with the classical many–variable functions introduced by Hermite [15], whose application within the context of the phase space approach to physical problems is suggested. Accordingly, in Sec. 2 a general view on the many–variable Hermite polynomials is presented. The possibility of exploiting the developed formalism within the context of the phase

space picture, which is becoming the context where many physical problems are naturally framed, is investigated in Sec. 3. In particular, the basic model of the harmonic oscillator is considered. General considerations and extensions are presented in Sec. 4.

## 2 Many–variable Hermite polynomials

One–variable Hermite polynomials $\mathcal{H}_n(x)$[1] can be defined by means of the relation

$$e^{-\frac{1}{2}(x-t)^2} = e^{-\frac{x^2}{2}} \sum_{n=0}^{\infty} \frac{t^n}{n!} \mathcal{H}_n(x) \ , \tag{1}$$

where they appear as the coefficients of the series expansion of the exponential of a quadratic form defined on the real domain.

The above expression can also be recast in the more usual form

$$e^{xt-t^2/2} = \sum_{n=0}^{\infty} \frac{t^n}{n!} \mathcal{H}_n(x) \ , \tag{2}$$

from which, exploiting the series development of the exponential function and appropriately rearranging the summation, the well known expression of the Hermite polynomials in form of a finite sum can be easily drawn:

$$\mathcal{H}_n(x) = n! \sum_{l=0}^{[n/2]} \frac{(-)^l x^{n-2l}}{l! 2^l (n-2l)!} \ , \tag{3}$$

where $[v]$ denotes the largest integer $\leq v$.

Also, according to the formula for the Taylor expansion, (2) provides the Rodriguez formula:

$$\mathcal{H}_n(x) = (-)^n e^{x^2/2} \frac{d^n}{dx^n} e^{-x^2/2} \ . \tag{4}$$

Taking the derivatives of both sides of (1) or (2) with respect to $x$ and $t$, it is easy to infer the recursion relations

$$\begin{aligned} \mathcal{H}_{n+1} &= x\mathcal{H}_n - n\mathcal{H}_{n-1} \ , \\ \mathcal{H}'_n &= n\mathcal{H}_{n-1} \ , \end{aligned} \tag{5}$$

linking the polynomial of order $n$ to the contiguous ones. The prime denotes derivative with respect to $x$.

It is immediate to get from the above relations the differential equation obeyed by $\mathcal{H}_n$'s:

$$\left( -\frac{d^2}{dx^2} + x\frac{d}{dx} \right) \mathcal{H}_n = n\mathcal{H}_n \ , \tag{6}$$

which allows to understood $\mathcal{H}_n$ as eigenfunction of the operator

$$\hat{\mathcal{D}} = -\frac{d^2}{dx^2} + x\frac{d}{dx} \ , \tag{7}$$

[1]The use of the script $\mathcal{H}_n$ to denote the Hermite polynomial is in order to avoid confusion with the more common polynomial $H_n$ : $H_n(x) = 2^{n/2}\mathcal{H}_n(\sqrt{2}x)$.

$n$ being the corresponding eigenvalue.

The operator $\hat{\mathcal{D}}$ is not self adjoint; the adjoint operator

$$\hat{\mathcal{D}}^+ = -\frac{d^2}{dx^2} - x\frac{d}{dx} - 1 \tag{8}$$

admits the eigenfunction $\mathcal{H}_n^+$, explicitly given as

$$\mathcal{H}_n^+(x) = \mathcal{H}_n(x)e^{-x^2/2} \tag{9}$$

belonging to the same eigenvalue as $\mathcal{H}_n$. Accordingly, the functions $(\mathcal{H}_n, \mathcal{H}_n^+)$ form a biorthogonal set in the usual sense that they satisfy the orthogonality relation

$$\int_{-\infty}^{\infty} \mathrm{d}x \mathcal{H}_n(x)\mathcal{H}_m(x)e^{-x^2/2} = n!\sqrt{2\pi}\delta_{nm} \ . \tag{10}$$

Generalizing the relation (1) to involve a bilinear form defined in $R^n$, Hermite introduced many–variable functions [15]. Adopting a matrix notation, we can write down

$$e^{-\frac{1}{2}(\underline{x}-\underline{h})^T \underline{\underline{M}}(\underline{x}-\underline{h})} = e^{-\frac{1}{2}\underline{x}^T \underline{\underline{M}}\underline{x}} \sum_{m_1,\ldots,m_n} \frac{h_1^{m_1}}{m_1!} \cdots \frac{h_n^{m_n}}{m_n!} \mathcal{H}_{m_1,\ldots,m_n}(\underline{x}) \ , \tag{11}$$

where $\underline{x}$ and $\underline{h}$ are elements of the vector space $R^n$:

$$\underline{x} = \begin{pmatrix} x_1 \\ \vdots \\ x_n \end{pmatrix} \ , \quad \underline{h} = \begin{pmatrix} h_1 \\ \vdots \\ h_n \end{pmatrix} \ , \tag{12}$$

the superscript $T$ meaning transpose.

Accordingly, $\underline{\underline{M}}$ is a real $n \times n$ matrix: $\underline{\underline{M}} = (a_{ij})$, $i, j = 1, \ldots, n$, which is required to be symmetric: $a_{ij} = a_{ji}$, not degenerate, i.e. $\det \underline{\underline{M}} \geq 0$ and positive definite: $a_{ii} > 0$, $i = 1, \ldots, n$.

The expression (11) can be rewritten in the alternative form

$$e^{\underline{x}^T \underline{\underline{M}}\underline{h} - \frac{1}{2}\underline{h}^T \underline{\underline{M}}\underline{h}} = \sum_{m_1,\ldots,m_n} \frac{h_1^{m_1}}{m_1!} \cdots \frac{h_n^{m_n}}{m_n!} \mathcal{H}_{m_1,\ldots,m_n}(\underline{x}) \ , \tag{13}$$

which is the $n$–variable analog of (2).

In passing, it is worth noticing that the above expression suggests considering the more general bilinear form

$$\phi(\underline{x}, \underline{h}) = \underline{x}^T \underline{\underline{A}}\,\underline{h} - \frac{1}{2}\underline{h}^T \underline{\underline{B}}\,\underline{h} \tag{14}$$

with the matrices $\underline{\underline{A}}$, $\underline{\underline{B}}$ being symmetric but in general different from each other. In this respect, let us recall that the Grassman Hermite functions have been introduced using the above quadratic form, with $\underline{\underline{A}}$ and $\underline{\underline{B}}$ being antisymmetric matrices and $\underline{x}$, $\underline{h}$ anticommuting variables. A further extension of (14) have been considered in ref. [6], with the intent of obtaining a class of functions, related to quantum groups.

In full analogy with the one–variable case, taking the derivative of (11) or (13) with respect to the components of both vectors $\underline{x}$ and $\underline{h}$, we get the recursion relations satisfied by $\mathcal{H}_{m_1,\ldots,m_n}(\underline{x})$:

$$\mathcal{H}_{m_1,\ldots,m_1+1,\ldots,m_n}(\underline{x}) = \left(\sum_{j=1}^{n} a_{ij}x_j\right)\mathcal{H}_{m_1,\ldots,m_n}(\underline{x}) - \sum_{j=1}^{n} a_{ij}m_j\mathcal{H}_{m_1,\ldots,m_j-1,\ldots,m_n}(\underline{x}) ,$$

$$\frac{\partial}{\partial x_i}\mathcal{H}_{m_1,\ldots,m_n}(\underline{x}) = \sum_{j=1}^{n} a_{ij}m_j\mathcal{H}_{m_1,\ldots,m_j-1,\ldots,m_n}(\underline{x}) , \tag{15}$$

with $i$ ranging from 1 to $n$.

Since corresponding to any quadratic form $\phi(\underline{x}) = \underline{x}^T\underline{\underline{M}}\,\underline{x}$ we can associate the adjoint form defined in terms of the inverse matrix, i.e. $\psi(\underline{\xi}) = \underline{\xi}\,\underline{\underline{M}}^{-1}\underline{\xi}$, it is possible to associate with the $\mathcal{H}_{m_1,\ldots,m_n}$'s the adjoint polynomials $\mathcal{G}_{m_1,\ldots,m_n}(\underline{x})$. The definition resembles the relation (11), but involves the transformed vectors:

$$\underline{\xi} \equiv \underline{\underline{M}}\,\underline{x} , \quad \underline{k} = \underline{\underline{M}}\,\underline{h} . \tag{16}$$

Explicitly, we have indeed

$$e^{-\frac{1}{2}(\underline{\xi}-\underline{k})^T\underline{\underline{M}}^{-1}(\underline{\xi}-\underline{k})} = e^{-\frac{1}{2}\underline{\xi}^T\underline{\underline{M}}^{-1}\underline{\xi}} \sum_{m_1,\ldots,m_n} \frac{k_1^{m_1}}{m_1!}\cdots\frac{k_n^{m_n}}{m_n!}\mathcal{G}_{m_1,\ldots,m_n}(\underline{x}) . \tag{17}$$

If $\underline{\underline{M}}$ is the identity matrix, the two polynomials coincide: $\mathcal{H}_{m_1,\ldots,m_n} = \mathcal{G}_{m_1,\ldots,m_n}$. Furthermore, they turn into the product of $n$ one–variable Hermite polynomials, i.e.

$$\mathcal{H}_{m_1,\ldots,m_n}(\underline{x}) = \prod_{i=1}^{n}\mathcal{H}_{m_i}(x_i) . \tag{18}$$

Taking the derivative of (17) with respect to $\underline{x}$ and $\underline{k}$, the following set of recursion relations can be obtained:

$$\mathcal{G}_{q_1,\ldots,q_i+1,\ldots,q_n}(\underline{x}) = x_i\mathcal{G}_{q_1,\ldots,q_n} - \frac{1}{\Delta}\sum_{j=i}^{n} A_{ij}q_j\mathcal{G}_{q_1,\ldots,q_j-1,\ldots,q_n}(\underline{x}) ,$$

$$\frac{\partial}{\partial x_i}\mathcal{G}_{q_1,\ldots,q_n}(\underline{x}) = q_i\mathcal{G}_{q_1,\ldots,q_i-1,\ldots,q_n}(\underline{x}) , \tag{19}$$

with $\Delta \equiv \det\underline{\underline{M}}$ and $A_{ij}$ the minor relevant to the element $a_{ij}$.

The relevance of the polynomials $\mathcal{G}_{q_1,\ldots,q_n}$ is clarified by the orthogonality relation, which can be proved in the form

$$\int_{R^n} \mathrm{d}\underline{x}\, e^{-\frac{1}{2}\underline{x}^T\underline{\underline{M}}\,\underline{x}}\mathcal{H}_{m_1,\ldots,m_n}(\underline{x})\mathcal{G}_{q_1,\ldots,q_n}(\underline{x}) = \frac{1}{\sqrt{\Delta}}\prod_{i=1}^{n} m_i!\sqrt{2\pi}\delta_{m_i,q_i} . \tag{20}$$

For the explicit derivation of the above relation the reader is addressed to ref. [8].

The orthogonality relation (20) can be conveniently exploited to express a given $n$–variable function $\rho(\underline{x})$ in form of a series involving $\mathcal{H}_{m_1,\ldots,m_n}$ and $\mathcal{G}_{m_1,\ldots,m_n}$. Accordingly, let us put

$$\rho(\underline{x}) = \sum_{m_1,\ldots,m_n} A_{m_1,\ldots,m_n}\mathcal{H}_{m_1,\ldots,m_n}(\underline{x}) , \tag{21}$$

or

$$\rho(\underline{x}) = \sum_{m_1,\ldots,m_n} B_{m_1,\ldots,m_n} \mathcal{G}_{m_1,\ldots,m_n}(\underline{x}) \ , \tag{22}$$

with the coefficients $A_{m_1,\ldots,m_n}$, $B_{m_1,\ldots,m_n}$ being specialized according to (20) into

$$A_{m_1,\ldots,m_n} = \frac{\sqrt{\Delta}}{(2\pi)^{n/2}} \frac{1}{m_1!} \cdots \frac{1}{m_n!} \int_{R^n} \mathrm{d}\underline{x} e^{-\frac{1}{2}\underline{x}^T \underline{\underline{M}}\, \underline{x}} \rho(\underline{x}) \mathcal{G}_{m_1,\ldots,m_n}(\underline{x}) \ ,$$

$$B_{m_1,\ldots,m_n} = \frac{\sqrt{\Delta}}{(2\pi)^{n/2}} \frac{1}{m_1!} \cdots \frac{1}{m_n!} \int_{R^n} \mathrm{d}\underline{x} e^{-\frac{1}{2}\underline{x}^T \underline{\underline{M}}\, \underline{x}} \rho(\underline{x}) \mathcal{H}_{m_1,\ldots,m_n}(\underline{x}) \ . \tag{23}$$

The explicit values of the entries of the matrix $\underline{\underline{M}}$ should be suggested by the specific problem under study.

It is needless to say that the theory of many–variable Hermite polynomials is very rich. However, the above considerations represent all the machinery we need for testing the possibility of using these functions as basis for the phase–space analysis of physical problems. For a more detailed discussion the interested reader is addressed to refs. [8, 15].

# 3 Two–variable Hermite polynomials and phase space picture of dynamical problems

Phase space picture is becoming the unifying language for both classical and quantum mechanics. Phase space formalism is indeed basic to the Hamiltonian formulation of classical mechanics. In this connection, the evolution of a dynamical system is described by a number $n$ of independent coordinate variables and on the same number of canonically conjugate momenta. The cartesian space of these $2n$ coordinates is just the *phase–space*.

Correspondingly, phase space picture of quantum mechanics is becoming increasingly popular. Although, the concept of phase–space is not compatible with quantum mechanics, $\hat{q}$ and $\hat{p}$ being noncommuting operators, the Wigner phase–space representation allows to overcome this problem, since in this representation both the coordinate and momentum variables are $c$–numbers. Accordingly, it is possible to perform phase–space canonical transformations as in the case of classical mechanics, which correspond to unitary transformations in the Schrödinger picture of quantum mechanics.

Phase space concept appears therefore as the unifying context, where classical as well as quantum mechanics can be naturally framed, thus suggesting the possibility to transfer concepts and methods from quantum to classical mechanics and viceversa.

Furthermore, as discussed in ref. [16], phase–space picture provides the natural language for quantum optics as well, offering a geometrical view to coherent and squeezed states as circles and ellipses respectively. In this connection, taking advantages from the symmetry of the relevant Wigner phase space distribution function it is possible to calculate expectation values and transition probabilities for the above quoted states [16].

Finally, let us recall that phase space is the context where the dynamics of electron beams moving through magnetic channels is studied and the Hamiltonian optics can be conveniently reformulated.

As already remarked, the paper is aimed at investigating the possibility of using the many–variable Hermite polynomials, briefly discussed in the previous section, as analytical tool in the phase–space approach to dynamical problems.

In the quantum framework, one–variable Hermite polynomials are intimately related to the harmonic oscillator dynamics. It is therefore natural to analyse, as first step for our investigation, the harmonic oscillator dynamics in the phase–space representation.

Let us consider therefore the quadratic Hamiltonian

$$H = \frac{1}{2}p^2 + \frac{1}{2}k(s)q^2 \ , \tag{24}$$

the variable $s$ playing the role of *time*. It is needless to stress the relevance of the above Hamiltonian as basic model for many physical problems as well as approximation in many of the existing theories.

As already stressed, in quantum mechanics the Hamiltonian (24) rules the evolution of a harmonic oscillator of unit mass and *time*–dependent frequency $k(s)$, $\hat{q}$ and $\hat{p}$ being the position and momentum operators. In classical mechanics, it describes for instance the betatron motion of a charged particle through a magnetic quadrupole, as in the ray optics it governs the propagation of an optical ray through a nonhomogeneous medium with a quadratic profile of the refractive index.

It is interesting to notice that in the configuration space picture the evolution of the system described by the Hamiltonian (24) is analysed within the context of conceptually and formally different approaches: the Schrödinger equation for the quantum wave function and the Hamilton equation of motion for the canonically conjugate variables $q$ and $p$. Conversely, the Von Neumann equation for the Wigner distribution function and the classical Liouville equation for the phase–space distribution are of the same form, so long as the Hamiltonian of the quantum system is quadratic. Hence, time evolution of the Wigner function can be obtained directly from the solution of the equation of motion of the corresponding classical system. Harmonic oscillator provides a unique example in which classical and quantum phenomenology overlap to a large extent.

Let us approach the problem within the context of classical mechanics. Accordingly, the Liouville equation for the phase space distribution function $\rho(q,p;s)$ is immediately written down as

$$\frac{\partial}{\partial s}\rho(q,p;s) = \left\{-p\frac{\partial}{\partial q} + k(s)q\frac{\partial}{\partial p}\right\}\rho(q,p;s) \ , \tag{25}$$

with an assigned initial condition: $\rho(q,p;s) = \rho_0(q,p)$.

As introduction to the forthcoming discussion, let us recall that an invariant quadratic form

$$I = \underline{x}^T \underline{\underline{T}}(s)\underline{x} \tag{26}$$

can be associated to any dynamics described by quadratic Hamiltonians in canonical coordinates and momenta. In passing, it is worth stressing that within a quantum context the quadratic form (26) is reported as the Ermakov–Lewis invariant [17], the vector $\underline{x}$ containing obviously the position and momentum operators, whilst in classical mechanics it is reported as the Courant–Snyder invariant [18], firstly introduced in the analysis of electron beam motion through magnetic channels. In the above expression, the two component vector $\underline{x} \equiv \begin{pmatrix} q \\ p \end{pmatrix}$ is acted by the real $2 \times 2$

matrix $\underline{\underline{T}}$, which furthermore is required to be symmetric and unimodular: $\det \underline{\underline{T}} = 1$. Just to share the language of accelerator physics, we refer to $\underline{\underline{T}}$ as the *Twiss* matrix[2] and report it in the form

$$\underline{\underline{T}} = \begin{pmatrix} \gamma & \alpha \\ \alpha & \beta \end{pmatrix} . \tag{27}$$

The entries $\alpha, \beta, \gamma$, usually named as *Twiss* parameters, play an important role in designing transport channels.

The quadratic form (26) can be depicted in the phase space as an ellipse, whose size and orientation are determined by the Twiss coefficients. The area of the ellipse, which is just the value of the invariant $I$, is usually denoted in accelerator physics as $I = \pi\varepsilon$, $\varepsilon$ being named as the *beam emittance*. It plays a crucial role in characterizing the quality and the dynamics of the $e$–beam. In a single particle analysis, $\alpha, \beta, \gamma$ defines the contour of the particle trajectory, as in an ensemble analysis they define the second order momentum of the phase space distribution function, thus providing information on its extent and maximum localization. Explicitly,

$$\begin{aligned} \varepsilon\gamma &= \sigma_{pp}^2 = \langle p^2 \rangle - \langle p \rangle^2 , \\ \varepsilon\beta &= \sigma_{qq}^2 = \langle q^2 \rangle - \langle q \rangle^2 , \\ \varepsilon\alpha &= -\sigma_{qp}^2 = -(\langle qp \rangle - \langle q \rangle \langle p \rangle) , \end{aligned} \tag{28}$$

the averages being understood on the distribution function. Accordingly, the emittance $\varepsilon$ can be given the further meaning:

$$\varepsilon^2 = \sigma_{qq}^2 \sigma_{pp}^2 - \sigma_{qp}^2 . \tag{29}$$

Let us stress now that the Liouville equation admits as particular solution the distribution function

$$\rho(q, p; s) = \frac{1}{2\pi\varepsilon} \exp\left\{ -\frac{1}{2\varepsilon} \underline{x}^T \underline{\underline{T}} \underline{x} \right\} , \tag{30}$$

shaped indeed in form of a Gaussian and therefore with a maximum localization within the ellipse of area $\varepsilon$.

The above considerations suggest to use the functions $\mathcal{H}_{m,n} e^{-\frac{1}{2\varepsilon} \underline{x}^T \underline{\underline{T}} \underline{x}}$ as basis in the phase–plane, the entries of the matrix $\underline{\underline{T}}$ being chosen as the second order momentum of the distribution. In other words we can use the above quoted functions to approximate a generic function defined in the phase space by means of two–variable Gaussians, further modelled by the Hermite polynomials $\mathcal{H}_{m,n}$, which give a different maximum localization. The process is perfectly similar to that used for one–variable functions using the Hermite functions.

Let us consider therefore generic distribution function $\rho(q, p; s)$. According to the results of Sec. 2, we can express $\rho(q, p; s)$ in form of a series:

$$\rho(q, p; s) = \sum_{m,n} a_{m,n}(s) \rho_{m,n}^H(q, p) , \tag{31}$$

[2]The quadratic form (26) can also been regarded as the transcription in phase space of the quantum invariant, the vector $\underline{x}$ being formed by the expectation values of the position and momentum operators and the matrix $\underline{\underline{T}}$ being linked to the *covariance* matrix.

with $a_{m,n}(s)$ and $\rho^H_{m,n}(q,p)$ being explicitly given as

$$a_{m,n}(s) = \int \mathrm{d}q \int \mathrm{d}p \rho(q,p;s) \mathcal{G}_{m,n}(q,p) \ ,$$
$$\rho^H_{m,n}(q,p) = \frac{1}{2\pi\varepsilon m!n!} \mathcal{H}_{m,n}(q,p) e^{-\frac{1}{2\varepsilon}\underline{x}^T \underline{\underline{T}}\, \underline{x}} \ . \tag{32}$$

The superscript $H$ specifies that the polynomials $\mathcal{H}_{m,n}$ have been used in the series expansion.

The alternative expansion in terms of the adjoint polynomials $\mathcal{G}_{m,n}(q,p)$ can be also used, thus leading to

$$\rho(q,p;s) = \sum_{m,n} b_{m,n} \rho^G_{m,n}(q,p) \ , \tag{33}$$

with

$$b_{m,n}(s) = \int \mathrm{d}q \int \mathrm{d}p \rho(q,p;s) \mathcal{H}_{m,n}(q,p) \ ,$$
$$\rho^G_{m,n}(q,p) = \frac{1}{2\pi\varepsilon m!n!} \mathcal{G}_{m,n}(q,p) e^{-\frac{1}{2\varepsilon}\underline{x}^T \underline{\underline{T}}\, \underline{x}} \ , \tag{34}$$

and the superscript $G$ specifying that the adjoint polynomials $\mathcal{G}_{m,n}$ have been used.

The entries of the *Twiss* matrix appearing in the above expression can be conveniently chosen, according to the previous discussion, as the second–order momenta of the distribution function $\rho_0(q,p)$ at the initial *time*. Then, the *emittance* $\varepsilon$ is just obtained according to (29).

Inserting the expression (31) into the Liouville equation (25), we get the set of equations for the coefficients $a_{m,n}(s)$, namely

$$\begin{aligned} \frac{d}{ds} a_{m,n} &= (\sigma^2_{pp} - k\sigma^2_{qq}) mn a_{m-1,n-1} + \sigma_{qp}[m(m-1)a_{m-2,n} - kn(n-1)a_{m,n-2}] \\ &+ m a_{m-1,n+1} - kn a_{m+1,n-1} \ , \end{aligned} \tag{35}$$

where the relations

$$\frac{\partial}{\partial q} \rho^H_{m,n} = -(m+1)\rho^H_{m+1,n} \ , \quad \frac{\partial}{\partial p} \rho^H_{m,n} = -(n+1)\rho^H_{m,n+1} \tag{36}$$

and

$$\begin{aligned} p\rho^H_{m,n} &= \rho^H_{m,n-1} + \sigma_{qp}(m+1)\rho^H_{m+1,n} + \sigma^2_{qq}(n+1)\rho^H_{m,n+1} \ , \\ q\rho^H_{m,n} &= \rho^H_{m-1,n} + \sigma^2_{pp}(m+1)\rho^H_{m+1,n} + \sigma^2_{qp}(n+1)\rho^H_{m,n+1} \end{aligned} \tag{37}$$

have been used, obtained from the recursive relations obeyed by $\mathcal{H}_{m,n}$ (see Appendix A).

Let us consider for instance the particular case where the quadrupole strength does not change along the direction of motion: $k(s) = k$, and the initial distribution function $\rho_0(q,p)$ has the form

$$\rho_0(q,p) = \frac{1}{2\pi\varepsilon} \exp\left\{ -\frac{1}{2\varepsilon} \underline{x}^T \underline{\underline{T}}\, \underline{x} \right\} \ . \tag{38}$$

The coefficients $a_{m,n}(0)$ are then given as

$$a_{m,n}(0) = \delta_{m,0}\delta_{n,0} \ . \tag{39}$$

In addition, assuming that the electron beam is matched to the quadrupole, namely

$$\sigma_{qp} = 0 \ , \quad \sigma_{pp}^2 - k\sigma_{qq}^2 = 0 \ , \tag{40}$$

it is easy to prove that the distribution function does not change during the motion:

$$\rho(q,p;s) = \rho_0(q,p) \ . \tag{41}$$

More general situations require the numerical handling of eq. (35), from which the evolution of $\rho(q,p;s)$ can be inferred according to the expansion (31).

# 4 Concluding remarks

The analysis developed in the previous sections has been aimed at testing the possibility of using many–variable Hermite polynomials as analytical tool, within the context of phase–space picture to dynamical problems.

The discussion has been limited, for illustrative purposes, to the harmonic oscillator dynamics. However, it can be easily realized that Hamiltonians containing higher order terms, accounting for non linear forces, can be treated by means of the same formalism as well.

Also, within a quantum mechanical context, the formalism developed might be used in connection with the Von Neumann equation, which, as already noticed, rules the evolution of the Wigner distribution function $W(q,p;s)$ according to [19]

$$\frac{\partial}{\partial s}W(q,p;s) = \left\{-p\frac{\partial}{\partial q} + \frac{1}{i\hbar}\left[V\left(q + \frac{1}{2}i\hbar\frac{\partial}{\partial p}\right) - V\left(q - \frac{1}{2}i\hbar\frac{\partial}{\partial p}\right)\right]\right\} W(q,p;s) \ . \tag{42}$$

Furthermore, let us say that, although in Sec. 3 we have considered 1–dimensional dynamics, problems with more than one degree of freedom can be analysed, as, for instance, the motion of electron–beams along magnetic channels with transverse coupling. In that case, the radial and vertical motions cannot be separated and the dynamics should be analysed in a 4–dimensional phase–space, the relevant elements consisting of the conjugate variables $x, p_x, y, p_y$.

## APPENDIX A
# Two–variable Hermite polynomials

This Appendix is devoted to discuss with some details the properties of the two–variable Hermite polynomials, which are used in Sec. 3 as illustrative of the usefulness of such functions within the context of the phase–space formalism.

Firstly, let us write down the explicit form of the recursion relations, reported in (15) for the general case of many–variable polynomials:

$$\begin{aligned}
&\mathcal{H}_{m+1,n}(q,p) = (aq+bp)\mathcal{H}_{m,n}(q,p) - am\mathcal{H}_{m-1,n}(q,p) - bn\mathcal{H}_{m,n-1}(q,p) \ , \\
&\mathcal{H}_{m,n+1}(q,p) = (bq+cp)\mathcal{H}_{m,n}(q,p) - bm\mathcal{H}_{m-1,n}(q,p) - cn\mathcal{H}_{m,n-1}(q,p) \ , \qquad (A.1) \\
&\frac{\partial}{\partial q}\mathcal{H}_{m,n}(q,p) = am\mathcal{H}_{m-1,n}(q,p) + bn\mathcal{H}_{m,n-1}(q,p) \ , \\
&\frac{\partial}{\partial p}\mathcal{H}_{m,n}(q,p) = bm\mathcal{H}_{m-1,n}(q,p) + cn\mathcal{H}_{m,n-1}(q,p) \ .
\end{aligned}$$

From the above relations after some algebra the following partial differential equation can be deduced

$$\left[-c\frac{\partial^2}{\partial q^2} - a\frac{\partial^2}{\partial p^2} + 2b\frac{\partial^2}{\partial q \partial p} + \Delta\left(q\frac{\partial}{\partial q} + p\frac{\partial}{\partial p}\right)\right]\mathcal{H}_{m,n} = \Delta(m+n)\mathcal{H}_{m,n} \ , \qquad (A.2)$$

in some sense reminiscent of eq. (6), which can be recovered in correspondence with $\underline{\underline{M}} = \underline{\underline{I}}$.

Consequently, the polynomials $\mathcal{H}_{m,n}$ can be understood as eigenfunctions of the operator

$$\hat{T} = -c\frac{\partial^2}{\partial q^2} - a\frac{\partial^2}{\partial p^2} + 2b\frac{\partial^2}{\partial q \partial p} + \Delta\left(q\frac{\partial}{\partial q} + p\frac{\partial}{\partial p}\right) \ , \qquad (A.3)$$

with eigenvalue $\Delta(m+n)$.

Let us consider now the adjoint polynomials $\mathcal{G}_{m,n}(q,p)$, for which the general relations (19) specialize into

$$\begin{aligned}
&\mathcal{G}_{m+1,n}(q,p) = q\mathcal{G}_{m,n}(q,p) - cm\mathcal{G}_{m-1,n}(q,p) + bn\mathcal{G}_{m,n-1}(q,p) \ , \\
&\mathcal{G}_{m,n+1}(q,p) = p\mathcal{G}_{m,n}(q,p) + bm\mathcal{G}_{m-1,n}(q,p) - an\mathcal{G}_{m,n-1}(q,p) \ , \qquad (A.4) \\
&\frac{\partial}{\partial q}\mathcal{G}_{m,n}(q,p) = m\mathcal{G}_{m-1,n}(q,p) \ , \quad \frac{\partial}{\partial p}\mathcal{G}_{m,n}(q,p) = n\mathcal{G}_{m,n-1}(q,p) \ ,
\end{aligned}$$

which provide the differential equation

$$\left[-c\frac{\partial^2}{\partial q^2} - a\frac{\partial^2}{\partial p^2} + 2b\frac{\partial^2}{\partial q \partial p} + \Delta\left(q\frac{\partial}{\partial q} + p\frac{\partial}{\partial p}\right)\right]\mathcal{G}_{m,n} = \Delta(m+n)\mathcal{G}_{m,n} \ , \qquad (A.5)$$

the same as for $\mathcal{H}_{m,n}$.

Finally, let us note that the orthogonality relation (20) in the case we are considering specialize as

$$\int dq \int dp \mathcal{H}_{m,n}(q,p)\mathcal{G}_{r,s}(q,p)\exp\left\{-\frac{1}{2}\underline{x}^T\underline{\underline{M}}\,\underline{x}\right\} = \frac{2\pi}{\sqrt{\Delta}} m!n!\delta_{m,r}\delta_{n,s} \ . \qquad (A.6)$$

## REFERENCES


[1] G.N. Watson, *A Treatise on the Theory of Bessel Functions*, (Cambridge University Press, London, 1958).

[2] A.F. Nikiforov and V.B. Uvarov, *Special Functions of Mathematical Physics*, (Birkhauser, Basel 1988).

[3] E.D. Rainville, *Special Functions*, (The Macmillan Company, N.Y. 1960).

[4] *Theory and Application of Special Functions*, ed. R. Askey (Academic Press, N.Y. 1975).

[5] W. Miller Jr., *Lie Theory and Special Functions*, (Academic Press, N.Y. 1968); N.J. Vilenkin, *Special Functions and the Theory of Group Representation*, (Academic Mathematical Society, Providence, RI 1968).

[6] R.J. Finkelstein, *J. Math. Phys.* **33**, 4259 (1992).

[7] K.M. Case, *J. Math. Phys.* **15**, 2166 (1974).

[8] P. Appell and J. Kampè de Ferièt, *Fonctions hypergeomètriques et hypersphèriques. Polynomes d'Hermite*, (Gauthier–Villars, Paris 1926).

[9] M.B. Jekhowsky, *Bull. Astr.*, XXXV, 134 (1918).

[10] G. Dattoli, L. Giannessi, L. Mezi and A. Torre, *Nuovo Comento* **B105**, 327 (1990); G. Dattoli, A. Torre, S. Lorenzutta, G. Maino and C. Chiccoli, *Nuovo Cimento* **B106**, 21 (1991).

[11] W. Miller Jr., *Comm. Pure Appl. Math.* **18**, 493 (1965).

[12] G. Dattoli, C. Chiccoli, S. Lorenzutta, G. Maino, M. Richetta and A. Torre, *J. Sc. Comp.* **8**, 69 (1993).

[13] G. Dattoli, C. Chiccoli, S. Lorenzutta, G. Maino and A. Torre, *Theory of Generalized Hermite Polynomials*, submitted for publication.

[14] A.W. Gould and A.T. Hopper, *Duke Math. J.* **29**, 5 (1962).

[15] Ch. Hermite, *Comptes Rendus*, t. 68, 93 (1864).

[16] D. Han, Y.S. Kim and M.E. Noz, *Phys. Rev.* **A37**, 807 (1988); D. Han, Y.S. Kim and M.E. Noz, *Phys. Rev.* **A40**, 902 (1989); D. Han, Y.S. Kim and M.E. Noz, *Phys. Rev.* **A41**, 6233 (1990); Y.S. Kim and M.E. Noz, *Phase Space Picture of Quantum Mechanics*, (World Publ., Co., Singapore 1991).

[17] H.R. Lewis Jr., *Phys. Rev. Lett.* **18**, 510 (1967); H.R. Lewis Jr., *J. Math. Phys.* **9**, 1976 (1968); H.R. Lewis Jr., and W.B. Reisenfeld, *J. Math. Phys.* **10**, 1458 (1969).

[18] E.D. Courant and H.S. Snyder, *Ann. Phys.* **3**, 1 (1958).

[19] E.P. Wigner, *Phys. Rev.* **40**, 749 (1932).

N95-13930

# UNDERSTANDING SQUEEZING OF QUANTUM STATES WITH THE WIGNER FUNCTION

Antoine Royer
*Département de Génie Physique, Ecole Polytechnique*
*Montréal, Québec H3C 3A7, Canada*

**Abstract**

The Wigner function is argued to be the only natural phase space function evolving classically under quadratic Hamiltonians with time-dependent bilinear part. This is used to understand graphically how certain quadratic time-dependent Hamiltonians induce squeezing of quantum states. The Wigner representation is also used to generalize Ehrenfest's theorem to the quantum uncertainties. This makes it possible to deduce features of the quantum evolution, such as squeezing, from the classical evolution, whatever the Hamiltonian.

## 1 Introduction

The Wigner function [1] can be used to get a visual understanding of why certain time-dependent Hamiltonians induce squeezing of quantum states. We first address the question: Why the Wigner function, rather than, say, the Husimi function [2]? It will be showed that although other phase space functions may evolve classically under certain *specific* quadratic Hamiltonians, the Wigner function is the only one to do so under quadratic Hamiltonians having a *time-dependent* bilinear part. We consider, as an example, squeezing by a periodically modulated harmonic oscillator. We then discuss a generalization of Ehrenfest's theorem applying to the quantum uncertainties. This allows to deduce aspects of the quantum evolution, such as squeezing, from the classical evolution even in the case of arbitrary Hamiltonians.

Phase space variables (position and momentum) are denoted by q and p. A caret is used to identify operators. Thus, $[\hat{q}, \hat{p}] = i$, where we take $\hbar = 1$. The time variable is denoted by t.

## 2 Quadratic Hamiltonians and phase space functions

Ehrenfest's theorem expresses the time derivatives of the expectations $\langle\hat{q}\rangle$ and $\langle\hat{p}\rangle$ in a way formally similar to Hamilton's equations. In the case of a Hamiltonian $\hat{H} = \frac{1}{2}\hat{p}^2/m + V(\hat{q})$, it reads

$$\frac{d}{dt}\langle\hat{q}\rangle = \langle\hat{p}\rangle/m, \qquad \frac{d}{dt}\langle\hat{p}\rangle = \langle F(\hat{q})\rangle \tag{1}$$

where $F(q) = -\partial V/\partial q$ is the force. If the potential $V(q)$ is quadratic, hence $F(q)$ linear (or, if the particle is in a state sufficiently localized on the scale of non-harmonic variation of V), then $\langle F(\hat{q})\rangle = F(\langle\hat{q}\rangle)$, and (1) become identical to Hamilton's equations, implying that $\langle\hat{q}\rangle$ and $\langle\hat{p}\rangle$ follow classical trajectories in phase space. This stays true in the case of a general quadratic Hamiltonian

$$\hat{H}(t) = \hat{H}_1(t) + \hat{H}_2(t) \tag{2}$$

where $\hat{H}_1(t)$ is linear, and $\hat{H}_2(t)$ is bilinear in $\hat{q}$ and $\hat{p}$ ($\alpha$, $\beta$, a, b, c scalar functions of time):

$$\hat{H}_1(t) = H_1(\hat{q},\hat{p},t) = \alpha(t)\hat{q} + \beta(t)\hat{p} \tag{3}$$

$$\hat{H}_2(t) = H_2(\hat{q},\hat{p},t) = a(t)\hat{q}^2 + b(t)(\hat{q}\hat{p}+\hat{p}\hat{q}) + c(t)\hat{p}^2 \tag{4}$$

Can one push this further, and associate with state vectors $|\psi\rangle$, or state operators $\hat{\rho}$, a phase space function $f(q,p,t)$ whose quantum evolution is classical for such Hamiltonians? That is, such that

$$\frac{\partial}{\partial t}f(q,p,t) = \{H, f\}_{PB} \equiv (\frac{\partial H}{\partial q}\frac{\partial}{\partial p} - \frac{\partial H}{\partial p}\frac{\partial}{\partial q})f(q,p,t) \quad \text{or} \quad f(q,p,t) = f(q_t,p_t,0) \tag{5}$$

where $(q_t,p_t)$ is the point which classically evolves into (q,p) in the time interval (0,t), under the Hamiltonian $H(q,p,t)$. It is natural to ask that $f(q,p)$ be linear in either $|\psi\rangle$ or $\hat{\rho}$, so that it has the form

$$f(q,p;\psi) = \langle\phi_{qp}|\psi\rangle \quad \text{or} \quad f(q,p;\hat{\rho}) = \mathrm{Tr}\{\hat{\Delta}_{qp}\hat{\rho}\} \tag{6}$$

where $|\phi_{qp}\rangle$ and $\hat{\Delta}_{qp}$ are kets and operators parametrized by phase space.

Introduce the unitary time-evolution operator $\hat{U}(t,t')$, defined by

$$\frac{\partial}{\partial t}\hat{U}(t,t') = -i\hat{H}(t)\hat{U}(t,t'), \quad \frac{\partial}{\partial t'}\hat{U}(t,t') = i\hat{U}(t,t')\hat{H}(t'), \quad \hat{U}(t,t')\hat{U}(t',t) = \hat{U}(t,t) = \hat{1} \tag{7}$$

and similarly $\hat{U}_1$ and $\hat{U}_2$ corresponding to $\hat{H}_1$ and $\hat{H}_2$. Let us first assure classical evolution under linear time-independent Hamiltonians $\hat{H}_1 = \alpha\hat{q}+\beta\hat{p}$: Here, $\hat{U}_1(t,0) = e^{-it(\alpha\hat{q}+\beta\hat{p})}$, and one gets classical evolution, $f(q,p,t) = f(q-\beta t, p+\alpha t, 0)$, up to a phase, iff

$$|\phi_{qp}\rangle = \hat{D}_{qp}|\phi\rangle, \qquad \hat{\Delta}_{qp} = \hat{D}_{qp}\hat{\Delta}\hat{D}_{qp}^{-1} \tag{8}$$

where

$$\hat{D}_{qp} = e^{ip\hat{q}-iq\hat{p}} \tag{9}$$

are phase space displacement operators, and $|\phi\rangle$ and $\hat{\Delta}$ are some fiducial ket and operator. We now note the relations ($[\ ]_+$ denotes anticommutators, $\{\ \}_{PB}$ Poisson brackets):

$$[\hat{H}_1, \hat{D}_{qp}] = H_1(q,p)\hat{D}_{qp}, \quad \tfrac{1}{2}i[\hat{H}_1, \hat{D}_{qp}]_+ = \{H_1, \hat{D}_{qp}\}_{PB} \equiv (\frac{\partial H_1}{\partial q}\frac{\partial}{\partial p} - \frac{\partial H_1}{\partial p}\frac{\partial}{\partial q})\hat{D}_{qp} \tag{10a}$$

$$i[\hat{H}_2, \hat{D}_{qp}] = \{H_2, \hat{D}_{qp}\}_{PB} \tag{10b}$$

where $H_{1,2} \equiv H_{1,2}(q,p)$. Using these results, and refering to (5), one finds that

$$\hat{U}(0,t)\,\hat{D}_{qp} = \hat{D}_{q_tp_t}\,\hat{U}_2(0,t)\,e^{i\chi(q,p,t)} \tag{11}$$

where $\hat{U}_2$ is the time evolutor for $\hat{H}_2$, and $\chi(q,p,t)$ is a phase determined by the equation

$$\frac{\partial}{\partial t}\chi - \{H(t),\chi\}_{PB} = \tfrac{1}{2}H_1(t), \qquad \chi(q,p,0) \equiv 0 \tag{12}$$

One verifies (11) by verifying that both sides of $\hat{U}(0,t)\hat{D}_{qp}\hat{U}_2(t,0) = \hat{D}_{q_tp_t}e^{i\chi}$ satisfy the same differential equation. We then get, from (6) and (11):

$$f_\phi(q,p;\psi(t)) \equiv \langle\phi|\hat{D}_{qp}{}^\dagger\hat{U}(t,0)|\psi\rangle = e^{-i\chi(q,p,t)}\,f_{\phi_t}(q_t,p_t;\psi(0)), \qquad |\phi_t\rangle \equiv \hat{U}_2(0,t)|\phi\rangle \tag{13}$$

$$f_\Delta(q,p;\hat{\rho}(t)) \equiv \mathrm{Tr}\{\hat{D}_{qp}\hat{\Delta}\hat{D}_{qp}{}^{-1}\,\hat{U}(t,0)\hat{\rho}\hat{U}(0,t)\} = f_{\Delta_t}(q_t,p_t;\hat{\rho}(0)), \quad \hat{\Delta}_t \equiv \hat{U}_2(0,t)\hat{\Delta}\hat{U}_2(t,0) \tag{14}$$

One sees that the function $f_\phi$ evolves classically iff $|\phi_t\rangle$ is stationary, i.e., if $\hat{H}_2$ is time-independent, and $|\phi\rangle = |E_n\rangle$ is an eigenket of it. For instance, if $\hat{H}_2$ is a harmonic oscillator, and $|\phi\rangle = |E_0\rangle$ is the ground state, then $|\phi_{qp}\rangle$ are coherent states, and

$$f_\phi(q,p;\psi(t)) = e^{-i\chi(q,p,t)+itE_0}\,f_\phi(q_t,p_t;\psi(0)) \tag{15}$$

is the Husimi function [2], which is well known to evolve classically under *that* $\hat{H}_2$ of which $|\phi\rangle$ is an eigenket. Clearly, no function $f_\phi$ linear in state *vectors* can possibly evolve classically if $\hat{H}_2$ is time-dependent. Consider now (14): Again, $f_\Delta$ evolves classically iff $\hat{\Delta}_t$ is stationary: For instance, if $\hat{H}_2$ is time-independent, and $\hat{\Delta} = |E_n\rangle\langle E_{n'}|$ or $\hat{\Delta} = g(\hat{H}_2)$, then the evolution is classical - but only for *that* specific time-independent $\hat{H}_2$. Is there an operator $\hat{\Delta}$ (apart from the unit operator) such that

$$\hat{U}_2(0,t)\,\hat{\Delta}\,\hat{U}_2(t,0) = e^{-i\varphi(t)}\,\hat{\Delta} \quad \Leftrightarrow \quad [\hat{H}_2(t), \hat{\Delta}] = \dot{\varphi}(t)\,\hat{\Delta} \qquad (\dot{\varphi}(t)=\partial\varphi/\partial t) \tag{16}$$

($\varphi$ a real phase) for time-dependent $\hat{H}_2(t)$? Yes, the parity operator $\hat{\Pi}$, since $\hat{q}\hat{\Pi} = -\hat{\Pi}\hat{q}$, $\hat{p}\hat{\Pi} = -\hat{\Pi}\hat{p}$ imply $[\hat{H}_2, \hat{\Pi}]=0$. Setting $\hat{\Delta} = \hat{\Pi}$ in (14) yields the *Wigner function* [1,3]

$$f_w(q,p;\hat{\rho}) = \pi^{-1}\mathrm{Tr}\{\hat{D}_{qp}\hat{\Pi}\,\hat{D}_{qp}{}^{-1}\,\hat{\rho}\}, \qquad f_w(q,p;\hat{\rho}(t)) = f_w(q_t,p_t;\hat{\rho}(0)) \tag{17}$$

The Wigner function is the only phase space function which evolves classically under (any) time-dependent $\hat{H}_2(t)$. One can see this as follows: Represent any $\hat{\Delta}$ by its Weyl symbol $\Delta_w(q,p)$, where

the Weyl symbol of an operator $\hat{A}$ is defined as [3,4]

$$A_w(q,p) = 2\mathrm{Tr}\{\hat{D}_{qp}\hat{\Pi}\,\hat{D}_{qp}^{-1}\,\hat{A}\} \tag{18}$$

We want $\hat{\Delta}_t$, hence its Weyl symbol, to be stationary for any $\hat{H}_2(t)$. Now, just as the Weyl symbol (17) of $\hat{\rho}$ evolves classically under $\hat{H}_2(t)$, so does that of $\hat{\Delta}_t$. The only possible way for $(\hat{\Delta}_t)_w(q,p)$ to be stationary under classical evolution with different $H_2$ 's (e.g., with orbits which are ellipses or hyperbolas of different eccentricities) is that it be be concentrated at the origin: We must thus have $\Delta_w(q,p) = (const)\delta(q)\delta(p)$; this implies [5b] that $\hat{\Delta} = (const)\hat{\Pi}$.

## 3 Squeezing by a Periodically Modulated Harmonic Oscillator

The classical evolution of the Wigner function under quadratic $\hat{H}(t)$ is very useful for understanding the quantum in terms of the classical evolution. As an example, consider a harmonic oscillator

$$\hat{H} = \tfrac{1}{2}m^{-1}\hat{p}^2 + \tfrac{1}{2}m\omega^2\hat{q}^2 = \tfrac{1}{2}\omega(\alpha\hat{p}^2 + \hat{q}^2/\alpha), \qquad \alpha = (m\omega)^{-1} \tag{19}$$

If $\alpha$=1 (in suitable units), the classical orbits $H(q,p) = constant$ are circles in the phase plane (q,p). If $\alpha \neq 1$, the orbits are ellipses (Fig.1), the ratio of the q semi-axis to the p semi-axis being $\alpha$. We will now let $\alpha$ alternate between two values, $\gamma$ and $\gamma^{-1}$ (where $\gamma > 1$), at every quarter of a period $2\pi/\omega$, while keeping $\omega$ fixed (i.e., only m changes). Let $\alpha = \gamma^{-1} < 1$ for the first quarter period: During that time interval, a point initially on the positive q axis (beginning of trajectory 1 on Fig.2) moves to the negative p axis, while receding away from the origin by a factor $\gamma$. Then let $\alpha = \gamma > 1$ during the next quarter period: The point moves to the negative q axis, receding away from the origin by another factor $\gamma$. And so on. One here has parametric amplification. On the other hand, points initially on the p axis (trajectory 2) close in on the origin. Thus, classically, the phase plane gets squeezed into the rotating q axis, by a factor $\gamma$ at each quarter period. Whence a corresponding squeezing of quantum states [5a,6].

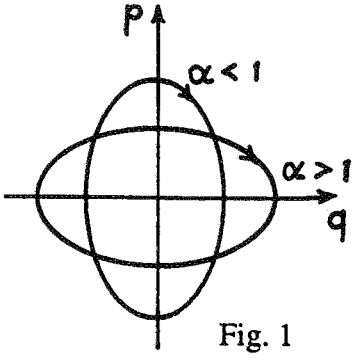

Fig. 1

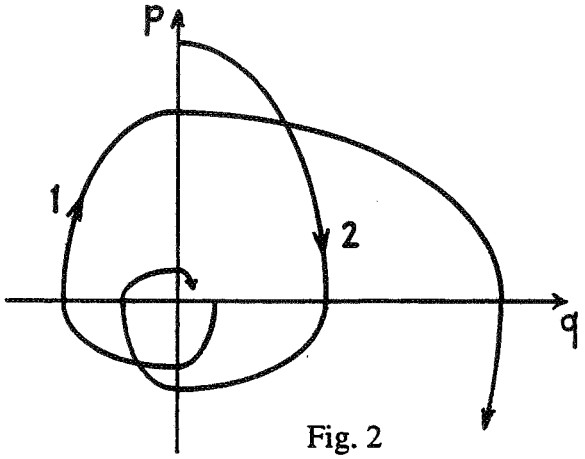

Fig. 2

## 4 Ehrenfest Theorem for the Quantum Uncertainties

The above concerned quadratic Hamiltonians. It will now be indicated that the Wigner-Weyl (WW) representation allows to reinterpret Ehrenfest's theorem, and to extend it to quadratic observables, hence to the quantum uncertainties. This makes it possible to deduce features of the quantum evolution from the classical evolution even in the case of arbitrary Hamiltonians. Let us first recall that in the WW representation, expectation values of operators $\hat{A}$ have the "classical" form [1,7]

$$\langle\hat{A}\rangle \equiv \mathrm{Tr}\{\hat{A}\,\hat{\rho}\} = \int dqdp\; A_W(q,p)\, f_W(q,p) \tag{20}$$

In particular, the quantum expectations of $\hat{q}$ and $\hat{p}$ are

$$\langle\hat{q}\rangle = \int dqdp\; q\, f_W(q,p), \qquad \langle\hat{p}\rangle = \int dqdp\; p\, f_W(q,p) \tag{21}$$

and the uncertainty matrix is

$$\begin{aligned} C_{qq} &= \langle(\hat{q} - \langle\hat{q}\rangle)^2\rangle = \int dqdp\; (q - \langle q\rangle)^2\, f_W(q,p) \\ C_{qp} = C_{pq} &= \langle\tfrac{1}{2}(\hat{q}\hat{p}+\hat{p}\hat{q}) - \langle\hat{q}\rangle\langle\hat{p}\rangle\rangle = \int dqdp\; (q-\langle q\rangle)(p-\langle p\rangle)\, f_W(q,p) \\ C_{pp} &= \langle(\hat{p} - \langle\hat{p}\rangle)^2\rangle = \int dqdp\; (p - \langle p\rangle)^2\, f_W(q,p) \end{aligned} \tag{22}$$

A quantum state (wave packet) may be roughly represented in phase space by an uncertainty ellipse

$$(u - \langle u\rangle)\cdot \mathbf{C}^{-1}\,(u - \langle u\rangle) = 1 \quad \text{where} \quad u = \begin{pmatrix} q \\ p \end{pmatrix}, \quad \mathbf{C} = \begin{pmatrix} C_{qq} & C_{qp} \\ C_{pq} & C_{pp} \end{pmatrix} \tag{23}$$

We also need the result [7]

$$[\hat{A}, \hat{B}]_W(q,p) = i\{A_W, B_W\}_{PB}(q,p) \quad \text{if} \quad \hat{A} \text{ or } \hat{B} \text{ is quadratic} \tag{24}$$

that is: The Weyl symbol of the commutator of two operators, one of which is quadratic, is equal to the Poisson bracket of the individual Weyl symbols. Let now $\hat{A}$ be an observable quadratic in $\hat{q}$ and $\hat{p}$. We then have, by (20) and (24), for any $\hat{H}(t)$:

$$\begin{aligned} \frac{\partial}{\partial t}\langle\hat{A}\rangle &= -i\mathrm{Tr}\{\hat{A}[\hat{H}, \hat{\rho}]\} = -i\mathrm{Tr}\{[\hat{A},\hat{H}]\hat{\rho}\} = \int dqdp\; \{A_W, H_W\}_{PB} f_W(q,p,t) \\ &= \int dqdp\; A_W(q,p)\{H_W, f_W\}_{PB} \qquad (\hat{A} \text{ quadratic, any } \hat{H}) \end{aligned} \tag{25}$$

where in the last line we performed an integration by parts. Eq.(25) says that the rate of change of the expectation of a quadratic observable is classical, in the sense that it is the same as if each point in

Wigner phase space instantaneously followed a classical trajectory. This does not mean that $\langle\hat{A}\rangle$ evolves classically over finite time intervals, because $f_w(q,p,t)$ in (25) is the exact *quantally* evolved Wigner function at time t, not one evolved classically during some finite time (unless $\hat{H}$ is quadratic); more specifically, the first time derivative of $\langle\hat{A}\rangle$ is classical, but not the higher order derivatives. By letting $\hat{A}$ stands for $\hat{q}$ or $\hat{p}$ in (25), one gets Ehrenfest's theorem:

$$\frac{\partial}{\partial t}\langle\hat{q}\rangle = \int dqdp\, q\{H_w, f_w\}_{PB} = \int dqdp\, \{q, H_w\}_{PB} f_w(q,p,t) = \langle\partial\hat{H}/\partial\hat{p}\rangle \qquad (26a)$$

$$\frac{\partial}{\partial t}\langle\hat{p}\rangle = \int dqdp\, p\{H_w, f_w\}_{PB} = \int dqdp\, \{p, H_w\}_{PB} f_w(q,p,t) = \langle-\partial\hat{H}/\partial\hat{q}\rangle \qquad (26b)$$

The last expressions in (26a,b) are the usual statement of Ehrenfest's theorem [equivalent to (1) if $\hat{H} = \frac{1}{2}\hat{p}^2/m + V(\hat{q})$], giving a formal quantum-classical analogy. The first expressions in (26a,b) tell us much more: That the rates of change of $\langle\hat{q}\rangle$ and $\langle\hat{p}\rangle$ *are classical*, but relative to a phase space distribution function. Eq.(25) generalizes Ehrenfest's theorem to quadratic observables, and thus to the uncertainties: Indeed, according to (21), (22) and (25), the uncertainty ellipse (23) evolves exactly as if each point in Wigner phase space instantaneously followed a classical trajectory. For instance, if the ellipse gets squeezed classically, during some small (infinitesimal) time interval, then so does it quantally. In general, one may expect that if the classical motion during a *finite* time interval squeezes the uncertainty ellipse, then so does the quantum evolution. The latter statement is of course rigorously true if $\hat{H}(t)$ is quadratic, in view of (17); it is also approximately true, in the case of arbitrary $\hat{H}(t)$, if $f_w(q,p,t)$ is sufficiently localized on the scale of non-harmonic variation of $H(q,p,t)$, for the evolution of $f_w(q,p,t)$ is then approximately classical [5b].

Let us mention, finally, that Ehrenfest's theorem for quadratic observables can also be written in a form corresponding to the last expressions in (26a,b), namely [5c]

$$\frac{\partial}{\partial t}\langle\hat{A}\rangle = \langle\{A_w, H_w\}_{PB}(\hat{q},\hat{p})_w\rangle \qquad (\hat{A} \text{ quadratic, any } \hat{H}) \qquad (27)$$

where the subscript w on the function $\{A_w, H_w\}_{PB}(\hat{q},\hat{p})$ of the non-commuting operators $\hat{q}$ and $\hat{p}$ signifies that they are ordered according to Weyl's ordering rule [4].


1. E.P. Wigner, Phys. Rev. 40, 749 (1932)
2. K. Husimi, Proc. Phys. Math. Soc. Jpn. 22, 264 (1940)
3. A. Grossmann, Commun. Math. Phys. 48, 191 (1976); A. Royer, Phys. Rev. A 15, 449 (1977)
4. H. Weyl, *The Theory of Groups and Quantum Mechanics* (Dover, New York, 1950), pp. 272-276
5. A. Royer, (a) Phys. Rev. A 42, 560 (1990);(b) *ibid* 43, 44 (1991);(c) Found. Phys. 22, 727 (1992)
6. J. Janszky, P. Adam and I. Foldesi, Phys. Lett. A 174, 368 (1993)
7. J.E. Moyal, Proc. Cambr. Phil. Soc. 45, 99 (1949)

# ON THE POSSIBILITY OF A QUANTUM MECHANICAL PHASE SPACE REPRESENTATION

Go. Torres-Vega
*Departamento de Física, Centro de Investigación y de Estudios Avanzados del IPN, Apartado Postal 14-740, 07000 México D.F.*

**Abstract**

Probability densities in phase space containing quantum dynamics information are very useful. However, is there a *true* phase space representation of Quantum Mechanics?

## 1 A Phase Space Representation

As in other representations, let us postulate that there exist a set of basis vectors $\langle\Gamma| = \langle p, q|$ and its adjoints $|\Gamma\rangle = |p, q\rangle$, where $\Gamma = (p, q)$ denotes a point in phase space. This set of vectors is orthonormal, $\langle\Gamma'|\Gamma\rangle = \delta(\Gamma' - \Gamma)$, and there is a closure relation, $\hat{I} = \int d\Gamma|\Gamma\rangle\langle\Gamma|$, for them. The inner product between a bra $\langle\psi|$ and a ket $|\phi\rangle$ is defined as $\langle\psi|\phi\rangle = \int d\Gamma\ \psi^*(\Gamma)\phi(\Gamma)$, fulfilling the expected properties for an inner product. Hence, the projection of an abstract ket $|\psi\rangle$, onto the basis vector $\langle\Gamma|$, results in a wave function dependent on both $p$ and $q$, $\psi(\Gamma) = \langle\Gamma|\psi\rangle$.

The momentum operator $\hat{P}$ is defined as $(p/2) - i\hbar(\partial/\partial q)$, and the coordinate operator $\hat{Q}$ is given by $(q/2) + i\hbar(\partial/\partial p)$. Momentum and coordinate operators comply with the commutator relationship, $[\hat{Q}, \hat{P}] = i\hbar\hat{I}$. These operators provide the foundation for the development of a quantum representation in phase space. In what follows, we present the consequences of this choice of operators.

These operators are the generators of change of phase and translation, $\exp(i\eta\hat{P}/\hbar)|p, q\rangle = \exp(i\eta p/2\hbar)|p, q - \eta\rangle$ and $\exp(i\xi\hat{Q}/\hbar)|p, q\rangle = \exp(i\xi q/2\hbar)|p + \xi, q\rangle$

With the definitions given above, we can write a Schrödinger equation in phase space,

$$i\hbar\frac{\partial}{\partial t}\psi(\Gamma; t) = \left[\frac{1}{2m}\left(\frac{p}{2} - i\hbar\frac{\partial}{\partial q}\right)^2 + V\left(\frac{q}{2} + i\hbar\frac{\partial}{\partial p}\right)\right]\psi(\Gamma; t)\,. \tag{1}$$

This is the equation on which the quantum theory in phase space is based.

The physical interpretation of the wave function in Eq. (1) is that its square magnitude times the volume element, $|\psi(\Gamma)|^2 d\Gamma$, gives the probability of finding the quantum system with momentum between $p$ and $p + dp$ and coordinate between $q$ and $q + dq$ *before* it is perturbed in any way. Even though the wave function depends on both coordinate and momentum, it is *not* possible to determine (to measure) them simultaneously (see below). Fig. 1 shows the interpretation of the Heisenberg's uncertainty principle in phase space. The diagonal matrix

elements of the quantum Liouville equation, when the potential function can be written as a power series in its argument, $V(x) = \sum_{n=0}^{\infty} V_n x^n$, is given by

$$\frac{\partial}{\partial t}\langle\Gamma|\hat{\rho}_t|\Gamma\rangle = -\frac{\partial}{\partial q}\frac{1}{2m}\left[\langle\Gamma|\hat{P}\hat{\rho}_t|\Gamma\rangle + \langle\Gamma|\hat{\rho}_t\hat{P}|\Gamma\rangle\right] + \frac{\partial}{\partial p}\sum_{n=1}^{\infty} V_n \sum_{l=0}^{n-1}\langle\Gamma|\hat{Q}^l\hat{\rho}_t\hat{Q}^{n-l-1}|\Gamma\rangle\,, \qquad (2)$$

where $\hat{\rho}_t$ is the density operator at time $t$.

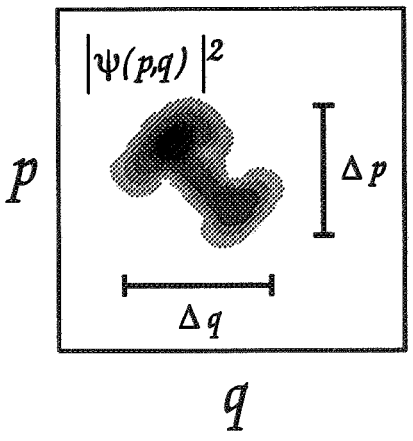


FIG. 1. Heisenberg's uncertainty relation, $\Delta p \Delta q \geq \hbar$, in phase space.

## 2 Time Reversal Properties

Time reversal is achieved by the replacements $t \to -t$, $p \to -p$, $q \to q$ and by taking the complex conjugation of wave functions. Under this transformation, the momentum operator $(p/2) - i\hbar(\partial/\partial q)$ transforms to its negative, the coordinate operator $(q/2) + i\hbar(\partial/\partial p)$ remains with no change, and the Schrödinger equation (1) becomes

$$i\hbar\frac{\partial}{\partial t}\psi^*(-p,q;-t) = \left[\frac{1}{2m}\left(\frac{p}{2} - i\hbar\frac{\partial}{\partial q}\right)^2 + V\left(\frac{q}{2} + i\hbar\frac{\partial}{\partial p}\right)\right]\psi^*(-p,q;-t)\,. \qquad (3)$$

Thus, if $\psi(p,q;t)$ is a solution to the Schrödinger equation, $\psi^*(-p,q;-t)$ is also a solution. Similarly, if $\langle p,q|\hat{\rho}_t|p,q\rangle$ is a solution to the quantum probability conservation equation, then $\langle -p,q|\hat{\rho}_{-t}|-p,q\rangle$ is also a solution to it.

## 3 Eigenfunctions of Momentum and Coordinate Operators

Let us consider the eigenfunctions of coordinate and momentum operators in phase space. A solution to the Eigenvalue equation $(p/2 - i\hbar\partial/\partial q)\langle\Gamma|u_{p'}\rangle = p'\langle\Gamma|u_{p'}\rangle$ is given by $\langle\Gamma|u_{p'}\rangle = (2\pi\hbar)^{-1/2}\exp[iq(p'-p/2)/\hbar]$. On the other hand, a solution to the eigenvalue equation $(q/2 + i\hbar\partial/\partial p)\langle\Gamma|u_{q'}\rangle = q'\langle\Gamma|u_{q'}\rangle$ is given by $\langle\Gamma|u_{q'}\rangle = (2\pi\hbar)^{-1/2}\exp[-ip(q'-q/2)/\hbar]$. As expected, there is no simultaneous eigenfunctions of coordinate and momentum operators.

# 4 Simultaneous Measurement of Momentum and Coordinate

Following the standard convention regarding measuring process, if one proceeds to determine the configuration of a given quantum system, the wave function, $\langle \Gamma|\psi\rangle$ reduces to the eigenstate $\langle \Gamma|u_{q'}\rangle$ of $\hat{Q}$ with probability $|\langle u_{q'}|\psi\rangle|^2$ of obtaining the value $q'$. If we then want to measure the momentum, we need to express the new state $\langle \Gamma|u_{q'}\rangle$ as an expansion in terms of the eigenstates of $\hat{P}$, i.e.,

$$\langle \Gamma|u_{q'}\rangle = \frac{1}{2\pi\hbar}\int dp' \exp\left(-\frac{i}{\hbar}p'q'\right)\langle \Gamma|u_{p'}\rangle \,. \tag{4}$$

According to this, once one determines the configuration of a quantum system, one can find it with any value for the momentum. Therefore, a wave function dependent on $p$ and $q$ need not violate the uncertainty principle.

# 5 Reduction to Momentum and Coordinate Representations

Coordinate or momentum representations can be recovered from the phase space representation proposed in this work. By taking the Fourier transform of the phase-space Schrödinger equation (1), over $q$, with kernel $(4\pi\hbar)^{-1/2}\exp(-ipq/2\hbar)$, we obtain

$$i\hbar\frac{\partial}{\partial t}\int dq\,\frac{e^{-ipq/2\hbar}}{\sqrt{4\pi\hbar}}\psi(\Gamma;t) = \left[\frac{p^2}{2m} + V\left(i\hbar\frac{\partial}{\partial p}\right)\right]\int dq\,\frac{e^{-ipq/2\hbar}}{\sqrt{4\pi\hbar}}\psi(\Gamma;t)\,, \tag{5}$$

where we have assumed that the potential function can be written as a power series in its argument, $V(x) = \sum_n V_n x^n$. Now, by taking the Fourier transform over $p$, with kernel $(4\pi\hbar)^{-1/2}\exp(ipq/2\hbar)$, we obtain

$$i\hbar\frac{\partial}{\partial t}\int dp\,\frac{e^{ipq/2\hbar}}{\sqrt{4\pi\hbar}}\psi(\Gamma;t) = \left[\frac{1}{2m}\left(-i\hbar\frac{\partial}{\partial q}\right)^2 + V(q)\right]\int dp\,\frac{e^{ipq/2\hbar}}{\sqrt{4\pi\hbar}}\psi(\Gamma;t)\,. \tag{6}$$

# 6 Classical Correspondence

In order to find what the classical analogues to quantum wave functions are, let us compare the quantum probability conservation equation in phase space (2) with the classical Liouville equation of motion,

$$\frac{\partial}{\partial t}\rho(\Gamma;t) = -\left[\frac{p}{m}\frac{\partial}{\partial q} + F(q)\frac{\partial}{\partial p}\right]\rho(\Gamma;t)\,. \tag{7}$$

We observe that the right hand side terms of the phase space quantum probability conservation equation (2) are just the symmetrizations of the classical products $p\,\rho(\Gamma;t)$ and $F(q)\rho(\Gamma;t)$ which appear in the classical Liouville equation (7). Therefore, the classical analogue to the quantum probability density $|\psi(\Gamma;t)|^2$ is the corresponding classical probability density $\rho(\Gamma;t)$.

The comparison between the quantum probability conservation equation in momentum representation,

$$\frac{\partial}{\partial t}\langle p|\hat{\rho}_t|p\rangle = \frac{\partial}{\partial p}\sum_{n=1}^{\infty} V_n \sum_{l=0}^{n-1}\langle p|\hat{Q}^l\hat{\rho}_t\hat{Q}^{n-l-1}|p\rangle \,, \tag{8}$$

and the coordinate average of the classical Liouville equation,

$$\frac{\partial}{\partial t}\int dq\,\rho(\Gamma;t) = -\frac{\partial}{\partial p}\int dq\,F(q)\rho(\Gamma;t) \,, \tag{9}$$

leads to the conclusion that the classical analogue to the quantum momentum probability density, $|\psi(p;t)|^2$, is the coordinate average of the classical probability density; $\int dq\,\rho(\Gamma;t)$. Similarly, the classical analogue to the quantum coordinate probability density $|\psi(q;t)|^2$ is the momentum average of the classical probability density, $\int dp\,\rho(\Gamma;t)$.

# 7 Step Potential

As a simple illustration, let us examine the dynamics of the scattering of a Gaussian wave packet, $\psi(\Gamma;0) = (2\pi)^{-1/2}\exp[-(q-q_0)^2/4 - (p-p_0)^2/4 + i(qp_0 - pq_0)/2]$, with $(p_0, q_0) = (\sqrt{2}, -3.5)$, from a potential step. In this calculation, the energy of the wave packet is 1 and the barrier height is 1. This model system illustrates the development of nodal structure due to quantum interference between the advancing and reflected parts of the wave packet when it encounters the step potential.

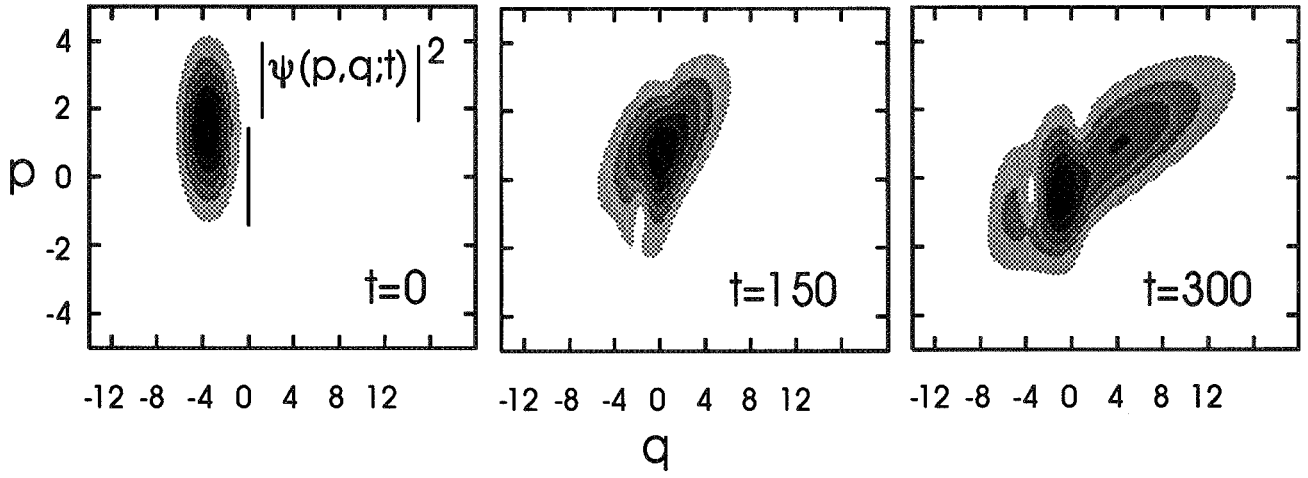


FIG. 2. Snapshots of the quantum evolution of the Gaussian density which is being scattered from a step potential at $q = 0$, in a dimensionless phase space.

Figure 2 shows density plots in phase space of the square magnitude, $|\psi(\Gamma;t=0)|^2$, of the time evolution of the Gaussian density. We can see that the wave packet breaks into three parts as it is evolving in time. First, there is a part whose momentum in near zero and which, consequently, moves very slowly. A second part of the wave packet smoothly changes its direction as it is reflected from the step, and combines with the part that stayed behind. Finally, a third

part of the wave packet has enough energy to overcome the barrier and continues moving past the step with smaller momentum.

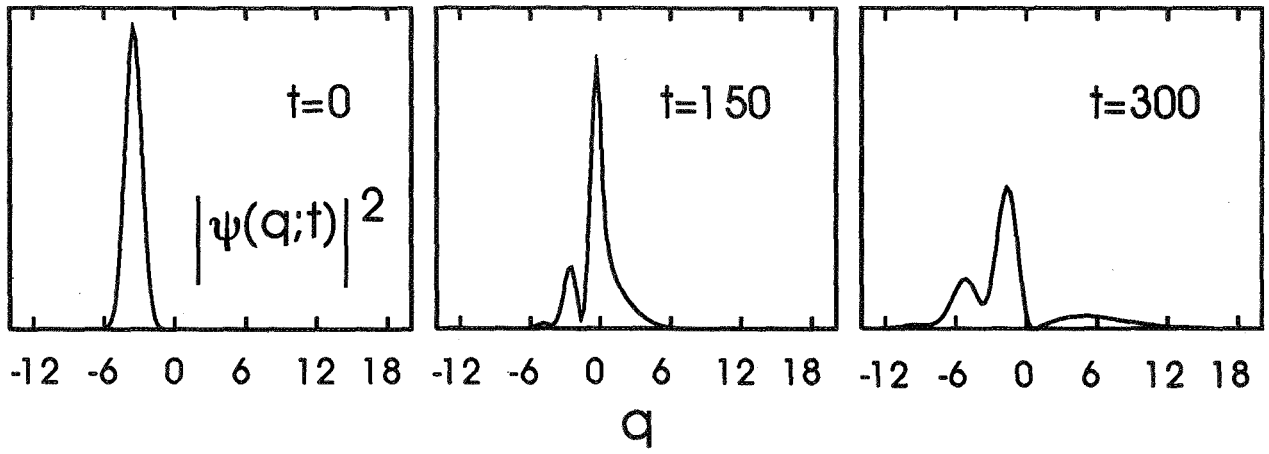


FIG. 3. Same calculation as the one in Fig. 2, but made in the coordinate representation.

Figure 3 shows the same type of calculation as in Figure 2 but made in coordinate representation. The analysis in phase space allows us a better understanding of the dynamics. Each peak appearing in the coordinate density corresponds to the different parts of the wave packet in phase space. These pictures suggest that, in this case, "quantum interference" effects may be partly explainable in classical terms. Each piece of the reflecting and transmitting wave packet resides in a different region of phase space and it is only when the wave function is projected onto coordinate or momentum space that one loses this perspective.

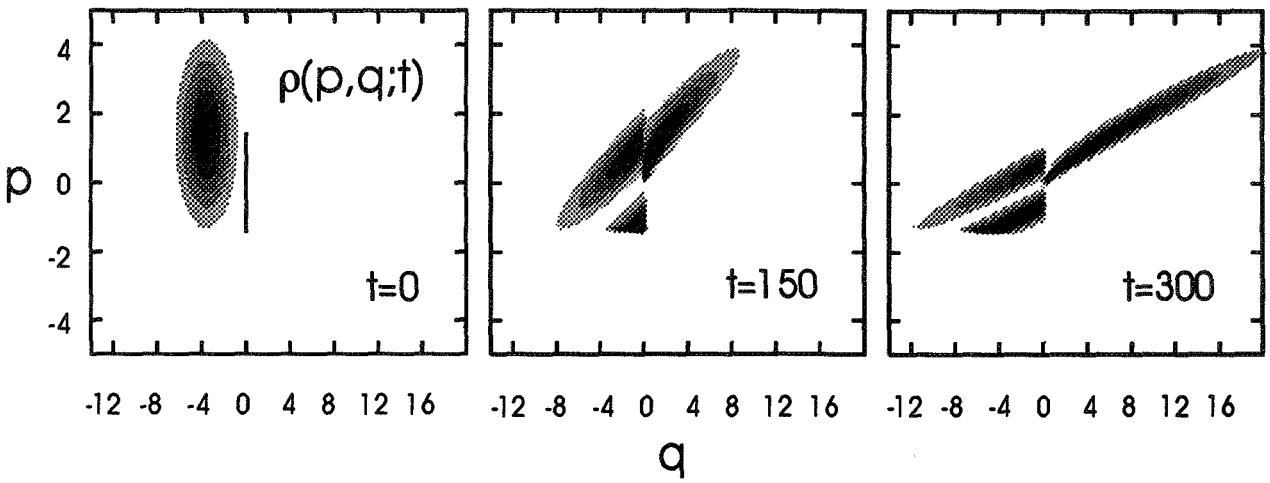


FIG. 4. Snapshots of the classical evolution of the classical analogue of the initial density in Fig. 2.

In a classical calculation, we have taken the Gaussian probability density $\rho(\Gamma;0) = (2\pi)^{-1/2}$ $\exp[-(q-q_0)^2/2 - (p-p_0)^2/2]$, with $(p_0, q_0) = (\sqrt{2}, -3.5)$, which is the classical analogue to the one in Fig. 2a, as an initial density to be propagated according to the classical Liouville equation 7. In Fig. 4, snapshots of the evolution of this density are shown at the same times as

in Fig. 2, and, in Fig. 5, the momentum average of the density in Fig. 4 (the classical analogue to the density in Fig. 3) is shown. By comparing figures 2, 3, 4 and 5 we conclude that the classical and quantum behavior are qualitatively the same with small quantitative differences. Since the classical averaging process is over real-valued functions, only constructive addition of the pieces of the distribution are permitted, thus, the interference effect wont appear in the classical analogue to the coordinate quantum density.

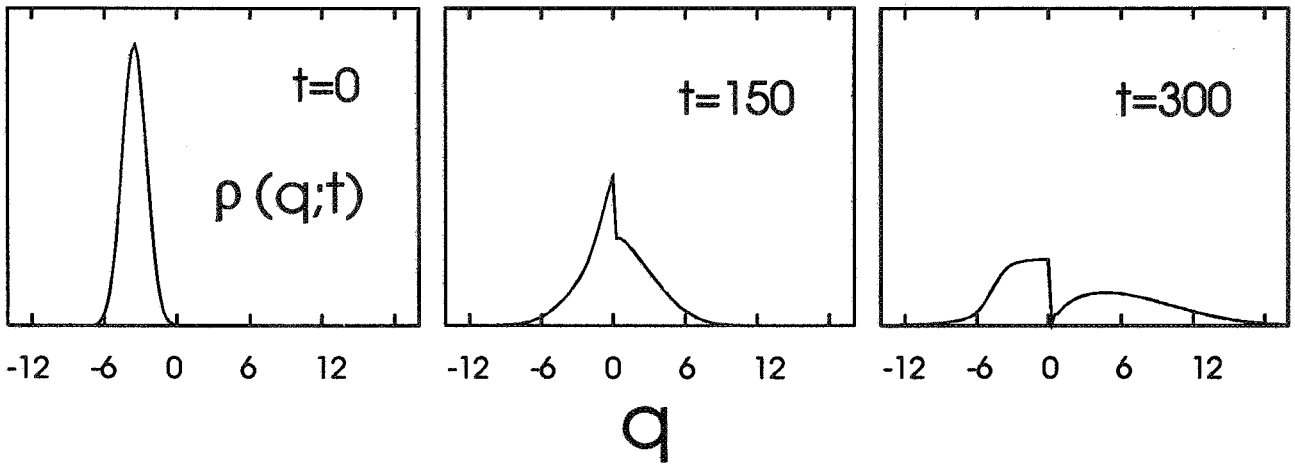


FIG. 5. Momentum averages of the densities in Fig. 4.

# 8 Acknowledgements

We would like to acknowledge financial support from CONACyT and SNI, México.

# References

[1] Go. Torres-Vega and J.H. Frederick, J. Chem. Phys. **93**, 8862 (1990).

[2] Go. Torres-Vega, J. Phys. Soc. Jpn. **60**, 714 (1991).

[3] Go. Torres-Vega and John H. Frederick, Phys. Rev. Lett. **67**, 2601 (1991).

[4] Go. Torres-Vega and John H. Frederick, J. Chem. Phys. **98**, 3103 (1993).

[5] Go. Torres-Vega, J. Chem. Phys. **98**, 7040 (1993).

[6] Go. Torres-Vega, J. Chem. Phys. **99**, 1824 (1993).

N95-13932

# PARTICLE LOCALIZATION, SPINOR TWO-VALUEDNESS, AND FERMI QUANTIZATION OF TENSOR SYSTEMS

Frank Reifler

Randall Morris

*Martin Marietta*

*Government Electronic Systems*

*Borton Landing Road*

*Moorestown, NJ 08057*

## Abstract

Recent studies of particle localization show that square-integrable positive energy bispinor fields in a Minkowski space-time cannot be physically distinguished from constrained tensor fields. In this paper we generalize this result by characterizing all classical tensor systems, which admit Fermi quantization, as those having unitary Lie-Poisson brackets. Examples include Euler's tensor equation for a rigid body and Dirac's equation in tensor form.

## 1. INTRODUCTION

It is a common misconception that fermions can only be represented in quantum field theory by bispinor fields. Recent studies of particle localization [1], [2], [3], [4] have shown that particle wave functions cannot vanish in regions of positive measure for any set of times of positive measure. This demonstrates that gedanken experiments, designed to observe the two-valuedness of bispinors, are not physically realizable since such experiments require absolute isolation of particle wave functions [4], [5], [6].

Moreover, in previous work we showed that square-integrable positive energy bispinor fields in a Minkowski space-time cannot be physically distinguished from constrained tensor fields. That is, the non-localization of particle wave functions implies that the two-valuedness of bispinors is unobservable in a Minkowski space-time. Thus, beam splitting experiments designed to observe the rotation properties of bispinors, in fact, describe the rotation properties of constrained tensor fields [4].

Furthermore, it was shown that Dirac's bispinor equation can be expressed, in an equivalent tensor form, as a constrained Yang-Mills equation in the limit of an infinitely large coupling constant. It was also shown [4], [7] that the free tensor Dirac equation is a completely integrable classical Hamiltonian system with (non-canonical) unitary Lie algebra type Poisson brackets, from which Fermi quantization can be derived directly without using bispinors.

In this paper we generalize this result by characterizing all classical tensor systems which admit Fermi quantization. As shown in Section 2, these tensor systems have Lie algebra type Poisson brackets

associated with a unitary symmetry group acting on the classical phase space. Two examples of classical tensor systems which admit Fermi quantization are Euler's equations for a rigid body and the tensor form of Dirac's equation. It is well known that Euler's equation can be Fermi (or Bose) quantized [8]. It is less well known that Dirac's equation can be written in a classical tensor form which can be directly Fermi quantized in the same manner as Euler's tensor equation.

## 2. FERMI QUANTIZATION OF CLASSICAL TENSOR SYSTEMS

In this section, Fermi quantization is derived for the Euler and Dirac tensor equations by representing their classical Lie-Poisson brackets as commutators of Heisenberg operators on a Fock space of Fermi occupation states.

We define a Fock space, that is, a Hilbert space $\mathcal{H}$ of occupation states of a single field, which is suitable for both fermions and bosons, as follows. We suppose that there exists a denumerable set of operators $A_p$, where $p = 1, 2, 3, \ldots$, such that all $A_p$ and their adjoints $A_p^*$ are defined on an invariant dense subspace $\mathcal{D} \subset \mathcal{H}$. For the fermion case, the operators $A_p$ and $A_p^*$ will be bounded, in which case $\mathcal{D} = \mathcal{H}$.

For each pair of indices p and q we define:

$$N_{pq} = A_p^* A_q \tag{1}$$

which is an operator defined on $\mathcal{D}$. The following can be taken as a set of axioms which are satisfied by fermions and bosons alike, when $p = 1, 2, 3, \ldots$ is interpreted as an index labelling the degrees of freedom (modes) of a single field, $N_p = N_{pp}$ as the occupation number operator, and $A_p^*$ and $A_p$ as creation and annihilation operators for the mode p.

a) There is a zero-occupancy state in $\mathcal{D}$, denoted by $|0\rangle$, such that for all modes p:

$$A_p |0\rangle = 0 \tag{2}$$

Furthermore, there are at least two distinct modes p and q such that $A_p \neq A_q$, and none of the operators $A_p$: $\mathcal{D} \rightarrow \mathcal{D}$ are the zero operator.

b) There are no states in $\mathcal{H}$ (except 0) which are orthogonal to all the occupation states:

$$|n_1, n_2, \ldots\rangle = (A_1^*)^{n_1} (A_2^*)^{n_2} \ldots |0\rangle \tag{3}$$

where $n_p = 0, 1, 2, \ldots$ is the occupation number for the mode p, and all but a finite number of $n_p$ are zero.

c) For all modes p, q, and r, the operators $N_{pq}$ and $A_r$ satisfy the following commutation relation on $\mathcal{D}$:

$$[N_{pq}, A_r] = -A_q \delta_{pr} \tag{4}$$

and its adjoint on $\mathcal{D}$

$$[N_{pq}, A_r^*] = A_p^* \delta_{rq} \tag{5}$$

where $\delta_{pq}$ equals one if $p = q$ and equals zero otherwise.

Note that axiom (c) is required for a quantum field theory in which field operators (Fermi or Bose) satisfy Heisenberg's equation [9]. Note also that axiom (c) does not involve any anti-commutation relations, and hence is applicable to tensor systems. We can prove that any Fock space satisfying (a), (b), and (c) is either Fermi or Bose, and for a given set of modes, the Fermi and Bose Fock spaces satisfying axioms (a), (b), and (c) are unique up to isomorphism [10].

Axioms (a) and (c), or equivalent axioms, are assumed in more general Fock spaces which have been used to derive parastatistics [10]. However, the parastatistical Fock spaces do not assume axiom (b). That is, in a parastatistical Fock space, there is more than one state for each set of occupation numbers. Since from the current state of knowledge, one can assume that the occupation numbers $n_1, n_2, \ldots$ determine a unique state $|n_1, n_2, \ldots>$, we do not consider Fock spaces with alternatives to axiom (b).

For a Fermi Fock space we add:

d) For each mode p, the occupation number $n_p = 0, 1$.

As a consequence of axiom (d), $A_p$ and $A_p^*$ are bounded operators defined on $\mathcal{H}$ (i.e., $\mathcal{D} = \mathcal{H}$).

Fermi quantization of tensor fields is derived from the following theorem:

THEOREM 1:

Given any denumerable set of modes p, q, r, s, . . ., there exists a Fermi Fock space $\mathcal{H}$ (unique up to isomorphism) satisfying (a), (b), (c), and (d). Moreover, let $\hat{H}$ be a self-adjoint operator whose domain is a dense subspace of $\mathcal{H}$. Then there exist operators $\hat{a}_{pq}(t)$ defined on $\mathcal{H}$, indexed by each pair of modes p an q, and depending on time $t \in R$ satisfying:

i) The adjoint relation:

$$\hat{a}_{pq}^* = \hat{a}_{qp} \tag{6}$$

ii) The (equal time) commutation relation:

$$[\hat{a}_{pq}, \hat{a}_{rs}] = \hat{a}_{ps} \delta_{rq} - \hat{a}_{rq} \delta_{ps} \tag{7}$$

iii) The Heisenberg equation:

$$\frac{d\hat{a}_{pq}}{dt} = -i [\hat{a}_{pq}, \hat{H}] \tag{8}$$

PROOF:

The (unique) Fermi Fock space exists by explicit construction [10]. Since $\hat{H}$ is self-adjoint, we may define the following operators on $\mathcal{H}$:

$$\hat{a}_{pq}(t) = e^{i\hat{H}t} N_{pq} e^{-i\hat{H}t} \tag{9}$$

Formulas (6) and (7) follow from formulas (1), (4), and (5). Formula (8) follows by differentiating formula (9) with respect to time t. Q.E.D.

Note that by formulas (6) and (7), the operators $\hat{a}_{pq}(t)$ generate a unitary Lie algebra [11]. For example, in the case of two modes, linear combinations of $\hat{a}_{pq}(t)$ for p, q = 1, 2 satisfy the commutation relations of angular momentum operators [12], which allows Euler's tensor equation to be Fermi quantized [8]. The following corollary of Theorem 1 characterizes all classical systems that can be Fermi quantized.

COROLLARY:

Classical systems that can be Fermi quantized are described by bimodal complex amplitudes[1] $a_{pq}(t)$ satisfying:

$$a_{pq}(t) = \overline{a_{qp}(t)} \tag{10}$$

(where the bar denotes ordinary complex conjugation), and a Hamiltonian function $H = H(a_{pq})$ which depends on the amplitudes $a_{pq}(t)$, such that the Hamiltonian equation is given by:

$$\frac{da_{pq}}{dt} = \{a_{pq}, H\} \tag{11}$$

where the Lie-Poisson brackets { , } are defined by:

$$\{a_{pq}, a_{rs}\} = -i\,(a_{ps}\,\delta_{rq} - a_{rq}\,\delta_{ps}) \tag{12}$$

Furthermore, Fermi quantization of such classical systems is unique up to isomorphism.

The chief application of Theorem 1 is the Fermi quantization of Dirac's equation in its tensor form. As previously shown [4], there is a double covering map which takes a bispinor field $\psi$ to a constrained set of SL(2,C) × U(1) gauge potentials $A^K_\alpha$ and a complex scalar field $\rho$, where Lorentz indices are denoted by $\alpha, \beta, \gamma = 0, 1, 2, 3$ and gauge indices by J, K, L = 0, 1, 2, 3. Repeated indices will be contracted using Minkowski metrics $g_{\alpha\beta}$ and $g_{JK}$. Since the Lie algebra of SL(2,C) is regarded as the complexification of the Lie algebra of SU(2), the gauge potentials $A^j_\alpha$ for j = 1, 2, 3 are complex, while the U(1) gauge potential $A^0_\alpha$ is real. $A^K_\alpha$ and $\rho$ satisfy the following constraint:

---

1 Note that the set of observables $\{a_{pq}\}$ defines a complex phase space $P_c$ for the classical system, which is a Lie algebra under the Lie-Poisson brackets (12). In general, the "physical" phase space P need not coincide with $P_c$. All that is needed is that P have Lie-Poisson brackets, and there is a homomorphism of $P_c$ onto P. All observables of P thus become observables of $P_c$. For a more complete discussion of Lie-Poisson brackets see reference [13].

$$A^K_\alpha \, A_{K\beta} = -|\rho|^2 \, g_{\alpha\beta} \tag{13}$$

With this constraint, Dirac's equation is obtained from the following Yang-Mills Lagrangian $L_g$ in the limit of an infinitely large coupling constant g:

$$L_g = -\frac{1}{4} \, \mathrm{Re} \, [A^{\alpha\beta}_K \, A^K_{\alpha\beta}] + \overline{(D_\alpha \rho)} \, (D^\alpha \rho) \, - \frac{g^2}{2} \, |\rho + 2m|^4 \tag{14}$$

where mg is the mass, and the covariant derivative $D_\alpha$ and curvature tensor $A^K_{\alpha\beta}$ are given by:

$$\begin{aligned} D_\alpha \rho &= \nabla_\alpha \rho + ig \, A^0_\alpha \rho \\ A^0_{\alpha\beta} &= \nabla_\alpha A^0_\beta - \nabla_\beta A^0_\alpha \\ \vec{A}_{\alpha\beta} &= \nabla_\alpha \vec{A}_\beta - \nabla_\beta \vec{A}_\alpha - g \, \vec{A}_\alpha \times \vec{A}_\beta \end{aligned} \tag{15}$$

where we denote $A^K_\alpha = (A^0_\alpha \, , \, \vec{A}_\alpha)$ with $\vec{A}_\alpha = (A^1_\alpha \, , \, A^2_\alpha \, , \, A^3_\alpha)$, and $\nabla_\alpha$ denotes the space-time partial derivatives. The tensor form of Dirac's equation L is given by:

$$L = \lim_{g \to \infty} \, g^{-1} \, L_g \tag{16}$$

By standard Yang-Mills formulas, we obtain the energy-momentum tensor $T^{\alpha\beta}_g$, the spin-polarization tensor $S^{\alpha\beta\gamma}_g$, and the electric current $J^\alpha_g$ derived from $L_g$. The corresponding bispinor observables, denoted by $T^{\alpha\beta}$, $S^{\alpha\beta\gamma}$, and $J^\alpha$, are given by (see formula (16)):

$$T^{\alpha\beta} = \lim_{g \to \infty} \, g^{-1} \, T^{\alpha\beta}_g \tag{17}$$

and similarly for $S^{\alpha\beta\gamma}$ and $J^\alpha$.

For quantum theory in a Minkowski space-time, it suffices [4] to consider tensor fields $(A^K_\alpha, \rho)$ that: (i) are enclosed in an arbitrarily large cube $K \subset R^3$ and (ii) satisfy periodic boundary conditions for all times $t \in R$. We quantize $(A^K_\alpha, \rho)$ by considering the classical fields to be defined on $K \times R$, and by defining the classical Hamiltonian H to be:

$$H = \int_K T^{00} \, (\vec{x}, t) \, d\vec{x} \tag{18}$$

where $T^{\alpha\beta}$ is the energy-momentum tensor (17), and where points in $K \subset R^3$ are denoted by $\vec{x} = (x^1, x^2, x^3)$ and $\vec{d}x = dx^1 \, dx^2 \, dx^3$ denotes the volume measure of K. Note that by conservation of energy, the Hamiltonian H is independent of time t.

By the map from bispinors to tensors [4], $T^{\alpha\beta}$, $S^{\alpha\beta\gamma}$, and $J^\alpha$ have expansions of the form:

$$T^{\alpha\beta} \, (\vec{x}, t) = \sum_p \sum_q \, T^{\alpha\beta}_{pq} \, (\vec{x}) \, a_{pq}(t) \tag{19}$$

(and similarly for $S^{\alpha\beta\gamma}$ and $J^{\alpha}$) where the sum is over all pairs of fermion modes p and q, and the amplitudes $a_{pq}(t)$ are complex functions of time satisfying the complex conjugate relation (10). The coefficients of the amplitudes $a_{pq}(t)$, denoted by $T^{\alpha\beta}_{pq}(\vec{x})$, are fixed complex functions of $\vec{x} \in K$. Thus, at any time t, the amplitudes $a_{pq}(t)$ suffice to specify $T^{\alpha\beta}$ (and similarly, $S^{\alpha\beta\gamma}$ and $J^{\alpha}$), and hence can be considered as classical phase space variables. Substituting (19) into formula (18), we get:

$$H = \sum_{p} \omega_p a_{pp} \tag{20}$$

where $\omega_p$ is the frequency of the mode p. The classical Hamiltonian equations (which are equivalent to the Euler-Lagrange equation for the tensor Dirac Lagrangian (16)) are given by formulas (10), (11), (12), and (20) which, by the corollary to Theorem 1, can be (uniquely) Fermi quantized.

This then reproduces the existing second quantized theory for fermions. This also shows that bispinors are not more fundamental than the tensor Hamiltonian equations (10), (11), (12), and (20), which we derived from the tensor Dirac Lagrangian (16).

## REFERENCES


1. G.C. Hegerfeldt, and S.N.M. Ruijsenaars, "Remarks on causality, localization, and spreading of wave packets," *Phys.* Rev. D, Vol. 22, No. 2 (15 July 1980), pp. 377-384.
2. G.C. Hegerfeldt, "Difficulties with causality in particle localization," Nuclear Physics B (Proc. Suppl.) 6 (1989), pp. 231-237.
3. A. Vogt and F. Reifler, "Unique continuation of some dispersive waves," Communications in Partial Differential Equations, (to appear).
4. F. Reifler and R. Morris, "Unobservability of Bispinor Two-Valuedness in Minkowski Space-time," *Ann. Physics* (N.Y.), Vol. 215, No. 2 (1992), pp. 264–276.
5. R. Geroch, "Spinor structure of space-times in general relativity I," J. of Math. Phys., Vol. 9, No. 11 (1968), pp. 1739-1744.
6. R. Penrose and W. Rindler, *Spinors and Space-Time, Volume 1*, Cambridge University Press, Cambridge (1986), pp. 46-47.
7. F. Reifler and R. Morris, "The Hamiltonian structure of Dirac's equation in tensor form and its Fermi quantization," Workshop on Squeezed States and Uncertainty Relations, NASA 3135 (1992), pp. 381-383.
8. D. Park, *Classical Dynamics and its Quantum Analogues*, Springer-Verlag, Berlin (1990), pp. 274-278.
9. F. Mandl and G. Shaw, *Quantum Field Theory*, John Wiley and Sons, New York (1984), pp. 62-64.
10. O.W. Greenberg and A. Messiah, "Selection rules for parafields and the absence of para-particles in nature," *Physical Review*, Vol. 138, No. 5B (1965), pp. 1155-1167.
11. B.G. Wybourne, *Classical Groups for Physicists*, John Wiley and Sons, New York (1974), pp. 270.
12. G. Baym, *Lectures on Quantum Mechanics*, Benjamin, Reading (1978), pp. 380-386.
13. J.E. Marsden, *Lectures on Mechanics*, Cambridge University Press, Cambridge (1992), pp. 4-11.

# SECTION 5

# UNCERTAINTY RELATIONS

# QUANTUM PHASE UNCERTAINTIES IN THE CLASSICAL LIMIT

J.D. Franson

*Applied Physics Laboratory, The Johns Hopkins University, Laurel, Maryland 20723*

**Abstract**

Several sources of phase noise, including spontaneous emission noise and the loss of coherence due to which-path information, are examined in the classical limit of high field intensities. Although the origin of these effects may appear to be quantum-mechanical in nature, it is found that classical analogies for these effects exist in the form of chaos.

## 1. Introduction

There are several sources of phase noise that may appear to be inherently quantum-mechanical in nature. One example is spontaneous emission noise, which is often attributed to vacuum fluctuations. Another example is the loss of coherence in which-path experiments, which can be shown to be due to the entanglement of one particle with another.

This paper addresses the question of whether or not these effects continue to exist in the macroscopic limit of high-intensity fields. If so, do they agree with the predictions of classical physics in that limit?

One motivation for considering these questions is to gain further insight into the origin of these effects. In addition, any disagreement with classical physics in the macroscopic limit would suggest an interesting experimental test of quantum mechanics in a new and untested situation.

It will be found that a classical analysis of these systems does give analogous effects due to classical chaos. This suggests that there is at least a loose connection between quantum noise and classical chaos.

On the other hand, classical physics cannot provide any analogy for nonlocal effects such as violations of Bell's inequality. The generalization of two-photon interferometry to high-intensity fields will be briefly discussed as an example of a situation in which no classical description exists even in the

macroscopic limit.

## 2. Which-Path Experiments

Wave-particle duality suggests that we cannot determine the path that a particle has taken through an interferometer without destroying the interference pattern. In most cases, it can be shown that the loss of coherence is actually due to the entanglement of the particle's wave function with a second particle or system located in one path or the other. No actual observation of the path taken is necessary in order to eliminate the interference pattern. An interesting feature of these which-path experiments is that it is often possible to restore the interference pattern using a "quantum eraser"[1].

An excellent example of a which-path experiment is shown in Figure 1. As suggested by Scully[2] et al., a single atom is incident upon a beam splitter that divides its wave function along two separated paths. A microwave cavity is located in each path and is coupled to the atom in such a way that a low-energy microwave photon will be emitted into whichever cavity the atom passes through.

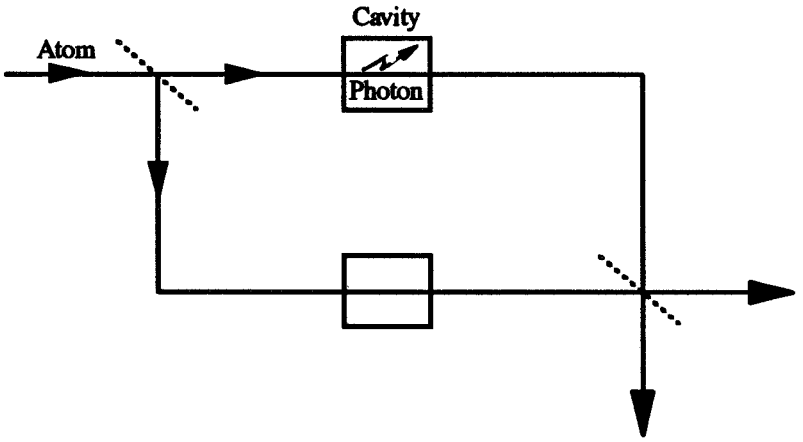


Fig. 1. A which-path experiment suggested by Scully et al. (Ref. 2) in which a microwave cavity is located in each arm of an atomic interferometer.

The interference pattern must be destroyed, since the path of the atom can be determined by detecting the location of the photon.

It can be shown that the change in the center-of-mass wave function of the atom has no significant effect and that the coherence is destroyed by the entanglement of the atom with the photon.

It is obvious that there can be no classical analogy for this kind of which-path experiment because an atom cannot be described by a wave in classical physics. But this begs the question of what is really responsible for the loss of coherence.

In order to allow a comparison with classical physics, consider instead the situation shown in Figure 2 in which the roles of the atom and photon have been interchanged[3]. Now a single photon is incident upon a beam splitter and its wave function propagates along two separated paths. A thin chamber containing gas atoms is located in each path and it is assumed that the photon is inelastically scattered, producing a secondary photon of low energy. The initial photon propagates with somewhat reduced energy toward a beam splitter and a single-photon detector. Once again, it can be shown that the change in the photon's wave function is irrelevant as long as $\delta k \delta x << \pi$, where $\delta k$ is the change in wave number and $\delta x$ is the thickness of the two chambers. The advantage of this which-path experiment is that it does allow a classical analysis if a large number of photons are incident, which corresponds to a classical light wave.

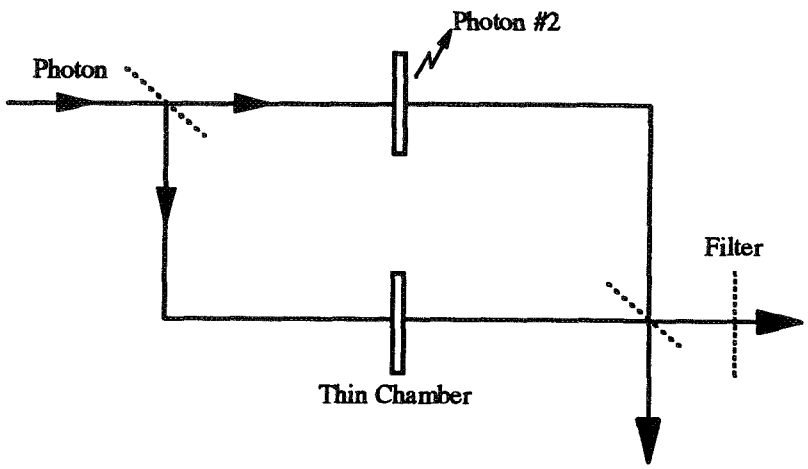


Fig. 2. A modified which-path experiment in which the roles of the atoms and photons have been interchanged to allow a comparison with classical physics.

The quantum-mechanical calculation is straightforward and has been described in more detail elsewhere[3]. Consider an operator $p^{\dagger}$

that creates a single photon in a short gaussian wave packet:

$$p^\dagger = \sum_i \beta_i a_i^\dagger \tag{1}$$

Here $\beta_i$ are complex coefficients and $a_i^\dagger$ creates a photon of frequency $\omega_i$. In order to achieve the macroscopic limit of high intensities, the quantum state will be taken to be a coherent state of the form

$$|\Psi_0\rangle = \gamma \sum_n \frac{(\alpha p^\dagger)^n}{n!} |0\rangle = \gamma \prod_i e^{\alpha \beta_i a_i^\dagger} |0\rangle \tag{2}$$

where $\alpha$ is a complex number sufficiently large that the pulse contains a large number of photons. The interaction Hamiltonian is given by

$$H' = \sum_i \sum_{jk} \epsilon_{ijk} (b_k^\dagger b_j^\dagger b_i + c_k^\dagger c_j^\dagger c_i) + h.c. \tag{3}$$

Here the operators b and c annihilate photons in the two paths through the interferometer and $\epsilon_{ijk}$ is a coefficient of no interest.

The intensity at the detector can then be shown to be

$$\langle I(x,t) \rangle = \langle E^- E^+ \rangle = \gamma' \sum_{ij} \sum_{i'j'} e^{i[(k_{j'} - k_j)x - (\omega_{j'} - \omega_j)t]} \epsilon^*_{ijk} \epsilon_{i'j'k'} \beta^*_i \beta_{i'} \tag{4}$$
$$(\alpha^* \alpha \langle b_k | b_{k'} \rangle + \alpha'^* \alpha' \langle c_k | c_{k'} \rangle - \alpha'^* \alpha \langle c_k | b_{k'} \rangle - \alpha^* \alpha' \langle b_k | c_{k'} \rangle)$$

The last two terms are the only ones that depend on the relative phase, as reflected by the coefficients $\alpha$ and $\alpha'$, and are proportional to the inner product of two states containing a photon in two different paths, which is zero. Thus the entanglement of the original photon with a secondary photon in one path or the other is responsible for destroying the interference pattern, as expected.

It is interesting to note, however, that it is not possible, even in principle, to determine which path a photon has taken, since the quantum uncertainty in the energy and number of photons in the coherent state of eq. (2) makes it impossible to associate the detected photons with individual secondary photons.

Any classical description of this experiment must be based on a nonlinear model, since a linear system cannot produce any change in the frequency of the light. With this in mind, consider a simple model consisting of three nonlinearly-coupled harmonic oscillators:

$$\begin{aligned} \ddot{x}_i &= -\omega_i^2 x_i + 4\epsilon (x_i - x_k)^3 - \eta \dot{x}_i + d(t) \\ \ddot{x}_j &= -\omega_j^2 x_j - 4\epsilon (x_k - x_j)^3 - \eta \dot{x}_j \\ \ddot{x}_k &= -\omega_k^2 x_k - 4\epsilon (x_i - x_k)^3 + 4\epsilon (x_k - x_j)^3 - \eta \dot{x}_k \end{aligned} \tag{5}$$

The three frequencies $\omega_i$, $\omega_j$, and $\omega_k$ correspond to the frequencies of the three light beams in Figure 2, $\epsilon$ and $\eta$ are adjustable constants, and d(t) represents an external driving field. This model is not intended to provide a realistic description of the response of an atom to an incident beam of light but does illustrate the kind of behavior that can occur in classical systems. It may be worth noting, for example, that the Coulomb force is a nonlinear function of the separation of two particles and naturally gives rise to nonlinear effects of this kind.

It was assumed that a nonlinear system of this kind is located in each path of Figure 2 and the above set of equations was solved numerically[3] for the case in which the incident field has frequency $\omega_d$. The resulting power spectral density for a sufficiently intense incident field is shown in Figure 3 and has a sharp peak at the incident frequency as well as a somewhat broader peak corresponding to fluorescence, as in the quantum description. The phase-space trajectory of the out-going field $x_j$ is plotted in Figure 4, where it can be seen that the motion is chaotic and unpredictable. This randomizes the phase of the field in a manner that is also similar to the quantum treatment.

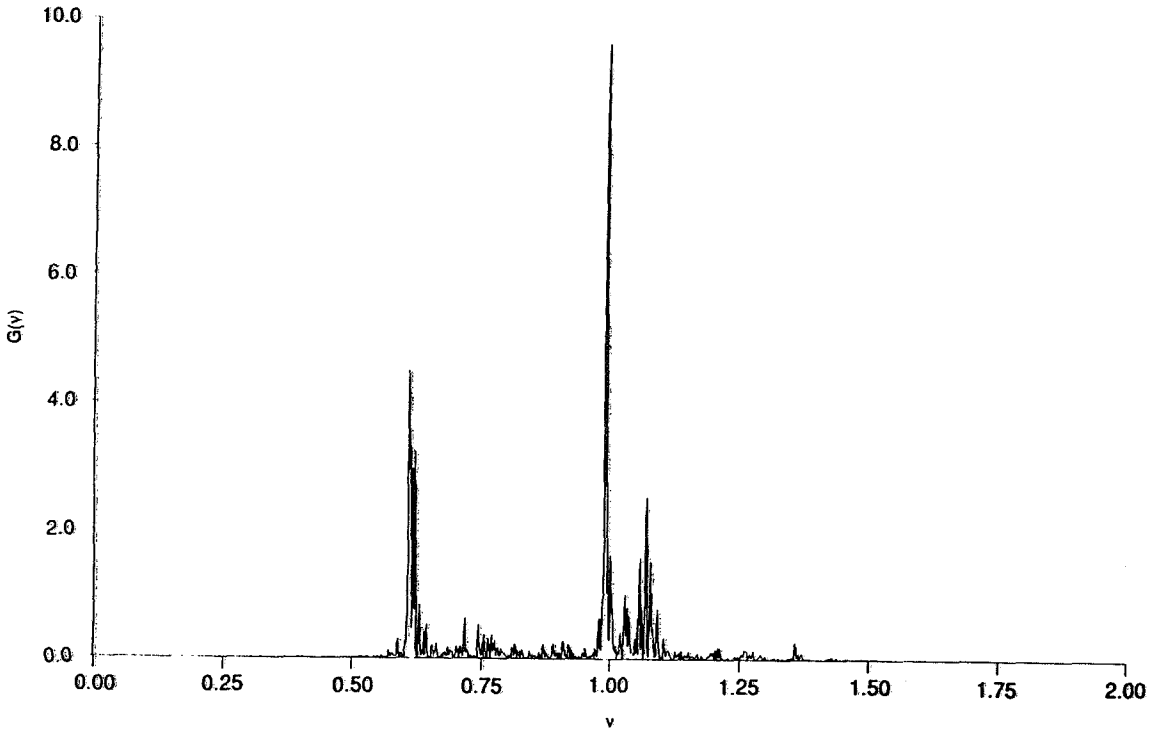


Fig. 3. Power spectral density $G(\nu)$ obtained from the classical model, showing the classical analog of fluorescence.

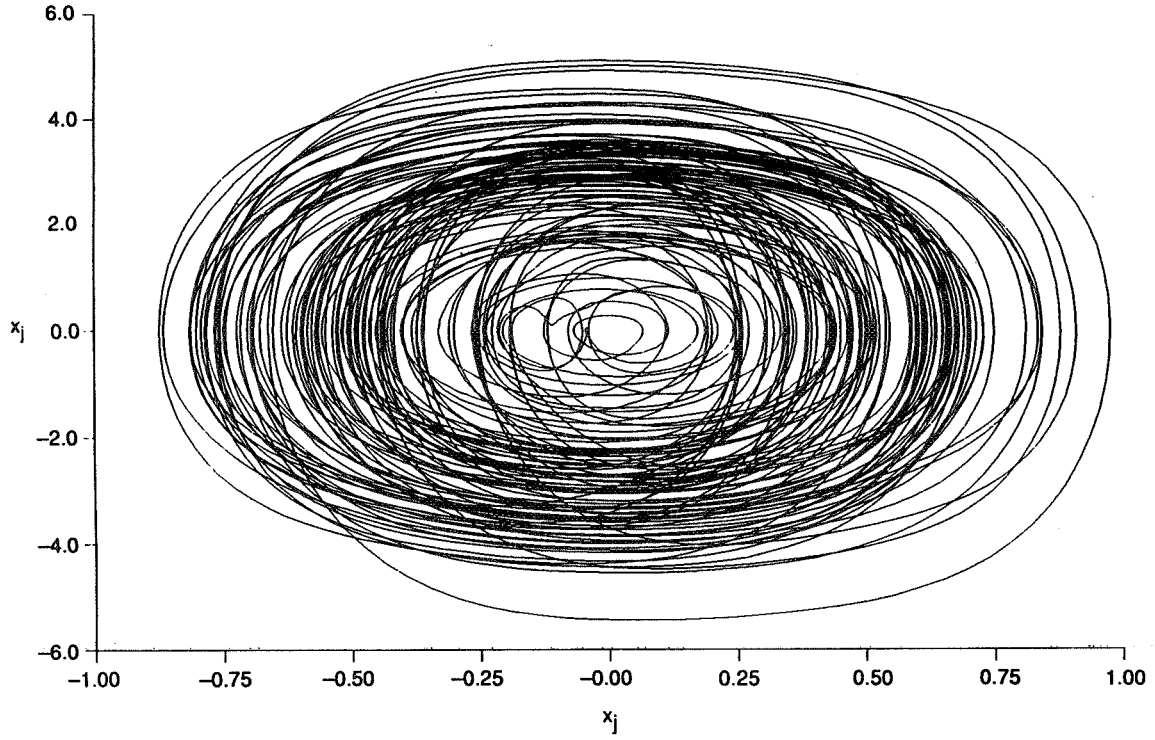


Fig. 4. Chaotic phase-space trajectory from the classical model, which randomizes the phase and destroys the interference pattern.

In the limit of low drive intensities the classical model produces a coherent response with no fluorescence. At sufficiently high intensities, chaos produces fluorescence at two frequencies that are analogous to the secondary photon and forward-propagating photons in Figure 2, both of which have random phase. Intermediate intensities produce more complicated behavior, including partial coherence at rational fractions of the drive frequency.

Thus the classical model gives loss of the interference pattern due to chaos in the macroscopic limit of high intensities. This suggests that there is at least a loose connection between quantum noise and classical chaos. It is important to note, however, that the classical model produces a random phase only for sufficiently high intensities, whereas a proper quantum-mechanical treatment eliminates the coherence for arbitrarily low intensities.

In many systems of this kind it is possible to implement a "quantum eraser" to restore the interference pattern[1]. This can be accomplished by letting the entangled secondary systems propagate

in time, measuring their state at some subsequent time, and selecting only those events for which the secondary systems were found to be in the same final state. For example, a quantum eraser can be implemented for the micro-maser cavity experiment shown in Figure 1 by connecting the two cavities with a small hole containing an atom and then selecting only those events for which the photon in one cavity or the other was absorbed by this atom.

Surprisingly enough, it may be possible to perform a similar procedure in the classical model discussed above. Suppose we consider a subset of the phase-space trajectories for which the other (non-detected) variables are the same in the two paths, i.e.

$$x_1 = x_1' \qquad (6)$$
$$x_2 = x_2'$$

where the primed and unprimed variables refer to the two different paths. In that case, it seems likely that

$$x_3 = x_3' \qquad (7)$$

If so, the out-going fields would be the same in the two paths and the coherence would be restored.

## 3. Spontaneous Emission Noise

The random phase associated with spontaneous emission of a photon by an atom is often attributed to vacuum fluctuations. Once again, this may seem to be inherently quantum-mechanical in nature. But returning to the example shown in Figure 2, it can be seen that both photons emitted by an atom in one path or the other of that interferometer are emitted by spontaneous emission. The classical model discussed above gave a random phase for both of these fields due to classical chaos in the limit of high field intensities, which is in qualitative agreement with the quantum-mechanical result.

This further suggests that there may be some connection between quantum noise and classical chaos. It must be kept in mind, however, that the classical model cannot produce these kinds of results in the limit of low intensities.

## 4. Nonlocal Effects

The preceding discussion suggests that certain kinds of quantum phase noise may have a classical analogy in the form of chaos. This analogy can only be taken so far, however, since the models used do not provide a realistic description of an atom and are qualitatively similar to the quantum-mechanical treatment only in the limit of high intensities.

In addition, quantum systems can exhibit nonlocal effects that violate Bell's inequality and obviously have no classical analog. Such effects are not limited to low-intensity fields, as can be

illustrated by considering the generalization of two-photon interferometry[4] to high-intensity fields as illustrated in Figure 5. A somewhat similar situation involving photon polarizations has also been discussed by Reid and Munro[5].

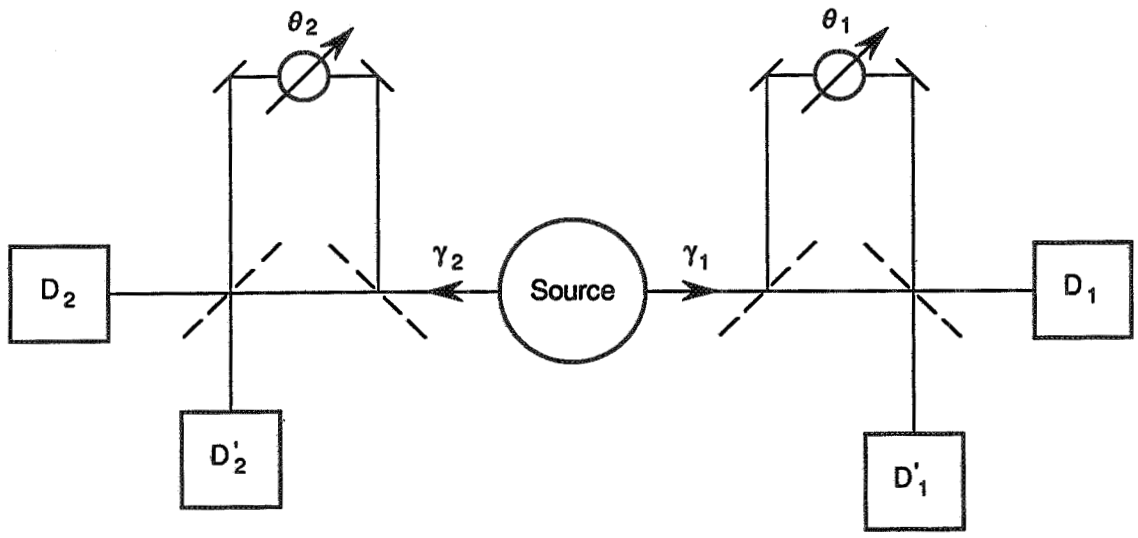


Fig. 5. Nonlocal interferometer consisting of two identical interferometers with a short path and a long path, capable of operation with high-intensity fields.

Nonlocal interferometry with high-intensity fields has been discussed in detail elsewhere[6] and only the main results will be reviewed here. Consider a quantum state of the electromagnetic field given by

$$|\Psi\rangle = \gamma \sum_n \frac{(\alpha c^\dagger)^n}{n!}|0\rangle = \gamma e^{\alpha c^\dagger}|0\rangle \tag{8}$$

where

$$c^\dagger = \sum_k f_k a_k^\dagger b_{k_0-k}^\dagger \tag{9}$$

Here $c^\dagger$ creates a pair of entangled photons in two paths via photon creation operators $a^\dagger$ and $b^\dagger$, $\gamma$ is a normalization constant, $\alpha$ is a

large complex number, and the coefficients $f_k$ describe the effects of filters inserted into the two beams.

Although eq. (8) resembles a coherent state, its properties are quite different. The probability $P_1$ of detecting a pair of coincident photons in the corresponding output ports of the two interferometers of Figure 5 can be shown to be given by

$$P_1 = \eta \cos^2\left[\frac{\phi_A+\phi_B+\omega_0\Delta t}{2}\right] \tag{10}$$

This is the same result obtained previously for the weak-field case but here the field can be extremely intense and contain a large number of photons.

The probability $P_N$ of detecting N pairs of coincident photons in the corresponding output ports of the two interferometers is

$$P_N = N!\,\eta^N \cos^{2N}\left[\frac{\phi_A+\phi_B+\omega_0\Delta t}{2}\right] = N!\,P_1^N \tag{11}$$

Eq. (11) also violates Bell's inequality. The factor of N! is due to the different ways in which photons can pair with each other and greatly enhances the probability of detecting a large number of pairs. No single pnoton detectors are required to observe such events, which correspond to large bursts of energy in the corresponding interferometer ports and which could be observed, at least in principle, with a bolometer. These effects are truly macroscopic in nature in that sense.

It is also possible to consider an EPR paradox involving quantum phase measurements performed on high-intensity fields with initially uncertain phases. Both classical and non-classical effects are obtained, as described elsewhere[7].

## 5. Summary

Several sources of quantum phase uncertainty have been considered in the limit of high field intensities where a comparison with a classical treatment is possible. It was found that classical analogies exist for the loss of coherence due to which-path information as well as the quantum noise associated with spontaneous emission. In both of these cases classical chaos randomizes the phase in a manner that is at least qualitatively the same as in the quantum description.

This suggests that there may be a loose connection between quantum noise and classical chaos. The classical treatment is only valid in the limit of high intensities, however, which is not too surprising in that classical physics would not be expected to provide an adequate description at the quantum level. In addition, violations of Bell's inequalities can also occur for high-intensity fields. Nevertheless, there does appear to be an analogy between quantum noise and classical chaos.

This work was supported by the Office of Naval Research.

## References

1. M.O. Scully and K. Druhl, Phys. Rev. A **25**, 2208 (1982).

2. M.O. Scully, B.G. Englert, and H. Walther, Nature **351**, 111 (1991); M.O. Scully, B.G. Englert, and J. Schwinger, Phys. Rev. A **40**, 1775 (1989).

3. J.D. Franson, Phys. Rev. A **45**, 8074 (1992).

4. J.D. Franson, Phys. Rev. Lett. **62**, 2205 (1989); Phys. Rev. Lett. **67**, 290 (1991).

5. M.D. Reid and W.J. Munro, Phys. Rev. Lett. **69**, 997 (1992).

6. J.D. Franson, to appear in Phys. Rev. A.

7. J.D. Franson, submitted to Phys. Rev. A.

# HOW TO DETECT AN EXCITED ATOM
## without disturbing it
*or*
# HOW TO LOCATE A SUPER-MINE
## without exploding it

Lev Vaidman
*School of Physics and Astronomy*
*Tel-Aviv University, Tel-Aviv 69978 ISRAEL*

**Abstract**

Possible realistic implementations of a method for interaction-free measurements, due to Elitzur and Vaidman, are proposed and discussed. It is argued that the effect can be easily demonstrated in an optical laboratory.

## 1 How to locate a Super-Mine

A "Super-mine" is a device which explodes if *anything* touches it. Proton, electron, photon, neutrino,... anything that reaches the mine, with any energy, triggers an explosion. Our task is to locate the mine. We have to find out where it *is*, not where it was. We have to check that the mine is in a certain location without exploding it. We have no additional information, except that there is nothing else except mines in the region. We are allowed to fail in our procedure, i.e. to explode a mine. In that case we can try again, in another region. But our measurement has to be reliable: we must not be mistaken when we say that there is a mine.

The task seems to be impossible: the mine interacts with the external world only by explosion when it is "touched," so how it can be found without an explosion? In classical physics this task is certainly impossible, since its solution leads to a paradox: to find the mine you have to touch it, but if you touch it, it explodes. Nevertheless, quantum mechanics allows a simple solution, which was suggested recently by Elitzur and myself [1].

Our method is based on a particle interferometer analogous to the Mach-Zehnder interferometer used in classical optics. In principle, it can work with any type of particle. The particle reaches the first beam splitter which has transmission coefficient $\frac{1}{2}$. The transmitted and reflected parts of the particle's wave are then reflected by the mirrors and finally reunite at another, similar beam splitter (Fig. 1*a*). Two detectors collect the particles after they pass through the second beam splitter. We can arrange the positions of the beam splitters and the mirrors such that because of destructive interference, no particles are detected by one of the detectors, say $D_2$, and all are detected by $D_1$. We position the interferometer in such a way that one of the routes of the particle passes through the region of space where we want to detect the existence of a mine (Fig. 2*b*). We send a single particle through the system. There are three

possible outcomes of this measurement:

i) no detector clicks, ii) detector $D_1$ clicks, iii) detector $D_2$ clicks.

In the first case, the particle explodes the mine. The probability for this outcome is $\frac{1}{2}$. In the second case (for which the probability is $\frac{1}{4}$), the measurement does not succeed either. The particle could have reached $D_1$ in both cases: when the mine is, and when the mine is not located in one of the arms of the interferometer. In this case there has been no interaction with the object, so we can try again. Finally, in the third case, when the detector $D_2$ clicks (the probability for which is $\frac{1}{4}$), we have achieved our goal: we know that there is a mine inside the interferometer without exploding it. If we wish to specify by the interaction-free procedure the exact position of the mine inside the interferometer, we can test (locally) that except for that region, the interferometer is empty.

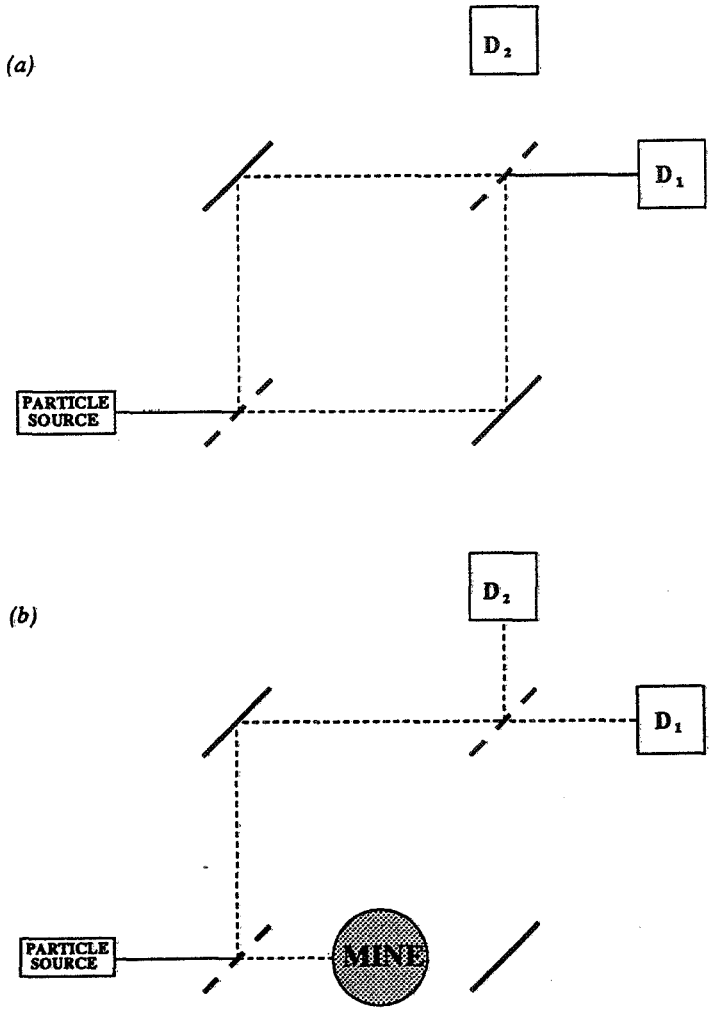


FIG. 1. ($a$) If there is no any object inside the interferometer, $D_2$ never clicks. ($b$). When $D_2$ clicks after sending just one particle we know that the mine is inside the interferometer and it is still intact.

## 2 What is the Probability for a Successful Experiment?

Even the ideal experiment does not always succeed. We have seen that the probability for success here is only 1/4. But we also have the probability 1/4 not to destroy the mine without finding it. Trying again and again, until success or an explosion, leads to the probability 1/3 of locating the mine without an explosion. We have shown [1] that by modifying the transmission coefficients of the beam splitters in the interferometer we can obtain (almost) the probability 1/2 for success.

This is, however, a gedanken experiment. A super-mine which is sensitive to everything, a Mach-Zehnder interferometer with complete destructive interference in one detector, a single particle source – these are not devices that can be found in a standard laboratory. Let us now discuss a few points which are relevant for a realization of the idea in a real laboratory.

We do not need a super-mine. The mine can be replaced by a fragile object which is nevertheless stable in the environment of the laboratory. It "explodes" (or clicks) if a photon with a certain energy hits it. Our task now is to detect the object without exploding it, using only such photons.

We do not need a source of single photons. We assume that the explosion (the click) is loud enough for us to hear, so all we need is a *weak* source of photons and *fast* switch that stops the beam when detector $D_2$ clicks. (The single-photon source is necessary if we want to locate an object and be sure that it was not disturbed in any way whatsoever, even if the object does not click.)

We do not need 100% efficiency in detector $D_2$. Of course, low efficiency will reduce the probability of detecting the object, but if the detector clicks, we are still 100% sure that the object is there.

If we have an ideal interferometer, then the photon which hits the object does not have to *invariably* explode it. It is enough for the photon to have just finite probability to be absorbed (to be scattered, to change its phase). Even the probability for the success remains unchanged, we only need to put more photons through the interferometer.

If we have an ideal equal-path interferometer, we do not need a monochromatic source: complete destructive interference occurs for all wavelengths.

Unfortunately, we do not have an ideal Mach-Zehnder interferometer. There is no possibility of obtaining 100% destructive interference in the detector $D_2$. Sometimes we will get clicks even if there is no object inside the interferometer. Also, we will get wrong clicks due to noise in the detector $D_2$.

What I have understood from my interaction with experimentalists [2] is that in a modern laboratory one can obtain the ratio of 1:100 for the number of clicks in the detectors $D_2$ and $D_1$ when there is no object inside the interferometer (instead of the theoretical 0 counts for detector $D_2$). This is the most important limitation on the proposed "interaction-free" measurement. The most optimistic estimate I heard [3] was the ratio of 1:1000. Therefore, we have to complete (one run of) our experiment while much fewer than a 1000 photons pass through the interferometer.

# 3 A Game

Consider a boy trying to catch a girl in a dark room. In order to catch her, he has to know where she is. But if she knows that she has been located, she has enough time to move to another location. She constantly looks in all direction, and any time she sees a photon, she moves. The girl can detect any photons the boy uses. Then, classically, the task of the boy is hopeless. However, quantum mechanics allows the boy to locate the girl without her being aware of, and thus, to catch her.

Let us now discuss a proposal for demonstration of such game in a laboratory. Instead of the girl we will take a high efficiency photo-detector. As I understand [4] there are detectors of up to 70% efficiency with noise of about one count per second. A student either puts or does not put this detector inside the interferometer. (Or, more realistically, she blocks or does not block the arm of the interferometer with a small mirror such that the reflected photons are absorbed by the photo-detector.) The output of the detector is connected to a bell. Our task is to find out if there is a detector without ringing the bell. We are allowed sometimes to fail, i.e. to ring the bell. Then we call the student to start everything from the beginning. But, when we claim that the detector is there, we must be correct with high probability.

In order to achieve this goal we tune the Mach-Zehnder interferometer for maximal destructive interference in detector $D_2$, see Fig. 2. We prepare a weak source of light (low intensity laser) such that it sends about $10^3$ photons per second. We add a fast electronic switch which stops the beam when the detector $D_2$ absorbs a photon. It is easy to get a switch with time of operation $\tau = 10^{-6}$sec. (Detector $D_1$ does not play any role in the experiment, so we can omit it.)

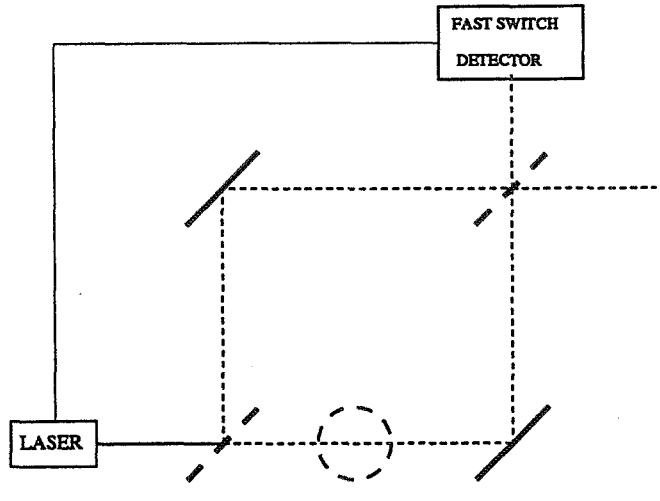


FIG. 2. A fast switch detector stops the beam when it detects a photon. We can learn about the existence of an object inside the interferometer by measuring the time it takes for the detector to click starting from the beginning of the run.

The experiment runs as follows: we switch on the laser and measure after what time the detector switch stops the laser. If it happens after about a second we can safely claim that the detector is not there: the probability for the mistake is about $2^{-1000}$. If, however, the time is about $10^{-3}$sec we can claim that the detector is there: the probability for a mistake now is also not large, about $10^{-3}$. If our device works properly, the only other probable outcome is that we will hear the bell first. If the detector is there, the probability for this is about 2/3. In this case we have to call the student to start again. But the other third is, roughly, the probability for a successful interaction-free measurement. It seems that all kind of noises which we have not taken into account cannot deny us a significant chance to perform this experiment successfully. If we are satisfied by a less reliable measurement (even 10% error is a sound experiment) we even do not need an extraordinarily precise Mach-Zehnder interferometer or ultrasensitive detectors.

# 4 How to Detect an Excited Atom

I believe that the proposed interaction-free measurement is more than just a demonstration of peculiarities of quantum mechanics. This is a measurement which can be performed on an infinitely fragile object without disturbing it in any way whatsoever. I believe that it can have practical applications. Now let us discuss one of the possible application: detecting an excited atom without changing its state.

Suppose we are going to investigate an exotic excited state which can be characterized by the ability to absorb a photon of certain energy. We want to know when an atom in such a state has appeared, but we do not want to change its state while detecting it. As far as we know, our method is the only one available. This is in contrast with the toy experiment of previous section where we always could locate the detector using photons which it cannot detect.

In order to detect an atom we can use exactly the same system, with laser and fast electronic switch on the detector (Fig. 2). But we encounter a serious problem: the cross section of absorption of a photon by an atom is much smaller than the cross section of the laser beam. Thus, many photons will come through the interferometer before one of them will be absorbed by the atom. Even more photons will pass before the click of detector $D_2$ signaling the existence of the excited atom. When more than 1000 photons pass the interferometer, we, most probably, will get a click just from noise, and therefore we will not be able to detect the atom. I am not familiar enough with the experimental possibilities, but there is hope of finding some focusing (squeezing ?) procedure to improve the ratio between the cross section for absorption and the cross section of the beam.

I have more hope in finding some other experimental implementations of interaction-free measurements. First, the Mach-Zehnder can be replaced by a Michelson-Morley interferometer, or any other two- (or several-) arm interferometer. But it can also be implemented in a single-beam interferometer with filters of polarization or some other degrees of freedom. Let me now state a general scheme for interaction-free measurements.

# 5 Generalization of Interaction-Free Measurement

Our task is to detect a system in a certain state, say $|\Psi\rangle$ . This state might cause some kind of explosion or destruction; destruction of a system, of a measuring device, or at least of the state $|\Psi\rangle$ itself. The states orthogonal to $|\Psi\rangle$ do not cause the destruction. Although the only physical effect of $|\Psi\rangle$ is an explosion which destroys the state, we have to detect it without any distortion. If we succeed in this task, we call the experiment an interaction-free measurement.

Let us assume that if the system is in a state $|\Psi\rangle$ and the measuring device is in a state $|\Phi_1\rangle$, we have an explosion. For simplicity, we will assume that if the state of the system is orthogonal to $|\Psi\rangle$ or the measuring device is in a state $|\Phi_2\rangle$ (which is orthogonal to $|\Phi_1\rangle$) than neither the system nor the measuring device changes their state:

$$\begin{aligned} |\Psi\rangle\ \ |\Phi_1\rangle &\rightarrow |explosion\rangle \\ |\Psi_\perp\rangle|\Phi_1\rangle &\rightarrow |\Psi_\perp\rangle|\Phi_1\rangle \\ |\Psi\rangle\ \ |\Phi_2\rangle &\rightarrow |\Psi\rangle\ \ |\Phi_2\rangle \\ |\Psi_\perp\rangle|\Phi_2\rangle &\rightarrow |\Psi_\perp\rangle|\Phi_2\rangle. \end{aligned} \tag{1}$$

Now, let us start with an initial state of the measuring device

$$|\chi\rangle = \alpha|\Phi_1\rangle + \beta|\Phi_2\rangle. \tag{2}$$

If the initial state of the system is $|\Psi\rangle$, then the measurement interaction is:

$$|\Psi\rangle|\chi\rangle \rightarrow \alpha|explosion\rangle + \beta|\Psi\rangle|\Phi_2\rangle = \alpha|explosion\rangle + \beta|\Psi\rangle(\beta^*|\chi\rangle + \alpha|\chi_\perp\rangle), \tag{3}$$

where $|\chi_\perp\rangle = -\beta^*|\Phi_1\rangle + \alpha|\Phi_2\rangle$. If, instead, the initial state of the system is orthogonal to $|\Psi\rangle$ , then the measurement interaction is:

$$|\Psi_\perp\rangle|\chi\rangle \rightarrow |\Psi_\perp\rangle|\chi\rangle. \tag{4}$$

To complete our measuring procedure we perform a measurement of the measuring device which distinguishes between $|\chi\rangle$ and $|\chi_\perp\rangle$. Since there is no component with $|\chi_\perp\rangle$ in the final state (4), it can be obtained only if the initial state of the system was $|\Psi\rangle$. This is also the final state of the system: we do not obtain $|\chi_\perp\rangle$ in the case of the explosion. The probability to obtain $|\chi_\perp\rangle$ (if the system was initially in the state $|\Psi\rangle$ ) is $|\alpha\beta|^2$. It is less than the probability for explosion, which is $|\alpha|^2$, but it is finite, and the ratio $|\beta|^2$ can be made as close as we want to 1. In this case, the measurements will detect the state $|\Psi\rangle$ with probability 1/2 (and with probability 1/2 will be the explosion).

A Mach-Zehnder interferometer (Fig. 3) is a particular implementation of this scheme. Indeed, the photon entering the interferometer can be considered a measuring device prepared by the first beam splitter in a state $|\chi\rangle = \frac{1}{\sqrt{2}}(|\Phi_1\rangle + |\Phi_2\rangle)$ at time $t_1$, where $|\Phi_1\rangle$ designates a photon moving in the lower arm of the interferometer, and $|\Phi_2\rangle$ designates a photon moving in the upper arm. Detector $D_2$ together with the second beam splitter tests for the state $|\chi_\perp\rangle = \frac{1}{\sqrt{2}}(|\Phi_1\rangle - |\Phi_2\rangle)$ at time $t_2$. Indeed, if the state $|\chi_\perp\rangle$ were measured at time $t_2$, it must be found with certainty.

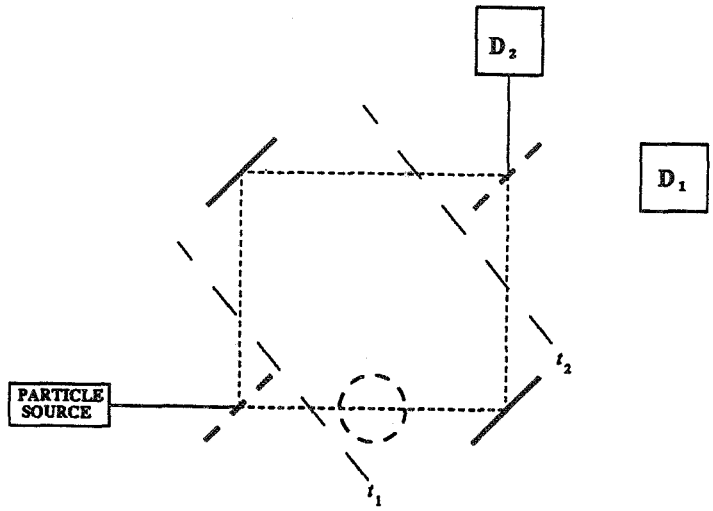


FIG. 3. The photon passing through the interferometer and detected by $D_2$ can be considered as a measuring device prepared at time $t_1$ in the state $|\chi\rangle = \frac{1}{\sqrt{2}}(|\Phi_1\rangle + |\Phi_2\rangle)$, and found at time $t_2$ in the state $|\chi_\perp\rangle = \frac{1}{\sqrt{2}}(|\Phi_1\rangle - |\Phi_2\rangle)$.

The difficulties of splitting and reuniting beams in the Mach-Zehnder interferometer can be avoided if our system is in a state $|\Psi\rangle$ which is sensitive, say, to a left circular polarization of light: it causes some kind of explosion, while right polarization causes no change. Then we can start with an $x$-polarized photon which interacts with the system and look for a $y$-polarized photon. If we do find such photon, we know that the system is in the state $|\Psi\rangle$.

Our method has remarkable property of not destroying infinitely fragile states and it is applicable to a wide class of physical systems. Therefore, although now we do not know where it can have practical applications, we are optimistic about finding such applications in the future.

# 6 Acknowledgements

It is a pleasure to thank Daniel Rohrlich and Avshalom Elitzur for very helpful suggestions. The research was supported in part by grant 425/92-1 of the the Basic Research Foundation (administered by the Israel Academy of Sciences and Humanities).

# References

[1] A. Elitzur and L. Vaidman, Found. Phys. **23**, 987 (1993).

[2] L. Mandel, A. Zeilinger, private communication.

[3] F. De Martini, private communication.

[4] P. Kwiat, private communication.

# THE STOKES LINE WIDTH AND UNCERTAINTY RELATIONS

A. I. Nikishov, V. I. Ritus
*Lebedev Physical Institute, Moscow 117924*

**Abstract**

For a function given by contour integral the two types (conventions) of asymptotic representations are considered: the usual representation by asymptotic series in inverse powers of large parameter and the special division of contour integral in contributions of high and low saddle points. It is shown that the width of the recessive term formation zone (Stokes strip) in the second convention is determined by uncertainty relation and is much less than the zone width in the first convention. The reasons of such a difference is clarified. The results of the work are useful for understanding of formation region of the exponentially small process arising on the background of the strong one.

## 1 Introduction

Many physical quantities are represented by contour integrals depending on two (or more) real parameters:

$$F(z) = A\int_C dt e^{f(t,z)}, \tag{1}$$

$z$ is one complex or a couple of two real parameters, $\nu$ and $\alpha$. The asymptotic representation of these integrals are considered when one of the parameters, $\nu$, tends to infinity where the integral has essential singularity, while another parameter, $\alpha$, is near the Stokes line [1] where $\alpha = 0$. We restrict ourselves to the case when $f(t,z)$ in (1) has only two saddle points $t_1$, $t_2$ where $f'(t_{1,2},z) = 0$, and denote

$$f_{1,2}(z) = f(t_{1,2},z), \qquad f''_{1,2}(z) = f''(t_{1,2},z). \tag{2}$$

Then the asymptotic representation consists of two terms:

$$F = D + R, \quad D \sim e^{f_2(z)}, \quad R \sim ig(z)e^{f_1(z)}, \quad \nu \gg 1. \tag{3}$$

The main (dominant) one $\sim e^{f_2}$ and the exponentially small relatively to it (recessive) one $\sim ige^{f_1}$, $\mathrm{Re}(f_2 - f_1) \gg 1$ when $\nu \gg 1$.

Qualitative distinction of the two terms lies in the different rates of change of their phases $\mathrm{Im}f_{1,2}(\alpha)$ with $\alpha$:

$$\omega_{1,2}(\alpha) = -\frac{\partial \mathrm{Im} f_{1,2}(\alpha)}{\partial \alpha}, \qquad \omega_1(0) \neq \omega_2(0). \tag{4}$$

Then from physical point of view $D$ and $R$ are the dominant and recessive waves with different frequencies $\omega_2$ and $\omega_1$ . Another qualitative distinction is the appearance (or disappearance) of $R$ when $\alpha$ crosses the Stokes line $\alpha = 0$. This appearance takes place in a certain interval $\Delta\alpha$ which may be called the Stokes line width [2,3,4]. According to these authors the switching function of recessive term coincides with error-function

$$g(\alpha) = \frac{1}{2}\mathrm{erfc}(w) = \frac{1}{\sqrt{\pi}}\int_w^\infty dx e^{-x^2}, \tag{5}$$

where $w = w(\alpha)$ is a certain odd function of $\alpha$, depending on convention [4] about dominant

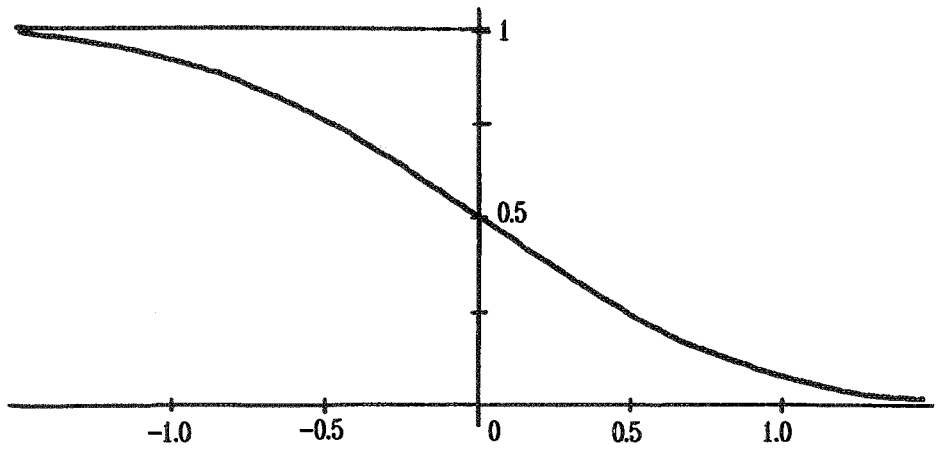


Figure 1:

term. The interval $\Delta\alpha$ defined by the condition

$$|w(\alpha)| \leq 1 \rightarrow \Delta\alpha \tag{6}$$

may be called the Stokes line width.

## 2 First convention about dominant and recessive terms

The 1-st convention [2,4] is based on asymptotic series expansion. Consider it on the example of standard Airy function expansion [5]

$$\mathrm{Ai}(z) = \frac{1}{2}\int_C dt e^{-i(zt+t^3/3)} \sim \frac{\sqrt{\pi}e^{-\zeta}}{2z^{1/4}}\sum_{k=0}^{\infty} c_k(-\zeta)^{-k}, \quad |\mathrm{arg}z| < \frac{2\pi}{3},$$

$$\sim \frac{\sqrt{\pi}e^{-\zeta}}{2z^{1/4}}\sum_{k=0}^{\infty} c_k(-\zeta)^{-k} + i\frac{\sqrt{\pi}e^{+\zeta}}{2z^{1/4}}\sum_{k=0}^{\infty} c_k\zeta^{-k}, \quad \frac{2\pi}{3} < \mathrm{arg}z < \frac{4\pi}{3}, \tag{7}$$

$$c_k = \frac{\Gamma(k+\frac{1}{6})\Gamma(k+\frac{5}{6})}{\pi 2^{k+1}k!}, \qquad \zeta = \frac{2}{3}z^{3/2}.$$

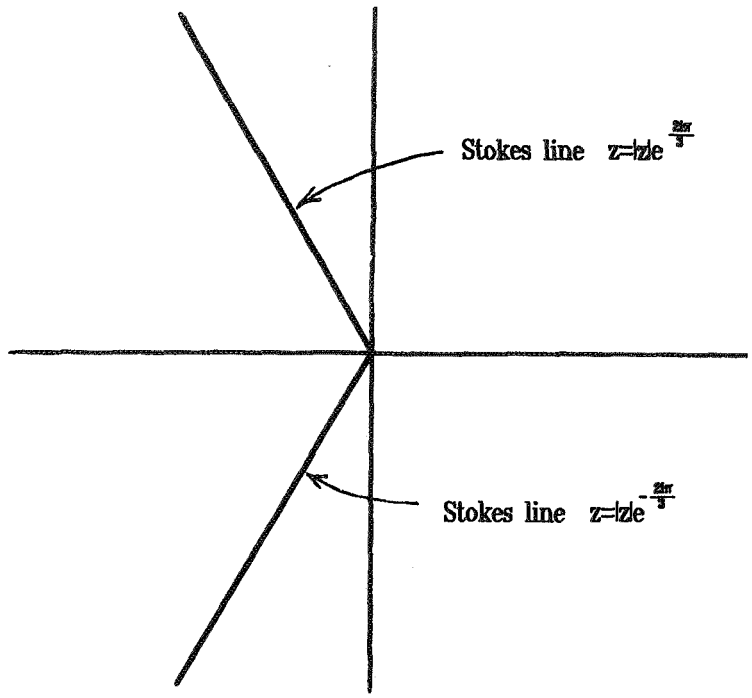


Figure 2:

Near the upper Stokes line $z=|z|e^{i(2\pi/3+\alpha)}$, $-\zeta = \frac{2}{3}|z|^{3/2}e^{i3\alpha/2}$. According to the 1-st convention the dominant wave $S_m$ is formed by asymptotic series trancated near its least term, while the recessive wave $R_m$ is represented by the remainder:

$$\mathrm{Ai}(z) = S_m(z) + R_m(z) =$$

$$= \frac{\sqrt{\pi}e^{-\zeta}}{2z^{1/4}} \sum_{k=0}^{m-1} c_k(-\zeta)^{-k} + \frac{2e^{-\frac{i\pi}{6}}}{\pi} \int_z^\infty dt f_m(t) \left[\mathrm{Ai}(z)\mathrm{Ai}(te^{-\frac{2\pi}{3}}) - \right.$$

$$\left. -\mathrm{Ai}(t)\mathrm{Ai}(ze^{-\frac{2\pi}{3}})\right], \tag{8}$$

$f_m(t) = (-1)^m\sqrt{\frac{3\pi}{2}}mc_m\zeta^{-m-1/2}e^{-\zeta}$, $m = m(z)$ – number of the least term. For $z \gg 1$ the $m = m(z) \gg 1$ and it is possible to find the asymptotic expression for $R_m(z)$. The investigation shows that for asymptotic series whose terms behave with number $k$ as

$$\Gamma(ak+b)(cz)^{-dk} \tag{9}$$

the ratio

$$\frac{R_m(z)}{S_m(z)} \sim i\frac{1}{2}\mathrm{erfc}(\xi)e^{f_1-f_2}, \tag{10}$$

where

$$\xi(z) \approx \frac{\mathrm{Im}(f_1 - f_2)}{\sqrt{2\mathrm{Re}(f_2 - f_1)}}. \tag{11}$$

So the recessive wave is switched on when $|\xi| \geq 1$, or when the phase difference of dominant and recessive waves becomes large:

$$|\mathrm{Im}(f_1 - f_2)| \geq \sqrt{2\mathrm{Re}(f_2 - f_1)} \gg 1. \tag{12}$$

# 3 Second convention and uncertainty relation

The 2-nd convention [4] based on contour integral representation and dividing contour integral at the height of recessive saddle. The dominant and recessive terms of $F(z)$ are nothing else than contributions of high and low saddles of the integrand. If $t_2$ and $t_1$ are the high and low saddle points and $z$ is near the Stokes line then the steepest decent lines going over the $t_2$ and $t_1$ ($\mathrm{SDL}_2$ and $\mathrm{SDL}_1$) on the complex $t$-plane are represented on the fig.3 together with the level line ($\mathrm{LL}_1$) of low saddle point $t_1$.

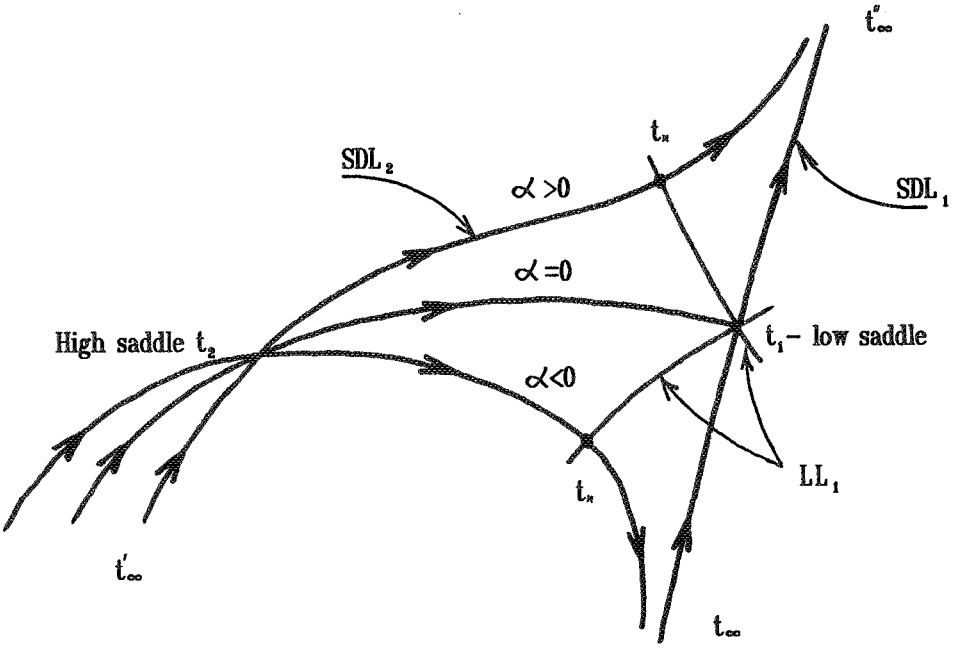


Figure 3:

The point $t_*$=$t_*(z)$ on the intersection of $\mathrm{SDL}_2$ and $\mathrm{LL}_1$ is a root of eqs.:

$$\begin{aligned} \mathrm{Im}f(t,z) &= \mathrm{Im}f_2, \\ \mathrm{Re}f(t,z) &= \mathrm{Re}f_1. \end{aligned} \tag{13}$$

The 2-nd convention defines the dominant $D$ and recessive $R$ terms of $F = D + R$ as integrals

$$D(z) = A\int_{t'_\infty}^{t_*} dte^{f(t,z)}, \qquad R(z) = A\int_{t_*}^{t''_\infty} dte^{f(t,z)} \tag{14}$$

Using in $R$ the Taylor expansion for $f(t,z)$ near saddle point $t_1$

$$f(t,z) = f_1 + \frac{1}{2}f_1''(t-t_1)^2 + \dots \tag{15}$$

we obtain

$$R(z) \approx A\sqrt{\frac{-2\pi}{f_1''}}e^{f_1}\cdot\frac{1}{2}\mathrm{erfc}(w), \tag{16}$$

where

$$w(\alpha) = \sqrt{i\,\mathrm{Im}(f_1 - f_2)} \tag{17}$$

is a complex function of $\alpha$. Hence, the switching function $g(\alpha)$ is complex and is given by a Fresnel type integral. The recessive wave switches on or off when $|w| \geq 1$ or

$$|\mathrm{Im}(f_1 - f_2)| \geq 1. \tag{18}$$

It is very natural condition: the phase difference of dominant and recessive waves is of the order of 1 or greater.

Near the Stokes line the phase is linear function of $\alpha$:

$$\mathrm{Im}f_{1,2}(\alpha) = \mathrm{Im}f_{1,2}(0) - \omega_{1,2}(0)\cdot\alpha + \dots, \tag{19}$$

and

$$\mathrm{Im}(f_1 - f_2) = \Delta\omega\cdot\alpha + \dots, \quad \Delta\omega = \omega_2(0) - \omega_1(0), \tag{20}$$

as on the Stokes line $\mathrm{Im}f_1(0)$=$\mathrm{Im}f_2(0)$. Two waves may be distinguished only outside of the Stokes line (Stokes strip)

$$|\mathrm{Im}(f_1 - f_2)| \geq 1 \quad \text{or} \quad \Delta\omega\cdot\Delta\alpha \geq 1, \tag{21}$$

when uncertainty relation is fulfilled. That is why the Stokes line width

$$\Delta\alpha \sim \frac{1}{\Delta\omega} \tag{22}$$

may be called natural.

In the first convention, where

$$F = S_m + R_m, \tag{23}$$

due to condition(12) or

$$\Delta\omega\cdot\Delta\alpha \geq \sqrt{2\mathrm{Re}(f_2 - f_1)} \gg 1 \tag{24}$$

the Stokes line width is much greater than natural

$$\Delta\alpha \sim \frac{\sqrt{2\mathrm{Re}(f_2 - f_1)}}{\Delta\omega} \gg \frac{1}{\Delta\omega}. \tag{25}$$

The slower formation of wave $R_m$ in comparison with $R$ is caused by the fact that the last $\sqrt{m} \sim \sqrt{2\mathrm{Re}(f_2 - f_1)} \gg 1$ terms in $S_m$ are coherent to $R_m$ and the disentanglement occurs slowly. This coherence disappears when $\alpha$ goes out of the more wider interval $\Delta\alpha \sim \sqrt{m}/\Delta\omega$ than natural one and then all recessive properties are concentrated in $R_m$.

# 4 T-parity and asymptotic expansions

T-transformation consists of the change $\alpha \to -\alpha$ and the complex conjugation. We consider here only the important case when functions $f_{1,2}$ in (2) satisfy the conditions

$$f_{1,2}(\alpha) \to f^*_{1,2}(-\alpha) = f_{1,2}(\alpha), \quad w(\alpha) \to w^*(-\alpha) = -w(\alpha), \tag{26}$$

and dominant wave $D$ goes into itself, $D \to D + \delta$, up to unimportant phase factor and exponentially small additional term $\delta$. One can say conditionally that $D$ has positive T-parity. At the same time

$$R \sim ig(w)e^{if_1} \to -ig(-w)e^{if_1} \tag{27}$$

and does not have definite T-parity inside the Stokes strip because

$$g(-w) = 1 - g(w). \tag{28}$$

Yet outside the Stokes strip, when $|w| \gg 1$,

$$ig(w)e^{f_1} \approx \begin{cases} ie^{f_1 - w^2}/(2\sqrt{\pi}w), & \mathrm{Re}w \gg 1, \\ ie^{f_1} + ie^{f_1 - w^2}/(2\sqrt{\pi}w), & \mathrm{Re}w \ll -1. \end{cases} \tag{29}$$

Then before Stokes strip the $R$ is $2\sqrt{\pi}|w|$ times less than its value $R_S$ on the Stokes line, does not change at T-inversion and has the phase of dominant wave shifted by the $\arg(iw^{-1})$, as $f_1 - w^2 = \mathrm{Re}f_1 + i\mathrm{Im}f_2$. After the Stokes strip the wave $R \approx 2R_S$, has the proper phase $\mathrm{Im}f_1 + \pi/2$, changes its sign at T-inversion and is accompanied by small additional term of the same type as $R$ itself was before the Stokes strip.

Therefore the Stokes strip is the forming region for recessive wave with frequency $\omega_1 \neq \omega_2$ and negative T-parity.

As to behaviour of dominant and recessive waves at T-transformation in the representation $F = S_m + R_m$, then for the examples considered in [4] the $S_m$ transforms into itself up to the same factor as for $D$ but without any additional term $\delta$,i.e. $S_m \to S_m$, while the $R_m$ behaves according to (29) with the change of $w$ by real $\xi$, see (11). Therefore the phase of forming wave $R_m$ equals to $\mathrm{Im}f_1 + \pi/2$ and its T-parity changes from positive to negative value being indefinite inside the Stokes strip. As $D = S_m + R_m - R$, the additional term $\delta$ having indefinite T-parity inside the wide Stokes strip vanishes outside it as $\delta \sim ie^{-\xi^2 + f_1}/2\sqrt{\pi}\xi$.

# 5 Stokes line width and the method of osculating parameters

It is instructive to see the appearance of Stokes width in the method of osculating parameters. According to this method the particular solution $y(\theta)$ of the differential equation of the second order with large parameter $\nu$ is sought as a superposition of quasiclassical solutions ${}^{\pm}f(\theta)$ with the correcting coefficient functions $a_{\pm}(\theta)$ defined by the relations

$$y(\theta) = a_+(\theta)\,{}^+f(\theta) + a_-(\theta)\,{}^-f(\theta), \tag{30}$$

$$y'(\theta) = a_+(\theta)\,{}^+f'(\theta) + a_-(\theta)\,{}^-f'(\theta), \tag{31}$$

and boundary condition

$$a_+(-\infty) = 1, \qquad a_-(-\infty) = 0. \tag{32}$$

The latter means that the solution in question is ${}_+y(\theta)$. As $a_{\pm}(\theta)$ are not differentiated in eq.(31) the differential equation of the second order is reduced to the system of two differential equations of the first order. This is sometimes useful for seeking out the appropriate approximation.

In physical literature there is a tendency to treat the two terms on the r.h.s. of (30) as two waves with $\pm$ frequencies for arbitrary $\theta$ and not only for $\theta \to +\infty$ (see [6] and references therein). This is done on the ground that quasiclassical solutions ${}^{\pm}f$ conserve the sign of frequency and the factors $a_{\pm}(\theta)$ should only correct the solutions. Yet this is true only in the case when ${}^+f(\theta)$, describing the strong wave, is taken with the accuracy up to the amplitude $a_-(\theta)$ of the weak wave $a_-(\theta)\,{}^-f(\theta)$, which under considered condition is exponentially small, for example $a_-(\theta) \sim e^{-\pi\nu}$.

To see this we note preliminarily that as follows from (31,32)

$$\begin{aligned} a_{\pm}(\theta) &= \pm\left(y(\theta)\,{}^{\mp}f'(\theta) - y'(\theta)\,{}^{\mp}f(\theta)\right)/D, \\ D &= {}^+f\,{}^-f' - {}^-f\,{}^+f'. \end{aligned} \tag{33}$$

We use now as an example the parabolic cylinder function $y(\theta)=CD_{i\nu-1/2}(-e^{-i\pi/4}2\sqrt{\nu}\theta)$. The constant $C$ is fixed by the condition $a_+(-\infty) = 1$. The first terms of the asymptotic expansion of $y(\theta)$ in power series in $\nu^{-1}$ can be obtained by Darwin method [7].

For the $n$-th approximation we have

$${}^+f_n(\theta) = e^{iS+\sigma_n}, \quad {}^-f = {}^+f^*, \quad S(\theta) = -\nu(\theta\sqrt{1+\theta^2} + \mathrm{Arsh}\theta), \tag{34}$$

$$\sigma_n = \sum_{k=0}^{n}(i\nu)^{-k}c_k(\theta), \quad c_0 = -\frac{1}{4}\ln(1+\theta^2).$$

Here $c_k$ are the real functions of $\theta$, bounded for $k \geq 1$ together with their derivatives and satisfying the relation

$$c_k(-\theta) = (-1)^k c_k(\theta).$$

It follows from (33,34) that $a_-(\theta)\,{}^-f_n(\theta)$ consists of positive- and negative-frequency terms which have the form

$$a_-(\theta)\ {}^-f_n(\theta) = \frac{e^{iS+\sigma_0}{c^*}'_{n+1}(\theta)}{4(i\nu)^{n+2}\sqrt{1+\theta^2}}\left(1+O(\nu^{-1})\right) -$$

$$-ie^{-\pi\nu}e^{-iS+\sigma_0}\left(1+O(\nu^{-1})\right). \tag{35}$$

As seen from here $a_-\ {}^-f$ becomes approximately the negative-frequency wave only when the first term on the r.h.s. is much smaller than the second one:

$$\frac{{c^*}'_{n+1}(\theta)}{4\nu^{n+2}\sqrt{1+\theta^2}} \ll e^{-\pi\nu}. \tag{36}$$

In notation of [8]

$$c'_n(\theta) = -2(-i\nu)^{n+\frac{1}{2}}h_{3n}X^{-3n-2}. \tag{37}$$

One can show that for $\theta \gg 1$ the function $c'_n(\theta) \approx a_n 2^{-2n}\theta^{-2n-1}$, $a_n \approx 2^{n-1}\Gamma(n+1)$, $n \gg 1$. Then the condition (36) takes the form

$$\theta^2 \gg \frac{1}{2\nu}\left[\frac{\Gamma(n+2)}{4}e^{\pi\nu}\right]^{\frac{1}{n+2}}. \tag{38}$$

So for $n \sim \nu \gg 1$ we have $\theta^2 \gg 1$. It is seen that with each successive step in approximation for ${}^{\pm}f_n$ the width, in which positive- and negative-frequencies are not separated, shrinks quickly, but only at the step $n \sim \nu$ the width approaches the barrier one — a physically reasonable result.

# References


[1] G. G. Stokes, Trans. Cambridge Philos. Soc., No 10, 106 (1864).

[2] M.V. Berry, Proc. R. Soc. London, Ser. A, **422**, 7 (1989), **427**, 265 (1990), **434**, 465 (1991).

[3] A. I. Nikishov, V.I. Ritus, in Sakharov Memorial Lectures in Physics. Proc. of the First Int. Sakharov Conf. on Physics, May21-31, 1991, Moscow, v.1, Nova Sci. Pub., New York.

[4] A. I. Nikishov, V.I. Ritus, Teor. Mathem. Fiz., **92**, 24 (1992).

[5] R. B. Dingle, *Asymptotic expansions: Their Derivation and Interpretation*, Academic Press, New York (1973).

[6] A. A. Grib, S. G. Mamaev, V. M. Mostepanenko, *Vacuum Quantum Effects in Strong Fields*, Energoatomizdat, Moscow (1988).

[7] M. Abramovitz, I. A. Stegun, *Handbook of Mathematical Functions with Formules, Grafs, and Mathematical Tables*, Dover (1964).

[8] J. C. P. Miller, in *Tables of Weber Parabolic Cylinder Functions*, Her Majesty's Stationary Office, London (1955).

# MAXIMUM PREDICTIVE POWER AND THE SUPERPOSITION PRINCIPLE

Johann Summhammer
*Atominstitut der Österreichischen Universitäten*
*Schüttelstr. 115, A-1020 Vienna, AUSTRIA*

**Abstract**

In quantum physics the direct observables are probabilities of events. We ask, how observed probabilities must be combined to achieve what we call maximum predictive power. According to this concept the accuracy of a prediction must only depend on the number of runs whose data serve as input for the prediction. We transform each probability to an associated variable whose uncertainty interval depends only on the amount of data and strictly decreases with it. We find that for a probability which is a function of two other probabilities maximum predictive power is achieved when linearly summing their associated variables and transforming back to a probability. This recovers the quantum mechanical superposition principle.

## 1 Introduction

Quantum theory is not yet understood as well as e.g. classical mechanics or special relativity. Classical mechanics coincides well with our intuition and so is rarely questioned. Special relativity runs counter to our immediate insight, but can easily be derived by assuming constancy of the speed of light for every observer. And that assumption may be made plausible by epistemological arguments [1]. Quantum theory on the other hand demands two premises. First, it wants us to give up determinism for the sake of a probabilistic view. In fact, this seems unavoidable in a fundamental theory of prediction, because any communicable observation can be decomposed into a finite number of bits. So predictions therefrom always have limited accuracy, and probability enters naturally. More disturbing is the second premise: Quantum theory wants us to give up the sum rule of probabilities by requiring interference instead. However, the sum rule is deeply ingrained in our thought, because of its roots in counting and the definition of sets: Define sets with no common elements, then define the set which joins them all. The number of elements in this latter set is just the sum of the elements of the individual sets. When deriving the notion of probability from the relative frequency of events we are thus immediately led to the sum rule, such that any other rule appears inconceivable. And this may be the reason why we have difficulties accepting the quantum theoretical rule, where probabilities are summed by calculating the square of the sum of the complex square roots of the probabilities. In this situation two views are possible. We may either consider the quantum theoretical rule as a peculiarity of nature. Or, we may conjecture that the quantum theoretical rule has something to do with how we organize data from observations into quantities that are physically meaningful to us. We want to adopt the

latter position. Therefore we seek to establish a grasp of the quantum theoretical rule with the general idea in mind that, given the probabilistic paradigm, there may exist an optimal strategy of prediction, quite independent of traditional physical concepts, but resting on what one can deduce from a given amount of information. We will formulate elements of such a strategy with the aim of achieving maximum predictive power.

## 2 Representing Knowledge from Probabilistic Data

Any investigative endeavour rests upon one natural assumption: More data from observations will lead to better knowledge of the situation at hand. Let us see whether this holds in quantum experiments. The data are relative frequencies of events. From these we deduce probabilities from which in turn we derive the magnitudes of physical quantities. As an example take an experiment with two detectors, where a click is registered in either the one or the other. (We exclude simultaneous clicks for the moment.) Here, only one probability is measurable, e.g. the probablity $p_1$ of a click in detector 1. After N runs we have $n_1$ counts in detector 1 and $n_2$ counts in detector 2, with $n_1 + n_2 = N$. The probability $p_1$ can thus be estimated as

$$p_1 = \frac{n_1}{N} \tag{1}$$

with the uncertainty interval [2]

$$\Delta p_1 = \sqrt{\frac{p_1(1-p_1)}{N}}. \tag{2}$$

From $p_1$ the physical quantity $\chi(p_1)$ is derived. Its uncertainty interval is

$$\Delta\chi = \left|\frac{\partial\chi}{\partial p_1}\right| \Delta p_1 = \left|\frac{\partial\chi}{\partial p_1}\right| \sqrt{\frac{p_1(1-p_1)}{N}}. \tag{3}$$

The accuracy of $\chi$ is given by the inverse of $\Delta\chi$. With the above assumption we expect it to increase with each additional run, because we get additional data. Therefore, for any $N$, we expect

$$\Delta\chi(N+1) < \Delta\chi(N). \tag{4}$$

However, this inequality cannot be true for an arbitrary function $\chi(p_1)$. In general $\Delta\chi$ will fluctuate and only decrease on the average with increasing $N$. To see this take a theory A which relates physical quantity and probability by $\chi_A = p_1$. In an experiment of $N = 100$ runs and $n_1 = 90$ we get: $\Delta\chi_A(100) = .030$. By taking into account the data from one additional run, where detector 2 happened to click, we have $\Delta\chi_A(101) = .031$. The differences may appear marginal, but nevertheless the accuracy of our estimate for $\chi_A$ has decreased although we incorporated additional data. So our original assumption does not hold. This is worrisome as it implies that a prediction based on a measurement of $\chi_A$ may be more accurate if the data of the last run are not included. Let us contrast this to theory B, which connects physical quantity and probability by $\chi_B = {p_1}^6$. With $N$ and $n_1$ as before we have $\chi_B(100) = .106$. Incorporation of the data from the additional run leads to $\chi_B(101) = .104$. Now we obviously don't question the value of the last run, as the accuracy of our estimate has increased.

The lesson to be learnt from the two examples is that the specific functional dependence of a physical quantity on the probability (or several probabilities if it is derived from a variety of experiments) determines whether our knowledge about the physical quantity will increase with additional experimental data, and that this also applies to the accuracy of our predictions. This raises the question what quantities we should be interested in to make sure that we get to know them more accurately by doing more experiments. From a statistical point of view the answer is straightforward: choose variables whose uncertainty interval strictly decreases, and simply *define* them as physical. And from a physical point of view? Coming from classical physics we may have a problem, as concepts like mass, distance, angular momentum, energy, etc. are suggested as candidates for physical quantities. But when coming from the phenomenology of quantum physics, where all we ever get from nature is random clicks and count rates, a definition of physical quantities according to statistical criteria may seem more reasonable, *simply because there is no other guideline as to which random variables should be considered physical.*

Pursuing this line of thought we want to express experimental results by random variables whose uncertainty interval strictly decreases with more data. When using them in predictions, which are also expressed by variables with this property, predictions should automatically become more accurate with more data input. Now a few trials will show that there are many functions $\chi(p_1)$ whose uncertainty interval decreases with increasing $N$ (eq.(3)). We want to choose the one with maximum predictive power. The meaning of this term becomes clear when realizing that in general $\Delta\chi$ depends on $N$ and on $n_1$ (via $p_1$). These two numbers have a very different status. The number of runs, $N$, is controlled by the experimenter, while the number of clicks, $n_1$, is solely due to nature. Maximum predictive power then means to eliminate nature's influence on $\Delta\chi$. For then we can know $\Delta\chi$ *even before* having done any experimental runs, simply upon deciding how many we will do. From eq.(3) we thus get

$$\sqrt{N}\Delta\chi = \left|\frac{\partial\chi}{\partial p_1}\right| \sqrt{p_1(1-p_1)} = constant, \tag{5}$$

which results in

$$\chi = C \arcsin(2p_1 - 1) + D \tag{6}$$

where C and D are real constants. The inverse is

$$p_1 = \frac{1 + \sin(\frac{\chi - D}{C})}{2}, \tag{7}$$

showing that the probability is periodic in $\chi$. Aside from the linear transformations provided by $C$ and $D$ any other smooth function $\alpha(\chi)$ in real or complex spaces will also fulfill requirement (5) when equally sized intervals in $\chi$ correspond to equal line lengths along the curve $\alpha(\chi)$. One particular curve is

$$\alpha(\chi) = \sin(\frac{\chi}{2})e^{i\frac{\chi}{2}}, \tag{8}$$

which is a circle in the complex plane with center at $i/2$. It exhibits the property $|\alpha|^2 = p_1$ known from quantum theory. But note, that for instance the function $\beta = \sin(\chi/2)$ does not fulfill the requirement that the accuracy only depend on $N$. Therefore the complex phase factor in eq.(8) is necessary [3][4].

# 3 Distinguishability

We have now found a unique transformation from a probability to another class of variables exemplified by $\chi$ in eq.(6). These unique variables always become better known with additional data. But can they be considered physical? We should first clarify what a physical variable is. A physical variable can assume different numerical values, where each value should not only imply a different physical situation, but should most of all lead to a different measurement result in a properly designed experiment. Within the probabilistic paradigm two measurement results are different when their uncertainty intervals don't overlap. This can be used to define a variable which counts the principally distinguishable results of the measurement of a probability. Comparison of that variable to our quantity $\chi$ should tell us how much $\chi$ must change from a given value before this can be noticed in an experiment. Following Wootters and Wheeler [5][6] the variable $\theta$ counting the statistically distinguishable results at detector 1 in $N$ runs of our above example is given by

$$\theta(n_1) = \int_0^{p_1(n_1)} \frac{dp}{\Delta p(p)} = \sqrt{N}\left[\arcsin(2p_1 - 1) + \frac{\pi}{2}\right]_{p_1=\frac{n_1}{N}} \tag{9}$$

where $\Delta p$ is defined as in eq.(2). When dividing $\theta$ by $N^{1/2}$ it becomes identical to $\chi$ when in eq.(6) we set $C = 1$ and $D = \frac{\pi}{2}$. This illuminates the meaning of $\chi$: It is a continuous variable associated with a probability, with the particular property that anywhere in its domain an interval of fixed width corresponds to an equal number of measurement results distinguishable in a given number of runs. With Occam's dictum of not introducing more entities than are necessary for the description of the subject matter under investigation, $\chi$ would be *the* choice for representing physical situations and can rightly be called physical.

# 4 A Simple Prediction: The Superposition Principle

Now we return to our aim of finding a strategy for maximum predictive power. We want to see whether the unique class of variables represented by $\chi$ indicates a way beyond representing data and perhaps affords special predictions. For the sake of concreteness we think of the double slit experiment. A particle can reach the detector by two different routes. We measure the probabilty that it hits the detector via the left route, $p_L$, by blocking the right slit. In $L$ runs we get $n_L$ counts. In the measurement of the probability with only the right path available, $p_R$, we get $n_R$ counts in $R$ runs. From these data we want to make a prediction about the probability $p_{tot}$, when both paths are open. Therefore we make the hypotheses that $p_{tot}$ is a function of $p_R$ and $p_L$. What can we say about the function $p_{tot}(p_L, p_R)$ when we demand maximum predictive power from it? This question is answered by reformulating the problem in terms of the associated variables $\chi_L$, $\chi_R$ and $\chi_{tot}$, which we derive according to eq.(6) by setting $C = 1$ and $D = \frac{\pi}{2}$. The function $\chi_{tot}(\chi_L, \chi_R)$ must be such that a prediction for $\chi_{tot}$ has an uncertainty interval $\delta\chi_{tot}$, which only depends on the number of runs, $L$ and $R$, and decreases with both of them. (We use the symbol $\delta\chi_{tot}$ to indicate that it is not derived from a measurement of $p_{tot}$, but from other measurements from which we want to predict $p_{tot}$.) In this way we can predict the accuracy of $\chi_{tot}$ by only deciding the number of runs, $L$ and $R$. No actual measurements need to have been done. Because

of

$$\delta\chi_{tot} = \sqrt{\left|\frac{\partial\chi_{tot}}{\partial\chi_L}\right|^2 \frac{1}{L} + \left|\frac{\partial\chi_{tot}}{\partial\chi_R}\right|^2 \frac{1}{R}} \tag{10}$$

maximum predictive power is achieved when

$$\left|\frac{\partial\chi_{tot}}{\partial\chi_j}\right| = constant, \quad j = L, R. \tag{11}$$

We want to have a real function $\chi_{tot}(\chi_L, \chi_R)$, and therefore we get

$$\chi_{tot} = a\chi_L + b\chi_R + c, \tag{12}$$

where $a$, $b$ and $c$ are real constants. Furthermore we must have $c = 0$ and the magnitude of both $a$ and $b$ equal to 1, when we wish to have $\chi_{tot}$ equivalent to $\chi_R$ or to $\chi_L$ when either the one or the other path is blocked. So there is an ambiguity of sign with $a$ and $b$. When rewriting this in terms of the probability we get

$$p_{tot} = \sin^2\left(\frac{\chi_L \pm \chi_R}{2}\right). \tag{13}$$

This does not look like the sum rule of probability theory. Only for $p_L + p_R = 1$ does it coincide with it. We may therefore conclude that the sum rule of probability theory does not afford maximum predictive power. But neither does eq.(13) look like the quantum mechanical superposition principle. However, this should not be surprising because our input were just two real valued numbers, $\chi_L$ and $\chi_R$, from which we demanded to derive another real valued number. A general phase as is provided in quantum theory could thus not be incorporated. But let us see what we get with complex representatives of the associated variables of probabilities. We take $\alpha(\chi)$ from eq.(8). Again we define in an equivalent manner $\alpha_L$, $\alpha_R$ and $\alpha_{tot}$. From $p_L$ we have for instance (from (8) and (7) with $C = 1$ and $D = \frac{\pi}{2}$)

$$\alpha_L = \sqrt{p_L}\left(\sqrt{p_L} + i\sqrt{1 - p_L}\right) \tag{14}$$

and

$$\Delta\alpha_L = \left|\frac{\partial\alpha_L}{\partial p_L}\right| \Delta p_L = \frac{1}{2\sqrt{L}}. \tag{15}$$

If we postulate a relationship $\alpha_{tot}(\alpha_R, \alpha_L)$ according to maximum predictive power we expect the predicted uncertainty interval $\delta\alpha_{tot}$ to be independent of $\alpha_L$ and $\alpha_R$ and to decrease with increasing number of runs, $L$ and $R$. Analogous to (11) we must have

$$\left|\frac{\partial\alpha_{tot}}{\partial\alpha_j}\right| = constant, \quad j = L, R, \tag{16}$$

yielding

$$\alpha_{tot} = s\alpha_L + t\alpha_R + u, \tag{17}$$

where $s$, $t$, and $u$ are complex constants. Now $u$ must vanish and $s$ and $t$ must both be unimodular when $p_{tot}$ is to be equivalent to either $p_L$ or $p_R$ when the one or the other route is blocked. We then obtain

$$p_{tot} = |\alpha_{tot}|^2 = |s\alpha_L + t\alpha_R|^2 = p_L + p_R + 2\sqrt{p_L p_R}\cos(\phi), \tag{18}$$

where $\phi$ is an arbitrary phase factor containing the phases of $s$ and $t$. This is exactly the quantun mechanical superposition principle. What is striking is that with a theory of maximum predictive power we can obtain the general form of this principle, but cannot at all predict $p_{tot}$ even when we have measured $p_L$ and $p_R$, because of the unknown phase $\phi$. So we are lead to postulate $\phi$ as a new measurable quantity in this experiment.

# 5 Conclusion

We have tried to obtain insight into the quantum mechanical superposition principle and set out with the idea that it might follow from a most natural assumption of experimental science: more data should provide a more accurate representation of the matter under investigation and afford more accurate predictions. From this we defined the concept of maximum predictive power which demands laws to be such that the uncertainty of a prediction is solely dependent on the number of experiments on which the prediction is based, and not on the specific outcomes of these experiments. Applying this to the observation of two probabilities and to possible predictions about a third probability therefrom, we arrived at the quantum mechanical superposition principle. Our result suggests nature's law to be such that from more observations more accurate predictions must be derivable.

# 6 Acknowledgments

I thank the Austrian Science Foundation (FFW) for financial support of ion double slit experiments (Project P8781-PHY) whose analysis led to this paper.

# References

[1] G. J. Whitrow, *The Natural Philosophy of Time, 2nd Ed.*, (Clarendon Press, Oxford, 1984).

[2] The uncertainty interval is derived from Chebyshev's inequality, e.g. William Feller, *An Introduction to Probability Theory and its Applications, 3rd Ed.*, (Wiley and Sons, New York, 1968), p.233. For reasons of simplicity we are using only the approximate form valid for large $N$.

[3] More details and variables that can be used to represent several probabilities can be found in: J. Summhammer, Found. Phys. Lett. **1**, 113 (1988).

[4] The statistical properties of $\chi$ are analyzed in: J. Summhammer, Phys. Lett. **A136**, 183 (1989).

[5] W. K. Wootters, Phys. Rev. **D23**, 357 (1981).

[6] J. A. Wheeler, Int. J. Theor. Phys. **21**, 557 (1982).

# CORRELATED QUADRATURES OF RESONANCE FLUORESCENCE AND THE GENERALIZED UNCERTAINTY RELATION

Henk F.Arnoldus
*Department of Physics, Mendel Hall, Villanova University*
*Villanova, Pennsylvania 19085*

Thomas F. George
*Departments of Chemistry and Physics, Washington State University*
*Pullman, Washington 99164-1046*

Rolf W. F. Gross
*Aerospace Corporation, P.O. Box 92957, Los Angeles, California 90009-2957*

Resonance fluorescence from a two-state atom has been predicted to exhibit quadrature squeezing below the Heisenberg uncertainty limit, provided that the optical parameters (Rabi frequency, detuning, laser linewidth, etc.) are chosen carefully. When the correlation between two quadratures of the radiation field does not vanish, however, the Heisenberg limit for quantum fluctuations might be an unrealistic lower bound. A generalized uncertainty relation, due to Schrödinger, takes into account the possible correlation between the quadrature components of the radiation, and it suggests a modified definition of squeezing. We show that the coherence between the two levels of a laser-driven atom is responsible for the correlation between the quadrature components of the emitted fluorescence, and that the Schrödinger uncertainty limit increases monotonically with the coherence. On the other hand, the fluctuations in the quadrature field diminish with an increasing coherence, and can disappear completely when the coherence reaches 1/2, provided that certain phase relations hold.

## I. RESONANCE FLUORESCENCE

We consider a two-state atom, with excited state $|e\rangle$, ground state $|g\rangle$, and level separation $\omega_0$, illuminated by an intense laser. The electric field at the position of the atom is assumed to have the form

$$\vec{E}_L(t) = E_o \, Re\, \vec{\varepsilon}_L \exp[-i(\omega_L t + \phi(t)] \quad , \tag{1.1}$$

where $\phi(t)$ is a stochastic phase which takes into account the laser linewidth. We shall assume that this is a diffusion process with independent increments. The driven atom

will emit resonance fluorescence, and the positive-frequency part of the electric field of this radiation is

$$E^{(+)}(t) = \gamma d^{+}(t) \quad , \tag{1.2}$$

with $d^{+}(t) = |g><e|$ the atomic lowering operator, and $\gamma$ an overall constant. The fluctuations in the amplitude (or phase) are measured by a homodyne detector with the driving laser as local oscillator. The slowly-varying operator under measurement is therefore[1]

$$E_\theta(t) = E^{(+)}(t)\exp[i(\omega_L t + \phi(t) - \theta)] \quad , \tag{1.3}$$

with $\theta$ the adjustable mixing angle of the detector. Essentially, the detector measures the variance of this quadrature operator, denoted by $\mathrm{var}(E_\theta)$.

The fluctuations in $E_\theta(t)$ will be expressed in terms of the parameter $r_\theta$, defined as

$$r_\theta = \mathrm{var}(E_\theta)/<E_\theta^2> = 1 - <E_\theta>^2 / <E_\theta^2> \quad . \tag{1.4}$$

Clearly, this parameter lies in the range $0 \le r_\theta \le 1$. For $r_\theta = 0$ we have $\mathrm{var}(E_\theta) = 0$, which corresponds to no fluctuations at all, and for $r_\theta = 1$ we have $<E_\theta> = 0$. This case corresponds to a pure random phase of the field (like in a number state).

## II. SQUEEZING

For Heisenberg's uncertainty relation we compare the quadrature field $E_\theta$ with the field $E_{\theta'}$, which is the same field except with a different mixing angle. Then the uncertainty relation can be written as

$$r_\theta r_{\theta'} \ge L_H^2 \quad , \tag{2.1}$$

with $L_H$ the Heisenberg lower limit, given by

$$L_H = \tfrac{1}{2}\frac{|<[E_\theta, E_{\theta'}]>|}{\sqrt{<E_\theta^2><E_{\theta'}^2>}} \quad . \tag{2.2}$$

If we insert the expression for the quadrature field in $L_H$, it follows that the dependence on the mixing angles $\theta$ and $\theta'$ has the form

$$L_H \propto |\sin(\theta - \theta')| \quad , \tag{2.3}$$

and therefore we take $\theta' = \theta + n\pi$ with $n$ as an integer. Then $E_\theta$ is said to be squeezed if

$$r_\theta < L_H \quad , \tag{2.4}$$

in view of (2.1).

The fluctuation parameter $r_\theta$ can be expressed in terms of matrix elements of the atomic density operator $\sigma$ (either in the rotating frame or not). We find

$$r_\theta = 1 - 4|\sigma_{eg}(t)|^2 \cos^2 \delta \quad , \tag{2.5}$$

with the angle $\delta$ equal to

$$\delta = \theta + \arg\gamma - \arg\sigma_{eg} \quad . \tag{2.6}$$

The Heisenberg lower limit can be written as

$$L_H = |n_g(t) - n_e(t)| \quad , \tag{2.7}$$

in terms of the populations $n_e$ and $n_g$ of the excited state and ground state, respectively. From (2.5) it then follows that the fluctuations in $E_\theta$ are minimum if the mixing angle $\theta$ is chosen such that $\delta$ becomes an integer multiple of $\pi$. This corresponds to maximum squeezing, given $\sigma$, because $L_H$ does not depend on $\theta$. For $\delta = n\pi$ the condition for squeezing becomes

$$1 - 4|\sigma_{eg}(t)|^2 < |n_g(t) - n_e(t)| \quad . \tag{2.8}$$

Whether squeezing occurs or not depends therefore on the populations of the atomic levels and the coherence between the levels.

## III. STEADY STATE

When the atom has spent a sufficient amount of time in the laser field, its density operator will reach a steady state. The Rabi frequency of the transition is defined as

$$\Omega = E_o|<e|\vec{\mu}\bullet\vec{\varepsilon}_L|g>|/\hbar \quad , \tag{3.1}$$

with $\vec{\mu}$ the dipole moment operator of the atom, and the laser linewidth $\lambda$ will be parametrized through the combination

$$\eta = \tfrac{1}{2} + \lambda / A \quad , \tag{3.2}$$

where $A$ is the Einstein coefficient for spontaneous decay. The detuning between the laser and the atomic resonance is

$$\Delta = \omega_L - \omega_o \quad . \tag{3.3}$$

In terms of these parameters, the absolute value of the coherence becomes[2]

$$|\sigma_{eg}| = \tfrac{1}{2}\Omega\frac{\sqrt{\Delta^2 + A^2\eta^2}}{\Omega^2\eta + \Delta^2 + A^2\eta^2} \quad , \tag{3.4}$$

and the difference in level population is

$$n_g - n_e = \frac{\Delta^2 + A^2\eta^2}{\Omega^2\eta + \Delta^2 + A^2\eta^2} \quad , \tag{3.5}$$

which equals the Heisenberg lower limit. The condition for squeezing, for $\delta = 0$, then becomes

$$(1-\eta)\Delta^2 > \eta^2(\Omega^2 + A^2(\eta-1)) \quad , \tag{3.6}$$

as in Ref. (2). It is easy to see that for $\eta > 1$, which is $\lambda > A/2$, squeezing never occurs. The fluctuation parameter $r$ is, for $\delta = 0$,

$$r = 1 - \Omega^2 \frac{\Delta^2 + A^2\eta^2}{[\Omega^2\eta + \Delta^2 + A^2\eta^2]} \quad . \tag{3.7}$$

For a given detuning $\Delta$ and laser linewidth $\lambda$, the fluctuations are minimum if we take the Rabi frequency, which is proportional to the laser power, equal to

$$\Omega^2 = (\Delta^2 + A^2\eta^2)/\eta \quad . \tag{3.8}$$

Then *r* becomes

$$r = 1 - 1/4\eta \quad , \tag{3.9}$$

which is independent of $\Delta$. This minimizes for $\lambda = 0$, which gives $r = 1/2$ and $\Omega^2 = 2(\Delta^2 + A^2/4)$.

A convenient parametrization follows by introducing the new variable

$$\xi = \frac{\Omega^2}{\Delta^2 + A^2\eta^2} \quad , \tag{3.10}$$

dimensionless and proportional to the laser power. Then *r* and $L_H$ can be written as

$$r = 1 - \frac{\xi}{(\xi\eta + 1)^2} \qquad (\delta = 0) \quad , \tag{3.11}$$

$$L_H = \frac{1}{\xi\eta + 1} \quad , \tag{3.12}$$

and the condition for squeezing becomes

$$\eta(\xi\eta + 1) < 1 \qquad (\delta = 0) \quad . \tag{3.13}$$

The dependence of *r* and $L_H$ on $\xi$ is shown in Fig. 1 for $\delta = \lambda = 0$. The difference $s = r - L_H$ is also shown, and a negative value of *s* corresponds to squeezing in the quadrature field below the Heisenberg uncertainty limit. Squeezing occurs for $\xi < 2$, and the maximum squeezing appears for $\xi = 2/3$, which gives $s = -1/8$. Notice that the minimum in *r* is located at $\xi = 2$, corresponding to $s = 0$. Hence, the best relative squeezing (minimum *s*) does not coincide with the smallest relative fluctuations in the field (minimum *r*).

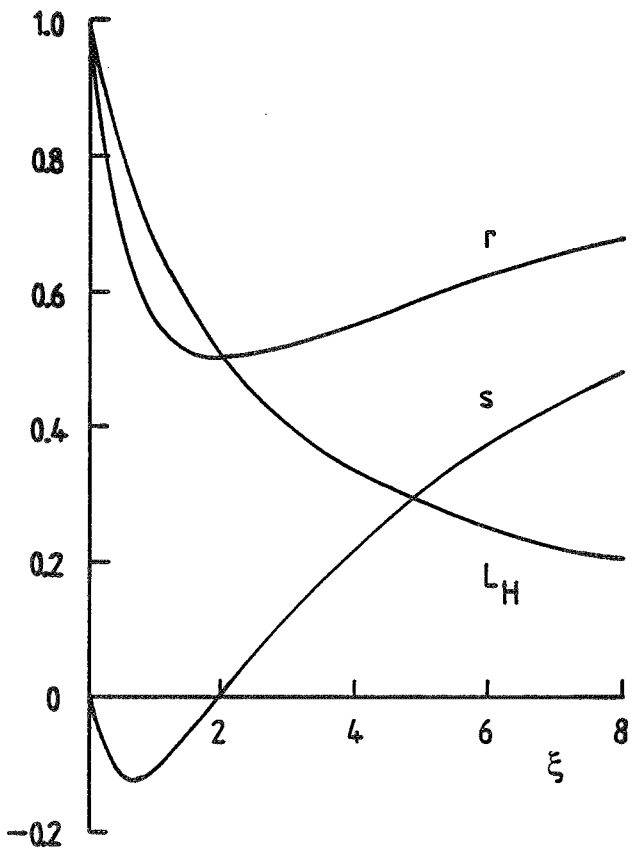


*Fig. 1. Plot of parameters* r, $L_H$, *and* s *as a function of* $\xi$.

## IV. SCHRÖDINGER UNCERTAINTY

Heisenberg's uncertainty relation (2.1) sets a lower bound on the product of two variances. It is well known, however, that this is not the sharpest lower bound. A different uncertainty relation, due to Schrödinger, is[3]

$$r_\theta r_{\theta'} \geq L_S^2 \quad . \tag{4.1}$$

The Schrödinger lower bound is related to the Heisenberg lower bound by

$$L_S = \frac{1}{\sqrt{1-c^2}} L_H \quad , \tag{4.2}$$

where the correlation coefficient $c$ is defined as

$$c = \frac{\frac{1}{2}<E_\theta E_{\theta'} + E_{\theta'} E_\theta> - <E_\theta><E_{\theta'}>}{\sqrt{\mathrm{var}(E_\theta)\,\mathrm{var}(E_{\theta'})}} \tag{4.3}$$

It can be verified that $c$ lies in the range

$$-1 \le c \le 1 \quad , \tag{4.4}$$

which then gives

$$L_S \ge L_H \quad . \tag{4.5}$$

This shows that the possible higher bound in Schrödinger's relation is due to the correlation between quadratures of the field with different values of $\theta$. We shall always take $\theta' = \theta + \pi/2$, as before.

For resonance fluorescence the correlation coefficient can be expressed in terms of the matrix elements of the atomic density operator. We obtain

$$c = \frac{2|\sigma_{eg}|^2 \sin(2\delta)}{\sqrt{\{1 - 4|\sigma_{eg}|^2 \cos^2\delta\}\{1 - 4|\sigma_{eg}|^2 \sin^2\delta\}}} \quad , \tag{4.6}$$

showing that $c$ is determined by the coherence between the levels only, and not by the populations of the atomic states. The relation between the Schrödinger limit and the Heisenberg limit then becomes

$$L_S = L_H \sqrt{1 + \frac{4|\sigma_{eg}|^4}{1 - 4|\sigma_{eg}|^2} \sin^2(2\delta)} \quad . \tag{4.7}$$

When $\delta$ is an integer multiple of $\pi/2$ or when the coherence is zero, we have $L_S = L_H$. When $\delta$ is not an integer multiple of $\pi/2$, the Schrödinger limit can become arbitrarily large when the coherence approaches 1/2 (any coherence, in absolute value, is smaller than 1/2 in a two-level system). Figure 2 shows the ratio $L_S/L_H$ for $\delta = \pi/4$, and as a function of the atomic coherence.

In terms of the parameters $\xi$ and $\eta$ the relation (4.7) becomes

$$L_S = L_H \sqrt{1 + \tfrac{1}{4}\left(\frac{\xi}{\xi\eta + 1}\right)^2 \frac{\sin^2(2\delta)}{(\xi\eta + 1)^2 - \xi}} \quad . \tag{4.8}$$

The laser power that minimizes $s$ for $\eta = 1/2$ and $\delta = 0$ is $\xi = 2/3$. Then the minimum value of $s$ is -1/8 and the minimum of $r$ is 5/8. Figure 3 illustrates the behavior of $r$, $L_H$, and $L_S$ as a function of $\delta$ for these values of $\xi$ and $\eta$.

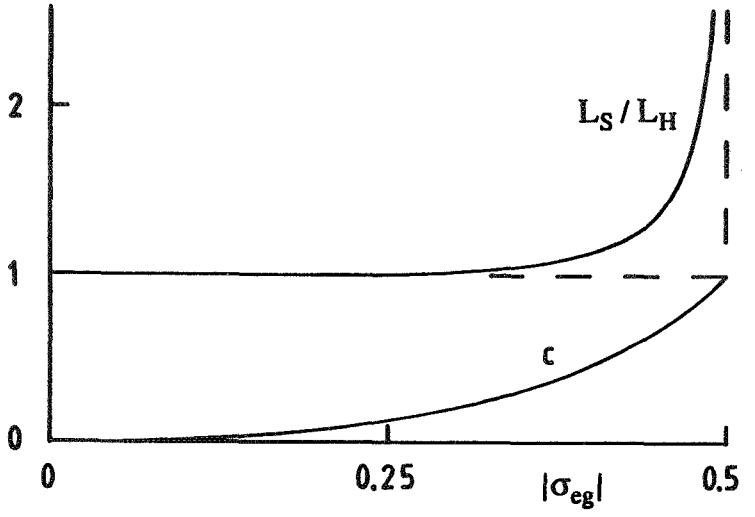


*Fig. 2. Ratio $L_S/L_H$ for $\delta = \pi/4$ as a function of the coherence.*

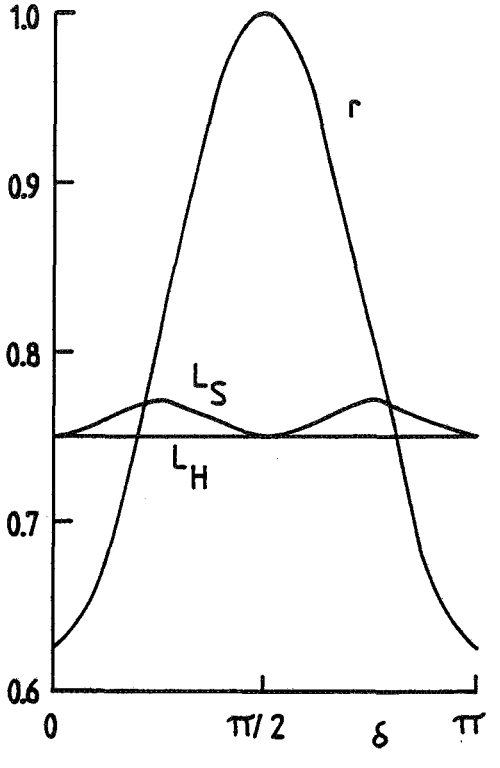


*Fig. 3. Plot of the Heisenberg- and Schrödinger limits and the fluctuation parameter r as a function of $\delta$.*

## V. CONCLUSIONS

We have studied the possibilities for squeezing in the quadrature components of resonance fluorescence from a two level atom. It was shown that the coherence between the two levels gives rise to a correlation between quadrature fields with a different mixing angle (in homodyne detection). This implies that the uncertainty limit on quantum fluctuations which is set by Schrödinger's relation can be considerably higher than the corresponding limit in Heisenberg's relation. It appears that in the steady state both limits are very close, as illustrated in Fig. 3. For pulsed-laser excitation, however, the coherence can approach its limiting value of 1/2, and this would increase the Schrödinger limit dramatically. Then the Heisenberg lower bound is an unrealistic lower limit, and squeezing should be defined with respect to the Schrödinger uncertainty relation.

Acknowledgment

This research was supported in part by the National Science Foundation under Grant No. CHE-9196214.

## REFERENCES

1. M. J. Collett, D. F. Walls and P. Zoller, *Opt. Commun.* **52**, 145 (1984).
2. H. F. Arnoldus and G. Nienhuis, *Optica Acta* **30**, 1573 (1983).
3. V. V. Dodonov, E. V. Kurmyshev and V. I. Man'ko, *Phys. Lett.* **79A**, 150 (1980).

# MINIMUM UNCERTAINTY AND SQUEEZING IN DIFFUSION PROCESSES AND STOCHASTIC QUANTIZATION

S. De Martino, S. De Siena, F. Illuminati, and G. Vitiello

*Dipartimento di Fisica, Università di Salerno, and*
*INFN Sezione di Napoli, 84081 Baronissi (Salerno), Italia*

**Abstract**

We show that uncertainty relations, as well as minimum uncertainty coherent and squeezed states, are structural properties for diffusion processes. Through Nelson stochastic quantization we derive the stochastic image of the quantum mechanical coherent and squeezed states.

## 1 Introduction

It is well known that the theory of stochastic processes is a powerful tool in the study of the interplay between probabilistic and deterministic evolution [1]. In quantum mechanics, and in particular in quantum optics, such interplay is expressed by the states of minimum uncertainty, the coherent [2] and squeezed states [3], which are viewed as the "most classical" states.

In this paper we report on a recent derivation [4] of uncertainty relations for classical stochastic processes of the diffusion type, and we determine the diffusion processes of minimum uncertainty (MUDPs). We find that a special class among them is associated to Gaussian probability distributions with time-conserved covariance and mean value with classical time evolution: we refer to them as strictly coherent MUDPs. We will also identify Gaussian MUDPs with time-dependent covariance and conserved expectation value: we refer to them as broadly coherent MUDPs. By exploiting Nelson's stochastic quantization scheme [5], we will show that the strictly coherent MUDPs provide the stochastic image of the standard quantum mechanical coherent and squeezed coherent states, while the broadly coherent MUDPs are associated with the phenomenon of time-dependent squeezing.

Our study is motivated by the possibility that the formalism of stochastic processes offers to treat on the same footing, in a unified mathematical language, the interplay between fluctuations of different nature, for instance quantum and thermal [6].

Beyond the case of diffusion processes, it is interesting to note that coherence and squeezing have recently emerged in other contexts wider than quantum mechanics ([7], [8]).

## 2 Uncertainty and Coherence in Diffusion Processes

In what follows, without lack of generality, we will consider a one-dimensional random variable $q$. The associated diffusion process $q(t)$ obeys

$$dq(t) = v_{(+)}(q(t),t)dt + \nu^{1/2}(q(t),t)dw(t)\,, \quad dt > 0\,, \tag{1}$$

where $v_{(+)}(q(t),t)$, is the forward drift, $\nu(q(t),t)$ is the diffusion coefficient, and $dw(t)$ is a Gaussian white noise, superimposed on the otherwise deterministic evolution, with expectation $E(dw(t)) = 0$ and covariance $E(dw^2(t)) = 2dt$. The forward and the backward drifts $v_{(+)}(x,t)$ and $v_{(-)}(x,t)$ are defined as

$$\begin{aligned} v_{(+)}(x,t) &= \lim_{\Delta t \to 0+} E\left(\frac{q(t+\Delta t) - q(t)}{\Delta t} \mid q(t) = x\right)\,, \\ v_{(-)}(x,t) &= \lim_{\Delta t \to 0+} E\left(\frac{q(t) - q(t-\Delta t)}{\Delta t} \mid q(t) = x\right)\,. \end{aligned} \tag{2}$$

The definitions of $v_{(+)}$ and $v_{(-)}$ are not independent, but related by [5]

$$v_{(-)}(x,t) = v_{(+)}(x,t) - \frac{2\partial_x(\nu(x,t)\rho(x,t))}{\rho(x,t)}\,. \tag{3}$$

It is now convenient to define the osmotic velocity $u(x,t)$ and the current velocity $v(x,t)$

$$\begin{aligned} u(x,t) &= \frac{v_{(+)}(x,t) - v_{(-)}(x,t)}{2} = \frac{\partial_x(\nu(x,t)\rho(x,t))}{\rho(x,t)}\,, \\ v(x,t) &= \frac{v_{(+)}(x,t) + v_{(-)}(x,t)}{2}\,. \end{aligned} \tag{4}$$

From the former definitions it is clear that $u(x,t)$ "measures" the non-differentiability of the random trajectories, controlling the degree of stochasticity. In the deterministic limit $u$ vanishes, and $v(x,t)$ goes to the classical velocity $v(t)$.

Finally, we have the continuity equation

$$\partial_t \rho(x,t) = -\partial_x(\rho(x,t)v(x,t))\,. \tag{5}$$

It is straightforward to check that $E(v_{(+)}) = E(v_{(-)}) = E(v)$, and $E(u) = 0$. Further,

$$E(v) = \frac{d}{dt}E(q) \qquad \forall t\,. \tag{6}$$

For the product $qu$, we have $|E(qu(q,t))| = E(\nu(q,t))$. By Schwartz's inequality, the r.m.s. deviations $\Delta q$ and $\Delta u$ satisfy

$$\Delta q \Delta u \geq E(\nu(q,t))\,. \tag{7}$$

Inequality (7) is the uncertainty relation for any diffusion process. Equality in (7) defines the MUDPs. Saturation of Schwartz's inequality yields $u(x,t) = C(t)(x - E(q))$, where $C(t)$ is an arbitrary function of time. Considering constant $\nu$ and time-dependent $\nu$, in both cases we obtain a Gaussian minimum uncertainty density:

$$\rho(x,t) = \frac{1}{\sqrt{2\pi(\Delta q)^2}} \exp\left[-\frac{(x - E(q))^2}{2(\Delta q)^2}\right], \tag{8}$$

where $2(\Delta q)^2 = -\nu(t)/C(t)$.

From eq. (5) we can determine the current velocity:

$$v(x,t) = \frac{d}{dt}E(q) + \frac{1}{\Delta q}\left(\frac{d}{dt}\Delta q\right) F(x,t)\,, \tag{9}$$

where

$$F(x,t) = x - E(q) + E(q) \exp\left[\frac{x^2 - 2xE(q)}{2(\Delta q)^2}\right]. \tag{10}$$

Eqs. (8)-(10) lead to the stochastic differential equation obeyed by any MUDP:

$$dq(t) = [A(t) + B(t)q(t)]dt + \nu^{1/2}(t)dw(t)\,. \tag{11}$$

It is interesting to observe that (11) defines the so-called *linear processes in narrow sense.* When $A(t) = 0$ they are the time-dependent Ornstein-Uhlenbeck processes. These last ones play a natural role in the theory of low noise systems [1], which are thus found to be related with MUDPs.

The possible choices of $E(q)$ and $\Delta q$ in (8) are not independent: taking the expectation value of in (9)-(10), and reminding (6) one has that either

$$\begin{cases} \Delta q & = \text{const.} \quad \forall t\,, \\ E(q) & = j(t)\,, \end{cases} \tag{12}$$

or

$$\begin{cases} \Delta q & = k(t)\,, \\ E(q) & = 0 \quad \forall t\,, \end{cases} \tag{13}$$

where $j(t)$ and $k(t)$ are arbitrary functions of time, and we have chosen for simplicity $q(t = 0) = 0$. Consider first case (12): $\Delta q$ does not spread; also, it is immediate to verify that the expectation value of the process $E(q)$ follows a classical trajectory:

$$v(x,t) = \frac{d}{dt}E(q) = v(t)\,, \tag{14}$$

As a consequence, MUDPs of the form (8) obeying (12) and (14) are coherent in a sense precisely analogous to that of quantum mechanical coherent states: we will refer to them as strictly coherent MUDPs and to processes (8) obeying (13) as broadly coherent MUDPs.

It is possible to discriminate on physical grounds the strictly coherent MUDPs from the broadly coherent ones by observing that (12) and (14) come as immediate consequence on imposing the Ehrenfest condition

$$v(E(q),t) = \frac{d}{dt}E(q)\,, \tag{15}$$

so that the strictly coherent MUDPs can be viewed as the most deterministic semi-classical processes.

Consider the scale transformation $x \to e^{-s}x$ which authomatically implies $u \to e^{s}u$, where $s$ is the scale parameter. The Gaussian distribution (8) is form-invariant under this transformation, while the uncertainty product (7) is strictly invariant with $\Delta q \to e^{-s}\Delta q$ and $\Delta u \to e^{s}\Delta u$. We will show next that in the framework of Nelson stochastic quantization this transformation is just the squeezing transformation of quantum mechanics. In this context, broadly coherent MUDPs are of special interest when considering time-dependent squeezing.

# 3 Nelson Diffusions

A very important class of diffusion processes (Nelson diffusions) in physics has been introduced by Nelson in his stochastic formulation of quantum mechanics [5].

To each single-particle quantum state $\Psi = \exp\left[R + \frac{i}{\hbar}S\right]$, Nelson stochastic quantization associates the diffusion process $q(t)$ with

$$\nu = \frac{\hbar}{2m}\,, \qquad \rho(x,t) = |\Psi(x,t)|^2\,, \qquad v(x,t) = \frac{1}{m}\frac{\partial S(x,t)}{\partial x}\,, \tag{16}$$

where $m$ is the mass of the particle. At the dynamical level, the Schroedinger equation with potential $V(x,t)$ is equivalent to the Hamilton-Jacobi-Madelung equation

$$\partial_t S(x,t) + \frac{(\partial_x S(x,t))^2}{2m} - \frac{\hbar^2}{2m}\frac{\partial_x^2 \rho^{1/2}(x,t)}{\rho^{1/2}(x,t)} = -V(x,t)\,. \tag{17}$$

It is well known [9] that for Nelson diffusions the uncertainties $\Delta q$ and $\Delta u$ are related to the quantum mechanical uncertainties $\Delta\hat{q}$ and $\Delta\hat{p}$ of the position and momentum operators $\hat{q}$ and $\hat{p}$ by

$$\Delta\hat{q} = \Delta q\,, \qquad (\Delta\hat{p})^2 = m[(\Delta u)^2 + (\Delta v)^2]\,, \tag{18}$$

$$(\Delta\hat{q})^2(\Delta\hat{p})^2 \geq (\Delta q)^2(\Delta mu)^2 \geq \frac{\hbar^2}{4}\,.$$

Minimum uncertainty Nelson diffusions (MUNDs) are MUDPs. Correspondingly, we will speak of strictly and broadly coherent MUNDs. By solving (17) for MUNDs we obtain $V(x,t)$ and the classical equations of motion for $E(q)$. For strictly coherent MUNDs (12) we have

$$V(x,t) = \frac{m}{2}\omega^2 x^2 + f(t)x + V_0(t)\,, \qquad \omega^2 = \frac{\hbar^2}{4m^2(\Delta q)^4}\,,$$

$$\frac{d^2}{dt^2}E(q) + \omega^2 E^2(q) = f(t)\,. \tag{19}$$

When the arbitrary constants $f(t)$ and $V_0(t)$ vanish, eqs. (19) are those of the classical harmonic oscillator and the associated quantum states are the standard Glauber coherent states; when $f(t) = \text{const.}$ we have the Klauder-Sudarshan displaced oscillator coherent states; finally, when $f(t)$ is truly time-dependent, we obtain the Klauder-Sudarshan driven oscillator coherent states [10].

For broadly coherent MUNDs we have instead

$$V(x,t) = \frac{1}{2}m\omega^2(t)x^2 + V_0(t)\,, \qquad \omega^2(t) = \dot{g}(t) + 2g^2(t) - \frac{\hbar^2}{8m^2(\Delta q)^4}\,, \tag{20}$$

where $g(t) = (\Delta q)^{-1}d\Delta q/dt$ must be such that $\omega^2(t)$ is positive. Eq. (20) describes the parametric oscillator potential, associated to the feature of time-dependent squeezing.

Furthermore, we can identify among MUNDs those corresponding either to Heisenberg or to Schroedinger minimum uncertainty. The key relation, easy to prove, is

$$E(vq) - E(v)E(q) = \frac{< \{\hat{Q}, \hat{P}\} >_\psi}{2}\,; \quad \hat{Q} = \hat{q} - < \hat{q} >_\psi\,, \quad \hat{P} = \frac{\hat{p} - < \hat{p} >_\psi}{m}\,, \tag{21}$$

where $< \{\cdot,\cdot\} >_\psi$ denotes the expectation of the anti-commutator in the state $\Psi$, i.e. the Schroedinger part of the quantum mechanical uncertainty.

Eqs. (18) and (21) show that the strictly coherent MUNDs (19) exhaust the Heisenberg minimum uncertainty states, while the broadly coherent MUNDs (20) form a subset of the Schroedinger minimum uncertainty states.

Finally, we investigate the possibility of letting $\nu$ be time-dependent in the context of quantum mechanics. From the first of equations (16) this means letting either $m$ or $\hbar$ be functions of time.

This latter case seems a bit speculative at this stage. We thus fix our attention on the case of time-dependent mass $m(t)$ and constant $\hbar$.

For such systems it can be immediately verified that the Nelson scheme (16)-(17) still holds with $m(t)$ replacing $m$. Considering the most interesting case of strictly coherent MUNDs, which means choosing $C(t) \propto \nu(t)$, and solving (17) we obtain

$$V(x,t) = \frac{1}{2}m(t)\omega^2(t)x^2 + f(t)x + V_0(t)\,, \qquad \omega^2(t) = \frac{\hbar^2}{4m^2(t)(\Delta x)^4}\,,$$

$$\frac{d^2}{dt^2}E(q) + \frac{\dot{m}(t)}{m(t)}\frac{d}{dt}E(q) + \omega^2(t)E(q) = \frac{f(t)}{m(t)}\,, \tag{22}$$

where $f(t)$, $V_0(t)$ are arbitrary functions of time. Eqs. (22) supplemented with $m(t) = m_0 e^{\Gamma(t)}$ define the dynamics of the damped parametric oscillator. The stochastic approach thus sheds new light in a unified treatment on the study of quantum dissipative oscillators, for it allows to derive for the expectation value the dynamical equation (22) that was so far unknown.

In conclusion, we have shown that the quantum mechanical concepts of uncertainty, coherence, and squeezing can be imported in the probabilistic arena of diffusion processes. This appears to be possible because of a subtle interplay between fluctuations, control, and optimization. Conversely, we may also say that these features of quantum mechanics can be traced back and related to general properties of diffusion processes.

Work on this subject is in progress, and includes application of our scheme to polymer dynamics and chemical reactions, uncertainty relations in field theory and dynamical systems on lattices and manifolds.

# References


[1] C. W. Gardiner, *Handbook of Stochastic Methods*, (Springer, Berlin, 1985).

[2] J. R. Klauder and B. S. Skagerstam, *Coherent States*, (World Scientific, Singapore, 1985).

[3] D. Stoler, Phys. Rev. **D1**, 3217 (1970); H. P. Yuen, Phys. Rev. **A13**, 2226 (1976).

[4] S. De Martino, S. De Siena, F. Illuminati, and G. Vitiello, *Diffusion Processes and Coherent States*, Preprint, University of Salerno, June 1993.

[5] E. Nelson *Dynamical Theories of Brownian Motion* (Princeton University Press, Princeton, 1967); *Quantum Fluctuations*, (Princeton University Press, Princeton, 1985); F. Guerra, Phys. Rep. **77**, 263 (1981); G. Parisi, *Statistical Field Theory*, (Addison-Wesley, New York, 1988).

[6] P. Ruggiero and M. Zannetti, Phys. Rev. Lett. **48**, 963 (1982).

[7] E. C. G. Sudarshan, in these Proceedings.

[8] E. Celeghini, M. Rasetti, and G. Vitiello, Phys. Rev. Lett. **66**, 2056 (1991); E. Celeghini, S. De Martino, S. De Siena, M. Rasetti, and G. Vitiello, in these Proceedings.

[9] D. De Falco, S. De Martino, and S. De Siena, Phys. Rev. Lett. **49**, 181 (1982); S. De Martino and S. De Siena, Nuovo Cimento **B79**, 175 (1984).

[10] J. R. Klauder and E. C. G. Sudarshan, *Fundamentals of Quantum Optics* (Benjamin, New York, 1970).

# SECTION 6

# FIELD THEORY AND GENERAL INTEREST

# APPLICATIONS OF SQUEEZED STATES: BOGOLIUBOV TRANSFORMATIONS AND WAVELETS TO THE STATISTICAL MECHANICS OF WATER AND ITS BUBBLES

B. DeFacio, S.-H. Kim and A. Van Nevel
Department of Physics & Astronomy
Missouri University
Columbia, MO 65211

## ABSTRACT

The *squeezed states* or *Bogoliubov transformations* and wavelets are applied to two problems in non-relativistic statistical mechanics: the dielectric response of liquid water, $\epsilon(\vec{q},\omega)$, and the bubble formation in water during insonnification. The *wavelets* are special phase-space windows which cover the domain and range of $L^1 \cap L^2$ of classical causal, finite energy solutions. The multi-resolution of discrete wavelets in phase space gives a decompostion into regions of time and scales of frequency thereby allowing the renormalization group to be applied to new systems in addition to the tired 'usual suspects' of the lsing models and lattice gasses. The Bogoliubov transformation: squeeze transformation is applied to the *dipolaron* collective mode in water and to the gas produced by the explosive cavitation process in bubble formation.

## 1. INTRODUCTION

Water is extremely important in chemistry and biology both as a solvent and as a neutral medium which is rich in possibilities.[1–19] The dielectric response of a medium, $\epsilon(\vec{q},\omega)$ is related to the index of refraction as, $n(\vec{q},\omega) = \sqrt{\epsilon\mu}$, whose real part controls wave propagation and whose imaginary part gives the attenuation. An August 1993 dissertation at Missouri University by one of us, S.-H. Kim[19], formulates a new model which is rather successful in accounting for the complex index of refraction $n(\omega) + i\alpha(\omega)$, over 14 to 15 decades of frequency. This model is a number-conserving relaxation-time,[7] Boltzmann transport equation model in phase space[5,6,9] based on Kubo's fluctuation-dissipation theorem [12] and a Kerr approximation.[11] The free rotation gives an IR peak at the correct frequency which is much larger than the one found experimentally by Simpson et al.[15] A phase-space analysis of our model based on wavelets will be presented here.

The problem of bubble formation in liquids is both old and difficult.[20–25] It is now known that two different mechanisms of bubble formation exist: **cavitation**, where the growth is explosive and **nucleation** where diffusion of molecules yields a slow growth. This work will be restricted to cavitation. All bubbles are interesting for electromagnetic wave propagation in water because they give additional spatial dispersion $\vec{q}$-dependence to the index of refraction of the medium through their Mie scattering.

The approach taken here will be to form a mean-field theory of a $\Phi^4$ theory in 4 space-time dimensions. It is a variant of an idea due to Kaup,[25] Wilhelmsson[26] and Glimm[27] that bubbles are non-linear, coherent effects in fluids. Kaup's clever title is, "Cavitons are solitons" for a plasma driven by both sound and electromagnetism. Our equations are completely different and have solitary wave solutions rather than solitons. These solitary waves will have finite lifetimes in contrast to the infinite lifetimes of Kaup's cavitons, which

he first showed were an integrable system. However, since both models are subject to other perturbations, this difference is not actually as serious as it first appears.[29]

There is also a practical reason for trying to understand bubble formation. Apfel[30,31], Nyborg[32], Rose and Goldberg[33] have shown that ultrasound at the frequencies used for medical diagnostics forms bubbles in water and tissue. They have raised questions about the safety of ultrasound but have not yet shown any evidence that these bubbles (or any other effect of ultrasound) are harmful. Trevena[34] has suggested that bubble collapse may occur through shock waves, which could damage cells.

Both of these problems will be analyzed using wavelets[36–51] which are a special class of **windows**

(i) which cover the domain $\Re^1$ or $\Re^2$ in refs. (36-49) and the Lorentzian manifold of special relativity in ref (50,51); and

(ii) are dense in the range of $L^2 \cap L^1$.

The first space $L^2$ is required classically for finite energy signals and for a probability interpretation of Hilbert space states in non-relativistic quantum mechanics, and the space $L^1$ is required classically for causality and is a major technical requirement in non-relativistic quantum mechanics which provides absolute continuity. Clearly, (i) assures the existence of measurability of the underlying space and (ii) places additional restrictions on the solutions for the correct dynamics and symmetries. In particular, the symmetry group is the set of **dilations**. In the continuous one-dimensional case dilations are generated by the transformation D

$$(D_{ab})(x) = ax + b \tag{1}$$

$$(D_{ab}\psi)(x) = |a|^{1/2}\psi\,(ax - b) \tag{2}$$

on the coordinates $x$ and solutions $\psi \in L^2 \cap L^1$, where $a \in \Re^1_+$ and $b \in \Re^1$. In the discrete case $(k, j) \in$ (the integers) with $a = 2$ (one choice, but not the only one)

$$(D_{jk})(x) = 2^j \cdot x + k \tag{3}$$

$$(D_{jk}\psi)(x) = : \psi_{jk}(x) = |2|^{j/2}\psi\left(2^j x - k\right) \quad . \tag{4}$$

In the discrete case, $L^2 \to \ell^2$ and $L^1 \to \ell^1$ and $\psi_{kj}$ "live in" $\ell^2 \cap \ell^1$. The choice of $a = 2$ gives the Lebeque covering of $\Re^1$ and extends to $\Re^n$ and thus any other integer with this property will suffice. To satisfy (2) the conditions (2a) completeness

$$\overline{V\psi_{jk}} = L^2 \cap L^1 \tag{5}$$

(2b) **mean zero** for $\psi$, mean one for $\phi$

$$\hat{\psi}(0) = \int_{-\infty}^{\infty} \psi(x)dx = 0 \tag{6}$$

$$\hat{\phi}(0) = \int_{-\infty}^{\infty} \psi(x)dx = 1 \tag{7}$$

where the multiresolution decompostion of Mallet satisfies $V_j = V_{j-1} \overline{\oplus} W_{j-1}$, i.e. $V_{j-1} \cup W_{j-1} = V_j$ and $V_{j-1} \cap W_{j-1} = \{0\}$. For fixed $j$, eqs. (3,4) reduce to a translation on $\ell^2$.

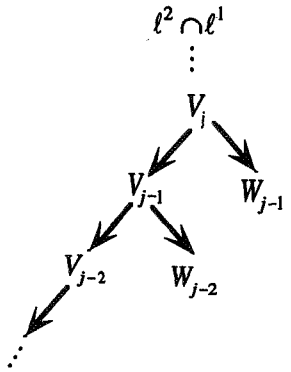


If $k$ is considered as a time (space) translation, $kt_0$, and $2^j$ as a frequency (wavenumber) scale, $2^j\omega_0$, with $t_0\omega_0 \geq 1$ then each fixed $j_0$ corresponds to a discrete translation group at frequency scale $2^{j_0}\omega_0$ and changing $j_0$ changes the frequency scale. Even if $\psi$ or $\phi$ are time (space) signals, the dilation operators $D_{ab}$ or $D_{jk}$ map them into the time (space)—frequency (wave number) **phase space**. Thus

$$\phi(x) \in V_j \quad \text{and} \quad \psi(x) \in W_j \tag{8}$$

implies that

$$\phi(2x) \in V_{j-1} \quad \text{and} \quad \psi(2x) \in W_{j-1} \quad . \tag{9}$$

The interpretation of the $V_j'$'s spanned by the $\phi_j'$'s is as a low band-pass window at frequency scale $2^j\omega_0$ whereas the higher frequencies are in the $W_j$'s spanned by $\psi_j$.'s at that frequency scale.

From this short discussion two things should be obvious. One is that although a wavelet is a window, **it is a great deal more** as it must cover each space-time point in order not to miss any point particles, or sources of charge or mass. The other is that all of the solutions allowed by the symmetries and dynamics of the system must be expressed in the wavelet basis, i.e. they must be a complete set. Kaiser[50] has formulated relativistic electrodynamics in terms of a wavelet based on analyicity and coherent states. D'Aranio and DeFacio[49] have formulated a class of squeezed states of quantum optics and provided a general inversion structure for a general density operator in terms of a suitable window, which was expressed in terms of a general basis of observables. Han, Kim and Noz[51] have presented a study of the relativistic phase space of light using compactly supported wavelet windows to clarify the relation between photons and light waves. Since there are many wavelet windows for any given problem, it is important to know which ones are natural and, if possible, if a "best one" exists.

In this paper, the application of wavelets and state squeezing, Bogoliubov transformations to the two statistical mechanics problems: $\in (\vec{q}, \omega)$ for water in **Section 2** and bubble formation will be described in **Section 3**, and our conclusions will be presented in **Section 4**.

## 2. STATISTICAL MECHANICS OF WATER, THE DIELECTRIC RESPONSE

In collaboration with Professor G. Vignale, we have published studies of a classical water-like polar fluid whose properties are chosen to mimic water. The starting point is the number-conserving relaxation-time approximation to the Boltzmann transport equation. Up to the first order deviation from equilibrium it has the form

$$\frac{\partial f_1}{\partial t} + \sum_\alpha \left[ \dot{q}_\alpha \left( \frac{\partial f_1}{\partial q_\alpha} \right) + \dot{p}_\alpha \left( \frac{\partial f_1}{\partial p_\alpha} \right) - \left( \frac{\partial v}{\partial q_\alpha} \right) \left( \frac{\partial f_0}{\partial p_\alpha} \right) \right] = - \frac{f_1 - f_1^{loc}}{\tau} \quad , \tag{10}$$

where overdots are time rate of changes, $\dot{q}_\alpha = \frac{\partial T}{\partial p_\alpha}$, $\dot{p}_\alpha = -\frac{\partial T}{\partial q_\alpha}$, $f_0 = e^{-\beta T}/Z$ is the equilibrium Boltzmann distribution function. $T$ is the kinetic energy of the molecule and includes translations, rotations and small amplitude vibrations, and $Z$ is the partition function. $f_1$ is the first order correction term to $f_0$ by a perturbed applied potential. The static response of the electric susceptibility $\chi(\omega = 0)$ is a $3 \times 3$ real matrix-valued quantity given by $-\beta f_0(q_\alpha)$.

Upon determining the dynamical self-response function $\chi_s(\omega)$ self-consistently from $f_1^{loc}$

$$\chi_s(\omega) = (1 + i/\omega\tau)\chi^0(\omega + i/\tau) \left[ 1 + \frac{i}{\omega\tau} \chi^0(\omega + i/\tau) \left\{ \chi^0(\omega = 0) \right\}^{-1} \right]^{-1} \quad , \tag{11}$$

where the Kubo fluctuation dissipation theorem for the single particle self-electric susceptibility

$$\chi^0(\omega) = \chi(0) \left[ 1 + i\omega \mathbf{G}(\omega) \right] \quad , \tag{12}$$

relates the electric susceptability to the van Hove correlation function $G(\omega)$. The total response from the Kubo theorem is

$$\chi(\omega) = \chi_s(\omega) \left[ 1 - \Psi(\vec{q}) \chi_s(\omega) \right]^{-1} \quad , \tag{13}$$

where $\Psi$ is the local field factor which describes the coherent many particle interactions. It is the analog of Lorentz's local field factor, in modern many-body theory. We have explored several choices and found Wei and Patey[17] to provide the best agreement with experiment. Indeed, various computer intensive molecular dynamics and Monte Carlo calculations gave $\epsilon_T(\vec{0}, 0)$ as 25-71 instead of the experimental value of $90.8 \pm 3.2$! The large experimental uncertainty is dominated by the spontaneous dissassociation $H_2O \rightleftharpoons H^+ + OH^-$ , which at $20°C$ yields an ion concentration of $8.33 \times 10^{-8}$ $moles/liter$. The high mobility of the $H^+$ species allows it to form a positively charged surface layer at the negative electrode which can distort the measured value of the electric permittivity, $\epsilon(\omega)$. By taking a limit as the moments of inertia approach zero, the Stockmayer fluid calculations were found comparable to the best computer studies. The causal dielectric permittivity values are

$$\frac{1}{\epsilon_T(\vec{q}, \omega)} = \frac{1}{[1 + 4\pi\chi_T(\vec{q}, \omega)]} \tag{14a}$$

and

$$\frac{1}{\epsilon_L(\vec{q}, \omega)} = [1 - 4\pi\chi_L(\vec{q}, \omega)] \tag{14b}$$



C-5

where $(T, L)$ denote the transverse and longitudinal components of the dielectric tensor $\epsilon$ and the electric susceptability tensor $\chi$. The directions $(T, L)$ are taken from the direction of the applied (vacuum) electric field $\vec{E}$. **Remark:** A wave propagation or scattering experiment is required to measure the $\vec{q}$ dependence of $n$ and $\alpha$, in contrast to the *ac* capacitance bridge which measures only the angular frequency, $\omega$, dependence. A graph from ref. (18) of the real part of the index of refraction will be shown later.

There is a collective mode in $\epsilon_L$ which Lobo, Robinson and Rodrigues[9] first suggested and Pollock and Alder[10] found in their simulation of a Stockmayer fluid model of water. It occurs in our model both in the symmetric rotor "waterlike" case[18] and in the realistic asymmetric rotor case.[19]

Considering the water molecule as a two-level system for simplicity, the composite Boson creation and destruction operators which create and destroy water molecules (*recall* that this analysis is at frequencies that are far below the breakup threshold energies) are written as $(\vec{a}_\alpha, \vec{a}_\beta^+)$ where their directions are those of the electric dipole moment, $\vec{\mu}$, of the molecule and $\alpha, \beta = 1, 2$ label which level. The collective dipolaron boson is created and destroyed by the Bogoliubov transformed operators $(b_\alpha,\ b_\beta^+)$. The frequency of the dipolaron is complex-valued

$$\omega_\alpha = \Omega_{q\alpha} - i\Gamma_{q\alpha} \tag{15}$$

and lies in the lower half $\omega$-plane because the response function $1/\epsilon_L(\vec{q}, \omega)$ is causal. The frequency in eq. (15) is determined from

$$Re\left[\epsilon_L\left(\vec{q}, \Omega_{q\alpha}\right)\right] = 0 \quad , \tag{16}$$

and the width from

$$\Gamma_{q\alpha} = \frac{\left|Im\left[\epsilon_L\left(\vec{q}, \Omega_q\right)\right]\right|}{\left|\left[\frac{\partial \epsilon_L(\vec{q},\omega)}{\partial \omega}\right]\right|_{\omega=\Omega_{q\alpha}}} \quad , \tag{17}$$

provided that $\Omega_{q\alpha} >> \Gamma_{q\alpha}$. The peak and its width are shown in Fig. 1, where one can see that $\Omega_{q\alpha} >> \Gamma_{q\alpha}$ is satisfied. The mechanism of this collective mode is high frequency coherent oscillations of the electric dipoles in self-consistent fields in the liquid. In order for the mode to be longitudinal, they oscillate 180° out of phase. Both $\Omega_{q\alpha}$ and $\Gamma_{q\alpha}$ were shown by Kim, *et al.*[18], to be almost *dispersion-free* (they only change by 1% over the entire range of validity). This mode depends on $q = |\vec{q}|$ being small but non-zero so it cannot be measured from any *ac* capacitance experiment such as those in ref. (3) and must await a light or neutron scattering experiment. Such an experiment would ***verify*** or ***falsify*** the model formulated in refs. (18,19).

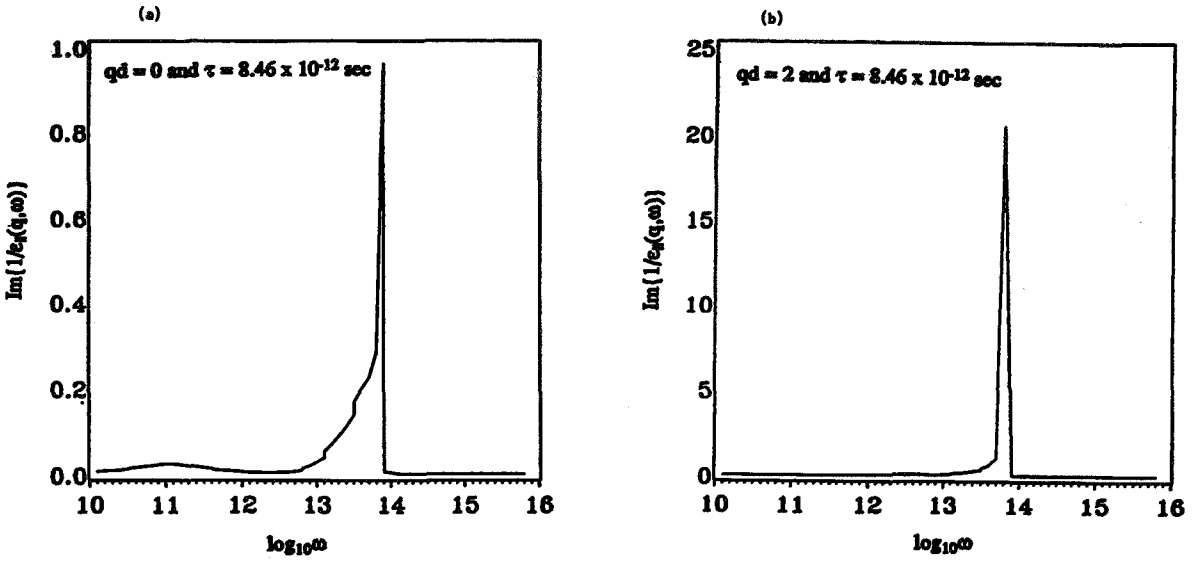


**Fig. 1.** The dipolaron collective mode in water.

Next, the reader is reminded that eq. (10) includes translations, rotations and vibrations in the $\dot{p}_\alpha \left(\frac{\partial T}{\partial p_\alpha}\right)$ terms. It is well known[52,53] that the renormalization group is based upon a scaling invariance. By expanding the single particle distribution function $f_1(\cdot)$ in a wavelet series

$$f_1(\cdot) = \sum_{j_i} C_{jk} \psi_{jk}(\cdot) \tag{18}$$

where $(\cdot)$ can stand for either the translation $\vec{x}$, rotation $(\theta, \phi)$ or vibrations $(q_1, q_2, q_3)$ in the real index of refraction $n(\omega)$. The three normal modes for vibration are given by group theory and are used in our calculation of $n(\omega)$. In Fig 2 the frequencies up to $10^{10} Hz$ are dominated by the translations, from $10^{10} \sim 10^{12} Hz$ at $(A, A')$ the collisions dominated Debye relaxation time dominates and at $10^{13} Hz$ the free rotor peak occurs at $(B_1, B')$. The free rotor peak at $(B')$ in our theory is much too large, so work is underway to try to bring this into better agreement with the experiment. Between $10^{13}$ and $10^{14} Hz$ the collective mode $(C')$ occurs with coherent oscillations of the dipoles as its mechanism. The small optical peaks at $(D_1, D_2)$ fail to resolve the two higher frequency modes in $(D_2)$ but we think that future experiments will. Thus, the wavelet phase space allows us to analyze the Boltzmann transport equation with a non-trival interaction.

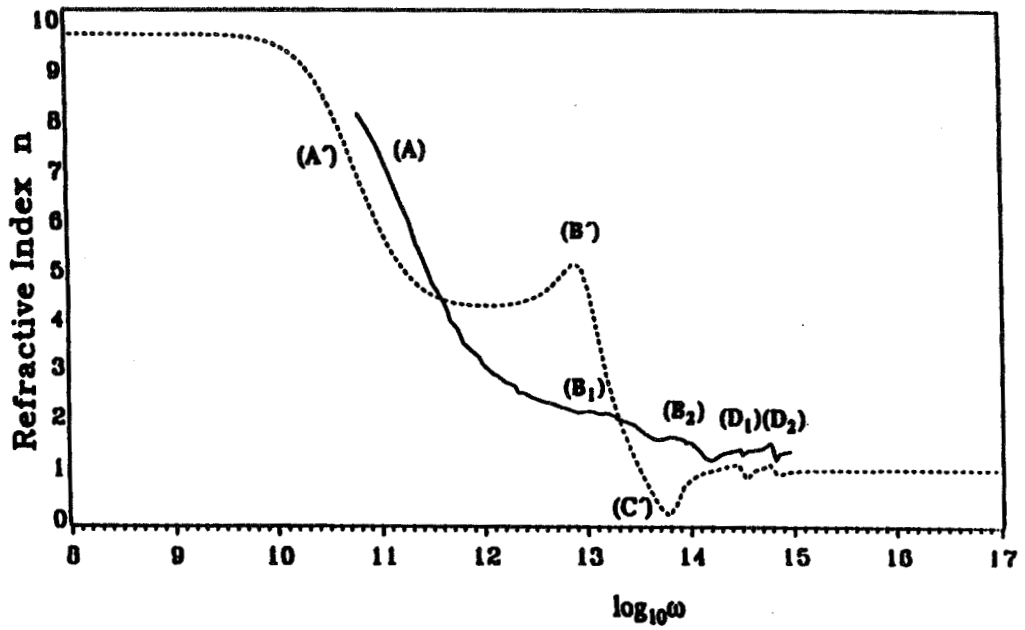


**Fig. 2.** The real index of refraction of water.

## 3. BUBBLE FORMATION IN WATER BEING INSONIFIED BY ULTRASOUND

The idea behind this calculation is to adapt the idea of Kaup to a solitary wave model by generalizing the work of Hammer, Shrauner and DeFacio where $\phi$ is a $1 \oplus 1$ fluid density field

$$L = -\frac{1}{2}\left[(\phi_x)^2 + (\phi_t)^2\right] - \frac{B}{4}\left(\phi^2 - u_0^2\right)^2 \quad , \tag{19}$$

with $u_0^2 = A/B$ where $A, B$ are real and positive coupling constants and $A$ is the strength of the negative mass, $B$ is the strength of the positive nonlinear quartic interaction to three space dimensions with a radial time independent potential. In $3 \oplus 1$ space-time dimensions

$$L_F = -\frac{1}{2}\left[\left(\vec{\nabla}\phi\right)^2 + \phi_t^2\right] - \frac{B}{4}\left(\phi^2 - u_0^2\right)^2 \quad , \tag{20a}$$

$$L_A = -\frac{1}{2}\left[\left(\vec{\nabla}p\right)^2 - p_t^2\right] - \frac{B_1}{4}\left(p^2 - u_{01}^2\right)^2 \quad , \tag{20b}$$

$$L_I = g\phi^2 p^2 + \mu\phi_t^2 \tag{20c}$$

where $L_F$ is the Lagrangian of the fluid, $L_A$ is the acoustic Lagrangian for the sound wave and $L_I$ is the interaction Lagrangian. If $\mu \approx 0$ and the sound waves are small enough in amplitude to be linear (see eq. (30a)) the field equations become

$$-(\Delta\phi + \phi_{tt}) - A\phi + B\phi^3 + gp^2\phi = 0 \quad , \tag{21a}$$

$$-(\Delta p - p_t t) - A_1 p + B_1 \rho^3 + g\phi^2 p = 0 \tag{21b}$$

The key role played by the nonlinear "potential" which acts as a *convection* term is our justification for calling this approach a *strong convection model.* The mechanism is that

the constant sound wave in the fluid produces gas under pressure as a new *phase* in the fluid. This is a non-equilibrium, open system and the gas density can be described by one Bogoliubov transformation and the non-zero temperature, $0°C$ to $100°C$, can be obtained from another Bogoliubov transformation. The entropy of this situation was discussed by DF, VN and Professor Brander[63] of the Institute for Theoretical Physics at Chalmers in the Göthenberg. The $\ell = 0$, radial solutions to eqs. (21a,b) are Jacobi elliptic functions with modulus $k_1$, $0 \leq k_1 \leq 1$, $\delta_{01}$ is a density defect where the local mass density is a minimum so that it is a site for cavitation and $(u, u_{01})$ are the amplitudes for the density and pressure wave, respectively.

Next a time-independent *mean field theory* for the density $\phi$ is formed by linearizing about the Jacobi elliptic functions according to

$$gp^2\phi \to gu_{01}^2 \left[Sn\left(\kappa_1 (r + \delta_{01}) \,|k_1\right)\right]^2 \phi \quad , \tag{22}$$

and

$$B\phi^3 \to B < \phi^2 > \phi \to Bu^2 \left[Sn\left(\kappa (r + \delta) \,|k\right)\right]^2 \quad . \tag{23}$$

This should be valid, provided it is not applied too close to a caviton 'explosion', and leads to the linearized field eqaution for the density $\phi$

$$\Delta\phi + \phi_{tt} + V_{MFT}(r)\phi = 0 \quad , \tag{24}$$

where

$$V_{MFT}(r) = A - Bu^2 \left[Sn\left(\kappa (r + \delta) \,|k\right)\right]^2 + gu_{01}^2 \left[Sn\left(\kappa_1 (r + \delta_{01}) \,|k_1\right)\right]^2 \tag{25}$$

Separation of variables using

$$\phi = R(r) Y_{\ell m}(\theta, \Phi) e^{-\omega_q t} \quad , \tag{25a}$$

and

$$R(r) = \frac{u(r)}{r} \tag{25b}$$

reduce eq. (25) to

$$u_{rr} + \left[V_{MFT} - \frac{\ell(\ell t^1)}{r^2} + \omega_q^2\right] u = 0 \quad . \tag{26}$$

This ODE satisfies Dirchlet zero boundary conditions on the dense domain $H^2(R_+^1)$ where $R_+^1$ is the positive half-line and $H^2$ is the Sobolev space of $L^2$ functions whose first two derivatives exist and are $L^2$. Thus, eq. (26) can be solved numerically using the Numerov algorithm. Then the density is constructed from the relation

$$\phi(\vec{r}, t) = \sum_{q\ell m} c_{q\ell m} R_{q\ell}(r) Y_{\ell m}(\theta, \phi) e^{-\omega_q t} \quad . \tag{27}$$

From eq. (27) the sound wave has modulus $k_1 \simeq 0$. One thing about this strong convection model which seems new is the inclusion of $\ell \geq 1$ multipoles which give deviations from spherical symmetry. The calculus of variation "proof" that bubbles are spherically shaped

only holds for thermal and fluid equilibrium, whereas the continous quasi-monochromatic sound wave makes this an open, non-equilibrium system. In Fig. 3 $V_{MFT}$ is plotted and

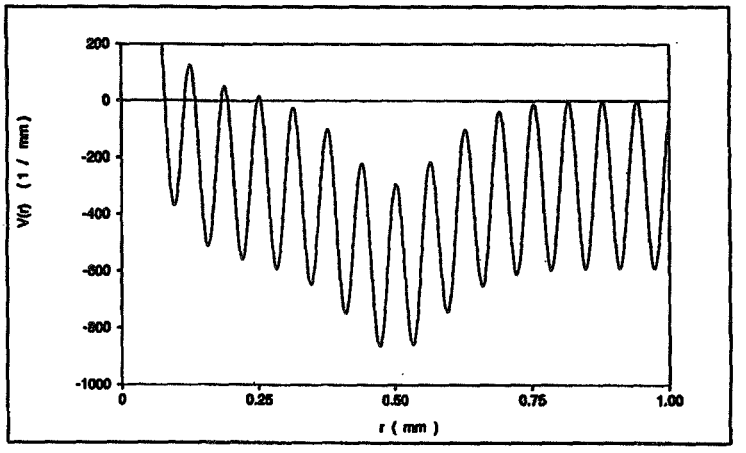


**Fig. 3.** An example of a mean field theory potential, $V_{MFT}$.

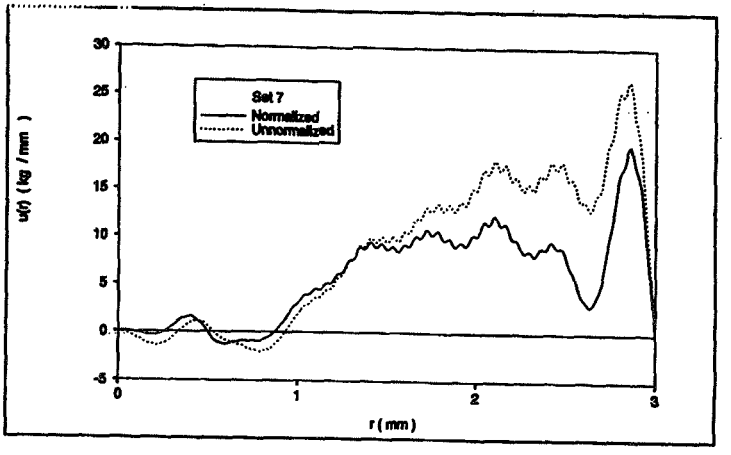


**Fig. 4.** The water density in a $3mm$ cell calculated from the mean field theory potential in the previous figure.

in Fig. 4 a bubble is shown which was found in the density, using the convection potential of Fig. 3. The parameters are consistent with those of water with a sound wave amplitude which is physically realizable. The bubble is centered at $\delta = 0.75mm$; and has radius $r_0 \simeq 300\mu$ ($\mu = 10^{-6}m$). The detection of bubble interfaces using wavelets is under study. Since some authors have questioned the safety of ultrasound in tissue,[31,34] it is important to understand bubble formation. In addition, the Mie scattering from bubbles adds spatial dispersion to the effective index of refraction.

## 4. CONCLUSIONS

Two different problems in non-equilibrium statistical mechanics were discussed:

(i) the dielectric response of water, $\epsilon(\vec{q},\omega)$, and

(ii) bubble formation in water under insonnification using Bogoliubov transformations: state squeezing maps and wavelets.

The multi-resolution structure of phase space permits the sort of analysis which the renormalization group has provided for lsing models and lattice gas models and little else. Thus, "squeezed states" are useful for more than quantum optics.


## ACKNOWLEDGEMENTS

This work was supported in part by the Missouri University Department of Physics and AFOSR grants 90-307 and 91-203. Professors Giovanni Vignale and Peter Pfeifer are thanked for many useful conversations. The figures were produced by the NeXT and Silicon Graphics Personal Iris work stations purchased by the two AFOSR grants. The organizers of the Third International Workshop on Squeezed States, Professors M.H. Rubin and Y.-H. Shih of UMBC and Dr. D. Han of NASA, Greenbelt are thanked for organizing an excellent conference which continues the traditions initiated by Professor Y.S. Kim and Professor W.W. Zachary.


## REFERENCES


1. D. Eisenberg and W. Kauzmann, **The Structure and Properties of Water** (Oxford University Press, Oxford, 1969).
2. A. Ben-Naim, **Water and Aqueous Solutions** (Plenum Press, New York and London, 1974).
3. E.H. Grant, R.J. Sheppard and G.P. South, **Dielectric Behavior of Molecules in Solution** (Oxford University Press, Oxford, 1978).
4. P. Debye, **Polar Molecules** (The Chemical Catalog Company, New York, 1929).
5. J. McConnell, **Rotational Brownian Motion and Dielectric Theory** (Academic, New York, 1980).
6. L.E. Reichl, Phys. Rev. A **24**, 1609 (1981); Phys. Rev. Lett. **49**, 85 (1982); L.C. Sparling, L.E. Reichl, and J.E. Sedlak, Phys. Rev. A **33**, 699 (1986).
7. N.D. Mermin, Phys. Rev. B **1**, 2362 (1970).
8. A. Rahman and F.H. Stillinger, J. Chem. Phys. **55**, 3336 (1971); **57**, 1281 (1972); J. Am. Chem. Soc. **95**, 7943 (1973); F.H. Stillinger, in *Liquid State of Matter*, edited by E.H. Montroll and J.L. Lebowitz (North-Holland, Amsterdam, 1982).
9. R. Lobo, J.E. Robinson, and S. Rodriquez, J. Chem Phys. **59**, 5992 (1973).
10. E.L. Pollock and B.J. Adler, (a) Physica A **102**, 1 (1980); (b) Phys. Rev. Lett. **46**, 950 (1981).

11. W.C. Kerr, Phys. Rev. **174**, 316 (1968).

12. R. Kubo, J. Phys. Soc. Jpn. **12**, 570 (1957): Rep. Prog. Phys. **29**, 255 (1966).

13. J.P. Hansen and I.R. McDonald, *Theory of Simple Liquids*, 2nd ed. (Academic, San Diego, 1986).

14. M.R. Querry, B. Curnutte, and D. Williams, J. Opt. Soc. Am. **59**, 1299 (1969); A.N. Rusk, D. Williams, and M.R. Querry, J. Opt. Soc. Am. **61**, 895 (1971).

15. O.A. Simpson, B.L. Bean, and S. Perkowitz, J. Opt. Soc. Am. **69**, 1723 (1979).

16. I. Thormahlen, J. Straub, J.M.H. Levelt Sengers, and J.S. Gallagher, J. Phys. Chem. Ref. Data **14**, 933 (1985); P. Schiebener, J. Straub, J.M.H. Levelt Sengers, and J.S. Gallagher, J. Phys. Chem. Ref. Data **19**, 677 (1990).

17. S.-H. Kim, G. Vignale and B. DeFacio, Phys. Rev. A **46**, 7548 (1992).

18. S.-H. Kim, B. DeFacio and G. Vignale, Phys. Rev. E **48** (Oct '93, in press).

19. S.-H. Kim, **The Dynamic Dielectric Response Function of Liquid Water**, Doctoral Dissertation, Missouri University, Department of Physics & Astronomy, Columbia, MO (August, 1993).

20. Alan Van Nevel, **A Model for Bubble Formation in a Fluid Undergoing Insonification** MS Thesis, Missouri University, Department of Physics & Astronomy, Columbia, MO (December, 1993).

21. M. Berthelot, Ann. Chim. Phys. **30**, 232-7 (1850).

22. F.M.L. Donny, Ann. Chim. Phys. **16**, 167-90 (1846).

23. Lord Rayleigh, Phil. Mag. **34** 9408 (1917).

24. G.K. Batchelor, **Introduction to Fluid Dynamics**, (Cambridge University Press Cambridge, New York, and Melbourne, 1967).

25. D.J. Kaup, Phys. Fluids **31** (6), 1465-70 (1988),

26. H. Wilhelmsson and J. Weiland, **Coherent Non-Linear Interaction of Waves in Plasmas**, (Pergammon, New York, 1977).

27. J. Glimm, SIAM Review **33**, 626-43 (1991).

28. C.L. Hammer, J.E. Shrauner, and B. DeFacio, Phys. Rev. B **23**, 5890-5903 (1981).

29. Private communication, Professor D.J. Kaup to BDF.

30. R. Apfel, **IEEE Transactions on Ultrasonics, Ferroelectrics, and Frequency Control**, Vol. UFFC-33, 139-42 (1986).

31. R.A. Roy, S. Madanshetty, and R. Apfel, J. Acoustic Soc. Am. **87** (6), 2451-58 (1990).

32. W. Nyborg and D. Miller, Appl. Sci. Res. **38**, 17-24 (1982).

33. J. Rose and B. Goldberg, **Basic Physics in Diagnostic Ultrasound** (Wiley and Sons, New York, 1979).

34. D.H. Trevena, **Cavitation & Tension in Liquids** (Adam Hilger, Bristol and Philadelpia, 1987).

35. Private communication, Dr. Richard Albanese, of Brooks AFB, to BDF.

36. A. Grossmann and J. Morlet, "Decomposition of Hardy Functions into Square-integrable Wavelets of Constant Shape," SIAM J. Math. Anal. **15**, 723-736 (1984).

37. J.M. Combes, A. Grossman and Ph. Tehamitchian, Editors, **Wavelets Time-Frequency Methods and Phase-Space**, (Springer-Verlag, Berlin and New York, (1989)).

38. M. Frazier, B. Jawerth and G. Weiss, **Littlewood-Paley Theory and the Study of Function Spaces** NSF-CBMS Conference at Auburn University, AL, Summer 1989, (SIAM, Philadelphia, 1991).

39. A. Daubechies, **Ten Lectures on Wavelets**, NSF-CBMS Conference at Lowell University MA, Summer 1990, (SIAM, Philadelphia, 1992).

40. B. DeFacio, C.R. Thompson and G.V. Wellan, "Wavelet Version of Fourier Optics," SPIE **1351**, **Digital Image Synthesis and Inverse Optics**, (Soc. Photo-Opt. Instr. Engr. Bellingham WA, 1990), 21-37.

41. C.E. Heil and D.F. Walnut, "Continuous and Discrete Wavelet Transforms," SIAM Rev. **31**, 628-666 (1989).

42. I. Daubechies, "Orthonormal Basis of Compactly Supported Wavelets," Comm. Pure Appl. Math. **41**, 909-996 (1988).

43. M. Frazier and B. Jawerth, "A Discrete Transform and the Decomposition of Distribution Spaces," J. Funct. Anal. **93**, 134-170 (1990).

44. B. DeFacio and C.R. Thompson, **Inverse Problems in Scattering and Imaging**, M. Bertero and E.R. Pike (Adam Hilger, Bristol United Kingdom, 1992), 180-203.

45. C.R. Thompson and B. DeFacio, **Inverse Problems in Scattering and Imaging**, SPIE **1767**, Editor, M. Fiddy (SPIE, Bellingham WA, 1992), 120-130 and *ibid*, 131-146.

46. G. Kaiser, SIAM J. Math Anal. **23**, 222-243 (1992).

47. D.M. Patterson, B. DeFacio, S.P. Neal and C.R. Thompson, **Rev. Prog. Quant. Non-Destructive Eval. 12**, 719-729.

48. B. DeFacio, in, **Workshop on Squeezed States and Uncertainty Retations**, NASA Conf. Proc. **3135**, Editors, D. Han, Y.S. Kim and W.W. Zachary (NASA, Greenbelt MD, 1992), 283-296.

49. G.M. D'Ariano and B. DeFacio, Nuovo Cim. **108B** (in press).

50. G. Kaiser, Phys. Lett. **A168**, 28 (1992).

51. D. Han, Y.S. Kim and M. Noz, **Second International Workshop on Squeezed States and Uncertainty Relations**, *NASA Conf. Proc.* **3219**, Editors, D. Han, Y.S. Kim and V.I. Man'ko (NASA, Greenbelt MD, 1993), 341.

52. K. Huang, **Statistical Mechanics 2/E** (Wiley, New York, 1987).

53. L.E. Reichl, **A Modern Course in Statistical Mechanics** (University of Texas Press, Austin, 1980).

54. G.M. D'Ariano, Int. J. Mod. Phys. **6**, 1291-1354 (1992).

55. G. D'Ariano, M. Rasetti and M. Vadacchino, Phys. Rev. D**32**, 1034-1037 (1985).

56. D. Han, Y.S. Kim and M. Noz, Phys. Rev. A**41**, 6233-6244 (1990).

57. Y.S. Kim and E.P. Wigner, Amer. J. Phys. **58**, 439-448 (1990).

58. H.P. Yuen, Phys. Rev. **A12**, 2226-2242 (1976).

59. A.O. Caldeira and A.J. Leggett, Physica **A121**, 587 (1983).

60. Y. Takahashi and H. Umezawa, Coll. Phenom. **2**, 55-80 (1975).

61. L. Yeh, in, **Workshop on Harmonic Oscillators**, *NASA Conf. Proc.* **3197**, Editors, D. Han, Y.S. Kim and W.W. Zachary (NASA, Greenbelt MD, 1993), 337-352.

62. L. Yeh and Y.S. Kim, LBL 31657 (1991).

63. B. DeFacio, A. Van Nevel and O. Brander, in Workshop on Harmonic Oscillators, *NASA Conf. Proc.* **3197**, Editors D. Han, Y.S. Kim and W.W. Zachary (NASA, Greenbelt MD, 1993) 309-322.

# Coherent States on the m-sheeted Complex Plane as m-photon states

A. VOURDAS

Department of Electrical Engineering and Electronics

University of Liverpool, P.O. Box 147,Liverpool, L69 3BX

## Abstract

Coherent states on the m-sheeted complex plane are introduced and properties like overcompleteness and resolution of the identity are studied. They are eigenstates of the operators $a_m^+, a_m$ which create and annihilate clusters of m-particles. Applications of this formalism in the study of Hamiltonians that describe m-particle clustering are also considered.

## 1. Introduction

Apart from the original (Glauber) coherent states which are associated with the Weyl group, other types of coherent states associated with other groups (e.g. SU(2), SU(1,1) etc.) have also been studied. In a recent publication [1] we extended these ideas in a different direction and introduced coherent states on the m-sheeted covering group of SU(1,1). From a physical point of view it can be used for the description of m-particle clustering. Here we extend the Glauber coherent states into coherent states

in the m-sheeted complex plane. The properties of these states (overcompleteness, resolution of the identity etc.) are explicitly considered. Using these states we extend the Bargmann [2] analytic representation into a new formalism that we call Bargmann analytic representation in the m-sheeted complex plane. Using this representation we introduce new creation and annihilation operators $a_m^+, a_m$ which create and annihilate clusters of m particles and show that the properties of our coherent states with respect to them, are similar to the properties of the ordinary (Glauber) coherent states with respect to the usual creation and annihilation operators $a^+, a$.

The above ideas are used in the description of m-particle clustering. which is a generalisation of the concept of pairing. They could be used to generalise two-photon states into m-photon states with even better properties. Some work in this direction but from a different point of view has already been presented [3, 4]

## 2. Coherent states on the m-sheeted complex plane

We consider the Riemann surface

$$R_m = C^* | Z_m \tag{1}$$

where $C^*$ is the punctured complex plane

$$C^* = C - \{o\} \tag{2}$$

and $Z_m$ is the discrete group of the integers modulo m. The punctured complex plane $C^*$ is the m-sheeted covering surface of the Riemann surface $R_m$.

The sheet number s(z) of a complex number z in $C^*$ is defined as

$$s(z) = IP\left[\frac{m\ Arg(z)}{2\pi}\right] \tag{3}$$

where IP stands for the integer part of the number. s(z) takes integer values from 0 to m - 1 (modulo m).

We also consider the harmonic oscillator Hilbert space H and express it as

$$H = \sum_{\ell=0}^{m-1} H_\ell \tag{4}$$

$H_\ell$ is an infinite-dimensional subspace spanned by the number eigenstates

$$H_\ell = \{\ |\ Nm + \ell >\ ;\ N = 0, 1, 2, \ldots\ \} \tag{5}$$

We call $\pi_\ell$ the projection operators on $H_\ell$

$$\pi_\ell = \sum_{N=0}^{\infty} |\ Nm + \ell >< Nm + \ell\ |$$

$$\pi_\ell\, \pi_j = \delta_{\ell j}\, \pi_\ell$$

$$\sum \pi_\ell = 1 \tag{6}$$

We now introduce the states

$$|z;m\rangle = \exp\left[-\frac{1}{2}|z|^{2m}\right] \sum_{N=0}^{\infty} z^{MN} (N!)^{-\frac{1}{2}} \mid mN + s(z) \rangle \qquad (7)$$

where s(z) is the sheet number of z defined in equ.(3). It is clear that if z belongs to the zero sheet the states $|mN\rangle$ should be used; if z belongs to the first sheet the states $|mN+1\rangle$ should be used; etc. The state $|z\rangle$ belongs to the Hilbert space $H_{s(z)}$. We refer to the states (7) as coherent states on the m-sheeted complex plane. We can prove

$$\langle z_1;m| \; z_2;m\rangle = \delta\,(s(z_1),\, s(z_2))\, \exp\left[-\frac{1}{2}|z_1|^{2m} - \frac{1}{2}|z_2|^{2m} + (z_1^{*} z_2)^m\right] \qquad (8)$$

where $\delta$ is the kronecker delta.

In order to give a resolution of the identity for these states we first prove a resolution of the identity within the Hilbert space $H_\ell$:

$$\int_{s_\ell} |z;m\rangle \langle z;m|\, d\mu_m(z) = \pi_\ell \qquad (10)$$

$$d\mu_m(z) = \pi^{-1}\, m^2\, |z|^{2(m-1)}\, d^2z \qquad (11)$$

$s_\ell$ is the $\ell$-sheet and $\pi_\ell$ is the projection operator (6). Summation over $\ell$ gives the resolution of the identity:

$$\int_{c} |z;m\rangle \langle z;m|\, d\mu_m(z) = 1 \qquad (12)$$

The states $|z;m\rangle$ with z in the sheet $S_\ell$, form an overcomplete set within the Hilbert space $H_\ell$.

## 3. Extended Bargman representation on the m-sheeted complex plane

Bargmann [2] introduced analytic representations in the complex plane which are based on ordinary coherent states. In refs. [5] analytic representations in the unit disc which are based on the SU(1,1) Perelomov coherent states, have been studied. This formalism has been extended in ref.[1] into analytic representations in the m-sheeted unit disc. In this section we study an analogous extension from the Bargmann representation in the complex plane into an analytic representation in the m-sheeted complex plane.

We generalise the Bargmann representation by representing the arbitrary (normalised) state $|f\rangle$ with the function

$$|f\rangle = \sum f_N \, | \, N\rangle$$

$$f(z;m) = \exp\left[\frac{1}{2}|z|^{2m}\right] \langle z^*;m|f\rangle = \sum_{N=0}^{\infty} f_{mN+s(z)} \, z^{mN} \, (N!)^{-\frac{1}{2}} \qquad (13)$$

where z takes values in $C^*$ and s(z) is the sheet number of z (equ.(3)). The f(z;m) is analytic in the interior of each sheet and has discontinuities across the cuts $C_\ell$.

As an example we consider the number eigenstates $|M = mN+\ell\rangle$ where N, $\ell$ are the integer part and remainder of M divided by m, correspondingly. They are represented by the function

$$f(z;m) = \delta(\ell,s(z))\ z^{mN}\ (N!)^{-\frac{1}{2}} \tag{14}$$

The kronecker $\delta(\ell,s(z))$ ensures that this function is non-zero only in the $\ell$ sheet.

As a second example we consider the states $|z_o;m\rangle$ of equ.(7) which are represented by the function

$$f(z;m;z_o) = \exp\left[\frac{1}{2}|z|^{2m}\right] \langle z^*;m|z_o;m\rangle =$$

$$\delta(s(z);s(z_o))\ \exp\left[-\frac{1}{2}|z_o|^{2m} + (zz_o)^m\right] \tag{15}$$

We next consider the operators

$$a_m = m^{-1}\ z^{1-m}\ \partial_z \tag{16}$$

$$a_m^+ = z^m \tag{17}$$

$$[a_m,\ a_m^+] = 1 \tag{18}$$

$$a_m^+\ |\ mN + \ell\ \rangle = (N+1)^{\frac{1}{2}}\ |\ m(N+1) + \ell\ \rangle \tag{19}$$

$$a_m\ |\ mN + \ell\ \rangle = N^{\frac{1}{2}}\ |\ m(N-1) + \ell\ \rangle \tag{20}$$

It is seen that they act as creation and annihilation operator within

each one of the Hilbert spaces $H_\ell$.

The operator

$$a_m^+ a_m - m^{-1} z\partial_z$$

$$a_m^+ a_m \mid mN + \ell > - N \mid mN + \ell > \tag{21}$$

can be considered as a number operator within the Hilbert space $H_\ell$.

We also consider the operator

$$R - a^+a - m\, a_m^+ a_m \tag{22}$$

$$R \mid mN+\ell> - \ell \mid mN+\ell> \tag{23}$$

which we call "remainder operator" or "number modulo m operator". Its eigenstates are the number states and its eigenvalues the remainders $\ell$ of the division of the number of the state over m. The operator R commutes with the operators $a_m$, $a_m^+$:

$$[R, a_m] - [R, a_m^+] - 0 \tag{24}$$

Note that the operators $a_m, a_m^+$ commute with the projection operators $\pi_\ell$ of equ.(7):

$$[a_m, \pi_\ell] - [a_m^+, \pi_\ell] - 0 \tag{25}$$

A consequence of that is that an "arbitrary" function of $a_m, a_m^+$ leaves each of the Hilbert spaces $H_\ell$ invariant in the sense that when it acts on a state which belongs in $H_\ell$ it produces another state which also belongs in the same

space.

We next consider the displacement operators with respect to the $a_m^+, a_m$

$$D_m(z_o) = \exp [z_o\, a_m^+ - z_o^*\, a_m] \tag{26}$$

They displace the operators $a_m, a_m^+$ by a constant and they commute with the operator R or equ.(22)

$$D_m(z_o)\, a_m\, D_m^+(z_o) = a_m - z_o \tag{27}$$

$$D_m(z_o)\, a_m^+\, D_m^+(z_o) = a_m^+ - z_o^* \tag{28}$$

$$[D_m(z_o),\ R] = 0 \tag{29}$$

We now act with the operators $D_m(z_o)$ on the number eigenstates $|\ell\rangle$ $(0 \le \ell \le m-1)$ and get the coherent states on the m-sheeted complex plane (7):

$$|z = (z_o)_\ell^{1/m}\ ;\ m\rangle = D_m(z_o)\ |\ \ell\rangle \tag{30}$$

The subscript $\ell$ indicates that among the m roots, the one which belongs to the sheet $S_\ell$ should be chosen. Equ.(30) can also be writen as

$$|z;m\rangle = D_m(z^m)\ |s(z)\rangle \tag{31}$$

where $|s(z)\rangle$ is number eigenstate and s(z) the sheet number of z (equ.(3)).

Using equs.(27), (31) we prove that the $|z;m\rangle$ are eigenstates of $a_m$

$$a_m\ |z;m\rangle = z^m |z;m\rangle \tag{32}$$

It should be pointed out that operators similar to $a_m^+, a_m$ have been considered in [6] and used in refs. [4] where the following states have been

studied

$$\exp\left[-\frac{1}{2}|z|^2\right]\sum_{N=0}^{\infty} z^N\,(N!)^{-\frac{1}{2}}\,|mN\rangle \tag{33}$$

They are a subset of our coherent states associated with the Hilbert space $H_\ell$ with $\ell = 0$; or equivalently with the zero sheet of our m-sheeted complex plane. It has been shown in [4] that the states (33) have very interesting quantum statistical properties.

## 4. m-photon states

We consider the Hamiltonian

$$H = \Omega\, a^+ a + \tau\, a_m^+ + \tau^*\, a_m = \Omega R + H_1 \tag{34}$$

$$H_1 = \Omega\, m\, a_m^+ a_m + \tau\, a_m^+ + \tau^*\, a_m \tag{35}$$

$$[R,\ H_1] = 0 \tag{36}$$

and express H as:

$$H = D_m\left[-\frac{\tau}{\Omega m}\right]\left[\Omega\, m\, a_m^+ a_m\right] D_m^+\left[-\frac{\tau}{\Omega m}\right] + \Omega R - \frac{|\tau|^2}{\Omega m} \tag{37}$$

We easily see that the eigenvectors and eigenvalues of H are:

$$H\, D_m\left[-\frac{\tau}{\Omega m}\right]|mN+\ell\rangle = \left[\Omega(mN+\ell) - \frac{|\tau|^2}{\Omega m}\right] D_m\left[-\frac{\tau}{\Omega m}\right]|mN+\ell\rangle \tag{38}$$

The physical significance of this Hamiltonian lies in the fact that the

operators $a_m^+, a_m$ create and annihilate clusters of m particles. Pairing of particles plays a very important role in various contexts in Physics. Generalisation from pairing into m-particle clustering can be described with various Hamiltonians. The obvious choice is

$$H = \Omega\, a^+ a + r\, (a^+)^m + r^*\, a^m \qquad (39)$$

There are certain difficulties associated with this Hamiltonian [3] and in any case it is useful to explore alternative models, especially if they are based on some symmetry which can be exploited to handle these highly non-linear terms. In ref. [1] a Hamiltonian associated with the SU(1,1) group, which describes m-particle clustering has been studied. In this section the Hamiltonian (34) which is associated with the Weyl group and which also describes m-particle clustering, has been studied.

## 5. Discussion

Coherent states on the m-sheeted complex plane have been introduced in equ.(7). The Hilbert space has been split into m subspaces (equ.(4)) and operators $a_m^+$, $a_m$ which play the role of creation and annihilation operators in each subspace, have been introduced. The $a_m^+$, $a_m$ are different from the usual creation and annihilation operators $a^+, a$. It has been shown that our coherent states have the usual properties of coherent states with respect to

the $a_m^+, a_m$. They are eigenstates of $a_m$ (equ.(32)); and they can be expressed as the product of the displacement operator times the lowest state (equ.(31)).

All these ideas can be used for the description of m-particle clustering. This is a generalisation of the concept of pairing which plays an important role in areas like squeezing in quantum optics, superconductivity, superfluidity, phase transistions etc. Consequently this formalism might be used for generalisations in all these areas. A Hamiltonian that describes m-particle clustering has been considered in equ.(34) and its eigenvalues and eigenfunctions have been calculated.

**References**


1. A. Vourdas, J.Math.Phys. 34, March (1993).

2. V. Bargmann, Commun.Pure Appl.Math. 14, 187, (1961).

3. R.A. Fisher, M.M. Nieto, V.D. Sandberg, Phys.Rev. D29, 1107, (1984).
   S.L. Braunstein, R.I. McLachlan, Phys.Rev., A35, 1659, (1987).
   M. Hillery, Phys.Rev., A42, 498 (1990).

4. J. Katriel, A.I. Solomon, G. D'Ariano, M. Rasetti, Phys.Rev. D34, 2332 (1986).
   J. Katriel, M. Rasetti, A. Solomon, Phys.Rev. D34, 1248, (1987).

G. D'Ariano, M. Rasetti, Phys.Rev. D35, 1239, (1987).

G. D'Ariano, S. Morosi, M. Rasetti, J. Katriel, A.I. Solomon, Phys.Rev. D36, 2399, (1987).

5. T. Paul, J.Math.Phys. 25, 3252, (1984).

J.R. Klauder, Ann.Phys. 188, 120, (1988).

A. Vourdas, Phys.Rev. A41, 1653, (1990); Phys.Rev. A45, 1943, (1992).

J.P. Gazeau, V. Hussin, J.Phys. A25, 1549, (1992).

6. R. Brandt, O.W. Greenberg, J.Math.Phys. 10, 1168, (1969).

N95- 13941

# SOME RULES FOR POLYDIMENSIONAL SQUEEZING

V. I. Man'ko
*Dipartimento di Scienze Fisiche Universita di Napoli "Federico II"and I.N.F.N.,Sez.di Napoli*
and
*Lebedev Physics Institute, Leninsky pr.,53, Moscow, 117333 Russia*

**Abstract**

The review of the following results of the Refs. [1] - [5] is presented: For mixed state light of $N$-mode electromagnetic field described by Wigner function which has generic Gaussian form the photon distribution function is obtained and expressed expliciltly in terms of Hermite polynomials of $2N$-variables.The momenta of this distribution are calculated and expressed as functions of matrix invariants of the dispersion matrix.The role of new uncertainty relation depending on photon state mixing parameter is elucidated.New sum rules for Hermite polynomials of several variables are found.The photon statistics of polymode even and odd coherent light and squeezed polymode Schrödinger cat light is qiven explicitly.Photon distribution for polymode squeezed number states expressed in terms of multivariable Hermite polynomials is discussed.

## 1 Introduction

In the Ref.[1] it was shown that the matrix elements of density matrix in number state basis for polymode oscillator are expressed in terms of Hermite polynomials of several variables for the density operator in the canonically transformed thermal state of the oscillator.In the recent works [2], [3] the photon distribution function for the generic Gaussian light described by the Wigner function which is the most generic Gaussian in quadrature phase space was found and expressed in terms of Hermite polynomials of 2 variables for one-mode case [2] and $2N$ variables for polymode case [3].The physical meaning of mixed Gaussian state of the light may be understood if one takes into account that the pure multimode Gaussian state corresponds to the generalised correlated state introduced by Sudarshan [6] who related those states to the symplectic dynamical group.The mixed Gaussian states studied above may be considered as the mixture of generalised correlated states plus thermal noise acting on each mode which has its own temperature. The photon distribution function for even and odd coherent states [7] or Schrödinger cat states [8] subject to squeezing both in one-mode and polymode cases has been found in Ref.[4].The polymode Schrödinger cat states and photon distributions for light in these states were introduced in [5].The aim of this work is to give a review of the photon distribution functions and related sum rules for one-mode and polymode Gaussian light and for the even and odd coherent states light using the results of [2] - [5]. It should be emphasized that the squeezed light is worth to be used in interferometric gravitational antennas [9] and the even and odd coherent light may play alternative role in gravitational wave experiment [10],[11].

## 2 Photon Distribution for Polymode Gaussian Light

The mixed squeezed state of the $N$-mode light with a *Gaussian* density operator $\hat{\varrho}$ is described by the Wigner function (see,for example,[12])

$$W(\mathbf{p},\mathbf{q}) = (\det \mathbf{M})^{-\frac{1}{2}} \exp\left[-\frac{1}{2}(\mathbf{Q}- < \mathbf{Q} >)\mathbf{M}^{-1}(\mathbf{Q}- < \mathbf{Q} >)\right], \tag{1}$$

where $2N$-dimensional vector $\mathbf{Q} = (\mathbf{p},\mathbf{q})$ consists of $N$ components $p_1,...,p_N$ and $N$ components $q_1,...,q_N$. $2N$ parameters $< p_i >$ and $< q_i >$, $i = 1,2,\ldots,N$, combined into vector $< \mathbf{Q} >$, are the average values of the quadratures.A real symmetric quadrature dispersion matrix $\mathbf{M}$ has $2N^2+N$ parameters

$$\mathcal{M}_{\alpha\beta} = \frac{1}{2}\left\langle \hat{Q}_\alpha\hat{Q}_\beta + \hat{Q}_\beta\hat{Q}_\alpha \right\rangle - \left\langle \hat{Q}_\alpha \right\rangle \left\langle \hat{Q}_\beta \right\rangle, \qquad \alpha,\beta = 1,2,\ldots,2N. \tag{2}$$

They obey certain constraints, which are nothing but the generalized uncertainty relations [12]. The photon distribution function in this state has the form [3],[1]

$$\mathcal{P}_\mathbf{n} = \mathcal{P}_0 \frac{H_\mathbf{nn}^{\{\mathbf{R}\}}(\mathbf{y})}{\mathbf{n}!}, \tag{3}$$

where vector $\mathbf{n}$ consists of $N$ nonnegative integers: $\mathbf{n} = (n_1, n_2, \ldots, n_N)$. The function $H_\mathbf{nn}^{\{\mathbf{R}\}}(\mathbf{y})$ is the Hermite polynomial of $2N$ variables. We introduced also notations

$$\mathbf{n}! = n_1!n_2!...n_N!. \tag{4}$$

The symmetric $2N$-dimensional matrix $\mathbf{R}$ and the $2N$-dimensional vector $\mathbf{y}$ are given by the relations

$$\mathbf{R} = \mathbf{U}^\dagger \left(\mathbf{I}_{2N} - 2\mathbf{M}\right)\left(\mathbf{I}_{2N} + 2\mathbf{M}\right)^{-1}\mathbf{U}^*, \tag{5}$$

$$\mathbf{y} = 2\mathbf{U}^t(\mathbf{I}_{2N} - 2\mathbf{M})^{-1} < \mathbf{Q} >, \tag{6}$$

where the $2N$-dimensional unitary matrix

$$\mathbf{U} = \frac{1}{\sqrt{2}}\begin{pmatrix} -i\mathbf{I}_N & i\mathbf{I}_N \\ \mathbf{I}_N & \mathbf{I}_N \end{pmatrix}$$

is introduced.The matrices $\mathbf{I}_N$ and $\mathbf{I}_{2N}$ are identity matrices of corresponding dimensions.

The probability to have no photons has the form

$$\mathcal{P}_0 = \left[\det\left(\mathbf{M} + \frac{1}{2}\mathbf{I}_{2N}\right)\right]^{-\frac{1}{2}} \exp\left[- < \mathbf{Q} > (2\mathbf{M} + \mathbf{I}_{2N})^{-1} < \mathbf{Q} >\right]. \tag{7}$$

It may be shown [3],[4] that the multivariable Hermite polynomial is the even function if the sum of its indices is the even number and the polynomial with the odd sum of indices is the odd function. Due to this pairity property of the polydimensional Hermite polynomials the "diagonal" multivariable Hermite polynomial is the even function since the sum of its indices is always even

number.Consequently the above photon distribution function is the even function. Thus the photon distribution function for generic mixed Gaussian light found in[3] is expressed in terms of multivariable Hermite polynomials and it depends on the quadrature means and dispersions.The photon number means and dipersion matrix corresponding to the found distribution (3) are of the form

$$< n_j >= \frac{1}{2}(\sigma_{p_jp_j} + \sigma_{q_jq_j} - 1) + \frac{1}{2}(< p_j >^2 + < q_j^2 >),$$
$$\sigma_{n_jn_j} = \frac{1}{2}(T_j^2 - 2d_j - \frac{1}{2}) + < \mathbf{Q}_j > \mathcal{M}_j < \mathbf{Q}_j >,$$

where $T_j$ and $d_j$ are the trace and the determinant of the 2x2-matrix $\mathcal{M}_j$,describing only j-th mode, and the 2-vector $\mathbf{Q}_j$ has the components $(p_j, q_j)$.

# 3 Pure Polymode States

The photon distribution for polymode squeezed correlated state may be expressed in terms of symplectic transform parameters relating boson operators as follows

$$\begin{pmatrix} \hat{\mathbf{b}} \\ \hat{\mathbf{b}}^\dagger \end{pmatrix} = \Omega \begin{pmatrix} \hat{\mathbf{a}} \\ \hat{\mathbf{a}}^\dagger \end{pmatrix} + \begin{pmatrix} \mathbf{d} \\ \mathbf{d}^* \end{pmatrix}, \qquad \Omega = \begin{pmatrix} \zeta & \eta \\ \eta^* & \zeta^* \end{pmatrix}, \tag{8}$$

where $\Omega$ is a symplectic $2N$x$2N$-matrix consisting of four $N$-dimensional complex square blocks, and $\mathbf{d}$ is a complex $N$-vector.Then we have for photon distribution in squeezed correlated polymode state $|\beta >$ labeled by the complex number vector with $N$-components

$$\mathcal{P}_\mathbf{n} = \frac{\mathcal{P}_0(\beta)}{\mathbf{n}!} \left| H_\mathbf{n}^{\{\zeta^{-1}\eta\}} \left(\eta^{-1}[\beta - \mathbf{d}]\right)\right|^2, \qquad \mathcal{P}_0(\beta) = |\mathcal{F}_0(\beta)|^2 \exp -|\beta|^2, \tag{9}$$

where

$$\mathcal{F}_0(\beta) = (\det \zeta)^{-\frac{1}{2}} \exp\left[\frac{1}{2}\beta\eta^*\zeta^{-1}\beta + \beta(\mathbf{d}^* - \eta^*\zeta^{-1}\mathbf{d}) + \frac{1}{2}\mathbf{d}\eta^*\zeta^{-1}\mathbf{d} - \frac{1}{2}|\mathbf{d}|^2\right]. \tag{10}$$

The photon doistribution function of the *squeezed number state* $|\mathbf{m} >$ is descibed by the formula

$$\mathcal{P}_\mathbf{n} = |\det \zeta|^{-1} \exp\left[\mathrm{Re}(\mathbf{d}\eta^*\zeta^{-1}\mathbf{d}) - |\mathbf{d}|^2\right] \frac{\left|H_\mathbf{nm}^{\{\mathbf{R}\}}(\mathbf{L})\right|^2}{\mathbf{n}!\mathbf{m}!}. \tag{11}$$

Here $\mathbf{m}$ is the label of the state, whereas $\mathbf{n}$ is a discrete vector variable. $2N$x$2N$-matrix $\mathbf{R}$ and $2N$-vector $\mathbf{L}$ are expressed now in terms of blocks of matrix $\Omega$ and vector $\mathbf{d}$ as follows,

$$\mathbf{R} = \begin{pmatrix} \zeta^{-1}\eta & -\zeta^{-1} \\ -\zeta^{-1} & -\eta^*\zeta^{-1} \end{pmatrix}, \qquad \mathbf{L} = \mathbf{R}^* \begin{pmatrix} -\zeta^{-1}\mathbf{d} \\ \mathbf{d}^* - \eta^*\zeta^{-1}\mathbf{d} \end{pmatrix}. \tag{12}$$

# 4 Even and Odd Coherent States

The one-mode even and odd coherent states have been introduced in Ref.[7].The polymode even and odd coherent states have been introduced in Ref.[5].The squeezed and correlated even and odd

coherent states have been introduced and studied in Ref.[4].We will discuss the photon statistics of the light in these states which are also called Schrödinger cat states [8].The multimode Schrödinger cat states are defined by the relation [5]

$$| \mathbf{A}_{\pm} >= N_{\pm}(| \mathbf{A} > \pm | -\mathbf{A} >), \tag{13}$$

where the multimode coherent state $| \mathbf{A} >$ is

$$| \mathbf{A} >=| \alpha_1, \alpha_2, \alpha_3, ....., \alpha_n >= D(\mathbf{A}) | \mathbf{0} >, \tag{14}$$

and $D(\mathbf{A})$ is the multimode displacement operator creating coherent state from the vacuum.The normalization constants are

$$\begin{aligned} N_+ &= \frac{e^{\frac{|\mathbf{A}|^2}{2}}}{2\sqrt{cosh \mid \mathbf{A} \mid^2}}, \\ N_- &= \frac{e^{\frac{|\mathbf{A}|^2}{2}}}{2\sqrt{sinh \mid \mathbf{A} \mid^2}}, \end{aligned} \tag{15}$$

where complex number $\mathbf{A}$ has the form

$$| \mathbf{A} |^2=| \alpha_1 |^2 + | \alpha_2 |^2 +.....+ | \alpha_n |^2= \sum_{m=1}^{n} | \alpha_m |^2 . \tag{16}$$

The photon distribution function has the form [5]

$$\begin{aligned} P_+(n) &= \frac{| \alpha_1 |^{2n_1} | \alpha_2 |^{2n_2} ... | \alpha_n |^{2n_n}}{(n_1!)(n_2!)....(n_n!)cosh \mid \mathbf{A} \mid^2}, \quad \mathrm{n_1 + n_2 + .... + n_n = 2k}, \\ P_-(n) &= \frac{| \alpha_1 |^{2n_1} | \alpha_2 |^{2n_2} ... | \alpha_n |^{2n_n}}{(n_1!)(n_2!)....(n_n!)sinh \mid \mathbf{A} \mid^2}, \quad \mathrm{n_1 + n_2 + .... + n_n = 2k + 1}, \end{aligned} \tag{17}$$

and the photon means corresponding to these distributions are

$$\begin{aligned} < \mathbf{A}_+ \mid n_i \mid \mathbf{A}_+ > &= | \alpha_i |^2 \, tanh \mid \mathbf{A} \mid^2, \\ < \mathbf{A}_- \mid n_i \mid \mathbf{A}_- > &= | \alpha_i |^2 \, coth \mid \mathbf{A} \mid^2 . \end{aligned} \tag{18}$$

The photon number dispersion matrix has the matrix elements

$$\begin{aligned} \sigma_{ik}^{+} &= | \alpha_i |^2 | \alpha_k |^2 \, sech^2 \mid \mathbf{A} \mid^2 + | \alpha_i |^2 \, tanh \mid \mathbf{A} \mid^2 \delta_{ik}, \\ \sigma_{ik}^{-} &= - | \alpha_i |^2 | \alpha_k |^2 \, cosech^2 \mid \mathbf{A} \mid^2 + | \alpha_i |^2 \, coth \mid \mathbf{A} \mid^2 \delta_{ik}. \end{aligned} \tag{19}$$

# 5 Squeezed Schrödinger Cat States

Let us find out the photon statistics of squeezed polymode Schrödinger cat state labeled by the complex $N$ -vector $\beta$.To do that let us difine transition amplitude from the polymode squeezed and correlated state $|\beta>$ to the polymode photon number state $|n>$

$$T_n(\beta) = \mathcal{F}_0(\beta)\frac{1}{\sqrt{n!}}H_{\mathbf{n}}^{\{\zeta^{-1}\eta\}}\left(\eta^{-1}[\beta - \mathbf{d}]\right), \tag{20}$$

where

$$\mathcal{F}_0(\beta) = (\det\zeta)^{-\frac{1}{2}}\exp\left[\frac{1}{2}\beta\eta^*\zeta^{-1}\beta + \beta(\mathbf{d}^* - \eta^*\zeta^{-1}\mathbf{d}) + \frac{1}{2}\mathbf{d}\eta^*\zeta^{-1}\mathbf{d} - \frac{1}{2}|\mathbf{d}|^2 - \frac{1}{2}|\beta|^2\right]. \tag{21}$$

Then the photon distribution function for polymode light in the squeezed Schrödinger cat state (even and odd) is given by the formula [4]

$$\mathcal{P}_n^{\pm}(\beta) = N_{\pm}^2(\beta)\left[|T_n(\beta)|^2 + |T_n(-\beta)|^2 \pm (T_n^*(\beta)T_n(-\beta) + T_n(\beta)T_n^*(-\beta))\right]. \tag{22}$$

If the shift parameter $d = 0$ the formula is simplified

$$\mathcal{P}_{2k}^{+}(\beta) = 4N_{+}^2\mathcal{P}_n(\beta), \tag{23}$$

if we have equality

$$\sum_{i=1}^{N} n_i = 2k, \tag{24}$$

and for even states

$$\mathcal{P}_{2k+1}^{+}(\beta) = 0, \tag{25}$$

if one has

$$\sum_{i=1}^{N} n_i = 2k + 1, \tag{26}$$

where $\mathcal{P}_n(\beta)$ is given by the formula (3).For the light in the odd squeezed Schrödinger cat state the photon distribution is

$$\mathcal{P}_{2k+1}^{-}(\beta) = 4N_{-}^2\mathcal{P}_n(\beta), \tag{27}$$

if the indices satisfy the equality (26) and

$$\mathcal{P}_{2k}^{-}(\beta) = 0, \tag{28}$$

if the indices satisfy relation (24).Thus the squeezed Schrödinger cat states if the shift parameter is equal to zero have highly oscillating distribution function.The influence of shift parameter decreases the oscillations of the distribution function. For Hermite polynomials the following sum rule may be found [3]

$$\begin{aligned}&\sum_{n_1=0}^{\infty}\cdots\sum_{n_N=0}^{\infty}\frac{\lambda_1^{n_1}}{n_1!}\frac{\lambda_2^{n_2}}{n_2!}\cdots\frac{\lambda_N^{n_N}}{n_N!}H_{n_1n_2\ldots n_Nn_1n_2\ldots n_N}^{\{\mathbf{R}\}}(\mathbf{R}^{-1}\mathbf{z})\\ &= \left[\det\left(\Lambda\Sigma_x\mathbf{R} + \mathbf{I}_{2N}\right)\right]^{-\frac{1}{2}}\exp\left[\frac{1}{2}\mathbf{z}\left(\Lambda\Sigma_x\mathbf{R} + \mathbf{I}_{2N}\right)^{-1}\Sigma_x\Lambda\mathbf{z}\right].\end{aligned} \tag{29}$$

Here $\mathbf{z} = (z_1, z_2, ...z_{2N})$, the $2N$x$2N$ matrix $\Sigma_x$ is the $2N$-dimensional analog of the Pauli matrix $\sigma_x$, and the diagonal $2N$x$2N$ - matrix $\Lambda$ has the matrix elements $\lambda_j$ in j-th and (N+j)-th rows. Let us consider the one mode case.Then the formula for the photon distribution function in terms of Hermite polynomials of two variables may be expressed in terms of usual Hermite polynomials

$$\mathcal{P}_n = \mathcal{P}_0 \frac{(T^2-4d)^{\frac{n}{2}}}{(2T+4d+1)^n} \sum_{k=o}^{n} \left( \frac{4d-1}{\sqrt{T^2-4d}} \right)^k \frac{n!}{[(n-k)!]^2 k!}$$

$$\times \left| H_{n-k} \left( \frac{(T+1)z + [\sigma_{pp} - \sigma_{qq} - 2i\sigma_{pq}]\, z^*}{\{(2T+4d+1)\,[\sigma_{pp} - \sigma_{qq} - 2i\sigma_{pq}]\}^{\frac{1}{2}}} \right) \right|^2 . \tag{30}$$

Here the parameters $\sigma_{pp}, \sigma_{qq}, \sigma_{pq}$ are matrix elements of the quadrature dispersion matrix $M$, $d$ is determinant of this matrix and $T$ is the trace of the matrix. The complex number $z$ is determined by the relation

$$z = \frac{1}{\sqrt{2}}(< q > + i < p >). \tag{31}$$

Formula (30) can be used also to illustrate the generalized uncertainty relation (for the Gaussian states). Indeed, it is obvious that the probability to find $n$ photons must be nonnegative. On the other hand, all but one terms in the right-hand side of eq. (30) are positive independently on the concrete values of the parameters determining the quantum state. The only exception is the term

$$\left( \frac{4d-1}{\sqrt{T^2-4d}} \right)^k .$$

Consequently, to guarantee the positiveness of the photon distribution function for all conceivable combinations of the parameters one should impose the restriction $d \geq \frac{1}{4}$.This inequality is the Schrödinger uncertainty relation (see, [6],[12] ).

# Acknowledgments

The author would like to acknowledge the University of Maryland at Baltimore County for kind hospitality and I.N.F.N.,Sez. di Napoli for support.

# References

[1] V. V. Dodonov, V. I. Man'ko, and V. V. Semjonov, Nuovo Cimento **B 83**, 145(1984); see also: V. I. Man'ko, *Proceedings of the International Workshop on Harmonic Oscillator*, University of Maryland at College Park,25-28 March,1992, D.Han and Y.S.Kim, eds. (Nasa Conference Publications,1993)

[2] V. V. Dodonov, O. V. Man'ko, and V. I. Man'ko, "Photon distribution for one-mode mixed light with generic Gaussian Wigner function", University of Naples Preprint INFN-NA-IV-93/35, DSF-T-93/35(1993) (submitted to Phys. Rev. A ).

[3] V. V. Dodonov, O. V. Man'ko, and V. I. Man'ko, "Multidimensional Hermite polynomials and photon distribution for polymode mixed light", University of Naples Preprint INFN-NA-IV-93/36, DSF-T-93/36(1993) (submitted to Phys. Rev. A ).

[4] V. V. Dodonov, V. I. Man'ko,and D.E.Nikonov,"Even and odd Coherent States (Schrödinger cat states) for Multimode Parametric Systems" (in preparation).

[5] Nadeem A. Ansari and V. I. Man'ko,"Photon statistics of multimode even and odd coherent light", University of Naples Preprint INFN-NA-IV-93/34,DSF-T-93/34(1993); (submitted to Phys. Rev. A).

[6] E. C. G. Sudarshan, *Proceedings of Second International Workshop on Squeezed States and Uncertainty Relations*, Moscow, 25-29 May, 1992,D.Han, Y. S. Kim, and V. I. Man'ko, eds., (NASA Conference Publication,**3219**,p.241, 1993).

[7] V. V. Dodonov, I. A. Malkin, and V.I.Man'ko,Physica **72**, 597 (1974).

[8] M. Brune, S. Haroche, J. M. Raimond, L. Davidovich, and N. Zagury, Phys. Rev. A **45**, 5193 (1992); C. C. Gerry and E. E. Hach III, Phys.Lett A **74**,185(1993).

[9] C. M. Caves, Phys.Rev. **D 23**, 1693 (1981).

[10] N. A. Ansari, L. Di Fiore, M. Man'ko, V.Man'ko, R. Romano, S. Solimeno, F. Zaccaria, *Technical Digests of EQEC'93-EQUAP'93*,**2**, Firenze, 10-13 September,1993, P.De Natale and R.Meicci, eds.
and S. Pelli, p.688 (1993); see also: N. A. Ansari, L.Di Fiore,M.Man'ko,V.Man'ko,R.Romano, S.Solimeno,and F.Zaccaria,"Optimal laser intensity for interferometric detection of gravitational waves", University of Naples Preprint INFN-NA-IV-93/16,DSF-T-93/16(1993).

[11] N. A. Ansari, L. Di Fiore, M. Man'ko, V. Man'ko, R. Romano, S. Solimeno, F.Zaccaria, "Quantum limits in interferometric GW antennas in the presence of even and odd coherent states", University of Naples Preprint INFN-NA-IV-93/20,DSF-T-93/20(1993); Phys. Rev. A (in press).

[12] V. V. Dodonov and V. I. Man'ko, *Invariants and Evolution of Nonstationary Quantum Systems*, Proceedings of Lebedev Physics Institute **183**, M.A.Markov, ed. (Nova Science Publishers, Commack, N.Y., 1989).

# SCHRÖDINGER OPERATORS WITH THE $q$-LADDER SYMMETRY ALGEBRAS[1]

Sergei Skorik
*Department of Physics, University of Southern California, Los Angeles, CA 90089-0484, U.S.A.*

Vyacheslav Spiridonov[2]
*Centre de Recherches Mathématiques, Université de Montreal, C.P. 6128-A, Montréal, Québec, H3C 3J7, Canada*

**Abstract**

A class of the one-dimensional Schrödinger operators $L$ with the symmetry algebra $LB^{\pm} = q^{\pm 2}B^{\pm}L$, $[B^+, B^-] = \mathcal{P}_N(L)$, is described. Here $B^{\pm}$ are the '$q$-ladder' operators and $\mathcal{P}_N(L)$ is a polynomial of the order $N$. Peculiarities of the coherent states of this algebra are briefly discussed.

## 1 Introduction

Exactly solvable spectral problems are of great importance. They have numerous applications in classical and quantum mechanics. In the last decades the theory of solitons once again exhibited their universal character. However, the definition of the notion of solvability (or integrability) itself is quite delicate. In particular, it involves the definition of functions which are allowed to enter the solution of the problem (in a sense these are two complementary things – it is common to define functions as solutions of some equations). Let us take for example the standard one-dimensional Schrödinger equation:

$$L\psi(x) \equiv (-d^2/dx^2 + u(x))\psi(x) = \lambda\psi(x), \tag{1}$$

endowed with some boundary conditions. The widely used tacit definition of solvability of this spectral problem consists in the requirement for $\psi(x)$ to be a finite sum of the hypergeometric functions ${}_2F_1(a, b; c; x)$ [1], or of their descendants. On the one hand, the ${}_2F_1$ indeed occupies a distinguished place among the classical special functions, but on the other hand, there are more complicated objects whose global structure has been well understood.

In the theory of nonlinear evolution equations the smooth bounded potential $u(x)$ is said to be solvable if it has a spectrum consisting of the $N + 1$ permitted bands, $N$ of the finite width and one infinitely large (these are the regions of $\lambda$ for which the wave functions $\psi(x)$ are bounded). In some cases this condition leads to the Lamé equation, which is a simplest generalization of the

[1]Talk presented by V.S. at the Third International Workshop on Squeezed States and Uncertainty Relations (Baltimore County, August 10-13, 1993)

[2]On leave of absence from the Institute for Nuclear Research, Russian Academy of Sciences, Moscow, Russia

second order differential equation for hypergeometric function. Another type of functions with known global analytical properties can be defined with the help of the nonlinear second order differential equations: the Painlevé transcendents PI-PVI are the simplest examples. Different and more rich classes of functions are defined by the second order (linear or non-linear) finite-difference equations, an example is given by the basic, or $q$-hypergeometric function. In the latter two cases, the corresponding special functions may be taken for definition of potentials and then the condition of solvability of (1) can be thought as the requirement for wave functions $\psi(x)$ to be related to $u(x)$ by some simple formulae which do not lead to the essentially new objects. This short discussion and the systems to be described below demonstrate that the problem of classification of all exactly solvable problems is far from completion even for a simple equation (1).

The integrability of a problem is related to its symmetry properties. Unfortunately, most of the symmetries are "hidden" and, as a result, the group-theoretical treatment of special functions often emerges as a secondary problem. Rarely new function was introduced primarily from the symmetry principles. The situation however changes when the classification problem is dealt with. The so-called characterization theorems are targeted to the enumeration of specific properties which define a taken system uniquely within the given class of equations. Using them one can see what properties should be abandoned in order to get more general systems. E.g., one may ask what are the most general potentials $u(x)$ for which there exist a differential operator $A$ of the order $N$ such that $[L, A] = 0$. For odd $N$ this happens to lead to the finite-gap potentials mentioned above (even $N$ cases contain generically a functional non-uniqueness).

Recently, the characterization of all potentials leading to the ordinary ladder algebra:

$$[L, A] = \mu A, \qquad \mu > 0, \tag{2}$$

where $A$ is the $N$-th order differential operator, has been given in [2]. For $N = 1$ it is easy to find that $u(x) \propto x^2$, i.e. a harmonic oscillator potential. For $N = 2$ one gets the singular oscillator potential $u(x) \propto \alpha x^2 + \beta/x^2$. The $N = 3$ case corresponds to the quite complicated situation when $u(x)$ involves the Painlevé IV transcendental function [2].

Already from (2) one expects that the spectrum of Hamiltonian $L$ is purely discrete and equidistant. This, however, depends on the structure of zero modes of $A$. If all of them are physical eigenstates of $L$ with different eigenvalues, and the conjugated operator $A^+$ does not break normalizability, then one has a spectrum composed from $N$ independent arithmetic series. The wave functions are explicitly expressed through $f(x)$, $f'(x)$ and $\int f(x)dx$, where $f(x)$ is *defined* by a system of $N$ first order nonlinear differential equations, i.e. the problem is solved exactly in the above sense. Although it is much harder to calculate physical observables of these systems than for the potentials related to the hypergeometric function, the principally important characteristics – the spectrum – is very simple and elegant.

The aim of this note is, however, to present even more complicated potentials than just mentioned ones [3-7]. The first class of them is connected with the algebra (2) but the operator $A$ is now a differential-difference operator [3]. The resulting potentials are more general than those of [2] since the corresponding characterization theorem does not apply. The second class is based on the $q$-deformed ladder relation:

$$LA = q^2 AL, \qquad q^2 \neq 0,\ 1, \tag{3}$$

which simply can not be realized with the help of differential operators of the finite order. Note that the limit $q \to 1$ does not necessarily mean that the operator $A$ will be an integral of motion – there may be a diverging constant entering additively into $L$ such that for $q = 1$ one gets (2) rather than $[L, A] = 0$.

## 2 Self-Similar Potentials

Let us briefly describe the definition of potentials leading to (3). The basic tool is the factorization, or dressing method based on the Darboux transformations. One takes a set of Hamiltonians, $L_j = -d^2/dx^2 + u_j(x)$, and represents them as products of the first-order differential operators,

$$A_j^+ = -\frac{d}{dx} + f_j(x), \qquad A_j^- = \frac{d}{dx} + f_j(x), \tag{4}$$

up to some constants $\lambda_j$:

$$L_j = A_j^+ A_j^- + \lambda_j, \tag{5}$$

i.e. $u_j(x) = f_j^2(x) - f_j'(x) + \lambda_j$. Then one imposes the following intertwining relations:

$$L_j A_j^+ = A_j^+ L_{j+1}, \qquad A_j^- L_j = L_{j+1} A_j^-, \tag{6}$$

which constrain the difference in spectral properties of $L_j$ and $L_{j+1}$ and are equivalent to the equations:

$$A_{j+1}^+ A_{j+1}^- + \lambda_{j+1} = A_j^- A_j^+ + \lambda_j. \tag{7}$$

Substitution of (4) into (7) yields the chain of differential equations [8]:

$$f_j'(x) + f_{j+1}'(x) + f_j^2(x) - f_{j+1}^2(x) = \lambda_{j+1} - \lambda_j \equiv \mu_j, \tag{8}$$

which is called the dressing chain.

The potentials we are interested in are defined by the following self-similarity constraints imposed upon the dressing chain [3, 6]:

$$f_{j+N}(x) = q f_j(qx + r), \qquad \mu_{j+N} = q^2 \mu_j. \tag{9}$$

The simplest example, defined by the reduction $f_j(x) = q^j f(q^j x)$, $\lambda_j = q^{2j}\lambda$, has been found in [4].

At the operator level, the relations (9) lead to the Schrödinger operators with non-trivial $q$-deformed symmetry algebras. Let us consider the products:

$$M_j^+ = A_j^+ A_{j+1}^+ \dots A_{j+N-1}^+, \qquad M_j^- = A_{j+N-1}^- \dots A_{j+1}^- A_j^-, \tag{10}$$

which generate the interwinings

$$L_j M_j^+ = M_j^+ L_{j+N}, \qquad M_j^- L_j = L_{j+N} M_j^-. \tag{11}$$

The structure relations complimentary to (11) look as follows:

$$M_j^+ M_j^- = \prod_{k=0}^{N-1} (L_j - \lambda_{j+k}), \qquad M_j^- M_j^+ = \prod_{k=0}^{N-1} (L_{j+N} - \lambda_{j+k}). \tag{12}$$

These identities show that if the operators $L_j$ and $L_{j+N}$ are related to each other through some simple transformation, e.g.

$$L_{j+N} = q^2 U L_j U^{-1} + \omega, \tag{13}$$

where $U$ is an invertable operator, then the combinations $B_j^+ \equiv M_j^+ U$, $B_j^- \equiv U^{-1} M_j^-$, map eigenfunctions of $L_j$ onto themselves, i.e. they are symmetry operators for $L_j$. The form of $U$ is restricted by the requirement that the $L_j$'s be of the Schrödinger form. Taking $U$ to be the affine transformation generator, $Uf(x)U^{-1} = f(qx + r)$, fixing the indices (e.g., $j \equiv 1$) and removing them, we get the symmetry algebra [6]:

$$LB^{\pm} = q^{\pm 2} B^{\pm} L, \qquad L \equiv -d^2/dx^2 + f_1^2(x) - f_1'(x) + \lambda_1 - \omega/(1-q^2), \tag{14}$$

$$B^+ B^- = \prod_{k=1}^{N} (L + \frac{\omega}{1-q^2} - \lambda_k), \qquad B^- B^+ = \prod_{k=1}^{N} (q^2 L + \frac{\omega}{1-q^2} - \lambda_k). \tag{15}$$

For $N = 1$ this is a $q$-analog of the Heisenberg-Weyl algebra which for special values of the parameters serves as the spectrum generating algebra [5]. For $N = 2$ this is a $q$-deformation of the $su(1,1)$ algebra, and for $N > 2$ we get polynomial relations describing symmetries of the self-similar potentials. Note that the limit $q \to 1$ is not trivial. If the parameter $r$ in (9) is not zero then we get the realizations of the algebra (2) which generalize the ones described in [2]. For $q \neq 1$ the parameter $r$ may be set equal to zero. If the operators $B^{\pm}$ are well defined and have $N$ normalizable zero modes, then the self-similar potentials have spectra consisting of $N$ independent geometric series. Moreover, $u(x)$'s are reflectionless and represent initial conditions for the infinite-soliton solutions of the KdV equation.

We conclude that the $N = 1$ case describes the deformation of harmonic oscillator potential, the $N = 2$ case corresponds to the $q$-deformed conformal quantum mechanics [3], and the $N \geq 3$ cases correspond to the $q$-deformation of the Painlevé type equations.

An interesting situation takes place when the parameter $q$ is a root of unity, i.e. $q^n = 1$. Generically these cases are related to the hyperelliptic potentials, the $N = 1$ system has been analyzed in detail in [7]. Depending on whether $q$ is a primitive root of unity of odd or even degree, the solution may be unique or non-unique. The $q = -1$ system exists only when the initial condition $f(0) = 0$ is imposed and it provides a non-standard realization of the Heisenberg-Weyl algebra. Indeed, the equation arising from (8), (9) at $N = 1, q = -1$:

$$\frac{d}{dx}(f(x) - f(-x)) + f^2(x) - f^2(-x) = \mu, \tag{16}$$

has the general solution $f(x) = \mu x/2$. This corresponds to the operators $B^{\pm}$ satisfying $[B^-, B^+] = \mu$ with the explicit form:

$$B^- = P(d/dx + \mu x/2), \qquad B^+ = (-d/dx + \mu x/2)P, \tag{17}$$

where $P$ is the parity operator $P\psi(x) = \psi(-x)$.

The general $q^3 = 1$ solution exists for arbitrary initial condition and is given by the equianharmonic Weierstrass function: $u_j(x) = 2\wp(x + \Omega_j), (\wp')^2 = 4(\wp^3 - 1)$, where $\Omega_{j+3} = \Omega_j$, and $q^j \Omega_j = \omega_2$ – the real semiperiod of the doubly periodic function $\wp(x)$. The analytical solutions at $q^4 = 1$ exist for special initial condition but they contain functional non-uniqueness. The particular

subcase of the $q^4 = 1$ system is defined by the (pseudo-)lemniscatic Weierstrass function satisfying the equation $(\wp')^2 = 4\wp^3 \pm \wp$. So, the group-theoretical treatment of the Schrödinger equation with these specific elliptic function potentials naturally leads to the $q$-oscillator algebra at roots of unity. Note that the algebra of symmetry operators in these cases does not have the spectrum generating meaning.

# 3 Coherent States of the $q$-Ladder Algebras

Coherent states are interesting objects of quantum mechanics [9]. Originally proposed for the harmonic oscillator potential, eventually they were generalized in many directions. Let us discuss briefly coherent states of the algebra (14), (15) which we define as eigenstates of the "annihilation" operator $B^-$:

$$B^-\psi_\alpha(x) = \alpha\psi_\alpha(x). \tag{18}$$

Looking at the definition of $B^-$ one can realize that this is quite complicated functional equation. The simplest case ($N = 1$) has the following explicit form:

$$(d/dx + f(x))\psi_\alpha(x) = \alpha\sqrt{|q|}\psi_\alpha(qx), \tag{19}$$

where $f(x)$ is a smooth solution of the differential equation with the deviating argument:

$$\frac{d}{dx}(f(x) + qf(qx)) + f^2(x) - q^2f^2(qx) = \mu.$$

The $\sqrt{|q|}$ factor appeared because we took $U$ to be unitary operator so that $(B^-)^\dagger = B^+$. We also assume that $0 < q^2 \leq 1$. (The $q^2 > 1$ choice is equivalent to analytical continuation of the $q^2 < 1$ potentials to the imaginary axis. This brings pole singularities into the potential and, as a result, operators $B^\pm$ are not well defined.) Coherent states of the $q$-oscillators have been widely discussed (see, e.g., [10]), but the realization (19) is a principally new one since it deals with the ordinary Schrödinger equation. Unfortunately, the structure of functions $\psi_\alpha(x)$, their minimal complete subsets, and many other things are not known at present.

As it was noticed in [7] there is a particular coherent state among $\psi_\alpha(x)$ which happens to be an eigenstate of the Hamiltonian! (Such situation is characteristic for the whole algebra (14), (15), i.e. for any self-similar potential at $q^2 < 1$.) It corresponds to the zero energy state, $L\psi_{cl}(x) = 0$, the formal existence of which follows from the boundedness of the potential $\int_{-\infty}^{\infty} |u(x)|dx < \infty$. So, we have the following representation of the $q$-oscillator algebra:

$$B^\pm\psi_{cl}(x) = re^{\pm i\theta}\psi_{cl}(x), \qquad r \equiv \sqrt{\mu/(1-q^2)}, \tag{20}$$

i.e. $B^\pm$ are pure complex conjugated numbers. Possible existence of such "classical" states of the $q$-oscillator algebra has been noticed also (in the different context) in [11]. Since for $\psi_{cl}(x)$ we have two equations: (19) with $\alpha = re^{-i\theta}$ and

$$(-d/dx + f(x))\sqrt{|q|}\psi_{cl}(qx) = re^{i\theta}\psi_{cl}(x),$$

we can remove the derivative part and get pure $q$-difference equation:

$$r|q|^{-1/2}[e^{-i\theta}|q|\psi_{cl}(qx) + e^{i\theta}q^{-1}\psi_{cl}(q^{-1}x)] = (f(x) + q^{-1}f(q^{-1}x))\psi_{cl}(x), \tag{21}$$

which, however, again is not easy to solve.

Finally, let us consider the case $q = -1$, i.e. the coherent states associated with the realization (17). We put for convenience $\mu = 2$ and renormalize $B^{\pm} \to \sqrt{2}B^{\pm}$. The $\psi_\alpha(x)$ states form a subset of solutions of $(B^-)^2\psi_\alpha(x) = \alpha^2\psi_\alpha(x)$. Because $(B^{\pm})^2$ are purely differential operators, one can easily solve this equation. Picking out the proper linear combination of the corresponding two independent solutions, one can find:

$$\psi_\alpha(x) = 2^{-1/2}(e^{-i\pi/4}|i\alpha\rangle + e^{i\pi/4}|-i\alpha\rangle), \tag{22}$$

where $|\alpha\rangle$ are the canonical coherent states of a harmonic oscillator:

$$|\alpha\rangle = \pi^{-1/4}\exp\left(\frac{\alpha^2 - |\alpha|^2}{2} - \left(\frac{x}{\sqrt{2}} - \alpha\right)^2\right). \tag{23}$$

The states (22) are not minimal uncertainty states for the variables $x$ and $p \equiv -id/dx$ for $\alpha \neq 0$:

$$\langle(\Delta x)^2\rangle = (1 - (\alpha - \alpha^*)^2 - (\alpha + \alpha^*)^2 e^{-4|\alpha|^2})/2,$$

$$\langle(\Delta p)^2\rangle = (1 + (\alpha + \alpha^*)^2 + (\alpha - \alpha^*)^2 e^{-4|\alpha|^2})/2,$$

$$\langle(\Delta x)^2\rangle\langle(\Delta p)^2\rangle > 1/4,$$

where $\Delta x = x - \langle x\rangle, \langle x\rangle = \int_{-\infty}^{\infty} x|\psi_\alpha(x)|^2 dx$, etc. However, it is easy to construct other canonical variables

$$\pi = i(B^+ - B^-)/\sqrt{2} = ixP, \quad \phi = (B^+ + B^-)/\sqrt{2} = -ipP, \quad [\phi, \pi] = i,$$

where $P$ is the parity operator, for which $\psi_\alpha(x)$ minimize their uncertainties, $\langle(\Delta\phi)^2\rangle\langle(\Delta\pi)^2\rangle = 1/4$. A detailed consideration of the properties of these coherent states will be given elsewhere [12].

Finally, we would like to point out that the procedure of determination of potentials with fixed symmetry properties presented here may be generalized to other spectral problems. In [13] it was applied to the second order finite-difference equation. In that case many features of the continuous considerations maintain but there are also few new ones. E.g., the algebras at $q > 1$ may now have spectrum generating meaning, i.e. one can find the systems with the exponentially growing spectra. Another advantage consists in the possibility to realize $q$-analogs of the compact unitary algebras like $su(2)$.

# 4 Acknowledgments

The authors benefitted from the stimulating discussions of the outlined results (during this workshop and the last years) with D.Fivel, A.Its, V.Kac, V.P.Karassiov, A.Mann, F.W.Nijhoff, A.Shabat, E.C.G.Sudarshan, S.Suslov, L.Vinet, and A.Zhedanov. The work of V.S. is supported by the NSERC of Canada and by the Fonds FCAR of Québec.

# References


[1] Erdélyi, A., Magnus, W., Oberhettinger, F., and Tricomi, F.G., *Bateman Manuscript Project. Higher Transcendental Functions.* Vol. 2. (McGraw-Hill, 1953).

[2] Veselov, A.P. and Shabat, A.B., Funkt. Anal. i ego Pril. **27**, n. 2, 1-21 (1993).

[3] Spiridonov, V., *in:* Proc. of the Workshop on Harmonic Oscillators (College Park, March 25-28, 1992). Eds. D.Han, Y.S.Kim, and W.W.Zachary (NASA Conf. Publ. 3197, 1993) pp. 93-108; Mod. Phys. Lett. **A7**, 1241-1251 (1992).

[4] Shabat, A., Inverse Prob. **8**, 303-308 (1992).

[5] Spiridonov, V., Phys. Rev. Lett. **69**, 398-401 (1992).

[6] Spiridonov, V., *in:* Proc. of the XIX$^{th}$ ICGTMP (Salamanca, 29 June - 4 July 1992). Eds. M.A. del Olmo, M.Santander, and J.M.Guilarte (CIEMAT/RSEF, Madrid 1993) Vol. I, pp. 198-201; Proc. of the CAP-NSERC Workshop on Quantum Groups, Integrable Models and Statistical Systems (Kingston, July 13-18, 1992). Eds. J.LeTourneux and L.Vinet (World Scientific, 1993).

[7] Skorik, S. and Spiridonov, V., Lett. Math. Phys. **28**, 59-74 (1993).

[8] Infeld, L. and Hull, T.E., Rev. Mod. Phys., **23**, 21-68 (1951).

[9] Klauder, J.R. and Skagerstam, B.-S. (eds), *Coherent States – Applications in Physics and Mathematical Physics* (World Scientific, 1985).

[10] Arik, M. and Coon, D., J. Math. Phys. **17**, 524-527 (1976); Biedenharn, L.C., J. Phys. **A22**, L873-L878 (1989); Kulish, P.P. and Damaskinsky, E.V., J. Phys. **A23**, L415-L419 (1990); Gray, R.W. and Nelson, C.A., J. Phys. **A23**, L945-L950 (1990); Floreanini, R. and Vinet, L., Lett. Math. Phys. **22**, 45-54 (1991); Phys. Lett. **A180**, 393-401 (1993); Bracken, A.J., McAnally, D.S., Zhang, R.B., and Gould, M.D., J. Phys. **A24**, 1379-1391 (1991); Fivel, D.I., J. Phys. **A24**, 3575-3586 (1991); Quesne, C., Phys. Lett. **A153**, 303-307 (1991); Zhedanov, A., J. Phys. **A24**, L1129-L1133 (1991), Teor. Mat. Fiz. **94**, 307-315 (1993); Askey, R. and Suslov, S.K., J. Phys. **A26**, L693-L698 (1993).

[11] Granovskii, Ya.I. and Zhedanov, A.S., Mod. Phys. Lett. **A8**, 1029-1035 (1993).

[12] Spiridonov, V., in preparation.

[13] Spiridonov, V., Vinet, L., and Zhedanov, A., Lett. Math. Phys. **29**, (1993).

# THE WAVE FUNCTION AND MINIMUM UNCERTAINTY FUNCTION OF THE BOUND QUADRATIC HAMILTONIAN SYSTEM

Kyu Hwang Yeon
*Department of Physics, Chungbuk National University*
*Cheongju, Chungbuk, 360-763, Korea*

Chung In Um
*Department of Physics, College of Science, Korea University*
*Seoul, 136-701, Korea*

T.F. George
*Department of Chemistry and Physics, Washington State University*
*Pullman, Washington 99164-1046*

**Abstract**

The bound quadratic Hamiltonian system is analyzed explicitly on the basis of quantum mechanics. We have derived the invariant quantity with an auxiliary equation as the classical equation of motion. With the use of this invariant it can be determined whether or not the system is bound. In bound system we have evaluated the exact eigenfunction and minimum uncertainty function through unitary transformation.

## 1 Introduction

In recent years an extensive effort has been devoted to obtaining an exact solution for the oscillator systems with time-dependent Hamiltonian [1)] and especially dissipative system, *i.e.*, damped free particle [2)], damped [3)] or damped driven harmonic oscillator [4)] and driven time-dependent harmonic oscillator[5)]. After Lewis and Riesenfeld[6)] first derived the relation between the eigenstates of the dynamical invariant and the solution of the Schrödinger equation, many authors have applied the dynamical invariant method to investigate the time-dependent oscillator system. The dynamical invariant is related directly to an auxiliary equation as the classical equation of motion for the Hamiltonian system, which is given as nonlinear second-order differential equation. Therefore the dynamical invariant can be determined by the particular solution to the auxiliary equation.

In this paper, employing the operator method, we derive the wave function and the minimum uncertainty function for the quadratic Hamiltonian system which includes canonical variables with time-dependent coefficients. Recently, we have investigated this system to obtain the wave function and propagator through path integral method [7)]. In Sec. 2, we derive the dynamical invariant from the equation of motion. We classify whether or not the system is bound in the consideration of our system as classical system and then find the conditions for bound and unbound. In Sec. 3, using the quantum invariant operator, we define the creation and annihilation operators and then evaluate the wave function and propagator of our system. In Sec. 4, we introduce new creation and annihilation operators from the old ones in Sec. 3, and evaluate eigenfunction of the unitary transformed system and minimum uncertainty function. Finally, we give the summary in Sec. 5.

## 2 The bound quadratic Hamiltonian system

The quadratic Hamiltonian of the system is given as

$$H = \frac{1}{2}[A(t)p^2 + B(t)(pq + qp) + C(t)q^2] \tag{1}$$

where $p$ and $q$ are canonical variables. $A(t)$, $B(t)$ and $C(t)$ is continuously differentiable function but $A(t)$ is nonzero. The classical equation of motion can be obtained from the Hamilton's equation of motion:

$$\ddot{q} + \zeta(t)\dot{q} + \xi(t)q = 0 \tag{2}$$

with

$$\zeta(t) = -\frac{\dot{A}(t)}{A(t)} \tag{3}$$

$$\xi(t) = A(t)C(t) + \frac{\dot{A}(t)B(t)}{A(t)} - B^2(t) - \dot{B}^2(t). \tag{4}$$

The general solution for Eq. (2) can not be found, but we may take the solution in the following form:

$$q = \rho(t)e^{i\gamma(t)} \tag{5}$$

here, $\rho(t)$ and $\gamma(t)$ are the functions to be determined from Eq. (2). The functions are real and depend only on time. Substitution of Eq. (5) in Eq. (2) offers the real and imaginary parts of this equation as

$$\ddot{\rho} - \rho\dot{\gamma}^2 + \zeta(t)\dot{\rho} + \xi(t)\rho = 0. \tag{6}$$

and

$$\ddot{\gamma} + 2\dot{\rho}\dot{\gamma} + \zeta(t)\dot{\gamma}\rho = 0. \tag{7}$$

The time invariant quantity can be found from Eq. (7) in the form:

$$\Omega = \frac{\rho^2\dot{\gamma}}{A(t)} \tag{8}$$

with auxiliary condition as the classical equation of motion, Eq. (2). With the use of Eq. (8), the nonlinear differential equation [Eq.(6)] can be written as

$$\ddot{\rho} + \zeta(t)\dot{\rho} + \xi(t)\rho = \frac{\Omega^2}{\rho^3}A^2(t). \tag{9}$$

We may find another classical time invariant quantity with an auxiliary equation as classical equation of motion. We assume that this invariant quantity depends on $p$, $q$ and $t$. Then, from Hamilton's equation of motion, the time derivative of $I(p, q, t)$ becomes

$$\frac{dI}{dt} = \frac{\partial I}{\partial t} + \frac{\partial I}{\partial q}\frac{\partial H}{\partial p} - \frac{\partial I}{\partial p}\frac{\partial H}{\partial q} = 0. \tag{10}$$

Combining Eq. (10) with Eq. (1) we may obtain the time invariant quantity as

$$I = \left(\frac{\Omega}{\rho}q\right)^2 + \left[\left(\frac{B(t)}{A(t)}\rho - \frac{1}{A(t)}\dot{\rho}\right)q + \rho p\right]^2. \tag{11}$$

$I(q,p,t)$ is an invariant quantity and thus we can express it in phase space. For $\Omega = 0$, Eq. (11) becomes a linear line in phase space and canonical variables $q$ and $p$ can occupy every region in phase space. Therefore the motion of the system is unbound. On the other and, for $\Omega \neq 0$, Eq. (11) becomes ellipse in phase space because the coefficient matrix of it has positive real eigenvalues. The canonical variables $q$ and $p$ can occupy some finite region in phase space, and thus the motion of the system is bound.

# 3 The Wave Function, Propagator and Uncertainty Values

For quantum mechanical treatment of our system, we may replace the canonical variables with the corresponding quantum operators in Eq. (7) and then we may also obtain the quantum invariant operator of the system as the same form of Eq. (11).

In order to obtain the eigenfunctions and eigenvalues of the invariant operator, we define the creation and annihilation operator, $a$ and $a^\dagger$ with auxiliary equations, Eq. (8) and Eq. (9) as

$$a = \sqrt{\frac{A}{2\hbar\dot{\gamma}}}\left\{\frac{1}{A}\left[\dot{\gamma} + i\left(B - \frac{\dot{\rho}}{\rho}\right)\right]q + ip\right\} \tag{12}$$

$$a^\dagger = \sqrt{\frac{A}{2\hbar\dot{\gamma}}}\left\{\frac{1}{A}\left[\dot{\gamma} - i\left(B - \frac{\dot{\rho}}{\rho}\right)\right]q - ip\right\}. \tag{13}$$

The invariant operator [Eq. (11)] can be expressed in terms of $a$ and $a^\dagger$ as

$$I = \hbar\Omega\left(a^\dagger a + \frac{1}{2}\right). \tag{14}$$

Since the $a$ and $a^\dagger$ satisfy the commutation relation, the normalized eigenstates and eigenvalues of Eq. (14) are given by

$$a^\dagger a|n> = n|n> \qquad n = 0, 1, 2, \cdots \tag{15}$$

$$\lambda = \hbar\Omega\left(n + \frac{1}{2}\right) \qquad n = 0, 1, 2, \cdots \tag{16}$$

The ground state must satisfy the condition that

$$au_0 = 0. \tag{17}$$

Solving Eq. (17) for $u_0$ we obtain

$$u_0 = \left(\frac{\dot{\gamma}}{\pi\hbar A}\right)^{1/4} e^{-\frac{1}{2\hbar A}\left[\dot{\gamma} - i\left(\frac{\dot{\rho}}{\rho} - B\right)\right]q^2}. \tag{18}$$

Operating $a^\dagger$ continuously to Eq. (18) we may obtain the n$th$ excited states:

$$\begin{aligned} u_n &= \frac{1}{\sqrt{n!}}(a^\dagger)^n u_0 \\ &= \sqrt{\frac{1}{2^n n!}}\left(\frac{\dot{\gamma}}{\pi\hbar A}\right)^{1/4} H_n\left(\sqrt{\frac{\dot{\gamma}}{\hbar A}}q\right) e^{-\frac{1}{2\hbar A}[\dot{\gamma}-i(\frac{\dot{\rho}}{\rho}-B)]q^2} \end{aligned} \tag{19}$$

where $H_n$ is a n$th$ order Hermite polynomial.

Eq. (19) is an eigenfunction of the invariant operator [Eq. (14)] with an auxiliary equation as classical equation of motion, but is not the solution of the Schrödinger equation;

$$i\hbar\frac{\partial\phi}{\partial t} = \frac{1}{2}[-\hbar^2 A(t)\frac{\partial^2}{\partial q^2} + \frac{\hbar}{i}B(t)\left(q\frac{\partial}{\partial q} + \frac{\partial}{\partial q}q\right) + C(t)q^2]\phi. \tag{20}$$

Comparision of Eq. (19) with (20) offers the exact wave function of the system:

$$\begin{aligned} \phi_n(q,t) &= e^{i\beta_n}u_n(q,t) \\ &= \left(\frac{1}{2^n n!}\right)^{1/2}\left(\frac{\dot{\gamma}}{\pi\hbar A}\right)^{1/4} e^{-i(n+\frac{1}{2})\gamma} H_n\left(\sqrt{\frac{\dot{\gamma}}{\hbar A}}q\right) e^{-\frac{1}{2\hbar A}[\dot{\gamma}-i(\frac{\dot{\rho}}{\rho}-B)]q^2}. \end{aligned} \tag{21}$$

Making use of the Mehler's formula together with Eq. (21), we can easily evaluate the propagator of the system given by

$$\begin{aligned} K(q,t,;q',t') &= \left[\frac{\dot{\gamma}^{1/2}\dot{\gamma}'^{1/2}}{2\pi i\hbar\sin(\gamma-\gamma')A^{1/2}A'^{1/2}}\right]^{1/2} \\ &\quad\times\exp\left\{\frac{i}{2\hbar A}\left[\frac{\dot{\rho}}{\rho}+\dot{\gamma}\cot(\gamma-\gamma')-B\right]q^2\right. \\ &\quad\left.+\frac{i}{2\hbar A'}\left[-\frac{\dot{\rho}'}{\rho'}+\dot{\gamma}'\cot(\gamma-\gamma')+B'\right]q'^2+\frac{i}{\hbar}\sqrt{\frac{\dot{\gamma}\dot{\gamma}'}{AA'}}\frac{qq'}{\sin(\gamma-\gamma')}\right\} \end{aligned} \tag{22}$$

where $\rho' = \rho(t')$, $\gamma' = \gamma(t')$, $A' = A(t')$, and $B' = B(t')$. Eq. (22) is the result that we obtained previously[7].

The uncertainty relation is defined by

$$(\Delta q\Delta p)_{m,n} = [|(< m|q^2|n > - < m|q|n >^2)(< m|p^2|n > - < m|p|n >^2)|]^{1/2}. \tag{23}$$

With the help of Eq. (21), we can express Eq. (23) as

$$(\Delta q\Delta p)_{n,n} = \hbar\left(n+\frac{1}{2}\right)\sqrt{1+\frac{1}{\dot{\gamma}^2}\left(\frac{\dot{\rho}}{\rho}-B\right)^2}. \tag{24}$$

# 4 The Minimum Uncertainty Function

The minimum value for $n = 0$ in Eq. (24) is larger than $\hbar/2$ and thus the coherent state of our system is not a minimum uncertainty state. To obtain minimum uncertainty state, we introduce the new creation and annihilation operators defined by

$$b = \mu a + \nu a^\dagger \tag{25}$$

for a pair of $c$ numbers $\mu$, $\nu$ obeying

$$|\mu|^2 - |\nu|^2 = 1. \tag{26}$$

The canonical transformation [Eq. (25)] which keeps the commutator invariant, is a unitary transformation. The properties of the $b$ and $b^\dagger$ are the same as those of $a$ and $a^\dagger$ [8].

Performing the same procedures in Sec. 3, we can obtain the wave function for n*th* excited states:

$$\begin{aligned}\psi_n &= \left(\frac{1}{2^n n!}\right)^{1/2} \left(\frac{\dot\gamma}{\pi\hbar A|\mu-\nu|^2}\right)^{1/4} \left(\frac{\mu^*-\nu^*}{|\mu-\nu|}\right)^n H_n\left(\sqrt{\frac{\dot\gamma}{\hbar|\mu-\nu|^2 A}}q\right) \\ &\quad \times \exp\left\{-\frac{q^2}{2\hbar A|\mu-\nu|^2}\left[\dot\gamma - i\left[\left(B-\frac{\dot\rho}{\rho}\right)|\mu-\nu|^2 + i(\mu\nu^*-\nu\mu^*)\,\dot\gamma\right]\right]\right\}. \end{aligned}\tag{27}$$

Substituting Eq. (26) into Eq. (24) and evaluating the diagonal element, the uncertainty relation for $(n,n)$ states can be obtained:

$$(\Delta q\Delta p)_{n,n} = \left(n+\frac{1}{2}\right)\hbar\left\{1+\left[\frac{1}{\dot\gamma}\left(B-\frac{\dot\rho}{\rho}\right)|\mu-\nu|^2 + i(\mu\nu^*-\nu\mu^*)\right]^2\right\}^{1/2}. \tag{28}$$

From Eq. (27) we can also find the condition of $\mu$ and $\nu$ for the minimum uncertainty

$$\mu = \frac{k}{\sqrt{k^2-1}} \tag{29}$$

$$\nu = \frac{1}{\sqrt{k^2-1}} e^{i\theta} \tag{30}$$

where

$$k = \frac{\alpha \pm \sqrt{\alpha^2 - \frac{4}{\dot\gamma^2}\left(B-\frac{\dot\rho}{\rho}\right)^2}}{2B} \tag{31}$$

$$\theta = \tan^{-1}\left[\frac{\frac{4}{\dot\gamma}\left(B-\frac{\dot\rho}{\rho}\right) \pm |\alpha|\sqrt{\frac{4}{\dot\gamma^2}\left(B-\frac{\dot\rho}{\rho}\right)^2 - a^2 + 4}}{\alpha^2-4}\right] \tag{32}$$

and

$$\frac{4}{\dot\gamma^2}\left(B-\frac{\dot\rho}{\rho}\right)^2 \le \alpha^2 \le \frac{4}{\dot\gamma^2}\left(B-\frac{\dot\rho}{\rho}\right)^2 + 4. \tag{33}$$

Here, $k$ is real and positive, and $\alpha$ must have the same sign of $\frac{1}{\dot\gamma}\left(B-\frac{\dot\rho}{\rho}\right)$. We can confirm that the minimum uncertainty is a function of one continuous parameter in the finite region.

# 5 Summary

Introducing the quadratic Hamiltonian system given in Eq. (1), we have derived the classical invariant quantity with an auxiliary equation as the classical equation of motion. With the use of this invariant, we can distinguish whether or not the system is bound. We transformed the invariant into an operator in the replacement of the creation and annihilation operator [Eq. (14)] and then evaluated the corresponding eigenfunction and eigenvalues. However, this eigenfunction is not the Schrödinger solution of the system. Though we obtain the exact wave function of the system [Eq. (21)] and propagator [Eq. (22)] the minimum uncertainty constructed by this wave function is larger than $\hbar/2$ and thus the coherent states of the system is not minimum uncertainty state. To obtain the minimum uncertainty we introduce the canonical transformation, which keeps the commutator invariant. Through this unitary transformation we obtained the eigenfunction and minimum uncertainty state of the system.

# Acknowledgments

This work was supported by the Center for Thermal and Statistical Physics, KOSEF under Contact No. 93-08-00-05 and by the BSRI Program, Ministry of Education, Republic of Korea, and by the U.S. National Science Foundation under Grant No. CHE-9196214.

# References

(1) J. G. Hartley and J. R. Ray, Phys. Rev. D **25**, 382(1982); D. C. Khandekar and S. S. Lawande, J. Math. Phys. **20**, 1870(1979): P. Camiz, A. Gerardi, C. Marehioso, E. Presutti and E. Scaeciatelli, J. Math. Phys. **12**, 2040(1971); P. G. L. Leach, J. Math. Phys. **21**,300(1980).

(2) K. H. Yeon and C. I. Um, J. Korean Phys. Soc. **23**, 82(1990).

(3) K. H. Yeon, C. I. Um and T. F. George, Phys. Rev. A **36**,5287(1987); V. V. Dodonov, T. F. George, O. V. Man'ko, C. I. Um and K. H. Yeon, J. Soviet Laser Research **12**(5), 385(1991); L. F. Landovitz, A. M. Lavine. E. Ozizmis and W. M. Schreiber, J. Chem. Phys. **78**, 291(1983); **78**, 6133(1983).

(4) V. V. Dodonov and V. I. Man'ko, Phys. Rev. A **20**, 550(1979); C. I. Um, K. H. Yeon and W. H. Kahng, J. Phys. A: Math. Gen. **20**, 611(1987).

(5) C. F. Lo, Phys. Rev. A **47**, 115(1993).

(6) H. R. Lewis, Jr. and W. B. Riesenfeld, J. Math. Phys. **10**, 1458(1969).

(7) K. H. Yeon. K. K. Lee, C. I. Um, T. F. George and L. N. Pandey, Phys. Rev. A in print.

(8) H. P. Yuen, Phys. Rev. A **13**, 2226(1976); J. von Neumann, Math. Ann. **104**, 570(1931)

# THE THERMAL-WAVE MODEL: A SCHRÖDINGER-LIKE EQUATION FOR CHARGED PARTICLE BEAM DYNAMICS [1]

R. Fedele and G. Miele
*Dipartimento di Scienze Fisiche, Università di Napoli "Federico II", and INFN Sezione di Napoli, Mostra d'Oltremare Pad. 20, 80125, Napoli, Italy*

**Abstract**

In this paper we review some results on longitudinal beam dynamics obtained in the framework of the *Thermal Wave Model* (TWM). In this model, which has recently shown the capability to describe both longitudinal and transverse dynamics of charged particle beams, the beam dynamics is ruled by Schrödinger-like equations for the beam-wave-functions, whose squared modulus is proportional to the beam density profile. Remarkably, the role of the Planck constant is played by a diffractive constant $\epsilon$, the emittance, which has a thermal nature.

## 1 Introduction

Recently, on pure basis of analogy with other similar subjects of physics, a new technique to derive the equation of motion for a thermal system, like a charged particle beam at finite temperature, which is able to take into account the collective behaviour of the ensemble has been obtained [1]-[5].
The starting point of this technique, *the Thermal Wave Quantization* (TWQ), are the equations of motion of the considered system, in the so called *single-particle approximation*, from which is possible to obtain the *single-particle hamiltonian* of the system. At this point, the formal analogy showed in the case of the transverse dynamics for relativistic charged particle beams, with the electromagnetic optics in paraxial approximation and with the two dimensional nonrelativistic quantum mechanics [1], suggests to replace the *single-particle hamiltonian*, with a differential operator, and the hamilton-equations with a Schrödinger-like equation, in which coordinate and particle momentum are replaced by a beam-wave-function.
This technique, applied to the longitudinal and transverse beam dynamics, has led to the formulation of the *Thermal Wave Model* (TWM) for relativistic charged particle beam propagation, which represents a useful *quantum-like* description of the total beam optics [1]-[5]. This model has already been successfully applied for estimating the effects of the aberrations in linear colliders [3], [5], as well as for describing nonlinear beam-plasma interaction [2], and nonlinear longitudinal dynamics in circular accelerating machines [4].

[1] presented by R. Fedele

## 2 TWM for longitudinal dynamics

Let us consider a single relativistic particle of electric charge $q$, within a stationary bunch, travelling with longitudinal velocity $\beta c$ ($\beta \simeq 1$) in a circular accelerating machine of radius $R_0 = cT_0/2\pi$ ($T_0$ being the revolution period). Its longitudinal motion is described, neglecting radiation damping and quantum excitations, by a pair of equations which, defining $s \equiv ct$ ($t$ being the time), can be put in the following dimensionless form [6]

$$\frac{dx}{ds} = \eta \frac{\Delta E}{E_0} \equiv \eta \mathcal{P} \quad , \tag{1}$$

$$\frac{d\mathcal{P}}{ds} = -\frac{q\Delta V}{cT_0 E_0} \quad , \tag{2}$$

where $x$ is the longitudinal particle coordinate and $\mathcal{P} \equiv \Delta E/E_0$ is the dimensionless longitudinal energy variation, after a turn in the ring. Note that $x$ ($-\pi R_0 \leq x \leq \pi R_0$) and $\mathcal{P}$ are both evaluated with respect to the synchronous particle ($\Delta E = 0$), and $E_0$ is the synchronous particle energy. The quantity $\Delta V$ represents the total voltage variation after a turn and it takes into account the interactions of the particles with the surrounding medium (RF-cavities, pipe, kickers, etc.). Consequently, the equations (1) and (2) describe the longitudinal bunch dynamics on time scale $t >> T_0$. Furthermore, in (1) the parameter $\eta$ is defined as $\eta \equiv (\Delta\omega/\omega_0)/(\Delta E/E_0)$ ($\omega_0 \equiv c/R_0$ and $\Delta\omega$ being the frequency shift with respect to $\omega_0$). By defining the *momentum compaction* $\alpha \equiv (\Delta R/R_0)/(\Delta E/E_0)$, where $\Delta R$ is the orbit radius variation with respect to $R_0$, it can be easily proved that $\eta = 1/\gamma^2 - \alpha$. From (1) and (2) we can easily write the following dimensionless *single-particle hamiltonian*

$$H = \frac{1}{2}\eta \mathcal{P}^2 + U \quad , \tag{3}$$

where

$$U \equiv \frac{1}{cT_0 E_0} \int_0^x q\Delta V \, dx' \quad . \tag{4}$$

In order to find an equation which describes the longitudinal evolution of the beam, taking into account its thermal spreading (longitudinal emittance) while it interacts with the surrounding medium (potential well and wake fields), we follow the *quantum-analogy*, which suggests to use in (3) the following correspondence rules

$$\mathcal{P} \rightarrow \hat{\mathcal{P}} \equiv -i\epsilon_L \frac{\partial}{\partial x} \quad and \quad H \rightarrow \hat{H} \equiv i\epsilon_L \frac{\partial}{\partial s} \quad , \tag{5}$$

where $\epsilon_L$ is the longitudinal beam emittance. Thus, by considering (3) and (5), the following Schrödinger-like equation for the *beam wave function* (bwf) $\Psi$ can be assumed

$$i\epsilon_L \frac{\partial \Psi}{\partial s} = \hat{H}\Psi \quad , \tag{6}$$

where $\hat{H} = \frac{\eta}{2}\hat{\mathcal{P}}^2 + U$. Consequently, (6) becomes

$$i\epsilon_L \frac{\partial \Psi}{\partial s} = -\frac{\epsilon_L^2 \eta}{2} \frac{\partial^2 \Psi}{\partial x^2} + U\Psi \quad . \tag{7}$$

Note that (7) describes the longitudinal beam dynamics in terms of the bwf $\Psi$, which we assume to be related to the longitudinal density number $\lambda(x,s)$ through the following relation: $\lambda(x,s) = \lambda_0|\Psi(x,s)|^2$, where $\lambda_0 = N/R_0$ ($N$ being the total number of particle in a bunch). According to the previous definitions, $|\Psi|^2$ gives the longitudinal beam density profile. Furthermore, the circular topology of the ring should requires periodic solutions for $\Psi$, with respect to $x$ ($\Psi(\pi R_0, s) = \Psi(-\pi R_0, s)$ and $\partial_x\Psi(\pi R_0, s) = \partial_x\Psi(-\pi R_0, s)$). In these conditions, from (7) the norm squared ($\mathcal{N}^2$) of bwf, defined as

$$\mathcal{N}^2 \equiv \int_{-\pi R_0}^{+\pi R_0} |\Psi(x,s)|^2 \, dx \quad , \tag{8}$$

is conserved ($U$ is assumed a real function), and it has been fixed for simplicity equal to $R_0$. This result is compatible with the physical requirement that $\int_{-\pi R_0}^{+\pi R_0} \lambda(x,s)\, dx = N$. However, in the following we restrict our analysis to consider bunched beam whose effective length is much smaller than $R_0$. Under this assumption, the above conditions of periodicity of $\Psi$ do not have a relevant role, because in this limit, for the bunch, the ring looks like an infinite linear accelerator. Thus we can define the effective bunch length $\sigma_L$, and the expectation value of the momentum $\hat{\mathcal{P}}$ as

$$\sigma_L(s) \equiv \left[\frac{1}{\mathcal{N}^2}\int_{-\pi R_0}^{+\pi R_0} x^2\,|\Psi|^2\,dx\right]^{1/2} \qquad \sigma_L^p(s) \equiv \frac{\epsilon_L}{\mathcal{N}}\left[\int_{-\pi R_0}^{+\pi R_0}\left|\frac{\partial\Psi}{\partial x}\right|^2 dx\right]^{1/2} \quad , \tag{9}$$

and in complete analogy to quantum mechanics the *uncertainty principle*

$$\sigma_L\,\sigma_L^p \;\geq\; \epsilon_L/2 \tag{10}$$

holds. Furthermore, note that (7) $1/\eta$ plays the role of an *effective mass.*

## 2.1 The interaction potential and synchrotron oscillations

As it has been shown in Ref. [4], the potential $U$ can be split in two parts (RF + Self-interaction) and (4) becomes: $U = U_{RF} + U_S$. Note that whereas in general $U_{RF}$ is a known function of $x$ and $s$, the explicit expression for $U_S$, depending on the bunch density (collective effects), needs particular assumptions about the beam interaction with the surrounding medium to be specified. This interaction can be parametrized in terms of the longitudinal coupling impedance [7]. In the special case of a linear approximation for the RF-potential, $U_{RF} = \frac{1}{2}\frac{K}{\eta}x^2$, where $K$ is the *cavity strength* ($\sqrt{|K|}$ is the synchrotron wave number), and for a purely reactive longitudinal coupling impedance $X$, the equation for bwf becomes

$$i\epsilon_L\eta\frac{\partial\Psi}{\partial s} \;=\; -\frac{\epsilon_L^2\eta^2}{2}\frac{\partial^2\Psi}{\partial x^2} \;+\; \frac{1}{2}Kx^2\Psi \;-\; \eta\frac{qI}{2\pi E_0}\left(\frac{X}{n}\right)|\Psi|^2\Psi \quad , \tag{11}$$

where $I$ is the beam current, and $n$ is the so-called *harmonic number* [8]. In the simplest case of ($X = 0$) and for $R_0 >> \sigma_L$, the Eq. (11) can be exactly solved, and the normalized solutions for bwf are the well known Hermite-Gauss modes as it occurs in complete analogy for electromagnetic optics in paraxial approximation [9]

$$\Psi_m(x,s) = \frac{\exp\left[-\frac{x^2}{4\sigma_L^2(s)}\right]}{[2\pi\sigma_L^2(s)]^{1/4}}\,H_m\left(\frac{x}{\sqrt{2}\sigma_L(s)}\right)\,\exp\left[i\frac{x^2}{2\epsilon_L\eta\rho_L(s)} + i(1+2m)\phi_L(s)\right] \quad . \tag{12}$$

In (12) the functions $\sigma_L(s)$, $\rho_L(s)$ and $\phi_L(s)$ are solutions of the following system of differential equations

$$\frac{d^2\sigma_L}{ds^2} + K\sigma_L - \frac{\epsilon_L^2\eta^2}{4\sigma_L^3} = 0 \quad , \tag{13}$$

$$\frac{1}{\rho_L} = \frac{1}{\sigma_L}\frac{d\sigma_L}{ds} \quad , \tag{14}$$

$$\frac{d\phi_L}{ds} = -\frac{\epsilon_L\eta}{4\sigma_L^2} \quad . \tag{15}$$

and $H_m(x)$ are the Hermite-polynomials with $m$ a non-negative integer. Note that $|\Psi_m|^2$ for $m = 0$ (fundamental mode) gives a Gaussian particle distribution. Remarkably, it can be easily proved that (13) is completely equivalent to

$$\frac{d^2\sigma_L^2}{ds^2} + 4K\sigma_L^2 = 4\mathcal{E} \quad with \quad \mathcal{E} = \frac{1}{2}\left(\frac{d\sigma_L}{ds}\right)^2 + \frac{\epsilon_L^2\eta^2}{8\sigma_L^2} + \frac{1}{2}K\sigma_L^2 = const. \tag{16}$$

In this form it is easily to recognize that the equation for $\sigma_L(s)$ (16), i.e. (13), describes the synchrotron oscillations. The equilibrium condition $d^2\sigma_L/ds^2 = 0$ gives

$$\sigma_L^0 = \frac{|\eta|}{\sqrt{|K|}}\sigma_L^{p0} = \frac{|\eta|R}{\nu_s}\sigma_L^{p0} \quad , \tag{17}$$

where $\sigma_L^0$ and $\sigma_L^{p0}$ are the equilibrium value of $\sigma_L$ and $\sigma_L^p$, respectively, and $\nu_s$ is the synchrotron number given by the ratio between the synchrotron frequency $\Omega_s \equiv c\sqrt{|K|}$ and the revolution frequency $\omega_0$ [10]. Equation (17) recovers the well known relationship between the bunch length $\sigma_L^0$ and the energy spread $\sigma_L^{p0}$ [10]. Since for the present case the bwf is Gaussian, in obtaining (17) we have introduced the minimum value $\sigma_L^0\sigma_L^{p0} = \epsilon_L/2$ of the product $\sigma_L\sigma_L^p$ consistently with disequality reported in section 2.

# 3 Coherent stability criterion and soliton solution

In this Section, we develop, within the framework of the thermal wave model, an analysis of some collective effects occurring when the bunch interacts with the surrounding medium. To this end, we consider the special case of RF cavity *off* and take into account both the space charge effect and a purely inductive coupling impedance. Consequently, (11) becomes

$$i\epsilon_L\eta\frac{\partial\Psi}{\partial s} = -\frac{\epsilon_L^2\eta^2}{2}\frac{\partial^2\Psi}{\partial x^2} - \eta\frac{qI}{2\pi E_0}\left(\frac{X}{n}\right)|\Psi|^2\Psi \quad . \tag{18}$$

Note that (18) is formally identical to the cubic NLS equation which describes the propagation of an e.m. pulse through a nonlinear medium in paraxial approximation [11],[12],[13]. In this analogy, the factor $\epsilon_L\eta$ plays the role of the diffraction parameter (the inverse of the wave number), $s$ corresponds to the time, and $-[\eta qI(X/n)/(2\pi E_0)]|\Psi|^2$ corresponds to a nonlinear refractive index. Thus, an analysis of the bunch coherent instability (stability) can be made in complete analogy to the electromagnetic case [11],[12]. To this aim, applying the well known method developed in

nonlinear e.m. optics to search for the sufficient conditions of modulational instability, we show that coherent instability for particle bunches is fully equivalent to modulational instability for e.m. bunches. Moreover, a soliton-envelope solution, very interesting for accelerator physics, is found.

As an example, we analyze the instability of a plane-wave ($\Psi_0(x,s) = \rho_0 \exp[i(k_0 x - \Omega_0 s)]$, where $\rho_0$ is a positive constant) solution of Eq. (18), when a small perturbation around it is introduced. Let

$$\Psi(x,s) = [\rho_0 + \rho_1(x,s)] \exp[i(k_0 x - \Omega_0 s) + i\theta_1(x,s)] \tag{19}$$

be the perturbed solution, being $\rho_1$ and $\theta_1$ real functions, and

$$\Omega_0 = \frac{\epsilon_L \eta}{2} k_0^2 - \frac{qI}{2\pi\epsilon_L E_0}\left(\frac{X}{n}\right)\rho_0^2 \quad . \tag{20}$$

In order to obtain the dispersion relation of the system we can assume

$$\rho_1(x,s) = \rho_1^0 \cos(kx - \Omega s + \phi_0) \qquad \theta_1(x,s) = \theta_1^0 \sin(kx - \Omega s + \phi_0) \quad , \tag{21}$$

where $\rho_1^0$, $\theta_1^0$, $k$, $\Omega$ and $\phi_0$ are real constants. By imposing that (19) is a solution of the linearized (18) we obtain the following dispersion relation

$$\Omega = \frac{\epsilon_L \eta}{2} k \left[2k_0 \pm \sqrt{\left(k^2 - \frac{4qI}{\eta\epsilon_L^2 2\pi E_0}\left(\frac{X}{n}\right)\rho_0^2\right)}\right] \quad . \tag{22}$$

Reminding that unstable modes occur for $\Im(\Omega) \neq 0$, namely

$$k^2 < \frac{2qI}{\pi\eta\epsilon_L^2 E_0}\left(\frac{X}{n}\right)\rho_0^2 \quad , \tag{23}$$

we get stability for $\eta X < 0$ and instability for $\eta X > 0$. This result recovers the well-known condition for coherent stability (instability) for monochromatic charged particle beams [14], in addition we remark that the above condition is fully similar to the Lighthill criterion, valid for modulational instability of an e.m. plane-wave travelling in a nonlinear medium [11],[12],[13].

For a bunched beam ($\sigma_L << R_0$), a solitary solution of (18) is found by looking for a solution of a relativistic envelope form:

$$\Psi(x,s) \;=\; G(x - \beta_0 s) e^{i\chi_0 x - i w_0 s} \quad , \tag{24}$$

with $\chi_0$, $w_0$, and $\beta_0$ real numbers. Thus, according to the general theory of NLS equations [11], the following soliton-like solution for the beam density ($\lambda = \lambda_0 G^2$), which satisfies (8), is possible under the condition $\eta X > 0$:

$$\lambda(x,s) = \frac{N^2 q^2 R}{4\epsilon_L^2 T_0 E_0}\frac{1}{\eta}\left(\frac{X}{n}\right) sech^2\left[\frac{Nq^2 R}{2\epsilon_L^2 T_0 E_0}\frac{1}{\eta}\left(\frac{X}{n}\right)(x - \beta_0 s)\right] \quad , \tag{25}$$

where

$$\chi_0 = \frac{\beta_0}{\epsilon_L \eta} \qquad w_0 = \frac{\epsilon_L \eta}{2}\chi_0^2 - \frac{1}{2\eta\epsilon_L}\left[\frac{Nq^2 R}{2\epsilon_L T_0 E_0}\left(\frac{X}{n}\right)\right]^2 \quad . \tag{26}$$

# 4 Conclusions

In this paper, we have reviewed some results and applications of the *Thermal Wave Model*, showing in particular, how it is possible to give a novel approach to the study of the nonlinear longitudinal dynamics of a relativistic particle bunch in circular accelerating machines. Neglecting radiation damping and quantum excitation, we have shown that the nonlinear interaction between the bunch and the surroundings (potential well and wake fields) is governed by an appropriate NLS equation (equation (11)), fully similar to the one that holds for the propagation of an e.m. bunch in a nonlinear medium in paraxial approximation [11], [12],[13]. Much remains to be done — like, for instance, the extension to 2- or even to 3-D, or the development of an iterable formulation — to make this model really interesting for the study of the typical, still unsolved, beam-dynamics problems. Nevertheless, its very innovative feature of allowing the treatment of the whole beam at the same time, makes it look extremely promising for a new, and more complete approach to the subject.

# References


[1] R. Fedele and G. Miele, Nuovo Cimento D **13**, 1527 (1991).

[2] R. Fedele and P.K. Shukla, Phys.Rev. A **44**, 4045 (1992).

[3] R. Fedele and G. Miele, Phys.Rev. A **46**, 6634 (1992).

[4] R. Fedele, G. Miele, L. Palumbo and V.G. Vaccaro, Phys. Lett. A **179**, 407 (1993).

[5] R. Fedele, G. Miele, and F. Galluccio, INFN/TC-93/12, to be published in Proc. 1993 Particle Accelerator Conference. Washington D.C. May 17-20, 1993.

[6] B.W. Montague, CAS Proc., CERN 77-13, 63 (1977).

[7] L. Palumbo and V.G. Vaccaro, LNF-89/035(P), May 1989.

[8] S. Hansen et al. , CERN/ISR-RF-DI-TH-OP/75-15, March 1975.

[9] S. Solimeno, B. Crossignani, and P. Di Porto *Guiding, Diffraction, and Confinement of Optical Radiation*, (Academy Press, London, 1986).

[10] M. Sands, SLAC Report 121 (1971).

[11] G.B. Whitham, *Linear and Nonlinear Waves*, (J. Wiley, New York, 1974).

[12] Y.R. Shen, *The Principles of Nonlinear Optics*, (Wiley-Interscience Publication, New York, 1984).

[13] S.A. Akhmanov, A.P. Sukhuorukov, and R.V. Khokhlov, Sov.Phys.Usp. **93**, 609 (1968).

[14] A. Hofmann, CAS Proc., CERN 77-13, 139 (1977).

# CAUSALITY PROBLEMS FOR FERMI'S TWO-ATOM SYSTEM

Gerhard C. Hegerfeldt
*Institut für Theoretische Physik*
*University of Göttingen, D37073 Göttingen, Germany*

**Abstract**

Let A and B be two atoms or, more generally, a 'source' and a 'detector' separated by some distance R. At $t = 0$ A is in an excited state, B in its ground state, and no photons are present. A theorem is proved that in contrast to Einstein causality and finite signal velocity the excitation probability of B is nonzero immediately after $t = 0$. Implications are discussed.

To study and check finite signal velocity, Fermi [1] considered two atoms A and B separated by a distance R. At time $t = 0$ atom A is assumed to be in an excited state $|e_A\rangle$ and B in its ground state $|g_B\rangle$, with no photons present. Atom A will decay to its ground state under the emission of a photon which may then be absorbed by atom B. Fermi asked when atom B will notice A and start to move out of its ground state. In accordance with Einstein causality, i.e. no propagation faster than the speed of light, he expected this to occur after a time $t = R/c$. This was indeed what Fermi found by his calculation.

More than thirty years later Shirokov [2] pointed out that Fermi's 'causal' result was the artefact of an approximation. Indeed, Fermi had replaced an integral over positive frequencies by an integral ranging from $-\infty$ to $\infty$. Without this approximation his calculation would not have given the expected result.

Moreover, Fermi had calculated the probability for a transition to A nonexcited, B excited and no photons, i.e. the transition probability from the state $|e_A\rangle|g_B\rangle|0_{ph}\rangle$ to the state $|g_A\rangle|e_B\rangle|0_{ph}\rangle$, which requires measurements on A, B and photons simultaneously. Hence this 'exchange' probability does not refer to finite signal velocity or Einstein causality but to 'local' or 'nonlocal' correlations. What is really needed for finite signal velocity is the probability of finding B excited, irrespective of the state of A and of possible photons.This will be called the excitation probability of B.

Fermi's problem was investigated by many authors in this or in a related form, e.g. by Heitler and Ma [3], Hamilton [4], Fierz [5], Ferretti [6], Milonni and Knight [7], Shirokov [2] and his review [8], Rubin [9], Biswas et al. [10], and Valentini [11]. The older papers confirmed Fermi's conclusion, while the results of the later papers depend on the model and the approximations used. At present there seems to be agreement that Fermi's 'local' result is not correct, but that this nonlocality cannot be used for superluminal signal transmission since measurements on A and B as well as on photons are involved.

Usually previous authors have used 'bare' states and a Hamiltonian of the form

$$H_{\text{bare}} = H_A + H_B + H_F + H_{AF} + H_{BF} \tag{1}$$

where $H_{AF}$ and $H_{BF}$ represent the coupling of atoms A and B to the quantized radiation field. The Hilbert space is simply a tensor product,

$$\mathcal{H}_{\text{bare}} = \mathcal{H}_A \times \mathcal{H}_B \times \mathcal{H}_F \,. \tag{2}$$

The initial state is then

$$|\psi_0{}^{\text{bare}}\rangle = |e_A\rangle|g_B\rangle|0_{ph}\rangle \,. \tag{3}$$

The probability of finding B in some excited state, irrespective of the state of A and photons, is a sum over all excited states $|e_B\rangle$ of B, over all states $|i_A\rangle$ of A and over all photon states $|\{\mathbf{n}\}\rangle$, i.e.

$$\begin{aligned}
&\sum_{e_B}\sum_{i_A}\sum_{\{\mathbf{n}\}} |\langle\{\mathbf{n}\}|\langle e_B|\langle i_A|\psi_t^{\text{bare}}\rangle|^2 \\
&= \langle\psi_t^{\text{bare}}| \{ \sum_{i_A,e_B,\{\mathbf{n}\}} |i_A\rangle|e_B\rangle|\{\mathbf{n}\}\rangle\langle\{\mathbf{n}\}|\langle e_B|\langle i_A|\} \; |\psi_t^{\text{bare}}\rangle \\
&= \langle\psi_t^{\text{bare}}| \; \mathbf{1}_A \times \sum_{e_B} |e_B\rangle\langle e_B| \times \mathbf{1}_F \; |\psi_t^{\text{bare}}\rangle
\end{aligned} \tag{4}$$

where the completeness relation for orthonormal bases has been used. The operator

$$\mathcal{O}_{e_B}^{\text{bare}} \equiv \mathbf{1}_A \times \sum_{e_B} |e_B\rangle\langle e_B| \times \mathbf{1}_F \tag{5}$$

represents the observable "B is in a bare excited state", and it is a projection operator. The expectation value of $\mathcal{O}_{e_B}^{\text{bare}}$ gives the excitation probability of B.

For bare states, however, there is a serious difficulty. Even with atom A absent and no photons present atom B will be immediately excited under simultaneous emission of photons! This well-known unphysical behavior is a consequence of the interaction term $H_{BF}$ because then the bare ground state $|g_B\rangle|0_{ph}\rangle$ is no longer an eigenstate of the bare Hamiltonian. Therefore, all results for bare states have to be considered with caution.

Valentini [11] and also Biswas et al. [10] have found the following interesting result for bare states by using perturbation theory and cutoffs. They calculated that for $t \leq R/c$ the bare ground state of B behaves as if the excited atom A were not present. This result seems to indicate a causal behavior and suggests a similar result for a properly renormalized theory. This, however, will be shown not to be the case.

Fermi's problem of finite signal velocity will now be treated under very plausible assumptions without bare states. Although a renormalized theory has yet to be constructed only two basic properties of such a supposedly existing theory are needed. The first is that the states of such a theory form a Hilbert space, denoted by $\mathcal{H}_{\text{ren}}$. The other property needed is a renormalized selfadjoint Hamiltonian $H_{\text{ren}}$ which is bounded from below, e.g. by 0. The assumption of positive energy is standard and physically well-motivated.

In general $\mathcal{H}_{\text{ren}}$ is no longer a tensor product,

$$\mathcal{H}_{\text{ren}} \neq \mathcal{H}_A \times \mathcal{H}_B \times \mathcal{H}_F, \tag{6}$$

and the initial state, denoted by $|\psi_0\rangle$, will not be a simple product state,

$$|\psi_0\rangle \neq |e_A\rangle\, |g_B\rangle\, |\phi_{\rm ph}\rangle\ .$$

Similarly, if the observable "B is in an excited state" makes sense and is represented by an operator $\mathcal{O}_{e_B}$ then in general $\mathcal{O}_{e_B} \neq \mathcal{O}_{e_B}^{\rm bare}$. However, $\mathcal{O}_{e_B}$ will still be a projection operator since its eigenvalues are 1 for 'yes' and 0 for 'no'. The excitation probability of B at time $t$ is then given by the expectation value

$$\langle \psi_t \mid \mathcal{O}_{e_B} \mid \psi_t \rangle\ .$$

Alternatively one may assume that the excitation probability of B is an expectation value of some positive operator, or one may measure the excitation through a positive observable which vanishes for the ground state, e.g. some operator related to the square of the dipole moment [12]. In all these cases one will run into difficulties with Einstein causality.

No point-like localization of A and B is required. As a generalization of Fermi's set-up A and B may be systems initially localized in two regions separated by a distance R with no (real) photons present. The ground state of B may be degenerate.

We note that measurements of the excitation probability of B involves measurements on B only and that $P_B^e(t=0) = 0$. One would expect, as Fermi, that

$$P_B^e(t) = 0 \ \text{ for } \ 0 \leq t \leq R/c\ . \tag{7}$$

However, in a slightly different context a theorem of the author [13] as well as prior [14] and later results [15, 16, 17, 18] showed difficulties with causality in particle localization [19]. Although the theorem is not applicable here – it applies to free particles or to the center-of-mass of systems – it makes one wary. Indeed, as a complement to this first theorem I will now show a second theorem which includes interactions.

**Theorem.** Let the Hamiltonian be positive or bounded from below and let the initial state at time $t = 0$ be

$$|\psi_0\rangle = \begin{cases} A & \text{in an excited state,} \\ B & \text{in a ground state, no photons.} \end{cases}$$

Let $P_B^e(t)$ be the probability of finding B excited,

$$P_B^e(t) = \langle \psi_t |\, \mathcal{O}_{e_B}\, |\psi_t\rangle \tag{8}$$

where $\mathcal{O}_{e_B}$ is a projection operator or, more generally, a positive operator.

Then either

(i) The excitation probability of B is nonzero for almost all $t$, and the set of such $t$'s is dense and open.

or

(ii) The excitation probability of B is identically zero for all $t$.

*Remarks.* Alternative (i) means that B starts to move out of the ground state immediately and is thus influenced by A instantaneously, in contrast to Einstein causality. Alternative (ii) is clearly unphysical since in this case B is never excited so that B is never influenced by A.

The proof is basically very simple and uses only the positivity of $H_{\rm ren}$, or rather its boundedness from below, and the fact that one deals with the expectation value of a positive selfadjoint operator.

*Proof of theorem.* Since $|\psi_t\rangle$ is continuous in $t$, so is $P^e_B(t)$. Hence, if for some $t_1$ one has $P^e_B(t_1) > 0$ then this also holds in a small interval around $t_1$, and therefore the set is open. Now let us assume that the set of $t$'s with $P^e_B(t) > 0$ is not dense. Then there is a small but finite interval $I$ such that

$$P^e_B(t) \;=\; 0 \quad \text{for} \quad t \in I\,. \tag{9}$$

It will now be shown that this implies that alternative (ii) holds. Eq. (9) can be written as

$$\langle\psi_t|\; \mathcal{O}_{e_B}\; |\psi_t\rangle \;=\; 0 \qquad \text{for} \quad t \in I\,. \tag{10}$$

If $\mathcal{O}_{e_B}$ is a projection operator then $(\mathcal{O}_{e_B})^2 \;=\; \mathcal{O}_{e_B}$. Therefore Eq. (10) can be written as

$$\begin{aligned} \langle\psi_t|\; (\mathcal{O}_{e_B})^2\; |\psi_t\rangle \;&=\; \|\; \mathcal{O}_{e_B}\; |\psi_t\rangle\;\|^2 \\ &=\; 0 \quad \text{for} \;\; t \in I\,. \end{aligned} \tag{11}$$

This means that

$$\mathcal{O}_{e_B}\; |\psi_t\rangle \;=\; 0 \quad \text{for} \quad t \;\in\; I\,. \tag{12}$$

For $\mathcal{O}_{e_B}$ a positive operator the argument is similar [20]. Now let $\phi$ be any fixed vector and define the auxiliary function $F_\phi(t)$ by

$$F_\phi(t) \;=\; \langle\phi|\; \mathcal{O}_{e_B}\; e^{-i\; H_{\rm ren} t/\hbar}|\psi_0\rangle\;. \tag{13}$$

Then, by Eq. (12),

$$F_\phi(t) \;=\; 0 \quad \text{for} \quad t \;\in\; I\,.$$

Since $H_{\rm ren} \geq -$ const, one has that the operator

$$e^{-i\; H_{\rm ren}(t+iy)/\hbar}$$

is well-defined for $y \;\leq\; 0$. Putting $z \;=\; t + iy$ one sees that $F_\phi(z)$ can be defined as a continuous function for $Im\; z \leq 0$, and, moreover, $F_\phi(z)$ is analytic for $Im\; z \;<\; 0$. However, such an analytic function cannot have boundary values vanishing on a real interval unless

$$F_\phi(z) \;\equiv\; 0$$

for $Im\; z \neq 0$ [21]. But then, by continuity, one also has $F_\phi(t) = 0$ for all real $t$. Hence the right side of Eq. (13) vanishes for all $t$. Since $\phi$ was arbitrary one has

$$\mathcal{O}_{e_B}|\psi_t\rangle \;\equiv\; 0 \quad \text{for all} \;\; t$$

and this gives $P^e_B(t) \;\equiv\; 0$, i.e. case (ii).

This proves that $P^e_B(t)$ is either nonzero on a dense open set or that it vanishes identically. In a slightly more sophisticated way it will now be shown directly that $P^e_B(t)$ is either nonzero for almost all $t$ or vanishes identically. Let the set of zeros of $P^e_B(t)$ be denoted by $\mathcal{N}_0$. The

same argument as before shows that $F_\phi(t)$ vanishes there too. As a boundary value of a bounded analytic function $F_\phi(t)$ satisfies, unless it vanishes identically, the inequality [22]

$$\int_{-\infty}^{\infty} dt \log |F_\phi(t)|/(1+t^2) \; > \; -\infty \; .$$

If $\mathcal{N}_0$ had positive measure the integral would be $-\infty$ and thus $F_\phi(t)$ would vanish identically in $t$, for each $\phi$. This would again imply case (ii). Hence if case (ii) does not hold $P_B^e(t)$ can only vanish on a null set [23]. This completes the proof of the theorem.

A typical behavior of the excitation probability of B according to (i) is shown in Fig. 3. No estimate of the actual magnitude of $P_B^e(t)$ is provided by the above argument, except that is nonzero for almost all $t$. It follows trivially for alternative (i) that the set of zeros of $P_B^e(t)$ is not only of measure 0 but also nowhere dense.

It should be noted that the above proof makes no use of any spatial separation of the two subsystems nor of its photon content. In fact, the theorem is a mathematically rigorous result which holds for any initial state $|\psi_0\rangle$, any positive Hamiltonian and expectation value of any positive operator [24]. Physics comes in only when one thinks of $|\psi_0\rangle$ as representing two spatially separated subsystems with no photons. Of course, if the systems are not spatially separated part (i) of the theorem comes as no surprise.

*Extensions.* The derivation does not need that A and B are atoms. The result clearly extends to more general situations:

a) Larger systems: A may be some "source" of photons and B a "detector".

b) A and B may move.

c) Other particles and other interactions may be included.

Other positive observables can be considered. E.g., for an excited localized atom (or system) with no real photons initially one obtains an acausal result for photons and electromagnetic energy in regions not containing the atom. This is in contrast to a result by Kikuchi [25] who, at the suggestion of Heisenberg, had studied this problem using the same approximation as Fermi [1]. The general case of a decaying particle or system can also be treated by the above approach.

*Discussion.* If the effect implied by the theorem were real it could in principle be used for superluminal signals, with all the well-known consequences. However, the result may also be viewed as a difficulty for the formulation of the underlying theory. The theorem is of the 'if-then' type. To avoid its physical consequences one has to check whether its conditions or any additional physical assumptions are fulfilled in a given situation. There are several possible ways out.

a) Systems localized in disjoint regions might not exist as a matter of principle, so that strictly speaking they always 'overlap'. Then an immediate excitation may evidently occur.

b) Renormalization will introduce a sort of photon cloud around each system. This essentially implies an overlap of the systems, leading back to case a).

c) The notion of 'ground state of B' in the presence of A may not make sense. Without A present one will expect a lowest energy state to exist for the system B plus radiation field, with no real photons. However, with A present, the lowest state of the complete system may change. Thus the 'ground state of B' may not be preparable independently of A. Effectively this also leads back to case a).

These possible ways out suggest implicitly that the problem is not well-posed, i.e. an experimental set-up to check the theorem might not be feasible. But without disjointly localizable sources and detectors how to check finite signal velocity at all?

One may argue that any violation of Einstein causality would be so rare or so small as to be unobservable in practice. But then a good theory should contain this from the beginning. Should quantum mechanics with its Hilbert space structure and its idealized measurements at sharp times therefore be modified? The above result is based on the use of Hilbert space and a selfadjoint time-development operator. This might not be appropriate any longer for systems with infinitely many degrees of freedom.

*Conclusion.* Fermi's original question on finite signal velocity has been generalized and analyzed in a model-independent way, without the use of any 'bare' theory or any approximations. Only positivity of the energy has been used. It has been shown that this leads to violation of Einstein causality if one assumes that two subsystems, 'source' and 'detector', can be localized in disjoint regions at some initial time. The view has been taken that this difficulty is of a theoretical nature, and possible ways out have been discussed.

# References


[1] E. Fermi, Rev. Mod. Phys. **4**, 87 (1932)

[2] M.I. Shirokov, Yad. Fiz. **4**, 1077 (1966). [Sov. J. Nucl. Phys. **4**, 774 (1967)]

[3] W. Heitler and S.T. Ma, Proc. R. Ir. Acad. **52**, 123 (1949)

[4] J. Hamilton, Proc. Phys. Soc. A **62**, 12 (1949)

[5] M. Fierz, Helv. Phys. Acta **23**, 731 (1950)

[6] B. Ferretti, in: *Old and New Problems in Elementary Particles*, edited by G. Puppi (Academic Press, New York, 1968), p. 108

[7] P.W. Milonni and P.L. Knight, Phys. Rev. A **10**, 1096 (1974)

[8] M.I. Shirokov, Sov. Phys. Usp. **21**, 345 (1978)

[9] M.H. Rubin, Phys. Rev. D **35**, 3836 (1987)

[10] A.K. Biswas, G. Compagno, G.M. Palma, R. Passante, and R. Persico, Phys. Rev. A **42**, 4291 (1990)

[11] A. Valentini, Phys. Lett. A **153**, 321 (1991)

[12] An operator is called positive if all its expectation values are nonnegative. It is then automatically selfadjoint and bounded if defined everywhere. For the expectation values to give probabilites the operator has to be bounded by 1, but this will not be used in the following.

[13] G.C. Hegerfeldt, Phys. Rev. D **10**, 3320 (1974)

[14] A.S. Wightman and S.S. Schweber, Phys. Rev. **98**, 812 (1955); B. Gerlach, D. Gromes and J. Petzold, Z.Phys. **221**, 141 (1969)

[15] B. Skagerstam, Int. J. Theor. Phys. **15**, 213 (1976); J.F. Perez and I.F. Wilde, Phys. Rev. D **16**, 315 (1977)

[16] G.C. Hegerfeldt and S.N.M. Ruijsenaars, Phys. Rev. D **22**, 377 (1980)

[17] G.C. Hegerfeldt, Phys. Rev. Lett. **54**, 2395 (1985); Nucl. Phys. B **6**, 231 (1989)

[18] B. Rosenstein and M. Usher, Phys. Rev. D **36**, 2595 (1987)

[19] Sometimes it is argued more directly that only the noncausally propagating positive-frequency field components are actually measured, as in the photon counting probabilities of Glauber. This argument is, however, not quite conclusive since positive-frequency components are a free-field concept and since, moreover, these counting probabilities hold only in an approximate way; cf. J.R. Klauder and E.C.G. Sudarshan, *Fundamentals of Quantum Optics* (Benjamin, New York, 1968).

[20] The positive root of a positive selfadjoint operator is uniquely defined and selfadjoint. Eq. (11) is then replaced by

$$\|(\mathcal{O}_{e_B})^{1/2}|\psi_0\rangle\|^2 \;=\; 0$$

which in turn implies Eq. (12).

[21] To see this directly one defines an extension of $F_\phi$ to the upper half plane by $F_\phi(z) = F_\phi(z^*)^*$, for $Im\ z > 0$. Since $F_\phi(t)$ is real for $t \in I$ it follows that the extension is continuous on $I$, and from this one can show that it is analytic for $z \notin I\!R \backslash I$. Hence $I$ is contained in the analyticity domain, and since $F_\phi(z) = 0$ for $z \in I$ it vanishes identically. This is a special case of the Schwarz reflexion principle, cf. e.g. N. Levinson, and R.M. Redheffer, *Complex Variables* (Holden-Day, San Francisco, 1970)

[22] G. Barnet, *Bounded Analytic Functions* (Academic, New York, 1981), p. 64

[23] $\mathcal{N}_0$ being a null set this implies also that its complement, the set of $t$'s with $P^e_B(t)$ positive, is dense. However, the proof of this fact given before is more transparent and has therefore been included.

[24] A frequently used model in quantum optics uses an electric dipole interaction, the rotating-wave approximation and cutoffs. Then the Hamiltonian is bounded from below, and thus the theorem applies. Hence without any further calculations one knows that in this model there is a violation of Einstein causality.

[25] S. Kikuchi, Z. Phys. **66**, 558 (1930)

# PSEUDOMASTER EQUATION FOR THE NO-COUNT PROCESS IN A CONTINUOUS PHOTODETECTION*

Ching Tsung Lee

Department of Physics, Alabama A & M University, Normal, Alabama 35762

The detection of cavity radiation with the detector placed outside the cavity is studied. Each leaked photon has a certain probability of propagating away without being detected. It is viewed as a continuous quantum measurement in which the density matrix is continuously revised according to the readout of the detector. The concept of pseudomaster equation for the no-count process is introduced; its solution leads to the discovery of the superoperator for the same process. It has the potential to become the key equation for continuous measurement process.

Quantum theory of measurement has been a highly controversial topic ever since the pioneer work of von Neumann. The process discussed in this original work is now classified as the first-kind (nondestructive) measurement, which is described by an instantaneous projection with projection operators as its principal mathematical tools. On the other hand, photodetection is a second-kind (destructive) measurement. To deal with photodetection the concept of quantum measurement must be extended to include continuous measurement process in which the quantum state of the subject system must be continuously revised to reflect our most up-to-date knowledge about the system resulting from the ongoing measurement process. Superoperators have been the principal mathematical tools for such study. It is the purpose of this paper to introduce a simple equation which has the potential to become the basic equation to describe the continuous measurement process.

There have been two different approaches to the theory of photoelectric detection. The first approach was initiated by Mandel [1] and followed by Kelley and Kleiner [2] and by Glauber [3]. The second approach was initiated by Mollow [4] and followed by Scully and Lamb [5], by She pherd [6], and by Srinivas and Davies [7]. In the first approach, light propagates in the open space, it encounters the photodetector, and any unabsorbed photons propagate away. In the second approach, both the radiation and the photodetector are enclosed in a cavity, and any photons not absorbed by the detector at one time are available for detection at later times. For obvious reason these two different approaches are classified by Mandel [8] as *open-system model* for the former and *closed-system model* for the latter.

The formula for the photoelectron distribution obtained in the open-system model was criticized by Srinivas and Davies [7] as being a short-time approximation only, it may lead to unphysical and meaningless results when time is large. In his response, Mandel [8] pointed out that, for the open-system model, it should be understood that the normalization volume must be large enough to satisfy the condition $L \gg ct$ at all times. He also pointed out that the circumstances modelled by the closed system are much less commonly encountered in practice.

In this paper we introduce a new model that is the hybrid of the two previous approaches. The radiation source is kept inside a cavity but the photodetector is taken outside of the cavity to detect only those photons leaked out of one end of the cavity, and any unabsorbed photons propagate away. We believe that this hybrid model not only keeps the merits of both previous models but also is a closer simulation of the circumstances more frequently encountered in practice. For example, if we want to study the statistical properties of photons in the output of a laser system, this hybrid model will describe the situation most closely.

In 1981 Srinivas and Davies [7] first considered the closed-system photodetection as a continuous quantum measurement. The information provided by the readout of the detector is used to adjust the density matrix continuously so that it always represents our most current knowledge about the cavity radiation. The counting process consists of *no-count* and *one-count* processes, the former lasts a finite duration while the latter occurs instantaneously. The effects of the two processes on the density matrix can be represented by two *superoperators* postulated to be as follows: (i) The one-count process is described by the superoperator $\mathcal{J}$ such that

$$\hat{\rho}(t^+) = \mathcal{J}\hat{\rho}(t) \equiv \frac{\hat{a}\hat{\rho}(t)\hat{a}^\dagger}{\mathrm{Tr}[\hat{\rho}(t)\hat{a}^\dagger\hat{a}]}. \tag{1}$$

where $\hat{\rho}(t)$ and $\hat{\rho}(t^+)$ are the density matrix for the radiation field immediately before and after the detection of a photoelectron while $\hat{a}$ and $\hat{a}^\dagger$ are the annihilation and creation operators, respectively, of a photon. (ii) The no-count process lasting for a duration $\tau$ is described by the superoperator $\mathcal{S}_\tau$ such that

$$\hat{\rho}(t+\tau) = \mathcal{S}_\tau\hat{\rho}(t) \equiv \frac{\exp\left(-\frac{\lambda}{2}\hat{a}^\dagger\hat{a}\tau\right)\hat{\rho}(t)\exp\left(-\frac{\lambda}{2}\hat{a}^\dagger\hat{a}\tau\right)}{\mathrm{Tr}\left[\hat{\rho}(t)\exp\left(-\lambda\hat{a}^\dagger\hat{a}\tau\right)\right]}, \tag{2}$$

where $\lambda$ is the coupling constant. It is obvious from Eqs. (1) and (2) that the evolution of the quantum state for the cavity radiation under continuous photon counting is nonunitary. These two postulates were verified very recently by Imoto *et al.* [9] by using some specific microscopic model. The system consists of a cavity radiation and a stream of two-level atoms described by the well-known Jaynes-Cumming Hamiltonian. More detailed theory has been further developed by Ueda *et al.* [10].

These two superoperators are valid for the closed-system model. To find the corresponding superoperators for the hybrid model is the initial motivation of the present study. We have discovered a general method to solve this type of problems, and we shall call it the method of *pseudomaster equation.*

For simplicity, we assume that the radiation inside the cavity is kept inactive except for possible leakage through one side of the cavity due to the less than perfect reflectivity of the mirror. Let $\mu$ be the rate of photon leakage or the inverse of the decay time. It can be expressed in terms of the speed of light $c$, the reflectivity of one end mirror $R$ and the distance between the two end mirrors $d$ as [11]

$$\mu = -c\ln R/2d. \tag{3}$$

Let $p(n,t)$ be the probability that $n$ photons remain inside the cavity at time $t$. Except for the difference in the physical meaning of the constant, the master equation for $p(n,t)$ in the hybrid model is exactly the same as the one first derived by Scully and Lamb [5] for the closed-system model, *i.e.*,

$$\frac{d}{dt}p(n,t) = -n\mu p(n,t) + (n+1)\mu p(n+1,t), \tag{4}$$

which describes the so-called *non-referring measurement process*, namely, the "free" evolution of the photon-number distribution without detection or without any adjustment of the quantum state according to the readout of the detector.

Assuming each leaked photon has the probability $\zeta$ of being detected, then we believe the no-count process can be described by the following difference-differential equation

$$\frac{d}{dt}q(n,t) = -n\mu q(n,t) + (n+1)\mu(1-\zeta)q(n+1,t), \tag{5}$$

where $(1-\zeta)$ is the probability that a leaked photon propagates away without been detected. Equation (5) is a modification of Eq. (4). One important characteristic of Eq. (5) is that it does not conserve the total probability. Because of this characteristic we call it pseudomaster equation. The physical meaning of $q(n,t)$ will become clear in later development.

By the way, the pseudomaster equation for the closed-system model is

$$\frac{d}{dt}q(n,t) = -\lambda n q(n,t), \tag{6}$$

which is quite trivial; so we shall focus our attention on Eq. (5) for the hybrid model.

The solution to Eq. (5) can be easily obtained through Laplace transformation. Let the no-count period begin at $t = t_1$ and let us make the identification

$$q(n,t_1) = p(n,t_1) \tag{7}$$

as the initial condition, then the solution to Eq. (5) at a later time $t = t_2$ can be written as

$$q(n,t_2) = \sum_{\ell=n}^{\infty} p(\ell,t_1)\binom{\ell}{n}\left\{(1-\zeta)\left[1-e^{-\mu(t_2-t_1)}\right]\right\}^{\ell-n} e^{-n\mu(t_2-t_1)}. \tag{8}$$

The first physical meaning of $q(n,t)$ is that it is the unnormalized form of $p(n,t)$ in no-count process, namely,

$$p(n,t) = q(n,t) \Big/ \sum_{n=0}^{\infty} q(n,t). \tag{9}$$

Let $P_m(t_1,t_2)$ be the probability that $m$ photoelectrons are detected during the period $(t_1,t_2)$. We are particularly interested in the special case $m=0$. We can obtain from Eq. (8) the probability that no photoelectron is detected during the period $(t_1,t_2)$ as

$$P_0(t_1,t_2) = \sum_{n=0}^{\infty} q(n,t_2) = \sum_{\ell=0}^{\infty} p(\ell,t_1)\left[1-\zeta+\zeta e^{-\mu(t_2-t_1)}\right]^{\ell}. \tag{10}$$

This is the second physical meaning of $q(n,t)$.

To be consistent, the no-count probability must satisfy the condition

$$P_0(t_1,t_2)P_0(t_2,t_3) = P_0(t_1,t_3). \tag{11}$$

Using Eqs. (8) and (10) in Eq. (9) we obtain

$$p(n,t_2) = \frac{1}{P_0(t_1,t_2)} \sum_{\ell=n}^{\infty} p(\ell,t_1)\binom{\ell}{n}\left[(1-\zeta)\left(1-e^{-\mu(t_2-t_1)}\right)\right]^{\ell-n} e^{-n\mu(t_2-t_1)}. \tag{12}$$

Replacing $t_1$ and $t_2$ in Eq. (10) by $t_2$ and $t_3$, respectively, and using Eq. (12), we obtain

$$\begin{aligned} P_0(t_2,t_3) &= \sum_{\ell=0}^{\infty} p(\ell,t_2)\left[1-\zeta+\zeta e^{-\mu(t_3-t_2)}\right]^{\ell} \\ &= \frac{1}{P_0(t_1,t_2)} \sum_{\ell=0}^{\infty} p(\ell,t_1)\left[1-\zeta+\zeta e^{-\mu(t_3-t_1)}\right]^{\ell} = \frac{P_0(t_1,t_3)}{P_0(t_1,t_2)}; \end{aligned} \tag{13}$$

so the condition of Eq. (11) is satisfied.

There are two kinds of waiting times, conditional and unconditional. We pick an arbitrary instant and ask: "How long do we have to wait until we detect a photoelectron?" This is the unconditional waiting time. If the waiting begins immediately after the detection of a photoelectron, then it is called conditional waiting time. From the expression for $P_0(t_1,t_2)$ we can also derive the unnormalized distributions for the two different waiting times according to [12]

$$W(t_1,t_2) = -\frac{\partial}{\partial t_2}P_0(t_1,t_2) = \mu\zeta e^{-\mu(t_2-t_1)}\sum_{n=1}^{\infty}p(n,t_1)n\Big[1-\zeta+\zeta e^{-\mu(t_2-t_1)}\Big]^{n-1} \tag{14}$$

and

$$\begin{aligned} V(t_1,t_2) &= -\frac{1}{\langle n\rangle_{t_1}}\frac{\partial^2}{\partial t_1\partial t_2}P_0(t_1,t_2) \\ &= \frac{\mu\zeta}{\langle n\rangle_{t_1}}e^{-\mu(t_2-t_1)}\sum_{n=2}^{\infty}p(n,t_1)n(n-1)\Big[1-\zeta+\zeta e^{-\mu(t_2-t_1)}\Big]^{n-2}, \end{aligned} \tag{15}$$

where $\langle n\rangle_t$ is the average number of photons remaining at time $t$.

The difference between unconditional and condition waiting times is that the latter begins immediately after the detection of a photons. Therefore we can see the effect on the quantum state of the radiation due to the detection of a photon by comparing Eqs. (14) and (15). If we replace $p(n,t_1)$ in Eq. (14) by

$$p(n,t_1^+) = \frac{n+1}{\langle n\rangle_{t_1}}p(n+1,t_1), \tag{16}$$

we obtain Eq. (15). On the other hand, if we try to use Eq. (1), we also have

$$p(n,t_1^+) = \langle n|\hat{\rho}(t_1^+)|n\rangle = \frac{\langle n|\hat{a}\hat{\rho}(t_1)\hat{a}^\dagger|n\rangle}{\langle n\rangle_{t_1}} = \frac{n+1}{\langle n\rangle_{t_1}}p(n+1,t_1), \tag{17}$$

which is identical to Eq. (16). So we conclude that the effect on the quantum state due to the one-count process in the hybrid model is the same as that in the closed-system model, and the superoperator for the one-count process in hybrid model remains the same as given in Eq. (1).

We now try to find the superoperator for the no-count process. Equation (12) provides the clue for this search. It turns out to be quite sophisticated because it involves the exponential of a superoperator. First let us define a superoperator $\mathcal{R}(\tau,\mu,\zeta)$ such that

$$\mathcal{R}(\tau,\mu,\zeta)\hat{\rho}(t) \equiv (1-\zeta)\big(1-e^{-\mu\tau}\big)\hat{a}\hat{\rho}(t)\hat{a}^\dagger. \tag{18}$$

Then we can define the exponential of this superoperator as

$$\exp\left[\mathcal{R}(\tau,\mu,\zeta)\right]\hat{\rho}(t) \equiv \sum_{\ell=0}^{\infty}\frac{\mathcal{R}^\ell(\tau,\mu,\zeta)}{\ell!}\hat{\rho}(t) = \sum_{\ell=0}^{\infty}\frac{1}{\ell!}\left[(1-\zeta)\big(1-e^{-\mu\tau}\big)\right]^\ell(\hat{a})^\ell\hat{\rho}(t)\Big(\hat{a}^\dagger\Big)^\ell, \tag{19}$$

which must be applied to both sides of the operand in lock step and cannot be split up into two separate parts, with one being the Hermitian conjugate of the other. Let us define another superoperator $\mathcal{S}(\tau,\mu)$ such that

$$\mathcal{S}(\tau,\mu)\hat{\rho}(t) \equiv \exp\Big(-\frac{\mu}{2}\hat{a}^\dagger\hat{a}\tau\Big)\hat{\rho}(t)\exp\Big(-\frac{\mu}{2}\hat{a}^\dagger\hat{a}\tau\Big), \tag{20}$$

which is slightly different from that defined in Eq. (2) in the physical meaning of the constant $\mu$ and in that it does not include the renormalization. We are now ready to present the superoperator $\mathcal{Q}(\tau,\zeta)$ for the no-count process such that

$$\mathcal{Q}(\tau,\mu,\zeta)\hat{\rho}(t) \equiv \mathcal{S}(\tau,\mu)\exp\left[\mathcal{R}(\tau,\mu,\zeta)\right]\hat{\rho}(t). \tag{21}$$

Then the density operator at the end of the no-count process can be written as

$$\hat{\rho}(n,t+\tau) = \mathcal{Q}_{\mathcal{N}}(\tau,\mu,\zeta)\hat{\rho}(t) \equiv \frac{\mathcal{Q}(\tau,\mu,\zeta)\hat{\rho}(t)}{\mathrm{Tr}\{\mathcal{Q}(\tau,\mu,\zeta)\hat{\rho}(t)\}}, \tag{22}$$

where the difference between the two superoperators $\mathcal{Q}(\tau,\mu,\zeta)$ and $\mathcal{Q}_{\mathcal{N}}(\tau,\mu,\zeta)$ is that the later includes the renormalization.

It should be pointed out that this superoperator must satisfy the following conditions:

$$q(n,t+\tau) = \langle n|\mathcal{Q}(\tau,\mu,\zeta)\hat{\rho}(t)|n\rangle, \tag{23}$$

$$P_0(t,t+\tau) = \mathrm{Tr}\{\mathcal{Q}(\tau,\mu,\zeta)\hat{\rho}(t)\}, \tag{24}$$

and

$$\mathcal{Q}(\tau_1+\tau_2,\mu,\zeta) = \mathcal{Q}(\tau_2,\mu,\zeta)\mathcal{Q}(\tau_1,\mu,\zeta). \tag{25}$$

The last semigroup condition is very critical because we have found at least two less sophisticated expressions for $\mathcal{Q}(\tau,\mu,\zeta)$, which satisfy the first two conditions, but must be abandoned because they do not satisfy the last condition. It can be easily verify that the expression given in Eq. (21) satisfy the first two condition. That it also satisfies the last condition can be shown as follows:

$$\begin{aligned}
&\mathcal{Q}(\tau_2,\mu,\zeta)\mathcal{Q}(\tau_1,\mu,\zeta)\hat{\rho}(t) \\
&\quad= \sum_{k=0}^{\infty}\sum_{\ell=0}^{\infty}\frac{(1-\zeta)^{k+\ell}}{k!\ell!}\left(1-e^{-\mu\tau_2}\right)^k\left(1-e^{-\mu\tau_1}\right)^\ell e^{-\mu\hat{a}^\dagger\hat{a}\tau_2/2}(\hat{a})^k e^{-\mu\hat{a}^\dagger\hat{a}\tau_1/2}(\hat{a})^\ell \\
&\qquad\qquad \times\hat{\rho}(t)\left(\hat{a}^\dagger\right)^\ell e^{-\mu\hat{a}^\dagger\hat{a}\tau_1/2}\left(\hat{a}^\dagger\right)^k e^{-\mu\hat{a}^\dagger\hat{a}\tau_2/2} \\
&\quad= \sum_{k=0}^{\infty}\frac{(1-\zeta)^k}{k!}\left[1-e^{-\mu(\tau_1+\tau_2)}\right]^k e^{-\mu\hat{a}^\dagger\hat{a}(\tau_1+\tau_2)/2}(\hat{a})^k\hat{\rho}(t)\left(\hat{a}^\dagger\right)^k e^{-\mu\hat{a}^\dagger\hat{a}(\tau_1+\tau_2)/2} \\
&\quad= \mathcal{Q}(\tau_1+\tau_2,\mu,\zeta)\hat{\rho}(t),
\end{aligned} \tag{26}$$

where we used the operator identity [13] $e^{x\hat{a}^\dagger\hat{a}}f(\hat{a},\hat{a}^\dagger)e^{-x\hat{a}^\dagger\hat{a}} = f\left(\hat{a}e^{-x},\hat{a}^\dagger e^{x}\right)$ to change the orders of some operators and used the summation identity $\sum_{k=0}^{\infty}\sum_{\ell=0}^{\infty}A(k,\ell) = \sum_{k=0}^{\infty}\sum_{\ell=0}^{k}A(k-\ell,\ell)$ to carry out one summation.

For a perfect detector with $\zeta = 1$, we have $\mathcal{Q}_{\mathcal{N}}(\tau,\lambda,1) = \mathcal{S}_\tau$ as given in Eq. (2) for the closed-system model. This means the present model with perfect detector is identical to the closed-system model as far as mathematics is concerned. On the other hand, when $\zeta = 0$ we obtain the superoperator for the non-referring measurement process, which always preserves the total probability, *i.e.*, $\mathrm{Tr}[\mathcal{Q}(\tau,\mu,0)\hat{\rho}(t)] = 1$; so no renormalization is necessary.

We can also consider a more general "closed-system" model with the detector inside the cavity but the cavity has some leakage. The pseudomaster equation for the no-count process of such a system can be written as

$$\frac{d}{dt}q(n,t) = -n(\lambda+\mu)q(n,t) + (n+1)\mu q(n+1,t), \tag{27}$$

where $\lambda$ is the coupling constant between the radiation field and the cavity and $\mu$ denotes the rate of photon leakage. Except for a slight change of constants, the calculations of this generalized closed-system model are almost exactly the same as the hybrid model. We just list the most significant results as follows:

$$q(n,t_2)=\sum_{\ell=n}^{\infty}p(\ell,t_1)\binom{\ell}{n}\left\{\frac{\mu}{\lambda+\mu}\left[1-e^{-(\lambda+\mu)(t_2-t_1)}\right]\right\}^{\ell-n}e^{-n(\lambda+\mu)(t_2-t_1)}, \tag{28}$$

$$P_0(t_1,t_2)=\sum_{\ell=0}^{\infty}p(\ell,t_1)\left[\frac{\mu}{\lambda+\mu}+\frac{\lambda}{\lambda+\mu}e^{-(\lambda+\mu)(t_2-t_1)}\right]^{\ell}, \tag{29}$$

and

$$\mathcal{Q}(\tau,\lambda,\mu)=\mathcal{S}(\tau,\lambda+\mu)\exp\left[\mathcal{R}(\tau,\lambda+\mu,\lambda/(\lambda+\mu))\right]. \tag{30}$$

In conclusion, we have introduced a hybrid model for photodetection which is the mixture of the previous open-system and closed-system models. It is without the defects of the former and more realistic than the latter. We have also introduced the concept of pseudomaster equation, the solution of which provides the clue to discovering the superoperator for the no-count process. It is obvious that, comparing with the superoperator approach, the method of pseudomaster equation is simpler, easier to see how to write it down and easier to handle. So we believe it has the potential to become the fundamental equation for analyzing various models of photodetections as continuous quantum measurement process.

---

*This work was supported by the U. S. Navy, Office of Naval Research, under Grant #N00014-89-J-1050.

[1] L. Mandel, Proc. Roy. Soc. London **72**, 1037 (1958); *ibid.* **74**, 233 (1959).
[2] P. C. Kelley and W. H. Kleiner, Phys. Rev. **A136**, 316 (1964).
[3] R. J. Glauber, in: *Quantum Optics and Electronics*, ed. by C. deWitt, A. Blandin, and C. Cohen-Tannoudji, Gordon and Breach, New York, 1965, p. 63.
[4] B. R. Mollow, Phys. Rev. **168**, 1896 (1968).
[5] M. O. Scully and W. E. Lamb, Phys. Rev. **179**, 368 (1969).
[6] T. J. Shepherd, Optica Acta **28**, 567 (1981); *ibid.* **31**, 1399 (1984).
[7] M. D. Srinivas and E. B. Davies, Optica Acta **28**, 981 (1981); *ibid.* **29**, 235 (1982).
[8] L. Mandel, Optica Acta **28**, 1447 (1981).
[9] N. Imoto, M. Ueda and T. Ogawa, Phys. Rev. A **41**, 4127 (1990).
[10] M. Ueda, Quantum Optics **1**, 131 (1981); Phys. Rev. A **41**, 3891 (1990); M. Ueda, N. Imoto and T. Ogawa, *ibid.* **41**, 3891 (1990).
[11] For a rigorous derivation of this expression see, for example, C. T. Lee, Opt. Communi. **27**, 277 (1978). The expression for the decay time is given in Eq. (33) as $\tau=-2\ell/c\ln R$, but it should be pointed out that this formula is for leakage through both ends and the separation between the two ends is $2\ell$.
[12] C. T. Lee, Phys. Rev. A **46**, 6100 (1992).
[13] See, for example, W. H. Louisell, *Quantum Statistical Properties of Radiation*, John Wiley & Sons, New York, 1973, p. 154.

# SQUEEZED STATES AND GRAVITON-ENTROPY PRODUCTION IN THE EARLY UNIVERSE

Massimo Giovannini
*Dipartimento di Fisica Teorica , Universita' di Torino*
*and INFN, Sezione di Torino, Turin, Italy*

**Abstract**

Squeezed states are a very useful framework for the quantum treatment of tensor perturbations (i.e. gravitons production) in the early universe. In particular, the non equilibrium entropy growth in a cosmological process of pair production is completely determined by the associated squeezing parameter and is insensitive to the number of particles in the initial state. The total produced entropy may represent a significant fraction of the entropy stored today in the cosmic blackbody radiation, provided pair production originates from a change in the background metric at a curvature scale of the Planck order. Within the formalism of squeezed thermal states it is also possible to discuss the stimulated emission of gravitons from an initial thermal bath,under the action of the cosmic gravitational background field. We find that at low energy the graviton production is enhanced, if compared with spontaneous creation from the vacuum; as a consequence , the inflation scale must be lowered, in order not to exceed the observed CMB quadrupole anisotropy. This effect is important, in particular, for models based on a symmetry-breaking transition which require, as initial condition, a state of thermal equilibrium at temperatures higher than the inflation scale and in which inflation has a minimal duration.

## 1 Introduction

In order to discuss the graviton production induced by a cosmological background transition, the starting point is the linearized wave equation for a tensor perturbation. For the sake of generality we will take into account also the variation of Newton constant [1], which corresponds, in a string cosmological scenario [2], to a time-dependence of the Fradkin-Tseytlin dilaton field $\phi(t)$. The linearized wave equation is then, in the Brans-Dicke (Stringy) frame [1]

$$\Box h_i^j - \dot{\phi}\dot{h}_i^j = 0 \tag{1}$$

where $h_i^j$ is the graviton field describing a tensor perturbation on a given curved background, represented by a homogeneous diagonal metric in which $d$ dimensions expand with the scale factor $a(t)$ and $n$ dimension contract with the scale factor $b(t)$:

$$g_{\mu\nu} \equiv diag\left(1, -a^2(t)\gamma_{ij}(x), -b^2(t)\gamma_{ab}(y)\right) \tag{2}$$

(conventions: $\mu, \nu = 1, ..., D = d + n + 1$; i,j=1,...,d; a,b=1,...,n; t is the cosmic time coordinate, ad $\gamma_{ij}$, $\gamma_{ab}$ are the metric tensors of two maximally symmetric euclidean manifolds, parametrized respectively by "internal" and "external" coordinates $x^i$ and $y^a$).

In terms of the conformal time coordinate $\eta$, defined by $dt/d\eta = a$, equation (1) becomes [1]

$$\psi_i^{j\prime\prime} + \left(k^2 - V(\eta)\right)\psi_i^j = 0 \tag{3}$$

where $\psi_i^j = h_i^j a^{\frac{d-1}{2}} b^{\frac{n}{2}} e^{-\frac{\phi}{2}}$ and V is

$$V(\eta) = \frac{(d-1)}{2}\frac{a''}{a} + \frac{n}{2}\frac{b''}{b} + \frac{1}{4}(d-1)(d-3)\left(\frac{a'}{a}\right)^2 + \frac{1}{4}n(n-2)\left(\frac{b'}{b}\right)^2 +$$

$$+ \frac{1}{4}\phi'^2 + \frac{1}{2}n(d-1)\frac{a'b'}{ab} - \frac{1}{2}(d-1)\frac{a'}{a}\phi' - \frac{n}{2}\frac{b'}{b}\phi' \tag{4}$$

This effective potential takes into account the contribution of the expanding dimensions ($a' \neq 0$), of the contacting dimensions ($b' \neq 0$) and of the possible variation in time of the gravitational coupling constant($\phi' \neq 0$). In the case of four expanding dimensions (without dilaton field and without contracting dimensions) we recover the standard result, a minimally coupled scalar field equation.

The quantum description of the amplification of scalar or tensor fluctuations, as discussed here (for other references see e.g. [11]), is based on the separation of the field into background solution and first order perturbations, and on the expansion of the solution to the perturbed wave equation into $|\ in\rangle$ and $|\ out\rangle$ modes. The complex coefficients of this expansion are interpreted in second quantization formalism as annihilation and creation operators for a particle $(b, b^\dagger)$ and the corresponding antiparticle $(\tilde{b}, \tilde{b}^\dagger)$. The relation between $|\ in\rangle$ and $|\ out\rangle$ mode solution can thus be expressed for each mode k as a Bogoliubov transformation between the $|\ in\rangle$ operators $(b, b^\dagger, \tilde{b}, \tilde{b}^\dagger)$ and the out ones $(a, a^\dagger, \tilde{a}^\dagger, \tilde{a})$ [3]

$$a_k = c_+(k)b_k + c_-^*(k)\tilde{b}_{-k}^\dagger \quad , \quad \tilde{a}_{-k}^\dagger = c_-(k)b_k + c_+^*(k)\tilde{b}_{-k}^\dagger \tag{5}$$

where $|c_+|^2 - |c_-|^2 = 1$. As noted by Grishchuk and Sidorov [3], by parametrizing the Bogoliubov coefficients $c_\pm$ in terms of the two real numbers $r \geq 0$ and $\theta$,

$$c_+(k) = \cosh r(k) \quad , \quad c_-^*(k) = e^{2i\theta_k}\sinh r(k) \tag{6}$$

the relations (1) can be re-written as unitary transformations generated by the (momentum-conserving) two-mode squeezing operator $\Sigma_k$,

$$\Sigma_k = \exp(z_k^* b_k \tilde{b}_{-k} - z_k b_k^\dagger \tilde{b}_{-k}^\dagger) \quad , \quad z_k = r(k)e^{2i\theta_k} \tag{7}$$

($r$ is the so-called squeezing parameter) as

$$a_k = \Sigma_k b_k \Sigma_k^\dagger \tag{8}$$

(and related expressions for $\tilde{a}^\dagger, \tilde{a}, \tilde{a}$)

The mean number of produced gravitons is then, according to equation (8)

$$\overline{N}_k = \langle 0|a_k^\dagger a_k|0\rangle = |c_-(k)|^2 = \sinh^2 r_k \tag{9}$$

From equation (5) is possible to compute the spectral energy density

$$\rho(\omega) = \omega(\frac{d\rho_g}{d\omega}) \simeq \omega^4 \overline{N}(\omega), \tag{10}$$

$\omega$ is the proper frequency related to the comoving one $k$ by $\omega = k/a(t)$ where a(t) is the scale of the expanding background metric.

We then insert the known expression of $c_-(\omega)$ in eq.(9) and measure $\rho(\omega)$, as usual, in units of critical energy density $\rho_c$, defining $\Omega(\omega) = \rho(\omega)/\rho_c$. We have, in four dimensions ($D = 4$) expanding with scale factor $a(\eta) \simeq \eta^{-\alpha}$ in conformal time [4]

$$\Omega(\omega, t_0) \simeq G{H_1}^2 \Omega_\gamma(t_0)(\frac{\omega}{\omega_1})^{2-2\alpha} \quad , \quad \omega_2 < \omega < \omega_1 \tag{11}$$

$$\Omega(\omega, t_0) \simeq G{H_1}^2 \Omega_\gamma(t_0)(\frac{\omega}{\omega_1})^{2-2\alpha}(\frac{\omega}{\omega_2})^{-2} \quad , \quad \omega_0 < \omega < \omega_2. \tag{12}$$

$\Omega_\gamma(t_0) \simeq 10^{-4}$ is the fraction of the critical energy density present today in the form of radiation; $\alpha \geq 1$ is a coefficient parametrizing (in conformal time) the power-law behaviour of the scale factor; $H_1 \equiv H(t_1)$ is the curvature scale at the time $t_1$ marking the end of inflation and the beginning of the radiation-dominated era; $\omega_0 \simeq 10^{-18}$ Hz is the minimum amplified frequency crossing today the Hubble radius $H_0^{-1}$; $\omega_2 \simeq 10^2\omega_0$ is the frequency corresponding to the matter radiation transition; $\omega_1$, finally, is the maximum amplified frequency, related to the inflation scale by $\omega_1 \simeq 10^{11}(H_1/M_P)^{1/2}$ Hz ($M_P$ is the Planck mass).

The computed spectra are constrained by the CMB anisotropy, by the pulsar timing data and by the closure density. The bounds on the variation of the spectral energy density becomes bounds on the variation of the squeezing parameter, which is given by [1],[3]

$$r(\omega) = |\delta|[25 - ln(\frac{\omega}{Hz}) + \frac{1}{2}\, ln(\frac{H_1}{M_P})] \tag{13}$$

($|\delta|$ is a model-dependent number of order of unity).

# 2 Thermal modification of the graviton spectrum

In this picture the crucial assumption is that the initial state of the gravitons is precisely the vacuum. The vacuum, however, is not the most general initial state for a gravity wave or for a generic scalar perturbation[5]. We can mimic a generic initial state with a squeezed number state, or, better with a statistical mixture of two mode squeezed number states [6]. In particular, any inflationary model based on a temperature dependent phase transition require as initial condition a homogeneous thermal state. So, a particularly relevant case is that of a thermal mixture of number states. Such initial condition will modify the mean number of particles and the spectral energy density .

For the spectral energy density we obtain [6]

$$\Omega(\omega,t_0) \simeq GH_1{}^2\Omega_\gamma(t_0)(\frac{\omega}{\omega_1})^{2-2\alpha}\coth(\frac{\beta_0\omega}{2}) \quad , \quad \omega_2<\omega<\omega_1 \tag{14}$$

$$\Omega(\omega,t_0) \simeq GH_1{}^2\Omega_\gamma(t_0)(\frac{\omega}{\omega_1})^{2-2\alpha}(\frac{\omega}{\omega_2})^{-2}\coth(\frac{\beta_0\omega}{2}) \quad , \quad \omega_0<\omega<\omega_2. \tag{15}$$

Here $\beta_0{}^{-1} \equiv \beta^{-1}(t_0)$ is the proper temperature of the initial thermal state, adiabatically rescaled down to the present observation time $t_0$ [$\beta_0$ is defined in terms of the comoving temperature $\overline{\beta}$ as $\beta(t_0) = \overline{\beta}a(t_0)$]. The effect of the initial finite temperature is to enhance graviton production at low frequency with respect to the high frequency sector of the spectrum. This effect depends on the value of the initial temperature which, in the context of inflationary models based on thermal symmetry breaking, is greater than the inflation scale. However, the modification of the spectrum is relevant only if the inflationary period is not too long (see [6] for a detailed discussion).

# 3 Entropy production from the cosmological amplification of vacuum fluctuations

Unlike the particle spectrum, which depends on the initial state, the non equilibrium entropy growth, associated with the process of particle production [7], is not affected by the particular choice of the initial conditions.

It is possible indeed to introduce a coarse graining approach to non equilibrium entropy, valid for squeezed states, in which the loss of information associated to the reduced density matrix is represented by the increased dispersion in the superfluctuant operators $x, \tilde{x}$ whose variance is amplified with respect to their initial value [8], [9]. In terms of these operators $a$ and $\tilde{a}$ have the following differential representation [10]

$$a_k = \frac{i}{2}e^{i\vartheta_k}\left[(\cosh r_k - \sinh r_k)(x - i\tilde{x}) + (\cosh r_k + \sinh r_k)(\partial_x - i\partial_{\tilde{x}})\right] \tag{16}$$

$$\tilde{a}_{-k} = \frac{i}{2}e^{i\vartheta_k}\left[(\cosh r_k - \sinh r_k)(x + i\tilde{x}) + (\cosh r_k + \sinh r_k)(\partial_x + i\partial_{\tilde{x}})\right] \tag{17}$$

(the relative phase has been chosen with respect to $\vartheta_k$, in such a way to identify the $x$ and $\tilde{x}$ operators with the superfluctuant ones) and the squeezed number wavefunctions (in the basis of the superfluctuant operators)becomes

$$\psi_{n_k,\tilde{n}_k}(x,\tilde{x}) = < x\tilde{x} \mid \Sigma_k \mid n_k n_{-k} > = < x\tilde{x} \mid \frac{(a_k^\dagger \tilde{a}_{-k}^\dagger)^n}{n!}\Sigma_k \mid 0 > = \left(\frac{\sigma_k}{\pi}\right)^{\frac{1}{2}} L_n^0\left(\sigma_k(x^2+\tilde{x}^2)\right) \times$$

$$\times\, e^{-\frac{\sigma_k}{2}(x^2+\tilde{x}^2)} = e^{in(\pi-2\vartheta_k)}\left(\frac{\sigma_k}{\pi}\right)^{\frac{1}{2}} e^{-\sigma_k(x^2+\tilde{x}^2)/2}\sum_{m=0}^{n}\frac{1}{m!(n-m)!}H_{2m}(\sqrt{\sigma_k}x)H_{2n-2m}(\sqrt{\sigma_k}\tilde{x}) \tag{18}$$

where $L_n$ and $H_n$ are the Laguerre and the Hermite polynomials, respectively and $\sigma_k = e^{-2r_k}$. It should be noted that, because of pair corrrelations, this wavefunction cannot be simply factorized

in terms of two decoupled squeezed oscillators in an excited state, which are known to provide the usual representation for the one mode squeezed number wavefunction.

It is interesting to point out, in passing, that the wave functions of a two mode squeezed state, as well as the transition probability between a generic two mode number state and a two mode squeezed number state, in the superfluctuant variables representation ($x$ , $\tilde{x}$) are the same as the corresponding quantities obtained in the context of the "squeezed" Landau levels problem for the electron in a uniform magnetic field [12]. In the Landau levels problem the two quantum numbers labelling the one particle wave functions are the energy of the electron and the component of the angular momentum perpendicular to the plane of the classical motion of the electron. Here the two quantum numbers in the many particle wavefunction are respectively the number of gravitons with four-momentum k ($n_k$) and with four-momentum -k ($n_{-k}$). Also to be mentioned is the fact that it is possible, within this formalism, to consider more general wavefunctions with $n_k \neq n_{-k}$

This is physically equivalent to consider, as initial condition for the gravitons, a state with non-zero number of particles and non zero four-momentum.

The entropy growth for a generic squeezed mixture of number states is the same as for the squeezed vacuum [10],

$$\Delta S_k = -Tr(\rho_{sk} \ln \rho_{sk}) + [Tr(\rho_{sk} \ln \rho_{sk})]_{r_k=0} = 2r_k \tag{19}$$

where $\rho_{sk}$ is the reduced density matrix for the mode k, and the integrated entropy over all the graviton spectrum is [8], [9] (from eq. (19), (13)):

$$S_g \simeq |\delta| S_\gamma (\frac{H_1}{M_P})^{3/2} \tag{20}$$

where $S_\gamma \simeq [a(t)\ell T_\gamma(t)]^3 = const$ is the usual black-body entropy of the CMB radiation (in terms of the to-day parameters, $(a_0 \ell T_{\gamma 0})^3 \sim (T_{\gamma 0}/H_0)^3 \sim (10^{29})^3$).

Particle production from the vacuum is thus a process able to explain the observed cosmological level of entropy provided the curvature scale at the inflation radiation transition is of the order of the Planck one [9], [10].

In the standard de Sitter inflationary scenario the curvature scale is bounded from the CMB anisotropy observations and has to be $H_1 \leq 10^{-5} M_{PL}$. This observation would seem to rule out the mechanism discussed here as a possible explanation of the entropy of the universe. On the other hand such constraints are evaded if the de Sitter phase (or the radiation dominated phase) is preceeded by a phase of growing curvature, like in the "pre-big-bang" models [2] which arise naturally in duality-symmetric string cosmology, and in which the curvature scale can approach Planckian values ($H_1 \leq M_{PL}$) [1],[2].

# 4 Acknowledgments

I am grateful to M.Gasperini and G.Veneziano for a fruitful collaboration which led to the many results reviewed in this paper, and for many helpful discussions. I whish also to thank the Istituto Nazionale di Fisica Nucleare, Sezione di Torino, for the financial support.

# References


[1] M.Gasperini and M.Giovannini Phys.Rev.D **47**,15119 (1993)

[2] M.Gasperini, N.Sanchez and G.Veneziano, Nucl.Phys.B **364**, 365(1991);
G.Veneziano, Phys.Lett.B **265**, 287(1991);
K.A.Meissner and G.Veneziano, Mod.Phys.Lett.A **6**, 3397 (1991);
M.Gasperini and G.Veneziano, Phys.Lett.B **277**, 256(1992);
M.Gasperini and G.Veneziano, Astropart.Phys. **1**,317 (1993)

[3] L.P.Grishchuk and Y.V.Sidorov, Phys.Rev.D **42** (1990)3413;
L.P.Grishchuk, "Squeezed states in the theory of primordial gravitational waves", in Proc. of the Workshop on squeezed states and uncertainty relations (Maryland Univ.), ed. by D.Han, Y.S.Kim and W.W.Zachary (Nasa Conf. Pub. No.3135, 1992) p.329
L.P.Grishchuk and Y.V.Sidorov, Class. Quantum Grav.6(1991) L161;
L.P.Grishchuk, in Proc of the VIth Brazilian School on cosmology and gravitation (Rio de Janeiro, July 1989)

[4] M.Gasperini and M.Giovannini, Phys.Lett.B **282**, 36 (1992);
B.Allen, Phys.Rev.D **37**, 2078 (1988);
V.Shani,Phys.Rev.D **42**, 453 (1990)

[5] I.Y. Sokolov, Class.Quant.Grav. **9**, L161 (1992)

[6] M.Gasperini, M.Giovannini and G.Veneziano, Phys.Rev.D**48**, R439 (1993)

[7] B.L.Hu and D.Pavon, Phys.Lett.B **180**, 329 (1986);
B.L.Hu and H.E.Kandrup, Phys.Rev.D **35** 1776 (1987)

[8] R.Brandenberger, V.Mukhanov and T.Prokopec, Phys.Rev.Lett.**69**, 3606 (1992); The entropy of gravitational field, Brown-Het-849 (August 1992);
T.Prokopec, Entropy of the squeezed vacuum, Brown-Het-861 (June 1992)

[9] M.Gasperini and M.Giovannini Phys.Lett.B **301**, 334 (1993)

[10] M.Gasperini and M.Giovannini Class.Quant.Grav **10**, (1993) (in press)

[11] "Inflationary cosmology" ed. by M.Abbott and S.Y.Pi (World scientific 1986) and references therein.

[12] I.A.Malkin, V.I.Manko and D.A.Trifonov Sov.Phys.JETP **31**, 386 (1970); Phys.Rev.D **2**, 1371 (1970)

# TIME-DEPENDENT VARIATIONAL APPROACH IN TERMS OF SQUEEZED COHERENT STATES —IMPLICATION TO SEMI-CLASSICAL APPROXIMATION—

Yasuhiko Tsue
*Department of Physics, Kochi University, Kochi 780, Japan*

**Abstract**

A general framework for time-dependent variational approach in terms of squeezed coherent states is constructed with the aim of describing quantal systems by means of classical mechanics including higher order quantal effects with the aid of canonicity conditions developed in the time-dependent Hartree-Fock theory. The Maslov phase occurring in a semi-classical quantization rule is investigated in this framework. In the limit of a semi-classical approximation in this approach, it is definitely shown that the Maslov phase has a geometric nature analogous to the Berry phase. It is also indicated that this squeezed coherent state approach is a possible way to go beyond the usual WKB approximation.

## 1 Introduction

In many-body problems, a great interest is paid to describe quantal systems in terms of a few classical variables because we are especially interested in some particular characteristic motions in quantal systems, for example, nuclear collective motions in nucleus and the dynamics of soliton models of baryons as the low energy effective theory of QCD. As is well known, in various quantal systems, if one takes the limit of "large $N$", the quantum theories are well described as the classical ones [1]. However, since, for example, we are interested in the nuclei as finite quantum many-particle systems, it should be noticed that the deviations from classical dynamics can never be neglected.

With the aim of establishing a possible framework for the classical description of quantal systems, we give a rather general framework to describe quantal systems by means of classical mechanics including the higher order quantal effects. Our basic idea is formulated with the use of the time-dependent variational principle utilizing the squeezed coherent states [2], paying strong attention to canonicity conditions developed in the TDHF theory [3][4].

In this paper, first, we briefly review our time-dependent variational approach with squeezed coherent states developed in Refs.[2] and [5]. Secondly, we show that, when we take a semi-classical limit in our framework, it is clearly realized that the Maslov correction occurring in the semi-classical quantization procedure in the usual WKB method can directly be interpreted as the Berry phase [6]. Although it has originally been pointed out that the Maslov correction is a kind of the Berry phase [7], it is possible to take account of the higher order quantum effects than that of the semi-classical approximation in our framework. Furthermore, it is understood that our approach is a possible way to go beyond the usual WKB approximation.

## 2 Formulation

In this section, we give the framework of the time-dependent variational approach in terms of squeezed coherent states [5][6]. We start with the general squeezed coherent state as

$$|\Phi(\alpha,\beta)\rangle \equiv \exp\{\sum_k(\alpha_k\hat{a}_k^\dagger - \alpha_k{}^*\hat{a}_k)\}|\Psi(\beta)\rangle\ , \tag{1}$$

$$|\Psi(\beta)\rangle \equiv \exp\Big\{\frac{1}{2}\sum_{k,k'}(\hat{a}_k^\dagger B_{kk'}\hat{a}_{k'}^\dagger - \hat{a}_k B_{kk'}{}^*\hat{a}_{k'})\Big\}|0\rangle\ . \tag{2}$$

Here, $|0\rangle$ is a vacuum state with respect to boson operators $\hat{a}_k$, and $\alpha_k$ and $B_{kk'}$ are the time-dependent $c$-number variables. The state $|\Psi(\beta)\rangle$ is called the squeezed vacuum. In the following consideration, we are restricted ourselves to deal with boson systems composed of one kind of boson. If we want to consider the systems described by su(2)-algebra such as the Lipkin model, it is enough to express the algebra by the use of two-kinds of boson operators, the representation of which is well known as Schwinger boson representation. Then, $B_{kk'}$ is taken as $B_{kk'} = B_k\delta_{kk'}(k = 1,2)$ [8].

With the aid of definitions of coordinate-momentum operators $\hat{Q} = \sqrt{\hbar/2}(\hat{a}+\hat{a}^\dagger)$ and $\hat{P} = (-i)\sqrt{\hbar/2}(\hat{a}-\hat{a}^\dagger)$, the above squeezed coherent state can be rewritten as the following Gaussian-type state :

$$\begin{aligned}|\Phi(t)\rangle &\equiv (2G)^{-\frac{1}{4}}\exp\Big\{\frac{i}{\hbar}(p\hat{Q}-q\hat{P})\Big\}\exp\Big\{\frac{1}{2\hbar}\Omega\hat{Q}^2\Big\}|0\rangle \\ &= e^{-i\varphi}|\Phi(\alpha,\beta)\rangle\ ,\end{aligned} \tag{3}$$

where we define the following variables as

$$q \equiv \sqrt{\frac{\hbar}{2}}(\alpha+\alpha^*)\ , \qquad p \equiv (-i)\sqrt{\frac{\hbar}{2}}(\alpha-\alpha^*)\ , \tag{4}$$

$$\Omega = 1 - \frac{1}{2G} + i2\Pi\ , \tag{5}$$

$$G \equiv \frac{1}{2}\Big|\cosh|B| + \frac{B}{|B|}\sinh|B|\Big|^2\ , \qquad \Pi \equiv \frac{i}{2}\frac{B^*-B}{|B|}\frac{\sinh|B|\cosh|B|}{\Big|\cosh|B| + \frac{B}{|B|}\sinh|B|\Big|^2}\ , \tag{6}$$

$$e^{-i2\varphi} \equiv \frac{1}{\sqrt{2G}}\Big(\cosh|B| + \frac{B}{|B|}\sinh|B|\Big)\ . \tag{7}$$

Here, $c$-number variable $\Omega$ is divided into real and imaginary parts, and for later convenience, the part "1" which represents the width of the wave packet of the original vacuum is extracted from real part. In the following, we will start with this expression of the squeezed coherent state in Eq.(3). Thus, we treat the variables $q, p, G$ and $\Pi$ as dynamical ones. Here, note that the variable $G$ is positive definite and never takes zero. This fact is important in order to present an interpretation of the usual WKB approximation within our framework.

In general, we can calculate the expectation values for arbitrary operators in terms of the Wigner transform :

$$\langle\Phi(t)|\hat{O}|\Phi(t)\rangle = \exp\{\hbar\hat{\mathcal{D}}\}O_W(q,p)\ . \tag{8}$$

Here, the derivative operator $\hat{\mathcal{D}}$ and the Wigner transform $O_W(q,p)$ are defined as

$$\hat{\mathcal{D}} \equiv \frac{1}{2}G\Big(\frac{\partial}{\partial q}\Big)^2+2G\Pi\Big(\frac{\partial^2}{\partial q\partial p}\Big)+\frac{1}{2}\Big(\frac{1}{4G}+4G\Pi^2\Big)\Big(\frac{\partial}{\partial p}\Big)^2 , \tag{9}$$

$$O_W(q,p) \equiv \int_{-\infty}^{\infty} ds e^{ips/\hbar}\langle q-\frac{s}{2}|\hat{O}|q+\frac{s}{2}\rangle , \tag{10}$$

where the relation $\hat{Q}|q\rangle = q|q\rangle$ is satisfied. The Wigner transform $O_W$ only depends on $q$ and $p$ and the variables $G$ and $\Pi$ are introduced by the operation of $\hat{\mathcal{D}}$.

We need to determine the time-development of the variables $q(t), p(t), G(t)$ and $\Pi(t)$, so that the time-development of the state $|\Phi(t)\rangle$ is determined. We can carry this out with the aid of the time-dependent variational principle similar to the TDHF theory :

$$\delta\int_{t_1}^{t_2} dt\langle\Phi(t)|i\hbar\frac{\partial}{\partial t}-\hat{H}|\Phi(t)\rangle = 0 . \tag{11}$$

Furthermore, we impose the canonicity conditions developed in the TDHF theory [4] in order to extract canonical variables. Taking the freedom of canonical transformations into account, we can express the canonicity conditions in the following form :

$$\langle\Phi(t)|i\hbar\partial_X|\Phi(t)\rangle = Y+\partial_X s(X,Y) , \qquad \langle\Phi(t)|i\hbar\partial_Y|\Phi(t)\rangle = \partial_Y s(X,Y) , \tag{12}$$

where $\partial_F \equiv \partial/\partial F$ is defined and $s(X,Y)$ which represents the freedom of the canonical transformation is an arbitrary function of canonical variables $X$ and $Y$. We can take possible solutions of the above canonicity conditions as $(X,Y) = (q,p)$ and $(\hbar G, \Pi)$. Therefore, the resultant equations of motion derived from the time-dependent variational principle are nothing but the canonical equations of motion due to the canonicity conditions :

$$\begin{aligned}
\dot{q} &= \frac{\partial H}{\partial p} = e^{\hbar\hat{\mathcal{D}}}\frac{\partial H_W}{\partial p} , \\
\dot{p} &= -\frac{\partial H}{\partial q} = -e^{\hbar\hat{\mathcal{D}}}\frac{\partial H_W}{\partial q} ,
\end{aligned} \tag{13}$$

$$\hbar\dot{G} = \frac{\partial H}{\partial \Pi} = \hbar e^{\hbar\hat{\mathcal{D}}}\Big\{2G\Big(\frac{\partial^2}{\partial q\partial p}\Big)+4G\Pi\Big(\frac{\partial}{\partial p}\Big)^2\Big\}H_W ,$$

$$\hbar\dot{\Pi} = -\frac{\partial H}{\partial G} = -\hbar e^{\hbar\hat{\mathcal{D}}}\Big\{\frac{1}{2}\Big(\frac{\partial}{\partial q}\Big)^2+2\Pi\Big(\frac{\partial^2}{\partial q\partial p}\Big)+\frac{1}{2}\Big(-\frac{1}{4G^2}+4\Pi^2\Big)\Big(\frac{\partial}{\partial p}\Big)^2\Big\}H_W . \tag{14}$$

Here, the dot denotes the time-derivative and the $c$-number Hamiltonian function $H$ is defined by $H \equiv \langle\Phi(t)|\hat{H}|\Phi(t)\rangle = e^{\hbar\hat{\mathcal{D}}}H_W(q,p)$. Thus, our main task is reduced to solving the classical equations of motion under appropriate initial conditions in the canonical form. As is seen from Eqs.(13) and (14), roughly speaking, the variables $q$ and $p$ represent the classical motion and $G$ and $\Pi$ may be regarded as the classical images of quantum fluctuations.

# 3 Maslov Phase as Berry Phase

In this section, we give a relation between the usual WKB approximation and our framework of the time-dependent variational approach with squeezed coherent states. Then, it is clearly shown

that the Maslov correction occurring in the semi-classical quantization procedure in the usual WKB method can directly be interpreted as the Berry or geometric phase.

In our framework, it is necessary to choose the initial conditions for newly-introduced variables as the classical image of quantum fluctuations, that is $G$ and $\Pi$. We adopt two criteria developed in our papers [2][6], namely the requirements of "Least Quantal Effects" and "Minimal Uncertainty" at initial time. As for the "classical parts" $q(t)$ and $p(t)$, we may select the initial conditions in a similar way to the usual TDHF theory [9].

Now, if the limit of $\hbar \to 0$ is taken in Eq.(13), then these equations are reduced to the usual classical Hamilton's equations of motion. Thus, it is expected that the variables $G$ and $\Pi$ represent the quantum fluctuations around the above-mentioned classical motions. Therefore, it is realized that the semi-classical limit in our framework is to take the limit of $\hbar \to 0$ in the equations of motion in Eqs.(13) and (14). In this limit, we can solve the equations of motion for $G$ and $\Pi$ in Eq.(14) and express these solutions in terms of the classical orbit $(q(t), p(t))$. The results are obtained as follows :

$$G = \frac{1}{2}\left[2G_0A^2 + \frac{B^2}{2G_0}\right], \qquad \Pi = \frac{1}{4G}\left[2G_0AC + \frac{BD}{2G_0}\right], \tag{15}$$

where $A \equiv \partial q/\partial q_0$, $B \equiv \partial q/\partial p_0$, $C \equiv \partial p/\partial q_0$ and $D \equiv \partial p/\partial p_0$ are defined and the variables with subscript 0 represent the initial values. Since the variables $G$ and $\Pi$ are always accompanied with $\hbar$, the expectation value of Hamiltonian should also be taken into account up to the order of $\hbar$ in this semi-classical limit. Namely, as the approximate energy expectation value, we adopt $H \simeq H_{\rm cl}(q,p) + \hbar H_{\rm ql}(q,p,G,\Pi)$.

In the usual WKB considerations, the energy is kept in the classical form which does not include $\hbar$. Therefore, in our framework of the time-dependent variational approach with the squeezed coherent states, $\hbar \int dt H_{\rm ql}$ in the action integral should be combined with the requantized phase factor $\int dt \langle \Phi(t)|i\hbar\partial/\partial t|\Phi(t)\rangle$ in order to compare our treatment with the usual WKB one properly. Thus, action function is written as

$$\begin{aligned} S &\equiv \int_0^{T_{\rm cl}} dt \langle \Phi(t)|i\hbar\frac{\partial}{\partial t} - \hat{H}|\Phi(t)\rangle = \int_0^{T_{\rm cl}} dt \left\{\frac{1}{2}(p\dot{q} - \dot{p}q) - \hbar\dot{\Pi}G - H\right\} \\ &\cong \int_0^{T_{\rm cl}} dt \left\{\left[p\dot{q} + \hbar\frac{\dot{A}B - A\dot{B}}{4G}\right] - H_{\rm cl}\right\} \quad (+\text{total time-derivative term}) , \end{aligned} \tag{16}$$

where it is assumed that the classical orbit is a periodic one, the period of which is written by $T_{\rm cl}$. According to the requantization procedure similar to the TDHF theory, we set the modified action integral except for the part of "energy" to integer $n$ times $2\pi\hbar$ :

$$\int_0^{T_{\rm cl}} dt \left\{p\dot{q} + \hbar\frac{\dot{A}B - A\dot{B}}{4G}\right\} = 2\pi\hbar n . \qquad n : \text{integer} \tag{17}$$

We rewrite the above relation as

$$\oint_C p dq = 2\pi\hbar\left(n - \frac{\dot{\Gamma}}{2\pi}\right), \tag{18}$$

where $\Gamma$ is defined and is explicitly calculated with the relation $G \equiv |z|^2/2$ :

$$\Gamma \equiv \int_0^{T_{\rm cl}} dt \frac{\dot{A}B - A\dot{B}}{4G}$$

$$= -\frac{1}{2}\mathrm{Im}\oint_C \frac{dz}{z} = -\pi\nu \ . \qquad \nu : \text{integer} \tag{19}$$

The above expression is nothing but a requantization condition in the semi-classical approximation. Here, $z$ ($G$) never passes through the point of origin $z = 0$ ($G = 0$) as is previously mentioned. Then, $G$ or $z$ undergoes the time-evolution accompanied with the classical motion $q(t)$ through the variables $A$ and $B$. The integer $\nu$, which corresponds to the Maslov correction occurring in the usual semi-classical quantization procedure in the WKB method, appears as the winding number around the origin $z = 0$ associated with the classical motion. These situations are analogous to the case encountered for the Berry phase [10][11]. Namely, it is understood that, in our squeezed coherent state approach, the Maslov correction or the Maslov "phase" corresponds to the Berry phase and the classical orbit plays a role of an "external parameter." The coefficient $\pi$ in the Maslov phase $\Gamma$ may be interpreted as a half of the solid angle that subtends at the "singular point" $G = 0$ ($z = 0$). Furthermore, the parameter governing the approximation is $\hbar$, so that $\hbar$ plays a role of an "adiabatic parameter" in the consideration of the Berry phase. Therefore, it is clearly realized in our approach that the Maslov correction has the similar geometric aspect to the Berry phase. It is thus shown that the quantum effects are automatically contained in the semi-classical limit in our squeezed coherent states approach.

# 4 Beyond the WKB Approximation

In the usual WKB method, the energy of the system is kept in the classical form which does not include $\hbar$ and the quantum effects are taken into account only through the requantization condition. On the other hand, in our time-dependent variational approach with the squeezed coherent states, the energy is the expectation value of the Hamiltonian with respect to the squeezed coherent state itself, that is $H = \langle\Phi(t)|\hat{H}|\Phi(t)\rangle$, so that the higher order quantum effects of $\hbar$ are already included. Thus, under the conception of our squeezed coherent states approach, the

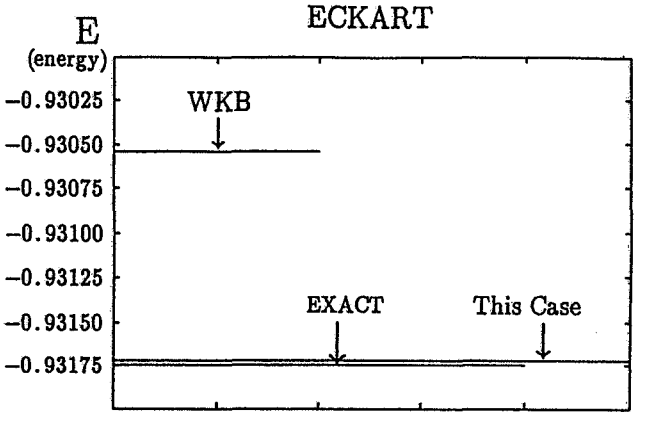


FIG. 1. The energies are shown in the case of Eckart potential $V(Q) = -U_0/\cosh^2\alpha Q$, in which we set the parameters $U_0 = 1$ and $\alpha = 0.1$ for simplicity. "This Case" represents the energy calculated numerically in our squeezed coherent state approach. "WKB" and "Exact" represent the energies obtained by the usual WKB approximation and exact eigenvalue of the ground state, respectively.

energy is calculated as follows : First, we analytically or numerically solve the self-consistent equations of motion in Eqs.(13) and (14). Secondly, we calculate the energy expectation value of the Hamiltonian with respect to the squeezed coherent state which includes the higher order effects of $\hbar$ than the quantum effects in the WKB approximation.

For example, in the case of Eckart potential, $V(\hat{Q}) = -U_0/\cosh^2 \alpha\hat{Q}$, the energy expectation value calculated numerically in our framework is compared with the exact energy eigenvalue and the usual WKB energy in Fig.1. Here, the initial conditions in our approach are taken as $q_0 = p_0 = 0$. Therefore, the energy thus obtained corresponds to the ground state one. It can be seen from Fig.1 that our treatment gives a fairly good result owing to the incorporation of the higher order effects of $\hbar$.

In summary, we have given the framework of the time-dependent variational approach in terms of the squeezed coherent states with the aim of describing quantal systems by means of the classical dynamics. In our squeezed coherent states approach, the Maslov correction that appears in the usual semi-classical quantization procedure is clearly realized as the Berry or geometric phase. Furthermore, our approach is a possible way to go beyond the WKB approximation.

# 5 Acknowledgments

The author is greatly indebted to Dr. Y. Fujiwara, Professor A. Kuriyama and Professor M. Yamamura for the collaboration at the early stage of this work. He also would like to thank Professor H. Horiuchi, Dr. T. Fukui and Dr. H. Fujii for fruitful discussions and comments.

# References

[1] L. G. Yaffe, Rev. Mod. Phys. **54**, 407 (1982).

[2] Y. Tsue, Y. Fujiwara, A. Kuriyama and M. Yamamura, Prog. Theor. Phys.'**85**, 693 (1991).

[3] T. Marumori, T. Maskawa, F. Sakata and A. Kuriyama, Prog. Theor. Phys. **64**, 1294 (1980).

[4] M. Yamamura and A. Kuriyama, Prog. Theor. Phys. Suppl. **93** (1987), and references therein.

[5] Y. Tsue and Y. Fujiwara, Prog. Theor. Phys. **86**, 443, 469 (1991).

[6] Y. Tsue, Prog. Theor. Phys. **88**, 911 (1992).

[7] R. G. Littlejohn, Phys. Rev. Lett. **61**, 2159 (1988).

[8] M. Yamamura, A. Kuriyama and Y. Tsue, Prog. Theor. Phys. **88**, 719 (1992).

[9] K.-K. Kan, J. J. Griffin, P. C. Lichtner and M. Dworzecka, Nucl. Phys. **A332**, 109 (1979).

[10] M. V. Berry, Proc. Roy. Soc. London **A392**, 45 (1984).

[11] *Geometric Phases in Physics*, edited by A. Shapere and F. Wilczek, (World Scientific, Singapore, 1989).

N95- 13949

# DECOHERENCE AND DISSIPATION FOR A QUANTUM SYSTEM COUPLED TO A LOCAL ENVIRONMENT

Michael R. Gallis
*Department of Physics, Penn State University/Schuylkill Campus*
*Schuylkill Haven, Pennsylvania 17972*
*Internet:mrg3@psuvm.psu.edu*

**Abstract**

Decoherence and dissipation in quantum systems has been studied extensively in the context of Quantum Brownian Motion. Effective decoherence in coarse grained quantum systems has been a central issue in recent efforts by Zurek and by Hartle and Gell-Mann to address the Quantum Measurement Problem. Although these models can yield very general classical phenomenology, they are incapable of reproducing relevant characteristics expected of a local environment on a quantum system, such as the characteristic dependence of decoherence on environment spatial correlations. I discuss the characteristics of Quantum Brownian Motion in a local environment by examining aspects of first principle calculations and by the construction of phenomenological models. Effective quantum Langevin equations and master equations are presented in a variety of representations. Comparisons are made with standard results such as the Caldeira-Leggett master equation.

## 1 Introduction and Motivation

Decoherence via coarse graining has been studied in the context of quantum measurement theory by Zurek[1] and by Hartle and Gell-Mann[2] as a mechanism which leads to the emergence of classical properties. Recent efforts have focused on the decoherence effects of a heat bath, which has also been examined in detail in the study of quantum brownian motion. Decoherence is identified as the (effective) suppression of interference terms in the density operator ($\rho(x,x')$, $x \neq x'$). It has been pointed out that most of the models which have been considered are somewhat simplistic and cannot reproduce the phenomenological features expected of a system which interacts locally with a homogeneous and isotropic environment[3]. In this paper I describe the perceived shortcomings of existing models and illustrate the construction of a phenomenological quantum master equation which contains many features expected from local coupling to a homogeneous environment[4].

Although decoherence is the most interesting feature of the effects of a heat bath, dissipation (and other effects) also generally appear in the dynamics of the density operator:

$$\frac{\partial \rho(x,x';t)}{\partial t} = \text{Hamiltonian terms} + \text{Dissipation terms} + \cdots - g(x,x')\rho(x,x';t). \tag{1}$$

The decoherence term appears as a (spatially dependent) decay term in the evolution equation, and can be understood in terms of effective fluctuating forces, or potentials: [5, 6]

$$g(x,y) = (\frac{1}{\hbar^2})(c(x;x) + c(y;y) - 2c(x;y),\ \langle V(x,t)V(y,s)\rangle = c(x;y)\delta(t-s). \tag{2}$$

Typical models have a quadratic form, $g(x,y) \propto (x-y)^2$ for the decoherence term, corresponding to a fluctuating force which is independent of position. However, for a local bath one expects the correlation function to die off at some characteristic length scale (the correlation length of the environment), which has some important ramifications for decoherence. For a quadratic form of decoherence, the decay rate of the interference terms in the density matrix increases without bound, while for a local model the decay rate saturates at separations (between $x$ and $x'$) much larger than the correlation length of the environment, reflecting the independence of environment fluctuations at large separations. As it turns out, the quadratic form can be considered a short length scale approximation of a more detailed model.

To consider the decoherence effects of an environment, simultaneous treatment of dissipation is necessary since decoherence and dissipative effects both generally arise from the same source (the interaction with a heat bath). For simplicity, I consider only linear dissipation, that is

$$m\dot{\mathbf{x}} = \mathbf{p}, \quad \dot{\mathbf{p}} = -\frac{\eta}{m}\mathbf{p} + \mathbf{F}. \tag{3}$$

As an example of quantum dissipative evolution, Dekker[7] has constructed a phenomenological master equation which includes ohmic dissipation and quadratic decoherence:

$$\frac{\partial \rho}{\partial t} = \tfrac{1}{i\hbar}[H,\rho] - i\tfrac{\lambda}{\hbar}[x,\{p,\rho\}] + \frac{(D_{xp}+D_{px})}{\hbar^2}[x,[p,\rho]] - \frac{D_{xx}}{\hbar^2}[p,[p,\rho]] - \frac{D_{pp}}{\hbar^2}[x,[x,\rho]]. \tag{4}$$

The Caldeira-Leggett[8] master equation is obtained from a first-principle calculation for the effects of a simple thermal bath. With an appropriate choice of parameters for the Dekker model, the Calderia-Leggett master equation can be reproduced.

Many open system models can reduce to the same classical phenomenology, particularly in the Markov regime, and yet have significant differences for a quantum sytem in that same regime. To illustrate this "richness" of quantum dissipative models, consider a rather generic oscillator bath model (following Zwanzig[9]):

$$L = \frac{1}{2}m\dot{x}^2 - U(\mathbf{x}) + \sum_\mu \frac{m_\mu}{2}[\dot{q}_\mu^2 - \omega_\mu^2(q_\mu - a_\mu(\mathbf{x}))^2]. \tag{5}$$

The classical calculations (the results of which are presumably reproduced in at least some limit of the quantum model) are relatively straightforward. The classical fluctuation-dissipation relation between the fluctuating forces and the nonlinear dissipation kernal emerges naturally, and in the usual Markov limit becomes:

$$\langle f_i(\mathbf{x},t) f_j(\mathbf{y},s)\rangle = k_B T \eta_{ij}(\mathbf{x},\mathbf{y};t-s) = \overline{\eta}_{ij}(\mathbf{x},\mathbf{y}) 2k_B T \delta(t-s), \tag{6}$$

and a simple langevin equation can (at least in principle) be obtained:

$$\ddot{x}_i(t) = -\frac{\partial U(\mathbf{x}(t))}{\partial x_i} + f_i(\mathbf{x}(t),t) - \overline{\eta}_{ij}(\mathbf{x}(t))\dot{x}_j. \tag{7}$$

For a homogeneous environment, the dissipation constant would be independent of position.

Some observations about the Markov limit are in order. For the classical picture, the spatial correlations of the fluctuating forces are irrelevant. After all, the particle can only be in one place

at one time. For a quantum system one must consider superpositions between the particle at different locations, i.e. superpositions between different trajectories for the particle. My point is that different models may produce the same classical phenomenology, but have some important differences for the quantum case, in particular for the effective decoherence due to the environment.

In order to help motivate some choices which will be required for the construction of the new model, consider a particle locally coupled to a scalar field. This particular model is a natural extension of one considered by Unruh and Zurek[10]. The action for this model is given by:

$$L = \int d^n r \left\{ \tfrac{1}{2} \left[ \dot{\phi}^2 - c^2 (\nabla_r \phi)^2 \right] + \delta(\mathbf{r} - \mathbf{x}) \left[ \tfrac{m\dot{\mathbf{x}}^2}{2} - \varepsilon \phi(\mathbf{r}, t) - V(\mathbf{x}) \right] \right\}. \tag{8}$$

This model produces approximately ohmic dissipation in one dimension[8, 11]. In addition, one can extract from the influence functional the effective correlation function of the fluctuating forces[5, 11]:

$$< \mathbf{F}(\mathbf{x}, \tau) \cdot \mathbf{F}(\mathbf{y}, s) > 0 = \frac{\hbar \varepsilon^2}{2(2\pi)^d} \int d^d k k^2 \left\{ \frac{\coth(\frac{\beta\hbar\omega}{2})}{\omega} \cos(\omega t) \cos(\mathbf{k} \cdot (\mathbf{x} - \mathbf{y})) \right\}. \tag{9}$$

This correlation function results from independent contributions from each mode of oscillation of the field. With some of the characteristics suggested by this local environment in mind, I now turn to the actual construction of the model.

# 2 The Phenomenological Model

The initial form of the evolution of the density operator is taken to be in the Lindblad[12] form (Schrödinger picture):

$$\frac{\partial \rho}{\partial t} = L[\rho] = \frac{1}{i\hbar}[H, \rho] + \frac{1}{2\hbar} \sum_{\mu} [V_\mu \rho, V_\mu^\dagger] + [V_\mu, \rho V_\mu^\dagger] = \frac{1}{i\hbar}[H, \rho] + \Delta L[\rho], \tag{10}$$

for which there is a corresponding form for the Heisenberg picture $L^*[O]$ which can readily be obtained from the cyclic properties of the trace. For a finite dimensional Hilbert space, this form is the most general for a completely positive dynamical semigroup. For infinite dimensional Hilbert spaces, it is a reasonable starting point. I will be focusing on the nonunitary part of the evolution, $\Delta L$.

The construction of the model is essentially the determination of the operators $V_\mu$, subject to the constraint that the dissipation is ohmic (expressed as an operator condition). This constraint produces the "correct" classical phenomenology, but does not completely determine the model. However, linear dissipation almost forces the $V_\mu$ to be at most linear in momentum, that is

$$V_\mu = A_\mu(\mathbf{x}) - \mathbf{B}_\mu(\mathbf{x}) \cdot \mathbf{p}. \tag{11}$$

Homogeneity and isotropy also serve to constrain the model. Assuming some sort of mode by mode interaction with a field, a reasonable choice is given by:

$$\{V_\mu\} = \{\alpha(k) e^{i\mathbf{k}\cdot\mathbf{x}} - \beta(k) e^{i\mathbf{k}\cdot\mathbf{x}} \mathbf{k} \cdot \mathbf{p}\}. \tag{12}$$

The discrete index $\mu$ has been replaced by the continuous index $\mathbf{k}$. The model is then completely specified by the complex functions $\alpha$ and $\beta$.

The resulting nonunitary contribution to the Schrödinger equation is given by the expression:

$$\begin{aligned}\Delta L[\rho] &= -\int d^dk \tfrac{|\alpha(k)|^2}{\hbar}(\rho - e^{i\mathbf{k}\cdot\mathbf{x}}\rho e^{-i\mathbf{k}\cdot\mathbf{x}}) - \int d^dk \tfrac{|\beta(k)|^2}{\hbar}(\tfrac{1}{2}\{(\mathbf{k}\cdot\mathbf{p})^2,\rho\} - e^{i\mathbf{k}\cdot\mathbf{x}}\mathbf{k}\cdot\mathbf{p}\rho\mathbf{k}\cdot\mathbf{p}e^{-i\mathbf{k}\cdot\mathbf{x}}) \\ &\quad - \int d^dk \tfrac{\mathrm{Re}[\alpha(k)^*\beta(k)]}{\hbar}(e^{i\mathbf{k}\cdot\mathbf{x}}\{\mathbf{k}\cdot\mathbf{p},\rho\}e^{-i\mathbf{k}\cdot\mathbf{x}}) - \int d^dk \tfrac{i\mathrm{Im}[\alpha(k)^*\beta(k)]}{\hbar}(e^{i\mathbf{k}\cdot\mathbf{x}}[\mathbf{k}\cdot\mathbf{p},\rho]e^{-i\mathbf{k}\cdot\mathbf{x}}). \quad (13)\end{aligned}$$

The position representation of the new model is given by:

$$\begin{aligned}\frac{\partial\rho(x,x';t)}{\partial t} &= \text{Hamiltonian terms} - \left(\int dk \frac{|\alpha(k)|^2}{\hbar}(1-\cos k(x-x'))\right)\rho(x,x';t) \\ &- \left(\frac{2}{\hbar}\int dk \mathrm{Re}[\alpha^*(k)\beta(k)]k\sin k(x-x')\right)\left(\frac{\partial}{\partial x}-\frac{\partial}{\partial x'}\right)\rho(x,x';t) \\ &- \left(i\int dk \mathrm{Im}[\alpha^*(k)\beta(k)]k\sin k(x-x')\right)\left(\frac{\partial}{\partial x}+\frac{\partial}{\partial x'}\right)\rho(x,x';t) \\ &+ \left(\int dk|\beta(k)|^2\hbar k^2\right)\left(\frac{\partial^2}{\partial x^2}-\frac{\partial^2}{\partial x'^2}\right)\rho(x,x';t) \\ &+ \left(\int dk|\beta(k)|^2\hbar k^2\cos k(x-x')\right)\left(\frac{\partial^2}{\partial x\partial x'}\right)\rho(x,x';t). \quad (14)\end{aligned}$$

The first nonhamiltonian term is responsible for decoherence. The corresponding noise spatial correlation is determined by $\alpha(k)$. The characteristic length should be on the order of the inverse of the "width" of $|\alpha(k)|^2$ in $k$ space. The second nonhamiltonian term is responsible for the dissipation. Clearly the dissipation and other terms are more complicated in this new model. However, that would also be expected from a more elaborate first principle calculation.

By examining the Eherenfest relations of physical quantities using $L^*$, some interesting physical features of the new model emerge. By construction, the average position and momentum obey relations corresponding to ohmic dissipation:

$$\frac{d\langle P\rangle}{dt} = \frac{i}{\hbar}\langle[H,P]\rangle - \frac{\eta}{m}\langle P\rangle, \quad \frac{d\langle x\rangle}{dt} = \frac{i}{\hbar}\langle[H,x]\rangle = \frac{\langle P\rangle}{m}, \quad (15)$$

where

$$\frac{\eta}{m} = \int dk 2\mathrm{Re}(\alpha^*(k)\beta(k))k^2. \quad (16)$$

With only limited constraints on $\alpha$ and $\beta$ ($\gamma$ must be positive), the kinetic energy is seen to be thermalized:

$$\frac{d}{dt}\langle(\frac{P^2}{2m}-\frac{k_BT}{2})\rangle = \langle\frac{i}{\hbar}[H,(\frac{P^2}{2m}-\frac{k_BT}{2})]\rangle - \gamma\langle(\frac{P^2}{2m}-\frac{k_BT}{2})\rangle, \quad (17)$$

where

$$\gamma \equiv 2\frac{\eta}{m} - \int d^dk \frac{|\beta(k)|^2}{d}\hbar k^4, \quad \frac{k_BT}{2} \equiv \frac{1}{\gamma}\int d^dk \frac{|\alpha(k)|^2}{2m}\hbar k^2. \quad (18)$$

The effective temperature is determined by $\alpha$ and $\beta$.

A low length scale approximation of the new model can be obtained by expanding the exponential terms in powers of $\mathbf{k}\cdot\mathbf{x}$:

$$\begin{aligned}\Delta L[\rho] \cong & -\int d^dk \frac{|\alpha(k)|^2}{2\hbar}[\mathbf{k}\cdot\mathbf{x},[\mathbf{k}\cdot\mathbf{x},\rho]] - \int d^dk \frac{|\beta(k)|^2}{2\hbar}[\mathbf{k}\cdot\mathbf{p},[\mathbf{k}\cdot\mathbf{p},\rho]] \\ & - \int d^dk \frac{i\mathrm{Re}(\alpha(k)^*\beta(k))}{\hbar}[\mathbf{k}\cdot\mathbf{x},\{\mathbf{k}\cdot\mathbf{p},\rho\}] + \int d^dk \frac{\mathrm{Im}(\alpha(k)^*\beta(k))}{\hbar}[\mathbf{k}\cdot\mathbf{x},[\mathbf{k}\cdot\mathbf{p},\rho]]. \quad (19)\end{aligned}$$

The lowest nonvanishing terms are second order, which exactly reproduces the Dekker master equation for 1 dimension. As a result, we can think of the Dekker or Caldeira-Leggett equations as a low length scale approximation for more general models.

On the other hand, the Caldeira-Leggett master equation,

$$\Delta L[\rho] = \frac{\eta}{i2m\hbar}[x,\{p,\rho\}] - \frac{\eta k_B T}{\hbar^2}[x,[x,\rho]], \quad (20)$$

can be considered a special case of the Dekker master equation, with the $D_{xp}$ terms equal to zero (which Dekker has argued should be the case) and an additional low momentum approximation which ignores the $D_{xx}$ term. With this type of special case in mind, we can construct a low momentum approximation for the new model which includes only the decoherence and dissipation terms:

$$\Delta L[\rho] = -\int d^dk \frac{|\alpha(k)|^2}{\hbar}(\rho - e^{i\mathbf{k}\cdot\mathbf{x}}\rho e^{-i\mathbf{k}\cdot\mathbf{x}}) - \int d^dk \frac{\mathrm{Re}(\alpha(k)^*\beta(k))}{\hbar}(\{\mathbf{k}\cdot\mathbf{p}, e^{i\mathbf{k}\cdot\mathbf{x}}\rho e^{-i\mathbf{k}\cdot\mathbf{x}}\}). \quad (21)$$

This would seem to be a likely starting point for applications of this model. However, this approximation is not a positive form for the dynamics.

Finally, I would like to look at the Wigner representation of the new model, which has some interesting features. If we expand the terms of the evolution equation in powers of $\hbar$ (in the same manner as is typically done with the potential),

$$\begin{aligned}\dot{W}(q,p) = & -\frac{1}{m}\frac{\partial}{\partial q}(pW) + \frac{\partial}{\partial p}(V'(q)W) + \sum_{n=1}^{\infty}\frac{(\hbar)^{2n}(-1)^n 2^{-2n}}{(2n)!}V^{(2n+1)}\frac{\partial^{2n+1}}{\partial p^{2n+1}}W \\ & + \lambda\frac{\partial}{\partial p}(pW) + \sum_{n=1}^{\infty}(\hbar)^{2n}\left(\int dk \frac{2\mathrm{Re}(\alpha^*\beta)k^{2n+1}}{(2n+1)!}\right)\frac{\partial^{2n+1}}{\partial p^{2n+1}}W \\ & + D_{pp}\frac{\partial^2}{\partial p^2}W + \sum_{n=1}^{\infty}(\hbar)^{2n+1}\left(\int dk \frac{|\alpha|^2 k^{2n+2}}{(2n+2)!}\right)\frac{\partial^{2n+2}}{\partial p^{2n+2}}W \\ & + (D_{xp}+D_{px})\frac{\partial^2}{\partial p\partial q}W + \sum_{n=1}^{\infty}(\hbar)^{2n+1}\left(\int dk \frac{\mathrm{Im}(\alpha^*\beta)k^{2n+2}}{(2n+1)!}\right)\frac{\partial}{\partial q}\frac{\partial^{2n+1}}{\partial p^{2n+1}}W \\ & + D_{xx}\frac{\partial^2}{\partial q^2}W + \sum_{n=1}^{\infty}(\hbar)^{2n-1}\left(\int dk \frac{|\beta|^2 k^{2n+2}}{(2n)!}\right)\frac{\partial^n}{\partial p^n}\left(\frac{\hbar^2}{4}\frac{\partial^2}{\partial q^2}+p^2\right)W, \quad (22)\end{aligned}$$

the lowest order terms correspond exactly to the Wigner representation of the Dekker equation. The Wigner representation of the Dekker equation is a standard classical type of diffusion equation. This illustrates the idea that the "classical" nature of the system emerges when coherent superpositions are not important in the dynamics. In this case, the relevant superpositions are

between different locations separated by distances on the order of the environment correlation length.

The convolution theorem can also be used to write down the Wigner representation of the evolution:

$$\begin{aligned} W(q,p) &= (\text{Hamiltonian terms}) - \frac{2}{\hbar}\int dp'(p-p')W(q,p-p')\frac{p'\mathrm{Re}[\alpha^*\left(\frac{p'}{\hbar}\right)\beta\left(\frac{p'}{\hbar}\right)]}{\hbar^2} \\ &- \left(\int dk\frac{|\alpha|^2(k)}{\hbar}\right)W(q,p) + \int dp'W(q,p-p')\frac{|\alpha\left(\frac{p'}{\hbar}\right)|^2}{\hbar^2} \\ &- \frac{\partial}{\partial q}\int dp'W(q,p-p')\frac{p'\mathrm{Im}[\alpha^*\left(\frac{p'}{\hbar}\right)\beta\left(\frac{p'}{\hbar}\right)]}{\hbar^2} \\ &+ D_{xx}(\frac{1}{4}\frac{\partial^2}{\partial q^2} - \frac{p^2}{\hbar^2})W(q,p) + \int dp'\frac{p^2|\beta\left(\frac{p'}{\hbar}\right)|^2}{\hbar^2}(\frac{1}{4}\frac{\partial^2}{\partial q^2} + \frac{(p-p')^2}{\hbar^2})W(q,p-p'). \quad (23) \end{aligned}$$

One apparent effect in the new model is a spreading induced by these convolution terms.

In summary, a new phenomenological master equation for ohmic dissipation and decoherence has been constructed which has completely positive dynamics. The new model has the features expected from local coupling to a homogeneous environment: specifically, the evolution is istropic and translationally invariant. Spatial correlations of the environment appear explicitly in the models. The new model also includes previous results as low length scale approximations.

# References


[1] W. H. Zurek, S. Habib and J. P. Paz, Phys. Rev. Lett. **70**, 1187 (1993). W. H. Zurek, Prog. Theor. Phys. **89**, 281 (1993).

[2] M Gell-Mann and J. B. Hartle, Phys. Rev. D **47**, 3345 (1993).

[3] M. R. Gallis and G. N. Fleming, Phys. Rev. A **42**, 38 1990.

[4] Some of these results have appeared in: M. R. Gallis, Phys. Rev. A **48**, 1028 (1993).

[5] M. R. Gallis, Phys. Rev. A **45**, 47 (1992).

[6] L. Diósi, Phys. Lett. **A 112**, 288 (1985).

[7] H Dekker, Phys. Rep. **80**, 1 (1981).

[8] A. O. Caldeira and A. J. Leggett, Physica (Utrecht) **121 A**, 587 (1983).

[9] R. Zwanzig, J. Stat. Phys **9**, 215 (1973).

[10] W. G. Unruh and W. H. Zurek, Phys. Rev. D**40**, 1071 (1989).

[11] M. R. Gallis, unpublished.

[12] G. Lindblad, Commun. Math. Phys. **48**, 119 (1976).

N95-13950

# GENERAL PROPERTIES OF QUANTUM OPTICAL SYSTEMS IN A STRONG FIELD LIMIT

**S. M. Chumakov**
*I.I.M.A.S. -Cuernavaca ,*
*Universidad Nacional Autónoma de México ,*
*Apartado Postal 139-B, 62191, Cuernavaca, Mor. México*

**A.B.Klimov**
*Fac. de Ciencias Físico-Matemáticas*
*Universidad de Guadalajara,*
*Corregidora 500, 44100 Guadalajara, Jal, México*

**Abstract**

We investigate the dynamics of an arbitrary atomic system ($n$ -level atoms or many $n$-level atoms) interacting with a resonant quantized mode of an em field. If the initial field state is a coherent state with a large photon number then the system dynamics possesses some general features, independently of the particular structure of the atomic system. Namely, trapping states, factorization of the wave function, collapses and revivals of the atomic energy oscillations are discussed.

# 1 Introduction

The Jaynes - Cummings Model is of principle importance in quantum optics. It consists of a single atom interacting with a single mode of quantized em field in a lossless cavity. The properties of JCM in the region of a strong coherent quantum field are:

1. Collapses and revivals of atomic inversion oscillations [1].
2. The existance of trapping states [2]. (These are initial atomic states which lead to the constant mean value of atomic energy in the course of the interaction with the field).
3. Wave Function (WF) factorization in the trapping states [3]. (This very unusual property of the JCM trapping states means that the field and atomic subsystems remain to a high accuracy in pure states, in spite of the presence of interaction).
4. WF factorization for an arbitrary initial atomic state at a half revival time. For this time moment the field state is a coherent superposition of macroscopically different states (so called Schrödinger cat) [4, 3].

Here, we address to ourselves the following question:
*Which phenomena from this list will survive for an arbitrary atomic system interacting with a strong quantum field ?*

## 2 What is an arbitrary atomic system ?

We start with some examples:

1. many two-level atoms in a cavity (the Dicke Model, [5]);
2. many three-level atoms of arbitrary level configurations in a cavity;
3. many $n$-level atoms of arbitrary degeneracy of the levels.

All these systems are described by Hamiltonians of the form:

$$\hat{H} = \omega\left(\hat{a}^{\dagger}\hat{a} + \hat{h}\right) + g\left(\hat{a}\hat{X}_{+} + \hat{a}^{\dagger}\hat{X}_{-}\right) \tag{1}$$

Here, $\hat{a}^{\dagger}, \hat{a}$ are photon operators; $\hat{h}$ is the bare Hamiltonian of the atomic system; $\hat{X}_{+}, \hat{X}_{-}$ are atomic transition operators. We suppose, that the following commutation relations are valid:

$$\left[\hat{h}, \hat{X}_{+}\right] = \hat{X}_{+} \qquad \left[\hat{h}, \hat{X}_{-}\right] = -\hat{X}_{-} \tag{2}$$

The model formulated in such a way implies the Rotating Wave Approximation and, therefore, the excitation number conservation:

$$[\hat{H}, \hat{N}] = 0, \qquad \hat{N} = \hat{a}^{\dagger}\hat{a} + \hat{h}. \tag{3}$$

It is usually the case in Quantum Optics. We do not impose any conditions on the commutator

$$[\hat{X}_{+}, \hat{X}_{-}]$$

which leads to a large freedom in the specification of the atomic subsystem.

We adopt also the exact resonance condition. It means that transition frequencies between neighboring levels are equal to the field frequency $\omega$. This condition is imposed with a sake of simplicity (the arbitrary detunings can be also involved in our approach). Stress, that the cavity is supposed to be a perfect one. We do not discuss the dissipation processes here.

## 3 The classical field limit

For to approach the classical field limit one has to take a coherent field states (CS) with large photon numbers. Then one may substitute

$$\hat{a} \to \alpha, \quad \hat{a}^{\dagger} \to \overline{\alpha},$$

where $\alpha \equiv \sqrt{\overline{n}}e^{i\phi}$ is a CS parameter. Then the quantum interaction Hamiltonian becomes proportional to the operator

$$\hat{H}_{int} \to \hat{H}_{cl} = e^{i\phi}\hat{X}_{+} + e^{-i\phi}\hat{X}_{-}.$$

$H_{cl}$ has the sense of the atomic Hamiltonian in a constant classical field. We will call the eigenvectors

$$\hat{H}_{cl} \mid \underline{p} >_{at} = \lambda_{p}^{0} \mid \underline{p} >_{at} \tag{4}$$

the *semiclassical eigenvectors.*

# 4 Factorization of the Wave Function

We now formulate our principle result [6]. *Let initial atomic state is semiclassical eigenstate and initial field state is CS with a large photon number:*

$$| in >=| \underline{p} >_{at} \otimes | \alpha > \tag{5}$$

*Then the WF will be approximately factorized for the time up to* $gt \sim \overline{n}$. The factorized WF has a form:

$$\begin{aligned} | \Psi(t) > &\cong | \Phi_p(t) > \otimes | A_p(t) >, \\ | \Phi_p(t) > &= \sum_n p_n e^{-igt\lambda_p^0\sqrt{n-C+1/2}} | n >_f, \\ | A_p(t) > &= e^{-ict} e^{-it\omega_p \hat{h}} | \underline{p} >_{at} \ . \end{aligned} \tag{6}$$

Here, $p_n$ - initial CS amplitudes, $C$ is the energy ground level of the bare atomic system, $e^{-ict}$ is a phase factor which we do not write down explicitly here.

We do not give here the proof of eqs.(6) (see [6]). Instead, let us qualitatively describe the system behavior. Eqs.(6) stand that the field and the atomic subsystem remain approximately in pure states in the course of the evolution (not in the mixed ones!). However, the two subsystems essentially interact. The field evolution depends on the semiclassical atomic eigenfrequency $\lambda_p^0$. The field state rotates along the circle of radius $\sqrt{\overline{n}}$ in the phase space slowly loosing the shape of the initial CS (spreading in phase).

The atomic subsystem is rotated by the free atomic hamiltonian $\hat{h}$ with the angular velocity

$$\omega_p \equiv \frac{g\lambda_p^0}{2\sqrt{\overline{n} - C + 1/2}} \tag{7}$$

dependent on the initial photon number $\overline{n}$.

We have proved eqs.(6) by means of the perturbation theory with the operator-valued small parameter $1/(\hat{N} + 1/2)$ . We neglected the terms of order $O(\overline{n}^{-1/2})$ the amplitudes. However, we kept higher accuracy in the frequencies (neglecting the terms of order $O(1/\overline{n})$ ). It means that our approximation holds for times up to $gt \sim \overline{n}$. It is a usual situation, that the system dynamics is more sensitive to the small corrections in frequencies, than in amplitudes.

# 5 Trapping states

It follows immediately from eqs. (6), that all the semiclassical eigenstates of an arbitrary atomic system are trapping states, i.e. the mean value of the atomic inversion does not evolve with time:

$$< \hat{h}(t) > = < \Psi(t) \mid \hat{h} \mid \Psi(t) > = < A_p(t) \mid \hat{h} \mid A_p(t) > =$$

$$_{at} < \underline{p} \mid \hat{h} \mid \underline{p} >_{at} = \ const.$$

This result holds with the accuracy $O(\overline{n}^{-1/2})$, due to our accuracy for the transition amplitudes.

# 6 Collapses and Revivals

This phenomenon, discovered initially for the JCM [1] appears for an arbitrary atomic system in a strong coherent field. Indeed, an arbitrary initial state of the atomic system can be expanded in the basis of the semiclassical eigenstates (4):

$$\mid \Psi >_{at} = \sum_p C_p \mid \underline{p} >_{at} .$$

Then, for the atomic inversion we get:

$$< \Psi(t) \mid \hat{h} \mid \Psi(t) > = \sum_{p,q} \overline{C}_q C_p < \Phi_q(t) \mid \Phi_p(t) >< A_q(t) \mid \hat{h} \mid A_p(t) > .$$

The atomic inversion is determined by the scalar products of the field states (6):

$$< \Phi_q(t) \mid \Phi_p(t) > = e^{-\overline{n}} \sum_n \frac{\mid \alpha \mid^{2n}}{n!} e^{-igt(\lambda_q^0 - \lambda_p^0)\sqrt{n-A/2+1/2}}.$$

This is a direct generalization of the well-known unharmonic series for the JCM, which also contains collapsing and reviving Rabi oscillations. The collapse, revival times and envelopes can be easily found.

The atomic matrix elements entering in eq.(6) are slowly varying functions oscillating with the frequency eq.(7). They may modulate the revival envelopes. However, for the Dicke model case these matrix elements to be equal to zero if $p \neq q \pm 1$ and the correspondent revivals disappear. If $p = q \pm 1$ , the atomic matrix elements equals to 1 just for the time moments of revivals.

# 7 Schrödinger Cat.

For the JCM case there are only two factorized states. An arbitrary initial state leads to the superposition of them. The two JCM atomic states $\mid A_p(t) >$, $p = 0, 1$ are nothing but two different spin-1/2 coherent states and they can be transformed one to another by rotation. It just happens at a half revival time $t_R/2$ [3]:

$$\mid A_0(t_R/2) > = \mid A_1(t_R/2) > = \mid \psi_0 >_{at},$$

and then the system WF is factorized for an arbitrary initial atomic state:

$$\mid \Psi(t_R/2) > = \mid \psi_0 >_{at} (\mid \Phi_0(t_R/2) > + \mid \Phi_1(t_R/2) >)$$

Therefore, at this time moment the field WF is the quantum superposition of macroscopically different states $\mid \Phi_p(t) >$, $p = 0, 1$.

It is clear, that for larger atomic system (say for spin-1) not all different atomic semiclassical eigenstates can be transformed one into another by rotation, and the Schrödinger cat is absent for arbitrary initial atomic state (as it has been recently noticed in the work [7]

# 8 Conclusions

We have solved the problem of the interaction of an arbitrary atomic system with the strong quantized em field in a lossless cavity. The key point of our solution is the wave function factorization (6) for the specially chosen initial states (4).

Since these states form a complete basis, this gives possibilities for an exhaustive description of the system dynamics.

Being reduced to the JCM, our results reproduce the treatment of J. Gea-Banacloche [3].

For the case of the Dicke model, they correspond to the first two orders of the perturbation theory proposed in the work [8] and can be treated as a direct generalization of that scheme for the arbitrary atomic system. From the mathematical point of view, our treatment is connected with the concept of dynamical symmetry group for the quantum optical systems [9]. (Note, that this dynamical symmetry is approximate rather than exact one).

Stress, that our method allows to make explicit analytical calculations of any physical quantities for the systems under study.

# 9 Acknowledgments

S.Ch. and A.K. acknowledge the support from CONACYT.

# References

[1] N.B. Narozhny, J.J. Sanchez-Mondragon and J.H. Eberly, Phys.Rev.A **23**, 236 (1981).

[2] K. Zaheer, M.S. Zubairy, Phys.Rev.A **39**, 2000 (1989);

[3] J. Gea-Banacloche, Phys.Rev.A **44**, 5913 (1991); *ibid.* **46**, 7307 (1992); *ibid.* **47**, 2221 (1993).

[4] S.J.D. Phoenix, P.L. Knight, Phys.Rev.A **44**, 6023 (1991).

[5] R.H. Dicke, Phys.Rev. **93**, 99 (1954).

[6] S.M.Chumakov, A.B.Klimov and J.J.Sanchez-Mondragon, submitted to Phys.Rev. A (1993).

[7] P.L.Knight, B.W.Shore, Phys.Rev.A **48**, 642 (1993).

[8] M. Kozierowski, A.A. Mamedov and S.M. Chumakov, Phys.Rev. A **42**, 1762 (1990); M. Kozierowski, S.M. Chumakov, J. Swiatlowski and A.A. Mamedov, Phys.Rev. A **46**, 7220 (1992).

[9] I.A. Malkin, V.I. Man'ko, *Dynamical symmetries and coherent states of quantum systems* (Nauka, Moscow, 1979, in russian ).

# PROBING THE ANTIFERROMAGNETIC LONG-RANGE ORDER WITH GLAUBER SPIN STATES

G. G. Cabrera
*Instituto de Física "Gleb Wataghin",*
*Universidade Estadual de Campinas (UNICAMP), C. P. 6165,*
*Campinas 13083-970, SP, Brazil*

**Abstract**

It is well known that the ground state of low-dimensional antiferromagnets deviates from Néel states due to strong quantum fluctuations. Even in the presence of long-range order, those fluctuations produce a substantial reduction of the magnetic moment from its saturation value. Numerical simulations in anisotropic antiferromagnetic chains suggest that quantum fluctuations over Néel order appear in the form of localized reversal of pairs of neighboring spins. In this paper, we propose a *coherent state* representation for the ground state to describe the above situation. In the one-dimensional case, our wave function corresponds to a two-mode Glauber state, when the Néel state is used as a reference, while the boson fields are associated to coherent flip of spin pairs. The coherence manifests itself through the antiferromagnetic long-range order that survives the action of quantum fluctuations. The present representation is different from the standard zero-point spin wave state, and is asymptotically exact in the limit of strong anisotropy. The fermionic version of the theory, obtained through the Jordan-Wigner transformation, is also investigated.

## 1 Introduction

The Heisenberg model has been extensively studied for many years as a non trivial many-body problem in quantum magnetism. For low dimensional systems, the ground state deviates from Néel ordering due to strong quantum fluctuations [1]. The determination of this ground state represents a fascinating problem, that in one dimension originated a whole branch of Mathematical Physics based in the so called "Bethe-Ansatz" technique [2]. However, exact solutions are extremely intricate, very often not susceptible of a direct physical intuition, and in the case of the Heisenberg model, they are restricted to one dimension.

In this contribution, we would like to present a novel approach based in a localized description of quantum fluctuations. If one takes as a reference the Ising limit, with a ground state of Néel type, switching the transverse part of the Heisenberg Hamiltonian may be visualized as a disordering process, where pairs of neighboring spins are simultaneously flipped, the ground state being a quantum superposition of admixtures contained in the manifold of total $S_z = 0$. This effect has been systematically observed in numerical simulations for anisotropic Heisenberg chains [3], and was used by Lagos and the author as the heuristic base for the construction of a trial solution [1]. To fix ideas, we will concentrate in the case of spin 1/2, and most of the examples will refer to a one-dimensional system. The theory can be extended to arbitrary dimension [4],

and to arbitrary value of the spin [5]. The antiferromagnetic Heisenberg Hamiltonian with axial anisotropic exchange can be written as:

$$\mathcal{H} = J \sum_{<ij>} \left[ S_z(i)S_z(j) + \frac{\alpha}{2} \{ S_+(i)S_-(j) + S_-(i)S_+(j) \} \right], \tag{1}$$

where $i, j$ are site indexes for nearest neighbors, $J > 0$ is the antiferromagnetic exchange, the $S$'s are spin $1/2$ operators, and $\alpha$ is the axial anisotropy parameter. Special cases of Hamiltonian (1) are: *i)* $\alpha = 0$, the Ising case; *ii)* $\alpha = 1$, the isotropic Heisenberg model; *iii)* $\alpha \to \infty$, the so called '$XY$-model'.

It is important to stress that the approach that will be proposed here is not perturbative, in spite that the Ising limit is considered as a departure point for its formulation. The method works successfully in the axial anisotropic regime, and is asymptotically exact for high anisotropy. Near the isotropic point, however, a delocalization transition occurs, and the linear spin wave theory becomes a better approximation when compared with exact results or numerical simulations [6]. However, the treatment can be extended in a variational way to account for the isotropic case, or the Heisenberg-$XY$ regime [7]. In particular, for two dimensions, isotropic exchange, and spin $S = 1/2$, the ground energy deviates less than 0.5% [7] from results obtained by elaborate Monte Carlo calculations [8].

## 2 The Wave Function

The Hamiltonian (1) is said to represent the so called $XXZ$ model, with the axial-anisotropy region confined to the interval $0 \leq \alpha < 1$. In the Ising limit ($\alpha = 0$), the ground state is of Néel type. For the infinite chain, there is a broken symmetry, and one of the two possible Néel states has to be chosen as a reference state. They both are connected by time inversion, the ground state of the infinite system being a doublet in the anisotropic region. The phase transition, with the presence of long-range order and a symmetry broken ground state, requires degeneracy. In contrast, in finite chains, the spectrum is not degenerate and the ground state is an eigenstate of the time-inversion operator (symmetric or antisymmetric, depending on the number of spins), with equal admixtures of both Néel kets.

For our developments here, we will choose the Néel state $|\mathcal{N}\rangle$, where the eigenvalues of the $S_z(m)$ operators for the linear chain are $\frac{1}{2}(-1)^m$. With the usual definition of spin ladder operators $S_\pm(m)$, we define boson-like operators by:

$$\phi_e^\dagger = \sqrt{\frac{2}{N}} \left\{ \frac{1}{4}\alpha N + \sum_{m \ even} S_+(m+1)S_-(m) \right\}, \tag{2}$$

$$\phi_o^\dagger = \sqrt{\frac{2}{N}} \left\{ \frac{1}{4}\alpha N + \sum_{m \ odd} S_+(m)S_-(m+1) \right\}, \tag{3}$$

where $N$ is the total number of sites in the chain. Operators defined by (2) and (3) flip pairs of neighboring spins when applied to the reference Néel state $|\mathcal{N}\rangle$. Two sequences with translational symmetry are possible, which we label by *even* and *odd*. It is apparent that a similar construction



C-6.

can be realized with the other Néel state $|\mathcal{N}\rangle'$ with $S_z \rightarrow \frac{1}{2}\,(-1)^{m+1}$, interchanging the roles of operators (2) and (3).

In the quasi-Ising limit, the ground state is close to $|\mathcal{N}\rangle$, and under this assumption we obtain the following algebra for the $\phi$'s:

$$\left[\phi_e, \phi_e^\dagger\right] = \left[\phi_o, \phi_o^\dagger\right] = 1, \quad [\phi_e, \phi_o] = \left[\phi_o, \phi_e^\dagger\right] = 0, \tag{4}$$

which are boson-like commutation relations. Within the same approximation, and restricting ourselves to the manifold $S_z = 0$, the Heisenberg Hamiltonian (1) can be written as a two-mode harmonic oscillator Hamiltonian [1]:

$$\mathcal{H} = J\left(\phi_e^\dagger \phi_e \; + \; \phi_o^\dagger \phi_o\right) \; + \; E_g(\alpha), \tag{5}$$

where $E_g(\alpha)$ is the ground state energy.

The Néel state satisfies the relations:

$$\phi_e|\mathcal{N}\rangle = \frac{1}{2}\alpha\sqrt{\frac{N}{2}}|\mathcal{N}\rangle, \quad \phi_o|\mathcal{N}\rangle = \frac{1}{2}\alpha\sqrt{\frac{N}{2}}|\mathcal{N}\rangle, \tag{6}$$

showing that the Néel state, or quasi-classical state, can be represented as a *Glauber state* [9], in terms of the $\phi$'s operators. The eigenvalue in (6), that also enters in the definitions (2,3), has been chosen so as to cancel the linear terms in Hamiltonian (5). Using a standard notation, we define *translation* operators by:

$$D(z) = \exp\left\{z\phi - z^*\phi^\dagger\right\}, \tag{7}$$

where $\phi$ may be the *even* or *odd* operator. A coherent state is thus obtained as:

$$|z_1, z_2\rangle = \exp\left\{z_1\phi_e - z_1^*\phi_e^\dagger\right\} \exp\left\{z_2\phi_o - z_2^*\phi_o^\dagger\right\}|0\rangle, \tag{8}$$

with $z_1, z_2$ two arbitrary complex numbers. If we write

$$z_1 = z_2 = \frac{1}{2}\alpha\sqrt{\frac{N}{2}},$$

we get a closed expression for the Néel state as a *minimum uncertainty wave packet* of the $\phi$'s operators. Of course, an equivalent representation can be constructed with the Néel ket as the vacuum, just by shifting the definitions of the $\phi$'s in a constant, and thus introducing linear terms in Hamiltonian (5).

Since the Néel state is a well defined state, we would like to represent the ground $|0>$, in terms of fluctuations over the Néel state $|\mathcal{N}\rangle$. This can be accomplished in closed analytic form, by inverting expression (8):

$$|0\rangle = \exp\left\{-\alpha\sqrt{\frac{N}{8}}\left(\phi_e^\dagger - \phi_e\right)\right\} \exp\left\{-\alpha\sqrt{\frac{N}{8}}\left(\phi_o^\dagger - \phi_o\right)\right\}|\mathcal{N}\rangle. \tag{9}$$

The structure displayed by (9) is quite interesting. Quantum fluctuations over the quasi-classical state $|\mathcal{N}\rangle$ are induced by the $\phi$'s operators. The distribution of fluctuations is Poissonian, the

anisotropy parameter $\alpha$ being related to the width of the wave packet. For $\alpha$ sufficiently small, the state (9) displays long-range order in spite of quantum fluctuations, but the effective magnetic moment is reduced from its saturation value. A vanishing magnetic moment signals at a phase transition as a function of the parameter $\alpha$.

In spite that the algebra given by (4) is obtained in the Ising limit, the trial state (9) results to be extremely accurate in describing the energy and correlation functions in the whole interval $0 \leq \alpha < 1$. The one dimensional case represents the most stringent test for the wave function, since, as we will sketch below, the accuracy of the method improves with the dimension [4]. The energy *per spin* and the staggered magnetic moment corresponding to our trial state (9) can be put in closed analytical form in terms of Bessel functions of integer order [5]:

$$E_g = \langle 0|\mathcal{H}|0\rangle = -\frac{J}{4}\left[J_0^2(2\alpha) + J_1^2(2\alpha) + 2\alpha J_1(2\alpha)\right], \tag{10}$$

$$M_z = \langle 0|S_z(m)|0\rangle = \frac{(-1)^m}{2} J_0(2\alpha). \tag{11}$$

The generalization to higher dimensions is rather straightforward [4]. If one assumes that the lattice is *bipartite*, *i.e.* not *frustrated* for Néel ordering, the corresponding boson-like operators are defined as:

$$\phi_\delta^\dagger = \sqrt{\frac{2}{N}} \sum_{\mathbf{R}} S_+(\mathbf{R}+\delta) S_-(\mathbf{R}) + \frac{\alpha}{2(z-1)} \sqrt{\frac{N}{2}} \tag{12}$$

where $\mathbf{R}$ labels sites in a sublattice, $\{\delta\}$ the set of nearest neighbors, and $z$ is the coordination number. The reference Néel state $|\mathcal{N}>$, in this case, assigns *up* spins to the $\mathbf{R}$ sublattice, and *down* spins to $\mathbf{R}+\delta$. The interesting formula is the analogue of (9) for the ground state:

$$|0\rangle = \exp\left\{-\frac{\alpha}{2(z-1)} \sqrt{\frac{N}{2}} \sum_\delta \left(\phi_\delta^\dagger - \phi_\delta\right)\right\} |\mathcal{N}\rangle. \tag{13}$$

Due to the $\frac{\alpha}{2(z-1)}$ factor in the exponential of (13), one realizes that the importance of quantum fluctuations diminishes with the coordination number $z$, and correspondingly with the dimensionality. However, closed form expression for arbitrary dimension and spin have not been obtained yet, even for the simplest lattice structure (like the square lattice) [10]. In spite of the above fact, using the Hellmann-Feynman theorem [5], one can show that the error in the energy, as calculated with the state (13), is proportional to $\alpha^4$. To go towards the isotropic point and to the Heisenberg-$XY$ region, one has to generalize the theory in a variational way [7].

# 3 The Jordan-Wigner transformation

The one-dimensional Heisenberg model for spin 1/2 can be mapped onto a spinless fermion model through the so called Jordan-Wigner transformation [11]. The two spin states are mapped onto fermion states with occupation numbers 0 and 1. Two fermions can not occupy a single site (one may think in a very large on-site Coulomb repulsion), and they hop in a lattice with nearest neighbors interactions. The transformation is accomplished by:

$$S_-(n) = \exp\left\{-i\pi \sum_{m<n} C_m^\dagger C_m\right\} C_m, \tag{14}$$

where the $C, C^\dagger$ are fermion operators. We readily obtain the relations:

$$S_+(m) \quad S_-(m+1) = C_m^\dagger C_{m+1},$$
$$S_+(m) \quad S_-(m) = S_z(m) + \frac{1}{2} = C_m^\dagger C_m = N_m,$$

that substituted in (1) yield the following fermion Hamiltonian:

$$\mathcal{H} = t \sum_m \left( C_m^\dagger C_{m+1} + h.c. \right) + V \sum_m \left( N_m - \frac{1}{2} \right) \left( N_{m+1} - \frac{1}{2} \right), \tag{15}$$

where $t = J\alpha/2, \quad V = J$. If $J > 0$, the fermion interaction $V$ is repulsive. For positive $\alpha$, Hamiltonian (15) describes hole-like fermions. An electron-like system is obtained by changing $\alpha \rightarrow -\alpha$. We already know that the properties of the Heisenberg Hamiltonian (1) are invariant under such a change [12]. Antiferromagnetic ordering implies that the total number of fermions is $\frac{N}{2}$, and the fermion ket that corresponds to the Néel state is the one with

$$\langle N_m \rangle = \frac{1}{2} [1 + (-1)^m].$$

We will call this state $|\mathcal{N}>$ to keep continuity with the previous sections. If one translates our ground state (9) into fermion language, one gets:

$$|0\rangle = \exp\left( -\frac{\alpha}{2} \mathcal{U} \right) |\mathcal{N}\rangle, \tag{16}$$

with

$$\mathcal{U} = \sum_m (-1)^m \left( C_{m+1}^\dagger C_m - C_m^\dagger C_{m+1} \right),$$

and mean occupation number given by

$$\langle 0 | N_m | 0 \rangle = \frac{1}{2} [1 + (-1)^m J_0(2\alpha)],$$

where $\alpha = 2t/V$. As in the spin case, most physical interesting quantities can be calculated in closed analytical form using the trial ket (16). For the fermion-fermion correlation functions, this has been done in Ref.[13]. A quantity which is important to investigate possible Fermi liquid behavior, is the one-particle momentum distribution [14]. In our case, this can be obtained analytically with (16), yielding:

$$\langle N_k \rangle_{holes} = \frac{1}{2} [1 - \sin(2\alpha \cos k)], \tag{17}$$

for hole-like fermions, and

$$\langle N_k \rangle_{part} = \frac{1}{2} [1 + \sin(2\alpha \cos k)], \tag{18}$$

for a particle-like system. The above distributions display a soft variation with the wave number $k$, and therefore no Fermi liquid behavior. The highly correlated limit $\alpha \rightarrow 0$, yields the constant value $1/2$, with the complete destruction of the Fermi surface of non-interacting particles.

# 4 Acknowledgments

The author acknowledges support from Fundação de Amparo à Pesquisa do Estado de São Paulo (FAPESP, Brazil), and Fundo de Apoio ao Ensino e Pesquisa (FAEP, UNICAMP, Brazil).

# References

[1] M. Lagos and G. G. Cabrera, Phys. Rev. B **38**, 659 (1988).

[2] H. A. Bethe, Z. Phys. **71**, 205 (1931); R. Orbach, Phys. Rev. **112**, 309 (1958); M. Gaudin, *La fonction d'onde de Bethe*, (Masson, Paris, 1983).

[3] D. Medeiros and G. G. Cabrera, Phys. Rev. B **43**, 3703 (1991); *ibid.* **44**, 848 (1991).

[4] G. G. Cabrera, M. Lagos, and M. Kiwi, Solid State Commun. **68**, 743 (1988).

[5] D. Gottlieb and M. Lagos, Solid State Commun. **79**, 551 (1991).

[6] G. G. Cabrera, Phys. Rev. B **43**, 13476 (1991).

[7] D. Gottlieb, M. Lagos, and M. Montenegro, Solid State Commun. **81**, 729 (1992).

[8] T. Barnes, D. Konchan, and E. S. Swanson, Phys. Rev. B **39**, 4357 (1989).

[9] R. Glauber, Phys. Rev. **131**, 2766 (1963).

[10] It appears that this problem is related to the formulation of the Wigner-Jordan transformation in two dimensions. See for example, Y. R. Wang, Phys. Rev. **46**, 151 (1992).

[11] P. Jordan and E. Wigner, Z. Phys. **47**, 631 (1928); E. Lieb, T. Schultz and D. Mattis, Ann. Phys. (N. Y.) **16**, 407 (1961).

[12] J. des Cloiseaux and M. Gaudin, J. Math. Phys. **7**, 1384 (1966).

[13] M. Lagos, M. Kiwi, E. R. Gagliano, and G. G. Cabrera, Solid State Commun. **67**, 225 (1988).

[14] G. G. Cabrera, to be published.

# BERRY PHASE IN HEISENBERG REPRESENTATION

**V.A. Andreev, A.B. Klimov**
*Optics Division*
*Levedev Institute of Physical Sciences*
*Moscow 117924*
and
**P.B. Lerner**
*T-4, MS K723*
*Los Alamos National Laboratory*
*Los Alamos, NM 87545*

**Abstract**

We define the Berry phase for the Heisenberg operators. This definition is motivated by the calculation of the phase shifts by different techniques. These techniques are: the solution of the Heisenberg equations of motion, the solution of the Schrödinger equation in coherent-state representation, and the direct computation of the evolution operator. Our definition of the Berry phase in the Heisenberg representation is consistent with the underlying supersymmetry of the model in the following sense. The structural blocks of the Hamiltonians of supersymmetrical quantum mechanics ("superpairs") [1,2] are connected by transformations which conserve the similarity in structure of the energy levels of superpairs. These transformations include transformation of phase of the creation-annihilation operators, which are generated by adiabatic cyclic evolution of the parameters of the system.

# 1 INTRODUCTION

The equivalence of the Schrödinger and Heisenberg pictures in quantum mechanics is something that is taken for granted. The specific choice of the Schrödinger, Heisenberg or interaction picture is usually regarded as a matter of convenience. Berry phase was defined initially and mostly for the Schrödinger picture as nonintegrable phase factor appearing in the wave-function after (adiabatic) evolution of the system's parameters. Here we investigate how one should define the analog of the Berry phase in the Heisenberg representation.

The traditional introduction to Berry phase includes the following construction. The Hamiltonian for the particular system $H(\vec{\lambda})$ is introduced, where the set of parameters, $\vec{\lambda}$, is considered to be changing adiabatically with time. Until now, most of the applications had in mind the discrete, though maybe degenerate, spectrum of the Hamiltonian, for all values of the paramters. Then, after the adiabatic cyclic evolution of the parameters, each eigenstate $\psi_n$ of a corresponding stationary problem

$$H(\vec{\lambda})\psi_n = E_n(\vec{\lambda})\psi_n \tag{1}$$

acquires a nonintegrable phase: $\psi_n \rightarrow e^{i\phi_n}\psi_n$. This phase usually admits geometric interpretation in terms of some contour in parameter space.

In the Heisenberg representation, the operators of observables, and not the eigenstates, do evolve in time. One can assume, that for particular observable, $a(t)$, the cyclic evolution of parameters results in the following relation after the period, $T$:

$$a(T) = S^{\dagger}a(0)S, \tag{2}$$

where $S$ is a unitary operator.

One supposes, that the operator, $S^{\dagger}$, in a basis of the eigenfunctions of the Eq. (1) has the form:

$$S^{\dagger} = \begin{pmatrix} e^{i\phi_0} & 0 & 0 & \cdots \\ 0 & e^{i\phi_1} & 0 & \cdots \\ \vdots & \vdots & \vdots & \vdots \\ 0 & \cdots & e^{i\phi_n} & \cdots \end{pmatrix} \tag{3}$$

It represents what can be naturally called matrix of a Berry phase in Heisenberg picture, although now it is a *unitary operator*, not a number. The rest of this paper is dedicated to demonstrating the usefulness of this notion.

We shall demonstrate for a simple exactly solvable model that this operator can be defined consistent with the (super)symmetry of a model. We cannot prove it in a general way, though we believe that the following proposition is true for any Hamiltonian $H$, for which Berry phase could be defined. Namely, if there exists the Hamiltonian, $H_1(\vec{\lambda}(t))$, after adiabatic cyclic transformation of its parameters it will be transformed into new Hamiltonian, $H_2$, which is a *superpair* to the initial Hamiltonian, $H_1$. The adiabatic theorem reappears in this approach as the identity of the eigenvalues of $H_1$, and $H_2$ (however, the degeneracy of zero eigenvalue, in general, may change). The wavefunctions, may, however undergo some unitary transformation.

This is in accord with general ideology of supersymmetric quantum mechanics, which usually includes the compound Hamiltonian, $\mathbf{H}$ , formed by two simpler Hamiltonians, $H_1$ and $H_2$ [1,2,3,4],

$$\mathbf{H} = \begin{bmatrix} H_1 & 0 \\ 0 & H_2 \end{bmatrix} \tag{4}$$

The properties of the Hamiltonians, $H_1$ and $H_2$, are closely related. Normally, these Hamiltonians have identical spectral structure, but, perhaps, only a finite number of energy levels. Consequently, almost all of the levels of the Hamiltonian $\mathbf{H}$ are doubly degenerate.

Previously [5], in this context, we studied the supersymmetric structure of the Jaynes-Cummings Model (JCM). The formal introduction of the supersymmetry in the JCM includes the replication of the JCM with a trivial phase transformation performed on the creation-annihilation operators of the boson:

$$a \rightarrow e^{i\phi}a, a^{\dagger} \rightarrow a^{\dagger}e^{-i\phi} \tag{5}$$

When $\phi$ is a real function of time, the Hamiltonians, $H_1$ and $H_2$, have identical spectra, and all the energy levels of the Hamiltonian $H$ are doubly degenerate.

The physical meaning of the phase shift, $\phi$, is not clear. It would be desirable to interpret it, analogous to Berry's interpretation of the Aharonov-Bohm effect [6], as a manifestation of a Berry

phase. Indeed, the JCM has a nontrivial Berry phase with potentially observable ramifications [7,8]. The interpretation of the phase shift (5) as Berry phase for some cyclic evolution in the JCM is not yet proven, however we demonstrate that this is true for somewhat simpler model of Section 3.

Thus, for our purposes we seek the transformations of phases of the Hermitian operators rather than wavefunctions. Therefore, we calculate Berry phase for our model using both the Schrödinger formalism for the wavefunctions and the Heisenberg formalism for the operators. Also, we calculate the phase shifts by an explicit expression of the evolution operator through SU(1,1) group operators. Both approaches are shown to be equivalent as the result of our analysis.

Because performing the adiabatic cyclic evolution of the system can be, under certain conditions, a valid quantum measurement, the result of the paper can be put in other form. Namely, the distinguishability of the systems described by the Hamiltonians forming a superpair is equivalent to the nontriviality of the Berry phase obtained during a cyclic evolution of the system's parameters. The separate measurements of the Berry phase of those two systems during the evolution distinguishes these systems.

The structure of paper is as follows. In Section II, we make a general definition of the cyclic evolution in the Heisenberg representation. In Section III, the supersymmetric family of Hamiltonians, similar to the Hamiltonian for degenerate parametric two-photon optical interaction, is considered. The calculation of the evolution of the Heisenberg operators shows that besides the dynamic phase shift (called self-modulation of phase in nonlinear optics) and amplitude change (amplification and de-amplification), there is an additional term. Unlike the previous ones this term has a nonzero value in the case of adiabatic cyclic evolution. However, the explicit proof of the identity of this phase to the phase, which is obtained by the wavefunction in course of adiabatic cyclic evolution is required. This is done by obtaining the explicit WKB solution of the Schrödinger equation in the coherent state formalism and comparing the results (Section IV). Following the recent tradition supported by the papers of Aharonov and Anandan, and Samuel and Bhandari [9,10] we identify the "slow" physical time of adiabatic evolution as a parameter of a closed contour. This definition is supported by the calculation of the Berry phase from Heisenberg equation of motion and through the explicit expression of the evolution operator in Section V.

# 2 BERRY PHASE IN THE HEISENBERG PRESENTATION

We consider the Hamiltonian, $H$, with time-dependent parameters, $\vec{\lambda}(t)$:

$$H = H(\vec{\lambda}(t)). \tag{6}$$

We assume that periodicity and adiabaticity of the evolution of the Hamiltonian can be represented in two ways. First, one can follow the evolution of $H(t)$ as a function of the time-dependent parameters. In this case, the Hamiltonian will undergo trivial transformation after the evolution.

$$H(0) = H(T) \tag{7}$$

The second way is to consider the change of the Hamiltonian as an observable with physical meaning of energy under the action of the evolution operator $U(t)$ which is engendered by the

Hamiltonian $H(t)$

$$\tilde{H}(t) = U^{-1}(t)H(0)U(t) \tag{8}$$

$$U(t) = Texp(i\int^t H(t)dt) \tag{9}$$

In this case the transformed Hamiltonian $\tilde{H}(T)$ can be different, unitarily equivalent to the initial Hamiltonian.

$$\tilde{H}(T) = U^{-1}(T)H(T)U(T) \tag{10}$$

The spectra of these Hamiltonians are therefore identical. However, other features can be different. This distinction can be extremely important if there are lines of singularity or other topological complications in the space of parameters.

In the case of adiabatic cyclic evolution, this operator doesn't depend on particular law of evolution of the system's parameters and we shall define this unitary operator as Berry phase in Heisenberg representation. It implies, that the difference from $\tilde{H}(T)$ and $H(T)$ can be expressed in terms of certain phase factors (eigenvalues of the operator $U(T)$). As a rule, they appear for a certain components of the Hamiltonian $H$. These phases are closely connected with the Berry phases in Schrödinger representation, indeed, in the example of the Section III they are identical.

The fact that the Hamiltonians $H(t)$ and $\tilde{H}(T)$ are forming a superpair is of primary importance. One of the simplest ways of representation follows from Eq. (7), which connects $H(T)$ and $\tilde{H}(T)$

$$H = \begin{pmatrix} H(T) & 0 \\ 0 & \tilde{H}(T) \end{pmatrix} = \begin{pmatrix} 0 & \sqrt{H}(0)U(t) \\ U^{-1}(T)\sqrt{H}(0) & 0 \end{pmatrix}^2 \tag{11}$$

One can then demonstrate using the formalism of that relationship implies superstructure [2,3]. This relation holds only in the case of nonnegative spectra of the Hamiltonians. Thus, we restrict ourselves by the Hamiltonians bounded from below, in which case we shift the zero level of energy to avoid negative eigenvalues.

The superstructure could be introduced in more sophisticated ways. A particular example would be demonstrated as well. The paper is dedicated to the connection between Berry phase and supersymmetry on the example of the simple model. More complicated examples such as the Jaynes-Cummings model (JCM) will be studied elsewhere.

In the paper [11], the authors proposed the generalization of Berry's concept, interpreting their phase, a factor similar to our symbol $V$ (Eqs. (20)-(21)), as a gauge transformation of the wavefunction. It is induced by the reparametrization of the Hamiltonian. The main result of this paper can be formulated in our language in the following way. The gauge transformation of Wilzcek and Zee while being applied to the Hamiltonian, regarded as observable, can result in other Hamiltonian, even if the evolution is adiabatic and cyclic. However, both Hamiltonians are unitary equivalent and the observable quantities are identical for both of them. The adiabatic theorem in the general quantum mechanics formalism is represented by supersymmetry in our paper and by the gauge invariance in their formalism.

# 3 BOSONIC FIELDS WITH SELF-ACTION: THE SUPERSYMMETRY OF THE SQUEEZING HAMILTONIANS

The problem is formulated for the simple model of two identical noninteracting bosonic fields described by the Hamiltonian

$$H_1 = \omega a^\dagger a \hat{I} + |\lambda| a^2 \begin{pmatrix} e^{i(\phi+\Theta)} & 0 \\ 0 & e^{i(\tilde{\phi}+\tilde{\Theta})} \end{pmatrix} + |\lambda| a^{\dagger 2} \begin{pmatrix} e^{i(\phi+\Theta)} & 0 \\ 0 & e^{-i(\tilde{\phi}+\tilde{\Theta})} \end{pmatrix} \begin{pmatrix} 1-c & 0 \\ 0 & c \end{pmatrix} \omega \tag{12}$$

The superpair of this Hamiltonian is

$$H_2 = \omega a^\dagger a \hat{I} + |\lambda| a^2 \begin{pmatrix} e^{i(\tilde{\phi}+\tilde{\Theta})} & 0 \\ 0 & e^{i(\phi+\Theta)} \end{pmatrix} + |\lambda| a^{\dagger 2} \begin{pmatrix} e^{-i(\tilde{\phi}+\tilde{\Theta})} & 0 \\ 0 & e^{-i(\phi+\Theta)} \end{pmatrix} + \begin{pmatrix} 1-c & 0 \\ 0 & c \end{pmatrix} \omega \tag{13}$$

The constant $c$ is defined from the equation

$$c(1-c) = \frac{|\lambda|^2}{\omega^2}$$

The system described by the Hamiltonian $\mathbf{H}$ in the form (4), where $H_1$ and $H_2$ have the form (12) and (13), respectively, are supersymmetric. This supersymmetry is generated by the following supercharges [5]:

$$Q = \begin{pmatrix} 0 & q_1 \\ q_2 & 0 \end{pmatrix}, Q^2 = H \tag{14}$$

$$q_1 = \begin{pmatrix} 0 & e^{i\phi} \\ |\lambda| e^{i\tilde{\Theta}} & 0 \end{pmatrix} a + \begin{pmatrix} 0 & \frac{c\omega}{|\lambda|} e^{-i\Theta} \\ (1-c)\omega e^{-i\phi} & 0 \end{pmatrix} a^\dagger \tag{15}$$

$$q_2 = \begin{pmatrix} 0 & e^{i\tilde{\phi}} \\ |\lambda| e^{i\Theta} & 0 \end{pmatrix} a + \begin{pmatrix} 0 & \frac{c\omega}{|\lambda|} e^{-i\tilde{\Theta}} \\ (1-c)\omega e^{-i\phi} & 0 \end{pmatrix} a^\dagger \tag{16}$$

$$H_1 = q_1 q_2 \quad H_2 = q_2 q_1 \tag{17}$$

The second supercharge has the form

$$Q_2 = \begin{pmatrix} 0 & -iq_1 \\ iq_2 & 0 \end{pmatrix} \tag{18}$$

This finishes the formal description of supersymmetry. The procedure of assigning a supersymmetric structure for an initial model remind our prescription for the JCM [5]. One should make a constant phase shift of the creation and annihilation operators and consider a replica of the initial system with transformed operators as a superpair for the initial system.

The described procedure has an obscure physical meaning. To clarify it we explicitly describe the unitary operator, which connects the components of the Hamiltonian in subsequent sections.

# 4 THE OPERATOR BERRY PHASE

Now we are prepared to study the Berry phase of the Heisenberg operators. We suppose the three parameters $\omega, Re\lambda, Im\lambda^*$ to undergo adiabatic periodic change in time. First, we calculate the nonintegrable phase attained by the wavefunction of the model, described in previous Sections, in coherent-state representation. Below, we shall demonstrate, that all the components of the Hamiltonian **H**, defined by Eqs. (12) and (13) can be obtained from one component of this Hamiltonian by applying the adiabatic cyclic evolution of the parameters of the system. Thus, the superpairs are connected by a unitary operator, which we call the Berry phase in Heisenberg representation. A single component of the Hamiltonian **H**, corresponds to the Schrödinger equation

$$i\frac{d}{dt}U = [\omega a^\dagger a + \lambda a^2 + \lambda^* a^{\dagger 2} + h_0]U \tag{19}$$

The contribution of the scalar term $h_0(t)$ is removed by the transformation

$$U = Vexp(i\int^t h_0(\tau)d\tau) \tag{20}$$

The wavefunction V is represented in the coherent state formalism by

$$V(\alpha*,\beta,t) = \langle\alpha|Texp(i\int^t (h-h_0)d\tau)|\beta\rangle \tag{21}$$

where $T$ is time ordering and $|\alpha\rangle, |\beta\rangle$ are coherent states:

$$a|\alpha\rangle = \alpha|\alpha\rangle \;\; a|\beta\rangle = \langle\alpha|a^\dagger = \langle\alpha|\alpha^* \tag{22}$$

For the quadratic Hamiltonian (5) the calculations can be done explicitly. The solution $V(\alpha^*,\beta,t)$ of the Eq. (19) in the coherent-state formalism has the form

$$V(\alpha^*,\beta,t) = (\xi(t))^{-1/2}exp[\frac{1}{2}\alpha^{*2}\frac{\eta}{\xi} + \alpha^*\beta\frac{1}{\xi} + \frac{1}{2}\beta^2\frac{\eta*}{\xi}] \tag{23}$$

where a,b are the parameters of the initial state. As usual for coherent-state representations [12], the solution is expressed in terms of auxiliary functions $\xi(t), \eta(t)$ which satisfy the following system of the equations [13]:

$$\begin{aligned} \dot{\xi}(t) &= i(\xi\eta - 2\eta\lambda) \\ \dot{\eta}(t) &= i(\lambda^*\xi - \eta\omega) \end{aligned} \tag{24}$$

with the initial conditions $\xi(0) = 1, \eta(0) = 0$.

The following system of equations is valid for the functions $\xi, \eta$

$$\ddot{\eta} - \frac{\lambda^*}{\lambda^*}\eta + [i\dot{\omega} - i\omega\frac{\dot{\lambda}^*}{\lambda^*} + \omega^2 - 4|\lambda|^2]\eta = 0.$$
$$\ddot{\xi} - \frac{\dot{\lambda}}{\lambda}\dot{\xi} + [i\dot{\omega} + i\omega\frac{\dot{\lambda}}{\lambda} + \omega^2 - 4|\lambda|^2]\xi = 0. \tag{25}$$

Below we shall demonstrate that WKB-solution of these equations will provide a multiplier with a nonintegrable phase.

The Hamiltonians $H_1, H_2$ include the creation-annihilation operators distinguished by some deterministic phase shift. For a description of the evolution of these operators we use one of the four components of the Hamiltonian $\mathbf{H}$, because all four Hamiltonians are independent and unitary-equivalent to each other,

$$h = \omega a^\dagger a + \lambda a^2 + \lambda^* a^{\dagger 2} + h_0,$$
$$\lambda = |\lambda| e^{i(\phi+\Theta)} \tag{26}$$

The Heisenberg equations have the form [14],

$$\begin{aligned} \dot{a} &= i[h, a] \\ \dot{a}^\dagger &= i[h, a^\dagger] \\ \dot{a} &= -i(\omega a + 2\lambda^* a^\dagger) \\ \dot{a}^\dagger &= i(\omega a^\dagger + 2\lambda a). \end{aligned} \tag{27}$$

It is again assumed that the parameters $\omega, \lambda, \lambda^*$ are slowly varying periodic functions of time. The operators $a, a^\dagger$ are satisfying the following equations:

$$\ddot{a} - \frac{\dot{\lambda}^*}{\lambda^*}\dot{a} + [i\dot{\omega} - i\omega\frac{\dot{\lambda}^*}{\lambda^*} + \omega^2 - 4|\lambda|^2]a = 0,$$
$$\ddot{a}^\dagger - \frac{\dot{\lambda}}{\lambda}\dot{a}^\dagger + [-i\dot{\omega} + i\omega\frac{\dot{\lambda}}{\lambda} + \omega^2 - 4|\lambda|^2]a^\dagger = 0. \tag{28}$$

One observes that equations (25), for the functions $\xi, \eta$ are identical to the system of equations (28) for the operators $a^\dagger, a$. By substitution

$$a = b exp(\frac{1}{2}\int^t \frac{\dot{\lambda}^*}{\lambda^*} d\tau) \tag{29}$$

one obtains for operator $b$ and its Hermitian conjugate, if the terms $(\dot{\lambda}^*/\lambda^*)^2, \frac{d}{dt}(\dot{\lambda}^*/\lambda^*)$ in the equation for $b$ are neglected

$$\ddot{b} + [i\dot{\omega} - i\omega\frac{\dot{\lambda^*}}{\lambda^*} + \omega^2 - 4|\lambda|^2]b = 0,$$

$$\ddot{b}^\dagger + [-i\dot{\omega} + i\omega\frac{\dot{\lambda}}{\lambda} + \omega^2 - 4|\lambda|^2]b^\dagger = 0. \tag{30}$$

The WKB approximation for the solution of Eqs. (28) yields

$$b = \frac{b_1(0)}{\sqrt{\Omega}} exp(\int_0^t (f(\tau) + i\psi(\tau))d\tau) + \frac{b_2(0)}{\sqrt{\Omega}} exp(\int_0^t (f(\tau) - i\psi(\tau)d\tau), \tag{31}$$

with

$$\begin{aligned} \Omega^2 &= \omega^2 - 4|\lambda|^2 \\ f(t) &= \frac{\dot{\omega} - \omega\frac{\dot{\rho}}{\rho}}{4(\omega^2 - 4\rho^2)^{1/2}} = \frac{\frac{d}{dt}(\frac{\omega}{\rho})}{4(\frac{\omega}{\rho} - 4)^{1/2}}, \rho = |\lambda|, \\ \psi(t) &= \omega\frac{(\dot{\phi} + \dot{\Theta})}{4\Omega} = \frac{\omega\dot{\kappa}}{4\Omega}dt, \end{aligned} \tag{32}$$

For cyclical evolution of the parameters the contribution of the function $f(t)$ is zero, because it is an exact differential. However, the integral of the function $\psi(t)$ yields the Berry phase.

$$\phi_B = \int_C \frac{\omega\dot{k}}{4\Omega}dt, \tag{33}$$

and $\tilde{\phi}_B$ is given by the same expression with $k \to \tilde{k} = \tilde{\phi} + \tilde{\Theta}$. The initial conditions can be chosen in such a way, that the phase transformations of the operators take place as a result of the evolution

$$a \to ae^{i\phi_B}, a^\dagger \to a^\dagger e^{-i\phi_B}, \tag{34}$$

then

$$h \to h = \omega a^\dagger a + \lambda a^2 e^{2i\phi_B} + \lambda^*(a^\dagger)^2 e^{-2i\phi_B}, \tag{35}$$

The calculation of the Berry phase for the model Hamiltonian **H** is now complete.

One observes that the superpairs $H_1$ and $H_2$, composing the supersymmetric Hamiltonian **H**, are distinguished by the Berry phase. As the Hamiltonian $H_2$ transforms as a result of cyclic evolution, the phases $(\phi + \Theta)$ and $(\tilde{\phi} + \tilde{\Theta})$ evolve in a different way. Berry phase is independent of the particular law of evolution, nevertheless it depends on the choice of the contour in parameter space. The contours can be chosen in such a way that the following relation is valid [15].

$$\phi + \Theta + \phi_B = \tilde{\phi} + \tilde{\Theta}, \tilde{\phi} + \tilde{\Theta} + \tilde{\phi}_B = \phi + \Theta$$

or

$$\phi_B = -\phi_B = (\tilde{\phi} - \phi) + (\tilde{\Theta} - \Theta) \tag{36}$$

Now we have found the geometric phase for the Hamiltonian **H** using the Heisenberg representation.

# 5 THE CALCULATION OF THE BERRY PHASE USING EVOLUTION OPERATOR

We have shown that creation-annihilation operators obtain phase shift according to Eqs. (34)-(35) as a result of adiabatic cyclic evolution which is identical with the Berry phase gained by the coherent phase. The substitution of the transformed operators in the Hamiltonian $h$ gives

$$h \to h_p = \omega a^\dagger a + \lambda a^2 e^{2i\phi} + \lambda a^{+2} e^{-2i\phi} + h_0 \tag{37}$$

This result can be obtained directly from computation of the action of evolution operator on Hamiltonian **H**.

One can rewrite the Hamiltonian **H** in the terms of SU(1,1) operators [16,17]:

$$h = \omega K_0 + \lambda K_- + \lambda^* K_+, \tag{38}$$

where

$$K_0 = 1/2(a^\dagger a + aa^\dagger), K_- = a^2, K_+ = (a^\dagger)^2$$
$$[K_0, K_+] = +K_+, [K_0, K_-] = -K_-, [K_+, K_-] = 2K_0. \tag{39}$$

To get rid of the T-exponent in the evolution operator:

$$U = Texp(\int^t h(\tau)d\tau),$$

one can rewrite it in the form [12]:

$$U = e^{\alpha K_+} e^{\beta K_0} e^{\gamma K_-}. \tag{40}$$

This decomposition expresses the evolution operator in terms of three time-dependent functions $\alpha(t), \beta(t) and \gamma(t)$. Using the commutation relations one obtains the following equations for these functions:

$$\begin{aligned} \dot{\alpha} - \alpha\beta + \alpha^2\gamma e^{-\beta} &= -i\mu^* \\ \dot{\beta} - 2\alpha\dot{\gamma}e^{-\beta} &= -i\omega \\ \dot{\gamma}e^{-\beta} &= i\mu. \end{aligned} \tag{41}$$

The quantity $\alpha(t)$ satisfies the equation

$$\dot{\alpha} + i\omega\alpha + i\mu\alpha^2 = -i\mu^*, \tag{42}$$

which can be rewritten after the substitution $\alpha = (1/i\mu)(\dot{\psi}/\psi)$ in the form

$$\begin{aligned} \ddot{\psi} &+ \dot{\psi}(-\frac{\dot{\mu}}{\mu} + i\omega) - |\mu|^2\psi = 0 \\ \kappa &= \psi exp[\frac{1}{2}\int^t d\tau(-\frac{\dot{\mu}}{\mu} + i\omega)] \\ \ddot{\kappa} &+ \kappa[\omega^2 - 4|\mu|^2 + i\omega\frac{\dot{\mu}}{\mu} - i\dot{\omega}] = 0. \end{aligned} \tag{43}$$

The equations (43) coincide in the form with the equations (25), (28) which were our starting point of obtaining expression of the Berry phase. The phase given by the equation (43) is identical to the Berry phase as defined above. Now one can study the behavior of the functions $\alpha, \beta, \gamma$ under cyclic adiabatic evolution of the parameters. The function $\kappa$ is the solution of the equation with the periodic potential. This implies that this function is quasiperiodic:

$$\kappa(t+T) = e^{i\phi_T}\kappa(t), \tag{44}$$

where $\phi_T$ is independent of t. Thus the ration $\dot{\kappa}/\kappa$ is a periodic function as well.

The function $\beta = -i\int d\omega - ln\psi$ is not periodic. According to Eq. (32) after the cyclic evolution $\beta$ changes by a constant $\phi_T$

$$\beta \to \beta - i\phi_T. \tag{45}$$

The function $\gamma$ is not periodic as well, however, it is not very important to us here.

One can now investigate the transformation of the primary Hamiltonian $h$ in course of evolution. Since we decomposed $h$ in the sum of three operators $K_0, K_+, K_-$, we can consider the action of the evolution operator on the single terms of the sum. It is quite necessary for Eqs. (41) not to be symmetrical with respect to the functions $\alpha, \beta, \gamma$. We can use the decomposition from Eq. (40) only for the study of the transformation of the operator $K_-$ :

$$\tilde{K}_-(T) = U^{-1}(T)K_-(0)U(T). \tag{46}$$

The initial conditions of the evolution were chosen as $\alpha(0) = \beta(0) = 0$ as a consequence of periodicity it implies $\alpha(T) = 0$. This means that $e^{\alpha K_+}$ and $e^{\gamma K_-}$ do not contribute to the periodic evolution of group operators. The only term with which changes is $e^{\beta K_0}$. Taking into account their relation $\beta(T) = -\phi_T$ one has

$$\tilde{K}_-(T) = e^{2i\phi_T a^\dagger a}K_0(0)e^{-2i\phi_T a^\dagger a} = e^{-2i\phi_T}K_0(0). \tag{47}$$

Similarly, choosing a different order of multiplication in the decomposition (40) one gets the transformation property for the other operators.

$$\begin{aligned} \tilde{K}_+(T) &= e^{2i\phi_T}K_+(0) \\ \tilde{K}_0 &= K_0(0). \end{aligned} \tag{48}$$

Consequently, the Hamiltonian $H$ is transformed under the evolution as

$$\begin{aligned} h \to h_\phi &= \omega K_0 + \lambda e^{-2i\phi_T}K_- + \lambda^* e^{2i\phi_T}K_+ \\ &= \omega a^\dagger a + \lambda e^{-2i\phi_T}a^2 + \lambda^* e^{2i\phi_T}(a^\dagger)^2 + h_0. \end{aligned} \tag{49}$$

This expression is the same one we obtained from the WKB solution of the operator equations (28). The phase shift is identical to the phase shift gained by coherent-state representation of the wavefunction. The reconciliation of all methods proved the correctness of the definition of Berry phase in Heisenberg picture. Because all of the components of the Hamiltonian **H** can be

obtained through the constant phase shift of the creation-annihilation operators or sign reversal of the phase factors $\Theta, \phi$ we finish up with the proposition that the trivial phase shifts in the supersymmetric Hamiltonian can be regarded as the Berry phases.

# 6 CONCLUSION

The present paper proposes the following definition of Berry phase in Heisenberg representation. Berry phase is the unitary operator connecting the Hamiltonian of the system with the initial Hamiltonian after adiabatic cyclic evolution of the system's parameters. We study the simplest model in which this unitary operator is independent of the particular quantum numbers of the system and reduces to a certain c-number phase factor. This definition is motivated by the identification of this number to the adiabatic phase factor gained by the wavefunction of the system in coherent-state representation. Since the model is exactly soluble, the direct computation of the evolution operator is possible and it confirms the calculations made by two other different methods: the WKB solution of the Heisenberg equations and the WKB-solution of the Schrödinger equation in coherent-state representation. This definition allows us to interpret the supersymmetric compound Hamiltonian as if it has been formed by images of the initial Hamiltonian, obtained as a result of an adiabatic cyclic evolution over a different contours in a parameter space.

# 7 ACKNOWLEDGEMENTS

The early stages of this work were sponsored in part by the University of Michigan Distinguished Visitors' fund and the Office of Naval Research Initiative for Accelerated Research.

# References


[1] E.Witten, Nucl. Phys. B 185 (1981) 513.

[2] A. Lesniewski, M. Lewenstein, A. Jaffe, Ann. Physics 78 (1987)

[3] I.E. Gendenstein, I.V. Krive Sov. Phys.-Uspechi 28 (1985) 645.

[4] R.W. Haymaker, A.R.P. Rau Am. Journ. Phys. 54 (1986) 928.

[5] Andreev V.A., Lerner P.B., Phys. Lett. A. 134 (1989) 507.

[6] Berry M.V. Proc. Roy. Soc. A 392 (1984) 45.

[7] Andreev V.A. Klimov A.B. Lerner P.B. JETP Lett, 50 (1989)

[8] ibid., Europhysics Lett. 12 (1990) 101.

[9] Y. Aharonov. J. Anandan. Phys. Rev. Lett. 58 (2986) 1574.

[10] J. Samuel, R. Bhandari, Phys. Rev. Lett. 60 (1988) 2339.

[11] F. Wilczek A. Zee, Phys. Rev. Lett. 52 (1984) 2111.

[12] A.M. Perelomov. *Coherent states and their applications.* (Springer-Verlag, Berlin, 1986.)

[13] Dodonov V. V., Man'ko V.I. Sov. Phys. Proc. FIAN, 183, (1988) 71.

[14] Abdalla M.S., Ahmed M.M.A., Obada A.-S.F. Physics A 162 (1990) 215.

[15] Andreev V.A., private communication

[16] K. Wodkiewicz, J.H. Eberly, JOSA B2 (1985) 458.

[17] Chris C. Gerry, P.K. Ma, E.R. Vrscay Phys. Rev. Lett. A 39 (1989) 668.

# SECTION 7

# INTERACTION OF LIGHT AND MATTER

# QUANTUM PROPAGATION IN SINGLE MODE FIBER

Lance G. Joneckis
*Laboratory for Physical Sciences*
*University of Maryland*
*College Park, MD 20740*

Jeffrey H. Shapiro
*Department of Electrical Engineering and Computer Science*
*Massachusetts Institute of Technology*
*Cambridge, MA 02139-4307*

**Abstract**

This paper presents a theory for quantum light propagation in a single-mode fiber which includes the effects of the Kerr nonlinearity, group-velocity dispersion, and linear loss. The theory reproduces the results of classical self-phase modulation, quantum four-wave mixing, and classical soliton physics, within their respective regions of validity. It demonstrates the crucial role played by the Kerr-effect material time constant, in limiting the quantum phase shifts caused by the broadband zero-point fluctuations that accompany any quantized input field. Operator moment equations—approximated, numerically, via a terminated cumulant expansion—are used to obtain results for homodyne-measurement noise spectra when dispersion is negligible. More complicated forms of these equations can be used to incorporate dispersion into the noise calculations.

## 1 Introduction

Optical fibers have long been considered for the generation of squeezed-state light, starting with the pioneering work of Levenson and coworkers in the mid 1980's, who observed 0.58 dB of continuous-wave (cw) squeezing [1], to recent measurements exhibiting over 5 dB of short-pulse squeezing [2]. In this paper we present a theory for quantum light propagation in single-mode optical fiber. Our development, which includes the effects of the Kerr nonlinearity, group-velocity dispersion, and linear loss, is guided by two overarching principles: the theory must include all relevant prior results, both classical and quantum mechanical, and, within reasonable limits, it must accommodate arbitrary input states. This theory [3] is an extension of our prior work on quantum propagation in a dispersionless, lossless, Kerr medium [4]. In that earlier study it was shown that a material time constant is crucial to a correct description of quantum nonlinear phase shifts beyond the four-wave mixing regime, a conclusion similar to that reached by Blow and coworkers [5]. The use of a finite Kerr-effect time constant is retained in the current treatment of lossy, dispersive fiber.

This paper is organized as follows. In Section 2 we review quantum propagation in a Kerr medium, concentrating on the structure of the theory and the necessity of a finite Kerr-effect time constant. We recount the principal result of [4], namely the limits on squeezed-state generation

in lossless, dispersionless fiber. Section 3 expands this theory to incorporate dispersion and linear loss via a split-step approach. Section 4 introduces the terminated cumulant expansion (TCE) as a technique for closing the infinite chain of coupled moment equations generated by the full theory. Using the TCE, the limits on quadrature-noise squeezing in lossy, dispersionless fiber are quantified. Finally, in Section 5, we discuss the relationship of our approach to other quantum propagation theories for single-mode fiber, focusing on the necessity of the Kerr-effect time constant.

## 2 Quantum Self-Phase Modulation

Our attention, in this section, is restricted to a linearly polarized field propagating in a lossless, dispersionless, single-mode fiber that exhibits the Kerr nonlinearity. Classically, the refractive index in this fiber can be written as follows,

$$n(z,t) = n_0 + \frac{n_2 \hbar\omega}{A}|E(z,t)|^2, \tag{1}$$

where $z$ is the axial coordinate along the fiber, $t$ is time, $n_0$ is the linear refractive index, $n_2$ is the Kerr coefficient, $A$ is the fiber's effective cross-sectional core area, and $E(z,t)$ is the normalized complex envelope of the single-mode field within the fiber. The field normalization we employ is such that $E(z,t)$ has units $\sqrt{\text{photons/sec.}}$ Note that the introduction of the photon energy, $\hbar\omega$, is strictly a convenience at this classical stage; it has no quantum significance as yet.

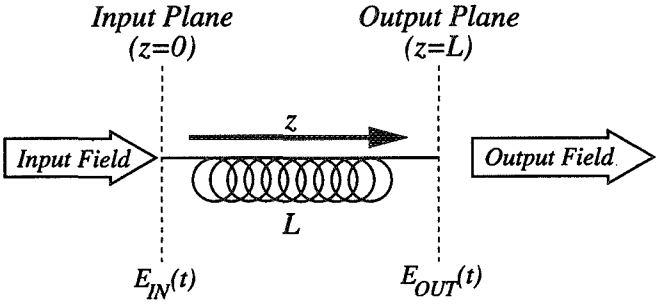


Fig. 1. Schematic configuration for Kerr-effect propagation in lossless, dispersionless fiber.

The classical propagation problem in lossless, dispersionless, Kerr-effect fiber is sketched in Fig. 1. The fiber is excited, at $z = 0$, by an input field $E_{IN}(t)$ that launches a $+z$-going wave $E(z,t)$ satisfying $E(0,t) = E_{IN}(t)$. In a reference frame moving at the group velocity, $v_g$, the complex field envelope within the fiber satisfies the following differential equation [6],

$$\frac{\partial E(z,t')}{\partial z} = i\kappa E^*(z,t')E(z,t')E(z,t'), \quad \text{for } z \geq 0, \tag{2}$$

where $t' \equiv t - z/v_g$ is the retarded time,

$$\kappa \equiv \frac{2\pi n_2 \hbar\omega}{A\lambda}, \tag{3}$$

is the nonlinear phase shift per unit length per unit photon flux, and $\lambda = 2\pi c/\omega$ is the center wavelength of the light. The intensity is a constant of motion for Eq. 2, so it is easily shown that

$$E(z,t) = \exp[i\kappa z E^*(0,t')E(0,t')]\, E(0,t'), \quad \text{for } z \geq 0. \tag{4}$$

Using the initial excitation condition that specifies $E(0,t')$, and directing our attention to $E_{OUT}(t) \equiv E(L,t)$, the field coupled out of the fiber at $z = L$, we obtain the classical input-output relation for a length $L$ lossless, dispersionless fiber exhibiting the Kerr nonlinearity, namely,

$$E_{OUT}(t) = \exp[irE^*_{IN}(t)E_{IN}(t)]\, E_{IN}(t), \tag{5}$$

where

$$r \equiv \kappa L, \tag{6}$$

is the nonlinear phase shift per unit photon flux and, for convenience, we have dropped the $L/v_g$ group delay.

Two well known results follow directly from Eq. 5: spectral broadening through self-phase modulation (SPM), and four-wave mixing (FWM). As an immediate consequence of Eq. 5, we see that an optical pulse propagating through the fiber acquires a time-varying phase shift, which is proportional to the pulse's intensity. The derivative of this time-varying phase constitutes an intensity-dependent instantaneous-frequency variation, implying, for sufficiently intense pulses or long fibers, significant spectral broadening. On the other hand, when the input field comprises a strong monochromatic pump, $E^P_{IN}$, at frequency $\omega$ plus weak sidebands at frequencies $\omega \pm \Omega$, FWM couples the sidebands. The input-output relation for classical FWM can be obtained, from Eq. 5, by replacing the exponential term with its two-term Taylor series approximation, and assuming that all nonlinear phase shifts other than the pump×pump term are small:

$$\tilde{E}_{OUT}(t) = \exp\left(ir|E^P_{IN}|^2\right)\left[(1 + ir|E^P_{IN}|^2)\tilde{E}_{IN}(t) + ir(E^P_{IN})^2\tilde{E}^*_{IN}(t)\right], \tag{7}$$

where $\tilde{E}(t) \equiv E(t) - E^P$ for the input and output fields.

In the quantum theory of the Kerr interaction the photon-units complex field envelope, $E(z,t)$, becomes a photon-units field operator, $\hat{E}(z,t)$. The input field operator—$\hat{E}_{IN}(t) \equiv \hat{E}(0,t)$—is a single-spatial mode, multitemporal-mode free field, and hence must satisfy the following $\delta$-function commutator rule [7],

$$\left[\hat{E}_{IN}(t), \hat{E}^\dagger_{IN}(u)\right] = \delta(t-u), \tag{8}$$

for photon-units field operators. The output field operator—$\hat{E}_{OUT}(t) \equiv \hat{E}(L,t)$—is *also* a single-mode free field, whose commutator must therefore mimic Eq. 8. This requirement is automatically met by quantizing Eq. 2 as follows,

$$\frac{\partial \hat{E}(z,t')}{\partial z} = i\kappa \hat{E}^\dagger(z,t')\hat{E}(z,t')\hat{E}(z,t'), \quad \text{for } z \geq 0. \tag{9}$$

Quantum FWM emerges from Eq. 9, in a manner that ensures commutator preservation, by decomposing the input field operator, $\hat{E}_{IN}(t)$, into a $c$-number pump, $E^P_{IN}$, plus a $\delta$-function commutator field operator, $\hat{\tilde{E}}_{IN}(t)$. Then, assuming that all nonlinear phase shifts other than the

pump×pump term are small, Eq. 9 can be linearized and solved to yield the quantum version of Eq. 7, namely,

$$\hat{\tilde{E}}_{OUT}(t) = \exp\left(ir|E_{IN}^{P}|^2\right)\left[(1+ir|E_{IN}^{P}|^2)\hat{\tilde{E}}_{IN}(t) + ir(E_{IN}^{P})^2\hat{\tilde{E}}_{IN}^{\dagger}(t)\right]. \tag{10}$$

Equation 10 is commutator preserving, does not require a Kerr-effect time constant, is consistent with the classical FWM theory, and agrees with experimental results in fiber squeezed-state generation [1].

We find that it is not possible to treat quantum SPM from Eq. 9, in a way that recovers the classical limit, without a modification of the theory. To highlight the failing of instantaneous-interaction quantum SPM, let us calculate the mean output-field for a coherent-state input field [4]. By direct substitution,

$$\hat{E}(z,t) = \exp\left[i\kappa z\hat{E}^{\dagger}(0,t')\hat{E}(0,t')\right]\hat{E}(0,t'), \quad \text{for } z \geq 0, \tag{11}$$

can be shown to be the solution to Eq. 9, leading to

$$\hat{E}_{OUT}(t) = \exp\left[ir\hat{E}_{IN}^{\dagger}(t)\hat{E}_{IN}(t)\right]\hat{E}_{IN}(t), \tag{12}$$

as the quantum version of Eq. 5 under an instantaneous Kerr-interaction model. The output mean field,

$$\begin{aligned}\overline{E}_{OUT}(t) &\equiv \langle E_{IN}(t)|\hat{E}_{OUT}(t)|E_{IN}(t)\rangle \\ &= \langle E_{IN}(t)|\exp\left[ir\hat{E}_{IN}^{\dagger}(t)\hat{E}_{IN}(t)\right]\hat{E}_{IN}(t)|E_{IN}(t)\rangle. \end{aligned}\tag{13}$$

for a coherent-state input field reduces to

$$\overline{E}_{OUT}(t) = \langle E_{IN}(t)|\exp\left[ir\hat{E}_{IN}^{\dagger}(t)\hat{E}_{IN}(t)\right]|E_{IN}(t)\rangle E_{IN}(t), \tag{14}$$

because a coherent-state input field obeys the eigenfunction relation

$$\hat{E}_{IN}(t)|E_{IN}(t)\rangle = E_{IN}(t)|E_{IN}(t)\rangle, \quad \text{for all } t. \tag{15}$$

For the rest of the calculation we employ a limiting argument,

$$\overline{E}_{OUT}(t) = \lim_{T\to 0}\left(\langle E_{IN}(t)|\exp\left[(ir/T)\int_{t-T}^{t} d\tau\, \hat{E}_{IN}^{\dagger}(\tau)\hat{E}_{IN}(\tau)\right]|E_{IN}(t)\rangle\right)E_{IN}(t) \tag{16}$$

$$= \lim_{T\to 0}\left(\exp\left[(\exp(ir/T)-1)\int_{t-T}^{t} d\tau\,|E_{IN}(\tau)|^2\right]\right)E_{IN}(t) \tag{17}$$

$$= E_{IN}(t), \tag{18}$$

where we have exploited the characteristic function for coherent-state photon counting [8] to obtain Eq. 17.

Equation 18 predicts that the instantaneous Kerr nonlinearity has *no* effect whatsoever on the mean field of a coherent-state input, regardless of how large the classical, peak nonlinear phase shift becomes! This result contradicts the classical theory, Eq. 5, and, more importantly, it contradicts

experiments which have confirmed the classical spectral-broadening predictions. In retrospect, the failure of Eq. 9 to reproduce SPM in the appropriate limit should not be too surprising as it arises from applying an instantaneous, spectral-broadening nonlinearity to a quantized field whose vacuum-state fluctuations extend to infinite bandwidth.

The classical SPM result can be recovered from our quantum mean-field calculation by introducing a phenomenological Kerr-effect time constant, $\tau_K$, as a lower-bound for $T$ in Eq. 16. In particular, with $T = \tau_K > 0$ and $r/\tau_K \ll 1$, Eq. 17 becomes

$$\begin{aligned} \overline{E}_{OUT}(t) &\approx \exp\left[(ir/\tau_K)\int_{t-\tau_K}^{t} d\tau\,|E_{IN}(\tau)|^2\right] E_{IN}(t) \\ &\approx \exp\left[ir|E_{IN}(t)|^2\right] E_{IN}(t), \end{aligned} \tag{19}$$

whenever $\tau_K$ is smaller than any classical time scale present in the field.

To incorporate $\tau_K$ into our quantum propagation theory for the lossless, dispersionless, Kerr effect in single-mode fiber, we employ the following partial mode expansion for the input-field operator:

$$\hat{E}_{IN}(t) = \sum_{n=-\infty}^{\infty} \hat{a}_n^{IN}\xi(t - n\tau_K), \tag{20}$$

where $\{\,\hat{a}_n^{IN} : -\infty < n < \infty\,\}$ is a set annihilation operators, and

$$\xi(t) \equiv \begin{cases} \frac{1}{\sqrt{\tau_K}}, & \text{for } 0 \le t < \tau_K, \\ \\ 0, & \text{otherwise,} \end{cases} \tag{21}$$

is a $c$-number, $\tau_K$-second duration, rectangular pulse. Suppressing the $L/v_g$-second group delay, the same expansion applies to the output field operator, $\hat{E}_{OUT}(t)$, with the input annihilation operators replaced by the output annihilation operators, $\{\,\hat{a}_n^{OUT} : -\infty < n < \infty\,\}$. These output annihilation operators are related to their corresponding inputs by

$$\hat{a}_n^{OUT} = \exp\left[(ir/\tau_K)\hat{a}_n^{IN\dagger}\hat{a}_n^{IN}\right]\hat{a}_n^{IN}, \quad \text{for } -\infty < n < \infty, \tag{22}$$

which should be compared with the instantaneous quantum Kerr model, Eq. 12.

Equations 20–22 comprise a coarse-grained time model for quantum Kerr-effect propagation in lossless, dispersionless, single-mode fiber. Introducing the Kerr time-constant as a simple phenomenological parameter, $\tau_K$, is arguably a distasteful ad hoc procedure, but the known existence of finite Kerr response times plus the inconsistency of an instantaneous quantum Kerr model mitigate against this deficiency. A more important consideration with respect to Eqs. 20–22 is that they are fundamentally incomplete; $\{\,\xi(t - n\tau_K) : -\infty < n < \infty\,\}$ is an orthonormal temporal mode set, but not a *complete* orthonormal mode set. Hence, in the coarse-grained time model, the input field commutator obeys

$$\begin{aligned} \left[\hat{E}_{IN}(t), \hat{E}_{IN}^{\dagger}(u)\right] &= \delta_{\tau_K}(t,u) \\ &\equiv \begin{cases} \frac{1}{\tau_K}, & \text{if } (n-1)\tau_K \le t,u < n\tau_K, \text{ for } n \text{ an integer,} \\ \\ 0, & \text{otherwise.} \end{cases} \end{aligned} \tag{23}$$

This expression is *not* the $\delta$-function commutator that a photon-units field operator should possess. However, as will be made clear below, it *can* be a reasonable approximation thereto. Moreover, from Eqs. 22 and 23, we see that the coarse-grained time quantum theory is consistent in that it preserves $\delta_{\tau_K}$-function commutators—we have that

$$\left[\hat{E}_{OUT}(t), \hat{E}^{\dagger}_{OUT}(u)\right] = \delta_{\tau_K}(t,u). \tag{24}$$

Given the approximate nature of the coarse-grained model's field commutator [4], what conditions suffice to ensure the accuracy of this model's moment predictions? Clearly, this model is a poor approximation for field dynamics occurring on time scales comparable to $\tau_K$, or, equivalently, over bandwidths of the order of $\tau_K^{-1}$. We expect $\tau_K$ to fall in the interval 1–100 fs—to match the known time scales of $n_2$—so our quantum input field, $\hat{E}_{IN}(t)$, must *not* have excited (non-vacuum state) modes at these time or bandwidth scales. Furthermore, because SPM causes spectral broadening, we must check that this same time/bandwidth scale condition is satisfied by the *output* field operator, $\hat{E}_{OUT}(t)$. Finally, we must limit any photodetection measurements that we make on the output field to be insensitive to $\hat{E}_{OUT}(t)$-behavior at $\tau_K$ time scales or $\tau_K^{-1}$ bandwidths. When all three of these conditions apply, we believe the coarse-grained time quantum Kerr model—with a proper value for $\tau_K$—should capture the full behavior of quantum Kerr propagation in lossless, dispersionless, single-mode fiber.

The output mean-field derivation—with a Kerr time-constant $\tau_K$—is virtually identical to the analysis of the instantaneous-interaction case. We find that

$$\overline{E}_{OUT}(t) \equiv \langle E_{IN}(t)|\hat{E}_{OUT}(t)|E_{IN}(t)\rangle = \exp\left[iR|E_{IN}(t)|^2\right] E_{IN}(t), \tag{25}$$

where we have defined the complex number, $R$, according to

$$iR \equiv [\exp(i\phi_q) - 1]\tau_K, \quad \text{for } \phi_q \equiv r/\tau_K. \tag{26}$$

Equation 25 bears a striking similarity to the classical formula, Eq. 5. Indeed, the two would be identical were $R = r$ to prevail.

We know that $r$ is the *classical* nonlinear phase shift per unit photon flux. Because $\tau_K$ is the time duration of a single, rectangular-pulse mode in our coarse-grained time model, we have that $\phi_q$ is *numerically* the classical phase shift produced by one photon in such a mode. Equation 25 applies to a coherent-state input field—which has vacuum-fluctuation noise in *all* its modes—so it is fair to regard $\phi_q$, *physically*, as the quantum nonlinear phase shift that is due to the vacuum fluctuations of a single mode.

The predictions of the quantum and classical theories are nearly coincident when we have $r \approx \mathrm{Re}(R)$ and $|\mathrm{Im}(R)| \ll 1$. These conditions hold for $\phi_q \ll 1$, as can be seen from Fig. 2, where we have plotted $\mathrm{Re}(R)/r$ and $\mathrm{Im}(R)/r$ vs. $\phi_q$. Assuming $\tau_K = 1\,\mathrm{fs}$, a 1 km fused silica fiber will have $\phi_q \approx 10^{-3}$ rad; from Fig. 2 we conclude that Eq. 25, the quantum coherent-state mean field, will then be in excellent agreement with Eq. 5, the classical mean field result. For $\phi_q > 10^{-1}$ rad, there is a pronounced divergence between $\mathrm{Re}(R)$ and $r$, caused by the intrinsic periodicity of $R$. Viewed as a function of $\phi_q$, Eq. 26 shows that $R$ is periodic with period $2\pi$. Physically, this periodicity constitutes a quantum state-recurrence for Kerr-effect propagation in lossless, dispersionless fiber and occurs when $L = L_q \equiv 2\pi\tau_K/\kappa$; for $\tau_K = 1\,\mathrm{fs}$ and fused-silica

fiber this implies $L_q \sim 10^4$ km, an experimentally inaccessible value for our assumptions of zero loss and zero dispersion.

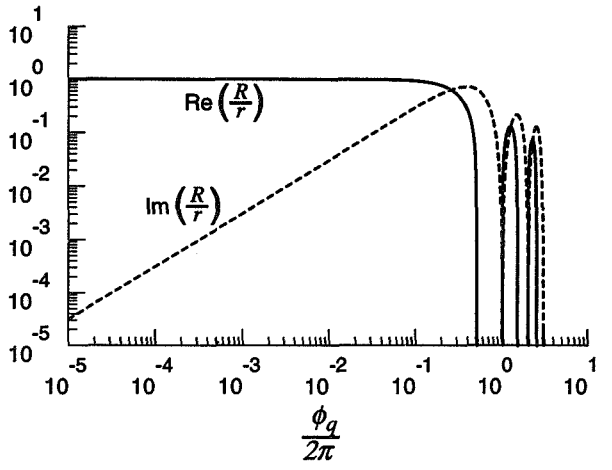


Fig. 2. Logarithmic plots of Re(R)/r and Im(R)/r vs. $_q$. The coherent-state mean field of coarse-grained time SPM reduces to the classical SPM result when R ≈ r; $_q$ is the quantum nonlinear phase shift, i.e., the Kerr-induced phase shift of one photon per $_K$ -second mode.

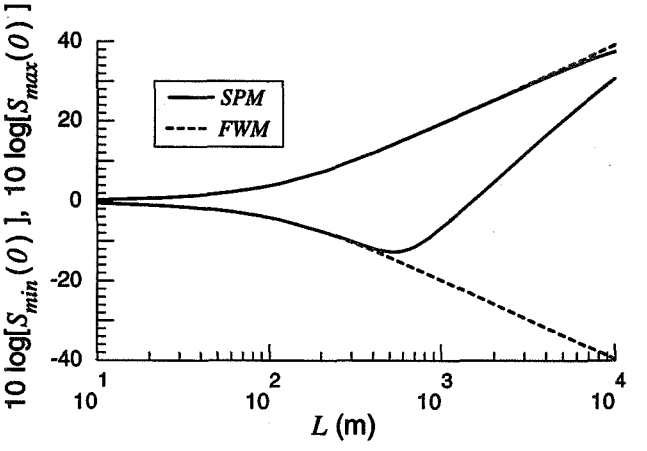


Fig. 3. Minimum and maximum low-frequency, homodyne-measurement noise spectra for a cw, coherent-state input vs. fiber length. The solid curves are the coarse-grained time SPM theory; the dashed curves are the instantaneous-interaction FWM theory. The parameter values employed are: $= 1.06\,\mu$m; A $= 3.56 \times 10^{-11}$ m$^2$; $n_2 = 3.2 \times 10^{-20}$ m$^2$/W; $P_{IN} = 1$ W; and $_K =$ 1 fs.

Expressions for the quantum output moments, up to the second order, have been derived for Gaussian-state inputs [4]. We note that these moments yield the correct results in the appropriate limits. Specifically, when $\phi_q \ll 1$ they are in agreement with the quantum FWM results. Furthermore, if we let $R \longrightarrow r$ and $\delta_{\tau_K}(t,u) \longrightarrow 0$ and use classical covariances in lieu of quantum covariances throughout, e.g., $\langle \hat{E}^\dagger_{IN}(t)\hat{E}_{IN}(u)\rangle \longrightarrow \overline{E^*_{IN}(t)E_{IN}(u)}$, etc., the resulting equations agree with classical stochastic SPM results. We note that *none* of these classical formulas depend on the Kerr-effect time constant, $\tau_K$. This is fully consistent with our assumption that the spectrum of the classical input excitation *and* the implied output-field spectrum are both narrower than $\tau_K^{-1}$. Under these circumstances we expect—in a classical theory—that the Kerr interaction is effectively instantaneous.

The implications of the full theory are readily ascertained by examining the output field's homodyne-detection statistics. An ideal homodyne measurement on $\hat{E}_{OUT}(t)$ yields a photocurrent whose statistics are proportional to those of the following abstract quantum measurement:

$$\hat{E}_\phi(t) \equiv \hat{E}_{OUT}(t)e^{i\phi} + \hat{E}^\dagger_{OUT}(t)e^{-i\phi}, \tag{27}$$

where $\phi$ is the local-oscillator (LO) phase. As is conventionally done in cw squeezing experiments, we shall focus on the minimum and maximum values of the homodyne-noise spectra as the LO phase is varied.

For a coherent-state input, both the instantaneous-interaction FWM and the coarse-grained time SPM theories imply frequency-independent homodyne spectra out to frequencies comparable to $\tau_K^{-1}$. In Fig. 3 we have plotted $S_{min}(0)$ and $S_{max}(0)$, vs. fiber length $L$, for both theories. These curves assume $n_2 = 3.2 \times 10^{-20}\,\mathrm{m^2/W}$, $A = 3.56 \times 10^{-11}\,\mathrm{m^2}$, $\lambda = 1.06\,\mu\mathrm{m}$, $P_{IN} \equiv \hbar\omega|E_{IN}|^2 = 1\,\mathrm{W}$, and, for the coarse-grained time case, $\tau_K = 1\,\mathrm{fs}$. Quantum FWM predicts complete noise suppression for one quadrature component, $S_{min}(0) \longrightarrow 0$, as the fiber length becomes infinite. Moreover, this transpires at minimum uncertainty product, $S_{min}(0)S_{max}(0) = 1$. These FWM features are clearly evident is Fig. 3; for long enough fibers, however, they are at odds with our coarse-grained time SPM theory. According to Fig. 3, the coarse-grained time SPM theory has an $S_{min}(0)$ which reaches a *nonzero* minimum at $L \approx 500\,\mathrm{m}$, and increases, for longer fibers, substantially above the coherent-state value of unity.

The precise location of the minimum in the low noise quadrature depends on $\tau_K$ with higher values of $\tau_K$ extending the region of agreement between the instantaneous interaction FWM and the coarse-grained time SPM theories. For various technical reasons, e.g., guided acoustic-wave Brillouin scatter, it is not feasible to perform such an experiment using a cw field. Nevertheless, the physical conditions corresponding to the minimum in Fig. 3, namely 1 Watt input power and roughly a 500-meter-long fiber, seem well within the realm of possibility for pulsed experiments. In fact, modeling Shelby's soliton-squeezing experiments [9] by using his peak intensity as the intensity in our cw theory, we find that conditions are right for a $\tau_K$-dependent deviation from quantum FWM. However, accurate analysis of a short-pulse experiment—especially one based on solitons—must surely account for group-velocity dispersion. In addition, a realistic quantum propagation theory for long fibers should address linear loss.

# 3 Inclusion of Dispersion and Loss

A split-step configuration for incorporating group-velocity dispersion (GVD) and linear loss (LL) into quantum propagation analysis for a Kerr-nonlinear fiber is shown schematically in Fig. 4. An infinitesimal length of fiber at $z$ is divided into two sub-segments. The first sub-segment exhibits only the Kerr nonlinearity and linear loss; the second has neither Kerr effect nor loss, but suffers from dispersion.

Let $\hat{E}(z,t)$ be the coarse-grained time, $+z$-going, photon-units field operator within the fiber, i.e., as before we have the mode expansion

$$\hat{E}(z,t) = \sum_{n=-\infty}^{\infty} \hat{a}_n(z)\xi(t - n\tau_K). \tag{28}$$

Over an infinitesimal, $\delta z$-meter-long fiber segment, the split-step procedure leads to the $z$-to-$(z+\delta z)$ annihilation operator transformation,

$$\hat{a}_n(z+\delta z) = \sum_{m=-\infty}^{\infty} h[n-m;\delta z]\hat{\tilde{a}}_m(z), \quad \text{for } -\infty < n < \infty, \tag{29}$$

where

$$\hat{\tilde{a}}_n(z) \equiv \exp\Big[i(\kappa\delta z/\tau_K)\hat{a}_n^\dagger(z)\hat{a}_n(z) + (\alpha/2)\delta z\Big]\,\hat{a}_n(z) + \sqrt{\alpha}\delta z\hat{b}_n(z), \quad \text{for } -\infty < n < \infty, \tag{30}$$

characterizes SPM and LL *alone* over the dispersionless sub-segment, and

$$h[n;\delta z] \equiv \begin{cases} -\frac{i\beta_2}{2\tau_K^2}\delta z, & \text{for } n=-1,1, \\ 1+\frac{i\beta_2}{\tau_K^2}\delta z, & \text{for } n=0, \\ 0, & \text{otherwise,} \end{cases} \tag{31}$$

is a discrete-time impulse response accounting for the dispersive sub-segment. In Eqs. 28–31, we have suppressed the group-velocity delay, and we have introduced the fiber's dispersion coefficient, $\beta_2$, and its power-attenuation coefficient, $\alpha$. More importantly, with the inclusion of a Langevin noise-operator $\hat{b}_n(z)$ required by the presence of the LL these equations preserve the $\delta_{\tau_K}(t,u)$-function commutator of a coarse-grained time input field operator, $\hat{E}_{IN}(t)$. So, if we drive the fiber at $z=0$ with such an input—forcing $\hat{E}(0,t)=\hat{E}_{IN}(t)$—and then iteratively apply Eqs. 28–31, we will arrive at an output field operator, $\hat{E}_{OUT}(t)\equiv\hat{E}(L,t)$ at $z=L$ with a proper coarse-grained time commutator. Furthermore, because the unitary operators that transform the $\{\hat{a}_n(z)\}$ into the $\{\hat{\tilde{a}}_n(z)\}$ are known, as are the operators for changing the $\{\hat{\tilde{a}}_n(z)\}$ into the $\{\hat{a}_n(z+\delta z)\}$, we can—in principle—calculate *all* the measurement statistics for $\hat{E}_{OUT}(t)$, given any state of $\hat{E}_{IN}(t)$.

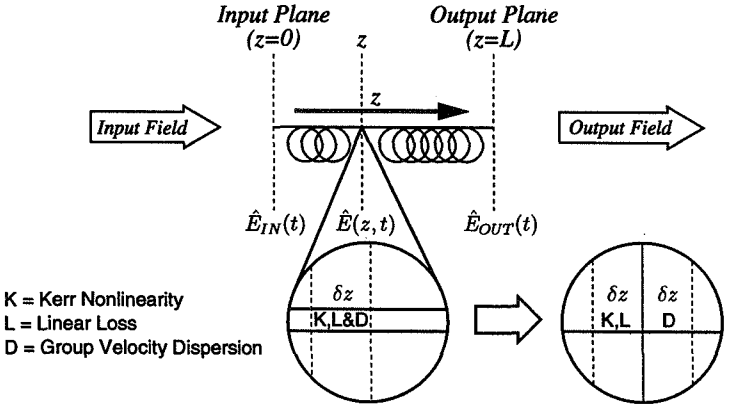


Fig. 4. Schematic split-step configuration for inclusion of group-velocity dispersion and linear loss into the coarse-grained time SPM theory.

We note that the only aspect missed in this split-step approach is a term proportional to the commutator of the Hamiltonians governing each step. It can be shown that this commutator is finite and its contribution goes to zero in $\delta z^2$; hence, in the limit of $\delta z \longrightarrow 0$ this is an exact theory. Taking the limit of $\delta z \longrightarrow 0$, the differential equation for the mode operator is

$$\begin{aligned} \frac{\partial}{\partial z}\hat{a}_n(z) &= -(\alpha/2)\hat{a}_n(z) + i(\kappa/\tau_K)\hat{a}_n^\dagger(z)\hat{a}_n^2(z) + \frac{i\beta_2}{2\tau_K^2}[2\hat{a}_n(z)-\hat{a}_{n-1}(z)-\hat{a}_{n+1}(z)] \\ &+ \sqrt{\alpha}\hat{b}_n(z), \quad \text{for } 0\le z\le L,\ -\infty<n<\infty. \end{aligned} \tag{32}$$

The coarse-grained time *cannot* be suppressed—it is essential to preventing the mean-field contradiction exhibited in Sect. 3.1—but it can be hidden. Returning to field operator notation, Eq. 32

can be recast as

$$\frac{\partial}{\partial z}\hat{E}(z,t) = i\kappa\hat{E}^\dagger(z,t)\hat{E}(z,t)\hat{E}(z,t) - i\frac{\beta_2}{2}\frac{\partial^2_{\tau_K}}{\partial_{\tau_K}t^2}\hat{E}(z,t) - \frac{\alpha}{2}\hat{E}(z,t) + \sqrt{\alpha}\hat{F}(z,t) \quad (33)$$

with the obvious, implied definitions for the $\tau_K$-approximation to the second partial derivative with respect to time and for the Langevin noise field-operator.

Equation 33 is extraordinarily appealing. Converting it, naïvely, to continuous-time classical form by merely dispensing with the operator carets, dropping the Langevin noise source, and the $\tau_K$ subscripts, we obtain

$$\frac{\partial}{\partial z}E(z,t) = i\kappa E^*(z,t)E(z,t)E(z,t) - i\frac{\beta_2}{2}\frac{\partial^2}{\partial t^2}E(z,t) - \frac{\alpha}{2}E(z,t), \quad (34)$$

the well-known starting point for the classical theory of solitons in fiber [6].

# 4 Moment Propagation and the Terminated Cumulant Expansion

Although it is possible to calculate the exact state transformation for the preceding quantum theory, it is a daunting numerical task in almost all cases of interest. Thus, we have elected to follow a much simpler and restrictive course—moment propagation. Taking the expectation value of Eq. 33 we find that the mean field develops according to

$$\frac{\partial}{\partial z}\langle\hat{E}(z,t)\rangle = i\kappa\langle\hat{E}^\dagger(z,t)\hat{E}(z,t)\hat{E}(z,t)\rangle - i\frac{\beta_2}{2}\frac{\partial^2_{\tau_K}}{\partial_{\tau_K}t^2}\langle\hat{E}(z,t)\rangle - \frac{\alpha}{2}\langle\hat{E}(z,t)\rangle, \quad (35)$$

which illustrates the fundamental problem of moment propagation—the Kerr nonlinearity couples each moment's differential equation to those of higher order. For example, in the single time case, the differential equation for the moment $\langle\hat{E}^{\dagger k}(t,z)\hat{E}^l(t,z)\rangle$ includes terms containing the moment $\langle\hat{E}^{\dagger k+1}(t,z)\hat{E}^{l+1}(t,z)\rangle$, leading to an infinite progression of coupled differential equations.

This infinite linkage of moment equations can be broken, in an approximate way, through a terminated cumulant expansion (TCE). (A brief review of cumulants—for classical random variables—is found in the Appendix. Here, we rely on normally-ordered quantum cumulants.) In the TCE-$K$ expansion, all normally-ordered quantum-field cumulants beyond the $K$-th order are set to zero:

$$\langle\langle\prod_k[\hat{E}^\dagger(z,t)]^{m_k}\prod_k[\hat{E}(z,t)]^{n_k}\rangle\rangle = 0, \quad \text{when } \sum_k(m_k+n_k) > K. \quad (36)$$

The TCE-$K$ assumption provides low-order moment expressions for all field-operator moments beyond $K$-th order. For example, the third-order cumulant relation,

$$\begin{aligned}\langle\langle\hat{E}^\dagger(z,t)\hat{E}^2(z,t)\rangle\rangle &= \langle\hat{E}^\dagger(z,t)\hat{E}^2(z,t)\rangle - 2\langle\hat{E}^\dagger(z,t)\hat{E}(z,t)\rangle\langle\hat{E}(z,t)\rangle \\ &- \langle\hat{E}^\dagger(z,t)\rangle\langle\hat{E}^2(z,t)\rangle + 2\langle\hat{E}^\dagger(z,t)\rangle\langle\hat{E}(z,t)\rangle^2, \end{aligned} \quad (37)$$

affords the following explicit expression for the TCE-2 expansion:

$$\langle\hat{E}^\dagger(z,t)\hat{E}^2(z,t)\rangle = \langle\hat{E}^\dagger(z,t)\rangle\langle\hat{E}^2(z,t)\rangle + 2\langle\hat{E}^\dagger(z,t)\hat{E}(z,t)\rangle\langle\hat{E}(z,t)\rangle - 2\langle\hat{E}^\dagger(z,t)\rangle\langle\hat{E}^\dagger(z,t)\rangle^2. \quad (38)$$

Substitution of this expression into the mean-field equation, Eq. 35, eliminates the third-order moment and leads, ultimately, to a closed system of differential equations for

$$\{\langle\hat{E}(z,t)\rangle, \langle\hat{E}^{\dagger}(z,t)\hat{E}(z,u)\rangle, \langle\hat{E}(z,t)\hat{E}(z,u)\rangle\}. \tag{39}$$

The accuracy of the TCE approximation depends upon both the initial state and its subsequent propagation. For a Gaussian state, such as a coherent state, all cumulants of order three or higher vanish. Moreover, a Gaussian state remains Gaussian under linear propagation—even if it is lossy and/or dispersive—so, for example, TCE-2 is *exact* for Gaussian-state inputs in the four-wave mixing limit. Higher-order TCE approximations track deviations from a Gaussian state, hence they should prove useful for Gaussian-state inputs even *beyond* the four-wave mixing regime. This is demonstrated, quantitatively, in Fig. 5, where we compare coherent-state input, homodyne-noise output spectra for a lossless, dispersionless Kerr-effect fiber computed via TCE-$K$, with the exact solution presented in the previous section. The coarse-grained time SPM curve (exact solution) represents a state that is very nearly Gaussian state up to the point of its minimum-noise curve departs from the instantaneous-interaction FWM curve. (As noted above, coherent-state FWM is always a Gaussian-state case.) The TCE-2 approximation misses the mark, as it always represents a minimum-uncertainty Gaussian state, which is plainly a bad approximation to the exact solution. However, the TCE-3 approximation captures the essential nature of the exact solution, viz. it correctly predicts the minimum noise level and its subsequent rise to the shot-noise-level. As expected, the TCE-4 and TCE-5 approximations show slightly better performance, but the meager improvement they provide hardly justifies their added computational burden.

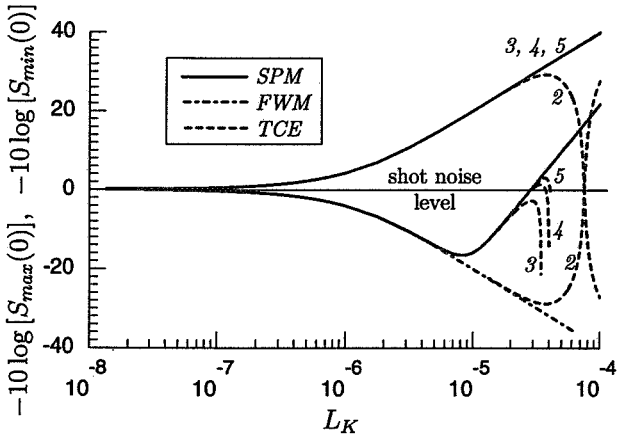


Fig. 5. Minimum and maximum low-frequency, homodyne-measurement noise spectra vs. $_q/2$ ( $_q$ = 2 for a fiber of length 3.25 × $10^5$ km, $_k$ = 1fs) at 1.55 μm in a dispersionless, lossless fiber. SPM denotes the exact calculation, FWM the four-wave mixing approximation, and TCE the terminated cumulant expansion (K = 2,3,4,5 shown). The input field is a 1-Watt, coherent state; 0 dB is the coherent-state noise level.

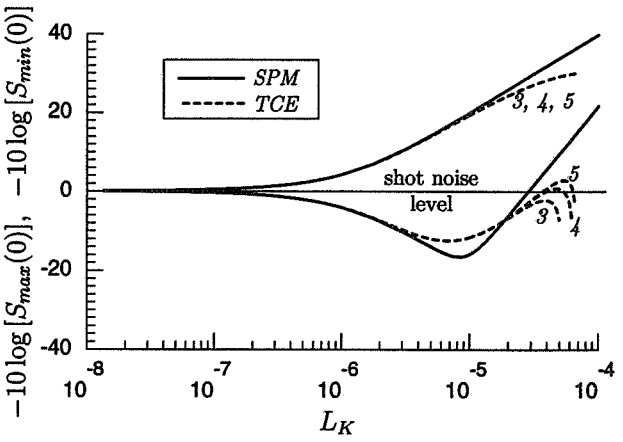


Fig. 6. Minimum and maximum low-frequency, homodyne-measurement noise spectra vs. $_q/2$ ( $_q$ = 2 for a fiber of length 3.25 × $10^5$ km, $_k$ = 1fs) at 1.55 μm in a dispersionless fiber. SPM denotes the exact, lossless calculation, and TCE the terminated cumulant expansion (K = 3,4,5 shown) with 0.2dB/km linear loss. The input field is a 1-Watt, coherent state; 0 dB is the coherent-state noise level.

Armed with the TCE approximation, we can obtain homodyne-noise spectra for situations in which the exact calculations are thwarted by moment linkage. Consider propagation in a lossy,

dispersionless Kerr-effect fiber. In Fig. 6 we have plotted the exact SPM result for the *lossless* case (solid curve) and the TCE solutions (dashed curves) for a fiber with a power loss coefficient of 0.2 dB/km. The regions of overlap follow the same trends seen in Fig. 4, and predict a 4 dB increase in the noise level over the lossless case.

Inclusion of dispersion couples time slots and greatly increases the complexity of TCE moment calculations, even with a coherent-state input. If we address $N$ time samples of the field, there are $(19N + 15N^2 + 2N^3)/3$ complex moments, or $(35N + 30N^2 + 4N^3)/3$ real quantities, to track. Each real quantity obeys one of 23 types of differential equation, which contain anywhere from 5 to 87 terms. For $N = 100$, there are thus 717,300 moments, or 1,434,500 real quantities, to be computed. We are working on these calculations at present, and expect to be reporting our results in the near future.

# 5 Conclusions

We have presented a general theory for quantum propagation of an optical field in a lossy, dispersive Kerr-effect fiber. Our approach leads to equations that are continuous in space, but discrete in time. The time granularity is set by a phenomenological Kerr-effect time constant needed to properly recover the known results of classical self-phase modulation. Other theories have been developed that describe propagation in such a fiber [11],[16], but ours is the first for which a material time constant has been specifically employed to temper the instantaneous interaction. It has been argued that the presence of dispersion provides a much more constrictive bandwidth limitation than $\tau_K^{-1}$, thereby eliminating the need for this Kerr-effect time constant [17]. We disagree, but in the interests of brevity, we shall confine our remarks to a few brief points. First, it has been shown that there is a four-wave mixing region in which dispersion enhances squeezing [18]; here we may expect that dispersion exacerbates the need for a finite $\tau_K$ to correctly determine the validity limit of FWM. On the other hand, if there are propagation regimes—such as soliton propagation—wherein dispersion renders a finite Kerr-effect time constant unnecessary, then that impotence should appear in our calculations, i.e., our noise results should be insensitive to the value we assign to $\tau_K$. Note that, even with loss and dispersion, the value of $\tau_K$ is irrelevant to linearized noise analysis, and this includes the linearized noise theory of quantum solitons. Finally, the theory we have presented handles the case of an arbitrary field, in either the normal or anomalous dispersion regimes, and is more encompassing than those restricted to soliton propagation.

# Appendix

For a real-valued classical random vector $\vec{X} \equiv (X_1, X_2, \ldots, X_n)$ whose joint characteristic function is $\phi(\vec{s}) \equiv \langle \exp(i\vec{s} \cdot \vec{X}) \rangle$, the cumulants are defined by:

$$\langle\langle \prod_k X_k^{m_k} \rangle\rangle = \left[ \prod_k \left( -i \frac{\partial}{\partial s_k} \right)^{m_k} \Phi(\vec{s}) \right]_{\vec{s}=\vec{0}}, \tag{40}$$

where the cumulant generating function is $\Phi(\vec{s}) \equiv \ln(\phi(\vec{s}))$. Higher order cumulants contain information of decreasing significance [10].

# References


[1] R.M. Shelby, M.D. Levenson, R.G. DeVoe, S.H. Perlmutter, and D.F. Walls, Phys. Rev. Lett. **57**, 691 (1986).

[2] K. Bergman and H.A. Haus, Opt. Lett. **16**, 663 (1991).

[3] L.G. Joneckis, and J.H. Shapiro, *Quantum Electronics and Laser Science Conference*, Vol. 12 of 1993 Technical Digest Series (Optical Society of America, Washington, D.C., 1993), p. 282.

[4] L.J. Joneckis, J.H. Shapiro, J. Opt. Soc. B **10**, 1102 (1993).

[5] K.J. Blow, R. Loudon, and S.J.D. Phoenix, J. Opt. Soc. B **8**, 1750 (1991).

[6] G.P. Agrawal, *Nonlinear Fiber Optics* (Academic, New York, 1989).

[7] H.P. Yuen and J.H. Shapiro, IEEE Trans. Inform. Theory **IT-24**, 657 (1978).

[8] H.P. Yuen and J.H. Shapiro, IEEE Trans. Inform. Theory **IT-26**, 78 (1980).

[9] R.M. Shelby, (personal communication).

[10] C.W. Gardiner, *Handbook of Stochastic Methods for Physics, Chemistry and Natural Sciences* (Springer-Verlag, New York, 1985).

[11] S.J. Carter, P.D. Drummond, M.D. Reid, and R.M. Shelby, Phys. Rev. Lett. **58**, 1841 (1987).

[12] S.J. Carter, and P.D. Drummond, J. Opt. Soc. B **4**, 1565 (1987).

[13] Y. Lai, and H.A. Haus, Phys. Rev. A **40**, 844 (1989).

[14] Y. Lai, and H.A. Haus, Phys. Rev. A **40**, 854 (1989).

[15] P.D. Drummond, Phys. Rev. A **42**, 6845 (1990).

[16] S.J. Carter, P.D. Drummond, Phys. Rev. Lett. **67**, 3757 (1991).

[17] H.A. Haus, and F.X. Kärtner, Phys. Rev. A **46**, R1175 (1992).

[18] B. Yurke, Phys. Rev. A **35**, 3974 (1987).

# QUANTUM AMPLIFICATION AND QUANTUM OPTICAL TAPPING WITH SQUEEZED STATES AND CORRELATED QUANTUM STATES

Z. Y. Ou
*Department of Physics, Indiana University-Purdue University at Indianapolis (IUPUI)*
*Indianapolis, IN 46202*

S. F. Pereira and H. J. Kimble
*Norman Bridge Laboratory of Physics 12-33, California Institute of Technology*
*Pasadena, CA 91125*

**Abstract**

Quantum fluctuations in a nondegenerate optical parametric amplifier (NOPA) are investigated experimentally with a squeezed state coupled into the internal idler mode of the NOPA. Reductions of the inherent quantum noise of the amplifier are observed with a minimum noise level 0.7 dB below the usual noise level of the amplifier with its idler mode in a vacuum state. With two correlated quantum fields as the amplifier's inputs and proper adjustment of the gain of the amplifier, it is shown that the amplifier's intrinsic quantum noise can be completely suppressed so that noise-free amplification is achieved. It is also shown that the NOPA, when coupled to either a squeezed state or a nonclassically correlated state, can realize quantum tapping of optical information.

# 1 Introduction

It has been known since the date when optical amplification was first realized that fundamental principles of quantum mechanics play an important role in the noise performance of a linear amplifier [1, 2]. For example, it was found [3, 4] that even in an ideal case when all the classical noise is eliminated, "extra" quantum noise from an amplifier's internal modes will add to the amplifier's output thus preventing noise-free amplification and degrading the output signal-to-noise ratio (SNR) relative to that of the input. Such "extra" quantum noise would destroy any coherent quantum superpositions that are often encountered in the microscopic world, should one try to amplify the microscopic quantum superposition to a macroscopic scale so as to produce a paradox such as Schrödinger's Cat [5].

However, Caves pointed out in a systematic analysis [6] of quantum noise in a linear amplifier that noiseless amplification is possible with a phase-sensitive amplifier (for which the gain depends on the phase of the input signal). On the other hand, for a phase-insensitive amplifier, although extra noise cannot be avoided as stated above, it may be rearranged, according to Caves' analysis. More specifically, a phase-insensitive amplifier is described by a general quantum model [6, 7]:

$$\hat{a}^{out} = \sqrt{G}\,\hat{a}^{in} + \hat{F}, \tag{1}$$

where $\hat{a}^{in,out}$ is the annihilation operator for the input and output signal, $G$ is the power gain of the amplifier and $\hat{F}$ is an operator related to the internal modes of the amplifier and satisfies $[\hat{F}, \hat{F}^\dagger] = 1 - G$. The quantum fluctuations in $\hat{F}$ will give rise to the "extra noise" added to the output signal. From Eq.(1), one can derive Caves' uncertainty relation [6]

$$(A_1 A_2)^{1/2} \geq \frac{1}{4}\left|1 - G^{-1}\right| \quad , \tag{2}$$

where $A_i \equiv \langle(\Delta\hat{F}_i)^2\rangle/G$ is the input equivalent noise added to the quadrature-phase amplitudes $X_i (i = 1, 2)$, with $X_1 \equiv (\hat{a}+\hat{a}^\dagger)/2, X_2 \equiv (\hat{a}-\hat{a}^\dagger)/2i, \hat{F}_1 \equiv (\hat{F}+\hat{F}^\dagger)/2$, and $\hat{F}_2 \equiv (\hat{F}-\hat{F}^\dagger)/2i$. Thus the noise in amplification in one quadrature-phase amplitude where the signal is encoded can be suppressed while the extra noise demanded by Eq.(2) is mostly coupled into the unused conjugate quadrature, with their noise product satisfying Eq.(2). By following this line of reasoning, it was suggested [8, 9, 10, 11] that by coupling the amplifier's internal modes to a squeezed vacuum instead of the usual vacuum state, the suppression of added noise for one quadrature can be achieved as stated above.

In the analysis of Caves, it was assumed that the input field $\hat{a}^{in}$ is independent of the internal modes of the amplifier described by $\hat{F}$. On the other hand, the situation will be totally different if $\hat{a}^{in}$ and $\hat{F}$ are correlated. Notice that the quantities in Eq.(1) are amplitudes of the relevant fields. Thus interference between the amplitudes of $\hat{a}^{in}$ and $\hat{F}$ may give rise to cancellation of their quantum fluctuations and lead to noise reduction in the amplifier's output. Quantum noise subtraction has been realized with various kinds of correlated quantum fields [12, 13, 14].

The distribution of information in the modern age requires division of incoming information into identical pieces for sharing by many users. An optical tap is a kind of information divider by optical means, with which one can extract the needed information while at the same time leaving the information readable by other users down the line [15]. The challenge is of course to tap the information without degradation of the signal-to-noise ratio (SNR) for both tapped and transmitted information. An optical divider or tap is usually a four-port device with two inputs and two outputs (the law of quantum mechanics requires there to be an extra input). A typical divider is simply a beamsplitter: information comes in one input and is divided into two outputs. However, the uncorrelated quantum noise from the other unused port will add to the outputs and degrade their SNRs. On the other hand, it is known that quantum noise can be suppressed with a squeezed state. Shapiro thus suggested [15] to couple the unused port to a squeezed vacuum to reduce its quantum noise. Another technique is to use two correlated quantum fields as the two inputs. Quantum correlation between the two inputs will subtract out the quantum noise in the outputs. Such techniques can be used in any four-port system for information division.

In the following sections, we will mainly discuss quantum fluctuations in a nondegenerate optical parametric amplifier (NOPA) which has only one internal mode called "idler". In section 2, we first describe an experiment in which we couple a squeezed light field into the internal idler mode of the NOPA and demonstrate quantum noise reduction by the scheme of rearranging the quantum noise between two conjugate quadrature-phase amplitudes. In section 3, we will discuss quantum noise cancellation in amplification with a correlated quantum state where noise-free amplification can be achieved with moderate correlation. In section 4, we will consider the NOPA as a four-port system (2 inputs and 2 outputs) and show that it can be used as a quantum optical information tap when the inputs are coupled either to a squeezed state or to a correlated quantum state.

# 2 Quantum Noise Reduction in Optical Amplification with a Squeezed State

A nondegenerate optical parametric amplifier (NOPA) is an optical amplifier that utilizes nonlinear coupling to convert energy in a pump beam(s) to a signal beam. It can be realized in either three-wave mixing or four-wave mixing processes. Besides the pump beam(s) and the input-output signal beams, another beam called "idler" is coupled to the pump and signal beams at the same time. This idler beam labled as $\hat{b}^{in}$ corresponds to the so-called internal mode of the amplifier discussed earlier. In terms of the quantities in Eq.(1), $\hat{F} = \sqrt{G-1}\ \hat{b}^{in\dagger}$ and $G$ is related to the pump beam. Fig.1 shows a NOPA with a coherent signal input and its idler mode coupled to a squeezed vacuum generated by a squeezer. Detailed descriptions of each device used in the diagram can be found in Ref.[14b]. In the linear operating regime (small input signal), the pump beam is undepleted and does not contribute any extra quantum noise to the output [16]. Thus Eq.(1) becomes

$$\hat{a}^{out} = \sqrt{G}\ \hat{a}^{in} + \sqrt{G-1}\ \hat{b}^{in\dagger}. \tag{3}$$

We can rewrite Eq.(3) with the quadrature-phase amplitude $\hat{X}_c(\theta) \equiv \hat{c}\ e^{-i\theta} + \hat{c}^{\dagger}e^{i\theta}$ $(c = a, b)$ as

$$\hat{X}_a^{out}(\theta) = \sqrt{G}\ \hat{X}_a^{in}(\theta) + \sqrt{G-1}\hat{X}_b^{in}(-\theta). \tag{4}$$

If the fields $\hat{a}$ and $\hat{b}$ are independent of each other, the output noise of the amplifier is then given by

$$N_a^{out}(\theta) = G\ N_a^{in}(\theta) + (G-1)N_b^{in}(-\theta), \tag{5}$$

where $N_i(\theta) \equiv \langle(\hat{X}_i - \langle\hat{X}_i\rangle)^2\rangle$ $(i = a, b)$.

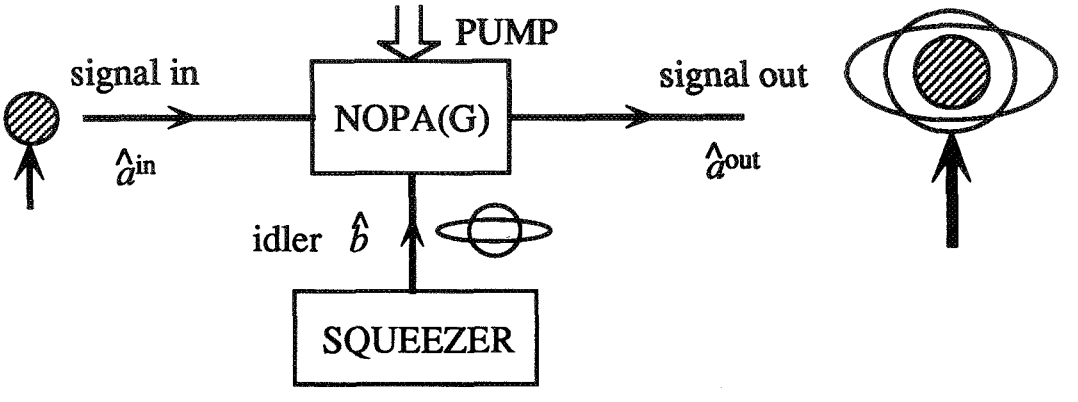


*FIG. 1. Diagram for the experiment of quantum noise reduction with a NOPA. The shaded part of the noise circle for the amplified signal corresponds to amplified input signal noise and the rest of the noise comes from the extra noise contributed by the amplifier's internal modes*

Usually, the idler mode $\hat{b}$ is coupled to empty vacuum and $N_b^{in}(-\theta) = 1$, resulting in extra noise $G - 1$ in the output. On the other hand, with the idler mode $\hat{b}$ coupled to a squeezed vacuum, for the squeezed quadrature of $\theta = \theta_-$, we have $N_{b-} \equiv N_b^{in}(-\theta_-) < 1$, thus the extra noise at the output due to the idler can be reduced. For the other quadrature, however, the extra noise will be enhanced. Therefore, as we change the phase and look at different quadratures, we will obtain a phase-sensitive noise level for the output with noise reduction at some phases and noise enhancement at other phases, as shown in Fig.2, where we plot the signal output noise level as a function of local oscillator phase. It is found that the minimum noise level in the phase-sensitive curve *ii* drops below the phase-insensitive curve *i*, which is the output noise level when the idler mode is coupled to the vacuum, thus demonstrating quantum noise reduction in the amplification process. The phase-insensitive curve *i* ($\Phi_G$) also gives a measure of quantum noise gain as compared to the vacuum noise level $\Psi_0$ ($G_q \equiv \Phi_G/\Psi_0$) [14b]. The dashed trace *iv* corresponds to the output noise level expected for a lossless system with perfectly squeezed idler at the same operating gain of the amplifier. To better quantify the noise reduction, we tune the phase to $\theta = \theta_-$ and block and unblock the injected squeezed light field. When the squeezed light is blocked, it corresponds to a vacuum state coupled to the idler mode. In Fig.3, we plot the output noise level as we turn "ON" and "OFF" the squeezed light. By performing the same measurement at different gains of the amplifier, we can plot the amount of noise redution $\Delta_- \equiv \Phi(\theta_-)/\Phi_G$ against the quantum noise gain $G_q$ as in Fig.4. The best noise reduction of $-0.7$ dB is observed at $G_q = 2.6$ (4.2 dB). The solid curve in Fig.4 is a theoretical prediction for our system with 0.3% internal round-trip loss for the NOPA and with 30% external loss (mainly propagation and detection losses), as determined by independent measurements [14b]. The amount of squeezing

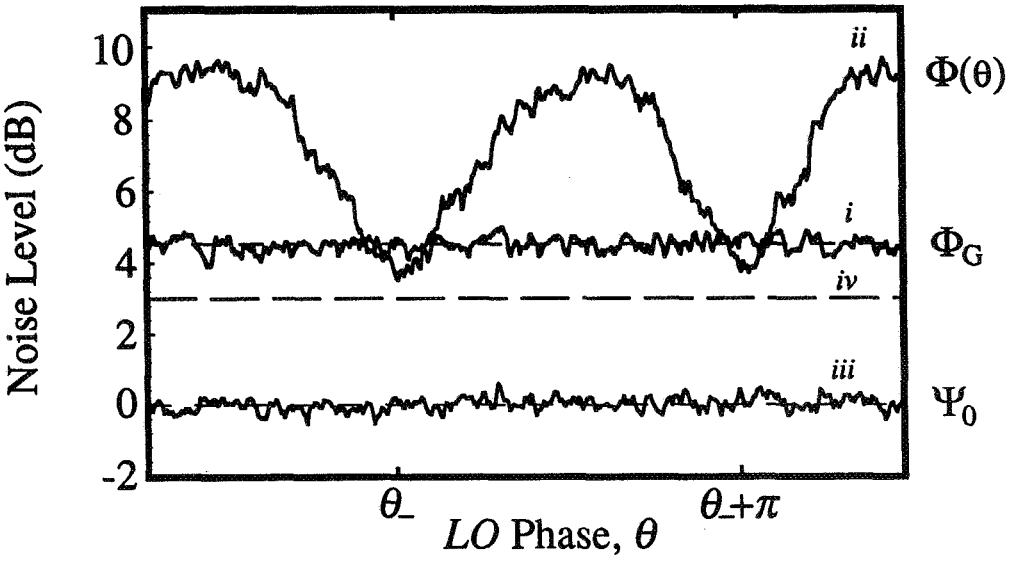


*FIG. 2. Spectral density of photocurrent fluctuations for $i_-$ generated by NOPA's signal output $\hat{a}^{out}$ as a function of the local oscillator phase $\theta$. Trace i is the amplified noise level $\Phi_G$ when the idler mode is in a vacuum state, while trace ii corresponds to the case when the idler is in a squeezed vacuum state. Trace iii is the vacuum noise level $\Psi_0$ and the dashed trace iv corresponds to the output noise level expected for a lossless system with perfectly squeezed idler.*

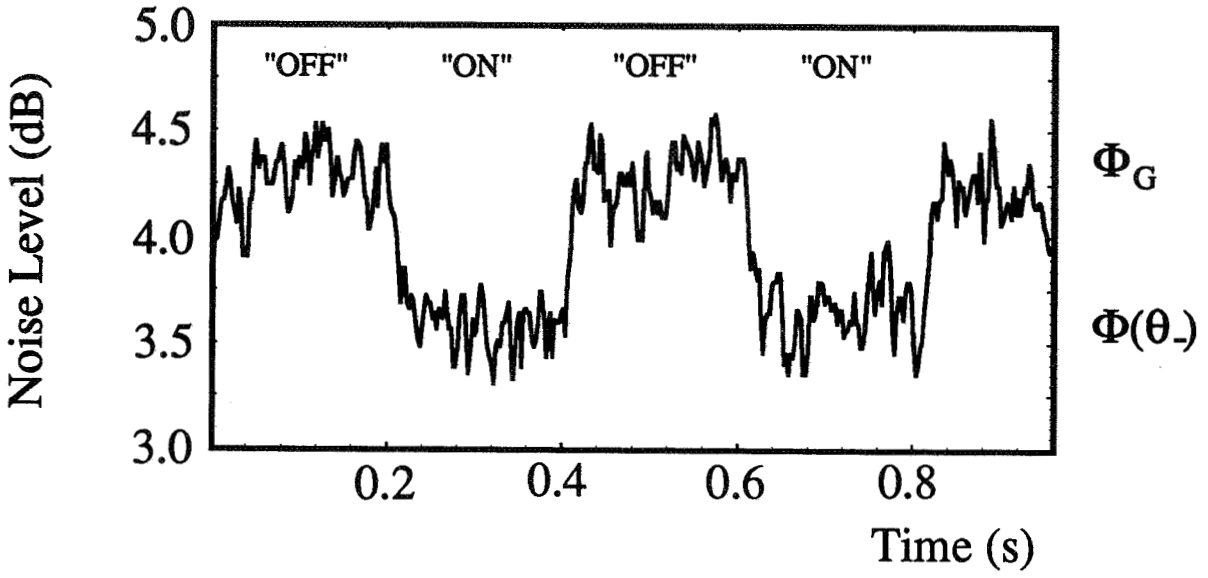


*FIG. 3. Amplified noise level of the signal output for NOPA. "OFF" correponds to the output noise level $\Phi_G$ for a vacuum state coupling to the idler mode. "ON" gives the output noise level $\Phi(\theta_-)$ for a squeezed state input to the idler. The noise levels are referenced to the vacuum noise level $\Psi_0$.*

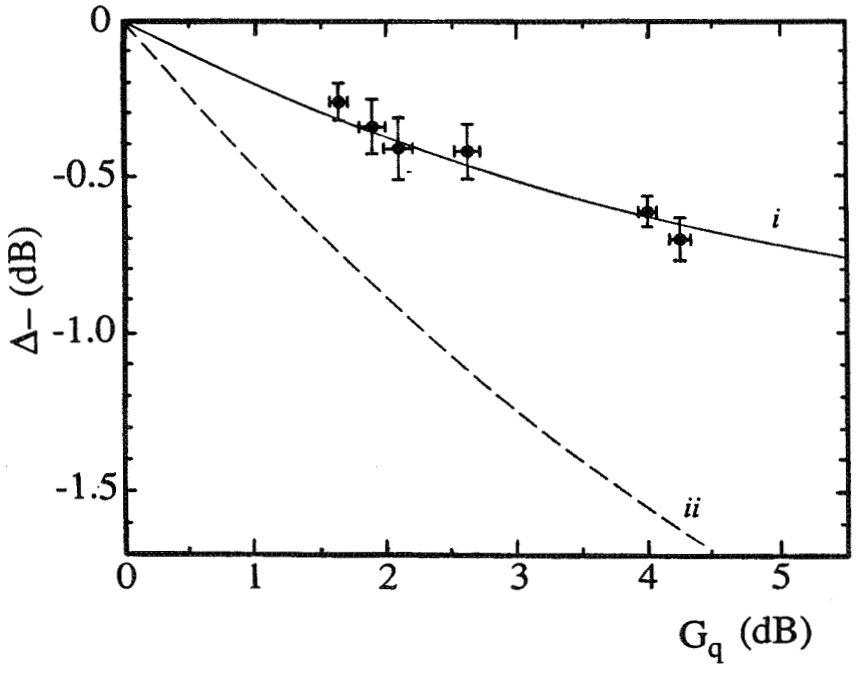


*FIG. 4. Quantum noise reduction $\Delta_-$ for the amplified output signal as a function of the detected quantum noise gain $G_q$ for a squeezed idler input of $N_- = 0.52$. The solid curve is the theoretical prediction for our system and the dashed curve ii is for a lossless system with perfect squeezing for the idler.*

that is coupled into the idler mode is also directly measured to be $N_b^{in}(\theta_-) = 0.52$. Thus all the relevant parameters in the theory for our experiment are measured independently. It is seen that the experimental data fit the theoretical prediction quite well. The dashed trace *ii* corresponds to the maximum possible noise reduction with a coherent signal input in a lossless system with perfect squeezing coupled to the idler mode ($N_b^{in}(\theta_-) = 0$), in which no extra noise is added to the amplified output.

# 3 Cancellation of Quantum Fluctuations in Optical Amplification with Correlated Quantum Fields

In the discussion of last section, we assumed that the quantum fluctuations in the signal input and the amplifier's internal idler mode are uncorrelated. When their quantum fluctuations are correlated, however, we cannot write the output noise as in Eq.(5) because the correlation between $\hat{X}_a^{in}(\theta)$ and $\hat{X}_b^{in}(-\theta)$ may result in cancellation (or enhancement) of their fluctuations through destructive (or constructive) interference.

The quantity to describe the degree of correlation between fields $\hat{a}$ and $\hat{b}$ is the correlation function defined as

$$C_{ab} \equiv \frac{\langle \Delta\hat{X}_a \Delta\hat{X}_b \rangle}{\sqrt{\langle \Delta^2\hat{X}_a \rangle \langle \Delta^2\hat{X}_b \rangle}} \quad (|C_{ab}| < 1). \tag{6}$$

Assume that $\Delta\hat{X}_a$ and $\Delta\hat{X}_b$ are positively correlated, that is, $C_{ab} > 0$ and that the fluctuations of field $\hat{a}$ are smaller than or equal to that of field $\hat{b}$, that is, $N_a \equiv \langle \Delta^2\hat{X}_a \rangle \leq \langle \Delta^2\hat{X}_b \rangle$. We will encode the signal only into the field $\hat{a}$ ($\langle \hat{X}_a \rangle \equiv A \neq 0$ and $\langle \hat{X}_b \rangle = 0$) because it has less noise. The signal-to-noise ratio (SNR) for the field $\hat{a}$ is then $R_a = A^2/N_a$. On the other hand, because the two fields are correlated, we have for the noise in the difference of the two fields:

$$N_d \equiv \langle (\Delta\hat{X}_a - \lambda_m \Delta\hat{X}_b)^2 \rangle = \langle \Delta^2\hat{X}_a \rangle (1 - C_{ab}^2) < N_a,$$

where we have minimized $N_d$ by choosing the optimized coefficient $\lambda_m = \langle \Delta\hat{X}_a \Delta\hat{X}_b \rangle / \langle \Delta^2\hat{X}_b \rangle$. $\lambda_m = C_{ab}$ when $\langle \Delta^2\hat{X}_a \rangle = \langle \Delta^2\hat{X}_b \rangle$. Thus the noise in the difference of two fields is smaller than the noise in the single field $\hat{a}$. So the optimized signal-to-noise ratio (SNR) is $R_d \equiv \langle \hat{X}_a - \lambda_m \hat{X}_b \rangle^2 / N_d = A^2/N_a(1 - C_{ab}^2)$ if both $\hat{a}$ and $\hat{b}$ fields are employed. Obviously, $R_d > R_a$.

Next let us consider the situation when the fields $\hat{a}$ and $\hat{b}$ are injected into the signal and idler ports of the amplifier, respectively. We adjust the phase of the pump beam so that Eq.(4) becomes

$$\hat{X}_a^{out} = \sqrt{G}\ \hat{X}_a^{in} - \sqrt{G-1}\hat{X}_b^{in}. \tag{7}$$

Thus the amplified signal becomes

$$\langle \hat{X}_a^{out} \rangle = \sqrt{G} \langle \hat{X}_a^{in} \rangle = A\sqrt{G}. \tag{8}$$

The noise of the amplified signal output is calculated as

$$N_a^{out} = \langle \Delta^2 \hat{X}_a^{out} \rangle = G \langle (\Delta\hat{X}_a^{in} - \sqrt{(G-1)/G}\Delta\hat{X}_b^{in})^2 \rangle, \tag{9}$$

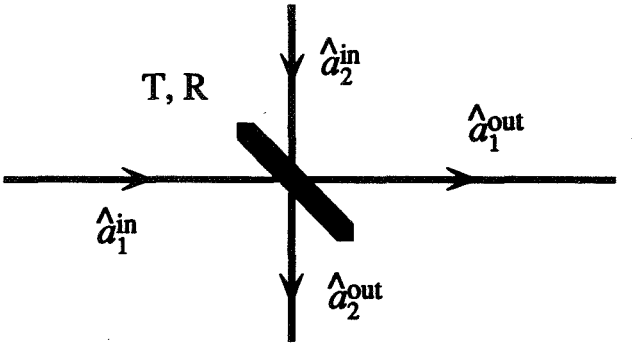


*FIG. 5. Diagram for a beamsplitter.*

which reaches minimum value of

$$N_{a_{min}}^{out} = G\langle(\Delta\hat{X}_a - \lambda_m\Delta\hat{X}_b)^2\rangle = G\langle\Delta^2\hat{X}_a\rangle(1 - C_{ab}^2) = GN_d, \tag{10}$$

when $\sqrt{(G-1)/G} = \lambda_m = C_{ab}$. Note that Eqs.(8) and (9) are for the signal beam alone; mixing of the field $\hat{a}$ with the field $\hat{b}$ as required for $N_d$ has taken place within the amplifier itself. Combining Eqs.(8,10), we obtain for the output SNR

$$R_a^{out} = \langle\hat{X}_a^{out}\rangle^2/N_{a_{min}}^{out} = A^2G/N_dG = R_d. \tag{11}$$

Therefore the output SNR $R_a^{out}$ is equal to the input SNR $R_d$ (and $> R_a$) with the signal amplified by the gain $G$. No extra noise is added in the amplification process. However, noise-free amplication can only be achieved at some specific gain $G = 1/(1 - \lambda_m^2)$ determined by the correlation function $C_{ab}$ between the two fields $\hat{a}$ and $\hat{b}$. When the two fields are close to perfect correlation with $\lambda_m = C_{ab} \to 1$, the gain $G$ can be arbitrarily large.

# 4 Quantum Optical Information Tapping with Squeezed States and Correlated Quantum Fields

The concept of quantum optical information tapping was first discussed by Shapiro [15] for a beamsplitter with squeezed state coupled to one of the input ports. Consider a beamsplitter shown in Fig.5, where the input port $\hat{a}_2$ is in a squeezed state with the degree of squeezing denoted by $S$. A coherent signal of size $A$ is injected into the other port labled as $\hat{a}_1$ with input SNR $R_1^{in} = A^2$. It can be easily calculated [15] that for a beamsplitter with transmissivity $T$ and reflectivity $R$, the output SNR at both output ports are given as

$$R_1^{out} = \frac{TA^2}{(T + RS)}, \quad R_2^{out} = \frac{RA^2}{(R + TS)}.$$

The efficiency of this information tapping scheme can be quantified [17] as the ratio of the output SNRs to the input SNRs:

$$\eta \equiv \frac{R_1^{out} + R_2^{out}}{R_1^{in}} = \frac{T}{T + RS} + \frac{R}{R + TS} = \frac{2TR(1 - S) + S}{TR(1 - S)^2 + S}, \tag{12}$$

which has maximum value of $\frac{2}{1+S}$ when $T = R = 1/2$. It is seen that

$$2 > \eta > 1 \tag{13}$$

for squeezed state input at port 2 ($S < 1$). On the other hand, for classical state ($S \geq 1$), we always have $\eta < 1$ [18]. Thus Eq.(13) is the criterion for realization of a quantum tap for optical information.

Quantum information tapping can also be achieved for a beamsplitter with correlated quantum fields $\hat{a}, \hat{b}$ as the two inputs. For this case, let us assume the two fields have the same noise level, that is, $\langle \Delta^2 \hat{X}_a \rangle = \langle \Delta^2 \hat{X}_b \rangle$. For a beamsplitter, we have for the quadratures of the fields:

$$\hat{X}_1^{out} = \sqrt{T}\hat{X}_a^{in} - \sqrt{R}\hat{X}_b^{in}, \tag{14a}$$

$$\hat{X}_2^{out} = \sqrt{T}\hat{X}_b^{in} + \sqrt{R}\hat{X}_a^{in}. \tag{14b}$$

where we only write down the $X$-quadratures, in which information is encoded.

It is easy to show that $R_1^{out} = R_d^{in}$ when $R/T = \lambda_m^2 = C_{ab}^2$ as before in Section 3. For output port 2, we find

$$R_2^{out} = R_d^{in} \frac{R(1 - C_{ab}^2)}{1 + 2\sqrt{TR}C_{ab}}$$

Thus the information tapping efficiency

$$\eta = 1 + \frac{R(1 - C_{ab}^2)}{1 + 2\sqrt{TR}C_{ab}} = 1 + \frac{(1 - C_{ab}^2)C_{ab}^2}{1 + 3C_{ab}^2} > 1. \tag{15}$$

Therefore quantum optical information tapping is achieved with correlated fields. Notice here we choose $R, T$ so that $R_1^{out} = R_d^{in}$. Of course, we could choose $R, T$ to maximize $\eta$. However, $\eta$ will never be close to the perfect value of 2 even for perfect correlation. This is because of the plus sign in Eq.(14b) required by unitarity for any beamsplitter; and it can not be changed to a minus sign no matter what you do with the relative phase of the two fields. In the following, we will see a different situation for the NOPA.

For the NOPA, there are also two inputs (signal and idler) and two corresponding outputs, as shown in Fig.6. With proper phase adjustment of the pump, the input-output relations for NOPA are given as

$$\hat{a}^{out} = \sqrt{G}\,\hat{a}^{in} - \sqrt{G-1}\,\hat{b}^{in\dagger},$$
$$\hat{b}^{out} = \sqrt{G}\,\hat{b}^{in} - \sqrt{G-1}\,\hat{a}^{in\dagger},$$

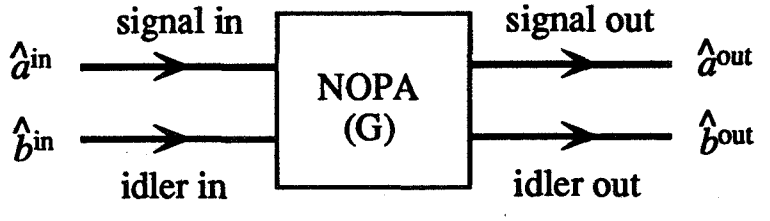


*FIG. 6. Diagram of NOPA as a four-port device.*

or in terms of the quadrature-phase amplitudes

$$\hat{X}_a^{out} = \sqrt{G}\,\hat{X}_a^{in} - \sqrt{G-1}\,\hat{X}_b^{in}, \tag{16a}$$

$$\hat{X}_b^{out} = \sqrt{G}\,\hat{X}_b^{in} - \sqrt{G-1}\,\hat{X}_a^{in}. \tag{16b}$$

First, let us assume that a coherent signal of size $A$ is injected into the signal port for amplification and squeezed state of squeezing $S$ is injected into the idler port. The input SNR is then $R^{in} = A^2$. From the input-output relations in Eqs.(16), we can calculate the output SNRs as

$$R_a^{out} = \frac{GA^2}{G+(G-1)S}, \quad R_b^{out} = \frac{(G-1)A^2}{GS+G-1}. \tag{17}$$

Hence the information tapping efficiency $\eta$ has the form of

$$\eta = \frac{G}{G+(G-1)S} + \frac{(G-1)}{GS+G-1} = \frac{2G(G-1)(1+S)+S}{G(G-1)(1+S)^2+S} \simeq \frac{2}{1+S} \quad \text{for} \quad G^2 \gg S. \tag{18}$$

Thus quantum optical information tapping is possible ($\eta > 1$) as long as $S < 1$. When $G^2 \gg S$, $\eta$ approaches $2/(1+S)$, which is the same as the result of Shapiro [15] for a beamsplitter. Of course, in this process, the signal is amplified.

As for the situation with correlated quantum fields as the inputs, for the parameters discussed in section 3, we know that $R_a^{out} = R_d$. From Eqs.(16), we can easily find out $R_b^{out}$ for the idler output. For the parameters given in section 3, we have

$$\langle \hat{X}_b^{out} \rangle = -A\sqrt{G-1},$$

and

$$\langle \Delta^2 \hat{X}_b^{out} \rangle = (1-\lambda_m^2)[\langle \Delta^2 \hat{X}_a^{in} \rangle - \langle \Delta^2 \hat{X}_b^{in} \rangle] + GN_d = GN_d \quad \text{for} \quad \langle \Delta^2 \hat{X}_a^{in} \rangle = \langle \Delta^2 \hat{X}_b^{in} \rangle.$$

Therefore, $R_b^{out} = R_d(G-1)/G$ and

$$\eta = 1 + \frac{G-1}{G} = 1 + C_{ab}^2 \to 2 \quad \text{for} \quad C_{ab} \to 1. \tag{19}$$

where the second equality follows since $G$ is chosen as in section 3, namely, $G = 1/(1-C_{ab}^2)$. Eq.(19) shows that we can always realize quantum optical information tapping in NOPA with correlated quantum fields.

In fact, for any linear four-port device with two inputs and two outputs, we can realize quantum optical information tapping with input of either a squeezed state or a correlated quantum state.

# 5 Acknowledgments

The work was supported by the Office of Naval Research and by the National Science Foundation.

# References


[1] K. Shimoda, H. Takahasi, and C. H. Townes, J. Phys. Soc. Jpn. **12**, 686 (1957).

[2] R. Serber and C. Townes, in *Quantum Electronics*, edited by C. H. Townes (Columbia Univ. Press, New York, 1959), pp.233-255.

[3] H. Heffner, Proc. IRE **50**, 1604 (1962).

[4] H. A. Haus and J. A. Mullen, Phys. Rev. **128**, A2407 (1962).

[5] R.J. Glauber, in *Frontiers in Quantum Optics*, edited by E. R. Pike and S. Sarkar (IOP, Bristol, 1986).

[6] C. M. Caves,Phys. Rev. D**26**, 1817 (1982).

[7] M. Ley and R. Loudon, Optica Acta **33**, 371 (1984).

[8] B. Yurke and J. S. Denker, Phys. Rev. A**29**, 1419 (1984).

[9] M.-A. Dupertuis, S. M. Barnett, and S. Stenholm, J. Opt. Soc. Am. B**4**, 1102 (1987).

[10] D. T. Pegg and J. A. Vaccaro, Opt. Comm. **61**, 317 (1987).

[11] G. J. Milburn, M. L. Steyn-Ross, and D. F. Walls, Phys. Rev. A**35**, 4443 (1987).

[12] A. Heidmann, R. J. Horowicz, S. Reynaud, E. Giacobino, and C. Fabre, Phys. Rev. Lett. **59**, 2555 (1987).

[13] O. Aytür,and P. Kumar, Phys. Rev. Lett. **65**, 1551 (1990).

[14] (a) Z. Y. Ou, S. F. Pereira, K. C. Peng, and H. J. Kimble, Phys. Rev. Lett. **68**, 3663 (1992). (b) Z. Y. Ou, S. F. Pereira, and H. J. Kimble, Appl. Phys. B**55**, 265 (1992).

[15] J. H. Shapiro, Opt. Lett. **5**, 351 (1980).

[16] M. J. Collett and D. F. Walls, Phys. Rev. Lett. **61**, 2442 (1988).

[17] J. Ph. Poizat and P. Grangier, Phys. Rev. Lett. **70**, 271 (1993).

[18] J. F. Roch, G. Roger, P. Grangier, J. -M. Courty, and S. Reynaud, Appl. Phys. **B55**, 291 (1992).

N95-13955

# QUANTUM NOISE LIMITS TO MATTER-WAVE INTERFEROMETRY

Marlan O. Scully

*Department of Physics, Texas A&M University*
*College Station, Texas 77843*
and
*Max-Planck-Institut für Quantenoptik, W-8046, Garching, Germany*

Jonathan P. Dowling

*Research, Development, and Engineering Center, AMSMI-RD-WS-ST*
*U. S. Army Missile Command, Redstone Arsenal, Alabama 35898*

**Abstract**

We derive the quantum limits for an atomic interferometer in which the atoms obey either Bose-Einstein or Fermi-Dirac statistics. It is found that the limiting quantum noise is due to the uncertainty associated with the particle sorting between the two branches of the interferometer. As an example, the quantum-limited sensitivity of a matter-wave gyroscope is calculated and compared with that of laser gyroscopes.

## 1. Introduction

Matter-wave interferometry dates from the inception of quantum mechanics, i.e., the early electron diffraction experiments [1]. More recent neutron interferometry experiments have yielded insight into many fundamental aspects of quantum mechanics [2]. Presently, atom interferometry has been demonstrated and holds promise as a new field of optics — matter-wave optics [3]. This field is particularly interesting since the potential sensitivity of matter-wave interferometers [4] far exceeds that of their light-wave or "photon" antecedents [5].

However, as was emphasized at the recent Solvay conference on quantum optics, there is at present no paradigm available for calculating or estimating the quantum noise limits to matter-wave interferometers, and therefore we have no basis for estimating the potential sensitivity of devices based on matter-wave interferometry (e.g., gyroscopes) [6].

In order to motivate the analysis and derive the quantum limits, we proceed as follows: First, we "set the stage" by considering a simple gyroscope and deriving the rotation-induced signal in matter-wave optics. Next, we proceed to develop the theory for atomic interferometers, cast in an operator formalism that is well suited to a quantum noise analysis, and then we obtain the quantum noise limits for matter-wave interferometry. Finally, we compare current laser gyroscope sensitivity to that of near-term, matter-wave devices.

We begin by considering an idealized atom interferometer used as a rotation detector or gyroscope, as shown in Fig. 1. From this diagram it is easy to see that the atomic path difference between the upper branch $\alpha$ and the lower branch $\beta$ is given by $\delta\ell = 2r\Omega t$, where $\Omega$ is the angular velocity of the interferometer, $r$ is the radius of the circle,

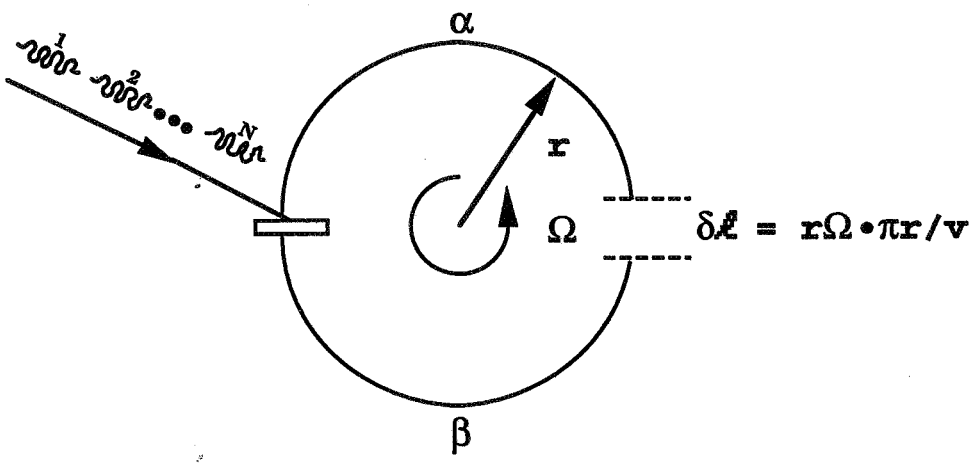


FIG. 1. A schematic illustration of an interferometer with semicircular arms to be used as a rotation sensor or gyroscope. The loop rotates with an angular frequency $\Omega$ about an axis through its center and normal to the loop plane. The path difference between counter- and copropagating beams can be easily seen to be $\delta\ell = r\Omega \bullet \frac{\pi r}{v}$, where $v$ is the atomic velocity. From these considerations the phase shift of Eq. (21) follows immediately. We may then use this result to estimate the minimum detectable rotation rate $\Omega^{\min}$, Eq. (23).

$v$ the particle velocity, and $t = \pi r / v$ is the particle transit time through the interferometer. This readily translates into a Sagnac phase difference of $\delta\varphi_{\alpha\beta} = k\left(\ell_\alpha - \ell_\beta\right)$ $= 2\pi r^2\Omega/\lambda\!\!\!^{-} v = 2A\Omega/\lambda\!\!\!^{-} v$, where $\lambda\!\!\!^{-} \equiv \hbar / mv$ is the atomic de Broglie wavelength [7] and $A$ the area enclosed by the arms. The phase signal is then given by $\varphi^{\text{signal}} = 2Am\Omega/\hbar$; independent of the interferometer shape as long as $A$ is the total area enclosed. This expression holds for both atom and light interferometers, if, in the photon case, we define an effective photon mass $m_\gamma$ implicitly by $m_\gamma c^2 = \hbar\omega$. Now, since the "mass" of a photon is governed by optical energies of a few electron volts — and atomic masses are of order $10^3$ MeV — we see that matter-wave gyroscopes potentially have a signal that is enhanced by many orders of magnitude, compared to light (laser) gyroscopes. Thus motivated, we next consider a detailed analysis of phase sensitivity in matter-wave interferometry.

## 2. A Simple Model

In accordance with current experiments [3], let us consider the model illustrated in Fig. 2. There, we see a stream of $N$ atoms passing one-at-a-time through a beam splitter into a simple interferometer with upper and lower branches labelled $\alpha$ and $\beta$, respectively. Upon recombining the two beams, we inspect the resultant interference pattern for phase shifts induced, say, by a gravitational potential between the two branches or a net rotation of the system. As in the optical dual [5], one might expect that the overall sensitivity of the device will be limited by the quantum limits imposed by particle number fluctuations $\Delta N$ on the phase noise $\Delta\varphi$ in the interferometer. It is

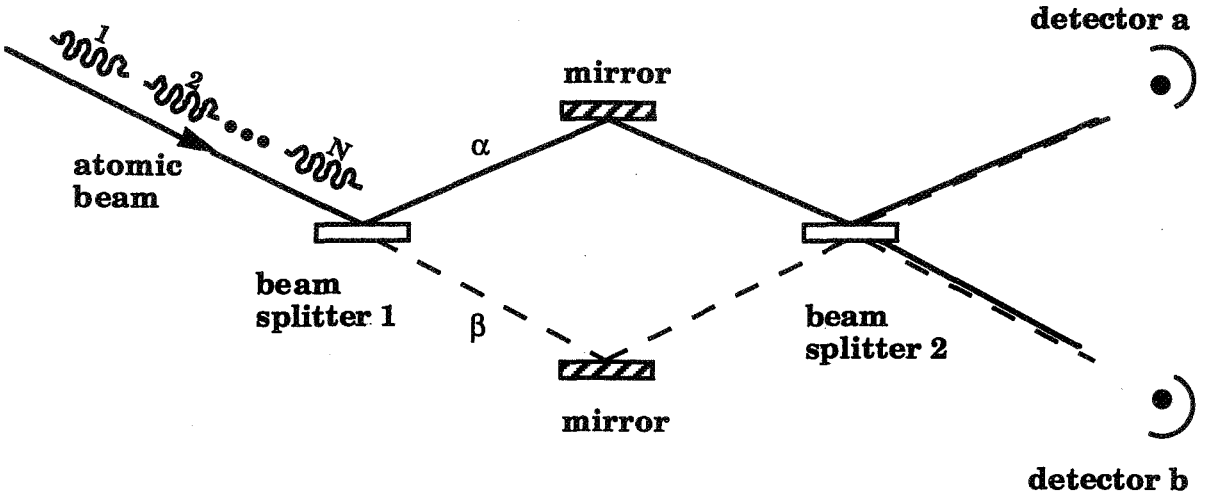


FIG. 2. We illustrate a scheme whereby a stream of $N$ atoms is sent through a simple interferometer during a measurement time $t_m$. The atoms are split at beam splitter 1, follow paths $\alpha$ or $\beta$, are reflected off the mirrors, and are then recombined at beam splitter 2. The recombined atoms are detected at upper detector $a$ or lower detector $b$ where interference fringes are recorded.

often stated that $\Delta N$ is to be associated with the fluctuations in the arrival time of atoms in the input beam, i.e., $\Delta N \sim \sqrt{\bar{n}}$ where $\bar{n}$ is the mean number of particles. However, we shall show that the particle number noise arises not from fluctuations in the input beam intensity but rather from beam splitter uncertainties pertaining to the lack of knowledge of which path, $\alpha$ or $\beta$ , the atom has taken through the interferometer.

## 3. The Quantum Signal

Let us continue developing our simple model depicted in Fig. 2. We assume that, upon reflection from a beam splitter surface, the particles undergo an unimportant phase shift that we take to be $\pi/2$, but that in reality depends upon the structure of the beam splitter. Upon passage *through* a beam splitter, however, the atom undergoes a phase shift of $\varphi_i$, $i = 1, 2$, for the first and second beam splitter, respectively. The cumulative effect in the interferometer of these various processes on the atomic wave function $\psi$ is depicted in Fig. 3, and leads to a wave function $\psi_a$ corresponding to the upper detector and $\psi_b$ for the lower detector, namely

$$\psi_a = \frac{\psi}{2} e^{i\theta_a}\left[1 - e^{-ik\left(\ell_\alpha - \ell_\beta\right)}\right] \quad , \quad \psi_b = \frac{\psi}{2} e^{i\theta_b}\left[1 + e^{-ik\left(\ell_\alpha - \ell_\beta\right)}\right] \qquad (1)$$

where $\theta_a \equiv \pi/2 + k\ell_\alpha + \varphi_2$ , and $\theta_b \equiv k\ell_\alpha + \varphi_1 + \varphi_2$, and where, without loss of generality, we let $\varphi_1 = \varphi_2 = \pi$ . Here, $k$ is the atomic wave number and $\ell_\alpha$ and $\ell_\beta$ are the

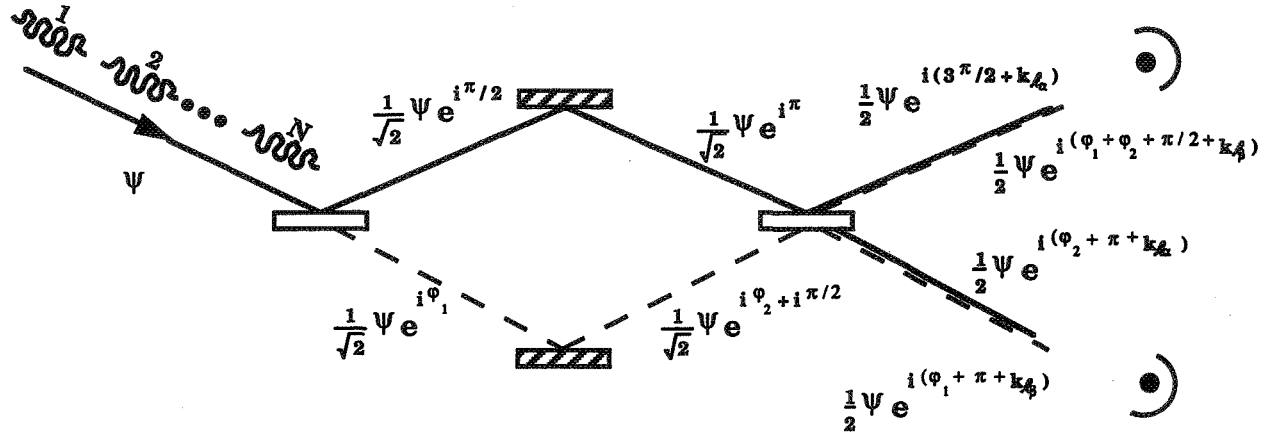


FIG. 3. Chasing phases through the interferometer accounts for accumulated phase shifts in the upper or lower detectors. The phase shift upon reflection is arbitrary, but we choose it here to be $\pi/2$ for simplicity. Upon transmission, a phase shift of $\varphi_1$ or $\varphi_2$ is assumed for beam splitter one or two, respectively, and without loss of generality we take $\varphi_1 = \varphi_2 = \pi$.

path lengths through the upper and lower branches, respectively. We imagine now that the beam is recombined by the second beam splitter and then the detectors $a$ and $b$ shown in Fig. 2 count the number of atoms as they arrive in the recombined upper beam or lower beam, respectively. If we label $N$ atoms with the index $i = 1, \ldots, N$, as those sent through the interferometer during a measurement time $t_m$, then the appropriate state vector $|\varphi\rangle_i$ for the $i^{th}$ atom in the interferometer, after recombination, is given by

$$|\varphi\rangle_i = \frac{e^{i\theta_a}}{2}\left(1 - e^{-i\varphi_{\alpha\beta}}\right)|1_a, 0_b\rangle_i + \frac{e^{i\theta_b}}{2}\left(1 + e^{-i\varphi_{\alpha\beta}}\right)|0_a, 1_b\rangle_i \ , \qquad (2)$$

where here $\varphi_{\alpha\beta} \equiv k(\ell_\alpha - \ell_\beta)$. We see that this state is an appropriate superposition of the number states $|1_a, 0_b\rangle$ and $|0_a, 1_b\rangle$ corresponding to an atom incident on the upper or lower detectors, respectively. The state vector $|\Phi\rangle_N$ for the $N$-atom state is then constructed via a direct product of the individual atomic states, namely

$$|\Phi\rangle_N \equiv \prod_{i=1}^{N} |\varphi\rangle_i \ . \qquad (3)$$

Let $\hat{c}^{\dagger}_{\sigma,i}$ and $\hat{c}_{\sigma,i}$, where $\sigma = a,b$, be the creation and annihilation operators, respectively, for the number states $|n_a, n_b\rangle_i$, where, corresponding to number operators $\hat{n}_{\sigma,i} \equiv \hat{c}^{\dagger}_{\sigma,i}\,\hat{c}_{\sigma,i}$, the eigenvalues $n_a$ and $n_b$ are $0$ or $1$. Then the number operator $\hat{N}_\sigma$ for the number of upper or lower atoms is determined by

$$\hat{N}_\sigma = \sum_{i=1}^{N} \hat{n}_{\sigma,i} \qquad (\sigma = a, b) \quad , \tag{4}$$

and the operators $\hat{c}$ obey the commutation relations

$$\left[\hat{c}_{\sigma,i}\, \hat{c}^{\dagger}_{\sigma,j} \pm \hat{c}^{\dagger}_{\sigma,j}\, \hat{c}_{\sigma,i}\right] = \delta_{ij} \ , \tag{5}$$

where the plus or minus sign indicates Bose or Fermi statistics, respectively. The statistical nature of the atoms will be important in circumstances where the density of particles in the interferometer is so large that there is more than one atom at a time within a single coherence length, or if the atoms are injected in a correlated manner into the input ports [9]. The expectation values $\langle \hat{N}_\sigma \rangle_N$ of these number operators, Eq. (4), are given by

$${}_N\langle \Phi |\, \hat{N}_a\, | \Phi \rangle_N = \sum_{i=1}^{N} \left| \frac{1 - e^{-i\varphi_{\alpha\beta}}}{2} \right|^2 {}_i\langle 1_a, 0_b |\, \hat{n}_{a,i}\, | 1_a, 0_b \rangle_i \ , \tag{6a}$$

$${}_N\langle \Phi |\, \hat{N}_b\, | \Phi \rangle_N = \sum_{i=1}^{N} \left| \frac{1 + e^{-i\varphi_{\alpha\beta}}}{2} \right|^2 {}_i\langle 0_a, 1_b |\, \hat{n}_{b,i}\, | 0_a, 1_b \rangle_i \ . \tag{6b}$$

This yields the expression for the mean number of atoms in the $\alpha$ and $\beta$ branches as

$$\langle \hat{N}_a \rangle_N = N \sin^2 \varphi_{\alpha\beta}/2 \quad , \qquad \langle \hat{N}_b \rangle_N = N \cos^2 \varphi_{\alpha\beta}/2 \ . \tag{7}$$

These expectations constitute the signal; we proceed to calculate the noise.

## 4. A Calculation of Poisson Noise

As noted earlier, it is frequently stated that number fluctuations $\Delta N$ in the interferometer should be just noise of the form $\sqrt{\bar{n}}$ due to fluctuations in the input beam. Let us briefly investigate this hypothesis. A reasonable assumption is that the distribution of the $N$ atoms in the input beam is Poissonian with a distribution function $P_n$, given by

$$P_n \equiv \frac{\bar{n}^n}{n!}\, e^{-\bar{n}} \ , \tag{8}$$

where $\bar{n}$ is the mean number of particles in the beam. The signal or expectation value of the operators $\hat{N}_\sigma$ is then given by

$$\langle \hat{N}_\sigma \rangle = \sum_{n=1}^{N} {}_n\langle \Phi | \hat{N}_\sigma | \Phi \rangle_n \, P_n = \bar{n} \begin{Bmatrix} \sin^2 \varphi_{\alpha\beta}/2 \\ \cos^2 \varphi_{\alpha\beta}/2 \end{Bmatrix} \tag{9}$$

where $\bar{n} = \sum_n n \, P_n$, and the upper and lower terms in braces are associated with detectors $\sigma = a$ and $\sigma = b$, respectively — a convention we shall use throughout. Hence, the fluctuations accompanying this signal are determined by the root variance $\langle \Delta \hat{N}_\sigma \rangle$, which is found to be

$$\langle \Delta N_\sigma \rangle = \sqrt{\bar{n}} \begin{Bmatrix} \sin^2 \varphi_{\alpha\beta}/2 \\ \cos^2 \varphi_{\alpha\beta}/2 \end{Bmatrix} \tag{10}$$

Now, to get a determination of minimum detectable phase shift, one usually equates the signal, Eq. (9), to the noise, given by Eq. (10). Regardless of the choice of $\varphi_{\alpha\beta}$, we see from Eqs. (9) and (10) that upon equating signal to error, the phase dependence cancels out and we have no determination of the minimum detectable phase. The point is that $N$ is not a random number, since we have the constraint $N_a + N_b = N = constant$, and fluctuations in the incoming atomic beam do not determine sensitivity. In other words, precise knowledge of the value of $N$ obviates the need for a Poisson analysis, since $N$ is clearly *not* a random variable. What, then, is the limiting noise mechanism in the interferometer?

## 5. The Quantum Noise

We compute the quantum noise fluctuations using the second quantized formalism developed earlier. Recalling the definitions for the number operator $\hat{N}$, Eq. (4), and the state vector $|\Phi\rangle_N$, Eq. (3), and using the commutation relations, Eq (5), we may write,

$$\langle \Delta \hat{N}_\sigma \rangle^2 = {}_N\langle \Phi | \hat{N}_\sigma^2 | \Phi \rangle_N - \left[ {}_N\langle \Phi | \hat{N}_\sigma | \Phi \rangle_N \right]^2$$

$$= {}_N\langle \Phi | \sum_{i=1}^{N} \hat{n}_{\sigma,i} \sum_{j=1}^{N} \hat{n}_{\sigma,j} | \Phi \rangle_N - \left[ {}_N\langle \Phi | \sum_{i=1}^{N} \hat{n}_{\sigma,i} | \Phi \rangle_N \right]^2$$

$$= \sum_{i=1}^{N} {}_i\langle\varphi|\ \hat{n}_{\sigma,i}\,|\varphi\rangle_i \sum_{\substack{j=1\\ j\neq i}}^{N} {}_j\langle\varphi|\ \hat{n}_{\sigma,j}\,|\varphi\rangle_j$$

$$+ \sum_{i=1}^{N} {}_i\langle\varphi|\,\hat{c}^{\dagger}_{\sigma,i}\left[1 \pm \hat{n}_{\sigma,i}\right]\hat{c}_{\sigma,i}\,|\varphi\rangle_i - \left[\sum_{i=1}^{N} {}_i\langle\varphi|\ \hat{n}_{\sigma,i}\,|\varphi\rangle_i\right]^2$$

$$= \frac{N}{4}\sin^2\varphi_{\alpha\beta} \pm \sum_{i=1}^{N} {}_i\langle\varphi|\ \hat{c}^{\dagger}_{\sigma,i}\ \hat{c}^{\dagger}_{\sigma,i}\ \hat{c}_{\sigma,i}\ \hat{c}_{\sigma,i}\,|\varphi\rangle_i \qquad (11)$$

where, as before, the upper and lower terms in braces correspond to $\sigma = a$ or $b$, respectively, and the $\pm$ sign refers to the statistics of the particles: a plus sign for bosons and a minus sign for fermions. We note that the last, statistics-dependent term of Eq. (11) is the sum of non-negative matrix elements and so itself is non-negative or non-positive, according to the plus sign or negative sign, respectively. A quantitative analysis of the contribution of this statistics-dependent term requires a specific model of the coherences between atoms in a dense beam. However, one can qualitatively state that for sufficiently high densities the use of fermionic atoms will tend to *lower* the quantum noise limit. This is because the last term will be negative. Bosons will have the opposite effect. Detailed analysis of the statistics-dependent contribution is beyond the scope of this letter, and will be left to a later work. Hence, since, in current experiments, the beam intensity is so low that there is only one atom at a time within a single coherence length. In this case, the statistics-dependent second term in the last line of Eq. (11) is zero, and we are left with the result

$$\langle\Delta N_\alpha\rangle = \frac{\sqrt{N}}{2}\sin\varphi_{\alpha\beta} \qquad (12)$$

We notice that this result depends on the total number of atoms $N$ and *not* the mean number $\bar{n}$ as in the Poisson-distribution argument given before. Now, the signal in either branch $N_\sigma$ is given by Eq. (7).

The quantum fluctuations in phase $\Delta\varphi_{\alpha\beta}$ in the measured phase difference $\varphi_{\alpha\beta}$ may be determined by [8]

$$\left|\Delta\varphi_{\alpha\beta}\right| \equiv \frac{\langle\Delta N_\sigma\rangle}{\left|\partial\langle N_\sigma\rangle/\partial\varphi_{\alpha\beta}\right|}$$

$$= \frac{1}{\sqrt{N}}\ , \qquad (13)$$

a result that is *independent* of $\varphi_{\alpha\beta}$. This independence might appear surprising at first, but it is a direct result of the fact that the *quantum* number state noise $\langle \Delta N_\sigma \rangle$ is proportional to the slope of the signal $\langle N_\sigma \rangle$ for the upper/lower number states considered here. (See, in particular, reference 8.) Again, we stress that $N$ is not the expectation value but rather the total number of atoms detected in the measurement time $t_m$. This is *not* then the expression one would expect from application of the uncertainty principle, for in that case $N$ would have to be replaced by $\langle N \rangle$. We reemphasize that it has not been clear what form of the uncertainty principle one should even use in an atom interferometer [6]. For light, the so called number-phase uncertainty principle, $\Delta\varphi\Delta N \gtrsim 1$, yields for a coherent state $\Delta\varphi \cong 1/\langle N \rangle$ – where the expectation $\langle N \rangle$ and not the total number $N$ is used. For atoms it is not obvious at all what the relationship should be, and we have shown that the result is unexpected in that Eq. (13) depends on the total number $N$ , that is precisely known for the atom interferometer, and where $\langle N \rangle$ has no meaning. In contradistinction, in a laser interferometer, it is impossible to know the total number of photons and only the mean can be specified. Hence, the atom result, Eq. (13), is quantitatively, qualitatively, and philosophically different from the optical result. Hence, Eq. (13) is indeed a novel result. We note that B. Yurke obtained a similar result for Fermions, using spin algebra techniques [9].

## 6. Comparing Laser and Matter Gyros

We conclude by applying this result to the gyroscope problem. Let us note that the atom number $N$ is given by $j\,t_m$, where $j$ is the atomic flux (in atoms per second) hitting the detector. We have from Eq. (14) the minimum detectable phase shift, $\varphi_{\min} = 2/\sqrt{j t_m}$, and equating this to the signal derived earlier, $\varphi^{\text{signal}} = 2Am\Omega/\hbar$ , we find the minimum detectable rotation rate $\Omega^{\min}$ is given by

$$\Omega^{\min} \cong \frac{\hbar}{Am}\,\frac{1}{\sqrt{j t_m}} \qquad \text{(matter)}. \tag{14}$$

This should be compared to the same result obtained from using an optical interferometer in which the flux $j$ is given by the power $P$ divided by the photon energy $\hbar\omega$ [5,7], in other words

$$\Omega^{\min} \cong \frac{\hbar}{Am_\gamma}\,\frac{1}{\sqrt{\frac{P}{\hbar\omega}\,t_m}} \qquad \text{(light)}, \tag{15}$$

where $m_\gamma$ is the effective photon mass, defined by $m_\gamma \equiv \hbar\omega/c^2$. In Table 1 we compare and contrast properties of the matter-wave and laser light interferometers in order to gauge their effectiveness in measuring $\Omega^{\min}$. As mentioned before, we note

that the typical photon effective mass gives an increase in sensitivity of $10^{10}$. This mass factor, however, is offset by the low particle flux available for atoms. This fact increases the laser gyroscope sensitivity over that of matter-wave devices by a factor of around $10^2$. In addition, the atoms make about one "round trip" through an interferometer, whereas in a ring laser gyroscope the photons make many ($\approx 10^4$) circuits around the ring and yield an additional sensitivity factor of $10^4$ in favor of the laser system. This still leaves the matter-wave device $10^4$ times more sensitive.

In summary then, we conclude that the phase uncertainty arising in an atomic interferometer arises from atomic number fluctuations associated with the sorting of the particles between the two arms of the interferometer. Applying our results to an interferometer used as a gyroscope, we find that a matter-wave gyroscope can be expected to be more sensitive to rotation by some *four orders of magnitude* than present laser devices.

| | Matter | Laser | Matter Over Light Sensitivity Factor |
|---|---|---|---|
| Mass Factor | $\sim 10^4$ MeV | $\sim 1$ eV | $\sim 10^{10}$ |
| Flux | $\rho v A \sim 10^{10} \cdot 10^4 \cdot 10^{-2}$ $= 10^{12} \frac{\text{particles}}{\text{sec}}$ | $\frac{P}{\hbar \nu} \sim \frac{10^{-3}}{10^{-19}}$ $= 10^{16} \frac{\text{photons}}{\text{sec}}$ | $\sim 10^{-2}$ |
| Round Trips | $\sim 1$ | $\sim 10^4$ | $\sim 10^{-4}$ |

TABLE I. Compared and contrasted are different properties of matter-wave and optical gyroscopes in terms of their sensitivity to phase differences — or equivalently — rotation rates. We see that the high mass of atoms initially contributes an increase of sensitivity of $10^{10}$, but that the low atomic beam intensity, compared to photon beams, removes some of this advantage, as does the reduced number of round trips possible in an atom interferometer. Nevertheless — a typical factor of a $10^4$ increase in rotation sensitivity can still be expected using atoms rather than photons.

## Acknowledgments

The authors would like to thank J. Clauser, J. Fransen, J. Kimble, P. Kumar, J. Mlynek, A. Overhauser, D. Pritchard, M. Reinsch, and S. Werner for many interesting discussions relating to this work. M. O. S. thanks the Office of Naval Research and J. P. D. acknowledges the National Research Council for financial support.

## References

[1] C. J. Davisson and L. H. Germer, Phys. Rev. **30**, 705 (1927); E. G. Dymond, Nature **118**, 336 (1926); G. P. Thomson, Proc. Roy. Soc. London A **117**, 600 (1928).

[2] R. Colella, A. W. Overhauser, and S. A. Werner, Phys. Rev. Lett. **34**, 1472 (1975); A. Zeilinger, Z. Physik B **25**, 97 (1976); H. Rauch, W. Treimer, and U. Bonse, Phys. Lett. A **47**, 369 (1977); S. A. Werner, J.-L. Staudenmann, and R. Colella, Phys. Rev. Lett. **42**, 1103 (1979); *Neutron Interferometry*, edited by U. Bonse and H. Rauch, (Oxford Univ. Press, New York, 1979); G. Badurek, H. Rauch, J. Summhammer, U. Kischko, and A. Zeilinger, Physica B **151**, 82 (1988).

[3] O. Carnal and J. Mylnek, Phys. Rev. Lett. **66**, 2689 (1991); D. W. Keith, C. R. Ekstrom, Q. A. Turchette, and D. E. Pritchard, Phys. Rev. Lett. **66**, 2693 (1991); F. Riehle, T. Kisters, A. Witte, J. Helmeche, and C. J. Bordé, Phys. Rev. Lett. **67**, 177 (1991); M. Kasevich and S. Chu, Phys. Rev. Lett. **67**, 181 (1991); *Optics and Interferometry with Atoms*, edited by J. Mylnek, V. Balkin, and P. Meystre, Appl. Phys. B **54** (1992), special issue.

[4] J. F. Clauser, Physica B **151**, 262 (1988).

[5] C. M. Caves, Phys. Rev. D **23**, 1693 (1981); R. J. Bondurant and J. H. Shapiro, Phys. Rev. D **30**, 2548 (1984); V. P. Chebotayev, B. Dubetsky, A. P. Kasantsev, and V. P. Yakovlev, J. Opt. Soc. Am. B **2**, 1791 (1985).

[6] *Quantum Optics*, Proceedings of the Twentieth Solvay Conference on Physics, Brussels, November 6–9, 1991, ed. by P. Mandel, in Phys. Rep. **219**, (3–6), 77 (1992).

[7] W. Schleich and M. O. Scully in *New Trends in Atomic Physics*, Les Houches lectures, session XXVIII, 1982, edited by G. Grynberg and R. Stora (Elsevier Science Publishers, New York, 1984), pp. 998–1124.

[8] D. J. Wineland, J. J. Bollinger, W. M. Itano, F. L. Moore, and D. J. Heinzen, Phys. Rev. A **46**, R6797 (1992).

[9] B. Yurke, Phys. Rev. Lett. **56**, 1515 (1986).

N95- 13956

# BLOCH VECTOR PROJECTION NOISE

L. J. Wang
*Department of Physics, Duke University, Durham, North Carolina, 27708-0305*

A. M. Bacon, H. Z. Zhao, and J. E. Thomas
*Department of Physics, Duke University, Durham, North Carolina, 27708-0305*

**Abstract**

In the optical measurement of the Bloch vector components describing a system of N two-level atoms, the quantum fluctuations in these components are coupled into the measuring optical field. This paper develops the quantum theory of optical measurement of Bloch vector projection noise. The preparation and probing of coherence in an effective two-level system consisting of the two ground states in an atomic three-level Λ-scheme are analyzed.

# 1 Introduction

The properties and generation of an optical squeezed state have been interesting subjects of study for a number of years. The Bloch vector model of a two-level atomic system interacting with a laser field, and the use of angular momentum components $J_j$ to represent the N two-level atoms [1], have also been widely investigated. It is known that quantum systems with dynamical variables in the form of nonlinear products of the position and momentum operators are different from those involving only the position and momentum operators. For instance, in a system of N two-level atoms, described by a Bloch vector spin angular momentum $\hat{\mathbf{J}}$, the uncertainty relation, $\Delta J_1 \cdot \Delta J_2 \geq \frac{1}{2}|\langle \hat{J}_3 \rangle|$, depends on the quantum state of the system, as opposed to that of $\Delta x \cdot \Delta p \geq \frac{\hbar}{2}$ for the two quadrature phase components of an optical field [2]. The quantum fluctuations in atoms hence provide an interesting system for the study of uncertainty relations, and are of practical importance. For example, the fluctuations in an atomic system contribute to noise that can in principle, limit the accuracy of atomic frequency standards [3].

As a simple example, let us consider the spin model for a single two-level atom with a ground state $|1\rangle$ and an excited state $|2\rangle$. The Bloch vector operators are

$$\begin{aligned} \hat{s}_1 &\equiv \frac{1}{2}(\hat{\sigma}_{12} + \hat{\sigma}_{21}), \\ \hat{s}_2 &\equiv \frac{i}{2}(\hat{\sigma}_{12} - \hat{\sigma}_{21}), \\ \hat{s}_3 &\equiv \frac{1}{2}(\hat{\sigma}_{22} + \hat{\sigma}_{11}), \end{aligned} \tag{1}$$

where

$$\hat{\sigma}_{ij} \equiv |i\rangle\langle j|, \quad i,j = 1,2.$$

These operators obey the usual commutation relation for angular momentum operators,

$$[\hat{s}_i, \hat{s}_j] = i\epsilon_{ijk}\hat{s}_k,$$

where $\epsilon_{ijk}$ is the Levi-Civita symbol. It is easy to show that $\hat{\mathbf{s}}$ describes a spin-$\frac{1}{2}$ system.

For a superposition state

$$|\varphi\rangle = \cos\frac{\theta}{2}|1\rangle + e^{i\phi}\sin\frac{\theta}{2}|2\rangle, \tag{2}$$

where $\theta$, and $\phi$ are some angles, we have

$$\begin{aligned} \langle\hat{s}_1\rangle &= \frac{1}{2}\sin\theta\cos\phi, \\ \langle\hat{s}_2\rangle &= -\frac{1}{2}\sin\theta\sin\phi, \\ \langle\hat{s}_3\rangle &= -\frac{1}{2}\cos\theta. \end{aligned} \tag{3}$$

Clearly, the vector $\mathbf{r} = (\langle\hat{s}_1\rangle, \langle\hat{s}_2\rangle, \langle\hat{s}_3\rangle)$ falls onto the surface of a sphere of radius $\frac{1}{2}$. The fluctuations in the components of $\mathbf{s}$ are,

$$\langle\Delta\hat{s}_j^2\rangle = \langle\hat{s}_j^2\rangle - \langle\hat{s}_j\rangle^2 = \frac{1}{4} - \langle\hat{s}_j\rangle^2, \quad j = 1,2,3, \tag{4}$$

with the fluctuation in the total Bloch vector

$$\langle\Delta\hat{\mathbf{s}^2}\rangle = \langle\hat{\mathbf{s}^2}\rangle - \langle\hat{\mathbf{s}}\rangle^2 = \frac{1}{2}.$$

It is also easy to show that

$$\langle\Delta\hat{\mathbf{s}_i^2}\rangle \cdot \langle\Delta\hat{\mathbf{s}_j^2}\rangle \geq \frac{1}{4}|\epsilon_{ijk}\langle\hat{\mathbf{s}_k}\rangle|^2. \tag{5}$$

Now let us consider the situation for N two-level atoms. If there is no mutual interaction between the atoms, the system can be described by the total spin angular momentum operator

$$\mathbf{S} = \sum_{n=1}^{N}\mathbf{s}_n.$$

We assume that all atoms are in the ground state $|1\rangle$ initially or, equivalently, the system is in the angular momentum eigenstate $|S = \frac{N}{2}, S_3 = -\frac{N}{2}\rangle$ (Fig.1a). Now we have

$$\langle\hat{S}_3\rangle = \sum_{n=1}^{N}\langle\hat{\mathbf{s}}_{3,n}\rangle = -\frac{N}{2},$$

and

$$\langle\hat{\mathbf{S}}^2\rangle = \frac{N}{2}(\frac{N}{2}+1).$$

We hence obtain

$$\langle\Delta\hat{\mathbf{S}}^2\rangle = \langle\hat{S}_1^2\rangle + \langle\hat{S}_2^2\rangle = \langle\hat{\mathbf{S}}_\perp^2\rangle = \frac{N}{2}. \tag{6}$$

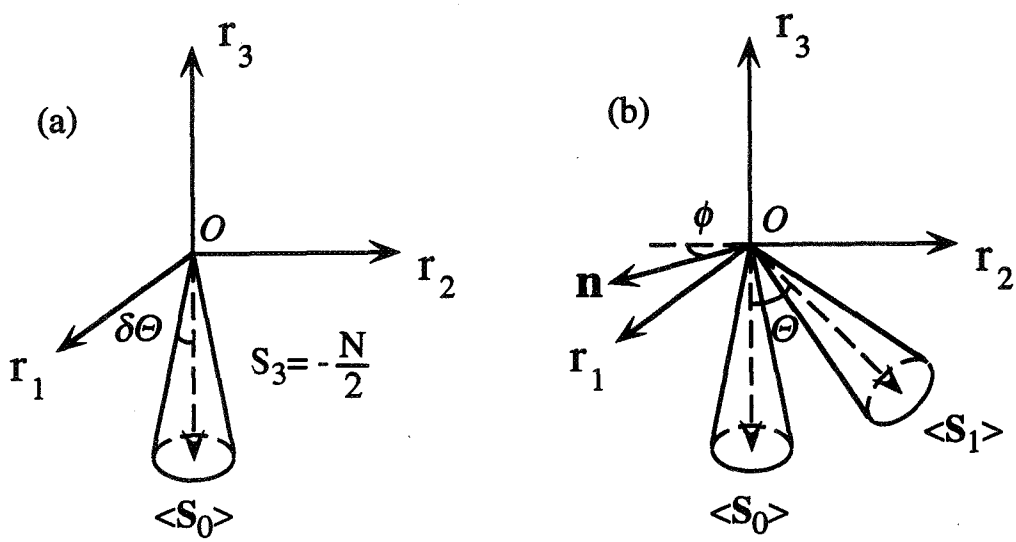


FIG. 1. Bloch vector for an N-atom system. In a), all atoms are in state $|1\rangle$, and the mean total Bloch vector $\langle \mathbf{S}_0 \rangle$ points down. b), $\langle \mathbf{S}_0 \rangle$ is rotated about an axis $\mathbf{n}$ to $\langle \mathbf{S}_1 \rangle$. The cones represent the fluctuations in Bloch vectors.

As is shown in Fig.1a, the uncertainty in $\mathbf{S}$ forms a cone centered on $\langle \mathbf{S}_0 \rangle$, pointing inversely along axis $r_3$, with a conic angle $\delta\theta \approx \sqrt{\frac{2}{N}}$. When a resonant laser field is applied, the Bloch vector $\mathbf{S}$ is rotated from $\langle \mathbf{S}_0 \rangle$ to $\langle \mathbf{S}_1 \rangle$, by angle $\theta$ about an axis $\mathbf{n}$ in the $Or_1r_2$ plane (Fig.1b). Now all atoms are in a superposition state as given in Eq.(2), and one can show that the mean square fluctuations in the components of the Bloch vector $\mathbf{S}$ are N times of that given by Eq.(4). Now let us take a closer look at Fig.1b. When the Bloch vector $\mathbf{S}$ is rotated from $\langle \mathbf{S}_0 \rangle$ to $\langle \mathbf{S}_1 \rangle$, the cone representing the fluctuations in $\mathbf{S}$ is also rotated. The projection of the base of the cone, which represents the fluctuation, onto an axis, say $r_1$, is merely

$$\begin{aligned} \Delta r_1^2 &= \frac{1}{2}\mathbf{S}_\perp^2 \left[1 - \left|\mathbf{r}_1 \cdot \frac{\langle \hat{\mathbf{S}}_1 \rangle}{|\langle \hat{\mathbf{S}}_1 \rangle|}\right|^2\right] \\ &= \frac{N}{4}\left(1 - \sin^2\theta\cos^2\phi\right). \end{aligned} \tag{7}$$

One can obtain similar results for the fluctuations along other axes. The fluctuations in the Bloch vector components are hence the projections of the Bloch vector uncertainty onto the corresponding axes. It has been pointed out that the shape of the cone (Fig.1b) can be altered, and turned to an ellipse, by introducing a non-uniform interaction between the external field with the atoms [4], or by mutual interaction between the atoms. We see from Eq.(7) that the noise in the Bloch vector component along $r_1$ reaches a minimum point at $\theta = \frac{\pi}{2}$ and $\phi = 0$ when the component is maximized. Yet the shot noise in the radiation field from the atomic medium is proportional to $\sqrt{r_1}$ and also maximized. It is predicted that the total noise consisting of the shot noise and the Bloch vector projection noise would reach its minimum value at $\theta = \frac{\pi}{3}$ [2].

## 2 Theory

In this section, we develop the quantum theory of optical measurement of atomic Bloch vector projection noise. We will consider the experimental situation of Λ-three-level atoms in a beam interacting with spatially separated laser fields. In a Λ-scheme three-level atom (Fig.2), we assume that dipole transitions between states $|1\rangle$ and $|0\rangle$, and $|2\rangle$ and $|0\rangle$ are both allowed, with resonant frequencies, $\omega_{01}, \omega_{02}$, and transition dipole moments $\mathbf{d}_{01}, \mathbf{d}_{02}$, respectively. We assume for simplicity that $\mathbf{d}_{01}$ and $\mathbf{d}_{02}$ are orthogonal. First, a resonant optical pumping field is applied to pump all atoms into state $|1\rangle$. Two co-propagating off-resonant laser fields of frequencies $\omega_1, \omega_2$, polarizations $\mathbf{e}_1, \mathbf{e}_2$, respectively, are applied downstream to prepare the atoms into a superposition state of $|1\rangle$ and $|2\rangle$. Level $|0\rangle$ adiabatically follows the ground state amplitudes and can be eliminated. Hence, we are left with an effective two-level system consisting only of ground states, which do not spontaneously decay. At a later point in the atomic beam, a probe field of frequency $\omega_2$, and polarization $\mathbf{e}_2$ is applied. This induces an $\mathbf{e}_1$-polarized radiation field, oscillating between states $|0\rangle$ and $|1\rangle$ which is homodyned with an external local oscillator field of frequency $\omega_1$. We will show that the homodyne output is proportional to the atomic Bloch vector components and carries its noise characteristics.

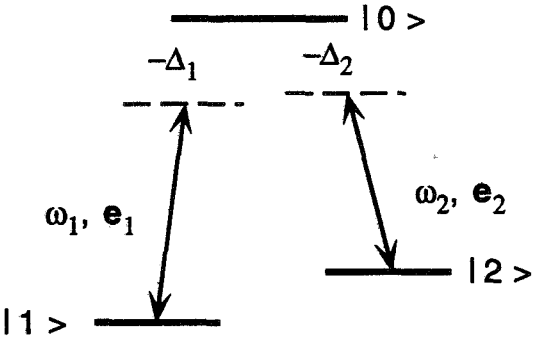


FIG. 2. Level diagram of a Λ-scheme three level atom.

We first treat the preparation process of the atomic ground state superposition. As illustrated in Fig.3.a, in the lab frame, atoms in the beam moving along axis $x$ with speed $v$, enter the coherence preparation region $I$, between $x = 0$ and $x = x_0$. It is more convenient, however, to calculate the atomic state in the atomic center-of-mass (CM) frame. Let us consider an atom that appears at an arbitrary position $x$ in the probe region $II$, at time $t'$. Referring to Fig.3.b, we see that the atom entered region $I$ at a previous time $t' - x/v$ and exits region at time $t' - (x - x_0)/v$.

We start from the effective Hamiltonian

$$\hat{H} = -\hbar\omega_{01}|1\rangle\langle 1| - \hbar\omega_{02}|2\rangle\langle 2| + \hat{V}. \tag{8}$$

and the interaction

$$\hat{V} = -\frac{\hbar\Omega_{01}}{2}e^{-i\omega_1 t}|0\rangle\langle 1| - \frac{\hbar\Omega_{02}}{2}e^{-i\omega_2 t}|0\rangle\langle 2| + H.c., \tag{9}$$

where we take

$$\Omega_{01} = \Omega_{10}^* = \frac{(\mathbf{e}_1 \cdot \mathbf{d}_{01})E_1}{\hbar},$$
$$\Omega_{02} = \Omega_{20}^* = \frac{(\mathbf{e}_2 \cdot \mathbf{d}_{02})E_2}{\hbar},$$

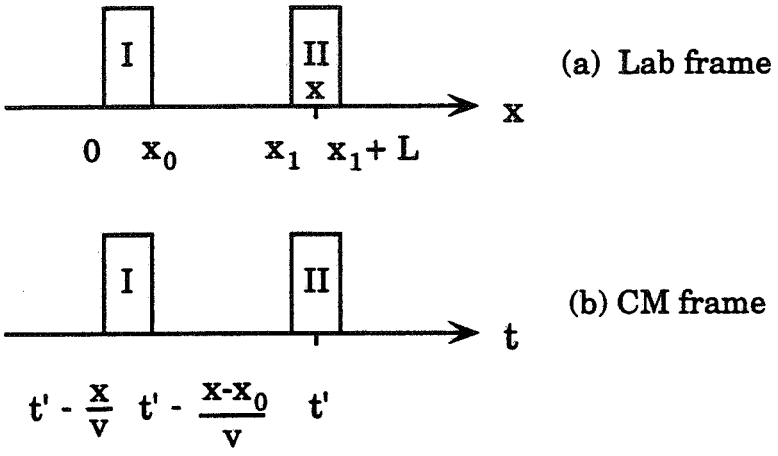


FIG.3, Schematic illustration of the experimental situation in a) the Lab frame, and b), in the atomic center-of-mass frame. Regions $I$ and $II$ are the coherence preparation and the probe region, respectively.

as the Rabi frequencies for the applied laser field given by

$$E(t) = \frac{\mathbf{e}_1 E_1}{2} e^{-i\omega_1 t} + \frac{\mathbf{e}_2 E_2}{2} e^{-i\omega_2 t} + c.c..$$

Taking the energy of state $|0\rangle$, $\tilde{E}_0 = 0$, the atomic state takes the form

$$|\psi(t)\rangle = a_0(t)\,|0\rangle + a_1(t)\,e^{i\omega_{01}t}\,|1\rangle + a_2(t)\,e^{i\omega_{02}t}\,|2\rangle. \tag{10}$$

We obtain from the Schrödinger equation,

$$\begin{aligned}
\dot{a}_0(t) &= i\frac{\Omega_{01}}{2}\,e^{-i\Delta_1 t}\,a_1(t) + i\frac{\Omega_{02}}{2}\,e^{-i\Delta_2 t}\,a_2(t), \\
\dot{a}_1(t) &= i\frac{\Omega_{01}^*}{2}\,e^{i\Delta_1 t}\,a_0(t), \\
\dot{a}_2(t) &= i\frac{\Omega_{02}^*}{2}\,e^{i\Delta_2 t}\,a_0(t),
\end{aligned} \tag{11}$$

where

$$\Delta_j \equiv \omega_j - \omega_{0j}, \qquad \text{j=1,2}$$

are the detunings. When $\Omega_1, \Omega_2 \ll \Delta_1, \Delta_2$, we may adiabatically eliminate level $|0\rangle$ by defining

$$a_0(t) = B_1(t)\,e^{-i\Delta_1 t} + B_2(t)\,e^{-i\Delta_2 t}, \tag{12}$$

where

$$B_1(t) = -\frac{\Omega_{01}}{2\Delta_1} a_1(t),$$
$$B_2(t) = -\frac{\Omega_{02}}{2\Delta_2} a_2(t).$$

Eq.(11) then becomes

$$\dot{a}_1(t) = -i\frac{|\Omega_{01}|^2}{4\Delta_1} a_1(t) - i\frac{\Omega_{10}\Omega_{02}}{4\Delta_2} e^{-i(\Delta_2-\Delta_1)t} a_2(t),$$
$$\dot{a}_1(t) = -i\frac{\Omega_{20}\Omega_{01}}{4\Delta_1} e^{i(\Delta_2-\Delta_1)t} a_1(t) - i\frac{|\Omega_{02}|^2}{4\Delta_2} a_2(t). \quad (13)$$

The initial condition of the atomic state as given in Eq.(10) is

$$a_1(t' - x/v) = 1,$$
$$a_2(t' - x/v) = 0, \quad (14)$$

or that the atom is in state $|1\rangle$ when entering region $I$ at time $t' - x/v$.

When the atomic ground splitting $\omega_{21} \ll \Delta_1, \Delta_2$, and $\Delta_1 \approx \Delta_2, |\Omega_{01}| \approx |\Omega_{02}|$, we may define the light shift frequency

$$\tilde{\Delta} \equiv \frac{|\Omega_{01}|^2}{2\Delta_1} \approx \frac{|\Omega_{02}|^2}{2\Delta_2},$$

the Raman Rabi frequency

$$\beta_R \equiv \frac{\Omega_{10}\Omega_{02}}{2\Delta_2} \approx \frac{\Omega_{10}\Omega_{02}}{2\Delta_1} = |\beta_R| e^{i\phi},$$

and the net detuning

$$\Delta \equiv \Delta_1 - \Delta_2 = (\omega_1 - \omega_2) - \omega_{21}.$$

Eq.(13) can be readily solved by changing variables

$$a_1(t) = A_1(t) e^{i\Delta t/2} e^{-i\int^t dt_1 \tilde{\Delta}(t_1)/2},$$
$$a_2(t) = A_2(t) e^{-i\Delta t/2} e^{-i\int^t dt_1 \tilde{\Delta}(t_1)/2}, \quad (15)$$

which yields when $\Delta \ll |\beta_R|$.

$$A_1(t) = \cos\left[\frac{1}{2}|\beta_R|(t - t' + x/v)\right],$$
$$A_2(t) = e^{i\phi} \sin\left[\frac{1}{2}|\beta_R|(t - t' + x/v)\right]. \quad (16)$$

Hence we obtain the atomic state for an atom which leaves region $I$ at time $t' - (x - x_0)/v$ and will arrive at position $x$ at time $t'$, as

$$|\psi(t' - \frac{x - x_0}{v})\rangle = A_1(t' - \frac{x - x_0}{v}) e^{i\frac{\Delta}{2}(t' - \frac{x-x_0}{v})} e^{i\omega_{01}(t' - \frac{x-x_0}{v})} |1\rangle$$
$$+A_2(t' - \frac{x - x_0}{v}) e^{-i\frac{\Delta}{2}(t' - \frac{x-x_0}{v})} e^{i\omega_{02}(t' - \frac{x-x_0}{v})} |2\rangle$$
$$= \cos\frac{\theta}{2}|1\rangle + e^{i\phi}\sin\frac{\theta}{2} e^{-i(\omega_1-\omega_2)(t' - \frac{x-x_0}{v})}|2\rangle, \quad (17)$$

where

$$\theta = |\beta_R| \frac{x_0}{v},$$

is the Raman Rabi area. All common time dependent phase factors in Eq.(17) are left out, as these will not affect the atomic coherence $\langle \hat{\sigma}_{12} \rangle$.

Now let us closely examine the probe region. As illustrated in Fig.4, a probe field

$$\mathcal{E}_p(t) = \mathbf{e}_2 \frac{\mathcal{E}_p}{2} e^{-i\omega_2 t} + c.c.$$

is incident onto the atomic beam at region $II$, and introduces an interaction Hamiltonian

$$\hat{V}^{(j)}(t) = -\frac{\hbar\Omega_2}{2} e^{-i\omega_2 t} \hat{\sigma}_{02}^{(j)} + H.c., \tag{18}$$

for the $j$-th atom at position $x$ at time $t$. Here $\Omega_2 = (\mathbf{d}_{02} \cdot \mathbf{e}_2)\mathcal{E}_p/\hbar$ is again the Rabi frequency for the probe field, and $\hat{\sigma}_{02}^{(j)} = |0\rangle\langle 2|$ is the Schrödinger picture operator for the $j$-th atom.

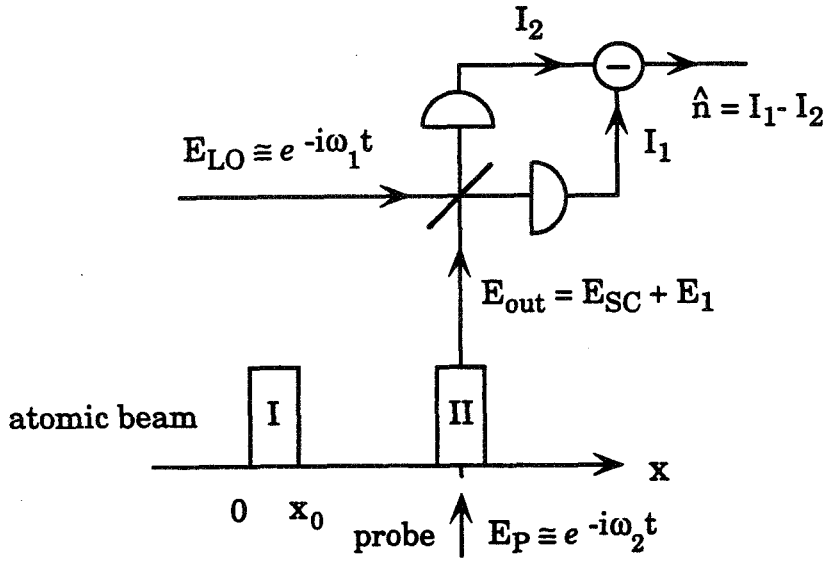


FIG. 4. Schematic diagram of the homodyne detection of the probe-field-induced Raman transition field.

It is convenient to use Heisenberg equations in the atomic CM frame for operators $\hat{\sigma}_{02}^{(j)}(x,t)$, etc., which are

$$\left(\frac{\partial}{\partial t} - i\omega_{21}\right) \hat{\sigma}_{21}^{(j)}(t) = 0, \tag{19}$$

and

$$\left(\frac{\partial}{\partial t} + \frac{\gamma}{2} - i\omega_{01}\right) \hat{\sigma}_{01}^{(j)}(t) = -i\frac{\Omega_2^*}{2} e^{i\omega_2 t} \hat{\sigma}_{21}^{(j)}(t), \tag{20}$$

where $\gamma$ is the spontaneous decay rate of state $|0\rangle$. $\gamma$ is small in the experiment so that noise terms in Eq.(20) will be neglected. Eq.(19) can be readily solved for the evolution between times

$t' - (x - x_0)/v$ when the atom leaves the preparation region $I$, and $t'$ in the atom frame:

$$\hat{\sigma}_{21}^{(j)}(t) = \hat{\sigma}_{21}^{(j)}(t' - \frac{x - x_0}{v})\, e^{i\omega_{21}[t - t' + \frac{x - x_0}{v}]}. \tag{21}$$

$\hat{\sigma}_{21}^{(j)}(t)$ is now determined from $\hat{\sigma}_{21}^{(j)}(t' - (x - x_0)/v)$ whose expectation value will be evaluated for the atomic state $|\psi(t' - (x - x_0)/v)\rangle$ in Eq.(17). Using Eq.(21), Eq.(20) is solved

$$\begin{aligned} \hat{\sigma}_{01}^{(j)}(t') &= -i\frac{\Omega_2^*}{2} \int_{t' - \frac{x - x_0}{v}}^{t'} dt_1\, e^{i\omega_2 t_1}\, e^{-(\frac{\gamma}{2} - i\omega_{01})(t' - t_1)}\, \hat{\sigma}_{21}^{(j)}(t_1) \\ &\approx -i\frac{\Omega_2^*}{2}\, e^{i\omega_2 t'}\, e^{i\omega_{21}\frac{(x - x_0)}{v}}\, \frac{1}{\frac{\gamma}{2} + i\Delta_2}\, \hat{\sigma}_{21}^{(j)}(t' - \frac{x - x_0}{v}), \end{aligned} \tag{22}$$

where we assumed that $\gamma\,(x - x_0)/v \gg 1$.

Note that in the lab frame, the $j$-th atom is at position $x$ at time $t'$. Hence we obtain from Eq.(22) the atomic polarization

$$\hat{\mathbf{P}}(x, t') \propto \sum_j \mathbf{d}_{10}\, \hat{\sigma}_{10}^{(j)}\,(x, t') + H.c., \tag{23}$$

where

$$\hat{\sigma}_{10}^{(j)}(x, t') = -\frac{\Omega_2}{2\Delta_2}\, e^{-i\omega_2 t'}\, e^{-i\omega_{21}\frac{(x - x_0)}{v}}\, \hat{\sigma}_{12}^{(j)}\,(t' - \frac{x - x_0}{v}), \tag{24}$$

under the assumption that the detuning $\Delta_2 \gg \gamma$, the spontaneous decay rate.

Now if the atomic dipole moment $\mathbf{d}_{10}$ and hence $\mathbf{P}$ are orthogonal to the polarization of the probe field $\mathbf{E}_p$, the optical radiation field due to the atomic polarization $\mathbf{P}$

$$\mathbf{E}_s = -2\pi i k l\, \mathbf{P}, \tag{25}$$

can be separated using a polarizer from $\mathbf{E}_p$. Here $kl$ is the optical thickness of the atomic beam.

Adding the vacuum field $\hat{E}_1$ of the same polarization as $\hat{E}_s$, we obtain for the positive frequency part of the total output field from the atomic medium

$$\hat{E}_{out}^{(+)}(t) = \hat{E}_1^{(+)}\,(t) + \hat{E}_s^{(+)}\,(t) \tag{26}$$

where

$$\hat{E}_s^{(+)}\,(t) = i\mathcal{T}\,\mathcal{E}_p(t) \sum_j e^{-i\omega_{21}\frac{(x - x_0)}{v}}\, \hat{\sigma}_{12}^{(j)}\,(x, t - \frac{x - x_0}{v}). \tag{27}$$

$$\mathcal{T} \propto \pi k l\, \rho\, \frac{(\mathbf{d}_{02} \cdot \mathbf{e}_2)\,(\mathbf{d}_{01} \cdot \mathbf{e}_1)}{\hbar\Delta_2}$$

is a dimensionless scattering coefficient, where $\rho$ is the number density of the atomic beam, and $\mathbf{e}_1, \mathbf{e}_2$ are the polarization unit vectors of the probe field $\mathcal{E}_p$ and the scattered field $\hat{E}_{out}$, respectively.

$\hat{E}_{out}$ is mixed with a local oscillator field $E_{LO}(t) \sim E_{LO}\, e^{-i\omega_1 t}$ in the homodyne detection scheme illustrated in Fig.4. The output signal $n$ can be written in the operator form as the difference of photo-currents $I_1$ and $I_2$,

$$\begin{aligned} \hat{n}\,(t) &= \hat{I}_1(t) - \hat{I}_2(t) \\ &\propto E_{LO}^*\,(t) \cdot \hat{E}_{out}^{(+)}\,(t) + E_{LO}\,(t) \cdot \hat{E}_{out}^{(-)}\,(t). \end{aligned} \tag{28}$$

Using Eq.(27), and (17) for the atomic state, we obtain

$$\langle \hat{n}\,(t)\rangle = |\mathcal{T} E_{LO}^{*} \mathcal{E}_p| \sum_{j}^{M} e^{i(\omega_1-\omega_2)t}\, e^{-i\omega_{21}\frac{(x-x_0)}{v}}\, \langle \hat{\sigma}_{12}^{(j)}\,(t-\frac{x-x_0}{v})\rangle + c.c., \tag{29}$$

where $\langle \hat{\sigma}_{12}^{(j)}\,(t-\frac{x-x_0}{v})\rangle$ is evaluated for the atomic state $|\psi(t-\frac{x-x_0}{v})\rangle$ given in Eq.(17). The photocurrent difference $\langle \hat{n}\,(t)\rangle$ can be written in terms of the Bloch vector components $\langle s_1\rangle$, and $\langle s_2\rangle$ of Eq.(1). Then Eq.(29) can be further simplified

$$\langle \hat{n}\,(t)\rangle = M|\mathcal{T} E_{LO}^{*} \mathcal{E}_p|\, \sin\theta\, \cos[(\omega_1-\omega_2-\omega_{21})\cdot\frac{(x-x_0)}{v}+\phi_0], \tag{30}$$

where $M$ is the number of atoms in the probe region, and $\phi_0$ some reference phase. Eq.(30) gives the usual Ramsey fringe pattern [5].

Now let us evaluate the fluctuations in the atomic Bloch vector components. We calculate the power spectrum of the homodyne output signal $n\,(t)$

$$S(\omega) = \frac{1}{2\pi}\int d\tau\, \langle \hat{n}\,(t)\,\hat{n}\,(t+\tau)\rangle\, e^{-i\omega\tau}. \tag{31}$$

After some algebra, we obtain

$$\begin{aligned} S(\omega) \;=\; & |E_{LO}|^2 - M|\mathcal{T}|^2\,|E_{LO}|^2\,|\mathcal{E}_p|^2\,A\,(\omega)\,\langle \hat{\sigma}_{11}-\hat{\sigma}_{22}\rangle_{\varphi} \\ & + M^2|\mathcal{T}|^2|E_{LO}|^2|\mathcal{E}_p|^2\,\langle \hat{\sigma}_{12}+\hat{\sigma}_{21}\rangle_{\varphi}^2\,\delta(\omega) \\ & + M\,|\mathcal{T}|^2\,|E_{LO}|^2\,|\mathcal{E}_p|^2 A\,(\omega)\,\left[1-\langle \hat{\sigma}_{12}+\hat{\sigma}_{21}\rangle_{\varphi}^2\right], \end{aligned} \tag{32}$$

under the assumption that the net detuning $\Delta$ is small so that $\Delta\cdot x_1/v \ll 1$, where $x_1$ is the distance between the preparation region $I$ and the probe region $II$. $|E_{LO}|^2$ is the intensity of the local oscillator field, and $|\mathcal{E}_p|^2$ the intensity of the probe field in units of photon number per second. $A(\omega)$ is a spectral function that centers at $\omega = 0$, with a spectral width of order of the transit bandwidth of the probe region. $\langle \hat{\sigma}_{11}-\hat{\sigma}_{22}\rangle_{\varphi} = \cos\theta$, and $\langle \hat{\sigma}_{12}+\hat{\sigma}_{21}\rangle_{\varphi} = \sin\theta\cos\phi$ are components of the Bloch vector expectation values evaluated for the atomic state $|\varphi\rangle$ given in Eq.(2).

Now let us closely examine the four terms in Eq.(32). The first term is clearly due to the shot noise in the homodyne process. The second term is the reduction of vacuum shot noise level due to Raman absorption. It can also be viewed as the shot noise associated with the spontaneous Raman transition. The third term is proportional to $M^2$, and centers at $\omega = 0$, represents the power spectrum of the stationary Ramsey fringe signal of Eq.(30). The last term is the phase $\phi$-dependent Bloch vector projection noise given in Eqs.(4) and (7).

# 3 Summary

In this paper, we developed the quantum theory for the experimental study of the Bloch vector projection noise. Eqs.(30) and (32) are the primary results. In a $\Lambda$-three-level atomic system, when two off-resonant Raman fields are applied, the upper state adiabatically follows the ground state

amplitudes and the Λ-scheme is hence reduced to an effective two-level system. Decayless ground state coherence is prepared. By probing with one optical transition, and detecting the induced transition between the other ground state and the upper level with a homodyne technique, we can measure the Bloch vector components as given in Eq.(30). The photo-current difference in the homodyne scheme also yields the noise characteristics of the Bloch vector components as given in Eq.(32).

An experimental study is currently being conducted using a wide-angled supersonic ytterbium (Yb) atomic beam. The 556 nm transition of $^{171}$Yb $^1S \rightarrow ^3P$ transition is used. In a 2.6 kG magnetic field, the $^{171}$Yb ground states of nuclear spin $I = \frac{1}{2}$ are split by 2 MHz and form a Λ-system with the upper state $|F = \frac{3}{2}, F_3 = \frac{1}{2}\rangle$. Doppler shifts in the corresponding $\sigma^+$ and $\pi$ transition in the wide angle atomic beam are Zeeman compensated [6] simultaneously by a quadrupole magnetic field. With this technique, the transition linewidth is narrowed to a few MHz for an interaction path length $l$ of 2.5 cm. The Ramsey fringe pattern of Eq.(30) has been observed.

# 4 Acknowledgments

This work is supported by NSF, RADC, and AFOSR.

# References

[1] R. H. Dicke, Phys. Rev. **93**, 99 (1954).

[2] K. Wodkiewicz and J. H. Eberly, J.O.S.A. **B 2**, 458 (1984).

[3] W. M. Itano et al., Phys. Rev. **A 47**, 3554 (1993).

[4] D. J. Wineland et al., Phys. Rev. **A 46**, R6797 (1992).

[5] N. F. Ramsey, *Molecular Beams* , (Oxford University Press, London, 1956).

[6] K. D. Stokes et al. Optics Lett. **14**, 1324 (1989).

N95- 13957

# New quantum properties of phonons and their detection

M. Artoni
*Photonics, NASA/Goddard Space Flight Center, Greenbelt, MD 20771, U.S.A.*

Joseph. L. Birman
*Physics Department, The City College of New York, Convent Avenue at 138th Street New York, N.Y. 10031, U.S.A.*

***Abstract***

We present a theoretical investigation on new and interesting properties of the phonon polarization field in solids. In particular, non-classical aspects of the phonon population and an experimental scheme that would enable one to detect them will be discussed.

## *1. Introduction*

In recent years much interest has been devoted to the investigation of quantum effects that have no classical analogs, of which optical squeezing is the most ubiquitous one [1]. In view of the successful generation and detection of squeezed states of the electromagnetic (e.m.) field it is natural to ask whether analogous states exist and can be observed for other boson fields. Condensed matter exhibits a variety of bosons that, via the interaction with an external field, can be excited into a squeezed state in much the same way as done with photons.

It was previously pointed out [2] that in a phonon-polariton [3,4], a mixed mode in which an optical phonon is coupled to a photon, the photon component exhibits non-poissonian quantum statistics and optical squeezing [2,5]. Owing to the quadratic nature of the transformation that takes one from coupled bare phonons plus bare photons to a polariton, where phonons and photons appear as exactly *dual* particles, we demonstrate that the phonon component of a polariton exhibits analogous properties. We further analyse an experiment that would enable one to detect such delicate features in solids with an appreciable effect.

## *2. Phonon-polariton*

Many topics in solids combine wave and particle aspects. Exactly as the photon describes the particle nature of the e.m. field, the phonon describes the particle nature of a lattice vibration [6]. Under certain conditions these two excitations may interact: at resonance, transverse optical phonons and photons couple and the character of the propagation inside the crystal is entirely changed. The pioneering work of Pekar [7], Fano [4], and Hopfield [8] has shown that eigenstates of the coupled system of a lattice vibration and radiation are composite *particles* made of photons and phonons, i.e. *phonon-polaritons* (polaritons hereafter). This represents the quantomechanical equivalent of the classical work of Huang [9] who first derived the dispersion for infrared active optical lattice vibrations of a cubic ionic crystal, showing that the actual modes propagating in the crystal are radiation-lattice coupled *waves*. A typical dispersion curve (no spatial dispersion) for a polariton is shown in Fig. 1 below.

## *3. Squeezed states*

Squeezed states are quantum states in which the fluctuations in one of the phase quadratures of the field are reduced below the vacuum noise limit [1]. *Single* and *two*-modes squeezed states have

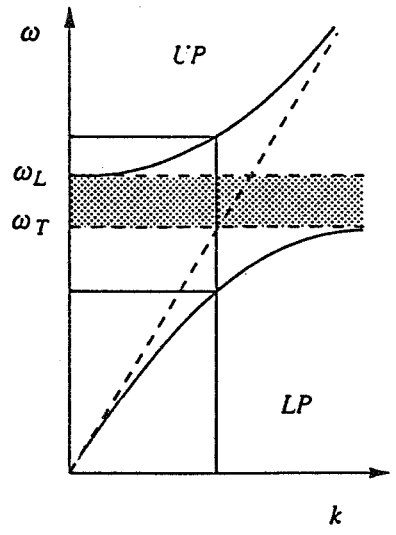


*Fig.1 Schematic polariton energy spectrum. UP and LP denote upper and lower dispersion branches. $\omega_T$ and $\omega_L$ are transverse and logitudinal phonon resonant frequencies.*

been extensively studied [1], and experiments [1] have already demonstrated their realizability in the case of an e.m. field.

If $\hat{a}_l$ and $\hat{b}_l$ denote two independent bosons, one can introduce [2] a two-mode squeezed state for the *mixed* boson $\hat{\gamma}_l = \alpha_l \hat{a}_l + \beta_l \hat{b}_l$ as a displaced state of the squeezed vacuum

$$|\gamma_{12}\rangle = \hat{D}(\gamma_{12}) \cdot \hat{S}_{12}^{\gamma}(r)|0\rangle =$$

$$= \{e^{-\frac{1}{2}(|\gamma_1|^2+|\gamma_2|^2)} e^{\gamma_1 \hat{\gamma}_1^\dagger} e^{\gamma_2 \hat{\gamma}_2^\dagger}\}\{e^{r(\hat{\gamma}_1 \hat{\gamma}_2 - \hat{\gamma}_1^\dagger \hat{\gamma}_2^\dagger)}\}|0\rangle \qquad (1)$$

$\hat{D}(\gamma_{12})$ and $\hat{S}_{12}^{\gamma}(r)$ are two-mode *displacement* and *squeeze* operators [10], respectively, whereas the other symbols have their usual meaning. $r$, the squeeze factor, mediates the coupling between the two modes 1 and 2. In the states $|\gamma_{12}\rangle$ these modes become so tightly correlated that they no longer fluctuate independently by even the small amount allowed in a coherent or vacuum state [1].

*4. Non-classical phonons*

The objective of this section is to show that a polariton state is a non-classical state and that the phonon counterpart associated with it exhibits non-classical features. We will restrict ourselves to *two-mode polariton coherent states*. In particular, these states are most suitable to describe the actual experimental scheme which we will discuss below. They can be constructed [2,11,12] from the polariton vacuum $|0\rangle_{pol}$, defined as $\hat{\eta}_{\pm k}|0\rangle_{pol} = 0$, $\hat{\eta}_{\pm k}$ being the polariton transformation [8]

$$|\eta_{\pm k}\rangle_{pol} = D(\hat{\eta}_k, \eta_k) D(\hat{\eta}_{-k}, \eta_{-k})|0\rangle_{pol}; \quad D(\hat{\eta}_{\pm k}, \eta_{\pm k}) \equiv e^{-|\eta_{\pm k}|^2/2} e^{\eta_{\pm k} \hat{\eta}_{\pm k}^\dagger} e^{-\eta_{\pm k}^* \hat{\eta}_{\pm k}} \qquad (2)$$

$|\eta_{\pm k}|^2 = |\gamma_{\pm k} c_r + e^{2i\phi} \gamma_{\mp k}^* s_r|^2$ yields the average number of polaritons in the state (2), where the $\gamma_{\pm k}$'s are the eigenvalues of the bose operator $\hat{\gamma}_{\pm k} = \alpha_k^{\pm} \hat{a}_{\pm k} + e^{i\chi_k^{\pm}} \beta_k^{\pm} \hat{b}_{\pm k}$. The $\hat{a}$'s and $\hat{b}$'s are respectively photon and phonon bare field annihilation operators. The real parameters $\{\alpha_k^{\pm}, \beta_k^{\pm}, \chi_k^{\pm}, \phi, r_k\}$ are *mode* and *material* dependent [2].

One should focus at this point on the structure of the polariton vacuum state. It has been the object of an exhaustive study not only by us [2,13], but also other workers [14] though within different contexts. In this rather interesting work a crucial common result emerged: the polariton vacuum $|0\rangle_{pol}$ is unitarily related to the bare particles vacuum $|0\rangle$ by a transformation of squeezing [1,10], that is

$$|0\rangle_{pol} = \hat{S}(\hat{\gamma}_{\pm}, r_k)|0\rangle = e^{r_k(\hat{\gamma}_k \hat{\gamma}_{-k} - \hat{\gamma}_k^\dagger \hat{\gamma}_{-k}^\dagger)}|0\rangle \qquad (3)$$

$r_k$ gives the amount of squeezing in the mode $k$. It is then clear from Eq.s (2) and (3) that a polariton coherent state is an instance of the two mode squeezed state defined in Eq. (1), 1 and 2 referring to counterpropagating wavevector modes.

It also follows from Eq.s (2) and (3) that for those $k$'s for which $S \cong 1$ the state $|\eta_{\pm k}\rangle_{pol}$ reduces to a bare particle coherent state, obtained by displacing the bare vacuum $|0\rangle$; but for those $k$'s for which $S \neq 1$, owing to purely quadratic terms in the photon and phonon creation and annihilation operators, $|\eta_{\pm k}\rangle_{pol}$ acquires a significantly more complicated structure. The non-classical character of a polariton state is clearly related to the parameter $r_k$. Owing to the wide breadth of values that $r_k$ can take on [2,5,15] one presume to create a polariton state with strong enough non-classical character so as to produce a sensitive result in the detection process. To this extent we recall from the results reported in [15] that, for a GaSb crystal, $r_k$ may vary across the polariton spectrum between values bigger than 1 to values that are even two orders of magnitude smaller.

Non-classical phonons in a polariton would be commonly characterised by a non-classical probability density distribution of the number of phonons in the polariton state [1,16]. In a polariton coherent state, unlike a polariton number state, no definite number of polaritons exists, but a well defined probability corresponds to each polariton number with a distribution of probabilities known to be *classical* [1,2,16]. Nonetheless, the distribution of its phonon component is in general *not classical*, with the most striking effects occurring where the squeezed structure of a polariton is most enhanced.

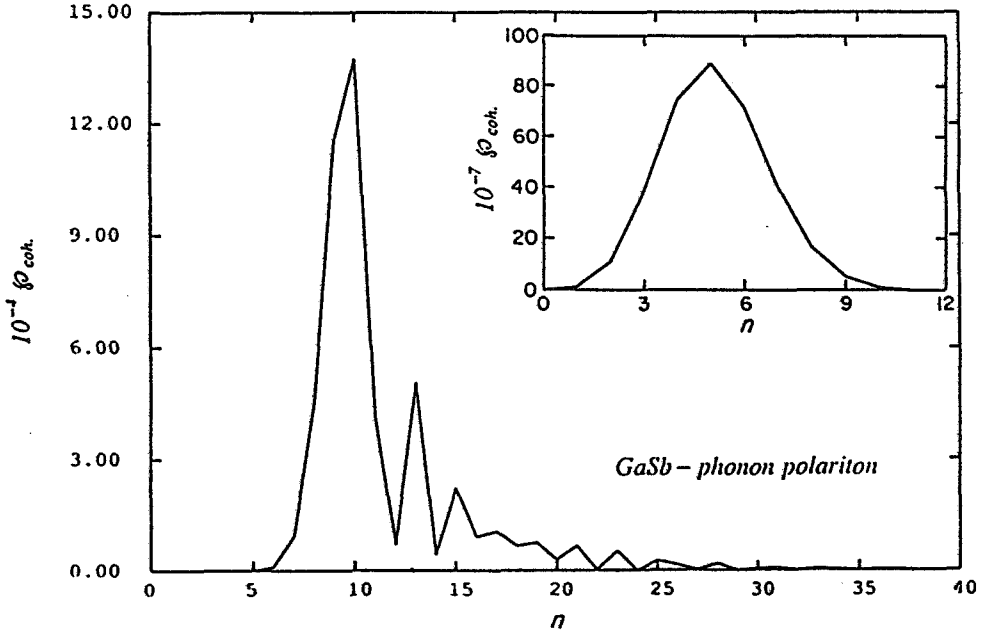


*Fig.2 Probability distributions for observing n phonons in a GaSb-polariton [15] for the two modes* $k_o = 10\,cm^{-1}$ $[r_o \approx 2.0]$ *(left) and* $k_o = 5.5 \cdot 10^3\,cm^{-1}$ $[r_o \approx 5 \cdot 10^{-2}]$ *(onset)*

The phonon number distribution in a polariton coherent state consists indeed of two contributions [15],

$$\wp_{coh} \equiv \wp_{coh}^{Poiss.}(n_{\pm k}) \cdot \wp_{coh}^{osc}(n_{\pm k}, r_k) , \qquad (4)$$

a Poisson one ($\wp_{coh}^{Poiss.}$) whose structure remains as such through the whole spectrum, and an oscillating one ($\wp_{coh}^{osc}$) whose size depends on the polariton dispersion. For those modes $k$'s for which $r_k \approx 0$ (Fig. 2 onset) $\wp_{coh}$ reduces to the Poisson distribution $\wp_{coh}^{Poiss.}$ (*classical limit*), whereas for those $k$'s for which $r_k \neq 0$ (Fig. 2) the component $\wp_{coh}^{osc}$ will contribute with strong oscillations in the large $n$ side of the distribution (*non-classical limit*). In this limit, quasi-periodic oscillations give rise to a remarkable effect of "quantization" in the phonon population which appears to be a distinctive non-classical feature of the phonon field in the polariton state (2). The two limits are illustrated in Fig. 2 through a numerical evaluation of Eq. (4) for GaSb polaritons [15].

*5. Detection*

The objective of this section is to address the question of how to probe the non-classical characteristics of the phonon field of a polariton discussed above. Probing the phonon number distribution associated with a specific structure of the polariton state is problematic if one decides to use particle-counting techniques analogous to those generally employed in the optical domain. *Conversely,* it would be possible to probe directly the non-classical structure of the polariton state that yields a non-classical phonon density distribution.

The idea consists in establishing coherence between two scattering processes that involve the absorption of two different wavevector phonon modes. Coherence would then produce constructive or destructive interference depending on whether the polariton is in a *non-classical* or *classical* state. Thus a measurement of the rate with which the probe scatters off of the phonon field of a polariton would provide a signature of the *non-classical* character of a polariton state.

This idea can be implemented as follows. Let a two-mode polariton be excited in a crystal, the modes referring to counterpropagating wavevectors of magnitude $|k_o|$ and frequency $\omega_o$. Then let a two-components probe beam, having high coupling efficiency to the phonon part of the polariton (neutrons e.g.), impinge on the crystal: both probe components have incident energy $\omega_{inc}$, but different wavevectors $k_d$ and $k_s$ (Fig. 3). The kinematics of the scattering process is described simply by the general conservation of energy and momentum (wavevector). Taking advantage of these laws, the input probe beam can be arranged so that the incoming probe is scattered into a given output state $|out\rangle_{pr}$ only when absorption off of the modes $k_o$ and $-k_o$ occurs as schematically illustrated in Fig.3.

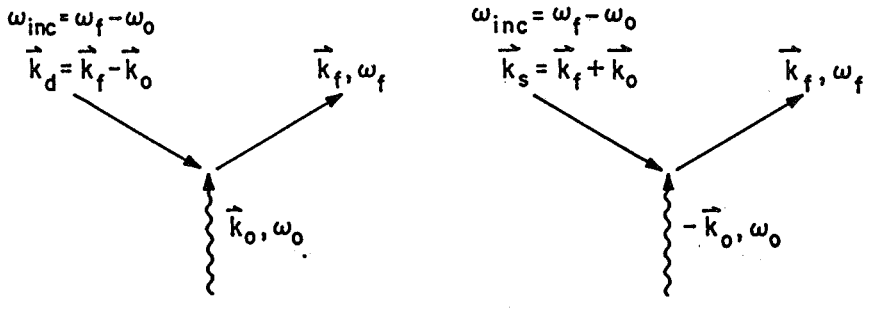


*Fig.3 Scattering processes involving the absorption of two counterpropagating phonons with energy $\omega_o$, and wavevectors $k_o$ and $-k_o$. With the probe in the state $|in\rangle_{pr}$ (Eq. 5), the two processes can coherently interfere when the phonon field is squeezed.*

Now let the detector be arranged so that only a probe in a final state of momentum $k_f$ and energy $\omega_f$ be detected and let the incoming probe be in a coherent superposition of states with wavevectors $k_d$ and $k_s$,

$$|out\rangle_{pr} = \hat{c}^{\dagger}_{k_f}|0\rangle_{pr} \qquad |in\rangle_{pr} = [A\hat{c}^{\dagger}_{k_d} + e^{i\varphi_{pr}} B\hat{c}^{\dagger}_{k_s}]|0\rangle_{pr} \tag{5}$$

$A, B$ and $\varphi_{pr}$ are respectively the real amplitudes and relative phase of the two components probe. These parameters can be all made to be controllable.

The relevant scattering rate (lowest order), when a polariton is initially excited into a coherent state, is

$$\sigma^{pol}_{coh}(k_o, A, f^o, \varphi_{pr}) = \sigma^{Poiss.}(k_o, A, f^o, \varphi_{pr}) + s^2_{r_o}\sigma^{osc.}(k_o, A, f^o, \varphi_{pr}) \tag{6}$$

denoting by $f^o$ the scattering amplitude for the process. The rate consists of two parts: one independent of $r_o \equiv r_{k_o}$ arising from the classical part of the distribution $\wp^{Poiss}_{coh}$ and one $r_o$-dependent coming from the oscillating counterpart $\wp^{osc}_{coh}$ (cf. Eq. 4). The relative size of these two contributions does play a significant role in determining the magnitude of the scattering rate. Namely, when polariton modes $|k_o|$ are populated for which is $r_o \approx 0$ Eq. (6) is approximated by

$$\sigma^{pol}_{coh}(k_o, A, f^o) = \sigma^{Poiss.}(k_o, A, f^o, \varphi) \tag{7}$$

In this case we can show [15] that for suitable values of the amplitude $A$ there exists a phase $\varphi_{pr}$ for which $\sigma^{Poiss.} \to 0$ so that the lowest-order scattering can be completely inhibited. On the *contrary*, when polariton modes $|k_o|$ are populated for which is $r_o \neq 0$ the second contribution ($\sim s^2_{r_o}$) in Eq. (6) is not negligible and can be shown to be always positive defined [15]. For these modes the rate turns out to be always greater or equal to $\sigma^{osc.}$, but never 0.

Hence rate measurements would permit one to discern the *non-classical* and *classical* character of a polariton coherent state. Destructive interference, able to suppress the rate with which a probe is scattered, is a signature of a classical polariton state, conversely constructive interference, yielding in principle a nonvanishing rate, is exhibited when the polariton state is non-classical (squeezed).

*6. Discussion*

Squeezed states, a familiy of pure quantum states having no classical analogue, have appeared in the literature since 1960's. In particular, extensive theoretical investigations for the realization of squeezed states of the electromagnetic field are also of long lasting. Only recently was the experimental realization of squeezed light with fewer quantum fluctuations than the vacuum achieved. To date there have been no reports, however, of the existence of non-classical states in condensed media, but the situation appears to be rather favorable for polaritons. This crystal mixed

quasiparticle appears to be indeed a promising place where to look for non-classical states of light and other bosons, such as e.g. phonons, especially if extremely low loss crystals can be obtained.

A further extension of this work would include considerations on the physical origin of the non-classical effects discussed above. Intermode correlation resulting from the quadratic transformation that takes one from coupled bare photon plus bare phonon to polaritons is a plausible origin for the squeezed structure of a polariton state and ultimately for the non-classical features of the phonon component associated with it.

In a real material elementary excitations and quasi-particles normally experience dissipation and phase destroying processes that may degrade the structure of the non-classical state inside the medium. For a complete treatment and in view of the possible experimental realizability of our findings the model presented here should further be extended to include various dissipative processes that randomize the phase of coherent superposition states on very short time scales. Such an investigation would afford the inclusion of irreversible couplings on the basis of the master equation.

Non-classical states have great fundamental significance and are extremely appealing in their own right as a test of basic quantum theories as well as perhaps for practical applications. The idea of searching for non-classical states of phonons in solids is certainly expected to add a new dimension to the search for non-classical behaviour.

## *7. Bibliography*


[1] "*Squeezed and non-classical light*", Ed.s P. Tombesi & R.P. Pike, NATO ASI-B, 190, (Plenum, 1989); J. Opt. Soc. Am. **B4**, No 10, (1987) and J. Mod. Opt. **34**, No 6, (1987) (special issues);

[2] M. Artoni, J.L. Birman, Phys. Rev. **B, 43**, 4221, (1991);

[3] "Polaritons", Eds. E. Burstein & F. De Martini, (Pergamon Press, 1972);

[4] U. Fano, Phys. Rev. **103**, 1202, (1956);

[5] M. Artoni, J. Birman, Optics Comm. **89**, 324 (1992);

[6] C. Kittel, in "Quantum Theory of Solids" (J. Wiley, New York, 1964)

[7] S.I. Pekar, "*Crystal Optics and Additional Light Waves*", (Benjamin/Cummings, 1983);

[8] J.J. Hopfield, Phys. Rev., 112, 1555, (1958); Here we adopt the Hopfield model for a phonon-polariton as the starting point of our work. A considerable success [3] has been achieved by this rather simple theoretical model which nevertheless encompasses the major relevant physics;

[9] K. Huang, Proc. Roy. Soc. (London) **A 208**, 352, (1951);

[10] C. Caves and B.L. Schumaker, Phys. Rev. A, **32**, 3068-3111, (1985);

[11] J. L. Birman, M. Artoni, B.S. Wang, Physics Report **194**, p. 367, (1990);

[12] A. Quattropani, L.C. Andreani, G.F. Bassani, Nuovo Cimento, Vol. **7D**, p. 55, (1986);

[13] M.Artoni, J.L. Birman Quantum Optics **1** (1989) 91;

[14] P. Schwendimann, A. Quattropani, Z. Hradil (preprint)

[15] M. Artoni, J. Birman, Optics Comm. (submitted) (1993);

[16] W. Schleich, J. Wheeler, Nature, **326**, 574, (1987), J. of Opt. Soc. Am. B, **4**, no 10 p. 1715, (1987);

N95-13958

# QUANTUM STATISTICS OF RAMAN SCATTERING MODEL WITH STOKES MODE GENERATION

B. Tanatar and Alexander S. Shumovsky[1]
*Bilkent University, Physics Department, 06533 Ankara, Turkey*

**Abstract**

The model describing three coupled quantum oscillators with decay of Rayleigh mode into the Stokes and vibration (phonon) modes is examined. Due to the Manley-Rowe relations the problem of exact eigenvalues and eigenstates is reduced to the calculation of new orthogonal polynomials defined both by the difference and differential equations. The quantum statistical properties are examined in the case when initially: the Stokes mode is in the vacuum state; the Rayleigh mode is in the number state; and the vibration mode is in the number or squeezed states. The collapses and revivals are obtained for different initial conditions as well as the change in time the sub-Poisson distribution by the super-Poisson distribution and vice versa.

## 1 Introduction

Recently quantum statistical properties of scattered light in the Raman process have attracted considerable interest.[1, 2] In particular, the anticorrelation between the Stokes and Rayleigh lines in the resonance scattering have been examined[3, 4], and the generation of squeezed light have been considered.[5, 6, 7] At the same time, the strong quantum fluctuations of energy have been observed[8, 9] experimentally. It is known that the Raman scattering is an example of optical parametric process in which one of the interacting waves is a medium vibration mode of boson type[10] (phonons). In the case of condensed matter, such a mode is usually in thermal equilibrium with a given temperature. The state of that mode is determined by different mechanisms of microscopic interactions in the medium and in some cases can lead to a strong number fluctuation.[11] An example is provided by a polariton–type system in which the equilibrium state is a squeezed one.[12] Evidently, the statistical properties of vibration mode must have influence on the statistics of scattered light.

In this paper we consider the quantum properties of scattered light, and its dependence on the type of statistical distribution function of the vibration mode in the Raman scattering. For simplicity, we suppose the resonance steady state process with generation of inelastic Stokes component only. The initial state of Rayleigh mode is assumed to be a number state, while vibration mode can be initially in a number state or in a squeezed vacuum state. The Stokes field is initially in the vacuum state. The simplest model of three bounded oscillators is used for description of process under consideration.[13] Using the representation of Schrödinger equation in terms of new orthogonal polynomials[14, 15], we examine the dynamics of the Mandel's factor

[1]On leave of absence from Bogolubov Laboratory of Theoretical Physics, JINR, Dubna, Moscow Region, Russia

of scattered light, and show the qualitative difference between two choices of initial states of the vibration mode.

The rest of this paper is organized as follows. We first introduce the model Hamiltonian for which we calculate the dynamical properties. Evaluation of the eigenvalues and eigenfunctions, and a discussion of how to construct the time dependent Mandel's factor is given in the next section. We then present our results, and conclude with an emphasis on the experimental implications.

# 2 Raman scattering model

To discuss some of the interesting statistical properties of light we study the Raman scattering model described by the Hamiltonian

$$H = \omega a^+ a + \omega_s a_s^+ a_s + \omega_b b^+ b + \gamma(b^+ a_s^+ a + a^+ a_s b) \tag{1}$$

where $a^+$ and $a_s^+$ are the creation operators for the Rayleigh and Stokes modes, respectively, with the corresponding frequences $\omega$ and $\omega_s$, $b^+$ is the creation operator for the vibration mode with frequency $\omega_b$, and $\gamma$ is the coupling constant. We consider here only the Stokes process because we will examine the case of low intensity initial field for which anti-Stokes component is negligible.

As a consequence of the Manley-Rowe relations, an exact eigenstate of the above Hamiltonian can be chosen as

$$|n,m>=\sum_{j=0}^{n} \lambda_j^{n,m} |n-j>_r |j>_s |m>_v \tag{2}$$

where $|... >_g$ is the number state of $g$-th mode. The coefficients $\lambda_j^{n,m}$ are determined by the recursion relation[15]

$$\lambda_{j+1}^{n,m}[(n-j)(j+1)(m+j+1)]^{1/2} = x^{n,m}\lambda_j^{n,m} - \lambda_{j-1}^{n,m}[(n-j+1)j(m+j)]^{1/2} \tag{3}$$

Here $x^{n,m} = (E^{n,m} - \omega_r n - \omega_v m)/\gamma$, and $E^{n,m}$ is an eigenvalue of the Hamiltonian corresponding to the eigenstate given above. The above relation [eq. (3)] can be represented in the form

$$P_{j+1}^{n,n}(x) = xP_j^{n,m}(x) - q_j^{n,m}P_{j-1}^{n,m}(x)\,; \qquad \text{with} \qquad q_j^{n,m} = (n-j+1)j(m+j)\,, \tag{4}$$

defining some orthogonal polynomials $P(x)$, which can be expressed in terms of the Bernoulli polynomials $B$ as

$$P_j^{n,m}(x) = \sum_{i=0}^{j} \beta_{ij}^{n,m} B_{ij}^{n.m} x^i\,, \tag{5}$$

where the coefficients $\beta$ satisfy

$$\beta_{ij}(j-i) = -jq_j\beta_{i,j-1}\,, \qquad \text{and} \qquad \beta_{i,j+1}(n-j)i = j\beta_{i-1,j}\,.$$

In terms of the polynomials $P(x)$, the equation for eigenvalues $E$ has now the form

$$P_{n+1}^{n,m}(x) = 0\,, \tag{6}$$

while the coefficients of the eigenstate given by eq. (2) are determined by the expression

$$\lambda_j^{n,m}(x_i) = \lambda_0^{n,m} \frac{P_j^{n,m}(x_i)}{F_j^{n,m}}, \qquad \text{with} \qquad F_j^{n,m} = \sqrt{[j!]^3 \binom{n}{j} \binom{m+j}{j}}. \tag{7}$$

The coefficient $\lambda_0$ is determined from the normalization condition.

Having constructed the solution to the eigenvalue and eigenstate problem, it is not hard to examine the dynamics of the system. In order to discuss our results, we shall use the time-dependent Mandel's $Q-$factor defined as

$$Q_r(t) = \frac{V_t(a_r^+ a_r) - < a_r^+ a_r >_t}{< a_r^+ a_r >_t}. \tag{8}$$

Here $a_r^+$ and $a_r$ are the Bose operators for the Rayleigh mode, $V_t(a_r^+ a_r)$ is the time-dependent number variance, and $< ... >_t$ denotes a time-dependent expectation value. $Q(t)$ is positive in the case of super-Poisson statistics and negative for sub-Poisson number distribution. Zero value corresponds to the coherent state (Poisson distribution). $Q-$factors for the other modes may be defined similarly. The time dependent terms in the Mandel's factor must be calculated as corresponding expectation values with time dependent wave function.

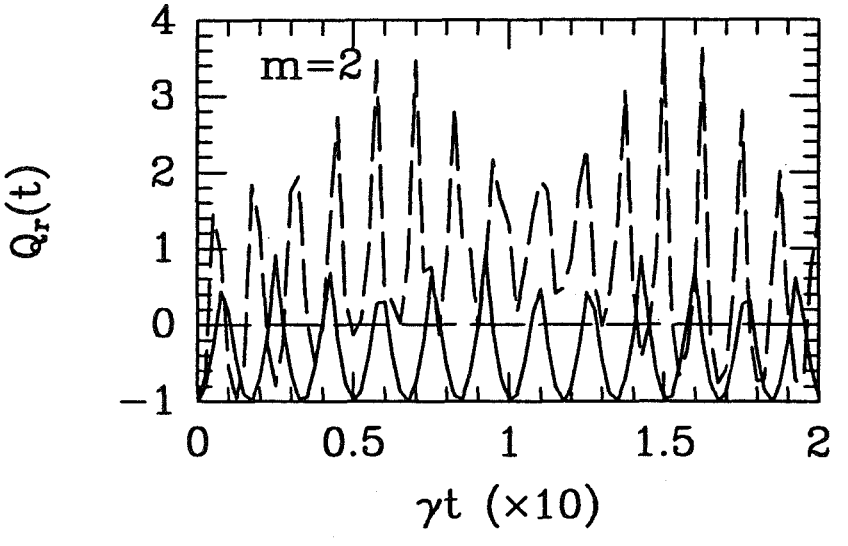


**Fig. 1.** $Q-$factor for Rayleigh mode initially in a number state with $n = 2$ (solid) and $n = 10$ (dashed), while the vibration mode is in a number state with $m = 2$.

# 3 Results and discussion

We have obtained qualitative differences in the quantum statistical properties of the Rayleigh mode depending on the initial state of the vibration mode. Using a number state for the Rayleigh mode, we consider uncorrelated (number state) and correlated (squeezed state) phonons in the vibration mode, and calculate the time evolution of the Mandel's $Q-$factor for the Rayleigh mode.

In Fig. 1 we show $Q_r(t)$ when the Rayleigh mode is initially in a number state with $n = 2$ and $n = 10$, indicated by solid and dashed lines, respectively. The vibration mode is also in the number state with $m = 2$. We observe that for a small value of $n$ $Q_r(t)$ periodically fluctuates between sub-Poisson and super-Poisson statistics. As $n$ is increased, quantum statistical distribution of the Rayleigh mode becomes more of super-Poissonian. The situation is qualitatively different, when the vibration mode is a correlated one described by a squeezed state as shown in Fig. 2. Here the squeezed state of the vibration mode is prepared such that the mean number of phonons is 2, viz., $|\nu|^2 = 2$. Solid, and dashed lines refer to the Rayleigh mode in the number state with $n = 2$ and $n = 10$, respectively. Here, we note that the distribution of photons remain mostly super-Poissonian, for large enough $n$. Similar results are obtained when the Rayleigh mode is initially in a coherent state.

To render the description of the vibration mode more realistic, we also use the Bose distribution at a given temperature. Here the mean number of phonons $\bar{m}$ may be regarded as a parameter. In Fig. 3 we show $Q_r(t)$ when the Rayleigh mode is initially in a number state with $n = 2$. Solid, dashed, and dotted lines refer to vibration mode parameter $\bar{m} = 0.1$, 1, and 10, respectively. We observe that for small values of $\bar{m}$ (low temperature) $Q_r(t)$ periodically fluctuates between sub-Poisson and super-Poisson statistics. As $\bar{m}$ is increased, quantum statistical distribution of the Rayleigh mode becomes entirely super-Poissonian.

We have also carried out calculations with large numbers of $n$, and observed the collapse-revival phenomenon occurs in the system for large enough $n$. Since an increase in $n$ implies an increase in the number of terms in the various sums, it is not surprising to observe the collapse-revival patterns as in the case of the Jaynes-Cummings model.[17, 18] It should be noted that similar behavior was obtained in the numerical calculations of Drobny and Jex[19], for the case of initial coherent state of the Rayleigh mode. In this connection, we emphasize that the collapse-revival phenomenon is a general property of the model described by the Hamiltonian irrespective of the initial state of the Rayleigh mode.

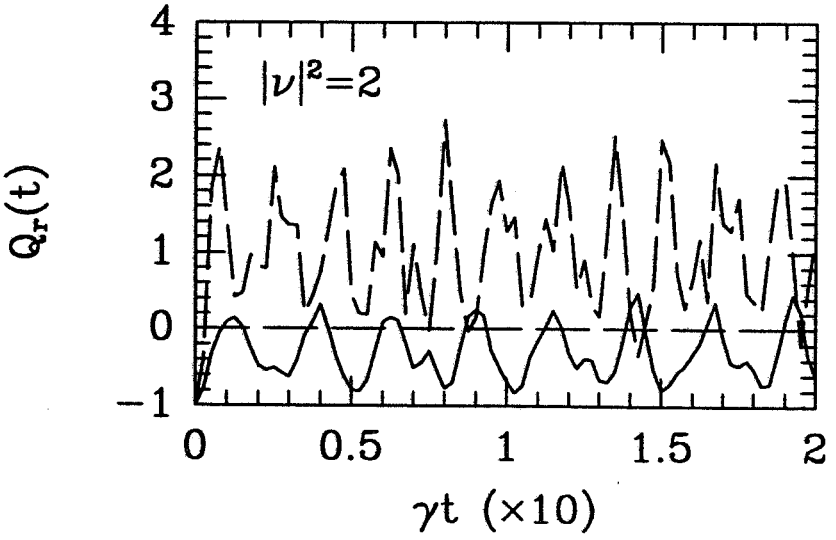


**Fig. 2.** Same as Fig. 1 when the vibration mode is initially in a squeezed state with parameter $|\nu|^2 = 2$.

We have obtained a qualitative difference in quantum statistical properties of scattered light depending on the statistics of the vibration mode. Our choice of initial state of the vibration mode can be considered as simulating correlated and uncorrelated phonons, and also phonons at finite temperature. We conclude stating that the experimental investigation of quantum statistical properties of scattered light in the Raman correlation spectroscopy with different types of incident light (e.g., in the number state or strongly sub-Poissonian) may yield important information about the correlations in the medium as well as in the molecules.

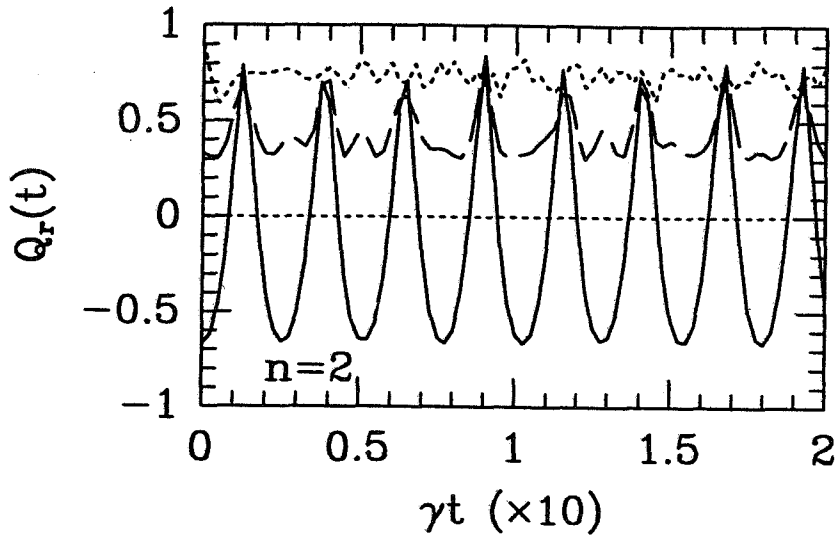


**Fig. 3.** $Q$−factor for Rayleigh mode initially in a number state ($n = 2$). Solid, dashed, and dotted lines indicate vibration mode parameter $\bar{m} = 0.1$, 1, and 10, respectively.

# Acknowledgments

B. T. thanks the Bilkent University for travel funds. A. S. acknowledges fruitful discussions with Professors C. Bowden, R. Bullough, S. Carusotto, O. Keller, F. Persico, and V. Rupasov.

# References

[1] A. S. Shumovsky and Tran Quang, in: Interaction of Electromagnetic Field with Condensed Matter, eds. N. N. Bogolubov, A. S. Shumovsky and V. I. Yukalov (World Scientific, Singapore, 1990) p. 103.

[2] J. Mostowski and M. G. Raymer, in: Contemporary Nonlinear Optics, eds. G. P. Agarval and R. W. Boyd (Academic Press, New York (1992)) p. 187.

[3] G. Agarwal and S. Jha, Z. Phys. B **25** (1979) 391.

[4] N. Bogolubov Jr., A. Shumovsky and Tran Quang, J. Physique **48** (1987) 1671.

[5] H. P. Yuen, Phys. Rev. A **13** (1976) 2226.

[6] A. Shumovsky and Tran Quang, Phys. Lett. A **131** (1988) 471.

[7] C. C. Gerry and J. H. Eberly, Phys. Rev. A **42** (1990) 6805.

[8] I. A. Walmsley and M. G. Raymer, Phys. Rev A **33** (1986) 382.

[9] M. D. Duncan, R. Mahon, L. L. Tankersley, and J. Reintjes, J. Opt. Soc. Am. B **7** (1990) 1336.

[10] Y. R. Shen, The Principles of Nonlinear Optics (Wiley, New York (1984)).

[11] A. S. Shumovsky, in: Modern Nonlinear Optics, ed. M. Evans (Wiley, New York (1993)).

[12] A. Chizhov, B. Govorkov Jr., and A. Shumovsky, Int. J. Mod. Phys. B, to be published.

[13] S. Carusotto, Phys. Rev. A **40** (1989) 1848.

[14] Yu. Orlov, I. Pavlotsky et. al., Int. J. Mod. Phys. B, to be published.

[15] A. Shumovsky and B. Tanatar, Phys. Rev. A, to be published.

[16] R. Loudon and P. L. Knight, J. Mod. Optics, **34** (1987) 709.

[17] H. I. Yoo and J. H. Eberly, Phys. Rep. **118** (1985) 239.

[18] Fam Le Kien and A. S. Shumovsky, Int. J. Mod. Phys. B **5** (1991) 2287.

[19] G. Drobny and I. Jex, Phys. Rev. A **46** (1992) 499.

# Evolution of Wave Function in a Dissipative System

Li Hua Yu
*National Synchrotron Light Source,*
*Brookhaven National Laboratory, N.Y.11973*

Chang-Pu Sun
*Institute of Theoretical Physics, State University of New York*
*Stony Brook, N.Y.11794*†

**Abstract**

For a dissipative system with Ohmic friction, we obtain a simple and exact solution for the wave function of the system plus the bath. It is described by the direct product in two independent Hilbert space. One of them is described by an effective Hamiltonian, the other represents the effect of the bath, i.e., the Brownian motion, thus clarifying the structure of the wave function of the system whose energy is dissipated by its interaction with the bath. No path integral technology is needed in this treatment. The derivation of the Weisskopf-Wigner line width theory follows easily.

The simplest example of a dissipative system, an harmonic oscillator coupled to the environment, which is a bath of harmonic oscillators, has been the subject of extensive studies[1-15]. We shall show in the present paper that in a special case, the Ohmic case (to be defined later), the dissipative system can be exactly treated both classically and quantum mechanically, thereby clarifying the sense in which the wave function is describable by an effective Hamiltonian. In this treatment path integral technology is not needed, and our presentation is self-contained.

We consider the problem discussed by Caldeira and Leggett (CL)[1], an harmonic oscillator system (the dissipative system) with coordinate q, mass M, and frequency $(\omega_0^2 + \Delta\omega^2)^{1/2}$, interacting with a bath of N harmonic oscillators of coordinates $x_j$, mass $m_j$, and frequency $\omega_j$., where $\Delta\omega^2$ is a shift induced by the coupling already discussed by CL. The Hamiltonian of the system and the bath is:

$$H = \frac{p^2}{2M} + \frac{1}{2}M(\omega_0^2 + \Delta\omega^2)q^2 + q\sum_j c_j x_j + \sum_j \left(\frac{p_j^2}{2m_j} + \frac{1}{2}m_j\omega_j^2 x_j^2\right) \tag{1}$$

The dynamic equation for operators in the Heisenberg representation leads to the following set of equations of motions:

$$M\ddot{q} = -M\omega_0^2 q - M\Delta\omega^2 q - \sum_j c_j x_j \,, \tag{2}$$

$$m_j\ddot{x} = -m_j\omega_j^2 x_j - c_j q \quad (j = 1, 2, ....N). \tag{3}$$

†Permanent Address: Department of Physics, Notheast Normal University, Changchun 130024, P.R.China

Now, applying the Laplace transform[2] (the bars are our notations for the Laplace transform, s is the Laplace transform of time t), equations (2), (3) can be used to eliminate bath variables $\bar{x}_j$ to obtain the equation for $\bar{q}$

$$M(s^2\bar{q} - sq_0 - \dot{q}_0) = -M\omega_0^2\bar{q} - M\Delta\omega^2\bar{q} - \sum_j c_j \frac{sx_{j0} + \dot{x}_{j0}}{s^2+\omega_j^2} - \sum_j \frac{c_j^2}{m_j(s^2+\omega_j^2)}\bar{q}\,, \tag{4}$$

where $q_0$, $\dot{q}_0$, $x_{j0}$, $\dot{x}_{j0}$ are the initial values of the respective operators in the Heisenberg representation. Assuming the number of bath oscillators is large enough so that we can replace the sum over j by an integration over $\omega_j$, the coefficient of the last term can then be separated into two terms:

$$\int_0^\infty \frac{\rho(\omega_j)c_j^2 d\omega_j}{m_j\,\omega_j^2} - s^2 \int_0^\infty \frac{\rho(\omega_j)\,c_j^2 d\omega_j}{m_j\omega_j^2(s^2+\omega_j^2)}\,, \tag{5}$$

where $\rho(\omega_j)$ is the bath oscillator density. Following an argument similar to the one pointed out by CL[1], the requirement that the system becomes a damped oscillator with frequency $\omega_0$ and damping rate $\eta$ in the classical limit, known as the "Ohmic friction" condition, leads to the following constraint:

$$\rho(\omega_j) = \frac{2\eta M}{\pi}\frac{m_j\omega_j^2}{c_j^2}. \tag{6}$$

By observing eq.(4) and eq.(5), it can be shown that the second term of eq.(5) leads to damping with the damping constant $\eta$, while the first term of eq.(5) represents a frequency shift. If the frequency renormalization constant $\Delta\omega^2$ is chosen to satisfy:

$$M\Delta\omega^2 = \int_0^\infty \frac{\rho(\omega_j)c_j^2 d\omega_j}{m_j\omega_j^2}\,, \tag{7}$$

the frequency is shifted to $\omega_0$. Then equation (4) is simplified, and its inverse Laplace transform gives the quantum Langevin equation, valid at time t >= 0+:

$$\ddot{q} + \eta\dot{q} + \omega_0^2 q = f(t)\ , \tag{8}$$

with the Brownian motion driving force:

$$f(t) = -\sum_j c_j(x_{j0}\cos\omega_j t + \dot{x}_{j0}\frac{\sin\omega_j t}{\omega_j})\ . \tag{9}$$

During the derivation, in order to carry out the integral in eq.(5), we used the requirement of the inverse Laplace transform that s must pass all the singular points from right of the complex plane, and hence real(s) >0.

Equation (8) and (9) are the equations of a *driven damped harmonic oscillator,* the solution of which is well known as a linear combination of the initial values at $q_0$, $\dot{q}_0$, $x_{j0}$, and $\dot{x}_{j0}$ :

$$q(t) = a_1(t)q_0 + a_2(t)\dot{q}_0 + \sum_j (b_{j1}(t)x_{j0} + b_{j2}(t)\dot{x}_{j0})\ , \tag{10}$$

$$x_i(t) = \alpha_{i1}(t)q_0 + \alpha_{i2}(t)\dot{q}_0 + \sum_j(\beta_{ij1}(t)x_{j0} + \beta_{ij2}(t)\dot{x}_{j0})\,,\ with \tag{11}$$

$$a_1(t) = \frac{\nu e^{-\mu t} - \mu e^{-\nu t}}{\nu - \mu}\,,\; a_2(t) = \frac{e^{-\mu t} - e^{-\nu t}}{\nu - \mu}\,, \tag{12}$$

$$\mu = \frac{\eta}{2} + \omega\, i\,,\; and\; \nu = \frac{\eta}{2} - \omega\, i\,, \tag{13}$$

and here $\omega = (\omega_0^2 - \eta^2/4)^{1/2}$ is the frequency shifted by damping. (All formulae are correct whether $\omega$ is real or imaginary. To avoid a minor detail of the initial value problem, we have redefined the initial time as t=0+.) The explicit expression for $b_{j1}$, $b_{j2}$, $\alpha_{i1}$, $\alpha_{i2}$, $\beta_{ij1}$, and $\beta_{ij2}$ are well known in freshmen physics.

We emphasize that the use of the Laplace transform instead of the Fourier transform allows us to express q(t) and $x_j(t)$ explicitly in terms of the initial values, as in eq.(10) and eq.(11).

The equations (10) and (11) serve as the starting point of subsequent discussions. We will proceed to find the Green's function of the full system, and hence the solution of the wave function in Schoedinger representation. The result tells us *in what sense the damped oscillator is described by an effective Hamiltonian without the bath variables* and gives its specific form, it also shows that under this condition, the wave function can be factorized, and the main factor relevant to the damped oscillator is a solution of the Schoedinger equation with an effective Hamiltonian.

Equations (10) and (11) are correct both in classical mechanics and in quantum mechanics in the Heisenberg representation. We notice that q(t) and $x_j$(t) are both linear superpositions of $q_0$, $\dot{q}_0$, $x_{j0}$, $\dot{x}_{j0}$ with c-number coefficients. The commutation rules between $q(t)$, $\dot{q}(t)$, $x_j(t)$, $\dot{x}_j(t)$ are $[q(t), \dot{q}(t)] = \frac{i\hbar}{M}$, $[x_j(t), \dot{x}_j(t)] = \frac{i\hbar}{m_j}$, and operators q(t) and $\dot{q}(t)$ commute with $x_j(t)$ and $\dot{x}_j(t)$. One can prove these commutation rules by two ways: (a). By direct computation, using the fact that at t=0, they are correct. (b). By the general principle that $q(t)$, $\dot{q}(t)$, $x_j(t)$, $\dot{x}_j(t)$ are related by a unitary transformation to $q_0$, $\dot{q}_0$, $x_{j0}$, $and\, \dot{x}_{j0}$.

Equation (10) and (11) show that the operators q(t) and $x_j(t)$ can each be written as a sum of two terms:

$$q(t) = Q(t) + \sum_j \xi_j(t)\,, \tag{14}$$

$$x_i(t) = \zeta_i(t) + \sum_j X_{ij}(t)\,, \tag{15}$$

where $Q(t)$ and $\zeta_i(t)$ are linear in $q_0$ and $\dot{q}_0$ and independent of $x_{j0}$ and $\dot{x}_{j0}$, and $\xi_j$ and $X_{ij}(t)$ are linear in $x_{j0}$ and $\dot{x}_{j0}$, and independent of $q_0$ and $\dot{q}_0$. Thus Q(t) and $\zeta_i(t)$ are operators in one Hilbert space $S_Q$, while $\xi_j(t)$ and $X_{ij}(t)$ are in an independent Hilbert space $S_X$, and the full Hilbert space is a direct product $S_Q \otimes S_X$.

We shall first analyze the structure of $S_Q$. We write that:

$$Q(t) = a_1 Q_0 + a_2 \dot{Q}_0 = a_1 Q_0 - a_2 \frac{i\hbar}{M}\frac{\partial}{\partial Q_0}\,. \tag{16}$$

To explicitly show that we are discussing the $S_Q$ space, we define $Q_0 \equiv q_0$, $\dot{Q}_0 \equiv \dot{q}_0$. The eigenfunction of Q(t) with an eigenvalue denoted by $Q_1$, in the $Q_0$ representation, is easily calculated to be:

$$u_{Q_1}(Q_0, t) = \left(\frac{M\omega e^{\frac{1}{2}\eta t}}{2\pi\hbar \sin\omega t}\right)^{\frac{1}{2}} exp\left[-\frac{iM}{2\hbar a_2}\left(a_1 Q_0^2 - 2Q_0 Q_1 + \phi(Q_1, t)\right)\right]\,, \tag{17}$$

with $\phi$ as an arbitrary phase, i.e., a real number. This eigenfunction is related to the Green's function $G(Q_1,Q_0;t,0) \equiv < Q_1|U_Q(t)|Q_0 >$, by $u_{Q_1}(Q_0,t) =< Q_0|U_Q^{-1}(t)|Q_1 > =< Q_0|U_Q^{\dagger}(t)|Q_1 >= G^*(Q_1,Q_0;t,0)$, where we denote the evolution operator by $U(t)$, which is unitary when we choose the eigenvectors of Q(t) to be orthonormal. Thus we have:

$$G(Q_1,Q_0;t,0) = \left(\frac{M\omega e^{\frac{1}{2}\eta t}}{2\pi\hbar \sin\omega t}\right)^{\frac{1}{2}} exp\left[\frac{iM}{2\hbar a_2}\left(a_1Q_0^2 - 2Q_0Q_1 + \phi(Q_1,t)\right)\right] \ . \tag{18}$$

Next, we shall determine the arbitrary phase $\phi(Q_1,t)$, which is the phase of the eigenvectors of Q(t). Using eq.(16), we find the commutation rule for $Q$ and $\dot{Q}$:

$$[Q,\dot{Q}] = (a_1\dot{a}_2 - \dot{a}_1a_2)[Q_0,\dot{Q}_0] = e^{-\eta t}[Q_0,\dot{Q}_0] = \frac{e^{-\eta t}}{M}i\hbar \ . \tag{19}$$

Thus we define the canonical momentum P(t) as:

$$P(t) = Me^{\eta t}\dot{Q}(t) = M\ e^{\eta t}(\dot{a}_1Q_0 + \dot{a}_2\dot{Q}_0) = \dot{a}_1Q_0 - \dot{a}_2\frac{i\hbar}{M}\frac{\partial}{\partial Q_0} \ , \tag{20}$$

and get the commutation rule: $[Q(t),P(t)] = i\hbar$. The eigenfunction of P(t) can be calculated in two ways: (a). We can calculate the eigenvector of P(t) in the $Q_0$ representation using eq. (20) and then use the Green's function eq.(18) to transform it into the Q(t) representation; (b). The commutation rule $[Q(t),P(t)] = i\hbar$ requires that P(t)=$-i\hbar\frac{\partial}{\partial Q}$, so the eigenfunction of P(t) with eigenvalue $P_1$ is $exp[i\frac{P_1}{\hbar}Q]$. By comparing these two solutions, the arbitrary phase $\phi(Q_1,t)$ in the Green's function is determined to within a phase $\phi(t)$, which is independent of $Q_1$. $\phi(t)$ is an arbitrary real function of time, except that $\phi(0) = 0$ so that it satisfies the condition that at t=0, the Green's function becomes $\delta(Q_1 - Q_0)$. Thus we obtain the Green's function in the $S_Q$ space:

$$G(Q_1,Q_0;t,0) = \left(\frac{M\omega e^{\frac{1}{2}\eta t}}{2\pi i\hbar \sin\omega t}\right)^{\frac{1}{2}} exp\left[\frac{iM}{2\hbar a_2}\left(a_1Q_0^2 + \dot{a}_2e^{\eta t}Q_1^2 - 2Q_0Q_1\right) - \frac{i\phi(t)}{\hbar}\right]. \tag{21}$$

It is then straight forward to derive the Hamiltonian $H_Q$ using the following relation:

$$H_Q = i\hbar\frac{\partial U_Q}{\partial t}U_Q^{-1} \ , \tag{22}$$

and remembering that the matrix elements of $U_Q$ and $U_Q^{-1}$ are the Green's function and its conjugate. The result is:

$$H_Q = e^{-\eta t}\frac{P^2}{2M} + \frac{1}{2}M\omega_0^2e^{\eta t}Q^2 + \dot{\phi}(t) \ . \tag{23}$$

Since $\phi$ is arbitrary except that $\phi(0) = 0$, we can take $\phi(t) = 0$. Therefore we have derived the well known effective Hamiltonian for the dissipative system. *We emphasize that the expression for $H_Q$ is here derived, while in usual literature it is introduced by more or less heuristic arguments.*

Next, we shall analyze the effect of the bath. Similar to eq. (17) we obtain the eigenfunctions $\theta_{\xi_{j1}}(x_{j0},t)$ for $\xi_j$. Using Dirac's notation we have: $Q|u_{Q_1} >= Q_1|u_{Q_1} >$, $\xi_j|\theta_{\xi_{j1}} >= \xi_{j1}|\theta_{\xi_{j1}} >$.

Thus $|u_Q> \prod_j \bigotimes |\theta_{\xi_j}>$ is an eigenvector of q(t), with eigenvalue of $Q + \sum_j \xi_j$. In other words, the eigenvector of q(t) with eigenvalue q is $|q, \{\xi_j\}> = |u_{q - \sum_j \xi_j} > \prod_j \bigotimes |\theta_{\xi_j}>$.

If initially the wave function is $|\Psi_0> = |\psi_0> \prod_j \bigotimes |\chi_{j0}>$, to calculate the wave function at time t, we should expand $\Psi_0$ in terms of the eigenvectors $|q, \{\xi_j\}>$, i.e., we should calculate

$$\psi(Q,t) \equiv < u_Q|\psi_0> = \int u_Q^*(q_0)\psi_0(q_0)dq_0 \,, \tag{24}$$

$$\chi_j(\xi_j,t) \equiv < \theta_{\xi_j}|\chi_{j0}> = \int \theta_{\xi_j}^*(x_{j0})\chi_{j0}(x_{j0})dx_{j0} \,. \tag{25}$$

Then the wave function in the Schoedinger representation at time t is

$$\Psi(q,\{\xi_j\},t) = < q,\{\xi_j\}|\Psi_0> = \psi(q - \sum_j \xi_j, t) \prod_j \chi_j(\xi_j,t) \,. \tag{26}$$

Notice that $\psi(Q,t)$ of eq.(24) is the wave function in the Schoedinger representation with the effective Hamiltonian eq.(23). Hence we have connected the effective Hamiltonian approach to the dissipative system problem with the other approaches that take both the system and the bath into account. We also notice that even though our $\Psi(q,\{\xi_j\},t)$ is in a different representation from that of $\Psi(q,\{x_j\},t)$, the usual probability interpretation is still valid: $\int\int ... \int |\Psi(q,\{\xi_j\},t)|^2 \prod_j d\xi_j$ is the probability density of finding the particle at q. Since this solution is very simple, it provides a simple way to analyze other complicated problems, e.g., study the influence of Brownian motion on interference, which we shall not elaborate because of space.

Under certain conditions, eg., at low temperature and when the system q is in highly excited states so the range of q is large enough that for all the values of $\xi_j$ which do not have vanishingly small probability, $q \gg |\sum_j \xi_j|$, we can approximately write: $\Psi(q,\{\xi_j\},t) = \psi(q,t) \prod_j \chi_j(\xi_j,t)$. That is, the wave function is factorized, the dissipative system q can be described by the wave function $\psi(q,t)$ only, and the Brownian motion can be ignored. Therefore it is interesting to examine the width of the argument of the wave function $\psi$, due to the Brownian motion, i.e., the mean value of $(\sum_j \xi_j)^2$ at time t. It can be calculated using its expression in the Heisenberg representation as introduced by (10) and (18). At temperature T, this width is :

$$< (\sum_j \xi_j(t))^2 > = \sum_j \frac{\hbar}{2m_j\omega_j}(|b_{j1}(t)|^2 + \omega_j^2|b_{j2}(t)|^2) \cot\left(\frac{\hbar\omega_j}{2kT}\right) \,. \tag{27}$$

This width is zero initially, then approaches its final equilibrium value in a time interval of the order of $1/\eta$. At low temperature limit, the equilibrium width is simplified to:

$$\sigma^2(t=\infty) = \frac{\hbar}{2\pi m\omega}\left[\frac{\pi}{2} + \arctan\left(\frac{\omega_0^2}{\eta\omega}\right)\right] \,. \tag{28}$$

If the damping rate $\eta$ is much smaller than the frequency of the oscillator $\omega_0$, this width happens to become the same as the width of the ground state of the system $\hbar/(2m\omega)$.

Finally, it is interesting to see the distribution of the dissipated energy of the harmonic oscillator in the bath, and check if it agrees with the Weisskopf-Wigner line width theory[16] For simplicity, we assume zero temperature. To calculate the energy dissipated by the system into the j'th bath oscillator, we use eq.(11) and its derivative to obtain the expression of $x_j(t)$ and $p_j = m_j\dot{x}_j(t)$, which are then substituted into the expression of the energy of the j'th oscillator: $h_j = \frac{p_j^2}{2m_j} + \frac{1}{2}m_j\omega_j^2 x_j^2$. We then calculate the expectation value of $h_j$, assuming initially the system is in the n'th excited state, and the bath oscillators in the ground state. We calculate the contribution to the expectation value of $h_j$ from the system, by keeping only terms which depend on $q_0$, and $\dot{q}_0$. The result is then the energy disspation by the system into the j'th oscillator. When multiplied by the density of states $\rho(\omega_j)$ eq.(6), it gives the dissipated energy spectrum. It is a function of $\omega_j$, with a narrow peak near the resonance $\omega_j = \omega$, if the damping is small, i.e., if $\eta \ll \omega$. It is oscillatory with a frequency of $2\omega_j$. Its time average over a period is :

$$E_j = (n + \frac{1}{2})\hbar\omega \frac{\eta}{\pi} \frac{1}{\frac{\eta^2}{4} + (\omega - \omega_j)^2} A(\omega_j), \tag{29}$$

where $A(\omega_j)$ varies slowly near the resonance, i.e., over the width $\eta/2$ of the peak it changes very little. Therefore, we can replace $\omega_j$ by $\omega$ near the peak, and the result is simplified to: $A(\omega) \approx 1$. Thus eq.(29) shows that the dissipated energy has a Lorenzian distribution near the resonance, in agreement with the Weisskopf-Wigner line width theory.


### Acknowledgements

We thank Prof.C.N. Yang for drawing our attention to the problem of dissipative systems, for spending his valuable time in many sessions of stimulating discussions on this subject, and for many suggestions which are critically important for the ideas of this paper. The part of work by Li Hua Yu is performed under the auspices of the U.S. Department of Energy under Contract No. DE-AC02-76CH00016. The part of work by Chang-Pu Sun is supported in part by a Cha Chi Ming fellowship through the CEEC program at the State University of New York at Stony Brook, and in part by the NSF of China through the Northeast Normal University.


# References


[1] A.O. Caldeira, A.J. Leggett, Ann. Phys. **149**, 374 (1983), and Physica **121A**, 587 (1983).

[2] A.O. Caldeira, Helvetica Phisica Acta **61**, 611 (1988).

[3] E. Kanai, Prog. Theor. Phys. **3**, 440 (1948).

[4] S. Nakajima, Prog. Theor. Phys. **20**, 948 (1958).

[5] R.Zwanzig, J. Chem. Phys. **33**, 1338 (1960).

[6] I.R. Senitzky, Phys. Rev. **119**, 670 (1960).

[7] R.P. Feynman, F.L. Vernon, Ann. Phys. **24**, 118 (1963).

[8] G.W. Ford, M. Kac, P. Mazur, Jour. Math. Phys. **6**, 504 (1965).

[9] M. D. Kostin, J. Chem. Phys. **57**, 3589 (1972).

[10] W.H. Louisell, *Quantum Statistical Properties of Radiation*, (John Wiley & Sons, 1973).

[11] M. Sargent III, M.O. Scully, W.E. Lamb, *Laser Physics*, (Addison-Wesley, 1974).

[12] K. Yasue, Ann. Phys. **114**, 479 (1978).

[13] R.H. Koch, D.J. Van Harlingen, J. Clarke, Phys. Rev. Lett. **45**, 2132 (1980).

[14] H. Dekker, Phys. Report **80**, 1 (1981).

[15] R. Benguria, M. Kac, Phys. Rev. Lett, 46, 1 (1981).

[16] V.F. Weisskopf, F.P. Wigner, Z. Physik **63**, 54 (1930); **65**, 18 (1930).

# NONRESONANT INTERACTION OF ULTRASHORT ELECTROMAGNETIC PULSES WITH MULTILEVEL QUANTUM SYSTEMS

E.Belenov, V.Isakov and A.Nazarkin
*Lebedev Physics Institute, Russian Academy of Sciences, Leninsky pr. 53, 117924 Moscow, Russia*

**Abstract**

Some features of the excitation of multilevel quantum systems under the action of electromagnetic pulses which are shorter than the inverse frequency of interlevel transitions are considered. It is shown that the interaction is characterized by a specific type of selectivity which is not connected with the resonant absorption of radiation. The simplest three-level model displays the inverse population of upper levels. The effect of an ultrashort laser pulse on a multilevel molecule was regarded as an instant reception of the oscillation velocity by the oscillator and this approach showed an effective excitation and dissosiation of the molecule. The estimations testify to the fact that these effects can be observed using modern femtosecond lasers.

## 1 Introduction

Progress in ultrashort pulse technique allows production of laser pulses of 5–10 femtosecond duration, i.e., of a few periods of electromagnetic wave [1]. The interaction of so short light pulses with matter must differ from the case of quasi-monochromatic resonant radiation because the pulse duration becomes shorter than the inverse frequancy of the transitions between vibrational levels of molecules $\omega_{ij}^{-1}$ or optical phonons in crystals, and under such conditions the result of interaction is practically independent of the real structure of matter. In particular, a Raman-active medium can be effectively excited by a single femtosecond pulse because its wide spectrum initially contains Stokes and anti-Stokes components of the field [2, 3].

We shall discuss here two effects which may occur if the light pulse is shorter than the time of vibrational transitions between molecule levels, i.e. under the condition $\tau_p \omega_{ij} \ll 1$. The first effect displays a specific selectivity of vibrational excitation of molecules by ultrashort light pulses, which is not connected with resonant properties of matter. The second effect is a possibility of effective excitation of high vibrational levels and even dissosiation of molecules in the field of an ultrashort electromagnetic pulse.

# 2 Selectivity of Molecule Excitation by Nonresonant Pulse Radiation

The selectivity of molecule excitation is connected with the fact that the probability of transitions between molecule levels cannot be presented already as a function of slowly varying amplitude E(t) of the light field similar to the case of quasimonochromatic resonant radiation but depends on its real temporal structure $\mathcal{E}$(t). The equations for ultrashort pulse propagation, in their turn, impose restrictions on such integral values as $\int_{-\infty}^{\tau} \mathcal{E}(t)dt$. As shown in Ref [4], the "area" of electromagnetic wave of limited aperture in a free space goes to zero, $\int_{-\infty}^{\infty} \mathcal{E}(t)dt = 0$. It results from the Gauss' integral theorem in the case of electromagnetic wave propagation in a space without electric charges. If $\mu_{nm}$ is a dipole moment of the transition between levels m and n, the amplitude of the transition $n \to m$ in the dipole approximation is of the form

$$a_m^{(1)}(\infty) = -\frac{i}{\hbar}\int_{-\infty}^{\infty} \mu_{nm}\mathcal{E}(t)e^{i\omega_{nm}t}dt \quad \overset{\tau_p\omega_{nm}\ll 1}{\longrightarrow} \quad -\frac{i\mu_{nm}}{\hbar}\int_{-\infty}^{\infty} \mathcal{E}(t)dt$$

and tends to zero for ultrashort pulses.

It means that excitation of vibrational levels of molecules by femtosecond pulses is mainly due to two-quanta processes over distant virtual levels

$$a_m^{(2)}(\infty) = -\frac{i}{2\hbar}\int_{-\infty}^{\infty} r_{nm}E^2(t)e^{i\omega_{nm}t}dt,$$

where $r_{nm} = \frac{1}{2\hbar}\sum_k \mu_{nk}\mu_{km}\left(\frac{1}{\omega_{kn}-\omega} + \frac{1}{\omega_{km}+\omega}\right)$ is a composite matrix element responsible for Raman effect at the transition $n \to m$, and the probability of excitation in the second order perturbation theory is proportional to the pulse energy $\int_{-\infty}^{\infty} |E(t)|^2\, dt \neq 0$. Thus, an ultrashort pulse provides "inverse" selectivity of molecule excitation — the transitions forbidden in the dipole approximation are stimulated much more effectively than the allowed ones.

As an illustration let us consider three-level quantum system, i.e. three lowest levels of the deformational vibrations of the $CO_2$ molecule ($00^00, 01^10$ and $02^00$). The model assumes that the condition of the ultrashort interaction $\tau_p\omega_{ij} \ll 1$ holds for i,j=1,2,3 and the other levels are distant in the energy scale, i.e. $|\omega_{ik} - \omega| \gg \tau_p^{-1}, k \neq 1,2,3$. Levels (1) and (3) are of the same parity and the transition between them is forbidden in the dipole approximation.

The condition $\tau_p\omega_{ij} \ll 1$ implies of course that the interaction of an ultrashort pulse with matter is coherent ($\tau_p \ll T_1, T_2$, pulse duration is shorter than times of longitudinal and transverse relaxcation) and can be described by equations for the probability amplitudes of the molecule to be at the level j(=1,2,3):

$$i\hbar\frac{da_1}{dt} = -\mu_{12}\mathcal{E}(t)a_2 - r_{13}\mathcal{E}^2(t)a_3, \tag{1}$$

$$i\hbar\frac{da_2}{dt} = -\mu_{21}\mathcal{E}(t)a_1 - \mu_{23}\mathcal{E}(t)a_3, \tag{2}$$

$$i\hbar\frac{da_3}{dt} = -\mu_{32}\mathcal{E}(t)a_2 - r_{31}\mathcal{E}^2(t)a_1. \tag{3}$$

Let the system be at the ground level (1) at the initial instant of time, i.e. $a_1(t=-\infty) = 1$ and $a_2(t=-\infty) = a_3(t=-\infty) = 0$. Under the action of ultrashort pulse, the transitions onto

level (2) occur due to the fast oscillating field $\mathcal{E}(t)$ which do not have a constant component, but transitions onto level (3) occur due to the interaction quadratic in field and $\overline{\mathcal{E}^2(t)} \neq 0$. We can assume that during the interaction the redistribution of population will be provided mainly by the transitions over level (3). Indeed, by integrating the second equation and saving here the amplitudes $\bar{a}_1$ and $\bar{a}_3$ whose time dependence is slow with respect to $\mathcal{E}(t)$, one obtains

$$a_2(t) \simeq \frac{i}{\hbar}\left[\mu_{21}\bar{a}_1(t) + \mu_{23}\bar{a}_3(t)\right]\int_{-\infty}^{t}\mathcal{E}(t)dt.$$

In other words, the population of level (2) is small ($a_2 \sim \mu_{ij}\mathcal{E}/\hbar\omega$) because of a nonresonant interaction of this level with the field of the ultrashort pulse. After substitution of $a_2(t)$ into the first and third equations one can obtain equations for slow components of the amplitudes $\bar{a}_1$ and $\bar{a}_3$, which do not contain parameters of dipole transitions $1 \rightarrow 2$ and $2 \rightarrow 3$:

$$\begin{aligned} i\hbar\frac{d\bar{a}_1}{dt} &= -\frac{r_{13}}{2}|E(t)|^2\bar{a}_3, \\ i\hbar\frac{d\bar{a}_3}{dt} &= -\frac{r_{31}}{2}|E(t)|^2\bar{a}_1. \end{aligned}$$

It is interesting to note that the solution of these equations

$$\begin{aligned} \bar{a}_1(t) &= \cos\Psi(t), \\ \bar{a}_3(t) &= i\sin\Psi(t), \\ \Psi(t) &= \frac{r_{13}}{2\hbar}\int_{-\infty}^{t}|E(t)|^2\,dt \end{aligned}$$

coincides formally with the solution for resonant coherent excitation of two-quanta transition, although in our case the interaction is nonresonant in principle.

The population of molecule levels after the action of ultrashort pulse is determined by the following expressions:

$$n_1(\infty) = \cos^2\left(\frac{r_{13}}{2\hbar}\int_{-\infty}^{\infty}|E|^2\,dt\right), \tag{4}$$

$$n_2(\infty) = \frac{1}{\hbar^2}\left[\mu_{12}^2 n_1(\infty) + \mu_{23}^2 n_3(\infty)\right]\left(\int_{-\infty}^{\infty}\mathcal{E}(t)dt\right)^2 = 0, \tag{5}$$

$$n_3(\infty) = \sin^2\left(\frac{r_{13}}{2\hbar}\int_{-\infty}^{\infty}|E|^2\,dt\right). \tag{6}$$

These equations display an evident selectivity of the interaction of an ultrashort light pulse with the three-level quantum system which produces the population inversion on the transition $3 \rightarrow 2$. If the energy of an ultrashort pulse corresponds to the value of the rotation phase $\Psi_\infty = \frac{r_{13}}{2\hbar}\int_{-\infty}^{\infty}|E|^2\,dt = \frac{\pi}{2}(2n+1)$, $n = 0, 1, 2, \ldots$ the quantum system will be moved onto the upper level (3) and all the energy stored can be picked up, for example, by two sequential $\pi$-pulses which are resonant to transitions $3 \rightarrow 2$ and $2 \rightarrow 1$.

Let us make some estimations for the molecule $CO_2$. It can be easily shown that if the initial population $n_{20}$ of the level (2) is not equal to zero, the inversion on the transition $3 \rightarrow 2$ appears if $\Psi_\infty > (n_{20}/n_{10})^{1/2}$. For a $CO_2$ molecule $\hbar\omega_{32} \simeq \hbar\omega_{21} \simeq 700cm^{-1}$ and under normal conditions $n_{20}/n_{10} \simeq 10\%$. Using data on Raman cross section ($r_{13} \simeq 10^{-24}\ cm^3, \lambda = 488\ nm$ [5]) one can estimate that a 10-femtosecond pulse provides inversion between vibrational levels $02^00$ and $01^10$ if its power exeeds $10^{12}\ W/cm^2$. This value can be easily satisfied by modern femtosecond technique.

# 3 Dissociation of Molecules by Femtosecond Pulses

The possibility of effective excitation of high vibrational levels makes topical the problem of transformation, for example, dissociation of molecules under the action of ultrashort laser pulse. Usually, collisionless excitation and dissociation of molecules by resonant radiation are investigated on the basis of the chain of equations for amplitudes of population probabilities of vibrational levels. This analisis is very complicated because of a large amount of levels which should be under consideration. In our case the condition $\tau_p \omega_{nm} \ll 1$ means that the result of interaction is not sensitive to the real vibrational structure of molecule spectrum and makes it convinient to investigate directly the equations for wave functions of vibrational Hamiltonian regarding it as a function of the distance between nuclei. The statement of the problem is quite similar to that solved by A. Migdal on excitation and ionization of atom after its nucleus received an instant impact [6, page 178]. For simplicity we consider a two-atom molecule and assume the pulse to be so short that during its action the nuclei acquire some velocity but their positions relative to electrons have no time to change. If at the initial instant of time the molecule is at the ground state then just after the pulse action it remains at the same vibrational level and its wave function is related to the initial one as

$$\varphi_0(Q, t=\infty) = \varphi_0(Q, t=-\infty) e^{-i\frac{\mathcal{P}Q}{\hbar}},$$

where $\mathcal{P} = -\frac{1}{4}\left(\frac{\partial \kappa_0}{\partial Q}\right) \int_{-\infty}^{\infty} |E(t)|^2 \, dt$ is the impulse transmitted to molecule under the action of ultrashort $\delta$-pulse; $\kappa_0$ is polarizability of the molecule, Q is vibrational coordinate.

The quantum state described by the wave function $\varphi_0(Q, \infty)$ is not already a stationary state of the molecule after receiving an instant impulse $\mathcal{P}$. The transition of the system to the stationary state is accompanied by excitation of the upper vibrational levels and the probability to find molecule at the level v is determined by the coefficient of expansion of $\varphi_0(Q, \infty)$ into series in terms of the stationary wave functions of the vibrational Hamiltonian:

$$w_{ov} = \left| \int_{-\infty}^{\infty} \varphi_v^*(Q) e^{-i\frac{\mathcal{P}Q}{\hbar}} \varphi_o(Q) dQ \right|^2 .$$

It is evident that the higher the pulse energy and consequently the transmitted momentum $\mathcal{P}$, the more is the difference between the quantum state of the molecule just after the pulse action and the stationary state and the higher are the levels to be involved into transition of the molecule to its stationary state.

Let us display it in framework of the model of anharmonic Morse oscillator, i.e. a particle of mass M which is moving in a field wth potential energy $U(R) = D\left(e^{-2\alpha R} - 2e^{-\alpha R}\right)$ [6]. The spectrum of positive energy of this particle is continuous and corresponds to a dissociated molecule. In the negative energy region there is a finite series of vibrational levels which is convergent to the dissociation energy D: $E_{v+1} - E_v = \hbar\omega_0 - v \cdot \hbar \triangle\omega_0$, where $\omega_0 = (E_1 - E_0)/\hbar = \alpha(\sqrt{2MD} - \alpha\hbar)/M$ is the fundamental frequancy of the oscillator and $\triangle\omega_0 = \alpha^2\hbar/M$ is the anharmonism of the molecule. The wave functions of Morse oscillator are of the form $\varphi_v(Q) \sim e^{-\xi/2}\xi^s F(-v, 2s+1, \xi)$, where $\xi = \frac{2\sqrt{2MD}}{\alpha\hbar} e^{-\alpha Q}$, $s + v = s_0 = \frac{\omega_0}{\triangle\omega_0} + \frac{1}{2} \simeq N$ and N is a total number of the oscillator levels.

The problem of excitation of anharmonic oscillator levels by an ultrashort radiation $\delta$-pulse has an exact solution. The probability of finding the molecule at the level v is

$$w_{ov} = \frac{\beta \sinh(\pi\beta)}{\pi\Gamma(2s_0)v!} \cdot \frac{|\Gamma(i\beta+v)|^2\,|\Gamma(i\beta+2s_0-v)|^2}{\Gamma(2s_0-v)}, \tag{7}$$

or, neglecting the difference between $s_0$ and N, — has the form

$$w_{ov} = \frac{\pi\beta}{(2N-1)!\sinh(\pi\beta)} \cdot \frac{\prod_{n=1}^{2N-1}[\beta^2+(n-v)^2]}{v!(2N-v-1)!}, \tag{8}$$

where $\beta = \mathcal{P}(\alpha\hbar)^{-1}\ln^{-1}\left[\frac{2\sqrt{2MD}}{\alpha\hbar}\right] \sim \int_{-\infty}^{\infty}|E|^2\,dt$.

For weak ultrashort pulses ($\beta \to 0$) the probability of exciting vibrational levels is small and proportional to the square of the pulse energy: $1 - w_{oo} = \beta^2\psi'(2N)$.

With elevation of the pulse energy the population of high vibrational levels increases and, therefore, the dissociation of the molecule becomes more probable. In the limit of superpower ultrashort pulses ($\beta \gg 2N$) the probability of dissociation is exponentially close to unity:

$$w_D = 1 - \sum_{v=0}^{N-1} w_{ov} \simeq 1 - 2\pi\left[\frac{2^{N-1}}{(2N-1)!}\right]^2 \beta^{4N-1}e^{-\pi\beta}.$$

Thus, under the action of femtosecond laser pulse molecules can be effectively excited on high vibrational levels, and moreover, when the pulse energy exceeds the threshold

$$\beta_v^2 = \frac{(2N-v)[2v(N-v-1)-1]}{2(N-v)}$$

the inversion takes place between levels v and v-1.

In conclusion let us present some estimations. For the CO molecule which is active in Raman scattering we shall estimate the energy of the laser pulse which provides inversion between the lowest levels ($v = 1$) $\to$ ($v = 0$). Using data on Raman cross section ($\partial\kappa_0/\partial Q \simeq 10^{-16}cm^2, \lambda = 488\ nm$[5]) and spectroscopic parameters ($D = 83777\ cm^{-1}, \alpha = 2.3904\ \AA^{-1}$) [7] we can estimate the pulse energy required for the inversion to be of the order of 0.1 $J/cm^2$.

The last estimation is connected with the energy of the ultrashort pulse which is necessary for an effective ($w_D \sim 1$) dissociation of a two-atom molecule. As an example we consider the molecule of $J_2$ whose dissociation energy is relatively small ($D \simeq 1.5eV$) and is of the same order of magnitude as the spectral width of a femtosecond pulse. From the condition $\beta \geq 2N$ we can obtain that the pulse energy required for dissociation exceeds 1 $J/cm^2$. This requirment is much stronger than the one for the inversion on the lowest levels but it can be satisfied by the modern femtosecond technique.

# 4 Acknowledgments

This research is supported in part by the Russian Basic Research Foundation under Grant No. 93-02-14271 and in part by Wissenschaftskolleg in Berlin, Schweizerische National-Versicherungs-Gesellschaft, Alusuisse-Lonza Holding AG and Mr. Helmut Hartmann (Augsburg). We would like to thank Professor M.H. Rubin and Professor Y.H. Shih for their kind invitation to participate in the Workshop. One of the authors (V.I.) is grateful to the American Physical Society for travel support.

# References


[1] S.A. Akhmanov, V.A. Vysloukh and A.S. Chirkin, *Optics of Femtosecond Laser Pulses.* (Nauka, Moscow, 1988, in Russian).

[2] Y.X. Yan, E.B. Gamble and K.A. Nelson, J. Chem. Phys.**83**, 5391 (1985).

[3] E.M. Belenov, A.V. Nazarkin and I.P.Prokopovich, JETP Lett. (Russia) **55**, 223 (1992).

[4] E.M. Belenov and A.V. Nazarkin, JETP Lett. (Russia) **53**, 188 (1991).

[5] W.R. Fenner, H.A. Hyatt *et al*, J. Opt. Soc. Am. **63**, 73 (1973).

[6] L.D. Landau and E.M. Lifshitz, *Quantum Mechanics*, (Nauka, Moscow, 1963, in Russian).

[7] I.I. Tugov, Proceedings of Lebedev Physics Institute.**146**, 17 (Nauka, Moscow, 1984, in Russian).

# SECTION 8

# EPR PROBLEM, BELL'S INEQUALITIES

# AND

# MULTIPHOTON INTERFEROMETRY

# Complementarity and Path Distinguishability: some recent results concerning photon pairs.

Abner Shimony
*Physics and Philosophy Departments, Boston University,*
*Boston, Massachussetts 02215*

Gregg Jaeger
*Physics Department, Boston University,*
*Boston, Massachussetts 02215*

**Abstract**

Two results concerning photon pairs, one previously reported and one new, are summarized. It was previously shown that if the two photons are prepared in a quantum state formed from $|A\rangle$ and $|A'\rangle$ for photon 1 and $|B\rangle$ and $|B'\rangle$ for photon 2, then both one- and two-particle interferometry can be studied. If $v_i$ is the visibility of one-photon interference fringes ($i = 1, 2$) and $v_{12}$ is the visibility of two-photon fringes (a concept which we explicitly define), then

$$v_i^2 + v_{12}^2 \leq 1.$$

The second result concerns the distinguishability of the paths of photon 2, using the known 2-photon state. A proposed measure $E$ for path distinguishability is based upon finding an optimum strategy for betting on the outcome of a path measurement. Mandel has also proposed a measure of distinguishability $P_D$, defined in terms of the density operator $\rho$ of photon 2. We show that $E$ is greater than or equal to $P_D$ and that $v_2 = (1 - E^2)^{1/2}$.

## 1 Introduction.

The idea of an entangled quantum state of a composite system – i.e., a state not factorizable into a product of one-particle states – was discovered by Schrödinger in 1926, and has been intensively studied as a result of analyses by Einstein-Podolsky-Rosen and Bell. A very convenient method for preparing entangled photon pairs by parametric down-conversion in laser-pumped nonlinear crystals was discovered by Burnham and Weinberg in 1970. Their discovery permitted the development of two-photon interferometry by Mandel and his school, Alley and Shih, Franson, Rarity and Tapster, Chiao and his school, and others.[1]

For subsequent discussion. it will be useful to refer to a schematic two-photon apparatus (Fig. 1), in which a pair of photons emerges from a source S, one of which propagates in beams A and/or



C-7

A′, and the other in beams B and/or B′, where the locution "and/or" is a brief way of referring to quantum mechanical superposition. For the work on path distinguishability that we shall report, this partial description of Fig. 1 provides the essence. For the work on the complementarity of one-photon and two-photon interference, some further elements are indispensable. There is an ideal symmetric beam splitter $H_1$ upon which each of the beams A and A′ impinge, from which emerge beams $U_2$ and $L_2$. We can speak equivalently of a photon "emerging" in beams $U_1$, $L_1$, $U_2$, $L_2$ or of its "detection by an ideal photo-detector" in the respective beams. Finally, there are variable phase shifters $\phi_1$ and $\phi_2$ inserted in beams A and B.

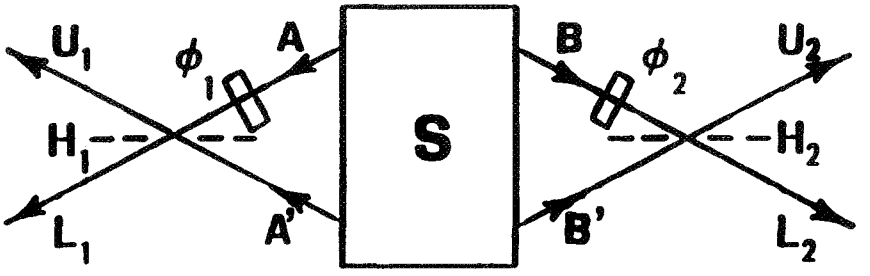


FIG.1. Schematic two-particle four-beam inteferometer.

## 2 Complementarity.

It was noticed in the past, for instance by Horne and Zeilinger,[2] that when the photon pair is prepared in the entangled state $|\Psi\rangle$,

$$|\Psi\rangle = \frac{1}{\sqrt{2}}\left[|A\rangle|B\rangle + |A'\rangle|B'\rangle\right] . \tag{1}$$

then probabilities of single detections in the various emerging beams are independent of phase shifts $\phi_1$ and $\phi_2$, specifically.

$$P(U_1) = P(L_1) = P(U_2) = P(L_2) = \frac{1}{2} . \tag{2}$$

whereas the probabilities of joint detection depend on $\phi_1$ and $\phi_2$, specifically,

$$P(U_1U_2) = P(L_1L_2) = \frac{1}{4}[1 - cos(\phi_1 + \phi_2)], \tag{3a}$$

$$P(U_1L_2) = P(L_1U_2) = \frac{1}{4}[1 + cos(\phi_1 + \phi_2)]. \tag{3b}$$

Since the probabilities in Eqs.(3a, b) vary from a minimum of zero to a non-zero maximum value, while those of Eq.(2) do not vary at all, it is reasonable to extend standard optical terminology and say that the visibility of one-photon "fringes" is zero and the visibility of two-photon fringes

is unity, where "fringe" is a generic way of referring to the dependence of detection probabilities upon variable phase shifts. When the quantum state of the two photons has the product form

$$|\Phi\rangle = \frac{1}{\sqrt{2}}\Big[|A\rangle + |A'\rangle\Big]\frac{1}{\sqrt{2}}\Big[|B\rangle + |B'\rangle\Big], \tag{4}$$

then

$$P(U_i) = \frac{1}{2}(1 - sin\phi_i), \quad i = 1,2, \tag{5a}$$

$$P(L_i) = \frac{1}{2}(1 + sin\phi_i), \quad i = 1,2, \tag{5b}$$

and the probabilities of joint detection are the products of respective single detections:

$$P(U_1U_2) = P(U_1)P(U_2) = \frac{1}{4}(1 - sin\phi_1)(1 - sin\phi_2), \ etc. \tag{6}$$

It is reasonable to say in this case that the visibility of one-photon fringes is unity, but the visibility of two-photon fringes is zero (the latter statement in spite of the fact that $P(U_1U_2)$ does vary with $\phi_1$ and $\phi_2$, because of the consideration that this variation is not a genuine two-photon effect but is derived from the one-photon variation).

The two extreme cases of $|\Psi\rangle$ and $|\Phi\rangle$ suggest that there is a complementarity of one-photon and two-photon interference visibility. Jaeger, Horne, and Shimony[3] raised the question of a general complementarity relation, holding for any two-photon state expressible in terms of $|A\rangle$, $|A'\rangle$, $|B\rangle$, $|B'\rangle$. A necessary condition for investigating this question was to define explicitly the "one-photon visibility" $v_i$ $(i = 1,2)$ and the "two-photon visibility" $v_{12}$. The former is straightforward, simply adapting the standard optical concept introduced by Rayleigh. We state it here only for the beams $U_1$ and $U_2$, but parallels hold for $L_1$ and $L_2$

$$v_i = \frac{[P(U_i)]_{max} - [P(U_i)]_{min}}{[P(U_i)]_{max} + [P(U_i)]_{min}} . \tag{7}$$

For $v_{12}$ Jaeger *et al.* suggested

$$v_{12} = \frac{[\bar{P}(U_1U_2)]_{max} - [\bar{P}(U_1U_2)]_{min}}{[\bar{P}(U_1U_2)]_{max} + [\bar{P}(U_1U_2)]_{min}} . \tag{8}$$

The "corrected" joint probability $\bar{P}(U_1U_2)$ is defined as

$$\bar{P}(U_1U_2) = P(U_1U_2) - P(U_1)P(U_2) + \frac{1}{4} , \tag{9}$$

where the second term on the right hand side removes the variability that is derived from the single probabilities $P(U_1), P(U_2)$ and the third term is a correction against excessive subtraction in order to agree with intuition in the extreme cases of $|\Psi\rangle$ and $|\Phi\rangle$.

In order to exhibit the desired complementarity relation, it is essential to calculate $v_i$ and $v_{12}$ in the most general two-photon state that can be prepared with $|A\rangle$, $|A'\rangle$ as basis states for photon 1 and $|B\rangle$, $|B'\rangle$ as basis states for photon 2, namely,

$$|\Theta\rangle = cos\alpha[cos\beta|A\rangle|B\rangle + e^{i\lambda}sin\beta|A'\rangle|B'\rangle] + sin\alpha[e^{i\mu}cos\gamma|A\rangle|B'\rangle + e^{i\nu}sin\gamma|A'\rangle|B\rangle] \ . \tag{10}$$

Note that only three phase angles $\lambda, \mu, \nu$ are used, because an overall multiplication by a phase factor does not change the quantum state, and this fact can be used to choose the coefficient of $|A\rangle|B\rangle$ to be real. In Ref. 3 it was fallaciously argued that a basis change of

$$|A\rangle = e^{i\rho}|\bar{A}\rangle \ , \quad |A'\rangle = e^{i\rho'}|\bar{A}'\rangle \ , \tag{11}$$

$$|B\rangle = e^{i\sigma}|\bar{B}\rangle \ , \quad |B'\rangle = e^{i\sigma'}|\bar{B}'\rangle \ ,$$

can be used to express $|\Theta\rangle$ in terms of $|A\rangle$, $|A'\rangle$, $|B\rangle$, $|B'\rangle$ with real coefficients. But Prof. Sheldon Goldstein pointed out to us (private communication) that in general only two of the three phase angles in Eq.(10) can be eliminated by a basis change, and therefore the greatest simplification that can be achieved in full generality retains one explicit phase angle, for instance,

$$|\Theta\rangle = cos\alpha[cos\beta|A\rangle|B\rangle + sin\beta|A'\rangle|B'\rangle] + sin\alpha[cos\gamma|A\rangle|B'\rangle + e^{i\tau}sin\gamma|A'\rangle|B\rangle] \ . \tag{12}$$

So far, we have not demonstrated a complementarity relation for the general case of Eq.(12). We therefore report the result in the restricted case of $\tau = 0$, which we have investigated. As stated in Ref. 3, Eqs.(29-32), we obtain

$$v_i^2 = \frac{1}{2}sin^2 2\alpha[1 + sin2\beta \ sin2\gamma + (-1)^i cos2\beta \ cos2\gamma] \ , \tag{13}$$

$$v_{12}^2 = cos^4\alpha \ sin^2 2\beta - 2sin^2\alpha \ cos^2\alpha \ sin2\beta \ sin2\gamma + sin^4\alpha \ sin^2 2\gamma \ , \tag{14}$$

whence

$$v_i^2 + v_{12}^2 \leq 1 \ , \tag{15a}$$

or equivalently,

$$0 \leq v_i v_{12} \leq \frac{1}{2} \ . \tag{15b}$$

Inequalities (15a,b) are our expressions of the complementarity of one-photon and two-photon visibilities. Although we have derived them only for the special case of $\tau = 0$, we are confident that they hold for any $\tau$ and hence for the most general $|\Theta\rangle$. Work is in progress on this important question.

# 3 Path Distinguishability.

We return now to Fig. 1 and ask a new question. Suppose that we are allowed to make any observation on photon 1, which is the left-going photon that propagates in A and/or A′; what is the best procedure for predicting which detector will be triggered by photon 2, if ideal detectors are inserted in beams B and B′? This question is related to a question recently raised by Mandel[4] concerning the distinguishability of the path of a photon that propagates in beams B and/or B′. There is, however, an important difference between Mandel's question and ours. He assumes only that one knows the density operator $\rho$ characterizing an ensemble of photons in the beams B and/or B′, and he asks for a measure of distinguishability expressed in terms of $\rho$. By contrast, we ask for a measure of distinguishability based upon the quantum state $|\Theta\rangle$ of the pair of photons 1 and 2, together with the outcome of an arbitrary measurement upon photon 1. It is possible to compare our result with Mandel's, because when $|\Theta\rangle$ is given a density operator for photon 2 can be calculated[5] by tracing out the appropriate variables of photon 1. But, of course, if only $\rho$ is given, there are many possible preparations of an ensemble of photons propagating in beams B and/or B′ that would yield the same $\rho$. In other words, the preparation of the ensemble provides additional information that is not included in $\rho$. Consequently, we anticipate a discrepancy between Mandel's measure of path distinguishability and ours.

As a preliminary to our proposed measure of path distinguishability we suppose that an observable $\mathcal{O}$ is measured on photon 1. Since the space of states that we have allowed for photon 1 is two-dimensional, there is no loss of generality if we restrict the observable $\mathcal{O}$ to the form

$$\mathcal{O} = |\phi_1\rangle\langle\phi_1| - |\phi_2\rangle\langle\phi_2| \ , \tag{16}$$

where $|\phi_1\rangle$ and $|\phi_2\rangle$ are orthonormal kets in the space spanned by $|A\rangle$ and $|A'\rangle$. (We are grateful to Prof. Lev Vaidman for suggesting that we consider any $\mathcal{O}$, rather than just $|A\rangle\langle A| - |A'\rangle\langle A'|$ as in our original preprint.) The eigenvalues of $\mathcal{O}$ are $+1$ and $-1$. Now formulate a strategy for betting on whether the detector in team $B$ or in beam B′ is triggered, letting the strategy depend upon the quantum state $|\Theta\rangle$ of the photon pair and the outcome $+1$ or $-1$ of measuring $\mathcal{O}$. If in a single case the correct detector is predicted, the observer wins one unit of utility; if the wrong detector is predicted, the observer loses one unit of utility. Once the strategy is specified, it is straightforward to calculate from $|\Theta\rangle$ the average gain per bet. Let $E_{\mathcal{O}}$ be the largest average gain thus calculated as the strategy is varied but $\mathcal{O}$ is fixed. Finally, our *measure of distinguishability of paths*, which we shall label $E$, is defined as

$$E = max\ E_{\mathcal{O}}\ \ (over\ the\ set\ of\ allowed\ observables)\ . \tag{17}$$

$E$ is thus the quantum mechanical estimate of the gain per bet when the optimum allowable strategy is followed, the bets being made concerning paths B and B′.

To calculate $E_{\mathcal{O}}$ we first rewrite $|\Theta\rangle$, assumed to be normalized, as

$$|\Theta\rangle = |\chi_1\rangle|B\rangle + |\chi_2\rangle|B'\rangle \ , \tag{18}$$

where, as before, $|B\rangle$ and $|B'\rangle$ are orthonormal, but $|\chi_1\rangle$ and $|\chi_2\rangle$ need not be; however,

$$\langle\chi_1|\chi_1\rangle + \langle\chi_2|\chi_2\rangle = 1 \ . \tag{19}$$

With no loss of generality we can assume that

$$\langle \chi_1|\chi_1\rangle \geq \langle \chi_2|\chi_2\rangle \ , \tag{20}$$

which can be achieved, if necessary, by interchanging the labels B and B′ of the two paths of photon 2. Then we can write

$$|\chi_2\rangle = \lambda|\chi_1\rangle + |\chi_3\rangle \ , \tag{21a}$$

where

$$\lambda = \frac{\langle \chi_1|\chi_2\rangle}{\langle \chi_1|\chi_1\rangle} \ , \tag{21b}$$

$$|\lambda| \leq 1 \ , \tag{21c}$$

and

$$\langle \chi_1|\chi_3\rangle = 0 \ . \tag{21d}$$

If we define

$$N_i = \langle \chi_i|\chi_i\rangle \ , \quad i = 1,3 \ , \tag{22a}$$

then the $|\bar{\chi}_i\rangle$, defined by

$$|\bar{\chi}_i\rangle = \frac{|\chi_i\rangle}{\sqrt{N_i}} \ , \quad i = 1,3 \ , \tag{22b}$$

are orthonormal. Furthermore,

$$N_1(1 + |\lambda|^2) + N_3 = 1 \ . \tag{23}$$

Any basis $|\phi_1\rangle, |\phi_2\rangle$ in the space of allowable states of photon 1 can be expressed as

$$|\phi_1\rangle = \mu|\bar{\chi}_1\rangle + \nu|\bar{\chi}_2\rangle \ , \tag{24a}$$

$$|\phi_2\rangle = \nu^*|\bar{\chi}_1\rangle - \mu^*|\bar{\chi}_2\rangle \ , \tag{24b}$$

where

$$|\mu|^2 + |\nu|^2 = 1 \ . \tag{24c}$$

This basis defines the observable $\mathcal{O}$ of Eq.(16). It will also be useful to write

$$\mathcal{B} = |B\rangle\langle B| - |B'\rangle\langle B'| \ , \tag{25}$$

an observable in the allowable space of states of photon 2; clearly $\mathcal{B}$ is observed to have values $+1$ and $-1$ according as photon 2 is detected in path B or B′.

If $\mathcal{O}$ is the observable chosen to be measured, then there are four pure strategies for bets on the path of photon 2:

(1) If $\mathcal{O} = +1$, predict $\mathcal{B} = +1$; if $\mathcal{O} = -1$, predict $\mathcal{B} = -1$.
(2) If $\mathcal{O} = +1$, predict $\mathcal{B} = -1$; if $\mathcal{O} = -1$, predict $\mathcal{B} = +1$.
(3) Predict $\mathcal{B} = +1$ regardless of the value of $\mathcal{O}$.
(4) Predict $\mathcal{B} = -1$ regardless of the value of $\mathcal{O}$.

In addition to these pure strategies there are mixed strategies, consisting of following (1), (2), (3), (4) with arbitrary probabilities summing to unity. But since the game is not being played against a rational opponent, the average gain in a mixed strategy cannot exceed the maximum of the average gain $E_{\mathcal{O}}^{(i)}$ of the pure strategies,[6] $i = 1, 2, 3, 4$. These are calculated as follows:

$$E_{\mathcal{O}}^{(1)} = P(\mathcal{O} = 1 \textit{ and } \mathcal{B} = 1) + P(\mathcal{O} = -1 \textit{ and } \mathcal{B} = -1)$$

$$-P(\mathcal{O} = 1 \textit{ and } \mathcal{B} = -1) - P(\mathcal{O} = -1 \textit{ and } \mathcal{B} = 1)$$

$$= |\langle\Theta|\phi_1\rangle|B\rangle|^2 + |\langle\Theta|\phi_2\rangle|B'\rangle|^2 - |\langle\Theta|\phi_1\rangle|B'\rangle|^2 - |\langle\Theta|\phi_2\rangle|B\rangle|^2$$

$$= S(|\mu|^2 - |\nu|^2) - T|\mu||\nu|\ cos(\theta_\lambda + \theta_\nu - \theta_\mu)\ , \tag{26}$$

where

$$S = N_1(1 - |\lambda|^2) + N_3\ , \tag{27a}$$

$$T = 4N_1^{1/2}N_2^{1/3}|\lambda|\ , \tag{27b}$$

$$\lambda = |\lambda|e^{i\theta_\lambda},\ \mu = |\mu|e^{i\theta_\mu},\ \nu = |\nu|e^{i\theta_\nu}\ ; \tag{27c}$$

$$E_{\mathcal{O}}^{(2)} = -E_{\mathcal{O}}^{(1)}\ ; \tag{28}$$

$$E_{\mathcal{O}}^{(3)} = P(\mathcal{B} = +1) - P(\mathcal{B} = -1) = \langle\chi_1|\chi_1\rangle - \langle\chi_2|\chi_2\rangle$$
$$= N_1(1 - |\lambda|^2) - N_3 = S - 2N_3\ ; \tag{29}$$

$$E_{\mathcal{O}}^{(4)} = P(\mathcal{B} = -1) - P(\mathcal{B} = +1) = -E_{\mathcal{O}}^{(3)}\ . \tag{30}$$

Note that $E_{\mathcal{O}}^{(3)}$ and $E_{\mathcal{O}}^{(4)}$ are independent of $\mathcal{O}$. Then

$$E_{\mathcal{O}} = max\Big\{|S(|\mu|^2 - |\nu|^2) - T|\mu||\nu|\ cos(\theta_\lambda + \theta_\nu - \theta_\mu)|\ ,\ |S - 2N_3|\Big\}. \tag{31}$$

In view of Eqs.(17) and (31) one finds the measure $E$ of path distinguishability by investigating $E_{\mathcal{O}}$ as $\mu$ and $\nu$ are varied, subject to Eq.(24c). We first note that for any $|\Theta\rangle$ there is an $\mathcal{O}$ such that

$$|E_{\mathcal{O}}^{(1)}| \geq |E_{\mathcal{O}}^{(3)}|\ , \tag{32}$$

so that the second option in Eq.(31) can be neglected when we maximize over all possible $\mathcal{O}$. To prove these statements, it suffices in Eqs.(24a,b) to let $\mu = 1$ and $\nu = 0$, determining an $\mathcal{O}'$ such that Eqs.(26), (27), (28) yield

$$|E_{\mathcal{O}'}^{(1)}| = |N_1(1 - |\lambda|^2) + N_3|\ , \tag{33}$$

and

$$|E^{(3)}_{\mathcal{O}'}| = |N_1(1-|\lambda|^2) - N_3| \ . \tag{34}$$

Since $N_1$ and $N_3$ are non-negative, and $(1-|\lambda|^2)$ is non-negative by Eq.(21c), we obtain

$$|E^{(1)}_{\mathcal{O}'}| \geq |E^{(3)}_{\mathcal{O}'}| \ , \tag{35}$$

the rhs being the same as $|E^{(3)}_{\mathcal{O}}|$ for all $\mathcal{O}$. $E$ is therefore obtained by maximizing the first option of Eq.(31) for allowable $\mu$ and $\nu$, and the result is

$$E = \frac{1}{2}(4S^2 + T^2)^{1/2}. \tag{36}$$

By Eqs. (27a), (27b), and (23) $E$ can be rewritten as

$$E = (1 - 4N_1^2|\lambda|^2)^{1/2}. \tag{37}$$

We can now make a comparison with Mandel's[4] measure of path distinguishability $P_D$. Mandel notes that in a two-dimensional Hilbert space, any density operator $\rho$ can be expressed uniquely in the form

$$\rho = P_{ID}\ \rho_{ID} + P_D\ \rho_D \ , \tag{38}$$

where $\rho_D$ is diagonal in the $|B\rangle$, $|B'\rangle$ basis, *i.e.*

$$\rho_D = c_{11}|B\rangle\langle B| + c_{22}|B'\rangle\langle B'| \ , \tag{39}$$

(after adaptation to our notation),

$$tr\ \rho_{ID} = tr\ \rho_D = 1 \ , \tag{40}$$

and

$$P_{ID} \geq 0,\ P_D \geq 0 \ . \tag{41}$$

Since $\rho_D$ is a diagonal density operator in the specified basis, one can prepare an ensemble with a definite proportion $c_{11}$ in the state $|B\rangle$ and a definite proportion $c_{22}$ in the state $|B'\rangle$ such that this ensemble is represented by $\rho_D$. It is this consideration that leads Mandel to identify $P_D$ as the degree of path distinguishability when $\rho$ is given. Mandel also shows that

$$P_D = 1 - \frac{|\rho_{12}|}{(\rho_{11}\rho_{22})^{1/2}} \ , \tag{42}$$

where $\rho_{ij}$ is the $ij^{th}$ matrix element of $\rho$ in the $|B\rangle, |B'\rangle$ basis.

Now let us consider the $|\Theta\rangle$ of Eq.(18), which we can rewrite as

$$|\Theta\rangle = N_1^{1/2}|\bar{\chi}_1\rangle|B\rangle + \lambda\, N_1^{1/2}|\bar{\chi}_1\rangle|B'\rangle + N_3^{1/2}|\bar{\chi}_3\rangle|B'\rangle\ . \tag{43}$$

By the standard procedure for writing the density matrix of particle 2 of a two-particle system,[5] we obtain (with the help of Eq.(23)),

$$\begin{aligned} \rho_{11} &= N_1\ , \\ \rho_{12} = N_1\lambda\ ,\ \rho_{21} &= N_1\lambda^*\ , \\ \rho_{22} = N_1|\lambda|^2 + N_3 &= 1 - N_1\ . \end{aligned} \tag{44}$$

Hence, Eq.(37) can be rewritten as

$$E = (1 - 4|\rho_{12}|^2)^{1/2}\ , \tag{45}$$

which can be shown as follows to be greater than or equal to $P_D$ of Eq.(42).

*Proof*: First note that if $x$ and $y$ are real numbers in the interval $[0,1]$ which sum to unity, then

$$xy \le \frac{1}{4}\ , \tag{46}$$

from which it follows that

$$(\rho_{11})^{1/2}(\rho_{22})^{1/2} \le \frac{1}{2}\ . \tag{47}$$

Furthermore, since, by Eq.(23)

$$N_1^2\ |\lambda|^2 \le N_1(1 - N_1 - N_3) \le N_1(1 - N_1)\ ,$$

we have

$$|\rho_{12}| = N_1|\lambda| \le \frac{1}{2}\ . \tag{48}$$

From Eqs.(47) and (48) we obtain

$$1 - 4|\rho_{12}|^2 \ge 1 - 2|\rho_{12}| \ge 1 - \frac{|\rho_{12}|}{(\rho_{11}\rho_{22})^{1/2}}\ , \tag{49}$$

where the lhs of this inequality is $E^2$ and the rhs is $P_D^2$. Since both $E$ and $P_D$ are non-negative, it follows that

$$E \ge P_D\ . \tag{50}$$

We note that when $E$ is unity, so is $P_D$: that is, perfect distinguishability (in our sense) on the basis of the two-photon state $|\Theta\rangle$ implies perfect distinguishability (in Mandel's sense) on the basis of the density operator. There is an intuitive reason for this agreement: $E = 1$ implies that there is perfect correlation between the behavior of photon 1 and the entrance of photon 2 into $|B\rangle$ or $|B'\rangle$, but perfect correlation requires the orthogonality of $|\chi_1\rangle$ and $|\chi_2\rangle$ in Eq.(18). This orthogonality, in turn, guarantees that the density operator of photon 2 is diagonal in the $|B\rangle, |B'\rangle$ basis.

If we look at the other extreme, however, we find that $P_D = 0$ does not imply that $E = 0$. Again there is an intuitive reason. When $P_D = 0$, then $\rho$ is a pure case, derived from a quantum state of the form

$$|\psi\rangle = c|B\rangle + c'|B'\rangle \ , \tag{51}$$

so that

$$\begin{aligned} \rho_{11} &= |c|^2 \ , \\ \rho_{12} = cc'^*, \ \rho_{21} &= c^*c' \ , \\ \rho_{22} &= |c'|^2 \ , \end{aligned} \tag{52}$$

Then

$$\begin{aligned} E - P_D &= -4|\rho_{12}|^2 + \frac{|\rho_{12}|}{(\rho_{11}\rho_{22})^{1/2}} \ , \\ &= -4|c|^2|c'|^2 + 1 \ , \end{aligned} \tag{53}$$

and this vanishes if and only if $|c|^2 = |c'|^2 = \frac{1}{2}$. But when the amplitudes of $|B\rangle$ and $|B'\rangle$ in the pure state $|\psi\rangle$ are equal, there is no strategy for betting on the path that will yield a net gain on the average. On the other hand, when $|c|^2$ and $|c'|^2$ are unequal, the strategy of betting on the path associated with the larger coefficient will yield a net gain on the average. The advantage of our $E$ over $P_D$ is the ability of the former to take advantage of inequalities in the amplitudes associated with the two paths.

Mandel also relates path distinguishability to the visibility $v_2$ of the interference pattern, where

$$v_2 = 2|\rho_{12}| \ . \tag{54}$$

He obtains the inequality

$$v_2 \leq P_{ID} = 1 - P_D \ , \tag{55}$$

with equality holding only when $\rho_{11} = \rho_{22}$. We obtain from the expressions for $E$ and $v_2$ in Eqs.(45) and (54) the equation

$$v_2 = (1 - E^2)^{1/2} \ , \tag{56}$$

which holds for any preparation of an ensemble of photons in states $|B\rangle$ and $|B'\rangle$ derived from a two-photon state of the form $|\Theta\rangle$. Hence, for the preparation of photon 2 that we have been studying, the visibility $v_2$ is a natural measure of path indistinguishibility.

# 4 Acknowledgments.

We are grateful to Profs. L. Vaidman, M. Horne, S. Goldstein, and L. Mandel for suggestions and encouragement. This research was supported in part by the National Science Foundation under grant no. PHY-90-22345.

# References


[1] References to the authors mentioned in this paragraph and to others are given in "Down Conversion Photon Pairs: A New Chapter in the History of Quantum Mechanical Entanglement," by M. Horne, A. Shimony, and A. Zeilinger, in *Quantum Coherence*, edited by J. Anandan (World Scientific, Singapore, 1990).

[2] M. A. Horne and A. Zeilinger, in *Microphysical Reality and Quantum Formalism*, Proceedings of the conference at Urbino, Italy, Sept. 25-Oct. 3, 1985, edited by A. van der Merwe, F. Selleri, and G. Tarozzi (Kluwer Academic, Dordrecht, 1988).

[3] G. Jaeger, M. A. Horne, and A. Shimony, "Complementarity of one-particle and two-particle interference," *Physical Review A* **48**, 1023 (1993).

[4] L. Mandel, "Coherence and Indistinguishability," in *Optics Letters* **16**, 1882 (1991).

[5] E. Beltrametti and G. Cassinelli, *The Logic of Quantum Mechanics*, Addison-Wesley, Reading, MA (1981), p.56.

[6] J. von Neumann and O. Morgenstern, *Theory of Games and Economic Behavior*, Princeton University Press, Princeton (1953), pp. 84-85, 145-146.

# Further Evidence For the EPNT Assumption

Daniel M. Greenberger
*City College of the City University of New York*
*New York, New York 10031*

Herbert J. Bernstein
*Hampshire College, Amherst, Massachusetts 01002*

Michael Horne
*Stonehill College, North Easton, Massachusetts 02357*

and

Anton Zeilinger
*Institut für Experimentalphysik*
*Universität Innsbruck, A-6020 Innsbruck, Austria*

## ABSTRACT

We recently proved a theorem extending the Greenberger-Horne-Zeilinger (GHZ) Theorem from multi-particle systems to two-particle systems. This proof depended upon an auxiliary assumption, the EPNT assumption (Emptiness of Paths Not Taken). According to this assumption, if there exists an Einstein-Rosen-Podolsky (EPR) element of reality that determines that a path is empty, then there can be no entity associated with the wave that travels this path (pilot-waves, empty waves, etc.) and reports information to the amplitude, when the paths recombine. We produce some further evidence in support of this assumption, which is certainly true in quantum theory. The alternative is that such a pilot-wave theory would have to violate EPR locality.

## INTRODUCTION

Recently, in trying to extend the GHZ (Greenberger-Horne-Zeilinger) Theorem[1,2] down to two-particle systems[3], we produced a proof that we realized depended on a further assumption, which went beyond the EPR (Einstein-Podolsky-Rosen) assumptions[4]. This assumption was the EPNT assumption-- the Emptiness of the Paths Not Taken. This assumption ruled out the possibility of any kind of information-bearing entity traveling down a path, provided one could produce an EPR element of reality connected with the path being empty. The EPR criterion depends on one being able to perform an experiment far away, without in any way affecting any particle that could possibly be travelling down this path. Then if this experiment shows that the path is empty, the path must be truly empty, according to EPR, since one has not interfered in any way with anything along the path. This fact of emptiness is then an "element of reality", because it is true independently of anything an experimenter might later do that might interfere with the path or particles along it.

One might be tempted to think that the EPNT assumption rules out any kind of interference at all, as when a particle passes through a beam splitter, and the two paths are later recombined and interfere. But for a single particle, one cannot produce an element of reality connected with the path, because any measurement on the particle to determine which path it takes will necessarily disturb it. So the EPNT assumption does not apply to one-particle systems. But for a two-particle system, one may make a measurement on one particle that determines which path the second particle takes, and here the EPNT assumption does apply, and it gives results that accord with quantum theory. Further questions concerning the applicability and plausibility of the EPNT assumption are dealt with in Ref. (3). The reason that the assumption is worth exploring in detail is that there are other theories, such as pilot wave theories, that compete with quantum theory and that do depend on inforation-bearing empty waves for their effects. It should also be pointed out that an alternative, complementary approach to this problem, not along the lines of GHZ, has been taken by L. Hardy, who can prove that for a certain percentage of particles in the beam, the GHZ theorem must be true for two particles[5].

## THE SITUATION IN QUANTUM THEORY

One can easily show that within quantum theory if a path is empty, it is truly empty, which means that if the amplitude for a particle to be travelling along a path is zero, then no information can be transmitted along that path. For example, in Fig. (1) we depict a unitary device which takes an incoming wave function that can be along either of the paths 1 or

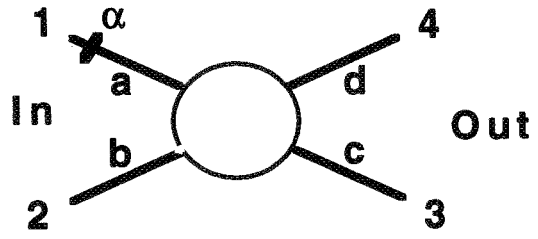


Fig. (1). Unitary Device for a 2-path Amplitude.
The particle enters from the left and exits to the right.
There is a phase shifter of angle $\alpha$ located on path 1.

2, with amplitudes $a$ or $b$ respectively, and converts it into a wave function travelling along the paths 3 and 4, with amplitudes $c$ and $d$ respectively.

Since the device is unitary, its most general form is

$$\begin{pmatrix} c \\ d \end{pmatrix} = e^{i\lambda} \begin{pmatrix} \cos\gamma & e^{i\beta}\sin\gamma \\ -e^{i\delta}\sin\gamma & e^{i(\beta+\delta)}\sin\gamma \end{pmatrix} \begin{pmatrix} a \\ b \end{pmatrix}.$$

If now a phase-shifting device, that shifts the phase by $\alpha$, is placed into beam 1, the incoming beam will change from amplitude $a$ to $ae^{i\alpha}$. An infinitesimal change in $\alpha$ will produce the result in beams 3 and 4,

$$\delta c = e^{i\lambda}\cos\gamma\, a e^{i\alpha} i\,\delta\alpha,$$

$$\delta d = e^{i((\lambda+\delta)}\sin\gamma\, a e^{i\alpha} i\,\delta\alpha.$$

One sees that both of these terms will be zero if $a$ is zero. This result shows that if the beam 1 is empty (i.e., $a$=0), there is no way to transmit any change in $\alpha$ to any amplitude

downstream of beam 1, even if there is a unitary connection between the beams. This result is easily generalized to any number of particles and amplitudes. It shows that according to quantum mechanics, no information can be transmitted through an empty beam. This of course is the essential content of the EPNT assumption.

We are assuming that quantum theory gives correct results and that it is the burden of any alternative theory to reproduce these results. The reason that the discussion cannot stop here is that one might choose not to believe quantum mechanics and say that there are indeed alternative ways to produce the results of the theory without accepting the unitarity and linearity of the theory. We shall show that multi-particle superpositions place a heavy burden on any such theory.

## INFORMATION PASSED ALONG EMPTY BEAMS VIOLATES THE UNCERTAINTY PRINCIPLE

We will now show that if one assumes that a beam is empty, as an EPR element of reality, but one still insists that it can carry information, then if this information can be operationally transmitted to another beam, this information can violate the uncertainty principle.

We shall work out a particular example, but it is obvious that the thrust of the argument is very general. Consider a particle at rest that can decay into two particles, as the one at point O in Fig. (2). The two

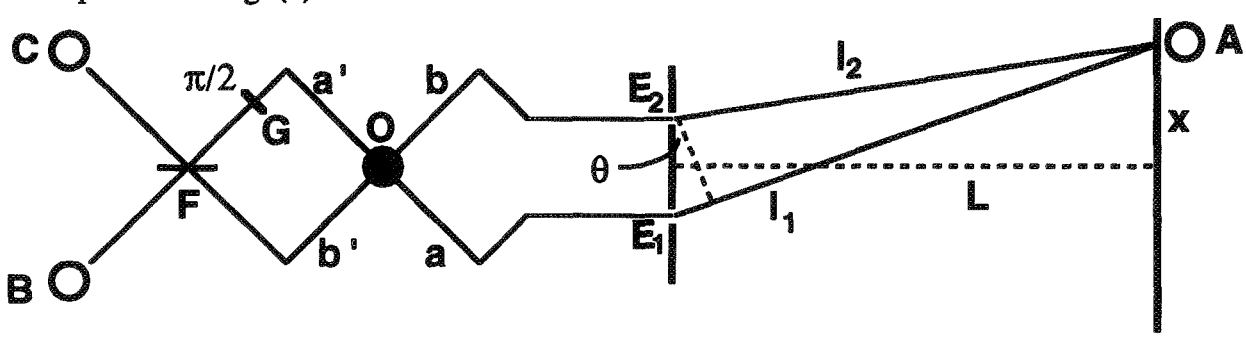


Fig. (2). Two-Slit Experiment With A Two-Particle Interferometer.
An interference pattern is produced by measuring coincidences between detectors A, B, and C.

particles come off in opposite directions, and are restricted by slits to the two sets of directions, *a*-*a'*, and *b*-*b'*. So the state of the system after decay is

$$\psi = \frac{1}{\sqrt{2}}(|aa'\rangle + |bb'\rangle).$$

The primed particle paths are directed through a beam-splitter at F toward the detectors B and C. (We assume, for unitarity, that the reflected ray picks up a $90^{o}$ phase). The paths of the unprimed particle are directed toward a screen with two slits, such that path *a* leads to one slit, $E_1$ while path *b* leads to the other slit, $E_2$. Each of the slits is of width d, and they are separated by a distance D, such that D » d. The diffraction pattern formed at a distance L from the slits is picked up by the detector A. We also assume that L » D, and that the position of A is given by *x*, as measured at L, perpendicularly from the center of the slits (see Fig. (2)).

An important feature of multi-particle beams that applies here should be noted. If the detector A is moved as a function of the distance x, there will be no diffraction pattern

observed, as there will be no single particle interference from this setup. Only if A is monitored in coincidence with the detector B or C will a pattern appear. We shall confirm this below. The reason we have used this two-particle setup to produce diffraction is that we can remove the beam-splitter at F. Then if detector B fires, we know that the particle had taken the path $a'$, and so its partner must have taken the path $a$. Thus this particle must have entered the slit $E_1$ and there will be only a one-particle interference pattern at A, of angular width $\theta \approx \lambda / d$, where we assume for convenience that $\lambda \ll d$. Similarly, if detector C fires, we know the particle must have entered the slit $E_2$ and will also produce a one-particle interference pattern at A. Since we can determine which path and slit the unprimed particle takes, without in any way interfering with the particle, this knowledge is an EPR element of reality. In other words, according to EPR, it is an objective fact. So even if we do not bother to remove the beam-splitter at F, EPR would conclude that the element of reality exists, because we could have removed the beam splitter without affecting the particle, and so the particle actually takes one slit or the other. They would conclude that because the particle takes one path or the other, but quantum theory is powerless to describe this fact, that quantum theory is therefore an incomplete theory.

But of course, according to quantum theory, whether we remove the beam-splitter or not is a crucial fact, one that completely changes the context of the experiment. If we remove it, then indeed the particle is in one path or the other. But if we do not remove it, the particle cannot be described as being in either path.

If we perform the experiment with the beam-splitter in place at F then the wave function $\psi$ becomes (we are also including a $\pi/2$ phase shifter at G, purely for computational convenience)

$$\begin{aligned}\psi &\to \tfrac{1}{\sqrt{2}}\varphi(k_x)\left(ie^{ik\ell_1}|Aa'\rangle + e^{ik\ell_2}|Ab'\rangle\right)\\ &\to \tfrac{1}{2}\varphi(k_x)\left(ie^{ik\ell_1}|A\rangle(|B\rangle + i|C\rangle) + e^{ik\ell_2}|A\rangle(|C\rangle + i|B\rangle)\right)\\ &= \tfrac{1}{2}\varphi(k_x)|A\rangle\left(i(e^{ik\ell_1} + e^{ik\ell_2})|B\rangle + (e^{ik\ell_2} - e^{ik\ell_1})|C\rangle\right).\end{aligned}$$

The probability for coincident counts at A and B, or at A and C is

$$P_{AB} = |\varphi(k_x)|^2 \cos^2 \tfrac{k\Delta\ell}{2}, \quad P_{AC} = |\varphi(k_x)|^2 \sin^2 \tfrac{k\Delta\ell}{2},$$

$$\Delta\ell = \ell_1 - \ell_2.$$

In this equation $\varphi(k_x)$ represents the Fourier Transform of the single slit pattern produced by each of the slits, for which $\theta \approx \lambda / d$, and it is much wider than one of the two-particle pattern maxima, whose width is of order $\theta \approx \lambda / D$. So in fact, in the region of the central maximum where the term $k\Delta\ell/2 \approx \pi D x / L\lambda$ contributes, $\varphi(k_x)$ can be considered to be a constant. (In this region, the minimum $x_m$ of the cosine term occurs when the argument equals $\pi/2$, or $x_m = L\lambda/2D \approx L\theta$, and $\theta \approx \lambda/2D$.) One can experimentally isolate this central maximum from the others, and since both slits contribute to it, one has $\Delta x \approx D$, while $\Delta p_x \approx p\theta \approx p\lambda / D \approx \hbar / D$. Thus this central maximum is of the order of a minimum uncertainty packet. Note also that if one only triggers the detector A, ignoring the detectors B and C, one will get a number of counts independent of the path difference $\Delta\ell$ between the beams, $P_A = P_{AB} + P_{AC} = const.$, which proves our original assertion that one must count coincidences to see the interference pattern in this experiment.

For the case when one removes the beam-splitter, one has only the top equation above for $\psi$,

$$\psi \rightarrow \tfrac{1}{\sqrt{2}}\varphi(k_x)\left(ie^{ik\ell_1}|Aa'\rangle + e^{ik\ell_2}|Ab'\rangle\right)$$

If then counter B fires in coincidence with A, one knows that the unprimed particle is in the beam $a'$ and similarly if counter C fires it is in beam $b'$, and so the coincidence counting rates will be $P_{AB} = \frac{1}{2}|\varphi(k)|^2$, $P_{AC} = \frac{1}{2}|\varphi(k)|^2$, which will be a constant on the scale of the two-particle pattern, but will fall off as $\theta \approx \lambda/d$. This is consistent with the uncertainty principle, since in this case, the particle is going only through one slit, so that $\Delta x \sim d, \Delta p \sim p\theta \sim \hbar/d$.

Now we come to the point of the argument. What if one were to believe that in the case of an ordinary single-particle two-slit experiment, when one can detect into which slit the particle enters one will obtain single slit patterns, as quantum theory predicts? But when one does not know which slit the particle enters there is some kind of information-bearing pilot wave that carries the information about the second slit, so that even though the particle travels through one slit only, nonetheless it is aware of the existence of the second slit through the intermediary of the pilot wave, and so one gets a two-slit diffraction pattern. It is for this case that we have devised our experiment above. For we can produce the EPR element of reality needed to prove the particle takes only one beam, by removing the beam-splitter. However if one believes that the element of reality persists when one does not remove the beam splitter, and also that a pilot wave of some sort carries information about the second slit, so that the diffraction pattern can occur, we believe that this leads to a contradiction in our experiment.

In our experiment, if one accepts another principle of EPR, that of locality, then one must accept the fact that the unprimed particle receives no information that can tell it whether in fact the beam splitter at F has been removed or not. So there is no way for the particle to know how to evaluate the information obtained from the pilot wave. Does it lead to a diffraction pattern or not? In an ordinary one-particle experiment, there is no way to observe that the particle has actually taken one slit or the other. But in our experiment, we can provide that information without disturbing the particle approaching the slit. According to the EPNT assumption, when one of the paths is truly empty in the EPR sense, there can be no information transmitted along the other path. The negation of this assumption implies that some information *can* be carried along this other path. If this is so, are there any experimental implications of this? If not, it is merely an idle statement.

The way to exploit these facts is to assume that the beam-splitter is present, but that there is another detector present, in beam $b'$. This detector will fire if the particle takes beam $b'$. If it does *not* fire, then we know that the particle is in beam $a$-$a'$. But there will be an empty wave in beam $b$-$b'$. Since the detector has not fired, the empty wave will presumably pass along to the beam splitter at F. Does it share any of its information with the other beam? To decide this, we assume that there is some parameter $\beta$ that determines how much information the pilot wave carries along one beam when it is known that the particle takes the other beam, through the other slit. In that case, the particle will produce a coincidence count probability for the counters A and B to fire,

$$P \propto \tfrac{1}{4}|\varphi(k_x)|^2\left|e^{ik\ell_1} + \beta e^{ik\ell_2}\right|^2,$$

where $\beta$ varies between 0 and 1.

This would lead to a diffraction pattern with a contrast of $C = 2\beta/(1+\beta^2)$. Not only would this disagree with quantum theory, but also with the uncertainty principle directly, since then $(\Delta p)^2 \sim \left[\beta^2(\hbar/D)^2 + (1-\beta^2)(\hbar/d)^2\right]$, while $(\Delta x)^2 \sim d^2$, since one knows which slit the particle actually took. For finite $\beta$, this violates the uncertainty

principle, giving in the limit of $\beta \rightarrow 1$ the result $\Delta x \Delta p \rightarrow \hbar d / D \ll \hbar$. The alternative is that the theory must violate EPR locality.

## THE IMPOSSIBILITY OF PILOT WAVES IN A THREE-PARTICLE SYSTEM

The argument supporting the EPNT assumption in a three-particle system is even stronger than for two particles. Again we shall work out a special example, but the results are generalizable. Consider a particle that decays into three particles. If the particles are of the same mass, and when they are counted, it is checked that each has the same energy, then they will come off at 120° apart. They are now restricted by slits to three sets of directions, *a-a'-a"*, *b-b'-b"*, and *c-c'-c"*. (Particle 1 is unprimed, particle 2 is primed, and particle 3 is double-primed. If particle 1 takes path *a*, then 2 must take path *a'*, and 3 takes path *a"*, etc.) (See Fig. (3)). This is a simple generalization of the two-particle process in

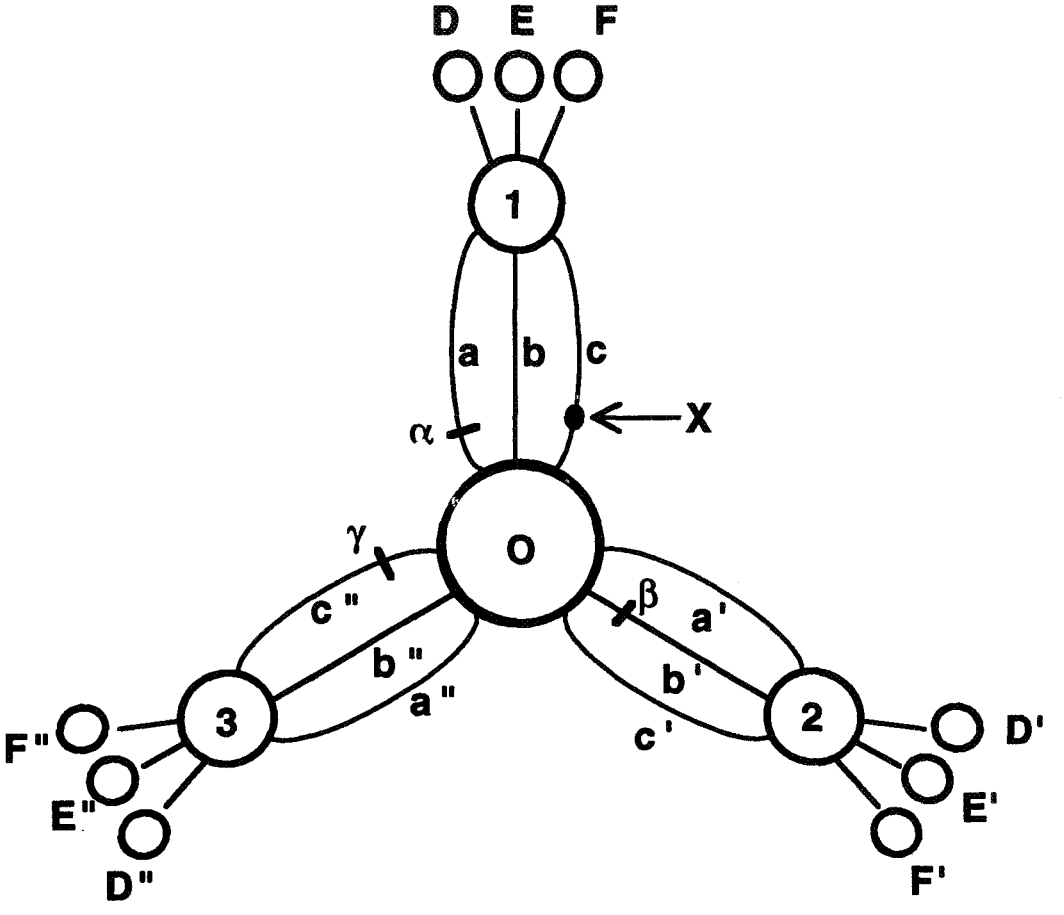


Fig. (3). A Three-Particle Interferometer With Three Tritters.
A particle at O decays into three particles which take the possible paths *a-a'-a"*, *b-b'-b"*, or *c-c'-c"*. The three paths for each particle converge at a tritter, and then pass to one of three detectors. Each particle has one phase shifter in one path, $\alpha, \beta$, or $\gamma$. In the second part of the experiment, a detector is placed at X to determine whether the particles have taken the paths *c-c'-c"*.

the previous example. Each particle is now refocussed into a unitary 3-way beam-splitter. (We have previously called such devices "multi-ports", or "critters", and in particular, a 3-way device is a "tritter"[6]. Such devices can emulate an arbitrary unitary transformation of the system.) For simplicity, our particular tritter is taken to have a specific unitary transformation (see Fig. (4)). If the beams

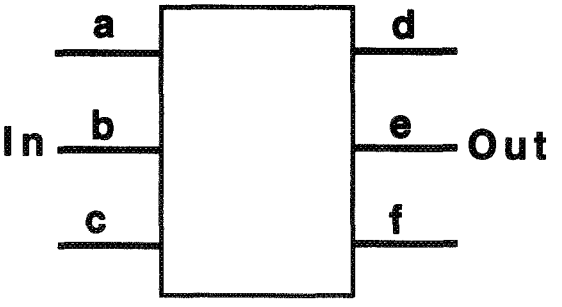


Fig. (4). A Three-Particle Unitary Device.
We call this device a "tritter". The three input beams a, b, c, are transformed unitarily into the output beams d, e, f.

a, b, c, are the incident beams, and d, e, f, are the outgoing beams, they will be related by the relations

$$|a\rangle \rightarrow \tfrac{1}{\sqrt{3}}(|d\rangle + |e\rangle + |f\rangle),$$

$$|b\rangle \rightarrow \tfrac{1}{\sqrt{3}}(|d\rangle + \lambda|e\rangle + \mu|f\rangle),$$

$$|c\rangle \rightarrow \tfrac{1}{\sqrt{3}}(|d\rangle + \mu|e\rangle + \lambda|f\rangle),$$

where 1, $\lambda = e^{2\pi i/3}$, and $\mu = e^{4\pi i/3}$ are the cube roots of unity, and

$$\mu^2 = \lambda, \lambda^2 = \mu, \lambda\mu = 1,$$

$$\mu^* = \lambda, \lambda^* = \mu, 1 + \lambda + \mu = 0.$$

The actual setup is as shown in Fig. (3). There is a tritter in the path of each particle. There is also a phase shifter, of phase $\alpha$ in beam $a$,one of phase $\beta$ in beam $b'$, and one of phase $\gamma$ in beam $c''$. The initial wave function of the three particles is

$$\psi = \tfrac{1}{\sqrt{3}}(e^{i\alpha}|aa'a''\rangle + e^{i\beta}|bb'b''\rangle + e^{i\gamma}|cc'c''\rangle).$$

Each of the tritter outputs goes to a detector, labelled D, E, F, for particle 1, and similarly, with primes, for the other particles. The amplitude after passing through the tritters and reaching the detectors is

$$\psi \rightarrow \tfrac{1}{9}\big[e^{i\alpha}(|D\rangle + |E\rangle + |F\rangle)(|D'\rangle + |E'\rangle + |F'\rangle)(|D''\rangle + |E''\rangle + |F''\rangle)$$

$$+e^{i\beta}(|D\rangle + \lambda|E\rangle + \mu|F\rangle)(|D'\rangle + \lambda|E'\rangle + \mu|F'\rangle)(|D''\rangle + \lambda|E''\rangle + \mu|F''\rangle)$$

$$+e^{i\gamma}(|D\rangle + \mu|E\rangle + \lambda|F\rangle)(|D'\rangle + \mu|E'\rangle + \lambda|F'\rangle)(|D''\rangle + \mu|E''\rangle + \lambda|F''\rangle)\big].$$

From this one can calculate the output to any set of detectors.

Rather than write down all possible outputs explicitly, we shall merely as an example write down all those that involve the counters D and D', namely DD'D", DD'E", and DD'F". They are

$$\psi \to \tfrac{1}{9}\left[(e^{i\alpha}+e^{i\beta}+e^{i\gamma})|DD'D''\rangle+(e^{i\alpha}+\lambda e^{i\beta}+\mu e^{i\gamma})|DD'E''\rangle+(e^{i\alpha}+\mu e^{i\beta}+\lambda e^{i\gamma})|DD'D''\rangle\right]$$

$+etc.$

So for example, the probability of counting a coincidence in the detectors DD'D" is

$$P_{DD'D''}=\tfrac{1}{81}(3+2\cos(\alpha-\beta)+2\cos(\beta-\gamma)+2\cos(\gamma-\alpha)).$$

The significant point here is that the counting rate associated with this set of coincidence counts depends symmetrically on the three phase shifts $\alpha,\beta,\gamma$.

As with the two-particle case, only coincidences between all three counters will lead to a diffraction pattern of counting. If one looks at only two detectors (or one), one will find a flat rate. For example, if one adds the rates (amplitudes squared) for the three counts given above, one will get for the probability of a count in DD',

$$P_{DD'}=P_{DD'D''}+P_{DD'E''}+P_{DD'F''}=const.$$

Now assume that a detector is placed into the beam $c$ at point X, so that if it fires, one knows that the first particle has taken this path, and therefore that particle 2 took path $c'$, and particle 3 took path $c''$.This establishes the path as an EPR element of reality, as one can determine the path of two of the particles by intercepting the third one. Thus in this experiment, the EPNT assumption applies and says that if a particular path is empty, then there is no entity associated with this path that can carry information through the system if the paths later happen to rejoin.

We shall be interested in the case where the detector is installed at X, but it does not fire. In this case, one knows that the particle is *not* located along the paths $c$-$c'$-$c''$. In other words, this set of paths is empty. Because the phase shifter $\gamma$ is located in the path $c''$, the EPNT theorem would predict that when the counter X does not fire, the counting rate for coincidences cannot depend upon the angle $\gamma$. The counter X will fire 1/3 of the time. If we keep the same normalization as before, so that the total probability for events in which X does not fire is 2/3, then the wave function reaching the set of tritters is

$$\psi_X=\tfrac{1}{\sqrt{3}}(e^{i\alpha}|aa'a''\rangle+e^{i\beta}|bb'b''\rangle).$$

Thus we see already that, quantum mechanically, it cannot depend on $\gamma$. The wave function reaching the counters will be

$$\psi_X \to \tfrac{1}{9}\left[e^{i\alpha}(|D\rangle+|E\rangle+|F\rangle)(|D'\rangle+|E'\rangle+|F'\rangle)(|D''\rangle+|E''\rangle+|F''\rangle)\right.$$

$$\left.+e^{i\beta}(|D\rangle+\lambda|E\rangle+\mu|F\rangle)(|D'\rangle+\lambda|E'\rangle+\mu|F'\rangle)(|D''\rangle+\lambda|E''\rangle+\mu|F''\rangle)\right].$$

Now the probability for a coincidence in DD'D" will be

$$\psi_X \to \tfrac{1}{9}\left[(e^{i\alpha}+e^{i\beta})|DD'D''\rangle+etc.\right],$$

$$P_{X,DD'D''}=\tfrac{2}{81}(1+\cos(\alpha-\beta)).$$

Not only is this independent of $\gamma$ but by a suitable choice of angles, one can make the result either greater or less than the result when the detector X was absent. For example, when $\alpha=\beta$, then $P_{X,DD'D''}=\tfrac{4}{81}$, while if $\gamma=\alpha=\beta$, then $P_{DD'D''}=\tfrac{8}{81}$; but if $\alpha=\beta=\gamma+\pi$, then $P_{DD'D''}=\tfrac{1}{81}$.

So, because there exists an element of reality connected with the fact that the path containing $\gamma$ is empty, this probability no longer depends on $\gamma$. However, if one looks at Fig. (4), one sees that the phase shifter $\gamma$ lies in the beam $c''$, while the detector X lies in the beam $c$. So according to EPR locality, there is no way in which particle 3, on one of the double-primed paths, could be made aware of whether the counter X has fired or not, or even whether it is present or not. Thus if there existed a pilot wave that sampled the

double-primed paths, there is no way in which it can have been notified to change the nature of the information it passes to the other beams when it reaches the tritter. In fact, the only difference between the cases when the detector X is present or not, is that now there is a label attached to the particle expressing the EPR element that the actual path of the particle excludes $c''$. And the existence of this element also must be responsible for the fact that the resulting count rate no longer depends upon $\gamma$. Similarly, the unprimed particle, one of whose paths contains the detector X, has no knowledge of $\gamma$ at all, and neither does the primed particle. So everything connected with this experiment can be explained by the EPNT assumption, but appears to be extremely implausible if one accepts EPR locality, and relies on a pilot wave type of explanation. Of course, if one drops EPR locality, one can use the Bohm-Hiley theory[7] to explain these events, as it is equivalent to quantum theory, and non-local.

We believe that if one accepts that pilot waves can exist in a local theory, then one necessarily will produce effects that violate quantum theory. The alternative EPNT assumption rules out such effects, even in two-particle systems, and is consistent with quantum theory.

## REFERENCES


1. D. M. Greenberger, M. A. Horne, and A. Zeilinger, *Bell's Theorem, Quantum Theory, and Conceptions of the Universe* M. Katafos, ed., Kluwer Academic, Dordrecht, 1989.
2. D. M. Greenberger, M. A. Horne, A. Shimony, and A. Zeilinger, Amer. J. Physics **58**, (1990) 1131.
3. H. Bernstein, D. M. Greenberger, M. A. Horne, and A. Zeilinger, Phys. Rev. **A47**, (1993), 78 .
4. A. Einstein, B. Podolsky, and N. Rosen, Phys. Rev. **47**, (1935), 777-780. We shall refer to this paper as EPR. It is reprinted in J. A. Wheeler and W. H. Zurek, *Quantum measurement Theory* Princeton U. P., Princeton, 1983.
5. L. Hardy, Phys. Lett. **A161**, (1992) 326.
6. A. Zeilinger, H. J. Bernstein, D. M. Greenberger, M. A. Horne, and M. Zukowski, in Proc. of *Fourth International Symposium of Foundations of Quantum Mechanics in the Light of New Technology*, H. Ezawa, Y. Murayama, *et al*, eds., World Scientific, Singapore, 1993.
7. This theory is discussed in great detail in D. Bohm and B. J. Hiley, *The Undivided Universe*, Routledge, London, 1993.

# THE PHOTON: EXPERIMENTAL EMPHASIS ON ITS WAVE-PARTICLE DUALITY

Y. H. Shih, A. V. Sergienko and M. H. Rubin
*Department of Physics, University of Maryland Baltimore County, Baltimore, MD 21228*

T. E. Kiess, C. O. Alley
*Department of Physics, University of Maryland, College Park, MD 20742*

**Abstract**

Two types of Einstein-Podolsky-Rosen experiments were demonstrated recently in our laboratory. It is interesting to see that in an interference experiment (wave-like experiment) the photon exhibits its particle property, and in a beam-splitting experiment (particle-like experiment) the photon exhibits its wave property. The two-photon states are produced from Type I and Type II optical spontaneous parametric down conversion, respectively.

We wish to report two EPR [1] type experiments. The first one is a two-photon interference experiment in a standard Mach-Zehnder interferometer. Another one is a two-photon beam-splitting type experiment for the measurement of polarization correlation. It is interesting to see that in the interference experiment (wave-like experiment) the photon exhibits its particle property, and in the beam-splitting experiment (particle-like experiment) the photon exhibits its wave property.

## I Two-photon interference in a standard Mach-Zehnder interferometer.

A pair of photons with different colors ( $\lambda_1 = 632.8\ nm, \lambda_2 = 788.7\ nm, 155.9nm$ difference in center wavelength) is directed to one input port of a Mach-Zehnder interferometer. Coincidence

measurement is made between the two output ports of the interferometer with the help of a 300 psec coincidence time window. The interference behavior was studied in a wide range of the optical path difference of the interferometer from white light condition, $\Delta L \cong 0$, to about $\Delta L \cong 127cm$ ($\cong 2 \cdot 10^3$ times the coherence length of the down converted beams). When the optical delay of the interferometer is greater than the coincidence time window, the amplitudes in which one photon follows the longer arm and the other follows the shorter arm of the interferometer are "cut off" by the coincidence time window. The particle property of the photon is demonstrated by means of more than 50% interference visibility.

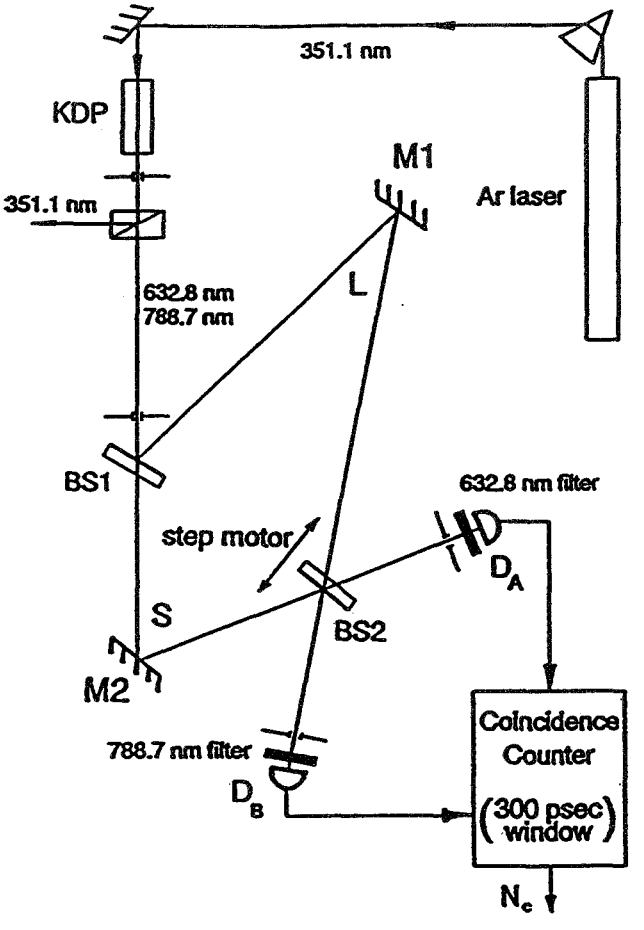


Figure I-1: Schematic diagram of the experiment.

The experimental arrangement is shown in fig. I-1. A $10cm$ long Type I phase matching KDP crystal pumped by a single mode $351.1nm$ CW Argon ion laser line is used to generate collinear photon pairs at wavelengths $632.8nm$ and $788.7nm$. The coherence length of the pump beam was measured to be longer than $5m$. The $351.1nm$ pump beam and the down converted beams were polarized in the extraordinary and ordinary ray directions of the crystal, respectively. A Glan-Thompson prism was used to separate the collinear down converted photon beams from the orthogonal polarized $351.1nm$ pump beam. Before the $351.1nm$ laser line was sent to pump the parametric down conversion, a quartz dispersion prism was used to separate out the radiation

lines of the laser plasma tube which are close to the $632.8nm$ and $788.7nm$ wavelengths.

The collinear $632.8nm$ and $788.7nm$ photon pair was then injected into a standard Mach-Zehnder interferometer. The optical path differences of the interferometer $\Delta L = L - S$ can be arranged to be shorter or longer than the coherence length, $l_{coh}$, of each beam of the down conversion field and the coincidence time window, $c \cdot \Delta T_{coin}$. The collinear photon pairs were injected onto the beamsplitter with an incident angle of about ten to twelve degrees (near normal), for which the reflected and transmitted intensities of the $632.8nm$ and $788.7nm$ beams were measured to be equal $(50\% - 50\%)$ within 5%.

Geiger mode avalanche photodiode detectors, operated at dry ice temperature, were used to record coincidences in the two output ports of the Mach-Zehnder interferometer. Each of the detector has a narrow band interference spectral filters. The central wavelengths of the filters are $632.8nm$ and $788.8nm$ with bandwidths of $1.4nm$ and $1.7nm$, respectively. The output pulses from detector A and detector $B$ were then sent to $N_1, N_2$ counter and a coincidence circuit to record coincidences. The coincidence time window $\Delta T_{coin}$ was about $300psec$.

We collected data for three regions of interest. In the first region, $\Delta L < l_{coh}$, i.e., the optical paths difference of the interferometer are equal to within the first order coherence length of the signal and idler. In the second region, $l_{coh} < \Delta L < c \cdot \Delta T_{coin}$. In the third region, $\Delta L > c \cdot \Delta T_{coin}$. The following reported data are all direct measured values without any noise reductions or theoretical corrections.

(1). The first region, $\Delta L < l_{coh}$.

Fig. I-2 shows the normalized counting rate of $N_c$ when the optical path difference changed from white light condition to about $4\mu m$. In this region, $N_1$ and $N_2$ both showed clear single wavelength, $632.8nm$ and $788.7nm$, respectively, first order interference pattern. However, $N_c$ shows a complecated interference pattern with $632.8nm, 788.7nm$, and the beating and the sum frequencies. The interference visibility is close to 100% with the $300psec$ coincidence window. The solid curve in fig. I-2 is a theoretical fitting of equation (I-10). Fig. I-3 shows a typical first order interference pattern of $N_2$ for detector B. The interference visibility is about 90%, with a period corresponding to wavelength $788.7nm$.

Fig. I-4 shows the typical interference patterns of $N_c$ at $\Delta L \cong 115\mu m$. The $N_c$ pattern in fig. I-4 is different than that in fig. I-2 in two ways, (A) the interference visibility is reduced and, (B) the beating component and the $632.8nm$ and $788.7nm$ components of the modulations are reduced and the sum-frequency modulation becomes predominant. The solid line in fig. I-4 is a theoretical curve resulting from Gaussian spectral filter functions in equation (I-10). The single detector counting rate is reported in fig. I-5. The interference visibility is reduced to about 42%.

(2). The second region, $l_{coh} < \Delta L < c \cdot \Delta T_{coin}$.

In this region both $N_1$ and $N_2$ become constant, however, $N_c$ shows clear interference with the sum frequency. Fig. I-6 shows the interference pattern of $N_c$ for $\Delta L \cong 0.5cm$. Compare to the 300 psec coincidence time window and the coherent length of the down converted beams, which satisfying $l_{coh} < \Delta L < c \cdot \Delta T_{coin}$. The interference visibility is $44\% \pm 3\%$ with modulation at a wavelength of $351.1nm$. In this region, all the measured interference patterns have modulation visibilities close to but less then 50%.

(3). The third region,$\Delta L > c \cdot \Delta T_{coin}$.

The interference patterns of $N_c$ in the final region of interest, $\Delta L > c \cdot \Delta T_{coin}$, is presented in fig. I-7. An interference visibility of $75\% \pm 3\%$ was measured at $\Delta L \cong 43cm$ with an interference

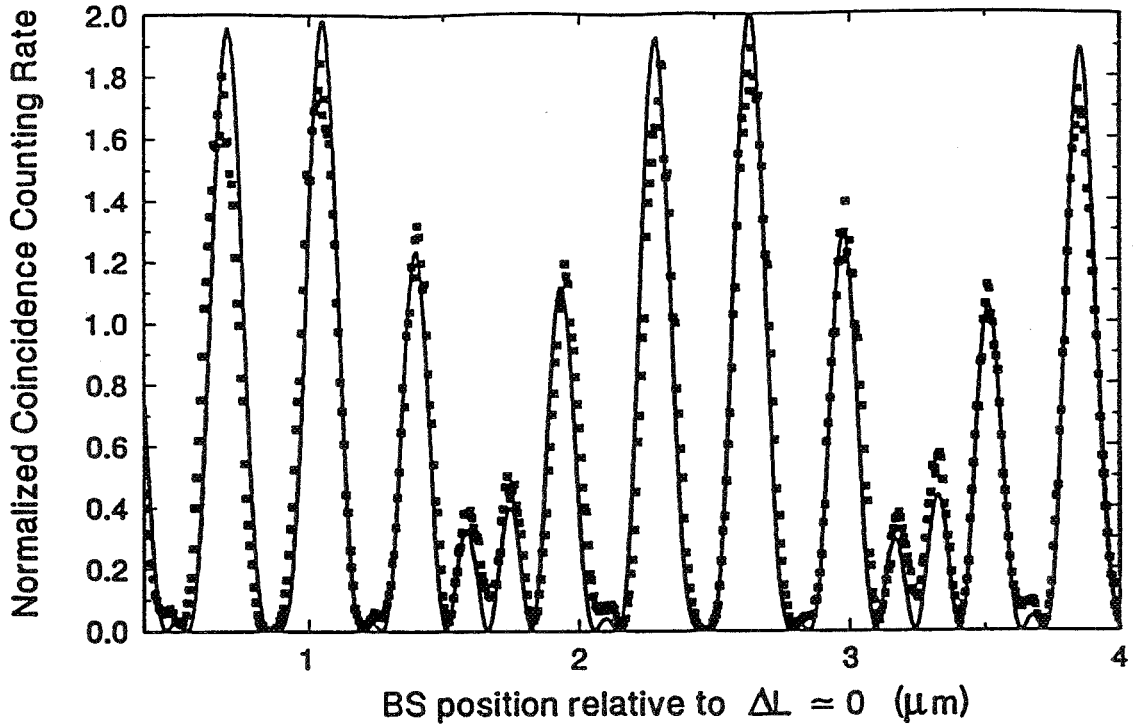


Figure I-2: Normalized coincidence counting rate of $N_c$at near white light condition ($\Delta L \cong 0$). The beting frequency,with $3.2\mu m$period, and sum frequency, with $351.1nm$period, are evident from the graph. Signal and idler frequencies, at periods $632.8nm$ and $788.7nm$ also contribute. The solid line is a theoretical curve of Eq. (I-10).

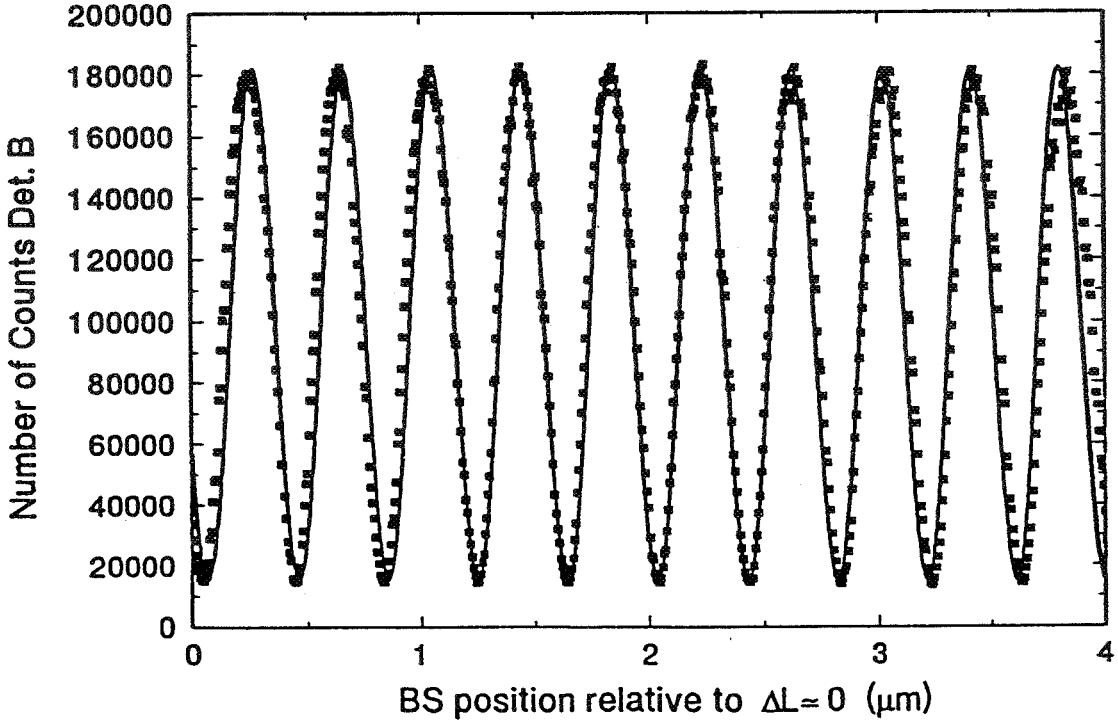


Figure I-3: Single detector counting rate $N_2$ at near white light condition ($\Delta L \cong 0$).

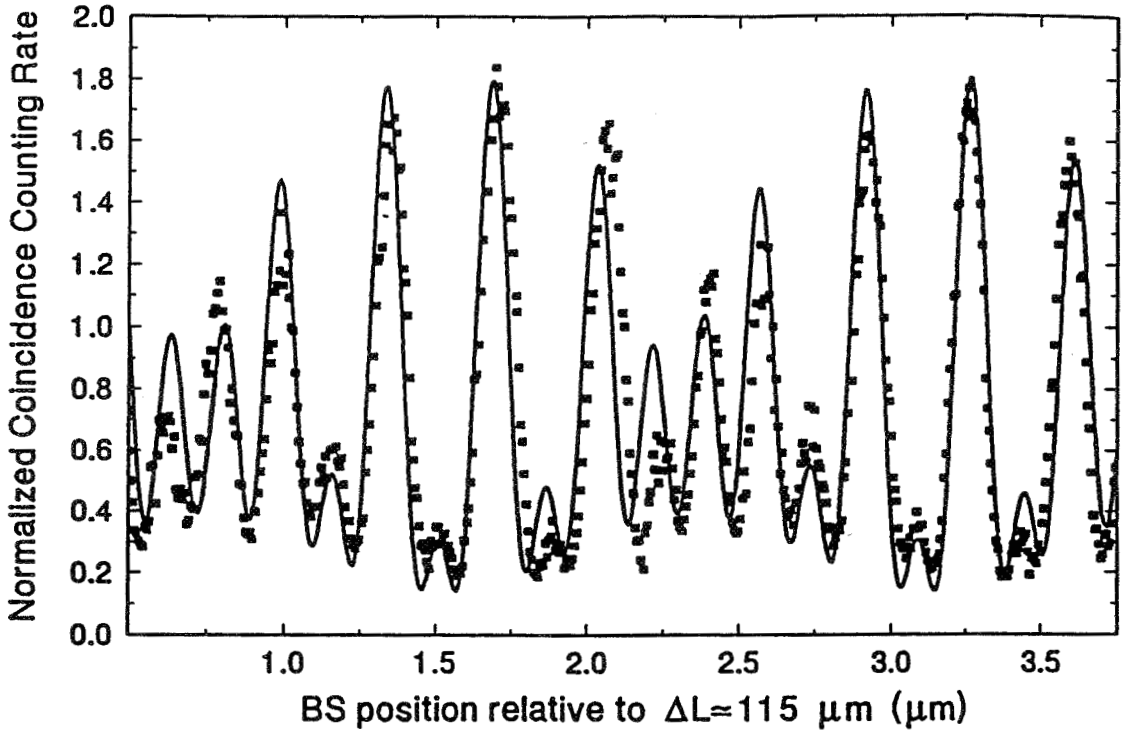


Figure I-4: Normalized coincidence counting rate of $N_c$ at $\Delta L \cong 115\ \mu m$. Compared with fig. I-2, the beating component and the $\omega_1$ and $\omega_2$ components of the modulation are reduced and the sum-frequency modulation becomes predominant. The solid line is a theoretical curve resulting from Gaussian spectral distributions in Eq. (I-10).

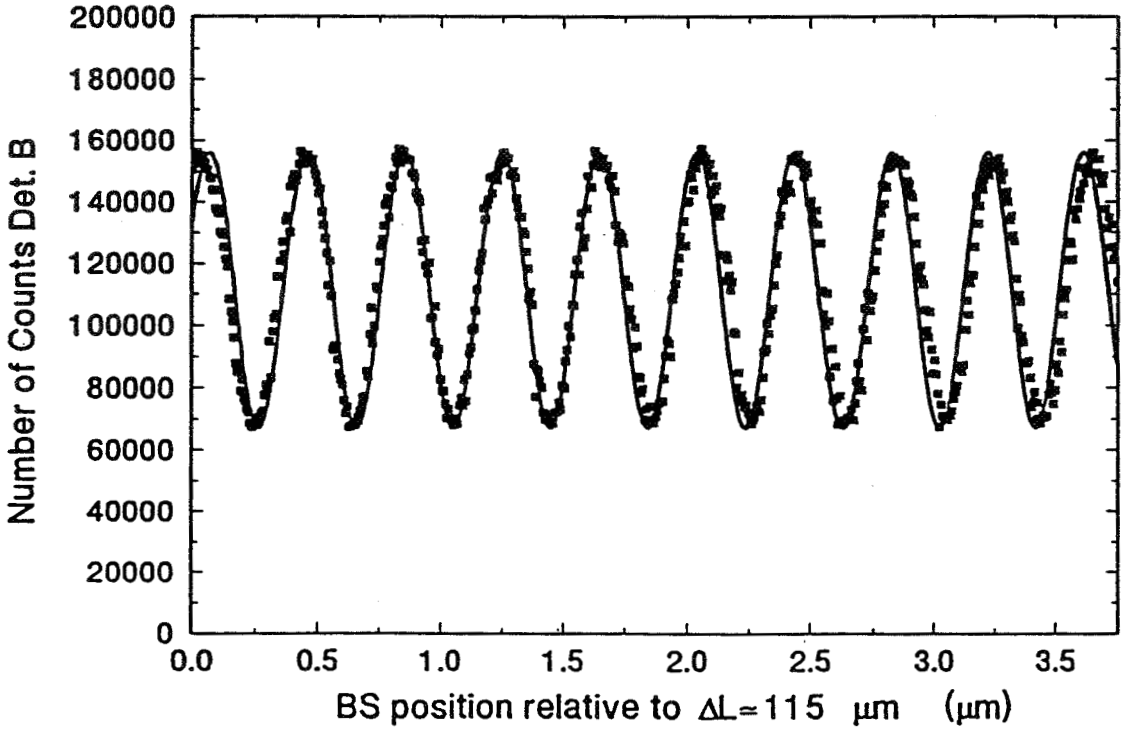


Figure I-5: Single detector counting rate $N_2$ at $\Delta L \cong 115\ \mu m$.

period of $351.1nm$. When $\Delta L$ increased to about $127cm$, the interference visibility was measured to be $56\% \pm 3\%$. In this region, no interference modulations were found for $N_1$ and $N_2$.

In our earlier paper [2] a general theory for a two photon interference experiment in two interferometers was developed. The experiment was suggested by Franson [3]. Experimental study for two independent interferometers have demonstrated more than 50% interference visibility by using short time coincidence time windows [4, 5]. The theory for this experiment is similar. The coincidence counting rate is calculated from the field fourth order correlation function:

$$G(r_1t_2, r_2t_2; r_2t_2, r_1t_1) =< E_1^{(-)}E_2^{(-)}E_2^{(+)}E_1^{(+)} > \qquad (\mathrm{I}-1)$$

where $E_j^{(+)}$ is the positive frequency part of the electric field in the Heisenberg picture evaluated at the position $r_j$ and the time $t_j$. $E_j^{(-)}$ is the hermitian conjugate of $E_j^{(+)}$,

$$E_j^{(+)}(t_j) = \int d\omega f_j(\omega)e^{-i\omega t}a_j(\omega) \qquad (\mathrm{I}-2)$$

$a_j$ is the destruction operator of the photons in the jth beam and $f_j$ is the pass band of the filter in the beam peaked at $\Omega_j$. We take $\Omega_1 + \Omega_2 = \omega_p$, the pump frequency. In this experiment the filters are chosen so that each detector only detects one of the down converted beam, i.e., $\Omega_1 - \Omega_2 >> \sigma$ the band width of the filters.

The average coincidence counting rate is given by

$$\begin{aligned} R_c &= \tfrac{1}{T}\iint_0^T dt_1dt_2G(r_1t_1, r_2t_2, r_2t_2, r_1t_1)S(t_1 - t_2, \Delta T_{coin}) \\ &= \tfrac{1}{T}\iint_0^T dt_1dt_2 \mid \langle 0 \mid E_1^{(+)}(t_1), E_2^{(+)}(t_2) \mid \Psi\rangle \mid^2 S(t_1 - t_2, \Delta T_{coin}) \end{aligned} \qquad (\mathrm{I}-3)$$

where $S(t, \Delta T_{coin})$ is a coincidence detection function, $\Delta T_{coin}$ is the coincidence time window, and the integrals are over the detection time T. A two photon amplitude, which is also called effective two-photon wavefunction, is defined in (I-3) by,

$$\Psi(t_1, t_2) =< 0 \mid E_1^{(+)}(t_1)E_2^{(+)}(t_2) \mid \Psi > \qquad (\mathrm{I}-4)$$

The two photon part of the state that emerging from the down conversion crystal may be taken to be [6],

$$\mid \Psi >= \iint d\omega_1 d\omega_2 \delta(\omega_1 + \omega_2 - \omega_p)a_1^\dagger(\omega_1)a_2^\dagger(\omega_2) \mid 0 > \qquad (\mathrm{I}-5)$$

where the $\delta$ function indicate a perfect frequency phase matching condition. The wave number phase matching condition is implicit in the choice of the location of the pinholes and the detectors. Substitute (I-4) and (I-5) into (I-3), it is straight forward to show that,

$$\Psi(t_1, t_2) = A(t_1, t_2) + A(t_1 - \Delta T, t_2 - \Delta T) + A(t_1, t_2 - \Delta T) + A(t_1 - \Delta T, t_2) \qquad (\mathrm{I}-6)$$

where $A(t_1, t_2)$ is calculated in (I-8), $\Delta L = c \cdot \Delta T$ is the optical path difference in the two arms of the interferometer. The first (second) term is the amplitude for which both photons follow the short (long) path through the interferometer, and the third (fourth) term is the amplitude for one photon follows the short (long) path and another photon follows the long (short) path. A simple calculation using Gaussian filters

$$f_j = \exp[-(\omega - \Omega_j)^2/2\sigma_j^2] \qquad (\mathrm{I}-7)$$

where $\sigma_j$ is the bandwidth of the jth filter, gives

$$A(t_1,t_2) = \exp[-i(\Omega_1 t_1 + \Omega_2 t_2)]u(t_1 - t_2)$$
$$u(t) = K\exp[-\Sigma^2 t^2/2]; 1/\Sigma^2 = 1/\sigma_1^2 + 1/\sigma_2^2 \qquad (I-8)$$

where $K$ is a constant.

If we now substitute equations (I-6) and (I-7) into (I-3) and take

$$S(t,\Delta T_{coin}) = \exp(-\mid t \mid /2\Delta T_{coin}) \qquad (I-9)$$

the average counting rate may be written in the form

$$R_c = R_0[J_0 + J_1\cos(\Omega_1\Delta T) + J_1\cos(\Omega_2\Delta T) +$$
$$J_+\cos(\Omega_1\Delta T - \Omega_2\Delta T) + J_-\cos(\Omega_1\Delta T + \Omega_2\Delta T) \qquad (I-10)$$

where

$$J_0 = C[2erfc(\Lambda) + \exp(-\Delta T/2\Delta T_{coin})erfc(\Lambda + \Sigma\Delta T/2)$$
$$+\exp(-\Delta T/2\Delta T_{coin})erfc(\Lambda - \Sigma\Delta T/2)$$
$$J_1 = 2C\exp(-\Sigma^2\Delta T^2/4)[\exp(-\Delta T/4\Delta T_{coin})erfc(\Lambda + \Sigma\Delta T/2)$$
$$+\exp(-\Delta T/4\Delta T_{coin})erfc(\Lambda - \Sigma\Delta T/2) \qquad (I-11)$$
$$J_+ = 2C\exp(-\Sigma^2\Delta T^2)erfc(\Lambda/2)$$
$$J_- = 2Cerfc(\Lambda)$$

where $\Lambda = 1/(4\Sigma\Delta T_{coin})$, $C$ is a constant that need not concern us. We remind the reader that the error function $erfc(x) \Rightarrow 0$ as $x \Rightarrow \infty$ and $erfc(x) \Rightarrow 2$ as $x \Rightarrow -\infty$. The key point to understand the behavior of the coincidence counting modulation is the variation of the J's with the increase of $\Delta T = \Delta L/c$.

(1). For $\Delta L < l_{coh}$, $J_0 = J_1 = 2J_+ = 2J_-$. From (I-10), the coincidence counting rate $R_c$ has oscillations at $\omega_1, \omega_2$, and their sum and difference frequencies. The visibility is 100% in this case. As is seen in fig. I-2. As $\Delta L$ increases $J_1$ and $J_+$ rapidly decrease becoming negligible when $\Delta L$ is approaching $l_{coh}$, the coherence length of the down converted beam. This can be seen in fig. I-4, when $\Delta L = 115\mu m$ which is about one half of the coherence length $l_{coh}$, the beating component and the $632.8nm$ and $788.7nm$ components of the modulations are reduced and the sum-frequency modulation becomes predominant.

(2). $l_{coh} < \Delta L < c \cdot \Delta T_{coin}$, as $\Delta L$ increases to be greater than $l_{coh}$ both $J_1$ and $J_+$ are zero and we left with

$$R_c = R_0[J_0 + J_-\cos(\Omega_p\Delta T)] \qquad (I-12)$$

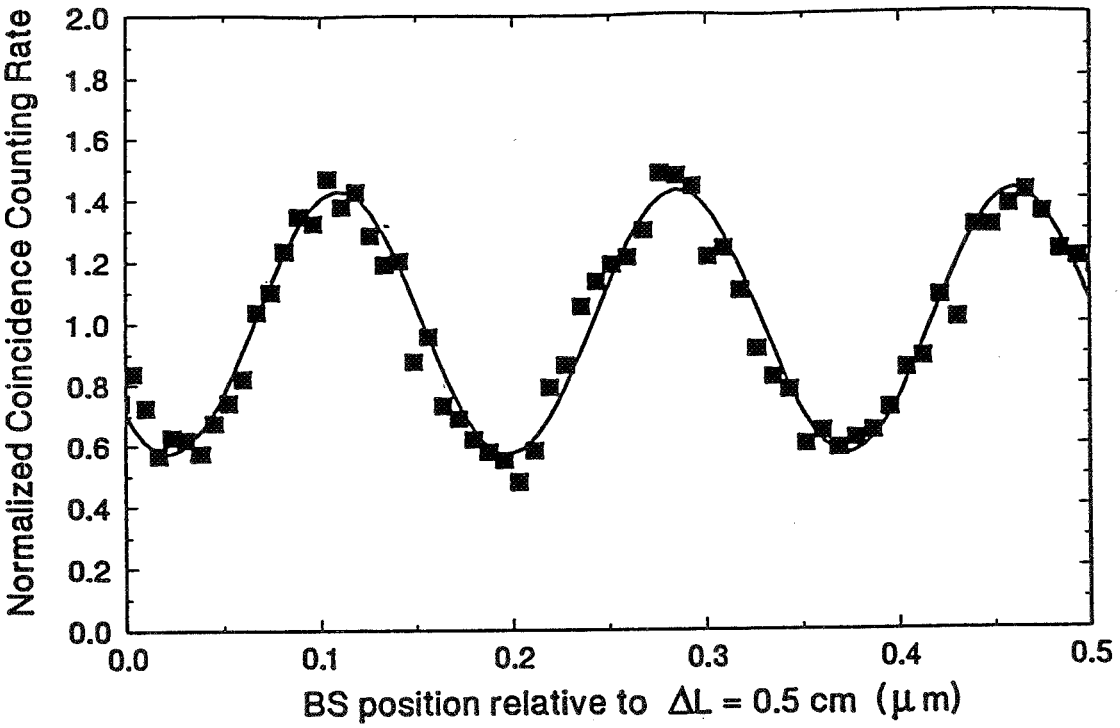


Figure I-6: Normalized coincidence counting rate of $N_c$ at $\Delta L \cong 0.5\ cm$ for a $\Delta T_{coin} = 300psec$ time window. The beating modulation and the $\omega_1$and $\omega_2$ modulations have completely disappeared. A visibility of $(44 \pm 3)\%$ was measured.

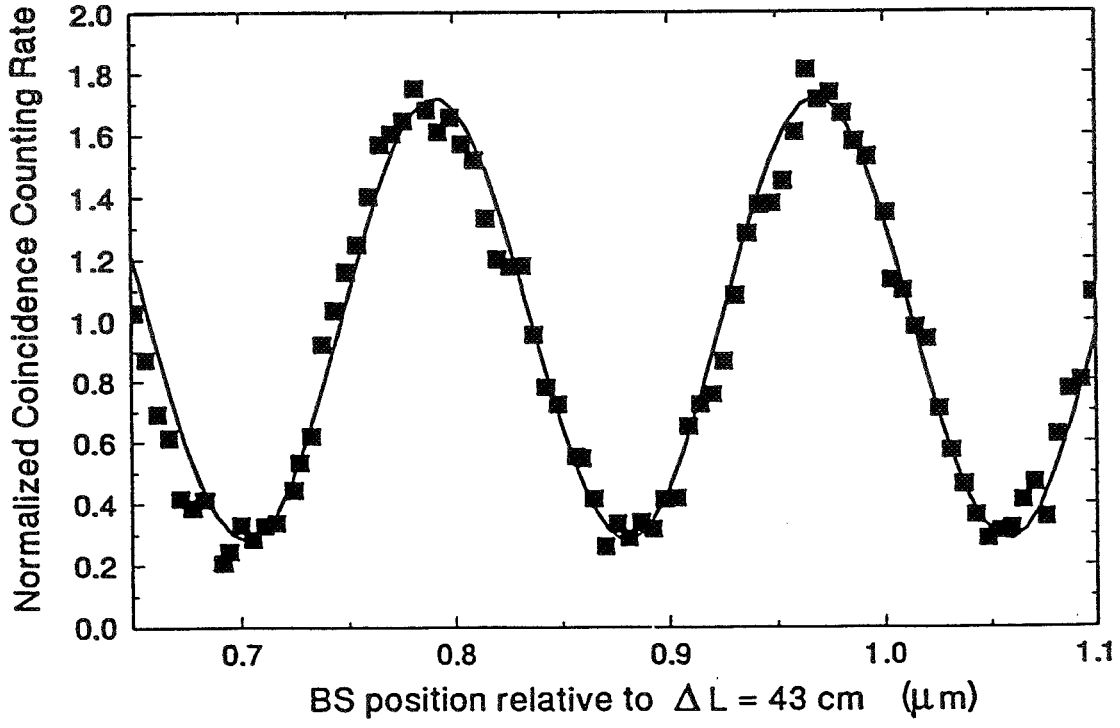


Figure I-7: Normalized coincidence counting rate of $N_c$at $\Delta L \cong 43cm$. The observed $(75 \pm 3)\%$ interference visibility marks the quantum interference effect. The modulation at $\lambda = 0.351\mu m$ is the sum frequency of the signal and idler light quanta.

which indicates that the modulation is only at the sum frequency. The modulation visibility can only approach to a maximum value of 50%, this is because the contribution of the last two terms in $J_0$ which arise from the state amplitudes in which one photon follow the longer and the other the shorter path of the interferometer. Fig. I-6 clearly shows this modulation.

(3). $\Delta L > c \cdot \Delta T_{coin}$. In this region, the interference pattern looks the same as in case (2), however, the interference visibility increases to more than 50%. This is because of the vanishing of the last two terms in $J_0$, the interference visibility is predicted to be 100% in idealized experimental conditions. This interference behavior is clearly demonstrated in fig. I-7.

The above simple theory of the quantum mechanical model provides a good quantitative understanding of what is happening in this experiment without the introduction of any artificial parameters. In the region of $\Delta L < l_{coh}$, all J's contribute to the interference pattern, which is not distinguishable from a classical model. In this region the first order interference pattern appears in both $N_1$ and $N_2$ counting. The coincidence modulation may explained as the result of the product of $N_1$ and $N_2$ modulations. When $\Delta L$ increases, $J_1$ and $J_+$ approach zero due to the vanishing of the factor $\exp(-\Sigma^2 \Delta T^2)$. This effect may be considered also to be a classical wave behavior. In the second region, $l_{coh} < \Delta L < c \cdot \Delta T_{coin}$, the coincidence interference behavior shown in (I-12) is expected. Since the $\omega_1$ and $\omega_2$ beams never meet at the same detector because of the filters, and each beam does not interfere with itself when $\Delta L > l_{coh}$, the coincidence modulation is a non-local two photon interference effect. In the third region, it is by now well known that under condition $\Delta L > c \cdot \Delta T_{coin}$, the interference is a purely quantum effect. It is impossible to have a classical model to explain the coincidence counting rate modulation of more than 50%. Mathematically the increase of the visibility is due to the vanishing of the factor $\exp(-\Delta T / 2\Delta T_{coin})$ in $J_0$. Physically this is due to the cut off by the coincidence time window of the state amplitudes in which one photon follows the longer path and other the shorter arm of the interferometer. This is equivalent to the projection of a quantum entangled EPR state [7, 8]

$$\Psi_{EPR} = A(t_1, t_2) + A(t_1 - \Delta T, t_2 - \Delta T) \qquad (\mathrm{I}-13)$$

from the initial state. For $\Delta L > c \cdot \Delta T_{coin}$, the entangled two-photon EPR state (I-13) is realized by the measurement, which takes advantage of the particle nature of the light quanta in a wave-like experiment.

# II Einstein-Podolsky-Rosen-Bohm Experiment By Splitting A Pair of Orthogonally Polarized Photon.

Type I parametric down conversion has drawn a great deal of attention since the first application [9] of it in an Einstein-Podolsky-Rosen-Bohm experiment [10]. The experimental study of Type II photon pairs was performed before Type I in our laboratory. However, the experimental results seemed to suggest that the orthogonally polarized signal and idler photon pair do not have the expected quantum entanglement. This phenomenon has troubled us and many other physicists with whom we have communicated in the past [11]. The entanglement of the Type II photon pair was demonstrated recently in our laboratory under two experimental conditions: (1) using a thin nonlinear crystal and (2) detecting coincidences in narrow spectral bandwidth [12, 13]. In

this section, we wish first to report the experimental study of this crystal length and detection bandwidth dependent entanglement of Type II down conversion. Then we report an experimental study of entangled two-photon EPR-Bohm states in Type II down conversion with linear, circular and elliptical polarizations.

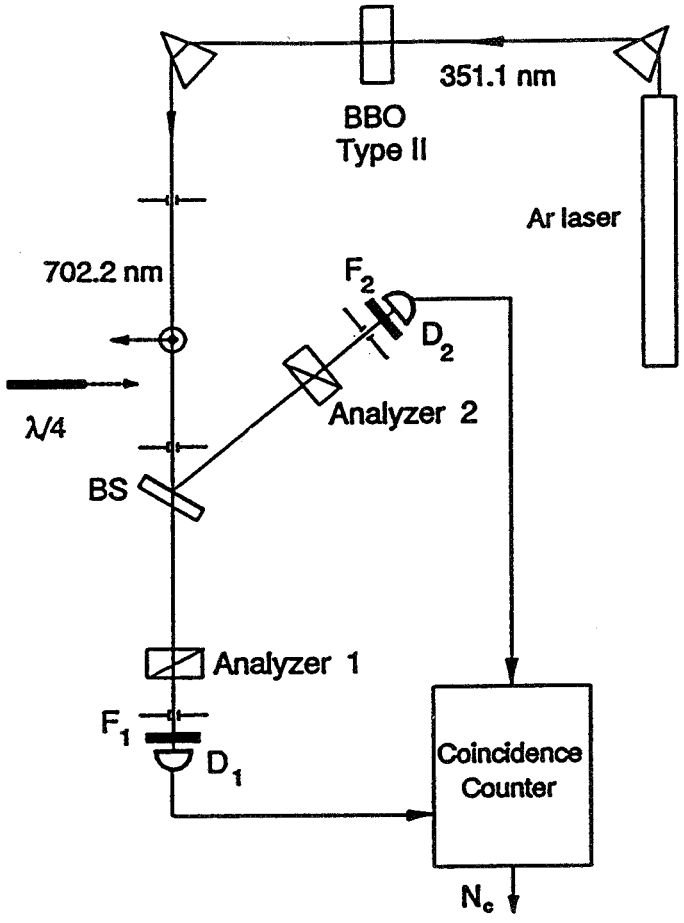


Figure II-1: Schematic experimental set up.

The experimental set up to study the effect of crystal length and detection bandwidth dependent entanglement is illustrated in fig. II-1. A single mode CW Argon ion laser line of $351.1nm$ was used to pump a BBO ($\beta - BaB_2O_4$) nonlinear crystal. The BBO was cut for a Type II phase matching condition to generate a pair of orthogonally polarized signal and idler photons collinearly and degenerately in $702.2nm$ wavelength. Two BBO crystals with lengths of $5.65mm$ and $0.5mm$, respectively, were used in the experiments. The $702.2nm$ pairs were separated from the pumping beam by a UV grade fused silica dispersion prism, then directed collinearly at a near normal incident angle to a polarization independent beam splitter which has $50\% - 50\%$ reflection and transmission coefficients. In each transmission and reflection output port of the beamsplitter a Glan Thompson linear polarization analyzer followed by a narrow bandwidth interference spectral filter were placed in front of a single photon detector. The photon detectors are dry ice cooled avalanche photodiodes operated in Geiger mode. The output pulses of the detectors were then sent

to a coincidence circuit with a $3nsec$ coincidence time window. The two detectors are separated by about $2m$, so that compared to the $3nsec$ coincidence window, the detections are space-like separated events. The coincidence counting rates were studied as functions of angles $\theta_1$ and $\theta_2$, where $\theta_i$ is the angle between the axis of the ith polarization analyzer and the direction, which is defined by the $o$-ray polarization plane of the BBO crystal. Keep in mind that a right-handed natural coordinate system with respect to the $k_i$ vector as the positive direction is employed for the discussions in this paper. The following form of coincidence rate as a function of $\theta_1$ and $\theta_2$ was observed in the experiments,

$$R_c = R_{c0}(\cos^2\theta_1 \sin^2\theta_2 + \sin^2\theta_1 \cos^2\theta_2 - \rho \sin\theta_1 \cos\theta_2 \sin\theta_2 \cos\theta_1) \qquad (\text{II}-1)$$

where $\rho$ is a parameter which depends on the crystal length, the detection bandwidth, and the group velocities of the $o-e$ beams inside the crystal. If $\rho = 2$, eq. (II-1) reduces to,

$$R_c = R_{c0} \sin^2(\theta_1 - \theta_2) \qquad (\text{II}-2)$$

which is the expected quantum correlation for the entangled two-photon EPR-Bohm state

$$|\Psi\rangle = 1/\sqrt{2}(|X_1\rangle \otimes |Y_2\rangle + |Y_1\rangle \otimes |X_2\rangle) \qquad (\text{II}-3)$$

$|\Psi\rangle$ quantum mechanically indicates a two-photon polarization state which is a superposition of the quantum probability amplitudes:

$$\begin{gathered}(1)\ |o-ray\ transmitted\rangle \otimes |e-ray\ reflected\rangle \\ (2)\ |e-ray\ transmitted\rangle \otimes |o-ray\ reflected\rangle\end{gathered} \qquad (\text{II}-4)$$

when the orthogonally polarized photon pair meets the beamsplitter. On the other hand, if $\rho = 0$ the interference cross term does not contribute. State (II-3) can not be concluded and no sign of the entanglement of the pair can be seen from the measurement.

Fig. II-2 reports the measured values of $\rho$ for BBO crystals with lengths of $5.65mm$ and $0.5mm$ for different bandwidths of the filters. Note that for the $5.65mm$ BBO crystal $\rho$ was always substantially less than 2 for the filters that used in the measurements. For the $0.5mm$ BBO, $\rho = 1.98$ was achieved with a $1nm$ bandwidth spectrum filter. The solid curves are the fits to a theoretical model which will be presented below. The values of $\rho$ were obtained from the measurements of coincidence rate as functions of $\theta_1$ and $\theta_2$. Fig. II-3, fig. II-4 are typical measurements which reflect the different coincidence behavior for $5.65mm$ and $0.5mm$ BBO crystals. In fig. II-3, $\theta_1$ was set to $45^\circ$ and the coincidence rate was mapped out as a function of $\theta_2$. In fig. II-4, both $\theta_1$ and $\theta_2$ were changed, keeping the sum of $\theta_1$ and $\theta_2$ equal to $90^\circ$. In both fig. II-3 and fig. II-4 the filters were $1nm$ bandwidth. By fitting many similar curves, $\rho = 0.72 \pm 0.07$ and $\rho = 1.98 \pm 0.04$ were determined for $5.65mm$ and $0.5mm$ crystals, respectively.

For Type II down conversion the two photon part of the state that exits the down conversion crystal may be calculated from the standard theory for parametric down conversion to be [6],

$$|\Psi\rangle = \iint d\omega_1 d\omega_2 \delta(\omega_1 + \omega_2 - \omega_p)\psi(\omega_1) a_o^\dagger(\omega_1(k_1)) a_e^\dagger(\omega_2(k_2)) \,|\, 0\rangle \qquad (\text{II}-5)$$

where $\omega$ and $k$ represents the frequency and the wave vector for signal (1), idler (2), and pump (p). The frequency phase matching condition is explicitly displayed by the delta function, and the

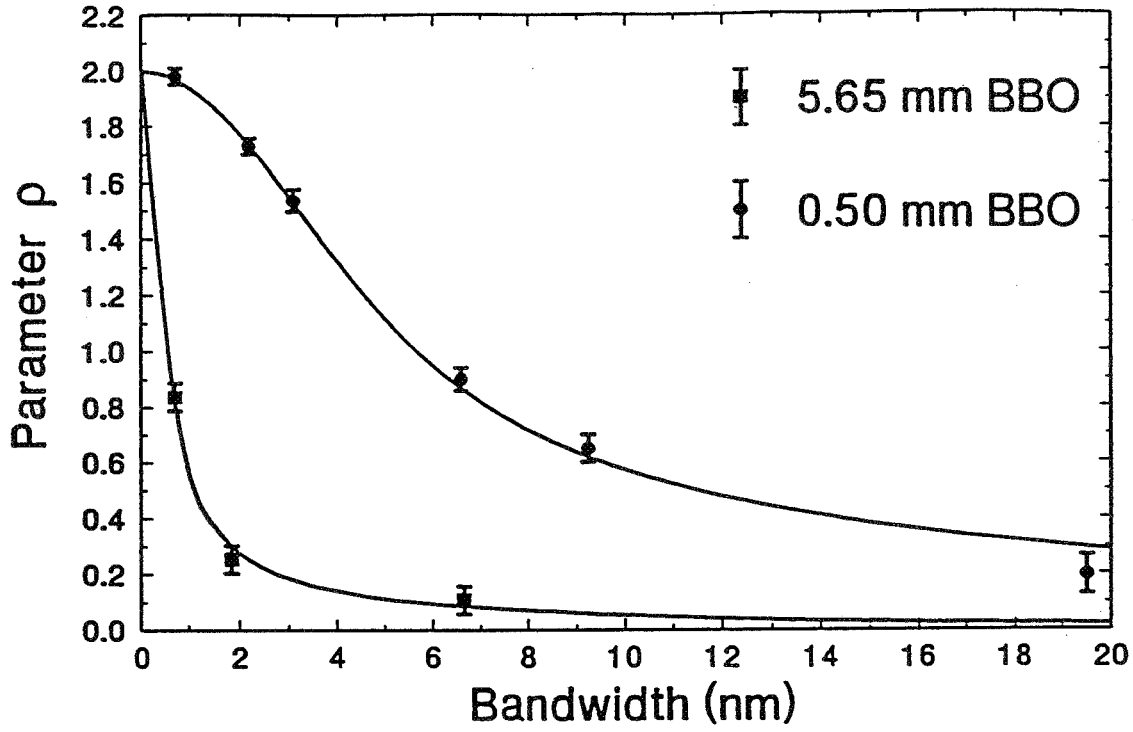


Figure II-2: Crystal Length and Detection Bandwidth Dependent Entanglement. The solid curve is a fitting of the theoretical mode.

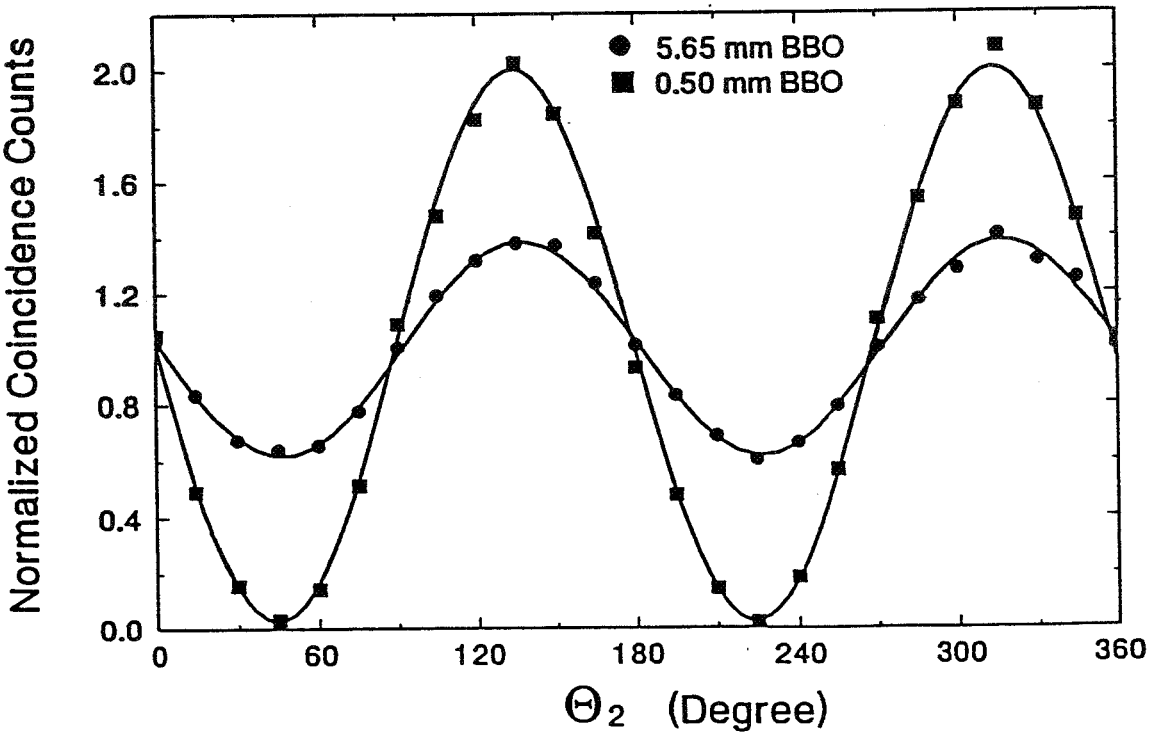


Figure II-3: Coincidence Measurements for Linear Polarization States when $\theta_1$ was set equal to 45°.

wave number phase matching condition is implicit in the choice of the location of the detectors, in this experiment we consider collinear down conversion. The function $\psi(\omega)$ is determined from the standard theory of down conversion. It depends on the length of the crystal, and $D = c/u_o - c/u_e$. We shall refer to $D$ as the two-photon dispersion. The subscript indies $o$ and $e$ for the creation operators indicate the ordinary and extraordinary rays of the down conversion, traveling along the same direction as the pump, the $z$-direction. The coordinate axes $x$ and $y$ are chosen along the the polarization direction of the $o$-ray and the $e$-ray, respectively.

The fields at the detectors 1 and 2 are given by

$$E_1^{(+)}(t) = \alpha_t \int d\omega f_1(\omega) \exp[-i\omega(t-\tau_1)] \sum_j \hat{e}_1 \hat{e}_j a_j(\omega)$$
$$E_2^{(+)}(t) = \alpha_r \int d\omega f_2(\omega) \exp[-i\omega(t-\tau_2)] \sum_j \hat{e}_2 \hat{e}_j a_j(\omega) \qquad (\text{II}-6)$$

where $a_j$ is the destruction operator of the photons, $j = o, e$, $i$ is in the direction of the ith linear polarization analyzer axis, $i = 1, 2$, $\alpha_t$ and $\alpha_r$ are the complex transmission and reflection coefficients of the beamsplitter. The function $f_i(\omega)$, $i = 1, 2$, is the spectral transmission coefficient function of the filter in front of the ith detector.

The counting rate can be written in terms of the square of the effective two-photon wave function (I-3), which has been used in the calculation of the first experiment. It is straight forward to show from (II-5),(II-6),

$$\Psi(t_1, t_2) = \alpha_t \alpha_r [\hat{e}_1 \cdot \hat{e}_o \; \hat{e}_2 \cdot \hat{e}_e A(t_1 - \tau_1, t_2 - \tau_2) + \hat{e}_1 \cdot \hat{e}_e \; \hat{e}_2 \cdot \hat{e}_o A(t_2 - \tau_2, t_1 - \tau_1)] \qquad (\text{II}-7)$$

where

$$A(t_1, t_2) = u(t_1 - t_2) \exp(-i\Omega_1 t_1) \exp(-i\Omega_2 t_2)$$
$$u(t) = A_0 \int d\omega f'(\omega) \psi'(\omega) \exp(i\omega t) \qquad (\text{II}-8)$$

where we have assumed that the filter $f_1$ and $f_2$ are peaked around $\Omega_1$ and $\Omega_2$, respectively, where $\Omega_1 + \Omega_2 = \omega_p$. For simplicity we take them to have the same shape so that $f'(\omega) = f_1(\omega + \Omega_1) = f_2(\omega + \Omega_2)$. $\psi$ can be computed from the standard theory of optical parametric down conversion. Taking the origin of the coordinates at the output side of the crystal, and letting $\psi'(\omega) = \psi(\omega + \Omega_1)$, we find

$$\psi'(\omega) = [1 - \exp(-i\omega DL)]/i\omega D \qquad (\text{II}-9)$$

The average coincidence counting rate is given by (I-2). In the following calculation we assume $S(t, \Delta T_{coin}) = 1$ for a $3nsec$ time window ($t_1 - t_2 << \Delta T_{coin}$). Taking the filters to be Gaussian

$$f'(\omega) = f_0 \exp(-\omega^2/2\sigma^2) \qquad (\text{II}-10)$$

it is not difficult to show that the coincidence counting rate becomes

$$R_c = R_{c0}[\cos^2\theta_1 \sin^2\theta_2 + \sin^2\theta_1 \cos^2\theta_2 - \rho \sin\theta_1 \cos\theta_1 \sin\theta_2 \cos\theta_2] \qquad (\text{II}-11)$$

where

$$\rho = 2(C_+ - C_-)/(C_+ + C_-) \qquad (\text{II}-12)$$

with

$$C_+ = K \int_{-\infty}^{+\infty} dt[erfc(s+t) + erfc(s-t)]^2$$
$$C_- = K \int_{-\infty}^{+\infty} dt[2erfc(t) - erfc(s+t) + erfc(t-s)]^2 \qquad (\text{II}-13)$$

where erfc is the error function, $K$ is a constant, and parameter

$$s = \sigma DL \qquad (\text{II}-14)$$

The only parameter that $\rho$ depends is $s$, which shows the dependence on $\sigma$, the bandwidth of the filters, $D$, the two-photon dispersion, and $L$, the length of the crystal. By sketching the integrals, it is not difficult to show that for a very long crystal $\rho \cong 0$, because $C_+ - C \cong 0$, and for a short crystal $\rho \cong 2$, because $C \cong 0$.

The functions in (II-13) are easily evaluated numerically and fit the data accurately with no free parameters. The solid lines in fig. II-2 are the theory curves for $5.65mm$ and $0.5mm$ BBO crystals. The curves agree with the measured values of $\rho$ within reasonable experimental error. One can achieve $\rho \cong 2$ with bandwidth filters less than $1nm$ for a $0.5mm$ BBO thin crystal.

Using a $0.5mm$ crystal and a $1nm$ bandwidth filter to achieve $\rho = 2$, measurements for two-photon polarization entangled EPR states were made. The use of a quarter wave plate and a beamsplitter easily can demonstrate the quantum mechanical entanglement of arbitrary elliptical polarization states in Type II down conversion. The experimental set up is the same as in fig. II-1, except a quarter wave plate is placed after the $0.5mm$ BBO crystal. If the fast axis of the quarter wave plate is oriented at angle $\Phi$ with respect to the direction, the orthogonal linear polarization states $\mid X\rangle$ and $\mid Y\rangle$ are transformed to orthogonal elliptical polarization states. After the beamsplitter a two-photon entangled state with elliptical polarizations is produced,

$$\mid \Psi\rangle = 1/\sqrt{2}\left[\begin{pmatrix} \cos\Phi \\ -i\sin\Phi \end{pmatrix}_1 \begin{pmatrix} \sin\Phi \\ -i\cos\Phi \end{pmatrix}_2 + \begin{pmatrix} \sin\Phi \\ i\cos\Phi \end{pmatrix}_1 \begin{pmatrix} \cos\Phi \\ i\sin\Phi \end{pmatrix}_2\right] \qquad (\text{II}-15)$$

where state $|\Psi\rangle$ is a superposition of the quantum probability amplitudes:

$$(1).\ (\cos\Phi \mid X'\rangle - i\sin\Phi \mid Y'\rangle)transmitted \otimes (\sin\Phi \mid X'\rangle + icos\Phi \mid Y'\rangle)reflected$$

$$(2).\ (\sin\Phi \mid X'\rangle + i\cos\Phi \mid Y'\rangle)transmitted \otimes (\cos\Phi \mid X'\rangle - i\sin\Phi \mid Y'\rangle)reflected$$

when the orthogonal elliptical polarized photon pair meets the beamsplitter.

The coincidence counting rate for linear polarization analyzers is then,

$$R_c = R_{c0}[\sin^2(2\Phi)\cos^2(\theta_1' + \theta_2') + \cos^2(2\Phi)\sin^2(\theta_1' - \theta_2')] \qquad (\text{II}-16)$$

where $\theta_i'$ is the angle between the axis of the ith polarization analyzer and the $|X_i'\rangle$ direction. Care has to be taken to follow the rules of natural coordinate system, especially for the reflected beam. Note that the direction of $|X_2'\rangle$ is opposite to that of $|X_1'\rangle$.

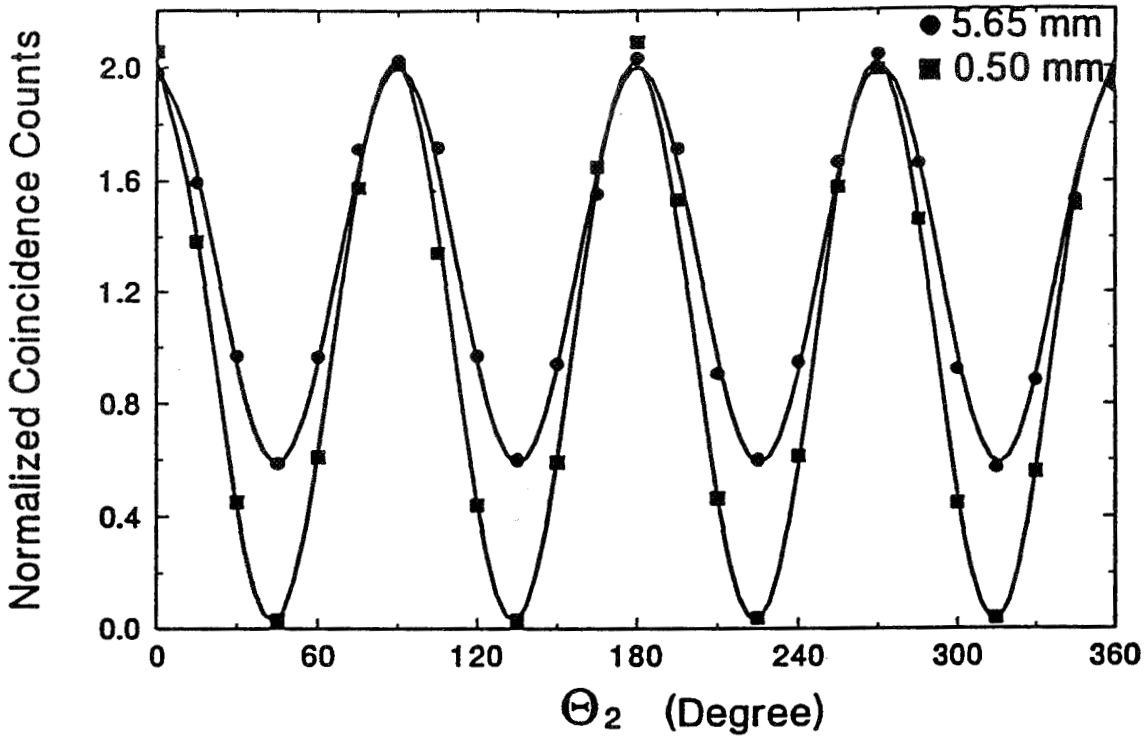


Figure II-4: Coincidence Measurements for Linear Polarization States when $\theta_1 + \theta_2 = 90°$was preserved.

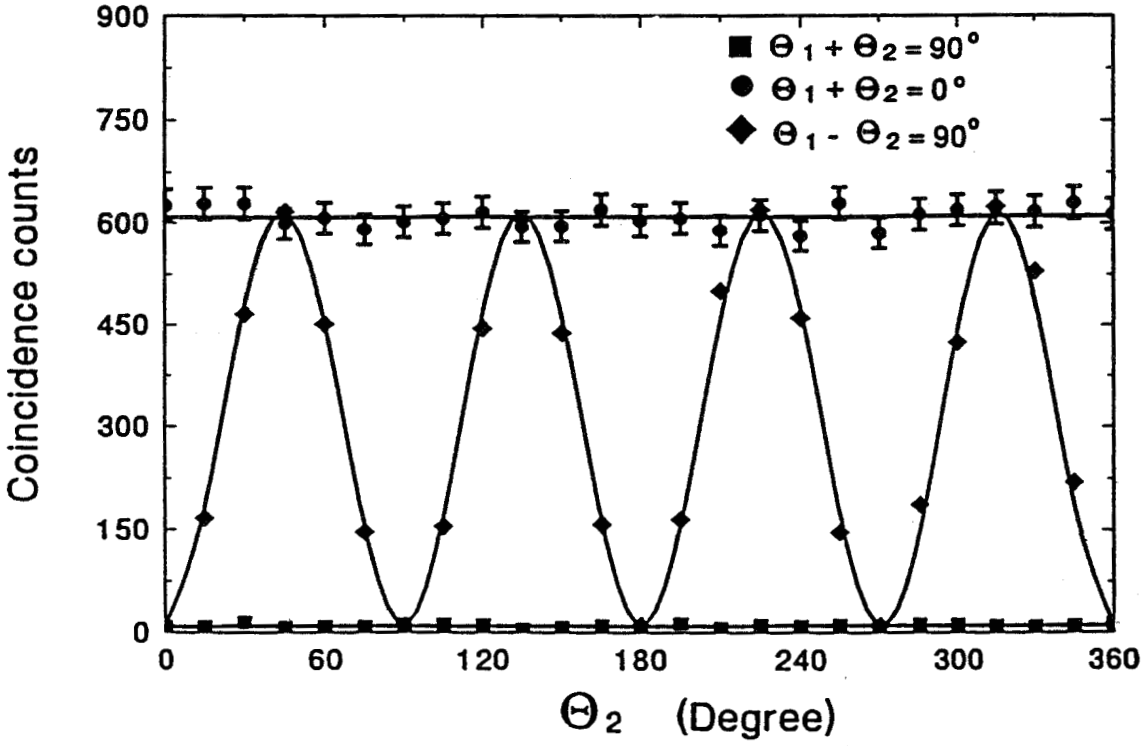


Figure II-5: Coincidence Measurements for Circular Polarization EPR-Bohm State.

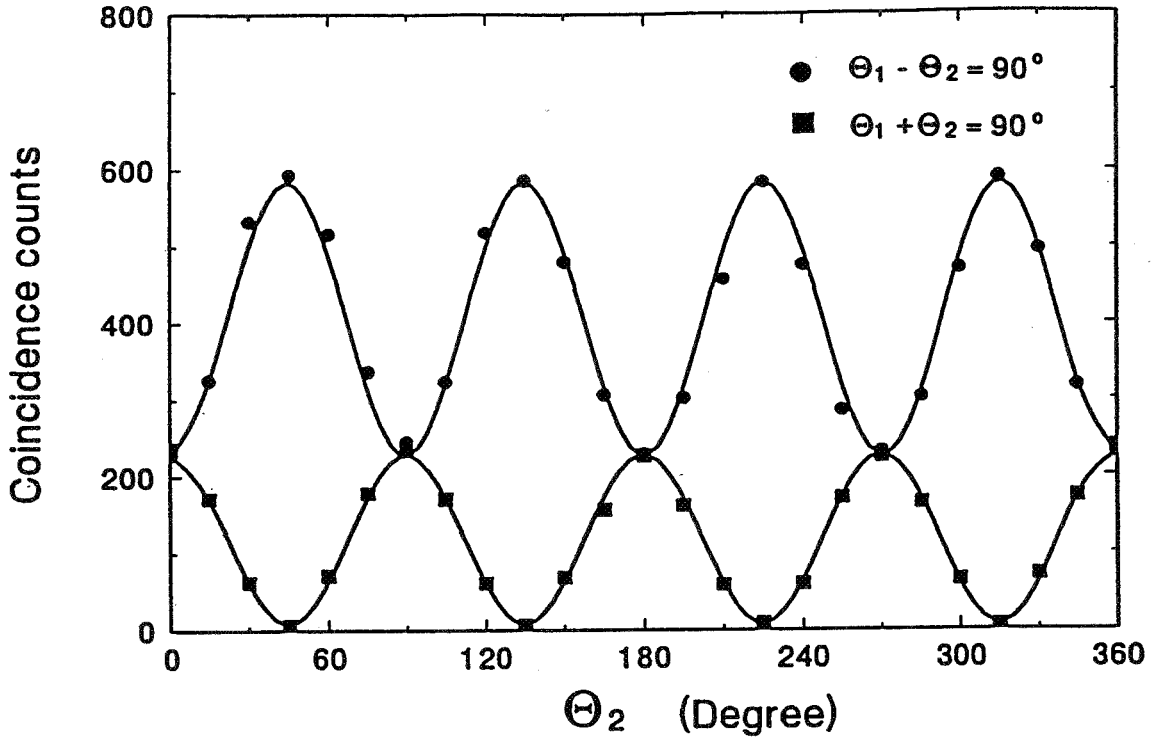


Figure II-6: Coincidence Measurements for Elliptical Polarization State with Quarter Wave-plate oriented at 26.5°.

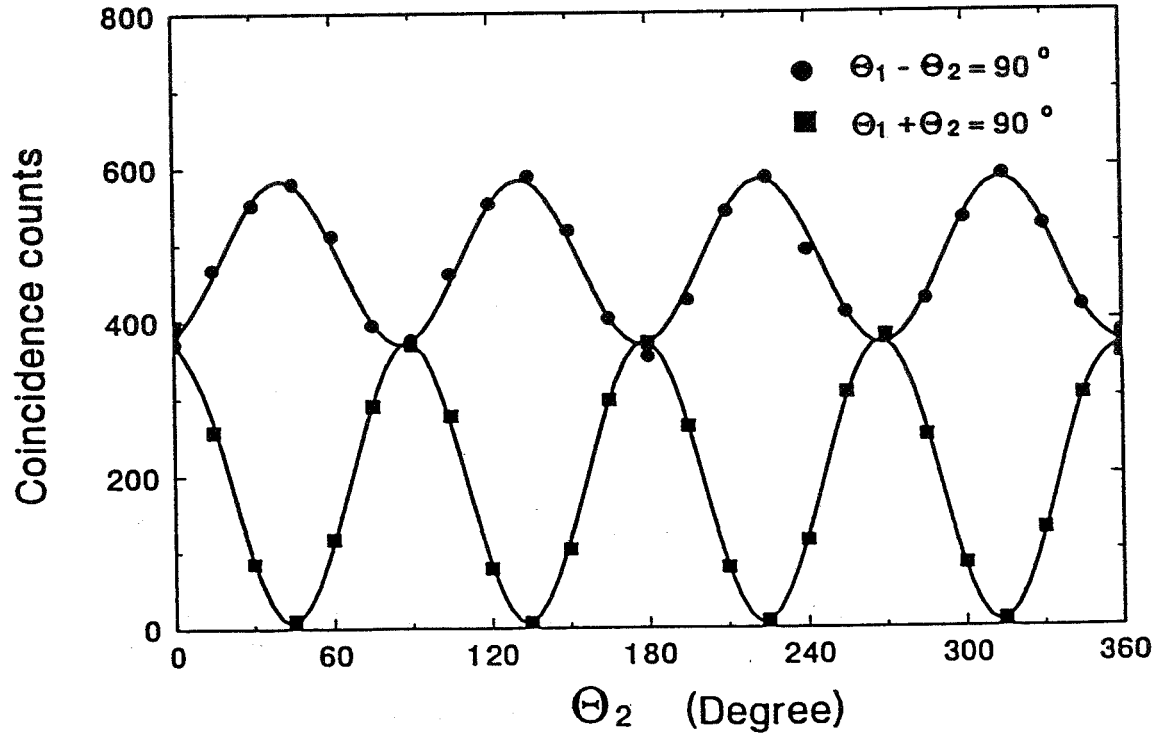


Figure II-7: Coincidence Measurement for Elliptical Polarization State with Quarter Waveplate oriented at 71.5°.

If $\Phi = 0°$, state (II-15) becomes state (II-3) which is a two-photon linear polarization entangled state. Quantum correlations given by eq. (II-2) were observed experimentally, see fig. II-3 and fig. II-4, with modulations about$(98 \pm 2)\%$.

For $\Phi = 45°$. State (II-15) becomes the circular polarization EPR-Bohm state,

$$| \Psi\rangle = 1/\sqrt{2}(| R_1\rangle \otimes | R_2\rangle + | L_1\rangle \otimes | L_2\rangle) \qquad (\text{II}-17)$$

The expected quantum correlations

$$R_c = R_{c0} \cos^2(\theta_1 + \theta_2) = R_{c0} \cos^2(\theta_1' + \theta_2') \qquad (\text{II}-18)$$

were measured experimentally. Fig. II-5 reports the measured results. The modulation is about $(98 \pm 2)\%$.

When the quarter wave plate was set to $\Phi = 26.5°$ and $71.5°$, fig. II-6 and fig. II-7 report four typical measurements which were taken under the conditions: $\theta_1' \pm \theta_2' = 90°$. The solid lines in these figures are the theory curves of (II-18). Note, here, we use $\theta'$ system to define the angles for the analyzers.

Contrary to the coincidence counting rate, the single detector counting rate remains constant for all the above measurement. Fig. II-8 reports a typical counting rate for detector 2 in a measurement.

A pair of orthogonally polarized light quanta enters a single port of a beamsplitter, if one of the photons, for example the transmitted one, is detected to be linearly polarized in a certain direction, $\theta_1$, the other one can be predicted with certainty to be linearly polarized in the direction $\theta_2$. This makes the experiment EPR type argument. Addition to this argument, it is also interesting to see that $\theta_2$ is not necessarily perpendicular to $\theta_1$, the value of $\theta_2$ depends on the EPR state prepared by the observer.

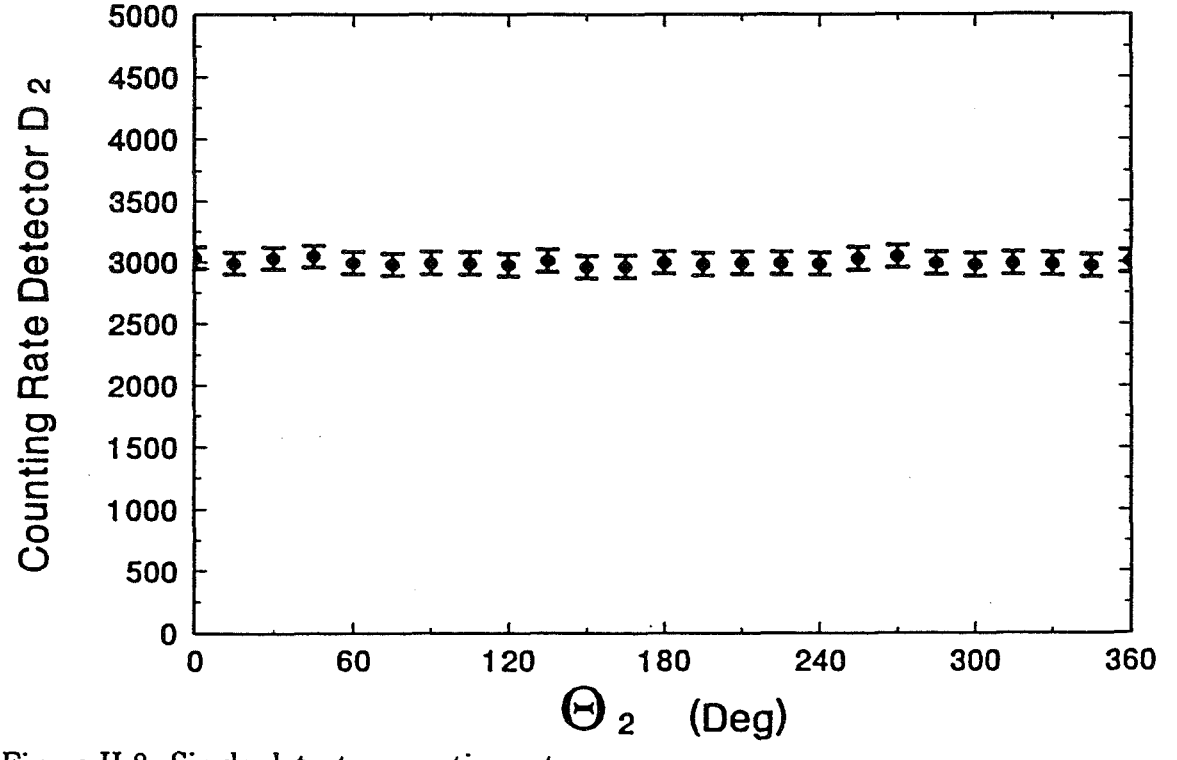


Figure II-8: Single detector counting rate.

This simple beam-splitting experiment is a particle-like experiment. Eq. (II-4) is based on the argument that the photon can be either transmitted or reflected by a beamsplitter. On the other hand this simple beam-splitting type experiment demonstrated the wave property of the photon. The 100% modulation of the coincidence counting rate is essentially an interference superposition of the two-photon amplitudes in (II-7). The overlap and non-overlap of the amplitudes $A(t_1 - \tau_1, t_2 - \tau_2)$ and $A(t_2 - \tau_2, t_1 - \tau_1)$ is a good measure of the wave packet picture of the photon, which results the crystal length and detection bandwidth dependent of the two-photon entanglement.

We wish to thank D.N. Klyshko for many useful discussions. This work was supported partially by the Office of Naval Research Grant No. $N00014 - 91 - J - 1430$.

# References

[1] A. Einstein, B. Podolsky and N. Rosen, Phys. Rev. 47, 777 (1935).

[2] M.H. Rubin and Y.H. Shih, Phys. Rev. A 45, 8138 (1992).

[3] J.D. Franson, Phys. Rev. Lett. 62, 2205 (1989).

[4] Y.H. Shih, A.V. Sergienko, and M.H. Rubin, Phys. Rev. A 47, 1288 (1993).

[5] P.G.Kwiat, A.M. Steinberg, and R.Y. Chiao, Phys. Rev. A 47, 2472 (1993).

[6] D.N. Klyshko, Photons and Nonlinear Optics, Gorden and Breach Science Publishers, N.Y., (1988).

[7] E.Schrödinger, Naturwissenschaften, 23, 807, 823, 844 (1935). A translation of these papers appears in J.A. Wheeler and W.H. Zurek, ed., Quantum Theory and Measurement, Princeton University Press, (1983).

[8] M.A. Horne, A. Shimony, and A. Zeilinger, Phys. Rev. Lett. 62, 2209 (1989).

[9] C.O. Alley and Y.H. Shih, Foundations of Quantum Mechanics in the Light of New Technology, ed. M.Namiki et. al., p. 47 (1986). Y.H. Shih and C.O. Alley, Phys. Rev. Lett. 61, 2921 (1988).

[10] D. Bohm, Quantum Theory, Prentice Hall, Englewood Cliffs, (1951).

[11] Private communications with J.A. Wheeler, E.P. Wigner, A. Shimony, J.D. Franson and others.

[12] T.E. Kiess, Y.H. Shih, A.V. Sergienko, and C.O. Alley, Phys. Rev. Lett., 71, 3893 (1993).

[13] Y.H. Shih, A.V. Sergienko, M.H. Rubin, T.E. Kiess and C.O. Alley, Submitted to Phys. Rev. A, (1993).

# THE GENERATION OF ENTANGLED STATES FROM INDEPENDENT PARTICLE SOURCES

Morton H. Rubin and Yanhua Shih
*Physics Department*
*University of Maryland Baltimore County, Baltimore, MD 21228-5398*

**Abstract**

The generation of entangled states of two systems from product states is discussed for the case in which the paths of the two systems do not overlap. A particular method of measuring allows one to project out the nonlocal entangled state. An application to the production of four photon entangled states is outlined.

## 1 Introduction

The importance of non-local entangled states in the study of the Einstein-Podolsky-Rosen paradox (EPR) has been stressed by Horne, Shimony, and Zeilenger (GHZ) [1]. These states are entangled states of two or more particles in which at least one pair of particles has space-like separation. Such states may be produced from independent sources by allowing the particles to scatter from one another and then separate, or by allowing their paths to overlap spatially such as by passing pairs of photons through a single beam splitter. The generation of entangled states from independent particle sources in which the entangled particles overlap has been discussed by Yurke and Stoler [2], and by Tan, Walls and Collett [3]. We consider the case in which the entangled particles are produced from independent sources and never overlap.

## 2 Independent Sources With Path Overlap

We briefly review the work of Yurke and Stoler. Two independent sources each emit a particle which is passed through a beam splitter and phase shifter. The detection system consists of a pair of detectors, labeled 1 and 2. Each detector is composed of a beam splitter which directs each particle to one of two particle counters denoted by R and G. The initial input state is a product state,

$$|\Psi>=|\alpha>_1 |\beta>_2 . \tag{1}$$

After passing through the system this state may be written as

$$\begin{aligned} |\Psi'> \;=\; & \frac{1}{4}\{e^{i\theta_1}(|\alpha\, R1>_1 + i|\alpha\, G1>_1) + i^2|\alpha\, R2>_1 + i|\alpha\, G2>_1\} \\ & i^2|\beta\; R1>_2 + i|\beta\, G1>_2 + e^{i\theta_2}(|\beta\, R2>_2 + i|\beta\, G2>_2)\} \end{aligned} \tag{2}$$

where the i's come from the reflection off the beam-splitters. If we consider the case in which only the R detectors register, the only part of the state that we look at is

$$e^{i(\theta_1+\theta_2)}|\alpha\, R1>_1 |\beta\, R2>_2 - |\alpha\, R2>_1 |\beta\, R1>_2 \tag{3}$$

which is an entangled state. By varying the phase shifters, interference between the two terms can be detected. This interference occurs because there are two distinct paths from the input state to the detection state that can not be distinguished by the detectors. From this point of view [4] the fact that "vacuum" enters the system through the beam splitters plays no role since the detectors do not see the vacuum states.

# 3 Independent Sources Without Path Overlap

We now turn to a different method of generating entangled states in which the independent sources are independently detected. The particle paths never cross. The entanglement is obtained by selective detection and the interference is caused by varying the phase shift in each path in a specific way. We shall see below that this allows us to consider the generation of an EPR state of the type envisioned by GHZ. We illustrate this technique for the simplest case, namely, two spin-1/2 particles. The input to the system is two independent particles polarized along the positive z-axis,

$$|\Psi>=|+z>_1 |+z>_2 . \tag{4}$$

Each particle is passed through a separate Stern-Gerlach apparatus which splits each state vector into a superposition of states polarized along the x-axis. After passing through the system we have

$$|\Psi'>=\frac{1}{2}\{|+x>_1 + e^{i\theta_1}|-x>_1\}\{|+x>_2 + e^{i\theta_1}|-x>_2\}, \tag{5}$$

where the phase shifter effect has been included. Multiplying (5) out gives

$$\begin{aligned}|\Psi'>=\frac{1}{2}\{&|+x>_1 |+x>_2 + e^{i(\theta_1+\theta_2)}|-x>_1 |-x>_2 + \\ &e^{i\theta_1}|-x>_1 |+x>_2 + e^{i\theta_2}|+x>_1 |-x>_2\}.\end{aligned} \tag{6}$$

Then we project this onto the detector states

$$|Dk>=|+zk>=\frac{1}{\sqrt{2}}(|+x>_k + |-x>_2),\ \text{k=1,2.} \tag{7}$$

The amplitude for detecting particle 1 at detector 1 and particle 2 at detector 2 is:

$$A=\frac{1}{4}(1+e^{i\theta_1})(1+e^{i\theta_2})=\frac{1}{4}\{(1+e^{i(\theta_1+\theta_2)})+(e^{i\theta_1}+e^{i\theta_2})\}, \tag{8}$$

which is still a product for independent choice of phases. Now if we choose $\theta_2=\theta_1+\pi$, then the second pair of terms in (8) cancel and the first shows interference as $\theta_1$ is varied,

$$A=\frac{1}{4}(1-e^{2i\theta_1}) \tag{9}$$

This is equivalent to producing the entangled state given by the first two terms of (6).

In this case the two independent particles never meet. Here the interference is between the pair of particles that went through the phase shifter and the pair that did not. From the point of view of indistiguishable paths, it is the paths of these *two-particle states* that are indistiguishable. Another way to look at this particular example is to note that the choice of the angles makes the first two term in (6) total spin 1 states and the second two form a total spin 0 state, the detector only detects the spin 1 part of the state.

This argument can be generalized to more than two particles and can be used to form the basis of many-particle interference experiments to test the theorem of Greenberger, Horne and Zeilenger [5]. The use of projection operators to pick off parts of state vectors, which is really what measurements do, is nothing new. It is fundamental to quantum theory. What is different is the means of picking off nonlocal entangled states from independent particles.

# 4 The Theory of the Four-Photon Experiment

We now apply this to a possible four-photon interference experiment. We wish to show how one can produce the highly correlated state necessary to carry out the experiment envisioned by Greenberger, Horne and Zeilenger. In fig. 1 we show the experiment envisioned. It is a double Franson interferometer [6]. The coincidence counting rate is proportional to

$$P = \int\int\int\int dt_1 dt_2 dt_3 dt_4 S(t_1,t_2,t_3,t_4)|\Phi_I(t_1,t_2)|^2|\Phi_{II}(t_3,t_4)|^2, \tag{10}$$

where the integrals are over the duration of the measurement. The function S expresses the fact that the coincidence time window is one when $t_2 - t_1$, $t_3 - t_1$ and $t_4 - t_1$ are all less than some small coincidence time $t_{coin}$ and rapidly goes to zero when this is not true.

$$\Phi_j(t_1,t_2) = \frac{1}{2}(\Psi_j(L_1,L_2) + \Psi_j(S_1,L_2) + \Psi_j(L_1,S_2) + \Psi_j(S_1,S_2)), \tag{11}$$

where j=I and II . The middle two terms can be discriminated against for $L - S = \Delta L$ if $\Delta L/c >> t_{coin}$. Then we can confine ourselves to considering

$$\Phi_j(t_1,t_2) = \frac{1}{2}\{\Psi_j(L_1,L_2) + \Psi_j(S_1,S_2)\}. \tag{12}$$

The amplitude in (12) is still a product,

$$\begin{aligned}\Phi_I(t_1,t_2)\Phi_{II}(t_3,t_4) \;=\; & \frac{1}{4}(\{\Psi_I(L_I,L_I)\Psi_{II}(L_{II},L_{II}) + \Psi_I(S_I,S_I)\Psi_{II}(S_{II},S_{II})\} + \\ & \{\Psi_I(L_I,L_I)\Psi_{II}(S_{II},S_{II}) + \Psi_I(S_I,S_I)\Psi_{II}(L_{II},L_{II})\}).\end{aligned} \tag{13}$$

This is in a form similar to that of (5). We now want to show how the last term in curly brackets can be made to vanish.

We have shown elsewhere [7] that the two-photon wave function is of the form

$$\Psi(t_1,t_2) = u(t_1 - t_2)v(t_1 + t_2). \tag{14}$$

The function u(t) describes the correlation of the photon pair in space and time. Its width is determined by the single photon bandwidth. This is usually fixed by filters in the output beams of the down-conversion crystal. The function v(t) is of the form

$$v(t) = A(t)e^{-i\frac{\Omega_p t}{2}}, \tag{15}$$

It expresses the fact that the pair is created somewhere within the overlap of the crystal and the pump beam. In general, if the pump beam is nearly monochromatic, A will be a slowly varying function of time.

Using these facts, the second term in curly brackets of (13) can be written as

$$u(t_1 - t_2)u(t_3 - t_4)\{v(t_1 + t_2)v(t_3 + t_4 - \frac{2\Delta L_{II}}{c}) + v(t_1 + t_2 - \frac{2\Delta L_I}{c})v(t_3 + t_4)\}. \tag{16}$$

The *key point* is that we can choose the path lengths so that

$$\Omega_p(\Delta L_I - \Delta L_{II})/c = \pi \tag{17}$$

making the relative phase between the two terms in the bracket of (16) negative. Since A(t) is constant over the measurement time this term will vanish. The first term in curly brackets has two terms with a relative phase of $\Omega_p(\Delta L_I + \Delta L_{II})/c$ which, under the condition stated, becomes $\pi + \Omega_p 2\Delta L_I/c$. Therefore varying the path length while keeping their difference fixed allows one to see interference with oscillations at half the pump wavelength.

The above experiment is for space-time variables. There is a more convenient way to proceed using the polarization of the photons.

# 5 Acknowledgments

After this paper was completed a related paper on the generation of entangled states from independent sources [8] was called to our attention. We thank Professor Zeilinger for giving us a preprint of this paper.

This work was supported by Office of Naval Research Grant No. N00014-91-J-1430.

# References

[1] M. A. Horne, A. Shimony, and A. Zeilenger, Phys. Rev. Lett. **62**, 2209 (1989). M. A. Horne, A. Shimony, and A. Zeilenger,*Quantum Coherence*, edited by J. S. Anandan, (World Scientific Co. Pte. Ltd, Singapore,1990).

[2] B. Yurke and D. Stoler, Phys. Rev. Lett. **68**, 1251 (1992) and Phys. Rev. A **46**, 2229 (1992).

[3] S. M. Tan, D. F. Walls and M. J. Collett, Phys. Rev. Lett. **66**, 252 (1991).

[4] This point of view is the natural one from the point of view of Feynman's approach to quantum mechanics, R. P. Feynman, R. B. Leighton, and M Sands, *The Feynman Lectures on Physics, Quantum Mechanics*, (Addison-Wesley, Reading,MA, 1965).

[5] D. M. Greenberger, M. Horne and A. Zeilenger, in *Bells Theorem, Quantum Theory and Conceptions of the Universe*, edited by M. Kaftos (Kluwer Academis, Dordrect, 1989).

[6] J. D. Franson, Phys. Rev. Lett.**62**, 2205 (1989).

[7] Y. H. Shih and Morton H. Rubin, to be published

[8] M. Zukowski, A. Zeilinger, M. A. Horne and A. K. Ekert, private communication.

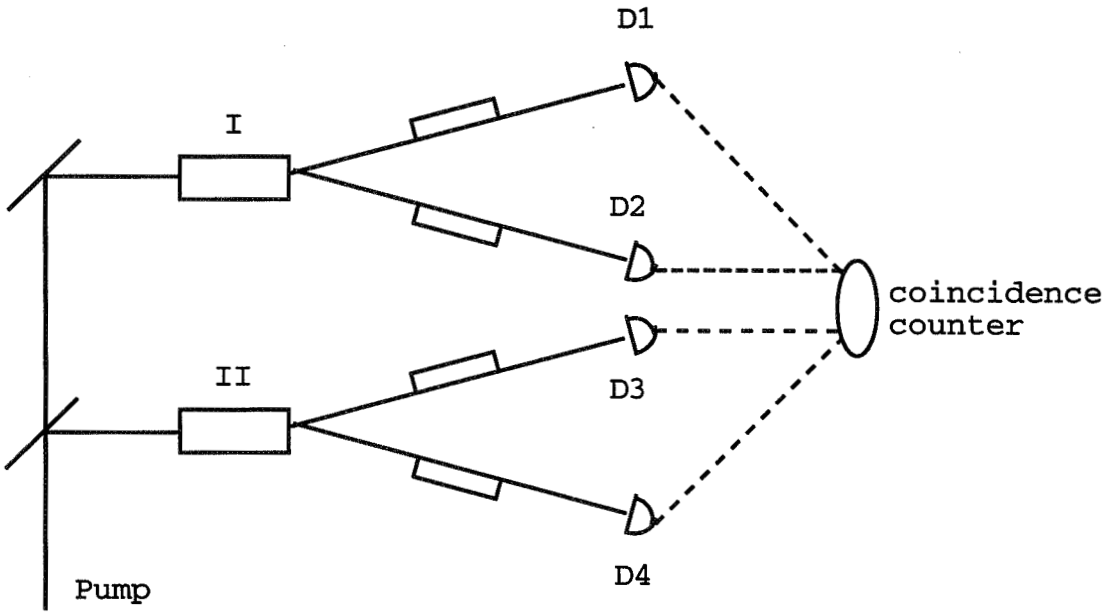


Figure 1: A pump beam enters two crystals which each produce a pair of photons by optical parametric downconversion. Each photon passes through an interferometer and is detected by one of the four detectors (Dk). A coincidence counter (C) gives a count only when all four photons arrive within a fixed time window.

# NONLOCAL EFFECTS ON THE POLARIZATION STATE OF A PHOTON, INDUCED BY DISTANT ABSORBERS

L.C.B. Ryff
*Universidade Federal do Rio de Janeiro, Instituto de Física*
*Caixa Postal 68528, 21945-970 Rio de Janeiro, RJ, Brazil*

**Abstract**

A variant of a Franson's two-photon correlation experiment is discussed, in which the linear polarization state of one of the photons depends on the path followed in the interferometer. It is shown that although the path difference is greater than the coherence length, the photon can be found in a polarization state represented by the superposition of the polarization states associated to the paths when there is coincident detection. Since the photons, produced via parametric down-conversion, are fairly well localized in space and time, the situation in which one of the photons is detected before the other can reach the interferometer raises an intriguing point: it seems that in some cases the second photon would have to be described by two wave packets simultaneously. Unlike previous experiments, in which nonlocal effects were induced by means of polarizers or phase shifters, in the proposed experiment nonlocal effects can be induced by means of variable absorbers.

Ever since Bell's theorem [1] and the important paper by Clauser, Horne, Shimony, and Holt [2], different experiments have been performed related to quantum mechanical nonlocality. In these experiments the photons of a correlated pair either are made to impinge on polarizers [3] or are made to pass through phase shifters [4,5]. Here I would like to discuss an experiment (represented in Fig. 1) in which nonlocal effects can be induced by means of variable absorbers (or variable beam-splitters). It is a modified Franson's experiment [5], in which a half-wave plate ($\lambda/2$), a two-channel polarizer, and two variable absorbers ($A_S$ and $A_L$) have been included. Photons $\gamma_1$ and $\gamma_2$, produced via parametric down-conversion, are in the same polarization state [6], which I will assume as being parallel to x. The orientation of the half-wave plate is chosen so that after passing it $\gamma_2$ is in a different polarization state, perpendicular to the state it was in. As has been shown [7], when there is coincident detection, the packets following the long ($L_2$) and the short ($S_2$) paths interfere. In the present proposal the relative amplitude of these packets is varied at a distance by means of $A_S$ and $A_L$. For our purposes, we only need to consider a field with one polarization component. When the beam-splitters $H_1, H_2, H_1'$ and $H_2'$; the absorber $A_S$; and the half-wave plate are removed, $\gamma_1$ and $\gamma_2$ can only follow the short paths, and the coincidence rate between the detectors at sites 1 and 2 is given by [8]

$$R_0 = k\langle t|\hat{E}_{2S}^{(-)}(t)\ \hat{E}_{1S}^{(-)}(t)\ \hat{E}_{1S}^{(+)}(t)\ \hat{E}_{2S}^{(+)}(t)|t\rangle\ , \qquad (1)$$

where $|t\rangle$ is the state of the field at time $t$; $\hat{E}_{2S}^{(+)}(t)$ is the annihilation part of the electric field operator at the detector at site 2; and so on, and $k$ is a proportionality constant. If, instead

of removing the beam-splitters, they are replaced by mirrors and $A_L$ is removed, $\gamma_1$ and $\gamma_2$ can only follow the long paths, and the coincidence rate between the detectors at sites 1 and 2 is given by

$$R_0 = k\langle t|\hat{E}_{2L}^{(-)}(t)\ \hat{E}_{1L}^{(-)}(t)\ \hat{E}_{1L}^{(+)}(t)\ \hat{E}_{2L}^{(+)}(t)|t\rangle\ . \tag{2}$$

$\hat{E}_L^{(+)}(t)$ and $\hat{E}_S^{(+)}(t)$ are related by the expression

$$\hat{E}_{jL}^{(+)}(t) = e^{i\phi_j}\ \hat{E}_{jS}^{(+)}(t-\Delta T)\ ,\ j=1,2, \tag{3}$$

where $\Delta T = (L-S)/c$, with $L = L_2 = L_1$ ($S = S_2 = S_1$) representing the length of the long (short) path, and $\phi_j$ is a phase shift. Since $L-S$ is much greater than the coherence lengths of the wave packets associated with $\gamma_1$ and $\gamma_2$,

$$\hat{E}_{1L}^{(+)}(t)\ \hat{E}_{2S}^{(+)}(t)|t\rangle = 0 \tag{4}$$

and

$$\hat{E}_{1S}^{(+)}(t)\ \hat{E}_{2L}^{(+)}(t)|t\rangle = 0\ . \tag{5}$$

Since $\Delta\omega\Delta T \ll 1$, where $\Delta\omega$ is the uncertainty in the sum of the frequencies of $\gamma_1$ and $\gamma_2$, it can be shown that [5]

$$\hat{E}_{1S}^{(+)}(t-\Delta T)\ \hat{E}_{2S}^{(+)}(t-\Delta T) = e^{i(\omega_{10}+\omega_{20})\Delta T}\ \hat{E}_{1S}^{(+)}\ \hat{E}_{2S}^{(+)}(t)\ , \tag{6}$$

where $\omega_1+\omega_2 = \omega_{10}+\omega_{20}\pm\Delta\omega$, and $\omega_{10}(\omega_{20})$ is the central frequency of $\gamma_1(\gamma_2)$.

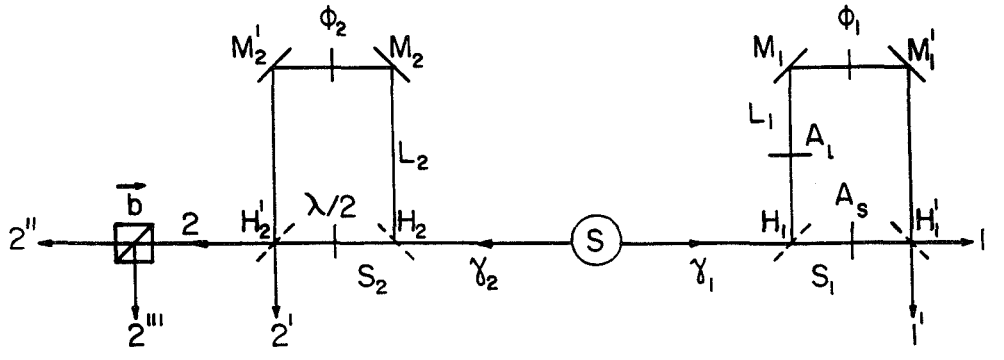


FIG. 1. Franson's experiment in which a half-wave plate, a polarizer, and two absorbers have been included.

To represent the action of the absorbers, I will introduce a parameter $\theta$, such that:

$$\hat{E}_{1S}^{(+)}(t) \xrightarrow{A_S} \sin\theta\ \hat{E}_{1S}^{(+)}(t) \tag{7}$$

and

$$\hat{E}_{1L}^{(+)}(t) \xrightarrow{A_L} \cos\theta\ \hat{E}_{1L}^{(+)}(t)\ . \tag{8}$$

Therefore, the transmissivities of the absorbers are varied in a correlated way. The field operator at site 1 in the experiment represented in Fig. 1. will then be given by

$$\hat{E}_1^{(+)}(t) = \frac{1}{2}\left[\sin\theta\ \hat{E}_{1S}^{(+)}(t) + \cos\theta\ \hat{E}_{1L}^{(+)}(t)\right]\ . \tag{9}$$

If $\mathbf{b}$ is the orientation of the polarizer and $\angle(\mathbf{b},\mathbf{x}) = \varphi$, then when the half-wave plate is in place, the field operators at sites $2''$ and $2'''$ are given by

$$\hat{E}^{(+)}_{2''}(t) = \frac{\alpha}{2}\left[\sin\varphi\ \hat{E}^{(+)}_{2S}(t) + \cos\varphi\ \hat{E}^{(+)}_{2L}(t)\right] \tag{10}$$

and

$$\hat{E}^{(+)}_{2'''}(t) = \frac{\beta}{2}\left[\cos\varphi\ \hat{E}^{(+)}_{2S}(t) + \sin\varphi\ \hat{E}^{(+)}_{2L}(t)\right], \tag{11}$$

where $\alpha$ and $\beta$ are phase factors.

It is then easy to show, using (1), (3), (4), (5), (6), (9), and (10) and choosing $\phi_1 + \phi_2 = -(\omega_{10} + \omega_{20})\ \Delta T + 2n\pi$ ($n$ is an integer), that the coincidence rate between the detectors at sites 1 and $2''$ is given by

$$R^{c}_{2''1} = k\langle t|\hat{E}^{(-)}_{2''}(t)\ \hat{E}^{(-)}_{1}(t)\ \hat{E}^{(+)}_{1}(t)\ \hat{E}^{(+)}_{2''}(t)|t\rangle = \frac{R_0}{16}\cos^2(\theta-\varphi)\ . \tag{12}$$

Similarly,

$$R^{c}_{2'''1} = k\langle t|\hat{E}^{(-)}_{2'''}(t)\ \hat{E}^{(-)}_{1}(t)\ \hat{E}^{(+)}_{1}(t)\ \hat{E}^{(+)}_{2'''}(t)|t\rangle = \frac{R_0}{16}\sin^2(\theta-\varphi)\ . \tag{13}$$

We see from (12) and (13) that, for coincident detection, whenever we have detection at site 1, if $\gamma_2$ follows the direction to 2, it impinges on the polarizer in a polarization state parallel to $\mathbf{c}$, such that $\angle(\mathbf{c},\mathbf{x}) = \theta$. (12) and (13) then follow from Malus' law. We can also easily verify that whenever we have detection at site $1'$, if $\gamma_2$ follows the direction to $2'$, it also impinges on the detector in a state parallel to $\mathbf{c}$. By a similar procedure we also easily verify that whenever we have detection at site $1(1')$, if $\gamma_2$ follows the direction to $2'(2)$, it impinges on the detector (polarizer) in a polarization state parallel to $\mathbf{d}$, such that $\angle(\mathbf{d},\mathbf{x}) = -\theta$. Since $\gamma_1$ and $\gamma_2$ are fairly well localized in space and time [9], these results are totally counterintuitive.

The nonlocal aspects of the experiment I am discussing can be made more evident by comparing the following two situations. In the first, the beam-splitter $H'_1$ is removed. To simplify the argument, we can consider the ideal situation in which all photons are detected. We then easily see that

$$R^{c}_{2''1} = \frac{1}{8}\sin^2\theta\sin^2\varphi \tag{14}$$

and

$$R^{c}_{2''1'} = \frac{1}{8}\cos^2\theta\cos^2\varphi\ , \tag{15}$$

which correspond, respectively, to the possibilities "$\gamma_1$ and $\gamma_2$ following the short paths" and "$\gamma_1$ and $\gamma_2$ following the long paths". In the second situation $H'_1$ is in place. Then, whenever $\gamma_1$ is detected, we know that, if $H'_1$ were not in place, $\gamma_1$ would have been detected either at site 1 or at site $1'$. Thus, $\gamma_2$ must either follow the long or the short path, as when $H'_1$ is not in place, according to the locality assumption, since, it is irrelevant whether $H'_1$ is in place or not. As a consequence, one must have

$$R^{c}_{2''1} = \frac{1}{16}(\sin^2\theta\sin^2\varphi + \cos^2\theta\cos^2\varphi)\ , \tag{16}$$

in strong disagreement with (12). In particular, when $\varphi = \pi/4$, (16) leads to $R^{c}_{2''1} = 1/32$, whilst (12) leads to $R^{c}_{2''1} = (1/16)\cos^2(\theta - \pi/4)$, where $0 \le \theta \le \pi/2$.

As I have emphazised elsewhere [7], the situation in which $\gamma_1$ is detected before $\gamma_2$ can reach the interferometer raises an intriguing point: it seems that $\gamma_2$ would have to be described by two wave packets simultaneously. When $\gamma_1$ is detected before $\gamma_2$ can reach the interferometer, the possibilities corresponding to "both photons following the long paths" and to "both photons following the short paths" remain indistinguishable, and results (12) and (13) are still obtained. (If this were not so, special relativity might be in trouble, since the detections of $\gamma_1$ and $\gamma_2$ are events separated by a space-like interval. Therefore, the order in which they occur depends on the Lorentzian frame in which the experiment is being described. On the other hand, the detection rates must be Lorentz invariant quantities). The packets associated with $\gamma_2$ correspond to the following two possibilities: $(L_1)\gamma_1$ follows path $L_1$; and $(S_1)$ $\gamma_1$ follows path $S_1$. These packets are split at $H_2$, producing four packets. The packet following $L_2$ in possibility $(L_1)$ — packet $(L_2, L_1)$ — interferes with the packet following path $S_2$ in possibility $(S_1)$ — packet $(S_2, S_1)$ — producing a packet (I) in a polarization state different from those that would have occurred, had $\gamma_2$ followed either path $L_2$ or path $S_2$. It is in this packet (I) that $\gamma_2$ is to be found when there is coincident detection. In the experiment that I am discussing, the amplitudes of the packets $(L_2, L_1)$ and $(S_2, S_1)$ depend on the parameter $\theta$. In the previous experiments, one acted either on the polarization [3] or on the phase [4,5] of the correlated photons to induce nonlocal effects. In the present proposal, the action is on the amplitudes. If we were to act also on the phases, polarization states different from those discussed here could be produced.

This experiment could be performed using the recently improved time resolution techniques [10].

# References


[1] J.S. Bell, Physics (Long Island City, NY) **1**, 195 (1964); J.F. Clauser and A. Shimony, Rep. Prog. Phys. **41**, 1881 (1978).

[2] J.F. Clauser, M.A. Horne, A. Shimony, and R.A. Holt, Phys. Rev. Lett. **23**, 880 (1969).

[3] S.J. Freedman and J.F. Clauser, Phys. Rev. Lett. **28**, 938 (1972); A. Aspect, P. Grangier, and G. Roger, ibid. **49**, 91 (1982); W. Perrie, A.J. Duncan, H.J. Beyer, and H. Kleinpoppen, ibid. **54**, 1790 (1985).

[4] M.A. Horne, A. Shimony, and A. Zeilinger, Phys. Rev. Lett. **62**, 2209 (1989); J.G. Rarity and P.R. Tapster, ibid. **64**, 2495 (1990).

[5] J.D. Franson, Phys. Rev. Lett. **62**, 2205 (1989); Z.Y. Ou, X.Y. Zou, L.J. Wang, and L. Mandel, ibid. **65**, 321 (1990); P.G. Kwiat, W.A. Vareka, C.K. Hong, H. Nathel, and R.Y. Chiao, Phys. Rev. A **41**, 2910 (1990).

[6] Z.Y. Ou and L. Mandel, Phys. Rev. Lett. **61**, 50 (1988).

[7] L.C.B. Ryff, Phys. Rev. A **48**, 1020 (1993).

[8] R.J. Glauber, in *Quantum Optics and Electronics*, edited by C. De Witt, A. Bladin, and C. Cohen-Tannoudji (Gordon and Breach, New York, 1965), p.62.

[9] D.C. Burnham and D.L. Weinberg, Phys. Rev. Lett. **25**, 84 (1970); S. Friberg, C.K. Hong, and L. Mandel, ibid. **54**, 2011 (1985); R. Ghosh, C.K. Hong, Z.Y. Ou, and L. Mandel. Phys. Rev. A **34**, 3962 (1986); Z.Y. Ou and L. Mandel, Phys. Rev. Lett. **61**, 54 (1988).

[10] J. Brendel, E. Mohler, and W. Martienssen, Europhys. Lett. **20**, 575 (1992); P.G. Kwiat, A.M. Steinberg, and R.Y. Chiao, Phys. Rev. A **47**, 2472 (1993).

# THE STRONG BELL INEQUALITIES A PROPOSED EXPERIMENTAL TEST

Edward S. Fry

*Physics Department, Texas A&M University*
*College Station, TX 77843*

**Abstract**

All previous experimental tests of Bell inequalities have required additional assumptions. The strong Bell inequalities (i.e. those requiring no additional assumptions) have never been tested. An experiment has been designed that can, for the first time, provide a definitive test of the strong Bell inequalities. Not only will the detector efficiency loophole be closed; but, the locality condition will also be rigorously enforced. The experiment involves producing two $^{199}Hg$ atoms by a resonant Raman dissociation of a mercury dimer ($^{199}Hg_2$) that is in an electronic and nuclear spin singlet state. Bell inequalities can be tested by measuring angular momentum correlations between the spin one-half nuclei of the two $^{199}Hg$ atoms. The method used to make these latter measurements will be described.

## 1 Introduction

Due to low detector efficiencies, previous experimental tests of Bell inequalities have required an auxiliary assumption in order to derive an experimentally testable inequality.[1-5] A new experimental concept has been developed that makes it possible to test the strong Bell inequalities (Bell inequalities without any auxiliary assumptions). It also leads directly to an extension that rigorously enforces locality.

This approach is an experimental realization of Bohm's version of the Einstein-Podolsky-Rosen *Gedankenexperiment*.[3, 6] Instead of photon pairs, it involves measurements of the correlations between angular momentum components of two atoms (actually spin one-half nuclei) of the isotope $^{199}Hg$. A brief description of the proposed experiment was recently published,[7] and a very detailed discussion has also been provided.[8]

In general, the measurement of components of spin suggests the use of Stern-Gerlach magnets. For spin one-half particles, there are two possible projections, + ("spin-up") and – ("spin-down"), of the spin on the axes of the magnets. As indicated in Figure 1, the magnetic field gradient deflects each spin one-half particle into one of two detectors depending on the projection of its spin on the magnet axis. To measure a spin component of a particle in any specified direction, one simply rotates the axis of the corresponding magnet to that direction. However, such an approach is unsuitable in the present work

for two reasons. First, to enforce Einstein locality, it would be necessary to rotate a magnet to an arbitrary direction in a time short compared to the time it takes light to travel from one magnet to the other - a few nanoseconds. This appears to be physically impossible. Second, based on available magnetic fields and the magnitude of the nuclear magnetic moment, the deflection produced by $^{199}$Hg nuclear spins is so small as to preclude this approach.

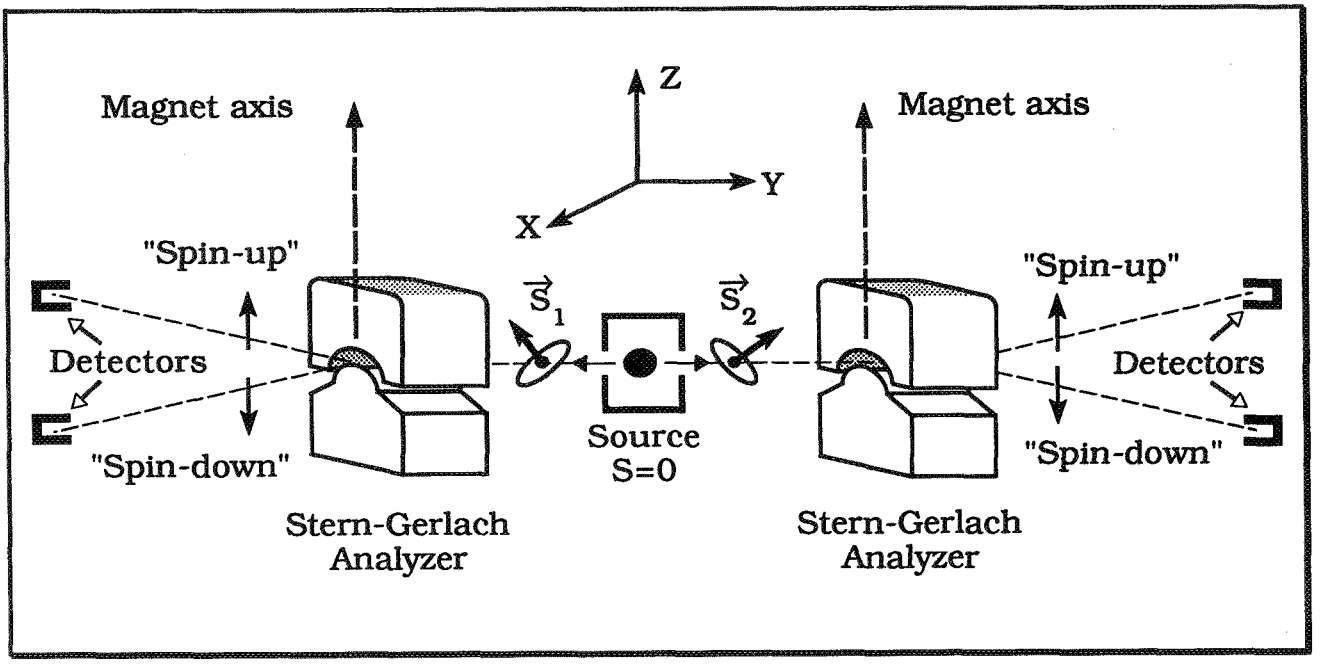


FIG. 1. Schematic of a Stern-Gerlach apparatus for measuring spin correlations. The diagram assumes spin one-half particles and the magnets are oriented for measurements of the spin components of both particles in the Z direction.

Other approaches to the measurement of spin components are possible. For example, a Bell inequality involving proton spin correlations has been tested using proton-proton scattering to determine the spin components.[9] However, this type of approach requires several auxiliary assumptions.

Efficient detection of atoms is combined with spin analysis in the approach to be described here. This approach takes advantage of the hyperfine structure interaction in $^{199}$Hg atoms in order to select nuclear spin components via electric dipole transitions. Detection efficiency is sufficiently high to close that loophole. And finally, this approach permits a very rapid change in the direction of the measurement of spin components; hence Einstein locality can be enforced.

## 2 Overview of the Proposed Experiment

The $^{199}$Hg atoms are produced by a stimulated Raman excitation to a dissociating state of the $X^1\Sigma_g^+$ ground state of a $^{199}$Hg dimer. The total electron and the total nuclear spin angular momenta are both zero in the initial rotational state of the Hg dimers, and are not changed in the dissociation process. The two mercury atoms resulting from the dissociation are both in $^1S_0$ ground states. Since the electronic

angular momentum is J=0 and the nuclear spin of $^{199}$Hg is I=1/2, each ground state atom therefore has a total angular momentum F=1/2. The component of total angular momentum (which is therefore the component of nuclear spin) in any given direction is measured by orienting excitation laser beams at 253.7 nm in that direction and using polarization selective excitation of one of the Zeeman sublevels. For left circularly polarized excitation, only atoms whose component of angular momentum, $M_F$=+1/2, in the direction of laser beam propagation are excited. Similarly, right circularly polarized light only excites atoms with $M_F$=-1/2. Excited atoms are photoionized via an auto-ionizing state using a laser at 197.3 nm. The resulting photoelectrons and ions are detected using Channeltron electron multipliers. Assuming a mercury atom has been detected if EITHER an electron OR an ion is observed, then the overall detection efficiency for the Hg atoms is greater than 96%. Figure 2 shows a schematic of the experiment indicating the relative directions of the dimer, atom, and laser beams.

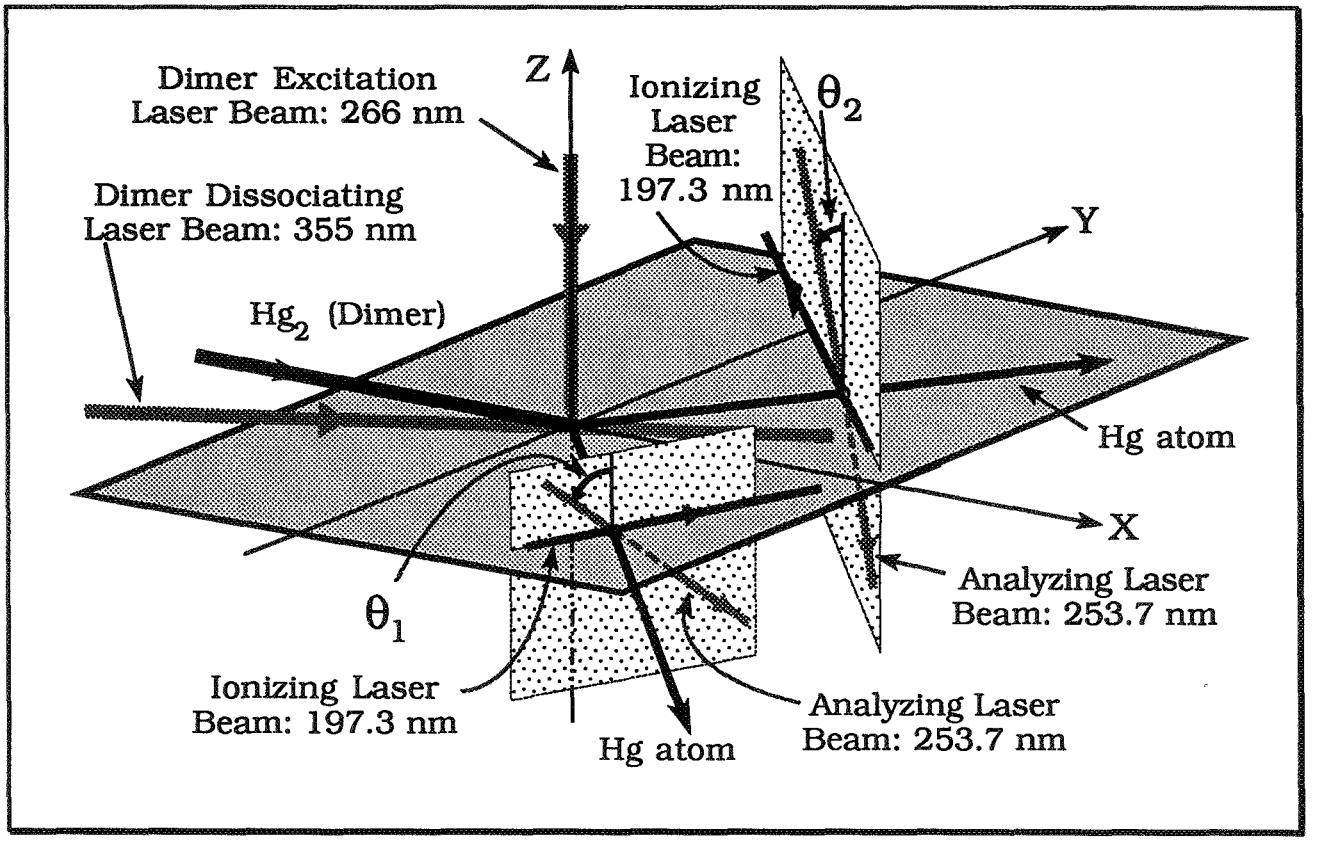


FIG. 2. Schematic of the experiment showing the direction of the mercury dimer beam together with a pair of the dissociated atoms and their respective detection planes. Relative directions of the various laser beams are also shown.

Rates for simultaneous detection (coincidence rates) of the two atoms are measured for components of their angular momenta in the directions $\theta_1$ and $\theta_2$, respectively (i. e. in the directions of the excitation laser beams). A set of four angles can be chosen that give a maximum violation of the strong Bell inequality.[7, 8] This experiment also lays the foundation for an experiment that enforces locality

since a combination of a Pockels cell and a beamsplitting polarizer can be used to stochastically change the direction of the exciting laser beams on the nanosecond time scale.

# 3 Measurement of the Nuclear Spin Components

Figure 3 shows the relevant energy levels of the mercury atom,[10] and the corresponding transitions at 253.7 nm for spin analysis and at 197.3 nm for detection via photoionization. The first transition is from the $(6s^2)\,6^1S_0$ $(F = \frac{1}{2})$ ground state (level 1) to the $(6s6p)\,6^3P_1$ $(F = \frac{1}{2})$ state (level 2); the second transition is from level 2 to the $(6p^2)\,^3P_0$ autoionizing state (level 3). Atom detection is via both the resulting ion and the photoelectron.

Assuming a Fano profile for the autoionizing transition, a calculated value for its oscillator strength, and a measured value for its width, a theoretical value of $\approx 2.3\times10^{-14}$ cm$^2$ is obtained for the peak cross-section.[7, 8] This is an unusually large cross-section, but is consistent with measured cross-sections for analogous transitions in Cd.[11] Since both transitions are so strong, laser pulse energies of only 60 μJ and 250 μJ, respectively, are sufficient to ionize all the atoms in a few nanoseconds.

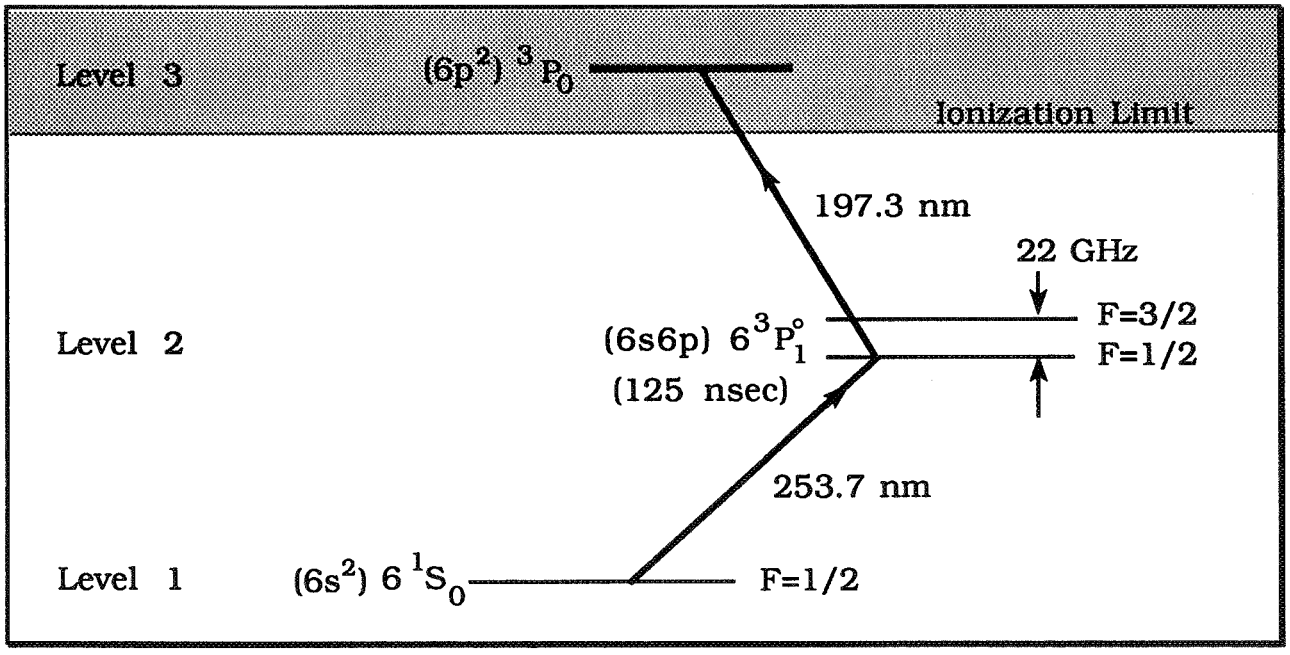


FIG. 3. Relevant energy levels of the mercury atom,[10] and the corresponding transitions for detection.

As shown in Figure 2, the laser beams for spin analysis have a wavelength of 253.7 nm and lie in planes perpendicular to the direction to the source. They are at angles $\theta_1$, $\theta_2$ to the +Z-axis. The angles $\theta_1$, $\theta_2$ of these laser beams define the directions in which each atom's angular momentum components is observed.

If we choose some arbitrary direction as the quantum axis for our system, then the quantum numbers for the two components of angular momentum in that direction are $M_F=\pm1/2$ (for an F=1/2 ground state

$^{199}$Hg atom). If the 253.7 nm laser beam is propagating in the direction of the quantum axis and has right circular polarization ($\sigma$+), then $M_F$ must increase by one in the transition. Thus, only ground state atoms for which the projection of the angular momentum in the direction of laser beam propagation is $M_F$=-1/2 can be excited to the $6^3P_1^\circ$ $(F = 1/2)$ state and ionized; see Figure 4. Similarly, for left circular polarization, only atoms with $M_F$=+1/2 are excited and ionized. In summary, by choosing an arbitrary direction and using a circularly polarized excitation laser, a Hg atom with either component of angular momentum in that direction can be selectively detected.

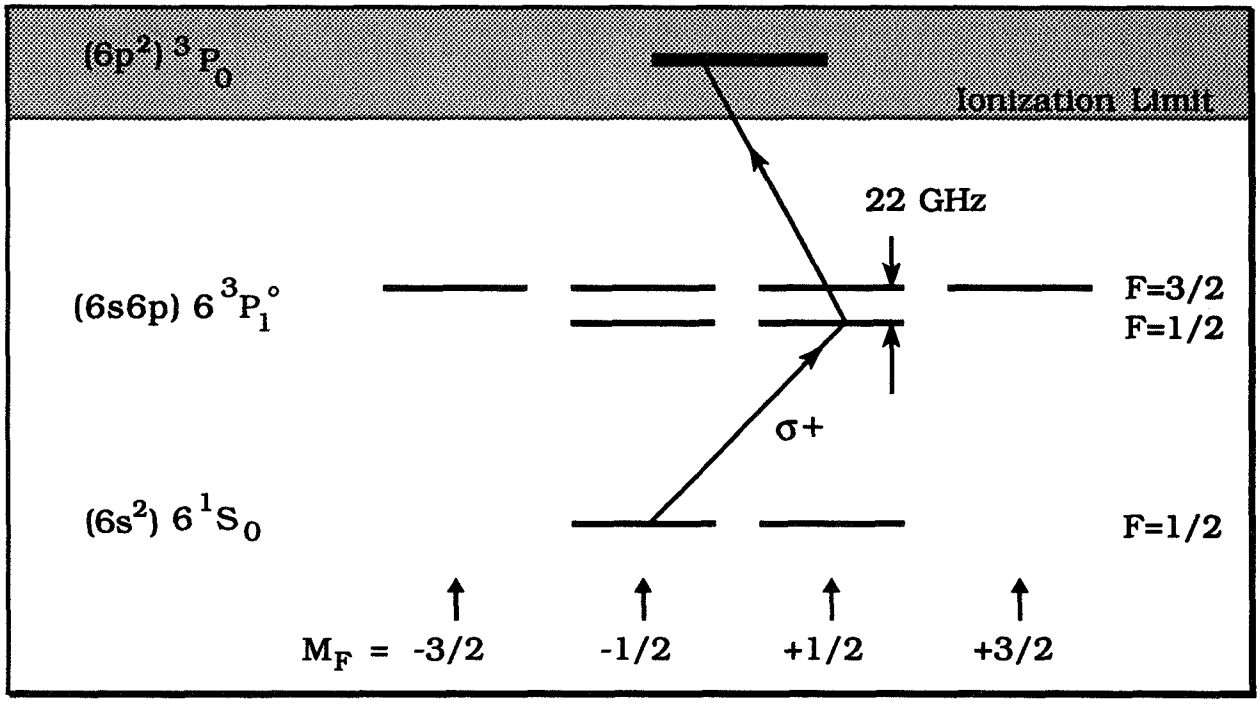


FIG. 4. Analysis scheme with right circularly polarized light. Since $M_F$ must increase by 1 in the transition, only ground state atoms with $M_F$=-1/2 can reach the $6^3P_1^\circ$ $(F = 1/2)$ state.

# 4 Summary

The use of electric dipole transitions to measure the component of nuclear spin of $^{199}$Hg in an arbitrary direction has been described. Its application to a definitive experimental test of the previously untested strong Bell inequalities is discussed. This novel approach makes it feasible to rigorously enforce Einstein locality.

# 5 Acknowledgement

This research was supported by the Robert A. Welch Foundation grant No. A-1218 and by the National Science Foundation grant PHY-9221038. The author also thanks Dr. Shifang Li for many helpful discussions and suggestions.

# 6 References


[1] C. O. Alley and Y. H. Shih, in *Proc. 2nd Int. Symp. Foundations of Quantum Mechanics*, 47 (Tokyo, 1987).

[2] A. Aspect, J. Dalibard, and G. Roger, Phys. Rev. Lett. **49**, 1804 (1982).

[3] J. F. Clauser and A. Shimony, Rep. Prog. Phys. **41**, 1881 (1978).

[4] Z. Y. Ou and L. Mandel, Phys. Rev. Lett. **61**, 50 (1988).

[5] J. G. Rarity and P. R. Tapster, Phys. Rev. Lett. **64**, 2495 (1990).

[6] D. Bohm, *Quantum Theory*, (Constable, London, England, 1954).

[7] E. S. Fry, in *Proceedings of the International Conference on Lasers '92*, 621 (Houston, TX, 1993).

[8] E. S. Fry, submitted to Phys. Rev. A (1994).

[9] M. Lamehi-Rachti and W. Mittig, Phys. Rev. D **14**, 2543 (1976).

[10] C. E. Moore, *Atomic Energy Levels*, Volume III, Circular 467 (National Bureau of Standards, Washington, DC, 1958).

[11] K. Miyazaki, T. Watanabe, and K. Fukuda, J. Phys. Soc. Japan **40**, 233 (1976).

# ON THE NONLOCAL PREDICTIONS OF QUANTUM OPTICS

Trevor.W.Marshall
Department of Mathematics, University of Manchester, Manchester, U.K.

Emilio Santos and Antonio Vidiella-Barranco
Departamento de Física Moderna, Universidad de Cantabria, Santander, Spain

We give a definition of locality in quantum optics based upon Bell's work, and show that locality has been violated in no experiment performed up to now. We argue that the interpretation of the Wigner function as a probability density gives a very attractive local realistic picture of quantum optics provided that this function is nonnegative. We conjecture that this is the case for all states which can be realized in the laboratory. In particular, we believe that the usual representation of "single photon states" by a Fock state of the Hilbert space is not correct and that a more physical, although less simple mathematically, representation involves density matrices. We study in some detail the experiment showing anticorrelation after a beam splitter and prove that it naturally involves a positive Wigner function. Our (quantum) predictions for this experiment disagree with the ones reported in the literature.

## 1. What is locality ?

The purpose of this paper is to investigate the conditions for the violation of locality in quantum optics. We shall show that these conditions are rather stringent and have not been fulfilled in those experiments where violations of locality have been claimed.

The first problem is that several, quite different, meanings have been given to the word "locality" (or "nonlocality"). In fact, there are people claiming that quantum mechanics never predicts nonlocality because it forbids sending signals at superluminal velocity. On the other hand, some authors include auxiliary hypotheses, related to the Clauser et al. [1] "no-enhancement" assumption, as a part of the concept of locality. With such a definition there are a lot of locality violations in the predictions of quantum optics. Here we shall use something intermediate between these extremes. We shall define locality in the following form based on Bell's work.

We should consider an EPR (Einstein-Podolsky-Rosen) experiment where some correlation is measured between properties, like spin, of two separated particles. Locality is satisfied if single probabilities ( $p_3$, $p_4$ ) and coincidence probabilities ($p_{34}$ ) can be obtained from a local hidden variables (LHV) model, i. e., if there are hidden variables, collectively represented by $\lambda$, which determine the above probabilities by means of

integrals of the form

$$p_3(\theta_1) = \int W(\lambda)\, P_3(\lambda,\theta_1)\, d\lambda\,, \quad p_4(\theta_2) = \int W(\lambda)\, P_4(\lambda,\theta_2)\, d\lambda, \tag{1}$$

$$p_{34}(\theta_1,\theta_2) = \int W(\lambda)\, P_3(\lambda,\theta_1)\, P_4(\lambda,\theta_2)\, d\lambda\,, \tag{2}$$

the functions $P_3$, $P_4$ and W fulfilling the conditions :

Normalization: $$\int W(\lambda)\, d\lambda = 1 \tag{3}$$

Positivity: $$W(\lambda) \geq 0,\ P_3(\lambda,\theta_1) \geq 0,\ P_4(\lambda,\theta_2) \geq 0 \tag{4}$$

Boundedness: $$P_3(\lambda,\theta_1) \leq 1\,,\ P_4(\lambda,\theta_2) \leq 1. \tag{5}$$

## 2. How to test locality ?

A test of locality involves performing an experiment where quantum optics predicts the violation of some genuine Bell inequality. Genuine means that the inequality can be derived from the conditions (1) to (5) alone, without adding auxiliary assumptions like "no-enhancement" :

$$P_3(\lambda,\theta_1) \leq P_1(\lambda)\,,\ P_4(\lambda,\theta_2) \leq P_2(\lambda) \quad \text{not assumed.} \tag{6}$$

Here $P_1(\lambda)$ and $P_2(\lambda)$ mean detection probabilities when no selector (e.g. polarizer) is inserted between the source and the detector.

Then, we stress that it is impossible to test locality in experiments measuring coincidences alone. In fact, it has been possible to construct a general LHV model giving the same coincidence probabilities as quantum optics for every EPR-type experiment in which only coincidences are measured [3]. Genuine Bell inequalities, therefore, should necessarily involve both singles and coincidences. In this respect, we do not agree with the usual statement that *there are loopholes in the experiments* to disprove LHV theories, because the word "loophole" suggests that the experiments have only practical difficulties. The fact is that these experiments have not been designed to test genuine Bell inequaltities, but inequalities involving additional assumptions, like (6). Therefore they can only refute restricted families of LHV models, namely those fulfilling those assumptions.

We also point out that a necessary condition [4] for the violation of locality is the existence of an entangled quantum state, i.e., a nonfactorable wavefunction. There are some experiments, where violations of locality have been claimed, which do not even fulfil this condition (e.g. the state vector (2) of Ref. 5 is factorable).

## 3. Single photon interferometry

The simplest "entangled state" in quantum optics appears in experiments of interference of a single photon (see Fig. 1) [6]. In an experiment of this class, a photon $\nu_2$ is sent to a beam splitter (represented by a dashed line in Fig.1). The state of the radiation field after the beam splitter is

$$|\psi\rangle = 1/\sqrt{2}\,\{\,|0\rangle|1\rangle + |1\rangle|0\rangle\,\} = 1/\sqrt{2}\,\{a_r^+ + a_t^+\}\,|0\rangle|0\rangle\,, \qquad (7)$$

which exhibits entanglement between a "single photon state" and the "vacuum state". In the anticorrelation experiment, represented in Fig. 1, no coincidences are predicted between the detectors $PM_r$ and $PM_t$, which seems to prove that the photon goes undivided into one channel.

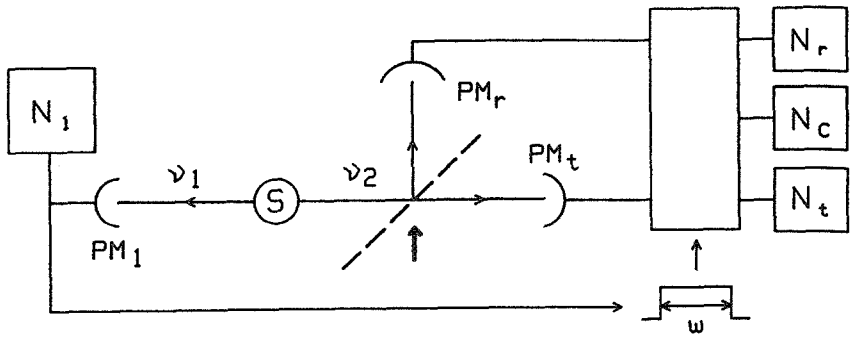


FIG. 1. Triggered experiment [6]. Atoms in the source S produce pairs of photons. The detection of the first photon of the cascade produces a gate during which the photomultipliers, $PM_t$ and $PM_r$, are active. The probabilities of the detection during the gate are $p_t = N_t/N_1$ and $p_r = N_r/N_1$ for singles and $p_c = N_c/N_1$ for coincidences, $N_j$ being the detection rates.

In the recombination experiment the two beams, produced at the beam splitter, are recombined at another beam splitter where they arrive with a different phase ( which may be changed by means of the phase shifter) and the detection probability at one of the outgoing channels depends on that phase difference. The standard way to "explain" this phenomenon is to say that there are two possible routes for the photon and that, according to quantum theory, "possibilities interfere". However, this is not a scientific explanation (at most, it may be considered as a poetic sentence or a practical rule). Later on we shall see how the phenomenon may be *really explained* using the Wigner representation of quantum optics.

## 4. The Wigner representation as a local hidden variables model

In order to understand the meaning of entanglement in quantum optics, we calculate the Wigner function of (7) and we obtain

$$W = N\,(\,2\,|\,\alpha_t + \alpha_r\,|^2 - 1\,)\,\exp(\,-\,2\,|\,\alpha_t\,|^2 - 2\,|\,\alpha_r\,|^2\,),\ N = \text{normalization} \qquad (8)$$

This function does not factorize, but this presents no problem; we may interpret W as a joint probability distribution for the amplitudes $\alpha_t$ and $\alpha_r$. We see that, in the Wigner representation, entanglement is just correlation, an obviously classical concept. Of course, there is another very well known problem, namely that (8) is not positive definite, as a probability should be. We shall return to this difficulty in detail later on, but for the moment let us ignore it proceed as if W were a genuine (non-negative definite)

probability.

In the Wigner representation fields propagate like in classical optics. In fact, the equations involving creation or annihilation operators become, in the Wigner representation, similar equations between field amplitudes:

$$a_t^+ = 1/\sqrt{2}\ (\ a_1^+ + i\ a_0^+) \quad \rightarrow \quad E_t = 1/\sqrt{2}\ (\ E_1 + i\ E_0),$$

$$a_r^+ = 1/\sqrt{2}\ (\ a_0^+ + i\ a_1^+) \quad \rightarrow \quad E_r = 1/\sqrt{2}\ (\ E_0 + i\ E_1). \qquad (9)$$

The picture that emerges is that of light as pure (Maxwellian) waves, but with a real zeropoint (background) radiation. Then, in the single photon interference experiment there is always "something" in both channels, because both $\alpha_t \neq 0$ and $\alpha_r \neq 0$.

Anticorrelation can be understood as a result of the interference between signal and zeropoint at the beam splitter. In fact, as shown by Eq. (9), the amplitudes of the fields in the outgoing channels contain a part coming from the signal (channel 1) and a part coming from the zeropoint (channel 0, arrow from below in Fig. 1). The superposition of amplitudes at channels r and t should produce interference, which will depend on the relative phases of the incoming channels. However, in any case the interference will be constructive in one channel and destructive in the other one, by conservation of energy. Now, quantum optics predicts that detectors are only sensitive to the intensity above the zeropoint level, which *explains* why there is detection only in one channel. Detection sensitive only to the intensity above the zeropoint level follows from the the normal ordering prescription of quantum optics. In the Wigner representation normal ordering becomes a subtraction of the zeropoint, as shown by the equality

$$a^+a = 1/2(a^+a + a\ a^+) - 1/2 \ \rightarrow \ |\ \alpha\ |^2 - 1/2 \qquad (10)$$

In this way we have a transparent picture of the anticorrelation, without any need of "photons". The explanation of the interference in the recombination experiment is rather easy, because we are dealing with a purely wave theory of radiation. Interference is produced between (correlated) signal and zeropoint at the second beam splitter. What we want to emphasize is that the only problem of the Wigner function is the lack of positivity, not entanglement. If the Wigner function of an entangled state is nonclassical, it is not because it contains correlation, but because it is not positive definite.

## 5. The meaning of enhancement and other nonclassical effects

Now it is easy to understand why "no-enhancement" (see Eq. (6) ) is violated. In fact from Eq. (7) it follows that

$$I_t = 1/2\ [\ I_1 + I_0 + 2\ \mathrm{Re}(E_1\ E_0^*)], \qquad I_j = |\ E_j|^2\ , \qquad (11)$$

and this intensity may be greater than the intensity $I_1$ of the incoming signal, if the relative phase of $E_1$ and $E_0$ is zero. A similar phenomenon happens at a polarizer. It is enough to assume that the detection probability increases monotonically with the incoming intensity to explain the origin of

"enhancement".

The existence of a real zeropoint electromagnetic radiation is, therefore, crucial for the explanation of enhancement. On the other hand, all LHV theories in which "no-enhancement" holds true have been refuted by the performed experimental tests of Bell's inequalities [7-9]. Consequently we may conlcude that LHV theories not involving zeropoint field are the ones actually refuted by these experiements. If one is fond of LHV theories, one should therefore look for theories involving a real zeropoint. It is very good that the Wigner represention of quantum optics, with the probabilistic interpretation above suggested, belongs to this class.

In the wave interpretation of quantum optics that we are suggesting (taking a positive Wigner function as a probability distribution) the interpretation of the nonclassical states of light is also transparent. According the usual definition, "nonclassical states of light" are those not having a positive Glauber-Sudarshan (P) representation. That is, for nonclassical states, the P-representation either does not exist or it is not non-negative definite. In contrast, any classical state of light has a positive P-representation, $P(\{\alpha_j\})$, which may be interpreted as a probability distribution of the amplitudes of the normal modes of the radiation. If we assume that there is a zeropoint radiation having a probability distribution $W_0(\{\beta_j\})$, in addition to the classical radiation, the question arises: What is the probability distribution of the full radiation present?. The answer is obvious, in every normal mode the total amplitude, $\gamma_j$, will be the sum of both amplitudes, i.e. $\gamma_j = \alpha_j + \beta_j$. Then the probability distribution of the full radiation will be

$$W(\{\gamma_j\}) = \int P(\{\alpha_j\})\ W_0(\{\gamma_j-\alpha_j,\})\ d^{2N}\alpha\ . \qquad (12)$$

This is just the Wigner function, which is known to be related to the P-function by Eq.(12). Therefore, classical states of light are those where the zeropoint is not modified; some additional radiation is added on top of the zeropoint. Consequently, "nonclassical states" are those where the zeropoint *is* modified.

## 6. Solution of the positivity problem

A very simple solution of the positivity problem, the problem that the Wigner function is not positive definite for all quantum states of light, is to sssume that only states with a positive Wigner function may be manufactured in the laboratory. That is, we assume that quantum states with a negative Wigner function are just mathematical constructions useful as intermediate steps in some calculations. Two main objections may be put to this assumption, namely that some of these forbidden states have been actually produced, e.g. single photon states, and that there are other representations in quantum optics, e.g. the Q -or positive P- representation, which are always positive and therefore better candidates than the Wigner function. We shall devote the remainder of the paper to answering the first objection. The answer to the second is that the Wigner function has a number of properties that make it the only good candidate. To quote just one, it is the only phase-space distribution which evolves according to a classical Liouville equation for any Hamiltonian quadratic in the creation and

annihilation operators. The Liouville equation corresponds to the classical Hamiltonian obtained from the quantum one by first putting all operators in symmetrical ordering (by using the standard commutation relations) and then replacing the operator $a_j$ ( $a_j^+$ ) by the classical amplitude $\alpha_j$ ( $\alpha_j^*$ ). Then, the amplitude $\hbar\ \alpha_j^*$ will be the canonical momentum conjugated to the coordinate $\alpha_j$.

Now for the first objection. In the first place we point out that we do not propose to interpret the Wigner function throughout quantum mechanics as a probability distribution in phase space. For instance, we do not apply it to the electrons in an atom. We make the proposal just for the electromagnetic field. In contrast with what happens in particle quantum mechanics, in quantum optics most of the states of the radiation have a positive Wigner function. For instance, this is the case for the vacuum, the coherent states, the chaotic state (thermal light) and even the squeezed states. Amongst the usual states of light, practically only Fock states (number states) have a non-positive Wigner function. Then the question arises: can pure Fock states really be produced in the laboratory?. What we conjecture is that Fock states are never produced as pure states, always as mixtures having a positive Wigner function. For instance, if we have a beam of "single-photon signals" such that within a time window w the probability of a signal is $p << 1$, then the state corresponding to the window is not the single photon state $| 1>$, but the mixture represented by the density matrix $\rho = (1 - p) | 0> < 0 | + p | 1> < 1 |$. The associated Wigner function is positive provided $p < 1/2$. If $p > 1/2$ the probability of having more than one photon within the window becomes relevant and again the Wigner function is positive. It may be argued that, with some effort, it is possible to monitor the single photon signals in such a way that the probability of having one in a time window is close to one whilst the probability of having more than one is negligible. We shall return to this later on.

## 7. Positivity of the Wigner function in parametric down conversion

There is a general argument showing that the Wigner function may be taken as positive in all experiments involving parametric down conversion. These experiments involve one or several nonlinear crystals where, in quantum language, the process takes place of converting a single photon of frequency $\omega_0$ into two photons of frequencies $\omega_1$ and $\omega_2 = \omega_0 - \omega_1$. The quantum Hamiltonian contains terms with an annihilation operator of the first type of photons and two creation operators. However, in all practical calculations the incoming beam (the pumping) is taken as classical, and the annihilation operator is replaced by a classical amplitude. Consequently, the full Hamiltonian becomes quadratic in the operators of creation and destruction of photons.

Now, it is well known that the Wigner function evolves according to a classical Liouville equation whenever the Hamiltonian is quadratic. On the other hand, the Liouville equation preserves positivity, in the sense that if the Wigner function is positive at a time then it remains positive at any later time. As the initial state (before switching on the pumping) is the vacuum, whose Wigner function is positive, the Wigner function remains positive forever. We should point out that the action of devices like lenses,

mirrors, beam splitters, etc. is linear and, consequently, all of them preserve the positivity of the Wigner function.

It is possible to argue that, strictly speaking, the Hamiltonian associated with the nonlinear crystal is cubic rather than quadratic, and a cubic Hamiltonian does not guarantee the positivity of the Wigner function. This is true, but then the "nonclassical" effects due to negative values of the Wigner function should be relevant in those experiments where a clear disagreement is obtained with the (approximate) quantum predictions obtained using a classical pumping. No experiment of this type has been performed to our knowledge.

## 8. State of the beam produced in an atomic source

In the following we investigate the positivity of the Wigner function in experiments involving photon beams produced by an atomic source. As a typical example we consider the experiment by Grangier et al. [6], represented in Fig. 1 where the authors claimed to have produced single photon signals, which seems to imply negative Wigner functions.

For simplicity we consider atoms with two states: $|g\rangle$ (ground) and $|e\rangle$ (excited). If at time t=0 we have $|e\rangle |0\rangle$ (excited atom plus radiation vacuum), then the evolution gives (to first order perturbation theory)

$$|\psi(t)\rangle = N \{|e\rangle + |g\rangle A^+(t)\}|0\rangle ; \qquad A^+(t) \equiv \Sigma_j c_j(t) \exp[-ik_j.x] a_j^+ \qquad (13)$$

where N is a normalization constant, j labels the radiation mode and $A^+(t)$ is the creation operator of a (localized, multimode) photon .

If we consider many atoms, which arrive at the source, are excited there (by the action of a laser) and decay at times $t_1, t_2, \ldots t_s, \ldots$, we should represent the atomic beam by the state vector

$$|\psi\rangle = N \Pi_s \{ |e_s\rangle + |g_s\rangle A^+(t-t_s) \} |0\rangle \qquad (14)$$

If the state of the outgoing atoms are not controlled, (14) is not the correct representation of the physical situation. In fact, we must take the partial trace of $\rho = |\psi\rangle\langle\psi|$ over the atomic states, which leads to

$$\rho = N \{ |0\rangle\langle 0| + \Sigma_s [A^+(t-t_s) |0\rangle\langle 0| A(t-t_s)] +$$

$$\Sigma_s \Sigma_r [A^+(t-t_s) A^+(t-t_r) |0\rangle\langle 0| A(t-t_r) A(t-t_s)] + \ldots \} \qquad (15)$$

Furthermore, if the emission times are not controlled, we must average over the times $t_1, t_2, \ldots$

After some algebra [11], we obtain that the final density matrix is

$$\rho_{\text{chaotic}} = \Pi_j \{ \Sigma_{nj} \bar{n}_j^{n_j} (1 + \bar{n}_j)^{-n_j-1} |n_j\rangle\langle n_j| \} \qquad (16)$$

which represents chaotic light, no matter how weak is the beam. The average photon number in mode j, $\bar{n}_j$, is related to the coefficient $c_j$ .Essential for

the result (16) is to take into account the interference between "photons" coming from different atoms.

It is interesting that the Wigner function of (16) is positive definite, a well known property of chaotic light.

The quantum predictions for the correlation and recombination experiments can be easily obtained. The recombination experiment shows interference with 100% visibility, which is not strange because the state (16) corresponds to "classical" light that can be treated by standard wave optics. The correlation experiment gives for the ratio of the coincidence probability to the product of singles:

$\alpha \equiv p_{coinc.} (p_r\, p_t)^{-1} = 2$ if detection window << lifetime of excited atom

$\alpha \equiv p_{coinc.} (p_r\, p_t)^{-1} = 1$ if detection window >> lifetime of excited atom

For intermediate situations we get values of $\alpha$ between 0 and 1. This result can be also explained by classical optics, as is well known since the early work of Brown-Twiss [10], who showed experimentally the photon bunching properties (i.e., $\alpha > 1$ ) of chaotic light.

## 9. "Single photon signals" in an atomic beam

The procedure used by Grangier et al. [6] in order to manufacture single photon signals was to monitor the photons by detecting them in coincidence with partner photon emitted by the atom in a cascade. Of course, our two state model for the atom is no longer adequate because a cascade implies at least three atomic states. However, it is still appropriate to represent the state of the beam by Eq.(15) provided that, in addition to taking the partial trace of the density matrix over the atomic states, we average over all emission times except one, say $t_0$.

We get a "single photon signal" superimposed to the chaotic light, which may be represented by the density matrix

$$\rho_{single\ photon} = N \{ \rho_{chaotic} + A^{+}(t-t_0)\, \rho_{chaotic}\, A(t-t_0) \} \qquad (17)$$

The interesting result is that the Wigner function of (17) is positive.

A straightforward but lengthy calculation[11] gives the quantum prediction for the commented experiments. With the parameters of the actual experiment [6] ( that is a coincidence window about twice the atomic lifetime) we predict that, when the beam is very intense, the "single photon" effect is lost and we get the asymptotic value $\alpha \rightarrow 1.57$ (pure chaotic light). In the performed experiment[6] values $\alpha > 1$ are not observed because, in the actual experimental conditions, the spacial coherence in the detector is lost[12]. However, we think that rather modest improvements of the apparatus will allow observing our prediction of interference between photons emitted by different atoms[11].

## 10. Discussion

We have shown that the interpretation of the Wigner function as a probability distribution provides a very attractive local realistic view of quantum optics. The main difficulty for this interpretation is the fact that the Wigner function is not positive definite for some quantum states. We conjecture that all states actually realizable in the laboratory have a positive Wigner function. In particular we have shown that this is the case for two typical situations where it is claimed that "single photon states" are produced, namely parametric down conversion and light beams produced by a (weak) atomic source. In the second case we argue that the correct representation of the light beam is by means of a density matrix, rather than a pure quantum state. We do not accept the so-called ignorance interpretation of the density matrix, that is as a probability distribution on the set of pure quantum states. On the contrary, we assume that most of the pure quantum states are not physical states.

Even if the above conjecture is correct, and the Wigner function of all physical states of light is nonnegative, some problems remain. We do not understand yet the processes of emission and detection of light or, more generally, the interaction of light with atoms. That is, we do not have a local realistic theory of atoms. In particular, we do not claim to interpret the Wigner function of the electrons in the atom as a probability distribution.

## Acknowledgements

We acknowledge financial support of DGICYT Project No. PB-92-0507 (Spain)

## References

1. J. F. Clauser and M. A. Horne, Phys. Rev. D **10**, 526 (1974)
2. J. S. Bell, Physics (N.Y.) **1**, 195 (1964)
3. E. Santos, Phys. Rev. A **46**, 3646 (1992)
4. V. Capasso, D. Fortunato and F. Selleri, Int. J. Mod. Phys. **7**, 319 (1973)
5. Z. Y. Ou and L. Mandel, Phys. Rev. Lett. **61**,50 (1988)
6. P. Grangier, G. Roger and A. Aspect, Europhys. Lett. **1**, 173 (1986)
7. J. F. Clauser and A. Shimony, Rep. Prog. Phys. **41**, 1881 (1978)
8. A. Aspect, P. Grangier and G. Roger, Phys. Rev. Lett. **47**, 460 (1981); **49**, 91 (1982); A. Aspect, J. Dalibard and G. Roger, Phys. Rev. Lett. **49**, 1804 (1981)
9. J. G. Rarity and P. R. Tapster, Phys. Rev. Lett. **64**, 2495 (1990)
10. R. Hanbury-Brown and R. Q. Twiss, Proc. Roy. Soc. A **242**, 300 (1957); **243**, 291 (1957)
11. T. W. Marshall, E. Santos and A. Vidiella-Barranco, to be published.
12. P. Grangier. Private communication.

# A Loophole-Free Bell's Inequality Experiment

Paul G. Kwiat, Aephraim M. Steinberg, and Raymond Y. Chiao
*Department of Physics, U.C. Berkeley*
*Berkeley, CA 94720*

Philippe H. Eberhard
*Lawrence Berkeley Laboratory, U.C. Berkeley*
*Berkeley, CA 94720*

**Abstract**

The proof of Nature's nonlocality through Bell-type experiments is a topic of long-standing interest. Nevertheless, no experiments performed thus far have avoided the so-called "detection loophole," arising from low detector efficiencies and angular-correlation difficulties. In fact, most, if not all, of the systems employed to date can never close this loophole, even with perfect detectors. In addition, another loophole involving the non-rapid, non-random switching of various parameter settings exists in all past experiments. We discuss a proposal for a potentially loophole-free Bell's inequality experiment. The source of the EPR-correlated pairs consists of two simultaneously-pumped type-II phase-matched nonlinear crystals and a polarizing beam splitter. The feasibility of such a scheme with current detector technology seems high, and will be discussed. We also present a *single*-crystal version, motivated by other work presented at this conference.

In a separate experiment, we have measured the absolute detection efficiency and time response of four single-photon detectors. The highest observed efficiencies were $70.7 \pm 1.9\%$ (at 633 nm, with a device from Rockwell International) and $76.4 \pm 2.3\%$ (at 702 nm, with an EG&G counting module). Possible efficiencies as high as 90% were implied. The EG&G devices displayed sub-nanosecond time resolution.

## 1 Introduction

It is now well known that quantum mechanics (QM) yields predictions which are inconsistent with the seemingly innocuous concepts of locality and reality. This was first shown by Bell in 1964 [1, 2] for the case of two quantum-mechanically entangled particles, e.g., particles in a singlet-like state, which do not possess definite polarizations even though they are always orthogonally polarized. As implied by Einstein, Podolsky, and Rosen (EPR) [3], it is straightforward to construct local realistic models that explain certain features predicted by QM (e.g., the total anti-correlation between detectors measuring the same polarization component of the two particles). The quantum mechanical contradiction with local realism becomes apparent only by considering situations of non-perfect correlations (i.e., measuring the polarization components at intermediate, non-orthogonal angles). More recently, Greenberger, Horne, and Zeilinger (GHZ) [4] and Mermin [5] have shown that QM and local realism are incompatible even at the level of perfect correlations,

for certain states of three or more particles. Hardy has also presented a clever gedanken experiment using electron-positron annihilation to achieve a contradiction with local realism without the need for inequalities [6], and has recently proposed an optical analog which may allow a feasible experimental implementation [7]. Unfortunately, none of these ingenious extensions and generalizations of the work of Bell reduces the experimental requirements for a completely unambiguous test. In fact, all of them seem to mandate even stronger constraints on any real experiment than do the original two-particle inequalities. One exception is the recent discovery that the detection efficiency requirement can be reduced by employing a state of two particles that are not maximally-entangled, i.e., with an unequal superposition of the two terms [8].

Experimental tests of Bell's inequalities have been extended to new systems, some relying on energy-time or phase-momentum entanglement [9-12]; nevertheless, regardless of the type of entanglement employed, *no test of Bell's inequalities to date has been incontrovertible*, due to several loopholes which severely reduce the true impact such an experiment might yield. One of these, the angular correlation problem, has essentially been solved by turning to down-conversion light sources over cascade sources, leaving the fast-switching loophole and the detection loophole. The former concerns the space-like separation of the different parts of the experiment. Clearly, no claims about nonlocality can be made if the pre-detector analyzers are varied so slowly that a signal traveling at the speed of light could carry the analyzer-setting information back to the source or to the other analyzer before a pair was produced or detected. To close this loophole, the analyzers' settings should be rapidly and randomly changed. Only one Bell-type experiment, that of Aspect *et al.* [13], has made any attempt at all to address this locality condition, but even in that experiment the loophole remains. Although the experiment used rapidly-varying analyzers, the variation was not random, and it has been argued that the rapidity of the polarization switching was not sufficient to disprove a causal connection between the analyzer and the source [14, 15].

The detection loophole arises from the non-unity detection efficiency in any real experiment (efficiencies in past tests were at best 10%), so that only a fraction of the emitted correlated pairs is detected. If the efficiency is sufficiently low, then it is possible for the subensemble of detected pairs to give results in agreement with quantum mechanics, even though the *entire* ensemble satisfies Bell's inequalities. Due to the non-existence of adequate detectors, experiments have so far employed an additional assumption, equivalent to the fair-sampling assumption that the fraction of detected pairs is representative of the entire ensemble [16, 17]. In order to experimentally close this loophole, one must have detectors with sufficiently high single-photon detection efficiencies. Formerly, it was believed that $\simeq$83% ($= 2\sqrt{2} - 2$) was the lower efficiency limit. However, one of us (P. H. E.) has shown that by using a non-maximally entangled state (i.e., one where the magnitudes of the probability amplitudes of the contributing terms are not equal), one may reduce the detector requirement to $\simeq$67%, in the limit of no background [8].

# 2 High-efficiency single-photon detectors

The highest *single-photon* detection efficiencies to date have been observed using avalanche photodiodes in the Geiger mode; until recently these have been limited to about 40%. We have measured efficiencies as high as 76%, and there are indications that these may be improved to 80% or even 90% [18, 19]. The technique used to measure the absolute efficiency of a single-photon detector is now fairly well known. It was proposed by Klyshko [20], and first used by Rarity *et al.* [21]

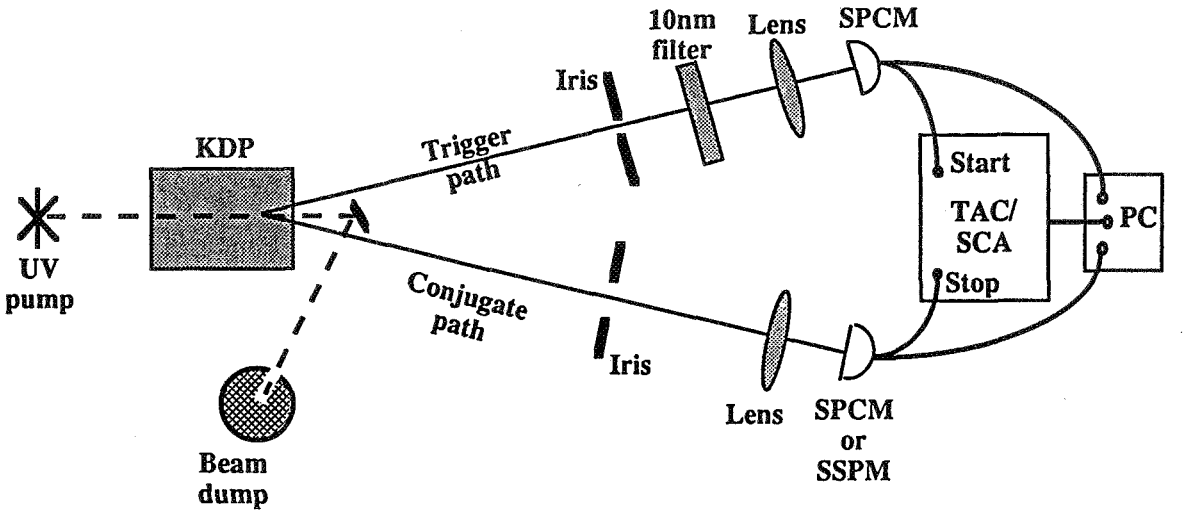


FIG. 1. A simplified schematic of the setup used to measure absolute quantum efficiencies. The 10-cm-long KDP crystal is pumped by the 351-nm line from an argon-ion laser. The smaller iris and interference filter on the path of the trigger photon serve (through phase-matching and energy conservation constraints) to define the path of the conjugate photons, which are all collected by the bottom detector (modulo losses en route). The outputs of the detectors are amplified and fed into the START and STOP channels of a Time to Amplitude Converter/Single Channel Analyzer. The coincidence rate output, as well as the two singles rates, are measured with a counter and stored on a computer. By comparing the coincidence and trigger singles rates, the efficiency of the bottom detector may be determined.

to characterize a silicon avalanche photodiode. The pairs of photons produced in spontaneous parametric down-conversion are highly correlated in time, and reasonably well collimated (i.e., constraining the direction of one photon of a pair determines within a few milliradians the direction of the other). One photon of each pair is directed to a "trigger" detector, and the collection optics are arranged to catch all of the "conjugate" photons with the detector whose efficiency is to be measured (see Fig. 1). The singles count rates at each detector ($R_t$ and $R_c$) are measured, as well as the rate of coincidence counts ($R_{t,c}$) between the detectors. In the ideal limit of no accidental counts (arising from photons from *different* pairs "accidentally" arriving within the coincidence timing window) and no background events (from unwanted external light, dark counts within the detector, or electronic noise), the efficiency of the "conjugate" detector is simply the ratio of coincidence rate to the "trigger" detector singles rate: $\eta_c = R_{t,c}/R_t$ . In the presence of accidentals, A, and trigger detector background, BG, the formula is modified slightly:

$$\eta_c = (R_{t,c} - A)/(R_t - BG). \tag{1}$$

In practice our correlated photon pairs resulted from pumping a potassium di-hydrogen phosphate (KDP) crystal, cut for type-I phase-matching. The down-converted photons typically exited

the crystal at a few degrees with respect to the axis of the pump beam. Using irises and filters to select the trigger photons, we were able to measure the efficiency at the wavelength pairs 702-702nm and 632nm-788nm (the energies of the down-converted photons must sum to the energy of the parent ultraviolet photon at 351nm). We examined four single-photon detectors: two Single Photon Counting Modules (SPCM-200-PQ, EG&G), and two Solid State PhotoMultipliers (SSPM, Rockwell International Corp.). The former devices use Geiger-mode silicon avalance photodiodes specially manufactured to have a very low "k", the ratio of hole- to electron-ionization coefficients [22]; our devices were also custom modified to employ a high overbias voltage of 30V. The SSPMs are also silicon devices, but operate using impurity-band-to-conduction-band impact-ionization avalanches, yielding a very sensitive response in the infrared. The avalanches are localized within areas several microns in size, and do *not* in general lead to device breakdown, so that these devices are capable of distinguishing between single-, double-, etc. photon detections [23].

The highest observed efficiencies were $70.9 \pm 1.9\%$ (with an SSPM, at 632 nm), and $76.4 \pm 2.3\%$ (with an SPCM, at 702 nm). We believe these to be the highest reported single-photon detection efficiencies in the visible spectrum; they are important for quantum cryptography and loophole-free tests of Bell's inequalities, as well as more prosaic applications such as photon correlation spectroscopy and velocimetry. It is important to note that associated with each of the detectors there are other sources of loss, which may yet be improved. Notably, the SPCM detector is housed in a can with uncoated glass windows, and the detector surface itself was broadband anti-reflection coated. Using multi-layer, wavelength-specific coatings, it should be possible to essentially eliminate losses at these interfaces, implying a detection efficiency of $\geq 82\%$. Moreover, a higher overbias is expected to increase the efficiency even further. The plastic optical fibers used to couple the light into the SSPMs were measured (after dismantling the apparatus) to possess unexpected losses—correcting for *all* of these losses would suggest SSPM efficiencies as high as $93 \pm 7\%$. (Since then, relative measurements of SSPM efficiencies of $90 \pm 5\%$ have been observed.) Work is currently underway to improve the fiber coupling scheme. In addition to high efficiency, a useful single-photon detector must have a low level of background, or noise. The SPCMs are internally cooled to about $-30°C$, and have rather small active areas (only $(0.1mm)^2$); their dark count rates are correspondingly low, typically $65s^{-1}$. The SSPMs are cryogenically cooled to 6 K, but have much larger active areas ($(1mm)^2$); typical dark count rates are $7{,}000s^{-1}$.

Previous measurements of the time correlation of the photon pairs have shown that they are emitted within 40 fs of each other [24]. Therefore, they can be used to accurately measure the intrinsic time resolution of single-photon detectors, by mapping out the coincidence rate as a function of electronic delay time. We found that the time profile for coincidences between the SSPM and the SPCM consisted of a main 3.5ns-FWHM peak preceded by a smaller peak by 11ns. A similar time profile between two SPCM's displayed only one peak, with 300ps FWHM. Afterpulses were detected in the SPCM's at a level of less than $10^{-4}$ of the counting rate, with an expontential falloff time-constant of $4.5\mu s$.

# 3 Proposed EPR-source

Even with *unit*-efficiency detectors, the down-conversion schemes used until now are inadequate for a completely unambiguous test of Bell's inequalities, because they must perforce discard counts. In the simplest of the down-conversion Bell-inequality experiments [25, 26], non-collinear corre-

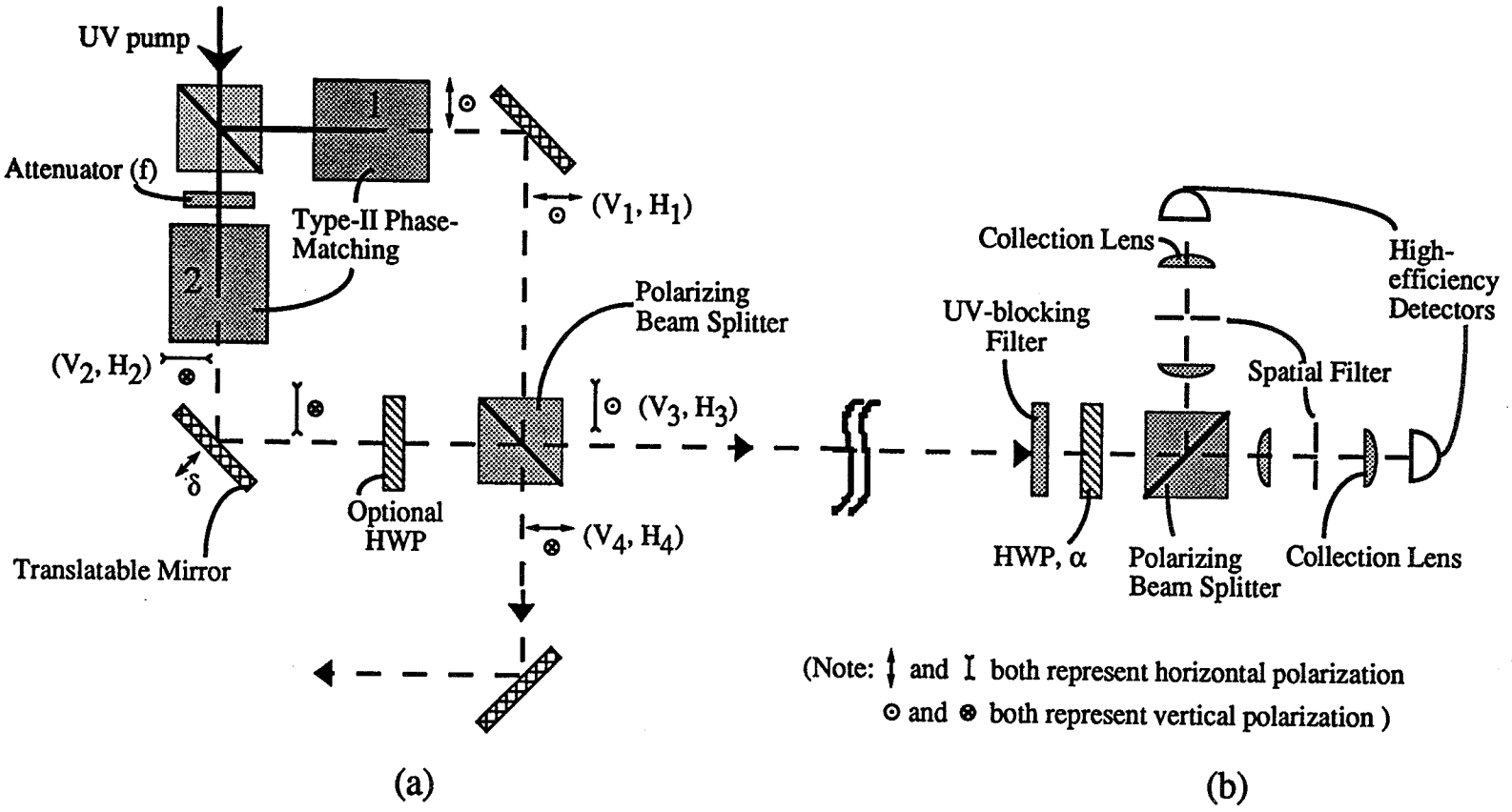
UV pump
1
Attenuator (f)
Type-II Phase-Matching
2
$(V_1, H_1)$
Polarizing Beam Splitter
$(V_2, H_2)$
$(V_3, H_3)$
δ
Optional HWP
$(V_4, H_4)$
Translatable Mirror
(a)
Collection Lens
High-efficiency Detectors
UV-blocking Filter
Spatial Filter
HWP, α
Polarizing Beam Splitter
Collection Lens
(b)
(Note: ↕ and I both represent horizontal polarization
⊙ and ⊗ both represent vertical polarization )

FIG. 2. Schematic of a novel arrangement in which a loophole-free test of Bell's inequalities is feasible. a) An ultraviolet pump photon may be spontaneously down-converted in either of two nonlinear crystals, producing a pair of orthogonally-polarized photons at half the frequency. One photon from each pair is directed to each output port of a polarizing beam splitter. When the outputs of both crystals are combined with an appropriate relative phase $\delta$, a true singlet- or triplet-like state may be produced. By using a half waveplate to effectively exchange the polarizations of photons originating in crystal 2, one overcomes several problems arising from non-ideal phase-matching. An additional mirror is used to direct the photons oppositely to separated analyzers. b) A typical analyzer, including a half waveplate (HWP) to rotate the polarization component selected by the analyzing beam splitter, and precision spatial filters to select only conjugate pairs of photons. In an advanced version of the experiment, the HWP could be replaced by an ultrafast polarization rotator (such as a Pockels or Kerr cell) to close the space-like-separation loophole.

lated photons were directed through equal path lengths to opposite sides of a 50-50 beam splitter, aligned so that the transmitted mode of one photon coincided with the reflected mode of the conjugate photon, and vice versa. A half waveplate prior to the beam splitter was used to rotate the polarization of one of the photons (which were initially horizontally polarized) by 90°. Coincidence rates between detectors looking at the two output ports were recorded, as a function of the orientation of polarizers at the detectors. In only measuring coincidence rates, the experimenters were able to effectively create a singlet-like state by discarding cases where both photon exited the same port of the beam splitter. However, it should be stressed that because of these discarded terms, the detection efficiency is inherently limited to 50% (unless the detector can reliably distinguish one photon from two), and no indisputable test of Bell's inequalities is possible. A similar problem arises in the single-crystal Bell-inequality experiment presented at this conference [27], as well as in experiments based on energy-time entanglement [11] and phase-momentum entanglement [12]. We propose here a setup which should permit for the first time closure of the loopholes. .A very different experiment by Edward Fry is just underway [28], using for the first time atoms from dissociated mercury dimers as the correlated particles. The advantage is that detection efficiencies of 95% are possible by photoionizing the atoms and detecting the photoelectrons.

A schematic of our proposed source is shown in Fig. 2a [29]. Two nonlinear crystals are simultaneously pumped by a coherent pump beam to induce spontaneous parametric down-conversion; the pumping intensity can be independently varied at each crystal. The crystals are cut for type-II collinear degenerate phase matching (i.e., the down-converted photons are collinear and orthogonally polarized, with spectra at roughly twice the pump wavelength). For example, we envisage using 1-cm long crystals of beta-barium borate (BBO), pumped by the 325-nm line from a HeCd laser incident at 54° to the optic axis. For clarity, we first assume a monochromatic pump beam (at frequency $2\omega_o$), and a single-mode treatment of the down-converted photons. Then the state after the crystals is

$$|\Psi>=\sqrt{1-|A|^2}|vac>+\frac{A}{\sqrt{1+|f|^2}}\left(|H,V>_{crystal\ 1}+f|H,V>_{crystal\ 2}\right)\ , \qquad (2)$$

where we have omitted higher order terms (for the very unlikely case in which more than one pump photon down-converts; by reducing the pump intensity, the contribution of these terms can be made as small as desired). $A$ includes the down-conversion efficiency into the modes we are considering, and also the pump field strength; $f$ represents a possible attenuation of the pump beam incident on crystal 2. The state (2) describes a photon pair [one photon polarized horizontally (H), the other vertically (V)] originating with probability amplitude $A/\sqrt{1+|f|^2}$ in crystal 1 and with probability $Af/\sqrt{1+|f|^2}$ in crystal 2. We now combine the modes from the two crystals at a polarizing beam splitter. For an ideal polarizing beam splitter, incident $p$-polarized light (horizontal in Fig. 2) is completely transmitted, while incident $s$-polarized light [vertical (out of the plane of the paper) in Fig. 2] is completely reflected; therefore, one photon of each pair will be directed to output port 3, while the conjugate photon is directed to output port 4. Including a phase shift $\delta = 2\omega_o \Delta x/c$ (where $\Delta x$, the difference in path lengths, may be varied by moving one of the mirrors slightly) between the two non-vacuum terms of (2), we then have

$$|\Psi> \approx \left(|V>_3 |H>_4 + f e^{i\delta} |H>_3 |V>_4\right) \quad , \tag{3}$$

where we have omitted the (predominant, but uninteresting) vacuum term and the prefactor $A/\sqrt{1+|f|^2}$. For the balanced case ($f = 1$), and for $\delta = 180^o$, (3) reduces to the familiar singlet-like state. (In practice, one should probably use a triplet-like state [$\delta = 0$], as this is far less sensitive to cross-talk effects in the polarizing beam splitter—see below.) Note that this contains *no* non-coincidence terms that must be intentionally discarded to prepare a singlet-like state. The source may thus find application in quantum cryptography [30, 31], as it doubles the signal-to-noise ratio of most previous down-conversion EPR schemes.

With the above source of correlated particles, one can now perform a polarization test of Bell's inequalities. Polarization analysis is performed using an additional polarizing beam splitter after each output port of the interferometer, and examining one or both channels of each analyzer with high efficiency detectors (see Fig. 2b). "Rotation" of these analyzers can be effectively accomplished by using a half waveplate before each one to rotate the polarization of the light. If the detectors are far separated from each other and from the source, and one uses some rapid, random means to rotate the light before the analyzers, (such as a Pockels or Kerr cell, whose voltage is controlled by a random signal), then one can close the space-like separation loophole. The signal could be derived, for instance, from the decay of a radioactive substance, or even from the arrival of starlight. Note that since the down-converted photons are emitted within tens of femtoseconds of one another [24] (unlike the photons in an atomic cascade), the limiting time factors will be the detector resolution (expected to be less than 10 ns) and the switching time (which can also be on the order of nanoseconds).

# 4 Other considerations

It has been shown that by using a non-maximally entangled state (i.e., one where the magnitudes of the probability amplitudes of the contributing terms are not equal), one may reduce the detector efficiency requirement [8]. The basic idea is that by making one term of (3) have a greater amplitude than the other, one effectively *polarizes* the source. For example, if $f$ is a

real number $\leq 1$, then a photon travelling to port 4 possesses a net horizontal polarization, while a photon travelling to port 3 appears somewhat vertically-polarized. By appropriately choosing the polarization-analyzer angles, one may reduce the contributions of the singles rates, while still violating a Bell's inequality, even for $\eta$ as low as 67%. It should be noted, however, that the *magnitude* of the violation is reduced as $f$ is reduced, increasing the relative importance of undesirable background counts. A background level (e.g., from any stray light or dark counts) of less than 1% is desired.

One problem that arises in the above scheme is the effect of walkoff of the down-converted photons in the birefringent parent crystal. While the birefringence of the nonlinear crystal is essential for achieving phase-matching, it also results in a relative *displacement* of the two down-converted photons: they propagate in the same direction after exiting the crystal, but are separated by a distance $d = L \tan \rho$, where $L$ is the propagation distance *inside* the crystal, and $\rho$ is the intra-crystal angle between the ordinary and extraordinary beams. Consequently, after the polarizing beam splitter, the *position* of a detected photon partially labels its origin, degrading coherence. Remarkably, insertion of an extra half waveplate after one of the crystals to rotate the polarization by 90° avoids this problem. Photons from either crystal exiting port 3 of the beam splitter would be initially extraordinary-polarized; photons exiting port 4 of the beam splitter would be initially ordinary-polarized. A similar situation occurs due to *longitudinal* walkoff: After propagation through some length of the birefringent down-conversion crystal, one of the down-converted photons will "pull ahead" of its conjugate. In the absense of the half waveplate, one could in principle determine from which crystal a given pair of photons originated by examining the timing of the coincident detection. This distinguishability of contributing paths removes quantum interference, just as in the transverse walkoff situation considered above. (This same effect was discussed by Sergienko *et al.* at this conference [32].) Fortunately, the extra half waveplate also removes this longitudinal walkoff effect. With the waveplate, an infinitely-fast detector looking at the originally extraordinary-polarized photons would *always* trigger before the detector looking at the originally ordinary-polarized photons; hence, interference remains. The waveplate also removes difficulties arising from finite bandwidth and vector phase-matching considerations [29].

For a plane-wave pump, the phase-matching constraints for down-conversion imply that with careful spatial filtering, one can in principle collect *only* conjugate pairs of photons from the crystals (i.e., essentially no unpaired photons, aside from stray light). Once we allow a more realistic, gaussian-mode pump, then this is no longer possible. For identical, finite-sized collection irises, there will always exist situations where one photon is detected while the other is not (even aside from the problem of inefficient detectors). This effect is mitigated by collecting over a larger solid angle. In particular, in order to keep the losses less than 2%, we must employ irises which accept light out to 30 times the pump divergence angle. For example, if we employed a 325-nm pump with a beam waist radius ($1/e^2$) of 3.5 mm, then we would need to accept all half-angles up to 1 milliradian. (In practice, this could be accomplished by use of a precision spatial filter system in each output port; see Fig. 2b.)

We have also investigated the effects of using various non-ideal optical elements. One of these investigations has led us to a novel interference effect. In considering an imperfect recombining polarizing beam splitter, we discovered that the singlet-like state is much more sensitive than the triplet-like state to beam-splitter "cross talk", when $f = 1$. By "cross talk" we mean the situation where photons exit the *wrong* port of the beam splitter (i.e., some fraction of the incident $p$-

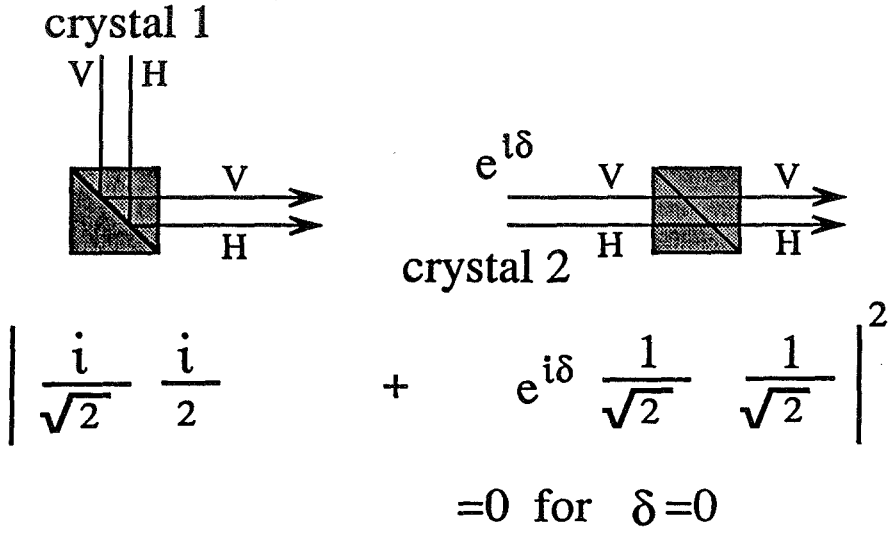


FIG. 3. The two processes that can lead to the final state of both photons going toward the same detector are indistinguishable; thus, we add their probability *amplitudes*. We assume that $f = 1$, and for simplicity that the transmission and reflection amplitudes are $1/\sqrt{2}$ and $i/\sqrt{2}$, respectively. When $\delta = 0$ (triplet-state), there is destructive interference.

polarized light is *reflected*, while some fraction of the incident *s*-polarized light is *transmitted*). Whenever this happens, we once again have a situation in which both photons can leave the same output port of the beam splitter – just as in the experiment discussed at the beginning of Sect. 3, this reduces the effective efficiency, making it more difficult to violate Bell's inequalities. However, in the special case for which the percentage of cross-talk for the two polarizations is equal (one example is the case of a non-polarizing 50-50 beam splitter), there is quantum interference which prevents the two photons from exiting the same port of the beam splitter; the interference only exists for the triplet arrangement ($\delta = 0^o$), not the singlet case ($\delta = 180^o$) [see Fig. 3]. This is, in some sense, the complementary effect to one in some one-crystal experiments (see, for instance, [24, 33]), in which the two-photons from a down-conversion crystal *always* take the same port of a 50-50 beam splitter. It would be interesting to demonstrate this phenomenon experimentally.

Using a scheme that was motivated by two of those presented at this conference [34, 35], it is possible to produce this EPR-source using only *one* down-conversion crystal. The key is to reflect the pump beam back through the crystal (see Fig. 4). Although this scheme has the advantage that it reduces the number of optical elements (most importantly the number of crystals) it does have a few difficulties not present in the 2-crystal approach. First, one must use an isolator to prevent the pump from coupling back into the laser. Next, the return path must be kept short compared to the pump coherence length (typically 10 cm for a HeCd laser), to maintain coherence between the processes in which the down-converted pair originated from a left-going or a right-going pump photon. Finally, one must find very good dichroic mirrors to separate the pump beam

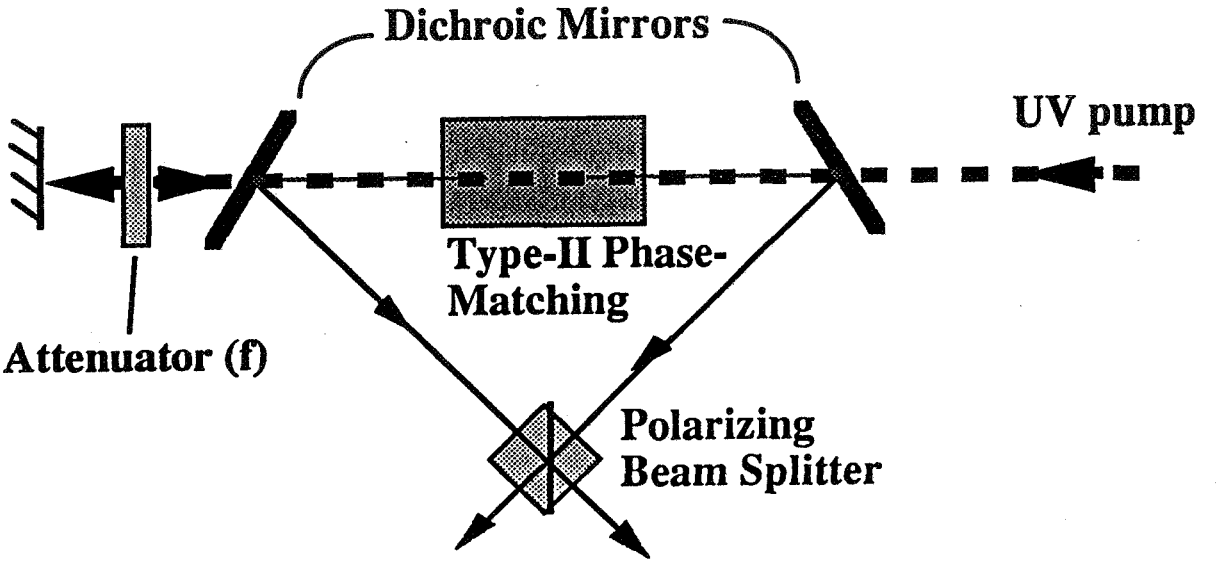


FIG. 4. Proposed one-crystal scheme to produce EPR-state.

from the down-converted photons. One solution is to use high-quality prisms (not shown in Fig. 4).

In conclusion, with the setup described herein it should be possible to produce an indisputable violation of a Bell's inequality. We have examined the effects of background, imperfect polarizing beam splitters, and phase-distorting optics. For $\lambda/20$-flatness optics, a background level of 1%, and custom-selected polarizing beam splitters (with an extinction ratio of at least 500:1), numerical calculation predicts that a violation should be possible as long as the net detection efficiency is greater than 82.6%. Naturally, all optics would be anti-reflection coated to minimize reflection losses; including a 0.25% loss for each interface, and the 2% loss from the gaussian nature of the beam, this means that the bare detector efficiency needs to be at least 88.6%, which may be achievable in light of our recent measurements [18, 19]. Of course, for a safety margin, one would like it to be even higher.

# 5 Acknowledgments

We would like to acknowledge the invaluable assistance of Joshua Holden. One of us (P.H.E.) was supported by the U.S. Department of Energy, Contract No. DE-AC03-76SF00098. The rest were supported by the Office of Naval Research under Grant No. N00014-90-J-1259.

# References


[1] J. S. Bell, Physics **1**, 195 (1964).

[2] J. F. Clauser and A. Shimony, Rep. Prog. Phys. **41**, 1881 (1978).

[3] A. Einstein, B. Podolsky and N. Rosen, Phys. Rev. **47**, 777 (1935).

[4] D. M. Greenberger, M. A. Horne and A. Zeilinger, in *Bell's Theorem, Quantum Theory and Conceptions of the Universe*, edited by M. Kafatos, (Kluwer, Dordrecht, 1989), p. 73.

[5] N. D. Mermin, Phys. Rev. Lett. **65**, 1838 (1990).

[6] L. Hardy, Phys. Rev. Lett. **68**, 2981 (1992).

[7] L. Hardy, Phys. Rev. Lett. **71**, 1665 (1993).

[8] P. H. Eberhard, Phys. Rev. A **47**, R747 (1993).

[9] J. D. Franson, Phys. Rev. Lett. **62**, 2205 (1989).

[10] J. Brendel, E. Mohler and W. Martienssen, Europhys. Lett. **20**, 575 (1992).

[11] P. G. Kwiat, A. M. Steinberg and R. Y. Chiao, Phys. Rev. A **47**, R2472 (1993).

[12] J. G. Rarity and P. R. Tapster, Phys. Rev. Lett. **64**, 2495 (1990).

[13] A. Aspect, J. Dalibard and G. Roger, Phys. Rev. Lett. **49**, 1804 (1982).

[14] J. D. Franson, Phys. Rev. D **31**, 2529 (1985).

[15] A. Zeilinger, Phys. Lett. A **118**, 1 (1986).

[16] J. F. Clauser, R. A. Holt, M. A. Horne and A. Shimony, Phys. Rev. Lett. **23**, 880 (1969).

[17] E. Santos, Phys. Rev. A **46**, 3646 (1992).

[18] P. G. Kwiat, A. M. Steinberg, R. Y. Chiao, P. H. Eberhard and M. D. Petroff, Phys. Rev. A **48**, R867 (1993).

[19] P. G. Kwiat, A. M. Steinberg, R. Y. Chiao, P. H. Eberhard and M. D. Petroff, to appear in Appl. Opt. (1993).

[20] D. N. Klyshko, Sov. J. Quantum Electron. **10**, 1112 (1980).

[21] J. G. Rarity, K. D. Ridley and P. R. Tapster, Appl. Opt. **26**, 4616 (1987).

[22] A. W. Lightstone, A. D. MacGregor, D. E. MacSween, R. J. McIntyre, C. Trottier and P. P. Webb, Electron. Eng. **61**, 37 (1989).

[23] M. D. Petroff, M. G. Stapelbroek and W. A. Kleinhans, Appl. Phys. Lett. **51**, 406 (1987).

[24] A. M. Steinberg, P. G. Kwiat and R. Y. Chiao, Phys. Rev. Lett. **71**, 708 (1993).

[25] Y. H. Shih and C. O. Alley, Phys. Rev. Lett. **61**, 2921 (1988).

[26] Z. Y. Ou and L. Mandel, Phys. Rev. Lett. **61**, 50 (1988).

[27] T. Kiess, A. V. Sergienko, Y. Shih, M. H. Rubin and C. O. Alley, in *Third International Workshop on Squeezed States and Uncertainty Relations*, edited by W.W. Zachary (1993).

[28] E. S. Fry, in *Third International Workshop on Squeezed States and Uncertainty Relations*, edited by W.W. Zachary (1993).

[29] P. G. Kwiat, P. H. Eberhard, A. M. Steinberg and R. Y. Chiao, submitted to Phys. Rev. A (1993).

[30] A. K. Ekert, Phys. Rev. Lett. **67**, 661 (1991).

[31] A. K. Ekert, J. G. Rarity, P. R. Tapster and G. M. Palma, Phys. Rev. Lett. **69**, 1293 (1992).

[32] A. V. Sergienko, T. Kiess, Y. Shih, M. H. Rubin and C. O. Alley, in *Third International Workshop on Squeezed States and Uncertainty Relations*, edited by W.W. Zachary (1993).

[33] C. K. Hong, Z. Y. Ou and L. Mandel, Phys. Rev. Lett. **59**, 2044 (1987).

[34] A. Zeilinger, in *Third International Workshop on Squeezed States and Uncertainty Relations*, edited by W.W. Zachary (1993).

[35] L. Mandel, in *Third International Workshop on Squeezed States and Uncertainty Relations*, edited by W.W. Zachary (1993).

# THE PROBABILISTIC ORIGIN OF BELL'S INEQUALITY

Günther Krenn
*Atominstitut der Österreichischen Universitäten*
*Schüttelstraße 115*
*A-1020 Wien*

**Abstract**

The concept of local realism entails certain restrictions concerning the possible occurrence of correlated events. Although these restrictions are inherent in classical physics they have never been noticed until Bell has shown in 1964 that in general correlations in quantum mechanics can not be interpreted in a classical way. We demonstrate how a local realistic way of thinking about measurement results necessarily leads to limitations with regard to the possible appearance of correlated events. These limitations, which are equivalent to Bell's inequality can be easily formulated as an immediate consequence of our discussion.

## 1 Introduction

Local realism denotes a certain way of thinking about the origin of experimental results which can be specified by the concepts of *locality* and *reality* as defined in the EPR paper [1]. For a system consisting of two spatially separated parts (e.g. in a singlet state) *locality* means that, "since at the time of measurement the two systems no longer interact, no real change can take place in the second system in consequence of anything that may be done to the first system." As a criterion for *reality* EPR give a reasonable proposition which reads as follows: "If,without in any way disturbing a system, we can predict with certainty (i.e. with probability equal to unity) the value of a physical quantity, then there exists an element of physical reality corresponding to this physical quantity."

Generalizing the EPR reality criterion in such a way that with regard to the singlet state (Bohm's version) the result of any spin-measurement has to be considered as predetermined, Bell has shown in 1964 [2] that local realism as defined above is "incompatible with the statistical predictions of quantum mechanics."

By applying the concepts of local realism to a three particle system, D.Greenberger,M.Horne and A.Zeilinger [3] (see also [4]) have shown that in this case a clear cut contradiction can be deduced on the level of perfect correlations. Although this approach provides the most expressive demonstration of the incompatibility of local realism with quantum mechanics it does not work for two-particle systems. There the incompatibility arises just on the statistical level. Hence an intuitive understanding of the contradiction between the idea of local realism and quantum mechanics is difficult, if one is not aware of the origin of this contradiction.

One attempt in order to demonstrate the basic idea of Bell's proof in a more expressive way has been made by E.P.Wigner [5], who derived a specific form of Bell's inequality by using only

simple settheoretical arguments. Recently another attempt has been made by Lucien Hardy [6] who showed that the probability for a contradiction of the GHZ-kind can be greater than zero for a two-particle system.

Nevertheless none of these approaches has provided a general argument based on the concepts of locality and reality which explicitly demonstrates the origin of the discrepancy between local realism and quantum mechanics. Thus our aim is to show the essential restrictions of local realism by discussing the results of a general two-particle experiment using the assumptions of *locality* and *reality*. As evident consequences the conditions for the fulfilment of these restrictions are equivalent to Bell's inequality.

## 2 Predictions based on the knowledge of correlations

We consider the following experimental setup (cf. Fig. 1): A source emits the two parts of a system in opposite directions. Measurements with the possible results $+1$ and $-1$ are performed on each part by two observers A and B. Each of them may select one of two possible values of a measurement parameter $\alpha$ and $\beta$, respectively. As a consequence four different experiments can be made, corresponding to the four different combinations of the measurement parameters $\alpha_1$, $\alpha_2$ and $\beta_1$, $\beta_2$.

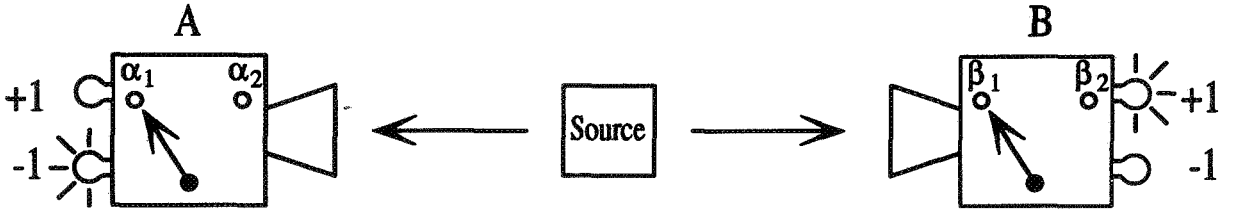


FIG. 1. The experimental setup consists of a source which emits the two parts of a system in opposite directions. Measurements with the possible results $+1$ and $-1$ are performed on each part by two observers A and B. Both A and B have a knob which selects one of two possible values of a measurement parameter. In such a way 4 different experiments can be made (cf. table I).

We assume that all four experiments have been made. The results are listed in table I.

TABLE I. The correlations of the results of the 4 experiments are listed. They might have been observed in actual experiments or calculated by quantum mechanics. $P_i^{\neq}$ is the probability for different results in experiment $i$. In consequence the probability for equal results $P_i^{=}$ is $1 - P_i^{\neq}$.

| Experiment | A | B | Correlation |
|---|---|---|---|
| 1 | $\alpha_1$ | $\beta_1$ | $P_1^{\neq}$ |
| 2 | $\alpha_1$ | $\beta_2$ | $P_2^{\neq}$ |
| 3 | $\alpha_2$ | $\beta_1$ | $P_3^{\neq}$ |
| 4 | $\alpha_2$ | $\beta_2$ | $P_4^{\neq}$ |

In experiment 1 with the parameters adjusted to $\alpha_1$ and $\beta_1$ the observers A and B got different results with probability $P_1^{\neq}$. In experiments 2, 3 and 4 the probabilities for different results are $P_2^{\neq}$, $P_3^{\neq}$ and $P_4^{\neq}$, respectively.

Knowing the correlations which have to be expected either from previous experiments or quantum mechanical calculations, A is able to predict the possible results of B and vice versa. This means that after A has for example performed a series of $n$ measurements with the setting $\alpha_1$ he can infer all possible results of B on the basis of his experimental data and the knowledge of the correlations in experiments 1 and 2 by the following reasoning.

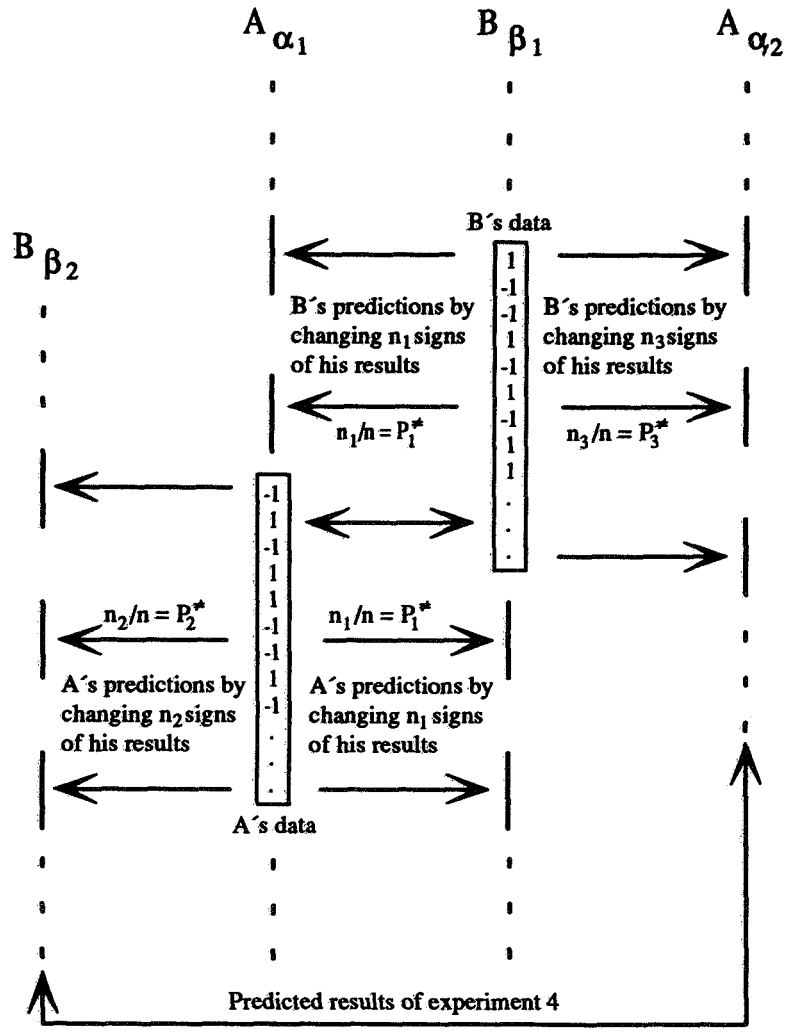


FIG. 2. A procedure is shown by which observer A (B) after having performed a series of $n$ measurements is able to predict the results of observer B (A) for the two alternative settings of the measurement parameter $\beta$ ($\alpha$). The actually measured results of observers A and B are listed in the two boxes. By changing a corresponding number of signs ($n_i = P_i^{\neq} \cdot n$ for experiment $i$) of the measured results the predictions are in agreement with the calculated or previously observed correlations listed in table I. Nevertheless it turns out immediately that the predicted results of experiment 4 are consistent with the actual correlations of experiment 4 (cf. table I) **only if** the inequality $n_1 + n_2 + n_3 \geq n_4$ (equivalent to Bell's inequality) is fulfilled.

If B selects the parameter $\beta_1$ (experiment 1) the probability for different results has to be $P_1^{\neq}$ (cf. table I). For $n \to \infty$ this means that $n_1 = P_1^{\neq} \cdot n$ results have to be different. By reversing $n_1$ signs of his results A arrives at a series of possible results of B which correspond to the known correlations. Because there are $\frac{n!}{n_1!(n-n_1)!}$ different ways of changing $n_1$ signs of $n$ numbers A ends up with a list of $\frac{n!}{n_1!(n-n_1)!}$ different predictions for the possible outcomes of B's measurements. In the same way A is able to infer the possible results B could get, if B selects $\beta_2$ (experiment 2) by changing $n_2 = P_2^{\neq} \cdot n$ signs of his results. In Figure 2 the results of A are listed in the box in row $A_{\alpha_1}$. The predictions he derives from these data are symbolized by vertical lines in rows $B_{\beta_1}$ and $B_{\beta_2}$. Each line corresponds to one way of changing $n_1$ and $n_2$ signs, respectively. By this means the predicted results correspond to the known correlations.

Now let's assume that observer B actually selects the parameter $\beta_1$ and performs a series of $n$ measurements. In figure 2 his results are listed in the box in row $B_{\beta_1}$. Of course they correspond to one of the predictions by A.

Not knowing what A has done observer B himself predicts all possible results A could get if he selects the parameter $\alpha_1$ (experiment 1) or $\alpha_2$ (experiment 3) (cf. table I) by considering all possible ways of changing $n_1$ or $n_3$ signs of his results. Again the actual results of A correspond to one of the predictions by B as it is shown in figure 2.

# 3 Bell's inequality

In the previous section we have shown how it is possible for A to predict all results B could obtain and vice versa. In the following we are going to apply the *locality* assumption that "no real change can take place in the second system in consequence of anything that may be done to the first system" [1]. Moreover we assume in agreement with *realistic* approaches that "unperformed experiments have results" [7] or in other words that predicted results have the status of potential reality.

If we now ask what A could have measured if he had selected the parameter $\alpha_2$ (experiment 3) instead of $\alpha_1$ (experiment 1), we just have to take into consideration the predictions by observer B to find the answer. Based on his actual results and the known correlation in experiment 3 (cf. table I) observer B has predicted all results A could have got if he had chosen $\alpha_2$ (cf. figure 2). As a consequence of the *locality* assumption the results of B, which are the basis of his predictions, are *independent* of anything that may be done by A. Because of this independence *all* of B's predictions have the status of potential reality, which means that if A had selected $\alpha_2$ he actually would have got one of the results predicted by B.

In the same way we find the answer to the question what B could have measured if he had selected the parameter $\beta_2$ (experiment 2) instead of $\beta_1$ (experiment 1) by considering the predictions by observer A (cf. figure 2). It is important to notice that because of the *locality* assumption we can make independent use of the predictions by B and A to answer the question what A and B could have measured if they had selected $\alpha_2$ and $\beta_2$, respectively.

Since we know all possible results A and B could have got if they had chosen $\alpha_2$ and $\beta_2$, respectively (experiment 4), we may now try to find out if these results are consistent with the known correlation of experiment 4 $P_4^{\neq}$ (cf. table I). For this purpose we take one of the results B could have got if he had selected $\beta_2$ (row $B_{\beta_2}$ in figure 2), change $n_2$ signs to get the actual results

of A (box in row $A_{\alpha_1}$), change $n_1$ signs to get the actual results of B (box in $B_{\beta_1}$) and change $n_3$ signs to end up with one of the results A could have got if he had selected $\alpha_2$ (row $A_{\alpha_2}$ in figure 2). Of course we could also do the same thing the other way round but anyway the results A could have got are connected to the results B could have got by the following transformation rule (cf. figure 2): Reverse $n_2$ signs in the first, $n_1$ signs in the second and $n_3$ signs in the last step or the other way round. Doing this the maximum number of signs one can change is simply $n_1 + n_2 + n_3$. This result of *local realistic* reasoning is consistent with the observed correlation in experiment 4 if and only if $n_1 + n_2 + n_3 \geq n_4 = P_4^{\neq} \cdot n$ . If this condition is violated, then not a single pair of the predicted results of experiment 4 (cf. figure 2) is correlated in agreement with experience because there is no pair with more than $n_1 + n_2 + n_3$ different signs.

It follows immediately that this condition is equivalent to Bell's inequality:

$$n_1 + n_2 + n_3 \geq n_4$$

$$\Big\Downarrow \frac{n_i}{n} = P_i^{\neq} \qquad i = 1,2,3,4$$

$$P_1^{\neq} + P_2^{\neq} + P_3^{\neq} \geq P_4^{\neq} \tag{1}$$

$$\Big\Downarrow P_i^{\neq} + P_i^{=} = 1 \qquad i = 1,2,3,4$$

$$1 - P_1^{=} + 1 - P_2^{=} + 1 - P_3^{=} \geq 1 - P_4^{=} \tag{2}$$

$$\Big\Downarrow E_i = P_i^{=} - P_i^{\neq} \qquad i = 1,2,3,4$$

$$\boxed{E_1 + E_2 + E_3 - E_4 \leq 2} \tag{3}$$

We get (3) by adding inequalities (1) and (2) and using the definition of the expectation value of the product of the results $E_i$ in experiment $i$ ($i = 1,2,3,4$).

# 4 Discussion

We have shown that just by discussing the possible results of a general two-particle experiment in a local realistic way one is directly led to a condition for the consistency between quantum mechanics and the concept of local realism.

The crucial point in the argumentation is on the one hand the assumption that A's and B's data are determined locally, which means that A's (B's) results are completely independent of the measurement parameter selected by B (A). On the other hand by assuming that unperformed experiments have results A's and B's predictions can be combined in order to get a prediction of experiment 4 (unperformed). It turns out that this kind of counterfactual reasoning is inconsistent with the results one obtains by actually making experiment 4.

# 5 Acknowledgments

I would like to thank Prof.Anton Zeilinger, Dr.Johann Summhammer, Dr.Marek Żukowski and Clemens Ulrich for useful discussions on this and related topics.

This work has been supported by the Austrian Fonds zur Förderung der wissenschaftlichen Forschung, grant No. P8781-PHY.

# References

[1] A.Einstein,B.Podolsky, and N.Rosen,"Can Quantum-Mechanical Description of Physical Reality Be Considered Complete?" Phys.Rev.**47**,777-780(1935).

[2] John S.Bell,"On the Einstein Podolsky Rosen Paradox" *Physics* 1,195-200(1964)

[3] D.M.Greenberger,M.Horne,and A.Zeilinger,"Going beyond Bell's theorem",in *Bell's Theorem,Quantum Theory,and Concepts of the Universe*,edited by M.Kafatos (Kluwer Academic,Dordrecht,The Netherlands,1989) ,pp.73-76

[4] D.M.Greenberger,M.Horne,A.Shimony,and A.Zeilinger, "Bell's theorem without inequalities",-Am.J.Phys.**58**,1131-1143(1990)

[5] Eugen P.Wigner,"On Hidden Variables and Quantum Mechanical Probabilities" Am.J.Phys. **38**,1005-1009(1970)

[6] Lucien Hardy,"A New Way to Obtain Bell Inequalities" Phys.Lett. A **161**, 21-25 (1991)

[7] Asher Peres, "Unperformed experiments have no results" Am.J.Phys. **46**, 745-747 (1978)

# EINSTEIN-PODOLSKY-ROSEN-BOHM EXPERIMENT AND BELL INEQUALITY VIOLATION USING TYPE II PARAMETRIC DOWN CONVERSION

T. E. Kiess,
*Department of Physics, University of Maryland, College Park, MD 20742*

Y. H. Shih, A. V. Sergienko,
*Department of Physics, University of Maryland, Baltimore County, MD 21228*

and C. O. Alley
*Department of Physics, University of Maryland, College Park, MD 20742*

**Abstract**

We report a new two-photon polarization correlation experiment for realizing the Einstein-Podolsky-Rosen-Bohm (EPRB) state and for testing Bell-type inequalities. We use the pair of orthogonally-polarized light quanta generated in Type II parametric down conversion. Using 1nm interference filters in front of our detectors, we observe from the output of a 0.5mm $\beta - BaB_2O_4$ (BBO) crystal the EPRB correlations in coincidence counts, and measure an associated Bell inequality violation of 22 standard deviations. The quantum state of the photon pair is a polarization analog of the spin-1/2 singlet state.

## 1 Introduction

The Einstein-Podolsky-Rosen-Bohm (EPRB) gedanken[1, 2] for two quantum particles has played an important conceptual role for viewing quantum-mechanical correlations that provide intrigue and challenge to classical intuition. In brief, the EPRB correlation considered here is contained in a two-particle, two detector setup in which a measurement is first made on one particle at one detector of a parameter that is indeterminate prior to the measurement. This outcome then implies with certainty the outcome of the measurement on the second particle. Demonstrations for spin-1/2 quanta[3], for photon polarization states [3, 4, 5, 6, 7, 8], and more recently for other variables [9, 10, 11, 12] have all shown these EPRB correlations in the coincidence registrations of two detectors.

The same quantum-mechanical state of two particles that generates an EPRB experiment also provides an enhancement of observed coincidence rates beyond a maximum bound set by Bell's two postulates[13, 3]. Violations of Bell-type inequalities are one application of EPRB states.

We have found a new and convenient way to generate quantum states that exhibit these EPRB correlations[1, 2], with an associated violation of two-particle Bell-type inequalities[13, 3]. Our source is the pair of light quanta generated in parametric down conversion with Type II phase matching. The pair is incident on one port of a nonpolarizing beamsplitter with output ports containing two linear analyzer-detector packages. The pair is orthogonally polarized, without the need for an interferometer or retardation plates. Our Bell Inequality violation in polarization variables is as large as 22 standard deviations.

# 2 Experimental Method

Our experimental configuration is shown in Fig. 1. A 351.1nm unfocussed Argon ion laser line is incident on a 0.5mm long BBO crystal oriented to achieve Type II phase matching in parametric down conversion, with the 702.2nm wavelength collinear with the pump. Pairs degenerate in propagation direction and frequency emerge from the BBO crystal and separate from the pump at a quartz prism. They are split at a nonpolarizing beamsplitter and sent to two Glan-Thompson analyzer-detector packages. Coincidence counts are collected in a 6nsec coincidence time window from two avalanche photodiode detectors operating in the Geiger mode.

Coincidence counts collected in a large time window are

$$N_{12} = N_o \left[ cos^2\theta_1 sin^2\theta_2 + sin^2\theta_1 cos^2\theta_2 - \lambda sin\theta_1 cos\theta_1 sin\theta_2 cos\theta_2 \right], \qquad (1)$$

for a constant $N_o$ and parameter $\lambda$ that is not a priori equal to two. Indeed, for filters of bandpass greater than 1nm, or for a BBO crystal of greater length (5.65mm), $\lambda$ was found to be less than two. We discuss this bandwidth and crystal length dependence elsewhere in greater detail. For the present conditions (filters with FWHM of 1nm, crystal length 0.5mm), the large visibility ($> 99\%$) in Figs. 2 and 3 is predicted from (1) only for $\lambda$ nearly two. We obtained $\lambda = 1.98 \pm 0.04$.

This value of $\lambda$ is within $1\sigma$ of 2, for which (1) reduces to $sin^2(\theta_1 - \theta_2)$, a function of only the difference angle, $\theta_1 - \theta_2$ This dependence on only one variable specifies an invariance with respect to the other, often referred to as a rotational invariance[3, 7].

This rotational invariance is a key property of our quantum state. Either the o-ray or the e-ray could trigger either detector, making detection of single counts ideally independent of analyzer angle. Once one detector has fired, the conditional probability of registering an event in the second detector is given by the coincidence probability, which for $\lambda = 2$ can be rewritten as $\propto cos^2(\theta_1 - \theta_2 + 90\,\mathrm{deg})$. This is Malus' law for detection of a linear polarization at angle $\theta_1 - \theta_2 + 90\,\mathrm{deg}$. The polarization at the second detector is known with certainty to be linear at this angle after the first detector has fired. This is a correlation of the EPRB type.

The $\lambda$–dependent mixing term in (1) foils any interpretation specifying the o-ray to be localized at detector 1 and the e-ray at detector 2, or vice-versa. Both of these quantum-mechanical amplitudes are present, and their interference generates the $\lambda-$ dependent term of (1) that represents an overlap of "o-ray resolved at D1, e-ray resolved at D2" ($\sim cos\theta_1 sin\theta_2$) with "e-ray at D1, o-ray at D2" ($\sim sin\theta_1 cos\theta_2$).

# 3 Results

We use the coincidence count expression (1) to exhibit Bell inequality violations. This application of (1) proceeds without any necessary regard to the underlying mechanism producing the $\lambda$–dependent interference term.

For the $\lambda = 2$ singlet state analog, we measured the Bell inequality expression as derived by Freedman[14, 3]

$$\mid \frac{N_{12}(\phi) - N_{12}(3\phi)}{N_{12}(-,-)} \mid \leq 0.25, \tag{2}$$

for $\phi \equiv \theta_1 - \theta_2 = 22.5\,\mathrm{deg}$ (see Table I).

It is possible to avoid exhibiting the aforementioned symmetry properties used to derive (2) by testing a more general Bell inequality form. We proceed from the inequality[15, 3, 8]

$$[-N_{12}(\theta_1', \theta_2') + N_{12}(\theta_1', \theta_2) + N_{12}(\theta_1, \theta_2') + N_{12}(\theta_1, \theta_2)] - (N_{12}(\theta_1, -) + N_{12}(-, \theta_2)) \leq 0, \tag{3}$$

in which the Clauser-Horne no-enhancement assumption[15] has already been imposed, and in which probabilities have been converted to coincidence counts $N_{12}$ accumulated in some time interval.

Although we have generated violations of (3), we advocate a stronger version in which the transmission losses of the analyzers are recognized and removed. The basis for this is a generalized version of the no-enhancement hypothesis, in which the passive, polarization-independent analyzer losses are assumed not to affect the behavior of the source whose coincidence properties are under study. We note that these analyzer losses must be controlled[15, 3, 16] in a rigorous Bell inequality test. For our purpose here of exhibiting the coincidence behavior of the source, we use this generalization to alter (3) to the form

$$[-N_{12}(\theta_1', \theta_2') + N_{12}(\theta_1', \theta_2) + N_{12}(\theta_1, \theta_2') + N_{12}(\theta_1, \theta_2)] - (\eta_2 N_{12}(\theta_1, -) + \eta_1 N_{12}(-, \theta_2)) \leq 0. \tag{4}$$

We deduced a choice of four angles ($\theta_1 = 22.5\,\mathrm{deg}, \theta_2 = 135\,\mathrm{deg}, \theta_1' = 67.5\,\mathrm{deg}, \theta_2' = 90\,\mathrm{deg}$) that would violate (3) or (4) maximally. Coincidence counts (Table II) in eight minutes are collected for these angles. Table III shows the deduced violation in these counts of both (3) and (4).

As has been noted[8], violations of (4) occur for any greater-than-zero value of the left hand side. For a relevant figure of merit in judging Bell inequality violations, we advocate the quantity Q-1, for Q the ratio of the term of (4) in square brackets to the term in parentheses. For Q-1>0, the form (4) is violated. We compare in Table III the measured Q-1 to the prediction generated from $\lambda$. As another consistency check, we list the ratio $\eta_2 N_{12}(\theta_1, -) : \eta_1 N_{12}(-, \theta_2)$, which should be 1:1, within experimental error.

In conclusion, we have identified a new source useful in realizing the EPRB gedanken and in testing Bell Inequalities. We achieve the EPRB correlations by virtue of a coincidence probability $\propto sin^2\phi$ for $\phi = \theta_1 - \theta_2$. We obtain a violation of the form (2) for polarization variables that is 22 standard deviations and limited here only by accumulation time. The quantum state is entangled[17] in polarization variables, leading to an interference term in coincidence counts that, because of EPRB correlations and Bell-type inequality violations, is manifestly quantum in nature.

# 4 Acknowledgements

This work was supported in part by the Office of Naval Research Grant No. N00014-19-J-1430.

# References

[1] A. Einstein, B. Podolsky, and N. Rosen, Phys. Rev. 47, 777 (1935).

[2] D. J. Bohm, *Quantum Theory*, (Prentice-Hall, Englewood Cliffs, N.J., 1951).

[3] For a review, see J. F. Clauser and A. Shimony, Rep. Prog. Phys. 41, 1881 (1978).

[4] A. Aspect, P. Grangier, and G. Roger, Phys. Rev. Lett. 49, 91 (1982), and 47, 460 (1981).

[5] A. Aspect, J. Dalibard, and G. Roger, Phys. Rev. Lett. 49, 1804 (1982), and references therein.

[6] W. Perrie, A. J. Duncan, H. J. Beyer, and H. Kleinpoppen, Phys. Rev. Lett. 54, 1790 (1985).

[7] C. O. Alley and Y. H. Shih, in Proceedings of the Second Internationa Symposium on Foundations of Quantum Mechanics in the Light of New Technology, Tokyo, 1986, ed. M. Namiki, et al (Physical Society of Japan, Tokyo, 1987), p. 47; Y. H. Shih and C. O. Alley, Phys. Rev. Lett. 61, 2921 (1988).

[8] Z. Y. Ou and L. Mandel, Phys. Rev. Lett. 61, 50 (1988).

[9] J. D. Franson, Phys. Rev. Lett. 62, 2205 (1989).

[10] J. Brendel, E. Mohler, and W. Martienssen, Europhys. Lett. 20, 575 (1992).

[11] Y. H. Shih, A. V. Sergienko, and M. H. Rubin, Phys. Rev. A47, 1288 (1993).

[12] P. G. Kwait, A. M. Steinberg, and R. Y. Chaio, Phys. Rev. A47, R2472 (1993).

[13] J. S. Bell, Physics 1, 195 (1965); Rev. Mod. Phys. 38, 447 (1966).

[14] S. J. Freedman and J. F. Clauser, Phys. Rev. Lett. 28, 938 (1972).

[15] J. F. Clauser and M. A. Horne, Phys. Rev. D 10, 526 (1974).

[16] For a recent discussion, see V. L. Lepore and F. Selleri, Found. Phys. Lett. 3, 203 (1990).

[17] M. A. Horne, A. Shimony, and A. Zeilinger, Phys. Rev. Lett. 62, 2209 (1989).

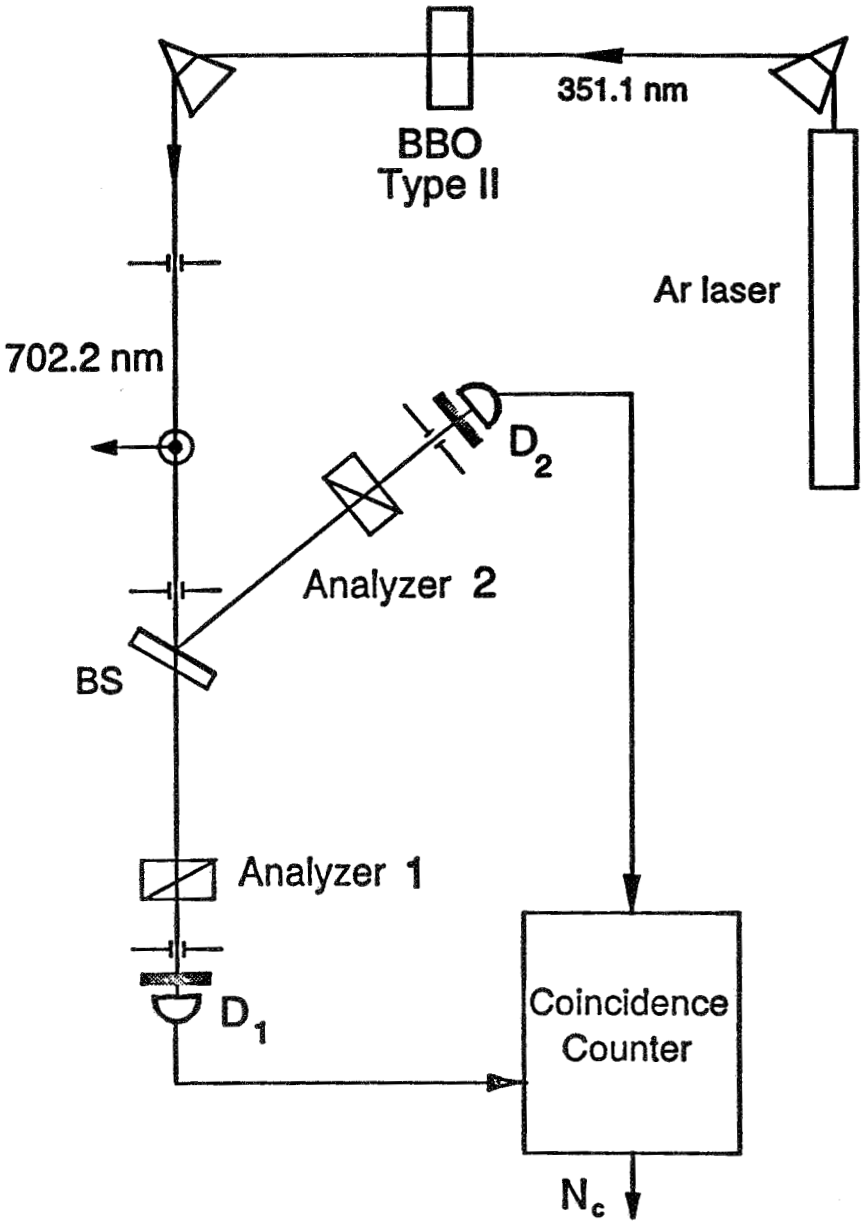


FIG. 1. Experimental Setup. Pairs from collinear Type II down conversion in a BBO crystal are separated from the pump at a prism and directed to a 50:50 beam-splitter. The coincidence registrations in detectors 1 and 2 are recorded as a function of the angles $\theta_1$ and $\theta_2$ of the Glan Thompson analyzers, for each bandwidth filter installed in front of the detectors.

Table I. Bell Inequality Measurements for $\phi = 22.5$ deg.

| $\theta_1$ | $N(\phi)$ | $N(3\phi)$ | $N(-,-)$ | Eq.(8) | |
|---|---|---|---|---|---|
| 0 deg | 1052 | 6054 | 16048 | 0.3117 | $\pm 0.0058$ |
| 0 deg | 1033 | 5931 | 15482 | 0.3164 | $\pm 0.0059$ |
| 45 deg | 902 | 5718 | 14915 | 0.3229 | $\pm 0.0061$ |
| 45 deg | 877 | 5424 | 14468 | 0.3143 | $\pm 0.0061$ |

Table II. Bell Inequality Measurements.

| $N(\theta_1', \theta_2')$ | $N(\theta_1', \theta_2)$ | $N(\theta_1, \theta_2)$ | $N(\theta_1, \theta_2')$ | $N(\theta_1, -)$ | $N(-, \theta_2)$ |
|---|---|---|---|---|---|
| 951 | 4060 | 3701 | 4054 | 4534 | 5060 |

Table III: Bell Inequality Violations Using Counts of Table II.

| Eq.(9) | Eq.(10) | $\eta_2 \cdot N(\theta_1, -)$ | $\eta_1 \cdot N(-, \theta_2)$ | $Q - 1$ | $Q_{pred} - 1$ |
|---|---|---|---|---|---|
| 1188 | 1778 | 4425 | 4579 | 0.198 | 0.207 |
| $\pm 143$ | $\pm 178$ | $\pm 97$ | $\pm 98$ | $\pm 0.022$ | $\pm 0.010$ |
| $(8\sigma)$ | $(10\sigma)$ | | | | |

## BANQUET TALK

# THE RELATION BETWEEN PHYSICS AND PHILOSOPHY

**A. Shimony**



C-8

# The Relation Between Physics and Philosophy

Abner Shimony
*Physics and Philosophy Departments, Boston University,*
*Boston, Massachussetts 02215*

It is an honor to be invited to give the banquet talk at this Workshop. The invitation by Profs. Shih and Rubin provides an opportunity to present to a new audience some theses to which I am devoted. I hope that you will hear some things that you have more or less believed for a long time but have never heard articulated explicitly.

Working physicists, I believe, almost inevitably have strong philosophical interests, regardless of whether they have taken courses labeled "Philosophy" and whether they have liked what they have sampled. Their interest is implicit in the discipline of physics itself. Peter Bergmann, in the introduction to his *Basic Theories of Physics I* attributed to Einstein the view that "a theoretical physicist is ... a philosopher in workingman's clothes." I would omit the adjective "theoretical" and apply the characterization to experimentalists as well. This claim depends, of course, on a conception of what philosophy is. I propose the following: philosophy is the systematic search for perspective, for connections among aspects of the world, and for depth of explanation. Some physicists are drawn into their profession from the beginning because they have been convinced by a few revealing examples that the procedures of physical investigation help to achieve perspective, connections, and depth of explanation. These are philosophers from the start. Others are drawn in because of their fascination with specific phenomena. In my case, the onset of curiosity about the physical world, so far as I can recall, came at the age of four, when I saw my father siphoning wine out of a barrel, and I was amazed that the wine went up in the siphon before it descended. But even if the route to professional physics is via wonder at specific phenomena, an approach to philosophy, in the sense mentioned, is unavoidable, because the physicist's understanding of phenomena goes beyond the phenomena themselves to underlying causes and to connections.

There are various ways to subdivide the discipline of philosophy, but the following will be convenient for our purposes:

1. epistemology, which assesses claims to knowledge;
2. metaphysics, which considers what kinds of things exist and what are the basic principles governing them;
3. theory of value.

I'll put greatest stress upon the relations between physics and metaphysics, because they are richer and more surprising than its relations to epistemology and value theory.

Epistemology:

Among the many problems of epistemology I shall focus on these: (i) what is the proper formulation of scientific method, and to what extent is that method rationally justified? (ii) To what extent can we disentangle subjective from objective contributions in our experience of the world? There were serious and highly intelligent figures in the history of thought, like Descartes,

who maintained that these and related questions in epistemology had to be answered before the substantive work of the sciences could begin, because a foundation is necessary before constructing the edifice of science. We can confidently say, I believe, that this architectural metaphor was mistaken, because all attempts to establish the foundations of knowledge without any substantive assertions about the world seem to have failed. Instead, work on the theory of knowledge and work on substantive science had to proceed in tandem, and – judging by the spectacular successes of the natural sciences – we can say that somehow human beings are capable of this remarkable and somewhat paradoxical intertwining of investigations.

As to problem (i), concerning scientific method, the great breakthrough occurred in the sixteenth and seventeenth centuries, and was inseparable from the development of the new physics and astronomy of Copernicus, Kepler, Galileo, Huygens, and Newton. It had been known from the time of the great Greek philosophers, and probably in a vague way many millennia earlier, that somehow human beings can learn by sense experience and also by reasoning. The division between Plato and his followers, on the one hand, and Aristotle and his followers on the other, concerned the primacy of sense experience or reason. In the work of the new physicists, culminating in Newton's *Principia*, the interplay of the contributions of experience and reason was clarified. These physicists recognized that human beings are not so constituted that they can have direct sensory experience of the fundamental structure of matter or of the fundamental forces among material things. However, if tentative propositions about fundamental physics are formulated in mathematical terms, then logical and mathematical reasoning leads to conclusions that can be checked by sense experience, notably the trajectories of terrestrial bodies and the apparent positions of planets in the celestial sphere. Newton's successful prediction that the orbit of Saturn would be distorted when that planet is close tc Jupiter, and Halley's successful prediction of the recurrence of a comet, and other spectacular verifications of predictions, indirectly confirmed the tentative propositions about fundamental physics which were incapable of direct check. Thus, in tandem with the substantive advance in physics and astronomy was the demonstration of the power of the scientific method summarized above, called the "hypothetico-deductive method." This method was not discredited by the significant refinements of scientific methodology in the centuries that followed, notably enrichment with probability theory. Reflection upon scientific practice was largely responsible for these refinements, since it was noticed by Gauss, Bessel, and others that experimental data are subject to random errors, and they realized that in addition to the dominant causes of a natural phenomenon there are always innumerable small perturbations that cannot be completely catalogued and yet can be treated rationally in terms of probability distributions. Further refinements of scientific method have been made in the twentieth century, and there are still controversial questions concerning inductive inference. Nevertheless, I would maintain that the great revolutions of physics of the twentieth century were accomplished essentially with a classical methodology. The propositions of relativity theory, quantum mechanics, elementary particle theory, etc. were established by applications of the hypothetico-deductive method, refined somewhat by probability theory, without a methodological revolution.

As to problem (ii), concerning the disentanglement of subjective from objective factors in experience, there was not – so far as I can see – a single critical breakthrough, but rather a long, intricate, progressive, and still incomplete development. As the human observer was recognized to be a natural system, the experiences of that observer could be studied as the termini of causal

chains, some of which are initiated within the observer, while others are initiated externally. Of course, all external stimuli eventually impinge upon the neural and psychic machinery of the observer. The naturalistic point of view regarding the human observer has made it possible for psychologists and neurophysiologists to understand such matters as optical illusions, the limited range of the visual and auditory spectra, and the distortion of perceptual judgments by emotional and conceptual bias. In turn, such understanding of the subjective element in experience permits scientists to take counter-measures, by instruments and procedures of observation, in order to enhance the revelation of objective factors in experience. Of course, the ultimate subjective elements of experience, such as sensory qualities, are entirely beyond present science, and will continue to be mysterious until we have a scientific world view that can accommodate consciousness. There has been, however, a capital negative achievement concerning the subjectivity of experience: namely, an accumulation of evidence that the structure of space and time are not imposed upon experience by the operation of the human mind, as Kant maintained in his doctrine of transcendental idealism. Kant's primary argument proceeds from the apparent necessity and universality of geometrical propositions, understood not as mere statements of a formal calculus but as assertions about physical space. The invention of non-Euclidean geometry by Lobatchevsky and Bolyai, the demonstration of its consistency relative to Euclidean geometry by Klein, and the success of its incorporation in general relativity theory are devastating to Kant's argument. Furthermore, when his exemplary geometric instances of synthetic a priori judgments are undercut, then his further claim, that the principles of causality, substance, etc. are necessary because they are imposed by the mind, is seriously weakened; and it is weakened even further by the triumph of a non-deterministic physics. In other words, the epistemological explanation of the basis of science – which was a major part of Kant's program –is undermined, and we are driven to recognize that in so far as science is valid, even as an approximation, it is so because it is a quite good description of the world as it is. The foregoing anti-Kantian argument is regrettably condensed, but it suffices to point to my next thesis: that there are important connections between physics and metaphysics.

Metaphysics:

This thesis may be disconcerting to many people, because the word "metaphysics" is commonly used as a pejorative by physicists, even by those who are sympathetic to epistemology. Until the beginning of the eighteenth century there were great scientists who were also metaphysicians, like Aristotle and Leibniz, and a case can be made for adding Newton to the list. The historical consequence of Kant's work at the end of the eighteenth century and Hegel's at the beginning of the nineteenth was a rift between science and philosophy, regardless of their intentions; and Hegel's grandiose and obscurely reasoned attempt at a "System" of thought engendered a negative reaction among many careful and critical scientists. The positivism of Mach and the Vienna Circle was a consequence of the quest for clarity of expression and rigor of demonstration, and to some extent it was a reaction against the excesses of Hegel. The enterprise of systematic philosophy – aiming at perspective, connections, and depth, as I proposed at the beginning of my talk – became generically suspect, because of the weaknesses of exposition, the excessive claims, and the remoteness from scientific practice of the most influential systematic philosopher of the nineteenth century. The Vienna Circle, which originally called itself the "Mach verein," was nearly unanimous in its condemnation of metaphysics as nonsense and its desire to purge scientific discourse of any residue of metaphysics. At the time of the great scientific revolutions of the early

twentieth century, positivism was a pervasive influence among scientifically oriented philosophers and philosophically oriented scientists. It is not surprising, then, that many of the revolutionaries gave an anti-metaphysical interpretation to their discoveries. Einstein for a long time expressed great sympathy with Mach's ideas, and some of his expositions of special relativity centered around the operationalist analysis of space-time concepts like "simultaneity." Heisenberg's initial formulation of quantum mechanics dispensed with position and momentum, which he regarded as unobservable on a microscopic scale, and tried to express his theory in terms of observables like frequency and intensity. Both Einstein and Heisenberg eventually deviated from positivism and both espoused some form of physical realism – Einstein in his argument for "elements of physical reality" and Heisenberg in a statement that the wave function of an atom can be regarded as a description of the atom as a "thing-in-itself." But Bohr to the end of his life gave interpretations of quantum mechanics with a positivistic flavor, e.g., saying of the wave function that "we are dealing here with a purely symbolic procedure, the unambiguous physical interpretation of which in the last resort requires a reference to a complete experimental arrangement." Bohr believed that the philosophical implications of quantum mechanics are epistemological, concerning limitations of human knowledge and renunciations of unitary pictures of the kind offered by classical physics. His consistent playing down of metaphysical interpretations of quantum mechanics reflect a pervasive suspicion of metaphysical speculation in the scientific community, and it is therefore not surprising that he maintained a strong grip upon the attitude of physicists towards quantum mechanics until fairly recently. I have to confess that in spite of my thesis about the relation of physics to metaphysics, I have respect and sympathy for the positivists' pursuit of clarity of concepts and rigor of demonstrations. I am skeptical, however, that criteria for the meaningfulness of sentences, such as "verifiability," "confirmability," or "falsifiability." can be formulated a priori without drastically damaging scientific investigation. Mach was right that there was an obscurity in Newton's concept of "absolute motion," but the reason is Galilean invariance, which precludes an absolute distinction between rest and uniform rectilinear motion; however, Galilean Invariance is entirely consistent with a clear concept of absolute acceleration. In sum, the clarification of scientific language must proceed in tandem with the progress of scientific knowledge, analogously to the linkage of scientific methodology and substantive science. If physics has progressed to the point where some of the traditional metaphysical problems can be formulated with precision, and even subjected to experimental treatment, then we are presented with a wonderful opportunity, that ought not be neglected because of a suspicion of the sterility of metaphysics. And I contend that modern physics has reached such a stage of development. We are fortunate enough to be invited to a great feast of ideas, and it would be a self-defeating austerity to decline the invitation.

Here is a partial list of results of modern physics having metaphysical implications. Of course, all of these results are subject to modification as science progresses, but it is most unlikely that any of them will cease to be good approximations (in the sense of the correspondence principle) to their successors. For this reasons, the implications that we can draw from them are likely to have a quasi-permanent status.

1. Modern physics (broadly understood to include chemistry) has established the granular character of matter, the present candidates for elementarity being quarks, leptons,. and various bosons. That the immense variety of kinds in the natural world can be understood in terms of combinations of these elementary units is a great vindication of the atomic vision of Democritus.

But the modern qualifications of the Democritean vision are as important metaphysically as the vindication, especially that none of the elementary units is immortal, but all are subject to creation and annihilation in allowable processes; and that certain quantities, notably energy and momentum, are conserved in all of these transformation processes, and others are approximately conserved.

2. The overwhelming evidence that the quantum state of a physical system is a complete description of it, without any need or place for supplementary "hidden variables," implies that various features of the quantum formalism must be attributed to individual physical systems and not just to ensembles. There is objective indefiniteness, because in any quantum state some physical variables have no definite value; there is objective chance, because the different behaviors of various systems with the same quantum state cannot be attributed to differences among hypothetical hidden variables; there is objective probability, because the chance behavior of an ensemble of systems in the same quantum state conforms to definite probability distributions. These three properties conjoined are called"potentiality," in Heisenberg's terminology. That the state of a physical system involves potentialities and cannot be fully understood in terms of actualities is one of the profound metaphysical implications of quantum mechanics. This interpretation of the quantum formalism, it may be noted, is entirely different from Bohr's, which is epistemological in character. For instance, the unceertainty principle is not interpreted in Bohr's fashion as a limitation upon human ability to measure both position and momentum, but rather as an acknowledgment of the objective fact that position and momentum cannot both be actual.

3. Quantum mechanics also has a remarkable implication for the relation between parts and wholes. There are states of composite systems, called "entangled" by Schroedinger, that cannot be expressed as the product of states of the individual components. Entanglement is manifested by the occurrence of correlations that cannot be accounted for by product states. By contrast, classical physics is pervasively analytic and characterizes the state of composite systems in terms of the states of components. Thus quantum mechanics has brought an unprecedented kind of holism into our view of the natural world.

4. When the parts of a composite system are spatially separated, the entanglement of its state implies a kind of non-locality: there is correlated behavior that cannot be explained by any propagation of causal influences that is not superluminal. Nevertheless, the probabilistic nature of quantum mechanics ensures that this kind of non-locality cannot be used to send a signal faster than light. For this reason, quantum non-locality can be characterized facetiously as "passion at a distance" rather than "action at a distance." In ways that are not fully understood, however, we can tentatively say that quantum non-locality requires some modification of classical ideas of causality.

5. The combination of quantum mechanics with the intrinsic indistinguishability of elementary particles of a given type leads to the conclusion that that a system of n identical integral spin particles are in an entangled fully symmetric state (except in the special case that all are in the same one-particle state), whereas n identical half-integral spin particles are in an entangled anti-symmetric state. There are important differences between these two types of entanglement, especially that the Pauli exclusion principle holds in the latter case and not in the former. In either case, however, the status of the individual particle is problematic. The individuality or thisness (Latin "haecceitas") does not seem to be manifested except in interactions with macroscopic

systems, as emphasized in Frisch's famous article, "Take a photon." (I suspect, incidentally, that the word "haecceitas" has seldom if ever occurred at a physics conference since the seventeenth century, but I use it to emphasize again the thesis that modern physics throws some light upon traditional metaphysical problems.)

5. Gauge field theories provide strong constraints upon the interactions permitted among elementary particles. This is an advance of great importance, since a perennial obscurity of the Democritean point of view has been the nature of interactions.

6. Both the special and the general theories of relativity transform our conception of space and time. The special theory asserts an inseparability of space and time in a much stronger sense than in classical kinematics. Classically, space-time is a four-dimensional affine space, with metric properties restricted to space separately and time separately, whereas the space-time of special relativity is a four-dimensional metric space (with a three-one metric). General relativity envisages a dynamical interaction of space-time with matter, instead of regarding the former as a fixed arena in which material dynamics occurs.

7. The interface of physics and biology has a metaphysical implication of great significance: that all biological processes not involving mentality can in principle be understood in terms of physical interactions. Even the program of pre-biotic evolution – of understanding the emergence of mutually catalytic molecules and eventually explaining the evolution of the genetic code in terms of ordinary physical processes – is very promising. I should note that the qualification "not involving mentality" was not inserted for the purpose of hedging but for the positive reason that, in my opinion, a further scientific revolution is needed in order to understand the place of mentality in the natural world.

8. Elementary particle theory and cosmology already have, or are on the verge of having, profound metaphysical implications. But since the assessment of these implications is beyond my expertise, I encourage others to make them explicit.

Finally, I wish to warn against construing this list of metaphysical implications as indicating that all is settled or nearly settled in fundamental physics, and that we need only read off the corollaries in order to do philosophy properly. Rather, there seem to me to be dark clouds showing the need for radical changes in physical theory. One dark cloud is the problem of the reduction of the wave packet, which I prefer to call the problem of the actualization of potentialities. Of course, the advocates of many-worlds and decoherence theories say that there is no such problem, but I am skeptical of their solution (which obliterates the distinction between potentiality and actuality), not for reasons of sophisticated physics, but because of a straightforward philosophical analysis of the relevant concepts. The outcome of this philosophical analysis is to provide a motivation for a modification of quantum dynamics, such as the stochastic modification advocated by Pearle, Ghirardi-Rimini-Weber, Piron, Karolyhazy-Frenkel, Gisin, Percival, Diosi, Penrose, and Bell. They all hope to provide a physical, rather than an epistemological, explanation of the actualization of potentialities. Here is an instance in which philosophical considerations may turn out to provide valuable heuristics for physical investigations. Another dark cloud is the problem of mentality. Before one takes too literally the phrase "theory of everything," applied to the hoped-for theory that explains all forces of nature, the spectrum of elementary particles, the values of all parameters, and the structure of space-time, one should inquire whether such a theory could even in principle account for the immediacy of consciousness.

Theory of value:

I shall say little about the relation between physics and theory of value, partly because of my lack of expertise. However, I do have a few strong opinions. There is, I believe, a real danger that our emotional and moral senses will be dulled by the advance of technology. The case is not hopeless, and the humanities and social sciences have serious suggestions for confronting this danger. But I think that the natural sciences can also make a contribution. A sense of wonder is one of the great motivations of the investigations of science, and the discoveries of science should provide much new nourishment of the sense of wonder. If physics is to offer an antidote against emotional flattening, however, it is essential that its discoveries be understood as revelations of the real structure of the world, to a good approximation, and not just as recipes for making laboratory predictions. My personal experience is that penetrating even a little into the secrets of the universe provides an emotional satisfaction that is like the satisfaction traditionally provided by religion. I suspect that others share this experience.

# REPORT DOCUMENTATION PAGE

*Form Approved*
*OMB No. 0704-0188*



| 1. AGENCY USE ONLY *(Leave blank)* | 2. REPORT DATE | 3. REPORT TYPE AND DATES COVERED |
|---|---|---|
| | May 1994 | Conference Publication |

**4. TITLE AND SUBTITLE**
Third International Workshop on Squeezed States and Uncertainty Relations

**5. FUNDING NUMBERS**
C-NAS5-30376
Code 910.1

**6. AUTHOR(S)**
D. Han, Y. S. Kim, N. H. Rubin, Y. Shih, and W. W. Zachary, Editors

**7. PERFORMING ORGANIZATION NAME(S) AND ADDRESS (ES)**
Goddard Space Flight Center
Greenbelt, Maryland 20771

**8. PEFORMING ORGANIZATION REPORT NUMBER**
94B00074

**9. SPONSORING / MONITORING ADGENCY NAME(S) AND ADDRESS (ES)**
National Aeronautics and Space Administration
Washington, DC 20546-0001

**10. SPONSORING / MONITORING ADGENCY REPORT NUMBER**
NASA CP-3270

**11. SUPPLEMENTARY NOTES**
Han: Goddard Space Flight Center, Greenbelt, Maryland; Kim: University of Maryland, College Park, Maryland; Rubin and Shih: University of Maryland Baltimore County, Baltimore, Maryland; Zachary: Howard University, Washington, D. C.

**12a. DISTRIBUTION / AVAILABILITY STATMENT**
Unclassified - Unlimited
Subject Category 74

**12b. DISTRIBUTION CODE**

**13. ABSTRACT** *(Maximum 200 words)*

The Third International Workshop on Squeezed States and Uncertainty Relations was held at the University of Maryland Baltimore County on August 10 - 13, 1993. This workshop was jointly organized by the University of Maryland and the Lebedev Physical Institute of the Russian Republic. These workshops were initiated by Y. S. Kim, of the University of Maryland, College Park. The first of these workshops was held in 1991 at the University of Maryland, College Park, and the second, in Moscow in 1992.

The purpose of these workshops is to bring together an international selection of scientists to discuss the latest developments in Squeezed States in various branches of physics, and in the understanding of the foundations of quantum mechanics. At the third workshop, special attention was given to the influence that quantum optics is having on our understanding of quantum measurement theory.

The fourth meeting in this series will be held in the People's Republic of China. The principal organizer will be Q. C. Peng, of the Shanxi University at Taiyun, P. R. C.

**14. SUBJECT TERMS**
Squeezed States, Quantum Optics, Uncertainty Relations, Group, Bell's Inequality

**15. NUMBER OF PAGES**
640

**16. PRICE CODE**

| 17. SECURITY CLASSIFICATION OF REPORT | 18. SECURITY CLASSIFICATION OF THIS PAGE | 19. SECURITY CLASSIFICATION OF ABSTRACT | 20. LIMITATION OF ABSTRACT |
|---|---|---|---|
| Unclassified | Unclassified | Unclassified | UL |

National Aeronautics and
Space Administration
**Goddard Space Flight Center**
Greenbelt, Maryland 20771

SPECIAL FOURTH-CLASS RATE
POSTAGE & FEES PAID
NASA
PERMIT No. G27